



Province of British Columbia
Ministry of Energy, Mines
and Petroleum Resources

MINERAL RESOURCES DIVISION
Geological Survey Branch

GEOLOGICAL FIELDWORK 1992

*A Summary of Field Activities
and Current Research*

Editors: B. Grant and J.M. Newell

PAPER 1993-1

MINERAL RESOURCES DIVISION
Geological Survey Branch

Parts of this publication may be quoted if credit is given. The following is the recommended format for referencing individual works contained in this publication:

Warren, M.J. and Price, R.A. (1993): Tectonic Significance of Stratigraphic and Structural Contrasts Between the Purcell Anticlinorium and the Kootenay Arc, East of Duncan Lake (82K); in *Geological Fieldwork 1992*, Grant, B. and Newell, J.M., Editors, *British Columbia Ministry of Energy, Mines and Petroleum Resources*, Paper 1993-1, pages 9-16.

British Columbia Cataloguing in Publication Data

Main entry under title:
Geological fieldwork. — 1974-

(Paper, ISSN 0226-9430)
Annual.

Issuing body varies: 1974-1980, Geological Division; 1981-1985, Geological Branch; 1986- , Geological Survey Branch.

Subseries, 1979- , of: Paper (British Columbia. Ministry of Energy, Mines and Petroleum Resources)

"A summary of field activities of the Geological Division, Mineral Resources Branch."

ISBN 0381-243X=Geological fieldwork

1. Geology — British Columbia — Periodicals.
2. Geology, Economic — British Columbia — Periodicals.
3. Mines and mineral resources — British Columbia — Periodicals. I. British Columbia. Geological Division. II. British Columbia. Geological Branch. III. British Columbia. Geological Survey Branch. IV. British Columbia. Ministry of Energy, Mines and Petroleum Resources. V. Series: Paper (British Columbia. Ministry of Energy, Mines and Petroleum Resources)

QE187.G46 557.11'05
Rev. Dec. 1987

VICTORIA
BRITISH COLUMBIA
CANADA

January 1993

PREFACE

The 1992 edition of *Geological Fieldwork: A Summary of Field Activities and Current Research* is the eighteenth in this annual publication series. It contains reports on Geological Survey Branch activities and projects in a year which saw a modest reduction in base-budget funding, in line with government-wide efforts to control the provincial deficit. The base budget of the Branch for the 1992/93 fiscal year was \$16.96 million, supplemented by an additional \$732 000 from the 1991-1995 Canada - British Columbia Mineral Development Agreement, (MDA) and by \$900 000 from a new government program, the British Columbia Corporate Resource Inventory Initiative (CRII) designed to improve resource inventories and assist land-use decisions.

The budget reduction resulted in the suspension of the British Columbia Geoscience Research Program, which is reflected in a sharp reduction in the number of university research papers published this year. However, the Branch has maintained a vigorous and diverse program of fieldwork and related research as demonstrated by the contents of this year's volume which include:

- Reports on nine 1:50 000-scale geological mapping programs: two in the Stikine district of northwestern British Columbia, three in the northern Quesnel trough, two on the central Interior Plateau, one on northern Vancouver Island and one in the sensitive Tatshenshini area in the northwest corner of the province.
- A report on the Katie alkaline porphyry copper prospect in the Salmo area of the West Kootenays, the first discovery of its type east of the Intermontane Belt.
- The work of the Branch's Environment Geology Section is reported in papers covering the on-going Regional Geochemical Survey program; surficial geology mapping in the central Interior Plateau and research on the viability of lake-sediment geochemistry as an exploration technique in this extensively drift-covered area; the Quaternary geology of buried gold placers in the Cariboo district; and evaluation of construction aggregate resources in the Howe sound area of the Lower Mainland.
- Progress reports on ongoing studies of the quality of British Columbia coals and the wind-up of the digital mapping program in the Northeast coalfield.
- Reports on three diverse industrial mineral occurrences: magnesite and talc in Cambrian carbonates in the Rocky Mountains, and graphite in the Coast Plutonic Complex.

The volume includes ten papers on the results of work by the Mineral Deposit Research Unit (MDRU) at The University of British Columbia. Seven cover ongoing research on the metallogenesis of the Iskut River area and related topics; three derive from research on the alkaline porphyry copper-gold systems at Copper Mountain, Mount Polley and the Iron Mask batholith.

Two major programs warrant special emphasis: the Tatshenshini and Interior Plateau projects. A proposal to develop the huge Windy Craggy copper-cobalt deposit in the Tatshenshini area of northwestern British Columbia has precipitated a major land-use conflict. The existing geoscience database in this remote and sensitive region is inadequate to fully evaluate its mineral potential. The Tatshenshini project, funded by CRII, is covered here by a four-part report. New geological and geochemical data to assist sound land-use management decisions are reported.

The Interior Plateau project, funded by MDA, is part of a cooperative effort between the Geological Survey Branch and the Geological Survey of Canada to expand the geoscience database in this thinly explored, heavily drift covered region. The Branch contribution, reported on in six papers in this volume, is an integrated program of bedrock and surficial geological mapping and lake-sediment geochemistry.

This volume of *Fieldwork* contains 48 articles, a modest decrease from last year, largely as a result of the reduced number of university research papers. Even so, meeting the January publication deadline demands a concerted and unstinting effort from our editorial and publications staff. We acknowledge the efforts of Doreen Fehr and Janet Holland on formatting and page layout, John Newell for timely edits, and Brian Grant for managing the entire process. We thank the staff of the Queen's Printer for their cheerful cooperation and enthusiasm.

W.R. Smyth
Chief Geologist
Geological Survey Branch
Mineral Resources Division

TABLE OF CONTENTS

		Page			Page
	PREFACE	3		ECONOMIC GEOLOGY	
	REGIONAL GEOLOGY			2-1 M.S. Cathro, K.P.E. Dunne and T.M. Naciuk: Katie - An Alkaline Porphyry Copper-Gold Deposit in the Rossland Group, Southeastern British Columbia (82F/3W)	233
1-1	M.J. Warren and R.A. Price: Tectonic Significance of Stratigraphic and Structural Contrasts Between the Purcell Anticlinorium and the Kootenay Arc, East of Duncan Lake (82K)	9	2-2	P. Stinson and D.R.M. Pattison: Petrology of the Evening Star Claim, Rossland, B.C. (82F/4)	249
1-2	G.T. Nixon, J.L. Hammack, J.V. Hamilton and H. Jennings: Preliminary Geology of the Mahatta Creek Area, Northern Vancouver Island (93L/5)	17	2-3	P.R. Bartholomew: Mineral Chemistry of Some Metamorphosed Shuswap-Alsea Mineral Deposits (82L, M)	255
1-3	J. Riddell, P. Schiarizza, R.G. Gaba, N. Cairn and A. Findlay: Geology and Mineral Occurrences of the Mount Tatlow Map Area (92O/5,6,12)	37	2-4	C.R. Stanley and J.R. Lang: Geology, Geochemistry, Hydrothermal Alteration and Mineralization in the Virginia Zone, Copper Mountain Copper-Gold Camp Princeton, British Columbia (92H/7)	259
1-4	L.J. Diakow and P. van der Heyden: An Overview of the Interior Plateau Program	53	2-5	G.E. Ray, I.C.L. Webster, G.L. Dawson and A.D. Ettlinger: A Geological Overview of the Hedley Gold Skarn District, Southern British Columbia (92H)	269
1-5	K.C. Green and L.J. Diakow: The Fawnie Range Project - Geology of the Natalkuz Lake Map Area (93F/6)	57	2-6	L.D. Snyder and J.K. Russell: Field Constraints on Diverse Igneous Processes in the Iron Mask Batholith (92I/9, 10)	281
1-6	C.H. Ash and R.W.J. Macdonald: Geology, Mineralization and Litho geochemistry of the Stuart Lake Area, Central British Columbia (Parts of 93K/7, 8, 10 and 11)	69	2-7	A. Panteleyev and V.M. Koyanagi: Advanced Argillic Alteration in Bonanza Volcanic Rocks, Northern Vancouver Island - Transitions Between Porphyry Copper and Epithermal Environments (92L/12)	287
1-7	J.L. Nelson, K.A. Bellefontaine, M.E. MacLean and K.J. Mountjoy: Geology of the Klawli Lake, Kwanika Creek and Discovery Creek Map Areas, Northern Quesnel Terrane, British Columbia (93N/7W, 11E, 14E)	87	2-8	T.M. Fraser, C.I. Godwin, J.F.H. Thompson and C.R. Stanley: Geology and Alteration of the Mount Polley Alkaline Porphyry Copper-Gold Deposit, British Columbia (93A/12)	295
1-8	F. Ferri, S. Dudka, C. Rees and D. Meldrum: Geology of the Aiken Lake and Osilinka River Areas, Northern Quesnel Trough (94C/2, 3, 5, 6 & 12)	109	2-9	A.A.D. Halleran and J.K. Russell: Rare-Earth Element Bearing Pegmatites in the Wolverine Metamorphic Complex: A New Exploration Target (93N/9E, 93O/12W, 5W)	301
1-9	J.M. Logan and J.R. Drobe: Geology and Mineral Occurrences of the Mess Lake Area (104G/7W)	135	2-10	A.J. Macdonald, P.D. Lewis, A.D. Ettlinger, R.D. Bartsch, B.D. Miller and J.M. Logan: Basaltic Rocks of the Middle Jurassic Salmon River Formation, Northwestern British Columbia (104A, B, G)	307
1-10	I. Neill and J.K. Russell: Mineralogy and Chemistry of the Rugged Mountain Pluton: A Melanite-Bearing Alkaline Intrusion (104G/13)	149	2-11	A.J. Macdonald: Lithostratigraphy and Geochronometry, Brucejack Lake, Northwestern British Columbia (104B/3E)	315
1-11	J.A. Bradford and D.A. Brown: Geology of the Bearskin Lake and Southern Tatsamenie Lake Map Areas, Northwestern British Columbia (104K/1 and 8)	159	2-12	T. Roth: Surface Geology of the 21A Zone, Eskay Creek, British Columbia (104B/9W)	325
1-12	J. Oliver and J. Gabites: Geochronology of Rocks and Polyphase Deformation, Bearskin (Muddy) and Tatsamenie Lakes District, Northwestern British Columbia (104K/8, 1)	177	2-13	R.D. Bartsch: A Rhyolite Flow Deme in the Upper Hazelton Group, Eskay Creek Area (104B/9, 10)	331
1-13	M.G. Mihalynuk, M.T. Smith and D.G. MacIntyre: Tatshenshini Project, Northwestern British Columbia (114P/11, 12, 13, 14; 114O/9, 10, 14, 15 & 16)	189			

TABLE OF CONTENTS *(Continued)*

	Page		Page
2-14 P. Metcalfe and J.G. Moors: Refinement and Local Correlation of the Upper Snippaker Ridge Section, Iskut River Area, B.C. (104B/10W and 11E)	335	4-6 V.M. Koyanagi and A. Panteleyev: Natural Acid-Drainage in the Mount McIntosh/Pemberton Hills Area, Northern Vancouver Island (92L/12)	445
2-15 D.A. Rhys and P.D. Lewis: Geology of the Inel Deposit Iskut River Area, Northwestern British Columbia (104B/11)	341	4-7 S.J. Sibbick and T.A. Delaney: Investigation of Anomalous RGS Stream Sediment Sites in Central British Columbia (92N, O and P)	451
2-16 A.W. Kaip and M.D. McPherson: Preliminary Geology of the Hank Property, Northwestern British Columbia (104G/1, 2)	349	4-8 V.M. Levson, R. Clarkson and M. Douma: Evaluating Buried Placer Deposits in the Cariboo Region of Central British Columbia (93A, B, G, H)	463
INDUSTRIAL MINERALS		4-9 S.J. Cook: Preliminary Report on Lake Sediment Studies in the Northern Interior Plateau, Central British Columbia (93C, E, F, K, L)	475
3-1 G. Benvenuto: Geology of Several Talc Occurrences in Middle Cambrian Dolomites, Southern Rocky Mountains British Columbia (82N/1E, 82O/4W)	361	4-10 T.R. Giles and D.E. Kerr: Surficial Geology in the Chilanko Forks and Chezacut Areas (93C/1, 8)	483
3-2 K.D. Hancock and G.J. Simandl: Geology of the Anzac Magnesite Deposit (93J/16W, 93O/1W)	381	4-11 D.N. Proudfoot: Drift Exploration and Surficial Geology of the Clusko River and Toil Mountain Map Sheets (93C/9, 16)	491
3-3 N. Marchildon, G.J. Simandl and K.D. Hancock: The AA Graphite Deposit, Bella Coola Area, British Columbia: Exploration Implications for the Coast Plutonic Complex (92M/15)	389	4-12 A.J. Sinclair and T.A. Delaney: Preliminary Evaluation of Multielement Regional Stream Sediment Data, Iskut River Area (104B)	499
APPLIED GEOCHEMISTRY AND SURFICIAL GEOLOGY		COAL	
4-1 W. Jackaman: 1992 Regional Geochemical Survey Program: Review of Activities	401	5-1 B.D. Ryan and J.T. Price: The Predicted Coke Strength After Reaction Values of British Columbia Coals, with Comparisons to International Coals	507
4-2 H.E. Blyth and N.W. Rutter: Quaternary Geology of Southeastern Vancouver Island and Gulf Islands (92B/5, 6, 11, 12, 13 and 14)	407	5-2 M.E. Holuszko: Washability of Lithotypes from a Selected Seam in the East Kootenay Coalfield, Southeast British Columbia (82J/2)	517
4-3 V.M. Levson: Applied Surficial Geology Program: Aggregate Potential Mapping, Squamish Area (92G)	415	5-3 M.E. Holuszko, A. Matheson and D.A. Grieve: Pyrite Occurrences in Telkwa and Quinsam Coal Seams (92F/4)	527
4-4 P.T. Bobrowsky, D.E. Kerr, S.J. Sibbick and K. Newman: Drift Exploration Studies, Valley Copper Pit, Highland Valley Copper Mine, British Columbia: Stratigraphy and Sedimentology (92I/6, 7, 10 and 11)	427	5-4 J.M. Cunningham and B.W. Sprecher: Peace River Coalfield Digital Mapping Project, 1992 Fieldwork (93I/9, 10)	537
4-5 D.E. Kerr, S.J. Sibbick and G.D. Belik: Preliminary Results of Glacial Dispersion Studies on the Galaxy Property, Kamloops, B.C. (92I/9)	439	EXTERNAL PUBLICATIONS AND UNIVERSITY RESEARCH	
		6-1 University Research in British Columbia	549
		6-2 Selected Recent External Publications by B.C. Geological Survey Branch Staff	551



TECTONIC SIGNIFICANCE OF STRATIGRAPHIC AND STRUCTURAL CONTRASTS BETWEEN THE PURCELL ANTICLINORIUM AND THE KOOTENAY ARC, EAST OF DUNCAN LAKE (82K)

By Marian J. Warren and Raymond A. Price, Queen's University

KEYWORDS: Regional geology, stratigraphy, Windermere Supergroup, Horsethief Creek Group, Hamill Group, deformation, thrust faults.

INTRODUCTION

The main goal of this study is to elucidate the nature and tectonic significance of the profound stratigraphic and structural changes that occur between the crest of the Purcell anticlinorium and the Kootenay Arc.

Reconnaissance (1:250 000) mapping by Reesor (1973) outlined conspicuous contrasts between the thick basal Paleozoic (Hamill-Badshot) succession that overlies the Windermere Supergroup in the western Purcell Range and the thin, condensed early Paleozoic succession with overlapping Upper Devonian strata that occurs in the eastern Purcell Range. Reesor also described the abrupt contrast between the tight upright fold structures in this area and the refolded, west-verging, recumbent isoclinal folds that occur immediately to the west in the Kootenay Arc. He also showed that several small granitic plutons in the area probably were emplaced while the folding was still underway.

The rocks exposed in this area (Figure 1-1-1) record both the Late Proterozoic - early Paleozoic birth and development of the Cordilleran miogeoclinal passive margin of North America (Bond and Kominz, 1984; Bond *et al.*, 1985), and the late Mesozoic - early Cenozoic deformation, regional metamorphism and granitic plutonism resulting from "collisions" between North America and a series of allochthonous terranes that have been accreted to it (Monger *et al.*, 1982).

Detailed geological mapping (1:50 000 and greater) was completed during July and August of 1991 and 1992 within an area of about 900 square kilometres in the western Purcell Mountains, between Duncan Lake and the headwaters of Toby and Jumbo creeks (Figure 1-1-2). This work will link the detailed mapping along the Kootenay Arc by Fyles (1964) to the detailed mapping by Root (1987) and Pope (1990) in the central and eastern Purcell anticlinorium.

The main objectives of this study are: (1) to establish the nature and tectonic significance of the stratigraphic relationships within the thick sequence of Windermere, Hamill and Badshot strata in the study area; (2) to investigate the stratigraphic and tectonic relationships between these strata and the condensed onlapping early Paleozoic succession that occurs on "the Windermere high" to the east, below the Mount Forster thrust fault in the central and eastern Purcell Mountains (Root, 1985; Reesor, 1973); (3) to establish the nature, evolution and regional tectonic significance of the change in structural style between the study area and the adjacent areas in the Kootenay Arc and in the central Purcell

Mountains; and (4) to investigate the relationship between the initial structural configuration of the rifted margin and the major structures that developed during Mesozoic terrane accretion and deformation of the margin.

SUMMARY OF STRATIGRAPHIC RELATIONSHIPS

WINDERMERE SUPERGROUP

The Windermere Supergroup in the study area comprises the Toby Formation and the overlying Horsethief Creek Group. Although the Horsethief Creek Group was previously undivided in this area, mappable units can be recognized within it at a scale of 1:50 000 or greater. Two markedly contrasting sequences of units have been defined by detailed mapping of the Horsethief Creek Group in the study area. Variations between the thin sequence exposed to the south and east, and the thicker sequence exposed to the north and west are summarized in Figure 1-1-4.

The southern and eastern sequence is exposed in the Jumbo, Toby, Glacier, and Hamill Creek drainages. It lies apparently conformably on cobble or boulder conglomerate of the Toby Formation, which in turn rests unconformably on the Dutch Creek and Mount Nelson formations of the Middle Proterozoic Purcell Supergroup. The lower part of the Horsethief Creek Group is in general characterized by fine-grained rocks. A laterally continuous unit of marble and calcareous slate (Ht1) lies at the base, overlain by a unit characterized by graded beds of slate and metasiltsstone (Ht2). The middle of the Horsethief Creek Group (Ht3) contains abundant discontinuous grit and pebble conglomerate beds (metre scale) and interbedded pelite. Both feldspar and mafic fragments or minerals are common in these rocks. The coarse facies fine upward to overlying pelitic rocks (Ht4). The sequence is overlain by a quartz grit unit, transitional to the overlying Hamill quartzite (Hmt). Total thickness of this sequence varies from a maximum of about 1500 metres in Jumbo Creek to less than 200 metres at Eagle Nest Lake.

The northern and western sequence is well exposed in Howser, Tea, and Rory creeks and on adjacent ridges. It consists of a lower sequence (Ht5) of rhythmically interbedded, thick (tens of metres) feldspathic grit or conglomerate and slate. These coarser clastic rocks are overlain by a sequence of dark marble and calcareous slate (Ht6) up to several hundred metres thick. The upper part of the Horsethief Creek Group (Ht7) contains abundant slate or pelitic schist, siliceous carbonates, minor grit, and a remarkable amount of graded quartz sandstone. Discontinuous greenstone lenses are common in Unit Ht7. Near the mouth of

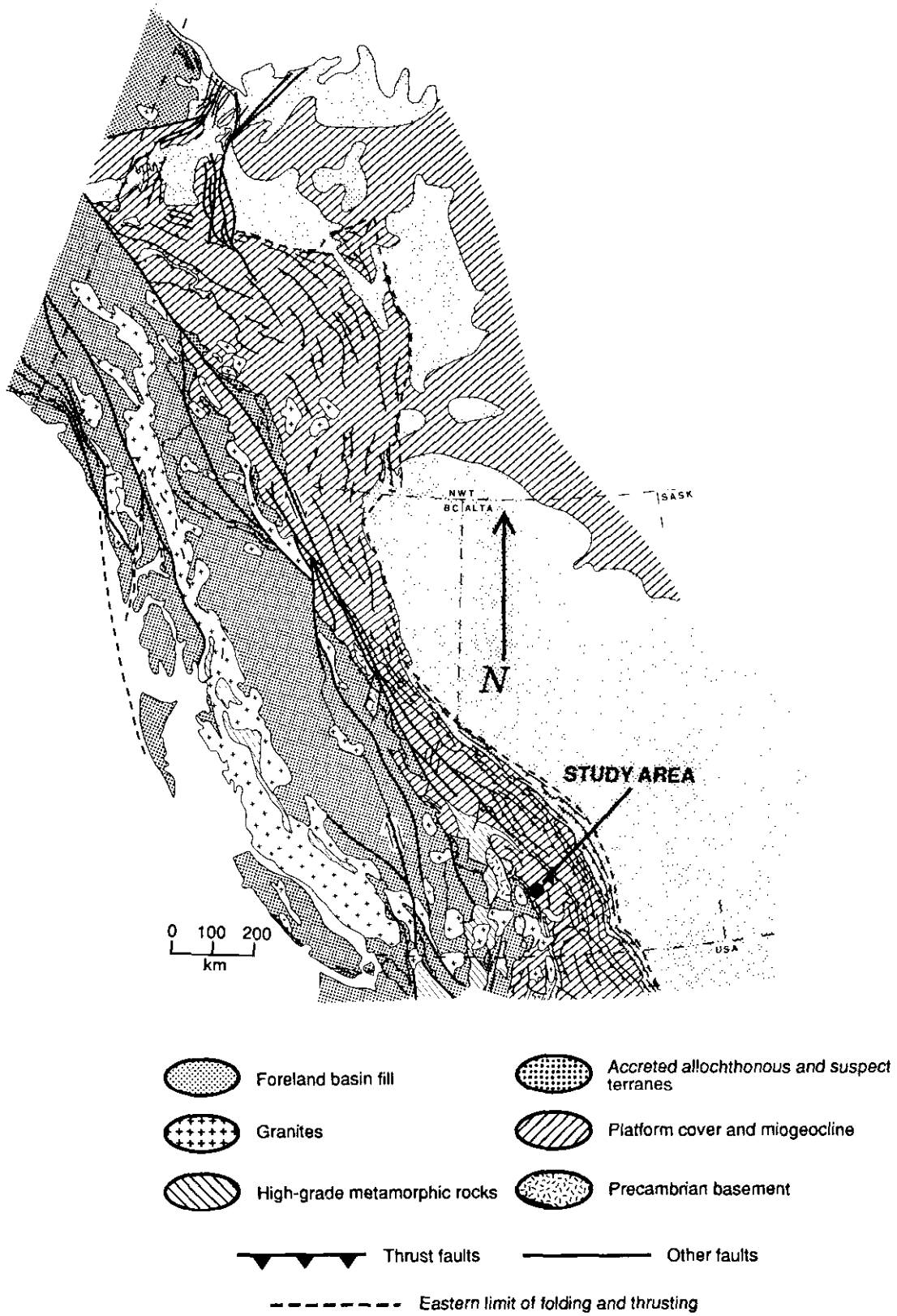


Figure 1-1-1. Tectonic map of the Canadian Cordillera showing location of the study area. Modified after Douglas (1968) and Price (1986).

Howser Creek, the Horsethief Creek Group is overlain by upper Hamill quartzite. In all other localities, the top of the sequence is not exposed. The bottom of the Horsethief Creek Group is nowhere exposed in this area. However, the thickness of the exposed strata exceeds 2000 metres, and individual units are in general both thicker and more continuous than to the south and east (as observed by Reesor, 1973).

The divisions of the Horsethief Creek Group in the Howser Creek area closely resemble the lower clastic, middle marble and upper clastic divisions described from areas to the north by other workers (Read and Wheeler, 1976; Brown *et al.*, 1978; Pell and Simony, 1987). The southern and eastern sequence is more similar to that mapped by Reesor (1973) in the eastern Purcells, although it is thicker and contains less coarse clastic material than observed to the east. The top two units of the southern and eastern sequence (Ht3, Ht4) grade laterally into the upper part of the northern and western sequence (Ht7). Lateral relationships between the lower parts of the two sequences are unknown.

HAMILL GROUP

TRANSITIONAL UNIT

The Hamill Group (Walker and Bancroft, 1929) lies stratigraphically above the Horsethief Creek Group. Stratigraphic relationships within the Hamill Group are summarized in Figure 1-1-5. The contact between the Horsethief Creek and Hamill groups is marked by a distinctive transitional unit, which is included in the base of the Hamill Group. The transitional unit is characterized by quartz and feldspar grit and pebble conglomerate in a quartz sand matrix. This unit thins to the west and north, and is absent near Howser Creek. Laterally continuous dolostone and quartz grit beds are common in this unit to the east, whereas dolostone-clast conglomerate and rapid facies variations occur to the west. The lower contact is more abrupt to the east, whereas the upper contact with the lower Hamill Group is more abrupt to the west. The transitional unit and its relationships to Horsethief Creek and Hamill groups are in many ways similar to the Three Sisters Formation to the south (Little, 1960), and the Jasper Formation to the north (Lickorish, 1992).

REMAINING HAMILL GROUP

The remainder of the Hamill Group, which overlies the transitional unit, is divisible within the study area into four map units, including the Mohican Formation (Fyles and Eastwood, 1962). The lowermost unit (Hm1) is a clean, crossbedded quartzite, with minor quartz grit and pebble conglomerate, and minor pelite. It lies conformably on the transitional unit. The middle Hamill Group (Hm2) contains pelitic schist, impure quartzite, minor carbonate and, most significantly, greenstone. This unit thins, and contains less abundant greenstone, to the east. In the Blockhead Mountain syncline, it contains little or no mafic material, and it pinches out. The upper part of the Hamill Group (Hm3) consists of clean, white quartzite at the base, and interbedded light and dark quartzite and pelite near the top. It is overlain by the Mohican Formation, a calcareous schist

which is transitional between the upper Unit Hm3 and the Badshot Formation. In the Blockhead Mountain syncline, the Mohican Formation contains a distinct, laterally continuous orthoquartzite marker unit.

The contacts between Units Hm1, Hm2, and Hm3 are abrupt, although where the less mature middle unit (Hm2) is absent, it is commonly difficult to distinguish between the lower (Hm1) and upper (Hm3) quartzite units. The contact between Unit Hm3 and the Mohican Formation is gradational. The total thickness of the Hamill Group varies from 900 to 1500 metres. The sequence described in this study area bears some marked similarities, as well as several differences, to those described by Höy (1974) to the south in the Kootenay Arc, and by Devlin (1989) to the north in the Dogtooth Range.

Within the Kootenay Arc (structural domain 1; Figure 1-1-3), Units Hm2 and Hm3 are exposed within the cores of recumbent anticlines, and no older rocks have been observed. An important relationship was documented in the adjacent western edge of the Purcell anticlinorium; upper Hamill Group (Hm3) directly overlies upper Horsethief Creek Group near the mouth of Howser Creek. This contact is apparently stratigraphic, and it is considered likely, therefore, that the lower part of the Hamill may be absent beneath the Kootenay Arc.

BADSHOT FORMATION

The Badshot Formation (Walker and Bancroft, 1929) stratigraphically overlies the Mohican Formation of the Hamill Group. The Badshot Formation is characterized by cliff-forming, white to medium grey, commonly laminated marble or dolomitic marble. At the eastern edge of the area mapped by Fyles (1964), marble horizons tens of metres thick may be separated by grey, locally calcareous schist.

PHYLLITE IN THE CORE OF THE BLOCKHEAD MOUNTAIN SYNCLINE

Silvery grey phyllite and interbedded an calcareous schist overlie the dolomitic marble of the Badshot Formation in the core of the Blockhead Mountain syncline. Root (1987) mapped this unit as lower Index Formation, of the Lardeau Group. The grey phyllite, however, differs in appearance from the lower Index Formation exposed to the west along Duncan Lake. The lower Index phyllite or schist is characteristically black, commonly graphitic, and contains abundant black or graphitic marbles above the contact with the Badshot Formation. Therefore, the schistose rocks in the core of the Blockhead Mountain syncline are included in the Badshot Formation.

LARDEAU GROUP

The Index Formation of the Lardeau Group is well exposed in tight map-scale folds within the Kootenay Arc on the east side of Duncan and Kootenay lakes (Fyles, 1964). The Formation as mapped by Fyles (1964) includes: black, commonly graphitic phyllite or schist of the lower Index Formation, with interbedded black marble at the base; green phyllite or quartz-muscovite-chlorite schist, grey mar-

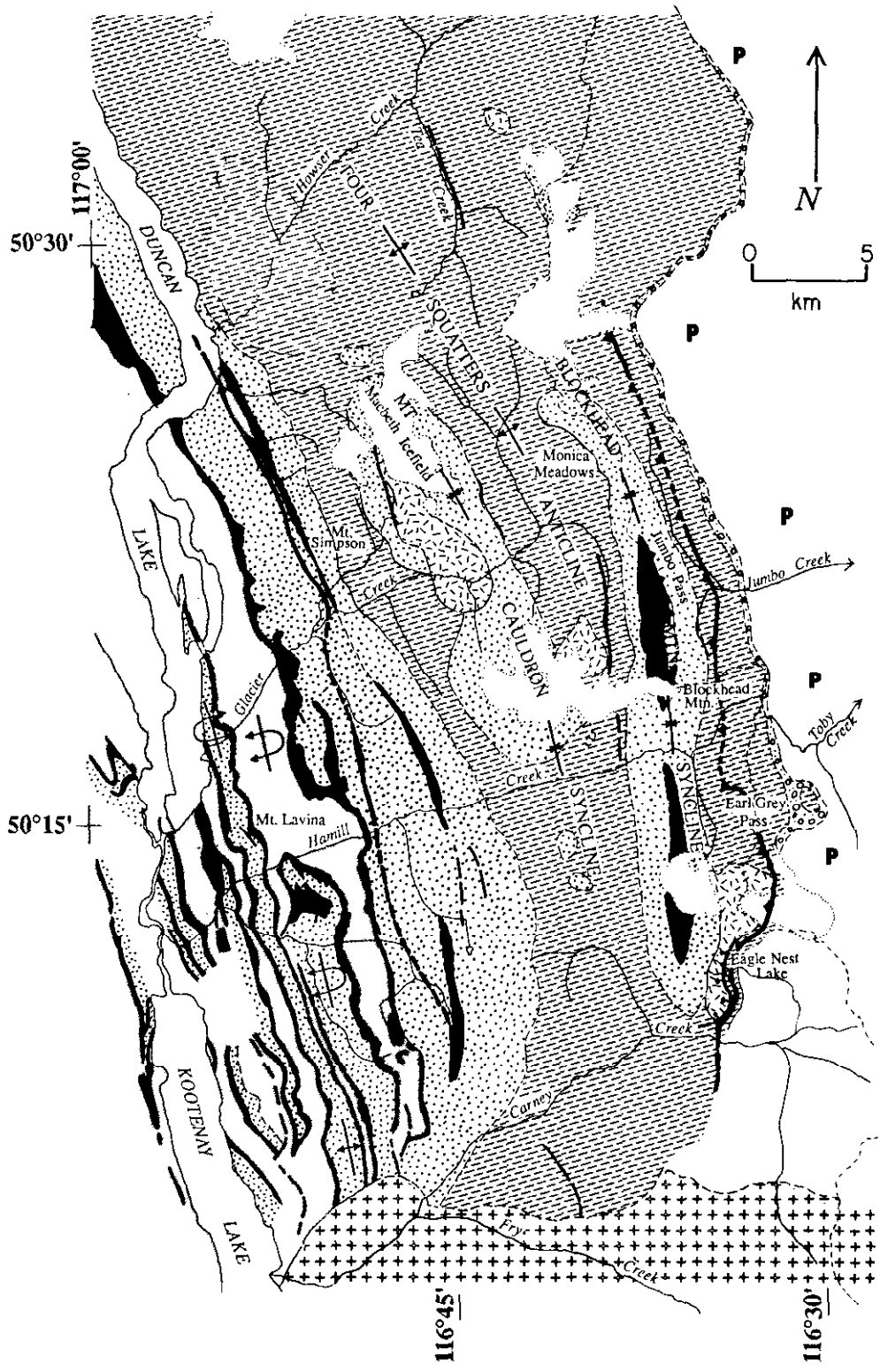
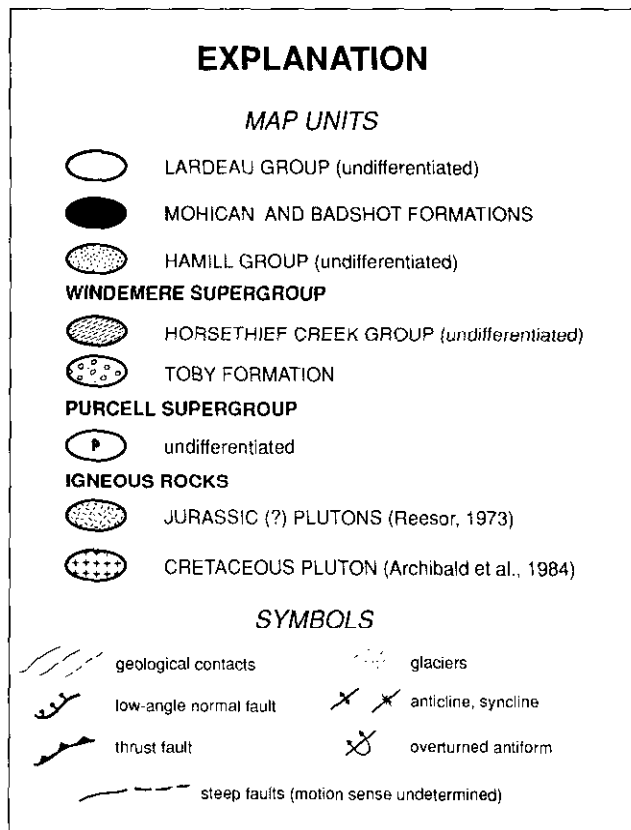


Figure 1-1-2. Simplified geological map of the study area and adjacent segment of the Kootenay Arc. Modified after Reesor (1973).



ble and minor greenstone of the upper Index Formation. The lower Index Formation, between the mouths of Glacier and Howser creeks, contains thin bands of ultramafic to mafic schist.

SUMMARY OF STRUCTURAL RELATIONSHIPS

The study area is divisible into three domains with contrasting structural styles and tectonic histories (Figure 1-1-3). These are, from east to west: the western Purcell anticlinorium; a thin transitional belt; and the western Kootenay Arc.

DOMAIN 1: PURCELL ANTICLINORIUM

The map pattern in Domain 1 is dominated by open to locally tight, upright folds, which deform an upward-facing stratigraphic sequence. The dominant regional schistosity or cleavage is axial planar to these folds. Locally developed shear zones are common and are parallel to the dominant foliation. Earlier east-verging recumbent folds are preserved in competent strata at outcrop scale, but do not affect the map pattern. A later crenulation or spaced cleavage commonly overprints the dominant foliation. The youngest observed structures are locally developed but widespread, east-striking left-lateral kink bands. Lower greenschist facies metamorphism accompanied the dominant phase of folding.

One significant fault was mapped within this domain, in the easternmost belt of Horsethief Creek Group. The fault is moderately west dipping and appears to cut the dominant

folds and axial planar cleavage. Stratigraphic relationships across the fault are striking and puzzling. Near Eagle Nest Lake, the fault juxtaposes the transitional unit at the base of the Hamill Group, in the hangingwall, against lowermost Horsethief Creek Group (Ht1) in the footwall. Approximately 1000 metres of Horsethief Creek Group strata are missing. Along strike to the north, in northernumbo Creek, the fault repeats part of the lower Horsethief Creek Group section. Both hangingwall and footwall units truncate against the fault toward the south. These relationships imply that the fault cuts a pre-existing structure.

DOMAIN 2: TRANSITIONAL

Domain 2 is a belt of subvertical rocks. The structural style is transitional between that of the Purcell anticlinorium to the east and the Kootenay Arc to the west. The stratigraphic sequence is upward facing and is deformed by upright isoclinal map-scale (km) folds and ductile high-strain zones. These structures deform earlier outcrop-scale isoclinal folds and an axial planar fabric, but no earlier map-scale structures have been observed in this domain. The

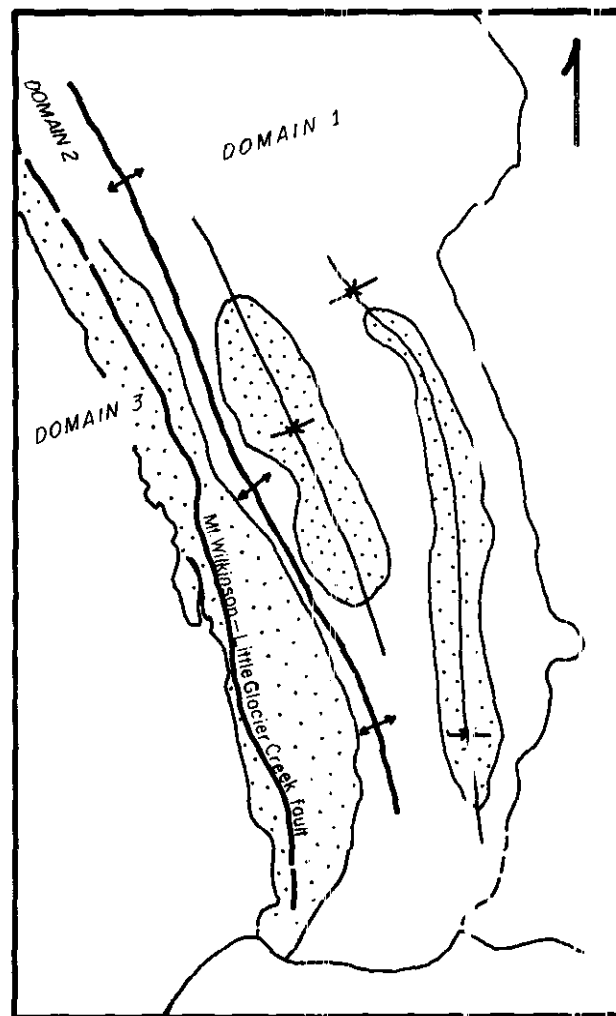


Figure 1-1-3. Sketch map showing locations of structural domains in the study area.

Windermere Supergroup Stratigraphy

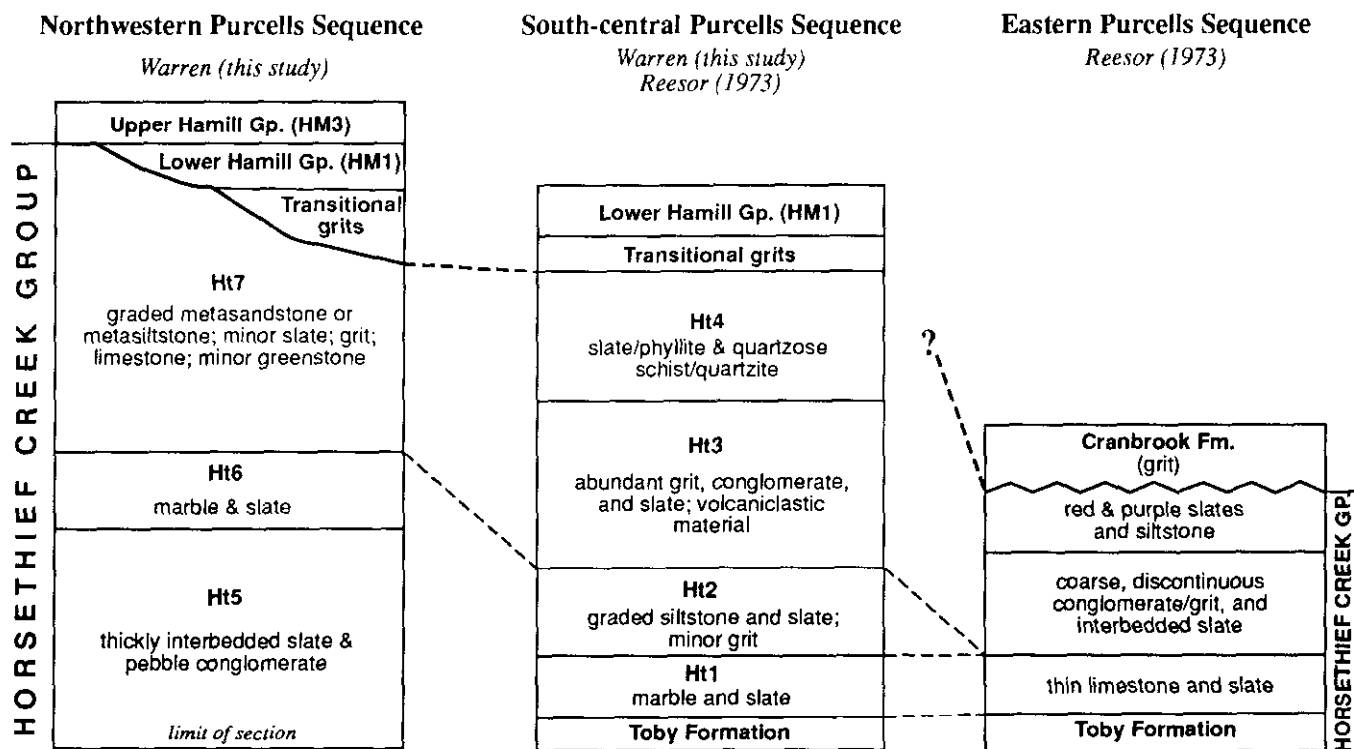


Figure 1-1-4. Stratigraphic relationships between sequences of Windermere Supergroup across the Purcell anticlinorium.

vergence of the early structures is unknown. The dominant deformation was accompanied by upper greenschist to amphibolite facies metamorphism.

DOMAIN 3: WESTERN KOOTENAY ARC

Domain 3, which was mapped in detail by Fyles (1964), is characterized by the more intense and complex deformation that is typical of the Kootenay Arc. Large-amplitude (10 km scale) west-verging recumbent folds were deformed by two phases of upright, tight to isoclinal folds, under conditions of amphibolite facies metamorphism. Much of the stratigraphic sequence is overturned, and along the eastern boundary of the domain, the sequence is everywhere overturned.

The boundary between Domains 1 and 2 is defined by the axial trace of an anticline cored by Horsethief Creek Group. Strata east of this boundary are gently to moderately dipping, whereas strata to the west are subvertical. Although no significant fault was mapped along this boundary, it represents an abrupt contrast in metamorphic grade and structural style.

NATURE OF DOMAIN BOUNDARIES

The boundary between Domains 2 and 3 is defined by a subvertical, locally mylonitic fault, which separates the Purcell anticlinorium from the Kootenay Arc. The fault is significant because it juxtaposes an upward-facing stratigraphic sequence to the east, against an overturned sequence to the west. Similar relationships have been

described along strike to the south by Höy (1974), along the West Bernard fault, and by Leclair (1988) along the Seeman Creek fault. The sense of motion along this fault has been a long-standing enigma, due primarily to the fact that the same map unit of the Hamill Group was observed on both sides of the fault. However, east of Duncan Lake, rocks of the middle and upper Hamill Group to the west, are juxtaposed against upper Hamill Group, and, where the fault intersects Duncan Lake, Index Formation. These relationships imply a west-side-up sense of motion, although this interpretation requires caution, as the fault cuts previously folded strata.

In all three structural domains, the second-phase structures are dominant. A poorly understood subhorizontal stretching lineation parallels the axes of second-phase folds in all three domains. It is important to note that the small early folds preserved in the eastern domain are east verging, whereas the large-amplitude early folds in the Kootenay Arc are west verging. The younger phase of upright folding in the Kootenay Arc is coplanar with the second-phase deformation, and similar in structural style. It probably represents a continuation of the dominant deformation. In Domain 1, the younger structures appear to have formed under slightly more brittle conditions than the dominant second-phase structures.

Granodiorite plutons were intruded late in the main phase of deformation in Domains 1 and 2 (Reesor, 1973; Warren and Price, 1992). Abundant granitic dikes or sills were intruded during the main phase of deformation in the southern part of Domain 3 (Fyles, 1964; Warren and Price, 1992).

Paleozoic Stratigraphy

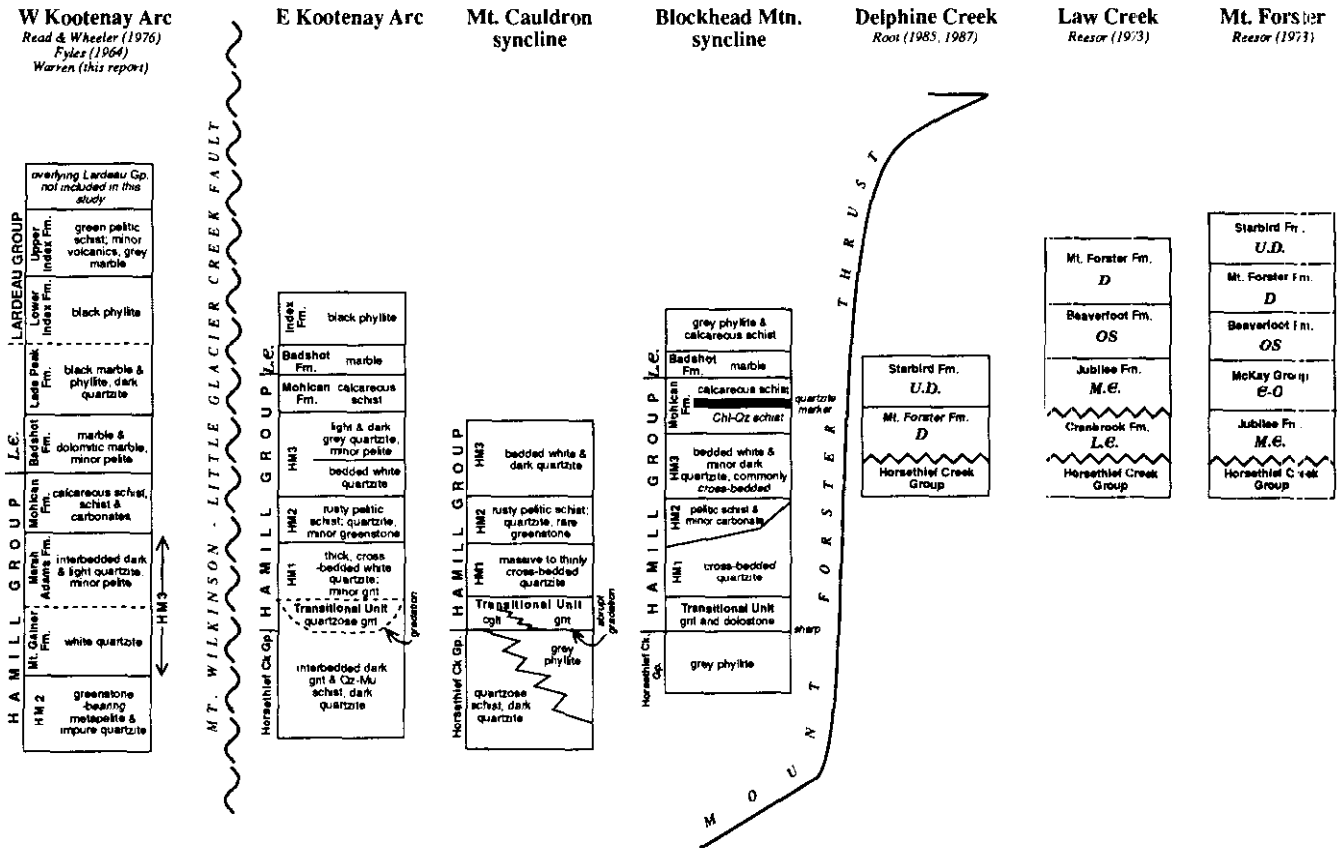


Figure 1-1-5. Stratigraphic relationships between lower Paleozoic rocks across the Purcell anticlinorium

A similar sill immediately south of the study area, on the west shore of Kootenay Lake, has yielded U-Pb zircon ages of 173 ± 5 Ma (Smith *et al.*, 1992).

SUMMARY

Stratigraphic relationships within and between Upper Proterozoic and Lower Cambrian rocks show that sedimentation during this interval was punctuated by several tectonic events, related to extension and/or rifting of the North American continental margin, and to emergence of "the Windermere high" (Reesor, 1973) as a high-standing continental crustal block. Regional sedimentation is disrupted at the base of the Windermere Supergroup, within the Horseshief Creek Group, beneath the Hamill Group, and again in the middle Hamill Group. Immature grit and greenstone within the Lardeau Group also imply tectonic events of an unknown nature. The duration of active tectonism was clearly longer than can be accounted for by recent models of continental rifting (*e.g.*, Bond and Kominz, 1984; Bond *et al.*, 1985). It is hoped that trace element and rare-earth element geochemical analyses of mafic igneous rocks in the Horseshief, Hamill and Lardeau groups will contribute to an understanding of the tectonic settings recorded by these rocks.

The boundary between the Purcell anticlinorium and the Kootenay Arc is a steep regional-scale fault, which separates rocks with early west-verging deformation, on the

west side, from rocks with early east-verging deformation, on the east side. Relationships within this study area strongly suggest that the west side moved up relative to the east side. Two other significant faults affect the western Purcell anticlinorium: a thrust fault in the Horseshief Creek Group near the Purcell divide, and the Mount Forster fault, which carries rocks of the study area in its hanging wall. Relationships between hanging wall and foot wall stratigraphy across all three faults suggest that they are influenced by structures related to the development of the "Windermere high" during Late Proterozoic/early Paleozoic extension.

ACKNOWLEDGMENTS

Funding for this project is provided by British Columbia Geoscience Research Grant RG91-05, Natural Sciences and Engineering Research Council Research Operating Grant OGP0092417 awarded to R.A. Price, and Queen's University School of Graduate Studies doctoral research and Geological Society of America student grants awarded to M. Warren. We are grateful for the services of Canadian Helicopters, Ltd. in Nelson, and Frontier Helicopters of Invermere. Anne Sasso provided assistance in the field. Thanks to Kathy Bossert of Howser for the use of her home, and for stimulating geological discussions. Dugald Carmichael and Maurice Colpron of Queen's University contributed enthusiastic comments and observations in the

field. Thanks to R. Madson of Invermere for a roof during the winter of early September. Hospitality and assistance from many people in the West Kootenays continues to be appreciated. M. Colpron helped with the figures.

REFERENCES

- Archibald, D.A., Krogh, T.E., Armstrong, R.L. and Farrar, E. (1984): Geochronology and Tectonic Implications of Magmatism and Metamorphism, Southern Kootenay Arc and Neighbouring Regions, Southeastern British Columbia. Part II: Mid-Cretaceous to Eocene; *Canadian Journal of Earth Sciences*, Volume 21, pages 567-583.
- Bond, G. and Kominz, M.A. (1984): Construction of Tectonic Subsidence Curves for the Early Paleozoic Miogeocline, Southern Canadian Rocky Mountains: Implications for Subsidence Mechanisms, Age of Breakup and Crustal Thinning; *Geological Society of America Bulletin*, Volume 95, pages 155-173.
- Bond, G.C., Christie-Blick, N., Kominz, M.A. and Devlin, W.J. (1985): An Early Cambrian Rift to Drift Transition in the Cordillera of Western North America; *Nature*, Volume 315, pages 742-746.
- Brown, R.L., Tippet, C.R. and Lane, L.S. (1978): Stratigraphy, Facies Change, and Correlations in the Northern Selkirk Mountains, Southern Canadian Cordillera; *Canadian Journal of Earth Sciences*, Volume 15, pages 1129-1140.
- Devlin, W.J. (1989): Stratigraphy and Sedimentology of the Hamill Group in the Northern Selkirk Mountains, British Columbia: Evidence for latest Proterozoic – Early Cambrian Extensional Tectonism; *Canadian Journal of Earth Sciences*, Volume 26, No. 3, pages 515-533.
- Douglas, R.J.W. (Compiler) (1968): Geological Map of Canada; *Geological Survey of Canada*, Map 1374A.
- Fyles, J.T. (1964): Geology of the Duncan Lake Area, Lardeau District, British Columbia; *B.C. Ministry of Energy, Mines and Petroleum Resources*, Bulletin 49.
- Fyles, J.T. and Eastwood, G.E.P. (1962): Geology of the Ferguson Area, Lardeau District, British Columbia; *B.C. Ministry of Energy, Mines and Petroleum Resources*, Bulletin 45.
- Höy, T. (1974): Structure and Metamorphism of Kootenay Arc Rocks around Riondel, British Columbia; unpublished Ph.D. thesis, *Queen's University*, Kingston.
- Höy, T. (1977): Stratigraphy and Structure of the Kootenay Arc in the Riondel Area, Southeastern British Columbia; *Canadian Journal of Earth Sciences*, Volume 14, pages 2301-2315.
- Leclair, A.D. (1988): Polyphase Structural and Metamorphic Histories of the Midge Creek Area, Southeast British Columbia: Implications for Tectonic Processes in the Central Kootenay Arc, unpublished Ph.D. thesis, *Queen's University*, Kingston.
- Lickorish, W.H. (1992): Structural and Stratigraphic Evidence for Lower Cambrian Rifting in the McNaughton Formation, Rocky Mountain Main Ranges, British Columbia and Alberta; in *Lithoprobe: Southern Cordillera Transect*; Report No. 24, pages 3-4.
- Little, H.W. (1960): Nelson Map-area, West half, British Columbia; *Geological Survey of Canada*, Memoir 308..
- Monger, J.W.H., Price, R.A. and Tempelman-Kluit, D.J. (1982): Tectonic Accretion and the Origin of Two Metamorphic and Plutonic Welts in the Canadian Cordillera; *Geology*, Volume 10, pages 70-75.
- Pell, J. and Simony, P.S. (1987): New Correlations of Hadrynian Strata, South-central British Columbia; *Canadian Journal of Earth Sciences*, Volume 24, pages 302-313.
- Pope, A. (1990): The Geology and Mineral Deposits of the Toby-Horsethief Creek Map Area, Northern Purcell Mountains, Southeast British Columbia (82K); *B.C. Ministry of Energy, Mines, and Petroleum Resources*, Open File 1990-26.
- Price, R.A. (1986): The Southeastern Canadian Cordillera: Thrust Faulting, Tectonic Wedging, and Delamination of the Lithosphere; *Journal of Structural Geology*, Volume 8, pages 239-254.
- Read, P.B. and Wheeler, J.O. (1976): Geology of the Lardeau Map-area, West-half, British Columbia; *Geological Survey of Canada*, Open File 432.
- Reesor, J.E. (1973): Geology of the Lardeau Map-area, East-half, British Columbia; *Geological Survey of Canada*, Memoir 369.
- Root, K.G. (1985): Reinterpretation of the Age of a Succession of Paleozoic Strata, Delphine Creek, Southeastern British Columbia; in *Current Research, Part A. Geological Survey of Canada*, Paper 85-1A, pages 727-730.
- Root, K.G. (1987): Geology of the Delphine Creek Area, Southeastern British Columbia: Implications for the Proterozoic and Paleozoic Development of the Cordilleran Divergent Margin; unpublished Ph.D. thesis, *University of Calgary*.
- Smith, M.T., Gehrels, G.E. and Klepacki, D.W. (1992): 173 Ma U-Pb Age of Felsic Sills (Kaslo River Intrusives) West of Kootenay Lake, Southeastern British Columbia; *Canadian Journal of Earth Sciences*, Volume 29, pages 531-534.
- Walker, J.F. and Bancroft, M.F. (1929): Lardeau Map-area, British Columbia. General Geology; *Geological Survey of Canada*, Memoir 161.
- Warren, M.J. and Price, R.A. (1992): Tectonic Significance of Stratigraphic and Structural Contrasts between the Purcell Anticlinorium and the Kootenay Arc, East of Duncan Lake (82K): Preliminary Results; in *Geological Fieldwork 1991*, Grant, B. and Newell, J.M., Editors. *B.C. Ministry of Energy, Mines and Petroleum Resources*, Paper 1992-1, pages 27-35.



**PRELIMINARY GEOLOGY OF THE MAHATTA CREEK AREA,
NORTHERN VANCOUVER ISLAND
(92L/5)**

By G. T. Nixon, J. L. Hammack, J. V. Hamilton and H. Jennings

(Contribution to the Canada - British Columbia Mineral Development Agreement 1991-1995)

KEYWORDS: Regional geology, Bonanza Group, Vancouver Group, Karmutsen Formation, Quatsino Formation, Parson Bay Formation, Longarm Formation, Island Plutonic Suite, Tertiary dikes, structure, mineral occurrences.

INTRODUCTION

A regional geological mapping program in the Quatsino Sound area was initiated in 1990 with a reconnaissance investigation (Massey and Melville, 1991). Mapping at 1:50 000-scale started this past summer on the Mahatta Creek (92L/5) sheet as part of a multiyear project aimed at improving our understanding of the geology and mineral potential of northern Vancouver Island. This report presents a brief account of the geological highlights of the field season. Fieldwork in 1993 will be conducted north of Quatsino Sound in parts of the 92L/12 and 102L/8-9 map sheets.

The Mahatta Creek map area is located near the north-western extremity of Vancouver Island due west of Port Alice (Figure 1-2-1). A base camp was established at Mahatta River, some 65 kilometres west of Port Alice at the north-central edge of the map area. A dense network of well-maintained logging roads provides access to most of the map area except in the extreme south (Kyuquot Provincial Forest) and northeast where access is poor. In addition to the road network, over 100 kilometres of coastline was investigated, stretching from Brooks Peninsula north to Quatsino Sound and east into the northern part of Neroutsos Inlet. The map area is covered by the 1:50 000-scale Vancouver Island aeromagnetic survey (Map 1733G) and the 1988 Regional Geochemical Survey (Matysek *et al.*, 1989).

The region boasts the largest producing mine on Vancouver Island, the Island Copper open-pit operation located on Rupert Inlet (Figure 1-2-1). The mine has been a major producer of copper and molybdenum ore since 1971 but is scheduled to close in 1996. Exploration activity in the region has recently increased in the continuing search for base and precious metal deposits. Mineral potential maps for Vancouver Island at 1:250 000-scale are currently in preparation as part of the recent Corporate Resource Inventory Initiative (CRII).

PREVIOUS WORK

The first geological investigations of northern Vancouver Island were made by Dawson (1887) who paid particular attention to Cretaceous coal-bearing strata on the north and south shores of Quatsino Sound. Subsequent studies of the geology and mineral deposits of the region include those of Dolmage (1919), Gunning (1930, 1932), Jeffrey (1962) and Northcote (1969, 1971). Detailed descriptions of shoreline

exposures of sedimentary rocks have been summarized by Jeletsky (1976) who made extensive fossil collections largely identified by Tozer (1967). However, the most recent comprehensive account of the regional geology of northern Vancouver Island (Alert Bay - Cape Scott) is provided by Muller *et al.* (1974; and see Muller and Roddick, 1983, for a coloured edition of their 1:250 000 geological map).

STRATIGRAPHIC NOMENCLATURE

In the descriptions that follow, we have adopted the stratigraphic nomenclature of Muller and co-workers (Muller *et al.*, 1974, 1981; Figure 1-2-2). There are, however, outstanding problems beyond the scope of this report that will need to be addressed at some future date. There is presently no continuous type section for the Quatsino Formation. The Parson Bay Formation, as used by Muller and co-authors, also has no complete section, and at its type locality on Harbledown Island across Johnstone Strait only the lowermost member is present. The Harbledown Formation has not been recognized as a mappable unit in the Quatsino Sound area, and appears to be largely correlative with the Bonanza volcanics (and interbedded sediments) of Quatsino Sound whereas these lithologies form two distinct formations on the east coast of Vancouver Island (Carlisle, 1972). As recognized by Muller, Jeletsky, and others, many stratigraphic sequences have been reassembled across intrusions, faults and other structural complexities without adequate control.

TECTONIC SETTING AND REGIONAL GEOLOGY

Vancouver Island lies within the southern part of the Insular Belt of the Canadian Cordillera and forms part of the Wrangellia tectonostratigraphic terrane which stretches northwards through the Queen Charlottes into Alaska (Wheeler *et al.*, 1991). Southern Wrangellia is bounded to the east by Cretaceous to Tertiary plutonic rocks of the Coast Belt and is underplated on the west by the Pacific Rim and Crescent terranes which form part of a subduction complex that is still being accreted today off the west coast of Vancouver Island (Riddihough and Hyndman, 1991). The amalgamation of Wrangellia and Alexander Terrane into the Insular Superterrane had apparently occurred by late Paleozoic (Late Carboniferous) time (Gardner *et al.*, 1988). Accretion of the Insular Superterrane to more inboard terranes of the Intermontane Belt (Intermontane Superterrane) may be as late as the mid-Cretaceous (Monger *et al.*, 1982)

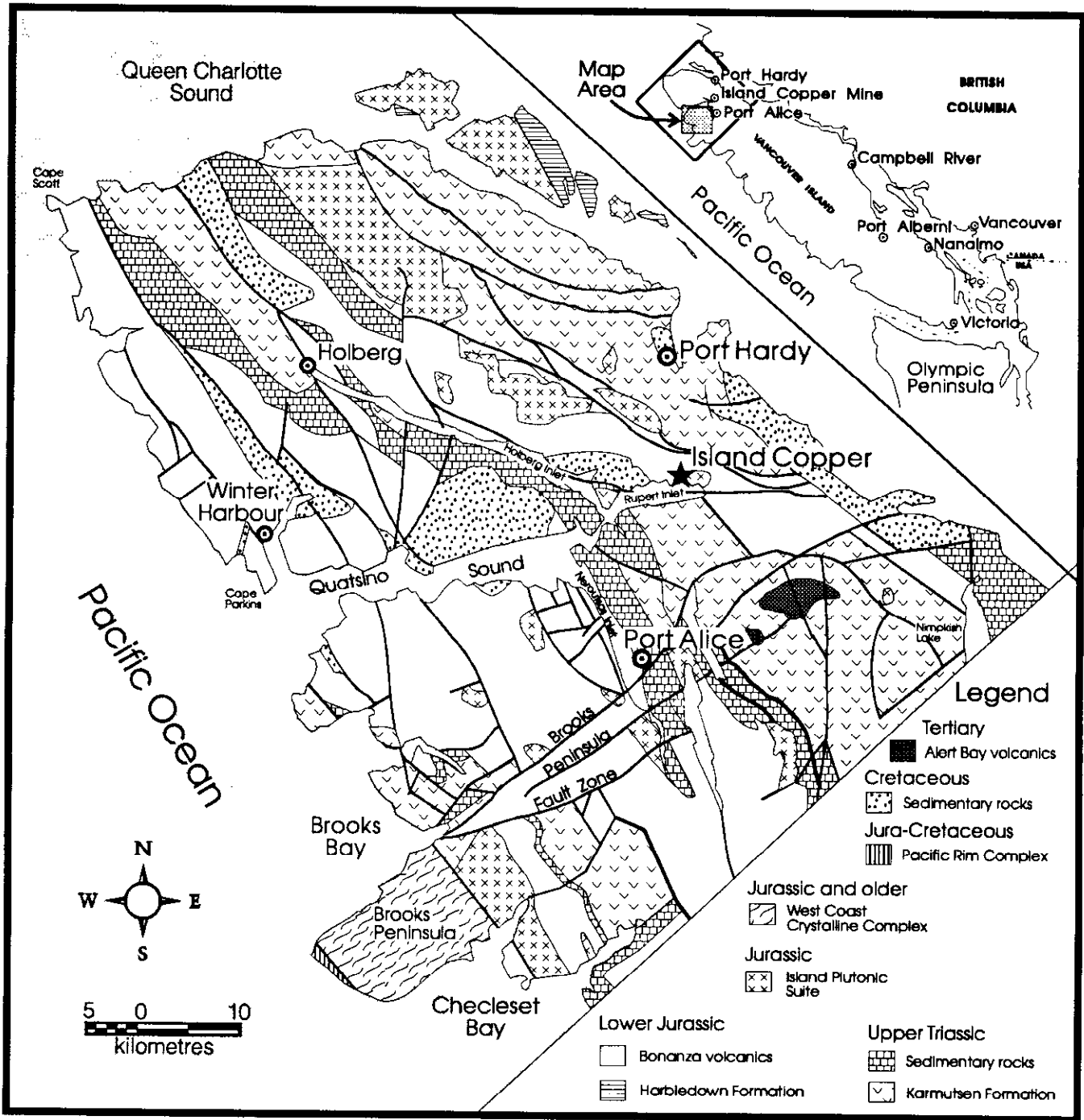


Figure 1-2-1. Generalized geology of northern Vancouver Island (modified after Muller *et al.*, 1974). Shaded inset shows location of Mahatta Creek map area.

or as early as the Middle Jurassic when a single Superterrane was attached to the North American continental margin (van der Heyden, 1991).

The crustal architecture and Mesozoic-Cenozoic stratigraphy of northern Vancouver Island are shown in Figures 1-2-1 and 1-2-2. A northwesterly trending structural grain is delineated by the major stratigraphic units, plutons and faults. The region is characterized by numerous fault-bounded blocks of homoclinal strata generally dipping westward (Muller *et al.*, 1974). The major northwesterly

trending faults are transected by a northeasterly trending high-angle fault system in the vicinity of Brooks Peninsula.

The Quatsino Sound area is largely underlain by weakly metamorphosed (subgreenschist) Triassic sedimentary rocks and Lower Jurassic volcanic-volcaniclastic sequences of the Vancouver Group and Bonanza Group, respectively (Figure 1-2-2). The base of the succession is marked by mid-Triassic (Ladinian) argillites ("Daonella beds" in Figure 1-2-2) intruded by numerous diabasic sills and lesser dikes ("sediment-sill" unit of Muller *et al.*, 1974) that have

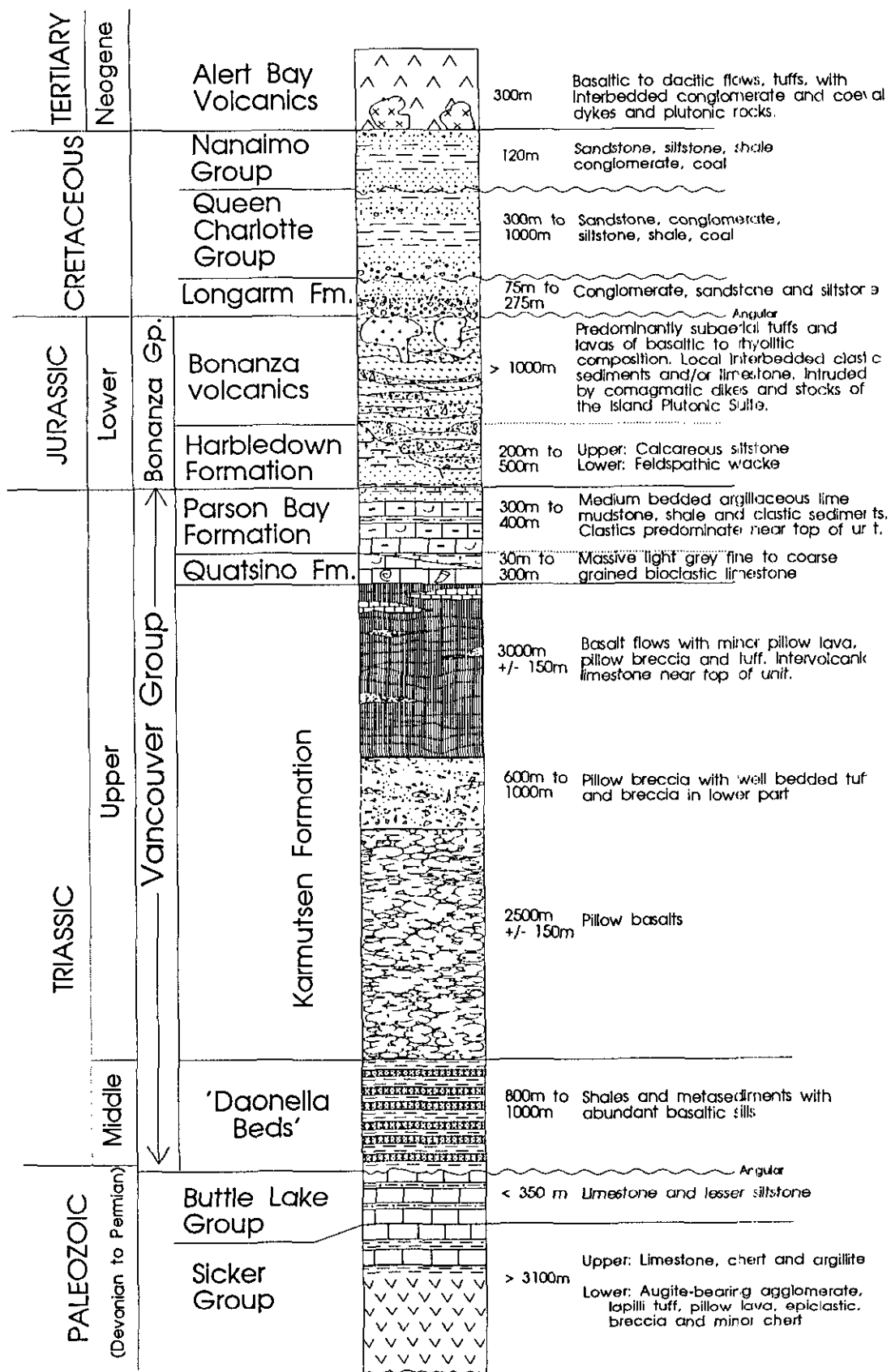


Figure 1-2-2. Generalized Mesozoic-Cenozoic stratigraphy of northern Vancouver Island (modified after Muller *et al.*, 1974, 1981).

fed a thick sequence of tholeiitic pillow basalts, submarine breccias and tuffs, and lava flows of the overlying Karmutsen Formation. In reference sections at Buttle Lake, a tripartite subdivision of the Karmutsen Formation has been recognized, comprising a basal pile of pillow lavas overlain by breccia and tuff and capped by massive lava flows with interlava limestone in the uppermost 300 metres of the section (Surdam, 1968; Carlisle and Suzuki, 1974). The lavas are conformably overlain by a succession of Upper Triassic marine sedimentary rocks comprising massive bioclastic limestone and thinly bedded, generally fine-grained clastics and impure limestone. The Triassic succession has been interpreted to represent a rapidly extruded (3.5-5 Ma) submarine flood basalt province (Karmutsen Formation) or back-arc rift sequence overlain by platformal limestone and shelf sediments (Quatsino and Parson Bay formations; Muller, 1977; Barker *et al.*, 1989). This sequence developed on a Devonian to Early Permian island-arc succession of calcalkaline volcanics and marine sediments (Buttle Lake and Sicker groups; Figure 1-2-2).

Marine sedimentation continued into the Lower Jurassic with the deposition of feldspathic wackes and calcareous siltstones (Harbledown Formation). These rocks are unconformably overlain by subaerial to submarine arc volcanics with minor interbedded sediments, and together comprise the Bonanza Group. The lower Mesozoic stratigraphy is intruded by Early to Middle Jurassic granitoid plutons (Island Plutonic Suite) considered to be comagmatic with the Bonanza volcanics. Variably deformed gabbro and granitoid intrusions in mid-crustal amphibolite-grade rocks of the Westcoast Crystalline Complex exposed on the Brooks Peninsula are probably genetically related to the Bonanza volcanics (Muller *et al.*, 1974). Cretaceous marine and fluvial sequences, including the Longarm Formation (Kyuquot Group) and Queen Charlotte Group, were deposited as clastic wedges on previously deformed and denuded basement rocks. During the Tertiary, localized felsic to mafic Alert Bay volcanics and dikes were emplaced across northern Vancouver Island in a fore-arc environment spatially coincident with the trend of the Brooks Peninsula fault zone (Armstrong *et al.*, 1985).

LOCAL STRATIGRAPHY

The Mahatta Creek map area is underlain principally by Bonanza Group volcanic and volcanoclastic rocks. Upper Triassic sedimentary rocks and Karmutsen basalts are restricted to the southwestern coastal regions except for a narrow strip of Parson Bay Formation along the west side of Neroutsos Inlet (Figure 1-2-3). Outliers of Cretaceous strata are preserved on the west coast and along the southern shores of Quatsino Sound. Outcrops of the Queen Charlotte Group on the north shore of Quatsino Sound were not investigated, and sediments belonging to the Upper Cretaceous Nanaimo Group appear to be absent. Intrusions of the Island Plutonic Suite occur throughout the map area whereas mafic dikes of presumed Tertiary age appear to be concentrated in the south.

KARMUTSEN FORMATION

The Karmutsen Formation is well exposed along the southwestern coast between Brooks Peninsula and Restless Bight (Figure 1-2-3) and extends farther north than shown by the mapping of Muller *et al.* (1974). The principal lithology comprises dark grey to maroon, aphanitic to finely porphyritic amygdaloidal basalt flows; pillow basalt, pillow breccias and bedded hyaloclastite deposits are comparatively rare as are coarsely porphyritic, plagioclase-phyric lavas. The preponderance of massive flows, the recognition of the overlying Quatsino Formation, and the local occurrence of limestone beds apparently intercalated with Karmutsen basalt in some fault blocks suggest that only the upper part of Karmutsen stratigraphy is exposed (Figure 1-2-3).

Textures observed in outcrop include a locally pronounced flow foliation defined by trachytic plagioclase or centimetre-scale alternating layers of amygdaloidal and compact lava (Plate 1-2-1). Amygdules may be concentrated at flow margins and localized vesicle trains are usually oriented within the flow foliation. The margins of flows are generally sharp and smooth; flow breccias are rare. Irregular joints are commonly lined with chlorite which is locally polished and exhibits slickensides; primary columnar jointing has not been observed.

In thin section, the primary phases of aphanitic basalts are plagioclase microlites (less than 0.5 mm), clinopyroxene, iron-titanium oxides (up to 10% by volume) and altered volcanic glass (typically 5-20%) displaying intergranular to subophitic or intersertal textures. Plagioclase (labradorite) phenocrysts and rare glomerocrysts in finely porphyritic variants reach 2.5 millimetres in length but may exceed 6 millimetres in coarsely porphyritic flows; clinopyroxene rarely attains 1 millimetre in diameter. The more holocrystalline flow interiors characteristically contain interstitial quartz typical of a tholeiitic residuum.

The Karmutsen Formation has been subjected to burial metamorphism ranging from zeolite facies near the top to prehnite-pumpellyite facies in the lower part (summarized by Greenwood *et al.*, 1991). Secondary mineral assemblages observed to date in the Mahatta Creek area commonly include chlorite, epidote/zoisite, carbonate, sericite, sphene/leucosene, quartz, pyrite and clays. In addition, zeolite, albite, prehnite(?) and rare potassium feldspar have been observed infilling amygdules, and fibrous actinolite is locally found in veinlets and basaltic groundmass. The occurrence of actinolite does not appear to be spatially related to granitoid intrusions and suggests that peak metamorphic conditions locally reached greenschist grade in the some parts of the Karmutsen pile.

QUATSINO FORMATION

The Quatsino Formation was named by Dolmage (1919) for a thick (750 m) limestone unit exposed at the eastern extremity of Quatsino Sound and in Rupert Inlet. Previous workers have noted that the formation can be informally subdivided into a lower massive and upper thinly bedded sequence that grades into overlying Upper Triassic clastic rocks of the Parson Bay Formation (Figure 1-2-2). Work by

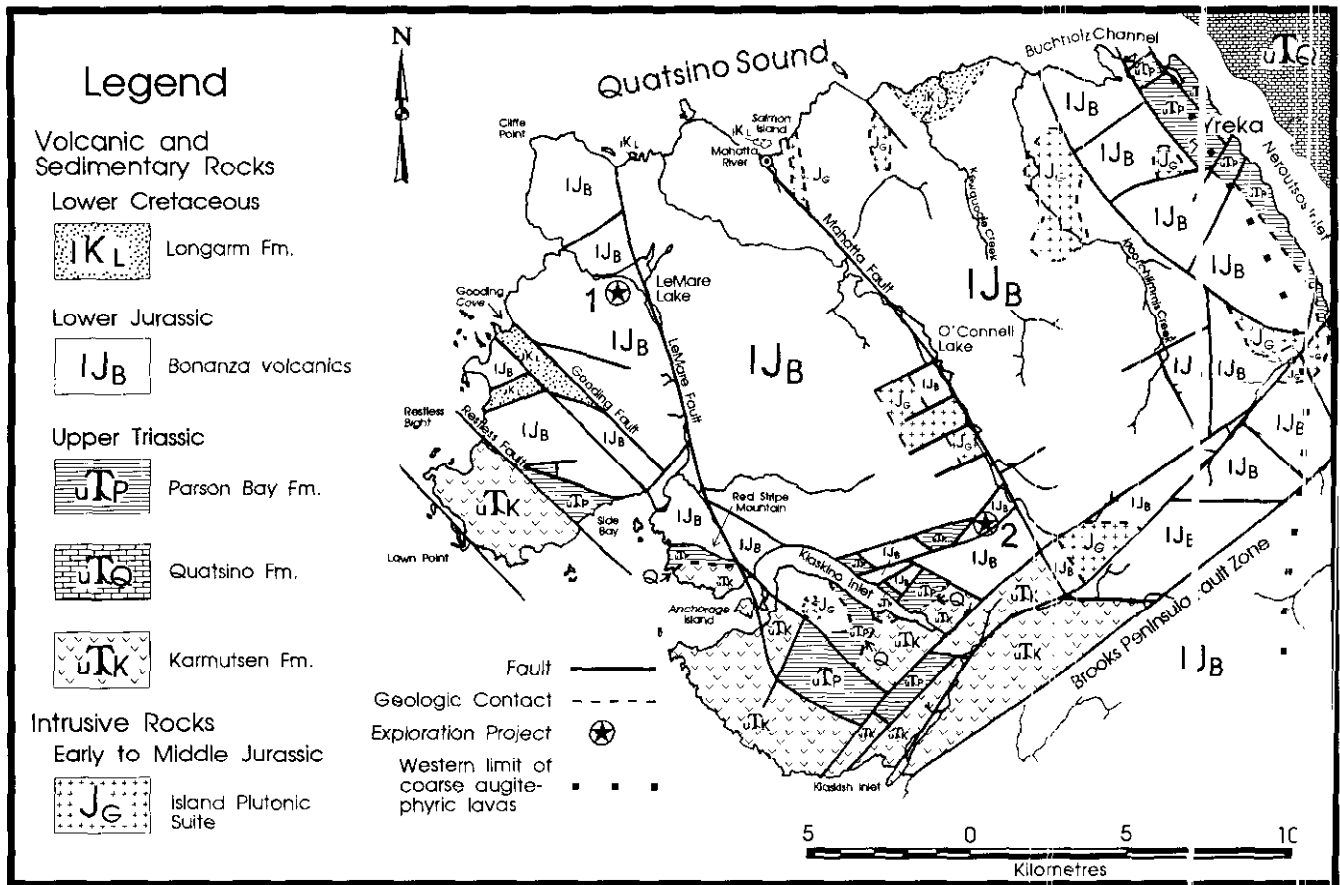


Figure 1-2-3. Generalized geology of Mahatta Creek area (92L/5); for detailed map see Open File 1993-10. Q indicates the presence of Quatsino limestone at the base of the Parson Bay Formation. The star indicates an exploration project. 1, LeMare Lake, Minnova Inc.; 2, Madhat, Pan Orvana Resources Inc.



Plate 1-2-1. Flow lamination in Karmutsen basalt defined by amygdaloidal and compact layers. Southeastern tip of unnamed island in Klaskino Inlet 0.4 kilometre northeast of Anchorage Island.

Jeletsky (1970, 1976) has shown that the substantial thickness of Quatsino limestone in the Rupert Inlet - Alice Lake area is drastically reduced in exposures on the west coast (and also to the east along Queen Charlotte Strait) which appear to represent a shorter time span. Anmonites place the Quatsino-Karmutsen contact in the upper Carnian; the contact with overlying Parson Bay Formation is diachronous, reaching a middle Norian age in the area where the Quatsino is thickest (Jeletsky, 1976; Tozer, 1967).

In the Mahatta Creek area, Quatsino limestone is exposed in the northeastern corner of the map area and as isolated outcrops around Klaskino Inlet where it is more extensive than previously recognized. Two new fossiliferous localities have been examined, on an island at the entrance of Klaskino Inlet, and another deep within it. The presence of the western facies of Quatsino limestone at the Karmutsen - Parson Bay contact is indicated symbolically in Figure 1-2-3.

Exposures on the eastern side of Neroutsos Inlet comprise a predominantly massive, though locally thinly bedded, medium to dark grey micritic limestone that weathers pale grey to white. Stylolitic structures are common and a pock-marked weathering surface is usually pronounced in shoreline exposures.

The Quatsino-Karmutsen contact is exposed on the southeastern shore of Klaskino Inlet and in a measured section



Plate 1-2-2. Thickly to thinly bedded, moderately dipping Quatsino limestone conformably overlying Karmutsen basalt.

just outside the entrance (Klaskino section of Muller *et al.*, 1974) where it is sharp and conformable or paraconformable (Plate 1-2-2). At the former locality (Figure 1-2-3), the Quatsino Formation rests on amygdaloidal basalt. The Quatsino and Parson Bay formations comprise a westward-dipping, westward-facing, continuous stratigraphic succession with some minor folding of Quatsino limestone and mafic Bonanza dikes near the Karmutsen contact. The basal part of the Quatsino comprises a massive, pale grey fine-grained limestone about 10 metres thick in gradational contact with very thinly bedded argillaceous limestone with laminae and concretions of black chert. These beds grade into very thinly bedded, medium grey, impure micritic limestone with black shaley partings which in turn passes into a laminated to very thinly bedded, dark grey siltstone-argillite sequence at the base of the Parson Bay Formation. The total thickness of the Quatsino Formation here appears to be about 30 metres. A thin limestone layer with abundant ammonites occurs less than 20 metres above the Karmutsen contact.

In the Klaskino section measured by Muller *et al.* (1974, Figure 5), the thicknesses of the lower and upper divisions of the Quatsino were estimated at approximately 24 and 48 metres respectively. Massive to locally thinly bedded limestone at the base of the section is interstratified with Karmutsen basalt regarded as sills by Muller *et al.* However, there are no obvious thermal or metasomatic effects at these

contacts and work in progress may establish an intercalated limestone-basalt flow succession as documented elsewhere (Figure 1-2-2). An isolated limestone horizon in Karmutsen basalt was discovered north of Lawn Point (Figure 1-2-3).

The Quatsino Formation can be traced from its coastal exposure in the Klaskino section across the top of Red Stripe Mountain where it runs into a fault. It is encountered again farther south near the northern tip of an unnamed island northeast of Anchorage Island. The Karmutsen-Quatsino contact has been intruded by Bonanza diorite and is not exposed. The succession here is very similar to that described above for southern Klaskino Inlet. Gastropods were recovered from the massive basal part of the Quatsino limestone which is at least 12 metres thick. The upper thinly bedded division is locally tightly folded; its thickness may reach 20 metres.

PARSON BAY FORMATION

The Parson Bay Formation is preserved in fault blocks surrounding Klaskino Inlet and northeast of Klaskish Inlet, in a westerly striking belt extending from Red Stripe Mountain to the coast (Klaskino section), at Side Bay, and on the south shore of the main channel of Quatsino Sound where it becomes Neroutsos Inlet. The formational name was advocated by Crickmay (1928) for Triassic sedimentary rocks originally comprising part of the Triassic-Jurassic Parson

Bay Group on Harbledown Island (Bancroft, 1913). Muller *et al.* (1974) were the first to apply this name to the Upper Triassic sediments of northern Vancouver Island. As used by these authors, the Upper Triassic Parson Bay Formation now incorporates the following units mapped by Jeletsky (1976) as part of his "Sedimentary Division of the Bonanza Subgroup", from base to top: a basal pelitic unit with minor impure limestone interbeds or "Thinly Bedded Member"; a clastic or "Arenaceous Member" comprising predominantly interbedded greywacke and argillite with minor tuff and pebble conglomerate, locally argillaceous at the top; an upper limestone unit with minor clastics or "Sutton Formation" present only in eastern Quatsino Sound; and a sequence of waterlain volcanic breccias and tuffs or "Hecate Cove Formation" (base of Jeletsky's "Volcanic Division of the Bonanza Subgroup") directly underlying Lower Jurassic Bonanza volcanics and also best exposed in the eastern part of Quatsino Sound. The age of the Parson Bay Formation in the area is well controlled by fossils and extends from lowermost to uppermost Norian.

The Klaskino section described by Muller *et al.* (1974, Figure 4 and Table 3) is considered to be the most complete. From south to north, laminated to thinly bedded dark grey to black impure limestones, calcareous siltstones and shales in gradational contact with Quatsino Formation pass into similar lithologies with local interbeds of normally graded, feldspathic wacke and minor intraformational limestone breccia. At the top of the section, a fault separates these thinly bedded sediments from coarser clastics comprising predominantly thickly bedded limestone breccias with a tuffaceous matrix with minor micritic limestone and pebble conglomerate. These beds are overlain by mafic to intermediate lavas of the Bonanza volcanics that appear to represent the Parson Bay - Bonanza transition. Jeletsky (1976, p.18) considered the latter rocks to be uppermost Triassic ("Hecate Cove Formation").

Outcrops of Parson Bay Formation in eastern Quatsino Sound at Buchholz Channel have a significantly higher proportion of carbonate beds and coarse volcanoclastic detritus than their counterparts on the west coast. These rocks, together with correlative units on the north shore of Quatsino Sound, were studied in detail by Jeletsky (1976) and formed his uppermost Triassic - lowermost Jurassic stratigraphy.

The northwesterly striking succession at Buchholz Channel generally dips and youngs to the west but is structurally complicated by faults and small-scale folds (Jeletsky, 1976, Figure 17). A wide variety of lithologies recur throughout the sequence: pale to medium grey, relatively pure fine-grained massive limestone, white to pale buff on weathered surfaces and locally exhibiting laminae and concretions of black chert; thinly bedded, impure micritic limestone commonly with interbeds of calcareous siltstone and black argillite; limestone breccias with angular fragments (up to 8 cm across) of dark grey limestone set in a micritic matrix; medium greenish grey, thinly bedded tuffaceous wackes; volcanic conglomerates and sandstones with carbonate-rich matrices; and grey-green volcanic breccias of epiclastic and pyroclastic origin. At the eastern end of Buchholz Channel, coarse epiclastic deposits including limestone breccias over-

lie dark greenish grey medium-bedded lapilli tuffs and massive augite-phyric mafic flows. Jeletsky (1975, p. 29) has also identified pillow lavas and pillow breccias at apparently the same stratigraphic horizon. A succession of augite-phyric lavas and thickly or indistinctly bedded volcanic breccias is also exposed along the western shore of Neroutsos Inlet where they appear to be intercalated locally with massive limestone and laminated to thinly bedded dark grey siltstones, mudstones and argillaceous limestones. Although there is little doubt that these carbonate-volcanoclastic sequences were laid down in shallow marine or littoral environments, the massive lavas may represent locally emergent or intratidal conditions. The Parson Bay Formation at Buchholz Channel thus appears to mark the transition from Upper Triassic marine sedimentation to Lower Jurassic Bonanza volcanism. The exact timing of this transition may be revealed by limestone samples currently being processed for microfossils.

The Parson Bay Formation cropping out on the north and south shores of Klaskino Inlet also contains the Parson Bay - Bonanza transition. Here, the strata comprise a generally westward-dipping, westward-facing succession of laminated to medium-bedded, dark grey to black, locally pyritic argillites, silicified siltstones, calcareous siltstones and argillaceous limestones. The sections are artificially thickened by faulting, folding and intrusion of Bonanza dikes and sills. In both sections, the uppermost beds of fine-grained clastics with minor carbonate are overlain by, or intercalated with, a structurally concordant sequence of well-bedded volcanoclastic-epiclastic deposits and lava flows. For mapping purposes, we have arbitrarily placed the contact shown in Figure 1-2-3 at the lowest stratigraphic horizon of lava, pyroclastic or coarse epiclastic material. Both Jeletsky and Muller and coworkers recognize an interfingering of Parson Bay and Bonanza lithologies.

On the north shore of Klaskino Inlet, the highest part of the Parson Bay Formation, a very thinly bedded, variably silicified argillite-siltstone succession, is in sharp contact with an aphanitic intermediate sill(?) and is overlain by a medium to thickly bedded, mixed epiclastic-pyroclastic succession of variegated maroon to pale green tuffaceous breccias, sandstones, lapilli tuffs and minor mafic amygdaloidal flows. The fragmental rocks contain angular to subrounded clasts (up to 5 cm across) of fine-grained mafic to silicic volcanic rocks and mark the base of the Bonanza Group as defined above. These clastics are overlain by a thick sequence of mafic amygdaloidal flows.

The contact between the Parson Bay Formation and Bonanza volcanics on the south shore of Klaskino Inlet is gradational. The top of the transition zone is marked by variably altered, pale greenish grey, massive vitric-lithic tuff (welded?) of silicic composition, overlain by aphanitic rhyolitic lavas with spherulitic devitrification textures. These lithologies overlies dark grey laminated to medium-bedded micritic limestones and calcareous mudstones with minor siltstone and argillite interbeds. Disseminated pyrite is locally concentrated in conformable layers up to 1 centimetre thick. These rocks are overlain by a less calcareous sequence of mudstones and siltstones intercalated with

tuffaceous sandstones and siltstones and medium-bedded crystal-vitric (water-washed?) intermediate to silicic tuffs. The exact thickness of the transition zone is uncertain due to intrusion and faulting, but it probably represents a minimum stratigraphic interval of several hundred metres. The more arenaceous and tuffaceous character of clastic sequences within the transition is reminiscent of lithologies in the uppermost part of the Parson Bay Formation at Side Bay.

BONANZA VOLCANICS

According to present definitions, the Bonanza Group (Gunning, 1932) comprises Lower Jurassic sedimentary rocks of the Harbledown Formation unconformably overlain by Bonanza volcanics (Muller *et al.*, 1981; Figure 1-2-2). Where the Harbledown Formation is missing, as appears to be the case in the Mahatta Creek area, Bonanza volcanics rest directly on Upper Triassic sediments of the Parson Bay Formation with no definitive evidence for a major erosional unconformity. In fact, as noted above, a narrow tuffaceous interval records the passage from a marine shallow-water to predominantly volcanic environment. Muller *et al.* (1974) measured a thickness of some 2500 metres for a section of Bonanza volcanics at Cape Parkins but expressed doubts as to its stratigraphic integrity.

The age of the Bonanza volcanics has been established as early Sinemurian to early Pliensbachian by ammonites and bivalves collected from intra-Bonanza sediments within the Mahatta Creek area (Muller *et al.*, 1974; Jeletsky, 1976), in a measured section at Cape Parkins (Muller *et al.*, 1974) and further south in Kyuquot Sound (Friebold and Tipper, 1970). Macrofossils in the Harbledown Formation yield a similar age range indicating that this formation is largely coeval with Bonanza volcanics and interbedded sedimentary rocks. Potassium-argon isotopic dates (103-161 Ma, mid-Cretaceous to early Late Jurassic) are minimum ages only (Muller *et al.*, 1974).

The Bonanza volcanics show many of the characteristics inherent to ancient volcanic terrains that prevent formal subdivision, not the least of which are the lack of distinctive lithostratigraphic markers, extreme variations or recurrence of lithologies in space and time, and inadequate fossil control. When combined with the structural complexities known to exist, it is not surprising that previous workers have had their respective difficulties in attempting to subdivide the Bonanza into regionally significant mappable units. It was for these reasons that Muller *et al.* (1974) decided to incorporate the Upper Triassic sedimentary units recognized by Jeletsky (1969, 1970, 1976) into the Parson Bay Formation, and placed little faith in Jeletsky's informal lithostratigraphic subdivision of Bonanza volcanics. At this time, we offer limited insight into these problems.

The Bonanza volcanics are an extremely diverse suite of extrusive and intrusive subvolcanic rock types that range in composition from basalt to rhyolite and reflect both subaqueous and continental volcanic and epiclastic environments. The main volcanic lithologies include basaltic flows, relatively minor pillow breccias and tuffs, and rare pillow lavas; rhyodacitic to rhyolitic flows; intermediate to silicic ash-flow tuffs, pyroclastic breccias and minor ash-fall mate-

rial; and intermediate porphyritic lavas of apparently minor volume. Intercalated sedimentary sequences include fine-grained clastics and carbonates, volcanic wackes, sandstones and conglomerates, and lahatic breccias. Descriptions of lithologies that illustrate the diverse nature of Bonanza volcanics in the Mahatta Creek area are given below along with some preliminary insights into potential regional differences in volcanic regimes that require further investigation.

The basaltic rocks are typically dark grey to greenish grey where freshest, and maroon to pale green where altered. They have aphanitic to fine-grained textures and are commonly amygdaloidal with carbonate, chlorite, epidote, zeolite and silica infillings. In thin section, aphanitic variants contain plagioclase microlites and microphenocrysts and clinopyroxene grains set in an oxide-charged groundmass. Plagioclase phenocrysts rarely exceed 2 millimetres in length in the more porphyritic lavas. Rare megacrystic flows contain phenocrysts of euhedral plagioclase and glomerocrystic intergrowths exceeding 1 centimetre in maximum dimension that may comprise up to 15 volume per cent of the rock (Plate 1-2-3). Some of these textures resemble those found in Karmutsen basalts. However, Bonanza basalts are usually less epidotized than Karmutsen lavas, which appears to reflect primary differences in bulk composition.

Excellent exposures of basaltic pillow breccias interbedded with shallow-water marine sediments occur on the unnamed point forming the northern tip of Restless Bight (Figure 1-2-3). Dark grey to bright red or pale green, altered, aphanitic basalt flows (2 to 6 m thick) with dense interiors that grade into amygdaloidal tops overlain by scoriaceous flow breccias form the lowest outcrops of a westward-dipping, westward-younging stratigraphic succession. These flows are overlain by a thinly to thickly bedded sequence of grey-brown weathering intercalated pillow breccias (Plate 1-2-4), pebble conglomerates and coarse tuffaceous sandstones with calcareous cement, including a thin (2 m) bed containing abundant crystals of gypsum (5 mm across). Some of the pillow breccias have been emplaced as submarine debris flows in which broken and whole pillows (up to 1 m long) are suspended in a calcareous sandy matrix. The gypsum bed probably represents a local sabkha-type environment. These beds are overlain by a succession of thin to medium-bedded sandy limestones and calcareous sandstones that contain large, coarsely corrugated clams identified as *Weyla* sp. (GSC locality C-208119, Haggart, 1992) which is consistent with an Early Jurassic (Sinemurian to Toarcian) age.

Viscous rhyolitic lavas are pale grey to greenish grey or maroon rocks with aphanitic to finely porphyritic textures. Dark grey to greenish black, partially devitrified obsidian is found in dikes and flows. Porphyritic varieties contain sparse (less than 5% by volume) euhedral feldspar phenocrysts less than 2 millimetres in length. Flow lamination and flow folds are usually conspicuous. Local flow breccias contain variably rotated, angular fragments of flow-laminated rhyolite up to 30 centimetres in length. Spherulitic devitrification textures are locally well developed with individual spherulites attaining 3 centimetres in diameter (Plate 1-2-5).



Plate 1-2-3. Coarsely plagioclase-phyric basalt flow showing glomerocrystic texture, Bonanza volcanics.

Pale grey-green to maroon, rhyolitic to dacitic or andesitic ash-flow tuffs and monolithic to heterolithic tuff-breccias and pyroclastic breccias are commonly associated with the rhyolitic lavas. Monolithic breccias typically contain abundant angular to subrounded clasts of flow-laminated rhyolite; most are lapilli-size although some blocks exceed a metre in length. Heterolithic breccias contain accidental clasts of basaltic lavas in addition to rhyolitic fragments. Vitroclastic matrices are nonwelded to strongly welded with dark green, collapsed pumice lapilli. These pyroclastic deposits most likely represent small-volume explosive phenomena associated with the growth of

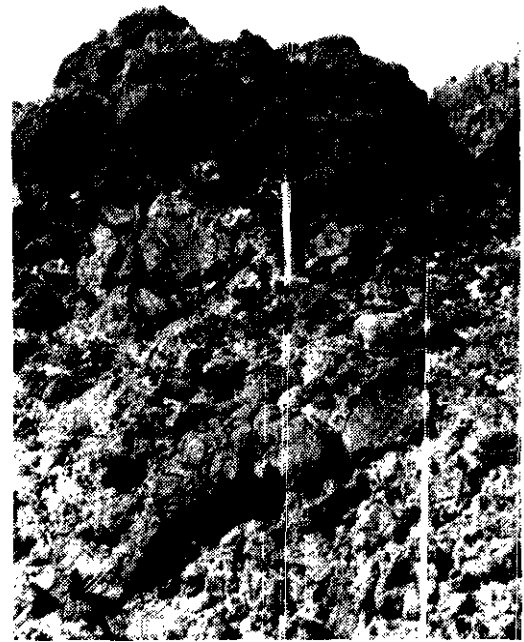


Plate 1-2-4. Basaltic pillow breccia containing whole pillow fragments, Bonanza volcanics, unnamed point at northern tip of Restless Bight.

rhyolitic flow-dome complexes. The ash-flow tuffs include vitric, vitric-lithic and crystal-lithic varieties and most are welded to some degree with locally pronounced eutaxitic pumice (Plate 1-2-6). The more intermediate compositions are generally crystal-lithic lapilli tuffs with up to 15 volume per cent accidental rock fragments, 20 per cent pumice lapilli and 15 per cent euhedral to broken crystals, mostly plagioclase (less than 3 mm long). Their decidedly heterolithic nature and finer average clast size with fewer flow-laminated rhyolite fragments suggests that these cooling units represent the far-travelled equivalents of rhyolitic breccias associated with flow-dome complexes or distal(?) outflow facies of caldera complexes. The widespread occurrence of densely welded textures in the silicic to intermediate pyroclastic rocks suggests that much of the Bonanza volcanism was continental. However, the total volume of silicic pyroclastic material appears to be substantially less than that of mafic lavas in the area.

Coarsely porphyritic, greenish grey to maroon augite-phyric lavas and associated tuffs are exposed along the eastern margin of the map area (Figure 1-2-3). These mafic to intermediate flows are characterized by up to 20 volume per cent euhedral phenocrysts of augite (up to 8 mm long), or augite and plagioclase, and exhibit seriate textures and amygdaloidal tops. They are intercalated with more finely porphyritic (<2 mm) augite and plagioclase-bearing lavas that may extend slightly farther west than the limit shown in Figure 1-2-3. The succession includes localized beds of augite-bearing lapilli tuff and tuff-breccia rich in fragments of fine-grained to porphyritic volcanic rocks. Some of these pyroclastic deposits may be waterlain.



Plate 1-2-5. Spherulitic devitrification in rhyolite flow, Bonanza volcanics.

Maroon to pale green laharc breccias are a minor but conspicuous component of the epiclastic rocks. They incorporate angular to well-rounded clasts (up to 0.8 m across) of the volcanic lithologies described above, in addition to minor sedimentary rocks including rare limestone. Flow imbrication or preferred orientation of clasts in the plane of the flow is locally apparent. The finer grained epiclastic detritus generally forms well-bedded sequences of tuffaceous pebble conglomerate, sandstone, siltstone and argillite. Marine sediments intercalated with Bonanza volcanics comprise dark grey to grey-green, laminated to medium-bedded impure limestone, calcareous mudstone and siltstone, and variably silicified siltstone and argillite. These limy sequences are very similar to Parson Bay sediments and recognition is dependant on fossil control where contacts with volcanic rocks are obscured.

Some interesting relationships are evident in the distribution of volcanic lithologies across the Mahatta Creek map sheet. The western two-thirds of the area is underlain by a seemingly bimodal aphanitic to finely porphyritic basalt-rhyolite association in which basaltic rocks appear to be much more volumetrically significant. Distinctively porphyritic, mafic to intermediate augite and plagioclase-bearing extrusive rocks appear more abundant in the east. As both assemblages are intimately associated with Upper

Triassic sedimentary rocks of the Parson Bay Formation, it seems probable that this spatial petrographic variation in lava types was established at the onset of Bonanza volcanism.

Geochemical data provide some insight into the possible significance of these petrographic variations. Muller *et al.* (1974, Table 4) presented 19 major element analyses of Bonanza "andesites", "dacites" and "rhyolites" from Cape Parkins at the entrance to Quatsino Sound (Figure 1-2-1) and concluded that the petrography and chemistry of these rocks was compatible with a calcalkaline affinity. It is worth noting, however, that based on silica content alone, almost all of the "andesites" in this table would be classified as basalts, the "dacites" are andesites, and the "rhyodacites" have rhyodacitic to rhyolitic compositions. Orthopyroxene was apparently confirmed in some samples but these were not identified. The titania content of the basalts (>1 weight %) is consistently high and unusually so for an arc-related calcalkaline suite. Muller *et al.* (1974) did note an alkalic affinity for the more mafic members of the suite on an alkali-silica plot but attributed this to alkali metasomatism. Recent geochemical analyses of basaltic to rhyolitic rock types by Minnova Inc. geologists at LeMare Lake, and work in progress, leave little doubt that alkali metasomatism is a factor, but the freshest basalts consistently exhibit a mildly alkalic affinity. This contrasts with the geochemistry of augite-phyric Bonanza volcanics in the Pemberton Hills area northwest of the Island Copper mine which are demonstrably subalkaline with a tholeiite (arc?) signature (Panteleyev and Koyanagi, 1993, this volume).

LONGARM FORMATION

The Longarm Formation was proposed by Sutherland Brown (1968) to include all sedimentary rocks of Early Cretaceous (Valanginian to Barremian) age on the Queen Charlotte Islands. Long Inlet, previously called the Long Arm of Skidegate Inlet on Graham Island, was defined as a type area for this formation. Lithostratigraphy described by Sutherland Brown includes shallow-water marine conglomerates fining upward to shale. A recently refined Cretaceous stratigraphy on the Queen Charlotte Islands (Haggart, 1989, 1991; Haggart and Gamba, 1990; Haggart *et al.*, 1991) may be similar to northern Vancouver Island stratigraphy, but scarcity of Cretaceous sedimentary rocks in the Mahatta Creek area allows for only the simplest of correlations at this time. The stratigraphy of the Longarm Formation on Vancouver Island has been subdivided by Jeletsky (1976) into five mappable facies. From oldest to youngest these lithologies are: fossiliferous calcareous greywacke; massive, calcareous, fossiliferous, concretionary siltstone; impure limestone, calcareous sandstone and conglomerate; bioclastic limestone and calcarenite; and calcareous concretionary greywacke with pebble conglomerate at its base.

Strata assigned to the Longarm Formation crop out along the northern and northwestern margins of the map area. Here, this unit represents a transgressive sequence ranging from basal shallow-marine fossiliferous conglomerates and lithic sandstones up to deeper water shales. The sequence onlaps Lower Jurassic Bonanza volcanic rocks with angular unconformity.



Plate 1-2-6. Welded, lithic-rich lapilli-tuff, Bonanza volcanics, LeMare Lake property. Minnova Inc.

Thick accumulations of Cretaceous sediments are common north of the study area (Figure 1-2-1). The scarcity of these sediments within the study area, and their distribution only along its northern margin, suggests that most of the region persisted as a paleohigh throughout Cretaceous time.

For the most part, Jeletsky's facies are not observed west of Mahatta River. Here, fossiliferous marine conglomerate and lithic arenite are the most common Cretaceous lithologies. At Gooding Cove, a structurally complex area at the western margin of the study area (Figure 1-2-3), the sequence fines upward from conglomerate into black fissile shale. The conglomerate is typically composed of well-rounded granule to cobble-sized clasts grading upward into and interbedded with massive, buff-weathering, medium to light grey, calcareous lithic arenite and wacke. Bivalve shells are very common. Conglomerate clasts are typically volcanic with the exception of rare medium-grained diorite clasts. Coarse-grained rocks grade upwards into unfossiliferous, thinly bedded, dark grey calcareous siltstone and fine-grained sandstone which in turn grades upward into orange-weathering, black fissile shale.

East of Mahatta River, at Kewquodie Creek (Figure 1-2-3), gently dipping, grey-green weathering, light grey to maroon siltstone and lithic wacke predominate. These beds are locally concretionary and have minor conglomerate interbeds; carbonate concretions are common locally.

Jeletsky placed rocks in this area within its uppermost (Barremian) subdivision of the Longarm Formation.

INTRUSIVE ROCKS

Granitoid intrusions of the Island Plutonic Suite occur throughout the map area and are the prime targets for skarn and porphyry copper exploration. The most common rock types are greenish grey to white weathering, medium-grained, equigranular hornblende diorite to quartz diorite, feldspar porphyries of dioritic composition, monzonite and minor granodiorite. The more mafic granitoids are chloritized and variably sericitized. Two varieties of porphyry are found: crowded porphyries with large (<1 cm) phenocrysts and glomerocrysts of plagioclase (30-40 volume %) and lesser hornblende (<5%); and porphyries with 5-10 per cent phenocrysts of euhedral plagioclase (<4mm). The latter intrusions locally show syenitic margins a few metres wide and some have local concentrations (up to 5 volume %) of pyrite cubes reaching 1 centimetre in diameter. The large monzonitic intrusion in Klootchlimmis Creek has a core of granodiorite. Weakly developed magnetite skarns are locally present at their margins.

Dikes of presumed Tertiary age cut through folded and faulted Upper Triassic and Lower Jurassic rocks. The vast majority are dark grey, weakly amygdaloidal basalts with

distinctive dark brown to buff spheroidal weathering of blocky joints; rhyolitic dikes are comparatively rare. The dikes reach 4 metres in width and commonly display chilled flow-laminated margins extending up to 15 centimetres from the contact. Most are aphanitic to sparsely porphyritic; plagioclase-phyric varieties containing up to 15 volume per cent phenocrysts with hiatal textures are rare. Pyrite is locally present along fractures but propylitic alteration is generally inconspicuous. The dikes are steeply dipping (65° - 90°) but appear to have no preferred regional orientation. They do, however, appear to be spatially restricted to the vicinity of the Brooks Peninsula fault zone where northeasterly trending, post-tectonic dikes of intermediate to rhyolitic composition have been mapped previously (Smyth, 1985). These intrusions may represent the conduits for Neogene extrusive rocks known farther east which have been related to near-trench plate-edge volcanism (Armstrong *et al.*, 1985).

STRUCTURE

Block faulting typifies the structural style within the study area where abundant faults of various orientations commonly dip steeply and exhibit both strike-slip and dip-slip displacement. Sedimentary and volcanic rocks within fault-bounded blocks almost invariably dip and face westward and describe a northwesterly trending homocline. Muller *et al.* (1974) have placed this area on the western flank of the Victoria arch, the culmination of which is located east of Nimpkish Lake, approximately 40 kilometres east of the study area (Figure 1-2-1). East of the arch, block-faulted strata dip and face eastward.

Rocks within the study area have undergone multiple stages of deformation ranging in age from Jurassic through to Tertiary as follows:

- The oldest episode of deformation recognized is a folding and block-faulting event which postdates Lower Jurassic volcanism but predates Lower Cretaceous sedimentation.
- Folding and faulting of Lower Cretaceous sedimentary rocks represents a second event apparently controlled by northwesterly trending, predominantly right-lateral transcurrent to transpressional faulting.
- Normal faults of Tertiary age truncate and reactivate many pre-existing structures.

Unfortunately, marker horizons are scarce and valley-fill masks most major faults making motion determinations difficult if not impossible to ascertain directly. Most progress has been made using kinematic indicators associated with minor faults found near the more dominant features.

UPPER TRIASSIC THROUGH LOWER JURASSIC

Volcanic rocks of the Upper Triassic Karmutsen Formation form the base of the stratigraphic succession exposed in the study area. Conformable contacts between the Karmutsen and overlying Upper Triassic Quatsino and Parson Bay Formation marine sediments, as well as the subaqueous to subaerial Lower Jurassic Bonanza volcanics, confirm that this time span represented a period of uplift, but otherwise

relative tectonic quiescence. Some faulting was certainly ongoing during Lower Jurassic volcanism as Bonanza-equivalent dikes have locally intruded along pre-existing faults.

PRE-LOWER CRETACEOUS DEFORMATION

The earliest recognizable deformational episode occurred prior to the deposition of the Lower Cretaceous Longarm Formation. The time period between Lower Jurassic volcanism and Lower Cretaceous sedimentation accounted for significant shortening and block-faulting. The apparent absence of volcanic and sedimentary rocks of Middle to Late Jurassic age suggests that this was also a period of extensive uplift and erosion.

Probably the earliest tectonic event was prompted by east to northeastward directed compressional stresses that caused widespread tilting of Lower Jurassic and older strata to form the northwesterly trending homocline recognized throughout the study area. Some of the northerly plunging mesoscopic and megascopic folds may also be attributed to this episode, as well as northwest to northeasterly striking reverse and thrust faults. Jeletsky (1976) assigned a Middle Jurassic age to this period of deformation, and more recent studies in the Queen Charlotte Islands have also defined a Middle Jurassic episode of folding and faulting (Thompson *et al.*, 1991; Lewis and Ross, 1991).

Within the Middle to Late Jurassic time-frame, folded and tilted sediments were cut by easterly striking, northerly dipping thrust faults and associated drag folds which formed in response to south to southwesterly directed compression. Southerly directed compression is supported by the presence of an east to southeast-striking, steeply dipping, pressure solution cleavage in Quatsino limestone on the eastern side of Neroutsos Inlet as well as in Parson Bay limestones in the southwest corner of the study area.

POST LOWER CRETACEOUS TO PRE-TERTIARY DEFORMATION

The Lower Cretaceous Longarm Formation is a fining upward, transgressive sequence which onlaps the older units with angular unconformity. As noted earlier, most of the study area was a paleohigh forming the southern flank of a Cretaceous basin.

Lower Cretaceous and older rocks have been displaced, sheared and folded by northwest-trending, steeply dipping faults which locally show right-lateral displacement. Deformation associated with these faults increases in intensity toward the western part of the study area. Drag folds along these faults, as well as faults of similar orientation, are believed to have formed in a north to northeasterly directed compressional regime. Longarm Formation sedimentary rocks typically have a shallow dip but are locally dragged into northwesterly plunging folds adjacent to these faults; this is particularly evident along the Gooding Cove fault. The Restless fault is another example of a northwesterly trending fault which shows a west-up and probably right-lateral sense of displacement (Figure 1-2-3). Parson Bay sediments adjacent to it have been thrown into a series of northwesterly plunging chevron folds (Plate 1-2-7).

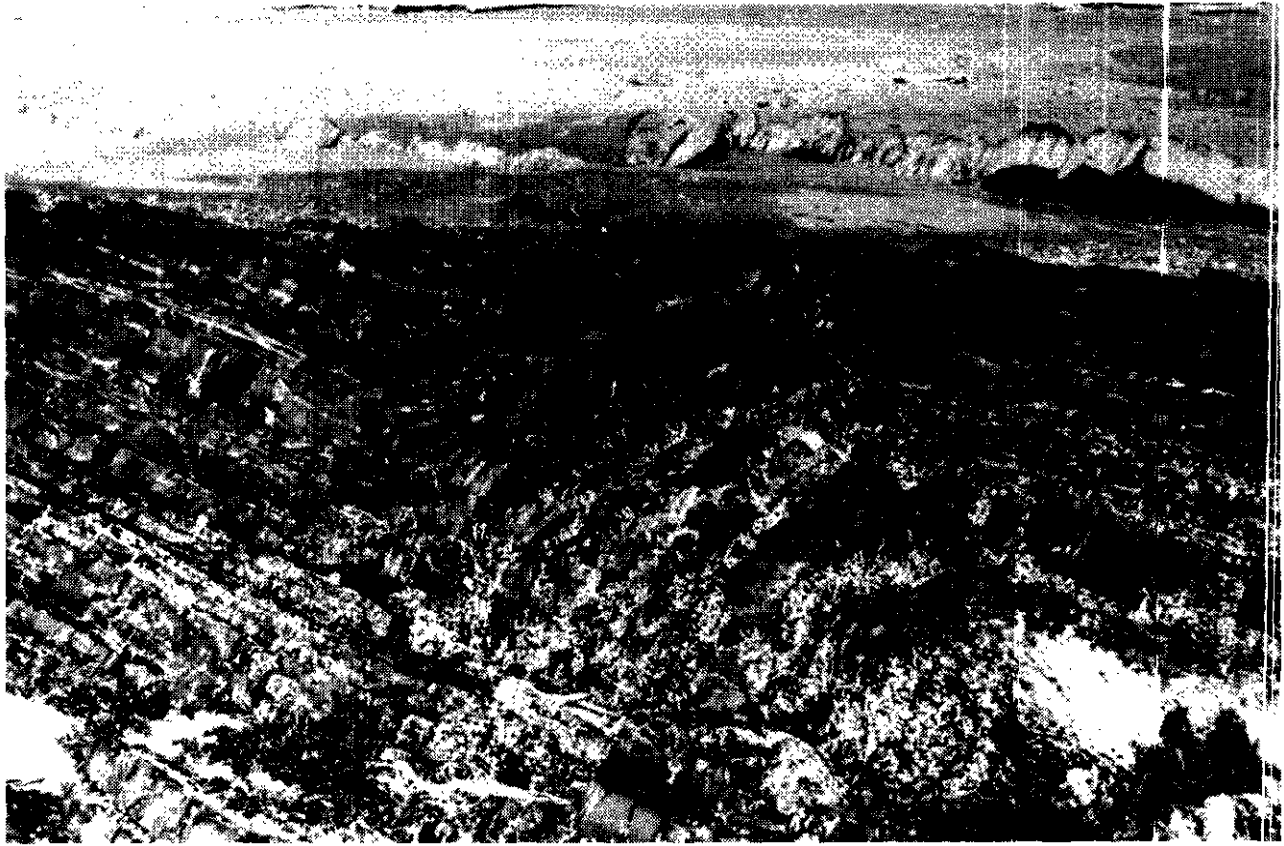


Plate 1-2-7. Chevron folds in thinly bedded Parson Bay sediments.

Steeply dipping, northwesterly trending faults form some of the most conspicuous lineaments within the study area. One of the most notable and intensely studied is the Mahatta River fault (Figure 1-2-3). North of the study area it offsets Cretaceous strata with right-lateral motion and, within the study area, there is some evidence for dip-slip motion bringing the southwest side up (Jeletsky, 1976).

The LeMare Lake fault is the only major fault in the Mahatta Creek area that displaces a known stratigraphic marker. At Red Stripe Mountain, Upper Triassic sedimentary rocks of the Quatsino and overlying Parson Bay formations are displaced to the south in a right-lateral sense by a system of subparallel faults. The magnitude of displacement across this composite fault trace, as indicated by the Quatsino limestone, is of the order of 5 kilometres. Subsidiary minor faults on the south side of the entrance to Klaskino Inlet locally exhibit subhorizontal slickensides consistent with late lateral motion.

TERTIARY NORMAL FAULTING

Northeasterly trending normal faults truncate and reactivate many pre-existing structures throughout the study area. The most intense zone of normal faulting lies along the Brooks Peninsula fault zone. Earliest movement along this fault is constrained by the truncation of major, northwesterly trending faults which cut Lower Cretaceous beds. Latest motion probably coincides with the eruption of Alert Bay volcanics and intrusion of coeval basaltic dikes.

KINEMATIC ANALYSIS

Motion determinations on major structures were difficult to assess due to the overall lack of marker horizons. However, kinematic features shown by many minor faults were analyzed. Most fault planes are slickensided, and a small percentage of faults show minor offsets or drag folds giving a definitive movement direction.

When poles to faults are plotted and contoured, what appears to be a somewhat random array of faults reveals a few consistent orientations (Figure 1-2-4A, B). Kinematic indicators on some of these faults (drag folds, offsets, slickensides) also reveal some consistencies as follows (Figure 1-2-4C):

- The majority of structures which revealed right-lateral motion are associated with steeply dipping, northwesterly trending faults (Figure 1-2-4C, 1-2-5A).
- Normal faults are more variable in orientation due to the reactivation of older structures. These faults typically trend northeast and dip steeply to moderately (Figure 1-2-4C, 1-2-5B).
- Structures which display thrust or reverse motion are also quite variable but are somewhat consistent with northeasterly directed and south to southwesterly directed compressional events (Figure 1-2-4C, 1-2-5C).

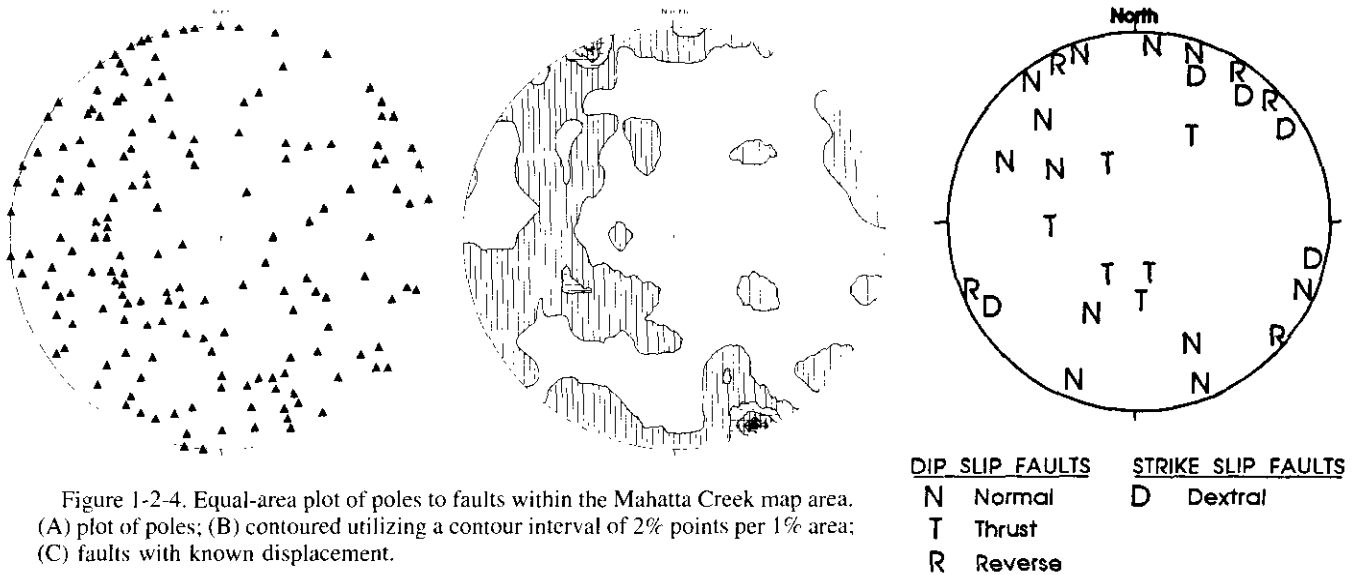


Figure 1-2-4. Equal-area plot of poles to faults within the Mahatta Creek map area. (A) plot of poles; (B) contoured utilizing a contour interval of 2% points per 1% area; (C) faults with known displacement.

LITHOLOGICAL CONTROLS ON STRUCTURAL STYLES

Thick, massive Karmutsen basalts, the stratigraphically lowest unit in the area, may have controlled the dominant structural style by accommodating strain by block faulting (Muller, 1974). This competent unit has formed a firm base which may have shielded the less competent overlying units from more intense deformation.

Bedded sediments of the Parson Bay Formation, and to a lesser extent the Quatsino Formation, have accommodated strain by flexural-slip folding and bedding-parallel shear. These folds are most evident in the west of the study area and typically verge toward the southwest or northeast. Locally, the overlying Bonanza volcanics are also broadly warped along similar fold axes. Bedded epiclastic and pyroclastic rocks within the Bonanza Formation commonly show bedding-parallel shear but mesoscopic folds are rare.

Poles to bedding planes have been plotted on equal-area stereonet for the Bonanza volcanics and Parson Bay, Quatsino and Longarm formations (Figure 1-2-6). The Triassic and Jurassic lithologies show fairly consistent northwesterly to southwesterly dips. The Parson Bay sediments have been more prone to accommodation of strain by folding along north-northeast to north-northwesterly trending fold axes. Longarm sediments are typically subhorizontal to gently dipping, except where they have been dragged along northwesterly trending faults.

ECONOMIC GEOLOGY AND EXPLORATION ACTIVITY

The prime economic targets in the Quatsino Sound area are gold-bearing iron and copper-rich skarns, precious metal bearing epithermal systems, porphyry deposits as characterized by the Island Copper orebody, and gold-enriched high-sulphidation systems transitional between porphyry

and epithermal environments (Panteleyev, 1992). Recent summaries of these deposit types can be found in McMillan *et al.* (1992) and Dawson *et al.* (1991), and the results of recent fieldwork in transitional environments west of Island Copper (Red Dog - Hushamu) are given by Panteleyev and Koyanagi (1993, this volume). Some 40 mineral occurrences in the map area are documented in the MINFILE database. Details of their locations and principal commodities are given in Open File 1993-10.

The Mahatta Creek area contains one past producer, the Yreka mine, situated just west of Neroutsos Inlet (Figure 1-2-3). Work began in 1898 and intermittent production between 1902 and 1967 totalled some 145 000 tonnes averaging 2.7 per cent copper, 31 grams per tonne silver and 0.34 gram per tonne gold. The ore is associated with an epidote-garnet skarn assemblage developed in limestones and augite-plagioclase-bearing limy tuffs of the Parson Bay Formation. The skarns are associated with quartz-plagioclase porphyry dikes and sills. Disseminated pyrrhotite and chalcopyrite with sparse pyrite, magnetite and hematite are locally controlled by faults or occur along stratigraphic horizons as lensoid replacement bodies (Wilson, 1955). Skarn occurrences in the surrounding area also contain minor amounts of sphalerite and galena.

Minor quartz feldspar porphyry intrusions are also found farther south near the eastern margin of a larger body of diorite near the mouth of Teeta Creek. Hydrothermal alteration is pronounced and hints of porphyry-style mineralization are found in local breccia pipes that contain disseminated chalcopyrite. The breccias contain rare sulphide fragments that signify a complex multi-stage history (C.I. Godwin, personal communication, 1992). Hydrothermal stockworks and veins containing copper and traces of molybdenum and precious metals are found elsewhere in the region.

Exploration activity in the Mahatta Creek area in 1992 was largely focused in the west, at LeMare Lake, on claims

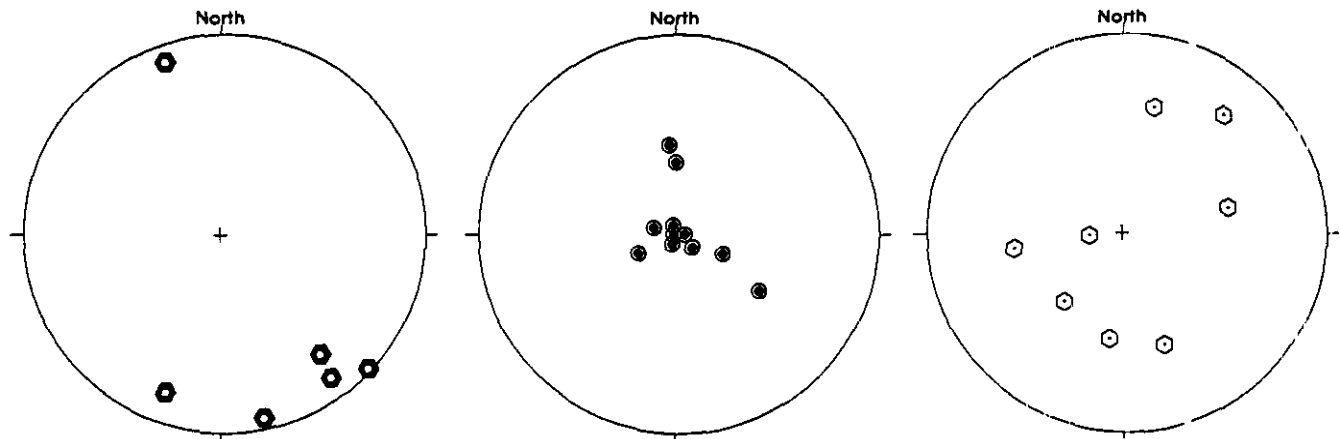


Figure 1-2-5. Displacement vectors on fault planes derived from drag folds, offsets and/or slickensides. (A) dextral faults; (B) normal faults; (C) thrust faults.

held by Minnova Inc., and on the Madhat property by Pan Orvana Resources Inc. Both properties were sampled extensively over the summer for soil and bedrock geochemistry, and drilling programs were conducted in the fall.

The Minnova property at LeMare Lake (Figure 1-2-3) covers an extensive zone of hydrothermal alteration. The hillsides west of the lake are underlain by a well-exposed, cyclical, basalt-rhyolite succession of intercalated flows, pyroclastic and epiclastic deposits which strike north-northwest and have westerly dips and facing directions. A typical lithological cycle, from bottom to top, includes: dark greenish grey to maroon, weakly amygdaloidal, aphanitic to finely porphyritic (<1 mm) basalt; volcanic siltstones, sandstones and minor granule conglomerates of predominantly mafic to intermediate heritage; greenish grey to pink, intermediate to predominantly rhyolitic, non-welded to strongly welded, lithic-rich lapilli tuffs and tuff-breccias, locally including rhyolitic base-surge deposits with shallow-angle cross-bedding and airfall(?) material, overlain by viscous, flow-laminated rhyolite. The epiclastic-pyroclastic succession is usually less than 20 metres thick, and the intermediate units generally comprise a mixture of rhyolite and basalt clasts. The common occurrence of densely welded textures involving flattened pumice lapilli indicates a subaerial environment of dominantly bimodal volcanism.

Alteration of these lithologies is most pronounced in a zone covering an area of more than a square kilometre just west of the southern tip of LeMare Lake. Widespread argillic, advanced argillic and more localized phyllic alteration commonly contain minor amounts of disseminated pyrite accompanied by rare malachite staining along fractures. The most intense alteration involves higher temperature, quartz-pyrophyllite assemblages that, unlike similar assemblages at the Island Copper mine, appear to lack dumortierite. These alteration zones are cut by a series of variably altered mafic dikes, some of which are quite fresh and appear to post-date the alteration. This strongly suggests that the alteration is syn-Bonanza or Early Jurassic in age.

Similar bimodal lithologies with more restricted zones of argillic alteration also occur southeast of LeMare Lake.

However, these alteration zones are unlikely to represent an extension of their counterparts to the west as they are separated from them by the LeMare fault, which shows some 5 kilometres of right-lateral offset. A small zone of potassic alteration containing rare chalcopryrite, possibly associated with porphyry-style mineralization at depth, is exposed in the northern part of the claim block in the low ground between LeMare Lake and Harvey Cove.

The Madhat property of Pan Orvana Resources Inc. is located approximately 5 kilometres south-southeast of O'Connell Lake (Figure 1-2-3). The claims cover a structurally complex region at the intersection of major east-northeast and northeast-trending faults. The northeast-trending faults are intruded by Bonanza(?) dikes of mafic to rhyolitic composition; the latter have chilled margins of greyish green partly devitrified obsidian. In addition, the lithological similarities of fault panels of volcanic and sedimentary rocks, currently assigned to the Pars on Bay Formation and Bonanza volcanics, remain to be firmly established by microfossils and geochemistry respectively. Structurally controlled quartz-carbonate alteration and veining with minor disseminated pyrite and chalcopryrite coincides with anomalous gold geochemistry in soils and bedrock; elevated copper values occur near the fringes of the gold anomalies. The mineralization appears to be related to a shallow hydrothermal source, possibly linked with dioritic intrusions in the vicinity.

ACKNOWLEDGMENTS

The crew of "Operation Rainforest" would like to thank Nick Massey for indoctrinating (innoculating?) us; Harvey Herd and the staff of Western Forest Products for easing our logistics at Mahatta River; Peter Bradshaw and Andy Laird (Pan Orvana Resources Inc.) for geological discussions and visits to the Madhat property; Cam DeLong, Dave Heberlein and Minnova Inc. for accommodating property visits and freely sharing geological data (Cam DeLong first suggested the possibility of an intra-Bonanza age for the mineralization and alteration at LeMare Lake based on dike relationships); the remainder of the Minnova crew,

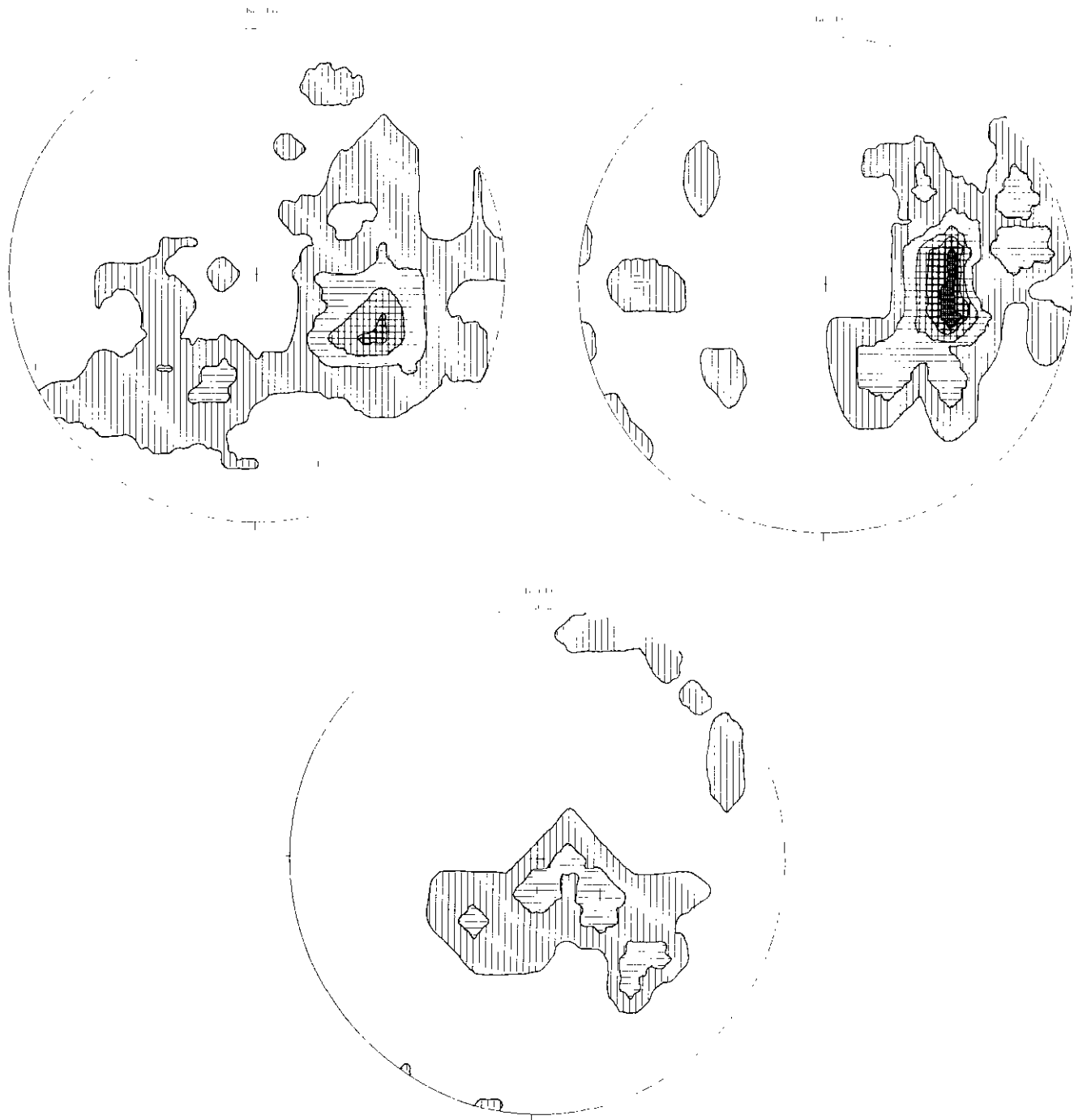


Figure 1-2-6. Poles to bedding planes for (A) Parson Bay Formation; (B) Bonanza volcanics; (C) Longarm Formation. Contoured utilizing a contour interval of 2% points per 1% area.

especially culinary wizard Lisa Horvat for barbecues, including an unforgettable "New England crab bake", and artiste extraordinaire Lloyd Cornish for cartooning our trials and tribulations (Plate 1-2-8), "sharing the wealth", and introducing us to the irrepressible beer-bottle saga; Fabrice Cordey for agreeing to join us in the field to share his radiolarian expertise, for showing us "features", and above all, for enhancing the beer-bottle saga; the staff of Quatsino Chalet, Port Alice, for a memorable stay; Alan Gilmour for logistical support and showing us precisely how to lose his crab trap; and El Niño for a wonderful summer. Thanks are extended to Brian Grant and John Newell for superb editorial handling.

REFERENCES

- Armstrong, R.L., Muller, J.E., Harakal, J.E. and Muehlenbachs, K. (1985): The Neogene Alert Bay Volcanic Belt of Northern Vancouver Island, Canada: Descending-plate-edge Volcanism in the Arc-Trench Gap; *Journal of Volcanology and Geothermal Research*, Volume 26, pages 75-97.
- Bancroft, J.A. (1913): Geology of the Coast and Island between Strait of Georgia and Queen Charlotte Sound, British Columbia; *Geological Survey of Canada*, Memoir 23.
- Barker, F., Sutherland Brown, A., Budahn, J.R. and Plafker, G. (1989): Back-arc with Frontal-arc Component Origin of Triassic Karmutsen Basalt, British Columbia, Canada; *Chemical Geology*, Volume 75, pages 81-102.
- Carlisle, D. (1972): Late Paleozoic to Mid-Triassic Sedimentary-Volcanic Sequence of Northeastern Vancouver Island; in Report of Activities, November 1971 to March 1972, *Geological Survey of Canada*, Paper 72-1B, pages 24-30.
- Carlisle D. and Suzuki, T. (1974): Emergent Basalt and Submergent Carbonate Clastic Sequences including the Upper Triassic Dilleri and Welleri Zones on Vancouver Island; *Canadian Journal of Earth Sciences*, Volume 11, pages 254-279.
- Crickmay, C.H. (1928): The Stratigraphy of Parson Bay, British Columbia; *University of California Publications, Bulletin of the Department of Geological Sciences*, Volume 18, pages 51-70.
- Dawson, G.M. (1887): Report on a Geological Examination of the Northern Part of Vancouver Island, B.C.; *Geological Survey of Canada*, Annual Report 1886, Part B, 129 pages.
- Dawson, K.M., Panteleyev, A., Sutherland Brown, A. and Woodsworth, G.J. (1991): Regional Metallogeny, Chapter 19; in *Geology of the Cordilleran Orogen in Canada*, Gabrielse, H. and Yorath C.J., Editors, *Geological Survey of Canada*, Geology of Canada, Number 4, pages 707-768.
- Dolmage, V. (1919): Quatsino Sound and Certain Mineral Deposits of the West Coast of Vancouver Island, B.C.; in Summary Report 1918, *Geological Survey of Canada*, Part B, pages 30B-38B.
- Frebold, H. and Tipper, H.W. (1970): Status of the Jurassic of the Canadian Cordillera in British Columbia, Alberta and Southern Yukon; *Canadian Journal of Earth Sciences*, Volume 7, pages 1-21.



Plate 1-2-8. "Operation Rainforest", rendition by Lloyd Cornish.

- Gardner, M.C., Bergman, S.C., Cushing, G.W., MacKevett, E.M. Jr., Plafker, G., Campell, R.B., Dodds, C.J., McClelland, W.C. and Mueller, P.A. (1988): Pennsylvanian Pluton Stitching of Wrangellia and the Alexander Terrane, Wrangell Mountains, Alaska; *Geology*, Volume 16, pages 967-971.
- Greenwood, H.J., Woodsworth, G.J., Read, P.B., Ghent, E.D. and Evenchick, C. A. (1991): Metamorphism, Chapter 16; in *Geology of the Cordilleran Orogen in Canada*, Gabrielse, H. and Yorath C.J., Editors, *Geological Survey of Canada*, *Geology of Canada*, Number 4, pages 533-570.
- Gunning, H.C. (1930): Geology and Mineral Deposits of Quatsino-Nimkish Area, Vancouver Island, British Columbia; in *Summary Report 1929, Geological Survey of Canada*, Part A, pages 94A-143A.
- Gunning, H.C. (1932): Preliminary Report on the Nimkish Lake Quadrangle, Vancouver Island, British Columbia; in *Summary Report 1931, Geological Survey of Canada*, Part A, pages 22-35.
- Haggart, J.W. (1989): Reconnaissance Lithostratigraphy and Biochronology of the Lower Cretaceous Longarm Formation, Queen Charlotte Islands, British Columbia; in *Current Research, Part H, Geological Survey of Canada*, Paper 89-1H, pages 39-46.
- Haggart, J.W. (1991): A Synthesis of Cretaceous Stratigraphy, Queen Charlotte Islands, British Columbia; in *Evolution and Hydrocarbon Potential of the Queen Charlotte Basin*, British Columbia, Woodsworth, G.J., Editor, *Geological Survey of Canada*, Paper 90-10, pages 253-278.
- Haggart, J.W. (1992): Report on Jurassic and Cretaceous Fossils from Northern Vancouver Island, British Columbia (Mahatta Creek Map-area, NTS 92L/5); *Geological Survey of Canada*, Fossil Report Number JWH-1992-09, 4 pages.
- Haggart, J.W. and Gamba, C.A. (1990): Stratigraphy and Sedimentology of the Longarm Formation, Southern Queen Charlotte Islands, British Columbia; in *Current Research, Part F, Geological Survey of Canada*, Paper 90-1F, pages 61-66.
- Haggart, J.W., Taite, S., Indrelid, J., Hesthammer, J. and Lewis, P.D. (1991): A Revision of Stratigraphic Nomenclature for the Cretaceous Sedimentary Rocks of the Queen Charlotte Islands, British Columbia; in *Current Research, Part A, Geological Survey of Canada*, Paper 91-1A, pages 367-371.
- Jeffery, W.G. (1962): Preliminary Geological Map, Alice Lake – Benson Lake Area; *B.C. Ministry of Energy, Mines and Petroleum Resources*.
- Jeletsky, J.A. (1969): Mesozoic and Tertiary Stratigraphy of Northern Vancouver Island, British Columbia (92E, 92L, 102I); in *Current Research Part A, Geological Survey of Canada*, Paper 69-1A, pages 126-134.
- Jeletsky, J.A. (1970): Mesozoic Stratigraphy of Northern and Eastern Parts of Vancouver Island, British Columbia (92-E, F, L, 102I); in *Current Research Part A, Geological Survey of Canada*, Paper 70-1A, pages 209-214.
- Jeletsky, J.A. (1976): Mesozoic and Tertiary Rocks of Quatsino Sound, Vancouver Island, British Columbia; *Geological Survey of Canada*, Bulletin 242, 243 pages.
- Lewis P.D. and Ross J.V. (1991): Mesozoic and Cenozoic Structural History of the Central Queen Charlotte Islands, British Columbia; in *Evolution and Hydrocarbon Potential of the Queen Charlotte Basin*, British Columbia, Woodsworth, G.J., Editor, *Geological Survey of Canada*, Paper 90-10, pages 31-50.
- Massey, N.W.D. and Melville, D.M. (1991): Quatsino Sound Project; in *Geological Fieldwork 1990, B.C. Ministry of Energy, Mines and Petroleum Resources*, Paper 1991-1, pages 85-88.
- Matysek, P.F., Gravel J.L. and Jackaman, W. (1989): 1988 British Columbia Regional Geochemical Survey, Stream Sediment and Water Geochemical Data, NTS 92L/102I – Alert Bay/ Cape Scott; *B.C. Ministry of Energy, Mines and Petroleum Resources*, RGS 23.
- McMillan, W.J., Höy, T., McIntyre, D.G., Nelson, J.L., Nixon, G.T., Hammack, J.L., Panteleyev, A., Ray, G.E. and Webster, I.C.L. (1992): Ore Deposits, Tectonics and Metallogeny in the Canadian Cordillera, *B.C. Ministry of Energy, Mines and Petroleum Resources*, Paper 1991-4, 276 pages.
- Monger, J.W.H., Price, R.A. and Templeman-Kluit, D.J. (1982): Tectonic Accretion and the Origin of Two Major Metamorphic and Plutonic Belts in the Canadian Cordillera; *Geology*, Volume 10, pages 70-75.
- Muller, J.E. (1977): Evolution of the Pacific Margin, Vancouver Island, and Adjacent Regions; *Canadian Journal of Earth Sciences*, Volume 14, pages 2062-2068.
- Muller, J.E. and Roddick, J.A. (1983): Alert Bay – Cape Scott; *Geological Survey of Canada*, Map 1552.
- Muller, J.E., Cameron, B.E.B. and Northcote, K.E. (1981): Geology and Mineral Deposits of Nootka Sound Map-area, Vancouver Island, British Columbia; *Geological Survey of Canada*, Paper 80-16, pages.
- Muller, J.E., Northcote, K.E. and Carlisle, D. (1974): Geology and Mineral Deposits of Alert Bay – Cape Scott Map-area, Vancouver Island, British Columbia; *Geological Survey of Canada*, Paper 74-8, 77 pages.
- Northcote, K.E. (1969): Geology of the Port Hardy – Coal Harbour Area; in *Report of the Minister of Mines and Petroleum Resources 1968, B.C. Ministry of Energy, Mines and Petroleum Resources*, pages 84-87.
- Northcote, K.E. (1971): Rupert Inlet – Cape Scott Map-area; in *Geology, Exploration and Mining in British Columbia 1970, B.C. Ministry of Energy, Mines and Petroleum Resources*, pages 254-258.
- Panteleyev, A. (1992): Copper-Gold-Silver Deposits Transitional Between Subvolcanic Porphyry and Epithermal Environments; in *Geological Fieldwork 1991*, Grant, B. and Newell, J.M., Editors, *B.C. Ministry of Energy, Mines and Petroleum Resources*, Paper 1992-1, pages 231-234.
- Panteleyev, A. and Koyanagi, V.M. (1993): Advanced Argillic Alteration in Bonanza Volcanic Rocks, Northern Vancouver Island – *Transitions Between Porphyry Copper and Epithermal Environments*; in *Geological Fieldwork 1992*, Grant, B. and Newell, J.M., Editors, *B.C. Ministry of Energy, Mines and Petroleum Resources*, Paper 1993-1, this volume.
- Riddihough, R.P. and Hyndman, R.D. (1991): Modern Plate Tectonic Regime of the Continental Margin of Western Canada; in *Geology of the Cordilleran Orogen in Canada*, Chapter 13, Gabrielse H. and Yorath C.J., Editors, *Geological Survey of Canada*, *Geology of Canada*, Number 4, pages 435-455.
- Smyth, W.R. (1985): Geology of the Brooks Peninsula, Vancouver Island (92L/4); in *Geological Fieldwork 1984, B.C. Ministry of Energy, Mines and Petroleum Resources*, Paper 1985-1, pages 161-169.
- Surdam, R.C. (1968): The Stratigraphy and Volcanic History of the Karmutsen Group, Vancouver Island, B.C.; *University of Wyoming*, *Contributions to Geology*, Volume 7, pages 15-26.

- Sutherland Brown, A. (1968): Geology of the Queen Charlotte Islands; *B.C. Ministry of Energy, Mines and Petroleum Resources, Bulletin 54*.
- Thompson, R.I., Haggart, J.W. and Lewis, P.D. (1991): Late Triassic Through Early Tertiary Evolution of the Queen Charlotte Basin, British Columbia, with a Perspective on Hydrocarbon Potential; Woodsworth, G.J., Editor, *Geological Survey of Canada, Paper 90-10*, pages 3-29.
- Tozer, E.T. (1967): A Standard for Triassic Time; *Geological Survey of Canada, Bulletin 156*.
- van der Heyden, P. (1991): A Middle Jurassic to Early Tertiary Andean-Sierran Arc Model for the Coast Belt of British Columbia; *Tectonics, Volume 11, Number 1* pages 82-97.
- Wheeler, J.O., Brookfield, A.J., Gabrielse, H., Monger, J.W.H. and Woodsworth, G. J. (1991): Terrane Map of the Canadian Cordillera; *Geological Survey of Canada, Map 1712A*.
- Wilson, P.R. (1955): The Geology and Mineralogy of the Yreka Copper Property, Quatsino Sound, British Columbia; unpublished M.Sc. thesis, *The University of British Columbia*, 81 pages.

NOTES



**GEOLOGY AND MINERAL OCCURRENCES OF
THE MOUNT TATLOW MAP AREA
(920/5, 6, and 12)**

By J. Riddell, P. Schiarizza, R.G. Gaba, B.C. Geological Survey Branch,
N. Caira and A. Findlay, Taseko Mines Limited.

(Contribution to the Interior Plateau Program
Canada - British Columbia Mineral Development Agreement 1991-1995)

KEYWORDS: Regional geology, Mount Tatlow, Cadwallader Terrane, Bridge River Complex, Methow basin, Tyaughton basin, Silverquick formation, Powell Creek formation, Yalakom fault, porphyry Cu-Au.

INTRODUCTION

The Mount Tatlow map area is located about 240 kilometres north of Vancouver (Figure 1-3-1), along the eastern boundary of the Coast Mountains. Elevations in the rugged mountainous western part of the study area range from 1300 metres to just over 3000 metres. To the north and east the physiography changes abruptly to the flat, open range terrain of the Interior Plateau; elevations there vary from 1300 to 1800 metres.

This report introduces the Tatlayoko project, and discusses the observations of the first of three proposed field seasons. The project is partially funded by the Canada - British Columbia Mineral Development Agreement 1991-1995, and is designed to provide a modern database for evaluating mineral potential in this part of the Coast Mountains. The project area is contiguous with the recently mapped Taseko - Bridge River area to the southeast (Schiarizza *et al.*, 1990a and references therein; Schiarizza *et al.*, in preparation) and the Chilko Lake area to the southwest (McLaren, 1990; Figure 1-3-1).

REGIONAL GEOLOGIC SETTING

The Mount Tatlow map area lies along the northeastern edge of the eastern Coast Belt (Monger, 1986; Journeay, 1990), which includes a number of distinct, partially coeval lithotectonic assemblages that originated in ocean basin, volcanic arc and clastic basin environments. These units are late Paleozoic to Cretaceous in age and are intruded by granitic rocks of mid-Cretaceous through Early Tertiary age. They are juxtaposed across complex systems of contractional, strike-slip and extensional faults of mainly Cretaceous and Tertiary age. Lithotectonic units and structures of the eastern Coast Belt extend southward into the Cascade fold belt of Washington State (Misch, 1966), and comprise a strongly tectonized zone between the Intermontane Belt to the east and the western Coast Belt and Wrangellia to the west (Monger, 1990). Stratigraphic relationships between lithotectonic assemblages of the eastern Coast Belt and coeval rocks to the east and west are uncertain or disputed.

The Mount Tatlow area is underlain by upper Paleozoic through Lower Cretaceous rocks of the Bridge River Complex, Cadwallader Terrane, and the Tyaughton and Methow basins, together with Upper Cretaceous sedimentary and volcanic rocks of the Silverquick and Powell Creek formations. These rocks are intruded by Cretaceous and Tertiary dikes and stocks, and are overlain by Neogene plateau lavas of the Chilcotin Group. The most prominent structural feature of the area is the northwest-striking Yalakom fault, which was the locus of more than 100 kilometres of Eocene(?) dextral strike-slip displacement.

LITHOLOGIC UNITS

BRIDGE RIVER COMPLEX

The Bridge River Complex is best exposed in the Bridge River drainage basin, 100 kilometres southeast of Mount Tatlow. There it comprises an assemblage of chert, argillite, greenstone, gabbro, blueschist, limestone and clastic sedimentary rocks with no coherent internal stratigraphy (Petter, 1986; Schiarizza *et al.*, 1989, 1990a). Cherts range from Mississippian to late Middle Jurassic in age (Cordey, 1991), and blueschist-facies metamorphism occurred in the Triassic (Archibald *et al.*, 1991). In its type area, the Bridge River Complex is structurally interleaved with Cadwallader Terrane, and is stratigraphically overlain by Tyaughton basin sedimentary rocks.

The Bridge River Complex is represented in the Mount Tatlow area by several poorly exposed creek outcrops of sheared ribbon chert that define a thin east-west strip through the forested slopes northeast of Mount Tatlow. The grey and black chert beds are 1 to 6 centimetres thick, and separated by thinner interbeds of dark grey argillite. Chert beds are intensely fractured in all directions normal to bedding surfaces. Beds are commonly crumpled (Plate 1-3-1). Associated with the chert beds are chert-rich sandstones, amygdaloidal greenstones, intensely foliated blue-green serpentinite lenses, and sheared muddy breccias containing boulders of greenstone, chert and marble. Shear foliations in all of these rocks strike east and are subvertical.

The Bridge River Complex within the Mount Tatlow area apparently comprises a fault-bounded lens that separates Cadwallader Terrane to the north from the Taylor Creek Group to the south. It is commonly associated with these same units in its type area, more than 100 kilometres to the southeast. The fault-bounded panels north of Mount Tatlow are truncated to the east by the Yalakom fault.

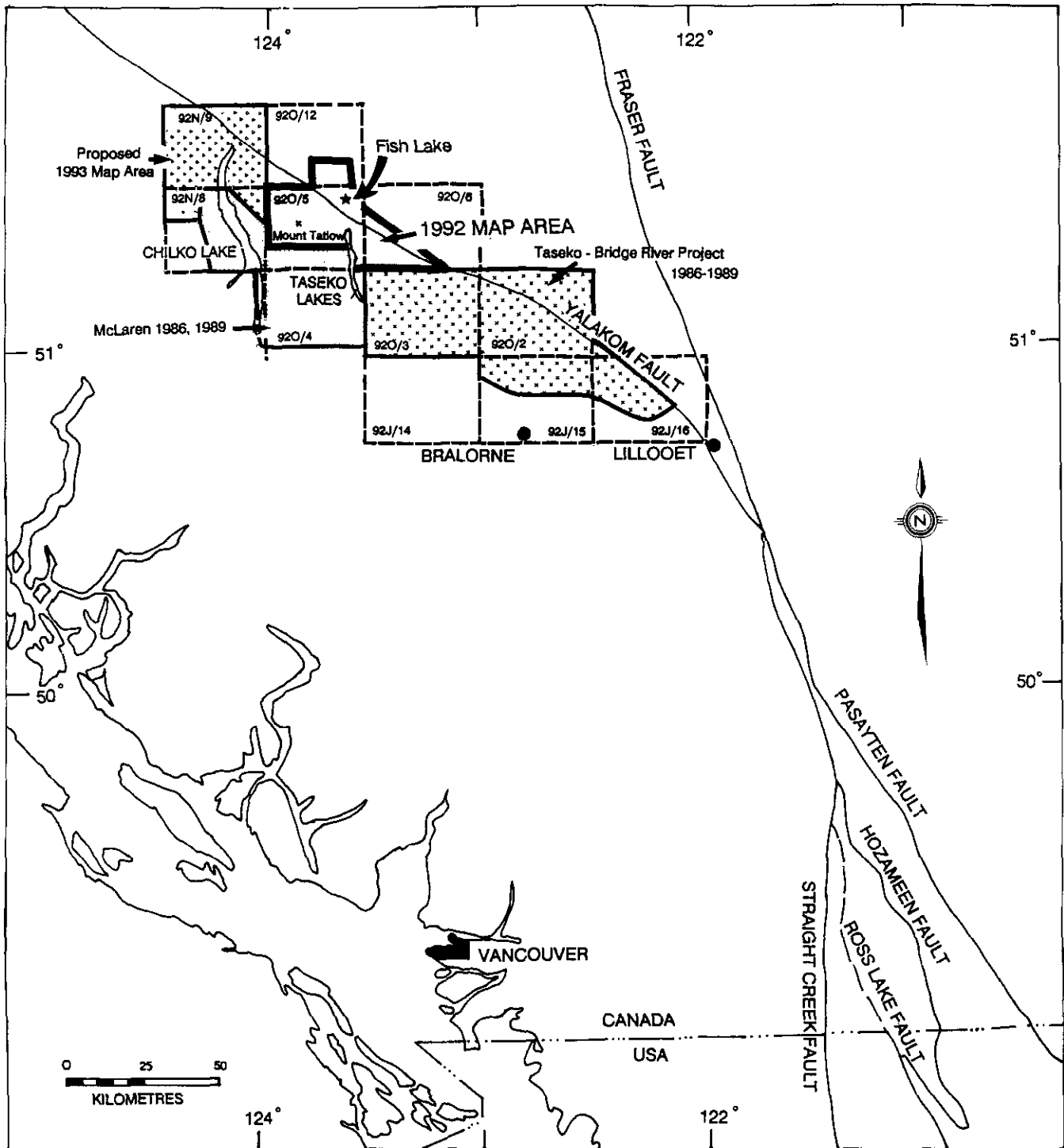


Figure 1-3-1. Location map.

CADWALLADER TERRANE

The Cadwallader Terrane, as defined 75 kilometres southeast of Mount Tatlow, consists of Upper Triassic volcanic and sedimentary rocks of the Cadwallader and Tyaughton groups, and Lower to Middle Jurassic clastic sedimentary rocks of the informally named Last Creek formation (Rusmore, 1987; Rusmore *et al.*, 1988;

Umhoefer, 1990). Trace element geochemistry of volcanic rocks and the composition of the clastic sedimentary rocks suggests that the rocks of Cadwallader Terrane accumulated on or near a volcanic arc.

Rocks assigned to the Cadwallader Terrane in the Mount Tatlow area include siltstones, sandstones, conglomerates and limestones correlated with the Upper Triassic Hurley



Plate 1-3-1. Bridge River ribbon chert.

Formation (Cadwallader Group), together with overlying siltstones and cherty argillites correlated with the Lower to Middle Jurassic Last Creek formation.

HURLEY FORMATION

Rocks assigned to the Upper Triassic Hurley Formation (uTRCH) are exposed in an east-striking band about 12 kilometres long and 2 kilometres wide, north of Mount Tatlow. They crop out in the lowest set of bluffs south of Konni Lake and in canyons in Tsoless and Elkin creeks near their confluence. Disrupted Hurley-type rock sequences (uTRCHy) and associated sheared serpentinite lenses crop out along the trace of the Yalakom fault east of Big Onion Lake and in Elkin Creek downstream from the confluence with Tsoless Creek.

The Hurley Formation in the Mount Tatlow area consists mainly of thinly bedded black-and-tan siltstones and shales with thin to medium interbeds of brown-weathering calcareous argillite, siltstone, sandstone and argillaceous limestone. These predominantly thin-bedded intervals are punctuated by thick, commonly graded beds of calcareous sandstone, and locally by limestone-bearing pebble to cobble conglomerates. The conglomerates have limy sand or mud matrix and also contain clasts of granitoid and volcanic rock, chert and calcarenite. Small carbonaceous fragments of plant debris were found in brown calcarenites in Tsoless Creek and Elkin Creek outcrops. The Hurley Formation also

includes massive, white-weathering limestone, which forms a lens several tens of metres thick within clastic rocks on the low slopes southeast of Konni Lake.

The belt of rocks we assign to the Hurley Formation was in large part mapped as Lower Cretaceous Taylor Creek Group by Tipper (1978), although he included the exposures of massive white limestone southeast of Konni Lake in the Upper Triassic Tyaughton Group. We have previously mapped the Hurley Formation from its type area near Eldorado Creek (Rusmore, 1985, 1987) eastward to the Yalakom River (Schiarrizza *et al.*, 1989, 1990a), and are confident that the belt north of Mount Tatlow is part of the formation. Collections of limestone and calcareous argillite are presently being processed for conodonts in an attempt to confirm the inferred Late Triassic age of the rocks.

LAST CREEK FORMATION

The Hurley Formation is stratigraphically overlain to the south by an east-striking belt of rocks that we assign to the Last Creek formation. Our assignment is consistent with that of Tipper (1978) who mapped these rocks as the Lower to Middle Jurassic portion of the Tyaughton Group (equivalent to the Last Creek formation in the revised nomenclature of Umhoefer, 1990). The formation is exposed in the Tsoless Creek canyon and northeast of Tatlow Creek, where it consists mainly of well-bedded grey to black cherty argillite. Pyrite is abundant in some beds, and they weather

rusty orange where sheared. The sequence also includes black micritic limestone beds 2 to 10 centimetres thick and minor cobble conglomerate with limy matrix and sedimentary and volcanic clasts. West of Tatlow Creek we mapped a discontinuous coquina bed 5 metres thick, and collected belemnites, radiolarians, shell fragments and ribbed bivalves from another limestone bed.

In its type area near Tyaughton Creek, the Last Creek formation comprises upper Hettangian to middle Bajocian conglomerate, sandstone and shale that disconformably overlies the Upper Triassic (middle to upper Norian) Tyaughton Group (Umhoefer, 1990). Correlative rocks have also been identified farther east, in the Camelsfoot Range, where they comprise cherty argillites and argillaceous limestones that overlie the Hurley Formation. These rocks were included in the Hurley Formation in the preliminary map and report by Schiarizza *et al.*, (1990a), but have subsequently yielded two collections of radiolaria of Early or Middle Jurassic and Middle Jurassic age, respectively. The Last Creek formation north of Mount Tatlow is specifically correlated with the Last Creek formation of the Camelsfoot Range, which it closely resembles in lithology and in its stratigraphic position directly above the Hurley Formation.

TYAUGHTON BASIN

The Tyaughton basin (Jeletzky and Tipper, 1968; Garver, 1992) includes shallow-marine clastic sedimentary rocks of the Middle Jurassic to Lower Cretaceous Relay Mountain Group, together with synorogenic marine clastic rocks of the Lower Cretaceous (Albian) Taylor Creek Group. Within the Mount Tatlow area, the Tyaughton basin is represented only by the Taylor Creek Group.

TAYLOR CREEK GROUP

The Taylor Creek Group outcrops as an east-trending belt north of the Mount Tatlow ridge system, where it is in fault contact with the Last Creek formation and Bridge River Complex to the north, and the Powell Creek and Silverquick formations to the south. It also underlies much of the southeastern part of the map area, in a belt that extends from Taseko Lake to Nadila Creek. Taylor Creek Group exposures in this area are cut by numerous intrusions, and unconformably overlain by Powell Creek volcanics and Quaternary cover.

The Taylor Creek Group consists largely of black shale and siltstone, together with chert-rich sandstone and pebble conglomerate. Olive-green muscovite-bearing sandstones, brown limy sandstone, and green ash and crystal tuffs also occur in the Taylor Creek sequence.

Pebble conglomerate is the most distinctive lithology. It contains clasts of white, grey, green, black and red chert, together with white and grey quartz, felsic volcanic rocks and, more rarely, calcarenite, black shale and siliceous argillite. Most of the conglomerates are clast supported, but sandy matrix-supported beds also occur. Pebbles are commonly 1 to 2 centimetres across, and rarely larger than 4 centimetres.

Black shale beds are commonly splintered and locally contain lighter coloured silty and sandy interbeds, resistant

carbonate-cemented interlayers, thin micrite beds, and limestone concretions. Small plant fragments and cone fragments are rare. Shales are commonly cleaved into paper-thin sheets near intrusions.

The Taylor Creek Group in the southeastern part of the Mount Tatlow map area is lithologically similar to, and in part continuous with, the Taylor Creek Group in the northwestern corner of the Warner Pass map area (Glover and Schiarizza, 1987). Those rocks were also mapped as Taylor Creek Group by Tipper (1978), but he assigned rocks we include in the group along Taseko Lake and north of Mount Tatlow to the sedimentary unit of the Kingsvale Group. McLaren and Rouse (1989) adopted the revised nomenclature of Glover *et al.* (1988a, b) and reassigned the sedimentary rocks along Taseko Lake to the Silverquick formation, which locally rests gradationally beneath the Powell Creek (Kingsvale Group) volcanics to the southeast. None of the rocks we include in the Taylor Creek Group are dated, but we did not note any lithologic distinction that warrants separation into two different units. Furthermore, our mapping along Taseko Lake west of Taseko Mountain reveals that the sedimentary rocks there lie beneath the Powell Creek formation across an angular unconformity; this corroborates their correlation with the Taylor Creek Group to the southeast, which is also unconformably overlain by the Powell Creek formation (Glover and Schiarizza, 1987).

SILVERQUICK FORMATION

The name "Silverquick" was introduced by Glover *et al.* (1988a, b) and Garver (1989) as an informal name for a thick succession of middle to Upper Cretaceous, predominantly nonmarine clastic sedimentary rocks that are well exposed in the Noaxe Creek and Bralorne map areas. There, the Silverquick formation consists of a lower unit of chert-rich conglomerates and associated finer grained clastic rocks, and an upper unit of predominantly volcanic-clast conglomerates; this succession rests unconformably on the Taylor Creek Group and grades upwards into andesitic breccias of the Powell Creek formation. The Silverquick formation is absent in the northwestern part of the Warner Pass map area and the contiguous part of the Mount Tatlow map area east of Taseko Lake, where the Powell Creek formation rests directly on the Taylor Creek Group. A succession of volcanic conglomerates and breccias at the base of the Powell Creek formation in the western part of the Mount Tatlow map area is, however, tentatively included in the formation, as it closely resembles the upper, volcanic-rich portion of the Silverquick formation in its type locality.

The Silverquick formation crops out in a westward-thickening wedge northwest of Mount Tatlow, where its pronounced stratification readily distinguishes it from the more massive and resistant flow breccias of the overlying Powell Creek formation (Plate 1-3-2). It consists mainly of volcanic conglomerates and breccias in beds ranging from tens of centimetres to more than 10 metres thick. Andesitic clasts are poorly sorted, angular to subrounded and generally vary in size from less than a centimetre to 30 centimetres; coarse conglomerates in the lower part of the unit, however, contain clasts more than 1 metre in size. The matrix is commonly sandy and rich in feldspar and

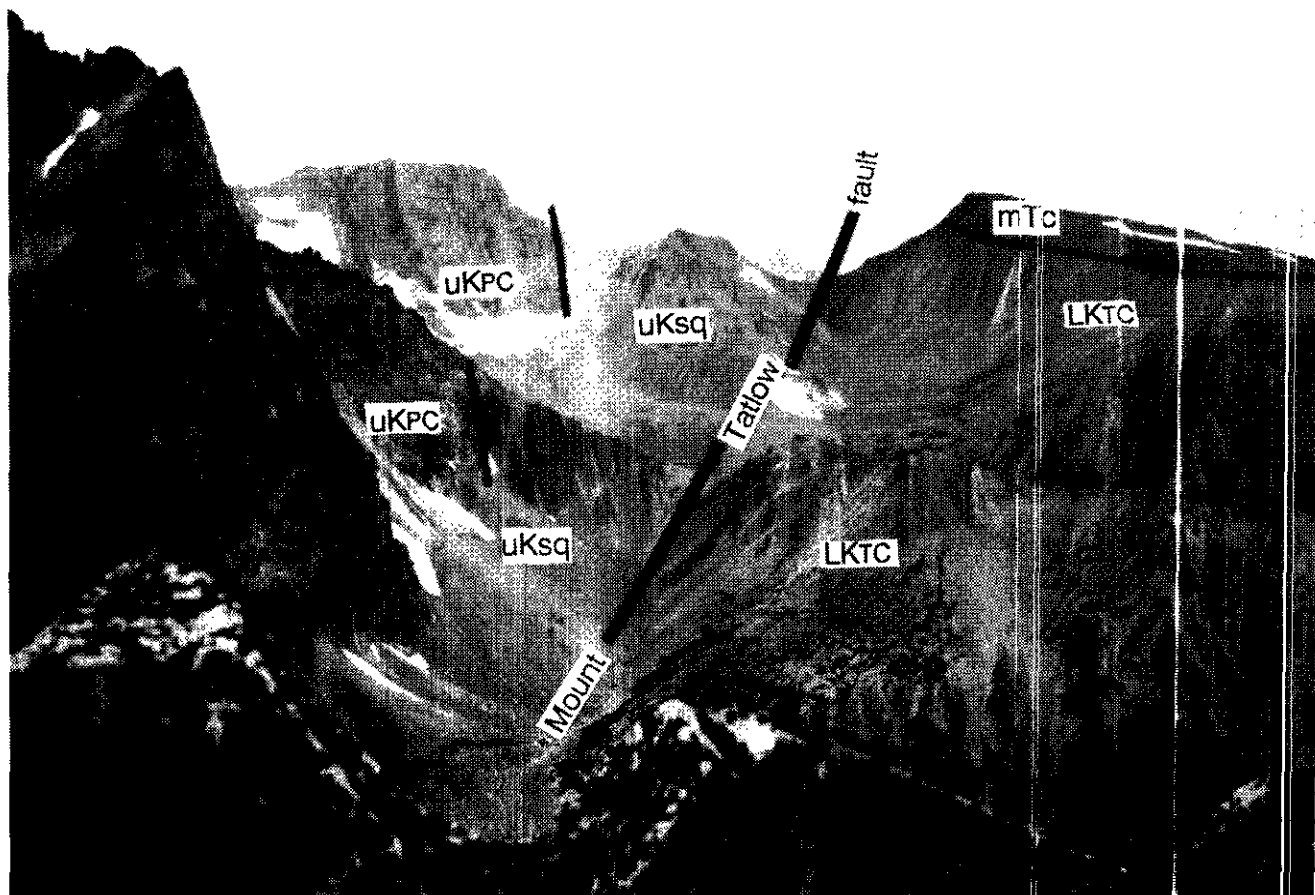


Plate 1-3-2. View to the west from the slope north of Mount Tatlow peak.

hornblende crystals. Stratification is accented by relatively thin interlayers of purplish siltstone. The base of the Silverquick formation is not seen as it is bounded to the north by the east-striking Mount Tatlow fault. The east-tapering outcrop geometry of the unit in part reflects truncation along this fault, but a primary depositional pinch-out is also inferred as this unit does not occur farther east, where massive breccias of the Powell Creek formation rest directly on the Taylor Creek Group.

POWELL CREEK FORMATION

The Powell Creek formation (informal) is a thick succession of Upper Cretaceous volcanic and volcanoclastic rocks. These rocks were assigned to the Kingsvale Group by Jeletzky and Tipper (1968) and Tipper (1978). The name "Powell Creek" was introduced by Glover *et al.* (1988a, b) following the work of Thorkelson (1985), who suggested that the term "Kingsvale Group" be abandoned as it is not a valid stratigraphic entity where originally defined by Rice (1947), and has not been used consistently by subsequent workers.

The Powell Creek formation underlies the steep peaks of Mount Tatlow and the adjacent mountains and ridges, and also outcrops in the hills east of Lower Taseko Lake and on ridges east and south of Anvil Mountain. It comprises more than 2000 metres of andesitic flow breccias, crystal and ash

tuffs, laharic breccias, flows, and volcanoclastic sandstones and conglomerates. Feldspar and hornblende-needle dikes and sills are common within the succession and may be coeval with the volcanics. Fragmental facies are far more abundant than flows. The sequence is notable for its compositional uniformity; fragmental materials in the breccias and tuffs do not represent any sources outside the unit itself.

Fragmental rocks are purple and green or green on fresh surfaces, and are rich in plagioclase crystals and crystal fragments. Many are rich in hornblende and some contain pyroxene. High hematite content is responsible for the purple colours which range from pale lilac and mauve to scarlet and maroon.

Flow breccias are massive, and the most resistant rocks in the sequence; they support the high peaks and form the steep cliffs. Clasts are normally 1 to 8 centimetres across; breccias with larger clasts occur locally. Epidote alteration is pervasive in the flow breccias on fracture planes and as clots.

Laharic breccias are a significant part of the section on the ridges south of Mount Tatlow peak (Plate 1-3-3). The lahars have a muddy matrix and are unsorted, with rounded cobbles and boulders of all sizes up to over a metre across. Muddy and sandy layers, centimetres to tens of metres thick, are intercalated with the coarse beds and delineate the bedding. On a gross scale, the bedded intervals are remarka-



Plate 1-3-3. Laharic breccias with muddy interbeds of Unit uKpc, south of Mount Tatlow peak.

bly planar; individual layers can be traced without disruption for thousands of metres. Muddy layers weather brown and maroon, and are brick-red in some sections.

Ash and crystal tuffs typically form relatively thin sections (<10 m) within sequences dominated by flow breccias or lahars. An exception to this is at the Vick property on the mountain directly west of the narrows at the foot of Lower Taseko Lake. There, the top 300 or 400 metres of section on the mountaintop are dominated by crystal tuffs, with lesser intercalated flow breccia. The tuffs are markedly less resistant than other rock types in the Powell Creek formation and the transition to tuffs from flow breccia is marked by an abrupt break in slope. Tuff matrix is commonly calcareous and in some places the rock is friable. The tuffs have a grainy or sugary appearance on weathered surfaces.

Most flows are andesitic, but dacites also occur, and thin bands of rhyolite are intercalated in the section at the Vick property. The andesite flows are green, and feldspar-hornblende or feldspar-pyroxene phytic. In the coarsest flows crowded feldspar crystals are up to 5 millimetres across.

The Powell Creek formation lies conformably above the Silverquick formation northeast of Mount Tatlow, but rests unconformably above the Taylor Creek Group east of Taseko Lake and in the contiguous part of the Warner Pass map area to the south (Plate 3-4-2 of Glover and Schiarizza,

1987). The age of the Silverquick and Powell Creek formations is constrained only by plant fossils, most of which indicate a general Albian to Cenomanian age (Jeletzky and Tipper, 1968; Schiarizza *et al.*, in preparation). As the unconformably underlying Taylor Creek Group includes middle and upper(?) Albian rocks (Garver, 1989), the Powell Creek formation is thought to be largely Cenomanian.

METHOW BASIN

The Methow basin includes Lower Jurassic to mid-Cretaceous rocks that crop out east of the Fraser fault in the Methow Valley of northern Washington State and contiguous southwestern British Columbia (McGroder *et al.*, 1990). Correlative rocks (mainly Lower Cretaceous Jackass Mountain Group) also crop out west of the Fraser fault, and extend from the Camelsfoot Range northwestward to the Mount Tatlow area. These exposures of the Jackass Mountain Group were included in the Tyaughton basin by Jeletzky and Tipper (1968) and Kleinspehn (1985), who considered the Methow and Tyaughton as parts of the same basin, fragmented by the Yalakom and Fraser fault systems. Thus the Tyaughton and Methow subdivisions have commonly come to reflect the present geographic distribution of rocks inferred to have been deposited in a once-continuous

basin, referred to as the Tyaughton-Methow basin (Kleinspehn, 1985).

We adopt a different approach and define the Tyaughton and Methow basins strictly in terms of their distinctive stratigraphies. Within the Taseko - Bridge River and Mount Tatlow map areas the Tyaughton basin comprises the uppermost Middle Jurassic to Lower Cretaceous Relay Mountain Group together with the Lower Cretaceous Taylor Creek Group. The Methow basin includes Middle Jurassic rocks correlated with the Ladner Group together with overlying Lower Cretaceous rocks of the Jackass Mountain Group (Schiarizza *et al.*, 1990a). The two assemblages are locally in contact across Cretaceous and Tertiary faults. Provenance studies indicate that the two basins received detritus from common source terrains in the mid-Cretaceous (Garver, 1992), but they had little in common prior to that time.

In the Taseko - Bridge River map area, Methow basin strata occur as two distinct facies, referred to as the Yalakom Mountain and Churn Creek facies respectively (Schiarizza *et al.*, in preparation). The lower part of the Yalakom Mountain facies consists of Middle Jurassic volcanic sandstones and rare volcanic breccias that Schiarizza *et al.* (1990a) correlate with the Dewdney Creek Formation of the Ladner Group (O'Brien, 1986, 1987). These Middle Jurassic rocks are disconformably(?) overlain by a lithologically similar succession that has yielded Barremian and Aptian fossils and is assigned to the lower part of the Jackass Mountain Group (this unit includes Unit 7b of Roddick and Hutchison, 1973, and Unit 3v of Glover *et al.* (1988a), but was included in the upper part of the Jurassic volcanic sandstone unit of Schiarizza *et al.*, 1990a). The Barremian-Aptian unit is in turn overlain by a distinct assemblage of arkosic sandstones and granitoid-bearing pebble conglomerates of Albian age [includes units 7c and 7d of Roddick and Hutchison (1973), Unit 3ak of Glover *et al.* (1988a), and the Jackass Mountain Group of Schiarizza *et al.* (1990a)].

The Churn Creek facies includes an interval of poorly exposed Middle Jurassic sandstones and siltstones that are overlain by two mappable units of the Jackass Mountain Group. The lower part of the group comprises volcanic sandstones rich in plant debris (Unit 3f of Glover *et al.*, 1988a) that have yielded plant fossils of probable Aptian age (Jeletzky and Tipper, 1968). The upper unit of the Jackass Mountain Group consists mainly of granitoid-bearing cobble and boulder conglomerates (Unit 3cg of Glover *et al.*, 1988a). This unit is not dated, but is correlated with the Albian arkose unit of the Yalakom Mountain facies.

Both the Churn Creek and Yalakom Mountain facies of the Methow basin are represented in the Mount Tatlow map area. The Churn Creek facies is exposed northeast of the Yalakom fault, where it was mapped as the Kingsvale Group sedimentary unit by Tipper (1978). The Yalakom Mountain facies outcrops southwest of the Yalakom fault on the slopes north of Konni Lake. Our mapping supports the interpretation of Kleinspehn (1985) that these exposures were displaced from the Camelsfoot Range by more than 100 kilometres of dextral movement along the Yalakom fault (*see section on Structural Geology*).

YALAKOM MOUNTAIN FACIES

The Yalakom Mountain facies is well exposed on the south-facing slopes of Konni Mountain and Mount Nemaiah, north of Konni Lake. The section dips steeply to the north and is right side up. It comprises two mappable units that correlate with the two units of the Yalakom Mountain facies mapped in the southwestern Camelsfoot Range (Schiarizza *et al.*, 1990a).

The lower unit (JKy) outcrops on the slopes directly north of Konni and Nemaiah lakes. It consists mainly of green to grey gritty sandstones and granule to small-pebble conglomerates which occur as medium to thick beds intercalated with lesser volumes of finer grained sandstone, siltstone and shale. The sandstones and conglomerates are well indurated, and contain feldspar, volcanic lithic fragments, some quartz and abundant shale rip-up clasts. The unit also includes a thin band (<10 m) of blue-green ardesitic lapilli tuff and breccia. Tipper (1969) reports a probable lower Bajocian ammonite from near the northeast end of Konni Lake, so Unit JKy is at least in part Middle Jurassic. The correlative unit in the Camelsfoot Range contains Aalenian and Bajocian ammonites (Schiarizza *et al.*, 1990a; Mahoney, 1992) but passes stratigraphically upward into lithologically similar rocks that have yielded Early Cretaceous (Barremian and Aptian) fossils (in part Unit 7b of Roddick and Hutchison, 1973).

The upper unit of the Yalakom Mountain facies (Unit KJMy) consists mainly of olive-green to blue-green feldspathic-lithic sandstones and gritty sandstones. The sandstones form massive resistant layers, tens of metres to more than 100 metres thick, that are intercalated with substantial intervals of grey siltstone and shale. Massive sandstone at the base of the unit forms the lowest set of prominent cliffs on the south flank of Konni Mountain. The contact was actually observed at only one locality, where it is marked by several metres of granitoid-bearing pebble to cobble conglomerate. A similar thin conglomerate interval marks the base of the correlative interval in the Camelsfoot Range (Jackass Mountain Group of Schiarizza *et al.*, 1990a). There, the unit locally contains fossils of Albian age (includes Units 7c and 7d of Roddick and Hutchison, 1973).

Tipper (1978) included the Jurassic rocks north and south of Konni Lake in the same unit, which he mapped as the Jurassic section of the Tyaughton Group (Last Creek formation in present terminology). However, the Jurassic rocks north of the lake, here assigned to the Methow basin, are lithologically distinct from the Middle Jurassic portion of the Last Creek formation, which consists of black calcareous shale or cherty argillite with only minor amounts of coarser grained clastic rocks (Umhoefer, 1990; Last Creek formation of this report). The Jurassic rocks of Unit JKy are lithologically more similar to the Middle Jurassic volcanic sandstones, conglomerates, tuffs and flows that comprise the Dewdney Creek Formation of the Ladner Group (O'Brien, 1986, 1987), with which they are here correlated.

CHURN CREEK FACIES

Rocks of the Churn Creek facies are restricted to the northeast side of the Yalakom fault. They crop out on the

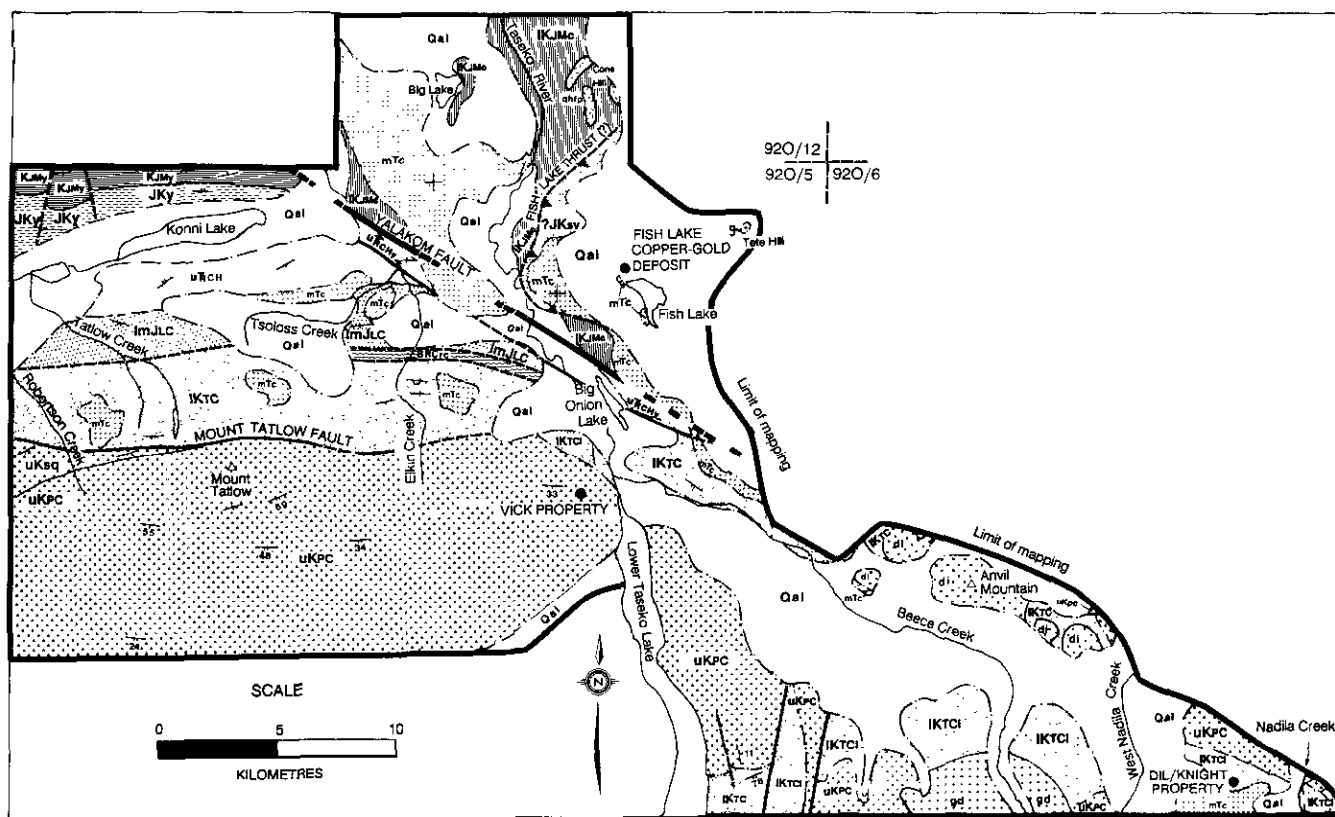


Figure 1-3-2. Generalized geology of the Mount Tatlow map area.

steep slopes on both sides of the Taseko River, in the Elkin Creek canyon, and in creek gullies east of the Taseko River below the level of the Chilcotin Group basalts (about 1600 m). Both the plant-rich volcanic sandstone unit and the overlying granitoid-bearing conglomerate unit of the Jackass Mountain Group are represented in these exposures. However the stratigraphic contact between them is difficult to follow due to poor exposure and numerous small faults. Consequently both units are included within one designation (IKJMc) on the geological map (Figure 1-3-2).

The lower unit is dominated by green, coarse-grained feldspathic sandstone with abundant carbonized logs, branches and twigs. Weathered surfaces are green, grey or brown. Sandstone grains include plagioclase crystals and felsic, intermediate and mafic volcanic lithic fragments. Quartz is present in most of the sandstones and in some locations is abundant. Black, angular rip-up clasts occur locally. The sandstones are thick to medium bedded, but are commonly massive with bedding that is conspicuous only from a distance; locally they are crossbedded. Granule to cobble conglomerates with a sandy matrix are also common within the unit. Clast/matrix ratios range from about 80/20 to 50/50. Conglomerate clasts include andesitic feldspar-crystal lithic tuff, quartzite, quartz-feldspar sandstone, silicified volcanic rock, hornblende and feldspar-phyric andesite, and rare, medium grey chert. Black shale beds also occur in the section, but they outcrop poorly.

Marine fossils were found in the lower unit of the Churn Creek facies east of Big Lake and in the Elkin Creek

canyon. The fossil assemblage includes shell fragments, gastropods, ribbed and smooth-shelled bivalves, and, at the Elkin Creek location, a large ammonite.

The upper conglomerate unit of the Churn Creek facies is well exposed in the bluffs along the east side of the Taseko River in the northernmost section of the map area. The conglomerates are poorly sorted with a sandy matrix. Well-rounded clasts of medium-grained granodiorite and dark to medium green feldspar-phyric volcanic rocks up to 60 centimetres across are most abundant. Feldspar-crystal tuff, dark grey massive basalt and green chert clasts were also observed. Granodiorite boulders are generally larger than other types. No plant or animal fossils were found in this unit.

VOLCANIC AND SEDIMENTARY ROCKS NEAR FISH LAKE CREEK

An enigmatic assemblage of volcanic and sedimentary rocks crops out south and east of the Churn Creek facies near the mouth of the creek that drains Fish Lake. It is designated Unit JKsv on Figure 1-3-2. This assemblage includes andesite with minor rhyolite layers, tuffaceous sandstone, pebbly sandstone with carbonaceous plant remains and limestone rip-ups, black argillite with shell fragments, and well-bedded flinty siltstone.

We speculate that these rocks are related to the volcanic and sedimentary package (observed only in drill core) that hosts the Fish Lake porphyry copper-gold deposit. The Fish

LEGEND

QUATERNARY

Qal unconsolidated glacial, fluvial and alluvial deposits

MIOCENE TO PLEISTOCENE

CHILCOTIN GROUP
mTc olivine basalt flows, debris flows

UPPER CRETACEOUS

POWELL CREEK FORMATION
uKpc purple and green andesitic flow breccia, crystal and ash tuffs, lahatic breccias, flows, and volcanic sandstone

SILVERQUICK FORMATION
uKsq well stratified volcanic conglomerate and breccia

TYAUGHTON BASIN

LOWER CRETACEOUS

TAYLOR CREEK GROUP
IKTC chert pebble rich conglomerate, black shale, siltstone, sandstone

IKTCi Taylor Creek Group sedimentary rocks intruded by numerous hornblende feldspar porphyry dikes and stocks

BRIDGE RIVER COMPLEX

MISSISSIPPIAN TO LATE MIDDLE JURASSIC
BRCr sheared ribbon chert, chert-rich sandstone, amygdaloidal greenstone, sheared muddy breccia containing boulders of greenstone, chert, and marble

CADWALLADER TERRANE

LOWER TO MIDDLE JURASSIC
LAST CREEK FORMATION
lmJLC well-bedded grey to black cherty argillite, thin fossiliferous micritic limestone beds, minor polymict cobble conglomerate with amy matrix

UPPER TRIASSIC

HURLEY FORMATION
uTrCh thinly bedded calcareous brown-weathering sandstone, black-and-tan siltstone and shale, sandstone with limestone interbeds, limestone-bearing polymict conglomerate

YALAKOM FAULT ZONE
uTrChy intensely deformed fragments of Hurley Formation strata, serpentinite lenses

METHOW BASIN

YALAKOM MOUNTAIN FACIES

ALBIAN (?)
IKJMy feldspathic lithic sandstone and gritty sandstone, grey siltstone, shale, granitoid-bearing pebble to cobble conglomerate

MIDDLE JURASSIC AND (?)/OJUNGER

JKy gritty feldspathic sandstone, granule and pebble conglomerate, siltstone, shale, minor lake-green andesite, breccia and tuff

CHURN CREEK FACIES

LOWER CRETACEOUS (?)
IKJMc green feldspathic sandstone with abundant carbonized plant remains, overlain by polystratified boulder and cobble conglomerate with volcanic and plutonic clasts

ROCKS NEAR FISH LAKE CREEK

JURASSIC OR CRETACEOUS?
JKsv andesite, tuffaceous sandstone, minor rhyolite, phyllite, pebbly sandstone with plant remains and limestone rip-up clasts, black argillite, well-bedded fine sandstone

INTRUSIVE ROCKS

MIDDLE EOCENE

BEECE CREEK PLUTON
gd light coloured medium-grained, gneissic to quartz monzonite

CRETACEOUS TO TERTIARY

di hornblende diorite, leucodiorite, and hornblende feldspar porphyry

qhfp Cone Hill/Fish Lake suite, zone hence feldspar porphyry with quartz

g Taseko granite

Lake host package forms the hangingwall of a gently southeast-dipping fault (the Fish Lake thrust of Cairn and Piroshko, 1992) that is intersected at about 750 metres depth in drill holes on the Fish Lake property. As sedimentary rocks that may correlate with the Churn Creek facies occupy the footwall, this same fault may constitute the boundary between Unit JKsv and exposures of Churn Creek facies to the west.

CHILCOTIN GROUP

Flat-lying basalt flows of the Chilcotin Group (Tipper, 1978; Bevier, 1983) crop out extensively in the map area. They unconformably overlie all older rock units and structures, including the Yalakom fault. They are part of the southwestern margin of an extensive belt of Early Miocene to early Pleistocene plateau lavas that covers 25 000 square kilometres of the Interior Plateau of south-central British Columbia (Mathews, 1989). The Chilcotin Group forms a blanket 50 to 200 metres thick that is preserved over much of northeastern part of Mount Tatlow map area, except in creek and river valleys that have cut down into the underlying rocks. Where the topographic relief is higher, Chilcotin Group flows form isolated erosional remnants that cap older rocks (Figure 1-3-2 and Plate 1-3-2).

The most common rock type is orange-brown weathered, black to dark grey basalt, locally with olivine and plagioclase phenocrysts. Flow thicknesses range from about 10 centimetres to 10 or 15 metres. Columnar jointing at the bases of flows is common and well developed, and flow tops are normally vesicular. In almost all locations, layering

is near horizontal, the rocks are undeformed and the minerals are unaltered.

Spectacular debris flows are exposed beneath columnar-jointed flows in the cliffs east of the Taseko River, south of the Fish Lake turnoff. They are unsorted and unstratified and contain clasts up to 50 centimetres across. Clasts include Chilcotin-type rocks (amygdaloidal basalt, black glassy shards and dense black basalt with glassy rims) and foreign rocks (feldspar-porphyrific andesite, feldspathic sandstone and limestone). Beds of spherulitic ash tuff, lapilli tuff, and pahoehoe and aa lavas are also exposed in the cliffs.

INTRUSIVE ROCKS

DIORITE AND HORNBLLENDE FELDSPAR PORPHYRY

Hornblende diorite, leucodiorite, and hornblende feldspar porphyry occur as stocks, plugs and dikes that intrude the Taylor Creek Group (Plate 1-3-4). They are most common along the Anvil Mountain ridge system and along the southern boundary of the map area east of Taseko Lake. However, they are represented in all areas where Taylor Creek Group rocks are exposed, including the north slopes of Mount Tatlow, near the headwaters of Elgin Creek, and along the Beece Creek road east of the foot of Lower Taseko Lake. These bodies were assigned tentative Eocene ages by Tipper (1978), but none are dated. Their abundance in the Taylor Creek Group and apparent absence in the Powell Creek formation suggests that at least some of the intrusive activity was mid-Cretaceous in age and preceded deposition of the Powell Creek formation.



Plate 1-3-4. Light-coloured feldspar-porphyry dikes cut sedimentary rocks of the Taylor Creek Group, southern boundary of the map area, east of Taseko Lake.

QUARTZ FELDSPAR PORPHYRY

Light grey felsic sills and dikes occur within all Mesozoic rock units but do not constitute mappable bodies. These rocks contain equant euhedral white plagioclase up to 1 centimetre across, slightly smaller pinkish quartz grains, and 1 to 3-millimetre mafic grains in a pale grey groundmass. Felsic sills are particularly prominent within the Powell Creek formation on the ridges south of Mount Tatlow peak, where they are up to 120 metres thick and can be traced through adjacent ridges for several kilometres.

BEECE CREEK PLUTON

The Beece Creek pluton consists of light-coloured medium-grained quartz monzonite to granodiorite of Middle Eocene age (44 Ma, Archibald *et al.*, 1989). It crops out on the ridges east and west of Beece Creek near its headwaters, and extends south into the Warner Pass map area (Glover and Schiarizza, 1987). The pluton intrudes rocks of the Taylor Creek Group and the Powell Creek formation; abundant quartz porphyry and rhyolite dikes intrude country rocks adjacent to the pluton.

FISH LAKE - CONE HILL INTRUSIVE SUITE

A number of small stocks and dikes intrude both the Jackass Mountain Group and Unit JKsv in the vicinity of Cone Hill and Fish Lake Creek. Most are hornblende feldspar porphyries with varying amounts of quartz phenocrysts in a grey aphanitic felsic groundmass. There are differences in composition and texture between the bodies, but none are dated so it is not possible to say whether they are related to

the same intrusive system. They resemble Fish Lake intrusive rocks in that they are feldspar porphyritic, often coarsely (>5 mm), and they generally contain quartz.

TÊTE HILL GRANITE

Tête Hill forms a solitary knob of hypabyssal granite that pokes up above the level of the Quaternary glacial deposits about 5 kilometres northeast of the Fish Lake deposit. The granite is fine grained; quartz, orthoclase and plagioclase crystals are less than 2 millimetres long. Some of the outcrops contain abundant miarolitic cavities. The miarolitic rocks are slightly coarser and contain plagioclase laths over 1 centimetre long that overprint the original rock texture. The age of the granite and its relationship with the Fish Lake intrusions are unknown.

STRUCTURE

STRUCTURE EAST OF TASEKO LAKE

The southeastern part of the Mount Tatlow map area is underlain mainly by the Taylor Creek Group and overlying Powell Creek formation. The contact is an angular unconformity that was observed 2 kilometres east of Taseko Lake, and is well exposed at several localities in the Warner Pass map area to the south (Glover and Schiarizza, 1987). The mid-Cretaceous deformation documented by this unconformity included southwest-vergent folding and thrusting that is well displayed in the Taseko - Bridge River area (Schiarizza *et al.*, 1990b).

The Taylor Creek Group in the Anvil Mountain - Nadila Creek area is overlain by the Powell Creek formation to the northeast and southwest, suggesting that it cores a broad northwest-trending anticline or arch. The abundant dioritic intrusions within the Taylor Creek Group in this area may be in part responsible for uplift along the axis of this structure; alternatively, the intrusions may predate the Powell Creek formation and the anticlinal fold. Other mappable structures in this area include a series of northerly striking faults along the southern boundary of the area east of Taseko Lake. These faults have apparent west-side-down displacement of the Powell Creek formation, but their actual sense of movement is unknown.

STRUCTURE OF THE KONNI LAKE - MOUNT TATLOW AREA

The structure southwest of the Yalakom fault and west of Lower Taseko Lake and Taseko River is dominated by four east-striking panels separated by east-striking faults. The northernmost panel comprises the Methow basin. It is separated from Cadwallader Terrane (Hurley and Last Creek formations) to the south by an inferred fault (the Konni Lake fault) in the valley of Konni and Nemaia lakes. The Cadwallader Terrane belt is also inferred to be bounded by a fault to the south, as it is at least locally separated from the Taylor Creek Group by a narrow lens of Bridge River rocks. The Taylor Creek Group is, in turn, faulted against the Powell Creek and Silverquick formations to the south; the trace of this fault is well defined in the vicinity of Mount Tatlow, where it is parallel to bedding in the Taylor Creek Group, but truncates the Silverquick/Powell Creek contact (Plate 1-3-2).

Methow basin rocks north of Konni Lake comprise a simple north-dipping homocline that, farther to the northwest, is folded through an east-northeast-trending, doubly plunging syncline (Tipper, 1969). The internal structure of the Powell Creek formation is also relatively simple, and comprises a broad east-trending syncline. The intervening Taylor Creek Group, Bridge River Complex and Cadwallader Terrane, however, are strongly deformed by east-plunging folds that are observed on the mesoscopic scale, and indicated on a larger scale by domains of opposing facing directions. Folds with both north and south vergence were mapped, but the macroscopic geometry of the belts is not well constrained. It is suspected, but not proven, that much of the internal deformation within these belts occurred during the mid-Cretaceous contractional deformation documented beneath the sub-Powell Creek unconformity to the southeast.

None of the inferred major east-striking faults between Konni Lake and Mount Tatlow was actually observed. The Mount Tatlow fault is Late Cretaceous or younger, while the two faults to the north are mid-Cretaceous or younger. A northerly dipping mesoscopic fault observed within the Taylor Creek Group along Elkin Creek has oblique reverse-sinistral movement, and a prominent north-dipping fault within the northernmost Silverquick exposure on the ridge west of Robertson Creek displays northeast-plunging slickensides compatible with a similar sense of movement. These observations are of interest because reverse-sinistral

faults have been documented in several areas in the Taseko - Bridge River area, including the Camelsfoot Range where they bound and imbricate structural panels that are inferred to be the offset equivalents of those at Konni Lake (see section on the Yalakom fault). The reverse-sinistral faults in the Taseko - Bridge River area are mainly Late Cretaceous in age, and are interpreted as later product of the same protracted deformational event that produced mid-Cretaceous thrust faults and folds. The major east-striking faults between Konni Lake and Mount Tatlow may also be products of this Late Cretaceous deformation, but this is not proven. Alternatively, or in addition, some of the east-trending structures in this area, such as the east trending synclines in the Methow basin and the Powell Creek formation, may have formed during Eocene or older dextral movement along the Yalakom fault.

STRUCTURE NORTHEAST OF THE YALAKOM FAULT

The structure of the Mesozoic rocks northeast of the Yalakom fault is poorly understood because much of the area is covered by flood basalts and thick glacial deposits. However, both north and northeasterly striking faults have been recognized. Major structures outlined by diamond drilling at the Fish Lake deposit include the Caramba fault, an east-striking subvertical fault that transects the southern part of the deposit, and a gently east-southeast-dipping fault that marks the base of the deposit. The latter fault places mineralized volcanic and intrusive rocks above unmineralized sedimentary rocks; it has been named the Fish Lake thrust by geologists working on the deposit, although the movement sense along it has not been established. The 10° to 25° dip of the fault suggests that it will intersect the surface 2 to 4.5 kilometres west of the deposit; thus it may constitute the boundary between exposures of Churn Creek facies along the Taseko River and Unit JKsv to the east, but this is speculative as this contact is not exposed.

THE YALAKOM FAULT

Leech (1953) first used the name Yalakom fault for a system of steeply dipping faults bounding the northeast margin of the Shulaps Ultramafic Complex along the Yalakom River. The fault system was traced northwestward through the Taseko Lakes and Mount Waddington map areas by Tipper (1969, 1978) who postulated that it was the locus of 80 to 190 kilometres of right-lateral displacement. It was traced southeastward through the northeastern corner of Pemberton map area by Roddick and Hitchison (1973), from where it extends into the western part of the Ascroft map area (Duffell and McTaggart, 1957; Monger and McMillan, 1989). There, it is truncated by the more northerly trending Fraser fault system, along which it is separated by about 90 kilometres from its probable offset equivalent, the Hozameen fault, to the south (Monger, 1985).

Within the Mount Tatlow area the Yalakom fault is well defined, although not well exposed, along lower Elkin Creek and on the slopes north of Big Onion Lake; elsewhere its trace is hidden beneath Miocene or Quaternary cover. The fault juxtaposes the Churn Creek facies of the Jackass

Mountain Group to the northeast against a number of different map units to the southwest. Where defined, the fault zone comprises up to several hundred metres of fractured and sheared sedimentary rock, most of which resembles Hurley Formation, structurally interleaved with lenses of serpentinite. No reliable shear-sense indicators were observed within the fault zone.

On its southwest side, the Yalakom fault truncates a succession of east-striking fault panels that include, from north to south: the Yalakom Mountain facies of the Methow basin; Cadwallader Terrane; and the Bridge River Complex. The same three-part structural succession is truncated on the northeast side of the Yalakom fault in the Camelsfoot Range, more than 100 kilometres to the southeast, and provides an estimate of dextral offset along the fault. This correlation strengthens the argument of Kleinspehn (1985) who postulated about 150 kilometres of displacement by matching only a part of this structural succession, the Jackass Mountain Group of Methow basin.

Geological relationships in the southwestern Camelsfoot Range are summarized in Figure 1-3-3. In this area the Yalakom fault, which to the northwest is well defined as a single strand separating the Shulaps Ultramafic Complex from the Methow basin, bifurcates to enclose a lens of thrust-imbricated Cadwallader Terrane structurally overlying the Bridge River Complex. The lens is juxtaposed against the Shulaps Complex to the southwest by a fault along the Yalakom and Bridge rivers that was referred to as the Bridge River fault by Schiarizza *et al.* (1990a), and is

interpreted to be the principal strand of the Yalakom fault by Schiarizza *et al.* (in preparation). Along the northeast boundary of the lens, Cadwallader Terrane is juxtaposed against the Yalakom Mountain facies of the Methow basin across a fault that was labelled Yalakom fault by Schiarizza *et al.* (1990a), but which Schiarizza *et al.* (in preparation) call the Camelsfoot fault, and interpret as an older structure that is truncated by the Yalakom fault. The Camelsfoot fault is not well exposed, but appears to dip northeast; it, together with northeast-dipping thrust and oblique (sinistral) thrust faults within structurally underlying Cadwallader Terrane and Bridge River Complex are thought to have formed during mid-Cretaceous contractional deformation that is well defined elsewhere in the area (Schiarizza *et al.*, 1990b). This interpretation is consistent with that of Miller (1988), who examined the structures in a relatively small area north of the confluence of the Bridge and Fraser rivers and concluded that they fit a strain ellipse for left-lateral slip along the Yalakom fault. His study area, however, is along the probable southeastern extension of the Camelsfoot fault whereas the Yalakom fault, interpreted to be the locus of younger dextral-slip displacement, is farther to the southwest. The interpretation shown in Figure 1-3-3 differs from that of Coleman (1990; Coleman and Parrish, 1991), who interpret the northeast-dipping Camelsfoot fault and underlying splays as the Yalakom fault.

Correlation of the Camelsfoot Range structural succession with that exposed around Konni Lake is based on: the gross three-fold succession comprising Methow basin/

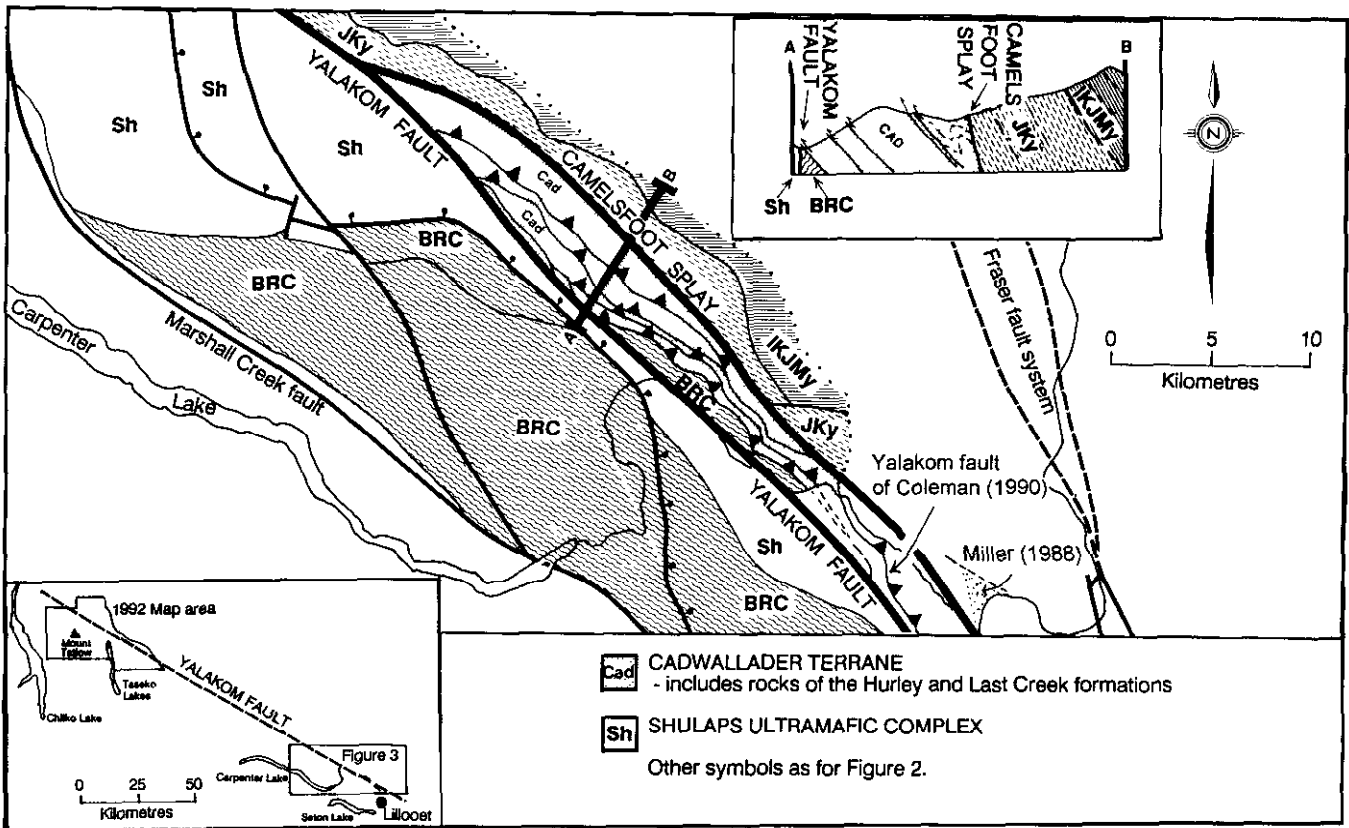


Figure 1-3-3. Geological relationships in the southwest Camelsfoot Range.

Cadwallader Terrane/Bridge River Complex; the internal stratigraphy of the Jura-Cretaceous Methow basin succession, which is virtually identical in the two areas; and the internal stratigraphy of the Cadwallader Terrane, which in each area comprises Hurley Formation directly overlain by cherty argillites of Last Creek formation (elsewhere in the region the Last Creek formation was deposited on the intervening Tyaughton Group). The dextral offset on the Yalakom fault derived from matching the cutoffs of the Konni Lake and Camelsfoot faults is 115 kilometres. This is considered approximate as the offset structures are not vertical and the synclinal disposition of the Jackass Mountain Group north of Konni Lake (Tipper, 1969) suggests that the Konni Lake fault may be folded and truncated again farther to the northwest. This estimate is similar to the lower limit of the 125 to 175 kilometre offset postulated by Kleinspehn (1985) whose criterion, similar facies of the Jackass Mountain Group, is one component of the structural succession used here. Other comparable estimates of dextral offset along the Yalakom-Hozameen fault system include the 120 kilometres between the Shulaps Ultramafic Complex and the Coquihalla serpentine belt (Schiarrizza *et al.*, in preparation), and 80 to 120 kilometres separation between belts of Middle Jurassic volcanics and associated plutons northwest of the Mount Tatlow area (Tipper, 1969; Schiarrizza *et al.*, in preparation).

The timing of movement along the Yalakom fault is not closely constrained in the Mount Tatlow area; it is post Lower Cretaceous and pre-Miocene. Movement is thought to have occurred mainly in the Eocene, based on the timing of deformation established in metamorphic complexes associated with the fault to both the northwest (Friedman and Armstrong, 1988) and southeast (Coleman and Parrish, 1991).

MINERAL OCCURRENCES

FISH LAKE (MINFILE 920 041)

Taseko Mines Limited drilled 7506 metres in ten holes on the Fish Lake porphyry copper-gold property in 1991, and in 1992 completed approximately 60 000 metres of NQ and BQ drilling in 121 holes. As a result of this work, on October 8, 1992, Taseko Mines announced a preliminary reserve estimate of 1.191 billion tons (1.08 billion tonnes) of ore with an average grade of 0.23 per cent copper and 0.41 gram per tonne gold.

The Fish Lake deposit is spatially and genetically related to an irregular, steeply dipping lenticular body of porphyritic quartz diorite which is surrounded by an east-west elongate complex of steep, southerly dipping, subparallel quartz feldspar porphyry dikes. This intrusive complex cuts andesitic flows and tuffs, together with a possibly coeval body of subvolcanic diorite porphyry. The potential orebody is essentially coextensive with a central zone of potassium silicate alteration, within which mafic minerals have been altered to biotite (which shows variable late alteration to chlorite). Secondary orthoclase is widely developed within the central porphyritic quartz diorite, mainly along quartz veinlets and microfractures.

An irregular annular zone of texture-destructive phyllic alteration occurs along the northern and eastern bodies of the deposit; variably developed propylitic alteration is widespread outside this phyllic zone. Numerous structurally controlled zones of late, pale sericite-ankerite alteration are also present, but are less abundant.

The Fish Lake deposit is oval in plan and is 1.5 kilometres long, up to 800 metres wide, and locally extends to a depth of 880 metres; its long axis parallels the east-west trend of the mineralizing intrusive complex. The deposit contains widespread bornite, almost everywhere subordinate to chalcopyrite, and is surrounded on its northern and eastern sides by a fairly well defined pyrite halo, which is essentially coextensive with the phyllic alteration zone. At least two-thirds of the deposit is in altered volcanic rocks, and in detail, high-grade intervals often envelope quartz feldspar porphyry dikes. A major low-angle fault forms the lower contact at depths between 750 and 850 metres.

VICK (MINFILE 920 027)

The Vick prospect is a polymetallic vein showing hosted by andesitic flow breccias and feldspar crystal tuffs of the Powell Creek formation. It is located on a steep mountain directly west of the narrows at the north end of Lower Taseko Lake. Two exploration adits were driven into the east side of the mountain at about 1700 metres (5500 feet) elevation in 1935 (Lalonde, 1987). Exploration in the area surrounding the 2407-metre (7898-foot) peak began in the early 1970s. A four-wheel-drive access road to the peak was built around the south side of the mountain in the early 1980s.

The showings are gold, silver and copper-bearing quartz-sulphide veins within a northeast-striking shear zone that can be traced across the top of the peak and down the steep cliffs to the lower adits on the east face. Diorite dikes roughly parallel the fault zone. The quartz veins contain iron carbonates, pyrite and chalcopyrite concentrations parallel to the walls of the veins. Malachite and azurite are common. Specularite pseudomorphs pyrite in the upper parts of the vein shear system. Significant precious metal assays (up to 72 grams per tonne gold, up to 86 grams per tonne silver; McLaren, 1990) are generally associated with the sulphide-rich sections of the veins (Deimage, 1936; Lalonde, 1987).

DIL/KNIGHT (MINFILE 920 002)

The Dil and Knight claims are located on the ridges between Nadila and West Nadila creeks on the southern border of map sheet 920/6. The area is underlain by shales and pebble conglomerates of the Taylor Creek Group, intruded by irregularly shaped bodies and dikes of hornblende feldspar porphyry.

Discovery of northeasterly trending boundary trains of banded, vuggy vein quartz sparked exploration for an epithermal precious metal target in the area in the early 1980s (McClintock, 1989). The vein quartz boulders are up to 50 centimetres across. Sulphides comprise less than 1 per cent of the veins, and include fine-grained pyrite and lesser arsenopyrite, stibnite and chalcopyrite. Samples contain

metal concentrations as high as 19.3 grams per tonne gold and 35.4 grams per tonne silver, and rock and silt geochemical studies identified coincident anomalies of gold, arsenic and molybdenum in the area (McClintock, 1989). McClintock studied thin sections of altered rock mixed with the quartz float and a sample of feldspar porphyry, and recognized two distinct types of alteration: phyllic alteration with associated pyritization, and intense argillic alteration with associated silicification and carbonate alteration.

To date, no mineralized quartz veins have been found in place.

A 1990 mapping and sampling program by Inco Limited (Bohme, 1990) identified the Knob showing, a hydrothermally altered pebble conglomerate. The conglomerate is hornfelsed and silicified, carbonatized and pyritized; assayed samples yielded up to 54.43 grams per tonne gold and 8.3 grams per tonne silver, together with anomalous levels of copper, arsenic and bismuth (Bohme, 1990). Associated argillaceous sedimentary rocks are intensely fractured and carbonatized, but do not carry any anomalous metal concentrations.

SUMMARY

The Mount Tatlow map area is underlain by Mesozoic sedimentary and volcanic rocks of the Cadwallader Terrane, the Bridge River Complex, the Methow basin, the Tyaughton basin, the Silverquick formation and the Powell Creek formation. These rocks are intruded by several suites of Cretaceous(?) and Tertiary dioritic to granitic plutons, and are overlain by flat-lying Neogene plateau basalts of the Chilcotin Group. The northwest-striking, dextral-slip Yalakom fault is the most prominent structural feature of the map area.

Rocks of the Upper Triassic Hurley Formation (Cadwallader Terrane) and the Mississippian to Jurassic Bridge River Complex had not been recognized within the map area prior to our study. Their recognition in fault-bounded panels south of Methow basin strata on the southwest side of the Yalakom fault provides a compelling match with the same structural succession mapped northeast of the fault in the Camelsfoot Range (Schiarizza *et al.*, 1990a); this correlation indicates that there has been about 115 kilometres of dextral offset along the Yalakom fault. It confirms the earlier work of Kleinspehn (1985) who matched just one component of the structural succession, the Jackass Mountain Group of the Methow basin.

The Fish Lake porphyry copper-gold deposit occurs in a poorly exposed area on the northeast side of the Yalakom fault. The deposit is hosted by a multiphase dioritic to quartz dioritic intrusive complex and andesitic volcanic and volcanoclastic rocks that are separated from underlying sedimentary rocks (Jackass Mountain Group?) by a gently east-dipping fault. Intrusive rocks similar to those of the Fish Lake deposit outcrop for a short distance to the west and north, but are restricted to the northeast side of the Yalakom fault. The volcanoclastic rocks may be related to a poorly understood succession (Unit JKsv) that crops out locally to the west and north of Fish Lake, but these rocks have no obvious correlatives elsewhere in the map area. If the east-

erly dipping fault that bounds the Fish Lake deposit is a thrust, then correlatives might be found to the northeast, where volcanic successions of both Early and Late Cretaceous age are known (Hickson, 1992).

ACKNOWLEDGMENTS

Much of the Mount Tatlow map area is the home of the native people of the Nemaiah Valley. We acknowledge the efforts of Chief Roger William in helping us to establish open communication and a spirit of mutual understanding during our presence in the area.

We would like to thank field assistant Dean Mason for his consistent enthusiasm and hard work. Our work benefited from discussions with C.J. Hickson (GSC, Vancouver) and her crew. We are grateful to Sherwood Henry and Beverly Manuel of Taseko Lakes Outfitters, and Udetta and Roland Class of Big Lake for their hospitality. J.R., P.S. and R.G.G. thank Nadia Caira and Alastair Findlay for taking time from their hectic schedule to share ideas about their project, and for writing the section on the Fish Lake deposit for this report. Bob Holt and Bob Thurston of Cariboo-Chilcotin Helicopters, and Rob Owens of Alpen Air, provided safe and punctual transportation.

REFERENCES

- Archibald, D.A., Garver, J.I. and Schiarizza, P. (1991): Ar-Ar Dating of Blueschist from the Bridge River Complex, SW British Columbia, and its Tectonic Implications: *Geological Society of America*, 1991 Annual Meeting, San Diego, California, Abstracts with Programs, Volume 23, No. 5, page A136.
- Archibald, D.A., Glover, J.K. and Schiarizza, P. (1989): Preliminary Report on $^{40}\text{Ar}/^{39}\text{Ar}$ Geochronology of the Warner Pass, Noaxe Creek and Bridge River Map Areas (92O/3, 2; 92J/16); in *Geological Fieldwork 1988, B.C. Ministry of Energy, Mines and Petroleum Resources*, Paper 1989-1, pages 145-151.
- Bevier, M.L. (1983): Regional Stratigraphy and Age of Chilcotin Group Basalts, South-central British Columbia; *Canadian Journal of Earth Sciences*, Volume 20, pages 515-524.
- Bohme, D.M. (1990): Geological and Geochemical Report on the Knight Claims; *B.C. Ministry of Energy, Mines and Petroleum Resources*, Assessment Report 20428.
- Caira, N. and Piroshko, D. (1992): Fish Lake Project Progress Report; *Taseko Mines Limited*, Volume 1; 50 pages.
- Coleman, M.E. (1990): Eocene Dextral Strike-slip and Extensional Faulting in the Bridge River Terrane, Southwest British Columbia; unpublished M.Sc. thesis, *Ottawa-Carleton Geoscience Centre and Carleton University*, 87 pages.
- Coleman, M.E. and Parrish, R.R. (1991): Eocene Dextral Strike-slip and Extensional Faulting in the Bridge River Terrane, Southwest British Columbia; *Tectonics*, Volume 10, pages 1222-1238.
- Cordey, F. (1991): Dating Otherwise Undatable Rocks II: Radiolarians - The 'Quartz Watches' of the Canadian Cordillera; *Geos*, Volume 20, pages 35-40.
- Dolmage, V. (1936): Vick, Taseko River Area, North of Taseko Lake; in Report of the Minister of Mines 1935, *B.C. Ministry of Energy, Mines and Petroleum Resources*, pages F26-F29.
- Duffell, S. and McTaggart, K.C. (1952): Ashcroft Map Area, British Columbia; *Geological Survey of Canada*, Memoir 262, 122 pages.

- Friedman, R.M. and Armstrong, R.L. (1988): Tatla Lake Metamorphic Complex: An Eocene Metamorphic Core Complex on the Southwestern Edge of the Intermontane Belt of British Columbia; *Tectonics*, Volume 7, pages 1141-1166.
- Garver, J.I. (1989): Basin Evolution and Source Terranes of Albian-Cenomanian Rocks in the Tyaughton Basin, Southern British Columbia: Implications for Mid-Cretaceous Tectonics in the Canadian Cordillera; unpublished Ph.D. thesis, *University of Washington*, 227 pages.
- Garver, J.I. (1992): Provenance of Albian-Cenomanian rocks of the Methow and Tyaughton basins, Southern British Columbia: a mid-Cretaceous Link between North America and the Insular Terrane; *Canadian Journal of Earth Sciences*, Volume 29, pages 1274-1295.
- Glover J.K. and Schiarizza, P. (1987): Geology and Mineral Potential of the Warner Pass Map Area (92O/3); in Geological Fieldwork 1986, *B.C. Ministry of Energy, Mines and Petroleum Resources*, Paper 1987-1, pages 157-169.
- Glover, J.K., Schiarizza, P. and Garver, J.I. (1988a): Geology of the Noaxe Creek Map Area (92O/2); in Geological Fieldwork 1987, *B.C. Ministry of Energy, Mines and Petroleum Resources*, Paper 1988-1, pages 105-123.
- Glover, J.K., Schiarizza, P., Garver, J.I., Umhoefer, P.J. and Tipper, H.W. (1988b): Geology and Mineral Potential of the Noaxe Creek Map Area (92O/2); *B.C. Ministry of Energy, Mines and Petroleum Resources*, Open File 1988-9.
- Hickson, C.J. (1992): An Update on the Chilcotin-Nechako Project and Mapping in the Taseko Lakes Area, West-central British Columbia; in Current Research, Part A, *Geological Survey of Canada*, Paper 92-1A, pages 129-135.
- Jeletzky, J.A. and Tipper, H.W. (1968): Upper Jurassic and Cretaceous Rocks of Taseko Lakes Map Area and their Bearing on the Geological History of Southwestern British Columbia; *Geological Survey of Canada*, Paper 67-54, 218 pages.
- Journey, J.M. (1990): A Progress Report on the Structural and Tectonic Framework of the Southern Coast Belt, British Columbia; in Current Research, Part E, *Geological Survey of Canada*, Paper 90-1E, pages 183-195.
- Kleinspehn, K.L. (1985): Cretaceous Sedimentation and Tectonics, Tyaughton-Methow Basin, Southwestern British Columbia; *Canadian Journal of Earth Sciences*, Volume 22, pages 154-174.
- Lalonde, C.M. (1987): Geological and Geochemical Surveys on the Vick Property; *B. C. Ministry of Energy, Mines and Petroleum Resources*, Assessment Report 16873.
- Leech, G.B. (1953): Geology and Mineral Deposits of the Shulaps Range; *B.C. Ministry of Energy, Mines and Petroleum Resources*, Bulletin 32, 54 pages.
- Mahoney, J.B. (1992): Middle Jurassic Stratigraphy of the Lillooet Area, South-central British Columbia; in Current Research, Part A, *Geological Survey of Canada*, Paper 92-1A, p. 243-248.
- Mathews, W.H. (1989): Neogene Chilcotin Basalts in South-central British Columbia: Geology, Ages, and Geomorphic History; *Canadian Journal of Earth Sciences*, Volume 26, pages 969-982.
- McGroder, M.F., Garver, J.I. and Mallory, V.S. (1990): Bedrock Geologic Map, Biostratigraphy, and Structure Sections of the Methow Basin, Washington and British Columbia; *Washington State Department of Natural Resources, Division of Geology and Earth Resources*, Open File Report 90-19.
- McLaren, G.P. (1986): Geology and Mineral Potential of the Chilko - Taseko Lakes Area (92O/4, 5; 92J/13; 92K/16; 92N/1); in Geological Fieldwork 1985, *B.C. Ministry of Energy, Mines and Petroleum Resources*, Paper 1986-1, pages 264-275.
- McLaren, G.P. (1990): A Mineral Resource Assessment of the Chilko Lake Planning Area; *B.C. Ministry of Energy, Mines and Petroleum Resources*, Bulletin 81, 117 pages.
- McLaren, G.P. and Rouse, J.N. (1989): Geology and Mineral Occurrences in the vicinity of Taseko Lakes (92O/3,4,5,6); in Geological Fieldwork 1988, *B.C. Ministry of Energy, Mines and Petroleum Resources*, Paper 1989-1, p.1: 3-158.
- McClintock, J.A. (1989): Geological and Geochemical Report on the Dil Claim Group; *B. C. Ministry of Energy, Mines and Petroleum Resources*, Assessment Report 19: 19.
- Miller, M.G. (1988): Possible Pre-Cenozoic Left-lateral Slip on the Yalakom Fault, Southwestern British Columbia; *Geology*, Volume 16, pages 584-587.
- Misch, P. (1966): Tectonic Evolution of the Northern Cascades of Washington State - A West-Cordilleran Case History; *Canadian Institute of Mining and Metallurgy*, Special Volume No. 8, pages 101-148.
- Monger, J.W.H. (1985): Structural Evolution of the Southwestern Intermontane Belt, Ashcroft and Hope Map Areas, British Columbia; in Current Research, Part A, *Geological Survey of Canada*, Paper 1985-1A, pages 349-358.
- Monger, J.W.H. (1986): Geology between Harrison Lake and Fraser River, Hope Map Area, Southwestern British Columbia; in Current Research, Part B, *Geological Survey of Canada*, Paper 86-1B, pages 699-706.
- Monger, J.W.H. (1990): Georgia Basin: Regional Setting and Adjacent Coast Mountains Geology, British Columbia; in Current Research, Part F, *Geological Survey of Canada*, Paper 90-1F, pages 95-107.
- Monger, J.W.H. and McMillan, W.J. (1989): Geology, Ashcroft, British Columbia (92I); *Geological Survey of Canada*, Map 42-1989, sheet 1, scale 1:250 000.
- O'Brien, J. (1986): Jurassic Stratigraphy of the Methow Trough, Southwestern British Columbia; in Current Research, Part B, *Geological Survey of Canada*, Paper 86-1B, pages 749-756.
- O'Brien, J.A. (1987): Jurassic Biostratigraphy and Evolution of the Methow Trough, Southwestern British Columbia; unpublished M.Sc. thesis, *University of Arizona*, 150 pages.
- Potter, C.J. (1986): Origin, Accretion and Post-accretionary Evolution of the Bridge River Terrane, Southwest British Columbia; *Tectonics*, Volume 5, pages 1027-1041.
- Rice, H.M.A. (1947): Geology and Mineral Deposits of the Princeton Map Area, British Columbia; *Geological Survey of Canada*, Memoir 234, 136 pages.
- Roddick, J.A. and Hutchison, W.W. (1973): Pemberton (East Half) Map Area, British Columbia; *Geological Survey of Canada*, Paper 73-17, 21 pages.
- Rusmore, M.E. (1985): Geology and Tectonic Significance of the Upper Triassic Cadwallader Group and its Founding Faults, Southwest British Columbia; unpublished Ph.D. thesis, *University of Washington*, 174 pages.
- Rusmore, M.E. (1987): Geology of the Cadwallader Group and the Intermontane-Insular Superterrane Boundary, Southwestern British Columbia; *Canadian Journal of Earth Sciences* Volume 24, pages 2279-2291.
- Rusmore, M.E., Potter, C.J. and Umhoefer, P.J. (1988): Middle Jurassic Terrane Accretion along the Western Edge of the Intermontane Superterrane, Southwestern British Columbia; *Geology*, Volume 16, pages 891-894.

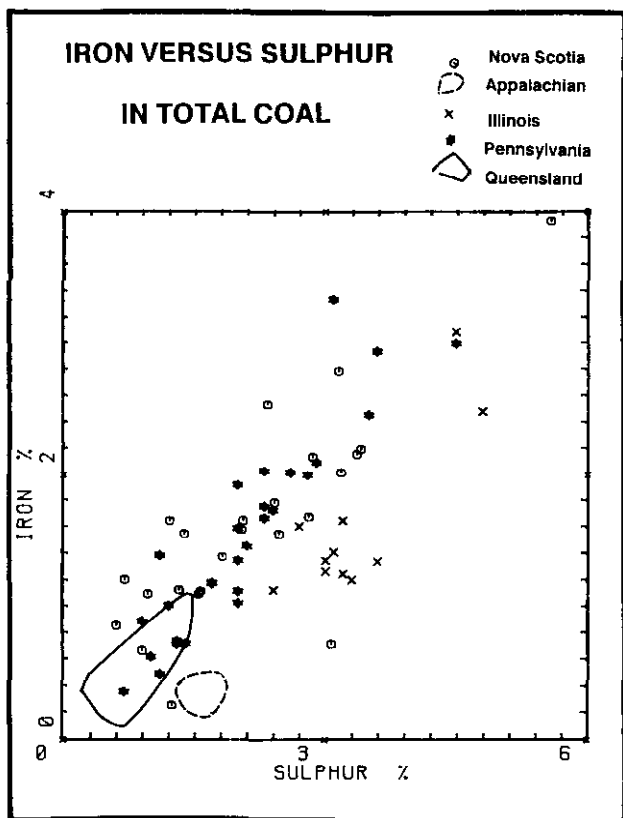


Figure 5-1-9. Plot of iron versus sulphur in some Canadian and international coals.

ratio correlates with iron, calcium and magnesium oxides and that iron oxide correlates with sulphur. Apparently most of the iron is in pyrite and the calcium and magnesium is in clays. In contrast to British Columbia coals calcium oxide correlates with base-acid ratios for the Queensland coals, possibly indicating a carbonate influence on base-acid ratio.

A plot of iron oxide versus sulphur concentrations (Figure 5-1-9) for Pennsylvania and Nova Scotia coals produces linear trends with data plotting near the pyrite line. Data from Illinois and Appalachian coals plot to the right of the pyrite line and indicate excess sulphur.

Base-acid ratios of eastern Canadian and eastern U.S.A. coals are high mainly because of varying amounts of pyrite and possibly iron carbonates. The coals do wash to a low ash and this provides flexibility for blending with British Columbia coals to reduce base-acid ratios.

BLENDING FOR IMPROVED CSR

Recent work investigated the effect on CSR values of coke of adding specific minerals to the parent coal samples (Price *et al.*, 1992). The addition of minerals such as calcite, pyrite and quartz changed the base-acid ratios of the doped coal sample and produced a change in the CSR values of the resultant coke. The CSR values were changed generally in amounts predicted by changes in the base-acid ratios and Equation A. This suggests that CSR values of coal blends can be estimated using the calculated blended base-acid

ratio as long as there is not a wide disparity of rank or rheology.

Equation A predicts that CSR decreases nonlinearly as base-acid ratio increases (Figure 5-1-3). This means that there will be a better than additive improvement in CSR if a high base-acid ratio coal is blended with a low base-acid ratio coal. Table 5-1-2 can be used to provide an example. If two coals A (57% of blend) and B (43% of blend) with BAR/CSR values of 0.06/70.5(A) and 0.20/32.5(B) (line 1, Table 5-1-2) are mixed, then the resulting BAR/CSR values are 0.12/59.3. This is an 82 per cent improvement in the CSR value of coal B and the blend has an acceptable CSR value. There is adequate flexibility to produce blends with good CSR values for the range of base-acid ratios of British Columbia coals.

The study by Price *et al.* (1992) also indicated that the mineral used to produce a change in CSR also had an effect on the CSR value independent of its effect on base-acid ratio. Thus if the base-acid ratio was changed a constant per cent by addition of the appropriate amount of apatite, gypsum, calcite or lime, the decrease in CSR value depended on the mineral (least for apatite most for lime). Similar results were observed for iron. Siderite addition had less effect than pyrite addition which had less effect than adding iron oxide.

This has interesting implications when considering the effect of weathering on CSR. For a property so dependent on ash chemistry one might expect it to be resistant to weathering, which mainly affects coal, not mineral matter. This is not the case, and an answer might be that weathering changes the form of some of the base oxides. For example, pyrite weathers to iron sulphate and in this way increases the detrimental effect of the ash on CSR without actually changing the base-acid ratio.

DISCUSSION

Coke strength after reaction is an important measure of coke quality, especially at a time when the ratio coke(kilogram)/ton hot metal is being decreased by the use of pulverized coal injection (PCI).

A sensitivity analysis using an empirical equation that predicts CSR values provides for a better understanding of the relative importance of ash content, base-acid ratio, rank and fluidity in influencing the resultant CSR. The base-acid ratio of the coal is one of the most important coal properties effecting the CSR of the resultant coke.

Correlation analysis of ash oxide data can indicate which oxides are responsible for variations in base-acid ratio. It then becomes important to identify the mineral host for these oxides. This can be achieved using correlation analysis, iron-sulphur plots, normative calculations or low-temperature ashing combined with x-ray diffraction. Often variations in base-acid ratio are correlated with variations in iron oxide concentration, probably present as pyrite or an iron carbonate. This information may lead to ways of selecting or washing run-of-mine coal for improved CSR.

On-line ash analyzers in coal wash-plants may be able to measure changes in iron content. From these data it might be possible to predict fluctuations in the CSR values of the clean coal before it reaches the customer.

AN OVERVIEW OF THE INTERIOR PLATEAU PROGRAM

By Larry J. Diakow, B.C. Geological Survey Branch and
Peter van der Heyden, Geological Survey of Canada

(Contribution to the Interior Plateau Program
Canada - British Columbia Mineral Development Agreement 1991-1995)

KEYWORDS: Regional geology, Interior Plateau, multi-disciplinary, bedrock mapping, surficial geology, geochemistry, airborne geophysics, biochemistry.

INTRODUCTION

The Interior Plateau program is a major new initiative that is funded and operated under the guidelines of the Mineral Development Agreement 1991-1995 (MDA) between the governments of Canada and British Columbia. During the program geoscientists from both the Geological Survey of Canada and the British Columbia Geological Survey Branch will collaborate on a number of multi-disciplinary projects throughout the Interior Plateau region of British Columbia (Figures 1-4-1 and 1-4-2). Mineral exploration in this region has been severely hampered by glacial drift, Neogene lava flows, an obsolete geological database, and lack of modern geophysical or geochemical coverage. Geological environments favourable for mineral deposits exist in neighbouring areas (e.g., porphyry style deposits such as Endako and Gibraltar, the Equity Silver deposit and epithermal precious metal deposits like Silver Queen and Blackdome). Extrapolation of plutonic suites

and stratigraphy suggests there is potential for similar, undiscovered deposits in the Interior Plateau region.

The projects include regional geochemical and aeromagnetic surveys, 1:50 000-scale bedrock and surficial geological mapping, airborne multiparameter surveys and a biogeochemical survey (Table 1-4-1). The objective of these projects is to upgrade the existing geological and geophysical databases in order to provide a more accurate assessment of mineral potential, and to accumulate modern data for providing information vital to informed resource management and land-use decisions in the Interior Plateau region.

Field-based projects initiated in 1992 will conclude in 1994. Annual reports accompanied by maps will be published for projects active during a given year. A final volume synthesizing the Interior Plateau program is planned for publication in 1995.

TABLE 1-4-1
SCHEDULE OF SUB-PROJECTS IN THE
INTERIOR PLATEAU PROGRAM

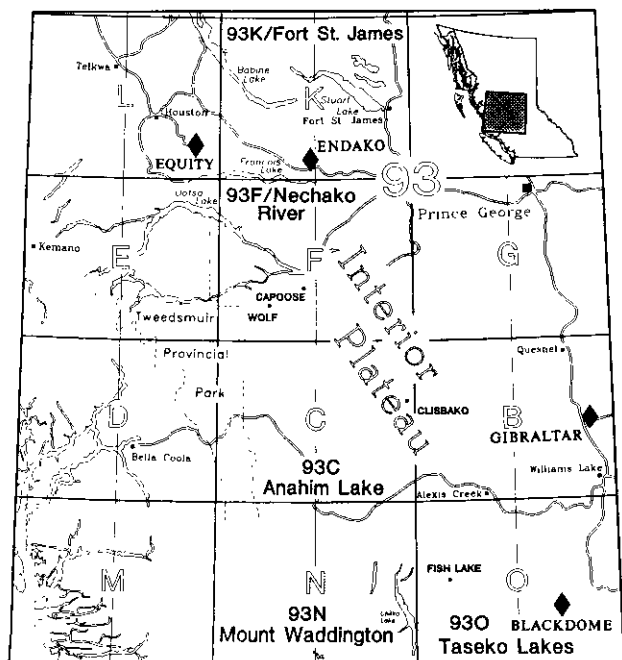


Figure 1-4-1. Major producing mines (shown by diamonds) and other significant mineral deposits in the Interior Plateau region.

Project/Coordinator	1992	1993	1994	1995
REGIONAL LAKE SEDIMENT GEOCHEMICAL SURVEY Wayne Jackman ¹ Steve Cook ¹	Orientation Survey			
	Full Survey			
	Report and Map Preparation			
AEROMAGNETIC TOTAL FIELD SURVEY Denis Teskey ²				
1:50,000 BEDROCK MAPPING Larry J. Diakow ¹ Peter van der Heyden ² Paul Schiarizza ¹ Cathy Hickson ²				
SURFICIAL GEOLOGY AND TILL GEOCHEMISTRY SURVEYS Peter Bohrowsky ¹ Alain Plouffe ²				
BIOGEOCHEMICAL SURVEY Colin Dunn ²				
AIRBORNE MULTIPARAMETER SURVEYS (Gamma ray, Magnetic and VLF) Robert Shives ² Ken Ford ² Bruce Ballantyne ² Don Harris ²				
				FINAL MAPS (1:50,000 1:100,000) and PROJECT VOLUME

Affiliation:
1. British Columbia Geological Survey
2. Geological Survey of Canada

REGIONAL GEOCHEMISTRY

In anticipation of a lake sediment Regional Geochemical Survey (RGS) covering the NTS 93C (Anahim Lake), 93F (Nechako River) and 93K (Fort St. James) map sheets, Stephen Cook, of the British Columbia Geological Survey Branch, carried out a lake sediment orientation study in the Vanderhoof-Houston region of the Interior Plateau in 1992. The purpose of this study is to evaluate the effectiveness of lake sediments as a sample medium for the regional sampling program. Studies were focused on sites that represent a variety of different lake types found draining each of two rock types most likely to be mineralized - plutons, with porphyry potential, and volcanic rocks of the Eocene Ootsa Lake Group with epithermal precious metal potential. Analyses from 625 lake-sediment samples obtained at 437 sites will determine the extent to which sediment geochemistry reflects the presence of nearby mineral occurrences, the effect of differing lake conditions, and the most effective sampling strategy for the RGS survey.

GEOPHYSICS

Denis Teskey of the Geological Survey of Canada is coordinating an aeromagnetic survey of an area in the Interior Plateau that will cover at least 30 adjoining 1:50 000 mapsheets. Data processing and interpretation, an integral part of this project, are necessary to minimize effects of thin but extensive sheets of Neogene flood basalts that may mask patterns due to older strata and deeper structures. Airborne geophysical surveys are planned for 1993. Processing of the digital data will follow with publication of a series of high-resolution residual total field maps at 1:50 000-scale and total field contour maps at 1:250 000-scale, planned for 1994.

Robert Shives, Ken Ford, Bruce Ballantyne and Don Harris of the Geological Survey of Canada initiated an applied geophysical study. They will carry out airborne gamma ray spectrometry (AGRS), magnetic and VLF-electromagnetic surveys over the two key mineral deposit types that represent likely exploration targets in the Interior Plateau region - the Clisbako epithermal precious metal occurrence and the Fish Lake porphyry copper-gold deposit.

Potassic alteration in rocks, present at both Clisbako and Fish Lake, provides excellent potential for successful application of the gamma ray spectrometric technique. Gamma ray spectrometry maps subtle variations in radioelement contents (K, U, Th) of bedrock and overburden. Where disruption of normal radioelement concentrations by mineralizing solutions can be recognized in bedrock or in derived surficial materials, the radioelements provide pathfinders to zones of alteration. Radioelement enrichment and depletion in concert with magnetic and VLF signatures can be interpreted and used as guides for mineral exploration.

Ground orientation and follow-up studies, in collaboration with other MDA projects, will include ground spectrometry, mineralogical studies and multimedia geochemical analyses, to explain the airborne patterns, to demonstrate practical applications of the data, and equally important, to foster the transfer of the relatively simple, inexpensive ground technique to the mapper and explorationist.

Ground tests were conducted in 1992 and aerial surveys will be completed in 1993. Colour contour and profile maps of radioelement, magnetic and VLF-EM data will be available at 1:50 000 and 1:100 000 scales for each area.

BEDROCK MAPPING

In 1992, two new bedrock mapping programs began along the eastern boundary of the Coast Belt and adjacent Intermontane Belt. Paul Schiarizza and Janet Riddell mapped about 1000 square kilometres in parts of the Mount Tatlow area (92O/5, 6, 12). This work established stratigraphic continuity with the recently mapped Chilkol Lake - Taseko Lakes - Bridge River area to the south-southeast. The Yalakom fault transects the map area; consistent stratigraphic relationships across the fault imply approximately 115 kilometres of dextral displacement. The Fish Lake porphyry copper-gold deposit is in the Tatlow area. Uranium-lead geochronometry on zircon from a mineralized phase of the intrusion will help to approximate the timing of intrusion-related mineralization at Fish Lake.

Farther northwest, Peter van der Heyden, of the Geological Survey of Canada, mapped the Charlotte Lake (93C/3), Junker Lake east-half (93C/4E), and parts of the Bussel Creek (92N/14) map areas. Exploration prospects in this area include epithermal precious metal bearing veins and porphyry copper-molybdenum showings. These mapping projects will be geographically linked in 1994, providing contiguous 1:50 000-scale geological coverage along a vast tract of the eastern Coast Belt and western Intermontane Belt.

In much of central British Columbia, Eocene magmatism is manifest as a broad field of continental volcanic rocks and associated calcalkaline plutons. Several former producing mines and scattered prospects throughout the Interior Plateau represent epithermal-type precious metal mineralization related to this magmatic episode. During the 1993 field season a new mapping project, coordinated by Cathie Hickson, of the Geological Survey of Canada, is scheduled to begin in the central region of the Interior Plateau (93C/9, 16 and 93B/12, 13). The focus will be to revise Eocene stratigraphy and identify metallotectics. Eocene rocks in the area contain several precious metal occurrences; the most notable at this time is at the Clisbako property.

During 1992, Larry Diakow and Kim Grein, of the British Columbia Geological Survey Branch, mapped the Natalkuz Lake (93F/6) area in the northern part of the Interior Plateau. This area is underlain by Middle Jurassic and older volcanic and sedimentary rocks that are cut by the Late Cretaceous Capoose batholith. The Natalkuz fault, a northeast-trending linear structure, cuts across the map area and juxtaposes older Jurassic strata against a dominantly Eocene and younger volcanic pile. At the Capoose property in the Fawnie Range, finely disseminated silver is found within rhyolite sills and, nearby, a number of porphyry copper-molybdenum showings are known in the Capoose batholith. Rhyolitic rocks of the Ootsa Lake Group contain sparse pyrite; their potential as hosts for epithermal precious metals is perceived to be low in the area mapped. In 1993, work will continue with expansion of the mapping farther

south into the Fawnie Creek area where silicified Eocene rocks contain precious metals at the Wolf property.

SURFICIAL GEOLOGY AND GEOCHEMISTRY

Peter Bobrowsky, of the British Columbia Geological Survey Branch, leads a surficial geological mapping project at 1:50 000-scale in parts of the Anahim Lake (93C) and Nechako River (93F) map sheets. Both areas have potential for mineral deposits in porphyry and epithermal environments; however, an extensive veneer of drift has significantly hampered exploration in both areas. The project will present surficial data in thematic formats that will aid drift prospecting. The maps will also integrate glacial process information into a format which will provide an additional tool for effective exploration of the drift-covered terrain.

In 1992, two field parties mapped the surficial geology in the four easternmost map sheets of the Anahim Lake area. Till samples were routinely collected throughout the map area for geochemical analysis and provenance studies. In 1993 surficial and bedrock mapping are proposed in the Fawnie Creek area (93F/3) which will result in a fully integrated terrain-bedrock map.

Alain Plouffe of the Geological Survey of Canada is engaged in a two-part project that addresses regional surficial geochemistry and Pleistocene glacial history. The project area comprises the northwest quadrant of Taseko Lakes (92O) and the northeast quadrant of the Anahim Lake (93C) map sheets. Further detailed surveys will be conducted around the Clisbako and Fish Lake properties to collaborate with and support studies of other projects in the area.

The till samples will be analyzed for a variety of elements and results compiled on regional reconnaissance geochemical maps. These maps will establish background concentrations of elements in till over different bedrock lithologies. Such maps have applications in drift prospecting. The historical aspect of the drift investigations is of primary importance for interpretation of the regional geochemical maps.

BIOGEOCHEMISTRY

Colin Dunn of the Geological Survey of Canada is undertaking a project to evaluate the effectiveness of biogeochemistry as a prospecting tool by sampling at several mineralized test sites that encompass an area roughly equivalent to two 1:50 000-scale map sheets. In a previous case study, over the QR deposit in the Quesnel trough, the biogeochemical survey demonstrated that reconnaissance level biogeochemical mapping is effective. Data were obtained from tree-top organic material by helicopter in a fast, cost-effective, and efficient program. This technique can detect mineralized bedrock concealed by dense forest and/or a veneer of overburden. The Interior Plateau program will involve detailed ground and airborne biogeochemical reconnaissance surveys at the selected test sites - the Clisbako and Fish Lake properties. The orientation survey done in 1992 will be followed up by the full survey in 1993. The work will be carried out in collaboration with other project leaders in the area. Approximately 50 elements will be analyzed. The maps produced will focus attention on areas with anomalous concentrations of metals.

GENERAL

Results of the various projects conducted by staff of the B.C. Geological Survey Branch in the Interior Plateau region are summarized in this volume. These include the following papers:

- Riddell, J., Schiariazza, P., Gaba, R.G., Cairn, N. and Findlay, A.: Geology and Mineral Occurrences of the Mount Tatlow Map Area.
- Diakow, L.J. and van der Heyden, P.: An Overview of the Interior Plateau Program.
- Green, K.C. and Diakow, L.J.: The Fawnie Range Project - Geology of the Natalkuz Lake Map Area.
- Cook, S.J.: Preliminary Report on Lake Sediment Studies in the Northern Interior Plateau, Central British Columbia (93C, E, F, K, L).
- Giles, T.R. and Kerr, D.E.: Surficial Geology in the Chilanko Forks and Chezacut Areas (93C/1,8).
- Proudfoot, D.N.: Drift Exploration and Surficial Geology of the Clusko River (92C/9) and Toil Mountain (93C/16) Map Sheets.



**THE FAWNIE RANGE PROJECT – GEOLOGY OF THE
NATALKUZ LAKE MAP AREA
(93F/6)**

By Kim C. Green and Larry J. Diakow

(Contribution to the Interior Plateau Program

Canada – British Columbia Mineral Development Agreement 1991-1995)

KEYWORDS: Regional geology, Fawnie Range, Natakuz Lake, stratigraphy, Capoose batholith, Capoose Au-Ag deposit.

INTRODUCTION

The Fawnie Range mapping project began in 1992 and is a component of the Interior Plateau program, a new multi-disciplinary study in the Interior Plateau physiographic region. The program is funded through the Canada-British Columbia Mineral Development Agreement (MDA) 1991-1995. The Interior Plateau program involves cooperative field investigations and research by geoscientists from the Geological Survey of Canada and the British Columbia Geological Survey (Diakow and van der Heyden; 1993, this volume).

The new Fawnie Range project is aimed at better understanding the stratigraphic and structural development of Mesozoic and Cenozoic volcanic sequences and assessing the geological controls of mineral deposits in the northern Interior Plateau.

Regional mapping at 1:50 000 scale, and at 1:20 000 scale in parts of the Fawnie Range, was completed in Natakuz Lake map area in 1992 (Figure 1-5-1). Much of the area is dominated by low rounded hills covered by forest

and mantled by extensive glacial deposits. Except for semi-continuous exposure in the Fawnie Range, outcrops tend to be widely separated and confined to the crests of hills and the shoreline of the Nechako Reservoir (Natakuz Lake, Knewstubb Lake, Euchu Reach).

ACCESS

A well-maintained network of logging roads connects the northeast corner of the map area with Vanderhoof, approximately 110 kilometres to the north-northeast. These roads, and the Nechako Reservoir which transects the northern part of the map area, provide good access to mainly Tertiary rock sequences. The oldest rock units crop out primarily southeast of the Nechako Reservoir in the Fawnie Range. This area is best reached by helicopter, although a barely passable four-wheel-drive road connects the southern segment of Fawnie Range and the Capoose prospect with an all-weather logging road. The drive to the Capoose prospect from Vanderhoof via the Kluskus-Ootsa Forest Service road is about 160 kilometres.

GENERAL GEOLOGY

Early geological investigations in the Natakuz Lake map area formed part of a systematic regional mapping program conducted in the Nechako River area (93F) during the late 1940s to early 1950s and later synthesized in a Geological Survey of Canada memoir (Tipper, 1963). Refinement of stratigraphic rock units and their distribution in the Natakuz Lake map area as determined in this study are shown in Figure 1-5-2.

The eastern and southeastern parts of the map area are underlain mainly by andesitic flows that are part of the lowest stratigraphic unit (Jv,s). Thin interflow sediments, we believe are well up-section in this unit, contain tentatively identified early Middle Jurassic fauna and suggest a possible correlation with the Early and Middle Jurassic Hazelton Group. Along the east-facing slope of the Fawnie Range these flows apparently constitute the base of a thin sequence of fine clastic sediments containing Callovian fauna which suggests a time-stratigraphic association with the Ashman Formation of the Bowser Lake Group. In turn the sedimentary unit passes up-section into a conformable package of andesitic fragmental rocks and minor inter-spersed flows. Although the age of these volcaniclastic rocks is uncertain, they may represent a previously unrecognized, spatially restricted volcanic unit of presumable Middle to Late Jurassic age. Collectively, layered rocks south of Natakuz Lake that form the backbone of the Fawnie Range

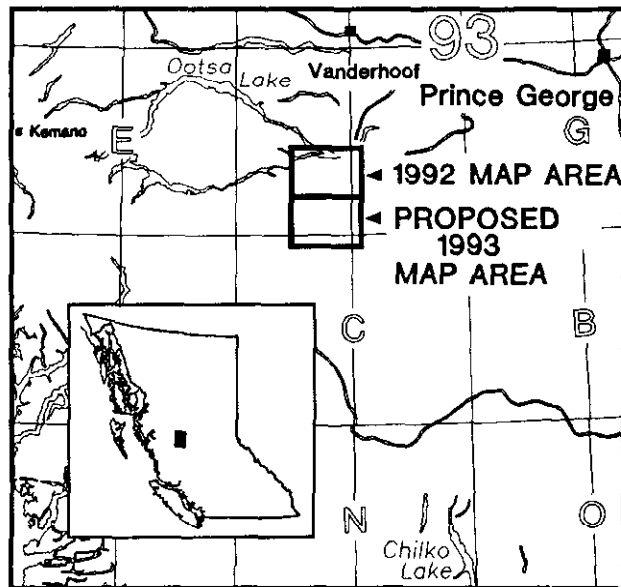


Figure 1-5-1. Location of Natakuz Lake map area (93F/6) and proposed 1993 map area (93F/3).

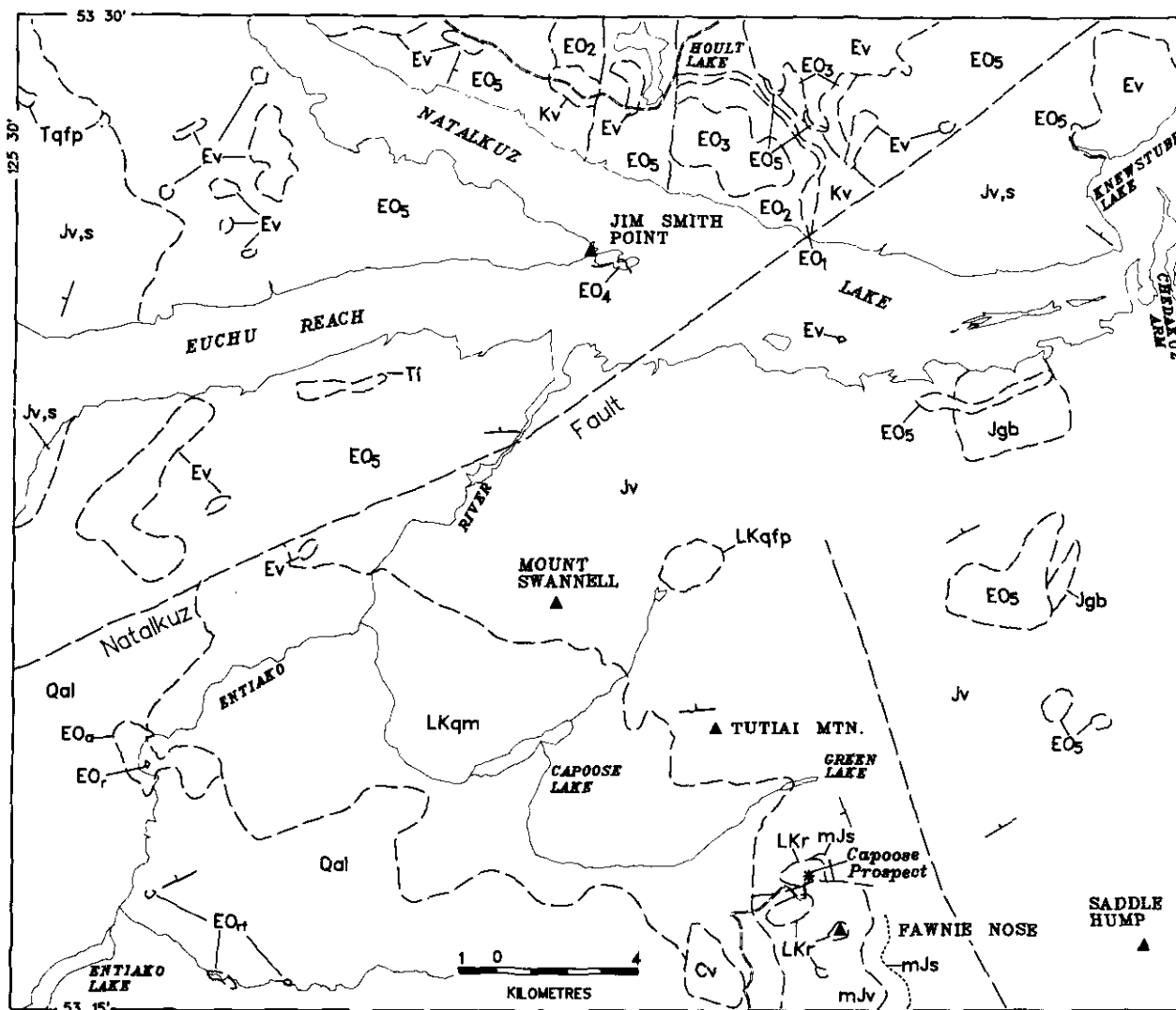


Figure 1-5-2. Distribution of rock units in the Natakuz Lake map area as determined in this year's study.

are intruded and thermally altered by the latest Cretaceous Capoose batholith.

The Natakuz fault, a regional northeast-trending extensional structure places pre-Tertiary successions and the Capoose batholith against predominantly volcanic rocks of the Eocene Ootsa Lake Group which underlies the west-northwest part of the map area. Basaltic flows of the Endako Group nonconformably overlie the Ootsa Lake Group. Basement for these Tertiary units is represented by generally small exposures of the Hazelton Group, hornblende-bearing pyroclastic deposits of the Upper Cretaceous Kasalka Group and one occurrence of Albian tuffaceous sediments.

The youngest rocks in the map area are fresh olivine tholeiite flows assigned to the Miocene and younger Chilcotin Group. A solitary erosional remnant of these flows rests nonconformably on the Capoose batholith along the southern margin of the map area.

STRATIGRAPHY

JURASSIC VOLCANIC AND SEDIMENTARY ROCKS (UNIT Jv,s)

Unit Jv,s is particularly well exposed along the axis of the Fawnie Range south of Natakuz Lake. The Late Cretaceous Capoose batholith intrudes and alters rocks of Unit Jv,s in a broad area of near continuous outcrop at Mount Swannell and Tutiai Mountain. Immediately east of the Fawnie Range numerous scattered outcrops are restricted to the crests of knolls. Adjacent to the narrow waterway connecting Natakuz and Knewstubb lakes thick glacial cover limits exposure to a few, widely spaced low hills. Neither the top nor the bottom of the unit is recognized in the map area. Its total thickness is difficult to ascertain; however, part of a homoclinal section at Tutiai Mountain is at least 1 kilometre thick. The most representative section of relatively unaltered lava flows and associated volcanoclastic rocks, about 350 metres thick, is exposed immediately west of

LEGEND

CENOZOIC QUATERNARY

Qal Area of thick glacial deposits.

TERTIARY AND YOUNGER Miocene to Pliocene CHILCOTIN GROUP

Cv Olivine basalt; dark grey; aphanitic or olivine-phyric; massive, columnar jointed or flow layered.

TERTIARY Late Eocene to Oligocene ENDAKO GROUP

Ev Basalt; black to dark grey-brown; pyroxene-phyric; massive to columnar jointed; rare flow breccia; locally vesicular or amygdaloidal.

Early to Middle Eocene OOTSA LAKE GROUP

EOrt Lapilli - crystal tuff; medium buff-grey; phenocrysts of quartz up to 30% by volume; angular lithic fragments, 3 to 5 mm; moderately consolidated ash groundmass.

EOr Rhyolite flows; light grey, quartz and feldspar-phyric; quartz phenocrysts up to 25% by volume.

EOa Andesite flows; maroon; feldspar-phyric; trachytic; interlayered finely laminated flows and flow breccias.

EO₅ Rhyolite flows and tuffs; white, cream pink; massive to laminated; aphanitic to porphyritic; feldspar, quartz, and biotite-phyric; spherulitic; locally contains pitchstone layers.

EO₄ Dacite flows; light pink to grey; porphyritic; feldspar and biotite-phyric.

EO₃ Dacite flows; light blue-grey; sparsely porphyritic; feldspar and biotite-phyric; weathering along flow surfaces imparts platy jointing in outcrops.

EO₂ Coarse feldspar andesite flows; dark grey to green; feldspar-phyric; phenocrysts up to 1cm long.

EO₁ Amygdaloidal andesite; dark grey; amygdaloidal and massive; aphyric; amygdules filled with silica, calcite and epidote.

MESOZOIC CRETACEOUS

LKr Late Cretaceous
Rhyolite sills, dikes, flows and tuffs; white, cream and pink; massive to laminated flows and sills; thickly to thinly bedded ash, crystal and crystal-lapilli tuffs; finely-crystalline red and brown garnet occurs in sills and flows.

Kv Andesite flows and tuffs; grey-green to purple; crystal, lapilli and block tuffs; clasts and groundmass are feldspar and hornblende-phyric.

JURASSIC Middle Jurassic (?)

mJv Andesite to dacite(?) crystal, lapilli and block tuffs; dark greyish-green, green and maroon; lapilli tuff locally with interbedded crystal and ash tuffs and minor sediments; clasts are feldspar-phyric andesite.

Middle Jurassic BOWSER LAKE GROUP ASHMAN FORMATION

mJs Interbedded argillite and siltstone, minor greywacke; dark grey to black; thinly bedded to massive; locally fossiliferous.

Early to Middle Jurassic HAZELTON GROUP

Jv,s Feldspar-augite-phyric andesite flows and lesser fragmental deposits; minor interlayered arkosic sediments; flows are dark grey to greenish-grey; massive or amygdaloidal; crowded feldspar texture; interbedded sediments include arkosic sandstone and siltstone; sediments are locally fossiliferous.

INTRUSIVE ROCKS

CENOZOIC TERTIARY

Tl Dacite subvolcanic intrusion; light grey, quartz and feldspar-phyric, biotite and hornblende as accessories.

Tqfp Quartz - feldspar porphyry; light grey to cream; quartz and feldspar-phyric; forms small stocks or dikes.

MESOZOIC CRETACEOUS

Late Cretaceous CAPOOSE LAKE BATHOLITH

LKqm Quartz monzonite to granodiorite; pinkish grey, coarsely crystalline, feldspar megacrystic, biotite and hornblende as accessories.

LKqfp Quartz - feldspar porphyry; grey to cream; quartz and feldspar-phyric; phenocrysts 1 to 3mm; euhedral; up to 20% by volume quartz.

JURASSIC (?)

Jgb Gabbro; grey to dark green, fine to medium-grained, salt-and-pepper texture; massive; contains phenocrysts of feldspar, pyroxene and olivine.

SYMBOLS

Geological boundary (approximate, assumed)	-----
Fault (approximate, assumed)	-----
Bedding, tops known	-----
Road	-----

Saddle Hump. This section can be reached on foot from the Top Lake Forest Service campsite 3.5 kilometres to the south.

A secondary assemblage of epidote-quartz-chlorite is ubiquitous and a significant feature that distinguishes this unit from younger, comparatively unaltered rock sequences in the map area. This assemblage of alteration minerals generally lines fractures, and less commonly occurs as irregular clots in the lavas. Microscopically, calcite and sericite, with or without epidote, incipiently alter plagioclase phenocrysts. This is often accompanied by chlorite and granular opaques which selectively replace ferromagnesian phenocrysts and the matrix.

Unit Jv is made up predominantly of lava flows. Fragmental deposits are prominent locally, but regionally they are minor and occur as comparatively thin beds that inter-finger with the lava flows. Rare interflow sedimentary rocks also occur sporadically throughout the unit.

Lava flows of Unit Jv are remarkably uniform in composition and texture. They are typical andesites with porphyritic and amygdaloidal textures, and contain plagioclase and relatively fresh pyroxene phenocrysts set in a dark green or maroon groundmass. Plagioclase phenocrysts typically vary from 1 to 3 millimetres in length and comprise between 15 and 35 volume per cent of the rock. The common occurrence of vitreous augite phenocrysts (1 to 5% by volume) is a diagnostic feature of these flows. Augite occurs in glomerocrysts with plagioclase and as microphenocrysts throughout the groundmass. Rare relict outlines of olivine grains may be present. The appearance of amygdules is variable in the porphyritic lavas from few volume per cent to 30 volume per cent of the rock. The amygdules are typically round and filled with chlorite, epidote and quartz. Hematite-rich breccia with calcite-filled interstices forms discontinuous layers up to 1 metre thick on some flows. At one locality a lens of grey limestone about 50

centimetres thick is exposed at the top of an amygdaloidal flow.

Fragmental deposits comprised of monolithic lapilli and blocks interleave the lava flows. The best continuous exposure of these deposits is immediately southwest of Chedakuz Arm on Knewstubb Lake. The fragments have a similar texture and bulk composition to the porphyritic andesite flows.

Porphyritic andesites are interlayered with dark green to black basaltic andesite flows in the volcanic section immediately west of Saddle Hump. Distinguished by a dense, fine granular aphyric texture, these rocks form largely structureless flows as much as 75 metres thick that weather to a smooth, orange-hued surface. In several places they contain resistant laminae that protrude from the weathered surface (Plate 1-5-1). Olivine microphenocrysts comprise up to 3 volume per cent and minute augite grains occupy interstices between the plagioclase microlites.

Interflow pyroclastic units are difficult to recognize in the hydrothermally altered and hornfelsed section adjacent to the Capoose batholith at Mount Swannell. Elsewhere, the fragmental rocks tend to be areally restricted in rather massive featureless sections less than 50 metres thick. In the area of the reference section immediately west of Saddle Hump, an apparently minor fault juxtaposes a sequence of

lavas and lapilli tuffs. The tuffs contain subangular maroon and mauve porphyritic and aphyric pyroclasts in an ash matrix charged with plagioclase crystal fragments. A superb bedded outcrop about 75 metres long on the north shore of Nataalkuz Lake exposes variegated maroon to green fragmental rocks. Lapilli tuff forms several thick beds that alternate with thinner, well-laminated ash-tuff beds, some of which contain accretionary lapilli (Plate 1-5-2). The lapilli comprise a heterolithic mixture of crowded porphyritic andesite, flow-laminated rhyolite, porphyritic dacite and aphyric siliceous fragments. A similar section of variegated tuffs interleaved with sparsely fossiliferous waterlain ash tuff crops out in road cuts in the extreme northwest corner of the map area.

Sedimentary rocks (Unit Js) directly underlie porphyritic andesite lavas at several widely spaced exposures immediately north of Nataalkuz Lake. The best outcrop is on the point that projects southward into the narrow waterway connecting Nataalkuz and Knewstubb lakes. At this location a well-bedded sedimentary section about 75 metres thick is abruptly and conformably overlain by coarse augite-bearing porphyritic andesite flows and associated fragmental rocks. The sedimentary rocks consist mainly of drab, olive-green arkosic sandstone and siltstone, and black mudstone. The arkosic sandstone is composed of well-sorted subangular grains of plagioclase, augite and lithic clasts. The detritus is



Plate 1-5-1. Fine-grained basaltic andesites of Unit Jv sometimes display protruding laminae on weathered surfaces.

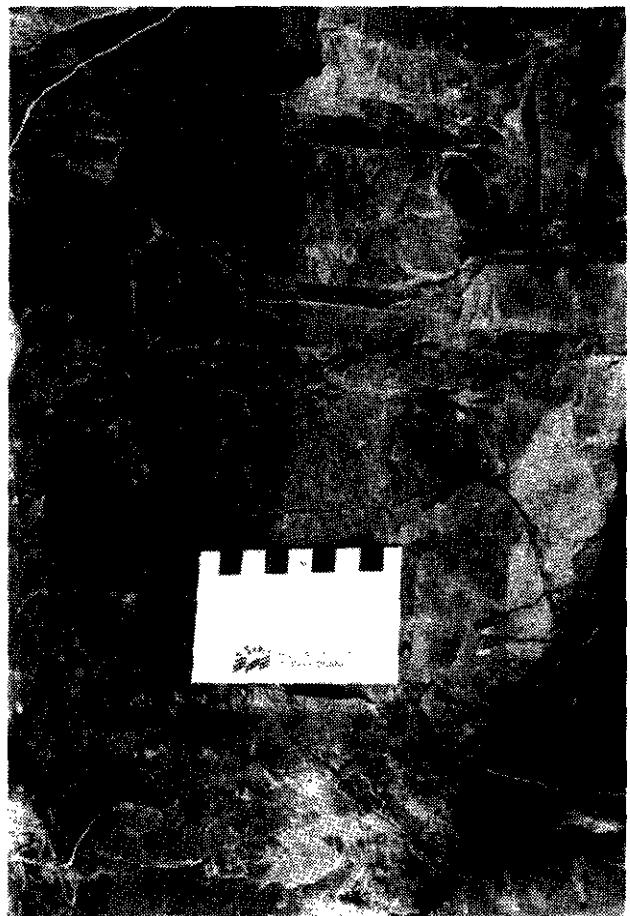


Plate 1-5-2. Accretionary lapilli in ash tuffs of Unit Jv.

undoubtedly derived from a local volcanic source, presumably from nearby augite-bearing porphyritic andesite flows. Concretions generally less than 10 centimetres in diameter on rare occasions reach 0.5 metre in diameter. The concretions are weakly calcareous and as a consequence weather recessively in the fine clastic beds. Conglomeratic sandstone with well-rounded siliceous (chert?) pebbles is exposed near the base of the section. A collection of pelicypod fossils, including *Trigonia* and scarce belemnites resembles some early Bajocian fauna (T.P. Poulton, personal communication, 1992). Moreover, the arkosic sedimentary beds replete with fossils resemble deposits of the Smithers Formation which crop out extensively 100 kilometres to the west, in the Whitesail Lake map area.

MIDDLE TO LATE(?) JURASSIC ROCKS

In the Fawnie Range, between Fawnie Nose and Green Lake a west-southwest-dipping monoclinical succession of sedimentary strata passes stratigraphically up-section into predominantly fragmental volcanic rocks that have been cut by a variety of felsic hypabyssal intrusions and also thermally metamorphosed by the nearby Capoose batholith. Topographically lower, and presumably comprising the stratigraphic base of this succession, are volcanic rocks tentatively assigned to Unit Jv. Near the midpoint of the ridge, an east-trending normal fault offsets the layered succession and in the uplifted northern block exposes a basal section about a kilometre thick. The stratigraphically lowest rock is a maroon and green block-lapilli tuff. The fragments are subangular to subrounded, monolithic and contain up to 40 volume per cent of feldspar phenocrysts. Up-section feldspar-phyric maroon and green crystal-lapilli tuff inter-layered with amygdaloidal flows predominates. At the Capoose prospect a succession of sedimentary rocks overlies the flows and tuffs with slight angular unconformity.

SEDIMENTARY ROCKS (UNIT mJs)

Sedimentary rocks crop out discontinuously from the Capoose prospect in the north to Fawnie Dome in the south. At the Capoose prospect sediments weather recessively in a section 120 metres thick and composed of interbedded argillite and tuffaceous siltstone (Tipper, 1963). To the south, lithologically similar rocks are exposed 0.6 and 1.4 kilometres east and southeast of Fawnie Nose. At these locations the section is over 300 metres thick and consists of alternating argillite and siltstone layers 1 to 2 centimetres thick with conspicuous massive interbeds of greywacke. A layer of black chert-pebble conglomerate less than 10 metres thick occurs locally near the top of the sedimentary sequence. The conglomerate contains subrounded quartz, chert, argillite and tuffaceous clasts up to 1.5 centimetres in diameter, supported by a fine-grained, dark grey matrix.

Fossil collections from sedimentary sections in the south as well as in the northern section include ammonites, bivalves and belemnites. The age of the sedimentary rocks near Fawnie Nose, as inferred from preliminary examination of the fossils, is tentatively Middle Jurassic, probably Bathonian or Callovian (T.P. Poulton, personal communication, 1992). This corresponds with the Callovian age for

fossils identified in the sediments from the northern locality (Tipper, 1963). This sedimentary unit is probably correlative with the Ashman Formation of the Bowser Lake Group as the ages and lithologic characteristics are broadly similar.

VOLCANIC ROCKS (UNIT mJv)

In the Fawnie Nose area the sediments of Unit mJs are overlain with slight angular unconformity by approximately 600 metres of crowded feldspar crystal tuff, crystal-lapilli tuff and local accumulations of maroon and green block-lapilli tuff. The stratigraphically highest member of the unit is crystal-lapilli tuff with distinctive chloritic flammé (Plate 1-5-3), that crops out for 1.5 kilometres along the ridge crest between Fawnie Nose and the Capoose prospect.

Hornfels alteration, caused by emplacement of the Capoose batholith, is extensive in the volcanic section exposed between Fawnie Nose and the Capoose prospect. The effects of the intrusion are indicated by the increased hardness of the rocks and accompanying destruction of primary volcanic textures to form massive and crudely bedded units in which the fragmental texture is totally obliterated or only faintly revealed on the weathered surface. Veinlets and clots of epidote and chlorite are ubiquitous throughout the section. The age of Unit mJv is loosely bracketed by underlying Callovian sedimentary strata of Unit mJs and a Maastrichtian date obtained from the Capoose batholith (Andrew, 1988).

CRETACEOUS VOLCANIC ROCKS (UNIT Kv)

Volcanic rocks of tentative Late Cretaceous age crop out mainly in the vicinity of Hoult Lake and extend as scattered outcrops in a belt trending southeastward towards Natukuz Lake. Several representative exposures of Unit Kv, one of which was sampled for U-Pb and K-Ar geochronometry, crop out adjacent to the road along the south shore of Hoult Lake.

The volcanic rocks comprise a structureless mass of block-lapilli tuff. The pyroclasts are characteristically monolithic, grey-green or purple hornblende-phyric andesite that are up to 15 centimetres in diameter. Plagioclase crystals between 1 and 3 millimetres long comprise up to 35 volume per cent and hornblende as long as 4 millimetres accounts for up to 5 volume per cent of the rock. Despite the presence of quartz-epidote veinlets cutting the tuffs and incipient replacement of plagioclase by epidote, the hornblende in many sections is remarkably fresh.

RHYOLITE (UNIT LKr)

Rocks of Units Jv,s, mJs and mJv, which underlie the ridge between Green Lake and Fawnie Nose are intruded by numerous rhyolitic dikes and sills (see Intrusive Rocks) and overlain by rhyolitic flows and tuffs. A Late Cretaceous age has been determined for the rhyolitic intrusions exposed at the Capoose prospect (Andrew, 1988).

Rhyolite flows and tuffs: South of the Capoose property rhyolite flows and tuffs overlie volcanic rocks of Unit mJv with apparent angular unconformity. The flows are white to light grey, finely laminated or brecciated and vary in texture from aphanitic to sparsely porphyritic. Quartz and feldspar

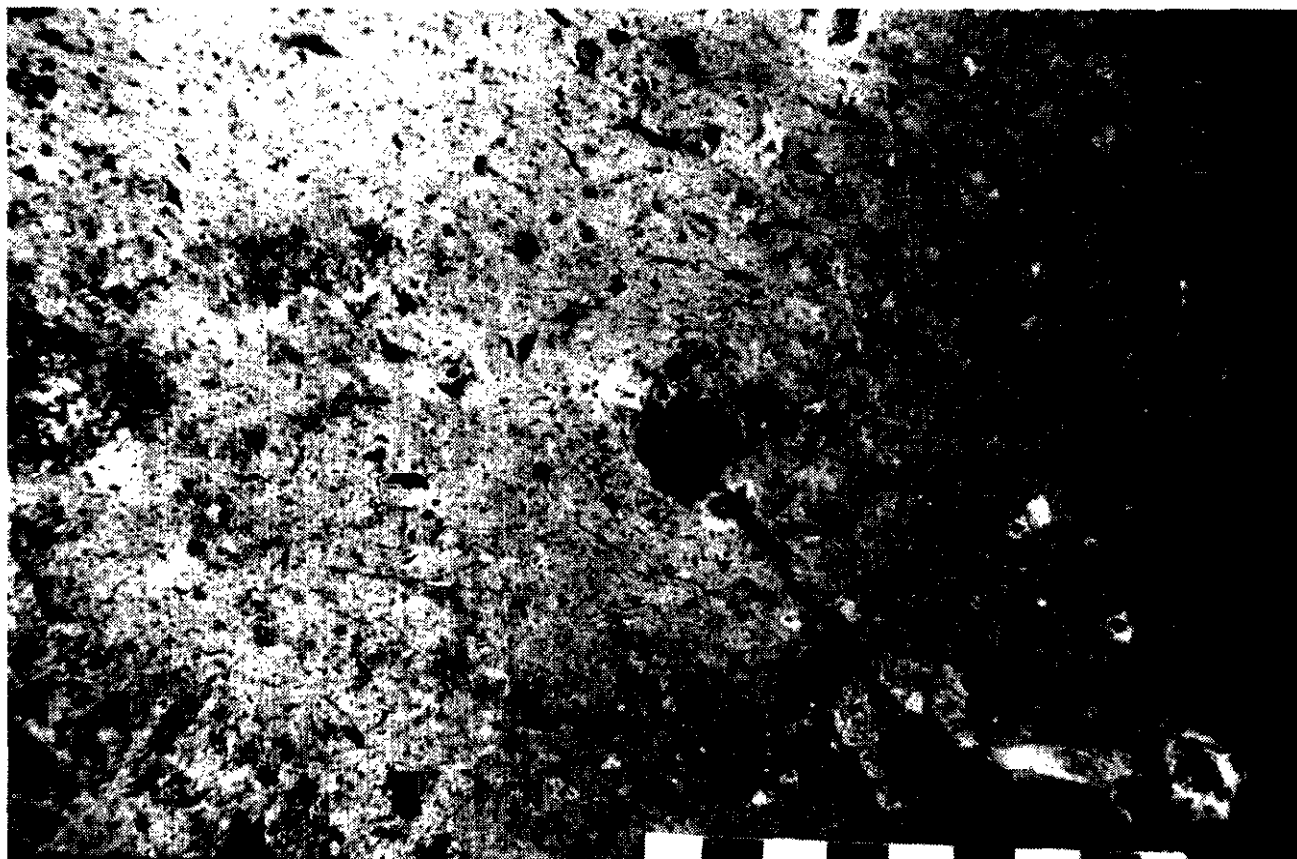


Plate 1-5-3. Chloritic fiammé are a distinctive feature in crystal-lapilli tuffs of Unit mJv.

phenocrysts, less than 1 millimetre in diameter, and finely crystalline brown garnet occur in the flows in concentrations of less than 5 per cent by volume.

Light grey to pink rhyolite ash, crystal and crystal-lapilli tuffs are interlayered with the flows. The tuffs are thickly to thinly bedded. The ash tuffs are very fine grained and appear cherty in outcrop. Crystal and crystal-lapilli tuffs contain euhedral to fragmented quartz (up to 30% by volume) and feldspar (<5% by volume) phenocrysts from 1 to 3 millimetres in diameter. Lithic fragments, 0.4 to 1.5 centimetres across, are predominantly angular, aphanitic, siliceous volcanic rocks.

EOCENE OOTSA LAKE GROUP

The Ootsa Lake Group is the name applied to a succession of continental calcalkaline basaltic to rhyolitic volcanic rocks of Eocene age (50.0 Ma) exposed in the Whitesail Range and Whitesail Reach areas (Duffell, 1959; Diakow and Mihalyuk, 1987a, b). Ootsa Lake Group volcanic rocks in the Nataalkuz Lake area are confined, for the most part, to the northwest side of the Nataalkuz fault. A 750-metre section of volcanic rocks consisting of amygdaloidal andesite, coarse feldspar-phyric flows and platy dacite unconformably overlies Upper Cretaceous volcanic rocks along the north side of Nataalkuz Lake. Rhyolite flows and lesser tuffaceous rocks underlie most of the northwestern

corner of the map area. Field relationships suggest that the rhyolite overlies older lithologies on a surface with significant paleotopography. Biotite-phyric dacite flows exposed on an island 1 kilometre east of Jim Smith Point either underlie or are interlayered with the rhyolite flows.

AMYGDALOIDAL ANDESITE FLOWS (UNIT EO₁)

North of Nataalkuz Lake, dark grey, massive and amygdaloidal andesite flows less than 75 metres thick unconformably overlie hornblende-bearing crystal-lapilli and block-lapilli tuffs of Unit Kv. The flows are aphanitic and locally brecciated with matrix infillings of chalcedonic quartz. Amygdules contain silica, calcite and epidote. Similar amygdaloidal flows are interlayered with bladed feldspar phyric flows of Unit EO₂.

BLADED FELDSPAR ANDESITE PORPHYRY FLOWS (UNIT EO₂)

Dark green-grey coarse feldspar-phyric andesite flows approximately 250 metres thick conformably overlie the amygdaloidal andesite flows. Alignment of tabular, 5-millimetre to 1.5-centimetre, feldspar phenocrysts impart a well-developed flow fabric to outcrops. Hand samples contain a phenocryst assemblage of plagioclase (20-40% by volume) and pyroxene (5-10% by volume). Phenocrysts are extensively replaced by calcite and chlorite. Epidote, hematite and silica occur on fracture surfaces. These flows are

lithologically similar to andesites of the Ootsa Lake Group mapped to the west in the Whitesail area (Unit 6, Diakow and Mihalyuk, 1987b)

SPARSELY PORPHYRITIC DACITE FLOWS (UNIT EO₃)

Sparsely feldspar-phyric dacite flows overlie the coarse feldspar-phyric andesites with apparent conformity. The dacite flows have an estimated thickness of 150 metres. However, this is a minimum thickness as the upper contact is not exposed. The dacite weathers readily along flow surfaces producing flaggy, porcellaneous fragments. The rock is medium to light blue-green or grey and contains tabular feldspar phenocrysts 2 to 3 millimetres long (5-10% by volume) and acicular hornblende phenocrysts 1 to 3 millimetres long. Alignment of the phenocrysts imparts a trachytic texture to the flows. Calcite and epidote have selectively replaced the feldspar phenocrysts. Hornblende phenocrysts are commonly replaced by chlorite and fine-grained opaque minerals.

DACITE FLOWS (UNIT EO₄)

Biotite-phyric dacite flows underlying or interlayered with rhyolite flows are exposed on an island approximately 1 kilometre east of Jim Smith Point. At this location dacite flows about 140 metres thick are exposed on the side of a hill directly above lake level. This represents a minimum thickness because the base of the dacite is not exposed. The dacite has a light grey to pinkish grey fine-grained groundmass and contains a phenocryst assemblage of plagioclase (20% by volume), anorthoclase (20% by volume) and biotite (5-10% by volume). Plagioclase phenocrysts (An₁₂) are white, euhedral, subvitreous to chalky and commonly up to 0.5 centimetre long. Anorthoclase phenocrysts range from 0.3 to 0.5 centimetre long and are colourless, euhedral and vitreous. In thin section anorthoclase is observed rimming plagioclase phenocrysts. Biotite occurs as vitreous, euhedral, 1 to 2-millimetre phenocrysts. Clots of intergrown fine-grained feldspar and biotite up to 1 centimetre across occur throughout the groundmass. A bulk sample has been collected for the purpose of determining a K-Ar age on biotite for the dacite flows.

RHYOLITE FLOWS AND TUFFS (UNIT EO₅)

Rhyolite flows and tuffaceous rocks comprise the most laterally extensive unit of the Ootsa Lake Group in the map area. Rhyolite flows outcrop along the north shore of Nataalkuz Lake; interlayered flows and tuffs predominate along the south side of Euchu Reach. Rhyolite flows are exposed on ridges at two locations southeast of the Nataalkuz fault unconformably overlying lava flows of Unit Jv. The thickest accumulation of rhyolite is exposed in the canyon walls along the Entiako River near its confluence with the Nechako Reservoir. At this location a fractured, pyritic subvolcanic plug domes the overlying sequence of flows, tuffs and sediments about 850 metres thick into a broad antiformal structure. This is a minimum thickness as the upper contact is not exposed.

Rhyolite Flows: Chalky white, pink and cream-coloured rhyolite flows are the most abundant rocks in the map area.

Textures in the rocks vary considerably over short distances. They include massive flows and flow breccias, planar and contorted laminated flows, spherulitic flows (1 mm to 1 cm spherulites) and interlayered pitchstones. The phenocryst assemblage in the flows is variable across the map sheet. Flows typically contain a phenocryst assemblage of plagioclase (up to 20% by volume), quartz (5-10% by volume), potassium feldspar (up to 20% by volume) and traces of biotite. Plagioclase is vitreous and occurs as euhedral, 2 to 3-millimetre phenocrysts. Quartz is almost always present as 1 to 2-millimetre euhedral phenocrysts. Salmon pink, 2 to 3-millimetre euhedral potassium feldspar phenocrysts are generally uncommon but locally comprise up to 20 per cent of hand samples. Biotite is usually present as euhedral, vitreous phenocrysts between 1 and 2 millimetres in diameter.

Rhyolitic Air-fall Tuffs: White and light green, massive to well-bedded ash, crystal, crystal-lapilli and lapilli-block tuffs are interlayered with rhyolite flows along the Entiako River and on low ridges south of Euchu Reach. Rhyolitic lapilli and ash-tuff beds are sharply overlain by Endako flows in Chedakuz Arm on Knewstubb Lake. A section of graded crystal-lapilli tuffs 300 metres thick crops out along the north side of Nataalkuz Lake almost directly north of Jim Smith Point. The tuffs contain a phenocryst assemblage of feldspar, quartz and biotite. Lithic fragments are fine-grained, subangular to angular and predominantly felsic volcanic rocks. Carbonized wood fragments and rare upright tree trunks occur in the tuffs at a number of locations in the map area indicating that the tuffs were, in part, subaerially deposited.

Tuffaceous sediments are preserved beneath basalt flows of the Endako Group at three locations north of Nataalkuz Lake. Locally they contain carbonaceous plant fragments and delicate bivalves. The thickest accumulation of sediments is exposed in a stream canyon 0.5 kilometre southwest of the western end of the road which runs along the northern edge of the map sheet. Here they are estimated to be 50 metres thick and grade upwards from laminated, quartz-rich tuffaceous siltstone to carbonaceous, coarse-grained lithic wacke.

EOCENE VOLCANIC ROCKS NEAR ENTIAKO LAKE

Andesite flows conformably overlain by rhyolite flows crop out in the southwestern corner of the map area along the Entiako River near Entiako Lake. We believe they are part of the Ootsa Lake Group, however, their depositional relationship with other stratigraphic units is uncertain. They are discussed separately because their mineralogy and texture differs from other volcanic units described as Ootsa Lake Group.

ANDESITE FLOWS (UNIT EO₆)

Maroon, feldspar-phyric flows crop out on a bend of the Entiako River approximately 5 kilometres downstream from Entiako Lake. The flows unconformably overlie quartz monzonite of the Capoose batholith. Flows are finely laminated with individual flow laminations averaging 0.5 cen-

timetre thick. Flow breccias consisting of dark red to black vitrophyric fragments are interlayered with the laminated flows through the andesite section. The andesite contains a phenocryst assemblage of plagioclase (15% by volume), biotite (1% by volume) and clinopyroxene (1% by volume). The phenocrysts are trachytically aligned in a very fine grained groundmass of feldspar microlites and devitrified volcanic glass.

RHYOLITE FLOWS (UNIT EO_r)

Quartz-phyric rhyolite flows directly overlie the laminated andesite flows along the top of a ridge at the bend in the Entiako River. The rhyolite flows are massive to thickly layered. The phenocryst assemblage comprises quartz (25% by volume), feldspar (5-10% by volume) and biotite (1% by volume). Quartz and feldspar phenocrysts are vitreous, euhedral and 2 to 4 millimetres in diameter. Biotite phenocrysts are 1 millimetre across and subhedral to euhedral. The groundmass is light grey, very fine grained and contains vugs lined with yellow clay.

RHYOLITE TUFFS (UNIT EO_r)

An isolated outcrop of rhyolitic lapilli-crystal tuff occurs approximately 1 kilometre downstream from Entiako Lake on the east side of the Entiako River valley. The tuff is well bedded with individual beds from 3 to 10 centimetres thick and has a buff-grey, moderately consolidated ash matrix. Crystals in the tuff include euhedral and fractured quartz phenocrysts (30% by volume), feldspar (5% by volume) and trace amounts of microscopic biotite, augite and sphene. Lithic fragments are 3 to 5 millimetres across and consist of devitrified siliceous glass shards, fine-grained rhyolite and fine-grained granitic rock.

ENDAKO GROUP (UNIT Ev)

The Endako Group, as originally defined by Armstrong (1949), included Oligocene or younger, flat-lying lava flows of variable composition up to 600 metres thick that underlie the Endako River drainage basin in the Babine Lake-Francois Lake areas. More recently, Diakow and Koyanagi (1988) have identified basalt flows dated at 41 Ma (whole-rock K-Ar) that unconformably overlie Ootsa Lake Group rocks in the Whitesail map area as Endako Group. Basalt flows mapped as Endako Group in the Natlakuz Lake map area nonconformably overlie rocks of the Ootsa Lake Group and infill pre-existing valleys within Ootsa Lake Group strata. These basalts occur less frequently as flat-lying erosional remnants capping hills and ridges in the northern part of the map area.

Exposures of the basaltic flows are generally massive but locally display columnar jointing. The flows are characteristically dense, black, aphyric to sparsely porphyritic but commonly include vesicular or amygdaloidal varieties. Black, glassy, feldspar-phyric flows that occur at a few localities are also included in the Endako Group. The phenocryst assemblage in the basalt flows includes plagioclase (An₆₀), augite, hypersthene and trace olivine. Clay minerals and chlorite occur as alteration products of both phenocrysts and groundmass phases. Amygdules are commonly filled with creamy opalescent silica, and calcite.

CHILCOTIN GROUP (UNIT Cv)

Early Miocene to early Pleistocene basalt flows cover an area of approximately 25 000 square kilometres extending from the Okanagan Highland northward to the Nechako Plateau (Mathews, 1989). Basalt flows mapped as Chilcotin Group are exposed in a valley, near the base of the western slope of Fawnie Nose. The basalt flows crop out as small, flat-lying, isolated knobs and boulder piles. Larger exposures occasionally display columnar jointing or flow layering. The flows are dark grey, fine grained and contain up to 15 per cent by volume yellow-green olivine phenocrysts (1 mm). Iddingsite, identified in thin section, is commonly pseudomorphous after olivine phenocrysts. Vesicles and amygdules, up to a centimetre in diameter, are often present; most are partially filled with fine-grained drusy quartz crystals. The zeolite natrolite, identified in thin section, is present in small (1 mm) amygdules.

INTRUSIVE ROCKS

The largest intrusion in the map area is the Capoose batholith (Unit LKqm) which underlies an area of approximately 100 square kilometres in the southern half of the area. The batholith has subdued relief and typically crops out along low ridges and in creeks. Exposed surfaces weather readily to produce rounded knobs and boulder piles. The batholith intrudes and pervasively alters Jurassic volcanic strata (Unit Jv) along the southwestern side of the Fawnie Range between Mount Swannell and Fawnie Nose. Alteration associated with the intrusion varies from intense silicification immediately adjacent to the contact to a zone of hornfels alteration up to 2 kilometres wide, characterized by destruction of primary volcanic textures and the local development of secondary biotite. The batholith has a bulk composition consistent with quartz monzonite but locally varies between quartz monzonite and granodiorite. Outcrops are typically light grey to salmon pink with a coarse-grained or feldspar-megacrystic texture. The phenocryst assemblage includes plagioclase, potassium feldspar, quartz, biotite and trace hornblende. Plagioclase and potassium feldspar typically occur as euhedral phenocrysts up to 1.5 centimetres in diameter. Chlorite has been identified in thin section partially replacing biotite and hornblende phenocrysts. The batholith is truncated along its western margin by the Natlakuz fault. A K-Ar date of 67.1 ± 2.3 Ma (on biotite) has been determined for the batholith (Andrew, 1988).

An oval-shaped, 1 by 2 kilometre quartz feldspar porphyry plug (Unit LKqfp) intrudes volcanic rocks of Unit Jv in the valley between Mount Swannell and Tutiai Mountain. We believe it is a satellite intrusion related to the Capoose batholith.

At the Capoose property rhyolitic dikes and sills (Unit LKr) intrude sedimentary rocks of Unit mJs and underlying volcanic rocks of Unit Jv. The intrusions are generally massive but locally are finely laminated. The texture in the intrusions varies from sparsely porphyritic to aphanitic. Euhedral, 1 to 2-millimetre quartz (7% by volume) and finely crystalline, anhedral, red and brown garnet (3% by volume) comprise the phenocryst assemblage. Potassium-

argon dates on three whole-rock specimens from the rhyolitic intrusions vary from about 64 to 70 ± 2.3 Ma (Andrew, 1988). These dates are concordant with the K-Ar age determined for the Capoose batholith.

Volcanic rocks of Unit Jv are intruded by a gabbro stock (Unit Igb) which underlies an area of approximately 9 square kilometres along the south side of Nataalkuz Lake near the eastern edge of the map area. A dike with a similar appearance and mineralogy underlies a prominent ridge 3 kilometres south of the stock. The gabbro is fine to medium grained displaying a salt-and-pepper texture and contains a phenocryst assemblage of plagioclase (50% by volume), chlorite pseudomorphs after olivine (15-20% by volume) and augite (20-25% by volume).

A number of quartz feldspar porphyry dikes (Unit Tqfp) are exposed in the northwestern corner of the map area intruding Jurassic volcanic and sedimentary rocks. The dikes contain phenocrysts of quartz, feldspar and biotite in a fine-grained siliceous groundmass.

A subvolcanic dacite plug (Unit Ti), compositionally similar to the dacite flows of Unit EO₄ crops out along the south shore of Euchu Reach. The plug is massive and has a porphyritic texture. The groundmass is light grey, fine grained and contains anorthoclase and plagioclase phenocrysts up to 1 centimetre long. Biotite is vitreous, euhedral and 3 to 5 millimetres across. Quartz (1-5% by volume) occurs as small 1 to 3-millimetre subhedral phenocrysts. Plagioclase phenocrysts commonly have anorthoclase rims.

STRUCTURE

Rocks in the Nataalkuz Lake map area are characterized by crudely layered sequences in which numerous small high-angle faults locally disrupt bedding. However, in general there is a problem recognizing throughgoing faults in the field because of sparse outcrop or broad areas underlain by homogeneous rock units that have only minor lithologic variations. For example, flow measurements and bedding attitudes from interflow sediments in Unit Jv south of Nataalkuz Lake indicate a consistent, gentle northward dip. This general trend in attitude deviates abruptly westward in a segment of the Fawnie Range south of Green Lake. A northerly trending fault immediately east of the Fawnie Range may account for this change in bedding attitude. The anomalous thickness of Unit Jv east of the Fawnie Range may be caused by subparallel northeast-striking normal faults with south-side-down movement. One such east-striking fault in the Fawnie Range displaces a distinctive fossiliferous sedimentary unit (mJs). South-side-down motion on this structure resulted in about 150 metres of displacement on the upper sediment-volcanic contact.

A major structure called the Nataalkuz fault is assumed to trend diagonally across the map area through heavily forested, low-lying terrain. Indirect evidence for this structure is the abrupt change from older Jurassic units and the Late Cretaceous Capoose batholith to the southeast, to mainly Tertiary volcanic units to the northwest. The age of this structure is uncertain; it may be synchronous with or post-date Ootsa Lake magmatism. Some obvious north-trending high-angle faults juxtapose Ootsa Lake rocks against

Jurassic and Cretaceous basement north of Nataalkuz Lake. The Endako Group appears to be unaffected by faults.

With the exception of disharmonic folds resulting from rheomorphism in viscous rhyolitic flows, the rocks in the map area lack evidence of compressional structures.

ALTERATION AND MINERALIZATION

Hydrothermally altered rocks occupy a belt about 7 kilometres long adjacent to the eastern contact of the Capoose batholith, from Tutiai Mountain in the north to Fawnie Range in the south. The most diagnostic altered rocks are white and stained with iron oxides on weathered surfaces. The contact between the Capoose batholith and country rocks appears to be a relatively planar surface inclined gently toward the east beneath the Fawnie Range. Generally, altered rocks nearest the contact are characterized by pervasive replacement of the primary minerals by silica, and destruction of primary textures. These rocks commonly grade imperceptibly, over just a few metres, into an assemblage of silica and pyrite with or without clay minerals. Disseminated pyrite is particularly abundant (up to 15% by volume) in rocks around Green Lake where it is oxidized and forms an extensive gossan. Minor sericite accompanies the quartz-pyrite assemblage in this area. On the southwest side of Tutiai Mountain the silicified zone is at least 100 metres thick and probably thicker as exposure continues down slope where it is obscured by cover. The silicified zone passes abruptly outward into a broad zone of hornfelsed propylite. The volcanic rocks are typically dark grey-green and recrystallized so that fresh surfaces have a fine granular or rare spotted appearance which obscures the primary textures. A secondary mineral assemblage of chlorite, epidote and calcite, with or without pyrite, is ubiquitous but rapidly diminishes in intensity outward from the silicified zone. Unit Jv, the most common country rock in contact with the batholith at Mount Swannel and Tutiai Mountain, contains a regional metamorphic epidote-quartz-chlorite assemblage which can be difficult to distinguish from intrusion-related alteration.

Metallic mineral occurrences in the map area all occur close to either the Capoose batholith or subvolcanic intrusions (Table 1-5-1). The main styles of mineralized showings include:

- Disseminated and fracture-controlled copper-molybdenum in the Capoose batholith and adjacent country rocks.
- Disseminated gold and silver in base metal bearing rhyolite sills (Capoose prospect).
- Minor lenses of pyrrhotite in hornfelsed propylite.
- Disseminated pyrite associated with an Eocene subvolcanic dome.

The Capoose base and precious metal deposit is the most extensively explored prospect in the map area. Rio Tinto Canadian Exploration Limited discovered the prospect in 1970 during a regional exploration program focused on the Capoose batholith and porphyry-style mineralization. Granges Exploration Ltd. explored the property from 1976 to 1985. An inventory of 28.3 million tonnes grading 0.91 gram per tonne gold and 36 grams per tonne silver was

TABLE 1-5-1
DOCUMENTED MINERAL OCCURRENCES IN THE
NATALKUZ LAKE MAP AREA

TYPE	NAMES	MINFILE NO.	ECONOMIC MINERALS	DESCRIPTION
VEIN	CAP	093F 021	chalcopyrite, molybdenite, covellite, pyrite	Sulphide mineralization occurs along fractures in quartz monzonite of the Capoose Lake Batholith. East - west trending dikes of probable Tertiary age occur proximal to mineralized fractures and may be associated with mineralization.
VEIN	CAPOOSE, CAP	093F 022	chalcopyrite, molybdenite, covellite, pyrite malachite	Northwest - southeast trending fractures within the Capoose Lake Batholith contain Cu-Mo sulphide mineralization. Best assays reported are 0.56% Cu and 0.007% MoS ₂ from a grab sample taken from one of 14 blast pits on the property.
DISSEMINATED	NED	093F 039	chalcopyrite, molybdenite, pyrite	The only outcrop on the property contains trace amounts of disseminated pyrite, chalcopyrite and molybdenite. The best intersection reported from a percussion drill hole assayed 0.044% MoS ₂ and 0.15 % Cu.
PORPHYRY	CAPOOSE, CAPOOSE LAKE (or CAPOOSE PROSPECT)	093F 040	pyrite, sphalerite, galena, chalcopyrite, arsenopyrite.	Mineralization at the Capoose prospect is hosted in and adjacent to Late Cretaceous garnet-bearing rhyolite sills which intrude Hazelton Group volcanic and sedimentary rocks. Sulphides occur mainly as disseminations but also as veinlets and fracture fillings within the rhyolite. Granges Exploration Ltd. has reported unclassified reserves of 28.3 million tonnes grading 0.51 g/t Au, and 36 g/t Ag.

reported (U.S. Securities and Exchange Commission, Form 10-K 1987).

Although the Capoose prospect was not studied in detail in 1992, its setting will be examined more closely during the field program in 1993. The reader is referred to thesis research by Andrew (1988) for a comprehensive review of the geology and genesis of this deposit. Briefly, precious metals occur in base metal sulphides disseminated in a series of rhyolitic sills. Isotopic evidence cited by Andrew favours a genetic association of the sills and the nearby Capoose batholith and a hydrothermal event involving both magmatic and meteoric fluids. She concludes that Capoose resembles "a low grade, epigenetic, intrusion-related, porphyry-style deposit".

Disseminated pyrite occurs locally within rhyolitic volcanic and subvolcanic rocks of the Ootsa Lake Group. The canyon near the confluence of the Entiako River and Euchu Reach exposes limonite-stained rhyolite with finely disseminated grains of pyrite. This rhyolite is homogeneous and well jointed; it is interpreted as an endogenous dome that may be cogenetic with an upwarped section of flanking rhyolitic flows and tuffs. The primary interest in this miner-

alization, albeit sparse, is as an indication of hydrothermal activity associated with Eocene magmatism in the map area.

ACKNOWLEDGMENTS

Fieldwork in the Natakuz Lake map area was funded by the Canada-British Columbia Mineral Development Agreement (MDA) 1991-1995.

Jack Whittles and Audrey Perry provided cheerful and able assistance in the field. We are especially grateful to Joyce of Northern Mountain Helicopters Inc., Vanderhoof, for tuning us in every morning and permitting the use of storage facilities at the base. Northern Mountain is also credited for the superb flying and courteous service maintained by pilots Joe Meier and Randy Diston. We also thank Dr. T.P. Poulton of the Geological Survey of Canada for promptly identifying fossil collections on short notice.

REFERENCES

Andrew, K.P.E. (1988): Geology and Genesis of the Wolf Precious Metal Epithermal Prospect and the Capoose Base and Precious Metal Porphyry-style Prospect, Capoose Lake Area.

- Central British Columbia; unpublished M.Sc. thesis, *The University of British Columbia*, 334 pages.
- Armstrong, J.E. (1949): Fort St. James Map-area, Cassiar and Coast Districts, British Columbia; *Geological Survey of Canada*, Memoir 252, 210 pages.
- Diakow, L.J. and Koyanagi, V. (1988): Stratigraphy and Mineral Occurrences of Chikamin Mountain and Whitesail Reach Map Areas (93E/6, 10), in *Geological Fieldwork 1987*, B.C. Ministry of Energy, Mines and Petroleum Resources, Paper 1988-1, pages 155-168.
- Diakow, L.J. and Mihalynuk, M. (1987a): Geology of the Whitesail Reach and Troitsa Lake Map Areas; B.C. Ministry of Energy, Mines and Petroleum Resources, Open File 1987-4.
- Diakow, L.J. and Mihalynuk, M. (1987b): Geology of the Whitesail Reach and Troitsa Lake Map Areas; in *Geological Fieldwork 1986*, B.C. Ministry of Energy, Mines and Petroleum Resources, Paper 1987-1, pages 171-179.
- Diakow, L.J. and van der Heyden, P. (1993): An Overview of the Interior Plateau Program; in *Geological Fieldwork 1992*, Grant, B. and Newell, J.M., Editors, B.C. Ministry of Energy, Mines and Petroleum Resources, Paper 1993-1, this volume.
- Duffell, S. (1959): Whitesail Lake Map-area, British Columbia; *Geological Survey of Canada*, Memoir 299, 119 pages.
- Mathews, W.H. (1989): Neogene Chilcotin Basalts in South-central British Columbia: Geology, Ages and Geomorphic History; *Canadian Journal of Earth Sciences*, Volume 26, pages 969-982.
- Tipper, H.W. (1963): Nechako River Map-area, British Columbia; *Geological Survey of Canada*, Memoir 324, 53 pages.

NOTES

GEOLOGY, MINERALIZATION AND LITHOGEOCHEMISTRY OF THE STUART LAKE AREA, CENTRAL BRITISH COLUMBIA (PARTS OF 93K/7, 8, 10 and 11)

By C.H. Ash and R.W.J. Macdonald

KEYWORDS: Regional geology, Cache Creek Terrane, Stuart Lake belt, ophiolitic remnant, subduction complex, mesothermal veins, gold.

INTRODUCTION

Economic mineral deposits found in oceanic terranes include: mesothermal gold-quartz veins, Cyprus-type massive sulphide, podiform chromite, platinum or cobalt associated with nickel sulphides, as well as asbestos and jade deposits. These are either hosted by, or otherwise closely associated with oceanic crustal or mantle lithologies. Mesothermal gold-quartz veins and related placers are historically the most economically significant in British Columbia. Ophiolitic crustal and upper mantle rocks are significant in that they delineate deep crustal faults, a first order control for the development of mesothermal veins. Recognition of these lithologies is therefore an important criterion in identifying areas of high mineral potential. Due to their tectonic formation these oceanic terranes are lithologically heterogeneous in detail and they remain undifferentiated on many current geological maps as a result of the small scale of previous mapping. This is particularly true for rocks of the Cache Creek Terrane (CC) in central British Columbia (Stuart Lake belt) where the existing geological database was compiled at 1:380 160 scale (1 inch to 6 miles) almost half a century ago (Armstrong, 1949; Rice, 1949).

During the 1992 field season three weeks were spent geological mapping at 1:50 000 scale in the Stuart Lake area, northeast of Fort St. James in central British Columbia (Figure 1-6-1). The area mapped occupies a northwest-trending belt to the southwest and northeast of Stuart Lake and includes parts of the NTS 93K/7 (Shass Mountain), 93K/8 (Fort St. James), 93K/10 (Stuart Lake) and 93K/11 (Cunningham Lake) map sheets. It was selected for mapping in order to provide a revised and more detailed geological database needed to evaluate its mineral potential. Stuart Lake itself, and an extensive network of logging roads with a high percentage of forest clear-cut to the west of the lake, provided easy access to a large area. Mapping has been compiled at 1:100 000-scale and combined with the geology of Paterson (1973) for the Pinchi Lake area east of Stuart Lake (Ash *et al.*, 1993).

Previous investigations by the authors in this area focused on characterizing the tectonic setting and timing of gold-quartz vein mineralization and associated felsic intrusive rocks at the Snowbird antimony-gold mesothermal vein deposit (Ash *et al.*, in preparation).

This report describes the geology and discusses the mineral potential of the area mapped. Whole-rock major, trace and rare-earth elemental data obtained for metabasalts from

the Pinchi and southern Stuart Lake area are presented and used to interpret the paleotectonic setting of these oceanic rocks.

PREVIOUS WORK

Earliest published geological maps of the region are those of Armstrong (1942a, 1944), which focused on a north-trending belt 20 kilometres wide, centred on the Pinchi fault zone. Armstrong (1949) also conducted the first systematic mapping of the region. He subdivided the Cache Creek rocks into two units, including both limestones and a mixed sedimentary suite of argillites and cherts with subordinate mafic volcanics. Ultramafic rocks throughout the belt were referred to as the "Trembleur intrusions", which he interpreted to be later, crosscutting plutons. Subsequently, Rice (1949) produced a 1:506 880-scale geological compilation and mineral occurrence map for the Smithers - Fort St. James area.

Paterson (1973; 1977) mapped and described the geology of the Pinchi Lake area and determined that the lithologies present were consistent with those of a dismembered

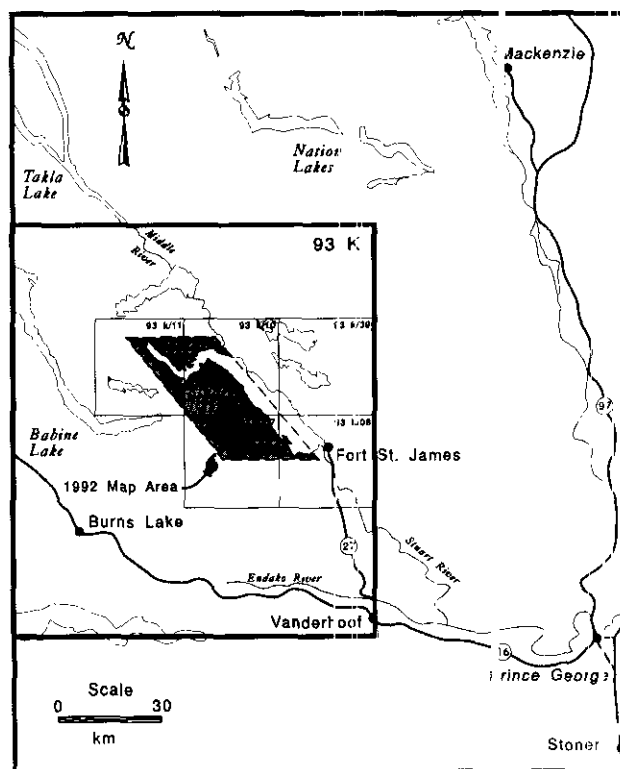


Figure 1-6-1. Location of the Stuart Lake map area.

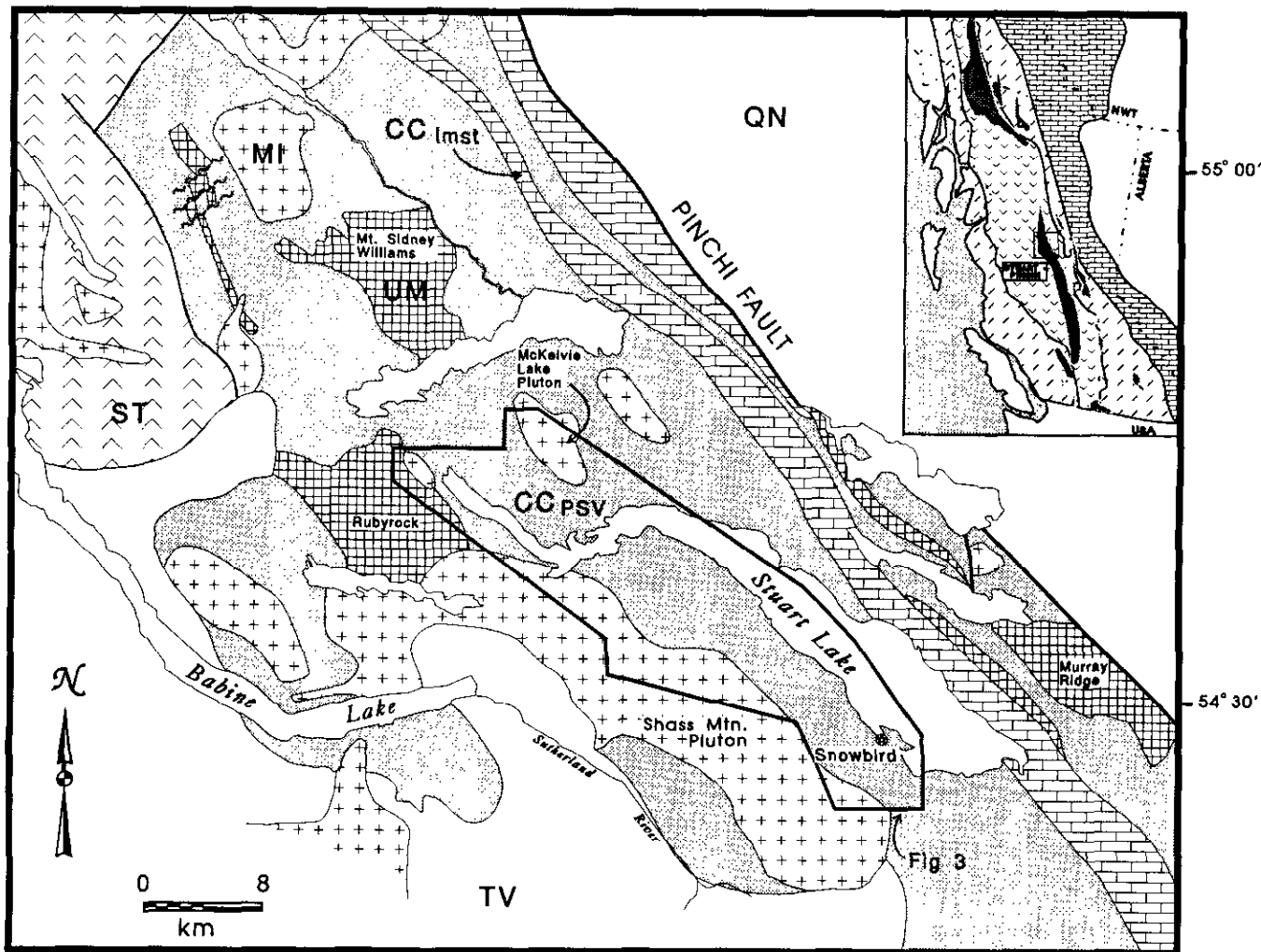


Figure 1-6-2. Regional geology of the southern Stuart Lake belt. CC = Cache Creek, PSV = Pelagic sediments and volcanics, lmst = Limestone, QN = Quesnellia, ST = Stkinia, TV = Tertiary Volcanics, MI = Mesozoic intrusions, UM = ultramafic rocks.

ophiolite suite. He suggested that the Pinchi fault may represent a fossil oceanic transform fault.

Ross (1977) documented the detailed structural history of ultramafic rocks underlying Murray Ridge to the southeast of Pinchi Lake. He defined three generations of fabric in the residual harzburgite and concluded that the two earlier fabrics were generated by mantle transport and the later fabric by high-level structural emplacement (obduction). Whittaker (1982a, b; 1983a, b) and Whittaker and Watkinson (1981; 1983; 1984; 1986) presented detailed petrological and phase chemistry data for the majority of the larger ultramafic bodies in the region which support the interpretation that they are obducted fragments of uppermost oceanic mantle material.

The geology of the Snowbird deposit (Game and Sampson, 1987a, b) and the area immediately to the west (Callan, personal communication, 1991) have been mapped in detail.

REGIONAL GEOLOGICAL SETTING

The study area covers late Paleozoic to early Mesozoic oceanic rocks of the Cache Creek Terrane (Figure 1-6-2). The Cache Creek Terrane in central British Columbia forms a north-trending belt, 450 kilometres long, which averages 60 kilometres in width, and is referred to as the Stuart Lake belt (Armstrong, 1949). Bounded by faults, this belt comprises a tectonically intercalated package of undifferentiated pelagic sediments, limestones and subordinate oceanic metavolcanic and plutonic ultramafic rocks.

The age of the Cache Creek rocks in this region is solely constrained by paleontological data. Limestones throughout the belt contain fusulinids that range in age from Pennsylvanian to Late Permian (Armstrong, 1949; Thompson, 1965). Conodonts from massive carbonate near Fort St. James indicate a middle Pennsylvanian (Moscovian) age (Orchard, 1991). Cherts collected from the shore of Stuart Lake within the town of Fort St. James contain upper Norian conodonts

(Orchard, 1991) and Carnian radiolaria (Cordey, 1990a, b). Available fossil evidence thus places the currently defined upper age of the Stuart Lake Belt at middle Upper Triassic (Norian). This interpretation is, however, based on a very limited number of samples. By comparison, the youngest fossils identified from siliceous pelagic sedimentary rocks in the Atlin Terrane are Early Jurassic in age (Cordey *et al.*, 1991) and the Stuart Lake belt probably has a similar age range.

Several large ultramafic bodies, including Murray Ridge, Mount Sydney Williams and Ruby Rock are exposed within the belt (Figure 1-6-2). These consist of harzburgite with subordinate dunite and pyroxenite or their serpentinized equivalents and are interpreted to represent residual upper-mantle material tectonically emplaced into their present positions (Paterson, 1973, 1977; Ross, 1977; Whittaker, 1982a, b, 1983a, b; Whittaker and Watkinson, 1981, 1983, 1984, 1986). Most commonly exposed as topographic highs, the inferred contacts of these ultramafic bodies tend to be circular, maintaining a consistent topographic elevation, suggesting that they may represent relatively flat-lying thrust sheets that form isolated klippen.

Cache Creek oceanic rocks are intruded throughout by Middle Jurassic and later felsic plutonic rocks that include diorites, granodiorites, tonalites and granites (Armstrong, 1949; Carter, 1981; Ash *et al.*, in preparation). These intrusions were initially divided into both the Topley and Omineca suites by Armstrong. Carter later subdivided the Topley intrusions of Armstrong into the Francois Lake and Topley suites which he defined on the basis of K-Ar mica age groupings at 173 to 206 Ma and 133 to 155 Ma, respectively.

Along its eastern margin the belt is separated from the early Mesozoic Takla rocks of the volcanic-plutonic arc terrane of Quesnellia by the Pinchi fault zone (Armstrong, 1949). Paterson (1977) described the fault zone in the Pinchi Lake area as a series of elongate fault-bounded blocks of contrasting lithology and metamorphic grade. It is interpreted as a high-angle transcurrent structure (Gabrielse, 1985) with the earliest movement occurring before the Late Cretaceous and recording a protracted history of displacement from Middle Cretaceous to Oligocene time. In the Pinchi lake area, Patterson (1973, 1977) described a belt of glaucophane-lawsonite-bearing mafic metavolcanics and metasediments within and paralleling the Pinchi fault zone that indicate a blueschist grade of metamorphism. Four K-Ar dates on muscovite from these blueschists range from 212 to 218 ± 7 Ma, indicating a Late Triassic metamorphic age (Paterson and Harakal, 1974). Referred to by Armstrong (1966) as the Pinchi mercury belt, the Pinchi fault is a strongly carbonatized zone with associated mercury mineralization occurring intermittently along most of its exposed length (Armstrong, 1942a, b, 1949, 1966; Rice, 1949). The Pinchi mine is the only significant mercury producer; during two periods of operation (1940-44, 1968-75) it produced 6.28 million kilograms (182 296 flasks) of mercury from 2.23 million tons of ore milled (I. A. Paterson, personal communication, 1992).

Contact relationships along the western margin of the central and southern parts of the belt are poorly defined, as

they are masked by both Tertiary volcanic rocks and heavy drift cover. To the north, the western boundary of the belt is marked by the Vital fault, an easterly dipping thrust fault which places Cache Creek rocks over the Sitlik assemblage (Paterson, 1974, Monger *et al.*, 1978) an enigmatic sequence of Upper Triassic to possibly Lower Jurassic volcano-sedimentary rocks (Paterson, 1974) which shows similar lithologic and tectonostratigraphic relationships to the Kutcho Formation along the southeast boundary of the Atlin Terrane (Thorstad and Gabrielse, 1986). These rocks are tentatively included with the Cache Creek Terrane (Gabrielse, 1991) and considered to be related to the destructive stage of the Cache Creek ocean basin. The unit is separated from arc-volcanic and plutonic rocks of Stikinia by the Takla fault to the west.

GEOLOGY OF THE STUART LAKE MAP AREA

The study area is underlain by accreted oceanic sedimentary, crustal and upper mantle lithologies which are cut by Middle Jurassic and possibly younger felsic plutonic rocks (Figure 1-6-3). Pelagic sediments with lesser limestone are the dominant rock types. Oceanic crustal lithologies, including mafic volcanic as well as mafic and ultramafic plutonic rocks, are found closely associated in several localities throughout the map area. Due to lack of exposure, contact relationships are poorly defined, however, most are interpreted to be tectonic.

SEDIMENTARY ROCKS

Pelagic sedimentary rocks including argillite and mixed argillite and siliceous siltstone with lesser ribboned chert dominate the map sheet. Limestone occurs in rare bedded sections but is most common as massive blocks within tectonized argillite. A geographically and lithologically distinctive bedded sandstone-argillite unit is also present.

ARGILLITE AND PHYLLITIC ARGILLITE

"Argillite" enclosing pods and slivers of limestone, ribboned chert and metavolcanic rocks is regionally the most widely exposed rock type and dominates the central, lower lying areas of the map sheet. This unit, although dominated by siltstone, contains variable amounts of finer grained mudstone and therefore the more general term argillite is used. In most outcrops it is homogeneous, variably cleaved to fissile and rarely retains any primary bedding (Plate 1-6-1). The rocks are dark grey to black and weather dark to light grey and occasionally rust-brown as a function of localized iron staining. More massive, lighter weathering lenses of chert or siliceous argillite (Plate 1-5-2) are common throughout the unit. Siliceous lenses are characterized by moderate to high aspect ratios and are usually from one to several centimetres wide and from ten to several tens of centimetres long, with long axes parallel to the dominant foliation fabric in the surrounding clastic rocks. The abundance of these lenses is both highly variable and erratic, ranging from a few identifiable lenses in more homogeneous exposures to locally comprising from 40 to 60 per cent of the outcrop. Exposures with abundant siliceous

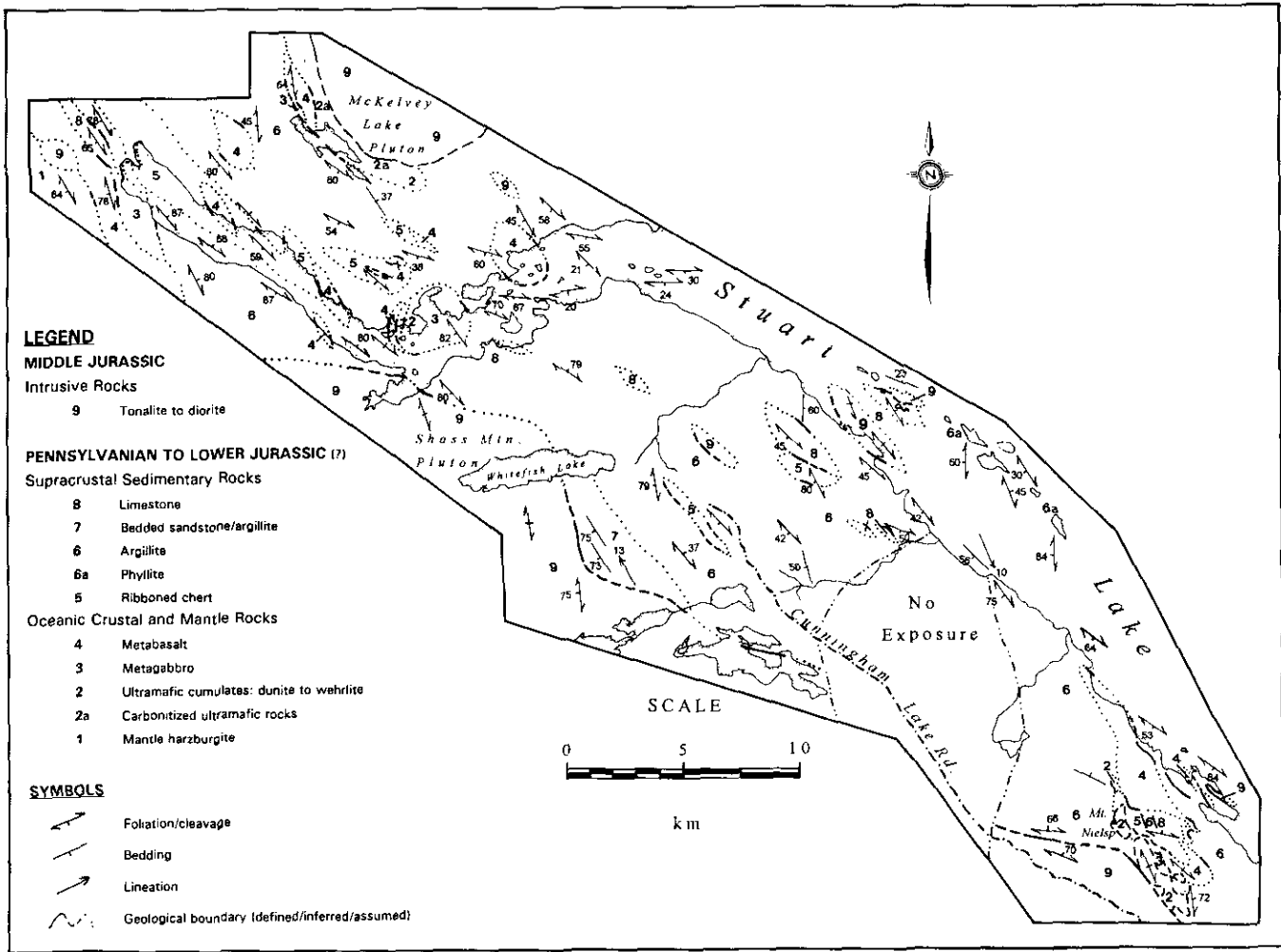


Figure 1-6-3. Generalized geology of the Stuart Lake map area.



Plate 1-6-1. Weathering appearance of strongly sheared, relatively homogeneous argillite.



Plate 1-6-2. Inhomogeneously sheared chert/siltstone and siliceous siltstone. Competent clasts are flattened, augened at their margins and are parallel to the dominant foliation fabric.

lenses were mapped as a distinct, mixed chert-argillite unit. The mixed unit rarely has any definable continuity at the present scale of mapping and is not distinguished on Figure 1-6-3.

Phyllitic varieties of the unit predominate along the shorelines of a northwest-trending chain of islands in Stuart Lake, in the east-central part of the map area. This subunit is clearly much more micaceous and weathered exposures have a silvery grey sheen reflecting their higher metamorphic grade. Siliceous or cherty lenses also characterize the phyllite but are much more attenuated and contorted than their counterparts in lower grade rocks. As the volume of siliceous lenses increases, an anastomosing fabric develops in the finer grained sediments accentuating the competency contrast between the two rock types (Plate 1-6-3).

RIBBONED CHERT

Ribboned chert is best exposed along the northeast side of the North Arm of Stuart Lake where it forms a belt of intermittent outcrops along the shoreline. It also occurs as isolated exposures throughout the argillite unit. Ribboned chert is commonly associated with the metavolcanic rocks, possibly reflecting a paleotectonic pre-emplacment stratigraphic relationship. It is very distinctive in outcrop, consisting of rhythmically layered massive chert beds with thinner interbeds of fissile argillite (Plate 1-6-4). Chert beds are buff-white to light grey to khaki and typically recrystallized. They weather a buff to chalk-white and less commonly maroon. Individual beds vary from 0.5 to 15 centimetres thick but are usually on the order of 1 to 4 centimetres. Argillaceous interbeds are dark grey and range from 0.5 to 1 centimetre in thickness. These interbeds weather preferentially and form recessive bands that impart a ribbed appearance to outcrops.

The unit is folded in most outcrops. Typically most deformational strain is accommodated by the argillaceous layers and as a result, close to tight similar folds predominate (Plate 1-6-5). Parasitic minor folds are common throughout the unit and are the clearest indication of the vergence and orientation of larger scale structures.

BEDDED SILTSTONE-SANDSTONE

Thinly laminated and rhythmically interbedded siltstone-sandstone occupies an isolated outcrop area marginal to the Shass Mountain pluton, south of Whitefish Lake. Siltstone layers are light grey to black, variably fissile, and usually form the thinnest laminations in the sections. Individual beds range from wispy crossbeds, less than 1 millimetre thick, in a sandstone matrix, to thicker, often fissile interbeds up to 2 centimetres thick. Biotite is a common accessory mineral and is interpreted to be metamorphic in origin, related to intrusion of the Shass Mountain pluton. Locally the siltstone is siliceous and cherty in appearance giving the rock a light grey colour. These layers are easily distinguished by colour, lack of fissility and more blocky fracture.

Sandstone layers are maroon, buff-weathering, fine to medium-grained quartz wacke. Beds are generally thicker than the siltstone layers and range from 0.5 to 10 centimetres in thickness.

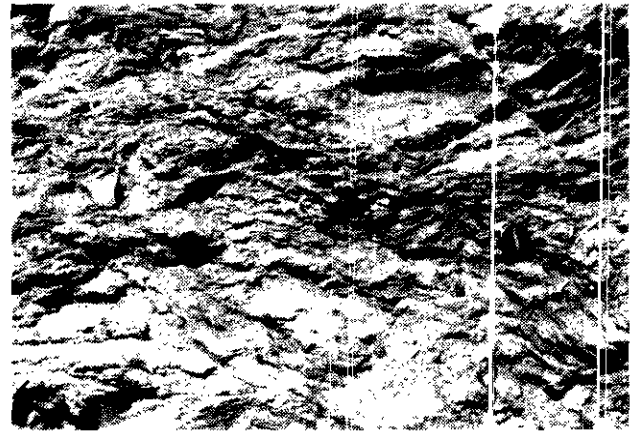


Plate 1-6-3. Competent lenses of siliceous argillite are parallel to the dominant foliation of the sheared argillaceous matrix.



Plate 1-6-4. Typical weathering appearance of the ribboned chert unit.



Plate 1-6-5. Folded ribboned chert, exposed along the western shoreline of the North Arm of Stuart Lake.

Contacts between the interbeds are sharp, and grading within the individual beds is uncommon. Sedimentary features such as crossbedding and flame structures are common. Locally the bedding is truncated by thick, massive beds of maroon biotite-bearing wacke suggestive of larger scale crossbedding. Finer and larger scale sedimentary structures observed in the unit suggest that it may be turbiditic.

LIMESTONE

Limestone forms a continuous northwest-trending belt 8 to 10 kilometres wide, immediately east of the area mapped (Figure 1-6-2). Locally throughout the map area, it is the only unit with clearly definable contact relationships, occurring most commonly as massive, isolated bodies that sit as blocks or rafts within a matrix of sheared phyllitic argillite or limy mudstone. It is typically recrystallized, weathers a buff-white to light to dark grey to blue-grey and is locally mottled. Blocks range in size from metres (Plate 1-6-6) to hundreds of metres (Plate 1-6-7) to kilometres in size.

Locally, 2 to 5-centimetre grey to buff-white massive limestone layers are interbedded with thinner 1 to 2-centimetre interbeds of tan-brown weathering, limy mudstone-siltstone. In these outcrops the limy mudstone layers are recessive and exposures have a ribbed appearance (Plate 1-6-8).

OCEANIC CRUSTAL AND UPPER MANTLE ROCKS

Oceanic crustal lithologies include metabasalts and mafic and ultramafic plutonic rocks and occur in close association with one another in four localities in the map area (Figure 1-6-3). All these areas contain the lithologic components of an idealized ophiolite or oceanic crustal section and are best characterized as "ophiolitic remnants" that have been intensely disrupted by folding and faulting during and after terrane collision. These remnants are the dominant unit in the topographically higher, northern part of the map area and along a ridge to the south. The most extensive ultramafic units mapped crop out at the highest topographic elevations. This relationship is interpreted to be a function of an inverted ophiolite stratigraphy produced by structural stacking during obduction of the oceanic lithosphere, however, currently available data are insufficient to prove this relationship.

METABASALT

Metabasalts are found in association with other crustal lithologies and in isolated localities with siliceous pelagic sedimentary rocks.

These rocks are typically grey green, fine grained, aphanitic to less commonly porphyritic and massive, however, brecciated and rare pillowed structures are identified locally. In some exposures the fine-grained aphanitic metabasalt grades into a slightly coarser, lighter weathering rock, representing a diabasic phase of the unit which is in part transitional to the metagabbroic unit described following.

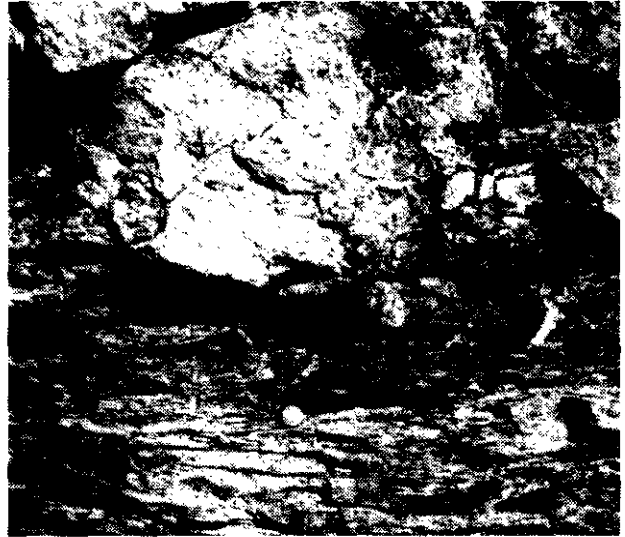


Plate 1-6-6. Massive limestone block within a sheared and flattened, limy mudstone containing small flattened massive limestone lenses.



Plate 1-6-7. Limestone block within sheared phyllitic matrix. Battleship Island, Stuart Lake.

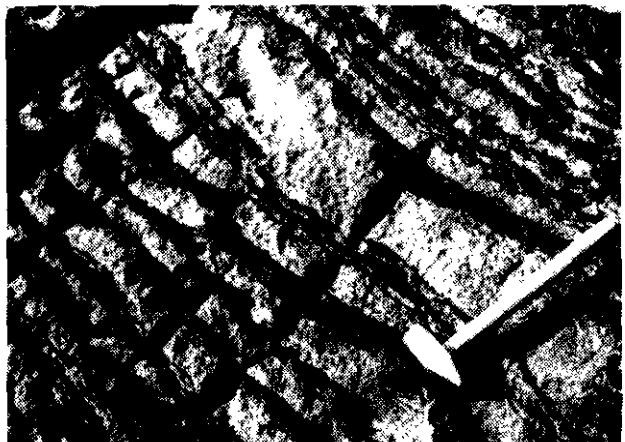


Plate 1-6-8. Bedded limestone with thinner and darker marly limestone interbeds.

The unit is microcrystalline with a felted texture. It is characterized by 40 to 60 per cent, randomly oriented, subhedral, tabular plagioclase microlites. These grains are variably sericitized and range from 0.1 to 0.5 millimetre in length. Intergranular, finer grained, variably chloritized pyroxene with trace to 2 per cent opaque minerals, forms the remainder of the rock. Augite microphenocrysts vary from subhedral to often euhedral 0.5 to 2-millimetre grains and comprise from trace to 10 per cent of the unit.

Quartz, chlorite, epidote and minor carbonate occur as the vein, vug and fracture filling material. In all but one of the thin sections examined, evidence of deformation is minimal with little or no preferential growth of secondary minerals.

METAGABBRO

Metagabbroic rocks are best exposed along the lake shore and on several islands in the middle arm of Stuart Lake. They also crop out along the eastern ridge of ultramafic rocks to the west of the Snowbird property and form a poorly defined belt between the Ruby Rock ultramafic body and the North Arm of Stuart Lake. Metagabbro in the McKelvey Lake area is confined to a few isolated exposures associated with the ultramafic rocks.

The gabbroic rocks are typically dull grey and weather a tan brown. They are medium to coarse grained, generally equigranular but locally varitextured and comprise roughly equal proportions of mafic and felsic minerals. Mafic minerals include 2 to 4-millimetre anhedral clinopyroxene replaced to varying degrees by secondary amphibole. Relict plagioclase, of similar grain size, is typically completely sericitized.

Mafic minerals in gabbroic rocks adjacent to the Shass Mountain pluton near Mount Nielsp have textures that appear to result from the close proximity of the pluton. Mafic grains are replaced by 1 to 2-millimetre tabular to highly irregular shaped amphibole (relict pyroxene?). Under cross nicols, individual grains are seen to comprise finer aggregates with a polygonal texture, suggestive of recrystallization.

ULTRAMAFIC ROCKS

The best and most continuous exposure of ultramafic rocks is along the upper levels of a series of northeast-trending ridges that include Mount Nielsp, to the west of the Snowbird property. They also form a continuous belt along the western margin of the McKelvey Lake pluton and are identified over a distance of several 100 metres in a single large cliff exposure near the large gabbro body on the north side of the middle arm of Stuart Lake.

Variably serpentinized and locally carbonatized dunitic to wehrlitic ultramafic cumulates are the most abundant ultramafic rock type. Harzburgite is only identified along the western margin of the Ruby Rock ultramafic body. The unit is black to dark green and weathers tan to dark brown where only moderately serpentinized. Where serpentinization is more complete, surfaces are light to dark grey to grey green with a characteristic mottled appearance. In several localities, incohesive sheared serpentinite has a characteristic anastomosing cleavage fabric.

Thin sections were reviewed only from the ultramafic rocks along the ridge to the west of the Snowbird deposit. These rocks locally preserve relict magmatic poikilitic texture with cumulate olivine and intercumulate pyroxene. Olivine comprises from 80 to 95 per cent of the unit as individual 1 to 3-millimetre euhedral grains which are from 40 to 75 per cent serpentinized. Relict grains form isolated kernels surrounded by mesh-textured antigorite, as serpentinization has developed along fractures. Development of secondary magnetite in association with serpentinization is minor to rare. Relict pyroxene is not preserved, as the intercumulate phase is totally replaced by fibrous aggregates of chlorite and talc. The relict cumulate poikilitic texture is, however, well preserved. Chromite spinel is a minor accessory mineral, comprising less than 1 per cent of the rock. Its habit is highly variable, forming 0.3 to 2-millimetre, anhedral to subhedral grains that are typically found in the altered intercumulate phase.

CARBONATIZED ULTRAMAFIC ROCKS

Carbonatized ultramafic rocks are exposed on the Snowbird property and locally developed marginal to the McKelvey Lake pluton. At the Snowbird property, carbonatized and potassium metasomatized ultramafic rocks occur as slivers or tectonic lenses closely associated with mineralized quartz veins along the Snowbird fault zone. These are buff-cream coloured, rusty orange-brown weathering rocks comprising coarse-grained aggregates of magnesite and quartz that are cut by a network of white dolomite and quartz veinlets. The alteration affecting these ultramafic rocks has completely obliterated any primary minerals and textures which would help to interpret the original protolith.

The extent of carbonate alteration affecting ultramafic rocks along the western margin of the McKelvey Lake pluton is not well established. Carbonatization is most pronounced immediately northeast of McKelvey Lake, in a cliff face 50 to 60 metres high. The effect of carbonate alteration diminish over a distance of approximately 1 kilometre north of this exposure.

INTRUSIVE ROCKS

The Middle Jurassic (165 Ma) Shass Mountain pluton (Ash *et al.*, in preparation) is the largest intrusive body in the region. It is an elongate northwest-trending intrusion exposed between Stuart Lake and Sutherland River (Figure 1-6-2) that metamorphoses oceanic rocks along the western edge of the map area. The western margin of a previously unnamed intrusion, informally referred to here as the McKelvey Lake pluton, crops out along the northeastern edge of the area. It is similar in weathering appearance, texture and mineralogy to the Shass Mountain body.

Isolated, small stocks that are compositionally and texturally similar to both the Shass Mountain and McKelvey Lake plutons are exposed northwest of the North Arm of Stuart Lake and a poorly constrained body crops out east of Whitefish Lake. Small, pervasively metasomatized stocks are identified in two other localities.

The Shass Mountain pluton is a medium to coarse-grained, equigranular white to buff-white weathering tonalite (Plate 1-6-9). The unit varies from being completely isotropic to locally displaying a well-developed flow fabric, most conspicuous near the margin of the body. Orientation of the fabric consistently parallels the intrusive contact and is characterized by a penetrative foliation defined by alignment of mafic minerals (Plate 1-6-10). Mafic xenoliths are also common near the margins of the pluton and include fragments of both hornfelsed sedimentary country rocks and more commonly, melanocratic, medium to coarse-grained amphibole-rich cognate xenoliths. Within undeformed areas of the intrusion, xenoliths are completely angular and range from several centimetres to several tens of centimetres across. In foliated areas of the pluton, mafic xenoliths are strongly attenuated and visually emphasize the fabric where they are elongated within foliation planes (Plate 1-6-11). Locally, these xenoliths are completely attenuated, giving the unit a banded or striped appearance.

Primary minerals, in decreasing order of abundance, are plagioclase, quartz, amphibole and biotite. Both felsic and mafic minerals show little or no sign of secondary alteration in thin section. Plagioclase occurs as 1 to 3-millimetre, lath-shaped subhedral to euhedral cumulate grains which comprise from 35 to 40 per cent of the rock. Quartz is typically anhedral, comprising from 35 to 40 per cent of the unit and occurs as both isolated 1 to 3-millimetre anhedral grains and as larger 3 to 5-millimetre grains which poikilitically enclose plagioclase, hornblende and biotite. Mafic mineral content locally varies from 15 to 30 per cent. Hornblende which forms 0.5 to 5-millimetre euhedral to subhedral grains is usually the dominant mafic mineral, however, biotite occurs locally in greater abundances.

The mineralogy and preliminary elemental analysis of the pluton supports an I-type classification corresponding to a biotite hornblende tonalite association (Ash *et al.*, in preparation).

METASOMATIZED SATELLITE STOCKS

Two small pervasively metasomatized linear felsic intrusive bodies are known in the map area. A northwest-trending elongate body near the lake shore east of the Snowbird property was mapped by Game and Sampson (1987a, b). The other outcrops as two small, isolated islands in the centre of Stuart Lake.

A finer grain size and a dull brown to flesh-tone weathering appearance clearly distinguish these bodies from the previously described felsic plutonic rocks. Disseminated 2 to 4-millimetre pyrite cubes, varying in abundance from 2 to 4 per cent, produce rusty brown weathering pits on exposed surfaces which are also diagnostic. Preliminary petrographic analysis indicates that secondary sericite and carbonate are also present in addition to pyrite.

The Snowbird stock is an oblong tonalite body, roughly 1 kilometre long and up to 200 metres wide, which intrudes deformed pelagic sediments and metabasaltic rocks between Stuart Lake and the main Snowbird showing (Figure 1-6-3). This intrusion was referred to as the "granite zone" by Faulkner and Madu (1990). This usage is discontinued here as petrographic review combined with potassium feldspar

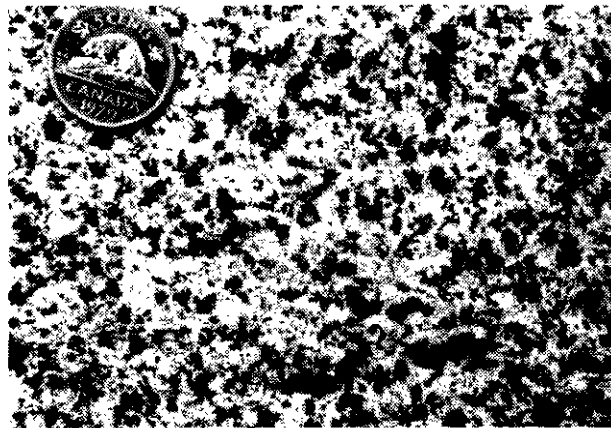


Plate 1-6-9. Isotropic, equigranular texture of the Shass Mountain pluton.

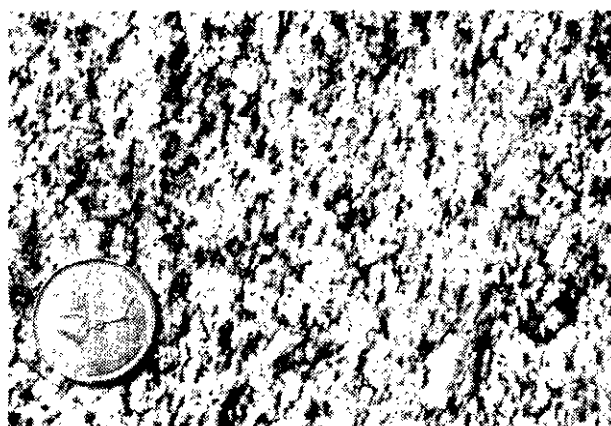


Plate 1-6-10. Alignment of mafic minerals defines a well-developed foliation fabric.



Plate 1-6-11. Strongly attenuated, mafic xenoliths aligned subparallel to foliation in the Shass Mountain pluton.

staining indicates that the intrusion is potassium-deficient and therefore not a granite. Quartz and feldspar occur in roughly equal proportions varying from 40 to 45 modal per cent. Mafic minerals which comprise from 10 to 20 modal per cent of the rock are pervasively carbonatized and weather orange brown.

Preliminary petrological analysis and whole-rock geochemical data for the Snowbird stock suggest that it is compositionally similar to the Shass Mountain pluton 5 kilometres to the west. Argon-argon isotopic analysis of sericite by laser step-heating methods indicates a Middle Jurassic (157 Ma) age of potassium metasomatism (Ash *et al.*, in preparation). This age is interpreted to represent alteration due to the effects of magmatic volatiles during the final stages of crystallization.

STRUCTURE

The map area is dominated by a prominent structural grain that is defined by the subparallel alignment of major structures, characteristic of the Stuart Lake belt as a whole (Armstrong, 1949). The grain trends predominantly to the north and northwest and is typically steeply dipping but locally flattens and rotates to a westerly orientation. This feature is most conspicuous in the centre of the map sheet at the bend in Stuart Lake and suggests that the shape of the lake may be structurally controlled.

Equal-area, lower hemisphere stereographic projections indicate several map-scale trends (Figure 1-6-4). The plots suggest the rocks are folded about subparallel axes that reflect the dominant structural grain. Cleavage and bedding mimic each other in distribution and orientation, striking northwest and dipping southwest and northeast, with moderate southwesterly dips predominating. Bedding-cleavage intersections and axes of small-scale parasitic folds plunge gently to moderately toward the southeast and northwest and are most easily recognized in the pelagic sedimentary sequences. Fold types range from open buckle folds in the thicker, more competent layers, to tight to isoclinal similar folds in the thinner bedded lithologies with the highest competency contrasts. A strong axial planar cleavage is associated with this folding and varies from gently inclined to upright, rotated around northwest-trending axes with changes in the attitude of the folds. Higher order, parasitic folds display characteristic S, M and Z-shapes and are a reflection of the asymmetry of the larger scale structures.

Folding is not as clearly recognizable in the more massive units such as thickly bedded limestone, and the plutonic and volcanic rocks, however, a foliation fabric paralleling the axial planar cleavage of the sediments is common and forms broad zones within these rocks. Similarly, flow fabrics in rocks of the Shass Mountain pluton and related stocks parallel this regional trend.

Discrete zones of intense shearing and foliation development are identified in all units and range in width from centimetres to tens of metres; they are most pronounced in silty layers. These shears locally disrupt bedding, fragmenting individual layers and isolating them as competent blocks within an anastomosing sheared matrix. Shearing appears to be related to folding as these fabrics roughly parallel the axial planar cleavages of the folds and is probably the result

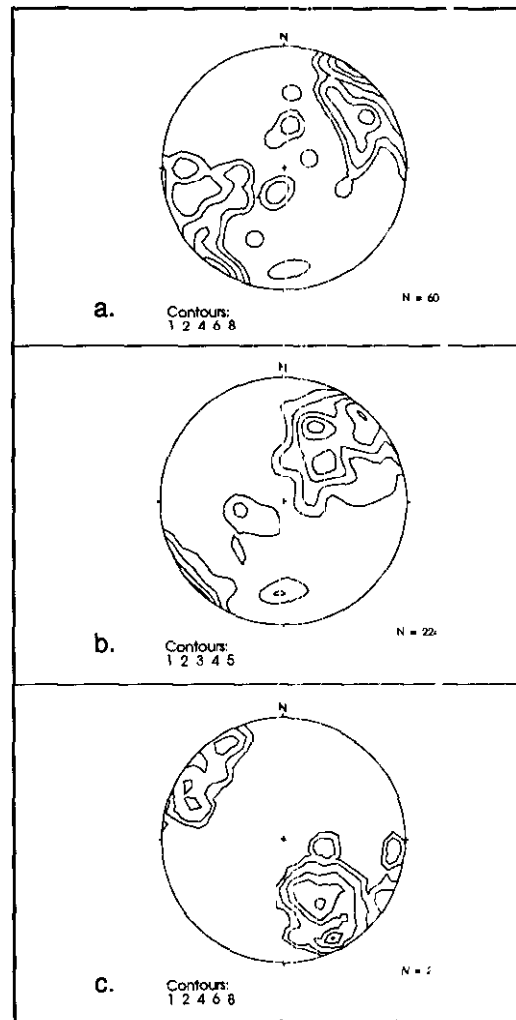


Figure 1-6-4. Equal-area, lower hemisphere stereographic projections of structural data from the Fort St. James map area; (a) plot of poles to bedding; (b) plot of poles to foliation and cleavage; (c) plot of lineations, includes axes of small-scale folds and bedding-cleavage intersections.

of a progressive increase in deformation of the folded layers.

BASALT GEOCHEMISTRY

The major element chemistry of basaltic rocks in the Pinchi Lake area has been presented and discussed previously by Paterson (1973). He established the presence of both alkali and tholeiitic basalts in the area.

A total of 25 mafic metavolcanic samples were collected from near Pinchi Lake and within the general vicinity of the Snowbird deposit (Figure 1-6-5). Major and rare-earth element (REE) analyses have been obtained for nearly all the samples collected, but trace element analyses are currently available for only 14 of the samples (Table 1-6-1). These chemical data are used to interpret the paleotectonic setting in which these rocks erupted.

All samples analyzed are basaltic in composition with silica contents varying between 45 and 51 weight per cent

(Figure 1-6-6a) and are divisible into both alkaline and subalkaline suites (Figure 1-6-6b). Trace element discriminant diagrams involving the immobile high field-strength elements (Y, Zr and Nb; Figure 1-6-7a, b and c) indicate that subalkaline and alkaline suites fall into the fields of mid-ocean-ridge (MORB) and within-plate basalts (WPB), respectively. This relationship is also evident on a plot using ratios of more incompatible to less incompatible elements (e.g., Ti/V, Figure 1-6-8). On the titanium *versus* vanadium plot the subalkaline basalts occupy a field which in part overlies the area of overlap between arc-tholiites and MORBs. The range in titanium and vanadium abundances of this suite, however, defines a field which clearly follows the hypothetical fractionation path (solid line) characteristic of MORBs (Shervais, 1982). Alkali basalts have Ti/V ratios greater than 50, consistent with ratios of Hawaiian alkali basalts and suggesting an ocean-island setting.

On a MORB-normalized multi-element plot (Figure 1-6-9) the two suites are clearly distinguished. Alkali basalts are enriched in most of the incompatible elements

relative to MORBs. The least incompatible elements (Y and Yb) show no enrichment relative to MORBs while the most incompatible elements (Th, Ta and Nb) show a humped pattern characteristic of within-plate basalts (Pearce, 1982, 1983). More specifically, they show abundance patterns which are indicative of ocean islands and a negative slope between Y and Yb clearly discriminates this suite from E-MORBs (Holm, 1985). The subalkaline suite displays characteristic N-MORB abundances for all the high field-strength elements. Unlike the high field-strength elements which are considered to be generally immobile during hydrothermal alteration or low-grade metamorphism (Cann, 1970; Pearce and Cann, 1973; Pearce, 1983), abundances of the low field-strength or large-ion lithophile elements (Sr, K, Rb and Ba) are highly variable in both suites. The mobility of these elements due to the effects of alteration and metamorphism is well established (Humphries and Thompson, 1978; Pearce 1980, 1982, 1983; Pearce and Cann, 1973; Saunders *et al.*, 1980) and not considered diagnostic. The MORB abundances for thorium, the least

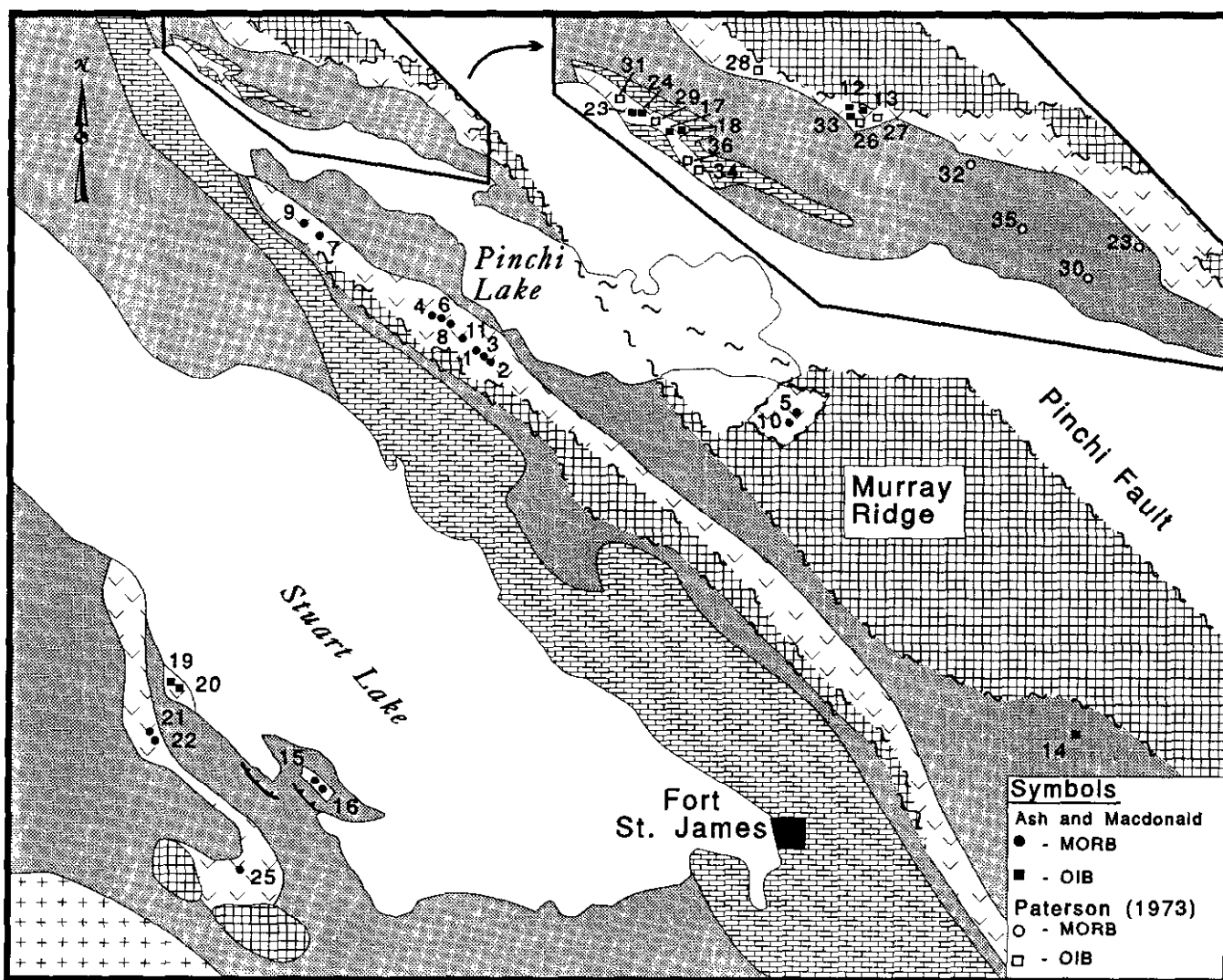


Figure 1-6-5. Generalized geology of the Stuart - Pinchi Lakes area illustrating the locations and geochemical character of sampled metabasaltic rocks. MORB = mid-ocean-ridge basalts, OIB = ocean island basalts.

TABLE 1-6-1
REPRESENTATIVE MAJOR, TRACE AND RARE-EARTH ELEMENT ANALYSES
OF METABASALTS FROM THE STUART-PINCHI AREA

Sample	C89-42 02	C89-42 03	C89-42 04	C89-42 05	C89-44 01	R89-13 02-03	R89-14 03	R89-13 02-01	R89-14 04-02	R89-15 02	C89-43 05	C89-46 04	C89-46 06	R89-17 03
Location	1	2	3	4	5	6	7	8	9	10	11	12	13	14
SiO ₂	49.48	48.49	49.65	50.97	49.06	49.85	50.19	49.42	49.41	50.13	45.17	48.72	45.60	45.56
TiO ₂	1.48	1.41	1.66	1.02	0.73	1.55	1.86	1.38	1.50	0.76	2.99	3.69	1.67	3.19
Al ₂ O ₃	13.91	13.94	13.76	14.32	13.44	13.57	13.07	14.22	14.26	15.41	12.54	12.71	12.34	12.50
Fe ₂ O ₃	11.94	11.10	12.16	11.53	9.29	13.34	14.23	12.05	12.91	8.99	12.46	12.90	11.20	12.38
MnO	0.16	0.20	0.22	0.19	0.22	0.19	0.26	0.19	0.24	0.19	0.15	0.13	0.12	0.14
MgO	7.30	7.95	6.33	6.14	6.59	9.48	7.32	5.82	7.14	5.93	5.16	4.54	4.58	7.48
CaO	5.38	10.84	9.07	6.75	8.42	5.01	8.29	7.54	9.08	8.76	6.99	7.21	7.75	9.73
Na ₂ O	4.32	3.42	4.13	3.95	3.10	3.94	3.36	3.16	3.25	3.80	1.98	4.96	2.27	2.41
K ₂ O	1.01	0.34	0.09	0.15	0.98	0.62	0.16	0.88	0.04	0.56	3.22	0.47	3.24	0.84
CO ₂	0.14	0.22	0.62	0.44	0.73	0.44	0.22	0.25	0.14	1.55	0.65	0.72	0.22	0.4
P ₂ O ₅	0.10	0.11	0.12	0.07	0.11	0.11	0.13	0.10	0.11	0.13	0.43	0.46	0.55	0.44
S	0.01	0.02	0.03	0.06	0.01	0.01	0.15	0.14	0.09	0.28	0.01	0.03	0.01	0.01
LOI	3.61	3.39	2.77	3.76	4.65	3.87	2.36	3.32	3.27	5.44	4.55	3.69	3.90	4.33
Total	98.84	101.43	100.61	99.35	97.33	101.98	101.60	98.47	101.44	101.93	96.30	100.23	6.45	99.95
FeO	7.18	6.24	7.13	7.68	5.81	9.97	7.97	8.18	9.11	5.60	6.89	7.89	6.53	8.18
Ni	39	42	39	47	51	25	23	51	25	22	320	195	69	121
Cr	122	192	130	136	313	76	51	146	53	90	389	240	75	211
Ba	56	16	11	29	1436	135	20	117	10	484	262	69	72	114
Sr	81	66	75	96	297	76	101	83	67	356	123	228	134	134
Rb	7	5	10	10	19	10	10	9	10	12	64	13	69	16
Zr	79	82	99	50	62	83	104	76	81	80	254	271	287	258
Y	31	33	39	25	20	36	40	32	34	21	28	32	31	28
Nb	6	7	6	4	5	4	7	4	4	5	31	33	53	36
Ca	3	4	4	4	6	4	4	6	6	5	5	6	6	6
La	7	8	1	4	15	2	9	14	4	15	38	34	46	32
Ce	11	15	18	8	25	17	17	12	23	23	59	61	94	79
V	341	338	353	337	249	361	393	344	362	210	249	250	326	282
Sc	38	42	41	37	40	37	43	40	41	30	27	26	27	31
Hf	1.6	2.2	0.0	1.3	1.6	0.0	0.0	0.0	0.0	5.9	6.3	6.5	2.0	2.0
Ta	0.3	0.3	0.39	0.3	0.3	0.16	0.16	0.23	0.23	1.6	1.9	3.0	0.3	0.3
Th	0.1	0.1	0.2	0.1	1.3	0.2	0.2	0.1	0.1	2.2	2.2	4.5	1.9	1.9
La	2.0	2.6	3.3	1.6	6.3	2.9	2.9	3.0	3.0	24.2	25.5	39.4	13.0	13.0
Ce	7	10	11.0	6	14	9.3	9.3	9.4	9.4	53	53	79	22	22
Pr			1.9			1.6	1.6	1.6	1.6			11.7		
Nd	7	8	10.9	5	8	9.2	9.2	9.1	9.1	32	32	40	11	11
Sm	2.1	2.8	3.8	1.7	2.2	3.3	3.3	3.4	3.4	7.2	7.6	8.2	2.8	2.8
Eu	0.80	0.99	1.4	0.65	0.61	1.3	1.3	1.3	1.3	2.39	2.40	2.70	0.38	0.38
Gd			5.1			4.9	4.9	4.4	4.4			9.2		
Tb	0.6	0.7	0.9	0.4	0.4	0.9	0.9	0.8	0.8	1.0	1.1	1.3	0.5	0.5
Dy			6.27			5.61	5.61	5.38	5.38			6.61		
Ho			1.30			1.18	1.18	1.15	1.15			1.08		
Er			3.89			3.52	3.52	3.35	3.35			2.73		
Tm			0.55			0.52	0.52	0.46	0.46			0.33		
Yb	2.28	2.90	3.43	2.03	1.42	3.31	3.31	3.05	3.05	1.75	1.73	1.90	1.60	1.60
Lu	0.35	0.43	0.56	0.30	0.22	0.50	0.50	0.45	0.45	0.24	0.23	0.27	0.25	0.25

Sample	CAS91 -71	CAS91 -75	CAS91 -78	CAS91 -79	RMA91 -15-3	RMA91 15-4	RMA91 -15-12	RMA91 -15-13	RMA91 17-1	RMA91 17-2	RMA91 -18-
Location	15	16	17	18	19	20	21	22	23	24	25
SiO ₂	48.62	55.95	46.05	45.52	44.94	50.86	47.33	49.29	46.67	44.80	57.93
TiO ₂	1.12	1.17	2.47	2.90	2.76	2.55	0.88	1.18	3.60	4.20	0.64
Al ₂ O ₃	14.42	12.84	10.37	11.33	14.42	13.09	15.19	13.87	12.38	13.61	15.05
Fe ₂ O ₃	10.66	10.24	12.14	10.79	14.84	13.52	9.86	11.85	11.13	11.80	10.23
MnO	0.19	0.20	0.17	0.14	0.17	0.14	0.16	0.21	0.10	0.12	0.16
MgO	6.80	6.48	10.81	10.17	7.36	5.70	6.05	5.97	7.59	5.67	5.40
CaO	7.32	6.39	10.32	10.60	5.20	5.55	11.08	9.09	8.50	9.26	4.34
Na ₂ O	3.70	3.61	1.60	1.41	2.45	2.13	3.51	3.82	2.91	3.52	3.41
K ₂ O	0.15	0.15	0.39	0.85	0.11	0.86	0.84	0.79	1.45	1.29	0.21
P ₂ O ₅	0.09	0.09	0.29	0.32	0.21	0.18	0.14	0.12	0.53	0.69	0.01
LOI	6.42	2.66	4.64	5.17	6.57	5.13	4.21	3.42	4.42	4.43	2.11
Total	99.49	99.78	99.25	99.20	99.03	99.71	99.25	99.61	99.28	99.39	99.61
La	2.3	3.7	19.8		11.2	11.1	2.2	2.8	31.1	41.2	1.1
Ce	7.5	12.8	46.6		30.5	29.1	5.2	6.8	75.4	93.0	4.1
Pr	1.3	1.7	6.1		4.3	4.0	1.0	1.3	10.0	11.7	0.1
Nd	7.3	9.0	28.3		21.1	19.5	5.5	7.2	46.4	50.2	4.1
Sm	2.5	2.9	6.4		5.7	5.3	2.1	2.8	10.0	10.7	1.1
Eu	0.8	0.9	2.1		1.9	1.8	0.8	1.0	3.2	3.5	0.1
Gd	3.6	3.8	6.4		6.5	6.0	3.4	4.4	9.7	14.1	2.1
Tb	1	1	1		1	1	1	1	1	1	1
Dy	4	5	5		6	5	4	5	6	6	6
Ho	0.92	1.00	0.86		1.02	0.96	0.92	1.14	1.07	1.04	0.51
Er	3	3	2		3	2	3	3	3	2	1
Yb	2.35	2.53	1.17		1.81	1.73	2.59	2.92	1.76	1.58	1.61

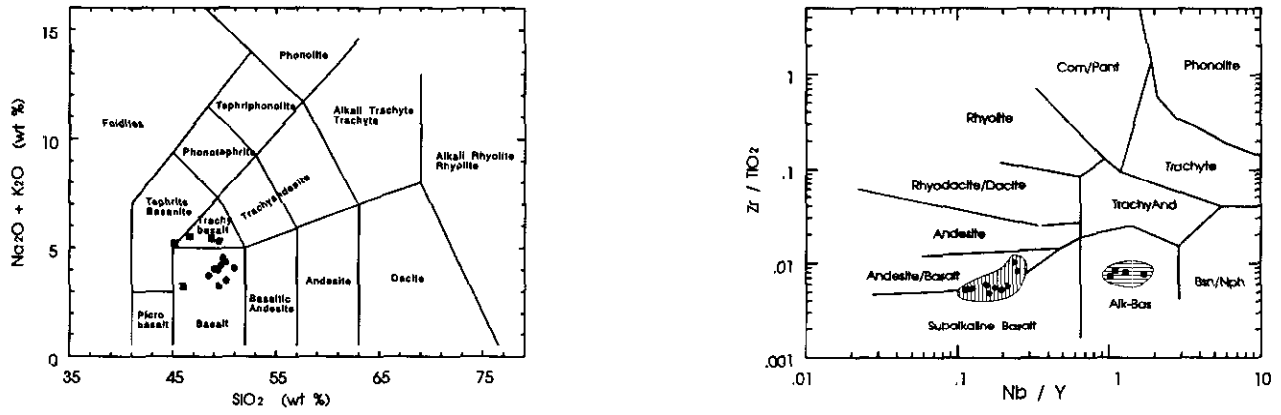


Figure 1-6-6. Classification of metavolcanic rocks from the Stuart - Fort St. James area using (a) $\text{Na}_2\text{O} + \text{K}_2\text{O} - \text{SiO}_2$ (after Le Maitre, 1984), and (b) $\text{Zr}/\text{TiO}_2 - \text{Nb}/\text{Y}$ (after Winchester and Floyd, 1977).

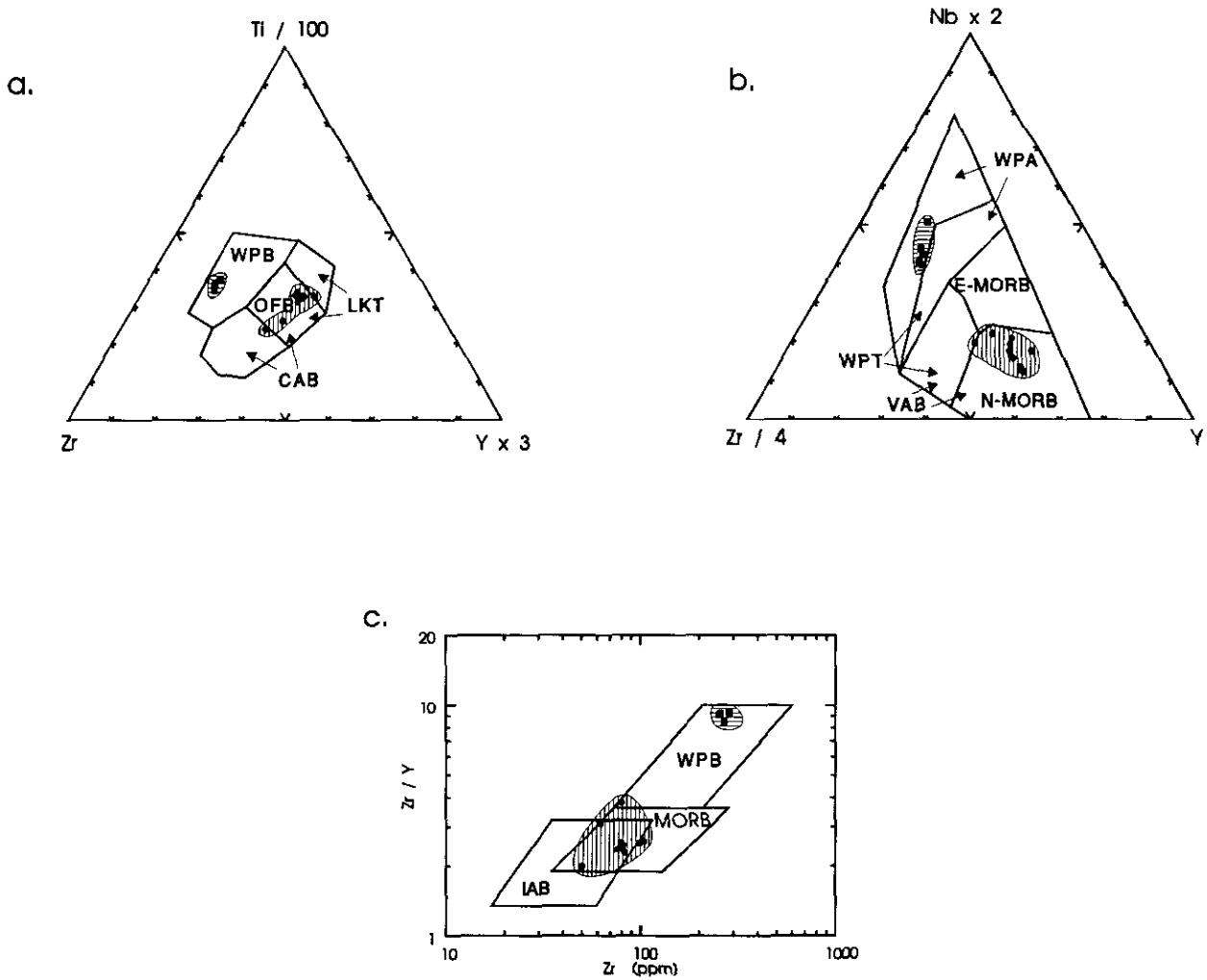


Figure 1-6-7. Trace element discriminant diagrams illustrating fields of metabasalts from the Stuart - Fort St. James area using (a) $\text{Ti} - \text{Zr} - \text{Y}$ (after Pearce and Cann, 1973) (b) $\text{Nb} - \text{Zr} - \text{Y}$ (after Meshede, 1986) and (c) $\text{Zr}/\text{Y} - \text{Zr}$ (after Pearce and Norry, 1979). WPA = within-plate basalts, OFB = ocean-floor basalts, LKT = low-K tholeiites, MORB = mid-ocean-ridge basalts (E = enriched, N = normal), VAB = volcanic arc basalts, IAB = island arc basalts.

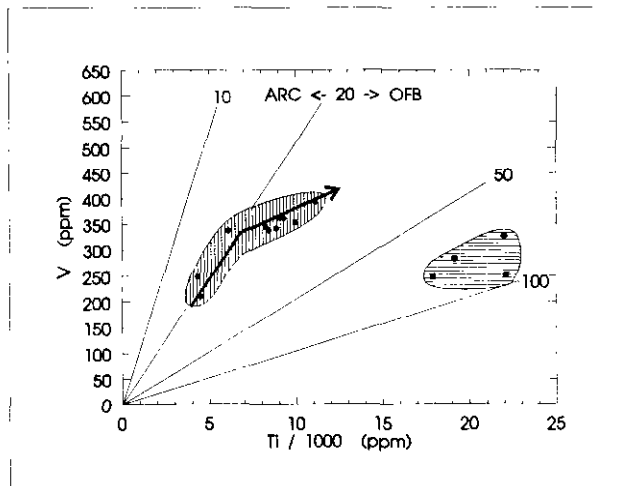


Figure 1-6-8. Plot of Ti vs V, illustrating fields of metabasalts from the Stuart - Fort St. James area (after Shervais, 1982).

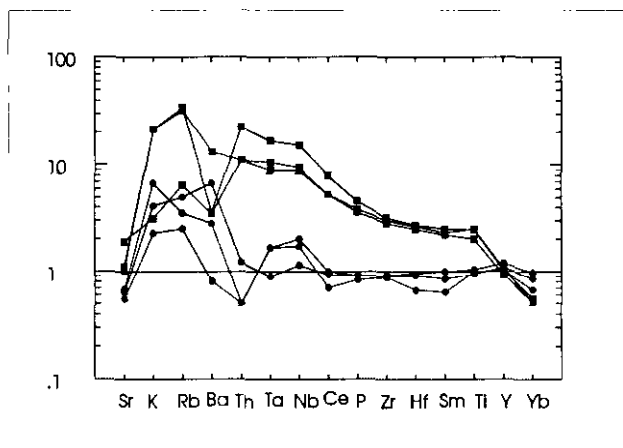


Figure 1-6-9. MORB-normalized multi-element distribution patterns for metabasalts from the Stuart - Fort St. James area. Normalization values from Pearce (1982).

mobile large-ion lithophile element (Wood *et al.*, 1979) are consistently compatible with or lower than N-MORB abundances, suggesting no suprasubduction zone influence.

Subdivisions of the samples for which only major and REE abundances are available (Table 1-6-1) are clearly defined by differences in their REE contents (Figure 1-6-10). The ocean-island suite has a negative slope characterized by light-REE enrichment accompanied by a less pronounced heavy-REE depletion. In contrast the MORB samples display relatively flat to slightly concave upward patterns. The two suites may also be discriminated on the basis of major element content using titanium abundances (Table 1-6-1) as illustrated by Figure 1-6-8. The MORB samples range from 0.73 to 1.86 weight per cent TiO_2 while rocks of ocean-island affinity vary from 2.5 to 5 weight per cent. This difference in TiO_2 abundances was used to subdivide major element analyses presented by Paterson (1973) for the Pinchi Lake area (Table 1-6-2, Figure 1-6-5, inset map).

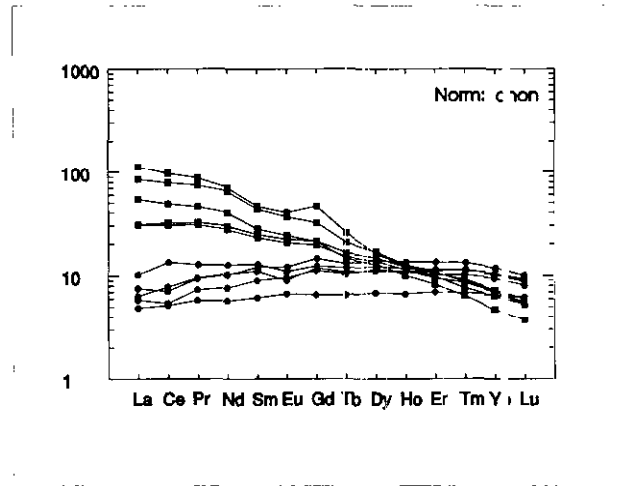


Figure 1-6-10. Chondrite normalized rare-earth elemental abundances of metabasaltic rocks from the Stuart - Fort St. James area. Normalization values from Andrews and Ebihara (1982).

DISCUSSION OF RESULTS

Available geochemical data suggest that mafic volcanic rocks in the Pinchi - southern Stuart Lake area record two distinct paleotectonic environments of basaltic volcanism. Regionally, basalts of mid-ocean ridge affinity are most prevalent (Figure 1-6-5). Except for one isolated locality, ocean-island basalts are localized along the Pinchi fault zone, while those of subalkaline composition occur both east and west of the fault and are predominant to the west.

The presence of basaltic rocks with geochemical signatures indicative of ocean islands, primarily along the eastern margin of the Stuart Lake belt in this region, may explain the presence of broad, thick sections of massive, shallow-water limestone. This relationship supports development of carbonate as reefs fringing ocean islands within the Cache Creek ocean, and is consistent with this ocean basin developing at a normal mid-ocean ridge spreading centre. It would clearly be of interest to determine the lateral extent of the ocean-island basalt-limestone association farther north along the eastern margin of the Stuart Lake belt.

MINERALIZATION

As previously indicated, mineral deposits identified in oceanic terranes are found in association with igneous oceanic crust or metamorphic upper mantle rocks. Four isolated areas of oceanic crustal rocks are present in the map area, three of which are not portrayed on the previous geological map of the area (Armstrong, 1945). The Snowbird mesothermal gold-stibnite-quartz-carbonate vein deposit is clearly associated with oceanic ultramafic crustal rocks and the most economically significant.

SNOWBIRD GOLD-STIBNITE DEPOSIT

The Snowbird deposit (MINFILE 093K 036) is the only significant mineral occurrence known in the map area. It is a shear-hosted mesothermal quartz-carbonate vein deposit,

TABLE 1-6-2
MAJOR ELEMENT CHEMISTRY OF METAVOLCANIC ROCKS FROM
THE PINCHI LAKE AREA (From Paterson, 1973)

Location	26	27	28	29	30	30	31	32	33	34	35	36
SiO ₂	43.80	44.60	44.20	45.60	33.10	32.30	42.90	47.90	42.70	44.80	46.70	47.50
TiO ₂	4.35	2.72	3.36	3.22	1.75	1.63	5.51	1.49	1.20	4.00	1.49	3.64
Al ₂ O ₃	14.70	13.10	18.10	13.70	9.10	9.20	10.50	14.40	13.80	16.40	14.10	14.60
Fe ₂ O ₃	3.90	5.00	3.10	5.60	5.20	5.00	4.20	4.10	4.40	5.20	5.10	3.60
FeO	9.60	6.70	6.80	6.30	4.30	4.30	8.10	7.80	5.50	5.20	7.00	7.60
MnO	0.13	0.16	0.18	0.17	0.20	0.21	0.11	0.14	0.10	0.06	0.14	0.13
MgO	4.50	7.20	3.00	5.40	6.20	6.00	7.30	5.60	7.00	4.40	7.50	4.90
CaO	6.50	9.50	8.60	9.80	20.00	21.00	11.10	7.90	13.80	8.80	9.20	8.90
Na ₂ O	4.80	2.00	5.10	2.60	3.20	3.10	2.90	2.90	1.10	2.70	1.90	3.30
K ₂ O	0.10	2.60	0.30	0.80	1.30	1.40	0.10	0.20	0.20	1.70	0.10	0.80
P ₂ O ₅	0.56	0.28	0.36	0.37	1.29	2.14	0.08	0.13	0.11	0.17	0.11	0.46
CO ₂	0.80	0.60	0.70	0.30	9.20	10.40	0.80	1.20	4.00	0.10	1.30	0.10
H ₂ O	4.70	4.30	4.60	4.50	3.90	3.80	4.80	5.10	6.00	5.70	6.60	5.00
Total	98.40	98.80	98.40	98.40	98.70	100.50	98.20	98.90	99.90	99.10	101.20	100.50

located 10 kilometres west of Fort St. James at the south-eastern end of Stuart Lake, several hundred metres inland from a small peninsula.

The geology of the Snowbird-Sowchea area has been mapped and in part compiled at a 1:10 000-scale (N. Callan, personal communication, 1992). The area of the main showing has been mapped in greater detail (Heshka, 1971; Game and Sampson, 1987a, b). Previous published descriptions of the deposit include those of Armstrong (1949), Faulkner (1988) and Faulkner and Madu (1990). Fluid inclusion and isotope data on mineralized quartz-carbonate veins have been presented by Madu *et al.* (1990).

The early history of the deposit, as briefly reviewed below, is taken from Armstrong (1949). The property was first staked in 1920 and initially referred to as the McMullen Group; it has obtained its current name from the Snowbird claim block covering the main showing (Plate 1-6-12). It was mined for antimony between 1939 and 1940, producing roughly 77 tonnes of hand-picked ore grading 60 per cent antimony. Mine development during that period included the sinking of a 45-metre inclined shaft and an unknown amount of drifting. The property was dormant from 1940 until 1963 when exploration aimed at determining its gold potential was first undertaken. This work is summarized in assessment reports filed with the British Columbia Ministry of Energy, Mines and Petroleum Resources (Poloni, 1974; Heshka, 1971; Dewonck, 1980; Game and Sampson, 1987a, 1987b).

VEIN MINERALIZATION

Mineralized veins are hosted by the Sowchea shear zone (Armstrong, 1949), a prominent northwest-trending fault zone which dips from 40° to 50° to the northeast. The character and orientation of this structure are well constrained by both drill-hole data (Poloni, 1974; Dewonck, 1980; Game and Sampson, 1987a, b) and excellent surface exposure. The southwest-facing slope of a ridge has been completely stripped of overburden and provides a near continuous exposure of the vein system. Information from assessment reports indicates that 57 diamond-drill holes totalling roughly 5000 metres have been drilled on the property. All drill holes were collared in the hangingwall of the Sowchea shear zone and the vein system. The fault zone



Plate 1-6-12. Adit on the Main vein at the Snowbird showing.

is up to several tens of metres wide and characterized by intense carbonatization, brecciation and shearing. Armstrong (1949) interpreted the structure as: "a zone of faulting, shearing and brecciation that provided channelways for later carbonatizing and mineralizing solutions". We fully support this interpretation. Pervasively carbonatized ultramafic rocks and mafic volcanic rocks occur as tectonic slivers within intensely sheared graphitic and variably pyritized argillite.

Ore shoots at the Snowbird deposit are hosted by three quartz-carbonate ± mariposite and/or illite veins, the Main, Pegleg and Argillite veins. Both the Main and Pegleg veins are structurally controlled by the Sowchea fault zone. The Argillite vein follows a high-angle cross-fault perpendicular to the main shear zone. Vein minerals include gold, stibnite, arsenopyrite, chalcopyrite and pyrite. Stibnite is the dominant sulphide mineral, occurring as a massive, grey, fracture-filling phase. Other sulphide minerals are only sporadically developed and a minor component of the vein mineralization. The Argillite vein is reported (Armstrong, 1949) to have carried a body of massive stibnite 10 metres long by 10 centimetres wide that was mined out by the Consolidated Mining and Smelting Company of Canada,

Limited during the short life of the mine. The outcrop of the Main vein contains a lens of massive stibnite 4 centimetres wide.

Significant gold values, assayed in drill core, are consistently from vein intercepts along the shear zone, either within, or adjacent to quartz-carbonate-mariposite-altered ultramafic or volcanic rocks. Gold values are highly erratic, with no definable continuity, a characteristic of bonanza style deposits. Game and Sampson (1987a) report that significant gold intersections on the main vein are all associated with massive stibnite. One 10-centimetre intersection of the Main vein, in contact with listwanite, contained visible gold and assayed 8500 grams per tonne gold and 2900 grams per tonne silver.

Fluid inclusion studies on the quartz-gold-stibnite veins (Madu *et al.*, 1990) suggest that the veins were formed from low-salinity, CO₂-rich aqueous fluids at temperatures greater than 240° C and in excess of 80 000 kilopascals (0.8 kilobar) pressure. As such, they fit into the global class of mesothermal vein deposits as defined by Bohlke (1989).

Argon-argon isotopic analysis of mariposite by laser step-heating methods on two samples of listwanite wallrock of the Main vein indicate that the age of carbonate alteration, and presumably gold mineralization, is Middle Jurassic, between 162 and 165 Ma (Ash *et al.*, in preparation). Based on the lithotectonic setting, and the age of the veins and spatially associated felsic intrusive rocks (Figure 1-6-11), it is proposed that vein minerals were precipitated from fluids generated by crustal thickening through partial melting, magmatism and metamorphic devolatilization during Middle Jurassic collision. Obduction of oceanic lower crustal and upper mantle lithologies provided deep through-going crustal fault zones active during the collisional event, most critically, during the period of fluid generation and mobilization.

MINERAL POTENTIAL

The only known mineral occurrence in the Stuart Lake area is the Snowbird deposit described previously. No other significant showings were noted during the course of mapping, however, an area of intensely carbonatized ultramafic rocks was identified to the east of McKelvey Lake, adjacent to the contact of the McKelvey Lake pluton in the northwest corner of the map area. Intense carbonatization with associated mariposite and minor 2 to 10-centimetre barren quartz veins together with carbonatized and pyritized felsic dike rocks were identified in numerous large angular boulders at the base of 40 to 50-metre cliff face several hundred metres to the northeast of the lake. The extent of the alteration zone in this area is not well constrained and deserves closer examination.

Potential for mineral occurrences in the northeastern sector of the map sheet cannot be ruled out as the area is heavily mantled with overburden and received only limited coverage, yet it has tectonic and lithologic characteristics conducive to gold-quartz vein mineralization.

We suggest that the lack of known mineral occurrences in the pelagic sedimentary rocks that dominate the central part of the map area reflects the lack of oceanic crustal and upper mantle "ophiolitic remnants" in the area.

The few quartz veins scattered throughout the map area are typically bull white with no visible mineralization. Several of the larger veins were sampled for gold and base metals. Assay results are not available at the time of writing of this report. Samples locations and assay results are tabulated on Open File Map 1993-9 (Ash *et al.*, 1993).

A number of gossanous zones were also identified and sampled. A zone of gossanous hornfelsed sediments adjacent to the Shass Mountain pluton, approximately 4.5 kilometres west-southwest of Mount Neilsp, is roughly 20 to 30 metres wide along a linear topographic trough that parallels the intrusive contact. The sediments are variably silicified and carry from 1 to 4 per cent finely disseminated sulphides, primarily pyrite.

A gossanous, brittle fault zone cuts an isolated cliff exposure of quartz diorite to the northeast of McKelvey Lake. It trends north-northeast, dips steeply and is possibly

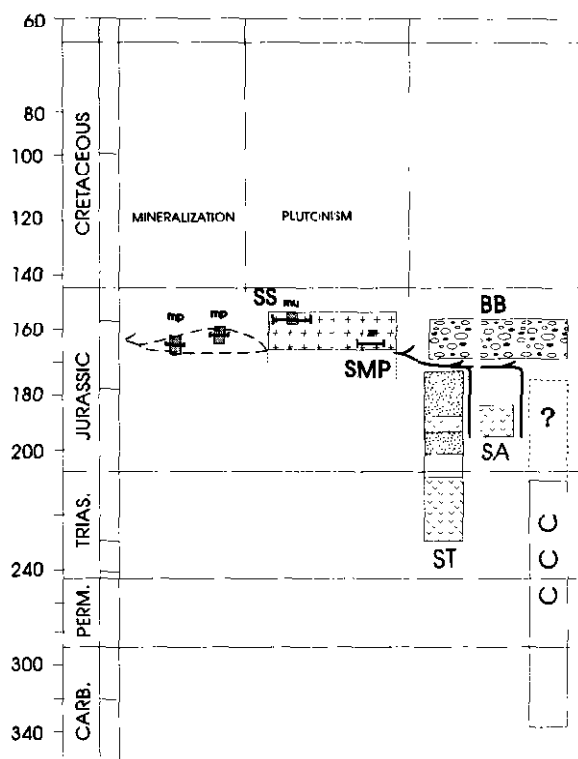


Figure 1-6-11. Geochronology of tectonism, mineralization and plutonism for the Snowbird gold-stibnite deposit.

CCCT – Central Cache Creek Terrane (Orchard 1991; Cordery *et al.*, 1991)

SAC – Stuhini arc complex (Tipper, 1984; L. Diakow, personal communication)

BB – Bowser basin (Currie, 1984)

SA – Sitlika assemblage (Paterson, 1974; Thorstad and Gabrielse, 1986)

SMP – Shass Mountain pluton (Ash *et al.*, in preparation)

SS – Snowbird stock (Ash *et al.*, in preparation)

zr – Zircon

mp – Mariposite

mu – Sericite

All mica ages are by ⁴⁰Ar-³⁹Ar.

up to several tens of metres wide; however, the limonite staining with associated trace pyrite is only 1 to 2 metres wide at the centre of the zone.

CONCLUSIONS

Regional geological mapping in the Stuart Lake area has established a geographic distribution of oceanic crustal and uppermost mantle "ophiolitic remnants" which are important to the development of mineral deposits in oceanic terranes. The only significant mineral occurrence, the Snowbird deposit, is spatially associated with one such ophiolitic remnant at the southern end of the map area. A lack of mineral occurrences in the lower lying central part of the map sheet is considered to be lithologically controlled and reflects the dominance of pelagic sediments and lack of ophiolitic remnants in the region. An increased abundance of oceanic crustal and upper mantle lithologies in the northern part of the map area suggests a higher mineral potential. A knowledge of the distribution of such remnants within the largely sedimentary Cache Creek Terrane is therefore necessary to adequately evaluate its mineral potential.

Combined geochemical data, petrographic analysis and potassium feldspar staining of felsic intrusions throughout the map area suggests that they are compositionally similar and are interpreted to have been intruded during a Middle Jurassic magmatic event which immediately followed emplacement of the oceanic terrane.

Geochemical data from mafic volcanic rocks in the Stuart-Pinchi area indicate that basalts of both mid-ocean-ridge and ocean-island affinity are present. Ocean-island basalts are concentrated along the eastern margin of the Stuart Lake belt and provide a reasonable explanation for the presence of thick sections of limestone along the belt. This interpretation clearly supports Monger's (1975) conclusion regarding the presence of shallow-water limestones in the Cache Creek Terrane of northwestern British Columbia.

ACKNOWLEDGMENTS

Geological maps of the Snowbird property and surrounding area provided by Chris Sampson and Nick Callan of X-Cal Resources Ltd. and Cominco Resources Ltd., respectively, were greatly appreciated. Thanks are extended to Dave Lefebure for helpful discussions during both field and write-up stages of this work. We acknowledge the enthusiastic corporation of Forest Service employees at Fort St. James for providing maps, aerial photographs and logistical support. Special thanks to Lauri Mathews, Mike MacDonell, Pete Hisch, Fred Hankins and Dave Cuzner. Grant Luck and Karl Scholz of Pacific Western Helicopters provided reliable and safe service. Trace and rare-earth elemental analysis were conducted at Memorial University of Newfoundland, Department of Earth Sciences by Dr. John Malpas. Thanks to Mario Rodrigues and family of the Pitka Bay Resort and Jack and Audrey Kelly of the Nakalat Lodge for their warm hospitality and providing comfortable accommodations. This paper has benefitted from scientific review and editorial comments by Dave Lefebure, Mitch

Mihalynuk, Ian Paterson, John Newell, Joanne Nelson and Brian Grant.

REFERENCES

- Andrews, E. and Ebihara, M. (1982): Solar-system Abundances of the Elements; *Geochimica et Cosmochimica Acta*, Volume 46, pages 2363-2380.
- Armstrong, J.E. (1942a): The Pinchi Lake Mercury Belt, British Columbia; *Geological Survey of Canada*, Paper 42-11, 18 pages.
- Armstrong, J.E. (1942b): Geology of the Pinchi Lake Mercury Belt, British Columbia; *Canadian Institute of Mining and Metallurgy*, Transactions, Volume 45, pages 311-323.
- Armstrong, J.E. (1944): Northern Part of the Pinchi Lake Mercury Belt, British Columbia; *Geological Survey of Canada*, Paper 44-5, 13 pages.
- Armstrong, J.E. (1949): Fort St. James Map-area, Cassiar and Coast Districts, British Columbia; *Geological Survey of Canada*, Memoir 252, 210 pages (Reprinted in 1965).
- Armstrong, J.E. (1966): Tectonics and Mercury Deposits in British Columbia; in *Tectonic History and Mineral Deposits of the Western Cordillera*; *Canadian Institute of Mining and Metallurgy*, Special Volume No.8, pages 341-348.
- Ash, C.H., McDonald, R.W.J. and Paterson, I.A. (1993): Geology of the Stuart - Pinchi Lake Map Area; *B.C. Ministry of Energy, Mines and Petroleum Resources*, Open File 1993-9.
- Ash, C.H. (in preparation): Origin and Tectonic Setting of Ophiolitic Ultramafic and Related Rocks in the Atlin Camp, Northwestern British Columbia; *B.C. Ministry of Energy, Mines and Petroleum Resources*, Paper.
- Ash, C.H., Macdonald, R.W.J. and Reynolds, P.R. (in preparation): Ophiolite-related Mesothermal Lode Gold in British Columbia: A Deposit Model; *B.C. Ministry of Energy, Mines and Petroleum Resources*, Bulletin.
- Böhlke, J.K. (1989): Comparison of Metasomatic Reactions Between a Common CO₂-rich Vein Fluid and Diverse Wall Rocks: Intensive Variables, Mass Transfers, and Au Mineralization at Alleghany, California; *Economic Geology*, Volume 84, pages 291-327.
- Cann, J. R. (1970): Rb, Sr, Y, Zr and Nb In Some Ocean-floor Basaltic Rocks; *Earth and Planetary Science Letters*, Volume 19, pages 7-11.
- Carter, N.C. (1981): Porphyry Copper and Molybdenum Deposits, West-central British Columbia; *B.C. Ministry of Energy, Mines and Petroleum Resources*, Bulletin 64, 150 pages.
- Cordey, F. (1990a): Radiolarian Age Determinations from the Canadian Cordillera; in *Current Research, Part E, Geological Survey of Canada*, Paper 90-1E, pages 121-126.
- Cordey, F. (1990b): Comparative Study of Radiolarian Faunas from the Sedimentary Basins of the Insular, Coast and Intermontane Belts; *Geological Survey of Canada*, unpublished in-house report, 57 pages.
- Cordey, F., Gordey, S.P. and Orchard, M.J. (1991): New Biostratigraphic Data for the Northern Cache Creek Terrane, Teslin Map Area, Southern Yukon; in *Current Research, Part E, Geological Survey of Canada*, Paper 91-1 E, pages 67-76.
- Currie, L. (1984): The Provenance of Chert Clasts in the Ashman Conglomerates of the Northeastern Bowser Basin; unpublished M.Sc. thesis, *Queens University*, Kingston, Ontario.
- Dewonck, B. (1980): Drilling Report, Snowbird Group, Omineca Mining District; *B.C. Ministry of Energy, Mines and Petroleum Resources*, Assessment Report 8613.

- Faulkner, E.L. (1988): Snowbird; in Exploration in B.C. 1987, *B.C. Ministry of Energy, Mines and Petroleum Resources*, pages B47-48.
- Faulkner, E.L. and Madu, B.E. (1990): Snowbird (93K 36); in Exploration in B.C. 1989, *B.C. Ministry of Energy, Mines and Petroleum Resources*, pages B171-174.
- Gabrielse, H. (1985): Major Dextral Transcurrent Displacements along the Northern Rocky Mountain Trench and Related Lineaments in North-central British Columbia; *Geological Society of America. Bulletin*, Volume 96, page 1-14.
- Gabrielse, H. (1991): Late Paleozoic and Mesozoic Terrane Interaction in North-central British Columbia; *Canadian Journal of Earth Sciences*, Volume 28, pages 947-957.
- Game, B.D. and Sampson, C.J. (1987a): Report on Geochemical Soil Sampling, Trenching and Drilling, Snowbird Group, Fort St. James, B.C., Omineca Mining Division; *B.C. Ministry of Energy, Mines and Petroleum Resources*, Assessment Report 15 732.
- Game, B.D. and Sampson, C.J. (1987b): Report on Snowbird Group, Fort St. James, B.C., Omineca Mining Division; *B.C. Ministry of Energy, Mines and Petroleum Resources*, Assessment Report 16 766.
- Heshka, W. (1971): Geological Report, Snowbird Group (#2589), Fort St. James, Omineca, B.C.; *B.C. Ministry of Energy, Mines and Petroleum Resources*, Assessment Report 3520.
- Holm, P.E. (1985): The Geochemical Fingerprints of Different Tectonomagmatic Environments Using Hydromagmatophile Element Abundances of Tholeiitic Basalts and Basaltic Andesites; *Chemical Geology*, Volume 51, pages 303-323.
- Humphries, S.E. and Thompson, G. (1978): Trace Element Mobility During Hydrothermal Alteration of Oceanic Basalts; *Geochimica et Cosmochimica Acta*, Volume 42, pages 127-136.
- Le Maitre, R.W. (1984): A Proposal by the IUGS Subcommittee on the Systematics of Igneous Rocks for a Chemical Classification of Volcanic Rocks Based on the Total Alkali Silica (TAS) Diagram; *Australian Journal of Earth Science*, Volume 31, pages 243-255.
- Madu, B.E., Nesbitt, B.E. and Muehlenbachs, K. (1990): A Mesothermal Gold-Stibnite-Quartz Vein Occurrence in the Canadian Cordillera; *Economic Geology*, Volume 85, pages 1260-1268.
- Meschede, M. (1986): A Method of Discriminating between Different Types of Mid-ocean Ridge Basalts and Continental Tholeiites with the Nb-Zr-Y Diagram; *Chemical Geology*, Volume 56, pages 207-218.
- Monger, J.W.H. (1975): Upper Paleozoic Rocks of the Atlin Terrane, Northwestern British Columbia and South-central Yukon; *Geological Survey of Canada*, Paper 74-47, 63 pages.
- Monger, J.W.H., Richards, T.A. and Paterson, I.A. (1978): The Hinterland Belt of the Canadian Cordillera: New Data from Northern and Central British Columbia; *Canadian Journal of Earth Sciences*, Volume 15, pages 823-830.
- Orchard, M.J. (1991): Conodonts, Time and Terranes: An Overview of the Biostratigraphic Record in the Western Canadian Cordillera; in Ordovician to Triassic Conodont Paleontology of the Canadian Cordillera, Orchard, M.J. and McCracken, A.D., Editors, *Geological Survey of Canada*, Bulletin 417, pages 1-25.
- Paterson, I.A. (1973): The Geology of the Pinchi Lake Area, Central British Columbia; unpublished Ph.D. thesis, *The University of British Columbia*, 263 pages.
- Paterson, I.A. (1974): Geology of Cache Creek Group and Mesozoic Rocks at the Northern End of the Stuart Lake Belt, Central British Columbia; *Geological Survey of Canada*, Paper 74-1, Part B, pages 31-42.
- Paterson, I.A. (1977): The Geology and Evolution of the Pinchi Fault Zone at Pinchi Lake, Central British Columbia; *Canadian Journal of Earth Sciences*, Volume 14, pages 1324-1342.
- Paterson, I.A. and Harakal, J.E. (1974): Potassium-Argon Dating of Blueschists from Pinchi Lake, Central British Columbia; *Canadian Journal of Earth Sciences*, Volume 11, pages 1007-1011.
- Pearce, J.A. (1980): Geochemical Evidence for the Genesis and Eruptive Setting of Lavas from Tethyan Ophiolites; in Ophiolites, Proceedings of the International Ophiolite Symposium, Cyprus, 1979, Panayiotou, A., Editor, *Cyprus Ministry of Agriculture and Natural Resources*, Geological Survey Department, pages 261-272.
- Pearce, J.A. (1982): Trace Element Characteristics of Lavas from Destructive Plate Boundaries; in Andesites, Thorpe, R.S., Editor, *John Wiley and Sons*, pages 525-548.
- Pearce, J.A. (1983): Role of the Sub-continental Lithosphere in Magma Genesis at Active Continental Margins; in Continental Basalts and Mantle Xenoliths, Hawkesworth, C.J., and Norry, M.J., Editors, *Shiva Publications*, Nantwich, pages 230-249.
- Pearce, J.A. and Cann, J.R. (1973): Tectonic Setting of Basic Volcanic Rocks Determined Using Trace Element Analyses; *Earth and Planetary Science Letters*, Volume 19, pages 290-300.
- Pearce, J.A. and Norry, M.J. (1979) Petrogenetic implications of Ti, Zr, Y and Nb Variations in Volcanic Rocks. *Contributions to Mineralogy and Petrology*, Volume 69, pages 33-47.
- Poloni, J.R. (1974): Report on Diamond Drilling, Stuart Lake Property, Westwind Mines Ltd; *B.C. Ministry of Energy, Mines and Petroleum Resources*, Assessment Report 5136.
- Rice, H.M.A. (1949): Smithers - Fort St. James, British Columbia; *Geological Survey of Canada*, Map 971A.
- Ross, V.R. (1977): The Internal Fabric of an Alpine Peridotite Near Pinchi Lake, Central British Columbia, *Canadian Journal of Earth Sciences*, Volume 14, pages 32-44.
- Saunders, A.D., Tarney, J., March, N.G. and Wool, D.A. (1980): Ophiolites as Ocean Crust or Marginal Basin Crust: A Geochemical Approach; in Ophiolites, Proceedings of the International Ophiolite Symposium, Cyprus, 1979, Panayiotou, A., Editor, *Cyprus Ministry of Agriculture and Natural Resources*, Geological Survey Department, pages 193-204.
- Shervais, J.W. (1982): Ti-plots and the Petrogenesis of Modern and Ophiolitic Lavas; *Earth and Planetary Science Letters*, Volume 59, pages 101-118.
- Thompson, M.L. (1965): Pennsylvanian and Early Permian Fusulinids from Fort St. James Area, British Columbia; *Canadian Journal of Paleontology*, Volume 39, pages 224-234.
- Thorstad, L.E. and Gabrielse H. (1986): The Upper Triassic Kutcho Formation, Cassiar Mountains, North-central British Columbia; *Geological Survey of Canada*, Paper 86-16, 53 pages.
- Tipper, H.W. (1984): The Allochthonous Jurassic - Lower Cretaceous Terranes of the Canadian Cordillera and their Relation to Correlative Strata of the North American Craton; in Jurassic-Cretaceous Biochronology and Paleogeography of North America, *Geological Association of Canada*, Special Paper 27, pages 113-120.
- Whittaker P.J. (1982a): Chromite Occurrences in Ultramafic Rocks in the Mitchell Range, Central British Columbia; *Geological Survey of Canada*, Paper 82-1A, pages 239-245.

- Whittaker P.J. (1982b): Chromite Occurrences in Mitchell Range Ultramafic Rocks of the Stuart Lake Belt, Cache Creek Group; in Geological Fieldwork 1981, *B.C. Ministry of Energy, Mines and Petroleum Resources*, Paper 1982-1, pages 234-243.
- Whittaker P.J. (1983a): Geology and Petrogenesis of Chromite and Chrome Spinel in Alpine-type Peridotites of the Cache Creek Group, British Columbia; unpublished Ph.D. thesis, *Carleton University*, Ottawa, 339 pages.
- Whittaker P.J. (1983b): Chromite in the Mount Sidney Williams Area, Central British Columbia (93K); in Geological Fieldwork 1981, *B.C. Ministry of Energy, Mines and Petroleum Resources*, Paper 1982-1, pages 315-319.
- Whittaker P.J. and Watkinson H.W. (1981): Chromite in some Ultramafic Rocks of the Cache Creek Group, British Columbia; *Geological Survey of Canada*, Paper 81-1A, pages 349-355.
- Whittaker P.J. and Watkinson H.W. (1983): Geology and Alteration Characteristics of Cr-spinel in Dunite at Mt. Sydney Williams, Central British Columbia; *Geological Survey of Canada*, Paper 83-1B, pages 177-184.
- Whittaker, P.J. and Watkinson, H.W. (1984): Genesis of Chromitite from the Mitchell Range, Central British Columbia; *Canadian Mineralogist*, Volume 22, pages 161-172.
- Whittaker P.J. and Watkinson H.W. (1986): Origin of Chromite in Dunitic Layer of the Mt. Sydney Williams Ultramafic Rock Complex, British Columbia; in *Metallogeny of Basic and Ultrabasic Rocks*, Gallagher, M.J., Ixer, R.A., Neary, C.R. and Prichard, H.M., Editors, *The Institution of Mining and Metallurgy*, pages 217-228.
- Winchester, J.A. and Floyd, P.A. (1977): Geochemical Discrimination of Different Magma Series and their Differentiation Products Using Immobile Elements; *Chemical Geology*, Volume 20, pages 325-343.
- Wood, D.A., Joron, J-L. and Treuil, M. (1979): A Reappraisal of the Use of Trace Elements to Classify and Discriminate Between Magma Series Erupted in Different Tectonic Settings; *Earth and Planetary Science Letters*, Volume 45, pages 326-336.



GEOLOGY OF THE KLAWLI LAKE, KWANIKA CREEK AND DISCOVERY CREEK MAP AREAS, NORTHERN QUESNEL TERRANE, BRITISH COLUMBIA (93N/7W, 11E, 14E)

By JoAnne L. Nelson, Kim A. Bellefontaine,
Mary E. MacLean and Keith J. Mountjoy

KEYWORDS: Regional geology, Nina Creek, Lay Range, Takla, Slate Creek, Inzana Lake, Witch Lake, Plughat Mountain, Chuchi Lake, Twin Creek, Jurassic sediments, mineralization, structural geology, Manson fault, Discovery fault, dextral transfer.

stratigraphy and structure around the Takla-Rainbow property, and a regional transcurrent fault system in the Discovery Creek map area. Exploration activity was quiet in the northern Quesnel belt following Placer Dome's decision to shelve the Mount Milligan project and the dissolution of B.P. Resources Canada Limited.

INTRODUCTION

This report covers 1:50 000-scale geological mapping of 93N/7 West Half, 93N/11 East Half and 93N/14 East Half, completed in the summer of 1992, the third and final mapping season of the Nation Lakes project. The maps are available as Open Files 1993-3, 4, and 5 (Nelson *et al.*, 1993a, b; Bailey *et al.*, 1993). The area, shown on Figure 1-7-1, links previously published map coverage by the Nation Lakes project (Nelson *et al.*, 1991b, 1992a) with that of the Manson Creek and Northern Quesnel Trough projects (Ferri *et al.*, 1988, 1989, 1992c; Ferri and Melville, 1990b).

Mapping highlights include a major northwest-trending aeromagnetic high in the Valleau Creek valley, Takla Group

MAPPING GOALS

Mapping goals in 1992 were directed toward resolution of the following problems:

- Work in 1990 and 1991 led to a fourfold stratigraphic subdivision of the Takla Group in map areas 93K/16, 93N/1, 93N/2E and 93N/7E (Nelson *et al.*, 1991a, 1992b). Do these informal formations, the Rainbow Creek, Inzana Lake, Witch Lake and Chuchi Lake, persist northward, or do gross facies changes intervene? In particular, what is the relationship between this stratigraphy and that proposed by Ferri and others in the Germansen Lake area (Ferri and Melville, in preparation).
- On the basis of mapping for Eastfield Resources Limited and Golden Rule Resources Limited, David Bailey (personal communication, 1991) reported a Triassic-Jurassic unconformity in the Twin Creek area on the Takla Rainbow property. Farther south, the contact between Triassic and Jurassic volcanic rocks is apparently transitional (Nelson *et al.*, 1992b). How could these conflicting observations be reconciled?
- Regional aeromagnetic coverage shows a very strong northwest-trending linear magnetic anomaly in the Valleau Creek valley. It terminates abruptly near Klawli Lake. What is the geological source of this anomaly? Does it bear any relationship to alkalic porphyry copper-gold deposits?
- Do potassic-propylitic alteration haloes, common around the Nation Lakes, persist northward within the Takla Group?
- The Discovery Creek area is transected by the northern extension of the Manson fault zone, a regional dextral transcurrent fault which apparently dies to the north near Wasi Creek (Figure 1-7-2; Ferri *et al.*, 1992c). A second array of dextral faults occurs in the Discovery Creek valley but dies southward near Germansen Lake. A reasonable structural model involves the transfer of motion from the Manson fault zone to the Discovery Creek valley but dies southward near Germansen Lake. A reasonable structural model involves the transfer of motion from the Manson fault zone to the Discovery Creek fault system. What is the nature of this transfer zone?

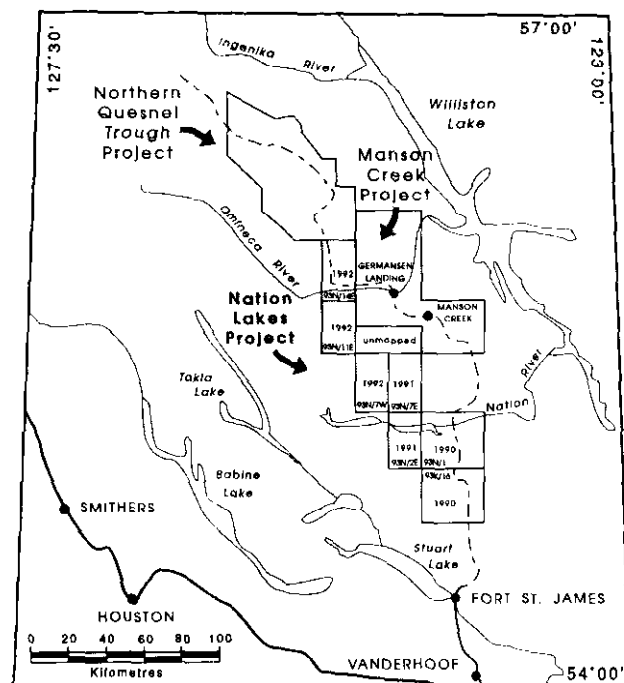


Figure 1-7-1. Location map showing Nation Lakes, Manson Creek and Northern Quesnel Trough projects. Shaded area depicts 1992 map area.

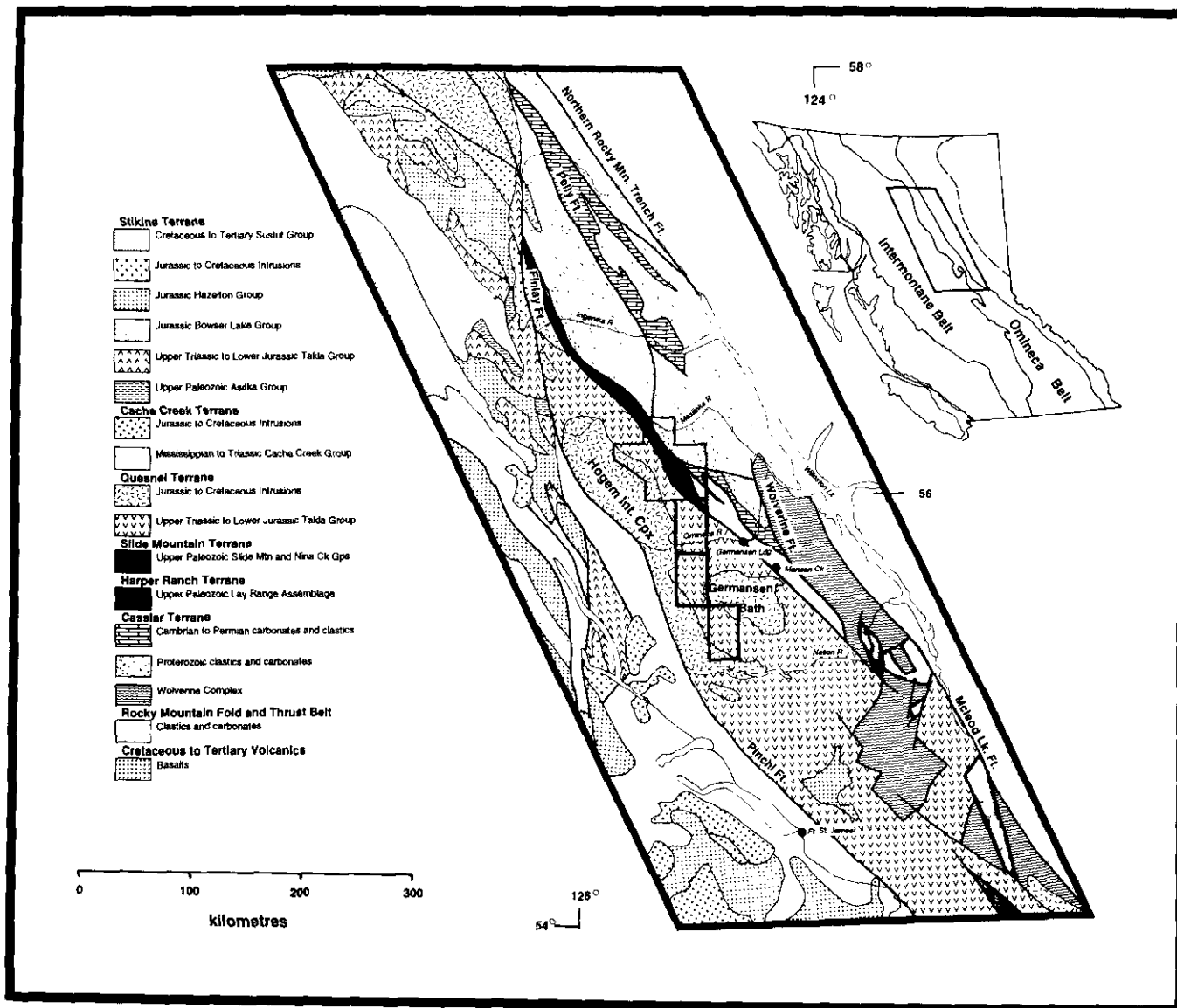


Figure 1-7-2. Regional geological setting of the Nation Lakes area. Small squares represent Nation Lakes 1992 mapping, The larger area depicts mapping of the Uslika Lake area (modified after Ferri *et al.*, 1992a).

GEOLOGIC OVERVIEW

Most of the mapped area is underlain by the Upper Triassic to Lower Jurassic Takla Group of the Quesnel Terrane (Figure 1-7-2). It is intruded to the west by the Hagem intrusive complex (Garnett, 1978; Nelson *et al.*, 1992b). Lower Jurassic sedimentary rocks, slightly younger than the volcanic Takla Group, form a single panel within the Discovery Creek fault zone 2 kilometres north of the Omineca River. They contain a rich ammonite fauna of latest Toarcian age (Table 1-7-1). Rocks of the upper Paleozoic Lay Range assemblage, part of the Harper Ranch Terrane, and Nina Creek group, belonging to the Slide Mountain Terrane, occur in fault-bounded panels east of the Discovery Creek fault system in 93N/14. Cretaceous to Early Tertiary units are restricted to the Discovery Creek fault zone.

STRATIFIED UNITS

NINA CREEK GROUP

Upper Paleozoic oceanic rocks of the Slide Mountain Terrane, termed the Nina Creek group, form a large klippe above the miogeoclinal Cassiar Terrane in the Nina Creek area (Ferri and Melville, in preparation). The Nina Creek group comprises a lower package of Pennsylvanian-Permian pelagic sedimentary strata with gabbro sills, termed the Mount Howell formation, and an upper, Pennsylvanian-Permian basaltic pile with minor chert and argillite called the Pillow Ridge formation. The age overlap between the two suggests that they are separated by a thrust fault rather than a stratigraphic contact. The two formations are probably facies packages that have been subsequently telescoped.

TABLE 1-7-1
FOSSIL IDENTIFICATION

REPORT J1-1992-GKJ

Report on Jurassic fossils from the Manson River map area (93N14) and submitted by J. Nelson (BCGS) in September 1992, for identification.

Field No.:	92-JN-24-1	G.S.C. Loc. No.:	C-189742
Locality:	Discovery Creek, Takla Group. UTM 368600E 6187000N.		
Identifications:	ammonites		
	<i>Pleydellia</i> n.sp.		
	<i>Lytoceras</i> sp.		
	Phymatoceratidae n.gen. et n.sp.		
	ammonite aptychi		
	bivalves		
Age & Comments:	late Late Toarcian		
<hr/>			
Field No.:	92-JN-21-4	G.S.C. Loc. No.:	C-189663
Locality:	Discovery Creek, approximately 2.25 km from road crossing. UTM 367500E 6187975N. Takla Group.		
Identifications:	pelecypods		
	rhynchonellid brachiopods		
	belemnite		
Age & Comments:	The presence of a belemnite with an internal radiating structure suggests an age younger than Middle Toarcian.		
<hr/>			
Field No.:	92-JN-21-5	G.S.C. Loc. No.:	C-189664
Locality:	Discovery Creek, approximately 2.25 km from road crossing. UTM 367525E 6188050N. Takla Group.		
Identifications:	ammonites		
	<i>Dumortieria</i> n.sp.		
	Phymatoceratidae n.gen. et n.sp.		
Age & Comments:	late Late Toarcian		
<hr/>			
Field No.:	92-JN-22-1	G.S.C. Loc. No.:	C-189665
Locality:	750 m northeast of Ron Repko's house. UTM 370000E 6186825N. Takla Group.		
Identifications:	crinoid columnals		
Age & Comments:	not diagnostic		

Note: Data contributed by G.K. Jakobs, Visiting Scientist, Geological Survey of Canada, Vancouver

The northeastern corner of 93N/14 is underlain by the Nina Creek group (Figure 1-7-3). Although outcrop control on the contact is poor, it apparently rests structurally on the lower Mississippian Gilliland felsic tuff unit of the Cassiar Terrane (Ferri and Melville, in preparation).

MOUNT HOWELL FORMATION (PPMH)

The lower part of the Nina Creek group is a monotonous sequence of grey to black argillite/chert and green chert that dips moderately to the southwest. It is overlain by 50 to 75

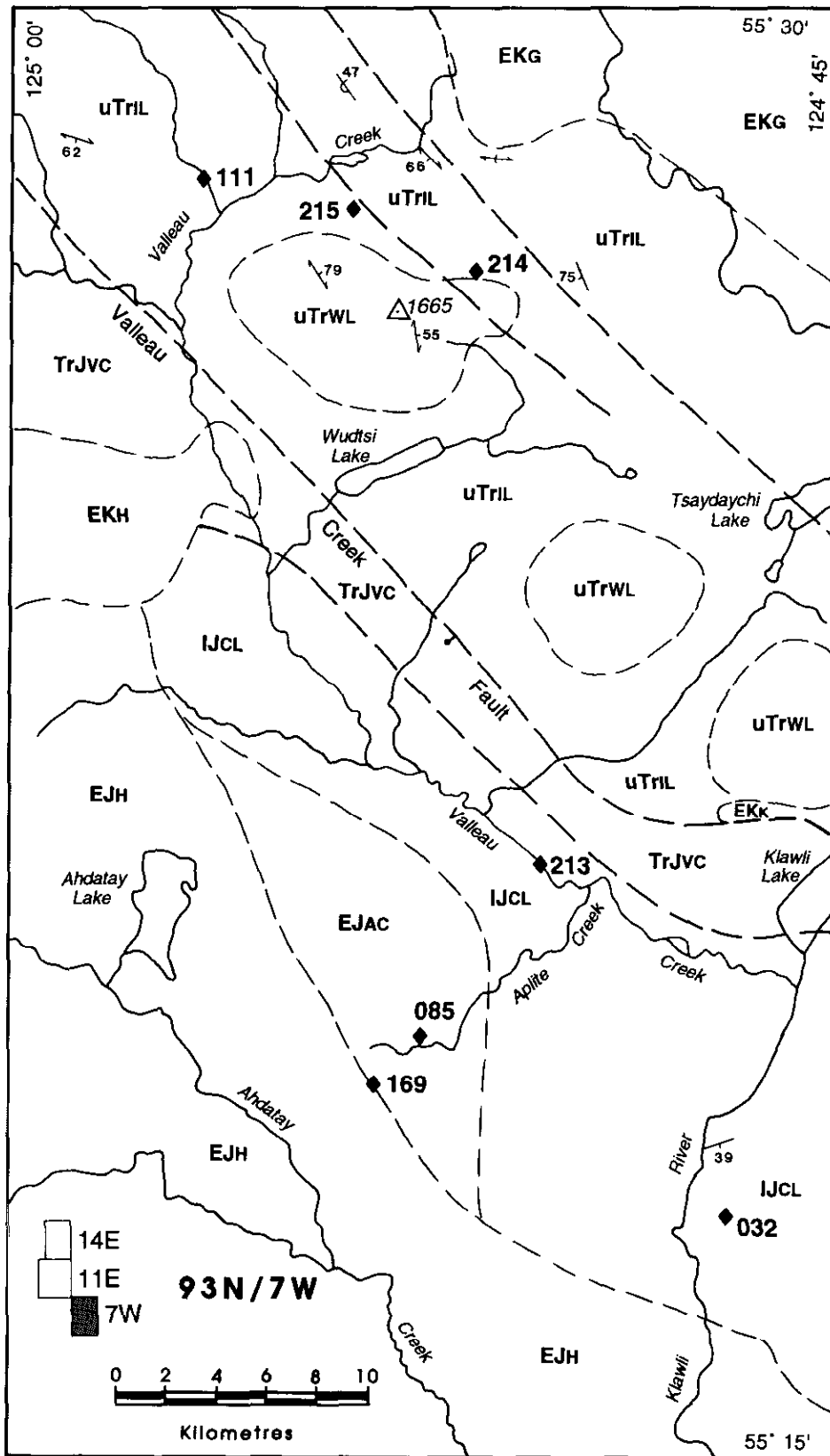
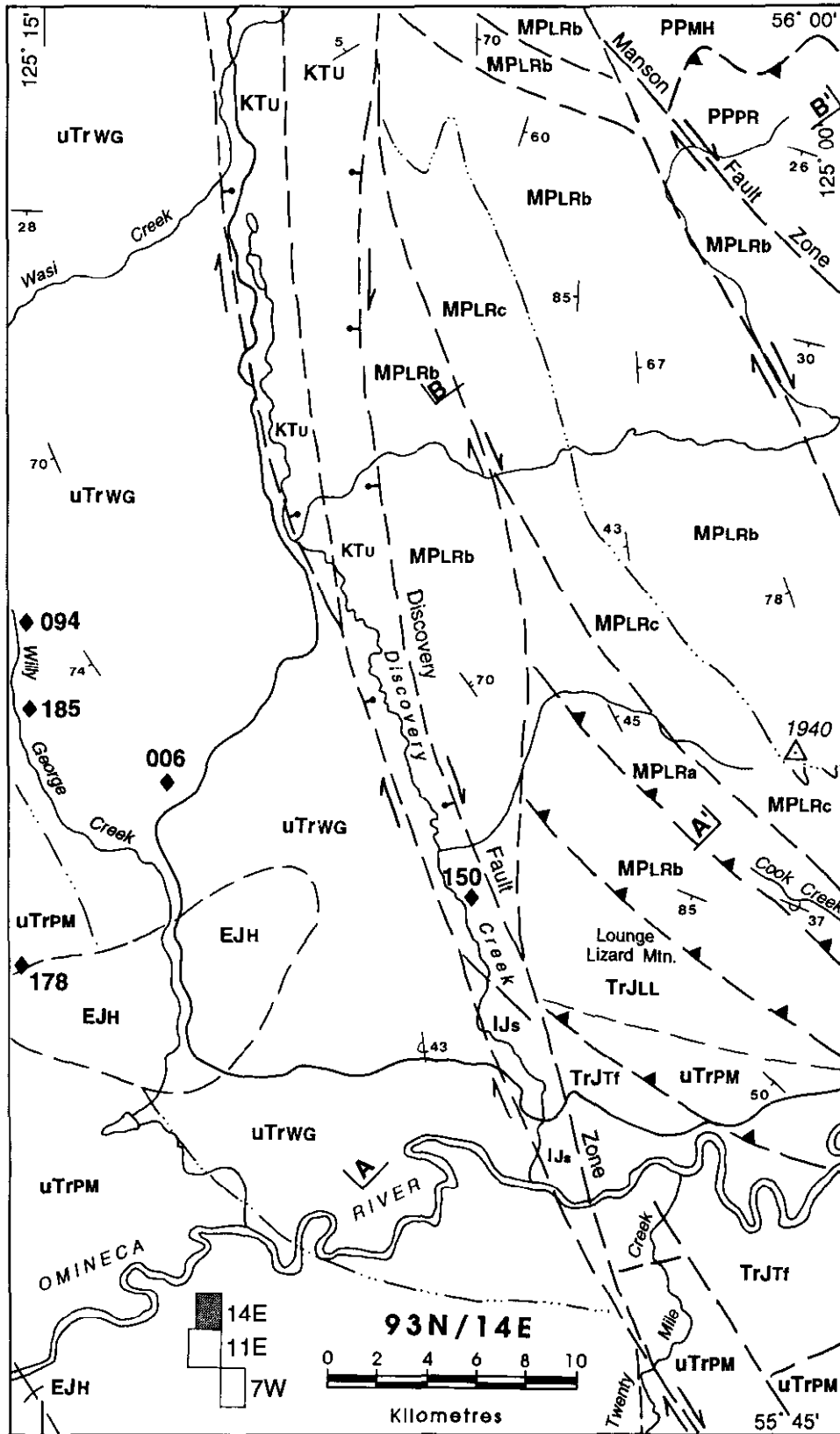


Figure 1-7-3. Geology of the Klawli River (93N/7W), Kwanika Creek (93N/11E) and Discovery Creek (93N/14E) map areas. See following pages for adjoining map sheets and legend.



LAYERED ROCKS

Cretaceous to Tertiary?

- KTv** maroon, orthoclase and quartz-bearing tuff with plagioclase-porphyrific volcanic fragments
- KTvs** plagioclase+hornblende+biotite, quartz-eye rhyolite tuff and flow, minor mafic lapilli tuff, siltstone, sandstone, quartzofeldspathic conglomerate
- KTu** **USLIKA FM:** conglomerate, sandstone, siltstone, mudstone, minor coal

Toarcian

- IJs** arkose, greywacke, sandstone, siltstone, minor conglomerate

Lower Jurassic Takia Group

- IJtc** **TWIN CREEK fm:** heterolithic lapilli tuff, plagioclase+quartz porphyritic flows and agglomerate/tuff breccia
- IJcl** **CHUCHI LAKE fm:** plagioclase ± augite porphyry flows and fragmental volcanics

Upper Triassic Takia Group

- TrJtj** **TAKLA FELSIC unit:** heterolithic lapilli tuff, agglomerate, conglomerate, amygdaloidal augite porphyry flow, crystal ash tuffs (plagioclase+augite); clasts of plagioclase-rich volcanics, monzonite intrusives, maroon augite porphyry and cherty tuffaceous sediments
- uTrpm** **PLUGHAT MOUNTAIN fm:** predominantly green augite+plagioclase-porphyrific basalt flows and fragmentals, maroon basalt, pillow basalt, amygdaloidal olivine porphyritic basalt, heterolithic lapilli tuff, volcanic sandstone and siltstone, limestone; uTrpmA: limestone; uTrpmB: maroon augite+olivine basalt flow, flow breccia, minor red sandstone
- uTrwl** **WITCH LAKE fm:** green and maroon, augite+plagioclase and hornblende+plagioclase porphyritic flows and volcanoclastics
- uTrwg** **WILLY GEORGE sequence:** augite-plagioclase lapilli tuff, crystal tuff, sedimentary breccia, arkose/wacke, argillite, siltstone
- uTrnl** **INZANA LAKE fm:** green tuff, lapilli tuff, grey siltstone and slate
- muTrsc** **SLATE CREEK fm:** grey slate and siltstone

Pennsylvanian to Permian Nina Creek Group

- PPMH** **MOUNT HOWELL fm:** grey to black argillite, green and red ribbon chert, diabase sills
- PPPR** **PILLOW RIDGE fm:** pillow basalt+variolites, diabase-gabbro sills

Mississippian to Permian Lay Range Assemblage

- MPLRc** **MAIN sequence:** green and maroon augite+plagioclase and augite+olivine porphyritic basalt
- MPLRb** **MAIN sequence:** crystal and lapilli tuff, volcanic sandstone, siltstone, siliceous argillite, chert and quartzite-bearing grit
- MPLRa** **COOK CREEK panel:** thin-bedded siliceous siltstone and argillite, sandstone, siliceous tuff and bedded chert

INTRUSIVE ROCKS

Early Cretaceous

- EKg** **GERMANSEN batholith:** coarse-grained hornblende-biotite granite, equigranular to orthoclase megacrystic
- EKk** **KLAWLI stock:** orthoclase-megacrystic, hornblende-biotite granite
- EKh** **HOGEM intrusive complex:** orthoclase-megacrystic granite, minor syenite

Early Jurassic

- EJH** **HOGEM intrusive complex:** monzonite, quartz monzonite, granodiorite, and diorite
- EJAC** **APLITE CREEK intrusive complex:** equigranular to porphyritic, fine to medium-grained diorite and gabbro, intrusive breccia, porphyritic monzonite

Late Triassic - Early Jurassic

- TrJll** **LOUNGE LIZARD intrusive complex:** variety textured diorite and gabbro, minor large plagioclase porphyritic diorite dykes
- TrJvc** **VALLEAU CREEK intrusive complex:** fine to coarse-grained diorite, gabbro, pyroxenite and hornblende

SYMBOLS

Geologic contact (approximate).....	
Lithologic contact (approximate).....	
Facies relationship (inferred).....	
Fault (approximate).....	
Bedding (tops known, unknown, overturned).....	
Foliation.....	
Strike-slip fault (motion indicated).....	
Normal fault (motion indicated).....	
Mineral occurrence & MINFILE number.....	◆ 215
Elevation in metres.....	△ 1818

metres of distinctive bright blood-red and bright green ribbon chert with argillite partings. This upper red chert unit is of regional extent and can be traced over 3 kilometres of strike length in the present map area. Identical cherts occur at the top of the Mount Howell formation from northwest of Nina Lake to south of Wasi Lake (F. Ferri, personal communication, 1992). Diabase-gabbro sills intrude both it and the underlying argillites and cherts.

PILLOW RIDGE FORMATION (PP_{PR})

To the west, near the Manson fault zone, red and green cherts of the Mount Howell formation are overlain by a 200-metre-thick sequence of gabbro and diabase sills with minor chert remnants (Figure 1-7-3). This unit thins to the northeast; at the eastern edge of the map area pillow basalts of the Pillow Ridge formation directly overlie the pelagic sequence.

The contact between the diabase-gabbro sill unit and the pillow basalts is well exposed and apparently transitional. The average grain size in the diabase decreases upwards. Chert disappears only tens of metres below the lowest occurrence of variolites that marks the first basalt flow. The sill unit is probably a feeder zone to the overlying flows and is included within the Pillow Ridge formation. A thrust fault between the sills and the underlying cherts and argillites cannot be demonstrated locally, but is inferred based on regional evidence.

The highest part of the Nina Creek Group is a 200-metre sequence of commonly pillowed basalt. These basalts are generally fine grained and equigranular, aphanitic or diabasic. Variolites are common in the finer grained and glassy flows. Pillow morphologies show upright tops that dip gently southwest. In one area pillow imbrications indicate a southerly paleoslope.

LAY RANGE ASSEMBLAGE

The Lay Range assemblage is named for extensive exposures in the Lay Range, 100 kilometres northwest of the present map area. There, it consists of a lower division of Mississippian to middle Pennsylvanian mixed siliciclastic, epiclastic, carbonate and pelagic-hemipelagic strata overlain by several kilometres of volcanic sandstone, fine lapilli tuff and ash tuff of Permian age (Ferri *et al.*, 1993a, b; and authors' 1992 observations). Ferri *et al.*, (1992a, c) recognized Lay Range sequences in the southern part of 94C/3, which adjoins the Discovery Creek map area. In 1992 we redefined contiguous parts of the Discovery Creek area as Lay Range assemblage that were previously included in the Takla Group by Armstrong (1949).

MAIN SEQUENCE (MPL_{Rb, c})

The Lay Range assemblage outcrops on the high ridges east of Discovery Creek (93N/14E; Figure 1-7-3). The regular bedding in the steeply dipping, generally west-facing panel results in the formation of ribby, ridge-top exposures. The assemblage consists of two conformable stratigraphic divisions; a lower siliceous fine-grained epiclastic division (MPL_{Rb}) and an upper volcanic division of lapilli tuffs, agglomerates and flows (MPL_{Rc}). The contact between the

two is transitional and is marked by an upward increase in coarse volcanic units over several hundred metres.

The lower division is dominated by olive green volcanic sandstone and siltstone, siliceous argillite and crystal, fine lapilli and ash tuff. Rare but diagnostic grit beds contain clasts of a variety of volcanic lithologies as well as chert, vein quartz, quartzite and/or metachert, minor limestone and plutonic lithologies. A few turquoise green and red beds of radiolarian chert form part of this sequence.

The upper division is dominated by heterolithic lapilli tuff containing variable volcanic clasts including plagioclase porphyry with an aphanitic green or, less commonly, maroon matrix; clinopyroxene porphyry with an aphanitic green or, less commonly, maroon matrix; clinopyroxene ± plagioclase crowded porphyry with clinopyroxenes larger and less abundant than plagioclase; and clinopyroxene and fresh olivine porphyry with an aphanitic groundmass. Other less abundant lapilli include brick-red aphanitic to glassy fragments and black cumulate clinopyroxenites. Green to maroon augite-olivine-porphyrific flows and flow breccias, and brown-weathering andesites with small, sparse plagioclase phenocrysts form an important part of the upper division in some areas. Epiclastic units such as sandstones and apple green ash tuffs are also present.

The smaller ridges northeast and north of Lounge Lizard Mountain are included within the Lay Range main sequence, based on lithologic similarities. Grits with rounded chert and quartz pebbles and clasts of green and red lapilli tuffs are found within these sequences.

In contrast with the type locality in the Lay Range, the lower heterogeneous sedimentary sequence of the Lay Range assemblage is missing in the Discovery Creek area. Instead, the tuff sequence, which is lithologically similar to the upper part of the type stratigraphy, passes upward into a volcanic section 2 kilometres thick and is not observed farther north. The presence of abundant coarse volcanic material in Discovery Creek could be a function of a higher structural level or the preservation of strata closer to a volcanic edifice, perhaps near the axis of the Paleozoic arc.

COOK CREEK PANEL (MPL_{Ra})

The valley at the head of Cook Creek is underlain by a distinctive lithologic assemblage that is bounded and also transected by faults (Figure 1-7-3). It contains more chert and less epiclastic detritus than the main Lay Range sequence. Lithologies include thin-bedded siliceous sandstone and siltstone, siliceous tuff, bedded chert and siliceous argillite. One sample of volcanic siltstone from the headwaters of Cook Creek contains approximately 1 per cent detrital muscovite. There is no source for muscovite in the Lay Range assemblage, thus it, together with quartzite and rare plutonic fragments in the main sequence, may provide a link to a pericratonic or continental terrane with a Paleozoic plutonic component. The Lay Range arc may have formed adjacent to a suspect pericratonic terrane similar to the Yukon-Tanana Terrane, or to the Kootenay Terrane on the margin of ancestral North America.

DISTINGUISHING LAY RANGE ASSEMBLAGE FROM TAKLA GROUP

The Lay Range assemblage and Takla Group are two very similar lithotectonic assemblages. They both represent primitive volcanic arcs consisting of basalt and andesite and related marine sediments. Individual rock textures can be strikingly similar, such as green and red heterolithic lapilli tuff, or olivine-augite-phyric basalt. Distinction at an outcrop scale is difficult, particularly in the upper, volcanic division of the Lay Range assemblage (MP1.Rc). Whole stratigraphic sequences must be examined. In this broader context, the differences between the Lay Range and Takla arcs are clear.

The Lay Range assemblage contains a number of lithologies that do not occur in the Takla Group. Most notable are the brightly coloured radiolarian cherts and the chert-quartz-quartzite grits. The very regular bedding and ribby outcrop aspect of the lower division distinguish it from most Takla exposures. Lay Range tuffs and sandstones are harder, more indurated and much more siliceous than those of the Takla Group.

Overall, the Triassic Takla and Lay Range arcs show parallel evolution. Both have progressed from deep marine deposition of epiclastic and fine pyroclastic material through a phase of basaltic volcanism and on to shallow marine conditions in which maroon volcanics are prominent. However, the abundance of maroon, plagioclase-phyric fragments in the lower Lay Range tuffaceous submarine sequence is not paralleled in the Takla arc. This suggests a shallow marine volcanic edifice that was shedding maroon volcanic material into the epiclastic submarine fans.

Chemically, the arcs show different trends. The Takla volcanics in this part of Quesnellia have characteristic island-arc signatures and chemistries that range from alkaline to transitional calcalkaline (Bellefontaine and Nelson, 1992). Preliminary data from the Lay Range assemblage suggest a transitional arc to ocean-floor setting with subalkaline volcanism (Ferri *et al.*, 1992b).

TAKLA GROUP

OVERVIEW AND STRATIGRAPHIC NOMENCLATURE

Previous mapping defined an informal fourfold stratigraphic subdivision of the Takla Group near the Nation Lakes (Nelson *et al.*, 1991a, 1992b). The Rainbow Creek formation comprises dark grey to black basinal shales and siltstones with subordinate epiclastic and pyroclastic strata and is assumed to be the oldest part of the Takla Group. The younger Inzana Lake formation is a mixed pyroclastic-epiclastic sequence in which lithologies range from augite-phyric lapilli tuff to fine-grained black siltstone and argillite. It has yielded three conodont collections, two of late Carnian age and one of middle Norian age. The Inzana Lake formation is overlain by and interfingers with the Witch Lake formation, a thick sequence of mostly augite-phyric, coarse pyroclastic basalt debris with lesser flows and minor plagioclase-dominant units and epiclastic sedimentary beds. It is overlain by plagioclase and augite-phyric fragmental rocks and flows of the Chuchi Lake formation.

Sedimentary units within the Chuchi Lake formation have yielded ammonites of early and late Pliensbachian age (Nelson *et al.*, 1992b).

Ferri and Melville (1988, 1989, 1990a, in preparation) developed a parallel but internally distinct Takla Group stratigraphy in the Manson Creek and GERMANSSEN Landing areas. The basal Slate Creek formation has yielded conodonts with ages ranging from late Anisian to Carnian. It is lithologically similar to the Rainbow Creek formation in the Nation Lakes area. The Slate Creek formation passes upward into an epiclastic-pyroclastic facies comparable to the Inzana Lake formation, which in turn is overlain by augite-phyric agglomerate and lapilli tuff. Both volcanic units are included within the Plughat Mountain formation. Jurassic intermediate to felsic volcanic rocks equivalent to the Chuchi Lake formation are not recognized.

The Plughat Mountain formation is similar to the Witch Lake formation in age and parental magma; both are dominated by augite-phyric porphyritic basalt. However, a number of striking differences between the two support the idea that they represent two separate volcanic piles. The volcanic sequence on Plughat Mountain includes at least 1500 metres of aphyric to weakly augite-phyric porphyritic basalt flows, in contrast with the almost wholly fragmental Witch Lake formation. Bright red, highly amygdaloidal augite±olivine-phyric flows are common in the Plughat Mountain formation but absent in the Witch Lake formation. Plagioclase phenocrysts are subordinate in the Witch Lake formation, but small crowded plagioclase porphyry fragments make up a significant proportion of clasts in many pyroclastic rocks of the Plughat Mountain formation. There are also contrasts in the chemistry of the volcanics. The Witch Lake basalts are alkaline while the Plughat Mountain basalts range from alkaline to calcalkaline (Ferri and Melville, in preparation; Bellefontaine and Nelson, 1992). Overall, the Plughat Mountain formation is a more heterogeneous package than the Witch Lake formation.

Both of these stratigraphies project into the 1992 map area (Figure 1-7-3). The Witch Lake formation caps the hills east of Valteau Creek in 93N/7, but does not continue into 93N/11. The Plughat Mountain formation outcrops almost continuously from its type area near GERMANSSEN Landing to GERMANSSEN Lake and into 93N/11. The Lower Jurassic Chuchi Lake formation extends into the lowlands east of Ahdatay Lake in southern 93N/7. A separate intermediate volcanic package, of presumed Early Jurassic age, overlies the Plughat Mountain formation near Twin Creek in 93N/11. Because of its distinct internal stratigraphy and lack of continuity with Chuchi Lake exposures, we have separately designated this volcanic sequence the Twin Creek formation.

SLATE CREEK FORMATION (muTrsc)

Grey slates, siltstones and minor tuffaceous sediments of the Slate Creek formation outcrop around the northern contact of the GERMANSSEN batholith in the GERMANSSEN Landing map area (Ferri *et al.*, 1989). They continue into the southeastern corner of 93N/11, around the western edge of the batholith (Figure 1-7-3). The slates are often strongly foliated and foliations appear to wrap around the margin of the

batholith. Exposure of the oldest unit of the Takla Group encircling most of the Germansen batholith might suggest that diapiric emplacement entrained and uplifted the base of the Mesozoic section. We have designated the basal strata in this area the Slate Creek formation instead of the Rainbow Creek formation because of continuity with the type locality (Ferri and Melville, in preparation).

INZANA LAKE FORMATION (uTrIL)

Well-foliated green tuff, lapilli tuff and grey siltstone and slate of the Inzana Lake formation extend from previously mapped exposures near Tsaydaychi Lake in 93N/7 East Half (Nelson *et al.*, 1992a) into the headwaters of Valleau Creek (Figure 1-7-3). Foliation and bedding strike northwest and dip steeply. In contrast, the contact with the overlying Witch Lake formation, defined in outcrops on the hills east of Valleau Creek, is nearly horizontal. This structural discordance between gross attitudes and attitudes within incompetent units is common in the Takla Group. It probably reflects strong disharmonic folding due to competency contrasts and the presence of décollements between massive and thin-bedded units.

WITCH LAKE FORMATION (uTrWL)

The Witch Lake formation east of Valleau Creek (Figure 1-7-3) consists of predominantly green and minor maroon augite porphyry flows, with lesser aphanitic flows, augite-plagioclase porphyry agglomerates, hornblende-porphyrific flows and plagioclase-phyric subvolcanic bodies. Subordinate volcanoclastics include tuffaceous sandstone, crystal tuff and lapilli tuff. The prominence of flows within these exposures is more akin to the Plughat Mountain formation than the Witch Lake formation to the south. However, the rocks lack olivine phenocrysts and large amygdules which are often present in the Plughat Mountain formation. This area may represent a mixing of volcanic styles between two different volcanic centres, or perhaps be the product of a centre with transitional characteristics.

PLUGHAT MOUNTAIN FORMATION (uTrPM)

The Plughat Mountain formation outcrops in most of eastern 93N/11 and on both sides of the Omineca River in 93N/14 (Figure 1-7-3). It is a lithologically and spatially highly variable, basalt-dominated volcanic pile. The most southerly exposures on Caribou Mountain, in eastern 93N/11, consist of interbedded green augite-porphyrific vesicular basalt flows and fragmentals with lesser maroon heterolithic agglomerate and flows. Minor quantities of plagioclase-phyric crystal tuff and a monzonite intrusive clast were noted on the north side of the mountain. The ridge north of West Dog Creek consists entirely of green augite±plagioclase-porphyrific agglomerate and lapilli tuff with one maroon augite-olivine porphyry flow at the base of the sequence near the road. Eaglenest Mountain is dominated by green augite±olivine±plagioclase-bearing flows and agglomerates. There are similar porphyritic flows and agglomerate on the mountain southeast of Eaglenest, as well as large outcrops of well-formed pillow basalt. The presence of pillow basalt in the heart of the Plughat Mountain formation may strengthen the case for the structural panel

hosting the Lounge Lizard intrusive complex as being part of the Plughat Mountain formation.

In the Omineca River valley lithologies include large-augite, small-plagioclase porphyry flows and agglomerates, large-amygdule flows, maroon and green amygdaloidal large-olivine porphyry flows and heterolithic lapilli tuffs that contain clasts in which plagioclase and augite are the primary phenocrysts. Limestone clasts occur within such lapilli tuffs near Twentymile Creek. Also along Twentymile Creek, aphanitic basalt flows, small-hornblende porphyry flows, augite and hornblende porphyry heterolithic lapilli tuffs and minor interbeds of tuffaceous sandstone form part of the sequence. In general, maroon colours are more common in the south while plagioclase contents of the volcanics increase to the north.

One thrust panel north of the Omineca River contains aphyric to small-olivine porphyry pillow basalts that are intruded by the Lounge Lizard intrusive complex. The southeastern continuation of this panel into 93N/15 is a narrow, fault-bounded sliver of pillow basalt and green and red basalt lapilli tuff. Although continuity cannot be established, this panel is assigned to the Plughat Mountain formation on the basis of lithologic similarities.

An Upper Triassic limestone reef (uTrPMA), viewed from a distance, resembles a kilometre-wide cliff nest, giving rise to the local name of Eaglenest Mountain (Plate 1-7-1). A well-used golden eagle nest is located on one of the limestone buttresses. The reef itself contains a rich and varied coralline fauna in discrete packstone beds that are interbedded with crinoid wackestones and calcirudites. Its intimate relationship with Plughat Mountain basalts is shown by abundant volcanic debris in the wackestones, and conversely by limestone clasts in nearby lapilli tuffs. Its perched position in the western cliffs of Eaglenest Mountain suggests that the mountain itself is part of an exhumed Late Triassic volcanic edifice. Identification of coral species is pending.

One continuous, mappable subunit was defined at the top of the Plughat Mountain formation west of Kwanika Creek. It is a bright red to maroon augite±olivine-phyric basalt flow (uTrPMB) that is often highly vesicular to scoriaceous. Flow breccia is common near its top. The presence of scattered bright red sandstone lenses overlying the breccia suggests reworking in shallow water. This maroon basalt marker unit overlies green augite±olivine porphyry agglomerates and flows of the main Plughat Mountain formation.

CHUCHI LAKE FORMATION (IJCL)

In the eastern half of 93N/7, the Chuchi Lake formation overlies the Witch Lake formation in a gently south-dipping homocline (Nelson *et al.*, 1992a). This continues into the lowlands west of Valleau Creek, east of Ahdatay Lake and in bank exposures along Valleau Creek where plagioclase-augite-porphyrific amygdaloidal flows, heterolithic plagioclase-dominant laharic agglomerates, plagioclase-porphyrific lapilli tuffs and a body of large plagioclase-phyric hypabyssal monzonite are exposed (Figure 1-7-3). The Chuchi Lake formation does not outcrop north of this area.

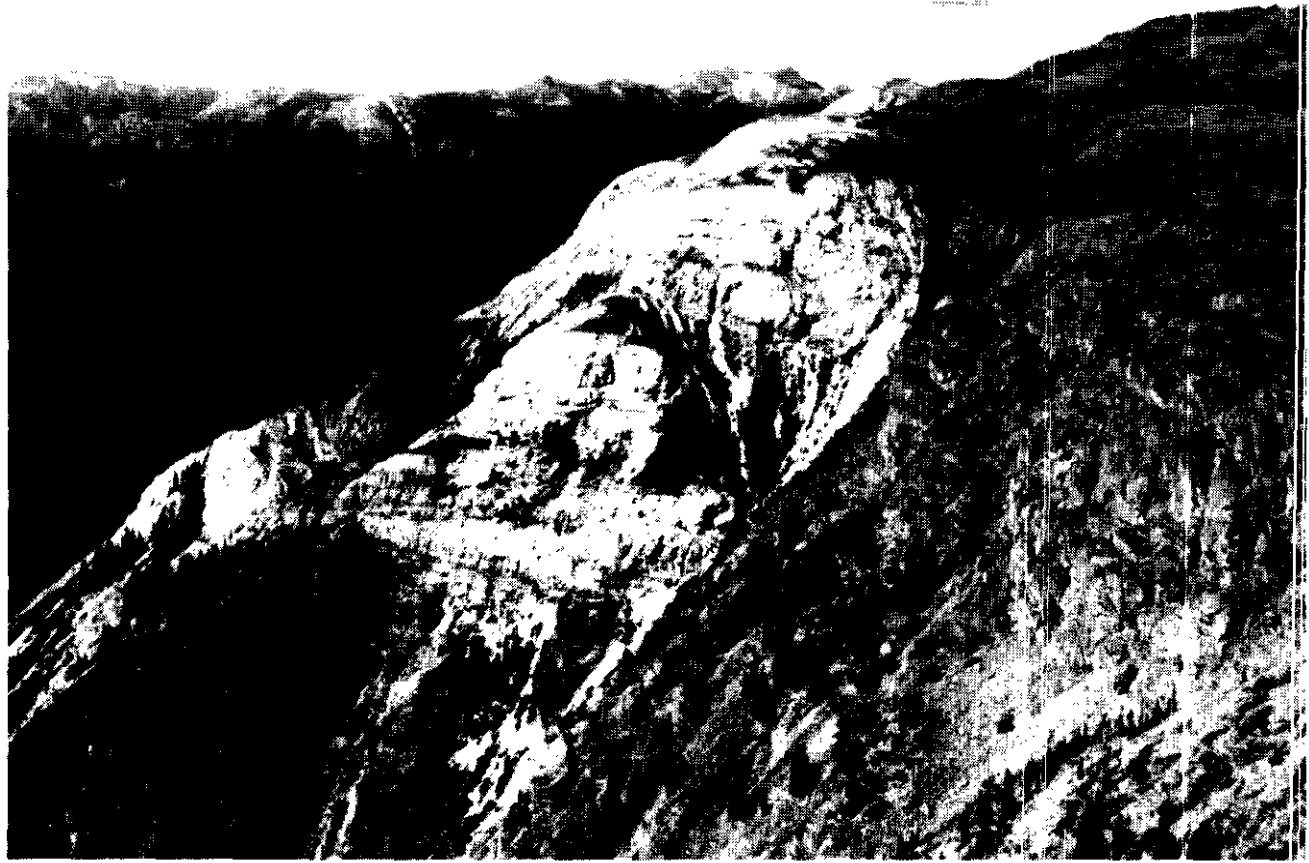


Plate 1-7-1. Eaglest limestone of probable Late Triassic age has reefoid appearance as it outcrops along the edge of a cliff exposing volcanic rocks of the Plughat Mountain formation (uTr_{mb}).

TWIN CREEK FORMATION (IJ_{rc})

West of Kwanika Creek, near Twin Creek, the red basalt at the top of the Plughat Mountain formation (uTr_{mb}) is overlain by heterolithic lapilli tuff, agglomerate, crystal tuff and local heterolithic volcanic conglomerate, all with significant to dominant plagioclase phenocrysts plus augite and hornblende (Figure 1-7-3). Augite-hornblende, plagioclase-augite, plagioclase and plagioclase ± quartz porphyry flows also occur. These are all included in the informal Twin Creek formation. Heterolithic lapilli tuffs predominate in the lower, more northerly exposures where augite is more prominent near the base. Less abundant, strongly heterolithic plagioclase-rich fragmental units are also present and high-level intermediate intrusive clasts occur in the conglomerate. Stratigraphically higher exposures southwest of Twin Creek include large-plagioclase and plagioclase ± quartz porphyry flows and related fragmental units. In general the section is consistent with progressive felsic differentiation of volcanic magmas through time. The presence of quartz is noteworthy.

The base of the heterolithic lapilli tuffs rests sharply on the red basalt. The contact is irregular on both minor and major scales. It undulates over 50 to 100 metres of elevation on mountain sides. In outcrop and hand sample scale the top of the basalt shows sharp irregularities, with clasts incorporated or partly incorporated in the overlying debris (Plate

1-7-2). Bedding in the red sandstones of the underlying basalt unit approximately parallels the overall attitude of the contact. Both dip very gently to the south. These attributes describe a low-angle unconformity or paraconformity, corresponding to a volcanic hiatus with no significant deformation.

We assume that the Plughat Mountain formation is entirely Late Triassic in age. By lithologic analogy with the Chuchi Lake formation we assign a provisional Early Jurassic age to the Twin Creek formation, pending zircon dating of one of the plagioclase porphyry flows near Groundhog Creek. The lapilli tuff - red basalt contact detailed above is considered to represent the Triassic-Jurassic boundary (Plate 1-7-2).

WILLY GEORGE SEQUENCE (uTr_{wl})

A distinctive pyroclastic-epiclastic sequence is exposed on the ridge east of Willy George Creek in western 93N/14E (Figure 1-7-3). Overall, this package is strongly heterolithic, although many of the individual lapilli tuff units within it are monolithic. The lapilli tuffs represent variations on a theme of augite-plagioclase, augite, plagioclase-augite and plagioclase porphyry volcanic clasts. Consistent volcanic textures within some units suggest sourcing from single volcanic events; others are strongly heterolithic and chaotic.

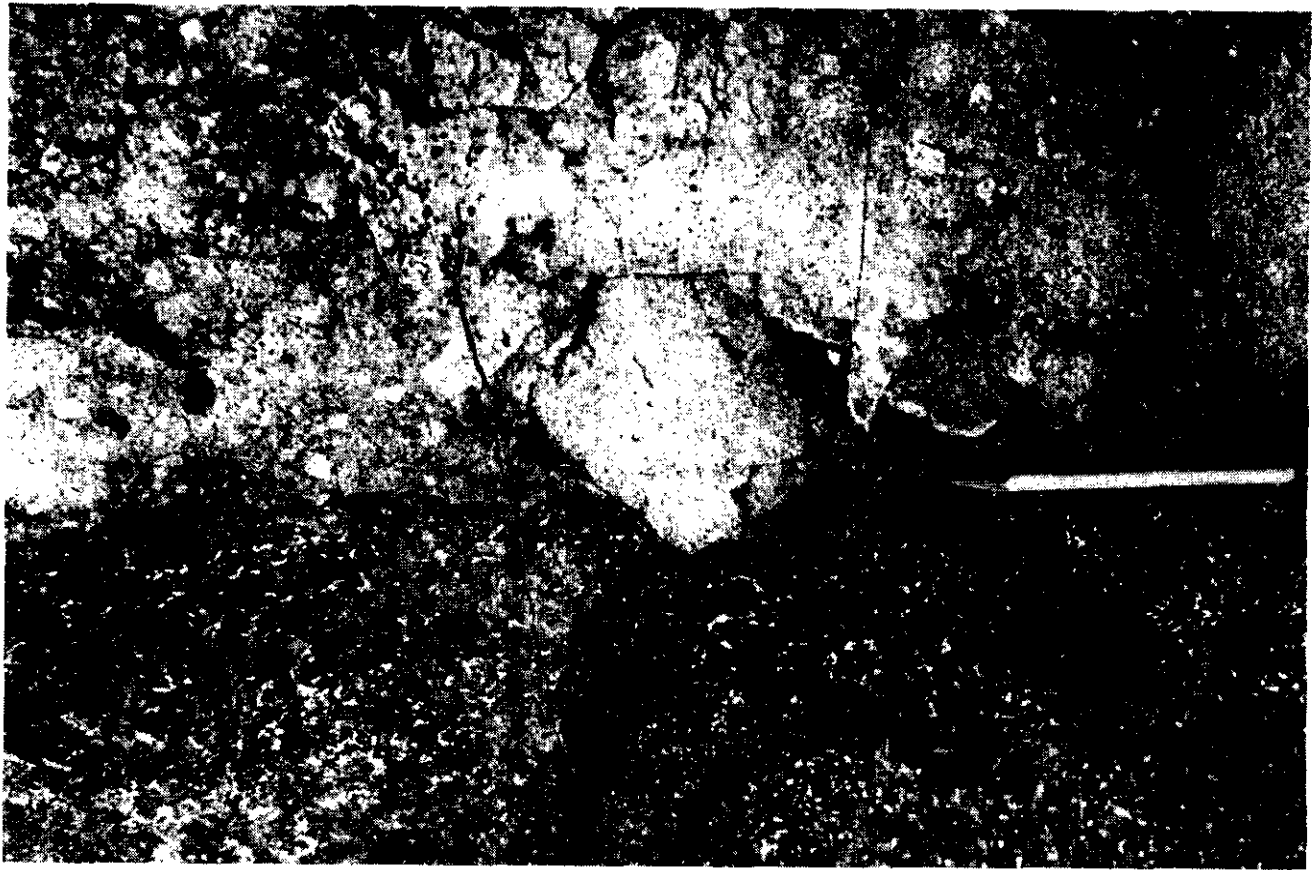


Plate 1-7-2. Triassic-Jurassic contact marked by an irregular surface between maroon basalt (uTr_{mb}) and overlying heterolithic agglomerate and breccia of the Twin Creek formation (J₁c).

One unit, traceable over several kilometres, contains white dacite blocks with sedimentary and other volcanic clasts.

The lapilli tuffs are interbedded with crystal tuffs and sandstones, which make up about half of the section. Sedimentary breccias like those in the Inzana Lake formation in 93K/16 (Nelson *et al.*, 1991a) are also present. Limestone clasts occur in the sedimentary breccias and also in the volcanic-dominated fragmental units. Some lapilli tuffs have a limy matrix. An interval of pale grey lithic arkose/wacke, argillite and siltstone lies within the sequence.

The Willy George sequence strikes northwest and dips and faces steeply west. Its uppermost unit is a fine to coarse monolithic pyroclastic rock, in which clasts show a distinctive texture of very large augite and tiny plagioclase phenocrysts in a grey groundmass. This unit apparently underlies the Plughat Mountain formation in exposures north of the Omineca River. Thus, the Willy George sequence is a stratigraphic and facies equivalent of the Inzana Lake formation, but the prominence of plagioclase within it contrasts strongly with the Inzana Lake. If it is Late Triassic in age, then it implies the existence of a so-far undocumented Late Triassic intermediate volcanic centre. Such centres must have existed in Late Triassic time, as plagioclase-porphyrific volcanic clasts, thin trachytic tuff beds and intermediate hypabyssal intrusive clasts occur in the Inzana Lake, Witch Lake and Plughat Mountain formations. The

Willy George sequence is the closest indication of a more felsic Triassic volcanic centre observed thus far in the Takla arc.

TAKLA FELSIC UNIT (Tr_{Jtr})

A Triassic or Jurassic mixed volcanic and volcanoclastic package crops out in the southeasternmost corner of 93N/14E (Figure 1-7-3). In contrast to the neighbouring Plughat Mountain formation, it has a large component of felsic material. Lithologies includes heterolithic lapilli tuff, agglomerate-conglomerate, amygdaloidal augite-porphyrific flows and crystal-ash tuffs with plagioclase dominant over augite phenocrysts. Fragments in the coarser units include plagioclase+subordinate augite-porphyrific volcanics, monzonite to diorite intrusives, maroon augite-porphyrific volcanics, silicified tuffaceous sediments and cherty argillite.

This unit continues beyond the Discovery Creek map area into low ridges northwest of Plughat Mountain (93N/15; Ferri *et al.*, 1989). Planar bedded, quartz-rich conglomeratic sandstones, sandstone, siltstone and cherty sediments together with maroon quartz-bearing amygdaloidal plagioclase-porphyrific volcanics attest to the felsic nature of this unit.

The age of this sequence is unknown. The presence of volcanic quartz in some of the volcanics and sediments

suggests a link to the Jurassic Twin Creek formation. However, the presence of the nearby Willy George sequence supports the possibility of a Triassic age for these felsic rocks.

UPPERMOST LOWER JURASSIC SEDIMENTARY SEQUENCE (IJs)

Lower Jurassic clastic sedimentary rocks form small cliffs along Discovery Creek for approximately 4 kilometres north of the road bridge (Figure 1-7-3). The most abundant lithologies are green to brown-weathering lithic arkose and greywacke with interbedded siltstones. Minor, local conglomerates contain green to maroon plagioclase-augite-porphyrific volcanic clasts. Many of the sandstones are composed of grit-sized grains and crystals of plagioclase, orthoclase, hornblende, biotite and augite that appear to be the immature eroded remnants of a plutonic source. The most likely candidate is the nearby Hogem intrusive complex. Less than 1 per cent detrital muscovite occurs in some of the beds.

Three fossil localities were identified on Discovery Creek. The macrofossil collections were examined by Giselle Jakobs and Howard Tipper of the Geological Survey of Canada. Two localities with ammonites similar to the one in Plate 1-7-3, yielded Toarcian ages. An internally radiat-

ing belemnite fossil suggests a post latest middle Toarcian age for the third locality (Table 1-7-1).

The presence of plutonic debris and detrital muscovite in these late Early Jurassic sediments provides important information on Jurassic tectonics. Potassium-argon mineral ages for the Jurassic phases of the Hogem intrusive complex range from 206 ± 8 to 171 ± 6 Ma (Garnett, 1978; data converted to new decay constants, R.L. Armstrong, unpublished data). Toarcian time is bracketed between 187 ± 15 and 178 ± 11 in the new time scale of Harland *et al.*, (1990). The plutonic debris in these late Toarcian sediments shows erosion of the Hogem intrusive complex while parts of it were still forming and cooling.

The positive identification of muscovite in this Toarcian sequence would require a pericratonic, miogeoclinal or cratonic source. The deposition of these sediments was approximately coeval with the emplacement of Quesnellia onto the North American margin (181 to 173 Ma; Murphy *et al.*, in press; or possibly as early as 186 Ma, G. Nixon, personal communication, 1992). They predate the subsequent uplift of metamorphic core complexes in the Omineca Belt. The oldest known cooling age for a metamorphic rock in the Ingenika Group is 174 Ma (K-Ar whole rock; Ferri and Melville, in preparation). The source of muscovite may lie farther east, perhaps in the craton; or alternatively within an accreted pericratonic terrane.



Plate 1-7-3. Hand sample of late late Toarcian ammonite from Discovery Creek sediments (IJs).

USLIKA FORMATION (KTU)

The Uslika Formation is a clastic package that occurs as a panel within the Discovery Creek fault zone. The rocks are contiguous with the Conglomerate Mountain exposures in 94C/3 (Ferri *et al.*, 1992c). In the northern part of 93N/14E (Figure 1-7-3) conglomerate and coarse sandstone predominate with minor occurrences of siltstone and mudstone with rare broadleaf and coniferous macrofossils. The conglomerate is composed of well-rounded coarse cobbles and boulders of monzonite, syenite, augite-porphyrific volcanics, plagioclase-porphyrific volcanics, green and maroon tuffs, green, red and pale beige chert, black and grey siliceous argillite, quartzite (often weakly foliated) and vein quartz. The rocks are clast supported, poorly sorted and very well indurated. Hematite in the matrix gives clasts a shiny coating and imparts a reddish hue to outcrops. Bedding is weakly visible in conglomerate beds and better defined in sandstones and conglomeratic sandstones. In general the stratigraphy strikes northwest to north. Dips vary from gentle to steep.

Approximately 15 kilometres south of these exposures in Discovery Creek, grey and black conglomerate occurs with interbeds of arkosic sandstone, siltstone, and mudstone. A bituminous coal bed 1 metre thick outcrops along the stream bank. The conglomerate contains small cobbles and pebbles of two main lithologies, dark grey to black chert and siliceous argillite, and lithified grey arkose. Minor components include vein quartz, turquoise green chert and quartz biotite granite. Bedding strikes northwest and dips steeply to the southwest.

Clasts in the Uslika Formation are probably derived from local sources: intrusive clasts from the Hogen intrusive complex, volcanic rocks from the Takla Group, quartzite from the Atan Group and cherts from the Lay Range assemblage and the Nina Creek group. Metamorphic clasts were not recognized in the study area, however, Roots (1954) documented rare clasts of quartz-mica schist and quartz-mica-feldspar gneiss less than 2 centimetres in diameter. The absence of abundant metamorphic clasts may indicate a more local source for the majority of clasts in the Uslika Formation; or perhaps the bulk of the metamorphic core complexes in the Omineca crystalline belt were not unroofed at the time of erosion and deposition. A syenite clast from the conglomerate yielded a 168 ± 1 Ma U-Pb zircon age (Parrish and Tipper, 1992), placing a maximum age of Late Jurassic on the Uslika Formation. Rare quartz-biotite-bearing intrusive rocks and coarse orthoclase porphyries are more akin to Cretaceous phases of the Hogen intrusive complex than Jurassic. This evidence supports a Cretaceous to Tertiary age for the Uslika Formation.

The Uslika Formation is bounded by faults of the Discovery Creek fault system. It is probable that it was deposited in graben structures along the fault in response to transcurrent motion (*see* Structure; Figure 1-7-5C; Ferri *et al.*, 1992a). The grabens are likely long-lived growth structures that contain different fans of clastic material derived from various areas. This structural scenario would also explain the large variation in inclination of beds in a seemingly undeformed sequence.

The Uslika Formation may be broadly correlatable with the Sustut Group in the area. Although Sustut clastics are less cemented and have better fossil control, the Sustut Group and the Uslika Formation are clastic packages of similar age, deposited in similar sedimentary and structural environments.

CRETACEOUS – TERTIARY(?) SEQUENCE WEST OF GERMANSEN LAKE (KTvs)

A variable suite of volcanic and clastic rocks is exposed at the west end of Germansen Lake in West Dog Creek (Figure 1-7-3). Pale pink-grey to buff-coloured hornblende-biotite-bearing, quartz-eye rhyolite is the most abundant lithology. It is locally flow banded and has a chalky weathering appearance. Less abundant but diagnostic quartzofeldspathic conglomerate with angular and rounded fragments of rhyolite, medium-grained equigranular biotite granite, volcanic quartz and vein quartz occurs with green sandstone, siltstone and volcanoclastics.

The contact of this unit with the Takla Group is not exposed. The steep dips in this section, its restricted aerial extent, and the lack of Takla volcanic fragments in the conglomerates, support deposition in a small, fault-bounded graben. The volcanic quartz is probably derived from the rhyolites and the vein quartz and intrusive clasts may have been shed from the Germansen batholith. This graben represents the southernmost extent of the Discovery Creek fault system and is most likely Cretaceous to Tertiary in age.

CRETACEOUS – TERTIARY(?) MAROON TUFFS IN DISCOVERY CREEK (KTv)

Bright maroon crystal-lithic tuffs outcrop in the lower part of Discovery Creek in narrow fault-bounded panels. The lack of bedding and the homogeneous texture of these tuffs suggests subaerial deposition, perhaps an ash flow. The volcanics contain phenocrysts of plagioclase, orthoclase and embayed quartz with lithic fragments of feldspar porphyry and carbonate. In one exposure the massive tuff grades into bedded red sandstone and mudstone. A similar unit is exposed in the eastern tributary creek next to a splay of the Discovery Creek fault.

The age of these rocks is unknown. They may be coeval with the Uslika Formation or as young as Tertiary. No evidence of interbedding with other lithologies was seen. These small felsic accumulations may have been localized along the faults, or in ancient stream valleys that followed faults.

INTRUSIVE UNITS

VALLEAU CREEK INTRUSIVE COMPLEX (TrJvc)

The Valleau Creek intrusive complex is a tabular, composite mafic to ultramafic body. It extends southeasterly from the southern part of 93N/11 along the Valleau Creek valley for 30 kilometres to the vicinity of Klawli Lake. There it turns abruptly eastwards and ends (Figure 1-7-3). This complex is reflected by a very strong linear north-

westerly trending aeromagnetic anomaly (Geological Survey of Canada, 1963). The most widespread lithologies are fine to medium-grained diorite and gabbro. Plugs or rafts of coarse-grained pyroxenite and hornblende with up to 10 per cent magnetite are scattered within it. The linear nature of the Valleau Creek complex and the presence of mylonitic float on its eastern margin suggest the complex is fault bounded and structurally controlled. A Late Triassic to Early Jurassic age for the complex is inferred as its northern end is truncated by a probable Early Jurassic monzonite phase of the Hogem intrusive complex.

LOUNGE LIZARD INTRUSIVE COMPLEX (TrJLL)

Most of Lounge Lizard Mountain north of the Omineca River and east of Discovery Creek is underlain by a composite diorite-gabbro body with a wide variety of textural variants (Figure 1-7-3). In general, the body shows increasing average grain size away from its southern margin, where it intrudes Plughat Mountain pillow basalt. Finer grained phases usually cut coarser units, although the reverse is sometimes observed. Near the southern margin, fine to medium-grained diorite is most abundant. The summit of the mountain is underlain by very coarse grained to pegmatitic diorite with areas of igneous layering, intruded by white plagioclase-clinzoisite pegmatites. Large plagioclase-phyric diorite dikes cut all other phases.

The age of this body is not known. It intrudes pillow basalts inferred to be Upper Triassic. Texturally, it resembles the diorite-gabbro border phase of the Hogem intrusive complex near Chuchi Lake (Nelson *et al.*, 1992a, b).

APLITE CREEK INTRUSIVE COMPLEX (EJAC)

The Aplite Creek intrusive complex is centred on a low mountain 5 kilometres southeast of Ahdatay Lake (Figure 1-7-3). Like the Valleau Creek complex, it is dominated by fine to medium-grained diorite and gabbro. Textures range from nearly equigranular to porphyritic with large augite phenocrysts. These rocks, mapped as volcanic in previous work (Paterson and Barrie, 1991), are distinguished by their holocrystalline matrix and lack of fragmental or amygdaloidal textures. Minor amounts of intrusive breccia, consisting of hypabyssal augite-hornblende-porphyritic monzodiorite and epidotized clasts, occur in Aplite Creek. Several small outcrops of hypabyssal crowded monzonite porphyry are present and later aplite, syenite and monzonite dikes are also part of the complex.

HOGEM INTRUSIVE COMPLEX (EJH, EKH)

The map area includes parts of the eastern edge of the Hogem intrusive complex. Two broad lithologic suites are present: a quartz-deficient suite of monzonite, quartz monzonite, granodiorite and diorite of probable Early Jurassic age (EJH) and a quartz-rich granite suite of probable Cretaceous age (EKH) with textures identical to those in the Germansen batholith (EKG) and Klawli stock (EKK; Figure 1-7-3). The quartz-deficient suite is characterized by medium to coarse-grained equigranular and rare porphyritic

textures. The quartz-rich suite is represented by two discrete granite plutons, one west of Valleau Creek that intrudes the Valleau Creek intrusive complex and one at the headwaters of Twin Creek. Orthoclase megacrysts are characteristic of these plutons. Orthoclase-megacrystic, medium-grained granite dikes intrude the Takla Group in and north of the Twin Creek valley. A small body of syenite west of Eaglenest Mountain is assigned to the Cretaceous suite.

A vertical mylonite zone, 250 metres wide with steep lineations, is exposed along the eastern margin of the Hogem complex 1 kilometre southwest of Goat Ridge. This substantiates structurally controlled emplacement of the Early Jurassic monzonite-granodiorite phase of the composite intrusion in this area.

GERMANSEN BATHOLITH (EKG)

The Germansen batholith outcrops on the eastern edge of 93N/11E near Moly Lakes and in the northern part of 93N/7W at the headwaters of Valleau Creek (Figure 1-7-3). At the first locality the batholith is a fine to medium-grained equigranular hornblende granite. It has intruded and metamorphosed black shales and slates of the Slate Creek formation to biotite schist and strongly hornfelsed phyllite. The contact is sheared and folded; kinematic indicators in the metasediments show southwest-side-down sense on moderate to steeply dipping foliation planes. This is consistent with the upward emplacement of the western margin of the Germansen batholith along a southwest-dipping contact zone.

Near Valleau Creek, the Germansen batholith is a coarse-grained equigranular to orthoclase-megacrystic biotite granite. Minor syenite and aplite dikes cut the intrusion. The host lithologies are sheared and foliated metauffs and meta-volcanics of the Inzana Lake formation. Minor amounts of molybdenite occur on fractures here and near Moly Lakes.

An Early Cretaceous, 106 ± 4 Ma age for the Germansen batholith has been obtained by a K-Ar dating on a biotite sample (Ferri and Melville, in preparation).

KLAWLI STOCK (EKK)

The Klawli stock extends onto 93N/7W from the area mapped in 1991 (Nelson *et al.*, 1992a). Orthoclase-megacrystic hornblende biotite granite outcrops in small glaciated gullies on the north side of Klawli Lake (Figure 1-7-3). The body has a rim of microdiorite and gabbro that probably represents the southeastern tail of the Valleau Creek intrusive complex and its associated aeromagnetic high. The Klawli intrusion is texturally identical to large parts of the Germansen batholith and is therefore assigned an Early Cretaceous age.

STRUCTURAL GEOLOGY

VALLEAU CREEK FAULT; A SYNVOCANIC STRUCTURE?

The tabular nature of the Triassic-Jurassic Valleau Creek intrusive complex (Figure 1-7-3) and the associated linear magnetic signature suggest a strong structural control for its

emplacement. This mafic-ultramafic complex is similar to the earliest identified phase of the Hogem intrusive complex and is probably synchronous with Takla volcanism. Long-lived synvolcanic structures are key to the generation of alkaline porphyry copper-gold systems (Nelson *et al.*, 1991a). The Valleau Creek fault may be one of the best examples of a synvolcanic structure in the Takla arc. The presence of Jurassic Chuchi Lake formation west of the complex and Triassic Inzana Lake formation to the east suggests that the fault was active until at least the Jurassic and had an overall displacement of roughly 1 kilometre, west side down. The lack of crowded porphyry intrusions and porphyry mineralization and alteration may be a function of a deep level of erosion. Minor disseminated malachite was noted south of Wudtsi Lake.

Another fault structure occurs east of the Valleau Creek complex near the headwaters of Valleau Creek. The fault is represented by an iron-carbonate, quartz and sericite alteration zone 1.5 to 2 kilometres wide with minor pyrite and

mariposite(?). Motion and offset on the structure are unknown as it lies entirely within the Inzana Lake formation. To the north this fault may have helped control the western margin of the Germansen batholith.

TWIN CREEK MAP AREA

The Twin Creek map area is characterized by predominantly subhorizontal Takla volcanic stratigraphy. High-angle faults near Groundhog Creek and north of Twin Creek have displacements in the order of a hundred metres or less, determined by the offset of the maroon basalt marker bed (uTrPmb; Figures 1-7-3, 1-7-4). The northwest-trending Twin Creek fault cuts these small-scale structures. Quartz-bearing potassium feldspar porphyry dikes and associated hydrothermal alteration and polymetallic sulphide mineralization are controlled by the Twin Creek shear zone (Bailey, 1991). Many of the dikes are deformed, suggesting a probable synplutonic Cretaceous motion on the Twin Creek fault.

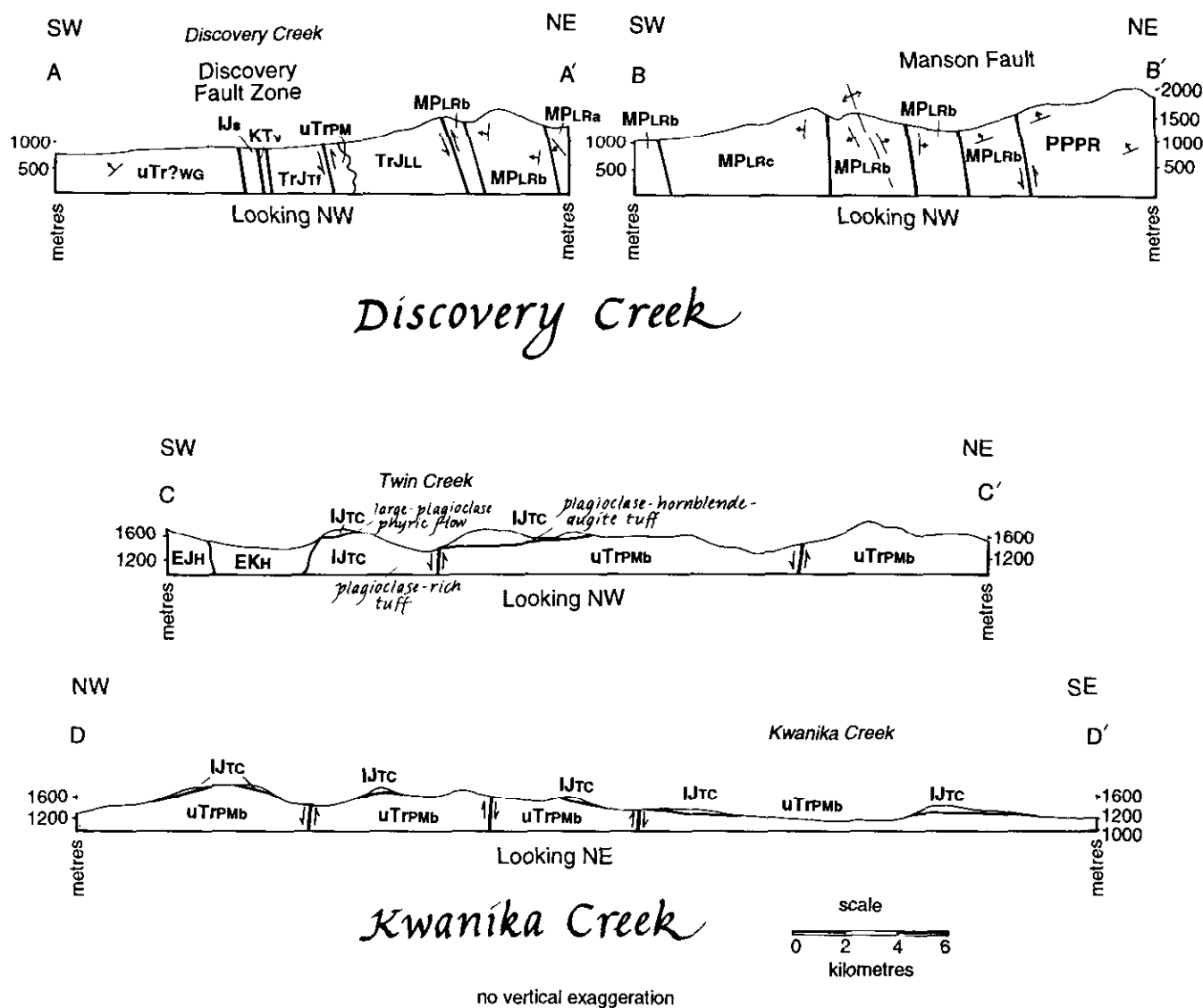


Figure 1-7-4. Cross-sections of map area. See Figure 1-7-3 for locations.

North-trending faults near Twentymile Creek merge into the transcurrent transfer zone in Discovery Creek (93N/14E).

THE MANSON CREEK – DISCOVERY CREEK DEXTRAL TRANSFER ZONE

The Discovery Creek area is transected by two major strike-slip fault systems; the Manson fault zone and the Discovery fault zone. The north-west-trending Manson fault zone is a vertical dextral strike-slip fault with an overall strike length of 150 kilometres. It continues southwards into the McLeod and Rocky Mountain Trench fault systems (Figure 1-7-2). Ferri and Melville (in preparation) suggest a Cretaceous age for most of the motion on this structure. The fault dies northward, as there is no apparent offset of stratigraphy across its projected location south of Wasi Lake (Ferri *et al.*, 1992c).

The Discovery Creek fault zone is a north-northwest-trending strike-slip system that is approximately 5 kilometres wide in the map area. Its southern extent is the west Germansen Lake graben where Cretaceous to Tertiary rhyolites and sediments (KTvs) outcrop. To the north, the fault swings slightly more northwesterly and joins the Lay Range fault system (Ferri *et al.*, 1993a) and then the Finlay-Ingenika-Pinchi fault system (Wheeler and McFeely, 1991).

The area between these two fault systems corresponds to a region of west-northwest-trending faults along the Omineca River. These faults divide stratigraphy into predominantly west-facing, steeply dipping, homoclinal packages that have a general trend of younging from northeast to southwest (Figure 1-7-4).

Kinematic indicators in the Discovery Creek area can be grouped into three categories consistent with various stress directions in a dextral transcurrent setting in which motion is stepping from one fault system to another. The result is a zone of compression linking the two fault strands (Figure 1-7-5A). Attitude *a* (Figure 1-7-5B) is perpendicular to the maximum stress (σ_1). It predicts pure compression or thrusting along west-northwest-trending faults. This corresponds to the major west-northwest-striking faults that divide the region into structural blocks. Kinematic indicators from the northeastern margin of the Lounge Lizard intrusive complex are consistent with northeast block up; that is a high-angle thrust fault. The general facing and younging of the structural panels towards the southwest is consistent with a steep southwest-verging thrust duplex. Regions where this younging trend is violated can be explained by less prominent west-side-up reverse faults or back thrusts, as in Cook Creek where limestone of the Middle to Upper Triassic Slate Creek formation is interleaved with Mississippian to Permian Lay Range assemblage.

Attitude *b* in the strain ellipse (Figure 1-7-5B) corresponds to an intermediate stress field in which dextral synthetic structures prevail. These structures are manifest as tight northwest-verging folds with steep southeast-plunging axes exposed in Discovery Creek (Plate 1-7-4; Figure 1-7-6). Their vergences support relative dextral motion for the Manson-Discovery fault system. Sinistral antithetic

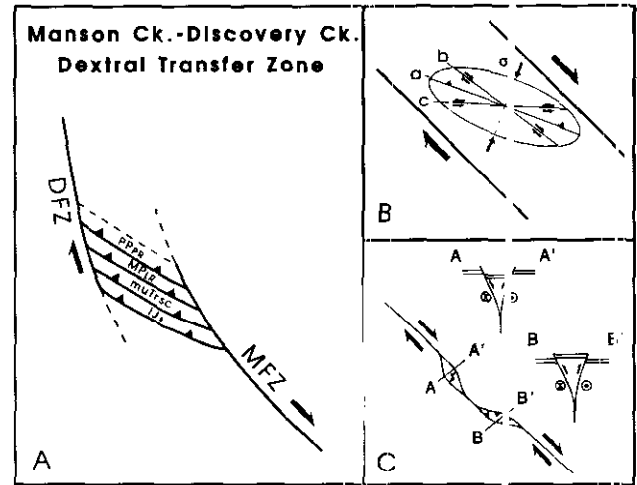


Figure 1-7-5. (A). Schematic diagram of a compressional transfer zone between the Manson Creek fault zone (MFZ) and the Discovery Creek fault zone (DFZ); stratigraphic abbreviations as in legend, Figure 1-7-3. (B). A strain ellipse for the compressional dextral transfer zone shows the maximum stress direction (σ_1) and predicts thrusting along direction *a*, dextral offset along orientation *b*, and sinistral offset in attitude *c*. (C). Figure showing changes in attitude of a dextral strike-slip fault (after Ferri *et al.*, 1992b). Cross-section A-A' depicts a negative flower structure forming grabens; an analogue would be the Uslika Formation (KTu). A positive flower structure (cross-section B-B') resulting in compression and thrusting as in the Manson Creek - Discovery Creek dextral transfer zone.

structures are expected along east-west trends (attitude *c*, Figure 1-7-5B). East-west sinistral shear is suggested by a fault zone 5 metres wide in Discovery Creek as well as numerous offset beds including a 1-centimetre layer of anthracite in the late Toarcian sediments. A carbonate alteration zone 20 metres wide, and smaller carbonate veins, also follow prominent east-west trends.

The structures observed near the Omineca River and southern Discovery Creek are consistent with the westward stepping of motion from the Manson fault zone to the Discovery fault zone through a zone of compression or positive flower structure (Figure 1-7-5C). In contrast, the Discovery Creek fault in the northern part of the map area is characterized by fault strands containing the Cretaceous to Tertiary Uslika Formation in simple grabens. This system continues northward into the Uslika Lake map area where Ferri *et al.*, (1992a) have concluded a northeist shift in the dextral fault has produced an extensional flower structure preserving younger sediments in grabens along fault strands (Figure 1-7-5C).

The change from compressional to extensional regimes along the Manson Creek - Discovery Creek dextral fault system occurs over a very short distance. This rapid change in orientation may reflect crustal-scale inhomogeneities, such as the first appearance of the Lay Range assemblage.

Timing of movement on the Manson Creek - Discovery Creek fault system is constrained to be as old as Cretaceous, based on the most probable age of the Uslika Formation and



Plate 1-7-4. Tight folds with steep southeast-plunging fold axes, Discovery Creek. These are consistent with dextral synthetic structures predicted by attitude **b** in strain ellipse (Figure 1-7-5B) for the Manson Creek - Discovery Creek dextral transfer zone.

the estimates of age of motion on the Manson fault zone (Ferri and Melville, in preparation). The fault probably continued to be active during the Tertiary with the deposition of the Sustut Group in the north (Ferri *et al.*, 1992c) and Cretaceous to Tertiary rhyolites at the west end of GERMANSSEN LAKE.

Minor fault-bounded, maroon, quartz-feldspar-bearing volcanics in southern Discovery Creek may represent later faulting along a north-northwest trend to open up small extensional structures.

MINERAL PROSPECTS

Mineral prospects in the map area are diverse and include epithermal, lode-gold, late-stage magmatic and skarn targets. Of these, the Aplite Creek (093N 085) and Takla Rainbow (093N 082) prospects have extensive exploration

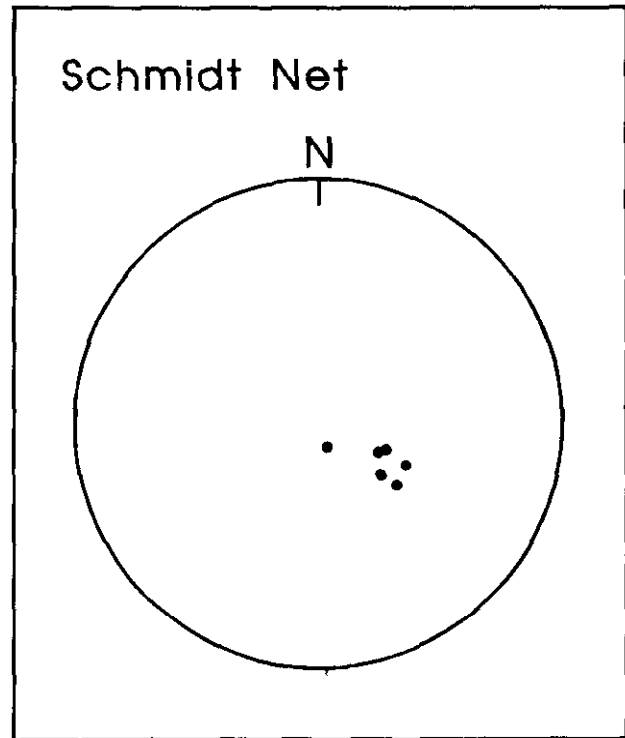


Figure 1-7-6. Steeply southwest plunging fold axes from tight folds in Discovery Creek, consistent with dextral synthetic structures in the Manson Creek - Discovery Creek dextral transfer zone.

histories. New mineral prospects include the Groundhog (093N 212), Vall (093N 213), Tsay (093N 214) and Wudtisi (093N 215). The abundant alkaline porphyry systems prevalent in the Nation Lakes area do not continue northwards into the area studied in 1992.

APLITE CREEK, AHDATAY (MINFILE 093N 085)

The Aplite Creek mineral prospect is situated 4.75 kilometres east-southeast of the southern end of Ahdatay Lake, along Aplite Creek. The area has received considerable exploration sporadically since the 1970s for porphyry copper-molybdenum, and most recently for porphyry copper-gold deposits. The prospect is within the Aplite Creek intrusive complex.

The area is cut by fracture zones trending northwest (345°) or northeast (060°). Deeply incised gullies with good outcrop exposures are coincident with these subvertical fracture zones and form prominent topographic linears. Moderate to intense propylitic and potassic alteration envelopes up to 20 to 25 metres thick occur around the fractures (Paterson and Barrie, 1991).

Mineralization consists of disseminated pyrite, pyrrhotite and chalcopyrite in anastomosing quartz-carbonate veins up to 4 centimetres thick. Sulphides are also present in the matrix of the country rocks, locally up to 100 metres away from the fractures (Paterson and Barrie, 1991). Various amounts of malachite, azurite, limonite and hematite are associated with the sulphide minerals.

TAKLA RAINBOW (MINFILE 093N 082)

The Takla Rainbow prospect lies at the headwaters of Twin Creek in 93N/11. This area was explored by various companies in the early 1970s. The Twin claims were staked in 1981 by L. Warren and N. Scarfe. Imperial Mines Limited optioned the claims in 1985 and explored them until 1989, identifying a significant zone of gold mineralization with associated copper and zinc on the West grid, referred to here as the Main zone. This zone is centred on the west-northwest-trending Twin Creek fault (Figure 1-7-3). The presence of abundant orthoclase-megacrystic granite dikes within the fault zone, many of them sheared, suggests syn-plutonic, probably Cretaceous, motion. Sulphides occur as disseminations in silicified, chloritized Takla Group and dikes within anastomosing shears of the Twin Creek fault zone. There are two other zones of alteration. The Red zone lies 1.2 kilometres northwest of the Main zone. It is an area of bleached tourmaline-matrix breccia developed in diorite of the Hogem intrusive complex. Eastfield Resources Limited drilled the Red zone in 1990. It reports low gold and copper values, propylitic alteration and disseminated sulphides that are suggestive of a porphyry-style system (Bailey, 1991). The ridge south of the Twin Creek fault is underlain by a strong quartz-kaolinite-pyrite alteration zone, capped by a discontinuous, horizontal alunite-quartz zone up to 5 metres thick that extends over 500 metres. It offers an as-yet unexplored epithermal target.

KLAWLI (MINFILE 093N 032)

The Klawli showing lies east of the Klawli River and is hosted by plagioclase±hornblende-porphyrific volcanics of the Chuchi Lake formation. In creek-bank trenches near old adits the volcanics are bleached and altered with zones containing pyrite, chalcopyrite, malachite and azurite. Although the rocks appear sheared and fractured, discrete shear zones and fabrics were not recognized. This showing was briefly described by Nelson *et al.*, (1992b). Three grab samples assayed greater than 2 per cent copper, 102.8 grams per tonne silver and 2.6 grams per tonne gold (Shaede, 1984).

GROUNDHOG (MINFILE 093N 212)

The Groundhog MINFILE locality is situated on a creek cut by the Tsayta - Germansen Lake road at Groundhog Pass, approximately 2 kilometres south of the confluence of Groundhog Creek and Twin Creek. A multi-element stream sediment anomaly was identified at the mouth of this creek during a Regional Geochemical Survey (RGS) in 1983. Follow-up assessment work by B.P. Resources Canada Limited in 1984 failed to locate the source of the anomaly (Humphreys, 1984).

Geological mapping in 1992 (this report) outlined fresh, maroon, amygdaloidal, plagioclase-porphyrific basaltic andesites underlying the Groundhog Pass area. The volcanics belong to the lower part of the Jurassic Twin Creek formation. Amygdules up to 1 centimetre in diameter are filled with massive magnetite. A grab sample from an amygdaloidal flow assayed 890 ppm copper, 100 ppm zinc and 12 ppm lead. The magnetite amygdules are the probable

source of the RGS anomaly. The magnetite was probably deposited by late-stage magmatic fluids. Minor malachite was noted on a fracture surface.

VALL (MINFILE 093N 213)

The Vall occurrence is located along the northeast bank of Valleau Creek approximately 5.5 kilometres from its confluence with the Klawli River. It is a skarn 20 centimetres wide with an attitude 000/78E, associated with a small, irregular carbonate vein system. A grab sample from the showing assayed 130 ppb gold and 176 ppm copper. The occurrence is hosted by hornfelsed coarse augite and minor plagioclase-porphyrific basalts of the Jurassic Chuchi Lake formation.

TSAY (MINFILE 093N 214)

The Tsay occurrence is hosted by a northwest-trending fault structure that extends 10 kilometres from the west end of Tsaydaychi Lake to the headwaters of Valleau Creek. The zone, 1.5 to 2 kilometres wide, lies entirely within the Inzana Lake formation and is characterized by iron carbonate and quartz-sericite alteration. Disseminated green mica (mariposite?) and pyrite occur in intensely altered, pale buff coloured, foliated sediments. A grab sample returned 135 ppm arsenic and 98 ppm copper.

The presence of anomalous arsenic values with carbonate-quartz-sericite alteration and mariposite suggests a listwanite association. The fault structure has potential for hosting gold-bearing quartz veins, and is thus an interesting regional exploration target.

WUDTSI (MINFILE 093N 215)

At the headwaters of Valleau Creek, approximately 5 kilometres north of the south end of Wudtsi Lake, a small, hybrid stock intrudes the Inzana Lake formation. The intrusive is a varitextured diorite-gabbro body. A hornfelsed mesocratic hornblende diorite phase contains pyrrhotite-bearing quartz stringers that yielded analysis of 190 ppm copper. Epiclastic sandstone and siltstone hosts are hornfelsed and altered (potassic?) and contain disseminated pyrite.

CONCLUSIONS

TAKLA GROUP INTERNAL STRATIGRAPHY AND VOLCANIC FACIES

The Nation Lakes mapping project now includes 4.5 standard 1:50 000 topographic sheets, extending over 150 kilometres along the northern Quesnel trough. Within this area, the Takla Group shows regional facies variations but an overall magmatic evolution from mainly basaltic in the Late Triassic to mixed, more differentiated volcanism in the Early Jurassic. As Upper Triassic Witch Lake augite-pyritic basalts are succeeded by the heterogeneous, Upper Jurassic Chuchi Lake volcanic suite, so is the dominantly basaltic Plughat Mountain formation succeeded by the intermediate Twin Creek volcanics, presumably of Early Jurassic age.

The Triassic and Jurassic volcanic suites probably did not form uniform blankets. Instead the Takla arc in the Nation Lakes area is composed of interfingering volcanic aprons with different volcanic styles and compositions. Significant differences occur between the Witch Lake and Plughat Mountain formations and between the Chuchi Lake and Twin Creek formations. The Plughat Mountain formation contains more flows, many with maroon colours and large amygdules, and a limestone reef. These suggest shallow marine conditions or partial emergence of the Plughat Mountain formation, in direct contrast to the Witch Lake formation. Compositional differences include abundant olivine in the Plughat Mountain and distinct trachyte flow units in the Witch Lake formation near Mount Milligan (Nelson *et al.*, 1991a, b).

The Twin Creek formation shows textural similarities to the Chuchi Lake, for instance in its heterolithic lapilli tuffs. It lacks interbedded basic flows and in particular the Pliensbachian sedimentary marker. Unlike the Chuchi Lake, quartz occurs in the more felsic units. This evidence for greater silica saturation in the north agrees with the contrast in chemistry between the shoshonitic Witch Lake formation and the transitional Plughat Mountain formation (Ferri and Melville, in preparation; Bellefontaine and Nelson, 1992).

JURASSIC TECTONICS

The Toarcian sedimentary sequence in Discovery Creek shows evidence for early uplift and exposure of monzonites in the Hogem intrusive complex, prior to emplacement of the Ducking Creek syenite. Muscovite in these sandstones requires either a pericratonic or a North American sedimentary source. In the latter case it would support the Toarcian accretion of Quesnellia to North America. If North American, the exact identity of the muscovite source is still difficult to pinpoint. It is probably not the metamorphic core complexes of the Omineca Belt, as they were not uplifted until post-Toarcian time.

LATE CRETACEOUS – EARLY TERTIARY STRIKE - SLIP TECTONICS

At the latitude of the Omineca River, dextral transcurrent motion steps westward from the Manson to the Discovery Creek fault zone. This step occurs across a transfer zone of high-angle southwest-directed reverse faults that juxtapose various stratigraphic levels of the Nina Creek group, Lay Range assemblage, Takla Group and younger sediments.

Motion on the Discovery Creek system may have accompanied deposition of the Lower Cretaceous to Tertiary Uslika boulder conglomerates. It also postdates Uslika deposition, as strands of the system transect the Uslika Formation, dividing it into moderately to steeply dipping panels. The southern end of the Discovery Creek fault system is a graben filled with rhyolites and siliciclastic sediments at the west end of Germansen Lake. A K-Ar age on one of the rhyolites may provide further age constraint on fault motion.

MINERALIZATION

Large propylitic and potassic alteration haloes like the Mount Milligan, Taylor, Witch and BP-Chuchi centres clus-

ter near the Nation Lakes area and do not extend north into the present map area. It appears that alkalic porphyries are not scattered evenly throughout the northern Quesnel trough but are instead concentrated in camps. Delineation of these mineralized camps is an important ongoing endeavor. What are the controls for the clustering of porphyry systems?

The Nation Lakes concentration of alkalic porphyries lies at the southern end of the Hogem intrusive complex, where it turns abruptly east and either plunges or terminates (Figure 1-7-2). Also, a northwesterly trending line of porphyry deposits follows the cryptic southern extension of the Val-leau Creek fault. Perhaps these regional-scale geologic features reflect fundamental discontinuities in the basement of the Takla arc. The proposed large-scale structures are shown by regional magnetic lineaments; they might also be modelled using gravity data.

ACKNOWLEDGMENTS

Dave Bailey gave freely of his expertise and experience in the Kwanika Creek area and co-authored the Kwanika Creek map sheet (Bailey *et al.*, 1993). Filippo Ferri, Chris Rees, Steve Dudka and Dan Meldrum helped in unravelling the structural complexities of the Discovery Creek area. Ron Repko pointed our noses at the choicest ammonites in Discovery Creek and Giselle Jakobs and Howard Tipper promptly identified them for us. We would also like to acknowledge Larry Erickson's songs, Inge Erickson's darn good rhubarb brew, Betty Howrys' pies, Bert Howrys' stories, Scott Müller's ice cream, and the professional and friendly service of Pacific Western pilots Karl Scholz and Spring Harrison.

REFERENCES

- Armstrong, J.E. (1949): Fort St. James Map-area, Cassiar and Coast Districts, British Columbia; *Geological Survey of Canada*, Memoir 252.
- Bailey, D.G. (1991): Qualifying Report on the Takla-Rainbow Property, Omineca Mining Division, North-central British Columbia; *B.C. Ministry of Energy, Mines and Petroleum Resources*, Assessment Report 20968.
- Bailey, D., Nelson, J.L., Bellefontaine, K.A. and Mountjoy, K. (1993): Geology and Geochemistry of the Kwanika Creek Map Area (93N/11E); *B.C. Ministry of Energy, Mines and Petroleum Resources*, Open File 1993-4.
- Bellefontaine, K.A. and Nelson, J.L. (1992): New Paleontologic and Lithogeochemical Data from the Nation Lakes Area and its Implications for the Quesnel and Stikine Arcs; Lithoprobe Southern Cordillera Transect Workshop and Cordilleran Tectonics Workshop, *University of Alberta*, Program with Abstracts, Report 24, page 84.
- Ferri, F. and Melville, D.M. (1988): Manson Creek Mapping Project (93N/9); in *Geological Fieldwork 1987*, *B.C. Ministry of Energy, Mines and Petroleum Resources*, Paper 1988-1, pages 169-180.
- Ferri, F. and Melville, D.M. (1989): Geology of the Germansen Landing Area, British Columbia (93N/10, 15); in *Geological Fieldwork 1988*, *B.C. Ministry of Energy, Mines and Petroleum Resources*, Paper 1989-1, pages 209-220.
- Ferri, F. and Melville, D.M. (1990a): Geology between Nina Lake and Osilinka River, North-central British Columbia (93N/15,

- North Half and 94C/2, South Half); in *Geological Fieldwork 1989*, B.C. Ministry of Energy, Mines and Petroleum Resources, Paper 1990-1, pages 101-114.
- Ferri, F. and Melville, D.M. (1990b): *Geology between Nina Lake and Osilinka River, North-central British Columbia 93N/15 (North Half) and 94C/2 (South Half)*; B.C. Ministry of Energy, Mines and Petroleum Resources, Open File 1990-17.
- Ferri, F. and Melville, D.M. (in preparation): *Geology of the Germansen Landing - Manson Creek Area*; B.C. Ministry of Energy, Mines and Petroleum Resources.
- Ferri, F., Melville, D.M., Malensek, G.A. and Swift, N.R. (1988): *Geology of the Manson Lakes Map Sheet, 93N/9*; B.C. Ministry of Energy, Mines and Petroleum Resources, Open File 1988-12.
- Ferri, F., Melville, D.M. and Arksey, R.L. (1989): *Geology of the Germansen Landing Area, 93N/10 and 93N/15*; B.C. Ministry of Energy, Mines and Petroleum Resources, Open File 1989-12.
- Ferri, F., Dudka, S. and Rees, C. (1992a): *Geology of the Uslika Lake Area, Northern Quesnel Trough, British Columbia (94C/3,4,6)*; in *Geological Fieldwork 1991*, Grant, B. and Newell, J.M., Editors, B.C. Ministry of Energy, Mines and Petroleum Resources, Paper 1992-1, pages 127-145.
- Ferri, F., Dudka, S. and Rees, C. (1992b): *The Lay Range Assemblage: Where, What and When? Lithoprobe Southern Cordillera Transect Workshop and Cordilleran Tectonics Workshop*, University of Alberta, Program with Abstracts, Report 24, page 80.
- Ferri, F., Dudka, S., Rees, C., Meldrum, D. and Wilson, M. (1992c): *Geology and Geochemistry of the Uslika Lake Area*; B.C. Ministry of Energy, Mines and Petroleum Resources, Open File 1992-11.
- Ferri, F., Dudka, S., Rees, C. and Meldrum, D. (1993a): *Geology of Aiken Lake and Osilinka River Areas, Northern Quesnel Trough, B.C. (094C/2, 3, 5, 6 & 12)*; in *Geological Fieldwork 1992*, Grant, B. and Newell, J.M., Editors, B.C. Ministry of Energy, Mines and Petroleum Resources, Paper 1993-1, this volume.
- Ferri, F., Dudka, S., Rees, C. and Meldrum, D. (1993b): *Preliminary Geology and Geochemistry of the Aiken Lake and Osilinka River Areas (094C/2, 3, 5, 6 and 12)*; B.C. Ministry of Energy, Mines and Petroleum Resources, Open File 1993-2.
- Garnett, J. A. (1978): *Geology and Mineral Occurrences of the Southern Hogen Batholith*; B.C. Ministry of Energy, Mines and Petroleum Resources, Bulletin 70, 75 pages.
- Geological Survey of Canada (1963): *Geophysics Paper 1595, Klawli Lake, British Columbia, 93N/7; Magnetic Survey, Map 1595G, scale 1:63 360*.
- Humphreys, N. (1984): *Assessment Report on the 1984 Geological and Geochemical Exploration Activities, Twin 1 Claims*; B.C. Ministry of Energy, Mines and Petroleum Resources, Assessment Report 13505.
- Harland, W.B., Armstrong, R.L., Cox, A.V., Craig, L.F., Smith, A.G. and Smith, D.G. (1990): *A Geological Time Scale 1989*; Cambridge University Press, 279 pages.
- Murphy, D.C., Gerasimoff, M., van der Heyden, P., Parrish, R.F., Klepacki, D.W., McMillan, W., Struik, L.C. and Gabites, J. (in press): *New Geochronological Constraints on Jurassic Deformation of the Western Edge of North America, Southeastern Canadian Cordillera*; in *Jurassic Magmatism and Tectonics of the North American Cordillera*, Miller, J.M., Editor, *Geological Society of America*, Special Paper.
- Nelson, J., Bellefontaine, K., Green, K. and MacLean, M. (1991a): *Regional Geological Mapping near the Mount Milligan Copper-Gold Deposit (93K/16, 93N/1)*; in *Geological Fieldwork 1990*, B.C. Ministry of Energy, Mines and Petroleum Resources, Paper 1991-1, pages 89-110.
- Nelson, J., Bellefontaine, K., Green, K. and MacLean, M. (1991b): *Geology and Mineral Potential of the Wittsichca Creek and Tezzeron Creek Map-areas (93N/1, 93K/16)*; B.C. Ministry of Energy, Mines and Petroleum Resources, Open File 1991-3.
- Nelson, J., Bellefontaine, K., MacLean, M. and Rees, C.J. (1992a): *Geology and Mineral Potential of the Chuchi Lake East Half (93N/2) and Klawli Lake East Half (93N/7) Map-areas*; B.C. Ministry of Energy, Mines and Petroleum Resources, Open File 1992-4.
- Nelson, J., Bellefontaine, K., Rees, C. and MacLean, M. (1992b): *Regional Geological Mapping in the National Lakes Area (93N/2E, 7E)*; in *Geological Fieldwork 1991*, Grant, B. and Newell, J.M., Editors, B.C. Ministry of Energy, Mines and Petroleum Resources, Paper 1992-1, pages 101-118.
- Nelson, J.L., Bellefontaine, K.A., Mountjoy, K. and MacLean, M.E. (1993a): *Geology and Geochemistry of the Klawli Lake, Map Area (93N/7W)*; B.C. Ministry of Energy, Mines and Petroleum Resources, Open File 1993-3.
- Nelson, J.L., Bellefontaine, K.A., Mountjoy, K. and MacLean, M.E. (1993b): *Geology and Geochemistry of the Discovery Creek Map Area (93N/14E)*; B.C. Ministry of Energy, Mines and Petroleum Resources, Open File 1993-5.
- Parrish, R.R. and Tipper, H.W. (1992): *U-Pb Zircon Age of a Clast from the Uslika Formation North-central British Columbia and Implications for the Age of the Uslika Formation in Radiogenic Age and Isotopic Studies: Report 5*; *Geological Survey of Canada*, Paper 91-2, pages 163-166.
- Paterson, W. and Barrie, C.T. (1991): *Assessment Report on Diamond Drilling on the Phil A Claim Group, Ahdatay Lake, British Columbia*; B.C. Ministry of Energy, Mines and Petroleum Resources, Assessment Report 20543.
- Roots, E.F. (1954): *Geology and Mineral Deposits of the Aiken Lake Map-area, British Columbia*; *Geological Survey of Canada*, Memoir 274, 246 pages.
- Shacde E. (1984): *Prospect Report on the Gold 1-4 Mineral Claims, Klawli River Area, Omineca Mining Division*; B.C. Ministry of Energy, Mines and Petroleum Resources, Assessment Report 12908.
- Wheeler, J.O. and McFeely, P. (1991): *Tectonic Assemblage Map of the Canadian Cordillera and Adjacent Part of the United States of America*; *Geological Survey of Canada*, Map 1712A, scale 1:2 000 000.

NOTES

GEOLOGY OF THE AIKEN LAKE AND OSILINKA RIVER AREAS, NORTHERN QUESNEL TROUGH (94C/2, 3, 5, 6 & 12)

By Filippo Ferri, Steven Dudka, Chris Rees
and Daniel Meldrum

(Canada - British Columbia Mineral Development Agreement 1991-1995)

KEYWORDS: Regional geology, Quesnel trough, Quesnel Terrane, Cassiar Terrane, Harper Ranch Terrane, Slide Mountain Terrane, Hogem intrusive complex, Takla Group, Lay Range assemblage, ultramafic intrusions, strike-slip faults, metamorphism, porphyry, copper-gold, carbonate-hosted, lead-zinc.

INTRODUCTION

This report summarizes the second year of the Aiken Lake project which is a 1:50 000-scale mapping program funded by the Canada - British Columbia Mineral Development Agreement (1991-1995). The project consists of three years of field mapping, covering an area extending from Uslika Lake northward to Johanson Lake (Figure 1-8-1). Mapping has focused on the northern limit of Mesozoic volcanics within the Quesnel trough (Quesnel Terrane), upper Paleozoic oceanic volcanics and sediments of the Harper Ranch Terrane and Paleozoic carbonates of the Cassiar Terrane. The project area has known porphyry copper-gold and carbonate-hosted lead-zinc occurrences and the potential for economic mineral concentrations. The primary goal of this project is to provide detailed geological base

maps in support of the search of new mineral discoveries. Secondary goals include an update of the mineral inventory database and the placement of known mineral occurrences within a geological framework. Stream-sediment samples from creeks and lithochemical samples of prospective lithologies were collected for the purpose of outlining areas of higher than average mineral potential and to assist in defining metallotects.

Mapping during the 1992 field season concentrated on the Aiken Lake and Osilinka River areas (Figure 1-8-1). The Aiken Lake map area includes most of NTS map sheet 94C/5 together with parts of 94C/6 and 94C/12. The Osilinka River map area includes parts of 94C/2 and 94C/3. These areas are located 200 to 250 kilometres north-northwest of Fort St. James (Figure 1-8-1). Road access is by the gravel, all-season Omineca mining access road from Fort St. James, or a similar forestry access road which originates at the southern end of Williston Lake. These roads follow the Mesilinka, Osilinka and Tena'chi drainages and connect to numerous secondary logging roads in the area. Almost all of the Osilinka map area is accessible by gravel roads. In contrast only 30 per cent of the Aiken Lake map area has road access. The Omineca mining access road follows the Mesilinka River and Lay Creek valleys in the Aiken Lake area. A major logging road almost reaches the mouth of Abraham Creek along the south side of the Mesilinka River. An old 4x4 track leads through the broad valley north of Black Pine Lake to the Ingenika mine on the Ingenika River.

This year's work in the Aiken Lake map area is contiguous with mapping completed during the 1991 field season (Ferri *et al.*, 1992a, b). The first geological map of the Aiken Lake area was produced by Lay (1940) who described the geology along the major drainages in the area. Roots (1954) produced a 4-mile geological map for the west half of the Mesilinka sheet in the first comprehensive geological study of the area. Detailed mapping within the map area has been produced by Zhang and Hynes (1991, 1992) who are studying the Takla Group on both sides of the Finlay fault. Bellefontaine (1989, 1990) carried out an in-depth structural study along the western margin of the Cassiar Terrane on the east side of the Swannell River. The east half of the Mesilinka sheet was mapped by Gabrielse (1975) and mapping to the south was published at 6-mile scale by Armstrong (1949). Detailed geological studies of Paleozoic rocks within the map area were completed by Monger (1973) and Monger and Paterson (1974) and were summarized, in part, by Monger (1977). Parrish (1976, 1979) carried out a structural and geochronological study of metamorphosed Ingenika Group rocks between Blackpine

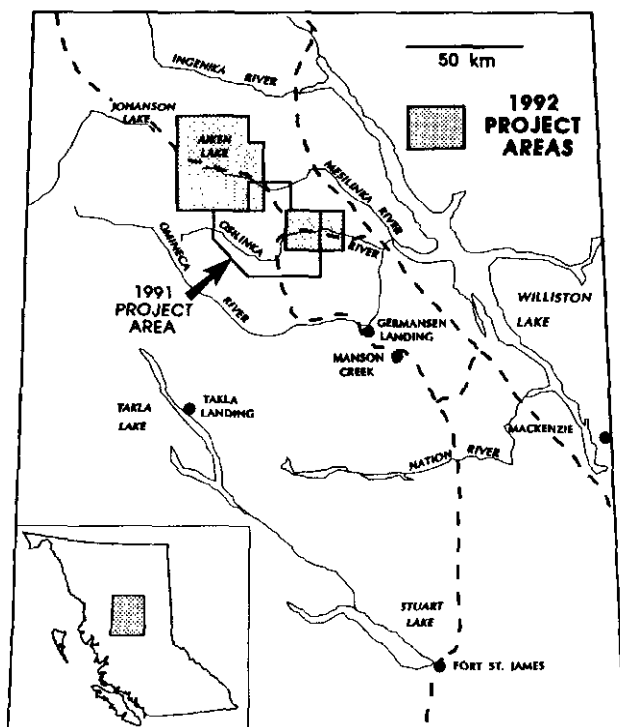


Figure 1-8-1. Location of the map area.

Lake and Chase Mountain. Irvine (1974, 1976) described Alaskan-type ultramafic bodies around Aiken Lake. Unpublished detailed geological maps of the Lay Range and surrounding areas compiled by J.W.H Monger of the Geological Survey of Canada were incorporated into this map. Garnett (1978) carried out a study of the southern Hogen intrusive complex and Meade (1975) mapped Takla Group rocks in the Germansen Lake area.

Detailed mapping by the British Columbia Geological Survey in this area includes the Manson Creek project (Ferri and Melville, 1988, 1989, 1990a, b, in preparation; Ferri *et al.*, 1988, 1989). The Manson Creek and Aiken Lake projects are contiguous with mapping by the Nation Lakes project (Nelson *et al.*, 1991, 1992, 1993). Nixon (1990) and Nixon *et al.* (1990a, b) produced detailed maps and descriptions of the Polaris Ultramafic Complex.

Mapping along the Osilinka River covered a small area of Paleozoic rocks north of End Lake. This provided complete coverage of these important Paleozoic rocks; it has also led to some reinterpretation of the complex geology in adjacent map areas covered during the Manson Creek and Aiken Lake projects.

Many of the unit names used in this paper are informal and have been defined by various authors in the region (*see*

Ferri *et al.*, 1992a; Nelson *et al.*, 1992; Ross and Monger 1978). This is reflected by the use of lower case lettering at the group and formation levels.

REGIONAL GEOLOGY

The project areas straddle the boundary between the Intermontane and Omineca geomorphological belts of the Canadian Cordillera. They are underlain by accreted volcanic rocks of the Intermontane Superterrane and displaced rocks of continental margin affinity (Wheeler and McFeely, 1991; Figure 1-8-2).

Parts of at least four tectonostratigraphic terranes are exposed in the map areas. The easternmost rocks are displaced continental rocks of the Cassiar Terrane. To the extreme west lies the Mesozoic island-arc terrane of Quesnellia. These terranes are separated by two upper Paleozoic terranes in the Osilinka River map area; the volcanic(arc?)-sedimentary Harper Ranch Terrane, and the oceanic Slide Mountain Terrane. The Slide Mountain Terrane is absent in the Aiken Lake map area.

Strata of the Cassiar Terrane include the Upper Proterozoic Ingenika Group through to the Mississippian to Permian Cooper Ridge group. These rocks are predomi-

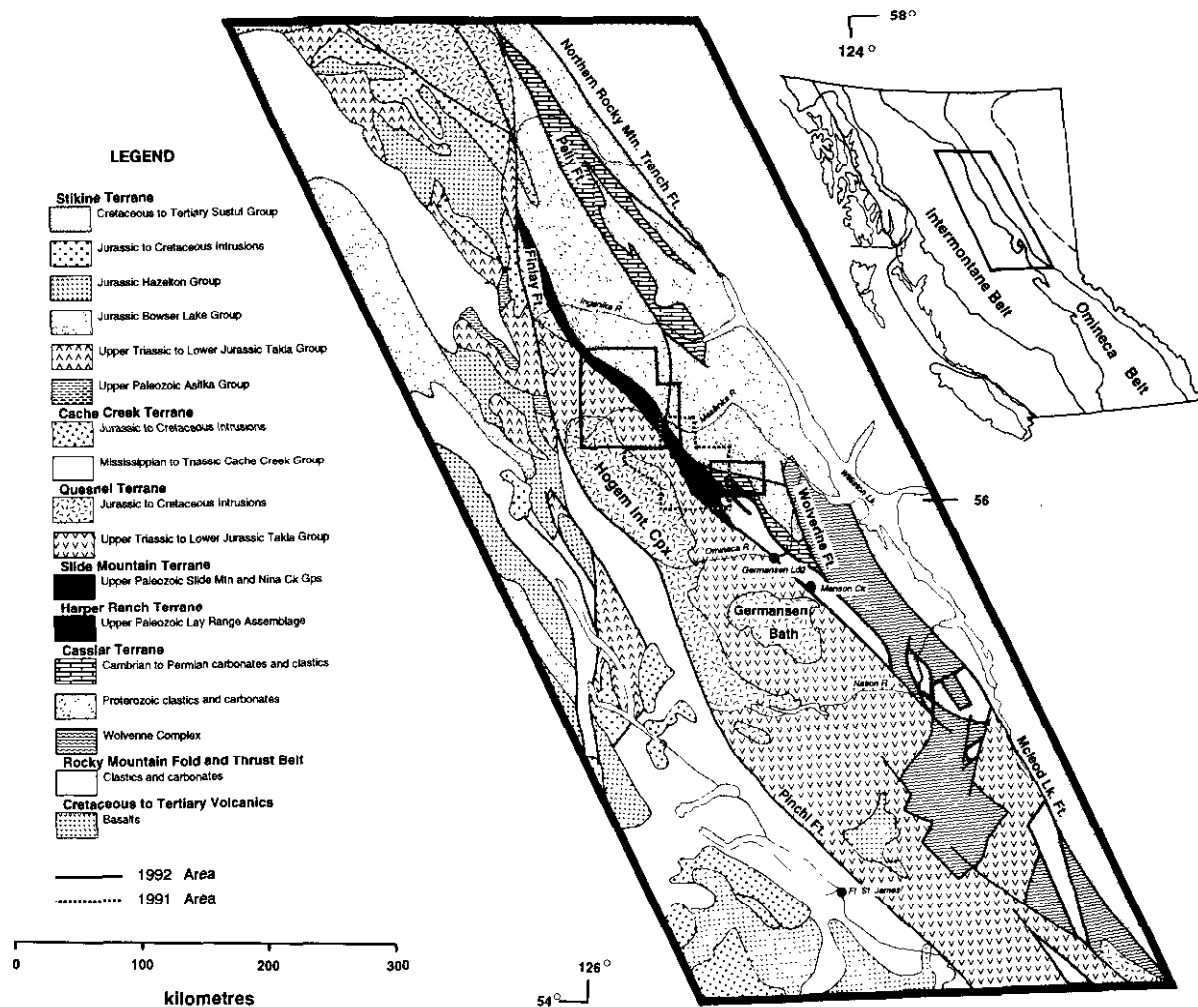


Figure 1-8-2. Regional geological setting of the Uslika map area. See text for details.

nantly clastic with carbonates becoming more common higher in the stratigraphy. The structurally and stratigraphically lower parts of this sequence are polydeformed and metamorphosed to sillimanite grade and outcrop as core complexes (Wolverine, Butler).

In the Osilinka River area the Slide Mountain Terrane lies structurally above the Cassiar Terrane. It is represented by the Pennsylvanian to Permian Nina Creek group (Ferri and Melville, in preparation). This package is composed of oceanic volcanic and sedimentary rocks (pillow basalts and cherty sediments) which have been thrust onto North American rocks.

The Quesnel Terrane is represented by the Upper Triassic to Lower Jurassic Takla Group (Roots, 1954). This is a volcanic and sedimentary arc sequence which is intruded along its western margin by the Triassic to Cretaceous Hogen intrusive complex (Garnett, 1978) and related intrusions. The eastern part of Quesnellia is further subdivided, in this area, into the Harper Ranch Subterrane (Wheeler and McFeely, 1991). This subterrane is represented by the enigmatic upper Paleozoic Lay Range assemblage, a package of volcanic and sedimentary lithologies with predominantly arc affinities although some of the sedimentary units suggest continental origins. Takla Group and Lay Range assemblage rocks are intruded by several ultramafic bodies, the most notable being the Polaris Ultramafic Complex.

OSILINKA RIVER AREA

LITHOLOGIC UNITS

NORTH AMERICAN CASSIAR TERRANE

An exhaustive description of Cassiar stratigraphy in this area will not be attempted here. Lithologic units are identical to those described in previous articles and the reader is referred to these for detailed descriptions (Ferri and Melville, 1989; Ferri *et al.*, 1992a; Figure 1-8-3). The discussion here will focus on new data or insights into each unit and any reinterpretation of previous work.

Ingenika Group to Big Creek group stratigraphy is recognized in the area straddling the Osilinka River. These rocks are exposed within a broad, northwest-trending syncline and can be traced across the Osilinka River into the Beveley Mountain area where they are cut by a series of steep normal faults and placed against higher grade rocks of the Swannell Formation.

Razorback rocks are seen in rubble along the main logging road on the north side of the Osilinka River and in several rubbly outcrops along the ridge to the north. The unit was also recognized along several logging-road cuts on the south side of the Osilinka River. These shales were originally thought to belong to the Echo Lake group but the recovery of Early Ordovician graptolites suggests that they are part of the Razorback group. Their occurrence within rocks of the Echo Lake group suggests a thrust fault repeating Echo Lake strata. The Razorback group is characterized by grey and dark grey slate, argillite and argillaceous limestone. Its thickness is approximately 50 to 75 metres and its exposure is quite poor. The trace of this unit is, in part,

based on the recessive notch it produces between carbonates of the Atan and Echo Lake groups.

Middle Ordovician shales on the east side of Wasi Creek, that were originally mapped as Echo Lake group, are now thought to be the Razorback group. This interpretation is based primarily on regional trends and on the reassessment of carbonates below these shales which are now believed to be the Lower Cambrian Mount Kison formation.

Two subdivisions of the Echo Lake group are recognized in the area: the basal limestone and dolomite up to 600 metres thick, and the succeeding sandy dolomite which can approach several hundred metres in thickness. The lower section is characterized by thick successions of grey to white fenestral dolomite (Plate 1-8-1). The Echo Lake group is commonly more dolomitic than carbonates of the Mount Kison formation, and contains areas of silica replacement. Thick sequences of massive limestone within this succession are difficult to distinguish from the Mount Kison formation.

The sandy dolomite unit is well exposed along the main logging road on the north side of the Osilinka River. Well-rounded, spherical quartz grains constitute up to 50 per cent of the rock and are found within thickly cross-stratified



Plate 1-8-1. Sample of typical Echo Lake group fenestral dolomite from the Osilinka River area. This lithology forms thick sequences in the lower part of the Echo Lake group and helps distinguish it from carbonates of the Atan Group.

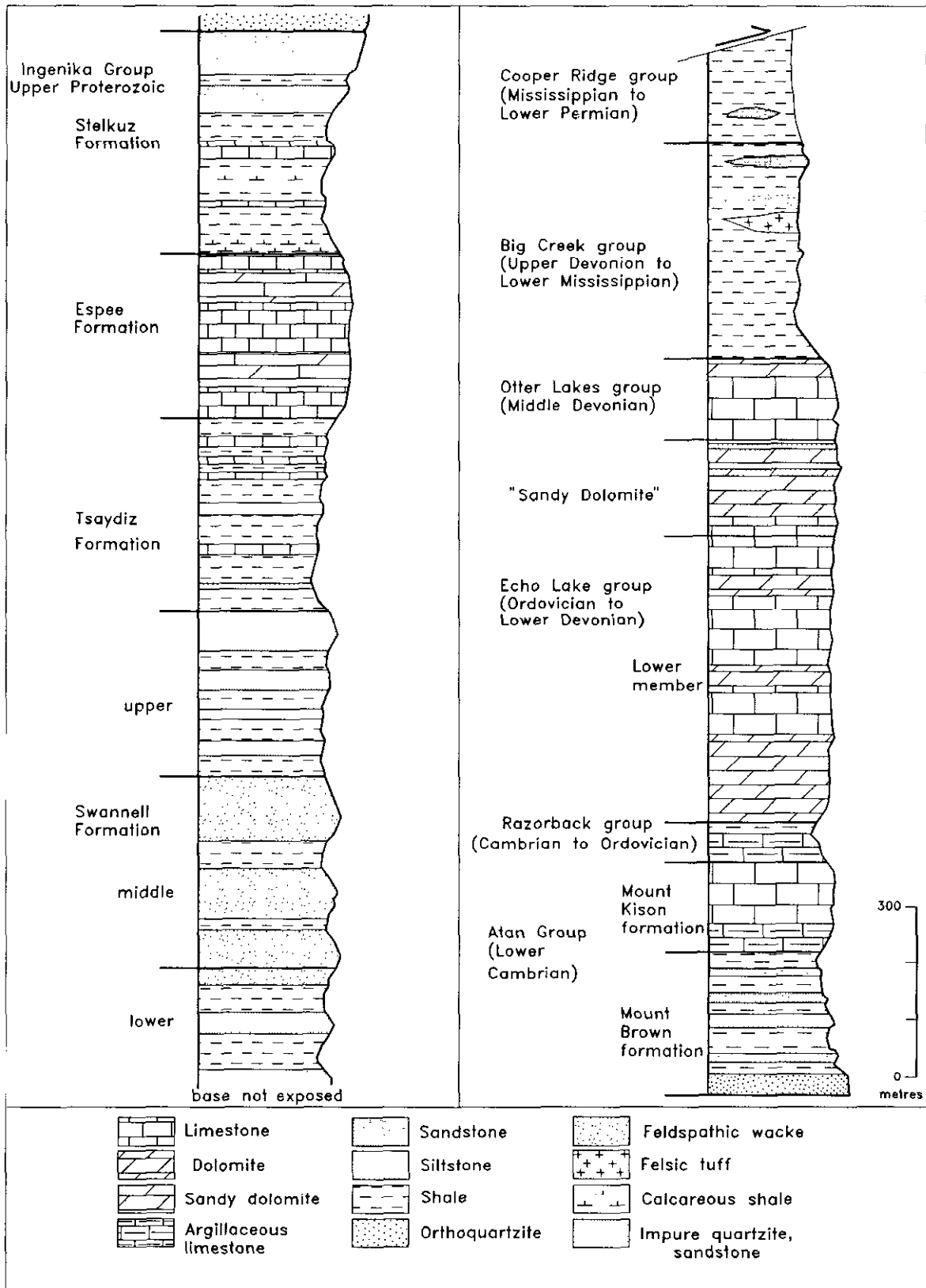


Figure 1-8-3. Generalized stratigraphic columns of Cassiar Terrane in the Osilinka River area (from Ferri and Melville, in preparation).

horizons. Twin-holed columns of several crinoid species were found at this locality and suggest a late Early Devonian (Emsian) age for the uppermost part of the Echo Lake group (B.S. Norford, personal communication, 1992). Middle Ordovician graptolitic shales, originally thought to be part of the Echo Lake group, are now known to belong to the Razorback group. This suggests that the lower age limit of the Echo Lake group is Middle Ordovician.

One of the distinguishing characteristics of the Echo Lake group in this area is the presence of carbonate breccia or conglomerate. Two types are seen: one which appears to be primary (*i.e.*, debris flows) and the other secondary. Primary breccia is characterized by locally derived carbonate clasts set in a limy mud matrix, or sandy matrix if found within the upper sandy dolomite unit. Clasts are up to tens of centimetres in size. The thickness of these deposits is difficult to deduce but is thought to be in the tens of metres.

Secondary breccia is characterized by metre-scale angular blocks separated by sparry dolomite or calcite which may display several generations of infilling. Some areas appear autoclastic (*i.e.*, fragmented in place). The origin of this breccia is not known. It may be either a solution collapse breccia or one related to faulting, though many features do not support a tectonic origin. A third possibility is that these occurrences are of debris-flow origin and the original limy mud has been selectively replaced by sparry carbonate.

Conodonts were recovered from the Otter Lakes group east and west of Wasi Creek. Both these localities yield faunas with a late Early to early Middle Devonian age range (Emsian to Eifelian; M.J. Orchard, personal communication, 1992) which is consistent with past interpretations of this unit.

The extent of the Big Creek group has increased in our present interpretation of the geology. Felsic tuff originally assigned to the Lay Range assemblage (dacitic tuff unit, MP1r4, in Ferri *et al.*, 1992a, b) is now known to be within the upper part of the Big Creek group. Mapping of Big Creek group stratigraphy in the Aiken Lake area has delineated a similar package of felsic tuff in support of this. The inferred fault separating Big Creek from Unit MP1r4 is not required and this contact is now reinterpreted as stratigraphic. This felsic tuff is known as the Gilliland tuff in the Germansen Landing area (Ferri and Melville, in preparation) and is lower Mississippian. Similar tuff is found east of Wasi Creek, but is much thinner. This tuff has regional extent as it has now been recognized from the Aiken Lake to Germansen Landing areas. The large expanse occupied by this unit west of Wasi Creek is not only a function of its substantial thickness but also due to broad, low-amplitude folding recognized immediately to the southeast.

The Big Creek group (and Gilliland tuff unit) is now thought to underlie the Nina Creek group east of Wasi Lake and Wasi Creek (Figure 1-8-4). Felsic tuff formerly mapped as Unit PPnhb of the Mount Howell formation (lower Nina Creek group, Ferri *et al.*, 1992b) is now grouped with the Gilliland tuff; shales and argillites below this are also considered part of the Big Creek group. Furthermore, shales, argillites, cherty argillites and tuffaceous units exposed at the mouth of the creek which flows into the northeast end of

Wasi Lake are now also believed to be part of the Big Creek group. These changes better reconcile the geology on either side of the Wasi Lake - Wasi Creek drainage, with the result that the offset on the fault along the lower part of Wasi Creek is not as large as previously interpreted.

Dark grey to grey, wavy to planar-bedded argillites and shales, and minor massive beds of brown to grey limestone are found above typical Big Creek lithologies on the east side of the syncline south of the Osilinka River. These rocks have been informally termed the Cooper Ridge group by Ferri and Melville (in preparation). This package was originally placed in the Slide Mountain Terrane as Unit PPsm1 by Ferri and Melville (1990b). However, conodonts subsequently recovered from the limestones in the upper part of this unit returned an Early Permian age; also, Ross and Monger (1978) recovered fusulinids of probable Early Permian age from limestones of this unit. This suggests continuous North American deposition in this area until at least the Early Permian and that the rocks of the Cooper Ridge group belong to the Cassiar Terrane. The presence of the Cooper Ridge group north and west of Whistler Mountain is less certain. Argillaceous rocks above the Otter Lakes group and below the Nina Creek group have been placed with the Big Creek group. The possible absence of Cooper Ridge rocks in this area may be due to lack of deposition or removal by the thrust fault at the base of the Nina Creek group.

Echo Lake group carbonates on the Osprey mineral claims are intruded by a small, grey, aphanitic and intermediate to felsic body. The intrusion is less than 10 metres in diameter, and associated with sulphide mineralization. Its undeformed nature suggests it is related to possibly Tertiary felsic intrusions into the Swannell Formation near Beveley Mountain.

SLIDE MOUNTAIN TERRANE

The lower part of the Nina Creek group was mapped south of the Osilinka River. These wavy bedded argillites, siliceous argillites and bedded cherts are part of the Mount Howell formation. Minor lithologies include: chert-quartz wackes (with 10% to 20% coarse clastic material) and brown argillaceous limestone. The uppermost exposed parts are intruded by gabbro sills.

STRUCTURE

Late northwest and northeast-trending normal faults are the most dominant structural elements in the Osilinka map area. These faults cut the broad syncline below Mount Howell and truncate it to the northwest against poly-deformed rocks of the Swannell Formation. The fault zones are quite wide, as exemplified north of the Childhood Dream mineral occurrence where several hundred metres of strongly fractured and crumbly carbonate of the Echo Lake group are placed against the Swannell Formation. The juxtaposition of garnet-grade Swannell Formation rocks against those of the Echo Lake group suggests that displacement on segments of these faults is in the order of kilometres.

Mapping along the Osilinka River has allowed the harmonization of the geology between the Beveley Mountain

area and that south of the river. In the Beveley Mountain area the northwest-trending, southwest-side-down normal fault that separates a wedge of carbonates from the Swannell Formation must connect with the similar, large northwest-trending fault (with similar sense of displacement) south of the Osilinka River (Ferri and Melville, 1990a, b). Furthermore, a similar fault to the southwest begins northeast of Wasi Lake, separating the Nina Creek group from Cassiar Terrane, and continues northwestward along Tenakihi Creek.

A northwest-trending, southwest-side-down normal fault inferred along the lower part of the Osilinka River (Ferri and Melville, 1990a, b) must exist and veer northward to separate the Paleozoic succession from Swannell rocks. It ultimately trends southeastward into the Wolverine fault zone, a steep brittle-ductile shear zone along the west side of the Wolverine Metamorphic Complex.

The major northeast and east-trending faults north of the Osilinka River are not parallel to any other major faults in the area.

A thrust fault (End Lake thrust) is now known to repeat Razorback and Echo Lake stratigraphy south of the Osilinka River and must continue northward. Evidence for this fault

is provided by the strongly brecciated Razorback and Echo Lake lithologies several kilometres south of the Osilinka River. This fault would help to explain the thickness of the Echo Lake group in this area. Displacement on the fault appears to decrease southward and the fault must terminate just south of the map area in Figure 1-8-4.

AIKEN LAKE AREA

LITHOLOGIC UNITS

NORTH AMERICAN CASSIAR TERRANE

Cassiar Terrane rocks described by Ferri *et al.*, (1992a) in the Usluka Lake area are also recognized in the Aiken Lake map area (Figure 1-8-5). Lithologies are similar except for minor differences which may reflect regional facies variations. Units of the Proterozoic Swannell Formation to the Devonian-Mississippian Big Creek group are exposed within a southwest-dipping panel cut by late normal faults. The Middle Devonian Otter Lakes group is not recognized. It is not certain whether this is due to lack of deposition or poor exposure.

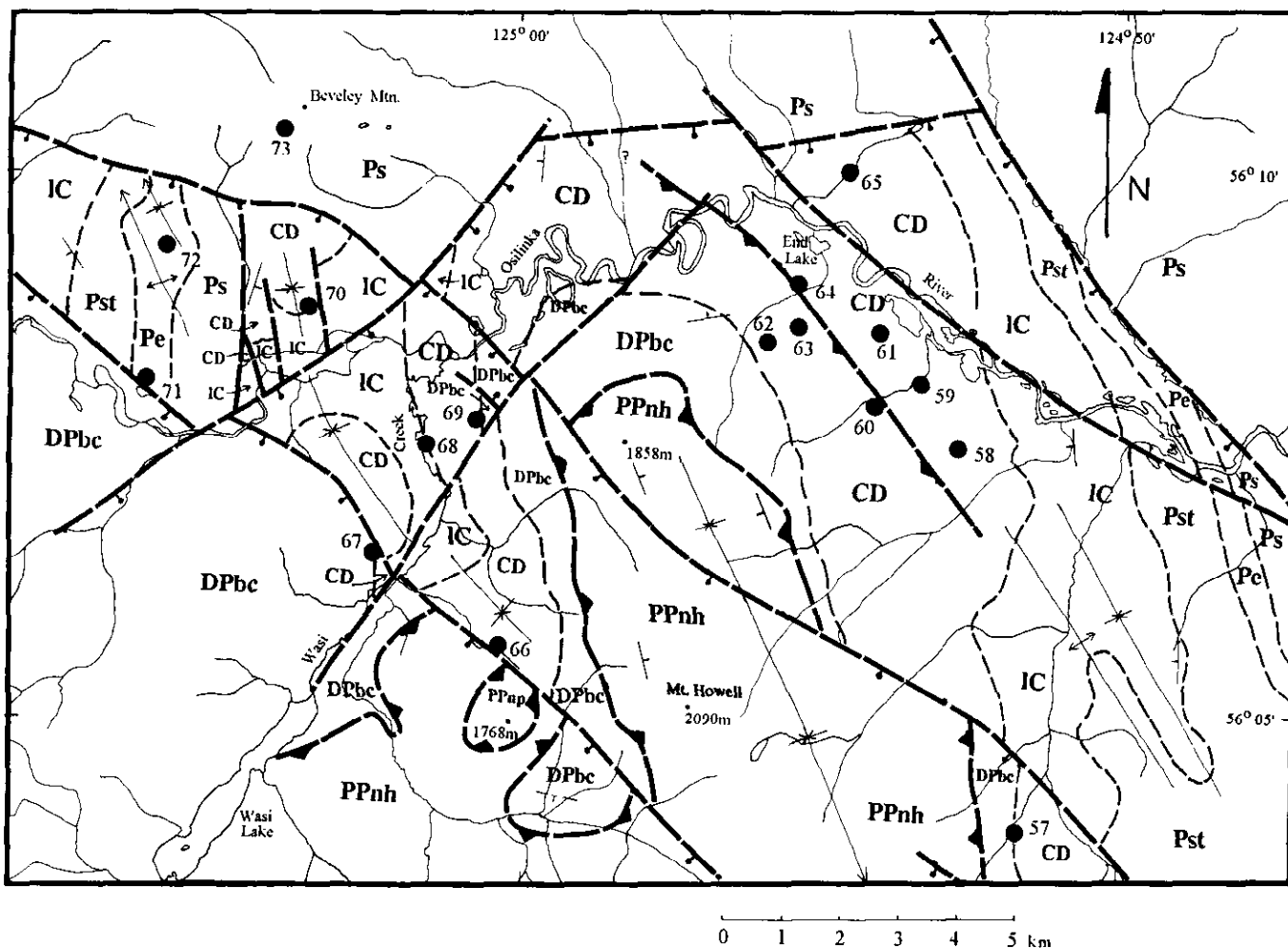


Figure 1-8-4. Geology of the Osilinka River map area.

LAYERED ROCKS

Upper Cretaceous to Tertiary

KTm *maroon conglomerate unit: conglomerate sandstone, siltstone*

Lower Cretaceous(?)

IKc *conglomerate, sandstone, siltstone, argillite, minor coal*

Triassic to Jurassic

Upper Triassic to Lower Jurassic

Takla Gp

uTrlJt *maroon tuff unit: maroon to green, tuffs agglomerates, plagioclase and augite-phyric*

Upper Triassic

uTrp2 *Plughat Mountain fm: augite-plagioclase phyric agglomerates, basalts, tuffs*

uTrp1 *Plughat Mountain fm: tuffs, tuffaceous, siltstone, argillite, agglomerate minor limestone*

Paleozoic or Mesozoic

PM *problematic unit: tuffs, argillites, siltstone, limestone, agglomerate*

Pennsylvanian to Permian

Nina Creek Gp

PPnp *Pillow Ridge fm: massive to pillowed basalt, lesser chert, argillite, gabbro*

PPnh *Mount Howell fm: argillite, chert, gabbro, minor basalt, wacke, felsic tuff*

Mississippian to Permian

Lay Range Assemblage

Middle Pennsylvanian to Permian

PPlru *upper mafic tuff division: tuffs to siltstones, agglomerate, basalt, argillite, gabbro, limestone*

Mississippian to Middle Pennsylvanian

MPIrl *lower sedimentary division: mixed argillite, conglomerate, limestone, sandstone, tuff*

Devonian to Permian

Upper Devonian to Lower Permian

Big Creek gp, Cooper Ridge gp

DPbc *shale, argillite, wacke, sandstone, felsic tuff, minor limestone*

Cambrian to Devonian

Cambrian to Middle Devonian

Razorback gp, Echo Lake gp, Otter Lakes gp

CD *limestone, dolomite, lesser cherty carbonate, sandy dolomite, argillite*

Lower Cambrian

Atan Gp

IC *limestone, shale, siltstone, quartzite*

Upper Proterozoic

Ingenika Gp

Pi *Undivided: impure quartzite, schist, phyllite, limestone, arkosic wacke and sandstone*

Pst *Stelkuz Fm: phyllite, slate, sandstone, limestone*

Pe *Espee Fm: limestone, dolomitic limestone*

Pts *Tsaydiz & Swannell Fms: phyllites, limestone, arkosic sandstone, phyllite, schist*

INTRUSIVE ROCKS

Late Triassic to Cretaceous

Hogem intrusive complex

TrKh *monzonite, quartz monzonite, syenite, granodiorite, granite, diorite*

Triassic or Jurassic

mafic-ultramafic body

TrJmg *gabbro*

TrJmp *Peridotite, pyroxenite, hornblende, gabbro*

Lower Jurassic

Polaris Ultramafic Complex

Up *Dunite, wehrlite, pyroxenite, gabbro*

Geologic contact	
Fault (undefined, normal, thrust)	
Bedding orientation (tops known, unknown)	
Bedding orientation, overturned	
Fold (anticline, syncline, overturned anticline)	
Limit of mapping	
Stratigraphic section location	A
Structural cross-section location	A - A'
Mineral occurrence	2

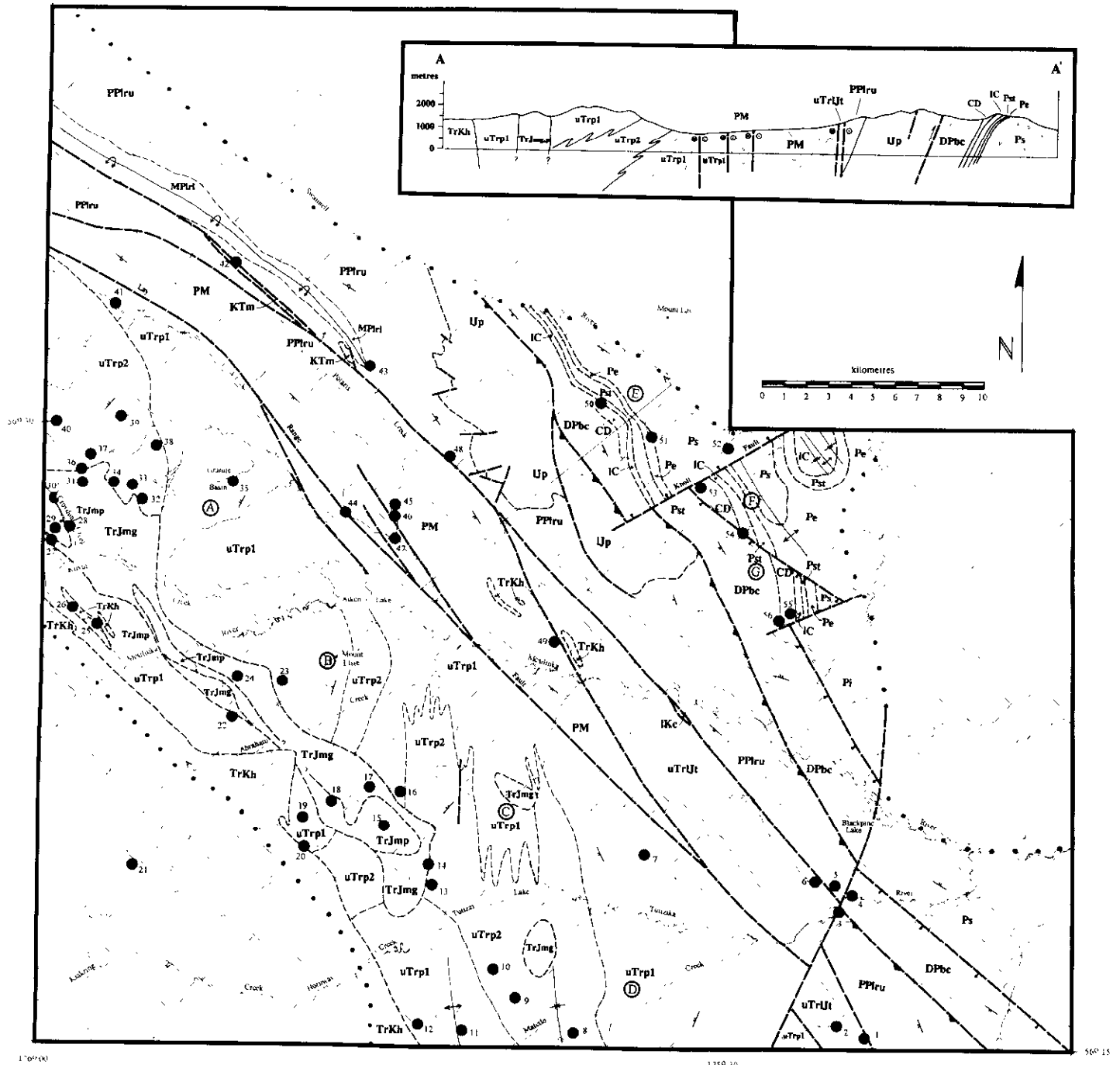


Figure 1-8-5. Geology of the Aiken Lake map area. Insert at top left is a cross-section through the middle of the map area.

Cassiar rocks are found in the northeastern part of the Aiken Lake map area and are dominated by the Proterozoic Ingenika Group. This is overlain by Paleozoic strata which show abrupt changes in thickness and lithology along strike. Paleozoic rocks in the map area include both a thick platformal sequence, typical of stratigraphy in the Osilinka River area, and a thin argillaceous basinal(?) succession which has not yet been mapped in this region.

INGENIKA GROUP (UPPER PROTEROZOIC)

The four formations of the Ingenika Group (defined by Mansy and Gabrielse, 1978) crop out in the map area. These are, from oldest to youngest, the Swannell, Tsaydiz, Espee and Stelkuz formations. Swannell rocks roughly correspond to the Tenakihi Group of Roots (1954) with the remaining formations being part of his lower Ingenika Group. The

thickness of this package is estimated to be a minimum of 2800 metres.

Swannell Formation: Approximately 700 metres of semicontinuous outcrop of the Swannell Formation is exposed along a ridge south of the Swannell River. A further, stratigraphically lower 1400-metre section is inferred from exposures along the Swannell River, indicating a total thickness approaching 2100 metres. This minimum thickness is in accordance with sections described elsewhere in the Cassiar Terrane (Roots, 1954; Mansy and Gabrielse, 1978; Ferri and Melville, 1990a).

An upper and lower sequence are recognized along the ridge section. The upper part is roughly 500 metres thick and composed of interlayered grey to tan, very fine to coarse-grained sandstone to feldspathic sandstone and grey to silvery grey or green phyllite to quartzitic phyllite. Phyllitic lithologies commonly make up less than 30 per cent of the outcrop. Sandstone beds are up to 1 metre thick and contain up to 40 per cent phyllitic material. This unit becomes schistose down-section as the metamorphic grade increases.

The lower sequence is composed of thick to massively bedded arkosic psammites (feldspathic grits) interlayered with thin to thickly bedded, green to brown phyllite or schist which may contain porphyroblasts of garnet, biotite and chloritoid. Pelitic rocks comprise less than 20 per cent of the outcrops. Only 200 stratigraphic metres of this unit was mapped.

Tsaydiz Formation: The Tsaydiz Formation is roughly 150 metres thick on the ridge south of the Swannell River and at least 300 metres thick in the core of the anticline north of the Swan mineral showing. It is characterized by grey to brown limestone thinly interlayered with light grey to grey slate. Minor beds of grey, recrystallized limestone, up to several metres thick, occur throughout the section.

Espee Formation: The Espee Formation is about 150 metres thick south of the Swannell River and over 300 metres thick north of the Swan mineral showing. Extensive outcrops occur within the core of the anticline northeast of the Swan mineral claims and good exposures are found along creeks cutting the southwest side of the syncline southeast of the Swannell River. It consists of grey to white, thin to moderately bedded and platy recrystallized limestone which locally is coarsely recrystallized and dolomitic. Thin micaceous partings are occasionally present along bedding surfaces.

Stelkuz Formation: The Stelkuz Formation is some 200 to 300 metres thick and is best exposed along a ridge south of the Swannell River. It is quite variable containing both siliciclastics and minor carbonate. The basal 100 metres is composed of dark brown to brown or grey-green phyllite, argillite and calcareous argillite with rare, grey siliceous limestone layers up to 2 metres thick. There are also thin layers or very fine grained sandstone. At the top of this sequence is a honey-coloured, coarse to finely recrystallized massive to thickly bedded limestone. The phyllite immediately below this carbonate has a distinctive deep green colour as do the gritty phyllites just above it. These distinctive limestone and green phyllitic horizons are a useful local

marker. The upper 100 metres of the formation begins with thin to thickly bedded quartz sandstone roughly 5 to 10 metres thick which gives way upwards to grey to dark grey phyllite.

ATAN GROUP (LOWER CAMBRIAN)

The Atan Group can locally be subdivided into two formations; the lower Mount Brown formation composed of siliciclastics and the upper Mount Kison formation made up of carbonates. The Atan section varies in thickness from 150 metres south of the Swannell River to 400 metres near the Swan mineral showings. Together with the Echo Lake group, it shows the greatest change in character north and south of the Knoll fault near the Swannell River (Figure 1-8-6).

Archaeocyathids have been recovered from the Mount Kison formation indicating an Early Cambrian age for the upper part of the Atan Group. The Mount Brown formation is similar to Lower Cambrian strata elsewhere in the Cassiar Terrane (Gabrielse, 1963).

Mount Brown formation: The Mount Brown formation ranges in thickness from 45 metres to approximately 150 metres. Near the Swan mineral showings it exhibits thicknesses and lithologies similar to those in the Csilinka River area (Figure 1-8-6): a basal grey to cream or brown quartzite or orthoquartzite up to 50 metres thick, succeeded by light green to olive green phyllite with minor light brown to brown, very thin to thin siltstone to fine sandstone layers.

The Mount Brown formation is considerably thinner immediately south of the Swannell River. The basal quartzitic unit is 5 metres thick and composed primarily of quartzose sandstone with pure orthoquartzite layers being less abundant and only 5 to 10 centimetres thick. The basal unit is succeeded by 40 metres of grey to green phyllite with traces of thin silty horizons. The contact with shales of the underlying Stelkuz Formation appears to be gradational over a distance of 5 metres.

Mount Kison formation: The Mount Kison formation is some 150 metres thick in the vicinity of the Swan mineral showings. It is composed of white to grey, finely recrystallized limestone which is locally coarsely recrystallized. Typically the unit is massive to moderately bedded featureless limestone with minor oolitic horizons in the upper part and thinner bedded sections in the lower part.

The Mount Kison formation is only 60 to 70 metres thick south of the Swannell River. It consists of a basal section of grey to dark grey, thin to thickly bedded, wavy to planar-bedded limestone. It is locally platy and has bands of alternating light and dark grey limestone. There are some very massive, coarsely recrystallized white limestone horizons in this section. Carbonate breccia or conglomerate of sedimentary origin (*i.e.*, syndepositional) are developed locally.

The top of the section is composed of grey to dark grey, thin to moderately bedded, argillaceous and graphitic, platy limestone. There are lesser massive beds of white limestone up to a metre thick. Horizons of sedimentary or primary carbonate breccia are also present.

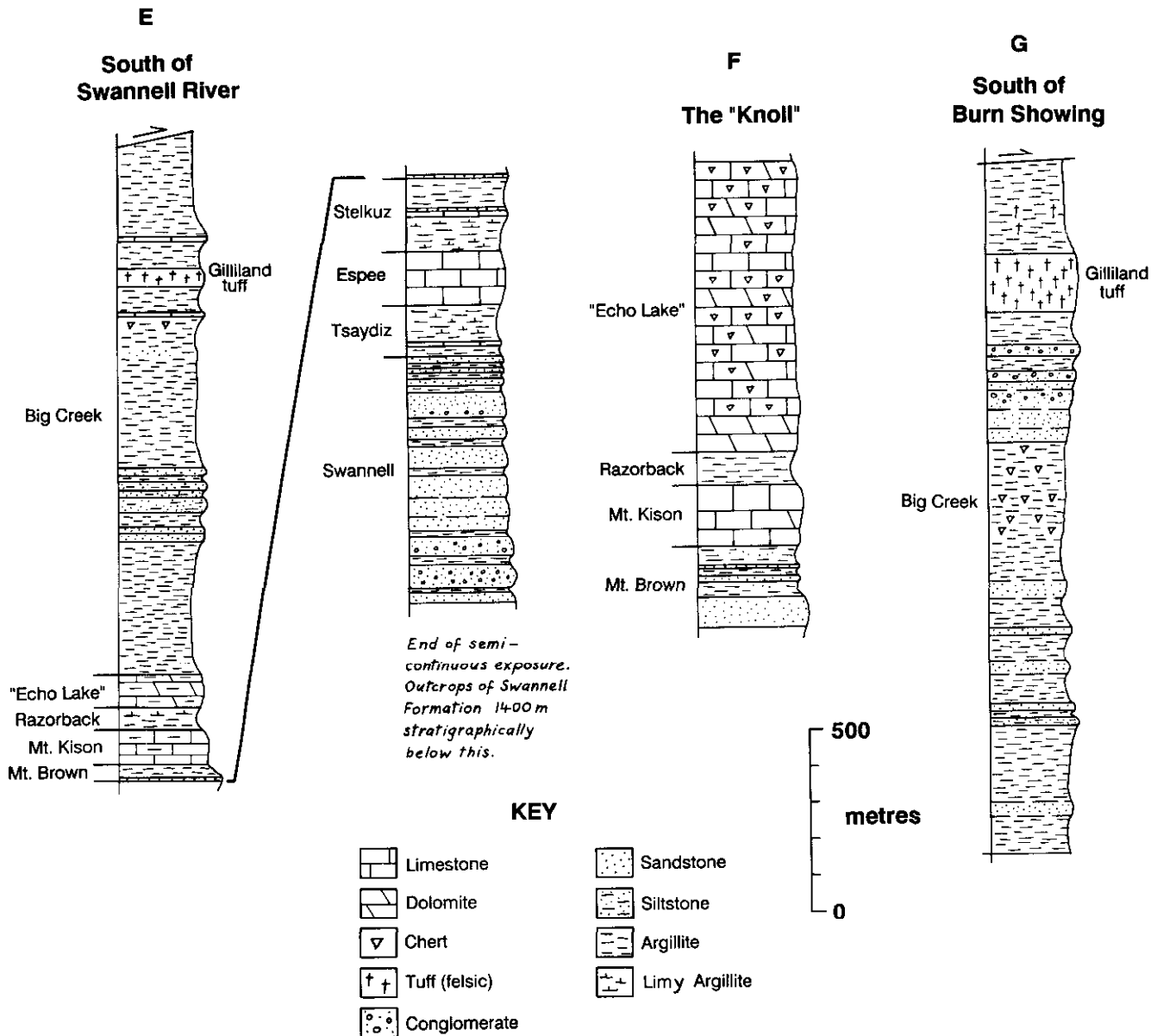


Figure 1-8-6. Stratigraphic columns of Upper Proterozoic to upper Paleozoic rocks in the northeast of the map area. Locations of columns E to G are shown in Figure 1-8-5. Columns E and F are northwest and southeast, respectively, of the Knoll fault; note the marked thinning of the Lower Cambrian (Mount Brown formation) to Devonian (Echo Lake group) succession across this fault.

RAZORBACK GROUP (CAMBRIAN TO MIDDLE ORDOVICIAN)

The Razorback group is 50 to 90 metres thick. It is poorly exposed throughout most of the map area. In the eastern part of the area it is characterized by grey to dark grey phyllite or slate in the few exposures that were observed. The best exposure is on the ridge south of the Swannell River. In this locality the basal part of the section is a green to light green phyllite with greyish phyllite in the middle part. The upper part is grey to greenish phyllite with brown limestone nodules which constitute up to 50 per cent of the rock. The uppermost 5 metres of the Razorback group is composed of silvery grey to dark grey or black phyllite with interlayers of dark grey limestone and argillaceous limestone.

No fossils were collected from this unit in the Aiken Lake map area. Lower and Middle Ordovician graptolites were recovered from the Razorback group in the Osilinka River area. The Cambrian lower age range is inferred from its position above the Atan Group and local similarities to Cambrian argillaceous facies elsewhere in the Cassiar Terrane.

ECHO LAKE GROUP (MIDDLE ORDOVICIAN? TO LOWER DEVONIAN)

Approximately 800 metres of limestone, dolomite, cherty carbonate and chert are assigned to the Echo Lake group. This unit is best exposed on a hill northwest of the Swan mineral claims. The lower part is composed of massive,

buff-grey to grey dolomite and limestone. It is moderately to coarsely recrystallized and poorly to well bedded. In the upper part the carbonate is replaced by grey to pale grey cherty quartz. This chert replacement occurs along layers and in some areas affects almost 100 per cent of the rock.

Along the ridge immediately south of the Swannell River, grey to pale grey, recrystallized dolomite and dark grey-brown to black argillaceous, thinly bedded, platy limestone overlie the Razorback group. The dolomite is at the base of the succession but also occurs locally in the upper argillaceous section. The argillaceous limestone succession contains lenses of primary carbonate breccia or conglomerate and some horizons are relatively rich in crinoid ossicles, sponge spicules and shell fragments. The entire succession in this area is only 200 metres thick. These lithologies are not typical of the Echo Lake group but they are found in the expected stratigraphic position suggesting they must be an unusual facies (Plate 1-8-2). The change between this section and the typical, thick Echo Lake group appears to occur across the northeast-trending Knoll fault (Figures 1-8-5, 1-8-6) immediately northwest of the Swan mineral claims. The change is abrupt, no transitional features were seen in these units. Alternatively, the apparent thinning of the Echo Lake group in this area may be the result of a northwest-trending normal fault, but no such fault appears to be present southeast of the Knoll fault and furthermore it would have to change stratigraphic position (*i.e.*, southeast of the Knoll fault it would be stratigraphically above the Echo Lake group whereas northwest of the fault it would have to be below it). Another possible explanation for this drastic change is an abrupt facies transition northwestward towards the Swannell River. Many of the Paleozoic units show marked thinning and change in lithologic character to the northwest, suggesting a facies change. The abundance of

argillaceous material points to a more basinal setting for the northern area. The Knoll fault, which forms the boundary, may be a long-lived structure which originally controlled local basin development and was later reactivated.

No definitive macrofossils were found in typical Echo Lake group rocks in the Aiken Lake area. Dark grey-brown to black argillaceous limestone and limestone south of the Swannell River, which are tentatively assigned to the Echo Lake group, have yielded crinoid and shell fragments spanning the Ordovician to Devonian time periods. In the Osilinka River area fossils suggest a Middle Ordovician to Lower Devonian age range (Ferri and Melville, in preparation, and this study).

BIG CREEK GROUP (UPPER DEVONIAN TO LOWER MISSISSIPPIAN)

The Big Creek group is perhaps the thickest unit within the Paleozoic succession of the Aiken Lake area. It is upwards of 1500 metres thick and dominated by argillaceous lithologies. This apparent thickness may be exaggerated due to tectonic thickening.

The basal 200 to 300 metres is composed of grey to blue-grey shale or argillite which locally is quite fissile. The middle part of the group contains beds of dark grey to black, chert-quartz wackes (black clastics). Typically the black clastic component of these strata is from 10 to 50 per cent but black quartzite layers are present locally. These black clastic units are usually fine to medium grained but some beds contain flattened chert grains up to several centimetres in length. It is difficult to estimate the thickness of this black clastic sequence but it is believed to be at least several hundred metres thick with clastic rocks constituting less than 30 per cent of the section.

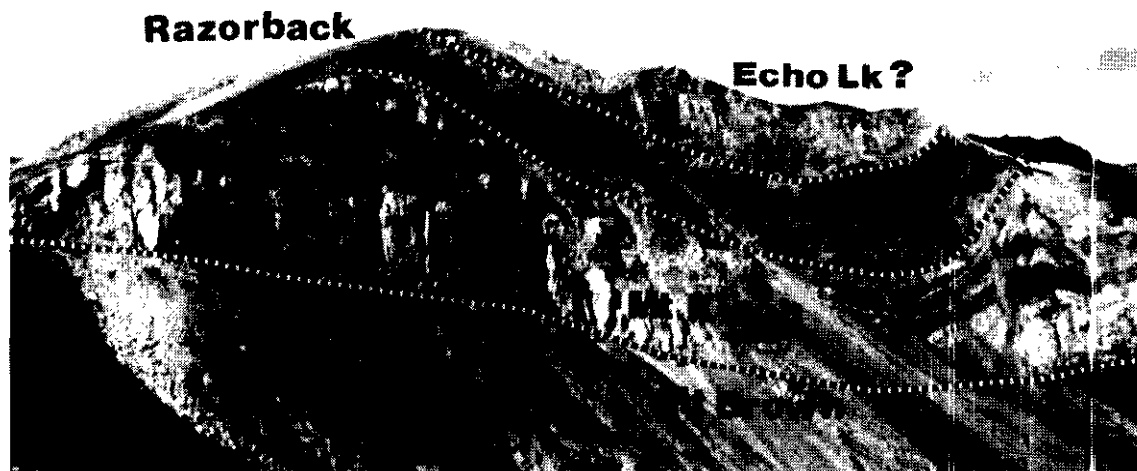


Plate 1-8-2. Looking northwest at the ridge immediately south of the lower part of the Swannell River. The viewer is standing on the Stelkuz Formation with siliciclastics of the Mount Brown formation in the immediate foreground. Mount Brown to Razorback rocks in this section are much thinner and more argillaceous than in other parts of the Cassiar Terrane in the map area. Argillaceous carbonates at the top of the hill occupy the same stratigraphic position as the Echo Lake group, but are much more argillaceous. See Figure 1-8-6 and text for details.

Approximately 200 to 300 metres of dark grey argillite or cherty argillite sits above the black clastic sequence. At the top of this succession are more clastics which locally contain a cobble to boulder conglomerate section 10 to 30 metres thick, with clasts of quartzite, limestone, argillite, tuff and augite-feldspar-porphyrific basalt. The restricted nature of these deposits suggests that they may be channel fills within the shale basin.

The upper part of the Big Creek group is composed predominantly of dark grey, wavy bedded argillite with minor beds of limestone and black clastics. The limestone is grey to dark grey, planar, very thin to moderately bedded and contains some very coarsely crystalline lenses. This sequence is over 50 metres thick south of the Mesilinka River. Limestone of this thickness is not typical of the Big Creek group as first described in the Nina Lake area (Ferri and Melville, 1990a; Ferri *et al.*, 1992a).

Grey, quartz \pm feldspar-bearing tuff, 50 to 200 metres thick is exposed towards the top of the upper part of the Big Creek group. Quartz and feldspar clasts make up less than 30 per cent of the tuff which may be strongly cleaved. The tuff is sometimes quite pyritic and rusty weathering. Argillites above, below and along strike with the tuff unit contain tuffaceous material either as thin, wispy horizons or as clasts. This tuff unit is now thought to be equivalent to the lower Mississippian Gilliland tuff of the Big Creek group described farther south in the Germansen Landing area (Ferri and Melville, in preparation) which has yielded an early Mississippian U-Pb date. There are no other age constraints for the Big Creek group in the map area except its similarities to the Upper Devonian to lower Mississippian Earn Group described elsewhere in the Cassiar Terrane (Gabielse, 1963).

Units MPlr3 and MPlr4 (argillite and dacitic tuff divisions) assigned to the Lay Range assemblage by Ferri *et al.* (1992b), are now thought to belong to the upper part of the Big Creek group. This interpretation is based primarily on their much stronger lithological similarities and affinities. This reinterpretation includes a section of Unit MPlr3 along the Tutizika River which can be traced into the Big Creek group south of the Swannell River. The Tutizika section contains lithologies in its northwestern section which may be part of the Lower Cambrian, although the upstream section resembles the Big Creek group. As well, felsic tuff known to be within the Big Creek group is probably equivalent to the original dacitic tuff division (MPlr4) formerly included in the Lay Range assemblage.

HARPER RANCH TERRANE

LAY RANGE ASSEMBLAGE (MISSISSIPPIAN TO PERMIAN)

Rocks of the upper Paleozoic Lay Range assemblage in the Uslika Lake area (Ferri *et al.*, 1992a, b) extend north-westwards into the present map area. Here they are well exposed in the Lay Range between Lay Creek and the Swannell River where mapping has led to a better understanding of the structure of the assemblage, and some revisions to last year's interpretation of the stratigraphy. The present work was helped considerably by unpublished maps and field notes generously made available by J.W.H. Monger of the Geological Survey of Canada.

Along the northwestern part of the Lay Range, a large northeasterly overturned anticlinal fold has been mapped (Plate 1-8-3). The core of this southeasterly plunging anticline, outcropping over a width of about 1 kilometre, contains the oldest rocks of the Lay Range assemblage, a Mississippian (?) to middle Pennsylvanian sequence of chert, tuff and clastic sedimentary rocks which are tightly folded, judging by strong cleavage development and numerous facing reversals. At the top of this sequence, referred to as the "lower sedimentary division", a fossiliferous limestone is overlain by distinctive maroon argillite and chert. This marker clearly outlines the core of the anticline on the northeastern limb but it is less easily traced on the southwest limb which is complicated by faulting.

Above the limestone - maroon argillite marker is a thick succession of tuff, agglomerate and volcanic flows, at least 2000 metres thick, referred to as the "upper mafic tuff division" which has an age range of middle Pennsylvanian to Permian. The northeast limb of the anticline is characterized by overturned strata of this division; facing indicators are less common on the right-way-up southwest limb. Southeast of this fold, in the rest of the Lay Range and the Mesilinka valley, only the upper mafic tuff division of the Lay Range assemblage is exposed.

East of Polaris Creek, the upper mafic tuff division is intruded by the Polaris Ultramafic Complex (Nixon, 1990; Nixon *et al.* (1990a, b). The contact aureole of the intrusion is commonly marked by hornfelsing and metamorphism to lower amphibolite grade, but on the northeastern margin contacts have been modified by shearing where both the Polaris Complex and the Lay Range assemblage have been thrust onto or faulted against the Big Creek group or older rocks (Nixon *et al.*, 1990a). This suggests a tectonic relationship between the Lay Range assemblage and the Cassiar Terrane; however, a primary stratigraphic relationship between them should not be ruled out.

A fault on the southwest side of the Lay Range assemblage separates it from a problematic rock unit which may be part of the Upper Triassic Takla Group. This fault zone is marked by strongly altered and fractured rocks.

Ferri *et al.* (1992a) tentatively included the dacitic tuff unit (MPlr4) and the argillite-grit-limestone unit (MPlr3) in the Lay Range assemblage, but they are now assigned to the Big Creek group.

Lower sedimentary division (Mississippian(?) to middle Pennsylvanian): The stratigraphy of the lower sedimentary division is not well defined, but it is important to recognize the probable continental derivation of some of the lithologies, in contrast to the upper volcanic-rich division. Fossil collections made by Roots (1954) probably came mostly from the this division; the oldest fossils were tentatively identified as Mississippian. The youngest unit, as defined here, is middle Pennsylvanian.

The division consists mainly of black and grey argillite and siltstone, bedded grey chert, thin-bedded feldspathic sandstone, chert-pebble conglomerate and 'grit', and less common fine to medium-grained quartzite, rhyolitic tuff, shaly or thin-bedded limestone, limy argillite and green tuffaceous rocks. The conglomerates are heterolithic, con-

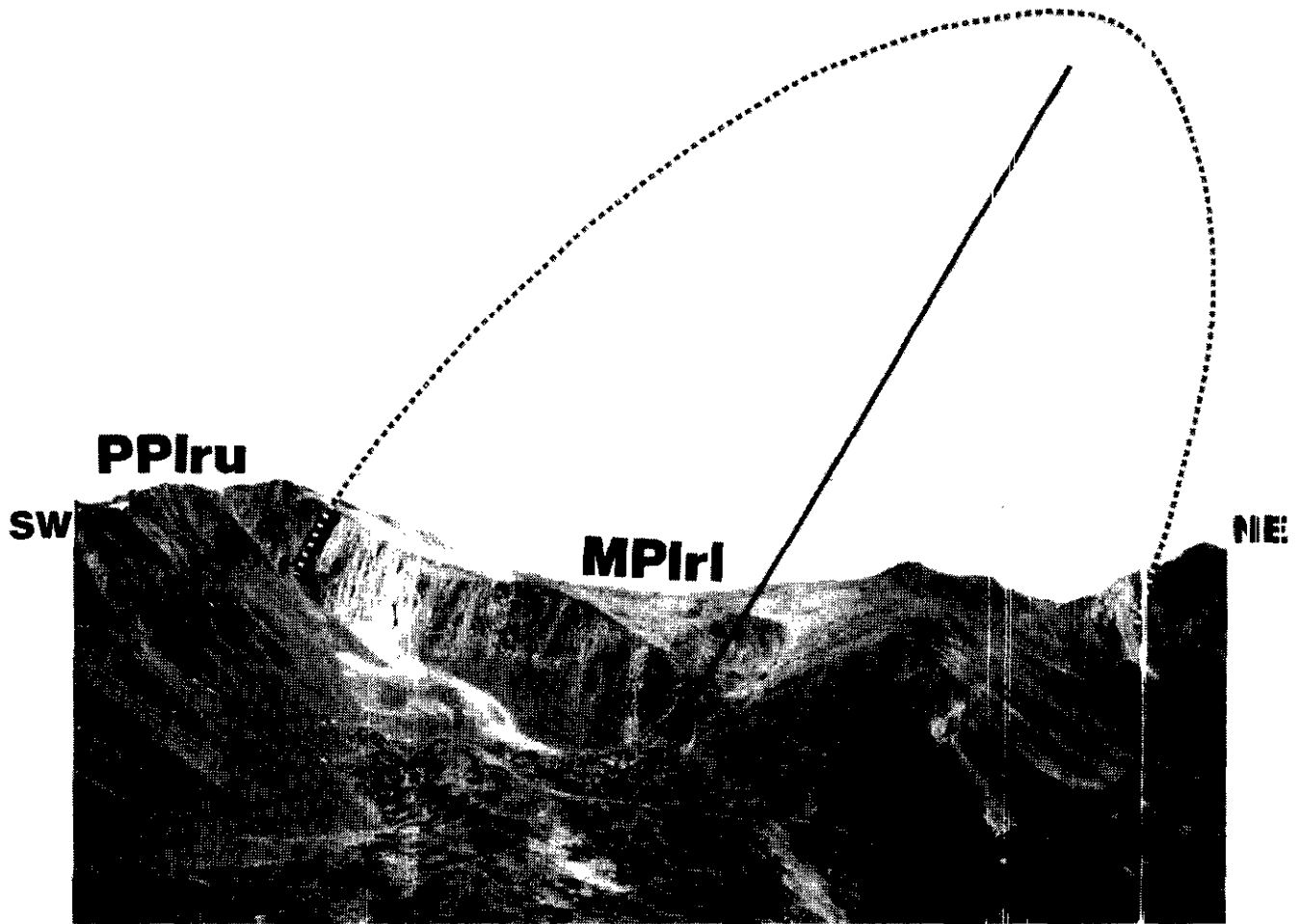


Plate 1-8-3. View to the northwest within the Lay Range, north of Polaris Creek. The mid-middle Pennsylvanian carbonate of the uppermost lower sedimentary division of the Lay Range assemblage is visible on both sides of this overturned, northeas verging fold. The viewer is from a carbonate at the nose of the fold. The distance between the carbonates is approximately 1 kilo metre.

taining up to cobble-size clasts of varicoloured chert, quartz, argillite, carbonate, green tuff and clinopyroxene-phyric volcanic rock (Plate 1-8-4). A thin, coarse-grained calcareous sandstone unit contains abundant fossil material, possibly crinoids. Locally there are small felsic or dioritic intrusions, and a narrow serpentinite body is exposed along a fault zone northeast of upper Polaris Creek.

The most distinctive limestone is at the top of the division. The largest body, in the hinge zone of the anticline, is 50 metres thick, but elsewhere the limestone may be only a few metres thick, or absent. It is a grey to white, massive to thinly bedded bioclastic limestone, locally rich in colonial and solitary horn corals, crinoidal material, fusulinids and foraminifera. Fusulinids collected by J.W.H. Monger indicate a middle Pennsylvanian age (early Moscovian, Ross and Monger, 1978). The limestone is locally dolomitic, and contains green tuffaceous layers and nodular masses of red or grey chert.

An interval of thinly bedded argillite, silty argillite and jasperoidal chert, several metres thick is usually present above the limestone. Some of these rocks are strikingly maroon to red, although shades of grey are also present.

This sequence is gradually succeeded by green tuffs of the upper division.

Upper mafic tuff division (middle Pennsylvanian to Permian): The Lay Range assemblage consists predominantly mafic crystal, lithic and lapilli tuffs, a conglomerate and volcanic flows, with subordinate interbedded green to grey argillite, siltstone, volcanic wacke and conglomerate, chert, limy siltstone and limestone, all of which comprise the upper mafic tuff division. One limestone unit, mapped near the base of this division on the southwestern limb of the anticline, contains middle Pennsylvanian fusulinids (late Moscovian, Ross and Monger, 1978), slightly younger than the limestone marker unit at the top of the lower sedimentary division. Permian conodonts were recovered from limy siltstone within mafic tuffs much higher in the division, in the Uslika Lake area (M.J. Orchard, personal communication, 1991; Ferri *et al.*, 1992a).

The volcanics are lithologically similar to the Upper Triassic Takla Group, but are distinguished in the field by their deeper green colour due to epidote, greater induration and stronger cleavage, and by the presence of quartz



Plate 1-8-4. Polymict conglomerate within the lower sedimentary division of the Lay Range assemblage. Large chert and carbonate clasts are visible. This conglomerate is much greener and more indurated than the younger maroon conglomerate illustrated by Plate 1-8-7.

(although rare) in coarser tuffs. The tuffs are bedded in units from several metres thick to centimetre-scale graded beds and fine laminations. Volcanic flows, locally pillowed, commonly have clinopyroxene and feldspar phenocrysts, and may be vesicular and amygdaloidal. They have the composition of basaltic andesite, and geochemical characteristics transitional between an island-arc and an ocean-floor origin. Rocks in this division, particularly the volcanics, are locally maroon, and maroon fragments are common in tuffs. Small felsic intrusions and gabbro occur in places.

QUESNEL TERRANE

TAKLA GROUP (UPPER TRIASSIC TO LOWER JURASSIC)

The Takla Group in the Aiken Lake area can be subdivided into the Plughat Mountain formation and the maroon tuff unit (Unit 1JuTrt, Ferri *et al.*, 1992b). These rocks are best exposed in the mountains southwest of Lay Creek and the Mesilinka River. They are a continuation of units described in the Uslika Lake area by Ferri *et al.*, (1992a, b). Plughat Mountain rocks are believed to be restricted to the Upper Triassic. Roots (1954) collected Upper Triassic faunas from Plughat rocks near Granite Basin and Carnian conodonts were recovered from limy horizons in the lower part of the Plughat formation near Uslika Lake. The maroon

tuff unit is thought to contain both Upper Triassic and Lower Jurassic rocks as it is equivalent to a unit of these ages to the southeast (Unit 1JuTrt, Ferri *et al.*, 1992b). The Takla Group is bounded on its northeast side by the strike-slip Lay Range fault (Wheeler and McFeely, 1991) along the Lay Creek - Mesilinka River drainages, and is intruded by the Hogem intrusive complex to the southwest. Takla rocks are hornfelsed and recrystallized along the margin of the Hogem intrusive complex. Calcareous lithologies may be altered to skarn and traces of copper are very common along the contact.

Plughat Mountain formation: The Plughat Mountain formation is at least 4000 metres thick and is composed of mafic tuffs, agglomerates and lesser tuffaceous sediments. Two broad subdivisions of the formation were delineated by Ferri *et al.* (1992 a, b) in the Uslika Lake area to the south: a lower, dominantly tuffaceous sequence which grades laterally and upwards into a thick and extensive upper agglomeratic succession. The Plughat Mountain formation in the present map area, however, is dominated by tuffaceous lithologies which in places comprise the entire thickness of the exposed Takla succession. Thick accumulations of agglomerate were seen only in the southern and northern parts of the map area. These pinch out laterally into

coarse tuffs over a distance of a few kilometres. Kilometre-thick tongues of agglomerate (as seen on Mount Elsie) are also present within the tuffaceous sequence but also quickly pinch out.

Major lateral facies variations also occur within the tuffaceous rocks. Coarse volcanoclastics in the syncline south of Tutizzi Lake quickly pinch out northward, along strike, into massive sections of coarse crystal-ash and lapilli tuff. These coarse tuffs continue to change in character northward, becoming finer grained, more distinctly bedded and containing sections of tuffaceous siltstone and argillite. A very similar transition is seen in the Granite Basin area northwest of Aiken Lake.

The absence of a clear tuff to agglomerate transition or any other marker within the Plughat Mountain formation means that the generalized stratigraphic columns north of Tutizzi Lake (Figure 1-8-7) cannot be correlated with any confidence. Nevertheless, given their en echelon position and the predominantly westerly dip, they can be projected into one another to suggest a total stratigraphic thickness in excess of 11 kilometres.

The lower part of the Plughat Mountain formation is dominated by blue-grey to grey, very fine to coarse crystal-ash tuffs to coarse lapilli tuffs with lesser agglomerate, tuffaceous siltstone, argillite and limestone. Layering tends to be massive to thickly bedded but finer grained sections of tuff display thinner bedding (Plate 1-8-5). Finer tuff sections are dominated by feldspar crystal fragments with subordinate pyroxene. Volcanic clasts are augite and plagioclase phyrific, though locally carbonate fragments are prominent. Tuffs and agglomerates in this section locally have a calcareous matrix.

The lower tuff sequence contains minor sections of finely bedded tuffaceous siltstone, siltstone, argillite, calcareous argillite and tuff, and limestone ranging from a few metres to 50 metres in thickness. These beds are rare in the upper and eastern part of the tuff section but become more prominent eastward and downward in the section. The lowest part of the tuffaceous section, exposed on the north-facing slopes above the Mesilinka River, is dominated by well-bedded, very fine grained crystal-ash tuffs, tuffaceous siltstones, siltstones, argillites, calcareous argillites and limestones. Sections of predominantly sedimentary lithologies up to 200 metres thick can be mapped over strike lengths of several kilometres within the fine tuffs.

Massive agglomerate and subordinate coarse lapilli tuff to crystal tuff several kilometres thick, generally rest above the tuffaceous sequence in the map area (Plate 1-8-6). Massive agglomerate interfingers with the tuffaceous section and is also present within it. The agglomeratic sequence is sometimes interrupted by very thin beds of siltstone, argillite and limestone, as seen west of Granite Basin. The agglomerate is typically monolithic being composed of *augite porphyry and sometimes feldspar porphyry clasts*. Heterolithic agglomerate with clasts of plagioclase and augite porphyry and sometimes plagioclase porphyry as well as intrusive feldspar porphyry is exposed on Mount Elsie. Feldspar porphyry agglomerate crops out north of Granite Basin. It is above a section of distinctive augite feldspar porphyry agglomerate with abundant carbonate

clasts up to 30 centimetres in size. The feldspar porphyry agglomerate appears to grade along strike into typical augite feldspar porphyry.

Maroon tuff unit: A fault-bounded package of maroon to green volcanics and minor sediments outcrops along the eastern boundary of the Takla Group. It is best exposed on a northwest-trending ridge between the Mesilinka and Tutizika rivers. The stratigraphy and thickness of this unit is not known but regional strikes and dips indicate it must be in the order of several kilometres thick.

The unit is characterized by maroon to green basaltic agglomerate, lapilli to ash tuffs and massive flows. The maroon colour is more dominant toward the south. Flows and coarse clastic material are composed of amygdaloidal hornblende or pyroxene ± feldspar porphyry. Dark grey to grey argillite is a minor constituent. Rare heterolithic pebble conglomerate with clasts of grey chert, black argillite, maroon feldspar porphyry, quartz and green volcanics is found along the southwestern boundary of the unit just north of the Tutizika River. This conglomerate is similar to younger pebble conglomerate found along the margins of this unit (*see section below*).

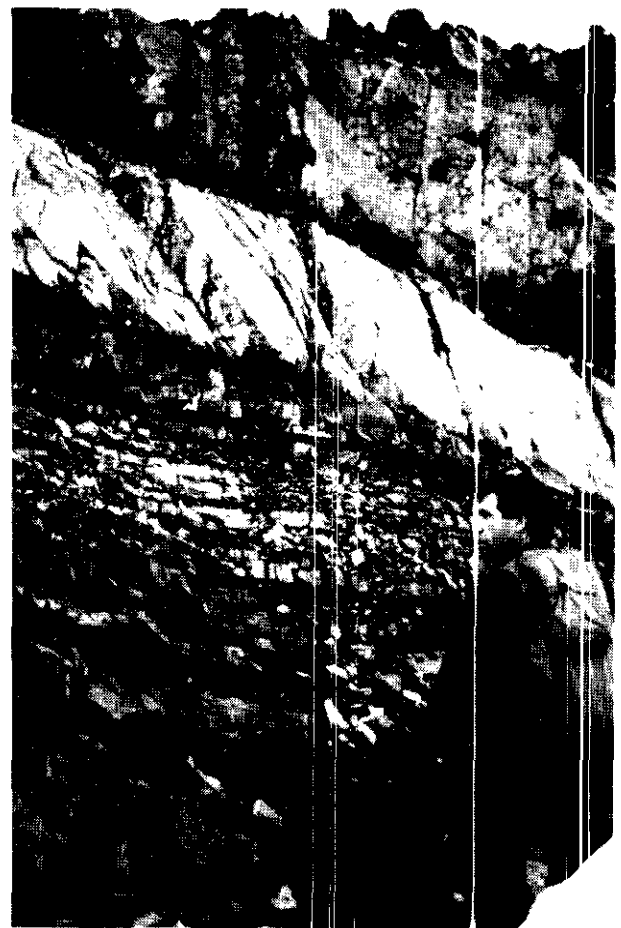


Plate 1-8-5. Well-bedded tuffs, tuffaceous siltstone and argillites near the top of Mount Elsie. This sequence is approximately 50 metres thick and lies within a thick section of agglomerate. These tuffs are more typical of the lower parts of the Takla Group.

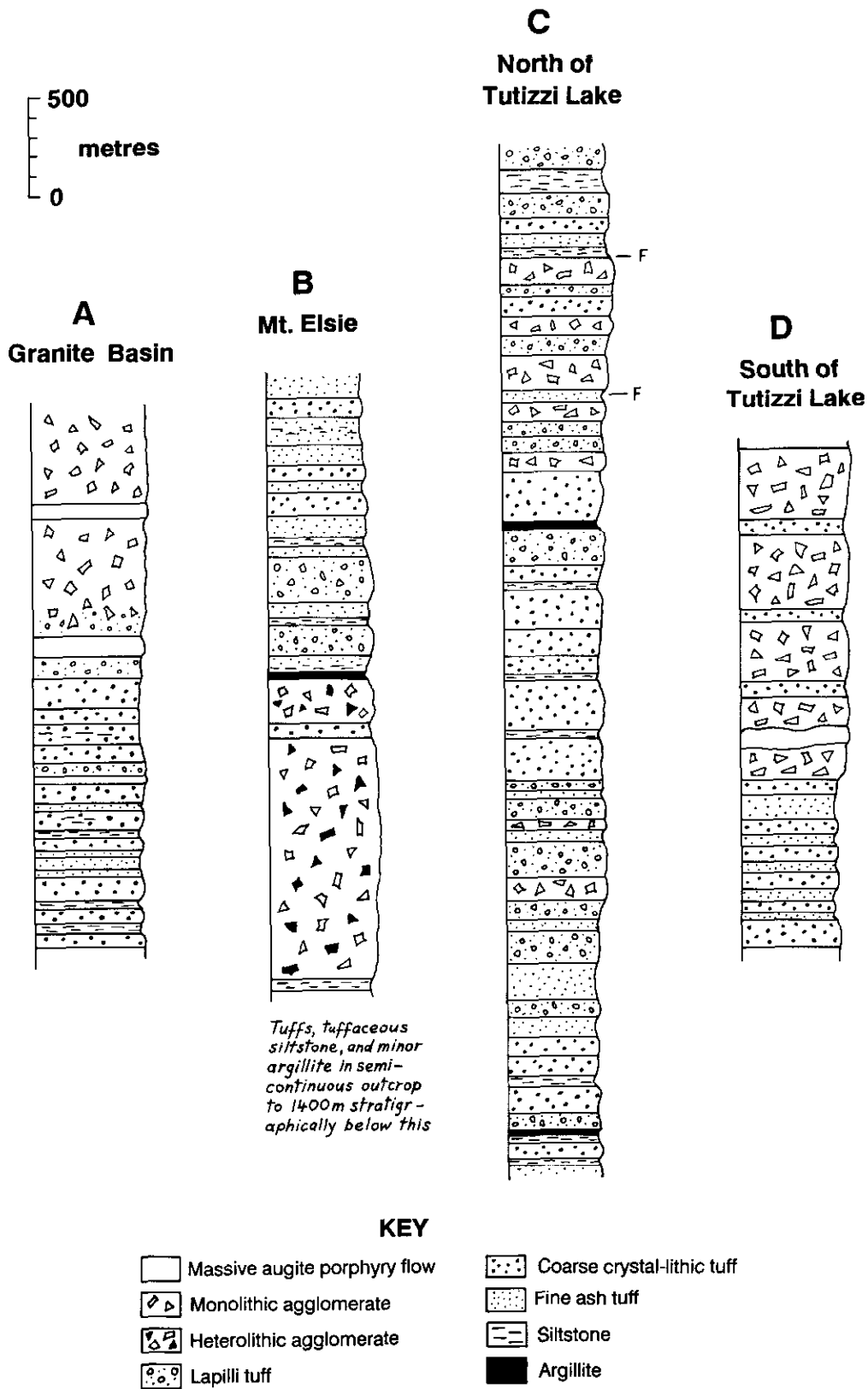


Figure 1-8-7. Representative stratigraphic columns of Takla Group rocks. Location of column A to D is shown in Figure 1-8-5. No common stratigraphic datum is implied. Note the predominance of tuffaceous lithologies over agglomeratic ones.

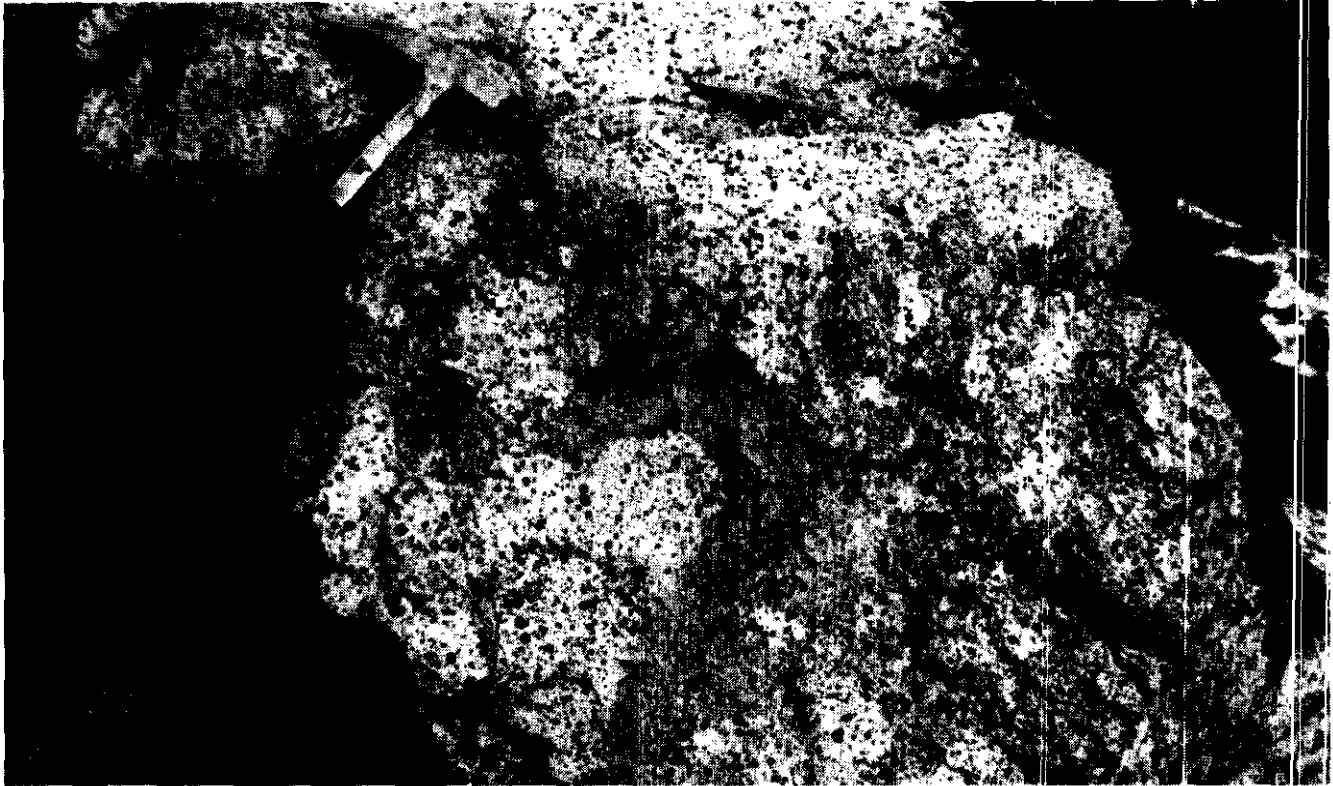


Plate 1-8-6. Augite-plagioclase-phyric agglomerate west of Granite Basin. Massive agglomerate, like this is more prevalent within the upper part of the Takla Group.

PROBLEMATIC UNIT (PALEOZOIC OR MESOZOIC)

A fault-bounded section of steeply dipping argillites, tuffs and minor coarse volcanoclastics outcrops on the ridge between Lay and Polaris creeks. The southwestern margin of this package is the Lay Range fault along Lay Creek. The character of the fault on the northeastern margin is not presently known though it *appears* to be less significant than the southwestern fault zone.

The overall appearance of these tuffs and sediments is very similar to the lower part of the Takla Group southwest of the Mesilinka River. The blue-grey to grey colour of the tuffs, lack of penetrative cleavage in finer grained lithologies, lack of continentally derived material and overall poorer induration indicate stronger affinities with the Takla Group than with the Lay Range assemblage. However, we believe that the lithologic similarities alone do not justify the relocation of a terrane boundary. More data, in the form of fossil ages, are required before these rocks can be definitely assigned to either the Takla Group or the Lay Range assemblage.

Rocks within this package are dominated by grey to blue-grey, very fine to coarse crystal-ash tuffs, tuffaceous siltstone, dark grey to black graphitic argillite, calcareous argillite and minor limestone. Lesser augite \pm plagioclase porphyry lapilli tuff and agglomerate are present within the northern part of the unit. These coarser volcanoclastics may be a fault sliver of Takla Group rocks. Layering is predominantly very thin to thickly bedded in the finer grained

lithologies and becomes more massive to the north within the lapilli tuffs. These rocks form a panel which generally is upright and steeply dipping to the southwest though locally bedding is overturned to the southwest.

OVERLAP ASSEMBLAGES

Several exposures of younger conglomerate, sandstone and siltstone are found primarily along the fault boundaries between terranes. Conglomerate is also exposed in the Lay Range. Many of these packages are too small to display on the map in Figure 1-8-5 but their presence may denote significant fault zones. Several varieties of these clastics are present but none have been dated, although their tectonostratigraphic position and overall similarity to Late Jurassic(?) to Tertiary conglomerate in the Ushika Lake area (Ferri *et al.*, 1992b) suggests a correlation.

MAROON CONGLOMERATE (CRETACEOUS TO TERTIARY)

Maroon pebble to boulder conglomerate is exposed in at least two places in the Lay Range north of Polaris Creek. The northern body forms a long, discontinuous outcrop which varies from 300 metres to less than 100 metres wide. It occurs within a high-angle strike-slip fault zone in its northern part where it is tectonically juxtaposed against strongly sheared serpentinite and volcanics of the Lay Range assemblage. In its southern part an unconformable

relationship with Lay Range tuffs was found along parts of its contact.

Another body of conglomerate to the southeast is roughly 1 square kilometre in area and more brown than maroon. It sits unconformably above rocks of the Lay Range assemblage although locally this contact is faulted.

The maroon conglomerate is composed of well-rounded clasts of quartzite, chert, argillite, phyllite, green tuff, amphibolite gneiss, schist and rare coralline limestone set in a coarse sandy matrix (Plate 1-8-7). This unit appears very similar to the Uslika Formation of the Uslika Lake area (Ferri *et al.*, 1992a, b; Roots, 1954) which has a poorly constrained age of Late Jurassic to Early Tertiary. The most obvious source of the metamorphic clasts is the Wolverine Metamorphic Complex. Unroofing and cooling of this complex appears to have occurred rapidly in the Late Cretaceous to Early Tertiary. This is substantiated by the presence of metamorphic clasts in the nearby Upper Cretaceous to Lower Tertiary Sifton Formation (Gabrielse, 1975; Roots, 1954) and from K-Ar cooling ages in these metamorphic rocks (Ferri and Melville, in preparation). These considerations help to further constrain the age of the conglomerate to Late Cretaceous to Early Tertiary.

CONGLOMERATE (LOWER CRETACEOUS?)

Pebble to cobble conglomerate is exposed on either side of the maroon tuff unit south of the Mesilinka River. Most

of these bodies are strongly sheared and indicates involvement in the shear zone in which they are found. Three areas are underlain by these younger clastics but their general similarity suggests they are related. The largest body, at the northeastern contact of the maroon tuff unit, is associated with maroon to black feldspathic sandstones and mudstones with coaly fragments and plant fossils. Clasts are composed of quartzite, chert, green tuff, siltstone and argillite. The two bodies to the south contain pebbles of only quartzite and chert.

The age of these conglomerate bodies is not known as no diagnostic fossils were found. Their location suggests that they may have filled a depression produced by erosion of softer rock along the fault zone or that they have been preserved in grabens along the fault zone. The maroon to black sandstone and siltstone along the northeastern boundary of the maroon tuff unit bears some resemblance to Early Cretaceous sediments in the Uslika Lake area (Ferri *et al.*, 1992 a, b).

INTRUSIVE ROCKS

HOGEM INTRUSIVE COMPLEX AND RELATED INTRUSIONS (LATE TRIASSIC TO MIDDLE JURASSIC, CRETACEOUS)

The Hogem intrusive complex is exposed in the southeastern part of the map area and intrudes rocks of the Takla



Plate 1-8-7. Maroon polymict conglomerate in the Lay Range. The age of this unit is inferred to be Late Cretaceous to Early Tertiary based on clast composition and its similarities to younger conglomerate farther south. It is far less indurated than conglomerate of the Lay Range assemblage (Plate 1-8-4).

Group. It is a multiphase complex with latest Triassic to Middle Jurassic alkaline phases and Cretaceous calcalkaline bodies (Garnett, 1978). Only a cursory examination of its margin was conducted during the 1992 field season.

The contact with the Takla Group is commonly an intrusive breccia. Takla rocks are hornfelsed and coarsely recrystallized for up to a kilometre away from the Hogem contact. Minor amounts of copper are commonly found along this contact.

Hogem rocks in the southern part of the map area are alkaline in composition and made up of tan to pink, medium to coarsely crystalline quartz monzonite to monzodiorite or syenite to monzosyenite with hornblende and/or biotite as accessories. Mottled pink and white, coarsely crystalline granodiorite crops out south of Abraham Creek. Coarsely crystalline gabbro is exposed along the ridges between Abraham Creek and the Mesilinka River. This body may be related to mafic and ultramafic intrusions along the margin of the Hogem complex (Irvine, 1974, 1976). Tan to pink, medium to coarsely crystalline granite to granodiorite, containing chloritized hornblende as an accessory, is exposed north of the Mesilinka River.

Two lenticular bodies of grey to green feldspar porphyry and related diorite are found north of the Mesilinka River and south of Kliyu Creek. They are locally rusty weathering to gossanous due to the presence of 1 to 5 per cent disseminated pyrite.

Hogem rocks are cut by numerous dikes of pink aplite or syenomonzonite from several centimetres to several metres in thickness. The relationship of these dikes to other bodies in the Hogem intrusive complex is not known. The Takla Group volcanics are also cut by numerous small dikes or irregular bodies of coarse feldspar porphyry. These rocks are characterized by feldspar phenocrysts up to several centimetres in length. The abundance and size of the dikes decreases away from the Hogem contact suggesting a genetic link to the complex.

One, and possibly two, bodies of poorly exposed grey, magnetic, hornblende-bearing monzonite intrude the problematic unit and the nearby maroon tuff unit north of the Mesilinka River. Argillites and fine tuffs in these packages are hornfelsed and pyritized. The monzonite is cut by diorite or gabbro dikes up to 1 metre wide.

POLARIS ULTRAMAFIC COMPLEX AND RELATED INTRUSIONS (EARLY JURASSIC)

The Lay Range assemblage is intruded by a large composite Alaskan-type ultramafic body called the Polaris Ultramafic Complex, covering an area of some 40 square kilometres. This transgressive sill-like body is composed of varying amounts of dunite, pyroxenite, hornblendite, wehrlite and gabbro, and is of late Early Jurassic age (G.T. Nixon personal communication, 1992). Only its margins were examined as it was recently mapped in detail by Nixon *et al.* (1989, 1990a, b; Nixon and Hammack, in preparation). The reader is referred to these publications for further details.

MAFIC-ULTRAMAFIC UNIT (EARLY JURASSIC OR OLDER?)

A composite body of gabbro, hornblendite, pyroxenite, orthopyroxenite and peridotite, over 20 kilometres long and 2 to 10 kilometres wide, intrudes the Takla Group near the Hogem contact. These rocks were examined in some detail by Irvine (1974, 1976) who described at least two separate bodies. Field data from this year's work, in conjunction with published aeromagnetic maps of the area, suggest that Irvine's two bodies are actually one. The aeromagnetic signature of the gabbro body south of Tutizzi Lake suggests it is related to this mafic-ultramafic unit. The age of this unit is not directly known. If it is an Alaskan-type ultramafic body and related to the nearby Polaris Complex then a latest Early Jurassic age is postulated (G.T. Nixon, personal communication, 1992). Alternatively if these bodies are related to mafic phases of the Hogem intrusive complex they may be as old as the latest Triassic (Garnett, 1978).

Very coarse to finely crystalline, multiphase hornblende gabbro is the most dominant lithology in the northern part of the large intrusion. The most mafic lithologies (peridotite, hornblendite and orthopyroxenite) form a long sinuous body along its western margin. Hogem rocks appear to cut this ultramafic intrusion.

A small body of dark green, very fine to coarsely crystalline gabbro intrudes the Takla Group south of the Mesilinka River, and is most likely related to the mafic-ultramafic unit.

STRUCTURE AND METAMORPHISM

Structural style and metamorphic grade are quite diverse in the Aiken Lake map area due to the varied terranes and rock packages present. Broad open folds and sub-greenschist grade metamorphism characterizes the Quasnel Terrane. The intensity of deformation and metamorphism is higher to the east in the Harper Ranch Terrane, and is most intense in rocks of the Cassiar Terrane where polyphase deformation is associated with metamorphism up to garnet grade.

Terranes are bounded and cut by major faults. The most important fault zone in the map area is the Lay Range fault (Wheeler and McFeely, 1991) a steep, northwest-trending strike-slip structure which trends roughly parallel to the Lay Creek valley. In this area strongly sheared and crumpled tuffs, tuffaceous siltstones and argillites of the Takla Group and the problematic unit are juxtaposed across an anastomosing fault zone about 1 kilometre in width. The fault zone is exposed on the northeast side of the upper part of Lay Creek; southeastward, it is covered by alluvium in the Mesilinka River valley but we believe it merges with the wide and intense shear zone mapped on the southwest side of the maroon volcanic package of the Takla Group. Several other parallel structures are found within the Takla Group and problematic unit.

The northeastern boundary of the problematic unit is a fault zone we believe to be related to the Lay Range fault. Although it is not as wide, and no kinematic indicators were observed, its steep dip and trend parallel to the Lay Range fault suggest they are genetically linked. This fault also

merges with shear zones south of the Mesilinka River valley which separate the maroon volcanic unit from tuffs of the Lay Range assemblage.

High-angle, strike-slip faults were also observed within the Lay Range assemblage. One, along the southwest flank of the lower sedimentary division, is marked by sheared serpentinite. Younger maroon Uslika-like conglomerate is also exposed within this fault zone.

We believe the various northeast-trending fault zones described here join structures mapped by Ferri *et al.* (1992a, b) in the Uslika Lake area. These fault zones ultimately connect with structures described by Nelson *et al.* (1993, this volume) along Discovery Creek. The Lay Range - Uslika Lake - Discovery Creek faults form a parallel structure en echelon with the Manson fault zone.

A major northeast-verging, ductile shear zone is exposed along the northeast contact of the Polaris Ultramafic Complex. This zone is upwards of 75 metres thick within peripheral gabbro of the complex and dips steeply to the southwest. A similar thickness of sheared argillite may be present within adjacent rocks of the Big Creek group but this is difficult to demonstrate due to the fine-grained, monotonous nature of these rocks. This shear zone was observed at several localities and was mapped by Nixon *et al.* (1989, 1990a, b). We believe it extends to the southeastern end of the Polaris Complex.

This shear zone represents the boundary between the Harper Ranch and the Cassiar terranes in this area as the Polaris Ultramafic Complex intrudes the Lay Range assemblage (Harper Ranch Terrane). To the southeast, the shear zone does not wrap around the southern end of the complex, but presumably continues southeastwards, separating the upper mafic tuff division of the Lay Range assemblage from the Big Creek group of the Cassiar Terrane. The absence of the lower sedimentary division anywhere between them supports the continuation of a fault along this contact, but without direct structural evidence for this, an unconformity is not precluded: it is possible that the lower sedimentary division was not deposited, or that it was eroded away between Big Creek and upper mafic tuff deposition. However, a fault is more likely. This contact would continue south of the present map area and onto the Uslika map sheet (Ferri *et al.*, 1992b) where the upper mafic tuff division (Unit MPlr2) is next to Unit MPlr3, now placed in the Big Creek group. Sheared tuffs of the upper mafic tuff division were mapped along this boundary south of the Tutizika River suggesting a fault contact between the two packages.

Normal faults are recognized mostly within Cassiar rocks. Two generations of normal faults have been identified; northwest-trending, southwest-side-down faults and later northeast-trending, southeast-side-down faults. The northeast-trending Knoll fault south of the Swannell River has considerable displacement as it juxtaposes garnet-grade rocks of the Swannell Formation against lower greenschist rocks of the Echo Lake group. Stratigraphic thicknesses and lithologic characteristics of units change across the fault suggesting that it may be a reactivated older structure which controlled basin development in the area. This fault also

displaces the major shear zone at the base of the Polaris Complex.

The northwest-trending fault cut by the Knoll fault has not been recognized to the northeast of Knoll fault, although it may be hidden within monotonous shales of the Big Creek group.

Structural attitudes within Quesnel rocks are relatively simple in comparison to the other rock packages. Bedding dips typically southwest to northwest, with variations outlining broad folds, as seen south of Tutizika River. The only deviance from this is along the northeast margin of the Quesnel Terrane where finer grained units define tighter folding. One such area is south of the Mesilinka River and southwest of the maroon tuff unit. At this locality, fine ash tuffs, tuffaceous sediments and argillites define steep, tight folding which on a macroscopic scale appears to be chevron-like. Northward, along this fault zone, bedding is steep to overturned. This may reflect its proximity to the fault zone.

Northeasterly bedding trends common in the Takla Group in the central and northern parts of the map area are different from the northwest-trending attitudes seen in the other terranes, which are more typical of the region. The regional significance of this is not yet resolved.

Folds within the problematic unit are upright or overturned to the northeast. Macroscopic fold structures were not observed directly and are inferred from dip reversals and overturned bedding.

The Lay Range assemblage locally contains a penetrative fabric or cleavage within the finer grained lithologies. The trace of the carbonate unit at the top of the lower sedimentary division outlines a megascopic southwest-plunging, northeast-verging, overturned fold which must represent the overall structural style of the package. Bedding reversals in the upper mafic tuff unit suggest the presence of similar megascopic folds but the monotonous nature of the tuffs precludes their accurate delineation.

In general, Cassiar rocks form a southwest-dipping panel. This is modified by several large-scale broad folds (F_2 ?) in the northeastern part of the map. The vergence of these megascopic folds is not known but Roots (1954) and Bellefontaine (1990) indicate that these structures are southwest verging. Mesoscopic folds (F_1) which have axial planes parallel to the dominant cleavage or foliation (S_1) show northeast vergence. This foliation is subparallel to compositional layering (S_0). The upright nature of the megascopic folds suggests that they are unrelated to the mesoscopic, northeast-verging structures. The dominant foliation in these rocks is cut by several sets of crenulations some of which are subparallel to S_1 and others which cut S_1 or S_0 at high angles.

Takla Group volcanics are characterized by sub-greenschist grade metamorphism at lower grade than rocks of the Lay Range assemblage. The more intense green to apple green colour of Lay Range volcanics results from the greater abundance of epidote which may be a reflection of the higher metamorphic grade (lower greenschist). The greater induration of Lay Range rocks is also a function of increased metamorphic grade.

Cassiar rocks display the most penetrative deformation and highest grade of metamorphism in the map area. Metamorphic grade along the Swannell River is upper greenschist in the lower parts of the Swannell Formation. High-grade assemblages consist of garnet±chloritoid-biotite-muscovite with the appearance of garnet and biotite essentially coinciding. Garnet porphyroblasts are idioblastic and appear to overgrow both the main foliation and a later crenulation cleavage, although in some areas the garnet porphyroblasts deflect the crenulation cleavage planes. This suggests several generations of crenulation cleavage formation. Garnet and biotite porphyroblasts are locally chloritized.

ECONOMIC GEOLOGY

A variety of mineral deposit styles are represented in the Aiken Lake and Osilinka River map areas. These include porphyry copper-gold, carbonate-hosted lead-zinc-barite±precious metals, and various vein deposits. Occurrences of lesser importance include ultramafic-hosted chromite, skarns and industrial minerals. The reader is referred to Table 1-8-1 for a brief description of the various occurrences in the map area.

Takla rocks host a large number of copper occurrences (some with associated gold) in both porphyry-style systems and hydrothermal veins often associated with shearing. At some occurrences there seems to be a direct correlation between copper mineralization and ultramafic dikes or sills that intrude the Takla volcanics. Porphyry mineralization is related to the syenite-monzonite-diorite-granitic-intrusive phases which comprise the Hogem intrusive complex. The Porphyry Creek and Granite Basin occurrences in the Aiken Lake map area are examples of this style of mineralization.

The Porphyry Creek occurrence, located on the extreme western boundary of the Aiken Lake map area, is the largest known porphyry system in the map area. Takla volcanics, sediments and limestones are intruded by diorite, quartz diorite, granodiorite and quartz monzonite of the Hogem intrusive complex and pyroxenite and gabbro of an ultramafic body. Sulphides include chalcopyrite, rare chalcocite and bornite together with native gold, galena, sphalerite and molybdenite occurring as disseminations, fracture fillings and in shears. Higher concentrations of gold and base metals are associated with late-stage intrusive activity. At least two complex mineralized systems are present on the Porphyry Creek property. The first is a calcalkaline porphyry molybdenum system with mineralization within a tabular, potassically altered and zoned granodiorite intrusion surrounded by a weak copper±tungsten halo. The second system is related to an intrusive breccia peripheral to the granodiorite stock and has potential for copper-gold mineralization of possible alkaline affinities (Grextan and Roberts, 1991).

There are many small copper (±gold±molybdenum) occurrences throughout Takla Group rocks (*see* Table 1-8-1) that are commonly related to an intrusive body and/or localized hydrothermal veining (usually quartz or ankerite). Mineralization is also frequently found along fractures and

in veins within mafic to ultramafic rocks of an ultramafic body.

Mineralization commonly consists of chalcopyrite, malachite and azurite±magnetite±molybdenite±specularite±galena±sphalerite in quartz and/or carbonate (commonly ankerite) veins. The amount of mineralization varies from a few specks of malachite to strongly mineralized quartz-carbonate vein systems several metres wide.

Carbonate-hosted lead-zinc occurrences occur within each of the various Paleozoic and Upper Proterozoic calcareous lithologies. Most showings appear to be stratabound replacements, although some are interpreted as stratiform (Ferri and Melville, in preparation), or related to hydrothermal activity, with remobilization and deposition in veins. Examples of carbonate-hosted lead-zinc occurrences include the PAR and Childhood showings in the Osilinka River area and the Swan, Rain and Crag showings in the Aiken Lake map area.

Recent mineral exploration in the Osilinka River area has centred on the PAR claims held by Cominco Exploration Limited. Lead, zinc, gold and silver mineralization with associated barite is found within and associated with the Lower Cambrian Mount Kison formation limestone, Cambrian to Middle Ordovician Razorback group limy shales to argillite, Ordovician to Lower Devonian Echo Lake dolostone and Middle Devonian Otter Lakes limestone. Trenching on the property in 1991 revealed thin lenses (less than 0.4 m) of 60 to 80 per cent sulphide rock intercalated with shales, phyllites and dolomite boudins of the Razorback group. Best assay results reported from trenching were: 6.7 per cent lead and 2.5 per cent zinc over 4.0 metres; 1.1 per cent lead and 3.2 per cent zinc over 18.0 metres; 6.1 per cent lead and 3.4 per cent zinc over 1.0 metre (Craig, 1991).

The Childhood Dream prospect is located north of the Osilinka River and east of Beveley mountain. Hosted in both primary and secondary breccia of the Echo Lake group (as described earlier in this article), it consists of massive to coarse-grained pyrite with disseminated galena and sphalerite. There are two exploration adits on the property with the best assay reported from a 1.8-metre chip sample returning 0.34 gram per tonne gold, 24.0 grams per tonne silver, 2.6 per cent lead and 11.2 per cent zinc (Lay, 1931).

Hydrothermal veining and mineralization are also attributed to faulting and shearing along the Lay Range fault. Occurrences related to the Lay Range fault include the Polaris and Polaris Zinc showings hosted by sheared volcanics and sediments of the Takla Group and possibly related to small diorite porphyry and quartz monzonite stocks mapped in the area. Mineralization consists of quartz-calcite veins with disseminated pyrite, arsenopyrite and pyrrhotite together with thick lenses of massive pyrite, pyrrhotite and chalcopyrite, and fracture coatings of chalcopyrite and molybdenite. The Jupiter and LCF prospects consist of quartz-carbonate-veined rock within the Lay Range fault zone.

The presence of skarn mineralization in some of the numerous limestone horizons within the Takla Group suggests a strong potential for similar mineralization along its contact with the Hogem intrusive complex.

**TABLE 1-8-1
TABLE OF MINERAL OCCURRENCES IN THE AIKEN LAKE
AND OSILINKA RIVER AREAS**

MAP NUMBER	STYLE OF MINERALIZATION	MINFILE NUMBER	OCCURRENCE NAME	COMMODITIES	GEOLOGICAL DESCRIPTION
1	Vein	094C 120	CR	Cu	Epidote alteration and malachite staining are found in massive maroon basalt flows of the Takla Group.
2	Vein	094C 121	Nuthatch	Cu	Epidote alteration and malachite staining are found in massive maroon basalt flows of the Takla Group. May have carbonate veining and flows are locally sheared and fractured. Minor azurite present. Mineralized zone is at least 15 m across.
3	unknown	094C 042	Mercury 2	Hg	Carbonatized fault zone contains some cinnabar, apparently in Lay Range sediments.
4	Vein?	094C 015	Stranger	Au	Pyrite occurs in quartz-calcite veins which cut Big Creek group calcareous black slaty argillite.
5	unknown	094C 041	Mercury 1	Hg	Carbonatized fault zone contains a little cinnabar (in upper Lay Range sediments).
6	Porphyry and vein	new	Zip	Cu	Takla Group tuffs are strongly fractured and pervasively cut by quartz-carbonate veins. Minor malachite staining seen in some places.
7	Vein	new	Ran	Cu	Takla Group volcanics and sediments are cut by a quartz vein 10-20 cm thick. Rusty fractures are coated with malachite and chalcocopyrite.
8	Vein	094C 135	Mat 3	Ag, Pb, Zn, Cu	Quartz vein hosting galena, sphalerite, chalcocopyrite, pyrite and silver sulpho-salts. A reported sample assayed 763g/t Ag. Similar to the MAT 1 occurrence (MINFILE NO. 094C 099). Hostrocks are volcanics and sediments of the Takla Group.
9	Porphyry and vein	new	Choice	Cu	Minor disseminated chalcocopyrite with malachite haloes and malachite on fracture surfaces of Takla Group volcanic tuffs and augite porphyry (flows?). Locally highly silica, carbonate and epidote altered.
10	Vein	094C 137	Tut 3	Au, Ag, Cu, Mo	Takla Group volcanics host a vuggy limonite-stained quartz vein with disseminated malachite and molybdenum.
11	Unknown	new	Ache	Cu	Blebs of chalcocopyrite and trace malachite occur on fracture surfaces and with epidote and calcite veining in augite porphyry agglomerate flows of the Takla Group.
12	Shear and porphyry(?)	094C 136	Tut 6	Cu, Au, Ag	Hosted in volcanics and tuffs of the Takla Group which are cut by sheared and silicified monzonite and syenite dikes with chalcocopyrite and pyrite mineralization. One reported sample assayed 0.89% Cu, 0.15g/t Au, 10.0g/t Ag.
13	Vein	094C 055	Tutizzi Lead	Pb, Cu	Reported occurrence of quartz veins north of Tutizzi Lake containing galena, commonly with chalcocopyrite or specularite, hosted in Takla Group volcanics and sediments.
14	Vein	094C 052	Tutizzi Copper	Cu,Pb	Reported occurrence of galena, chalcocopyrite and/or specularite in quartz veins within the mafic-ultramafic unit (possibly related to the Hogem intrusive complex) near the contact with volcanics and sediments of the Takla Group.
15	Vein	094C 053	Tutizzi Lake	Pb,Cu,Ag	Mafic intrusives possibly related to the Hogem intrusive complex host a 90 cm wide brecciated quartz pod mineralized with galena and chalcocopyrite. Reported assays have returned values up to 0.26 g/t Au, 176.2 g/t Ag, 1.44% Cu and 50.38 % Pb.
16	Unknown	094C 056	Izzi	Au, Cu	A gossan zone within hornblende-bearing pyroxenite, possibly related to the Hogem intrusive complex, contains chalcocopyrite, malachite, hematite and pyrite. Reported chip samples assayed as high as 1.525g/t Au.
17	Unknown	new	Ant	Cu	A pyritic zone in a pyroxenite body, possibly related to the Hogem intrusive complex, hosts malachite staining; also a nearby gabbroic phase shows trace malachite.
18	Unknown	new	Welt	Cu	Malachite occurs at the contact between Takla Group volcanics and monzodiorite possibly related to the Hogem intrusive complex.
19	Porphyry	094C 064	Grouse North	Mo	Fine to medium-grained pink syenite hosts molybdenite in two well developed fracture sets.
20	Vein	094C 078	Grouse	Mo	A 40 cm wide quartz vein within the Hogem intrusive complex contains minor molybdenite.
21	Vein	094C 054	Abraham Creek	Pb, Cu	Reported occurrence of quartz veins west of Abraham Creek containing galena, commonly with chalcocopyrite or specularite, hosted in hornblende diorite and appanite of the Hogem intrusive complex.
22	Vein	new	Misty	Cu	Hydrothermally altered volcanics and sediments of the Takla Group are cut by a carbonate vein mineralized with malachite and azurite.
23	Porphyry?	new	Bell	Cu	Takla Group volcanics and sediments are intruded by medium to coarse-grained gabbro in which a small area has malachite disseminated throughout and very minor chalcocopyrite.
24	Porphyry and vein	new	Shot	Cu	Fine to medium-grained gabbro contains rusty zone with malachite and azurite staining with possible chalcocopyrite in a small 1m square area. Quartz veining and silica alteration are present.
25	Shear and/or vein	new	Anorak	Cu	Malachite on fracture surfaces at the foliated/sheared contact between Takla Group volcanics and a diorite body. The diorite can be siliceously altered with 1-5% pyrite.
26	Porphyry and vein	094C 040	Mes(Link)	Cu, Mo	The showing is hosted by Takla Group rocks near the contact with the Hogem intrusive complex. Phyllic and argillic alteration are common with local silicification and pyritization (up to 20% of volume). Within the gossan zone, pyrite averages 1-3%. Malachite, molybdenite, azurite and tenorite have been identified in the area of the showing.

27	Porphyry	094C 007	Porphyry Creek	Cu, Au, Pb, Mo, Zn	Widely altered (chlorite, epidote, biotite, silica) volcanics and sediments of the Takla Group are intruded by primarily mafic phases probably related to the Hogem intrusive complex. Widespread copper mineralization comprising chalcopyrite, with or without malachite, azurite, and rare chalcocite or bornite occurs as disseminations, fracture fillings and in shears. Specks of native gold have been found in pan concentrates and in quartz-carbonate veins. Galena +/- sphalerite occurs locally in quartz-carbonate veins. Molybdenum is also found in quartz-carbonate +/- potassium feldspar veins.
28	Shear and vein	094C 008	Croydon	Au, Cu, Mo	Hostrocks are altered hornblende diorite and amphibolite, possibly part of the Hogem intrusive complex. Mineralization occurs in four fracture zones partially filled with vein quartz, with pyrite and chalcopyrite being the main metallic minerals. Lesser magnetite molybdenite and gold are also present, in local areas of almost massive sulphide.
29	Unknown	094C 065	Porphyry Creek Molybdenum	Mo	Reported molybdenum showing in mafic rocks related to the Hogem intrusive complex.
30	Unknown	094C 066	Croydon North	Au	Two reported assays showed 10.29 and 4.11 g/t Au. Mineralization is hosted in mafic and ultramafic rocks possibly related to the Hogem intrusive complex.
31	Porphyry?	new	Lonely	Cu	Takla Group volcanics and sediments are intruded by diorite and gabbro, likely part of the Hogem intrusive complex. Malachite and pyrite are found disseminated throughout and along fracture surfaces.
32	Disseminated and/or porphyry	new	Jump	Cu	Minor occurrences of malachite and possibly chalcopyrite hosted in Takla Group volcanics and flows. Appears to be some association with mafic-rich marginal phase of hornblende porphyry dike which cuts flows of augite/feldspar porphyry agglomerate. There is some local shearing but its relationship to the mineralizing event is unclear.
33	Vein	094C 128	South Sarah	Cu, Au, Ag, Hg	Takla Group volcanic rocks are propylitically altered and minor showings of chalcopyrite are common. A reported grab sample from quartz-carbonate veins contains 6.06% Cu, 78.4 g/t Ag, 1.6 g/t Hg and 13.5 g/t Au.
34	Skarn	094C 084	Bloom Cirque Skarns	Cu, Fe	Sparse and erratic chalcopyrite with malachite and azurite occur in four occurrences of magnetite skarn... along the margins of Bloom cirque. Host rocks are calcic silicate horizons within Takla Group rocks. Diorite phases of the Hogem intrusive complex outcrop 100 m west of the occurrence.
35	Porphyry and vein	094C 009	Granite Basin	Au, Ag, Cu	Takla Group rocks are intruded by phases of the Hogem intrusive complex. Pyrite, chalcopyrite and possibly bornite and tetrahedrite are present in four pyritic zones. Assays reportedly reach up to 11.4 g/t Au over 9 m.
36	Porphyry and vein	094C 039	Bloom Cirque	Co, Cu	Minor cobalt bloom on fracture surfaces in small quartz veins and minor occurrences of fracture-controlled and disseminated chalcopyrite, malachite and pyrite are present throughout fine-grained hornblende diorite and quartz diorite. Widespread weak to strong propylitic alteration accompanies the mineralization.
37	Vein and porphyry	094C 075	Sarah	Cu, Au, Ag	The occurrence consists of fracture coatings and disseminations of pyrite, chalcopyrite and malachite with minor bornite in mafic intrusives of the Hogem intrusive complex. One 30 cm wide vein assayed 5.28% Cu, 7.5 g/t Au and 55.5 g/t Ag. Epidote and chlorite alteration are present.
38	Unknown	new	Rave	Cu	An extensive gossan zone in the Takla Group volcanics and sediments carries small amounts of malachite and chalcopyrite.
39	Porphyry	094C 127	Raven	Cu, Pb, Zn	Chalcopyrite is found in monzonite porphyry dikes with magnetite, pyrrhotite and pyrite as fracture-controlled blebs and pods in Takla Group tuffs. Also present are minor galena and sphalerite.
40	Porphyry and vein	new	Howl	Cu	Takla Group volcanics and sediments are cut by small (2-10 cm) quartz-carbonate veins. Malachite and chalcopyrite are found in the veins and minor malachite on fracture surfaces in the area. Some mineralization appears to be associated with small ultramafic dikes which cut the Takla Group.
41	Shear and vein	094C 122	LCF	Au, Ag	Altered and quartz-carbonate veined Takla Group rocks yielded a geochemical analysis of 6.68 g/t Au and 4.4 g/t Ag.
42	Shear	new	Webb	Cu	Malachite staining occurs on fracture surfaces in an ankerite-altered fault zone within a massive serpentinite body in the Lay Range assemblage.
43	Shear	new	Hoot	Cu	The upper unit of the Lay Range assemblage sediments are strongly sheared and locally silicified. A small amount of malachite staining occurs on fracture surfaces associated with the shearing.
44	Shear and vein	094C 012	Jupiter	Au, Ag, Cu, Pb, Zn	A quartz-carbonate-cemented fault breccia zone hosts Au, Ag, Cu, and Zn mineralization. Another area of quartz and calcite fissure veins is heavily mineralized with sphalerite, tetrahedrite, galena, and minor chalcopyrite, covellite, and pyrrhotite. The main showing has been explored with a 242 m adit with several crosscuts.
45	Porphyry and vein	094C 091	Polaris Cu-Mo	Cu, Mo	Small quartz monzonite bodies intrude pyritized volcanics of the problematic unit. Chalcopyrite and minor molybdenite are hosted in fractures within both lithologies. A reported grab sample assayed 0.234% Cu and 0.004% Mo.
46	Shear and vein	094C 013	Polaris	Au, Ag, Cu, Mo	Small quartz and quartz-calcite veins containing disseminated, banded or blebby pyrite, arsenopyrite and pyrrhotite are hosted by calcareous and cherty black argillite. Assays of more than 100 g/t Au are reported. Also reported are lenses of massive sulphide up to 9 m thick and 30 m long consisting of pyrrhotite with minor pyrite and chalcopyrite. A third zone contains chalcopyrite and molybdenite in fractures in quartz monzonite and pyritized volcanic rock.
47	Unknown	094C 059	Polaris zinc	Zn, Cu	Volcanics tuffs and sediments of the Takla Group are sheared by the Lay Creek fault and reportedly host zinc and copper mineralization. No further information is available on the occurrence.
48	Ultramafic hosted	094C 090	Aiken Lake	Cr, asbestos	The Polaris Ultramafic Complex carries flexible, asbestiform chrysotile and a few minor occurrences of disseminated to banded cronite within serpentinitized seridotite, dunite and pyroxenite intrusions.

49	Unknown	094C 081	Mes	Cu	Pyrite and minor chalcopyrite occur in fractures in the problematic unit volcanics near quartz monzonite intrusions.
50	Carbonate-hosted base and precious metals	094C 074	Rain	Pb, Zn, Ag, Ba	Tan dolomitic zones occur in a grey limestone and Pb-Zn-Ba mineralization occurs in a white crystalline phase of dolomite. Two showings 750 m apart assayed 0.82 % Pb, 3.68 % Zn, 3.4 g/t Ag and 14.5 % Ba and, 4.53 % Pb, 4.2 % Zn, 3.12 g/t Ag and 31.0% Ba respectively. Host lithology is uncertain, but believed to be either Echo Lake group or Mount Kison formation limestone.
51	Vein and shear	new	Ritz	Cu	Interbedded thinly layered brown limestone and phyllite of the Tsaydz Formation of the Ingenika Group are cut by quartz veins, up to 50 cm thick, which contain carbonate and sulphides with malachite staining.
52	Shear and vein	094C 079	Nel	Ag, Cu, Zn, Pb, Au	Galena, tetrahedrite, pyrrargyrite, argentite, chalcopyrite and pyrite have been identified in quartz veins and breccias. Silicification, sericite-pyrite alteration and mineralized strongly leached gouge material are also described at the occurrence which is hosted by quartzites, grits and schists of the Swannell Formation of the Ingenika Group.
53	Carbonate-hosted base and precious metals (replacement)	new	Knoll	Pb, Zn, Ba	Sphalerite, galena and barite mineralization occurs in a rusty sparry dolomite section of the dolomitic and siliceous dolomite breccias of the Echo Lake group.
54	Carbonate-hosted base and precious metals (replacement)	094C 082	Crag	Pb, Zn, Ag, Ba	Fine-grained galena with minor sphalerite and pyrite occurs in a 1m wide dolomitic zone which crosscuts massive white limestone of the Mount Kison formation. A grab sample reportedly assayed 5.0% Pb, 2.8% Zn, 188.6 g/t Ag and 0.48% Ba.
55	Carbonate-hosted base and precious metals (replacement)	new	Sing	Pb, Ba	Coarsely recrystallized limestone in the Echo Lake group hosts coarsely crystalline barite and finely disseminated galena.
56	Carbonate-hosted base and precious metals (replacement)	094C 073	Swan	Pb, Zn, Ag	Scattered lenses of galena and light brown sphalerite are hosted by a tan-weathered cream-coloured band near the top of the massive white limestone unit. The highest reported assay is 0.48% Pb, 1.72% Zn, and 4.11 g/t Ag across 1.5 m.
57	Carbonate-hosted base and precious metals (replacement)	094C 096	Whistler	Zn, Pb	Galena, sphalerite, pyrite and barite occur in coarsely crystalline dolomite within the Otter Lakes group. Two showings occur along a stream cut just below the contact with Big Creek group sediments.
58	Carbonate-hosted base and precious metals (replacement)	094C 033	Gordon	Zn, Pb	Primary and secondary breccias of the Echo Lake group host sphalerite, galena and pyrite as replacements of the dolomite or as disseminations. Barite is also present. A reported chip sample across 2 m assayed 2.6% Pb.
59	Carbonate-hosted base and precious metals (replacement)	new	Upper Osprey	Cu, Zn, Pb?	Primary and secondary breccias of the Echo Lake group have been strongly mineralized by veining and replacement. A large gossanous zone at least 10 m by 20 m contains several zones of massive sulphide each exposed over 10 m by 5 m and greater. Sulphides include pyrite, chalcopyrite, sphalerite, +/- galena and bornite. A second occurrence less than 100 m away, is strongly mineralized with pyrite +/- chalcopyrite and malachite. This appears to be a quartz latite intrusion, pipe-like in shape and about 8 m across.
60	Carbonate-hosted base and precious metals (replacement)	new	Thrust	Cu, Zn	Patchy sphalerite and blebs of chalcopyrite occur in recrystallized dolostone in the middle of the brecciated zone of the End Lake thrust. The thrust places Razorback group on top of dolomite breccias of the Echo Lake group.
61	Carbonate-hosted base and precious metals (replacement)	094C 129	Osprey	Pb, Zn	An 80 m long gossanous outcrop of primary and secondary breccias of the Echo Lake group hosts pervasive sphalerite with higher grade sections found in apparent shear zones. A 2 m chip sample reported 15.8% Zn and 0.34% Pb.
62	Carbonate-hosted base and precious metals (replacement)	094C 031	Molly	Zn, Ag, Pb, Ba	Sphalerite and barite with minor galena, quartz, calcite and pyrite occur as disseminations and in irregular patches replacing the limestone. Locally mineralization appears conformable to bedding. A 4 m chip sample from a trench reportedly assayed 6% Zn, 0.015% Pb and 20 g/t Ag.
63	Carbonate-hosted base and precious metals (replacement)	094C 032	Gwynn	Pb, Ba	Galena with barite and minor quartz are exposed in trenches within the Echo Lake group dolostones.
64	Carbonate-hosted base and precious metals (replacement)	094C 030	Elizabeth	Pb, Zn	Echo Lake group dolostones host sphalerite with minor galena and barite. A reported 15 m trench sample assayed 2% Zn.
65	Carbonate-hosted base and precious metals (replacement)	094C 029	Childhood Dream	Ag, Au, Zn, Pb	Primary and secondary breccias of the Echo Lake group host massive to coarse-grained pyrite with disseminated galena and sphalerite as replacement and breccia infillings. There are two exploration adits, one 5 m and one 10 m long. The best chip sample reportedly assayed 0.34 g/t Au, 24.0 g/t Ag, 2.6% Pb and 11.2% Zn.
66	Carbonate-hosted base and precious metals (replacement)	094C 080	Greg	Zn, Pb	Disseminated sphalerite and galena reportedly occur within blackish limestone, which is mapped as Echo Lake group but may be Otter Lakes group rocks.
67	Carbonate-hosted base and precious metals (replacement)	094C 130	Carie	Pb, Zn, Ag, Ba	The showing is hosted within a dolomitized carbonate breccia (probably primary) of the Echo Lake group, near a fault contact with Big Creek sediments. Disseminated and massive galena, disseminated sphalerite, hydrozincite and smithsonite and locally massive crystalline barite are present.
68	Carbonate-hosted base and precious metals (replacement and stratabound)	094C 024	Par / Weber	Zn, Pb, Au, Ag	The area of the prospect is underlain by the Lower Cambrian Mount Kison formation and the Ordovician to Middle Devonian Razorback, Echo Lake and Otter Lakes groups. Mineralization in variable amounts is found in each of the above mentioned strata. By far the most interesting and prospective mineralization found to date consists of thin lenses of 60-80% sulphide rock intercalated with shales, phyllites and dolomite boudins of the Razorback group.
69	Stratabound carbonate-hosted base metals	094C 103	Critter	Zn, Ba?	Disseminated sphalerite with possible barite found in recrystallized and brecciated sections of light to dark grey dolomite of the Otter Lakes group.

70	Carbonate-hosted base and precious metals and vein/ replacement	094C 023	Bevely	Pb, Zn, Ag, Ba	Disseminated to massive galena, sphalerite, barite and argentiferous galena occur as veins and veinlets, in fractures and shears within the Mount Kison formation of the Aikén Group, the Echo Lake group and possibly the Otter Lakes group in several zones on the Bevely prospect. Mineralization appears to be localized in minor fold flexures and warps on larger scale folds in the area.
71	Veins	094C 104	Quarry	Pb, Zn, Cu, Au, Sb	Recrystallized and dolomitized limestones of the Espee Formation host quartz vein mineralization. Minerals identified in hand samples include sphalerite, galena, cerussite, chalcopyrite, bournonite, malachite, azurite and possibly stibnite. Fire assays on two grab samples from this location returned values of 890 ppb and 385 ppb Au.
72	Vein/ replacement?	094C 038	Regent	Pb, Ag	Massive, argentiferous, crystalline galena occurs in an irregular pod-shaped vein and is hosted in Espee Formation dolomite and limestone (assay: 1575 g/t Ag).
73	Shear-controlled quartz vein	094C 105	Gael	Ag, Au, Cu	Disseminated fine-grained argentite and arsenopyrite are hosted by a shear-controlled quartz vein within the Swannell Formation of the Ingenika Group.

The Polaris Ultramafic Complex is host to minor chromite and chrysotile asbestos mineralization. Chromite at the Aiken Lake showing consists of ball-like masses up to 5 centimetres across, as disseminated grains up to 3 millimetres in diameter and in layers up to 30 centimetres thick with up to 5 per cent chromite. Platinum group elements have been detected by stream sediment sampling around the Polaris Complex but have not been found in outcrop.

CONCLUSIONS

- Mapping in Cassiar rocks of the Aiken Lake area has delineated a sequence of Paleozoic siliciclastics and carbonates very similar to those in the Osilinka River area. Basinal and platformal facies may be present.
- A re-examination of the Lay Range assemblage in its type locality has led to recognition of a lower sedimentary division and an upper mafic tuff division. The dacitic tuff unit (MPlr4) and argillite unit (MPlr3) are now believed to be part of the North American Cassiar Terrane.
- Takla Group volcanics are dominated by tuffs at least 4000 metres or more thick. Coarse volcanoclastic units are subordinate. Abrupt lateral facies variations between the various lithologies are present within the map area.
- A package of rocks east of Lay Creek, originally mapped as Lay Range assemblage, is probably part of the Takla Group.
- Major strike-slip structures cut through the map area and are part of the Lay Range fault system. This fault zone joins fault zones mapped south of the area.
- Mineral occurrences in the map area are dominated by porphyry copper-gold prospects within the Takla Group and at the Hogem-Takla contact, and by carbonate hosted lead-zinc showings in carbonates of the Cassiar Terrane.

ACKNOWLEDGMENTS

We would like to thank Pacific Western Helicopters Ltd., particularly Grant Luck and Jim Reed, for excellent service. Ken Hudson of Omineca Transfer Ltd. is also acknowledged for excellent service and his ability to anticipate our weekly rations. Special thanks also go out to Jim and Sharon Reed, Karen Voll and Dale Scott for making our stay at Aiken Lake one of our most enjoyable summers yet in the

north. Honourable mention goes to Mike Scholz for allowing us to rent his beautiful cabin at Aiken Lake.

Geological concepts in the map area benefited from the input of several people. These include Jim Monger, JoAnne Nelson, Kim Bellefontaine, Bert Struik and Hugh Gabrielse. The donation by Jim Monger of unpublished geologic maps covering much of the Lay Range is greatly appreciated.

REFERENCES

- Armstrong, J.E. (1949): Fort St. James Map Area, Cassiar and Coast Districts, British Columbia; *Geological Survey of Canada*; Memoir 252, 210 pages.
- Bellefontaine, K. (1989): Tectonic Evolution of Upper Proterozoic Ingenika Group, North-central British Columbia (94C/12); in Geological Fieldwork 1988, *B.C. Ministry of Energy, Mines and Petroleum Resources*, Paper 1989-1, pages 221-226.
- Bellefontaine, K. (1990): The Tectonic Evolution of the Ingenika Group and its Implications for the Boundary between the Omineca and Intermontane Belts, North-central British Columbia; unpublished M.Sc. thesis, *McGill University*, 94 pages.
- Craig, D.L. (1991): Geology - Geochemistry of Part Mineral Claim Group; *B.C. Ministry of Energy, Mines and Petroleum Resources*, Assessment Report 21211.
- Ferri, F. and Melville, D.M. (1988): Manson Creek Mapping Project (93N/9); in Geological Fieldwork 1987, *B.C. Ministry of Energy, Mines and Petroleum Resources*, Paper 1988-1, pages 169-180.
- Ferri, F. and Melville, D.M. (1989): Geology of the Germansen Landing Area, British Columbia (93N/10, 1); in Geological Fieldwork 1988, *B.C. Ministry of Energy, Mines and Petroleum Resources*, Paper 1989-1, pages 109-220.
- Ferri, F. and Melville, D.M. (1990a): Geology between Nina Lake and Osilinka River, North-central British Columbia (93N/15, North Half and 94C/2, South Half); in Geological Fieldwork 1989, *B.C. Ministry of Energy, Mines, and Petroleum Resources*, Paper 1990-1, pages 101-114.
- Ferri, F. and Melville, D.M. (1990b): Geology between Nina Lake and Osilinka River, British Columbia, 93N/15 (North Half) and 94C/2 (South Half); *B.C. Ministry of Energy, Mines and Petroleum Resources*, Open File 1990-17.
- Ferri, F. and Melville, D.M. (in preparation): Geology of the Germansen Landing - Manson Creek Area; *B.C. Ministry of Energy, Mines and Petroleum Resources*, Bulletin.
- Ferri, F., Melville, D.M., Malensek, G.A. and Swift, N.R. (1988): Geology of the Manson Lakes Map Sheet, 93N/9; *B.C. Ministry of Energy, Mines and Petroleum Resources*, Open File 1988-12.

- Ferri, F., Melville, D.M. and Arksey, R.L. (1989): Geology of the Germansen Landing Area, 93N/10 and 93N/15; *B.C. Ministry of Energy, Mines and Petroleum Resources*, Open File 1989-12.
- Ferri, F., Dudka, S. and Rees, S. (1992a): Geology of the Uslika Lake Area, Northern Quesnel Trough. B.C. (94C/3, 4, 6); in *Geological Fieldwork 1991*, Grant, B. and Newell, J.M., Editors, *B.C. Ministry of Energy, Mines and Petroleum Resources*, Paper 1992-1, pages 127-146.
- Ferri, F., Dudka, S., Rees, C., Meldrum, D. and Willson, M. (1992b): Geology and Geochemistry of the Uslika Lake Area, British Columbia (94C/3, 4, 6); *B.C. Ministry of Energy, Mines and Petroleum Resources*, Open File 1992-11.
- Gabrielse, H. (1963): McDame Map-area, Cassiar District, British Columbia; *Geological Survey of Canada*, Memoir 319, 138 pages.
- Gabrielse, H. (1975): Geology of Fort Grahame E1/2 Map-area, British Columbia; *Geological Survey of Canada*, Paper 75-33, 28 pages.
- Garnett, J.A. (1978): Geology and Mineral Occurrences of the Southern Hogen Batholith; *B.C. Ministry of Energy, Mines and Petroleum Resources*, Bulletin 70, 75 pages.
- Grextton, P.L. and Roberts, P. (1991): Porphyry Creek Property: 1990 Prospecting, Mapping and Sampling; *B.C. Ministry of Energy, Mines and Petroleum Resources*, Assessment Report 21521.
- Irvine, T.N. (1974): Ultramafic and Gabbroic Rocks in the Aiken Lake and McConnell Creek Map-areas. B.C.; *Geological Survey of Canada*, Paper 1974-1, Part A, pages 149-152.
- Irvine, T.N. (1976): Studies of Cordilleran Gabbroic and Ultramafic Intrusions. B.C.; *Geological Survey of Canada*, Paper 1976-1, Part A, pages 75-81.
- Lay, D. (1931): North-eastern Mineral Survey District (No. 2) in Minister of Mines Annual Report 1930, *B.C. Ministry of Energy, Mines and Petroleum Resources*, page 152.
- Lay, D. (1940): Aiken Lake Area, North-central British Columbia; *B.C. Ministry of Energy, Mines and Petroleum Resources*; Bulletin 1, 32 pages.
- Mansy, J.L. and Gabrielse, H. (1978): Stratigraphy, Terminology and Correlation of Upper Proterozoic Rocks in Omineca and Cassiar Mountains, North-central British Columbia; *Geological Survey of Canada*, Paper 77-19, 17 pages.
- Meade, H.D. (1975): Geology of the Germansen Lake Area; *B.C. Ministry of Energy, Mines and Petroleum Resources*, Preliminary Map 19.
- Monger, J. W. H. (1973): Upper Paleozoic Rocks of the Western Canadian Cordillera; *Geological Survey of Canada*, Paper 73-1 Part A, pages 27-28.
- Monger, J.W.H. (1977): Upper Paleozoic Rocks of the Western Canadian Cordillera and their Bearing on Cordilleran Evolution; *Canadian Journal of Earth Sciences*, Volume 14, pages 1832-1859.
- Monger, J.W.H. and Paterson, I.A. (1974): Upper Paleozoic and Lower Mesozoic Rocks of the Omineca Mountains; *Geological Survey of Canada*, Paper 74-1, Part A, pages 19-20.
- Nelson, J., Bellefontaine, K., Green, K. and MacLean, M. (1991): Regional Geological Mapping near the Mount Milligan Copper-Gold Deposit (93N/1, 93K/16); in *Geological Fieldwork 1990*, *B.C. Ministry of Energy, Mines and Petroleum Resources*, Paper 1991-1, pages 89-110.
- Nelson, J., Bellefontaine, K., Rees, C. and MacLean, M. (1992): Regional Geological Mapping in the Nation Lakes Area, (93N/2E, 93N/7E); in *Geological Fieldwork 1992*, Grant, B. and Newell, J.M., Editors, *B.C. Ministry of Energy, Mines and Petroleum Resources*, Paper 1992-1, pages 103-118.
- Nelson, J., Bellefontaine, K., Mountjoy, K. and MacLean, M. (1993): Geology of the Klawli Lake, Kwanika Creek and Discovery Creek Map Areas, Northern Quesnel Terrane, British Columbia (93N/7W, 11E, 14E); in *Geological Fieldwork 1992*, Grant, B. and Newell J.M., Editors, *B.C. Ministry of Energy, Mines and Petroleum Resources*, Paper 1993-1, this volume.
- Nixon, G.T. (1990): Geology and Precious Metal Potential of Mafic-Ultramafic Rocks in British Columbia: Current Progress; in *Geological Fieldwork 1989*, *B.C. Ministry of Energy, Mines and Petroleum Resources*, Paper 1990-1, pages 353-358.
- Nixon, G.T., Ash, C.H., Connelly, J.N. and Case, G. (1989): Preliminary Geology and Nobel Metal Geochemistry of the Polaris Mafic-Ultramafic Complex; *B.C. Ministry of Energy, Mines and Petroleum Resources*, Open File 1989-17.
- Nixon, G.T., Hammack, J.L., Connelly, J.N., Case, G. and Paterson, W.P.E. (1990a): Geology and Nobel Metal Geochemistry of the Polaris Ultramafic Complex, North-central British Columbia (94C/5, 12); in *Geological Fieldwork 1989*, *B.C. Ministry of Energy, Mines and Petroleum Resources*, Paper 1990-1, pages 387-404.
- Nixon, G.T., Hammack, J.L., Ash, C.H., Connelly, J.N., Case, G., Paterson, W.P.E. and Nuttall, C. (1990b): Geology of the Polaris Ultramafic Complex; *B.C. Ministry of Energy, Mines and Petroleum Resources*, Open File 1990-13.
- Nixon, G.T. and Hammack, J.L. (in preparation): Geology and Platinum-group Element Mineralization of Alaskan-type Ultramafic-Mafic Complexes in British Columbia; *B.C. Ministry of Energy, Mines and Petroleum Resources*, Paper.
- Parrish, R.R. (1976): Structure, Metamorphism and Geochronology of the Northern Wolverine Complex near Chase Mountain, Aiken Lake Map-area, British Columbia; unpublished M.Sc. thesis, *The University of British Columbia*, 89 pages.
- Parrish, R.R. (1979): Geochronology and Tectonics of the Northern Wolverine Complex, British Columbia; *Canadian Journal of Earth Sciences*, Volume 16, pages 1428-1438.
- Roots, E. F. (1954): Geology and Mineral Deposits of Aiken Lake Map-area, British Columbia; *Geological Survey of Canada*, Memoir 274, 246 pages.
- Ross, C.A. and Monger, J.W.H. (1978): Carboniferous and Permian Fusulinaceans from the Omineca Mountains, British Columbia; *Geological Survey of Canada*, Bulletin 267, pages 43-64.
- Wheeler, J.O. and McFeely, P. (1991): Tectonic Assemblage Map of the Canadian Cordillera and adjacent parts of the United States of America; *Geological Survey of Canada*, Map 1712A.
- Zhang, G. and Hynes, A. (1991): Structure of the Takla Group East of the Finlay-Ingenika Fault, McConnell Creek Area, North-central, B.C. (94D/8, 9); in *Geological Fieldwork 1990*, *B.C. Ministry of Energy, Mines and Petroleum Resources*, Paper 1991-1, pages 121-129.
- Zhang, G. and Hynes, A. (1992): Structures Along Finlay-Ingenika Fault, McConnell Creek Area, North-central British Columbia; in *Geological Fieldwork 1991*, Grant, B. and Newell, J.M., Editors, *B.C. Ministry of Energy, Mines and Petroleum Resources*, Paper 1992-1, pages 147-154.

GEOLOGY AND MINERAL OCCURRENCES OF THE MESS LAKE AREA (104G/7W)

By J.M. Logan and J.R. Drobe

KEYWORDS: Regional geology, Mess Creek, Schaft Creek, calcalkaline porphyry, Stikine assemblage, Stuhini Group, Mount Edziza Volcanic Complex.

INTRODUCTION

The Schaft Creek project culminates three years of 1:50 000-scale regional mapping in the Stikine-Iskut rivers area. Current mapping completed the west half of Mess Lake map area (104G/7), in which the large-tonnage Schaft Creek porphyry copper-molybdenum-gold deposit is located (Figure 1-9-1); the east half lies within Mount Edziza Provincial Park. Fieldwork was completed in a 5-week season.

Project objectives include provision of an updated 1:50 000-scale geological map with mineral occurrences and metallogenesis, determination of the timing of mineralization at the Schaft Creek porphyry copper-molybdenum deposit through a U-Pb zircon date, and ultimately a mineral potential map of the area west of Mount Edziza Park. Preliminary accomplishments and geological highlights include the recognition of a Lower Permian calcalkaline volcanic succession and a middle Pennsylvanian basaltic volcanic succession. The age of both packages is indicated by intercalations of fusulinid limestone. The Forrest Kerr

pluton, now known to be as old as Late Devonian (Drobe *et al.*, 1992) was traced to the north edge of the map area. In addition, the thick granite and quartz-bearing conglomerate, interpreted to be Permian by Logan *et al.* (1992a), has been reassigned an Early Jurassic age as originally suggested by Souther (1972).

The map area straddles the physiographic boundary between the rugged Coast Mountains and Tahltan Highlands of the Stikine Plateau. East of Mess Creek, the Tahltan Highlands are dominated by the volcanic shield of Mount Edziza (Souther, 1972). West of Mess Creek, there is a significant increase in topographic relief and the summits are more rugged and underlain by Mesozoic volcanics of the Stuhini Group. Mess Creek, which flows north within a fault-controlled valley, contains tufa deposits and actively discharging hot springs.

REGIONAL GEOLOGY AND PREVIOUS WORK

The map area contains some of the oldest and youngest known rocks of Stikinia. Relatively few intervals are missing from Early Devonian to Recent time. Faults divide the area into four dominant lithotectonic packages. From east to west these are Devonian to Mississippian, Early Permian, Pennsylvanian and older, and Triassic to Jurassic. Volcanic outliers of the Pleistocene and Recent Mount Edziza Volcanic Complex overlie these packages as far west as Mess Creek.

Geology south of the map area is described by Logan *et al.* (1989, 1990a, b, 1992a, b), Logan and Koyanagi (1989) and that to the immediate west by Brown and Gunning (1989a, b) (Figure 1-9-1). Regional studies include 1:250 000-scale mapping of the Telegraph Creek sheet (Souther, 1972) and detailed studies of the Mount Edziza Volcanic Complex (Souther and Symons, 1974; Souther, 1970, 1988).

STRATIGRAPHY

The geology of the Mess Lake area is illustrated in Figure 1-9-2 with only minor simplifications. Figure 1-9-3 summarizes the stratigraphic and structural relationships in two schematic cross-sections across the north and south parts of the map area.

STIKINE ASSEMBLAGE

Monger (1977) defined the Stikine assemblage to include all late Paleozoic rocks peripheral to the Bowser Easin. These rocks form the basement of Stikinia and record its history before and after accretion to the North American continent. The Early Devonian through Carboniferous rocks of the Mess Lake area record more than 100 million years of

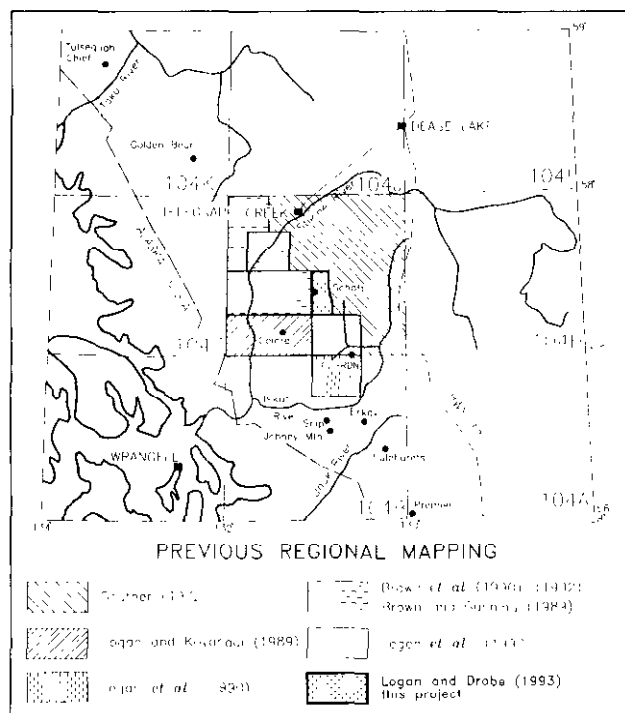


Figure 1-9-1. Location map showing previous and current field areas for Iskut North (Logan *et al.*) and Stikine (Brown *et al.*) projects.

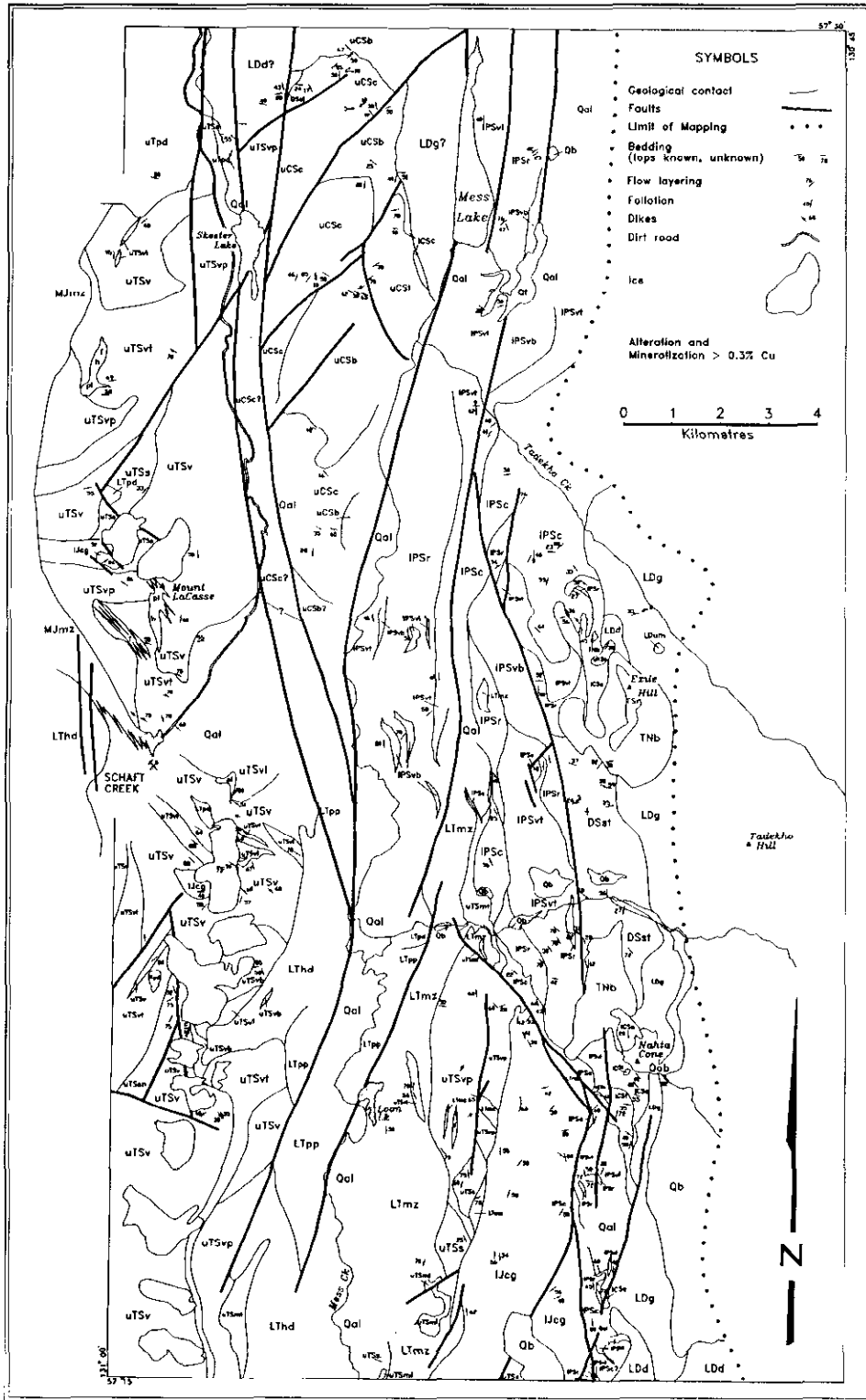


Figure 1-9-2. Simplified geology of the Mess Lake area. See facing page for legend.

LEGEND
LAYERED ROCKS

**QUATERNARY
PEISTOCENE AND RECENT**

Qt hot-spring deposit, tufa

BIG RAVEN FORMATION

Qob olivine basalt, pyroclastic cone and tephra, lava flow

Qal unconsolidated glacial till and poorly sorted alluvium

ARCTIC LAKE FORMATION

Qb olivine-plagioclase-augite basalt, tuff breccia and flow; intra-flow fluvial and glacial deposits

**TERTIARY
PLIOCENE**

SPECTRUM FORMATION

TSr leucocratic peralkaline rhyolite

NIDO FORMATION - KOUNUGU MEMBER

TNb aphyric and olivine-phyric basalt, subaerial flows, intercalated fluvial gravel

UPPER CRETACEOUS TO TERTIARY

uKSe **SUSTUT GROUP**
chert-pebble conglomerate, quartzose sandstone and siltstone

LOWER TO MIDDLE JURASSIC

lJcg cobble to boulder conglomerate and coarse sandstone, quartz-rich, well-bedded;
lower section of quartz-feldspar crystal-lithic tuff

UPPER TRIASSIC

STUHINI GROUP

uTSa well-bedded green dust tuff, tuffaceous siltstone-sandstone turbidites, minor limestone and conglomerate

uTSv augite-phyric, plagioclase-phyric and aphyric basaltic andesite flows and equivalent subvolcanic intrusives

uTSvt massive to weakly stratified, polyolithic lapilli tuff, bedded epiclastics

uTSvp plagioclase-phyric basalt flows and subvolcanic gabbro

uTSmt mafic tuff and lesser flows

STIKINE ASSEMBLAGE

LOWER PERMIAN

IPSc dark grey and buff, medium-bedded to massive fossiliferous carbonate, thin-bedded sections contain intercalated tuff and chert

IPSr flow-layered and spherulitic rhyolite lava; quartz-feldspar-phyric rhyolite lava, autobreccia, ashflow tufts

IPSt feldspar-phyric lapilli and crystal tuff, interbeds of limestone near top

IPSub plagioclase and pyroxene-phyric andesite flows, basalt flows and related breccias

UPPER CARBONIFEROUS

uCSa grey, thin-bedded, fetid and dolomitic limestone, maroon and green lapilli tuff and cherty siltstone

uCSb amygdaloidal green, grey and maroon basalt, aphyric to sparsely plagioclase-phyric

LOWER CARBONIFEROUS

lCSa tuffaceous wacke, siltstone, sandstone and volcanic conglomerate

lCSb grey, medium-bedded to massive, bioclastic limestone; buff dolomitic and ferruginous units

LOWER DEVONIAN

DSst green and red-purple schistose tuff and minor flow, thin interbeds recrystallized grey and buff limestone (DSs)

DSqa chlorite schist, quartz-sericite schist

INTRUSIVE ROCKS

DIKES (a) aphyric andesite and basalt; (pp) mafic plagioclase ± pyroxene porphyry; (f) felsic ± quartz dykes; (h) hornblende; orphyritic diorite; (pl) plagioclase porphyry

MIDDLE JURASSIC

MJmz **YEHINIKO PLUTON**
pink equigranular hornblende-biotite monzonite, monzodiorite

LATE TRIASSIC OR YOUNGER

LTpd medium-grained equigranular augite diorite and gabbro

LTpp grey to green, stubby-plagioclase porphyritic hornblende pyroxene diorite

LTmz salmon-orange crowded plagioclase hornblende monzonite porphyry, trachytic and equigranular phases

LThd **HICKMAN PLUTON**
equigranular, pink and grey, medium-grained hornblende monzonite and diorite

LATE DEVONIAN

LDg **FORREST KERR PLUTON**
biotite granite to tonalite

LDd hornblende diorite, quartz diorite

LDum coarse-grained gabbro, hornblende, clinopyroxene etc.

island arc volcanism and carbonate accumulation interrupted by tectonism and uplift. Calcalkaline volcanism, in part subaerial, was followed by carbonate deposition during the Early Permian interval (Brown *et al.*, 1991).

DEVONIAN OR OLDER (DSst, DSqs)

Penetratively foliated, polydeformed intermediate to mafic volcanic rocks underlie a narrow belt along the eastern margin of the area mapped (Figure 1-9-2). These rocks crop out sparsely between Nahta Cone and Eidle Hill where they are overlain by Tertiary lava flows. Contact relationships with Early Carboniferous and younger rocks are either faulted or hidden beneath overburden. To the east, Early Devonian hornblende diorite and biotite granodiorite (units **LDd** and **LDg**) intrude the volcanic rocks (Figure 1-9-3b).

Purple and green tuffs, aphyric to plagioclase-phyric flows and rare silicified, ankeritic carbonate horizons (**DSst**) are exposed in a west-flowing creek 3 kilometres north of Nahta Cone. Farther north are plagioclase-phyric volcanic rocks, including lapilli ash flow tuff (**DSst**) and intermixed phyllite, chlorite and quartz-sericite schists (**DSqs**). These volcanic rocks are variably foliated and crenulated and distinguished from younger rocks in the map area by their degree of deformation.

LOWER CARBONIFEROUS (lCSa, lCSb)

A distinctive orange-weathering belt of limestone extends southward 7 kilometres from Tadekho Creek to just north of Arctic Lake in the Forrest Kerr map area (Logan *et al.*,

1992a). The belt is split from the southern edge of the map area to Nahta Cone (Figure 1-9-2). Fossils indicate that the eastern branch is Lower Carboniferous and the western Lower Permian (E.W. Bamber, personal communication, 1992). Small patchy outcrops of Lower to mid-Carboniferous limestone (ICSc) can be traced 6 kilometres north from the map border to Nahta Cone, where it rests conformably on medium-grained pink granite of the Late Devonian Forrest Kerr pluton (Figure 1-9-3b). The base of the limestone is limonitic and contains quartz grains and granitic grit, although no basal conglomerate was observed. Elsewhere, the limestone overlies penetratively foliated mafic volcanic rocks, tuff and chlorite and sericite schist of Devonian and older age. The contact relationship is not clear.

At its northmost extent, the limestone is unconformably overlain by Pliocene columnar basalts and Pleistocene and Recent tephra and basalt of Nahta Cone (Plate 1-9-1). Preliminary fossil identifications from the limestone give early mid-Carboniferous (Serpukhovian) ages (E.W. Bamber, personal communication, 1992).

Well-bedded, pale green to khaki greywacke and cherty volcanic siltstone of Unit ICSt overly limestone in apparent conformity south of Nahta Cone and in a small exposure north of Exile Hill (Figure 1-9-3b). Macrofossils collected

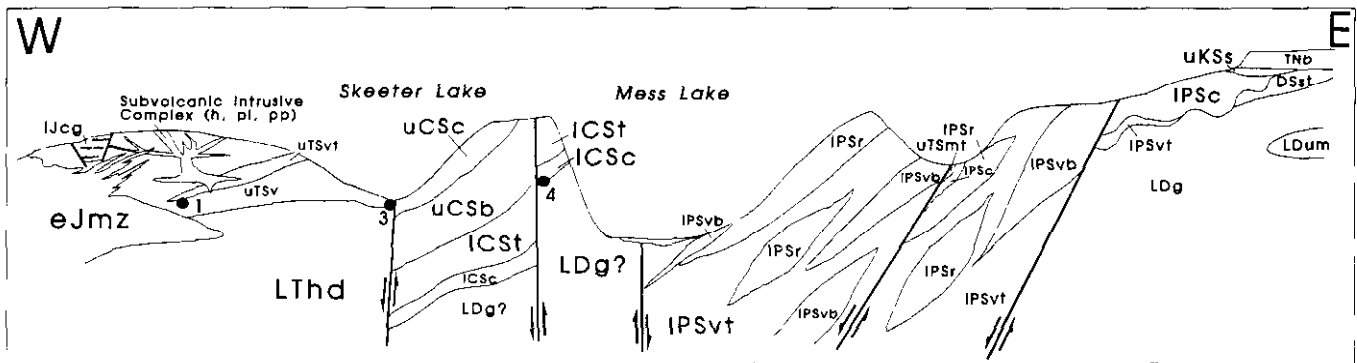
from these sediments are non-diagnostic. West of Mess Creek, similar limestone and volcanoclastics correlate on the basis of lithology and stratigraphy. Fine-grained aphyric lapillistone tuff, ash and dust tuff grading to thinly interbedded sandstone and siltstone of Unit ICSt crop out along the top and extending down the eastern side of the plateau west of Mess Lake. Limestone (ICSc) is interbedded within this volcanoclastic sequence, but the thickest accumulation parallels the top of the Mess Lake pluton. This succession forms the footwall of a faulted contact with Late Carboniferous mafic volcanic rocks.

UPPER CARBONIFEROUS (UCSB, UCSC)

Upper Carboniferous rocks are confined to a narrow, north-trending, high plateau west of Mess Creek, in the northwest corner of the map area between Mess and Skeeter lakes (Figure 1-9-2). They are separated from Upper Triassic rocks to the west and Lower Permian rocks to the east by northerly trending regional faults.

A succession consisting of polydeformed, structurally thickened limestone, chert and siliceous tuff (uCSc) is exposed east of Skeeter Lake and extends to the top of the plateau. It structurally overlies a lower package of massive, amygdaloidal basalt flows and tuffs (uCSb) (Figure 1-9-3a). These rocks are in fault contact with Lower Car-

- A -



- B -

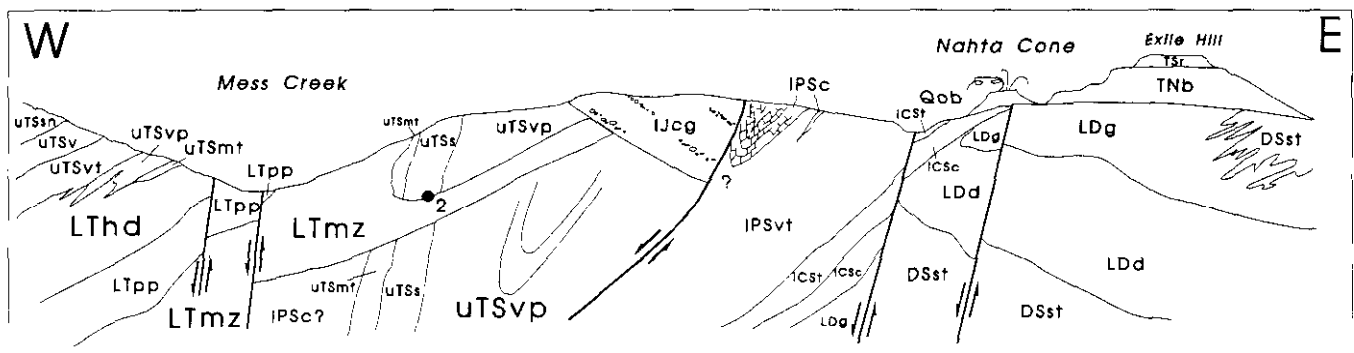


Figure 1-9-3. Schematic representation showing stratigraphic relationships of the various units across the northern (3a) and southern (3b) part of the Mess Lake field area. Mineral occurrences are shown in their respective stratigraphic positions. See text and Figure 1-9-2 for description of units. Numbers correspond to mineral occurrences; 1 = Schaft Creek; 2 = Run, Mix, Run North; 3 = BB 38 and 57; 4 = Cot & Bull.



Plate 1-9-1. Tufa terraces east of Mess Creek, near the south end of Mess Lake.

boniferous volcanic wacke, tuff and limestone. The upper unit of limestone, tuff and cherty sediments has accommodated much of the deformation. At the top of the volcanic package are maroon basaltic tuff and interbedded limestone containing Pennsylvanian (Kasimovian to Gzhelian) fusulinacean foraminifers (E.W. Bamber, personal communication, 1992).

LOWER PERMIAN (IPSvb, IPSvt, IPSr, IPSc)

Lower Permian rocks underlie a fault-repeated, north-trending belt 4 to 5 kilometres wide east of Mess Creek and extending south to the boundary of the map (Figure 1-9-2). Medium-bedded Lower Permian packstones form the uppermost unit and are underlain in depositional conformity by a characteristically maroon, in part subaerial, calc-alkaline volcanic succession (Figure 1-9-3a, b). Interbedded limestone horizons containing abundant Wolfcampian fusulinacean foraminifers crop out near the top of the volcanic package (E.W. Bamber, personal communication, 1992).

A moderately west-dipping, fault-duplicated section of Lower Permian volcanics is exposed 3 kilometres west of Exile Hill. The western section is 200 metres thick and forms a dip slope down to Mess Creek. Aphyric purple and green amygdaloidal basalt, plagioclase and pyroxene-phyric andesite breccia flows and associated volcanoclastics form what appears to be the lowest unit (IPSvb), but also occur at various levels within this section (Figure 1-9-3a). Well-

bedded, feldspar-phyric intermediate and felsic tuffs and epiclastic rocks comprise the characteristically pale maroon weathering medial unit (IPSvt). Interbedded quartz-bearing polyolithic epiclastic rocks and rare accretionary lapilli tuffs and ash-flow tuffs record contemporaneous submarine and subaerial depositional environments. The uppermost volcanic unit (IPSr) consists of mauve to brown flow-layered and spherulitic rhyolite, quartz-feldspar-phyric rhyolite flows, autobreccia and ash-flow tuffs. These felsic rocks are resistant and form most of the prominent ridges and the dip slope east of Mess Creek.

Medium-bedded to massive Lower Permian packstone (IPSc) forms prominent knobs and discontinuous ridges extending as far north as Tadekko Creek. It overlies epiclastic rocks of Unit IPSvt and flow layered rhyolite of Unit IPSr, in apparent conformity. 6 kilometres south and 2 kilometres northwest of Nahta Cone, respectively. Thin-bedded limestone contains an abundant Lower Permian fauna of rugose and tabulate corals, productoid brachiopods, pelecypods, bryozoa and fusulinacean foraminifers.

UPPER TRIASSIC STUHINI GROUP (uTSmt, uTSvp, uTSvt, uTSv, uTSs)

Volcanic rocks of the Stuhini Group underlie Mount La-Casse and most of the rugged mountainous area west of Mess Creek. They also crop out in a narrow north-trending belt east of Mess Creek, where they are less well exposed

(Figure 1-9-2). They lie unconformably on Lower Permian limestone 3 kilometres northwest of Nahta Cone. They are unconformably overlain by Lower Jurassic conglomerate southwest of Nahta Cone and in two localities west of Mess Creek (Figure 1-9-3a, b). They are truncated on both east and west sides by several large intrusions.

West of Mess Creek, Upper Triassic rocks are divided into five volcanic and one sedimentary unit (Figure 1-9-3b). The lowermost unit is green-blue, recessive weathering, mafic lapilli tuff with minor flows (**uTSmt**). The scoriaceous lapilli are altered to serpentine, talc and chlorite. East of Mess Creek, Unit **uTSmt** overlies Lower Permian carbonate of Unit **IPSc** in two areas; the contact in one is partly faulted. Volcanic rocks of Unit **uTSvp** were not observed to directly overlie Unit **uTSmt**, but they usually crop out nearby. Dark grey, massive, plagioclase-phyric basalt flows and related similarly textured intrusive rocks crop out south of the Schaft Creek porphyry copper deposit. Contacts with other units are poorly exposed, except where Unit **uTSvp** is intruded by Unit **LThd**. Tuffs of Unit **uTSvt** were observed to overlie these basaltic rocks in only one place. Unit **uTSvt** comprises massive to weakly stratified, polyolithic, grey to mauve lapilli tuff and crystal tuff that form thick sections underlying the east-facing slope above Mess Creek. Both plagioclase and augite crystals are common, although augite is generally less than 5 per cent of the rock. Measurable bedding attitudes are rare; the few measured indicate steep dips. The thickest Upper Triassic unit comprises augite-phyric, plagioclase-phyric, augite and plagioclase-phyric, and aphyric basaltic andesite flows (**uTSv**). It extends the full length of the western edge of the map area and hosts the Schaft Creek deposit. Subvolcanic intrusive rocks are difficult to distinguish and separate from the extrusive rocks and are included with them. Tuffs and flows occur subequally and vary in colour from maroon to green; it is common for purple tuff to be interbedded with green tuff. The basaltic andesite is pillowed for 3 kilometres both northeast and southeast of Schaft Creek. All bedding attitudes of intercalated tuffs observed were steeply inclined to the northeast and southwest. Locally the unit is very likely tightly folded, but the lack of good stratification makes the extent of this difficult to ascertain. Unit **uTSs** comprises about 150 metres of well-bedded green dust tuff, tuffaceous siltstone-sandstone and wackes which crop out on the eastern flank of Mount LaCasse, 4 kilometres northeast of the Schaft Creek deposit. Near its western margin, the well-bedded section thins considerably where it is faulted against Unit **uTSv**. The tuffs also apparently thin to the northeast, limiting their usefulness as a marker unit. Steeply dipping, tightly folded sediments consisting of volcanic conglomerate, interbedded sandstone and siltstone, pyroxene crystal sandstone and limy siltstone (Unit **uTSs**) are exposed about 4 kilometres south of the Schaft Creek deposit. A thin maroon quartz and limestone-bearing volcanoclastic unit (possibly Unit **IJcg**) may overlie these sediments conformably but is faulted against pyroxene-phyric volcanics of Unit **uTSv** farther east. Fossils from thin interbedded siltstone, sandstone and conglomerate are identified as Upper Triassic (Norian; E.T. Tozer, personal communication, 1992).

East of Mess Creek, Upper Triassic rocks are limited to units **uTSmt**, **uTSvp** and **uTSs** (Figure 1-9-3b). Unit **uTSmt** is highly visible in creek exposures where alteration and weathering have produced characteristic dun to bluish green hues. It is intruded along its western limit by the Loon Lake stock (Unit **LTmz**) and may be overlain by silicified dust tuff and turbiditic siltstone of Unit **uTSs**, as it is west of Mess Creek on the More Creek sheet (Logan *et al.*, 1992a, b). Massive tuffs and flows of Unit **uTSvp** include associated subvolcanic intrusive rocks which could not be mapped separately. Both are predominantly plagioclase-phyric with lesser pyroxene. Pillowed and breccia flow textures occur locally in the massive sequence of plagioclase-phyric basaltic andesite. The unit is unconformably overlain by Lower Jurassic conglomerate.

LOWER TO MIDDLE JURASSIC (**IJcg**)

West of Mess Creek, Lower to Middle Jurassic rocks rest with angular unconformity on volcanics of the Upper Triassic Stuhini Group (Figure 1-9-2). East of the Schaft Creek porphyry deposit, on Mount LaCasse, the Jurassic unit comprises conglomerate with equal proportions of well-rounded crowded plagioclase porphyritic andesite and aphyric basalt clasts, interbedded with coarse sandstone containing high proportions of quartz and potassium feldspar. The conglomerate overlies propylitically altered pyroxene volcanics. The nature of the contact is uncertain, but the conglomerate appears to occupy a fault-bounded graben (Figure 1-9-3a). The conglomerate itself is pervasively epidotized (due in part to its permeability). Alteration is probably related to dike swarms associated with the Middle Jurassic Yehiniko pluton.

Moderately south-dipping Jurassic conglomerates rest unconformably on steeply dipping Upper Triassic pyroxene-phyric flows and volcanoclastics in a second exposure 3 kilometres south of the Schaft Creek deposit (Figure 1-9-2). The section comprises 90 metres of quartz-bearing polymictic volcanic conglomerate above a lower quartz and feldspar crystal tuff layer 20 metres thick. The sediments are well-bedded granule or weakly stratified to massive boulder conglomerates and lesser sandstones. Clasts are generally subangular, purple, maroon and green plagioclase and/or pyroxene-phyric andesite. Epidotized clasts are common and clasts of quartz feldspar crystal tuffs increase in abundance down section. The volcanic lower zone is a pale maroon, pink-weathering feldspar and quartz-eye crystal-lapilli tuff. Upper and lower contacts are gradational and therefore conformable with the conglomerate.

East of Mess Creek, the conglomerates outcrop in a belt 2 to 2.5 kilometres wide extending north from Arctic Lake to Nahta Cone (Figure 1-9-2). At the northern end of this exposure, they overlie volcanic rocks of the Stuhini Group with structural conformity, but farther south they unconformably overlie Late Triassic plagioclase hornblende porphyritic diorite (**LTmz**). The conglomerate is at least 250 metres thick. In general, the lowermost sections are maroon, well-bedded, immature, volcanic-derived conglomerate. In places they are graded and consist entirely of maroon plagioclase-phyric andesite clasts in a plagioclase-rich

groundmass. Up section, quartz and potassium feldspar grains and granite clasts appear then increase in abundance. Layers of coarse carbonate boulders are prominent within the unit. The 4 to 5-metre well-rounded boulders are Mesozoic reefoid limestone. Rare interbedded limestone and sandstone lenses have been sampled for radiolaria.

UPPER CRETACEOUS TO TERTIARY SUSTUT GROUP

Small isolated remnants of Sustut Group sediments (Unit **uKs**) are preserved on Exile Hill and north of Nagha Creek (Souther, 1988). On Exile Hill, they are well-bedded, pale green weathering and friable quartzose sandstone and poly-lithic chert-granule conglomerate that rest unconformably on Late Devonian diorite of Unit **LDd** (Figures 1-9-2 and 1-9-3a). The sediments are limonitic, and thoroughly fractured and veined by calcite. Granitic, aphyric volcanic, chert and quartz clasts comprise roughly equal proportions of the granule conglomerate.

PLIOCENE – NIDO (TNb) AND SPECTRUM (TSr) FORMATIONS

Subaerial flows of aphyric and olivine-phyric basalt with intercalated fluvial gravel of the Nido Formation (**TNb**) and peralkaline rhyolite flows of the Spectrum Formation (**TSr**) underlie the Arctic Lake plateau and Quaternary members of the Mount Edziza Volcanic Complex on the eastern border of the map area (Figure 1-9-2). These Pliocene rocks were not specifically examined because they were mapped by Souther (1988) at a scale of 1:50 000. The Nido Formation unconformably overlies Paleozoic carbonate, intrusive and volcanic rocks and also Upper Cretaceous sedimentary rocks (Figure 1-9-3a, b). It is overlain by the Spectrum Formation. Flows in both formations are essentially flat lying. At one locality, an intraflow cobble conglomerate is exposed between flows of the Nido Formation.

QUATERNARY

ARCTIC LAKE FORMATION (Qb)

Basalt flows of the Arctic Lake Formation (**Qb**) form erosional outliers east of Mess Creek (Figure 1-9-2). Most are exposed at elevations above 1000 metres (3500 feet), but one flow crops out on the floor of Mess Creek valley. A whole rock K-Ar date of 0.45 ± 0.07 Ma was obtained from flows at the head of More Creek. Unit **Qb** is characterized by flat to gently inclined, brown to grey weathering, thick, usually vesicular beds of plagioclase, augite and olivine-phyric basalt.

BIG RAVEN FORMATION (Qob)

The youngest consolidated unit in the map area consists of olivine basalt flows of the Big Raven Formation (Unit **Qob**) which form Nahta Cone (Figures 1-9-2 and 1-9-3b). The cone is approximately 70 metres high and consists mainly of black and brick-red scoria blocks. Nahta Cone was breached on its east side and at least two highly fluid lavas flowed to the north along a drainage where they are still preserved. Levees of flow breccia mark the path of the

flows down the creek. The cones are situated on the contact between Lower Devonian volcanic rocks of Unit **ICSt** and granitic rocks of Unit **LDg**. A V-shaped apron of lapilli-sized tephra covers these units for a distance of about 700 metres north and 500 metres west of the main cone. The apron provides evidence that the cone erupted on two occasions with differing wind directions. Souther (1970) carbon dated the flows at 1340 years b.p.

HOTSPRING DEPOSITS (Qt)

Hot spring deposits of tufa (Unit **Qt**) occupy an elongate area of about 50 hectares southeast of Mess Lake (Plate 1-9-1). The hot springs are located along north-trending faults. They are discharging and depositing tufa into a connected series of poorly drained flat-bottomed valleys. Water percolating in the active springs is below body temperature. Most of the deposits are of the low-rill, terraced type, but six small circular cones 1 to 4 metres high and a hill of travertine up to 10 metres high are also present. Many of the tufa terraces have raised pressure ridges presumably reflecting recent fault movement. The ridges have relief on the order of 10 to 40 centimetres and lengths on the order of 50 to 100 metres. According to a local trapper, new ridges appear each year, suggesting the faults are still active.

INTRUSIVE ROCKS

Three intrusive episodes are recognized in the Mess Lake area: Late Devonian, Late Triassic or younger, and Middle Jurassic. These correspond in part with episodes described by Anderson and Bevier, (1990); Holbek (1983) and Logan *et al.*, (1990a, 1992a).

LATE DEVONIAN

Tonalite, granodiorite, diorite and hornblende diorite crop out along the eastern margin of the map area (Figure 1-9-2). These rocks are the northward extension of the Late Devonian Forrest Kerr pluton that is exposed around Arctic Lake in the More Creek map area (Logan *et al.*, 1992b). Outcrop of the intrusion extends north as far as Talekho Creek, where the pluton is covered by Lower Carboniferous and Lower Permian limestone and volcanic rocks and Tertiary lava flows. Tertiary and Recent lava flows also cover the eastern edge of the pluton. Along the western edge, it is faulted against Lower Permian volcanic rocks and is locally unconformably overlain by Lower Carboniferous carbonate (Figure 1-9-3b).

As to the south (Logan *et al.*, 1990a, 1992a), the pluton comprises three phases: a granitic phase of coarse-grained biotite tonalite, granite and granodiorite (**LDg**), chloritized hornblende diorite (**LDd**) and minor hornblende/gabbro (**LDum**). Most of the rock has an equigranular texture. Weakly foliated and passively folded gneissic textures occur close to intrusive contacts and phase boundaries within the intrusion. The pluton intrudes penetratively foliated, schistose metatuffs of Unit **DSst**.

Pink, coarse-grained, equigranular granite west of Mess Lake resembles rocks of the Forrest Kerr pluton, but has an unclear relationship with overlying carbonate of probable Early Carboniferous age. The Mess Lake body crops out

only on the east side of the ridge between Skeeter and Mess lakes and, therefore, presumably has a moderate to steep westerly dip (Figure 1-9-2 and 1-9-3a). The granite, limestone and tuffaceous wacke (**ICSc** and **ICSt**) are cut by a north-trending west-dipping diorite dike swarm. From a distance this gives the cliffs a bedded appearance. The contact between the intrusive and the limestone strikes north-northwest and dips moderately southwest.

LATE TRIASSIC OR YOUNGER

HICKMAN PLUTON

A medium to fine-grained, pink or grey elongate stock of monzonite to diorite (**LTHd**) is exposed 10 kilometres south of the Schaft Creek deposit (Figure 1-9-2). It crops out on the east-facing slope above Mess Creek and is probably an eastern extension of the Hickman pluton. Along its western margin numerous aplitic dikes extend from the main stock into Upper Triassic volcanic rocks of the Stuhini Group (Unit **uTSv**). The eastern contact is more problematic. The stock is monzonite near the top (i.e., western margin) where it intrudes Upper Triassic rocks, but grades eastward and downward into hornblende diorite, commonly with occurrences of dark grey hornblende. To the north, it appears to be faulted against grey plagioclase-porphyrific diorite of unknown age. It is possible that the plagioclase porphyry is a border phase of the equigranular stock or plagioclase porphyry of Unit **LTmz**.

The monzonite portion of the stock is pink and equigranular with up to 15 per cent oxidized hornblende. Where the percentage of hornblende is higher, pink, fine-grained, equigranular dikes to about 30 centimetres wide are common. The mafic content of the stock increases until the rock is fine to coarse-grained hornblende, with hornblende crystals up to a centimetre in length. The crystals are mostly weakly chloritized, though vitreous hornblende is present. Narrow carbonate-epidote and zeolite veinlets are a common alteration feature.

UNIT **LTmz** – LOON LAKE STOCK

A north-trending hypabyssal stock of plagioclase hornblende monzonite porphyry (**LTmz**) forms the eastern slope above Mess Creek (Figure 1-9-2). On its eastern side it intrudes Upper Triassic sediments and volcanic rocks of Units **uTSvp** and **uTSs** and, farther north, Lower Permian rocks. The intrusion is unconformably overlain by Lower Jurassic conglomerate of Unit **IJcg** in a creek exposure, about 1.5 kilometres north of the south boundary of the map sheet. The western limit of the Loon Lake stock appears to be faulted against intrusive Unit **LTpp** but the contact may be in part intrusive (Figure 1-9-3b).

The typical texture of the Loon Lake stock is crowded porphyry with 20 to 40 per cent euhedral plagioclase laths to 7 millimetres in length and 0 to 10 per cent hornblende to 3 millimetres in length. The rock is mostly salmon pink to mauve grey. Common variations in the texture include darker grey, less crowded plagioclase porphyry and fine to medium-grained, equigranular grey diorite.

UNIT **LTpp**

Hypabyssal plagioclase diorite, not unlike the monzonitic Loon Lake stock, crops out along the lower slopes of Mess Creek valley, west of the creek between the Loon Lake stock and intrusive unit **LTHd** (Figure 1-9-2). It was mapped as a separate body, but may be a border phase or related to the Loon Lake stock. The diorite is typically pale green and contains stubby plagioclase phenocrysts to 4 millimetres in length and rare chloritic hornblende or pyroxene.

UNIT **LTpd**

Plugs of pyroxene diorite crop out in several areas west of Mess Creek (Figure 1-9-2). About 5 kilometres south of the Schaft Creek deposit, a small plug intrudes Upper Triassic sediments. About 2 kilometres south of the deposit, and also about 5 kilometres north of the deposit, similar plugs intrude Upper Triassic volcanic rocks. A similar, larger stock intrudes Upper Triassic volcanic rocks in the north-west corner of the map area.

The plugs are mainly medium-grained, green-grey augite plagioclase diorite. They are generally associated with plagioclase-phyric and coarse pyroxene-phyric dikes and are probably related to them.

YEHINIKO PLUTON (**MJmz**)

Middle Jurassic monzonite of the Yehiniko pluton intrudes volcanic rocks of the Stuhini Group east of Schaft Creek and north of the Schaft Creek deposit. Most of the contact is gradational and consists of numerous aplite and/or rhyolite apophyses in the country rock (Figures 1-9-2 and 1-9-3a). In places the contact is a simple curvilinear surface. Several small outcrops of the intrusion on the north edge of the Schaft Creek deposit are mineralized together with adjacent volcanic rocks. The southern contact with the Late Triassic Hickman batholith is covered by overburden.

The main phase of the Yehiniko pluton is pink, medium to coarse-grained biotite granite (Brown and Gunning, 1989a). Near its contacts with Upper Triassic volcanic rocks, the texture is finer, more fractured and the colour is grey to orange. Within the Schaft Creek deposit, the intrusion is white, argillically altered, equigranular monzonite to quartz monzonite. North of the deposit, the apophyses of the intrusion are aphanitic to fine-grained, flow-layered pink rhyolite dikes and sills of quartz-eye feldspar porphyry that are possibly younger. These alter the country rock locally.

DIKES

West of Mess Creek, at least four distinct dike and/or sill suites are recognized within the Upper Triassic Stuhini Group. Most are 1 to 10 metres wide. Plagioclase-phyric dikes (**pl**) are the most common. They typically have 5 to 10 per cent opaque, pale green plagioclase crystals averaging 2 to 6 millimetres in length. Pyroxene diorite dikes (**pp**) have textures very similar to those of extrusive rocks within the Stuhini Group and are probably in part coeval with them. In the larger dikes, plagioclase averages 2 to 4 millimetres, augite 5 to 10 millimetres, and the groundmass is finely

crystalline rather than aphanitic, as it is in the equivalent extrusive rocks. Hornblende-porphyrific diorite (**h**) is less common and forms irregular bodies (plugs or small dike/sill complexes), mainly north of the Schaft Creek deposit. Vitreous hornblende to 10 per cent and averaging 3 to 10 millimetres long forms glomerocrysts in a grey, aphyric vitreous or sparsely feldspar-phyric groundmass. The age relationships of these dikes is not known. The felsic aphyric and quartz-feldspar-phyric apophyses (**f**) of the Yehiniko pluton cut them. The youngest dikes are aphyric andesite and basalt. These are typically green to grey in colour, average less than 3 metres wide, and are commonly amygdaloidal near the margins. They postdate mineralization at the Schaft Creek deposit.

STRUCTURE

FOLDS

Lower Devonian rocks of Unit **DSst** are penetratively foliated and schistose. The foliation dips gently to the west and is folded isoclinally about northwest-trending axes. Folds are typically recumbent and northeast verging. Macrofolds are overprinted by nonpenetrative and penetrative crenulation folds on millimetre and centimetre scales respectively; related crenulation cleavage is present.

Lower Carboniferous carbonate rocks (**ICSc**) east of Mess Creek, which unconformably overlie Units **LDg** and **DSst**, are unaffected by this penetrative deformation. The rocks are deformed into open gentle folds on a scale of hundreds of metres. The folds are the only deformation recognized in the carbonates and may reflect movement in the underlying rocks.

The same fold geometry and relationships of Lower Devonian rocks are seen in Upper Carboniferous rocks underlying the plateau between Skeeter and Mess lakes. Foliated, thin-bedded tuffs and carbonates display recumbent isoclinal and tight parallel folds in cliff exposures on both sides of the plateau. Most folds have amplitudes on a scale of several metres. Fold axes plunge gently either northwest or southeast, and vergence appears to be to the northeast. Schistose and slaty beds also have millimetre and centimetre-scale crenulation folds. The massive basalt of Unit **uCSb** is weakly foliated but shows no evidence of folding.

The poor correlation between stratigraphic position and deformation suggests strata forming the ridge between Skeeter and Mess lakes have undergone a localized deformational event, possibly related to unrecognized thrust faulting.

Lower Permian volcanic rocks and carbonates east of Mess Creek are homoclinal; minor deviations in attitude are due to brittle faulting and disruption by intrusion of the Loon Lake stock. On the south slope of Tadekho Creek, the carbonate is involved in some large open folds. It is also drag folded adjacent to a minor north-trending fault about 4 kilometres southwest of Exile Hill. The most extensive deformation is adjacent to a well-exposed listric fault that places Lower Jurassic conglomerate against Lower Permian

limestone. Approaching the fault from the east, bedding dips in the carbonate steepen from west to vertical, and become east dipping adjacent to the fault. The east-dipping beds are either overturned or the carbonate is tightly folded into an upright syncline in which the closure is not exposed.

Upper Triassic rocks east of Mess Creek have steep westerly dips. Most of the variation in attitudes in these rocks is probably caused by intrusion by the Loon Lake stock. Exposure is too poor to recognize large-scale folds; minor folds were observed in a small creek about 7 kilometres southwest of Nahta Cone. West of Mess Creek, Upper Triassic rocks dip steeply to the southwest and northeast, suggesting tight folding. The paucity of bedding attitudes in much of the section hinders recognition of folding. Tight noncylindrical folds do occur in well-bedded sandstone of Unit **uTSsn**. Well-bedded tuffs of Unit **uTSs** are drag folded into a shallow, open anticline against a normal fault, 5 kilometres north of the Schaft Creek deposit.

FAULTS

Curvilinear north-trending faults are the most significant structures in the Mess Lake area. They control topography and affect the distribution of nearly all rock units. Northeast-trending splays cut the ridge between Skeeter and Mess Lake valleys.

Movement along the faults took place during at least two separate episodes. The first episode of normal faulting uplifted rocks east of Mess Creek and Skeeter Lake relative to rocks to the west. The second episode had an opposite sense of displacement and uplifted rocks west of Mess Creek and Skeeter Lake relative to rocks to the east. The first episode brought Devonian rocks to the surface in Eocene time. Most of the movement was along faults presently located in Mess Creek and Skeeter Lake valleys. However, rocks as young as Early Jurassic were preserved in a listric fault block east of Loon Lake. The trace of the listric fault is well exposed and can be traced along the edge of the Arctic Lake plateau from just south of Nahta Cone to west of Arctic Lake in the More Creek map area. The fault juxtaposes a tilted block of east-dipping conglomerate of Unit **IJcg** and west-dipping volcanic, sedimentary and intrusive rocks of Units **uTSvp**, **uTSs** and **LTm** against west-dipping Lower Permian carbonate of Unit **IPSc**. A maroon, quartz-bearing fragmental unit is exposed along the entire length of the fault and appears to underlie Unit **IPSc**. We believe that the fragmental unit may be fault breccia (i.e., milled Unit **IJcg**).

The second episode of faulting uplifted rocks west of Mess Creek and Skeeter Lake along faults mainly to the east of the creek. The uplift was young enough to affect the distribution of Eocene and younger rocks to the east, and to cause the dramatic difference in topography across Mess Creek. East of Mess Creek, west-side-up faults repeat Lower Permian stratigraphy south of Tadekho Creek. Evidence of the sense of movement along these faults is found in a minor creek 4 kilometres southwest of Exile Hill, where drag folds in Unit **IPSc** clearly indicate west-side-up movement along a minor north-trending structure (Plate 19-2).

MINERAL PROPERTIES

The locations of mineral properties are shown in Figure 1-9-4. Their stratigraphic positions are shown in Figure 1-9-3 and details are summarized in Table 1-9-1.

SCHAFT CREEK PORPHYRY DEPOSIT

The Schaft Creek porphyry copper-molybdenum deposit is situated at the western edge of the map area, at an elevation of 1000 metres on the west-facing slope above Schaft Creek (Figures 1-9-1 and 1-9-4; Plate 1-9-3). Since its discovery in 1957, successive drill programs by Silver Standard Mines Ltd., American Smelting and Refining Company, Hecla Mining Company and Teck Corporation, the present owner, tested the property. The deposit is classified as a high-level calcalkaline volcanic porphyry (Linder, 1975; Fox *et al.*, 1976). It consists of a linear intrusive tourmaline breccia pipe, the Breccia zone, and the Main zone, a fracture-controlled zone of mineralization. Both are hosted in andesite flows and epiclastic rocks. Mineralization includes pyrite, chalcopyrite, bornite and molybdenite. Reserves are 910 million tonnes grading 0.3 per cent copper, 0.03 per cent molybdenum, 0.113 gram per tonne gold and 0.992 gram per tonne silver (Melville *et al.*, 1992).

The geology of the deposit is complicated and poorly exposed. Our visit consisted of one day looking at drill core and one day mapping drill roads and outcrops along the

eastern edge of the deposit. Regional mapping traced the stratigraphy along ridges from the north and south into the deposit area. The following discussion presents our observations but the reader is directed to Linder (1975) and Fox *et al.* (1976) for discussions of the genesis, stratigraphy and mineralogy of the deposit.

Our observations of the Upper Triassic stratigraphy in the area of the deposit agree with observations of Fox *et al.* (1976). They note that 90 per cent of the deposit is in plagioclase-phyric and aphyric basalt flows and associated subvolcanic intrusions (**uTSvp**), massive tuffs, and bedded green and purple epiclastics (**uTSvt**). The epiclastic rocks are overlain by weakly mineralized mixed purple and green flow breccias and tuffs of units **uTSvt** and **uTSv**. Dike swarms of plagioclase porphyry, pyroxene plagioclase porphyritic diorite, felsite (aplite and quartz-eye feldspar porphyry) and hornblende porphyry, in order of abundance, cut the Upper Triassic volcanic rocks (Figure 1-9-3a). The felsic intrusives are bleached, altered and mineralized with disseminated and fracture-controlled sulphides.

No simple lithologic or stratigraphic difference was recognized between the purple volcanics and the mineralized green andesitic volcanics distinguished by earlier workers. The colour difference may reflect proximity to the intrusive and the centre of alteration and mineralization. Epidote clasts, originally probably mafic pumice fragments that have been completely replaced by epidote, and volcanic and

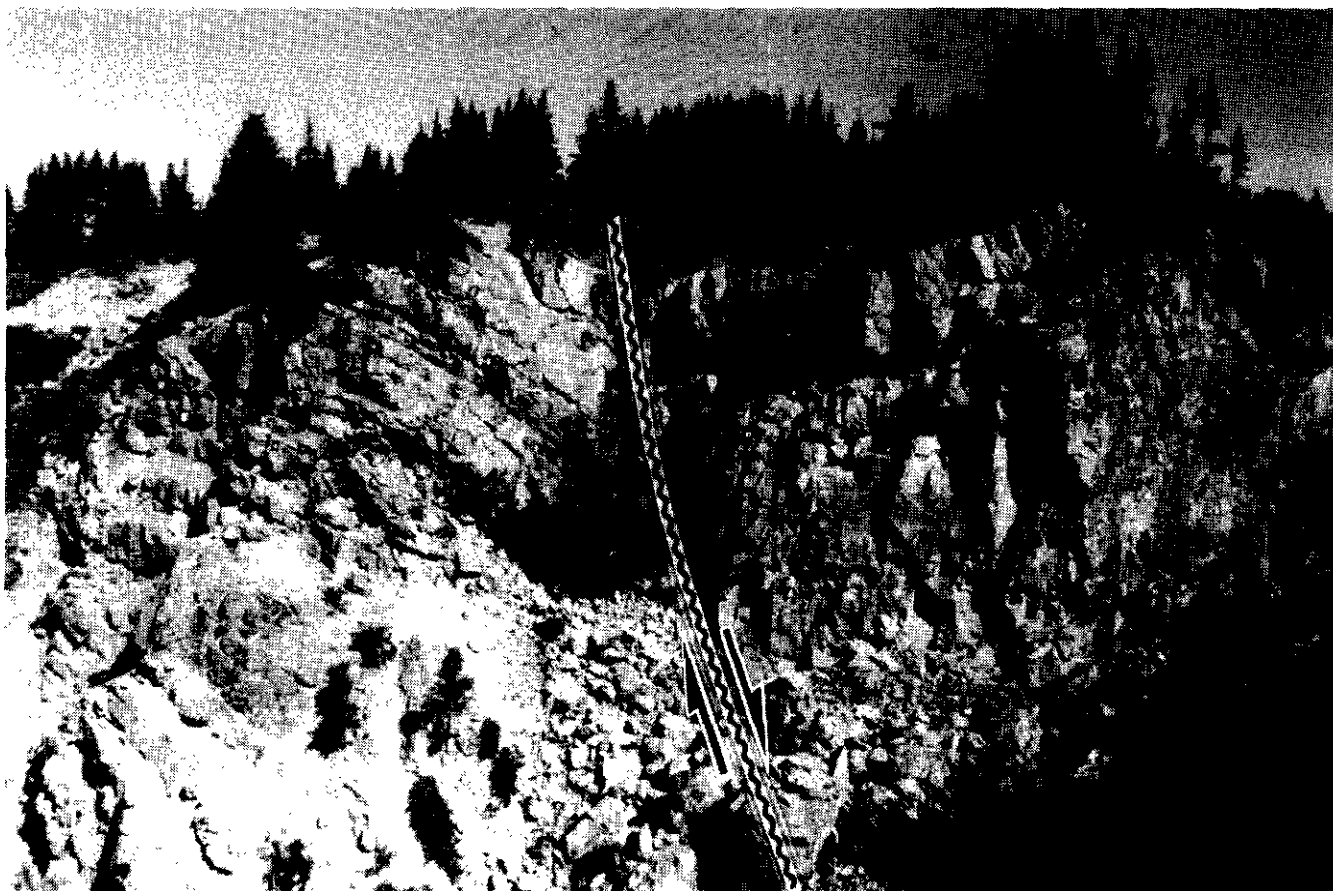


Plate 1-9-2. Drag folds in Lower Permian limestone of Unit IPSc indicating west-side-up movement along a north-trending fault east of Mess Creek. View is to the north.

TABLE 1-9-1
MINERAL OCCURRENCES FOR THE MESS CREEK MAP AREA (104G/07W)

TYPE/ PROB. AGE	MINFILE 104G	NAME	HOST	COMMODITY	DESCRIPTION	REFERENCE
GOLD-COPPER PORPHYRY						
Late Triassic - Middle Jurassic ?	015	SCHAFT CREEK	uTSvp, uTSvt LTmz	Cu, Mo, Au, Ag	Disseminated and fracture-controlled chalcopyrite, molybdenite, gold and silver mineralization is related to a high-level intrusive complex of felsic to intermediate dike swarms and a breccia pipe. Mineralization is discordant to volcanic stratigraphy. Unclassified reserves of 510 million tonnes grading 0.3% Cu, 0.03% Mo, 0.113 g/t Au, and 0.992 g/t Ag.	Linzer (1975), Fox et al. (1976), Me ville et al. (1992)
Late Triassic ?	040, 41	RUN, MIX, RUN NORTH	uTSvp, LTmz	Cu, Au, Mo	Chalcopyrite, magnetite and pyrite disseminations and molybdenum on fracture selvages and in quartz veinlets cut crowded plagioclase porphyries and mafic volcanic rocks. Steep fracture and breccia zones control mineralization.	Guthrie (1971), Panteleyev (1973) Clo tier (1976)
Late Triassic ?	118	BB 57	uTSvp, LTpd	Cu	Trace amounts of disseminated chalcopyrite, magnetite, pyrite and bornite occur in fractured and sheared propylitic andesite, augite porphyritic diorite and monzodiorite.	Hc use (1971)
Late Triassic ?	119	BB 38	uTSvt, uTSv	Cu	Trace amounts of disseminated chalcopyrite, magnetite and pyrite occur in fractured and sheared andesite.	Hc use (1971)
GOLD-SILVER-QUARTZ VEINS						
Jurassic	057	COT & BULL	uCSc	Ag, Cu, Au	Disseminated blebs of tetrahedrite, chalcopyrite and pyrite occupy fractures and breccia zones in a bedding-parallel, east-trending fault cutting limestone. Mineralization either predates or is syngenetic with a north-trending basalt dike swarm.	Betrakis (1981), Hewgill and Wilton (1986)

intrusive fragments that are variably replaced by epidote, occur within purple volcanic flows and tuffs of Units **uTSvt** and **uTSv**. The presence of epidote defines a propylitic alteration zone marginal to mineralization. South of the deposit, this stratigraphy is unconformably overlain by quartz-eye felsic tuffs and quartz-bearing Lower Jurassic conglomerates that contain epidote clasts and clasts of epidotized volcanic rocks.

In the areas south and east of the deposit, the overall strike of bedding is north-northwesterly with easterly and westerly dips that average 70°. Locally strikes are north-easterly, also with steep dips, suggesting tight folds. Other workers describe gentle east dips for bedding in the western part of the deposit, suggesting a simple synclinal structure. Northwest, north and northeast-trending faults truncate the deposit and produce a mosaic of fault blocks with varying internal structure and stratigraphy.

The deposit is hosted by Upper Triassic volcanic rocks of the Stuhini Group adjacent to the eastern contact of the coeval Hickman pluton, where it is cut by the Middle Jurassic Yehiniko pluton. These intrusive events are well constrained by K-Ar dates (Holbek, 1988). The timing of mineralization is not well constrained. It could be related to either plutonic event or perhaps in between and Early Jurassic. A whole-rock K-Ar date for hydrothermal biotite

is 185 ± 5 Ma (Panteleyev and Dudas, 1977). This may reflect: the age of mineralization, argon lost due to Middle Jurassic resetting, or excess argon. In the hope of establishing an age for the deposit, we collected a zircon sample from quartz monzonite porphyry intrusive known to be spatially and temporally associated with the mineralizing system.

OTHER PORPHYRY PROSPECTS - RUN

The Run property is located approximately 10 kilometres southeast of the Schaft Creek deposit, on the east side of Mess Creek (Figure 1-9-4). No active exploration was carried out on the Run claims during the summer of 1992.

The claims are underlain by a salmon-pink weathering plagioclase hornblende porphyritic monzonitic intrusion (**LTmz**). Rafts of hornfelsed lapilli and crystal tuff are exposed where creeks are incised into the main intrusive body. Farther upslope, dikes of pink monzonite intrude a thick package of plagioclase-phyric basalt flows, tuffs and subvolcanic gabbro dikes and plugs of Late Triassic age (Figure 1-9-3b).

Fractures, faults and intrusive breccias control alteration and stockwork mineralization. The monzonite contains magnetite to several per cent, partly altered to hematite.

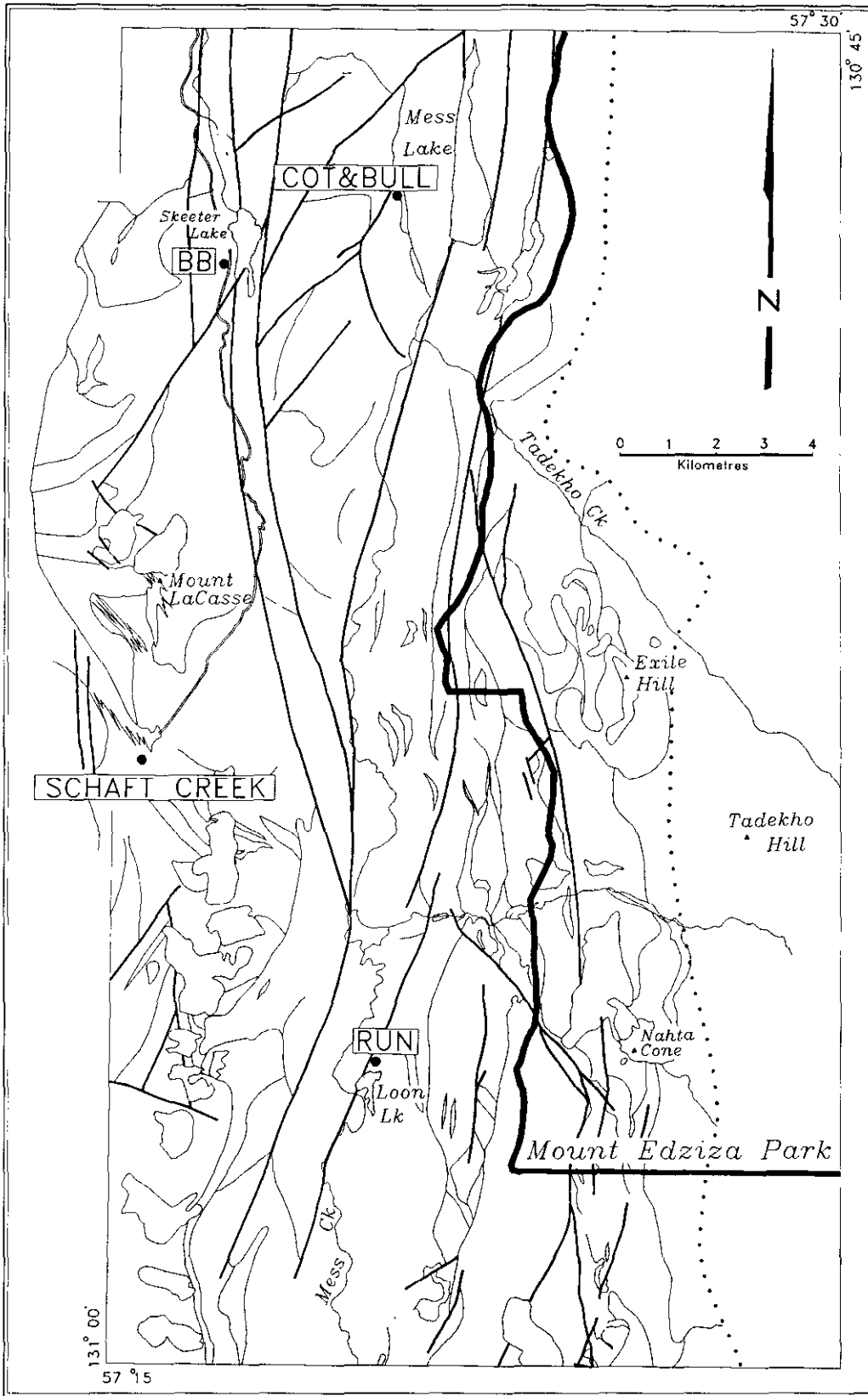


Figure 1-9-4. Mineral occurrence map showing locations of occurrences discussed in text and shown in stratigraphic position in Figure 1-9-3.

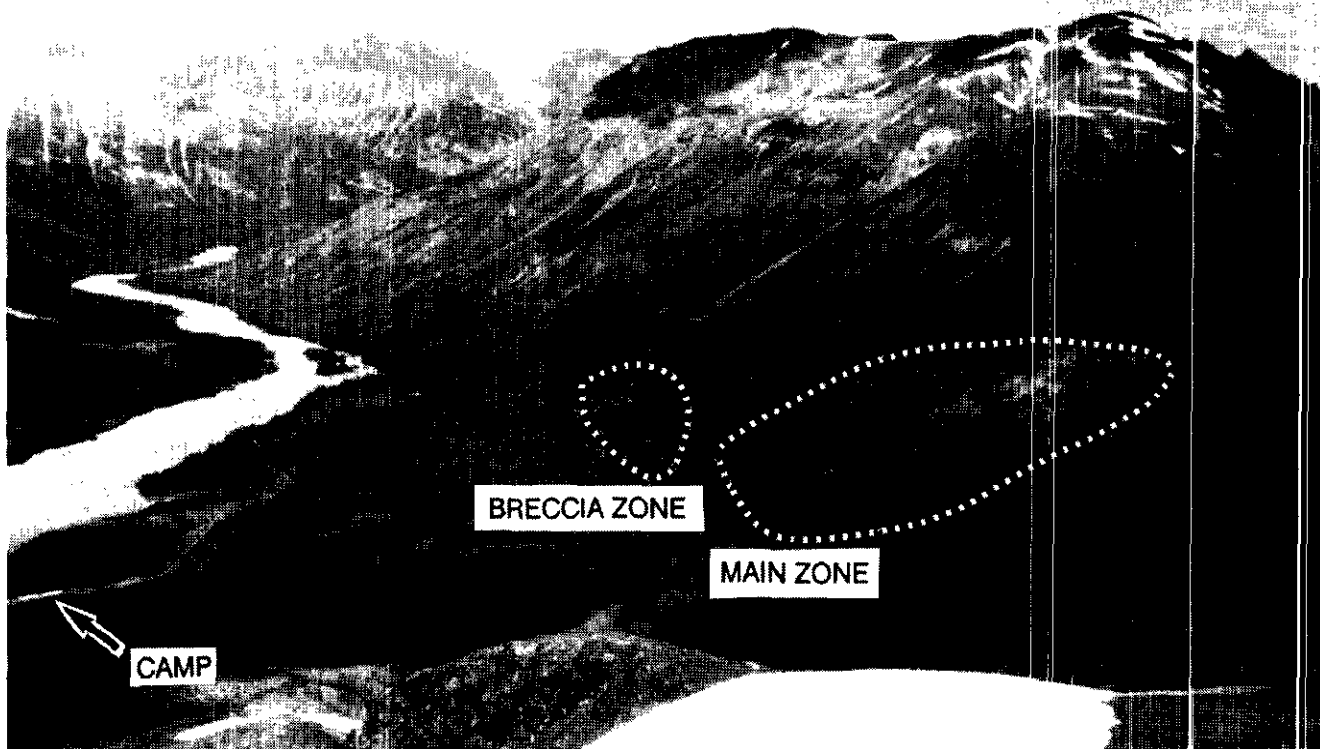


Plate 1-9-3. The Schaft Creek porphyry deposit lies east of Schaft Creek, on the lower slopes of Mount LaCasse. View is to the north.

Locally pyrite ranges to 10 per cent. Chalcopyrite, molybdenite and local chalcocite occur as disseminations and fracture fillings in the monzonite and in quartz veinlets in the volcanic rocks.

ACKNOWLEDGMENTS

Our thanks to Wayne Spilsbury and Andy Betmanis of Teck Exploration Ltd. for providing maps and drill sections, and for geological discussions about the Schaft Creek deposit. Ken Cottrel provided lodging and hospitality at Mess Lake. The safe flying provided by Bob Paul and Daryl Adzich of Vancouver Island Helicopters Ltd. was gratefully appreciated, as was Norma Jeans baking and expediting expertise. Fossils were promptly identified by E.T. Tozer (GSC, Vancouver), W.E. Bamber, Lin Rui and S. Pinard (ISPG-GSC, Calgary). Critical reviews of the manuscript by Bill McMillan, John Newell and Brian Grant improved the final product.

REFERENCES

- Anderson, R.G. and Bevier, M.L. (1990): A Note on Mesozoic and Tertiary K-Ar Geochronometry of Plutonic Suites, Iskut River Map Area, Northwestern British Columbia; in *Current Research, Part E, Geological Survey of Canada, Paper 90-1E*, pages 141-147.
- Betmanis, A.I. (1981): Prospecting Report on the Cot and Bul Claims, Mess Lake Area. *B.C. Ministry of Energy, Mines and Petroleum Resources, Assessment Report 947-9*
- Brown, D.A. and Gunning M.H. (1989a): Geology of the Seud River Area, Northwestern British Columbia. in *Geological Fieldwork 1988, B.C. Ministry of Energy, Mines and Petroleum Resources, Paper 1989-1*, pages 21-267.
- Brown, D.A. and Gunning M.H. (1989b): Geology, Geochemistry and Mineral Occurrences of the Seud River Area, Northwestern British Columbia (104G/5,6); *B.C. Ministry of Energy, Mines and Petroleum Resources, Open File 1989-7*
- Brown, D.A., Greig, C.J. and Gunning M.H. (1990): Geology and Geochemistry of the Stikine River - Yehinico Lake Area, Northwestern British Columbia (104G/11W, 2E); *B.C. Ministry of Energy, Mines and Petroleum Resources, Open File 1990-1*.
- Brown, D.A., Logan, J.M., Gunning, M.H., Orchard, M.J. and Bamber, W.E. (1991): Stratigraphic Evolution of the Paleozoic Stikine Assemblage in the Stikine and Iskut Rivers Area, Northwestern British Columbia; *Canadian Journal of Earth Sciences*, Volume 28, pages 958-972.
- Brown, D.A., Harvey-Kelly, F.E.L., Neill, I. and Timmerman, J. (1992): Geology of the Chuine River - Tah tan Lake Area, Northwestern British Columbia (104G/12 and 13, in *Geological Fieldwork 1991*, Grant, B. and Newell, J.M., Editors, *B.C. Ministry of Energy, Mines and Petroleum Resources, Paper 1992-1*, pages 179-195.

- Cloutier, G.A. (1976): Geological and Geochemical Report on the May Property, May Groups 1,2 and 5; *B.C. Ministry of Energy, Mines and Petroleum Resources*, Assessment Report 6162.
- Drobe, J.R., Logan, J.M. and McLellend, W.C. (1992): Early Carboniferous Plutonism in Stikinia, Stikine and Iskut Rivers Area, Northwestern British Columbia; *Lithoprobe*, Report No. 24, page 85.
- Fox, P.E., Grove, E.W., Seraphim, R.H. and Sutherland Brown, A. (1976): Schaft Creek; in Porphyry Deposits of the Canadian Cordillera, Sutherland Brown, A., Editor, *Canadian Institute of Mining and Metallurgy*, Special Volume 15, pages 219-226.
- Gutrath, G.C. (1971): Report on the Run Claim Group; *B.C. Ministry of Energy, Mines and Petroleum Resources*, Assessment Report 3093.
- Hewgill, W. and Walton, G. (1986): Bud Claim; *B.C. Ministry of Energy, Mines and Petroleum Resources*, Assessment Report 1582.
- Holbek, P.M. (1988): Geology and Mineralization of the Stikine Assemblage, Mess Creek Area, Northwestern British Columbia; unpublished M.Sc. thesis, *The University of British Columbia*, 174 pages.
- House, G.D. (1971): Geological, Geochemical and Magnetic Surveys of the BB #31, MV#5 and MV#11 Claim Groups; *B.C. Ministry of Energy, Mines and Petroleum Resources*, Assessment Report 3640.
- Linder, H. (1975): Geology of the Schaft Creek Porphyry Copper Molybdenum Deposit, Northwestern British Columbia; *Canadian Institute of Mining and Metallurgy*, Bulletin, Volume 68, pages 49-63.
- Logan, J.M. and Koyanagi, V.M. (1989): Geology and Mineral Deposits of the Galore Creek Area, Northwestern B.C. (104G/3,4); in *Geological Fieldwork 1988*, *B.C. Ministry of Energy, Mines and Petroleum Resources*, Paper 1989-1, pages 269-284.
- Logan, J.M., Koyanagi, V.M. and Rhys, D. (1989): Geology and Mineral Occurrences of the Galore Creek Area, (104G/3,4); *B.C. Ministry of Energy, Mines and Petroleum Resources*, Open File 1989-8.
- Logan, J.M., Koyanagi, V.M. and Drobe, J.R. (1990a): Geology of the Forrest Kerr Creek Area, Northwestern British Columbia (104B/15); in *Geological Fieldwork 1989*, *B.C. Ministry of Energy, Mines and Petroleum Resources*, Paper 1990-1, pages 127-140.
- Logan, J.M., Koyanagi, V.M. and Drobe, J.R. (1990b): Geology, Geochemistry and Mineral Occurrences of the Forrest Kerr – Iskut River Area, Northwestern British Columbia (104B/10,15); *B.C. Ministry of Energy, Mines and Petroleum Resources*, Open File 1990-2.
- Logan, J.M., Drobe, J.R. and Elsby, D.C. (1992a): Geology of the More Creek Area, Northwestern British Columbia, (104G/2); in *Geological Fieldwork 1991*, *B.C. Ministry of Energy, Mines and Petroleum Resources*, Paper 1992-1, pages 161-178.
- Logan, J.M., Drobe, J.R. and Elsby, D.C. (1992b): Geology of the More Creek Area, Northwestern British Columbia, (104G/2); *B.C. Ministry of Energy, Mines and Petroleum Resources*, Open File 1992-5.
- McDonald, J. (1978): Hotsprings of Western Canada – A Complete Guide; *Waterwheel Press*, Vancouver, 162 pages.
- Melville, D.M., Faulkner, E.L., Meyers, R.E., Wilton, H.P. and Malott, M-L. (1992): 1991 Producers and Potential Producers, Mineral and Coal; *B.C. Ministry of Energy, Mines and Petroleum Resources*, Open File 1992-1.
- Monger, J.W.H. (1977): Upper Paleozoic Rocks of Northwestern British Columbia; in Report of Activities, Part A, *Geological Survey of Canada*, Paper 77-1, pages 255-262.
- Panteleyev, A. (1973): Run; in *Geology, Exploration and Mining in British Columbia 1972*, *B.C. Ministry of Energy, Mines and Petroleum Resources*, pages 504-505.
- Panteleyev, A. and Dudas, B.M. (1973): Schaft Creek; in *Geology, Exploration and Mining in British Columbia 1972*, *B.C. Ministry of Energy, Mines and Petroleum Resources*, pages 527-528.
- Souther, J.G. (1970): Volcanism and its Relationship to Recent Crustal Movements in the Canadian Cordillera; *Canadian Journal of Earth Sciences*, Volume 7, pages 553-568.
- Souther, J.G. (1972): Telegraph Creek Map Area, British Columbia; *Geological Survey of Canada*, Paper 71-44, 38 pages.
- Souther, J.G. (1988): Mount Edziza Volcanic Complex, British Columbia; *Geological Survey of Canada*, Map 1623A.
- Souther, J.G. and Symons, D.T.A. (1974): Stratigraphy and Paleomagnetism of Mount Edziza Volcanic Complex, Northwestern British Columbia; *Geological Survey of Canada*, Paper 73-32, 48 pages.

MINERALOGY AND CHEMISTRY OF THE RUGGED MOUNTAIN PLUTON: A MELANITE-BEARING ALKALINE INTRUSION (104G/13)

By Ian Neill and J.K. Russell
The University of British Columbia

KEYWORDS: Petrology, mineral chemistry, Rugged Mountain, syenite, pyroxenite, silica undersaturated, melanite.

INTRODUCTION

The Rugged Mountain intrusion is a small (14 km²), zoned alkaline pluton located in northwestern British Columbia, 25 kilometres southwest of Telegraph Creek (Brown *et al.*, 1992a, b). The pluton is exposed on the north side of Shakes Creek, a southeasterly flowing tributary of the Stikine River and on the south flank of Rugged Mountain from which it takes its name.

The Rugged Mountain pluton was first mapped by F.A. Kerr (1948). In his exploration of the Stikine River, Kerr mapped a series of seven alkaline bodies stretching down river from Telegraph Creek to the Iskut River. The northernmost of these bodies, referred to in his paper as the Shakes Creek mass, is known as the Rugged Mountain pluton. Souther (1972) also studied the Rugged Mountain intrusion while mapping the Telegraph Creek map sheet at 1:250 000 scale. Porphyry copper-gold exploration of the intrusion was undertaken during the 1988 and 1989 field seasons by Homestake Mineral Development Company as a joint owner with Equity Silver Mines Limited. Several samples of magnetite-rich pyroxenite with malachite staining returned copper values as high as 2.32 per cent with 1.58 grams per tonne gold.

Subsequent 1:50 000-scale mapping of the Chutine and Tahltan map sheets by the British Columbia Geological Survey Branch (Brown *et al.*, 1992b) provided an opportunity for detailed mapping of the intrusion by the senior author (Figures 1-10-1 and 1-10-2). Rocks of the Rugged Mountain pluton have similar mineralogy throughout and, in particular, have igneous melanite garnet in all phases of the intrusion. Other common minerals include aegirine-augite, potassium feldspar, magnetite, apatite and titanite. The field petrographic and chemical observations described in this paper suggest that the suite is cogenetic. Furthermore, these same field, mineralogical and chemical characteristics are found in other alkaline intrusions within the Cordillera of British Columbia, suggesting a common mechanism is dominant in the genesis of this type of alkaline pluton.

REGIONAL GEOLOGICAL SETTING

The Rugged Mountain intrusion is one of a chain of alkaline plutons located within the western margins of the Intermontane Belt, just east of the Coast Plutonic Complex (Kerr, 1948; Woodsworth *et al.* 1991; Brown *et al.*, 1992a). It lies within Stikinia and is hosted by Upper Triassic volcanic and sedimentary rocks of the Stuhini Group. The

major tectonic structures of the region include the Stikine arch, the Skeena arch, the Bowser Basin (which separates these two features) and the Atlin horst (Souther and Armstrong, 1966). The Rugged Mountain intrusion is part of the Stikine arch. The arch forms a northeasterly trending structural high of crystalline and metamorphic rocks between the Coast and the Cassiar crystalline belts and is a source of sediments for basins to the north and south.

The basal sections of the Stikine arch comprise upper Paleozoic rocks of the Stikine assemblage (Monger, 1977). This assemblage is characterized by Middle Devonian to Permian flows and pyroclastics, interbedded with thick carbonate sections, argillite and minor chert. The thick limestone sequences in the western part of the arch locally reach thicknesses of over 2800 metres (Brown *et al.*, 1992a), suggesting stable shelf conditions during the Permian (Souther, 1971). The rocks of the Stikine assemblage suffered uplift, metamorphism, intrusion and deformation during the Middle to Late Triassic Tahltanian orogeny, leaving a marked unconformity between Stikine assemblage and younger strata.

The Upper Triassic marked the end of the Tahltan orogeny and the onset of arc magmatism, leading to the formation of sequences of subaerial volcanic rocks interfingering with clastics and limestone. These rocks comprise the Stuhini Group and are the host of the Rugged Mountain intrusion. The Stuhini Group is thought to have formed from the buildup of volcanic islands, with predominantly subaerial deposition in active periods. Fringing carbonate reefs with sediment reworking mark periods of quiescence (Souther, 1971).

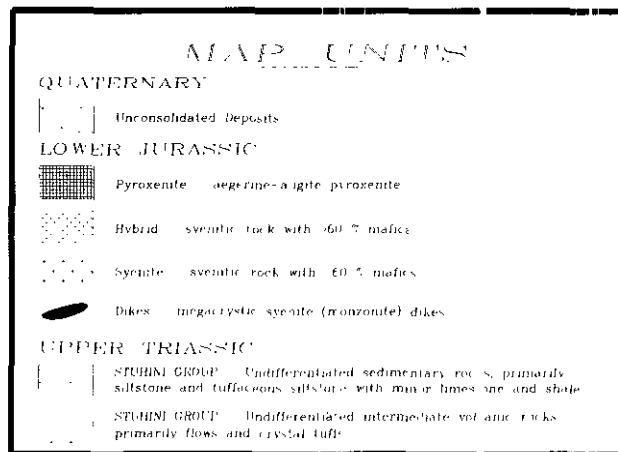


Figure 1-10-1. Map units for geological map of Rugged Mountain pluton presented as Figure 1-10-2.

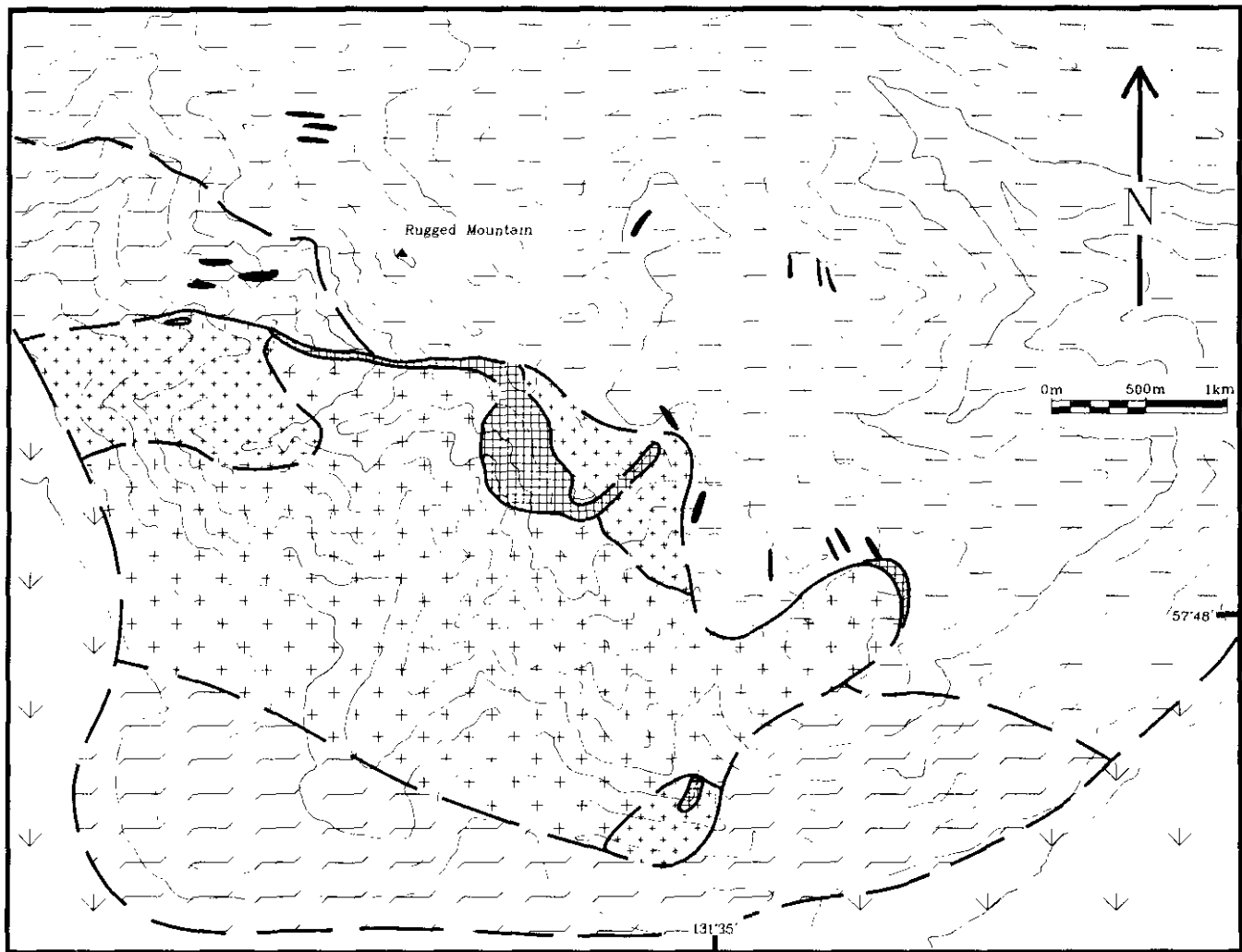


Figure 1-10-2. Geological map of Rugged Mountain intrusion.

The maximum age of the Rugged Mountain intrusion is constrained by the Upper Triassic Stuhini Group that it intrudes. Potassium-argon dating of the Ten Mile Creek syenite (Morgan, 1976), 40 kilometres to the northeast, yields an age of 209 ± 7 Ma. Mineralogical and petrological similarities between these two plutons suggest that Rugged Mountain is coeval, implying Early Jurassic emplacement.

THE RUGGED MOUNTAIN INTRUSION

The Rugged Mountain pluton is emplaced into Upper Triassic Stuhini Group rocks. Close to the pluton, Stuhini rocks comprise four distinct rock types, including: eastward dipping, unmetamorphosed, green and white banded crystal-ash tuff to the north of the intrusion; deformed and hornfelsed, blue-grey tuffaceous, pyritic siltstone inter-layered with shale and limestone; crystal-lapilli tuff; and intermediate volcanic flows.

The pluton itself contains four main rock types with variable contact relationships including: pyroxenite, syenite, "hybrid" and a later set of dikes (Figure 1-10-1). The

intrusion is concentrically zoned, with a syenite core and pyroxenite forming an incomplete border between the remainder of the intrusion and the country rocks (Figure 1-10-2). The hybrid phase is characteristically in contact with the pyroxenite and has gradational contacts with the less mafic syenitic rocks. Contacts between either syenite or hybrid and the pyroxenite are commonly sharp, such as along the thin strip of pyroxenite in the northwest part of the pluton. In other areas the syenite and hybrid clearly disrupt and brecciate the pyroxenite. Late potassium feldspar megacrystic syenite to monzonite dikes cut the intrusion as well as the country rocks.

Samples were collected from all rock types of the Rugged Mountain intrusion. Each sample was cut and stained for potassium feldspar content. Feldspathoid staining on a subset of samples using the method of Shand (1939) proved inconclusive, as the only stain which adhered to the samples appeared to be bonded to alteration assemblages. Further study of stained thin sections provided no evidence of primary feldspathoid minerals. A summary of mineral occurrence in thin section is presented in Table 1-10-1.

PYROXENITE PHASE

The pyroxenite generally occurs at the margins of the pluton, but also outcrops in a single large mass in the northern part of the intrusion (Figure 1-10-2). At the north-west limit of the pluton a continuous strip of pyroxenite, 5 to 10 metres wide, separates country rock to the north from the syenitic rocks to the south. In this locality, contact relationships between syenite and pyroxenite are sharp, unfaulted and steeply dipping to the north. Near the eastern and southeastern contacts of the intrusion, the pyroxenite also occurs as a border phase, with the mafic content of the syenitic rocks increasing with increasing proximity to the pyroxenite. The pyroxenite is brecciated by both syenite and hybrid and locally is cut by pink-weathering potassium feldspar veins.

The unit is dark green to black in colour, medium grained and weathers recessively. Pyroxene and biotite are identifiable in hand sample and the unit varies from strong to weakly magnetic. In places (e.g., the northern contact) the pyroxenite has malachite staining and pyrite which correlate to the copper and gold anomalies reported by Homestake (Marud, 1990).

In thin section the primary mineralogy of the pyroxenite includes aegirine-augite, magnetite, apatite, titanite and biotite. Garnet also occurs as small anhedral crystals and in fractures. Aegirine-augite is the most common mineral and occurs as aligned, elongate euhedral crystals forming a cumulate texture. Optically the grains are strongly pleochroic and have discernible chemical zoning. Magnetite and apatite are the next most common phases: the former occurs as interstitial subhedral crystals or as irregularly shaped infillings between aegirine-augite and the latter forms small elongate prisms and stubby euhedral crystals. Biotite and titanite are less common euhedral grains. Red-brown melanite garnet occurs as small euhedral grains inferred to represent primary magmatic crystallization.

Secondary and alteration minerals include chlorite after aegirine-augite (Sample INE 91-80-2), calcite fracture fillings and space-filling brown-coloured andradite. The habit and composition of this garnet indicates that it is a secondary mineral.

SYENITE PHASE

Syenite forms the core of the complex and generally lies in contact with the hybrid phase. The syenitic rocks placed within this map unit are felsic to intermediate, varying in colour index from 10 to 60. They weather light grey to pink, are medium grained and porphyritic with potassium feldspar crystals up to 2 centimetres in length.

Primary mineralogy of the syenitic rocks includes potassium feldspar, aegirine-augite, garnet, apatite, titanite, magnetite, biotite and hornblende. Plagioclase was not observed, which may be due to sericitization. Alkali feldspar occurs as phenocrysts and as large interstitial grains. Hornblende occurs both as a primary phase and as a partial replacement product of aegirine-augite. Melanite garnet has two habits; euhedral, dark red crystals suggesting a primary occurrence and light-brown space fillings commonly including feldspar, apatite and pyroxene. The latter habit is also primary. Titanite occurs as diamond-shaped, high-relief phenocrysts, identical to those seen in the pyroxenite phase. Biotite forms green and brown pleochroic subhedral to euhedral crystals and is commonly spatially associated with apatite and/or magnetite. Secondary minerals include sericite after feldspar, chlorite and hornblende after pyroxene and calcite infilling fractures.

HYBRID PHASE

The hybrid phase generally occurs between the pyroxenite and the syenite core. It is gradational in composition to the syenite and is arbitrarily separated from the syenitic

TABLE 1-10-1
MINERAL ASSEMBLAGES OBSERVED IN THIN SECTION FOR RUGGED MOUNTAIN INTRUSIVE ROCKS.

Sample No.	Rock Type	Primary Phases								Secondary/Replacement Phases						
		Px	Hbl	Bi	Ksp	Pl	Gt	Ttn	Ap	Opq	Hbl	Gt	Chl	Cc	Q	Ser
INE 78-2	Pyroxenite	X		X				X	X	X				X		
INE 80-2	Pyroxenite	X					X	X	X	X		X	X	X		
INE 76-2	Hybrid	X	X	X	X	X	X	X	X	X	X		X	X		
INE 115	Hybrid	X			X		X	X	X	X						X
INE 119	Hybrid	X		X	X	X	X	X	X	X						X
INE 336	Hybrid	X		X	X	X			X	X	X					X
INE 121	Syenite	X	X	X	X		X	X	X	X	X					X
INE 122	Syenite	X			X			X	X	X			X	X		X
INE 316	Syenite	X	X	X	X		X	X	X	X	X					X
INE 317	Syenite	X		X	X		X	X	X	X	X		X			X
INE 320	Syenite	X	X	X	X		X		X	X	X			X		X
INE 322	Syenite			X	X		X	X	X	X						X
INE 324	Syenite	X		X	X		X		X							X
INE 64	Dike	X			X	X	X	X		X						X
INE 73-2	Dike	X			X				X	X			X			X
INE 82	Dike	X	X		X	X		X	X	X	X				X	X

Px - pyroxene, Hbl - hornblende, Bi - biotite, Ksp - potassium feldspar, Pl - plagioclase, Gt - garnet, Ttn - titanite, Ap - apatite, Opq - opaques, Chl - chlorite, Cc - calcite, Q - quartz, Ser - sericite.

rocks on the basis of percentage of mafic minerals. The hybrid phase contains greater than 60 per cent dark-coloured minerals making it mafic in composition. The geological map for the Rugged Mountain intrusion (Figure 1-10-2) marks regions where either the syenite or hybrid phase dominates. Much of the actual contact between the two phases could not be mapped because parts of the intrusion are inaccessible.

The hybrid phase of the intrusion is fine grained, equigranular and weathers a dull pinkish grey. Primary mineralogy of the hybrid includes feldspar, aegirine-augite, garnet, biotite, apatite, titanite, magnetite and hornblende. The most abundant mineral in this rock type is potassium feldspar, which occurs as phenocrysts and as interstitial grains. One sample contains myrmekitic intergrowths in the groundmass. The intergrowth may be between potassium feldspar and a feldspathoid (*e.g.*, Kwak, 1964), although this has not yet been confirmed by x-ray diffraction. Aegirine-augite phenocrysts are less elongate than in the pyroxenite and occur in clusters with biotite and subordinate apatite and magnetite. Garnet varies from deep red to light brown in colour and is commonly euhedral. Apatite is a late-stage crystallization product with euhedral titanite and commonly occurs as inclusions in garnet, pyroxene or biotite. Secondary and replacement minerals in the hybrid are identical to those in the pyroxenite and syenite.

DIKE PHASE

The dikes of the Rugged Mountain intrusion represent the last intrusive event. They intrude the sedimentary rocks that surround the pluton and in places cut the intrusion itself (Figure 1-10-2). The dikes are diverse in texture and in phenocryst mineralogy and probably represent a series of injections, although for this study they are grouped together. Included within this unit are trachytic to non-trachytic dikes, megacrystic to non-megacrystic dikes and dikes that are dominated by potassium feldspar or sodium feldspar phenocrysts. Also included in this group are a series of syenite pegmatites which outcrop at the margins of the pluton. Feldspar megacrysts in the dikes and pegmatitic syenite reach 7 centimetres in length.

In thin section the rocks are seen to contain feldspar, plagioclase, garnet, hornblende, apatite, titanite, magnetite and augite. Biotite was observed in several hand specimens of the dike phase but was absent in the samples for which thin sections were prepared. Pyroxene occurs infrequently in this unit as small fractured phenocrysts. Titanite is common in the dike rocks, but has a different habit than seen in the other intrusive phases. It occurs as elongate prisms with simple twinning along {100}. Garnet is present as large euhedral poikilitic grains. The garnet phenocrysts show euhedral growth banding and reach 1 centimetre in diameter. Titanite occurs as inclusions in the garnet and is aligned parallel to the crystal edges of the garnet.

Secondary and alteration mineralogy seen in the dikes consists of sericite after feldspar and chlorite, and hornblende after pyroxene. Secondary quartz was seen in one section.

GEOCHEMISTRY

Chemical compositions, including major, minor and trace element concentrations of each phase of the Rugged Mountain intrusion were measured by inductively coupled plasma analysis with reported detection limits of 0.01 per cent. Ferrous iron was measured volumetrically for each sample and ferric iron calculated from the total iron oxide. Chemical compositions are reported with the computed normative characteristics in Table 1-10-2.

CHEMICAL CHARACTER OF THE RUGGED MOUNTAIN SUITE

Figure 1-10-3 is a chemical plot of alkalis against silica and indicates the definite alkaline nature of the Rugged Mountain rock suite. Silica content in the rocks ranges from 35 to 60 per cent and spans the compositional range of ultramafic to intermediate rocks (*e.g.*, Philpotts, 1990). Within the intrusion, the syenitic rocks are the most alkaline and the pyroxenites plot as mildly alkaline. The dike rocks are similar in alkali content to the syenites.

Chemically, the rock suite is strongly undersaturated with respect to silica. The calculated normative mineralogy (Table 1-10-2) shows all intrusive rocks to be nepheline to nepheline-leucite normative. Calculations in Table 1-10-2 reflect the measured ferrous and ferric iron contents of the rocks, however, the undersaturated character of the normative mineralogy is maintained regardless of the treatment of iron. These normative characteristics are somewhat at odds with the fact that neither nepheline nor leucite were observed in thin section. This may be due to alteration of intergranular feldspathoids in the original rock.

There are several notable chemical trends within this suite of igneous rock compositions. Firstly, the pyroxenites have high concentrations of $\text{Fe}_2\text{O}_3(\text{T})$, CaO and P_2O_5 relative to other phases of the Rugged Mountain intrusion. Within the rock suite, the concentrations of these oxides strongly decrease with increasing SiO_2 content. Both TiO_2 and MgO, although less strikingly enriched in the pyroxenite, exhibit similar patterns when examined against SiO_2 . Constituents characteristic of alkali feldspar, Al_2O_3 , Na_2O and K_2O , all increase in concentration with increasing SiO_2 (*e.g.*, from pyroxenite to dike rocks).

Trace element data are plotted on a trace element discrimination diagram to differentiate between volcanic-arc granites, syncollisional granites, within-plate granites and orogenic granites (Figure 1-10-4). All Rugged Mountain rocks, save one of the hybrids, fall within the field of volcanic-arc granites. This correlates well with the tectonic setting proposed for the area (*e.g.*, Souther, 1971; Monger, 1977).

The same chemical data are plotted on an AFM diagram, which is generally used to differentiate between calcalkaline and tholeiitic rock series. Figure 1-10-5 is used here to illustrate one of the remarkable chemical characteristics of the Rugged Mountain suite: as a whole the series is extremely iron enriched. The dike rocks and syenites plot

TABLE 1-10-2
MAJOR ELEMENT OXIDES, TRACE ELEMENT COMPOSITIONS AND CALCULATED NORMATIVE
MINERALOGY OF RUGGED MOUNTAIN INTRUSIVE ROCKS.

Sample No.	78-2	80-2	76	115	336	121	122	316	317	320	322	324	64	73-2	82
SiO ₂	38.90	37.59	46.43	47.73	48.56	51.86	52.51	53.72	50.42	51.17	54.12	51.52	60.28	57.09	53.74
TiO ₂	1.54	1.47	0.97	0.99	0.92	0.64	0.76	0.52	0.63	0.85	0.68	0.99	0.14	0.54	3.28
Al ₂ O ₃	3.20	4.47	15.24	15.23	15.52	19.29	19.26	20.78	18.93	18.71	20.35	20.09	21.06	19.21	13.88
Fe ₂ O ₃	9.80	8.05	4.23	4.10	3.66	2.53	3.12	2.25	2.67	3.30	1.18	2.43	0.80	2.03	1.04
FeO	10.10	9.45	4.93	5.21	5.09	2.81	2.19	2.03	2.77	3.6	3.25	3.21	0.85	2.33	1.07
MnO	0.34	0.32	0.20	0.17	0.18	0.15	0.17	0.13	0.15	0.18	0.13	0.12	0.03	0.10	3.08
MgO	9.96	7.91	3.43	3.33	3.88	1.41	1.51	0.99	1.41	1.78	0.70	1.32	0.14	1.06	3.40
CaO	21.33	20.24	10.79	10.33	9.91	6.33	5.51	4.91	6.71	7.74	4.59	4.98	2.88	4.86	2.62
Na ₂ O	0.81	0.87	1.16	0.79	1.38	2.45	3.24	2.96	2.23	1.75	2.25	2.34	5.29	3.79	1.87
K ₂ O	0.06	1.23	7.73	7.03	7.54	8.68	8.27	9.03	8.49	8.51	10.70	10.24	7.49	8.00	11.78
P ₂ O ₅	2.58	2.31	0.83	0.82	0.91	0.29	0.28	0.24	0.34	0.46	0.16	0.32	0.01	0.22	0.01
LOI	0.18	4.83	3.71	2.61	1.73	2.32	3.67	2.58	4.06	2.01	2.39	2.93	1.44	1.39	1.76
Total	98.80	98.74	99.65	98.34	99.28	98.76	100.49	100.14	98.81	100.06	100.50	100.49	100.41	100.62	95.53
Fe ₂ O ₃ (T)	21.02	18.55	9.71	9.89	9.32	5.65	5.56	4.51	5.75	7.30	4.79	6.00	1.74	4.62	2.23

Trace Element Concentrations (ppm)															
Sr	1038	1247	1909	2932	2554	1603	1762	1505	2095	2157	1105	1498	1624	2377	2155
Rb	<10	24	152	150	179	175	135	145	169	200	204	274	132	134	210
Zr	52	68	81	61	58	85	93	77	80	80	67	48	105	134	76
Y	26	23	22	21	19	20	22	26	20	22	17	18	<10	18	11
Nb	7	10	<5	<5	<5	10	8	6	<5	<5	<5	6	5	13	7
Sn	29	23	19	28	15	<15	<15	<15	<15	18	16	<15	<15	15	<15

Calculated Normative Mineralogy															
Or	-	-	20.09	37.53	32.67	53.26	50.59	54.78	53.03	49.58	58.60	48.67	44.78	47.69	11.30
Ab	-	-	-	-	-	2.00	7.99	6.79	0.55	-	-	-	33.30	19.94	8.71
An	4.99	4.96	14.11	18.03	14.22	16.61	14.07	17.20	17.52	18.44	13.91	14.58	11.77	11.91	11.37
Lc	0.28	6.07	21.62	4.62	10.21	-	-	-	-	1.40	4.00	11.08	-	-	-
Ne	3.76	4.24	5.54	3.78	6.48	10.56	11.02	10.23	10.49	8.18	10.37	11.11	6.46	6.70	4.05
Dp	62.67	57.17	26.61	25.12	25.08	11.83	9.21	5.45	11.47	14.81	7.04	7.78	2.10	9.24	2.19
Wo	-	-	1.58	-	-	0.03	0.54	-	0.81	0.11	-	-	0.31	0.22	-
Ol	2.47	0.93	-	0.67	1.89	-	-	0.78	-	-	0.91	1.99	-	-	0.52
Cs	2.29	4.70	-	-	-	-	-	-	-	-	-	-	-	-	-
Mt	14.61	13.40	6.77	6.66	5.80	3.97	4.63	3.37	4.30	5.01	3.63	2.28	1.19	3.04	1.57
Il	2.97	2.97	1.92	1.96	1.79	1.26	1.49	1.01	1.26	1.65	1.30	1.95	0.27	1.03	0.54
Ap	6.21	5.83	2.06	2.04	2.22	0.72	0.69	0.59	0.86	1.12	0.38	0.79	0.02	0.53	0.02

Sample numbers are without INE- prefix. Major and trace elements determined by ICP. FeO was measured by volumetric analysis.

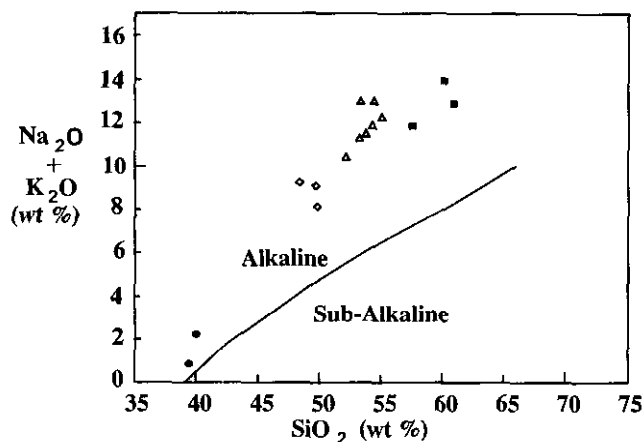


Figure 1-10-3. Compositions of Rugged Mountain intrusive rocks are plotted as per cent Na₂O+K₂O versus SiO₂. Symbols correspond to pyroxenite (filled circles), hybrid rocks (diamonds), syenitic rocks (triangles) and dikes (solid squares).

toward the alkali apex but the hybrid rocks and pyroxenites define a strong iron-enrichment trend that is chemically distinct from most other rock series.

COMPARISON TO OTHER SIMILAR INTRUSIONS

Chemically the Rugged Mountain intrusive rocks are very similar to rocks from the Averill intrusion, a small zoned, alkaline intrusion in the Franklin mining camp comprising pyroxenite, monzogabbro, monzodiorite, monzonite and syenite (Keep, 1989, Keep and Russell, 1989; in press). Compositions of rocks from the Averill intrusion are plotted on an AFM diagram for comparison against the Rugged Mountain chemical compositions (Figure 1-10-6). The chemical patterns are very similar and share the prominent iron-enrichment trend established by the pyroxenites. This same chemical pattern is seen in the Kruger Complex (Currie, 1976) and the Duckling Creek body (Garnett, 1978; Woodsworth *et al.*, 1991), both of which have mafic to ultramafic, silica-undersaturated rock types.

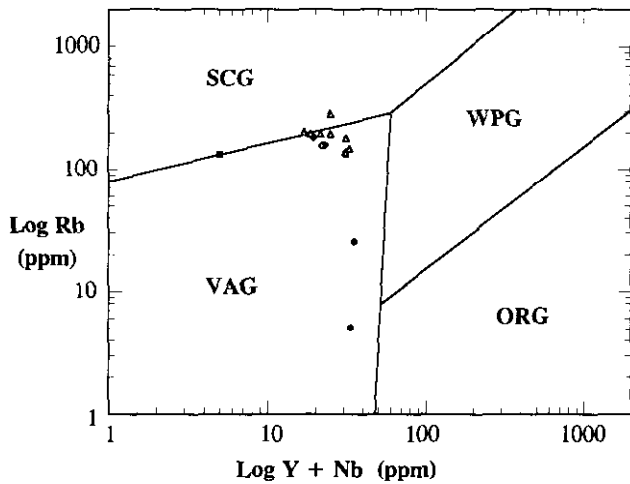


Figure 1-10-4. Trace element chemical compositions of Rugged Mountain intrusive rocks using symbols as in Figures 1-10-3.

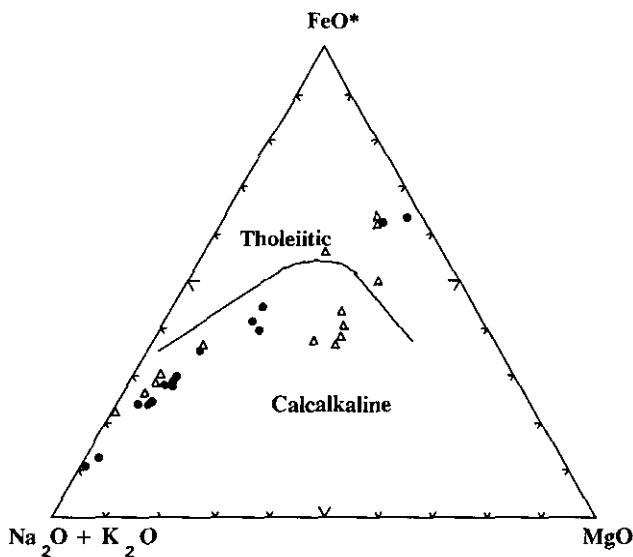


Figure 1-10-5. AFM diagram with chemical compositions of Rugged Mountain rocks plotted with same symbols as used in Figure 1-10-3.

MINERAL CHEMISTRY

Pyroxenes and garnets from each of the four different intrusive rock types were chemically analyzed with the Cameca SX-50 electron microprobe at the The University of British Columbia. Standard operating conditions (Keep, 1989) were used including a 15 kilovolt acceleration voltage and a 20 nanoampere beam current. Count time on standards and unknowns was 20 seconds and K-alpha peaks were used for analysis. Identical standards were used for analysis of the garnet and pyroxene unknowns. Where possible, grain cores and rims were analysed.

The K-beta peak of titanium overlaps the K-alpha peak of vanadium, thus an empirical correction factor is commonly

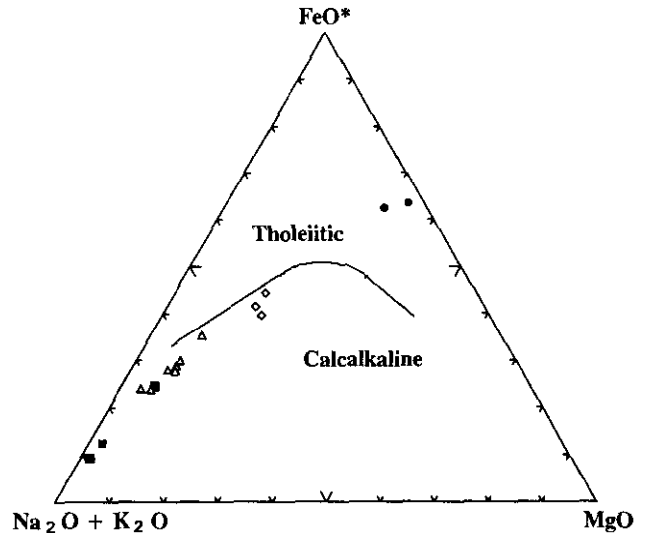


Figure 1-10-6. AFM diagram of Rugged Mountain igneous rock compositions (filled circles) and chemical compositions of Averill plutonic rocks (Keep, 1989; Keep and Russell, in press; Neill, 1991).

required to eliminate the "apparent vanadium" counts induced by the presence of titanium. This factor was measured by analyzing a titanite standard containing no vanadium and calculating the correction factor from the ratio of "apparent measured vanadium" to "known titanium". This value was used to correct the vanadium measured in unknown phases containing titanium (e.g., melanite garnet). The magnitude of corrections required was insignificant suggesting that, unlike many other instruments, the analysing crystals of the Cameca SX-50 are capable of discriminating between the two overlapping peaks.

PYROXENE ANALYSES

Pyroxenes were analyzed for the elements Si, Al, Ca, Na, Fe, Mg, Ti, Mn and Cr. Representative chemical analyses are listed in Table 1-10-3 with the calculated structural formulas: chromium was below detection limits in all samples. Structural formulas were computed on the basis of four cations with adjustment of ferric-ferrous iron to obtain a best fit.

Pyroxene compositions from the pyroxenite, the syenite and the hybrid are plotted in Figure 1-10-7, which represents the ideal solid solution series augite to aegirine (solid line). The $Fe^{+2} - Fe^{+3}$ distinction derives strictly from the structural formulas calculation. Most pyroxenes are augitic in composition although in some pyroxenes there is up to 20 mole per cent substitution of the aegirine molecule $NaFe^{+3}Si_2O_6$. Deviations below the ideal solid solution line represent the presence of other substitutions such as Ca-tschermaks pyroxene $[CaAl(SiAl)O_6]$. There is little chemical variation between cores and rims of analysed pyroxene grains; where chemical zoning is present, mineral grains have rims with higher sodium and lower calcium contents.

GARNET ANALYSES

Garnets from each rock type were analyzed for the elements Si, Al, Ca, Fe, Mn, Mg, Ti, Na, Cr and V. Sodium and chromium were below detection limits in all samples. Representative chemical analyses are reported with calculated structural formulas in Table 1-10-4. Mineral formulas are based on eight cations with all iron treated as ferric.

Two compositional varieties of garnet are found in Rugged Mountain rocks. Melanite, a titanium-rich andradite, is the most common type analysed and commonly occurs as an igneous crystallization product in silica-undersaturated systems (*e.g.*, Dingwell and Brearly, 1985). The melanite garnet is also interpreted to be a primary magmatic phase on the basis of texture. In the dike rocks melanite occurs as euhedral, 1-centimetre, chemically zoned crystals with titanite inclusions in a fine-grained sub-volcanic groundmass. The second and rarer type of garnet lies within the andradite-grossular solid solution which is commonly associated with hydrothermal alteration, metasomatism, contact metamorphism or other nonmagmatic origins. Commonly these compositions are encountered on the rims of melanite crystals or as fracture fillings. The titanium content of these garnets varies from 0.2 to 0.6 cations per formula unit. Representative analyses of both melanite and andradite are included in Table 1-10-4.

Within the Rugged Mountain intrusion, melanite garnet has a wide range in titanium content (Figure 1-10-8). Dingwell and Brearly (1985) state that titanium substitution occurs primarily in the tetrahedrally coordinated site replacing silica, but that titanium can also occur in the octahedrally coordinated site. The electron microprobe analyses of Rugged Mountain melanites are compared against a model solid solution line in Figure 1-10-8. The data plot significantly above the model line representing Si-Ti exchange. The figure shows that, even though there is a strong negative correlation between the two elements, the

TABLE 1-10-3
REPRESENTATIVE ELECTRON MICROPROBE PYROXENE ANALYSES FROM RUGGED MOUNTAIN INTRUSIVE ROCKS.

Unit Sample No.	Pyrox. 79	Pyrox. 79	Hybrid 119	Hybrid 115	Syenite 121	Syenite 121
SiO ₂	47.64	52.34	48.71	44.70	42.80	47.00
TiO ₂	1.03	0.03	1.20	1.53	2.07	1.56
Al ₂ O ₃	4.08	0.20	3.50	5.89	7.90	4.03
FeO	11.19	9.69	10.69	13.33	14.56	13.85
MnO	0.34	1.14	0.26	0.43	0.49	0.43
MgO	10.46	11.61	10.80	9.30	7.23	8.80
CaO	22.60	23.63	22.16	22.28	22.09	21.82
Na ₂ O	0.92	0.32	1.33	1.10	0.92	1.33
Total	98.26	98.96	98.65	98.56	98.06	98.82

Mineral Structural Formulae Calculated on Basis of 4 Cations						
Si	1.82	2.00	1.85	1.72	1.67	1.81
Al(IV)	0.18	0.00	0.15	0.27	0.33	0.18
Al(VI)	0.01	0.00	0.01	0.00	0.03	0.00
Ti	0.03	0.00	0.03	0.04	0.06	0.05
Fe ⁺³	0.18	0.02	0.17	0.29	0.24	0.21
Mg	0.60	0.66	0.61	0.53	0.42	0.50
Fe ⁺²	0.18	0.29	0.17	0.13	0.23	0.24
Mn ⁺²	0.01	0.04	0.01	0.01	0.02	0.01
Na	0.07	0.02	0.10	0.08	0.07	0.10
Ca	0.93	0.97	0.90	0.92	0.92	0.90
Σ Oxygen	5.91	5.99	5.91	5.85	5.88	5.90

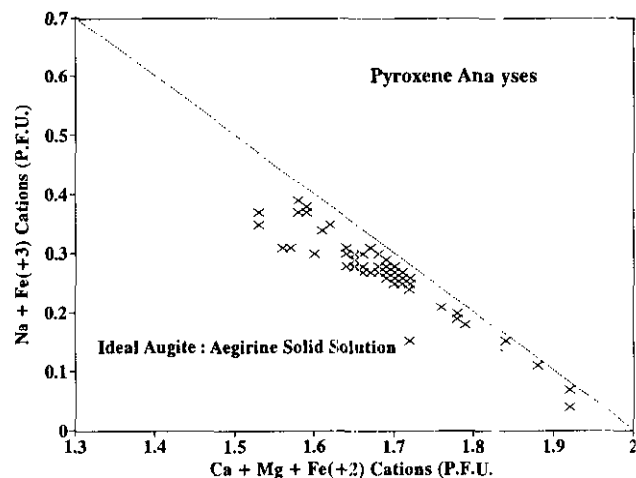


Figure 1-10-7. Electron microprobe analyses of pyroxenes from all units of the Rugged Mountain intrusion. Line represents the solid solution between ideal augite and aegirine.

melanites contain more titanium than can possibly be explained by vacancies on the tetrahedral site. Possibilities for accommodating the titanium include replacing some of the ferric iron with ferrous, thereby creating vacancies in the octahedrally coordinated site for titanium. Vanadium was also detected in the melanite and is assumed to occur in the trivalent state and assigned to the octahedral site (Gomes, 1969; Meagher, 1982).

Melanite appears to be an important accessory phase in a number of other alkaline intrusions in British Columbia. In addition to having similar rock types (pyroxenite/syenite) and chemical compositions to the Rugged Mountain pluton the following intrusions contain melanite; Ten Mile Creek (Morgan, 1976), Duckling Creek (Garnett, 1978; Woodsworth *et al.*, 1991), Zippa Mountain (R.G. Anderson, personal communication, 1992), Galore Creek (Allen *et al.*, 1976; Meetch, 1965) and the Averill (Keay and Russell, 1988, 1989, in press). Two other alkaline intrusions reported to have brown-coloured garnet as an accessory phase are the Kamloops syenite (Kwak, 1964) and the Fayfield River intrusion (McLean, 1973). The presence or absence of melanite has two consequences. Firstly, it is a clear indication of the degree of silica understauration in these alkaline magmas, where the feldspathoids are no longer preserved. Secondly, it may form a solid petrological basis for subdividing or classifying Cordilleran alkaline plutons more finely. It appears to us that the Copper Mountain suite (Woodsworth *et al.*, 1991), which includes the Rugged Mountain intrusion, includes many petrologically dissimilar bodies which could be separated on the basis of accessory phases.

CONCLUSIONS

The Rugged Mountain pluton comprises a suite of alkaline, strongly undersaturated melanite-bearing intrusive rocks. The intrusion is crudely zoned and comprises four rock types: pyroxenite, syenite, hybrid and syenite to monzonite dikes. The zonation is from pyroxenite at the

TABLE 1-10-4
 REPRESENTATIVE ELECTRON MICROPROBE MELANITE GARNET ANALYSES
 FROM RUGGED MOUNTAIN INTRUSIVE ROCKS.

Unit Sample No.	Pyrox. 78	Pyrox. 78	Hybrid 119	Hybrid 115	Hybrid 115	Syenite 322	Syenite 322	Dike 64	Dike 64	Gr - And 115
SiO ₂	32.57	32.35	31.09	33.48	34.87	34.06	30.92	35.12	33.83	35.92
TiO ₂	6.62	3.70	8.07	4.41	2.63	2.24	8.94	2.12	4.34	0.61
Al ₂ O ₃	2.47	2.54	2.50	2.46	4.00	1.62	1.93	7.37	6.68	16.72
V ₂ O ₅	0.79	0.86	0.87	0.00	0.32	0.31	1.12	0.67	0.47	0.23
Fe ₂ O ₃	23.41	25.21	23.36	25.48	23.86	28.36	24.99	22.45	21.03	8.27
MnO	0.41	0.41	0.43	0.29	0.39	0.57	0.75	2.44	1.94	0.36
MgO	0.39	0.31	0.52	0.12	0.21	0.20	0.37	0.25	0.32	0.02
CaO	32.16	32.39	31.70	32.61	32.78	31.95	30.92	29.90	30.86	36.66
Total	98.82	97.77	98.54	98.85	99.06	99.31	99.44	100.32	99.47	98.79

Mineral Structural Formulae Calculated on the Basis of 8 Cations

Si	2.77	2.78	2.66	2.84	2.92	2.89	2.61	2.89	2.81	2.82
Al(IV)	0.23	0.22	0.25	0.16	0.08	0.11	0.20	0.11	0.19	0.18
Ti	0.42	0.24	0.52	0.28	0.17	0.14	0.58	0.13	0.27	0.04
Al(VI)	0.02	0.03	0.00	0.09	0.32	0.05	0.00	0.61	0.46	1.36
Fe ⁺³	1.50	1.63	1.51	1.63	1.50	1.81	1.61	1.39	1.31	0.49
V	0.04	0.05	0.05	0.00	0.02	0.02	0.06	0.04	0.03	0.01
Mg	0.05	0.04	0.07	0.02	0.03	0.03	0.05	0.03	0.04	0.00
Ca	2.93	2.98	2.91	2.97	2.94	2.91	2.84	2.64	2.75	3.08
Mn ⁺²	0.03	0.03	0.03	0.02	0.03	0.04	0.05	0.05	0.17	0.02
Σ Oxygen	12.14	12.03	12.14	12.06	12.06	12.05	12.18	12.13	12.11	11.89

margins to syenite at the core. The zonation of the pluton suggests a relatively simple genetic relationship between the syenite, pyroxenite and the transitional hybrid. Mineralogically, the rocks of the Rugged Mountain pluton share the same critical mineral assemblage of aegirine-augite, potassium feldspar, magnetite, apatite, titanite and magmatic melanite garnet. The continuity in mineral assemblage and continuum in modal proportions further suggests a cogenetic relationship between all phases of the intrusion. The chemical character of the intrusion mirrors the field and mineralogical patterns. The chemical trends are smooth and continuous and the chemical characteristics (normative mineralogy) are consistent throughout the suite.

The presence of melanite garnet and aegirine-augite throughout all phases of the intrusive further suggests the presence of a single evolving magma chamber. Electron microprobe analysis has shown a strong chemical linkage between pyroxenes from the syenite, the hybrid and the pyroxenite. The pyroxenes lie along the aegirine-augite to augite solid solution line. Similarly, electron microprobe analysis of melanite garnets in all phases of the intrusion has delineated a continuum in mineral chemistry: high titanium contents in garnets occur throughout the rock suite.

These observations suggest that the pyroxenite represents a cumulate phase of the original Rugged Mountain intrusion and that it is comagmatic the syenite. The hybrid appears to represent a transitional unit derived from later interaction between the syenite and pyroxenite. The syenite and monzonite dikes are later yet and probably represent the last stages of magmatic activity.

Other alkaline intrusions of British Columbia show some of the same characteristics, including: petrological zoning, a

similar pyroxenite-syenite association, strong silica under-saturation, strong iron-enrichment trends, aegirine-augite and potassium feldspar dominated mineralogies and the presence of accessory melanite garnet. Several show enough of these attributes to suggest a separate sub-class of alkaline intrusion (perhaps within the Copper Mountain suite of Woodsworth *et al.*, 1991). At the very least, the repetition of these chemical, petrographic and field relationships in other Cordilleran intrusions in British Columbia suggests a common mechanism operating throughout time and space.

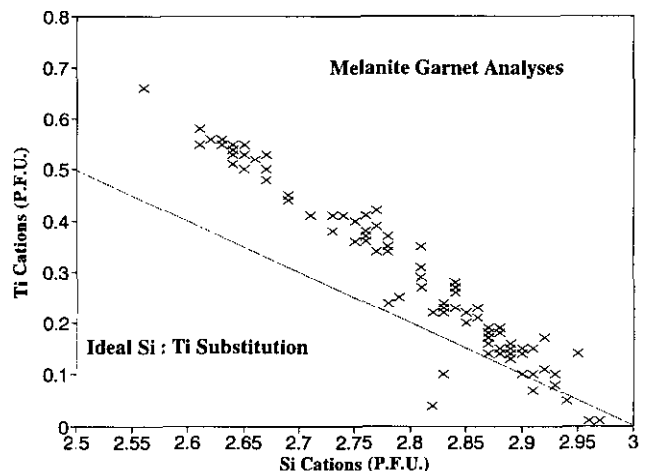


Figure 1-10-8. Electron microprobe analyses of garnets from all units of the Rugged Mountain intrusion. Line represents the effects of cationic exchange between tetrahedrally coordinated Si and Ti (*see text*).

ACKNOWLEDGMENTS

Field mapping by the senior author was completed in the summer of 1991 with the support of the British Columbia Ministry of Energy, Mines and Petroleum Resources and the supervision and support of Derek Brown. Additional research funding derived from the Natural Sciences and Engineering Research Council through Operating Grant A0820 and Infrastructure Grant (Electron Microprobe Laboratory) INF000992. The EMP analytical work of I.N. was facilitated immensely by Dr. Mati Raudsepp.

REFERENCES

- Allen, D.G., Panteleyev, A. and Armstrong, A.T. (1976): Galore Creek, in Porphyry Deposits of the Canadian Cordillera, Sutherland Brown, A., Editor, *Canadian Institute of Mining and Metallurgy*, Special Volume 15, pages 402-414.
- Brown, D.A., Harvey-Kelly, F.E.L., Neill, I. and Timmerman, J. (1992a): Geology of the Chutine River - Tahltan Lake Area, Northwestern British Columbia (104G/12W and 13); in *Geological Fieldwork 1991*, Grant, B. and Newell, J.M., Editors, *B.C. Ministry of Energy, Mines and Petroleum Resources*, Paper 1992-1, pages 179-195.
- Brown, D.A., Neill, I., Timmerman, J. and Harvey-Kelly, F. (1992b): *Geology and Geochemistry of the Chutine River and Tahltan Lake Areas, Northwestern B.C. (104G/12W, 13)*; *B.C. Ministry of Energy, Mines and Petroleum Resources*, Open File 1992-2.
- Currie, K.L. (1976): The Alkaline Rocks of Canada; *Geological Survey of Canada*, Bulletin 239, 278 pages.
- Dingwell D.B. and Brearly, M. (1985): Mineral Chemistry of Igneous Melanite Garnets from Analcite-bearing Volcanic Rocks, Alberta, Canada; *Contributions to Mineralogy and Petrology*, Volume 90, pages 29-35.
- Garnett, J.A. (1978): Geology and Mineral Occurrences of the Southern Hogem Batholith; *B.C. Ministry of Energy, Mines and Petroleum Resources*, Bulletin 70, 75 pages.
- Gomes, Celso de Barros (1969): Electron Microprobe Analysis of Zoned Melanites; *American Mineralogist*, Volume 54, pages 1654-1661.
- Keep, M. (1989): *The Averill Plutonic Complex, near Grand Forks, British Columbia*; unpublished M.Sc. thesis, *The University of British Columbia*, 167 pages.
- Keep, M. and Russell, J.K. (1988): Geology of the Averill Plutonic Complex, Franklin Mining Camp; in *Geological Fieldwork 1987*, *B.C. Ministry of Energy, Mines and Petroleum Resources*, Paper 1988-1, pages 49-53.
- Keep, M. and Russell, J.K. (1989): *The Geology of the Averill Plutonic Complex, Grand Forks, British Columbia*; in *Geological Fieldwork 1988*, *B.C. Ministry of Energy, Mines and Petroleum Resources*, Paper 1989-1, page 27-31.
- Keep, M. and Russell, J.K. (in press) Mesozoic Alkaline Rocks of the Averill Plutonic Complex; *Canadian Journal of Earth Sciences*.
- Kerr, F.A. (1948): Lower Stikine and Western Isku River Areas, B.C.; *Geological Survey of Canada*, Memoir 46, 94 pages.
- Kwak, T.A.P. (1964): A Garnet-bearing Syenite near Kamloops, B.C.; unpublished M.Sc. thesis, *The University of British Columbia*, 53 pages.
- Marud, D. (1990): Report of Activities on the Rugged Mountain Property; *B.C. Ministry of Energy, Mines and Petroleum Resources*, Assessment Report 20154.
- McLean, D.C. (1973): A Zoned Syenite Intrusion, Dayfield River, South-central B.C.; unpublished B.Sc. thesis, *The University of British Columbia*, 50 pages.
- Meagher, E.P. (1982): Silicate Garnets; in Orthosilicates, Ribbe, P.H., Editor, *Reviews in Mineralogy*, Volume 11, pages 25-66.
- Meetch, L. (1965): A Garnet-bearing Syenite Porphyry, Galore Creek, British Columbia; unpublished B.Sc. thesis, *The University of British Columbia*, 32 pages.
- Monger, J.W.H. (1977): Upper Paleozoic Rocks of the Western Canadian Cordillera and their Bearing on Cordilleran Evolution; *Canadian Journal of Earth Sciences*, Volume 14, pages 1832-1859.
- Morgan, J.T. (1976): *Geology of the Ten Mile Creek Syenite-Pyroxenite Pluton, Telegraph Creek, B.C.*; unpublished B.Sc. thesis, *The University of British Columbia*, 41 pages.
- Neill, I. (1991): Geology, Petrography and Chemistry of the Rugged Mountain Alkaline Pluton, Northwestern British Columbia (104G/13); unpublished B.Sc. thesis, *The University of British Columbia*, 75 pages.
- Philpotts, A.R. (1990): Principles of Igneous and Metamorphic Petrology; *Prentice Hall*, New Jersey, 498 pages.
- Shand, S.J. (1939): On the Staining of Feldspatoids; *American Mineralogist*, Volume 24, pages 508-513.
- Souther, J.G. (1971): Geology and Mineral Deposits of Tulsequah Map-area, British Columbia; *Geological Survey of Canada*, Memoir 362, 84 pages.
- Souther, J.G. (1972): Telegraph Creek Map Area, B.C.; *Geological Survey of Canada*, Paper 71-44, 34 pages.
- Souther, J.G. and Armstrong, J.E. (1966): North Central Belt of the Cordillera of British Columbia; in *Tectonic History and Mineral Deposits of the Western Cordillera*, *Canadian Institute of Mining and Metallurgy*, Special Volume 8, pages 171-189.
- Woodsworth, G.J., Anderson, R.G. and Armstrong, R.L. (1991): Plutonic Regimes, Chapter 15; in *Geology of the Cordilleran Orogen in Canada*, Gabrielse, H. and Yorath, C.J., Editors, *Geological Survey of Canada*, Geology of Canada, Number 4, pages 491-531.

NOTES



GEOLOGY OF THE BEARSKIN LAKE AND SOUTHERN TATSAMENIE LAKE MAP AREAS, NORTHWESTERN BRITISH COLUMBIA. (104K/1 and 8)

By J.A. Bradford and D.A. Brown

KEYWORDS: Regional geology, Golden Bear, Stikine assemblage, Stuhini Group, Moosehorn batholith.

INTRODUCTION

The Golden Bear project was designed to provide a regional geological framework for exploration in the vicinity of the Golden Bear mine, and to expand on recent 1:10 000-scale mapping by Jim Oliver (Oliver and Hodgson, 1989, 1990). Mapping of the Bearskin Lake (104K/1) and the southern third of the Tatsamenie Lake map sheet (104K/8) was completed at 1:50 000 scale during the 1992 field season. The project area is northwest of the Tahltan Lake sheet (104G/13), mapped under the Stikine project in 1991 (Brown *et al.*, 1992; Figure 1-11-1).

The Golden Bear mine has produced about 3 504 000 grams (112 670 ounces) of gold from 271 230 tonnes of ore

milled from its opening in late 1989 to August, 1992. The mine is located above the north side of Bearskin (Muddy) Lake, about 140 kilometres west of Dease Lake. Access along the company road is restricted and takes approximately 4 hours from Dease Lake. A private gravel airstrip is located just west of Bearskin Lake and serves the mine. During the 1992 field season a helicopter was based at the airstrip and provided access to most of the map area.

Much of the area is a rolling Early (?) Miocene peneplain comprising part of the Tahltan Lake Plateau (Ryder, 1984) and is deeply dissected by U-shaped and hanging valleys. Large alluvial fans characterize the upper reaches of the Samotua River and parts of Bearskin valley. Alpine glaciers have carved a rugged landscape of arêtes and cirques in the southwest quadrant of 104K/1. Numerous large rock slides are found throughout the map area, the most prominent being the Bearskin slide (Souther, 1971), currently the loca-

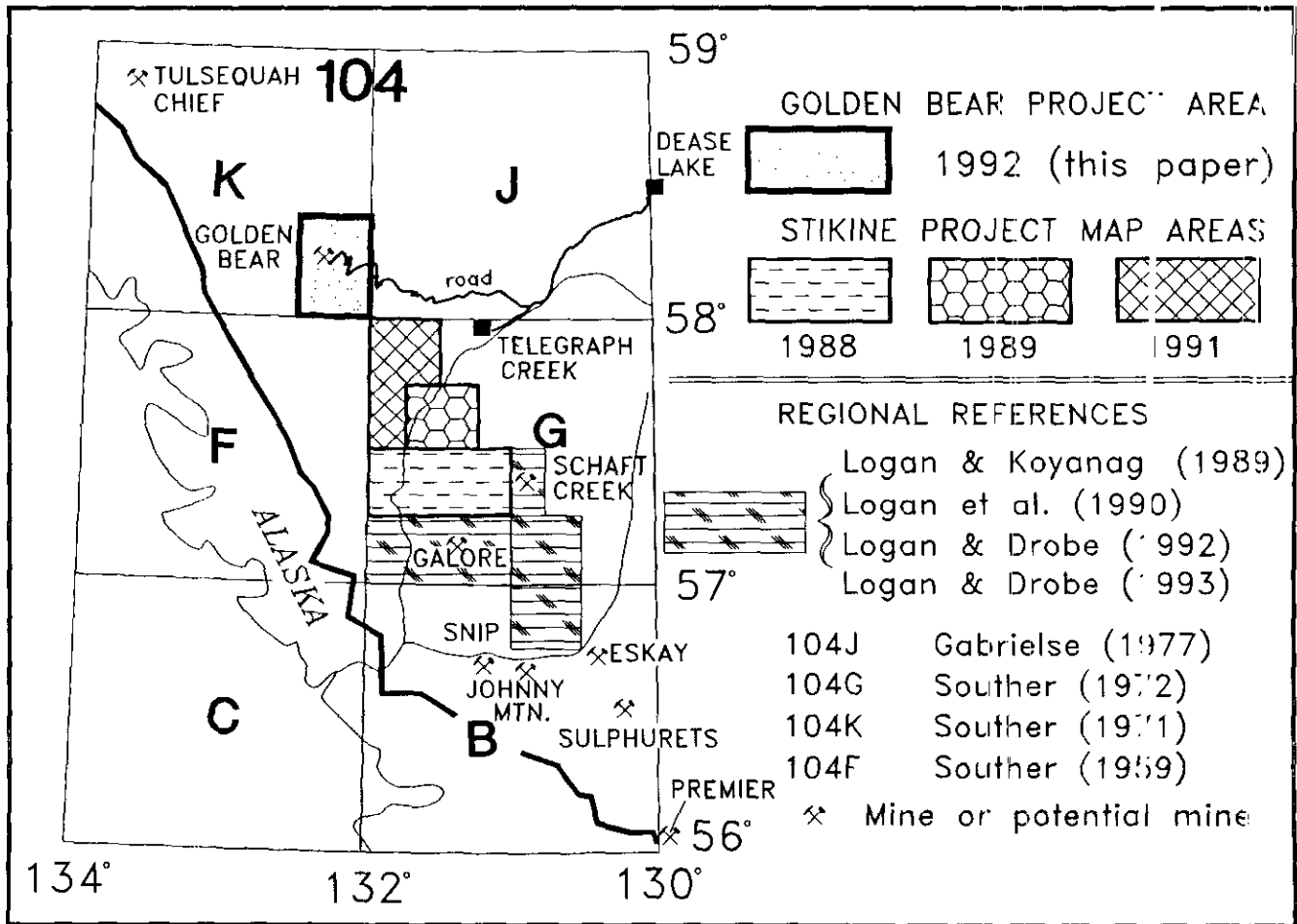


Figure 1-11-1. Location of the Golden Bear project map area relative to previous regional geological studies.

tion of the Golden Bear mine buildings and haul road. Debris from this slide dammed the creek to form Bearskin Lake and now covers about 2 square kilometres. It was derived from the area immediately east of the open pit.

Accomplishments during the 1992 field season include: documentation of pre-Late Triassic deformation; division of Upper Triassic and older volcanic and sedimentary rocks into Stuhini Group and Stikine assemblage; and discovery of potential volcanogenic stratabound alteration within pre-Upper Triassic volcanic rocks. Interpretation of stratigraphic and structural relationships among lithologic units remains tentative due to the paucity of age controls. Sampling for conodonts (36 samples), radiolaria (2), macrofossils (4), and U-Pb (4) and K-Ar (2) dating should cast light on problem areas.

GEOLOGICAL SETTING

The project area is situated along the western edge of the Intermontane Belt. It lies within Stikinia, with the possible exception of metamorphic rocks in the southwest corner of 104K/1. Previous mapping at 1:250 000-scale by Souther (1971) identified an extensive unit of Triassic and older volcanic and sedimentary rocks (his Unit 4) containing Permian limestone in structural culminations. This unit has been subdivided into Upper Triassic Stuhini Group and Paleozoic Stikine assemblage. These rocks are intruded by Triassic, Jurassic and Eocene plutons, and are overlain by Tertiary volcanic rocks. The only Jurassic stratigraphy in the project area consists of a small, fault-bounded wedge of clastic sedimentary rocks of the Takwahoni Formation.

STRATIGRAPHY

PALEOZOIC(?) METAMORPHIC ROCKS (Pm)

Amphibolite-grade metamorphic rocks (Unit 5 of Souther, 1959, 1971) were briefly examined just south of the map area in the northwest corner of the Chutine Peak map area (104F/16). A high-angle reverse(?) fault between these rocks and lower greenschist grade metavolcanic rocks (possibly Stuhini Group) was projected north to intersect a knife-edged nunatak in the southwest corner of 104K/1.

The amphibolite-grade rocks include well-foliated poly-deformed schists of variable compositions, including: rusty brown weathering quartzofeldspathic biotite schist, amphibole(?) - chlorite schist (mafic metavolcanic rocks), marble, and orthogneiss (felsic sills?).

This succession is tentatively correlated with the Boundary Ranges Metamorphic Suite that lies west of lower grade rocks of the Laberge and Stuhini groups and Stikine assemblage, as described in the Tutshi Lake and Tulsequah Glacier areas (Mihalynuk and Rouse, 1988; Smith and Mihalynuk, 1992). This belt of rocks may represent metamorphosed Stikine assemblage as advocated by Currie (1992) for the Tagish Lake area (104M).

PALEOZOIC - STIKINE ASSEMBLAGE

CARBONIFEROUS(?) LIMESTONE (CSIs)

Undated limestone exposed in structural culminations in the Samotua River valley and along the western margin of

the Moosehorn batholith (Figure 1-11-2) is provisionally interpreted as the oldest unit in the project area, based on regional and stratigraphic considerations. The unit comprises massive to thin and thick-bedded, white to medium grey, recrystallized limestone with dull grey siliceous layers and lenses. No bioclastic material or macrofossils were noted, possibly due to recrystallization and deformation of the limestone. On the west side of the large antiform straddling the Samotua River in 104K/8 ("Samotua antiform"), well-bedded siliceous carbonate with chloritic laminae at the top of the limestone grades into overlying chloritic metavolcanic rocks with carbonate layers. Although the contact is sheared, it is interpreted as stratigraphic.

These limestone bodies, interpreted as Permian by Souther (1971), are overlain by a significant thickness of polydeformed metavolcanic and metasedimentary rocks. Significant sub-Stuhini volcano-sedimentary sections overlying Permian limestone are virtually unknown in Stikinia, but lithologically similar sequences below the Permian limestone have been described in the Scud River area and elsewhere (Brown *et al.*, 1991). If the overlying sequence is pre-Permian, then the Samotua limestone could be Carboniferous or older, assuming an upright stratigraphic succession. In the absence of definitive fossil evidence, a Carboniferous age is assumed.

CARBONIFEROUS(?) - FOLIATED METAVOLCANIC ROCKS (CSv)

Foliated, chloritic metavolcanic rocks of the Stikine assemblage contain lithologies similar to Stuhini Group in part, but are distinguished from them by the following criteria:

- strong, penetrative flattening foliation (especially evident in lapilli tuffs and pillow basalt) and phyllosilicate fabrics;
- well-developed mullions and stretching lineations;
- a "chloritic" green weathering colour, lacking the distinctive red-brown weathering of Stuhini rocks;
- in general, more andesitic compositions;
- greenschist metamorphic grade;
- bright green colours on fresh surfaces.

The dominant pre-Upper Triassic volcanic lithologies include: andesitic ash to lapilli tuff; feldspar and lesser augite-phyric tuff and flows; massive andesitic flows; laminated green and white, locally calcareous tuff; maroon and green tuff and flows; rare pillow basalt and argillite. In places, thin to thick-bedded grey and white recrystallized limestone up to 25 metres thick is present.

A phyllitic foliation is common, but strain is variable and some outcrops have only a very weak foliation. Near the Bandit showing (Figure 1-11-2), and southeast of the Samotua antiform, relatively unstrained tuff and massive flows locally resemble Stuhini Group, and transitions from phyllitic to very weakly foliated rocks are abrupt. In some cases, massive diabasic rocks may represent Stuhini feeder dikes and sills.

The age of the Stikine assemblage metavolcanic rocks is poorly constrained. Chloritic metavolcanic rocks at Sam Creek (Figure 1-11-2) structurally overlie Upper Car-

boniferous (Moscovian) felsic volcanic rocks in what could be an inverted structural sequence; if so, a Moscovian or older age is implied. Green and maroon phyllitic andesites in southeastern 104K/8 resemble poorly dated pre-Permian volcanic rocks in the Chutine and Little Tahltan culminations in 104G/13 (Brown *et al.*, 1992).

CARBONIFEROUS(?) - TUFF, VOLCANIC SEDIMENTARY ROCKS AND ARGILLITE (CSvs)

A distinctive unit of well-bedded tuff and sedimentary rocks crops out along the Samotua River south of the mouth of Bearskin Creek. Similar rocks are exposed east of the Samotua Glacier in the south-central part of 104K/1. The unit consists of thin to medium-bedded, felsic to intermediate ash tuff, tuffaceous sandstone and argillite. Interbedded volcaniclastic rocks and argillite are characterized by graded bedding, flame structures and argillite rip-ups. Heterolithic pebble conglomerate with abundant chert and metavolcanic clasts is present locally. Minor limestone, calcareous ash tuff and foliated pyroxene-phyric sills also occur within the sequence. The interbedded tuff and sediments of Unit CSvs resemble the "siliceous unit" in the Scud River area (104G/5, 6), which stratigraphically underlies Permian limestone (Brown and Gunning, 1989).

CARBONIFEROUS(?) - SEDIMENTARY ROCKS (CSs)

Strongly deformed argillaceous sedimentary rocks occur within the Stikine assemblage metavolcanic sequence near the mouth of Bearskin Creek. They consist dominantly of slate to argillaceous phyllite, with minor ash tuff, siltstone, and brown-weathering limestone beds and lenses up to 0.5 metre thick. The contact with overlying foliated volcanic rocks appears to be stratigraphic.

A unique stretched-pebble conglomerate occurs near the top of the sediment package and is exposed along the Golden Bear mine road. This matrix-poor pebble to cobble conglomerate consists almost entirely of subrounded felsic volcanic clasts, with minor black chert or cherty argillite and black silty limestone. Volcanic clasts include well-laminated felsic tuffs and plagioclase-phyric dacite. All volcanic clasts are intensely altered to an assemblage of fine-grained quartz, sericite and pyrite. The conglomerate coarsens upward over a thickness of about 5 metres. Clasts have undergone marked ductile strain, with a length to width ratio averaging 3.4:1. The source of the felsic volcanic clasts is unknown.

UPPER CARBONIFEROUS - FELSIC TO MAFIC VOLCANIC ROCKS AND SEDIMENTARY ROCKS (uCSvs1)

A heterogeneous section of foliated felsic to mafic volcanic rocks, argillaceous phyllite and limestone structurally overlies thick Permian limestone at the head of Sam Creek (Figure 1-11-2). Similar felsic phyllite and carbonate can be traced to the west side of Misty Mountain, where they also overlie a thick limestone package.

At Sam Creek, Lower Permian limestone is overlain by a thin (100 m) unit of chloritic metavolcanic rocks with intercalated pink marble. This is in turn overlain by a thick section (300-400 m apparent thickness) of pale grey, tan or

brown-weathering, varicoloured (green, grey, brown, pink), thin-bedded to laminated felsic phyllite (felsic metatuff). Intercalated with the felsic rocks are lesser dark green, chloritic, intermediate to mafic metavolcanic rocks, tan to orange-weathering dolostone and dolomitic phyllite, argillaceous phyllite, and blue-grey to white and pinkish marble. A sericite and/or chlorite foliation is characteristic of the felsic unit, but lithologies can be massive to fissile. Thin, potassium feldspar - quartz layers occur in some laminated felsic rocks. Plagioclase and quartz-phyric rhyolite is present locally.

Unit uCSvs1 contains the oldest dated rocks in the map area. Preliminary U-Pb dating of zircons from felsic tuff on the north side of Sam Creek yields an age of $302 \pm 2/-4$ Ma (Oliver and Gabites, 1993, this volume; locations shown on Figure 1-11-2). Similar rocks on the north shore of Tetsamenic Lake have a minimum age of 307 ± 2 Ma (*ibid.*). Age and structural relationships imply either that the basal contact of Unit uCSvs1 is a flat-lying thrust, or that large-scale recumbent folding has inverted the section at Sam Creek and elsewhere above the Permian limestone. The contact with structurally underlying Permian limestone was not seen in outcrop, and significant shear fabrics were not observed above or below the contact. Silica-sealed brecciation is extensively developed along the contact west of Misty Mountain; however, this is interpreted as hydrothermal in origin. Zircon U-Pb dating of units structurally overlying Unit uCSvs1 may help constrain structural interpretation in this area.

PERMIAN LIMESTONE (PSIs)

Massive to thin-bedded, white to dark grey limestone underlies an 8 square kilometre area between Bearskin Lake and Sam Creek. This and smaller limestone bodies scattered throughout the map area have been assigned a Permian age on the basis of poorly preserved fusulinids and rugosan corals (Souther, 1971). In general, carbonate in the project area is less fossiliferous than in other areas of Stikinia, perhaps due to more intense deformation and metamorphism.

Internal stratigraphy of the Bearskin Lake limestone was described by Oliver and Hodgson (1989). Dark grey, carbonaceous limestone and black siltstone occurs near the top of the unit above Bearskin Lake. A black chert described in the Fleece Bowl area might be a silicified correlative unit. The carbonaceous limestone overlies tan to orange-weathering dolomitic limestone, which also occurs near the top of the section at Sam Creek, where it contains abundant crinoid columnars. A "silicæ facies", described as stratigraphically overlying Permian limestone in the Totem zone, north of the Golden Bear deposit (Oliver and Hodgson, 1989), was not interpreted as a stratigraphic unit in our mapping. This zone is a product of hydrothermal silicification, as both crosscutting and stratabound silica zones with limestone remnants are evident.

Large, partially silicified fusulinids from a locality just west of the Totem area were identified as Early Permian, possibly Guadalupian forms (Figure 1-11-2 Rui Lin, personal communication, 1992).

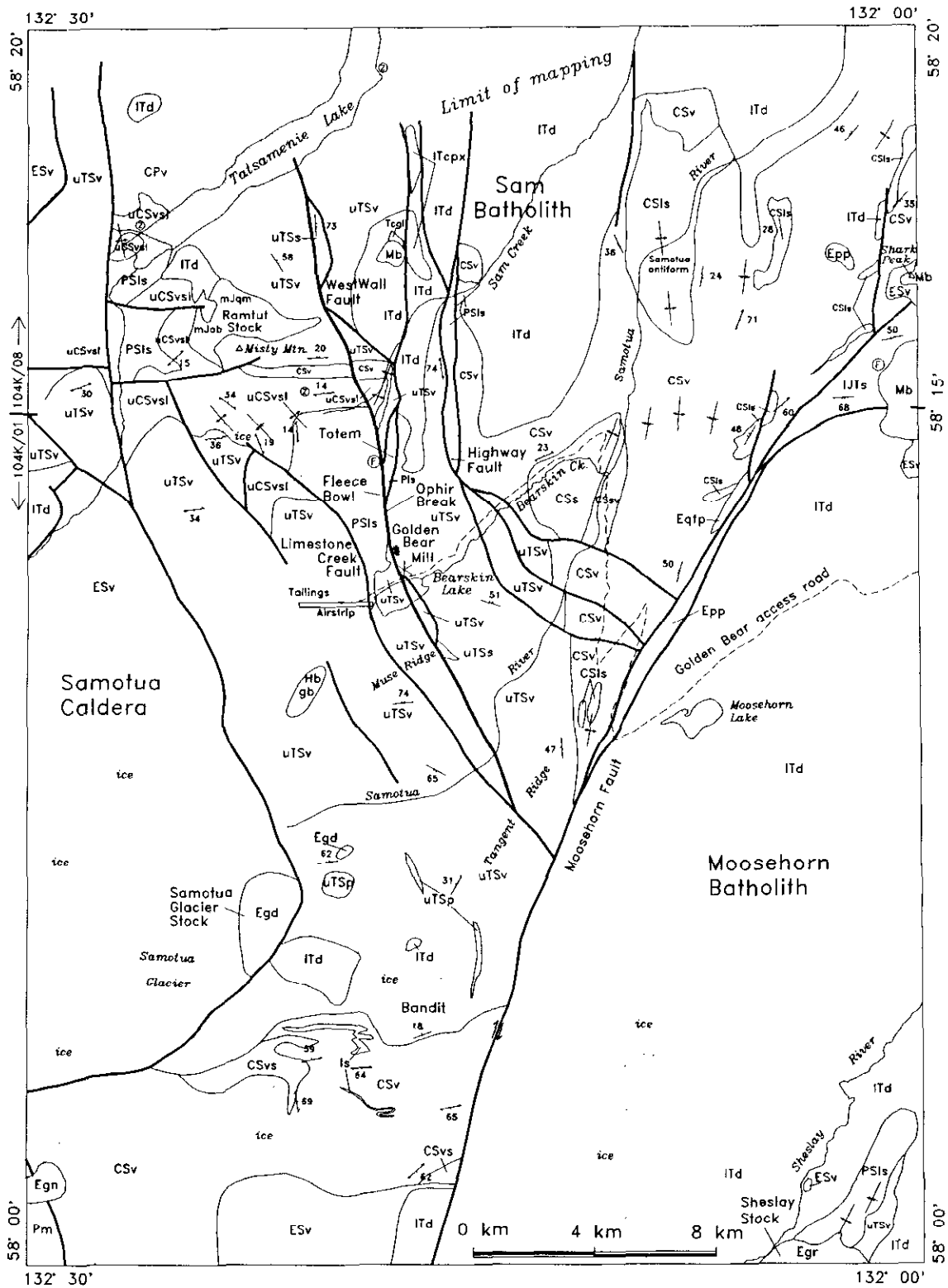


Figure I-11-2. Geology of the Bearskin Lake and Tatsamenie Lake map areas (104K01/08), simplified from Open File 1993-1.

LEGEND	
STRATIFIED ROCKS	
MIOCENE	
▭ Mb	Basalt -- flat lying, columnar jointed
EOCENE	
▭ ESv	SLOKO GROUP -- intermediate to felsic volcanic breccia, tuff & lesser flows
TERTIARY	
▭ Tcg	Polymictic conglomerate -- poorly indurated
LOWER JURASSIC	
▭ IJTs	TAKWAHONI FORMATION -- sandstone, siltstone, polymictic conglomerate
UPPER TRIASSIC	
▭ uTSv	STUHINI GROUP -- volcanics, volcanoclastics uTSp -- megacrystic, "bladed" plagioclase porphyry uTSs -- argillite, siltstone, limestone Hbgb -- hornblende gabbro
PERMIAN & OLDER STIKINE ASSEMBLAGE	
Lower Permian	
▭ PSIs	Limestone -- variably recrystallized
UPPER CARBONIFEROUS	
▭ uCSvsl	Felsic to mafic volcanics, phyllite, limestone
CARBONIFEROUS (?)	
▭ CSs	Slate, siltstone, limestone
▭ CSvs	Andesitic tuff, argillite, tuffaceous sandstone
▭ CSv	Mafic to intermediate metavolcanic rocks ls = limestone
▭ CSIs	Limestone
PALEOZOIC (?)	
BOUNDARY RANGES (?) METAMORPHIC SUITE	
▭ Pm	Amphibolite and greenschist grade metapelite, amphibole-charite schist, orthogneiss, marble
INTRUSIVE ROCKS	
EOCENE	
▭ Egr	Biotite hornblende granite Epp = plagioclase porphyritic granite Egd = biotite hornblende granodiorite Eqfp = quartz plagioclase porphyritic rhyolite
MIDDLE (?) JURASSIC	
▭ mJqm	Hornblende biotite quartz monzonite mJab = albite
LATE TRIASSIC	
▭ ITd	Hornblende diorite, monzodiorite, quartz diorite
▭ ITcpX	Clinopyroxenite
⊙	Zircon U-Pb sample locality
⊙	Fossil locality

UPPER TRIASSIC - STUHINI GROUP (UTSV)

The Stuhini Group comprises a thick package of volcanic and sedimentary rocks underlying most of the central portion of 104K/1 and part of 104K/8. Stuhini rocks overlie a variety of older units, including an inverted section at Sam Creek, along a pronounced regional unconformity. The basal contact is well exposed in two areas: Sam Creek and near the Bandit showing. At Sam Creek, weakly foliated pyroxene and plagioclase-phyric Stuhini volcanic rocks overlie polydeformed chloritic phyllite, dolomitic limestone, argillaceous phyllite and siliceous phyllite along a foliation-parallel discontinuity. At Bandit, gently northeast dipping pyroxene crystal-lithic lapilli tuff unconformably overlies strongly folded and foliated metavolcanic rocks,

argillaceous phyllite and limestone. There is no basal conglomerate at either location.

The Stuhini Group consists mainly of red-brown weathering, plagioclase and augite-bearing volcaniclastic rocks. Flows are subordinate to clastic rocks, in contrast to the Trapper Lake section (104K/7) described by Souther (1971), where over 1200 metres of pillow basalt are exposed. In the project area, pillow basalt was not seen south of Bearskin Lake, but occurs just west of the Golden Bear pit, overlying Permian limestone (D. Reddy, personal communication, 1992). Pillowed flows were also mapped between Tatsamenie Lake and the Sam batholith by Oliver (Oliver and Hodgson, 1990).

Volcaniclastic sequences are typically heterogeneous, comprising intercalated massive to finely laminated ash tuff, ash and crystal tuff, lapilli tuff and block and ash tuff, as well as more massive "greenstones" which could be flows or sills. Lapilli tuff commonly contains augite and/or plagioclase crystals as well as mafic lithic clasts. Augite-phyric lithic clasts are common, while intermediate to felsic volcanic, plagioclase-phyric hypabyssal intrusive and chert clasts are rare. Massive, homogeneous crystal tuff or tuffaceous sandstone units can be mistaken for dioritic intrusive bodies, but locally contain thin beds of finer crystals, ash laminae, or scattered lithic clasts. Intercalated sedimentary rocks suggest that the volcaniclastic sequences are submarine.

Epilastic rocks comprise at least 10 per cent of the Stuhini Group south of Bearskin Lake. Epilastic sequences include thin to medium bedded, dark green-grey volcanic siltstone and sandstone, locally interbedded with argillite and minor limestone. Crossbedding and graded bedding occur within sandstone-argillite sections, which may be turbiditic deposits. A distinctive "ribby" weathering calcarenite is interbedded with green to purplish tuff, crossbedded tuffaceous sandstone and conglomerate on Muse Ridge.

A continuous, west-facing section, about 4 kilometres north of the Bandit showing, has a thickness of about 2000 metres. It includes a thick, lower, dominantly epilastic sequence of well-bedded, graded tuffaceous sandstone, ash tuff and lesser argillite. Within this is a conglomerate unit with fine-grained basalt and rare felsic clasts. The epilastic sequence is overlain by massive to well-bedded ash and crystal tuff with lesser pyroxene-phyric flows, which are overlain by lapilli tuff with lesser ash and crystal tuff, coarsening upward into block and lapilli tuff with amygdaloidal basalt clasts.

South of Tatsamenie Lake, the Stuhini Group consists predominantly of pyroxene-phyric mafic flows and tuffs. Intercalated sediments include white to grey limestone, black, carbonaceous, slightly fetid calcisiltite and argillite. Buff to grey ribbon chert was noted at one locality. The Stuhini Group between Sam Creek and Tatsamenie Lake is generally more intensely deformed than south of Bearskin Lake. Both steeply dipping and bedding-parallel shear fabrics are common.

Sills, dikes and plugs of megacrystic, bladed plagioclase augite(±hornblende?) porphyry intrude Stuhini volcanic rocks east of the Samotua Glacier and north of the Bandit

showing (Figure 1-11-2; Unit uTSp). Plagioclase crystals range up to 4 centimetres in length. These hypabyssal intrusions are interpreted as subvolcanic bodies within the Stuhini section.

Brittle/ductile shear fabrics are locally present in Stuhini rocks throughout the map area. Bedding-parallel schistose fabrics, augen-like sheared feldspar phenocrysts, and flattened and stretched lapilli are evident north of the Golden Bear airstrip. This area is interpreted as a contractional zone related to strike-slip faulting. Elsewhere, shear fabrics in Stuhini rocks are generally confined to steeply dipping, sharply delimited shear zones. Within these zones, intensely foliated chloritic schists contain layers and lenses of unfoliated rock. A series of such zones east of the Samotua Glacier contains steeply plunging "lozenges" of unsheared rock and steeply plunging shear-related folds with dextral asymmetry.

LOWER JURASSIC - TAKWAHONI FORMATION (IJTs)

A fault-bounded block of clastic rocks in the southeast corner of Tatsamenie Lake map area is correlated with the Takwahoni Formation (Laberge Group), after Souther (1971). The sedimentary rocks consist of dark grey to pale brown weathering, thin to medium-bedded, turbiditic, fine to coarse-grained arkosic wacke and interbedded shale and siltstone. Graded bedding, flame structures and argillite rip-ups are common. Belemnoids and small, poorly preserved ammonites and carbonized plant stems were collected from the unit, suggesting an influx of terrestrial material into a marginal marine basin. A facies of subangular to subrounded polymictic pebble to cobble conglomerate containing felsic to intermediate volcanic, chert, granodiorite and limestone clasts is intercalated with the finer sediments. Subrounded limestone clasts, up to a metre in diameter, attest to the high-energy setting for the conglomeratic facies.

Structure within the fault wedge is complex, with well-exposed folds and complex high and low-angle faults. Outcrops are locally strongly sheared and fractured, and a spaced cleavage is evident in places. Clasts in the conglomerate unit are unstrained, in contrast to those in Unit CSs.

A single collection of ammonites obtained from the Takwahoni succession in 1992 were Early Jurassic (latest Pliensbachian) in age (H.W. Tipper, personal communication, 1992). This is the most southerly occurrence of Takwahoni Group in the Tulsequah map sheet (Souther, 1971).

EOCENE - SLOKO GROUP (ESV)

Sloko Group volcanic rocks are exposed in fault-bounded blocks along the western part of the map area and in isolated areas below Miocene basalts along its eastern edge. The Sloko Group consists primarily of rhyolitic to dacitic pyroclastics, including heterolithic tuff-breccia to lapilli tuff, welded crystal-vitric tuff and ash tuff. Minor andesitic tuff is also present. Flow rocks are less common, but include plagioclase and hornblende-phyric, massive or columnar

jointed dacite. Very coarse breccias (clasts 1 m across) occur close to the bounding faults, and contain a variety of volcanic and granitoid clasts, quartz, feldspar and hornblende crystals, ash and vitric fragments. An extensive section of brown, rhyolitic volcanic glass with abundant drusy cavities is exposed north-northwest of Tatsamenie Lake.

A large, subcircular volcanic subsidence feature (here called the Samotua caldera) underlies an extensive area north of the Samotua Glacier (Figure 1-11-2). Faults bounding the eastern part of this structure dip steeply inward at 60° to 80°. The western limit is outside the map area. Stuhini rocks adjacent to the bounding faults are intensely sheared to chloritic schist, and locally brecciated by post-shearing brittle deformation. In the northwest corner of 104K/1, down-dropped blocks of Stuhini schist, up to 200 metres long, occur entirely within Sloko tuffs.

Uranium-lead dates overlapping the Paleocene-Eocene boundary have been obtained for rhyolite near Graham Inlet, 125 kilometres to the northwest (104M, M.G. Mihalynuk, unpublished data, 1992). Potassium-argon dates are slightly younger, ranging from 48 to 53 Ma for Sloko tuff in the Yehiniko Lake area and for the correlative Bennett Lake extrusive rocks (D.A. Brown, unpublished data; Lambert, 1974, respectively).

TERTIARY(?) - POLYMICTIC CONGLOMERATE (Tcg)

A poorly indurated, polymictic conglomerate forms an isolated subcrop under Miocene flows in south-central Tatsamenie Lake map area. It resembles unconsolidated gravel, however, some clasts are cemented to each other and medium-grained wacke talus was also found. The clasts include dacite, felsite and plagioclase-porphyritic andesite, believed to be derived from Sloko Group. Granitoid and pre-Stuhini phyllite clasts are also present.

The poor induration and abundance of presumable Sloko-derived clasts suggests this unit is Eocene or younger. It may correlate with Tertiary, fault-controlled deposits such as those in the Yehiniko valley (Brown and Greig, 1990) and Tuya River (Ryan, 1991) areas.

MIOCENE(?) - BASALT FLOWS (Mb)

Subhorizontal, columnar jointed olivine basalt flows occur in two areas, along the eastern edge of the map area and as a small erosional remnant southwest of Tatsamenie Lake. These basalt flows have been correlated with the Level Mountain Group (Souther, 1971). The Level Mountain edifice (Hamilton, 1981) is a continental sodic alkali basalt shield volcano. Potassium-argon dates from Level Mountain span a range 14.9 to 5.3 Ma (T.S. Hamilton, unpublished data, 1981).

Age dating of columnar jointed basalt and intercalated felsic tuff at "Shark Peak", in the southeast corner of 104K/8, suggests that at least some of the basalt flows are Eocene. At Shark Peak, thin vitric-crystal tuff lenses are overlain by columnar jointed, porphyritic olivine basalt. This is in turn overlain by a distinct white-weathering

rhyolite ash and vitric crystal-lithic lapilli tuff unit, which is capped by similar porphyritic, vesicular or amygdaloidal basalt flows (A. Panteleyev, 1964; Figure 1-11-3). A biotite K-Ar date of 54.5 ± 1.6 Ma was obtained from the middle rhyolite tuff, while whole-rock K-Ar dates of 49.0 ± 1.4 Ma and 38.9 ± 1.2 Ma were obtained from the lower and upper basalt flows (A. Panteleyev, unpublished data, 1976). The whole-rock K-Ar dates from the basalt may be significantly older than the true age due to excess radiogenic argon and isotopic fractionation during analysis (cf. Souther *et al.*, 1984). However, the stratigraphic bracketing of the Sloko-age rhyolite tuffs is good evidence for an Eocene age.

INTRUSIVE ROCKS

Intrusive rocks underlie approximately 25 per cent of the map area and fall into three broad age groups: Late Triassic, Jurassic and Eocene. Most of the southeast quadrant of the Bearskin Lake sheet is underlain by part of a large body, here called the Moosehorn batholith, which shares many attributes with the Hickman batholith in the Telegraph Creek map area. As in the Chutine River - Tahltan Lake map area, the plutons are quartz poor compared to some of those in the Scud River area. Foliation defined by aligned hornblende crystals is another characteristic of many of these plutons.

Available age constraints include Late Triassic K-Ar dates on the Kaketsa stock, just east of the project area, and two new, Late Triassic U-Pb age determinations from plutons north of the project area (Oliver and Gabites, 1993, this volume). An additional four samples are being processed for U-Pb and K-Ar dating as part of this project.

LATE TRIASSIC

MOOSEHORN BATHOLITH

The Moosehorn batholith underlies an area of about 560 square kilometres, including the entire southeast third of the

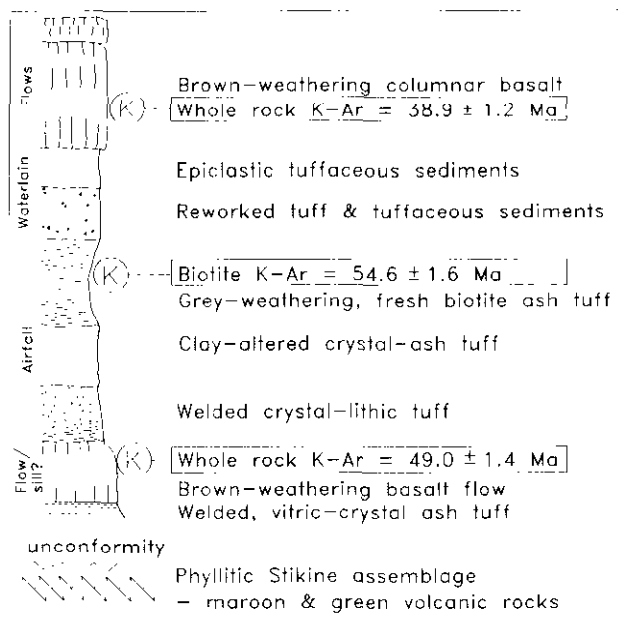


Figure 1-11-3. Schematic stratigraphic column in the Shark Peak area, from A. Panteleyev (unpublished data).

Bearskin Lake map area, and parts of the Chutine Peak (104F/16) and Kennecott Lake and Ketchum Lake (104J/4 and 5) map areas. It is characterized by massive, light to dark grey weathering, variably foliated hornblende monzodiorite to quartz monzodiorite, with minor hornblende monzonite. Up to 5 per cent primary biotite occurs in parts of the pluton, especially south of Moosehorn Lake. Patches of interstitial primary potassium feldspar are evident on cut surfaces stained with sodium cobaltinitrite. Parts of the batholith are strongly magnetic.

The Moosehorn batholith is generally unaltered, although epidote patches and stringers occur locally. A zone of fracture-controlled to pervasive epidotization with minor malachite occurs about 2 kilometres north of Moosehorn Lake. Zones of quartz-carbonate alteration are related to Tertiary high-angle faults or Sloko felsic dikes.

The batholith is correlated with the Late Triassic Stikine Plutonic Suite, which includes the Hickman (Holbek, 1988) and Hotailuh (Anderson, 1983) batholiths. The smaller Kaketsa stock, in the northwest corner of the Kennecott Lake sheet (104J/04) has been dated at 214 to 218 Ma by hornblende K-Ar (Panteleyev, 1975). The Kaketsa stock is slightly more quartz rich than the Moosehorn and is host to several porphyry copper prospects (McMillan *et al.*, 1976).

SAM BATHOLITH

The Sam batholith, so named because Sam Creek bisects the western half of the pluton, extends from Tatsamenie Lake to Camp Island Lake in the Ketchum Lake map area (104J/5). It has complicated and irregular boundaries and is lithologically more diverse than the Moosehorn batholith. It intrudes Stuhini Group and Stikine assemblage volcanic rocks. Most of the batholith is grey weathering, variably foliated hornblende diorite, grading into melonodiorite and, locally, hornblendite. Parts of the pluton are strongly magnetic. Margins of the stock are not always sharply defined, consisting of interfingering diorite and amphibolitized mafic volcanic rocks.

A compositionally and texturally heterogeneous zone of hornblendite blocks in diorite extends along the eastern edge of Highway Creek northeast to the mouth of Sam Creek. Angular, irregular hornblendite blocks comprise up to 70 per cent of the exposure, and range up to 4 metres in length. The hornblendite varies from fine to very coarse grained (crystals up to 8 cm), and locally grades into texturally variable diorite; it is interpreted to represent an early mafic phase of the batholith.

Pink and white, medium to coarse-grained granite pegmatite dikes crop out in several locations near the southernmost lobe of the Sam batholith, about 3 kilometres north-east of the Golden Bear mine. North of Fleece Creek, these occur as sigmoidal, sheared lenses in intensely chloritized mafic volcanic rocks. They may represent a late phase of the batholith.

The age of the pluton is 218 ± 3.6 Ma (Oliver and Gabites, 1993, this volume), based on zircon U-Pb dating of a sample obtained north of the project area, on the east side of Tatsamenie Lake.

SAM ULTRAMAFITE

Elongate ultramafic bodies along the southwestern edge of the Sam batholith probably represent an early or marginal phase. A marginal zone of pyroxenite and hornblende blocks and irregular blobs within the diorite grades outward into fine to coarse-grained olivine clinopyroxenite, locally with minor interstitial plagioclase. The western contact of the largest of the ultramafites is faulted, with serpentinite along the fault. Fibrous serpentinite occurs in narrow veinlets in one of the smaller ultramafic pods. The Sam ultramafite is correlated with the Polaris Ultramafic Suite, which includes Alaskan-type ultramafites, such as the Gnat Lakes and Hickman ultramafic complexes (Nixon *et al.*, 1989). Differences include the lack of a concentric zoning and the absence of dunite at the Sam body.

Previous interpretations considered these ultramafic bodies to be slivers within deep-seated fault zones which delineated the northern extent of the fault systems.

MIDDLE(?) JURASSIC RAMTUT STOCK

The Ramtut stock comprises a quartz monzonite phase and an "albitite" phase, which intrude weakly foliated hornblende diorite of probable Late Triassic age. The diorite is similar compositionally and texturally to the Moosehorn batholith. The quartz monzonite, interpreted as Early Tertiary by Wheeler and McFeeley (1991), is believed to be Middle Jurassic, on the basis of its unfoliated character, sharp contacts, and relationship to the albitite phase, from which a whole-rock K-Ar date of 171 ± 6 Ma was obtained (Hewgill, 1985). The quartz monzonite phase has been sampled for U-Pb and K-Ar dating.

QUARTZ MONZONITE PHASE

Medium to fine-grained hornblende quartz monzonite underlies a triangular peak northeast of Misty Mountain. It appears to grade westward into the albitite phase. In contrast to the Triassic plutons, the Ramtut stock is massive and unfoliated, with sharp, discordant contacts. Contact metamorphic effects include actinolite needles identified up to 3 kilometres away from the intrusion, and skarnified limestone and calcareous tuff at the toe of the glacier north of Misty Mountain.

ALBITITE PHASE

The albitite phase is a sill-like projection from the Ramtut stock which follows the contact between Upper Carboniferous phyllite and carbonate and overlying mafic tuff. It comprises euhedral albite and quartz in a fine-grained groundmass of albite, quartz and hornblende, together with accessory apatite, sphene and ilmenite (Hewgill, 1985). The albite content varies from 60 to 95 per cent, and texture varies from porphyritic to subequigranular. Bright green hornblende is variably chloritized. Comparison of major element analyses of the albitite and quartz monzonite shows an increase in Na_2O (to an average of 8.8%) in the albitite with a corresponding decrease in K_2O (Hewgill, 1985). The albitite is interpreted as a product of magmatic-hydrothermal sodium metasomatism.

MINOR INTRUSIONS

Numerous plagioclase porphyry and hornblende plagioclase porphyry dikes crop out east of the Ramtut stock near the West Wall fault. A Middle to Late Jurassic age for some of these dikes is inferred on the basis of a hornblende K-Ar date of 156 ± 5 Ma (Schroeter, 1987).

Numerous small plugs and dikes of possible Jurassic or Eocene age intrude the western margin of the Moosehorn batholith. Many of them are buff to orange-weathering, subcrowded plagioclase-phyric monzonite to quartz monzonite with small primary biotite and hornblende grains. Abundant fine-grained potassium feldspar in the groundmass may be of secondary origin. A strong carbonate-sericite alteration overprint is common.

Coarse-grained hornblende gabbro outcropping northeast of the mine above the Bearskin slide was assigned a Jurassic age by Oliver and Hodgson (1989), presumably because of its lack of a tectonic foliation.

TERTIARY

The voluminous Eocene plutons that comprise much of the Coast Belt lie west of the map boundary; however, two small granitic stocks, and numerous plagioclase-porphyrific and felsite dikes are interpreted to be related to this intrusive suite.

SAMOTUA GLACIER STOCK

A small (10 Km²), plagioclase-phyric granodiorite stock underlies the eastern side of the lower part of the Samotua Glacier, along the margin of the Samotua caldera. The stock comprises medium-grained, subcrowded to uncrowded plagioclase porphyry, with 25 to 75 per cent plagioclase phenocrysts up to 1 centimetre long in a matrix of plagioclase, quartz, minor potassium feldspar and up to 15 per cent biotite and hornblende.

SHESLAY STOCK

The Sheslay stock intrudes Permian (?) limestone, mafic metavolcanic rocks and the Moosehorn batholith in the southeast corner of 104K/1. The stock consists of massive, very fresh, coarse-grained, potassium feldspar megacrystic biotite hornblende granite. Prominent jointing is characteristic here as in other Eocene plutons west of the Stikine River (Brown and Gunning, 1889).

MINOR INTRUSIONS

Dikes of probable Sloko age occur throughout the map area. These are commonly plagioclase and/or quartz-phyric rhyolite or dacite, ranging up to 10 metres wide. A swarm of felsic dikes occurs along the margin of the Samotua caldera, dipping steeply inward toward the bounding faults. These dikes also intrude Sloko pyroclastic rocks, and therefore represent a late stage of caldera development. A prominent iron carbonate alteration halo extends about 30 metres into mafic volcanic rocks (Unit CSv) on either side of a 10-metre-wide Sloko rhyolite dike, 2 kilometres south of the Bandit showing. A narrow swarm of buff-weathering, locally silicified dacitic dikes trending northeasterly across

the Moosehorn batholith 9 kilometres south of Moosehorn Lake is also included in this suite. Elsewhere, Sloko dikes are locally clay-altered and associated with silicified, pyritized or clay-altered haloes. These examples indicate that at least some of the prominent alteration zones in the area can be attributed to Eocene intrusions and hydrothermal activity.

STRUCTURE

Structural interpretation of the Golden Bear area is hindered by the lack of stratigraphic control in sub-Stuhini units and by the paucity of Jurassic or younger stratigraphy. Inversion of stratigraphy beneath the basal Stuhini unconformity, and a significantly greater amount of strain in rocks of the Stikine assemblage is consistent with at least one and possibly two pre-Late Triassic phases of deformation, followed by an erosional interval. Post-Stuhini, Early Jurassic deformation is consistent with an Early to Middle Jurassic age for mineralization at Golden Bear. Faulting is complex and dominated by a strike-slip regime. Preliminary interpretation of timing of various deformation events relative to stratigraphy and intrusive episodes is illustrated in Figure 1-11-4.

FOLDING

PHASE 1 (D₁)

The oldest structures recognized are centimetre to metre-scale recumbent isoclinal folds (F₁) of compositional layering. These are especially common in thin-bedded siliceous phyllite and carbonate of Unit uCSvs1, but occur in all pre-Stuhini lithologies. A micaceous penetrative fabric (S₁) parallels axial planes of F₁ folds (Plate 1-11-1). The orientations of D₁ folds and fabrics vary widely, depending on the effects of later folding. No large-scale recumbent structures were defined, but their presence could explain possible inversion of Paleozoic stratigraphy at Sam Creek. Alternatively, if the basal contact of Unit uCSvs1 is a thrust, thrusting may have occurred during D₁, as the contact is deformed by F₂ folds (Figure 1-11-2). Age of D₁ is loosely constrained as post-Early Permian to pre-Late Triassic.

PHASE 2 (D₂)

Penetrative fabrics developed during Phase 1 deformation are refolded by Phase 2 chevron folds (F₂). Phase 2 folds are upright to gently dipping, gently to moderately plunging, tight to open folds. Penetrative fabric development associated with Phase 2 deformation is uncommon, although a spaced cleavage (S₂) is evident locally. Phase 2 linear fabrics, including mullions, crenulation lineations, mineral lineations and stretched clasts, are common in lithologies with well developed S₁ foliations. The stretching direction is colinear with F₂ fold axes.

Small-scale F₂ folds are ubiquitous in thin-bedded lithologies of Units CSv and CSvs along the Samotua River and south of the Bandit showing. Orientation of these folds varies widely between domains. A domain of tight, north to northeast-trending F₂ folds with an east-vergent asymmetry occurs west of the Moosehorn batholith along the Samotua

River. Folds of very similar structural style trend east-northeast, south of the Bandit showing. The differing orientations may reflect pre-existing F₁ fold shapes. At Sam Creek, a series of northwest-plunging antiforms and synforms deforms the contact between Units uCSvs1 and uCSvs1.

Unequivocal F₂ folds were not observed in Stuhini Group rocks, and no major F₂ fold axes were traceable from the Stikine assemblage into the Stuhini Group. The intensity of F₂ folding in Unit CSv implies significantly greater contraction in Stikine assemblage than Stuhini Group rocks. These observations suggest that D₂ may represent a second episode of pre-Stuhini deformation. Although truncations of F₂ folds were not observed at the basal Stuhini unconformity, at the Bandit showing, steeply dipping, foliated Stikine assemblage metavolcanic rocks locally underlie gently dipping, unfoliated Stuhini Group pyroxene crystal-lithic tuff. North of Sam Creek, Stuhini bedding is structurally conformable with S₁ foliations and recumbent isoclinal fold axial planes in the underlying Stikine assemblage.

PHASE 3 (D₃)

Evidence for a third phase of folding is found at Sam Creek, where an open, northeast-trending fold ("Sam Creek

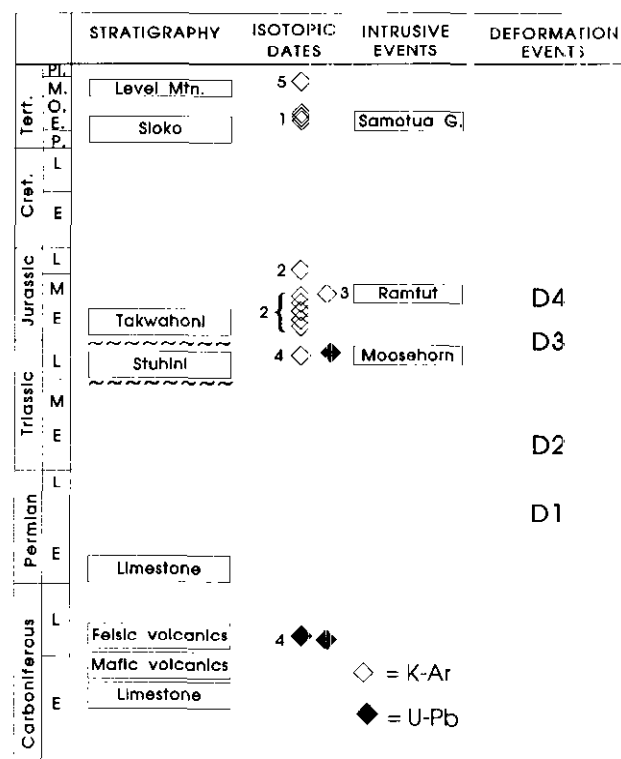


Figure 1-11-4. Schematic stratigraphic column compared with regional intrusive and deformational events. Isotopic dates are from: (1) Panteleyev (unpublished data); (2) Schroeter (1987); (3) Hewgill (1985); (4) Oliver and Gabites (1993, this volume); (5) Hamilton (unpublished data). Preliminary attempts to delineate the structural features of the map area suggest: D₁=recumbent and isoclinal folding (also thrusting?); D₂=folding metamorphic foliations, chevron-style; D₃=refolding to produce D₂/D₃ interference patterns; and D₄=folds and faults in Takwahoni Formation.



Plate 1-11-1. Phase I recumbant isoclinal folds, Unit uCSvs1, southwest of Misty Mountain.

antiform") is defined by a conspicuous limestone unit in chloritic metavolcanic rocks (Unit CSv). This fold, and related northeast-trending folds above Bearskin Lake, clearly involve rocks interpreted here as Stuhini Group. Interference between F_2 and F_3 folds produces a broad dispersion of S_{0-1} fabrics, and a square, domal surface exposure of the Permian limestone. Phase 3 folding modifies the orientation of F_2 axes, which are commonly doubly plunging throughout the map area. Variable orientations observed for F_2 fold axes are compatible with broad, chevron-style refolds, although this variation may also be due to the influence of F_1 fold geometries.

There is no overlying Jurassic stratigraphy to constrain the timing of D_3 . However, if mineralization at Golden Bear is late Early to Middle Jurassic, then it is probable that deformation involving Stuhini Group took place in latest Triassic to Early Jurassic time. This might have involved both F_3 folding and sinistral (?) movement along the "Ophir break". Evidence for Norian to Hettangian deformation has recently been documented in the Iskut area (Henderson *et al.*, 1992), and post-Norian, pre-Toarcian deformation is described in the Yehiniko Lake area (Brown and Greig, 1990).

PHASE 4 (D_4)

If pre-mineral deformation at Golden Bear is Early Jurassic, then east-trending chevron folds and faults in the Pliensbachian Takwahoni Formation probably represent a fourth phase of deformation. South-directed folding and thrusting south of the King Salmon fault is linked to Middle

Jurassic (Bajocian) convergence of the Cache Creek and Stikine terranes (Gabrielse, 1991). Deformation of the Takwahoni may plausibly be ascribed to this event.

Late kink and box folds of highly variable orientation (but generally trending northeast to southeast) affect most of the phyllitic rocks. These may also be related to the Middle Jurassic event, although a younger (Tertiary?) extensional origin is also possible.

FAULTS

Faulting in the Golden Bear area is dominated by north to northwest-trending high-angle, strike-slip faults, which are significant in representing first order structural controls on gold mineralization. Excellent exposures in the Golden Bear open pit (Plate 1-11-2) shed some light on the structural style of these faults, but the direction and amount of slip are controversial. A northeast-trending, dextral fault (Moosehorn fault) bounds the west side of the Moosehorn batholith, and post-dates the north to northwest-trending faults. Eocene normal faults bound the Samotua caldera, and coeval faults affect older units to the east.

OPHIR BREAK

The "Ophir break" is an economically important fault zone that extends at least 15 kilometres from Bearskin Lake to Tatsamenie Lake, and possibly another 10 kilometres to the Samotua River. The break is the primary structural control for the Golden Bear deposit. In the mine area, it comprises several anastomosing fault strands across a width

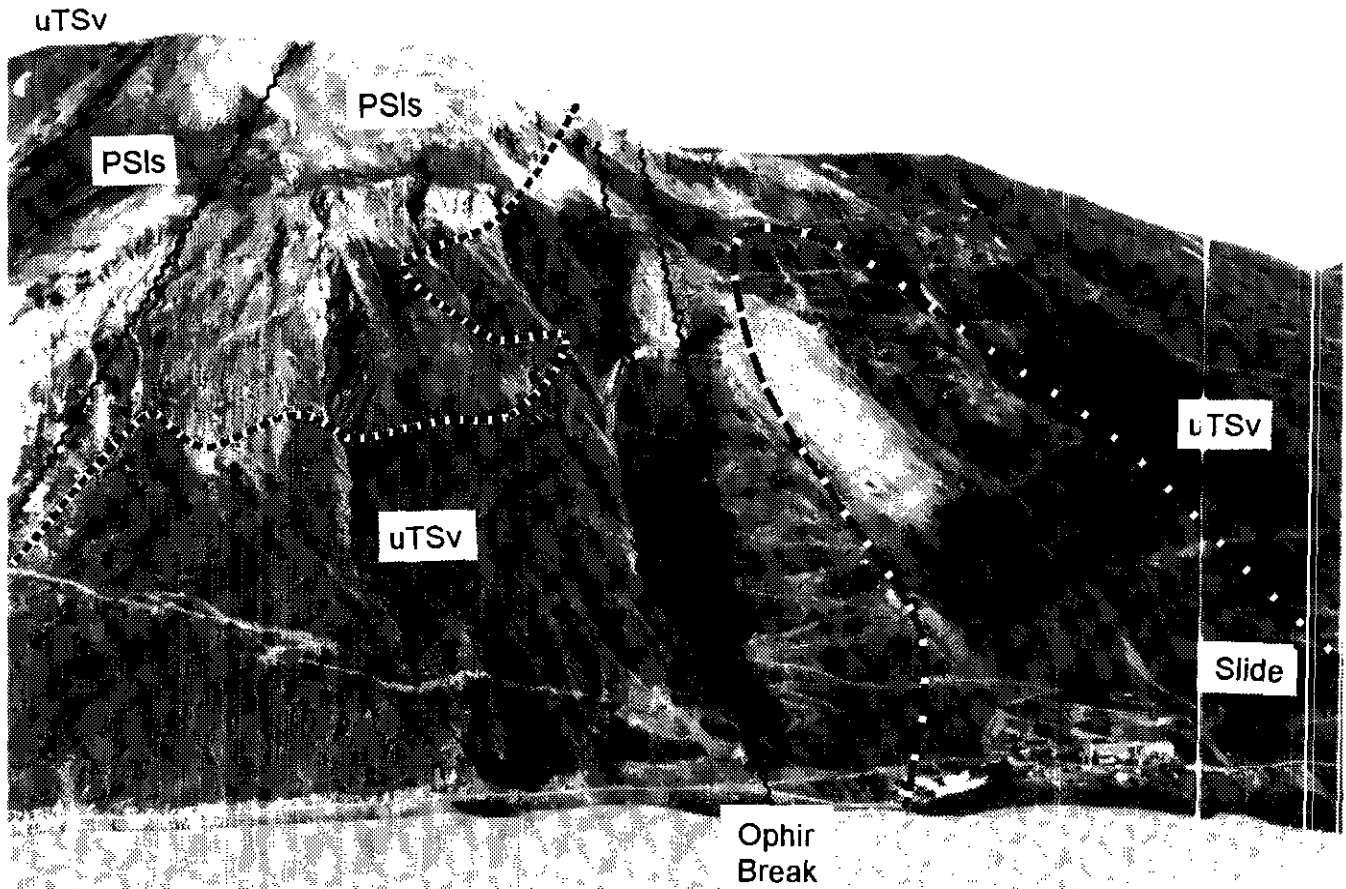


Plate 1-11-2. Golden Bear mine area, north side of Bearskin Lake, illustrating the main fault structures that comprise part of the Ophir break.

of 50 to 100 metres or more. Fault dips within the zone range from 65° to the east through vertical to locally overturned to the west. Small-scale flats along fault bends are believed to constitute dilational zones significant in localizing gold deposition (Schroeter, 1986), suggesting local reverse slip. Faults in the mine area typically comprise up to several metres of brecciated pyritic rock and sulphide-rich gouge.

Fault strands in the deposit area bound at least two major silicified carbonate lenses. The main carbonate lens in the pit is up to 50 metres wide, and is in contact across the Bear fault with carbonate-altered Stuhini Group mafic volcanic rocks to the east (Plate 1-11-2). About 1.5 kilometres north of the mine, in the Fleece Bowl area, the break diverges into two main strands, the eastern Black fault and the western Fleece fault. The Fleece fault is called the West Wall fault north of Sam Creek (Figure 1-11-2)

Fault grooves and slickensides on faults along the Ophir break have dominantly shallow plunges. Reconstruction of offsets required to produce the Totem silicified carbonate lens and the smaller lenses in the deposit area suggests the possibility of both sinistral and dextral motion at different times. Faults bounding the Totem lens dip steeply outward, giving the lens an "inverted canoe" morphology (D. Reddy, personal communication, 1992). Its configuration suggests a possibility for oblique-sinistral slip along the west-dipping

fault which is the western boundary to the lens. Dextral slip, on the order of 1500 metres, could produce the series of smaller carbonate lenses which occur south of the intersection of the fault zone with the main body of Permian limestone.

Timing of movement along the Ophir break is poorly constrained. Although it clearly cuts Stuhini Group, it is possible that pre-Stuhini faulting accompanied F_1 and F_2 folding. The main period of strike-slip movement post-dated Stuhini Group, possibly accompanying F_3 folding in a transpressional tectonic regime. This is consistent with an Early to Middle Jurassic (Schroeter, 1987) age for the main period of mineralization. Post-mineral fault movement is indicated by the juxtaposition of intensely silicified carbonate and very weakly altered volcanic rock at Totem, as well as by brecciated silicified limestone and pyritic gouge within brittle shears. Latest motion could be Eocene or younger.

FAULTS WEST OF THE OPHIR BREAK

Northwest-trending, left-stepping en echelon dextral faults bound a contractional zone northwest of Bearskin Lake. The Limestone Creek fault juxtaposes Permian limestone on the east with Stuhini Group on the west at the west end of the lake. Feldspar-phyric basalt west of the fault contains a strong, south-dipping shear fabric with asym-

metrical porphyroblasts indicating top-to-the-north shear. Shear fabrics die out down-section to the north. About 4 kilometres to the north, felsic phyllites correlated with Unit uCSvs1 overlie mafic to intermediate metavolcanics along a steep reverse fault. Feldspar and augite-phyric tuffs and diorite in the footwall of this fault are also strongly sheared, with asymmetric feldspar porphyroblasts again indicating top-to-the-north motion. Steeply plunging fault lineations along the Limestone Creek fault indicate probable late (Eocene?) normal slip.

HIGHWAY FAULT

The Highway fault (so-called because it parallels Highway Creek in south-central 104K/8) trends subparallel to the Ophir break and dips steeply to the northeast. East of the mine, in the Fleece Creek area, the Highway fault has an apparent reverse sense of motion, putting hangingwall Stikine assemblage foliated volcanic rocks, phyllite and limestone on Stuhini Group mafic ash tuff. North of Sam Creek, the Highway fault forms a prominent linear of brecciated, iron carbonate altered rock where it cuts through the Sam batholith. The partially fault-bounded sliver of limestone south of Sam Creek may represent the sheared-out limb of an F_2 fold. South of Bearskin Creek, the Highway fault appears to split into several splays with an apparent reverse sense of motion, while changing in orientation from north to northwest. This is consistent with dextral slip.

MOOSEHORN FAULT

The Moosehorn fault is a north-northeast trending zone of brittle and brittle-ductile shearing intruded by numerous dikes along the west side of the Moosehorn batholith. Iron carbonate and hematitic alteration, silicification and brecciation affect some of the intrusive rocks along the fault. Copper mineralization associated with intense quartz-carbonate alteration and quartz veining was noted within the fault zone west of Moosehorn Lake. In the northeast corner of 104K/1 the fault curves toward a more easterly orientation. Dextral slip is inferred by preservation of a down-dropped block of Takwahoni sediments in an extensional fault-bend graben in this area, and by the northeast-trending dike swarm south of Moosehorn Lake.

MINERAL OCCURRENCES

Prior to this study, 25 known showings in the project area were listed in MINFILE. The most striking visual features are prominent brown-weathering and extensive iron carbonate alteration zones, including those mapped by Souther (1971) on the north and east side of Tatsamenie Lake. Known showings and alteration zones are shown in Figure 1-11-5. The most significant category of showings, which includes the Golden Bear mine, consists of silicified zones in limestone that are associated with high-angle faults and contacts with volcanic rocks. Occurrences are summarized in Table 1-11-1.

STRUCTURALLY CONTROLLED SILICIFIED ZONES IN LIMESTONE

The Golden Bear deposit is one of several silicified zones in carbonate hostrocks in the map area. Others include the

Fleece and Totem zones on the Ophir break, the Ram-Tut and Slam, as well as new zones in the Sheslay limestone (southeast corner of 104K/1; Figure 1-11-5), and west of Shark Peak (southeast corner of 104K/8). Mineralization occurs as irregular, fine-grained silica replacement zones with lesser dolomite, rather than as discrete quartz zones. Skarn mineralogy is absent. Multiple phases of silicification are indicated by silica-healed breccias. Chalcedonic quartz is present at the Slam showing, and may occur at Golden Bear (D. Reddy, personal communication, 1992). Volcanic rocks in fault contact with silicified zones are commonly iron carbonate or pyrite-sericite-chlorite altered.

Significant differences exist among the showings in this category. Golden Bear and Fleece are unique in having gold grades in excess of 8 grams per tonne, while only erratic values in the 1 to 3 grams per tonne range have been obtained from the Totem, Slam and Ram-Tut prospects. At Golden Bear, while good grades are obtained in silicified limestone, a significant portion of the ore is pyritic fault gouge, suggesting possible upgrading of gold values during post-mineral faulting. Golden Bear and, to a lesser extent, Fleece, contain abundant pyrite, while Totem and Slam are sulphide poor. A small massive sulphide pod has been reported at Ram-Tut. Golden Bear and Fleece are characterized by a typical epithermal geochemical signature (elevated Ag, As, Sb, Hg and Te) and no base metals. Slam is similar, although tellurium has not been reported, while Ram-Tut contains both high arsenic, antimony and mercury and local base metals (Zn, Pb and Cu). It is not known whether the base metal and precious metal mineralization at Ram-Tut represent a single mineralizing event.

The Golden Bear, Fleece and Totem zones all have an obvious relationship to faulting along the Ophir break, which has controlled emplacement of fault-bounded carbonate lenses as well as creating pathways for hydrothermal fluids. Ram-Tut and Slam also appear to be associated with high-angle faults. At Ram-Tut, brecciation and silicification are concentrated along the contact between Permian limestone and structurally overlying phyllitic rocks.

Various relationships to intrusions are evident, making generalizations about timing controversial. At Golden Bear, Fleece and Totem, five K-Ar dates on sericitic alteration range from 177 to 205 Ma (Schroeter, 1987), providing strong evidence for an Early to Middle Jurassic mineralizing event. Mineralization at Ram-Tut occurs beneath the albitized phase of the Ramtut stock, suggesting a possible relationship with Jurassic intrusive activity. At Slam, clay-altered Eocene quartz feldspar porphyry dikes trending subparallel to major fault structures occur within the main silicified zone. At Fleece, a Tertiary (?) sericite-pyrite-altered feldspar porphyry dike is mineralized in the hangingwall of the Fleece fault. This suggests that at least some hydrothermal remobilization of gold occurred in the Tertiary, possibly due to Eocene motion along the Ophir break together with coeval intrusion of Sloko dikes.

The Ramtut stock represents the only surface expression of Jurassic plutonism in the map area. A genetic link with the Golden Bear deposit is possible, but difficult to prove. Better data on the age of the pluton and tighter constraints on timing of mineralization are needed. Analysis of regional

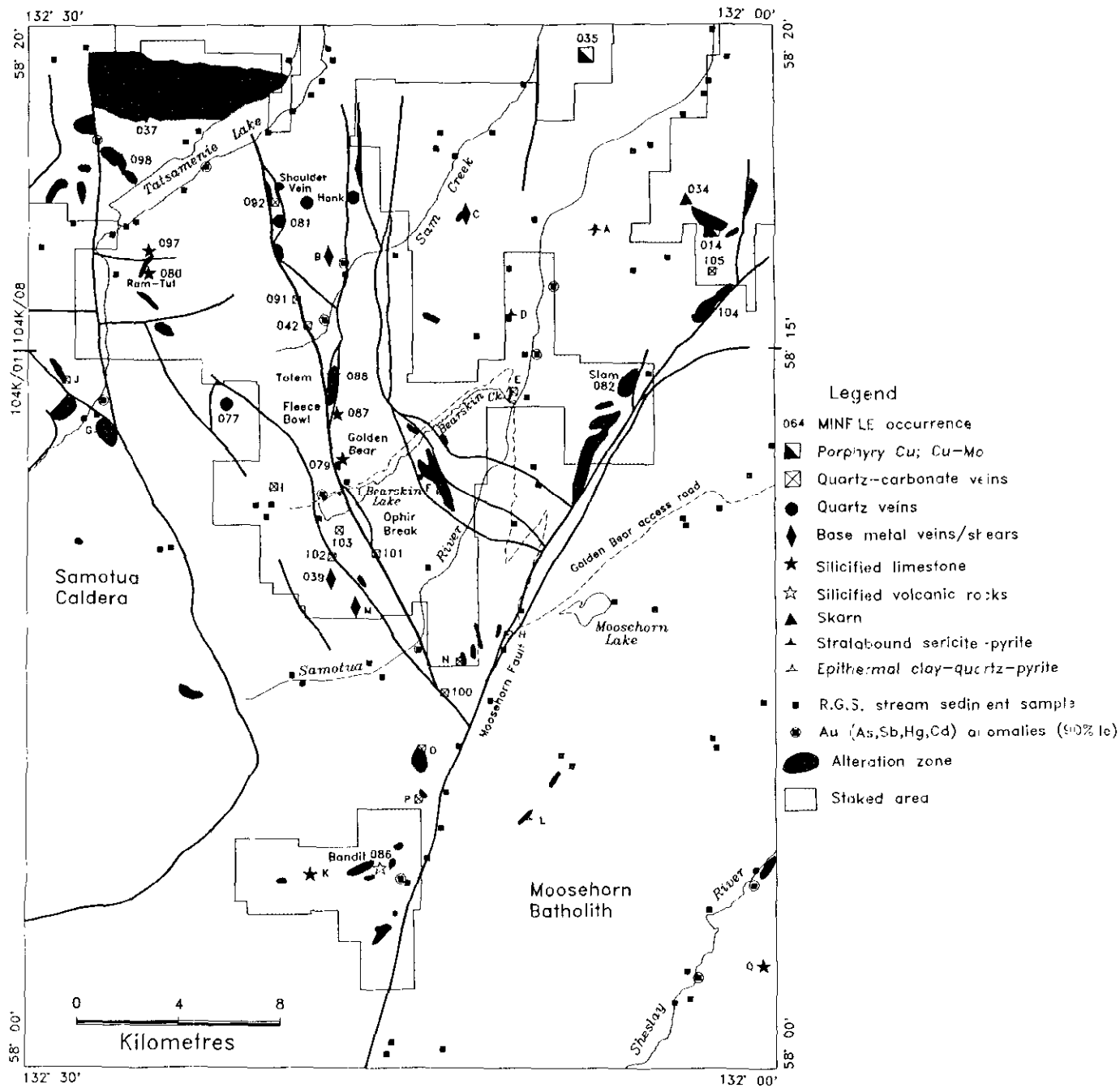


Figure 1-11-5. Mineral occurrence localities from MINFILE database, RGS sample sites, and approximate claim distribution illustrated by hatched area (based on June, 1992 records). Occurrences are described in Table 1-11-1.

geochemical survey (RGS) stream-sediment geochemistry for the project area shows that seven out of twelve multi-element anomalies involving gold, silver, arsenic, antimony, copper, lead and zinc occur in drainages centred on the Ramtut stock. This suggests that it may represent the thermal centre which generated hydrothermal fluid circulation focused along major faults as far away as Golden Bear. However, the evidence presented above suggests that this style of mineralization may also be related to Eocene intrusive activity.

IRON CARBONATE (-QUARTZ - SULPHIDE - ALBITE - K-FELDSPAR - HEMATITE) ZONES IN VOLCANIC ROCKS AND INTRUSIONS

Large gossans are widespread in volcanic rocks throughout the project area, from the north side of Taisamenie Lake to the Bandit property at the south end of the Bearskin Lake map area. For the most part, these zones are controlled by steep north-northwest-trending faults, although north of Taisamenie Lake an east-west structural

TABLE 1-11-1A
DESCRIPTIONS OF MINERAL OCCURRENCES IN THE BEARSKIN LAKE MAP AREA (104K/1) NTS ZONE 08

MINFILE	Name	UTM	Description	References
104K 039 104K 101-3	Oro, Tan 3-4	6450550 N 659150 E	Sheared mafic volcanics and diorite with disseminated and fracture-controlled chalcopyrite.	Simpson and Jones (1984a)
104K 077	Thor	6457150 N 654450 E	Siliceous phyllite and carbonaceous phyllite with minor tetrahedrite in silicified zones. Up to 58.9 g/t Ag (grab sample).	Thicke and Shannon (1983)
104K 079	Golden Bear	6455200 N 659100 E	Silicified carbonate lenses and fault gouge along a north trending fault zone have yielded over 3.5 million grams Au (1989-1992).	Schroeter, (1986)
104K 082	Slam	6458400 N 670300 E	Silicified zone 200 x 30 m in limestone, locally brecciated with chalcadonic quartz veining; associated with clay-altered Eocene dikes. Values to 1.3 g/t Au/1 m (chip sample).	Thicke and Shannon (1983)
104K 086	Bandit	6439150 N 660750 E	Silicification and pyritization along alteration/vein zone 50 x 1000 m in Stuhini Group tuffs, with Au values to 4.7 g/t/2 m. Two ddh.	Thicke and Shannon (1982)
104K 087	Fleece Bowl	6457050 N 658900 E	Silicified carbonate lenses and fault gouge along a north-trending fault zone. Indicated (probable) reserves: 416,000 tonnes of 8.2 g/t Au.	Schroeter, (1986)
104K 088	Totem	6458600 N 658800 E	200 x 1000 metre zone of intensely silicified limestone; minor pyrite; locally intense stratabound and crosscutting breccias.	Schroeter, (1986)
104K 100	Oro 4	6446450 N 663650 E	Quartz-carbonate veins and alteration zones in Stuhini Group tuffs. Pyritized tuff with 2.3 g/t Au (grab).	Simpson and Jones (1984b)
	E	6458000 N 665700 E	Quartz-carbonate epithermal breccias and veins in slates; trace pyrite.	
	F	6454000 N 663300 E	Quartz-carbonate-hematite-clay alteration in Stuhini Group tuffs; 300 x 1500 metres; pyrite stringers.	
	G	6456000 N 650000 E	Clay-quartz-pyrite alteration in Sloko Group felsic tuffs along caldera margin faults.	
	H	6448500 N 665800 E	Fine grained sulphides and quartz with malachite in steeply dipping fault zone along edge of Moosehorn batholith; associated with Tertiary dikes; 5 ppm Ag (grab).	
	I	6453900 N 656800 E	Quartz vein with 5% pyrite, chalcopyrite, in strongly fractured mafics; 1.08% Cu (grab).	
	J	6457900 N 648150 E	1.0 km long gossan in Stuhini Group with 1-3% disseminated and fracture controlled pyrite.	
	K	6439150 N 658550 E	Clay altered, silicified, carbon-rich fault breccia.	
	L	6441500 N 666900 E	Clay altered felsite dikes with chalcadonic quartz veining, trace pyrite cut Moosehorn batholith.	
	M	6450100 N 660100 E	Fractured, chloritized mafic volcanics with 2% disseminated pyrite, chalcopyrite; 0.32% Cu (grab).	
	N	6447050 N 664100 E	Quartz vein 0.5 m wide with chalcopyrite in tuff, argillite; 0.26% Cu (grab).	
	O	6444000 N 662600 E	Quartz-carbonate veins with pyrite, tetrahedrite in iron-carbonate altered tuffs; 1.17 g/t Au, 0.84% As (grab).	
	P	6442500 N 663000 E	Chalcopyrite-pyrite-epidote in fractures in aphanitic mafic volcanics; 1.24% Cu, 3.0 ppm Ag (grab).	
	Q	6436000 N 676500 E	Variably silicified and brecciated limestone; minor sulphide.	

TABLE 1-11-1B
DESCRIPTIONS OF MINERAL OCCURRENCES IN THE SOUTHERN TATSAMENIE LAKE MAP AREAS (104K/8) NTI, ZONE 03

MINFILE	Name	UTM	Description	References
104K 014	Fae	6464800 N 673500 E	Clay alteration, quartz veining with pyrite, molybdenite, chalcopyrite in quartz feldspar porphyry quartz monzonite stock. 0.024% Mo, 0.026% Cu/24 m (chip sample).	Stevenson (1976)
104K 034	Norm	6465660 N 672800 E	Magnetite pods up to 3 m wide along quartz monzonite-limestone contact; minor pyrite, chalcopyrite.	Stevenson (1972)
104K 035	Bing	6471500 N 668200 E	Disseminated chalcopyrite-molybdenite in quartz-feldspar alteration zones; skarn with pyrite, chalcopyrite, molybdenite adjacent to feldspar porphyry stock.	Grath (1965)
104K 037	Tot 2	6468250 N 650900 E	Chalcopyrite veinlet to 10 cm wide in chlorite schist; assayed > 1.0% Cu, 14.8 g/t Ag.	Brown and Valton (1983b)
104K 042	Sam	6460450 N 657650 E	Pyrite, arsenopyrite, stibnite in quartz-carbonate veinlets in metavolcanics.	Sannon (1982)
104K 080 104K 097	Ram, Tut	6462310 N 651120 E	Disseminated and fracture-controlled pyrite, stibnite, tetrahedrite and semimassive sphalerite in silicified brecciated zones near top of limestone. Six ddh, with values to 2.4 g/t Au, 33.5 g/t Ag/1.6 m.	Bisset (1984)
104K 081	Two Ounce Notch	6464400 N 656400 E	North-trending quartz vein up to 1 m wide with semimassive pyrite in graphitic sediments along the West Wall fault. Up to 14.0 g/t Au/0.3 m.	Saw (1984)
104K 091	Misty	6461400 N 657200 E	Scattered Au values to 10.0 g/t in pyritized tuff near West Wall Fault.	Brown and Valton (1983a)
104K 092	Spire, Nie 3	6465500 N 656300 E	Quartz-carbonate breccia zones with pyrite, sphalerite, chalcopyrite, galena. Up to 2.7 g/t Au, 13.8% Zn in grab samples.	McBean (1990)
104K 098	Tot	6465880 N 650450 E	Pyrite, chalcopyrite, stibnite in phyllitic felsic volcanics cut by fault. One ddh with up to 3.81 g/t Au/2.26 m.	Moat and Valton (1987)
104K 104	Taker	6461800 N 673450 E	Iron carbonate altered metatuffs with up to 2.7 g/t Au in grab samples.	Valton (1984b)
104K 105	Giver	6463150 N 673500 E	Iron carbonate altered metatuffs with up to 7.3 g/t Au in grab samples.	Valton (1984b)
	Honk	6465800 N 659200 E	Quartz vein with semimassive pyrite, local chalcopyrite in sheared mafics. Up to 18.1 g/t Au in grab samples.	McBean (1990)
	Shoulder Vein	6464200 N 657400 E	Quartz veins with semimassive Pyrite, Gn, stibnite, Chalcopyrite, Sp in chloritized mafics. Up to 15.3 g/t Au in grab samples.	McBean (1990)
	A	6464500 N 668850 E	Stratabound quartz-sericite-pyrite alteration zone in foliated mafic volcanics; 3.0 ppm Ag (grab).	
	B	6463000 N 658550 E	Semimassive pyrrhotite, chalcopyrite in sheared, silicified diorite, mafics along shear; 6 ppm Ag, 1.48% Cu (grab).	
	C	6464800 N 663450 E	150 x 300 metre gossan in sheared diorite; up to 10% pyrite, pyrrhotite.	
	D	6460450 N 664500 E	Stratabound quartz-sericite-pyrite alteration in foliated mafic tuff and limestone; cm-thick pyrite-arsenopyrite layers; trace chalcopyrite.	

grain becomes more prominent. Lithologies represent a significant secondary control, as on Tangent Ridge, where alteration is locally subparallel to bedding in Stuhini tuff.

These zones comprise a variety of alteration assemblages, including iron carbonate, quartz-carbonate, quartz-carbonate-pyrite, and quartz-sericite-pyrite. Iron carbonate alteration appears to be the most common, although some iron carbonate zones contain quartz vein and silicified breccia zones, representing more tightly focused, higher temperature portions of the systems. At the Bandit prospect, silicified zones contain significant albitic alteration (J. Howe, personal communication, 1992): albite or potassium feldspar may be more widespread in many of these zones. Quartz-poor, carbonate-rich assemblages tend to have very little sulphide, although specular hematite is ubiquitous. Quartz veins commonly contain pyrite and tetrahedrite, with stibnite reported from several localities.

Several quartz veins with gold and base metal sulphides occur north of Sam Creek between the Highway fault and the Ramtut stock. These include the Two Ounce Notch, Shoulder Vein and Honk showings. Semimassive pyrite, lesser chalcopyrite, and locally sphalerite, galena and stibnite occur in these veins, which locally contain gold in excess of 15 grams per tonne.

Numerous shear zones with chlorite-pyrite or iron carbonate alteration contain fracture controlled and disseminated chalcopyrite. These are most common in the Stuhini Group, especially on Muse Ridge west of the Highway fault, and in Late Triassic diorite. Although widespread, these do not appear to represent systems of appreciable size.

The iron carbonate gossans were probably produced by the same hydrothermal systems that produced silicified zones in carbonate hostrocks. The different style of alteration reflects lithological control. Evidence for timing of mineralization in these zones is equally equivocal. Although Sloko-age dikes are associated with some of these zones, it is not always clear that there is a genetic link. It is possible that more deeply seated Jurassic intrusions were heat sources for most of these systems.

STRATABOUND PYRITIC ALTERATION ZONES IN STIKINE ASSEMBLAGE VOLCANIC ROCKS (VMS ?)

A previously unreported, prominent pyritic alteration zone occurs in Stikine assemblage foliated mafic to intermediate tuff east of the Samotua antiform in southeastern 104K/8. The metavolcanic rocks structurally underlie cherty argillite in a tightly folded sequence. The alteration zone is up to 10 metres thick, subparallel to foliation and compositional layering, and is exposed along a strike length of at least 50 metres. Assemblages grade from chlorite-pyrite with minor epidote and carbonate, to sericite-pyrite and quartz-sericite-pyrite. Up to 5 per cent disseminated pyrite occurs locally. Although no massive sulphide is exposed at this location, the style and orientation of this alteration zone suggest the possibility of a volcanogenic massive sulphide system. A similar, thinner stratabound alteration zone with centimetre-thick pyrite-arsenopyrite layers was noted near

the southeast edge of the Sam batholith north of the Golden Bear mine road.

The volcanogenic massive sulphide potential of Paleozoic volcanic rocks of northern Stikinia is well known; however, very little exploration for this type of deposit has been done in the southeastern quarter of the Tulsequah sheet.

CLAY (-PYRITE) ALTERATION ZONES IN SLOKO GROUP

Several conspicuous acid sulphate alteration zones up to 1 kilometre across are exposed along the margin of the Samotua caldera in Sloko Group lapilli tuff and breccia. Alteration is dominated by clay, with minor sericite, quartz, and locally 2 to 3 per cent disseminated pyrite. Hydrothermal activity was probably late synvolcanic, with fluids focused along active faults near the caldera margin. Similar alteration occurs locally as haloes around Sloko dikes cutting volcanic rocks or diorite. Little exploration has been done on Sloko volcanic rocks in the project area, although the geologic setting suggests potential for both bulk-tonnage and bonanza epithermal gold mineralization.

PORPHYRY COPPER AND MOLYBDENUM

Several porphyry copper and molybdenum occurrences in southeastern 104K/8 and northwestern 104J/4 were explored in the 1960s and 1970s. Molybdenum-copper showings include the Fae (MINFILE 104K 014) and Bing (104K 035). Although neither showing was visited, mapping in the vicinity suggests that both are related to young (probably Eocene) quartz monzonite porphyry intrusions (cf. Souther, 1971). Very fresh dikes intruding Triassic diorite and Stikine assemblage near the Bing showing contain embayed quartz and abundant fine-grained biotite. Near the Fae prospect, an intensely clay-altered feldspar porphyry cut by quartz stockworks is interpreted as an Eocene plug. Work by Kennco in the early 1960s identified equigranular biotite quartz monzonite and potassium feldspar porphyry phases of this intrusion. Disseminated molybdenite, chalcopyrite and minor galena and sphalerite occur along its western flank. Magnetite pods occur in meta-volcanic and sedimentary rocks northwest of the plug (Norm showing: MINFILE 104K 034).

Numerous copper-only occurrences to the east of the map area in 104J/4 centre around the Kaketsa stock and several smaller Late Triassic diorites. Only minor chalcopyrite was noted locally in Triassic diorite bodies in the Golden Bear area.

MINING AND EXPLORATION ACTIVITY

North American Metals Corporation continued mining from the Golden Bear open pit this summer. The mill was running at up to 500 tonnes per day, well above its designed 350 tonnes per day capacity. Underground mining along the Bear fault and parallel structures is proceeding and plans for next summer include open-pit mining the headwall of the current pit (D. Reddy, personal communication, October 1992).

In addition to mining, North American Metals had a three component exploration program: drilling along the Ophir break aimed at defining additional underground ore reserves; detailed 1:1000-scale mapping of the Totem and Fleece Bowl prospects; and mapping and sampling on all peripheral claims included in its mining lease. Activity outside the immediate mine area was conducted by the parent company, Homestake Exploration Limited, on the Ram-Tut, Bandit and Slam claim groups. This included detailed mapping, soil and rock sampling, induced polarization surveys and trenching.

ACKNOWLEDGMENTS

Additional mapping and assistance were ably provided by Dean Barron, Todd Parsons and Jonathan Rouse. Our mapping was supplemented and guided by the earlier detailed work of Jim Oliver completed between 1988 and 1990; his exchange of data and ideas was of great benefit to the project. Homestake geologists Darcy Marud, Jane Howe and Ron Britten, and North American Metals geologists Doug Reddy, Jennifer Smith, and Duncan McBean are thanked for their ideas, comments and support during the fieldwork. Bill McClelland contributed to a lively week of traverses and stimulating discussions. Fossil identifications by Howard Tipper (GSC, Vancouver) and Rui Lin (ISPG, Calgary) provided essential age constraints. Editorial improvements are due to thorough reviews by John Newell and Bill McMillan. The Golden Bear mine staff are thanked for their logistical support and hospitality.

REFERENCES

- Anderson, R.G. (1983): The Geology of the Hotailuh Batholith and Surrounding Volcanic and Sedimentary Rocks, North-central British Columbia; unpublished Ph.D. thesis, *Carleton University*, 669 pages.
- Brown, D.A. and Greig, C.J. (1990): Geology of the Stikine River - Yehiniko Lake Area, Northwestern British Columbia (104G/11W, 12E); in *Geological Fieldwork 1989, B.C. Ministry of Energy, Mines and Petroleum Resources*, Paper 1990-1, pages 141-151.
- Brown, D.A. and Gunning, M.H. (1989): Geology of the Scud River Area, Northwestern British Columbia (104G/5,6); in *Geological Fieldwork 1988, B.C. Ministry of Energy, Mines and Petroleum Resources*, Paper 1989-1, pages 251-267.
- Brown, D.A. and Walton, G. (1983a): Geological and Geochemical Survey, Misty Group; *B.C. Ministry of Energy, Mines and Petroleum Resources*, Assessment Report 11,408.
- Brown, D.A. and Walton, G. (1983b): Geological, Geochemical Survey and Trenching, Tot Group; *B.C. Ministry of Energy, Mines and Petroleum Resources*, Assessment Report 11,779.
- Brown, D.A., Logan, J.M., Gunning, M.H., Orchard, M.J. and Bamber, W.E. (1991): Stratigraphic Evolution of the Paleozoic Stikine Assemblage in the Stikine and Iskut Rivers Area, Northwestern British Columbia; *Canadian Journal of Earth Sciences*, Volume 28, pages 958-972.
- Brown, D.A., Neill, I., Timmerman, J. and Harvey-Kelly, F. (1992): Geology and Geochemistry of the Chutine River and Tahltan Lakes Areas, Northwestern British Columbia (104G/12W, 13); *B.C. Ministry of Energy, Mines and Petroleum Resources*, Open File 1992-2.
- Bruaset, R.U. (1984): Geological, Geochemical Survey, Ram-Tut, Tot Claims; *B.C. Ministry of Energy, Mines and Petroleum Resources*, Assessment Report 13,068.
- Currie, L.D. (1992): Metamorphic Rocks in the Tagish Lake Area, Northern Coast Mountains, British Columbia: A Possible Link Between Stikinia and Parts of the Yukon-Tanana Terrane; in *Current Research, Part A; Geological Survey of Canada*, Paper 92-1A, pages 199-208.
- Gabrielse, H. (1977): Dease Lake Map Area; *Geological Survey of Canada*, Open File 707.
- Gabrielse (1991): Late Paleozoic and Mesozoic Terrane Interactions in North-central British Columbia; *Canadian Journal of Earth Sciences*, Volume 28, pages 947-957.
- Gutthath, G. (1965): Report of Geochemical and Geophysical Surveys, Bing No. 48 and Bing No. 83 Claim Groups; *B.C. Ministry of Energy, Mines and Petroleum Resources*, Assessment Report 668.
- Hamilton, T.S. (1981): Late Cenozoic Alkaline Volcanics of the Level Mountain Range, Northwestern British Columbia Geology, Petrology and Paleomagnetism; unpublished Ph.D. thesis, *University of Alberta*, 490 pages.
- Henderson, J.R., Kirkham, R.V., Henderson, M.N., Payne, J.G., Wright, T.O. and Wright, R.L. (1992): Stratigraphy and Structure of the Sulphurets Area, British Columbia; *Geological Survey of Canada*, Paper 92-1A, pages 323-332.
- Hewgill, W.V. (1985): Geochronology and Rare Earth Element Geochemistry of a Metasomatic Albitite in Northwestern British Columbia, unpublished B.Sc. thesis, *The University of British Columbia*.
- Holbek, P. (1988): Geology and Mineralization of Stikine Assemblage Mess Creek Area, Northwestern British Columbia; unpublished M.Sc. thesis, *The University of British Columbia*, 174 pages.
- Lambert, M.L. (1974): The Bennett Lake Cauldron Subsidence Complex, British Columbia and Yukon Territory; *Geological Survey of Canada*, Bulletin 227, 213 pages.
- Logan, J.M. and Drobe, J.R. (1992): Geology, Mineralization and Geochemistry of the More Creek Area, Northwestern British Columbia (104G/2); *B.C. Ministry of Energy, Mines and Petroleum Resources*, Open File 1992-5.
- Logan, J.M. and Drobe, J.R. (1993): Geology and Mineral Occurrences of the Mess Lake Area (104G/7W) in *Geological Fieldwork 1992*, Grant, B. and Newell, J.M., Editors, *B.C. Ministry of Energy, Mines and Petroleum Resources*, Paper 1993-1, this volume.
- Logan, J.M. and Koyanagi, V.M. (1989): Preliminary Geological and Mineral Deposits of the Spnaler Creek and Flood Glacier (104G/3, 4); *B.C. Ministry of Energy, Mines and Petroleum Resources*, Open File 1989-8.
- Logan, J.M., Koyanagi, V.M. and Drobe, J.R. (1990): Geology of the Forrest Kerr Creek Area, Northwestern British Columbia (104B/15); *B.C. Ministry of Energy, Mines and Petroleum Resources*, Open File 1990-2.
- McBean, D. (1990): Geological and Geochemical Report on the Nie Group; *B.C. Ministry of Energy, Mines and Petroleum Resources*, Assessment Report 20,655.
- McMillan, W.J., Panteleyev, A. and Preto, V.A. (1976): Geochemical Sampling, Geology and Magnetism of the Kaketsa Stock; in *Geological Fieldwork 1975, B.C. Ministry of Energy, Mines and Petroleum Resources*, Paper 1976-1, pages 63-68.
- Mihalynuk, M.G. and Rouse, J.N. (1988): Preliminary Geology of the Tutshi Lake Area, Northwestern British Columbia

- (104M/15); in Geological Fieldwork 1987, *B.C. Ministry of Energy, Mines and Petroleum Resources*, Paper 1988-1, pages 217-231.
- Moffat, L. and Walton, G. (1987): Diamond Drilling and Physical Work, Tot and Ram-Tut Groups, Tatsamenie Lake Area, B.C.; *B.C. Ministry of Energy, Mines and Petroleum Resources*, Assessment Report 16.525.
- Nixon, G.T., Ash, C.J., Connelly, J.N. and Case, G. (1989): Alaskan-type Mafic-Ultramafic Rocks in British Columbia: The Gnat Lakes, Hickman and Menard Creek Complexes; in Geological Fieldwork 1988, *B.C. Ministry of Energy, Mines and Petroleum Resources*, Paper 1989-1, pages 429-442.
- Oliver, J.L. and Hodgson, C.J. (1989): Geology and Mineralization, Bearskin (Muddy) and Tatsamenie Lake District (South Half), Northwestern British Columbia (104K); in Geological Fieldwork 1988, *B.C. Ministry of Energy, Mines and Petroleum Resources*, Paper 1989-1, pages 443-453.
- Oliver, J.L. and Hodgson, C.J. (1990): Geology and Mineralization, Tatsamenie Lake District, Northwestern British Columbia (104K); in Geological Fieldwork 1989, *B.C. Ministry of Energy, Mines and Petroleum Resources*, Paper 1990-1, pages 163-173.
- Oliver, J.L. and Gabites, J. (1993): Geochronology of Rocks and Chronology of Polyphase Rock Deformation, Bearskin (Muddy) and Tatsamenie Lake District, Northwestern British Columbia (104K/8. 1); in Geological Fieldwork 1992, Grant, B. and Newell, J.M., Editors, *B.C. Ministry of Energy, Mines and Petroleum Resources*, Paper 1993-1, this volume.
- Panteleyev, A. (1964): A Late Tertiary Volcanic Sequence in the Sheslay River Vicinity, Stikine Area, unpublished B.Sc. thesis, *The University of British Columbia*, 32 pages.
- Panteleyev, A. (1975): Geochemistry and Age of Kaketsa Stock; in Geological Fieldwork 1974, *B.C. Ministry of Energy, Mines and Petroleum Resources*, Paper 1975-1, pages 77-78.
- Ryan, B. (1991): Geology and Potential Coal and Coalbed Methane Resource of the Tuya River Coal Basin (94J/2. 7); in Geological Fieldwork 1990, *B.C. Ministry of Energy, Mines and Petroleum Resources*, Paper 1991-1, pages 419-429.
- Ryder, J.M. (1984): Terrain Inventory for the Stikine-Iskut River Areas (NTS 104F, 104G and parts of 104B and 104H); *B.C. Ministry of Energy, Mines and Petroleum Resources*, Technical Report 11, 85 pages.
- Schroeter, T.G. (1986): Muddy Lake Prospect (104K/1); in Geological Fieldwork 1985, *B.C. Ministry of Energy, Mines and Petroleum Resources*, Paper 1986-1, pages 175-184.
- Schroeter, T.G. (1987): Golden Bear Project (104K/1); in Geological Fieldwork 1986, *B.C. Ministry of Energy, Mines and Petroleum Resources*, Paper 1987-1, pages 103-109.
- Shannon, K. (1982): Geological and Geochemical Survey, Sam Claims 1 and 2; *B.C. Ministry of Energy, Mines and Petroleum Resources*, Assessment Report 10.158.
- Shaw, D. (1984): Geological, Geochemical and Geophysical Survey, Nic, Misty and Snic Groups, Duck and Nie 8; *B.C. Ministry of Energy, Mines and Petroleum Resources*, Assessment Report 12.688.
- Sevensma, P.H. (1972): Norm Group, Geological and Geochemical Report; *B.C. Ministry of Energy, Mines and Petroleum Resources*, Assessment Report 3842.
- Simpson, R.H. and Jones, H.M. (1984a): Geological - Geochemical - Geophysical Report on the Oro Claims; *B.C. Ministry of Energy, Mines and Petroleum Resources*, Assessment Report 12.628.
- Simpson, R.H. and Jones, H.M. (1984b): A Geological Report on the Oro 4 Claim; *B.C. Ministry of Energy, Mines and Petroleum Resources*, Assessment Report 13.251.
- Smith, M.T. and Mihalynuk, M.G. (1992): Tulsequah Glacier: Maple Leaf; in Exploration in British Columbia 1991, *B.C. Ministry of Energy, Mines and Petroleum Resources*, pages 133-141.
- Souther, J.G. (1959): Chutine, British Columbia; *Geological Survey of Canada*, Map 7-1959.
- Souther, J.G. (1971): Geology and Mineral Deposits of Tulsequah Map Area; *Geological Survey of Canada*, Memoir 362, 76 pages.
- Souther, J.G. (1972): Telegraph Creek Map Area, British Columbia; *Geological Survey of Canada*, Paper 71-44, 38 pages.
- Souther, J.G., Armstrong, R.L. and Harakal, J. (1984): Chronology of the Peralkaline, Late Cenozoic Mount Edziza Volcanic Complex, Northern British Columbia, Canada; *Geological Society of America*, Bulletin, Volume 95, pages 337-349.
- Stevenson, R.W. (1976): Report on Rock, Soil and Silt Geochemical Survey, Fae No. 1 Claim Group; *B.C. Ministry of Energy, Mines and Petroleum Resources*, Assessment Report 5924.
- Thicke and Shannon (1982): Geological and Geochemical Survey, Bandit 1 and 2 Claims; *B.C. Ministry of Energy, Mines and Petroleum Resources*, Assessment Report 10,755.
- Thicke and Shannon (1983): Trench, Geological and Geochemical Survey, Thor Group; *B.C. Ministry of Energy, Mines and Petroleum Resources*, Assessment Report 11,963.
- Walton, G. (1984a): Geological, Geochemical Survey, Slam Group; *B.C. Ministry of Energy, Mines and Petroleum Resources*, Assessment Report 12.775.
- Walton, G. (1984b): Geological, Geochemical Surveys, Giver, Taker Claims; *B.C. Ministry of Energy, Mines and Petroleum Resources*, Assessment Report 12,975.
- Wheeler, J.O. and McFeeley, O. (1991): Tectonic Assemblage Map of the Canadian Cordillera and adjacent parts of the United States of America; *Geological Survey of Canada*, Map 1712A.

GEOCHRONOLOGY OF ROCKS AND POLYPHASE DEFORMATION, BEARSKIN (MUDDY) AND TATSAMENIE LAKES DISTRICT, NORTHWESTERN BRITISH COLUMBIA (104K/8, 1)

By Jim Oliver, Teck Exploration Ltd. /Queen's University
and Janet Gabites, The University of British Columbia

KEYWORDS: Geochronology, zircon, U-Pb dating, Tatsamenie, Sam Creek, Icy Pass.

INTRODUCTION

This report presents the preliminary results of a series of zircon dates on the supracrustal and intrusive rocks between Bearskin (Muddy) Lake and Tatsamenie Lake in northwestern British Columbia. These dates are used in conjunction with a geological map to develop a hypothesis for the sequence of polyphase rock deformation in this area.

Although the dates in this paper are preliminary, only one may change significantly with the results of further analysis which is in progress.

The project area is located approximately 140 kilometres west of Dease Lake (Figure 1-12-1). During 1988, 1989 and 1990 detailed 1:5000 and 1:10 000-scale maps were completed across an area extending from the north side of Bearskin (Muddy) Lake to the north shore of Tatsamenie

Lake. These maps form a portion of a Ph.D. project by Oliver and are available in an open file format (Oliver, 1993). Map coverage of this and related areas at a 1:50 000 scale has recently been completed by Bradford and Brown (1993, this volume).

PREVIOUS WORK

The general stratigraphic and structural relationships of the upper Paleozoic and Mesozoic rocks in the Tatsamenie Lake area were first documented by Souther (1971). The first paleontological confirmation of the Early Permian age of the limestones and other carbonate rocks on the north side of Tatsamenie Lake was made by Monner and Ross (1977).

The study area has been the focus of reconnaissance exploration programs for base and precious metals conducted intermittently since the 1960s. The geology of porphyry copper-molybdenum and gold occurrences in the northwestern parts of the map area was described by Holby (1976) and Cukor and Sevensma (1971). Precious metals reconnaissance programs conducted by Chevron Minerals Limited during the early 1980s culminated in the discovery and development of the Golden Bear deposit. The results of these field programs are documented in a series of assessment reports (Brown and Walton, 1983; Shaw, 1984 and others). Stratigraphic and structural characteristics of the Golden Bear mine area have been described by Schroefer (1987) and Oliver and Hodgson (1989). Geological relationships in the northern half of the study area have been outlined by Oliver and Hodgson (1990).

U-Pb GEOCHRONOLOGICAL METHODS

Zircons are separated from finely crushed (0 to 40 kilogram rock samples using a wet shaking table, heavy liquids and magnetic separator. The concentrates are split into magnetic (M) and nonmagnetic (NM) fractions and hand picked to 100 per cent purity as required. Concordance is improved by air abrasion techniques (Krogh, 1982). Chemical dissolution and mass spectrometry follow the procedures of Krogh (1973). A mixed ^{205}Pb - ^{233}U - ^{235}U spike is used (Parrish and Krogh, 1987; Roddick *et al.*, 1987). Uranium-lead date errors are obtained by individually propagating all calibration and measurement uncertainties through the entire date calculation and summing the individual contributions to the total variance (Nines, 1980). The isotopic composition of initial common lead is based on the Stacey and Kramers (1975) common lead growth curve. The decay constants are those recommended by the IUGS Subcommis-

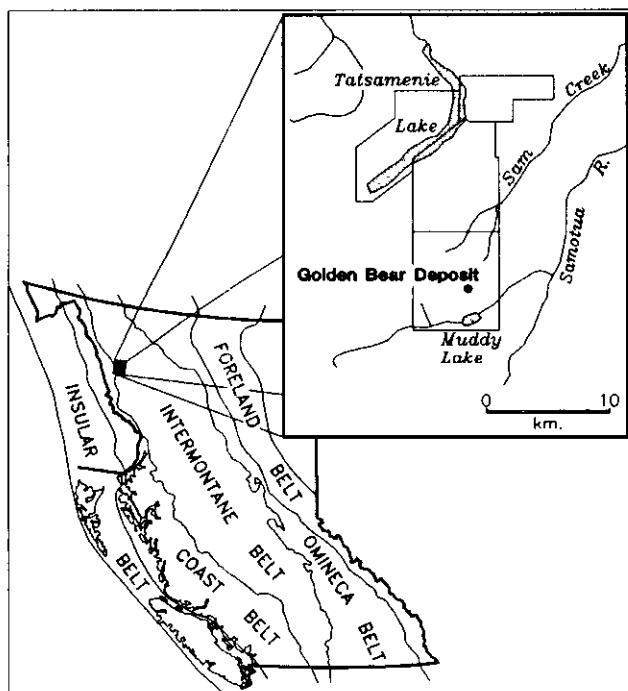


Figure 1-12-1. Location of the Tatsamenie Lake - Muddy (Bearskin) Lake map area within the tectonic framework of the Canadian Cordillera. The position of four 1:10 000-scale detailed Open File geological maps (Oliver, 1993) is also shown.

TABLE 1-12-1
U-Pb ZIRCON DATA FROM SAMPLES IN THE MUDDY (BEARSKIN)
AND TATSAMENIE LAKE AREAS

Fraction: ^{1,2} Magnetic & size split	wt mg	U ³ ppm	Pb ³ ppm	²⁰⁸ Pb %	²⁰⁶ Pb/ ²⁰⁴ Pb Measured ⁴	²⁰⁶ Pb/ ²³⁸ U ratio±%1σ Date±2σ	²⁰⁷ Pb/ ²³⁵ U ratio±%1σ Date±2σ	²⁰⁷ Pb/ ²⁰⁶ Pb ratio±%1σ Date±2σ
ID 2								
Felsic pyroclastic				Lat 58° 18'18" Long 132° 26'12"				
a NM2A/3°abr -94+74μ	0.21	94.4	5.46	16.69	319	0.04879(0.342) 307.1±2.0	0.3544(0.662) 308.0±3.5	0.05268(0.501) 315.1±23
b M2A/1°abr -94+74μ	0.3	41.4	2.05	11.60	943	0.04808(.120) 302.7±0.7	0.3499(.336) 304.7±1.8	0.05279(.295)4 319.7±13.5
c M2A/1°abr -74+44μ	0.1	126	7.01	16.96	289	0.04692(.186) 295.6±1.1	0.3361(.889) 294.2±4.5	0.05196(.797) 283.7±36.9
d M2A/1°abr -74+44μ	0.41	124	6.42	13.04	1147	0.04871(.363) 306.6±2.2	0.3540(.405) 307.7±2.1	0.05270(.124) 316.0±5.7
ID 5								
Felsic pyroclastic				Lat 58° 15'24" Long 132° 21'15"				
a NM2A/1°abr -74μ	0.23	80.1	4.41	15.48	360	0.04779(.336) 300.9±2.0	0.3438(.573) 300.0±3.0	0.05218(.406) 293.3±18.6
b NM2A/1°abr -74+44μ	0.1	49.6	2.94	17.58	206	0.04903(.202) 308.6±1.2	0.3622(.878) 313.8±4.7	0.05357(.779) 353.0±36
c M2A/1°abr -74+44μ	0.24	89.7	7.96	29.14	95	0.04930(.785) 310.2±4.8	0.3576(2.62) 310.4±14	0.05261(2.18) 312±103
d M1.5A/3°abr -74+44μ	0.62	79.8	3.98	11.54	2132	0.04842(.407) 304.8±2.4	0.3534(.422) 307.3±2.2	0.05294(.090) 326.2±4.1
89-254								
Granodiorite				Lat 58° 21'30" Long 132° 18'00"				
a NM2A/1°abr +104μ	0.9	302	11.1	7.94	2431	0.03706(.065) 234.6±0.3	0.2678(.110) 240.9±0.5	0.05242(.066) 303.6±3.0
b NM2A/1°abr -104+74μ	0.1	631	32.2	22.52	140	0.03459(.448) 219.2±1.9	0.2493(1.58) 226.0±6.4	0.05228(1.29) 297.5±60
c NM2A/1°abr -74+44μ	0.3	154	5.49	9.07	921	0.03484(.061) 220.8±0.3	0.2447(.216) 222.3±0.9	0.05095(.182) 238.4±8.4
d M2A/1°abr +74μ	1.01	355	12.1	8.07	14180	0.03475(.393) 220.2±1.7	0.2424(.394) 220.4±1.6	0.05060(.016) 222.5±0.8
I90-HD								
Hornblende diorite				Lat 58° 22'15" Long 132° 11'30"				
a NM2A/1°abr -104+74μ	0.2	286	18.3	29.17	86.5	0.03393(.739) 215.1±3.1	0.2420(2.60) 220.0±10.3	0.05172(2.15) 273±102
b NM2A/1°abr -74+44μ	0.4	81.7	2.92	10.53	872	0.03457(.133) 219.1±0.6	0.2550(.307) 230.7±1.3	0.05351(.249) 350.4±11.3
c M2A/1°abr -74μ	0.10	448	18.1	16.42	271	0.03353(.452) 212.6±1.9	0.2502(1.19) 226.7±4.8	0.05412(873) 376±40

Notes: Analyses by J. Gabites, 1992, in the geochronology laboratory, Department of Geological Sciences, U.B.C..

IUGS conventional decay constants (Steiger and Jäger, 1977) are: $^{238}\text{U}\lambda = 1.55125 \times 10^{-10} \text{a}^{-1}$,

$^{235}\text{U}\lambda = 9.8485 \times 10^{-10} \text{a}^{-1}$, $^{238}\text{U}/^{235}\text{U} = 137.88$ atom ratio.

1. Column one gives the label used in the Figures.
2. Zircon fractions are labelled according to magnetic susceptibility and size. NM = non magnetic at given amperes on magnetic separator, M = magnetic. Side slope is given in degrees. Abr = air abraded. The - indicates zircons are smaller than the stated mesh (in microns), + crystals are larger than the stated mesh.
3. U and Pb concentrations in mineral are corrected for blank U and Pb. Isotopic composition of laboratory Pb blank is 206:207:208:204 = 18.16:15.614:38.283:1.00, based on ongoing analyses of total procedural blanks of 37 ± 5 pg (Pb) and 6 ± 0.5 pg (U).
4. Initial common Pb is assumed to be Stacey and Kramers (1975) model Pb of the age of the $^{207}\text{Pb}/^{206}\text{Pb}$ date for each fraction.

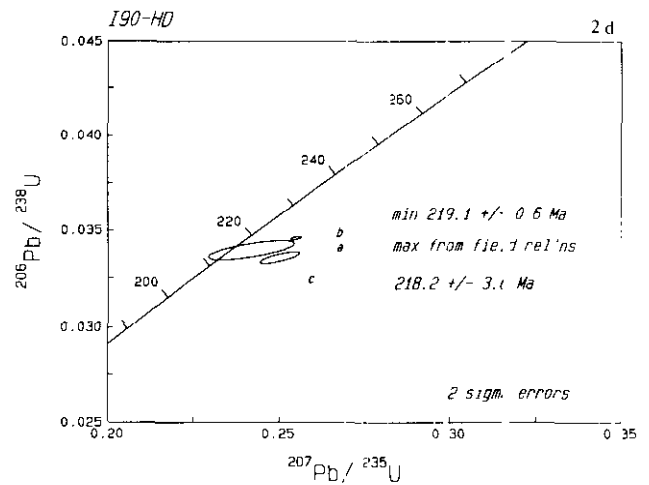
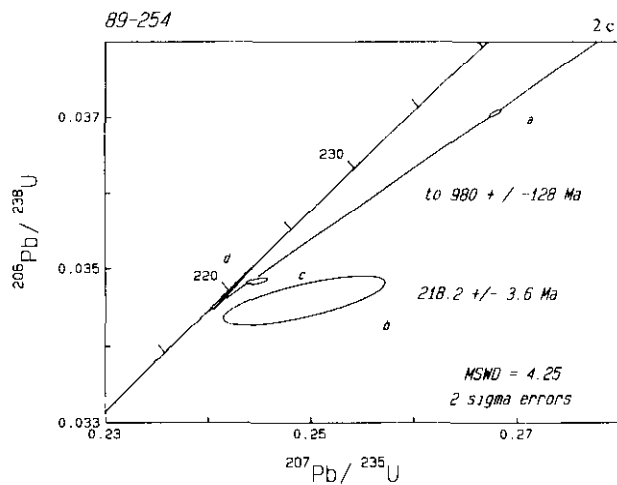
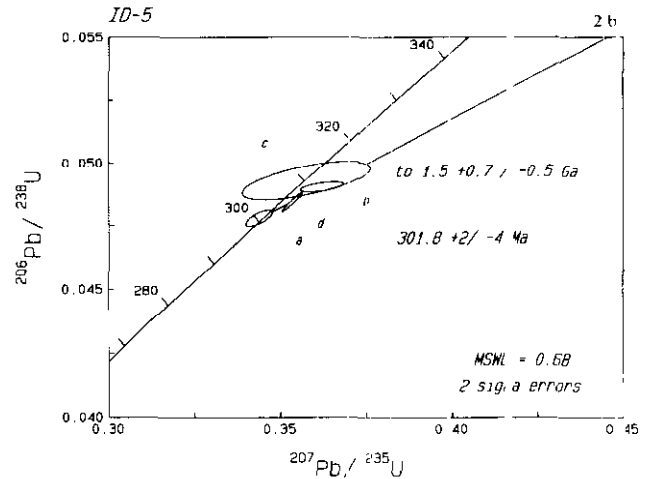
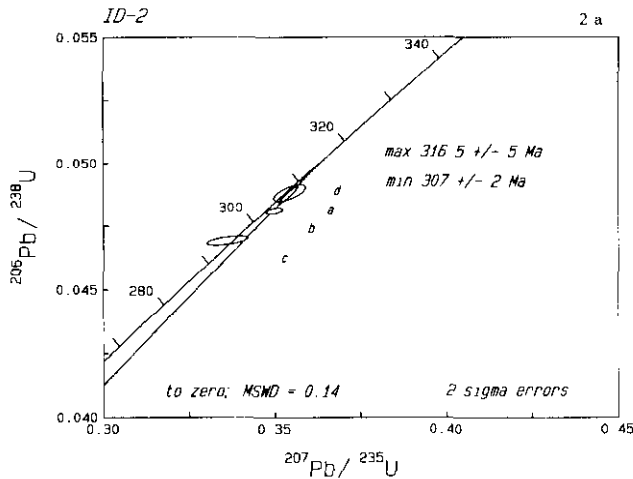


Figure 1-12-2. U-Pb concordia diagram for felsic rocks north of Tatsamenie Lake (Figure 1-12-2a, sample ID-2), for felsic rocks north of Sam Creek (Figure 1-12-2b, sample ID-5), for granodiorite of the Sam batholith (Figure 1-12-2c, sample 89-254), and for the Icy Pass porphyry, (1-12-2d, sample 190-HD).

sion on Geochronology (Steiger and Jäger, 1977). Concordia intercepts are based on the York (1969) regression and Ludwig (1980) error algorithm. Errors reported for the raw U-Pb data are one sigma; those for final dates and shown on concordia plots are two sigma (95% confidence limits).

The analytical results for zircon from four rock samples are summarized on Table 1-12-1 and depicted graphically on Figure 1-12-2 (a-d). Sample locations are shown on Figure 1-12-3.

SAMPLE CHARACTERISTICS AND INTERPRETATION OF U-Pb DATA

TATSAMENIE LAKE FELSIC VOLCANICS (SAMPLE ID-2)

Sample ID-2 was taken from the massive, poorly bedded felsic volcanic rocks which structurally overlie the carbonate rocks exposed on the northwest shore of Tatsamenie

Lake. Felsic flows and ash tuffs are the likely protolith. These rocks are strongly deformed and in this section are observed to be composed of weakly compositionally layered and recrystallized quartz, with lesser feldspar lamellae, and a weak, micaceous, slightly correlated foliation. The zircons separated from this rock are clear, colourless, doubly terminated prisms. Their aspect ratios are typically 1:1.5 to 3. Fluid inclusions and apatite lathes are visible in some crystals; where possible crystals containing inclusions were not used in the analysis.

The four fractions analyzed all plot close to concordia (Figure 1-12-2a). Two fractions (b and c) have lost lead. There is no indication of inherited zircon in this sample. The lower limit on the age of this sample, 307 ± 2 Ma, is given by the mean of the $^{206}\text{Pb}/^{238}\text{U}$ dates from the two most concordant fractions (a and d). These analyses are least affected by analytical error in the determination of ^{204}Pb . The sample cannot be older than the $^{207}\text{Pb}/^{235}\text{Pb}$ from the most concordant fraction; thus the upper limit on the age of

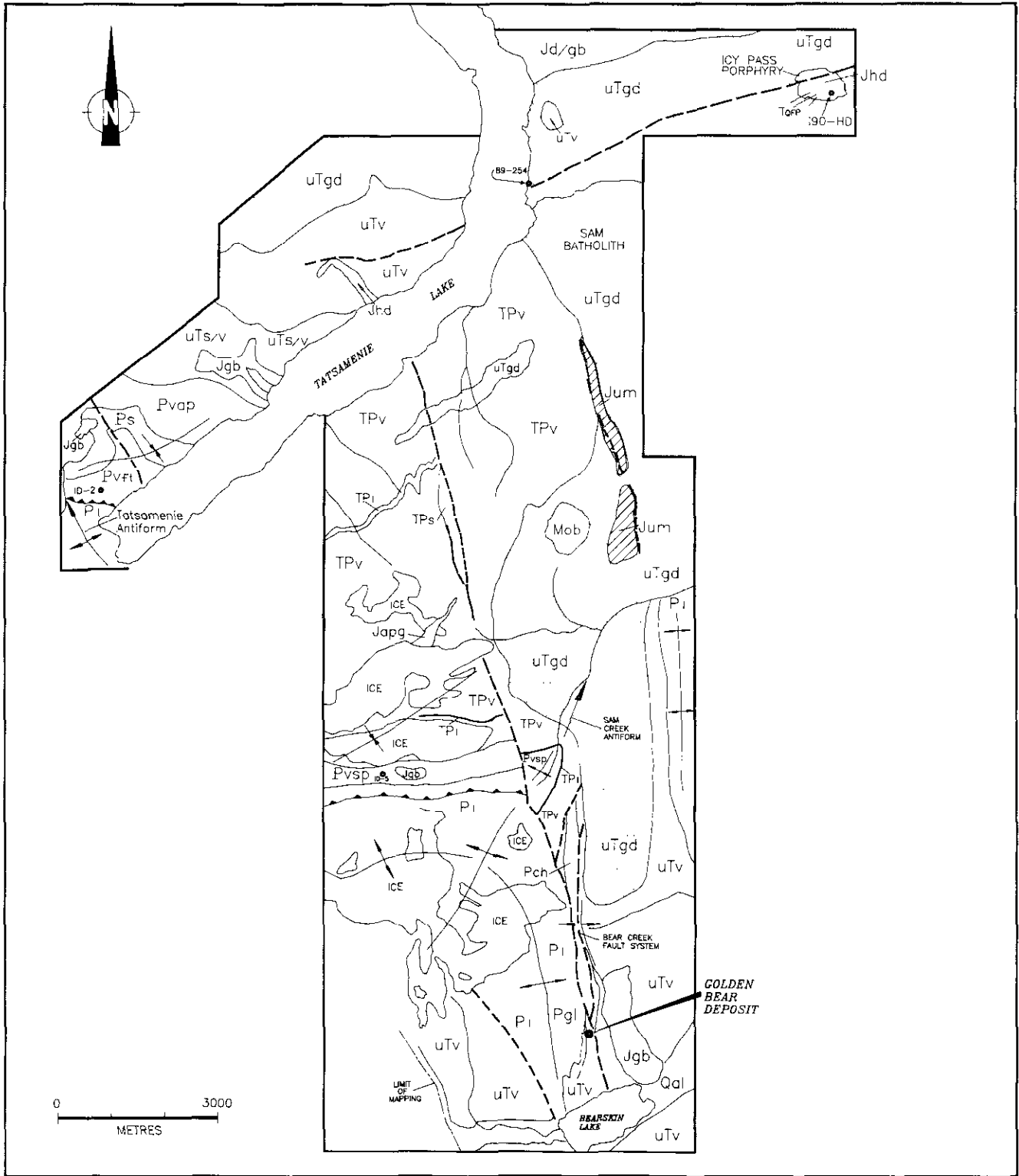


Figure 1-12-3. Inferred lithological and structural relationships for rocks in the Muddy (Bearskin) Lake - Tatsamenie Lake map area. See facing page for legend to map.

INTRUSIVE ROCKS

EARLY TERTIARY

Tqfp Quartz feldspar porphyritic dikes, Sloko equivalent (?).

MIDDLE TO EARLY JURASSIC(?)

Jgb Massive hornblende pyroxene gabbros.

Jagg Potassium feldspar rich, aplitic dikes.

Jhd Hornblende diorite.

Jum Magnetite clinopyroxenite, Alaskan-type ultramafic rocks.

UPPER TRIASSIC

uTgd Weakly foliated hornblende biotite granodiorites to diorites.

this rock is given by the mean of the $^{207}\text{Pb}/^{206}\text{Pb}$ dates for fractions (a) and (d) at 316.5 ± 5 Ma. Field relationships do not provide further constraints on the age of this volcanic rock.

SAM CREEK FELSIC VOLCANICS (SAMPLE ID-5)

This sample was selected from a felsic volcanic rock exposed immediately north of Sam Creek. These rocks differ macroscopically from those exposed on the north side of Tatsamenie Lake only in the slight increase in the percentage of mafic mineral phases and more intensely developed phyllitic cleavage. They are interpreted to be fine-grained, poorly stratified felsic pyroclastics.

The zircons separated from this sample are clear, colourless to light tan euhedral prisms with aspect ratios of 1:2 to 3. Clear fluid inclusions and apatite laths are visible in about 20 per cent of the crystals. No inherited cores are visible.

The four fractions analyzed cluster near concordia (Figure 1-12-2b) between 300 and 310 Ma, similar to sample ID-2. The zircons in ID-5 clearly contain an inherited zircon component and appear not to have lost lead. The best estimate of the age of the rock is given by the lower intercept of a least squares regression at $301.8 \pm 2/-4$ Ma. The average age of the inherited lead is 1.5 ± 0.7 Ga. Errors are increased slightly by including fraction (c) with a large error ellipse, but the date is not changed.

SAM BATHOLITH, GRANODIORITE (SAMPLE 89-254)

A weakly foliated to unfoliated granodiorite extends across the eastern edge of the map area. The intrusion cuts rocks as young as the Upper Triassic Stuhini Group. The batholith is cut by albite dikes which have given a K-Ar

STRATIFIED ROCKS

QUATERNARY

Qal Unconsolidated sediments.

MIOCENE (?)

Mob Olivine basalt flows.

UPPER TRIASSIC -- STUHINI GROUP

uTv Undifferentiated volcanic rocks

uTs Undifferentiated sedimentary rocks

TRIASSIC TO PERMIAN (ROCKS OF POORLY CONSTRAINED STRATIGRAPHIC AGE)

TPv Undifferentiated volcanic rocks

TPs Undifferentiated sedimentary rocks, (TPI limestone).

LOWER PERMIAN -- STIKINE ASSEMBLAGE

Pl Buff to grey; massive to thin-bedded limestone.

Pch Chert and strongly silicified dolomites.

PENNSYLVANIAN

Pvft Felsic volcanic dust and ash tuffs.

Ps Undifferentiated clastic and carbonate rocks.

Pvap Strongly actinolite porphyroblastic mafic volcanic rocks.

PvsP Siliceous phyllites of volcanic origin.

whole-rock age of 171 ± 6 Ma (Hewgill, 1985), and by elongate, clinopyroxene-rich, Alaskan-type ultramafic bodies of indeterminate age.

The zircons separated from this sample were almost all broken fragments of clear, colourless, stubby euhedral crystals. Three of the four fractions analyzed define a chord with a lower intercept of 218 ± 3.6 Ma (Figure 1-12-2c). Inherited lead is indicated with an average age of 0.98 Ga. The fourth fraction has a large error ellipse and low $^{206}\text{Pb}/^{204}\text{Pb}$ ratio. The zircons in this fraction have probably suffered lead loss and contain inherited old lead. Additional fractions from this sample are presently being analysed to improve these age constraints.

ICY PASS DIORITE (SAMPLE I90-HD)

The sample is taken from one of the larger porphyry copper-molybdenum and gold occurrences in the north-western part of the map area. Away from the main hydrothermal alteration zone, these rocks are medium-grained hornblende and plagioclase-phyric diorites. They are foliated only along their contact margins and are cut by quartz-feldspar-porphyritic dikes and rhyolite dikes. The dike rocks are probably equivalent to, or younger than, Sloko-type intrusions.

The zircons separated from sample 190-HD are clear, colourless, euhedral, stubby prismatic crystals. Approximately half of the crystals were broken and a small proportion contain clear fluid inclusions or apatite laths. No inherited cores were present. The three fractions analyzed thus far are discordant and form a cluster such that a least squares regression is not possible (Figure 1-12-2d). The discordance of the three fractions suggests the presence of an inherited zircon component. It is unusual for three discordant fractions with different sizes and magnetic susceptibilities to cluster in this way.

The data set is insufficient to establish a precise emplacement age for the body, and analysis of additional zircon fractions is now in progress. A maximum age limit for the rock is established by field relations. The hornblende diorite intrudes the Sam batholith which we have dated at 218.0 ± 3.6 Ma.

STRATIGRAPHIC AND STRUCTURAL OVERVIEW, AND U-Pb CONSTRAINTS ON ROCK DISTRIBUTION AND DEFORMATION

Schematic structural and stratigraphic relations of Palaeozoic and Mesozoic rocks in the Tatsamenie Lake area are shown on Figure 1-12-3. This figure is simplified from the detailed map of Oliver (1993). Detailed characteristics of the stratigraphy in the area are discussed by Bradford and Brown (1993). Several significant geological features are shown on this figure and assist in the interpretation of zircon data.

- The distribution of felsic rocks is asymmetric across the deformed carbonate rocks which form the core of the Tatsamenie antiform. Felsic rocks are exposed on the northern and eastern limits of the deformed limestone suite. They do not appear to crop out on the western limb of the antiform. On the western side the felsic rocks are commonly truncated by north-trending faults.
- A minimum of two major folding events deform the rocks in the study area. One of these map-scale structures is the Tatsamenie antiform. This and related early folds are characterized by north-trending axial surfaces and tight, upright to weakly east-overtaken limbs. This antiform is deformed across broad, upright, northeast-plunging antiform-synform pairs. The interaction of these two fold styles produces well-defined Type II interference patterns (Ramsay, 1967).
- The Sam Creek antiform is faulted and offset by apparent right-lateral motion on a north-trending fault which forms part of the north-trending Bear fault system.

Geochronological data, summarized in Table 1-12-1, place important constraints on interpretations of volcanic stratigraphy and the timing of rock deformation in this area. Geological interpretations integrating these and other age data with field relationships lead to the following conclusions:

- Felsic rocks structurally above Early Permian carbonate rocks are dated at 301.8 ± 2 – 4 Ma to 316.5 ± 5 Ma. In this map area, the presence of felsic volcanic

rocks overlying limestones was first documented by Oliver and Hodgson (1990). The Early Permian age of the carbonate rocks, which structurally underlie the felsic rocks, initially documented by Monger and Ross (1977) has recently been confirmed by Bradford and Brown (1993).

We believe that the older felsic rocks have been emplaced on top of the Permian section through the action of a south-verging thrust fault. We correlate the felsic package with the felsic volcanic sequence that stratigraphically underlies the Permian limestones regionally, as has been described in the Scud River area by (Brown and Gunning, 1989).

- Geochronological constraints on the timing of the formation of the north-trending Tatsamenie antiform and of the development of overthrust rock sequences are limited. We believe that there is a close relationship between thrusting and the development of tight north-trending major folds such as the Tatsamenie antiform. Souther (1971) used field relationships to infer the presence of a deformational event older than the Middle Triassic, which he termed the Tahltanian orogeny. Brown *et al.* (1992) also inferred an Early Triassic deformational event using observations relating to changes in the intensity of rock fabric, metamorphic grade and truncation of early rock fabrics. The data of this report suggest that formation of the Tatsamenie antiform and the emplacement of overthrust rock sequences is compatible with this Permo-Triassic deformational event.
- The Sam batholith has been dated at 218.2 ± 3.6 Ma. In the region of Sam Creek, this intrusive stock appears to be deflected across the axial surface of a northeast-trending antiform. Deformation of this intrusive body suggests that open, upright fold structures with northeast-trending axial surfaces were initiated later than 218 Ma.
- The Sam Creek antiform is cut by a north-trending fault zone, part of the Bear fault zone. Whole-rock sericite K-Ar dates on hydrothermal alteration envelopes are 205 ± 7 Ma to 179 ± 6 Ma (Schroeter, 1987). These dates may place an upper limit on the timing of the development of northeast-trending structures such as the Sam Creek antiform.

The timing of this event significantly pre-dates Middle Cretaceous folding which affects rocks on the western edge of the Bowser Basin (Evenchick, 1991). It is better correlated to an Early Jurassic deformation which has been documented in the Sulphurets area (Henderson *et al.*, 1992). Brown and Grieg (1990) have documented an undeformed latest Late Triassic to Early Jurassic unconformity in the Stikine River - Yehiniko Lake area. This post-Stuhini Group, pre-Early Jurassic deformational event may also have affected the Tatsamenie Lake area.

- The Sam Creek antiform deforms both the early Tatsamenie antiform and its overthrust sequence. This thrust surface probably had a west-verging orientation prior to its rotation into south-verging positions across structures like the Sam Creek antiform.
- The fault, locally termed the Limestone Creek fault, which defines the western edge of the carbonate strat-

igraphy due north and west of Muddy Lake (Figure 1-12-3) has not been significantly deflected by the southern continuation of the Sam Creek antiform. As is the case for the Bear fault, movement across this fault post-dates the formation of the antiform.

- The presence of pre-Permian felsic rocks north of Tatsamenie Lake and north of Sam Creek raises interesting questions concerning the age of the mafic volcanic rocks between these two points. The exact thickness of the pre-Permian volcanic section is difficult to define solely on the basis of field relationships. This rock package has some similarity to Pennsylvanian volcanic rocks mapped by Nelson and Payne (1984) in the Tulsequah area. The resolution of the age of this suite, and the position of other detachment or unconformable surfaces, requires age constraints based on either isotopic or paleontological data.

ACKNOWLEDGMENTS

The authors wish to thank the British Columbia Ministry of Energy, Mines and Petroleum Resources for its support of this project through Geoscience Research grants in 1988, 1989 and 1991. Funding for portions of this project has also been provided for by Teck Exploration Inc., Placer Dome Inc. and by Rea Gold Corporation. Additional logistical support for Oliver's fieldwork was provided by Canamera Geological Ltd. The consistent support of Homestake Canada Ltd. throughout the evolution of this project is recognized and appreciated. Oliver wishes to thank Teck Exploration for its substantive financial support in the preparation of these dates and in the preparation of this paper.

Thanks are also extended to Derek Brown and John Bradford for their participation in cooperative and open discussions on the many nuances of the geology of this part of northern Stikinia.

The technical assistance and advice of Jim Mortensen at The University of British Columbia's geochronology laboratory is gratefully acknowledged.

REFERENCES

- Bradford, J.A. and Brown, D.A. (1993): Geology of the Bearskin Lake and Southern Tatsamenie Lake Map areas, Northwestern British Columbia (104K/01 and 08); in Geological Fieldwork 1992. Grant, B. and Newell, J.M., Editors, *B.C. Ministry of Energy, Mines and Petroleum Resources*, Paper 1993-1, this volume.
- Brown, D.A. and Greig, C.J. (1990): Geology of the Stikine River - Yehiniko Lake Area, Northwestern British Columbia (104G/11W and 12E); in Geological Fieldwork 1989, *B.C. Ministry of Energy Mines and Petroleum Resources*, Paper 1990-1, pages 127-140.
- Brown, D.A. and Gunning, M.H. (1989): Geology of the Scud River Area, Northwestern British Columbia (104G/5); in Geological Fieldwork 1988, *B.C. Ministry of Energy, Mines and Petroleum Resources*, Paper 1989-1, pages 251-267.
- Brown, D.A., Harvey-Kelly, F.E.L. and Timmerman, J. (1992): Geology of the Chutine River - Tahltan Lake Area, Northwestern British Columbia (104G/12W and 13); in Geological Fieldwork 1991. Grant, B. and Newell, J.M., Editors, *B.C. Ministry of Energy, Mines and Petroleum Resources*, Paper 1992-1, pages 179-195.
- Brown, D.A. and Walton, G. (1983) Geological and Geochemical Survey, Misty Group; *B.C. Ministry of Energy, Mines and Petroleum Resources*, Assessment Report 1408, 10 pages.
- Cukor, V. and Sevensma, P.H. (1971): Brinex: Skyline Project - MC Group, 104K-8, Atlin Mining Division, British Columbia. Geological - Geochemical Report; *B.C. Ministry of Energy, Mines and Petroleum Resources*, Assessment Report 3475, 11 pages.
- Evenchick, C.A. (1991): Geometry, Evolution and Tectonic Framework of the Skeena Folc Belt, North Central British Columbia; *Tectonics*, Volume, 10, pages 527-546.
- Henderson, J.R., Kirkham, R.V., Henderson, M. J., Payne, J.G., Wright, T.O. and Wright, R.L. (1992): Stratigraphy and Structure of the Sulphurets Area British Columbia; in Current Research, Part A; *Geological Survey of Canada*, Paper 92-1A, pages 323-332.
- Hewgill, W.H. (1985): Geochronology and Rare Earth Element Geochemistry of a Metasomatic Albite in Northwestern British Columbia; unpublished B.Sc. thesis, *The University of British Columbia*, 57 pages.
- Holby, M. (1976): Icy Lake Option, 104K/8E, Geological and Soil Geochemical Report; *B.C. Ministry of Energy, Mines and Petroleum Resources*, Assessment Report 3019, 27 pages.
- Krogh, T.E. (1973): A Low-contamination Method for Hydrothermal Decomposition of Zircon and Extraction of U and Pb for Isotopic Age Determinations; *Geochimica et Cosmochimica Acta*, Volume 37, pages 485-494.
- Krogh, T.E. (1982): Improved Accuracy of U-Pb Zircon Ages by the Creation of More Concordant Systems Using an Air Abrasion Technique; *Geochimica et Cosmochimica Acta*, Volume 46, pages 637-649.
- Ludwig, K.R. (1980): Calculation of Uncertainty of U-Pb Isotope Data; *Earth and Planetary Science Letters*, Volume 46, pages 212-220.
- Monger, J.W. and Ross, C.A. (1971): Distribution of Fusulinaceans in the Western Canadian Cordillera; *Canadian Journal of Earth Sciences*, Volume 8, pages 259-278.
- Nelson, J. and Payne, J.G. (1984): Paleozoic Volcanic Assemblages and Volcanogenic Massive Sulfide Deposits near Tulsequah, British Columbia; *Canadian Journal of Earth Sciences*, Volume 21, pages 379-381.
- Nines, P.D. (1980): The Ontario Geological Survey Geochronology Research Program - An Overview; *Ontario Geological Survey*, Miscellaneous Paper 92, pages 4-6.
- Oliver, J.L. (1993): Geology of the Muddy Lake - Tatsamenie Lake Areas. (104K/8, 1; 1:10 000-scale); *B.C. Ministry of Energy, Mines and Petroleum Resources*, Open File 1993-11.
- Oliver, J.L. and Hodgson, C.J. (1989): Geology and Mineralization, Bearskin (Muddy) Lake and Tatsamenie Lake District (South Half), Northwestern British Columbia (104K); in Geological Fieldwork 1988, *B.C. Ministry of Energy Mines and Petroleum Resources*, Paper 1989-1, pages 443-453.
- Oliver, J.L. and Hodgson, C.J. (1990): Geology and Mineralization, Tatsamenie Lake District, Northwestern British Columbia (104K); in Geological Fieldwork 1989 *B.C. Ministry of Energy, Mines and Petroleum Resources*, Paper 1990-1, pages 163-173.
- Parrish, R.R. and Krogh, T.E. (1987). Synthesis and Purification of ²⁰⁵Pb for U-Pb Geochronology; *Chemical Geology, Isotope Geoscience Section*, Volume 66, pages 111-121.

- Ramsay, J.R. (1967): *Folding and Fracturing of Rocks*; McGraw Hill Book Company, 568 pages.
- Roddick, J.C., Loveridge, W.D. and Parrish, R.R. (1987): Precise U/Pb Dating of Zircon at the Sub-nanogram Pb Level; *Chemical Geology, Isotope Geoscience Section*, Volume 66, pages 111-121.
- Schroeter, T.G. (1987): Golden Bear Project (104K 1); in *Geological Fieldwork 1986, B.C. Ministry of Energy, Mines and Petroleum Resources*, Paper 1987-1, pages 103-110.
- Shaw, D. (1984): Geological, Geochemical and Geophysical Survey, Nic, Misty and Snic Groups, Duck and Nie 8; *B.C. Ministry of Energy, Mines and Petroleum Resources*, Assessment Report 12688, 19 pages.
- Souther, J.G. (1971): Geology and Mineral Deposits of the Tulsequah Map Area; *Geological Survey of Canada*, Memoir 362, 76 pages.
- Stacey, J.S. and Kramers, J.D., (1975): Approximation of Terrestrial Lead Isotope Evolution by a Two-stage Model; *Earth and Planetary Science Letters*, Volume 26, pages 207-221.
- Steiger, R.H. and Jäger, E. (1977): Subcommittee on Geochronology: Convention on the Use of Decay Constants in Geo- and Cosmochronology; *Earth and Planetary Science Letters*, Volume 36, pages 359-362.
- York, D. (1969): Least-squares Fitting of a Straight Line with Correlated Errors; *Earth and Planetary Science Letters*, Volume 5, pages 320-324.

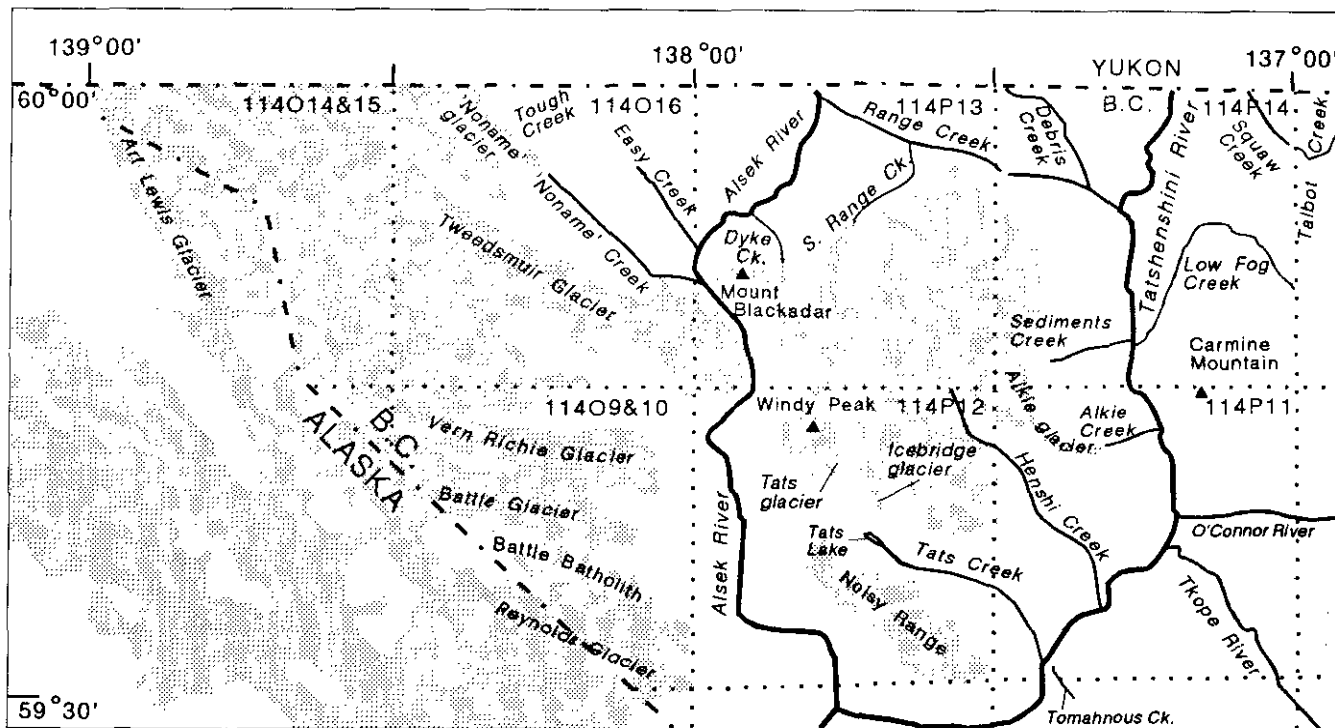


Figure 1-13-2. Geographic location names referred to in Parts A to D of this report that are within the area mapped in 1992.

sheets, or approximately 482 000 hectares. It was mapped in sufficient detail to warrant publication at 1:50 000 scale. At this scale, we are able to outline previously undefined rock units which are now known to cover large portions of the area. Nearly 300 samples collected from various rock units will, when analyses are complete, provide a basis for evaluating the mineral potential of the units. No such "baseline" regional geochemical data previously existed.

During the course of mapping, several significant, previously unknown copper showings were discovered (see Part D). Isolated occurrences of anomalous concentrations of other metals, particularly lead, silver and gold were also identified. Samples from these occurrences are in the process of being analysed. Currently available, but incomplete analytical results are tabulated in Part D.

Discovery of some 20 new fossil localities has added significantly to an understanding of the stratigraphy of the area. More than 60 samples are presently being analysed for microfossils. This will help us to further refine the geological history of the area as more fossil ages are determined.

Preliminary mineral potential findings, based mainly upon geological observations and initial geochemical data, have been submitted to the Commission on Resources and the Environment (CORE) to aid in land-use decisions.

LOCATION, ACCESS AND PHYSIOGRAPHY

The study area covers that part of British Columbia west of, and including, a corridor 10 kilometres wide along the Haines Highway. This comprises a triangular area occupied

by the rugged St. Elias Mountains and drained by the Tatshenshini and Alsek rivers. It is bounded to the south and west by Alaska and to the north by Yukon Territory. We report here on observations from the northern half of this area (Figure 1-13-1).

The paved Haines Highway, which links Haines Junction, Yukon Territory, with Haines, Alaska, provides year-round access to the eastern part of the area. Several loose-surface roads in varying condition extend west from the highway. A maintained gravel road provides access to placer mining operations in the northern Squaw Range, but requires fording the Tatshenshini River at Dalton Post, Yukon. Abandoned bulldozer-trails extend up Chuck Creek to the O'Connor River gypsum occurrence just east of the study area, up the Parton River to the headwaters of Low Fog Creek, and up Goldrun and Talbot creeks.

The area is most readily accessible by air. A 1000-metre gravel airstrip at the exploration camp of Geddes Resources Limited will accommodate a DC-3 aircraft and provides access to the north-central area. Tats, Low Fog and Range lakes are all large enough for float planes to land and take off. The nearest centres for supplies and services are: Whitehorse, Yukon, some 190 kilometres east-northeast; Atlin, British Columbia, about 225 kilometres to the east; and Haines, Alaska, 135 kilometres to the southeast. Helicopters are the most effective means of transportation within the study area and are available for charter in Atlin, Whitehorse and Haines Junction.

A diversity of biogeoclimatic zones characterizes the Alsek-Tatshenshini area. These result from the interplay of interior and Arctic climates which give way to a coastal

influence both to the south and west. Glaciers are small and relatively uncommon in the east, but in the west they cover over 80 per cent of the area and exert a major influence on the weather. In this western area the permanent snow line extends down to 1000 metres elevation. Low overcast and persistent precipitation are typical weather conditions. Snow is common at any time of the year at higher elevations, with winter accumulations in excess of 10 metres. Cornice build-up on the northern sides of ridge crests is common, and failure of cornices throughout the early summer makes work on north slopes hazardous.

Two major north-south valleys transect the Alsek Ranges, and a third separates the western Alsek Ranges from the Icefield Ranges. From east to west the valleys are occupied by the upper Tatshenshini, lower Tatshenshini and Alsek rivers. Willows and boreal and black spruce occupy the Tatshenshini valley and impede travel on foot. Major tributaries of this river are forested mainly by poplar, alpine birch and juniper and are more easily travelled. Much of the Alsek Valley is recently deglaciated and barren of vegetation, but the lower reaches are forested.

PREVIOUS WORK

Work in the Tatshenshini-Alsek area has been hampered by poor access, generally inclement weather and, prior to an aerial photogrammetric survey in 1979, a lack of accurate topographic base maps. The first prospectors entered the area around 1898 in search of placer gold and discovered lode silver-gold showings in the Rainy Hollow area, leading to intermittent copper production between 1908 and 1922. Coarse gold was found along Squaw Creek in 1927 (James, 1928, p. C110) where placer operations have continued to the present.

Earliest geological mapping in the project area focused mainly on the areas surrounding the Windy Craggy deposit following its discovery by J.J. McDougall in 1958, then agent for the Ventures-Falconbridge group (Downing and McDougall, 1991). Exploration at Windy Craggy proceeded intermittently until the 1980s when underground development and detailed mapping (e.g., Prince, 1983) led to the delineation of a deposit containing nearly 300 million tonnes of massive sulphide (Geddes Resources, 1992). Geological mapping of the East Arm Glacier area in the mid-1970s by Swiss Aluminum Mining Company of Canada Ltd. (Scheilly *et al.*, 1976) focused on locating the source of massive sulphide boulders near the toe of the glacier. Subsequent drilling by St. Joe Canada Inc. proved the existence of a massive sulphide lens beneath 340 metres of ice (Brisco, 1987).

Earliest regional mapping was conducted by the Geological Survey of Canada during Operation St. Elias in 1974 (Campbell and Eisbacher, 1974; Campbell and Dodds, 1979, 1983a, b) which relied heavily on application of aerial reconnaissance mapping. More detailed follow-up mapping in subsequent years by Dodds covered parts of map sheets 114P/9, 11, 13, 14 and 15 (Campbell and Dodds, 1983a) and 114P/10 and 12 (Dodds, 1988). British Columbia Geological Survey Branch studies in the area include investigations by MacIntyre (1983, 1984, 1986), MacIntyre and Schroeter (1985) and Peter (1989) and focused mainly on mineral

occurrences. An extended investigation of the Windy Craggy volcanogenic massive sulphide deposit (114P/12) by MacIntyre (1983, 1986) addressed its regional stratigraphic and structural setting, and the geochemistry of enclosing basalts. Isotopic age controls in the area (Dodds and Campbell, 1988; Jacobsen *et al.*, 1986) are mainly based on K-Ar isotopic techniques for dating minerals in plutonic rocks.

TECTONIC SETTING

Much of the Canadian Cordillera is an amalgamation of large, commonly unrelated geologic provinces or terranes that may have originated far from their present location and subsequently collided and accreted to the margin of ancestral North America (Coney *et al.*, 1980). The Alexander Terrane is one of the largest of these terranes. It is composed largely of platformal and basinal rocks and underlies over 95 per cent of the central map area, extending hundreds of kilometres to the north and south (Berg *et al.*, 1978). Submarine volcanic and sedimentary rocks, interpreted to be fragments of Wrangellia Terrane underlie several tens of square kilometres in the northeastern map area. An even smaller area is underlain by clastic rocks alternatively interpreted to be part of the Chugach Terrane (Wheeler *et al.*, 1991) or Wrangellia (Campbell and Dodds, 1983a, b). These rocks are exposed in an irregular strip along the Alaska border, extending less than 2 kilometres into British Columbia at the latitude of the map area. Our mapping in this border area confirmed a highly variable belt of rocks with uncertain terrane affinities. Resolution of this terrane problem is not possible on the basis of current data. Overall, however, the rocks most closely resemble the Tarr Inlet suture zone (Brew and Morrell, 1976) which may contain fragments of both the Chugach and Wrangellia terranes.

Faults that apparently separate terranes include the Duke River fault east of the Alexander Terrane (also known as the Denali fault, of which it is a splay), and the Hubbard (or Art Lewis, of Plafker *et al.*, 1976)-Border Ranges fault system west of the Alexander Terrane. Our mapping raises some questions about the nature and location of these terrane-bounding(?) structures. Resolution of these tectonic problems is important because the regional distribution of geologic provinces must be considered when defining tracts of high and low mineral potential.

PROJECT PROCEDURE

Key steps in the mineral potential evaluation process are identification of the distribution of rock packages or "tracts" with distinct geological features, their stratigraphic setting and age, their geochemical profile and tectonic events that may have modified both the rock characteristics and their potential for economic mineralization. Where such data are unavailable, sparse or obsolete, they are gathered principally by field-based geological mapping and collection of samples for laboratory analysis. Mineral potential maps can then be constructed by integration of all sources of data (e.g., rock distribution, geochemistry, fossil ages).

Key steps in a geological mapping program are: compilation of existing data, identification of limitations in existing data, establishing objectives for the collection of new data, optimized collection of field data, collection of samples for laboratory analysis aimed at meeting specific objectives, data analysis and synthesis, and production of maps and reports.

At the beginning of the project, 2 months were spent compiling all available pertinent data onto 1:50 000-scale topographic base maps which would form a starting point for field studies. Over 320 person-days were spent collecting field data in the Tatshenshini-Alsek area during a 2-month period commencing July 4. Initial orientation surveys were conducted along the Haines Highway with a four-person crew. Heavy snowpack precluded fieldwork in the western area until mid-July, at which time an eight-person mapping crew was moved into the centrally located Geddes Resources Limited exploration camp. In early August, the field crew was reduced to four geologists who used mainly short traverses or spot checks in combination with "vantage-point mapping". Mapping and geochemical sampling, generally at a more detailed scale, were also undertaken around significant showings in the region. Litho-geochemical sample coverage and mineral occurrence inventory resulting from this first phase of the project extend beyond the area reported on here.

Fieldwork was supported by an on-site helicopter. Traverses were conducted in accessible areas where critical geological relationships could be established using daily helicopter set-outs and pick-ups. Only four field days were lost due to inclement weather or mechanical problems. In July and August most of the area was also covered by a companion Regional Geochemical Survey (RGS) program which focused on collection of stream sediment and water samples for multi-element analysis (Jackaman, 1993, this volume).

Completion of 1992 Tatshenshini project objectives within the allotted time frame required regional map coverage at a rate of three to six times that of a standard 1:50 000 geological mapping program in similar terrain. This was in part made possible through the increase in mapping efficiency resulting from use of an on-site helicopter, but was also accomplished by limiting mapping in widespread, homogeneous rock units (such as intrusions) to a few representative spot checks. Mapping within such rock

units is not, therefore, commensurate with Geological Survey Branch 1:50 000 mapping standards.

EXPECTED RESULTS

Fundamental to fulfilling the objectives of the project is production of 1:50 000 geological maps which represent an integration of all existing data. These will be augmented by geochemical and fossil data as they continue to become available. Complete geochemical results are not available at the time of writing, however, available assay results from samples collected within the Upper Triassic assemblage and elsewhere (reported in Part D) serve to highlight the mineral potential of these rocks. Assay data from this project will eventually be complemented by regional stream-sediment geochemical data collected as part of the companion RGS program. Together they will form the basis for geochemical characterization of mineral potential tracts.

Major oxide and rare-earth element (REE) analyses of specific volcanic units are pending. When available they will assist in the interpretation of the tectonic environment of volcanism. Such chemical analyses may help to constrain the answers to many geological questions which bear on the distribution of, and relationships between, similar rock packages. For example, are probable Upper Triassic pillow basalts enclosing massive sulphide lenses in the placer-rich Squaw Creek valley chemically related to pillow basalts that host the Windy Craggy deposit? Are poorly understood metabasites west of the Alsek River chemically distinct from undeformed and dated basalts to the east? In what tectonic environment did they form? Given the environment of formation, what types of mineral deposits might be expected? Do chemical differences or similarities support the notion of an intervening major tectonic contact or terrane boundary?

OUTPUT PLANNED

Initial products arising from the Tatshenshini-Alsek project include this report (Parts A to D) and a 1:50 000-scale Open File map series featuring the geology and litho-geochemistry of the area described in this report. These will be accompanied at a later date by Open File mineral potential maps of the same area.

Rare-earth element, and fossil and isotopic age data, will be released in the form of government or external publications as data are compiled and interpreted.



**PART B: STRATIGRAPHIC AND MAGMATIC SETTING
OF MINERAL OCCURRENCES**

By M.G. Mihalynuk, M.T. Smith, D.G. MacIntyre and M. Deschênes

INTRODUCTION

Magmatic and stratigraphic settings exert a first order control on the formation of various mineral deposit types. Some settings are rich in mineral wealth while others are barren. Stratigraphic setting is of particular importance where stratiform or stratabound mineral deposits are concerned as orebodies are commonly restricted to specific stratigraphic intervals. For example, within the area bounded by the Alsek and Tatshenshini Rivers, Upper Triassic rocks include a stratigraphic interval that is spectacularly endowed with massive sulphide copper mineralization. On the other hand, no significant mineral occurrences have yet been recognized in either the thick and extensive Paleozoic limestones or the widespread Jura-Cretaceous granodioritic bodies. Thus, an understanding of the stratigraphic and magmatic setting of mineral occurrences is the first step toward accurate delineation of mineral potential tracts, a primary objective of the Tatshenshini project, as outlined in Part A. Structural and deformational events affecting the distribution of rocks formed within various stratigraphic and magmatic settings are discussed in Part C.

FUNDAMENTAL SUBDIVISIONS

The Tatshenshini project study area is largely underlain by rock of units of the accreted Alexander Terrane, bounded to the east and west respectively by small slivers of the Wrangellia Terrane, and possibly the Chugach Terrane. Four major lithologic packages are represented within the Alexander Terrane: Cambro-Ordovician clastic strata and associated mafic sills and pillow basalts; a thick Ordovician to Silurian carbonate succession; lithologically variable terrigenous, marine, and minor volcanic strata of Silurian to Permian age; and Upper Triassic, moderately deep water, marine carbonate and fine-grained clastic strata with associated rift-related(?) basalts. Two additional metavolcanic and metasedimentary assemblages of probable Alexander Terrane affinity underlie the southwestern part of the study area.

No mineral occurrences are known to have formed during deposition of lower Paleozoic strata. By contrast, Upper Triassic Alexander Terrane lithologies are host to the most significant mineral occurrences in the study area, including the huge Windy-Craggy copper-cobalt deposit. Upper Triassic strata of Wrangellia have many characteristics in common with contemporaneous rocks in the Alexander Terrane and also have demonstrated high mineral potential.

Two major intrusive suites are exposed within the map area. Dominantly granodioritic, but compositionally variable Jura-Cretaceous intrusions comprise the Saint Elias Plutonic Suite (Campbell and Dodds, 1983a) in the western part of the area. To the east, the Oligocene Tkopec Plutonic Suite is also compositionally variable, but is dominated by granite to granodioritic phases. Tkopec intrusions thermally

metamorphose postaccretionary stratified units including deformed Early Tertiary clastic rocks.

Early Tertiary terrigenous sedimentary rocks occupy small, fault-controlled basins along Tats Creek and the western Tatshenshini River valley. The lower Tertiary strata host thin coal seams in both of these basins.

STRATIGRAPHY

**CAMBRO-ORDOVICIAN SHEET SANDSTONE
AND BASALT (COzsb)**

Well-bedded clastic strata (COzsl; Figures 1-13-3 and 1-13-4) and intercalated basaltic sills (COzd) and pillowed and unpillowed flows (COzb) attain a structural thickness of at least 2000 metres where they are well exposed on both sides of the Alsek River within 114P/13. Clastic units form distinct couplets composed of fine sandstone to siltstone, commonly with a calcareous matrix. They display exquisitely preserved, intricately interwoven crosslamination and planar topsets (2-35 cm) interbedded with olive-grey mudstone (1-20 cm; Plate 1-13-1). Load casts and ball-and-pillow structures are common. Elsewhere the unit is dominated by very fine grained, parallel-laminated, siliceous (possibly tuffaceous) pyritic strata. Grading is uncommon.

Concordant, intermediate to basaltic sills and subaqueous, generally unpillowed flows 0.5 to more than 12 metres thick are commonly intercalated with the clastic succession. Locally they make up more than 80 per cent of the section over intervals of hundreds of metres. Sills and flows are difficult to distinguish from one another, as both have sharp contacts and either aphanitic or vesicular texture. Thicker sills are dioritic or diabasic in character. Other parts of the section are dominated by pillowed flows with associated flow-top breccias or coarse tuff.

Carbonate content of the clastic unit increases up section, and massive carbonate beds a metre or more thick are exposed at a few localities. The clastic strata are overlain (conformably?) by thick, platformal carbonates of Ordovician to Devonian age, providing a minimum age limit for the underlying unit. An inarticulate bivalve fossil recovered from a sandstone layer during the course of this study confirms a Cambrian or younger age (Morford, 1992; C-208163).

The base of the succession may be exposed where the Alsek River crosses the British Columbia - Yukon Territory border. At this locality it is structurally underlain by well-bedded, compositionally variable carbonate with tuffaceous and cherty interlayers. This unit extends into Yukon where it has been previously mapped as part of the overlying Cambrian to Ordovician package (Campbell and Dodds, 1983c).

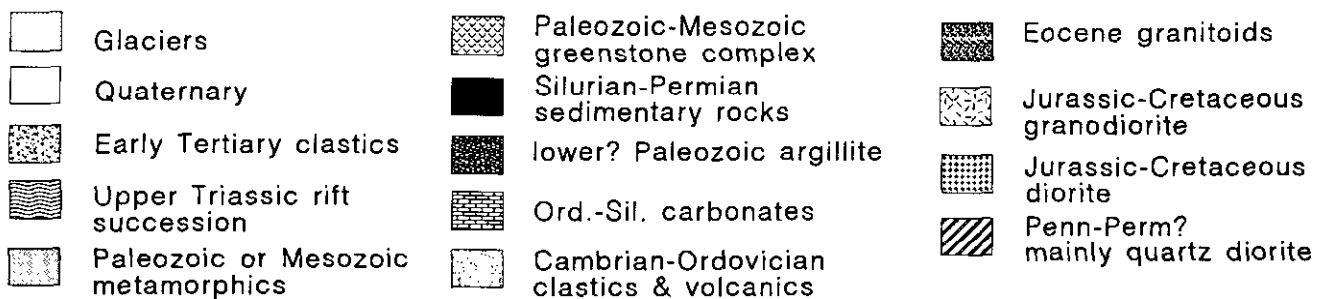
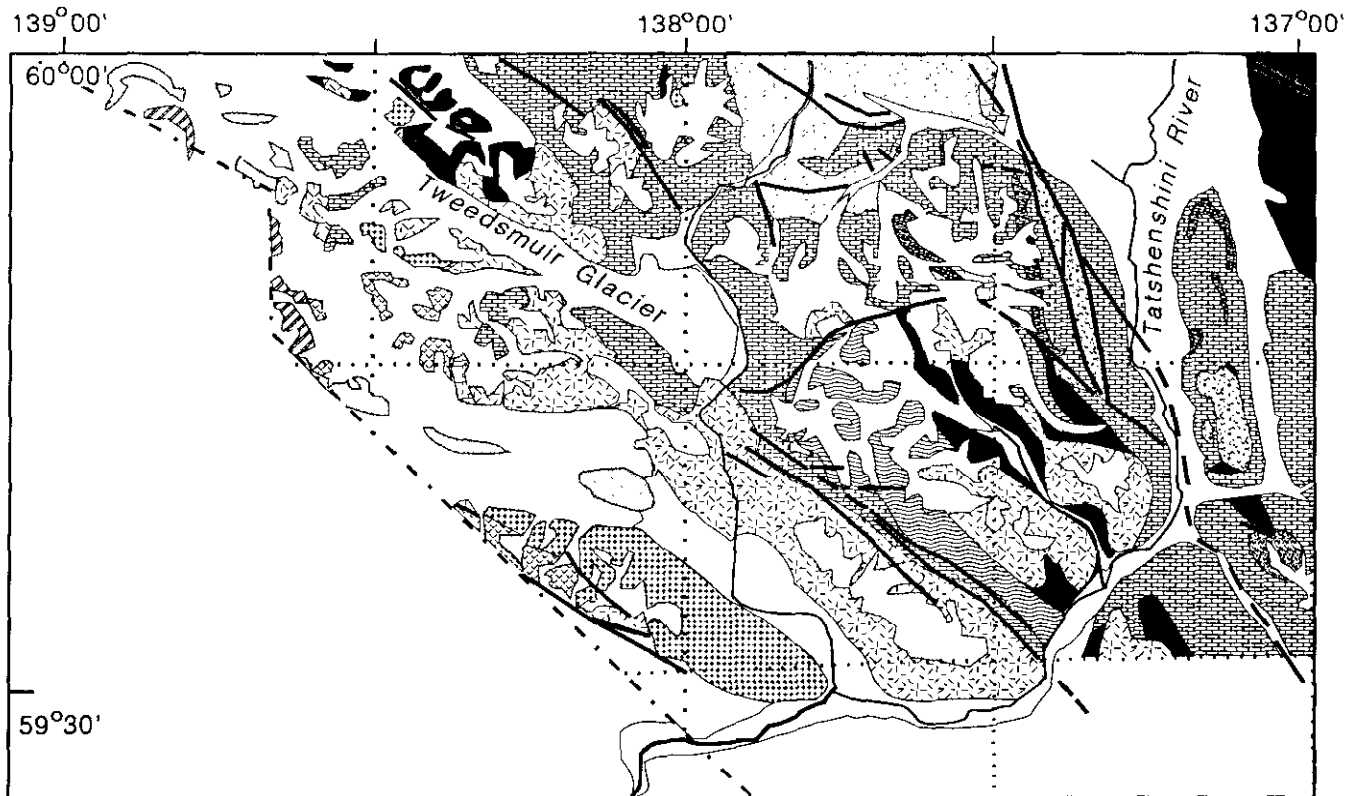


Figure 1-13-3. Much-simplified geological map showing only the most broadly defined units. Detailed 1:50 000-scale Open File maps are scheduled for release in early 1993.

Preserved bed-forms point to a sublittoral, wave or current-dominated environment (*e.g.*, Johnson, 1981). Sparse paleoflow determinations are largely unimodal to the north-northwest, indicating onshore wave-surge or long-shore current direction. The large number of concordant sills within the stratigraphic section supports a nearby magmatic source.

ORDOVICIAN TO SILURIAN CARBONATE (IPzc)

Volumetrically the most significant stratigraphic entity in the map area is a thick succession of limestones and silty limestones. It was formerly divided by Campbell and Dodds (1983a, b) into two broadly defined units; Ordovician to Devonian massive to laminated carbonate and siltstone (ODcs) and Silurian to Devonian massive limestone and marble (SDc). In this study, we further divide the succession on the basis of bedding thickness, per cent chert or siltstone,

the presence of macrofossils, and relationships with overlying and underlying strata and diagenetic textures, in order to attempt a more complete understanding of the structural relationships and facies changes within the depositional basin. Most of the units are interpreted to have been deposited in a relatively shallow, subtidal marine environment, but there is little evidence of widespread bioturbation or skeletal debris, perhaps pointing to restricted or hypersaline waters.

Several of the following units may be coeval, but representative of different facies. Unfortunately, facies changes are difficult to document as the rocks are strongly deformed (Part C) and thermally metamorphosed near the contacts of plutons and thick dikes. Several lithologies are known to occur at more than one stratigraphic interval (Figure 1-13-4). Volcanic rocks, including lenses of dark green pillow basalt and tuffaceous rocks, are present in at least two localities within the carbonate-dominated succession and cherty layers may have a tuffaceous component.

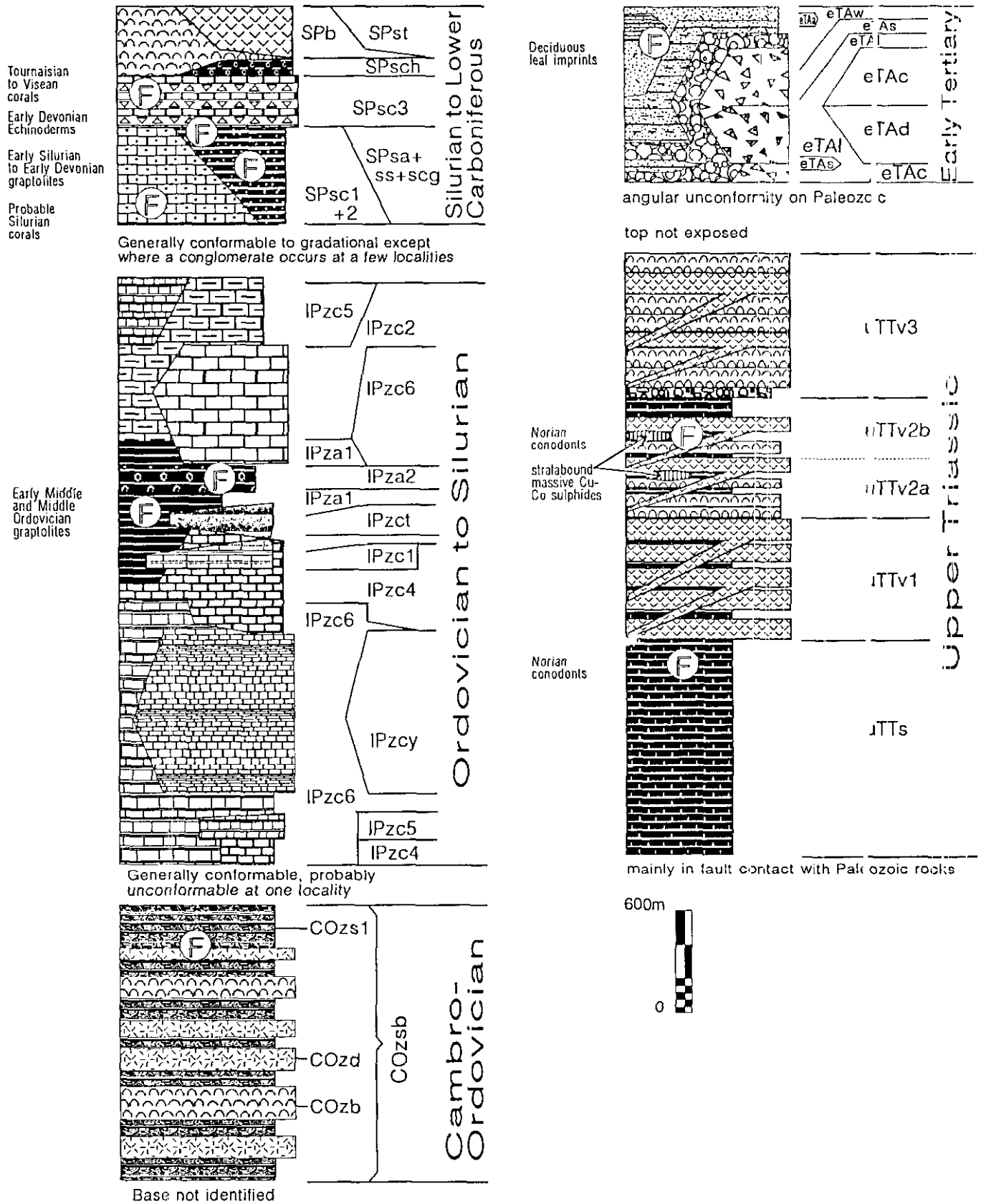


Figure 1-13-4. Stylized stratigraphic column showing relations and approximate average thickness of regionally mappable units within the Alesk-Tatshenshini area. Minor units of limited extent or those of unknown stratigraphic position are not shown. Some facies relationships are schematically shown as if the column represents a condensed west to east cross-section.



Plate 1-13-1. Cambro-Ordovician sheet sandstones (COzs1) showing low-angle trough cross-stratification, climbing ripple cross-stratification and hummocky(?) cross-stratification are interbedded with phyllitic argillite (dark). This combination of features probably formed in a sublittoral, current-dominated environment. View is to the west, and divisions on the scale card are 1 centimetre.

HETEROLITHIC LINSEN CARBONATE (IPzc0)

Two end-member lithologies comprise this unit. Most abundant is very well bedded medium to dark grey, tan-weathering calcareous mudstone that forms 1 to 3-centimetre beds with tan, silty lenses 1 to 2 centimetres thick. Of lesser importance, but dominating the section in a few localities, is interlayered, cross-stratified calcarenite grading into micrite in 2 to 10-centimetre sets. At one locality the unit is capped by limestone-cobble conglomerate. These sediments are interpreted to have been deposited in a sublittoral environment.

DARK, THIN-BEDDED LIMESTONE (IPzc1)

Thin-bedded, dark grey to black, slatey, carbonaceous to fetid limestone grades into or is interlayered with argillaceous limestone and light grey, cross-stratified calcarenite. This unit includes minor but distinct "scoriaceous" carbonate. All lithologies comprising this unit are pyrite

rich, with pyrite cubes several millimetres across. These rocks may represent a transgressive cycle and could be correlative with argillite containing Middle Ordovician graptolites.

TIGER-STRIPE CARBONATE (IPzc2)

A tiger-stripe pattern is created in these rocks where cryptocrystalline to finely recrystallized, irregular, medium grey, 1 to 5-centimetre beds are interlayered with 0.5 to 2-centimetre, relatively recessive, tan partings. Very fine laminae are preserved within the tan arenaceous layers (Plate 1-13-2a), although in places these layers are very irregular due to soft-sediment deformation resulting from regularly spaced, elongate, centimetre-scale diapirs (Plate 1-13-2b). Very fine grained, medium-bedded, buff siliceous interbeds are locally present. Near the faulted contact with Upper Triassic Tats group (informally named) stratigraphy, this unit is strongly recrystallized, light grey to white with a second foliation axial planar to centimetre-scale parasitic chevron folds outlined by millimetre-scale tan laminae.

Tiger-stripe carbonate probably occurs at several stratigraphic intervals. However, it consistently occurs beneath massive, fossiliferous, blue-grey limestone of probable Silurian age (*see* DPsc1).

MASSIVE CARBONATE (IPzc3)

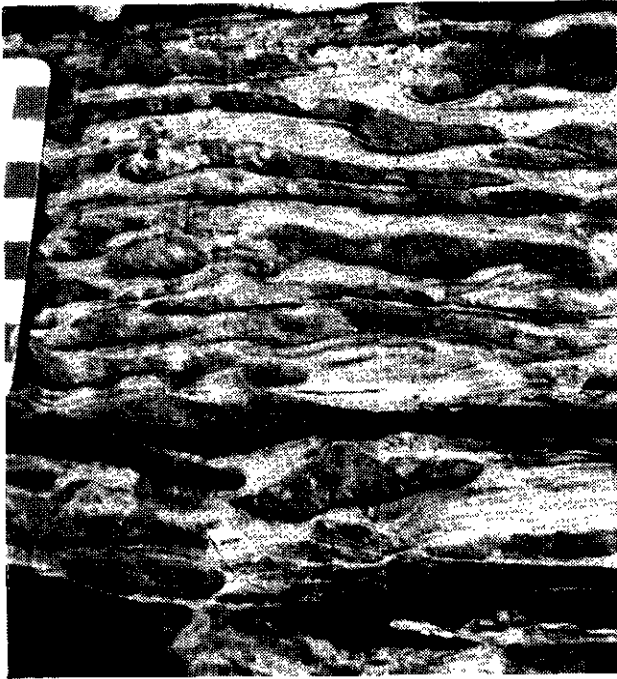
This unit consists of massive, medium grey to tan limestone and marble with rubbly to hackly weathering characteristics, which breaks into irregular fist to pebble-sized pieces or platy fragments where strongly foliated. It is commonly white weathering where adjacent to intrusive contacts and locally contains abundant, dark green waxy dikes which are discordant to totally transposed (*e.g.*, Part C; Plate 1-13-10). We believe that, in places, this unit is in part equivalent to recrystallized megacyclic carbonate (*see* Unit IPzcy below).

THINLY INTERBEDDED CHERTY ARGILLITE AND CARBONATE (IPzc4)

Light to medium grey, thinly interbedded (<5 cm) carbonate and resistant cherty argillite layers form a distinctive unit which attains thicknesses of tens of metres. This unit is generally reddish weathering and commonly fissile. Small-scale structures are beautifully outlined by the contrasting lithologies with cherty layers behaving in a more brittle fashion than the intervening carbonate (Plate 1-13-3). These rocks were deposited in a quiet, moderately deep marine environment that experienced episodic influx of fine-grained clastic detritus. In some instances the resistant layers may be altered ash beds.

RIBBED CARBONATE (IPzc5)

Buff-weathering limestone with interbedded, resistant ribs (0.5-2 cm) of orange argillaceous to silty carbonate and well-laminated, buff silty argillite beds is a coarser variety of the preceding unit and in some localities is interlayered with it. Locally it overlies the Cambro-Ordovician section and may also be injected with mafic dikes. It may have been in part penecontemporaneous with the Cambro-Ordovician



unit, but deposited in a more carbonate-rich and lower energy environment. It is also overlain by Unit IPzc4 in part and is known to occur at higher stratigraphic intervals.

LIMESTONE-PEBBLE CONGLOMERATE (IPzcc)

Light to medium grey carbonate chips, ranging from small pebble to cobble size, occur in a tan to medium grey carbonate matrix in a clast-supported conglomerate. These conglomerates form beds 0.5 to 2 metres or more thick (up to 30 m at the mouth of Alkie Creek). The beds may form sets within a dominantly argillite or carbonate host and do not appear to be restricted to specific stratigraphic intervals but rather record intrabasinal erosional events of various ages. In at least one locality a set of these conglomerate beds marks the break between carbonate and argillite deposition, probably through migration of the facies boundary rather than in response to a tectonic event.

MARBLE AND DIKE COMPLEX (IPzcd)

Light to medium grey weathering, compositionally layered marble or limestone with abundant dark green boudinaged basaltic dikes comprising as much as 50 per

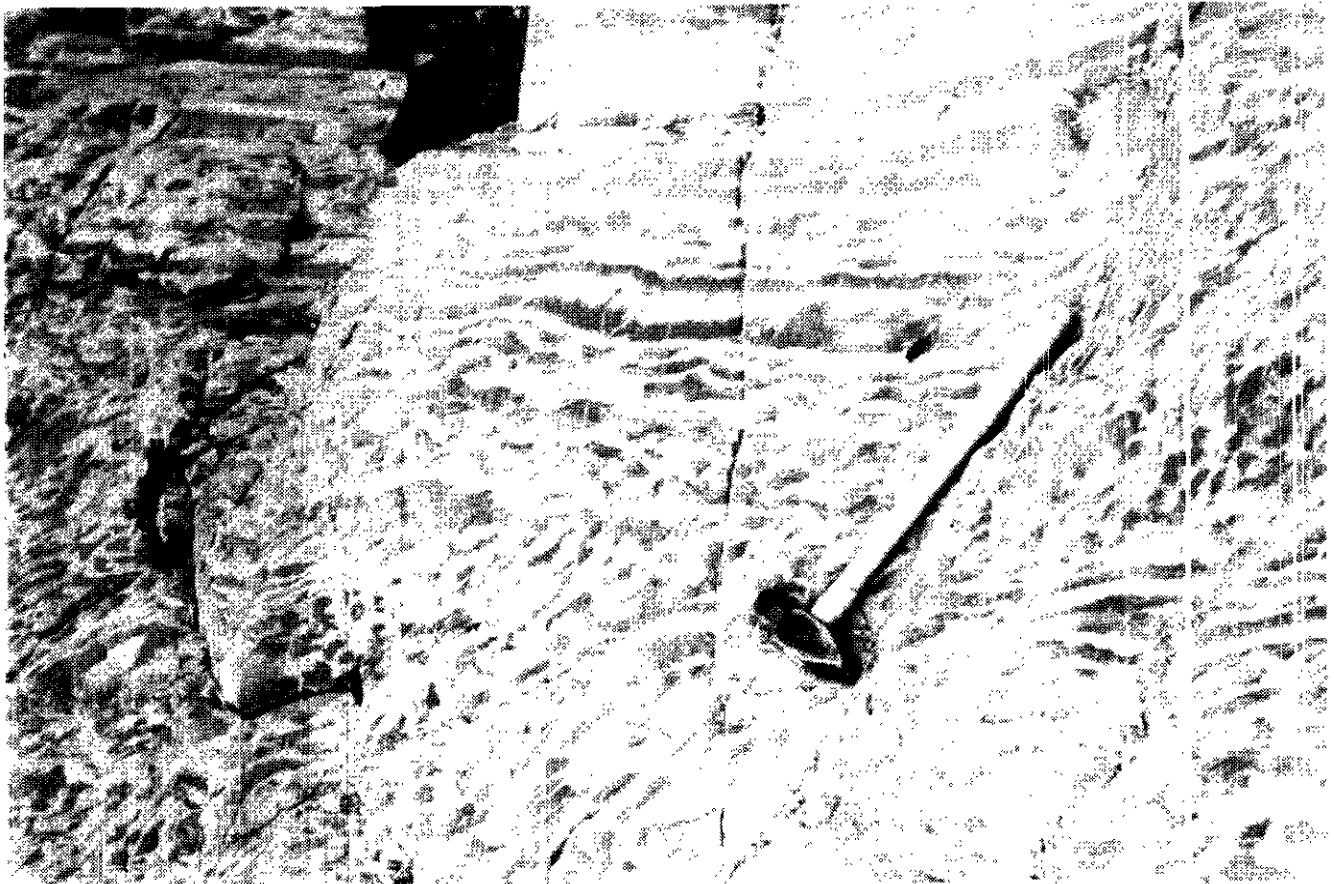


Plate 1-13-2. (a) A weathered outcrop of tiger-stripe carbonate (IPzc2) showing preservation of cross laminae within calcarenite beds and resistant nature of the more siliceous beds. (b) A glacially polished outcrop with distinctive disrupted beds. At least part of the disruption is thought to be due to soft-sediment deformation by slumping and decimetre-scale diapirism, perhaps resulting from deposition on a paleoslope.



Plate 1-13-3. Interbedded cherty argillite and carbonate (IPzc4) typically displays inhomogeneous deformation. Resistant cherty argillite layers deform brittly while thicker carbonate layers deform by plastic flow.

cent of the section, is a conspicuous and widespread lithologic association not restricted to a specific stratigraphic interval. White-weathering rinds of calesilicate-altered marble commonly rim larger dikes, particularly in zones where dikes are abundant. Although the dikes clearly postdate deposition of host carbonate, they appear to be correlative to an overlying mafic complex that is in apparent depositional contact at one locality.

CALCAREOUS TURBIDITES (IPzct)

This unit consists of brown to rust and grey-weathering, calcareous, lithic turbidites, ranging from well bedded with crosslaminations and graded bedding well preserved, to thick pebbly massive beds. Complete Bouma sequences are locally preserved with divisions A B C ± D and E, A B C or distal C D E and A E turbidites being the most common. Thicknesses range from 5 to 70 centimetres, with thicker beds generally corresponding to the more complete sequences. This unit grades into argillite containing Ordovician graptolites.

CARBONATE MEGACYCLE SUCCESSION (IPzcy)

Depositional cycles with brown, argillaceous carbonate bases that grade upwards into light to medium grey, massive to well-bedded hackly weathering carbonate over thicknesses of 10 to 60 metres are very well developed near the confluence of Alsek River and Easy Creek. Distinct

argillaceous bases weather with resistant, dark brown cherty argillite layers spaced 1 to 15 centimetres apart and stand out 1 to 3 centimetres from recessive yellow-brown carbonate (Plate 1-13-4a). Each cycle is composed of dozens of argillite partings rhythmically interlayered with carbonate, with a decrease in the argillaceous component structurally up section. Where best exposed north of Turnback Canyon there are at least ten of these units stacked in succession (Plate 1-13-4b).

In carbonate shelf environments worldwide, laterally persistent, evenly bedded shallowing-upward cycles containing algal mats are among the most commonly encountered carbonate lithologies. They are interpreted to be products of subtidal to supratidal carbonate deposition which exceeds subsidence rates (James, 1984). Cyclic deposition combined with preservation of possible algal mats within some of the cycles of Unit IPzcy point to a similar depositional environment, but several key features are lacking. Subaerial features such as desiccation cracks or evidence of cross-stratification or intercycle conglomerate identified in other cyclic successions (James, 1984) have yet to be identified. Perhaps Unit IPzcy was deposited in a very quiet, lower intertidal to subtidal environment seaward of a periodically exposed part of the platform.

LOWER PALEOZOIC ARGILLACEOUS STRATA (MAINLY ORDOVICIAN, IPza)

Rocks of Unit IPza, which lies within the carbonate sequence, were previously mapped as part of the "Icefield Ranges pelitic assemblage" by Campbell and Dodds (1983a, b) which included rocks ranging in age from Late Triassic to Devonian and older. Once an extensive map unit, this pelitic assemblage has been greatly reduced, with inclusion of much of this unit with the lower Paleozoic carbonate and middle Paleozoic mixed sequences. Rocks still included within this unit are here referred to as lower Paleozoic argillaceous strata (IPza). They consist primarily of silty, black, grey or rusty argillite, which is commonly well laminated (IPza1). Rust coloration is primarily due to the oxidation of iron sulphides such as pyrite occurring as cubes up to 0.5 centimetre in diameter or as pyrrhotite blebs and wisps. A slaty to phyllitic cleavage with a well-developed micro-crenulation occurs locally. Thickness of this unit is difficult to estimate as much strain has been accommodated by these rocks and they may be tectonically thickened by more than 100 percent.

Two other end-member lithologies are also common. A chert and siliceous argillite subunit is locally mappable, for example, northeast of Carmine Mountain where it is associated with early Middle Ordovician (Norford, 1992; sample C-168133) graptolite fauna (IPza2). Also, a light to dark grey calcareous argillite exposed at the headwaters of Tough Creek is a mappable subunit (IPza3). Various proportions of the three compositional end members may occur over intervals of less than 100 metres.

LOWER PALEOZOIC VOLCANIC ROCKS (Pzb)

Volcanic flows and tuffs comprise a minor portion of the lower Paleozoic succession at several localities. Cherty intervals within Middle Ordovician shale north of Carmine

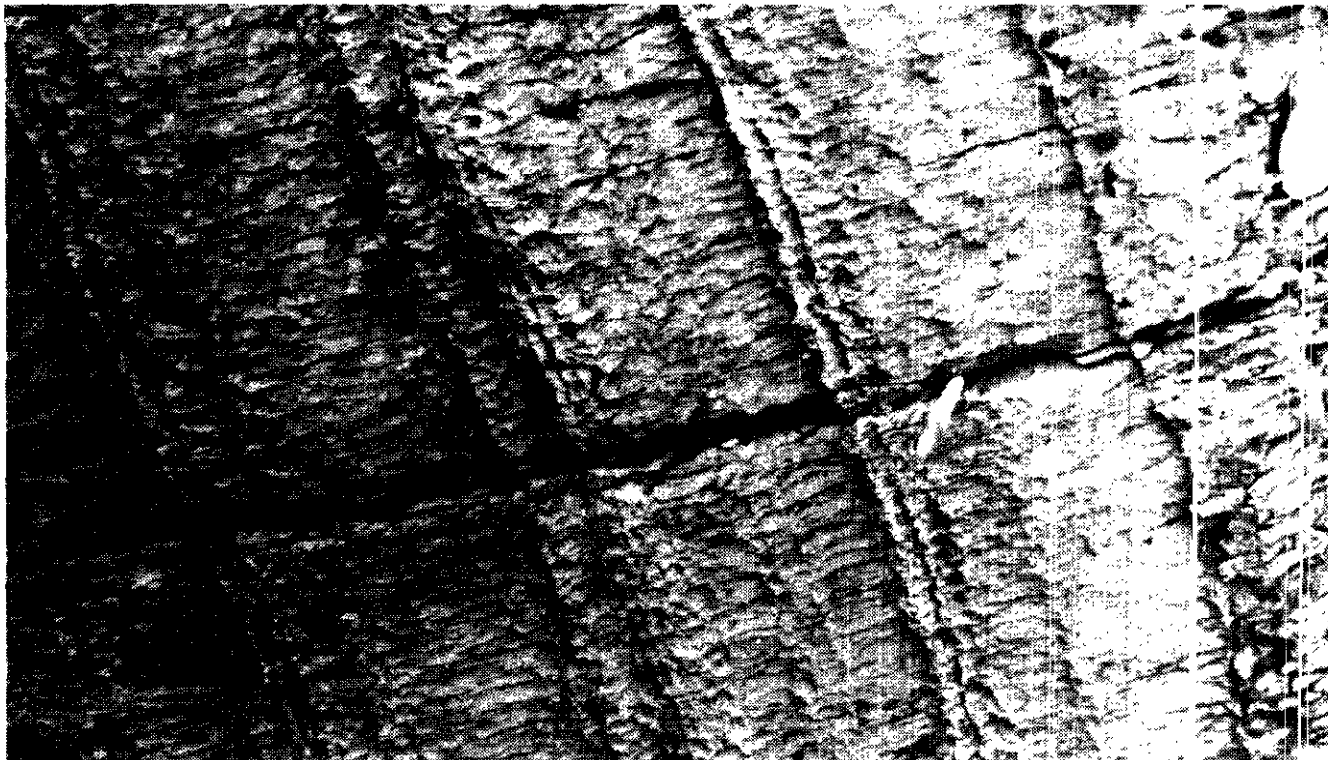


Plate 1-13-4. (a) Widely spaced, resistant argillaceous partings within the fine-grained portion of a megacycle succession (IPzcy). Normally carbonate beds between rhythmically interlayered argillite partings are 4 to 10 centimetres thick, whereas these are up to 20 centimetres thick. Felt-tipped marker is approximately 1 centimetre thick. (b) Stacked megacycles near the confluence of Easy Creek and the Alsek River. Approximately 1000 metres of relief is exposed in the foreground beneath the glacier.

Mountain (114P/14) locally contain ash-tuff layers. In the upper Tats Creek valley (114P/12) scoriaceous basaltic lapilli tuff and light green, siliceous, metamorphosed ash tuff (Plate 1-13-5a) are apparently interbedded with foliated Paleozoic carbonate. North of the headwaters of Sediments Creek (114P/13) a tabular body of pillow basalt (Plate 1-13-5b) 50 to 100 metres thick is enclosed in Paleozoic limestone. Stratigraphic tops may be indicated where a red-weathering, tuffaceous basal(?) section is in contact with recrystallized carbonate to the east while carbonate in contact to the west is not contact metamorphosed.

MIDDLE TO UPPER PALEOZOIC SEDIMENTARY ROCKS

A sequence of limestone, argillite, sandstone, conglomerate and volcanic rocks of known and presumed middle to upper Paleozoic age overlies the carbonate succession in the Henshi Creek (114P/12), O'Connor River (114P/11), Easy Creek and upper Tweedsmuir Glacier (114O/16) and western Squaw Range (114P/14) areas. Siliciclastic rocks in other areas such as Sediments Creek, lower Henshi Creek and south of Tkope River may be the same age. Mappable units within this package are described following, in approximate order of abundance.

ARGILLITE AND SANDSTONE (SPsa, SPss, SPscg)

This unit consists of noncalcareous to calcareous black argillite (SPsa) or black limestone which is laminated to thin bedded, with or without medium to thick, orange weathering interbeds of fine to coarse-grained lithic sandstone (SPss) and granule to pebble conglomerate (SPscg). The proportion of coarser clastic rocks in a given section ranges from almost none to over 60 per cent, depending on location, with the thicker and coarser beds corresponding to the more sandstone-rich sections. Other horizons are dominated by coarse sandstone and conglomerate, and in the O'Connor River area, contain abundant plant fossils (swamp grass and fern fronds). Sandstone and conglomerate preserve sedimentary structures ranging from massive, pebbly to graded beds to planar to ripple cross-stratification. Black chert, graphitic argillite and light grey and rust-coloured pyritiferous volcanic(?) clasts are common. Pebble imbrication at one locality indicates westerly paleoflow.

Details of the argillite unit (SPsa) are less well known elsewhere, but in most localities the jet-black, highly fissile carbonaceous nature is apparent and serves to distinguish it from the more indurated, rusty weathering argillite of lower Paleozoic age. On the other hand it strongly resembles parts of the Upper Triassic sedimentary unit (uTTs).

LIMESTONE (SPsc1, SPsc2, SPsc3)

Limestone ranges from light to medium blue-grey and thin to medium bedded (SPsc1) to dark grey to black, fine grained, massive to medium-thin bedded (SPsc2), to medium-bedded, buff-weathering, black, fresh limestone with thinner recessive argillaceous interbeds (SPsc3).

Unit SPsc1 is typically blue-grey weathering, fossiliferous, and occurs as lenses up to 100 metres thick and a few kilometres long surrounded by sooty argillite. Fossils

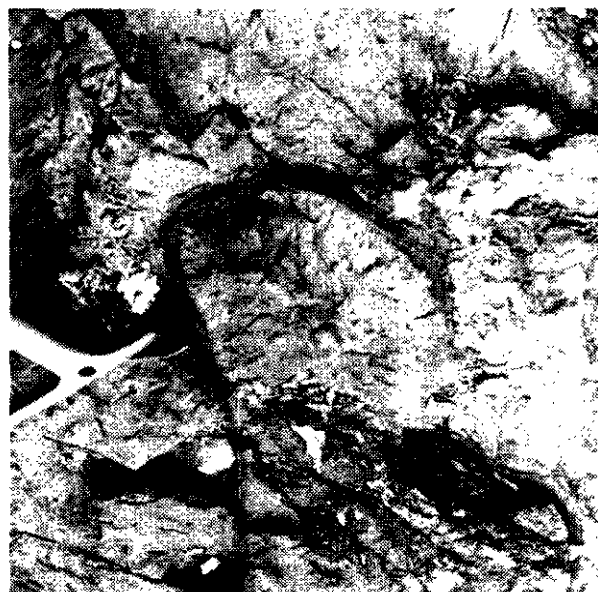


Plate 1-13-5. (a) Folded siliceous tuff layer within Paleozoic carbonate in the upper Tats Creek valley. (b) Pillows within a flow unit 50 to 100 metres thick, north of the headwaters of Sediments Creek.

are prolific, locally forming crinoid columnal and stem packstone and rugosan coral packstone. Brachiopods and bryozoans are also abundant locally. Although recrystallization has masked many of the primary features, preliminary identification of these fossils suggests that the rocks are mainly Early Devonian (*e.g.*, Norris, 1992) to Early Carboniferous (W. Bamber, personal communication, 1992), although they could be as wide ranging as Silurian to Late

Carboniferous and Permian. Limestone lenses of Unit SPsc1 are one of the most characteristic features of the middle to upper Paleozoic sequence, and are easily distinguished from the lower Paleozoic carbonates which are massive, unfossiliferous, and generally buff weathering.

ANDESITIC TUFF (SPst)

Green-weathering lapilli tuff with some ash and block tuff is exposed in the upper Tweedsmuir Glacier area, where it lies (depositionally?) between the basalt and chert units. Analogous lithologies occupy a similar structural(?) position in the Squaw Range where they are also associated with a greywacke unit (*see* SPsw below) and near the mouth of the O'Connor River where they structurally overlie graptolite-bearing carbonaceous and gypsiferous shales of Silurian to Devonian age that contain white, clay-altered ash layers. Clast composition ranges from dark green (basaltic?) to light green and siliceous (dacitic?).

CHERT AND SILICEOUS ARGILLITE (SPsch)

A sequence of black to grey, thin-bedded chert and siliceous argillite 10 metres thick and with slaty partings is exposed in the upper Tweedsmuir Glacier area. It appears to structurally overlie the andesitic tuff unit and underlies a thick sequence of limestone (SPsc1) and argillite (SPsa). Tan to white, recrystallized chert and siliceous argillite, with associated phyllitic quartzite, are also present within a sequence of argillite and limestone in the Squaw Range.

BASALT (SPb)

A unit consisting of lensoidal, dark green, aphanitic, vesicular basalt flows crops out in the upper Tweedsmuir Glacier area. Fingering is indicated by a presumed upward increase in the number and size of vesicles within individual flows 2 to 3 metres thick. The basalt flow unit appears to depositionally overlie a carbonate unit of unknown age, and is separated from the rest of the units described above by ice cover. Hence it may be one of the oldest units in the package or be unrelated to the remainder of the section. Basaltic flows are also exposed in the Squaw Range south of the Duke fault, where they are presumed to be late Paleozoic in age. They range from massive to rarely pillowed, and are associated with tuff and greywacke.

METAGREYWACKE (SPsw)

In the Squaw Range, brown to greenish metagreywacke varies from massive to thinly interbedded with slate. It is associated with tuff, argillite and basalt flows. Foliation is generally outlined by the development of chlorite and muscovite (phengite?), but locally garnet-biotite grade is attained. Higher metamorphic grade may be related to intrusion of thick gabbroic sills.

ARGILLITE AND CARBONATE COUplet (SPsac)

A distinctive sedimentary couplet of carbonate-rich argillite overlain by orange-weathering carbonate is well exposed near the mouth of the O'Connor River and in a gorge south of Sediments Creek. Black carbonate inter-layered with graphitic argillite may be microlaminated.

Argillite is jet black, highly friable, gypsiferous, and contains white clay-altered ash layers with rare vesicular basaltic(?) bombs. Argillite contains graptolites of probable Early Silurian to Early Devonian age (Norford, 1992; sample C-168134), which are present in abundance above white to tan ash horizons. The upper carbonate is generally strongly disrupted, veined and, at one locality, talcose. The sedimentary couplet is found in association with the the argillite unit (SPsa) and sandstone unit (SPs) which contains rare ash-tuff horizons.

CONTACT RELATIONS AND FACIES INTERPRETATION

The relationship of this sequence of rocks to the underlying lower Paleozoic carbonate sequence appears to be complex. In the upper Tweedsmuir Glacier area (1140/16W), fossiliferous limestone overlies a section of the sandstone and argillite sequence, which in turn appears to overlie and in part be interbedded with the lower Paleozoic tiger stripe carbonate (JPzc2a). In the Easy Creek area argillite and fossiliferous limestone of the middle to upper Paleozoic package overlie tiger stripe limestone or buff-weathering fine-grained facies of the carbonate megacyclot unit (JPzcy). In the O'Connor River and Alkie Creek areas the contact is adjacent to medium to dark grey limestone of unknown age, with distinct, very fine, buff laminations (algalmats?). This facies seems to be present both in the upper part of the lower Paleozoic sequence and in the lower part of the middle to upper Paleozoic sequence.

Middle to upper Paleozoic sedimentary sequences represent a distinct departure from the carbonate-dominated platform environment of the lower Paleozoic sequence. Silurian rocks in the O'Connor River area include interbedded carbonates and graptolite-bearing argillite of presumed marine origin, as well as sandstones with abundant plant fossils of probable nonmarine origin. This suggests a swampy near-shore or deltaic environment, with marine incursions due to subsidence or channel abandonment. In the Alkie Creek area, the section includes thick to thin graded sandstone, laminated argillite, and thin to thick beds of limestone, including graded calcarenite. Beds are typically planar, and these rocks are perhaps marine turbidites such as those deposited at delta fronts.

Fossiliferous carbonate lenses within a section dominated by sooty calcareous and noncalcareous argillite, typical of the upper Henshi Creek and upper Tweedsmuir Glacier areas, suggest a reef to back-reef environment. Organic-rich argillite probably accumulated in anoxic lagoonal areas surrounded by biohermal patch reefs. Volumetrically minor *tuffaceous units are common throughout the area and point to a magmatic episode(s), perhaps related to a tectonic event(s).*

Overall, the middle to upper Paleozoic sequence appears to represent marine regression and clastic influx, with shallow-water platform carbonate sedimentation giving way to deltaic, possibly nonmarine environments and reef to back-reef (lagoonal) deposition. The laminated carbonate sequence that marks the transition in the Alkie Creek and O'Connor River areas is suggestive of a dry, periodically subaerial (tidal flat) environment.

UPPER TRIASSIC TATS GROUP (informal, uTT)

The nomenclature of Upper Triassic strata within northern Alexander Terrane, which comprise a submarine rift assemblage of fine-grained sediments and mafic volcanics, has undergone several revisions in recent years. Originally mapped by Campbell and Dodds (1983a), this stratigraphy was later refined by MacIntyre (1984) who included it in the informally named Tats group (MacIntyre, 1986). Rapid facies changes, abundant syndepositional and later faulting and folding and sedimentary-volcanic interfingering have prompted other workers to refer to these rocks as the Tats volcanic complex (Gammon and Chandler, 1986). However, a coherent stratigraphy does seem to exist, and is believed (Monger *et al.*, 1991) to be correlative with the Hyd Group (Gehrels *et al.*, 1987) in southeast Alaska. Our preference is to maintain use of "Tats group".

Tats group stratigraphy is of critical economic significance in the region because it hosts the Windy Craggy volcanogenic massive sulphide deposit, which contains nearly 300 million tonnes of copper-cobalt ore reserves (Geddes Resources, 1992; Part D). Tats group strata are mainly restricted to a fault-bounded basin between Tats Creek on the west and Henshi Creek on the east. Mapping in 1992 established the presence of Tats group stratigraphic elements south along Tats Creek to the Tatshenshini River. In this report the Tats group is divided into regionally mappable units including a lower sedimentary unit and three major volcanic units following the subdivisions of MacIntyre (1984).

The Tats group lower sedimentary division (uTTs) has a structural thickness of 1000 to 1500 metres and is dominantly composed of black to dark grey or brown, thinly bedded, fissile and platy weathering calcareous siltstone and argillaceous limestone with calcalkaline basaltic sills. Also present are minor but conspicuous debris flows and quartz-lithic calcarenite beds. Accurate stratigraphic details and thicknesses are difficult to determine as this unit is everywhere strongly contorted.

The lower volcanic division (uTTv1) is generally not more than 1000 metres thick, and consists mainly of massive sills and perhaps structureless basalt flows with minor interbeds of sedimentary rocks like those of lower sedimentary division. Dark green to black flows and sills are locally porphyritic with a microdioritic, felted texture. Adjacent sedimentary strata are commonly hornfelsed. This unit is transitional between the sedimentary division and the middle volcanic division, and is absent in some localities.

A middle volcanic division (uTTv2) can be divided into a lower volcanic and sill-dominated section (uTTv2a) and an upper sediment-dominated sequence (uTTv2b) in order to facilitate mapping in some areas. Volcanogenic massive sulphide horizons in the Icebridge Glacier area are thought to occur in the upper sequence, at a stratigraphic position similar to the Windy Craggy massive sulphide horizon.

The middle volcanic division ranges from 600 to approximately 2200 metres thick, and consists of interbedded pillow basalt and calcareous siltstone with minor tuff, chert and limestone-clast debris flows. Basaltic sills are present in

some locations and are particularly conspicuous in the upper sediment-dominated division. Some "sills" may actually be massive flows. Careful along-strike observations have shown that some units that in one place appear to be sills, can be traced into demonstrably pillowed lavas. Both sills and thick flows may hornfels sediments at their margins.

Volcanic flows and sills of the middle division are cogenetic (Peter, 1992) and calcalkaline (MacIntyre, 1986). Peter determined that the basalts are tholeiitic, but this conclusion was based upon major element geochemistry of altered samples. Less altered sills consistently plot within the calcalkaline field and analysis of the relatively immobile elements (Hf, Th, Ta) shows that most samples are calcalkaline.

The upper volcanic division (uTTv3) ranges from 500 to 1000 metres thick, and consists almost entirely of massive to pillowed basalt flows. This unit also includes basaltic sills, but sedimentary rocks are very minor to absent. An agglomerate unit, 50 or more metres thick, is locally present near the base of the unit, but identical rocks probably occur throughout the upper volcanic division.

Equivalent Upper Triassic strata also outcrop south and east of the map area. In addition, a Paleozoic to Mesozoic greenstone complex in the Vern Ritchie Glacier area has protoliths similar to the Tats group and hosts a newly discovered copper occurrence (Part D). Until an age of the metamorphic rocks is firmly established, correlation with Tats group stratigraphy should be regarded as tenuous at best.

PALEOZOIC OR MESOZOIC GREENSTONE-CARBONATE COMPLEX

A Paleozoic or Mesozoic Greenstone-Carbonate Complex is exposed within 1140/9, 15 and 16. It consists primarily of dark green to black, aphanitic to bladed feldspar porphyritic flows. Textures vary from massive to amygdaloidal, with rare remnant pillows which are commonly masked by a moderate to strong foliation or patches of epidote-chlorite alteration. Interbedded(?) marine sedimentary rocks include carbonates, including brown to white-weathering marble layers up to several hundred metres thick, sharpstone volcanic conglomerate with calcareous matrix, dark grey chert(?) and wacke, and at one locality, a pyritic sericite schist. Greenstone-dominated rocks give way westward to structurally underlying thin to medium-bedded calcareous to siliceous(?) wacke with interbedded argillite, a unit which is characteristically red-brown to greenish weathering. All components of the complex are intruded by Jurassic-Cretaceous granitoid rocks, and are thus no younger than Middle Jurassic, but may be as old as early Paleozoic. A predominance of metabasalt suggests a protolith such as the Upper Triassic Tats group, but thick carbonate horizons are more typical of the Paleozoic succession. More work is needed to resolve these possibilities.

A newly discovered copper showing, the Vern occurrence, contains up to 15 per cent chalcopyrite, but its extent could not be determined due to precipitous terrain. Two kilometres northwest of the Vern showing is a gossanous

cliff face approximately 50 metres high. This zone was not examined because it is located below a potentially hazardous icefall (see also Part D).

PALEOZOIC OR MESOZOIC SCHIST AND GNEISS

Rocks mapped as Paleozoic or Mesozoic schist and gneiss are primarily exposed in the western part of the map area (114O/9 and 15) and locally around the margins of batholiths, where protolith textures are no longer evident. The latter grade into less recrystallized rocks, which include the upper and lower Paleozoic carbonate and clastic sequences.

A northwest-trending linear belt of relatively coarse, amphibolite-grade rocks crops out along the International Boundary. Retrograde greenschist facies recrystallization has affected some of these rocks. Except where they can be traced into identifiable lithologies, protolith ages are unknown, although they may be largely late Paleozoic in age and derived from the Devonian to Permian sequence. Mapping during 1992 permitted definition of the following units:

- Metapelite, metasilstone, calcareous metapelite and quartzite(?), which is generally buff or light grey to dark grey, schistose, and often brown weathering. Schistose varieties include biotite-actinolite (or hornblende)-plagioclase-quartz-muscovite schist;
- Medium-grained, strongly foliated metabasite, primarily hornblende-plagioclase or actinolite-plagioclase schist, with minor secondary epidote and quartz. In 114O this unit includes low-grade equivalent chlorite-epidote-actinolite schist;
- Coarse white to orange marble, with associated calcareous skarn and calcsilicate gneiss. Calcsilicate layers commonly include epidote, diopside, wollastonite and grossular in bands;
- Medium grey pyritiferous phyllite and semischist with calc-phyllite and thin to thick phyllitic limestone interbeds;
- Quartz-rich metasediments, including quartzite and siliceous meta-argillite. As mapped, this unit includes subordinate phyllite and carbonate;
- Green-grey weathering, dark green, gneissic banded amphibolite, which may be cut by epidote-feldspar±quartz veins, and is interlayered with the metapelite and carbonate units;
- Strongly foliated, fine to coarse-grained dioritic orthogneiss.

EARLY TERTIARY CLASTIC SUCCESSION

A folded and faulted but unmetamorphosed sequence of presumed Early Tertiary age is preserved in a north-trending basin, 2 to 3 kilometres wide, along the west side of the Tatshenshini River valley and in small (1 km²) grabens in the Tats Creek valley. The Early Tertiary succession is relatively easily distinguished by lack of a pervasive cleavage and by locally abundant plant fossils including decid-

uous leaf imprints and coal. It is primarily of nonmarine alluvial, fluvial and possibly lacustrine(?) origin.

The Early Tertiary clastic succession consists of the following interfingering units: dark brown weathering argillite; light brown weathering platy wacke, which locally contains black, well-rounded pebbles of vesicular basalt; laminated to medium-bedded shale, siltstone, and sandstone with coal-bearing interbeds and minor conglomerate; pebble conglomerate, made up of subangular to subrounded clasts of black argillite, chert, shale, limestone and intermediate to felsic volcanics in a muddy matrix; and angular to well-rounded coarse cobble to boulder conglomerate.

Three coarse conglomerate end-members are recognized on the basis of the type of substrate eroded: limestone clasts in a carbonate matrix, diorite-clast conglomerate and breccia, and green volcanic clasts in a red, oxidized matrix. Limestone conglomerate may contain up to 50 per cent well-rounded, unfoliated basalt clasts. Lack of a fabric in volcanic clasts suggests that they may be derived from relatively young volcanic rocks like those that cap Carmine Mountain.

Very coarse rocks comprise the bulk of the section in the northeastern part of the depositional basin, and are essentially absent at the southwestern end, where a relatively thin basal unit consists of mixed lithic-pebble and rare argillite-cobble conglomerate. Overall, rocks in this basin fine from east to west and north to south. Stratification in the conglomerates ranges from absent to crude and subhorizontal, locally with pebble imbrication. Within the coal-bearing section of sandstone, shale and conglomerate, sandstone beds are medium to thick, lensoidal, and vary from trough cross-stratified to ripple cross-stratified to planar bedded, with laminated shale to fine sandstone interbeds. Locally abundant plant fossils, including fragments of leaves and stems of broadleaf and less commonly needle-leaved plants are most common in this part of the section. Coal seams, generally less than 50 centimetres thick, occur within the shaly parts of the section. The wacke unit makes up perhaps 70 per cent of the section in the southern end of the basin. It consists of a monotonous sequence of poorly bedded, fissile sandstone with rare plant fossils. Argillite is only a minor constituent, most closely associated with the wacke unit.

The type and distribution of facies (Plate 13-6) suggests that the lower Tertiary section was deposited in a fault-bounded basin, with alluvial fans derived from a large fault scarp bounding the eastern side of the basin, grading westward into fluvial deposits. During part of the basin history the northern part of the fault scarp evidently had greater relief than the southern part. Wacke and argillite units in the southwestern part of the basin represent lower energy, possibly lacustrine, environments.

Coarse arkose (probably locally derived from adjacent Jura-Cretaceous plutonic rocks) and conglomerate, locally with interbedded coal, are found in association with massive, light grey to light yellow, clay-rich units, several metres thick, in small basins along the Tats Creek valley. Clay beds of this type generally have a volcanic source, suggesting a possible tie with Eocene and Oligocene (?) volcanic strata east of the immediate study area (Campbell



Plate 1-13-6. Coarse angular limestone conglomerate of probable Early Tertiary age was probably deposited not far from a basin-bounding fault scarp.

and Dodds, 1983a). Basin formation is probably contemporaneous with major Late Cretaceous to Early Tertiary north to northwest-trending strike-slip faulting in the region.

TERTIARY(?) CARMINE MOUNTAIN VOLCANICS

On Carmine Mountain (114P/11) a relatively flat-lying volcanic and sedimentary sequence unconformably overlies lower Paleozoic marble, and apparently includes stratigraphic elements of both middle and late Paleozoic and Early Tertiary age. Units that directly overlie the Paleozoic marble are slightly foliated and include: medium to dark green lapilli tuff and agglomerate; carbonate-matrix limestone cobble to boulder conglomerate; subangular argillite-chip pebble conglomerate; and well-rounded polymictic pebble conglomerate. Limestone float with corals of possible Devonian age was found in a covered area between the first two units. Carmine Mountain is capped by massive andesite and lesser basalt flows, massive to columnar jointed dacite and rhyolite flows, and light to medium grey or grey-green dacitic to rhyolitic ash and lapilli tuff. Together with the conglomeratic rocks these felsic volcanic

strata are essentially undeformed, and may be Early Tertiary in age, possibly correlative with the "Oligocene and older" volcanics of Campbell and Dodds (1983a).

INTRUSIVE ROCKS

Intrusive rocks underlie about 25 per cent of the map area, increasing in abundance to the west. Basic intrusive rocks range from Cambro-Ordovician to Tertiary age. Intermediate to felsic intrusives are dominantly Mesozoic or younger.

JURASSIC(?) AND OLDER

Intrusive units of presumed pre-Jurassic age range in composition from diorite to gabbro and are commonly foliated. They underlie parts of the westernmost and easternmost map area. Age is constrained by their crosscutting relationship with carbonate strata at least as young as Ordovician, while some evidence supports transitional relationships with basaltic rocks interbedded with upper Paleozoic(?) strata. At two localities in the upper Tats Valley (114P/12), map patterns suggest that these rocks are crosscut by part of the Jura-Cretaceous plutonic suite. Such

an interpretation is supported by observations at one locality where a mafic border phase apparently intrudes older basaltic rocks. The rocks include an amphibolite unit, an agmatite unit, and a greenstone, gabbro and diorite complex.

VARIABLY FOLIATED, POLYPHASE BASALT-GABBRO COMPLEX

Previously unmapped rocks of a basalt-gabbro complex form elongate bodies less than a kilometre across (114P/12) but several kilometres long, which display intrusive relationships with each other and enclosing Paleozoic carbonates west of Tats Glacier. Intrusive phases included in this complex are a brecciated, medium-grained hornblende-feldspar-porphyrific gabbro or diorite, and a crowded feldspar-porphyrific hypabyssal body with a black groundmass which is intruded by and intrudes a dark green, aphanitic basaltic phase. A weak to strong foliation is locally developed and all units are chloritized and epidotized.

These rocks may be correlative with nearby basalt agglomerate which apparently forms part of the Paleozoic stratigraphy. They may also be related to the Paleozoic to Mesozoic greenstone-carbonate complex or the Squaw-Datlasaka Ranges gabbro-diorite sills of Campbell and Dodds (1983a). However, both the aphanitic and porphyritic phases are lithologically similar to flows within the Tats group volcanic stratigraphy. Current age controls do not provide a basis for favouring one or the other of these alternative correlations.

SQUAW-DATLASAKA GABBRO-DIABASE

Several lithologies are included in this unit which is widely exposed in the Squaw Range (114P/14). It is composed of variably foliated, medium-grained, aphanitic to feldspar-porphyrific basalt, diorite and gabbro. South of Talbot Creek the unit is mainly dark green to black weathering and grades both south and west into a dike complex within Ordovician carbonate with a steady increase in the number of screens of marble (and felsic tuff?). They are locally cut by coarse quartz-carbonate veins up to 20 centimetres wide. These rocks are interpreted as Paleozoic to Mesozoic intrusive rocks by Campbell and Dodds (1983a).

Rocks north of Talbot Creek that were included with this unit by Campbell and Dodds (1983a) are mainly bright green due to ubiquitous chlorite-epidote alteration. They intrude intercalated wacke and other marine sediments, flows and tuffs. Mylonitic fabrics are locally well developed on the margins of these bodies, particularly the structurally lower contacts. As a consequence, we attribute at least some repetition of these sills to west-dipping thrust faults.

JURASSIC-CRETACEOUS PLUTONS

Intrusive rocks of Jurassic to Cretaceous age comprise the volumetrically most significant intrusions in the central and western parts of the map area. These include the Noisy Range batholith, Battle Glacier batholith, Easy pluton and the Not Yet pluton, which form north-northwest-trending, elongate bodies conforming to the regional structural fabric.

In most intrusions of this age it is possible to demonstrate an early, foliated, dominantly dioritic border phase and a later granodioritic to quartz monzonitic phase. Foliated zones are also present in the relatively younger, more felsic phases.

Potassium-Argon cooling ages from these bodies fall within the 130 to 160 Ma range (Dodds and Campbell, 1988), and place them in the Saint Elias Plutonic Suite of Campbell and Dodds (1983a).

DOMINANTLY DIORITIC (BORDER) PHASES

Dominantly dioritic rocks occur as homogeneous bodies in the westernmost part of the map area (Battle Glacier batholith) or as heterogeneous border phases around relatively homogeneous granodioritic to quartz monzonitic bodies, and as small plutons in 114P/13 and 14 and 114O/16. They are dominated by orange to green-weathering, medium to coarse-grained, epidote and chlorite-altered diorite. Adjacent the Ender Ranges fault they are particularly strongly deformed and are intruded by variably deformed fine-grained porphyritic dikes with black to white, tabular plagioclase phenocrysts.

Where these dioritic phases are restricted mainly to the borders of more felsic bodies or to small plutons, several distinct phases are typically present. These range from hornblende to hornblende-rich quartz diorite or hornblende leucogabbro containing rare coarse, euhedral plagioclase crystals. Each phase or mixture of phases may vary from fine to very coarse grained and unfoliated to strongly foliated. Foliation generally follows a northwest to northeast trend, concordant with the foliation in the intruded Paleozoic to Mesozoic metasedimentary country rocks, suggesting forceful emplacement. The intrusions commonly contain up to 25 per cent irregularly shaped, foliated, melanocratic xenoliths composed mainly of hornblende, biotite and plagioclase. Unfoliated aplitic to pegmatitic dikes and epidote-calcite-quartz veins commonly cut the border phase (Plate 1-13-7).

Skarn associated with dioritic phases is best developed north of the Windy Craggy area (114P/13) where mineralized garnet-epidote-diopside-wollastonite skarn hosts irregularly distributed pods and lenses of massive and disseminated pyrrhotite, chalcopyrite, sphalerite and magnetite at the contact between carbonate and clastic sediments (see Part D).

GRANODIORITE TO QUARTZ MONZONITE PHASE

Leucocratic phases dominate the relatively homogeneous interiors of many of the large Jura-Cretaceous plutons. Medium to coarse-grained, weakly to strongly foliated biotite hornblende granodiorite or tonalite to hornblende-biotite quartz monzonite are most common. Both end-member compositions are light to medium grey and blocky weathering. Average outcrops are composed of 60 to 70 per cent fresh, equigranular feldspar, 10 to 30 per cent interstitial quartz, and 20 to 30 per cent hornblende and biotite. Hornblende crystals are usually shiny black, prismatic and subidiomorphic. Biotite forms hypidiomorphic booklets up to 1 centimetre in diameter. These rocks occasionally con-



Plate 1-13-7. (a) Polyphase intrusive border phase typical of the Saint Elias Plutonic Suite. Several foliated and unfoliated mafic phases are cut by late aplitic phases. (b) Zones rich in platy xenoliths, such as the one shown here, are common within Jura-Cretaceous plutons, particularly near margins or screens.

tain potassium feldspar megacrysts up to 2 centimetres in size, which may be zoned. The potassium feldspar content of the matrix is not known.

Paleozoic carbonate-rich sediments in contact with leucocratic intrusions are only weakly altered, in contrast with the well-developed skarn alteration associated with the dioritic intrusive phases. Contacts are usually concordant with compositional layering in the country rocks and the contact zones may contain up to 80 per cent decimetre to metre-sized, rounded, elongate or equidimensional, mafic-rich xenoliths. The xenoliths are mainly composed of hornblende, biotite and lesser plagioclase and tend to decrease in quantity away from the contact. Narrow aplite and felsic pegmatite dikes are common. Where a foliation is developed it is generally concordant with layering in the country rocks, indicating forceful emplacement. Weak chlorite-epidote-altered zones occur locally.

OLIGOCENE (?) TKOPE PLUTONIC SUITE

The southeastern part of the map area (114P/11E, south of the O'Connor River) is partially underlain by the Tkope River batholith (Jakobsen *et al.*, 1980), which occupies the western margin of a series of much larger, epizonal, polyphase but dominantly granitic intrusions of the Oligocene Tkope Plutonic Suite (Campbell and Dodds, 1983a).

Within the map area, the batholith is homogeneous, unfoliated and dominated by pinkish, fine to medium-grained, equigranular, hornblende biotite granite. Biotite occurs as glomerocrysts. Weathered surfaces are greenish grey and blocky. Volumetrically less significant biotite-hornblende granodiorite and alaskite are also present. Batholith borders are unfoliated, medium-grained gabbro and diorite. An intrusion in the extreme northeast corner of 114P/11, consisting of orange to pink-weathering medium-grained granite, may also be part of the Tkope suite.

PART C: DEFORMATION AND STRUCTURAL STYLES

By M.T. Smith, M.G. Mihalynuk, and D.G. MacIntyre

INTRODUCTION

The Tatshenshini project is a mapping and mineral potential study of portions of NTS map sheets 114O and 114P lying west of the Haines Highway, and centred on the Windy Craggy copper-cobalt volcanogenic massive sulphide deposit. Goals of the project, field methodology, and field season statistics are outlined in Part A of this paper, and lithologic descriptions are provided in Part B; Part D describes the major areas of mineral potential. We have emphasized collection of structural data in our field program, as a clear understanding of the structural geology of the region is critical to predicting its mineral potential, both in terms of defining structures that host mineral deposits and more generally, defining areas of favorable geology. In order to avoid redundancy, the reader is referred to summary diagrams in Parts A and B of this paper for names of geographical features, detailed geology, locations of major terranes, etc. (Figures 1-13-1, 1-13-2).

The deformational history and structural styles evident within the Tatshenshini map area are complex and highly variable. An early (pre-Triassic?) phase of ductile deformation is manifest primarily by isoclinal folds of variable orientation. The main phase of ductile deformation, evidenced by tight to isoclinal folds and low-grade greenschist facies metamorphism, postdates deposition of the informally named Upper Triassic Tats group. It both predates and is coeval with Late Jurassic to Early Cretaceous plutonism, as some plutons contain a foliation parallel to the regional trend of deformation, while others crosscut some fabric elements. Emplacement of Jurassic-Cretaceous plutons resulted in additional folding, elevated synkinematic metamorphic grade and/or postkinematic contact metamorphism near the margins. The last (composite) phase of deformation is ductile to brittle in nature and resulted in the local development of penetrative shear fabrics and crenulation cleavage, and discrete faults and shear zones, including large northwest-trending faults. Some faults record early sinistral and later dextral strike-slip movement. The latter are associated with east-trending (antithetic?) cross faults. This phase of deformation is suspected to be in part Early Tertiary, based on the presence of fault-related sedimentary rocks of this age in small graben-like structures, and by association with other large dextral strike-slip faults in the region such as the Denali and Border Ranges faults (e.g., Lanphere, 1977; Roeske *et al.*, 1990). A separate domain of northwest-striking amphibolite grade gneiss and schist is exposed along the western border of the study area in 114O/15 and 114O/9. Its relationship to the rest of the map area is unclear.

A CAUTIONARY WORD

Foliation types and orientations, and fold sets, are difficult to classify because of dramatic contrasts in the relative competency of different units, a condition which is present on all scales. Bedding in the Paleozoic carbonate sequence

is often transposed, and these rocks readily deform into a confusing array of seemingly randomly orientedptygmatic folds, particularly adjacent to intrusive contacts (Plate 1-13-8). By contrast, sedimentary structures are well preserved in the relatively resistant Cambrian-Ordovician volcanic sequence, where most of the deformation is taken up by brittle faults in the hinge zones of large kink folds. Another extreme example of competency contrasts is in the Upper Triassic sequence, where the Tats group lower sedimentary sequence is tightly folded and sheared, but pillows in the overlying basalt sequence are almost undeformed. On an outcrop scale, competency contrasts are well displayed in large carbonate and (to a lesser extent) argillite domains that are intruded by 10 to 50 per cent mafic dikes (Plates 1-13-9 and 1-13-10). The latter are broken and boudinaged, while the carbonate has flowed around the competent layers, resulting in complex fold patterns. On an even smaller scale, thin bedded argillite and limestone units show spectacular examples of brittle-ductile behavior in rocks that are folded or display shear fabrics (see Part B, Plate 1-13-3).

Large strain gradients are in evidence even in relatively homogeneous rocks. Plate 1-13-11 illustrates the effects of simple shear(?) on a marker bed consisting of rugosan packstone. Over an interval of approximately 20 centimetres, the corals range from nearly undeformed to almost unrecognizable, with a minimum of several hundred per cent elongation of the corals at the bottom of the bed. As this phenomenon would probably pass unrecognized in a monotonous sequence of argillite or limestone, it underscores the need for caution when interpreting the thickness, nature and distribution of sedimentary sequences (and stratiform mineral deposits) in this area.

BEDDING, CLEAVAGE AND FOLIATION

All strata with the exception of the Tertiary are cleaved or foliated. Rocks south of the Vern Ritchie Glacier and along the western border of 114O/15 are completely recrystallized, and lack protolith textures; the dominant planar element is a gneissic to coarse schistose layering. In all other areas, protolith textures are at least locally preserved, with bedding commonly parallel or subparallel to foliation. As already mentioned, bedding may be transposed into the foliation direction, particularly in thin-bedded carbonates. This phenomenon is primarily restricted to areas adjacent to the high-grade metamorphic rocks, the margins of plutons and to the Squaw Range. Elsewhere, metamorphic layering usually takes the form of a weakly to strongly developed axial planar cleavage, ranging from slaty to phyllitic in nature.

Representative orientations of planar elements (including bedding and foliation) are illustrated in Figure 1-13-5, together with orientations of folds. In much of the area, foliation and bedding strike north to north west, roughly parallel to the regional trend of major faults. Notable exceptions are the southwest part of 114O/16, where an east-

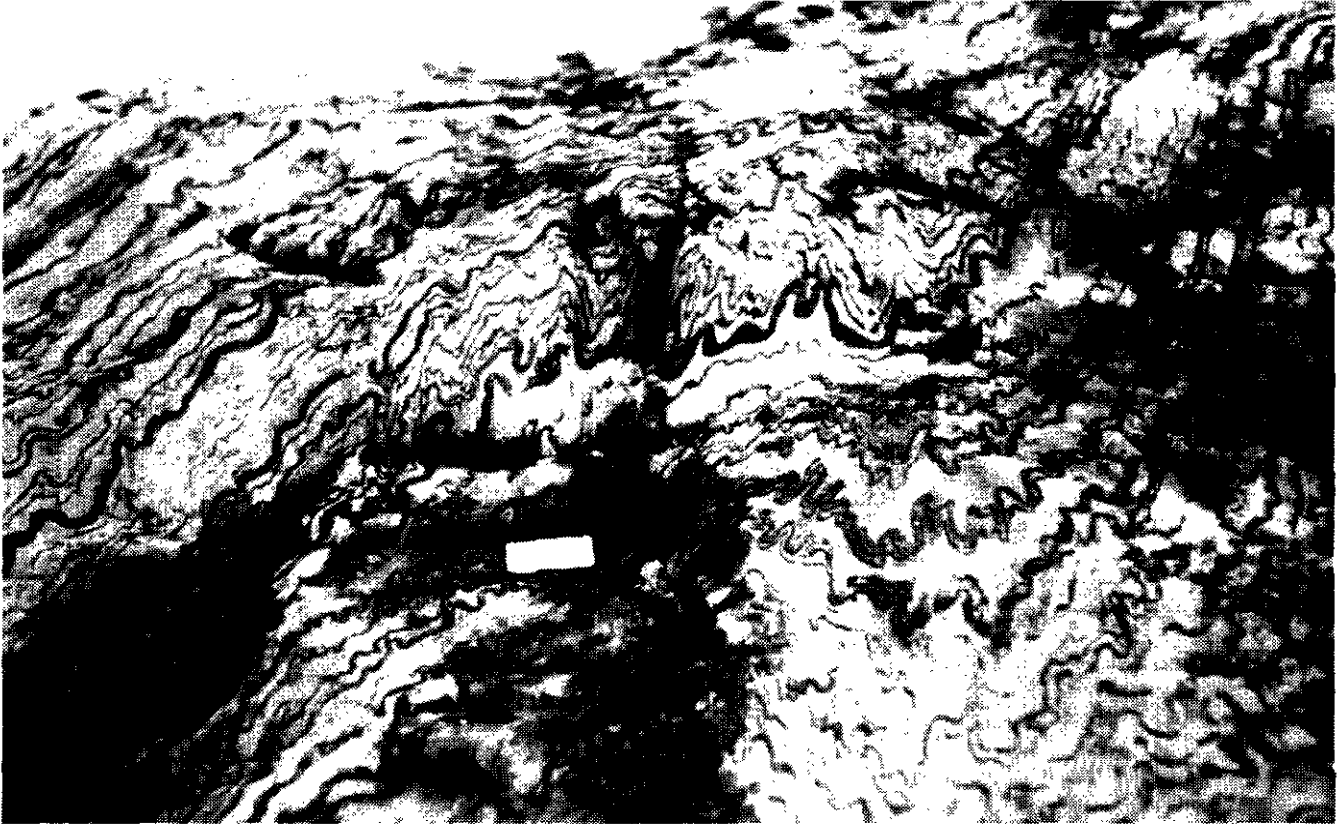


Plate 1-13-8. Pygmic folds in marble adjacent to a pluton. The rectangular card is 10 cm long.

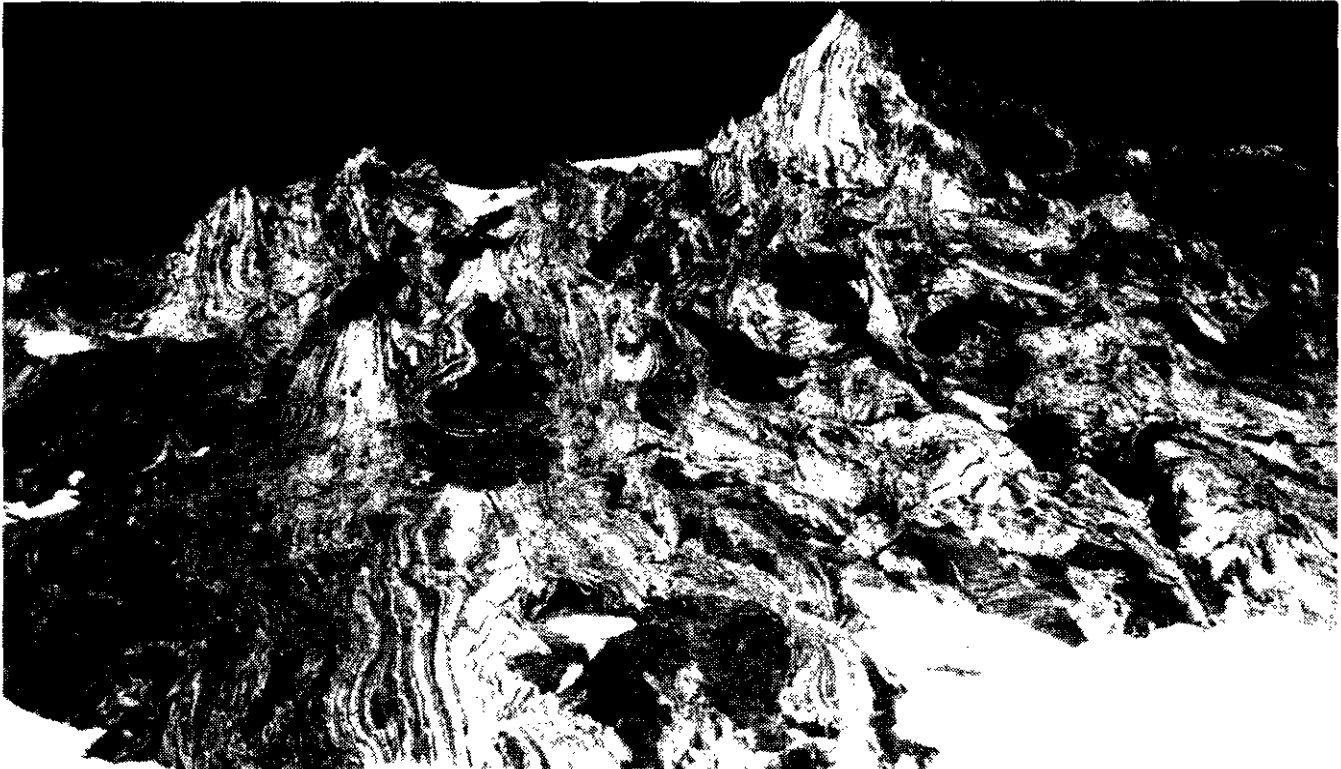


Plate 1-13-9. Boudinage of mafic dikes in marble. View is up and to the north, with the total elevation gain from the bottom to the top of the photo approximately 800 metres. Dark coloured boudins are 3 to 10 metres thick. Note the complex fold patterns produced in response to necking and boudinage of relatively brittle dikes. Photo was taken near the head of Henshi Glacier.



Plate 1-13-10. Boudinaged mafic sill in ductily deformed argillite. Rectangular card is 10 centimetres long.



Plate 1-13-11. Evidence of strain partitioning in limestone. Rugosan corals in the middle part of the photograph are essentially undeformed, and become extremely elongated over an interval of only a few centimetres.

northeast strike prevails, and in the southeast part of 114P/11, where the complex interaction of plutons, folds and faults produces a diverse pattern of foliation orientations.

FOLDS

The earliest generally recognized phase of folding is manifest as a set of centimetre to metre-scale intrafolial isoclines of variable (though often gently plunging) orientation, reflecting variability in foliation orientation (Plate 1-13-12). This set is primarily restricted to the lower Paleozoic carbonate section, and is not clearly present in the Upper Triassic section, and thus may predate it.

The second protracted "phase" of folding resulted in mostly upright to steeply inclined, tight to isoclinal folds, often with tight (chevron) fold hinges. These folds range from map scale to tens of metres in amplitude, to centimetre scale. Representative fold axes from the map area are plotted on Figure 1-13-5. In many areas, notably in the southern part of 114P/14, the southeastern half of 114P/13, and the northern part of 114P/11, the axes of kilometre to decametre-scale folds are near vertical to steeply or moderately inclined to the north or south (Figure 1-13-5 and Plate 1-13-13). In much of 114P/12, the folds tend approximately northwest and dip moderately. In 114O/16 north,

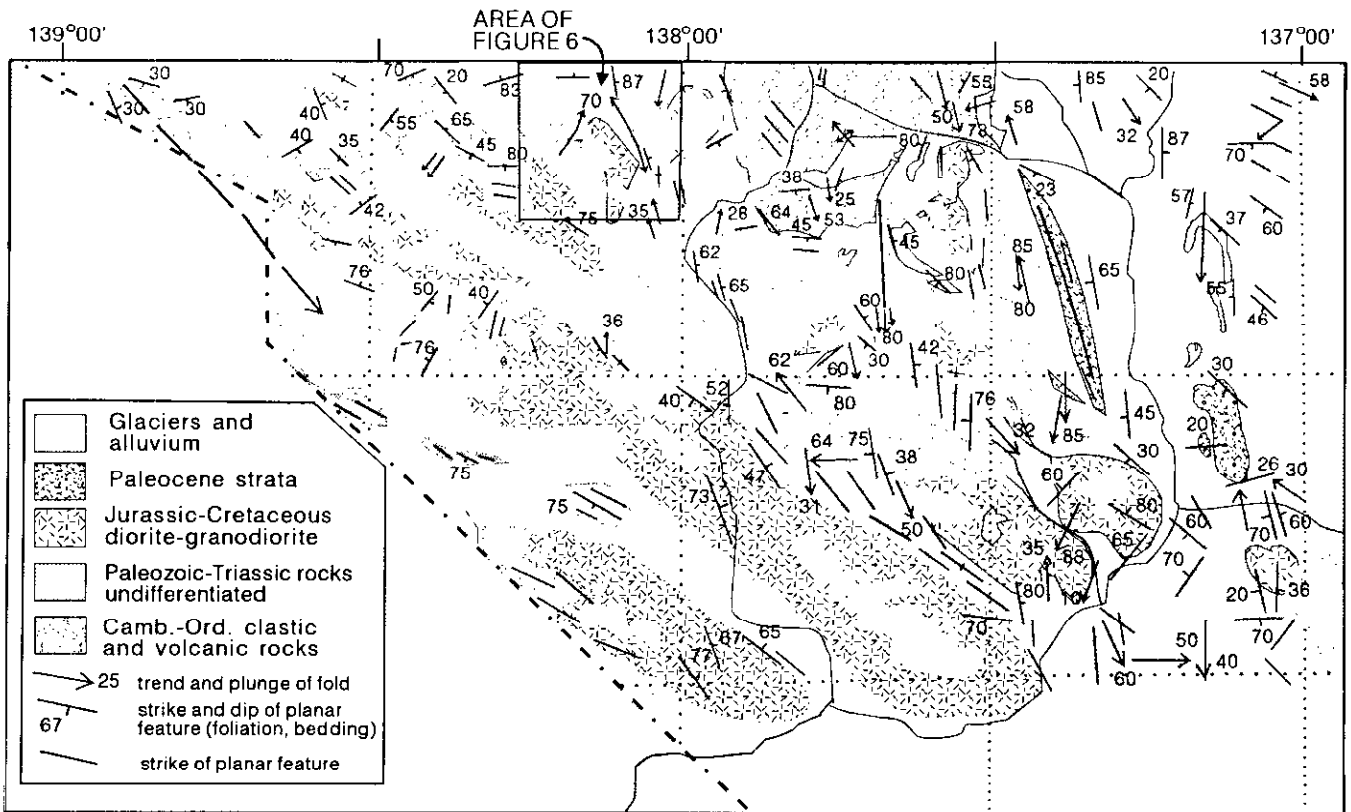


Figure 1-13-5. Simplified geological map showing major fold axes and foliation trends within the map area. See Part B, Figure 1-13-4 for a more detailed geological map.



Plate 1-13-12. First phase intrafolial isoclinal folds in the Paleozoic carbonate unit. View is to the northwest. Photo is taken a few kilometres north of Tats Lake.

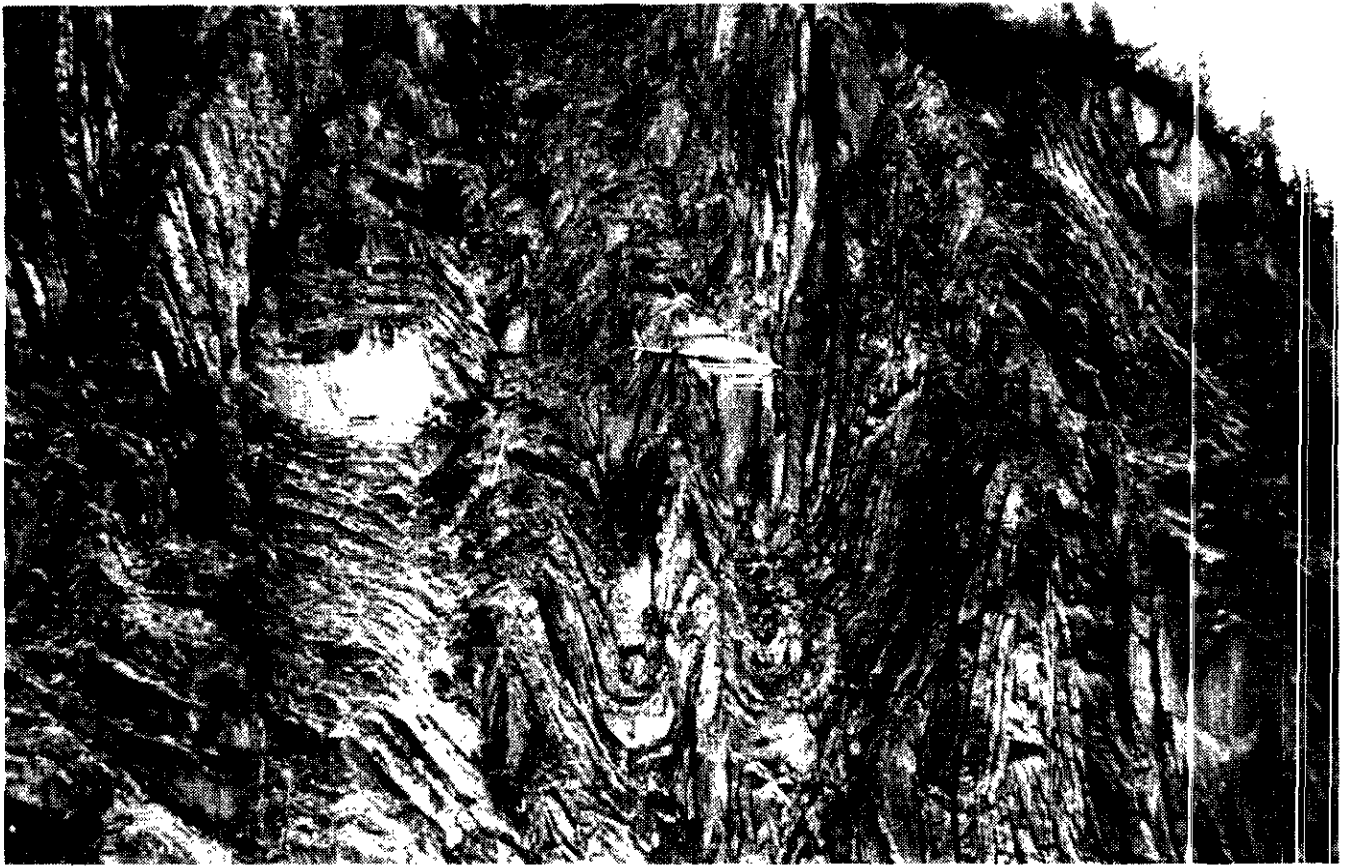


Plate 1-13-13. Second phase folds with steeply inclined axes, exposed on a cliff face. Helicopter for scale. Photo taken along the O'Connor River, south of Carmine Mountain

several large folds in the vicinity of Easy and Tough creeks range from open to tight and have gently to steeply plunging axes (Plate 1-13-14). The hinge lines and/or axes of these folds parallel the margins of several plutons (Figure 1-13-6). This suggests that the folds formed prior to Late Jurassic time and were shouldered aside during pluton emplacement, or were formed in response to intrusion during Late Jurassic to Early Cretaceous time. This interpretation of the timing of folding is substantiated by observations from other areas, where folds crosscut and are contact metamorphosed by intrusions (*e.g.*, Tatshenshini River valley north of the mouth of Henshi Creek), and by areas where the axial planar cleavage is manifest as a foliation in adjacent intrusive bodies.

In the gneissic package of rocks in 114O/9 and 10, folds trend northwest but have horizontal to gently plunging hinge lines. Their relationship to the steeply plunging folds to the east and northeast is unclear.

A number of "cross" folds with moderately east to north-northeast or west to north-northwest plunging hingelines postdate the earlier folds by an unknown time interval. Folds of this type are common in the northwestern half of 114O/16, where they are relatively open and have wavelengths of up to several hundred metres.

A late phase crenulation cleavage or kink banding is developed in some areas, largely restricted to the immediate

vicinity of thrust faults at the contact of Triassic and Paleozoic rocks in 114P/12. In these areas, depositional laminae in argillite and limestone are deformed by centimetre-scale chevron folds (Plate 1-13-15) and may be transposed and thickened by densely spaced folds with wavelengths of up to 1 centimetre and amplitudes of up to 10 centimetres. Crenulation cleavage is also locally present in phyllitic argillite units in the Range Creek and Tatshenshini Valley areas.

Lastly, open, north to north-northwest-trending chevron folds with subhorizontal axes deform lower Tertiary strata west of the Tatshenshini River, and thus indicate deformation of Early Tertiary or younger age.

FAULTS

NORTHWEST-TRENDING FAULTS

The dominant fault set in the map area dips steeply and strikes north to northwest, parallel to the trend of crustal-scale, terrane-bounding, dextral strike-slip faults, including the Denali-Duke fault system (in the extreme northeastern corner of 114P/14) and Border Ranges fault (in the southwest corner of 114P/12 and 114O/9). Regionally, motion along these faults is interpreted to be mainly dextral strike-slip, mid-Cretaceous to Tertiary, and both ductile and brittle in nature (*e.g.*, Lanphere, 1977; Roeske *et al.* 1990). Other



Plate 1-13-14. Folded argillite (dark) and limestone (light) near the confluence of Tough Creek and Supercub Creek. View is to the east-northeast. Note thrust fault within the limestone sequence at left.

large northwest-trending faults in the study area are designated the Tats Creek, Sediments Creek and Debris fault zones (Figure 1-13-7).

BORDER RANGES FAULT

The Border Ranges fault is a major structure separating the Alexander Terrane from the outboard Chugach Terrane. To the south, Roeske *et al.* (1990) and Brew and Morrell (1979) describe the fault zone as a complex feature at least 10 kilometres wide. Brew and Morrell called this feature the Tarr Inlet suture zone, consisting of sheared phyllite, slate, conglomerate, chert and greenstone, interpreted to be Permian in age and part of the Wrangellia Terrane. They interpreted the northeastern boundary of this zone to be the Art Lewis fault of Campbell and Dodds (1983a), which trends down the Art Lewis and Battle glaciers but does not extend south of the terminus of the Battle Glacier, and the southern boundary to be the Border Ranges fault mapped by Campbell and Dodds (1983a) to south of the Reynolds Glacier.

A fault zone and related rocks that we interpret as part of the Tarr Inlet suture zone crops out long the northern margin of the Reynolds Glacier (114O/9) as a series of anastomosing brittle shear zones which cut the Jurassic-Cretaceous (148 and 172 Ma K-Ar hornblende ages; Dodds and Campbell, 1988) Battle Glacier batholith and the sedimentary rocks (chert, greenstone, greywacke and argillite of uncertain age and affinity) that it intrudes. At one location on

114P/12, discrete strands of the fault zone are up to 10 metres wide, outlined by strongly sheared quartz-graphite mylonite. In other areas the strain is more widely distributed to include other lithologies and silicic, argillic and chloritic alteration with disseminated sulphides are variably developed. A more intact sequence of rocks, similar to those involved in the fault zone is present in the northern Battle Range, intruded by plutonic rocks. We are unsure at this time whether they represent an intact "boudin" in the Tarr Inlet suture zone and are part of Wrangellia (as might be consistent with the interpretation of Brew and Morrell, 1979), or lie north of the zone and are part of the Alexander Terrane.

DUKE FAULT

The Duke fault, a strand of the Denali fault system as mapped by Campbell and Dodds (1983b), trends down Squaw Creek in the extreme northeast corner of 114P/14 and juxtaposes the Alexander Terrane and a small sliver of the Wrangellia Terrane. Our mapping indicates a northwest-trending, imbricate zone of high-angle and southwest-dipping thrust faults in this area. Some rock types exposed to the south of the original mapped trace of the fault are similar to some to the north. However, as our mapping covers less than 10 kilometres of the interpreted fault trace, we are reluctant to question its status as a terrane-bounding structure. Nevertheless, most deformation within the fault



zone appears to be younger (*e.g.*, Lamphere, 1977) than the Pennsylvanian stitching (Gardner *et al.*, 1988) of Wrangella and Alexander terranes.

TATS CREEK FAULT ZONE

The Tats Creek fault zone consists of a series of parallel, steep, northwest-trending faults that cut the Noisy Range pluton and Paleozoic and Mesozoic strata to the northeast (Figure 1-13-8), dissecting the latter into a series of narrow fault panels. Some of the fault strands, including one contact between the Noisy Range pluton and Paleozoic carbonates, have a ductile mylonitic fabric with sinistral shear sense, overprinted by more brittle dextral shears. Other fault strands contain only brittle fabrics. One such fault is continuous over a length of more than 12 kilometres within the Noisy Range batholith, and is manifest by a red and green zone of brecciation and cataclasis up to 30 metres wide, accompanied by chloritic and hematitic alteration of the country rocks. It may merge with or be related to a series of closely spaced parallel faults exposed at the north end of the Tats Creek valley, and may also be temporally related to a wide, mineralized gouge zone in plutonic rocks exposed near the mouth of Tomanous Creek, south of the Tatshenshini River (Figure 1-13-10).

At least three small (1 km²) graben structures are present along these faults, containing poorly consolidated sedimen-

tary rocks including sandstone, conglomerate and light grey to buff claystone. These rocks contain coal and other plant remains, and are interpreted to be Early Tertiary and of nonmarine origin on the basis of correlation with other similar coal-bearing units in the region. They are assumed to be contemporaneous with faulting and representative of local transtensional conditions (*i.e.*, small pull-apart basins).

Although post Early Tertiary movement on these faults cannot be interpreted with certainty, the possibility of Miocene to Recent movement is suggested by numerous topographic lineaments parallel to the faults and offset stream channels in the Tats Creek valley. Microseismicity studies of the Windy Craggy region over a recent 2-year period showed no significant seismic activity in this valley (Horner, 1989).

The full extent and distribution of faults in the Tats Creek valley is difficult to elucidate due to heavy brush and drift cover. However, at the mouth of Tats Creek, numerous closely spaced shear zones disrupt a section of rocks 3 kilometres wide exposed along the northwest bank of the Tatshenshini River.

DEBRIS FAULT SYSTEM

The Debris fault system consists principally of two north-northwest-trending faults which in part enclose a down-dropped, trough-like depositional basin filled with lower

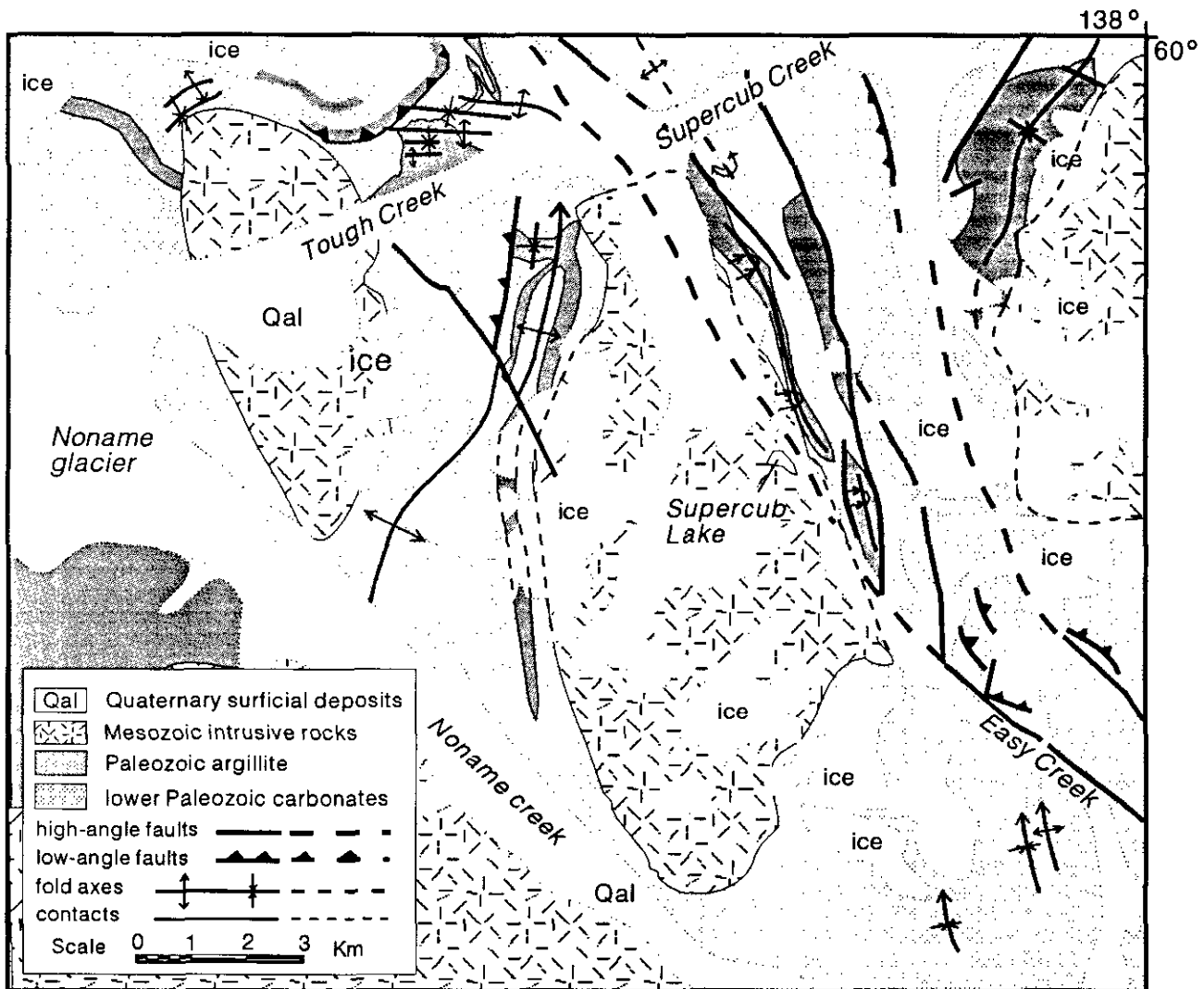


Figure 1-13-6. Detail of Supercub Lake area (1140/16) showing inter-relationship of folds and intrusions.
See Figure 1-13-5 for location.

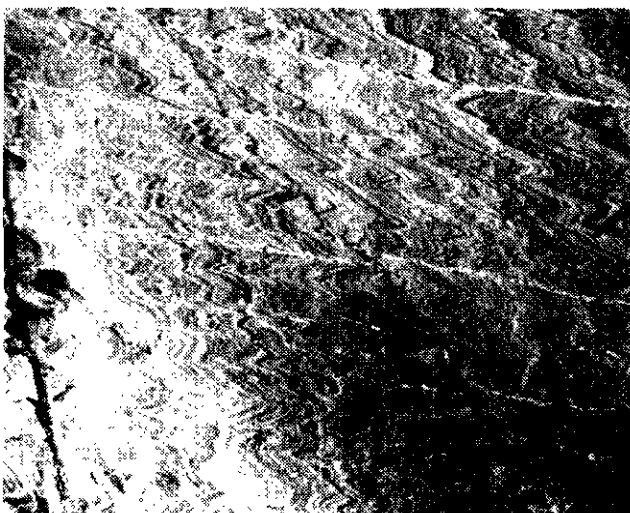


Figure 1-13-5. Simplified geological map showing major fold axes and foliation trends within the map area. See Part B, Figure 1-13-3 for a more detailed geological map.

Tertiary sedimentary rocks (Figure 1-13-10). The two bounding faults enclose numerous smaller faults, which may merge to the south into a single, moderately southwest-dipping fault. The westernmost fault is, in part, a west-dipping, high-angle reverse fault that places the Paleozoic carbonate sequence over the lower Tertiary sedimentary rocks. Facies distribution (*i.e.*, lack of coarse detritus adjacent to the fault) of sedimentary rocks in the Early Tertiary basin suggests that most of the dip-slip motion on this fault postdates sedimentation. Maximum syndepositional displacement is on the easternmost fault, as evidenced by a boulder conglomerate and breccia unit within the sedimentary sequence adjacent to the fault, suggesting derivation from a fault scarp and down-to-the-west displacement. A brittle shear zone at least 50 metres wide is in part contained within bluish, chlorite-altered volcanoclastic rocks and marks the main fault trace. Cumulative down-to-the-west dip-slip motion across the fault is estimated to be at least a kilometre; the magnitude of strike-slip motion is unknown. Quaternary cover within the Tatshenshini and Tkope River valleys obscures the southern continuation of the fault.

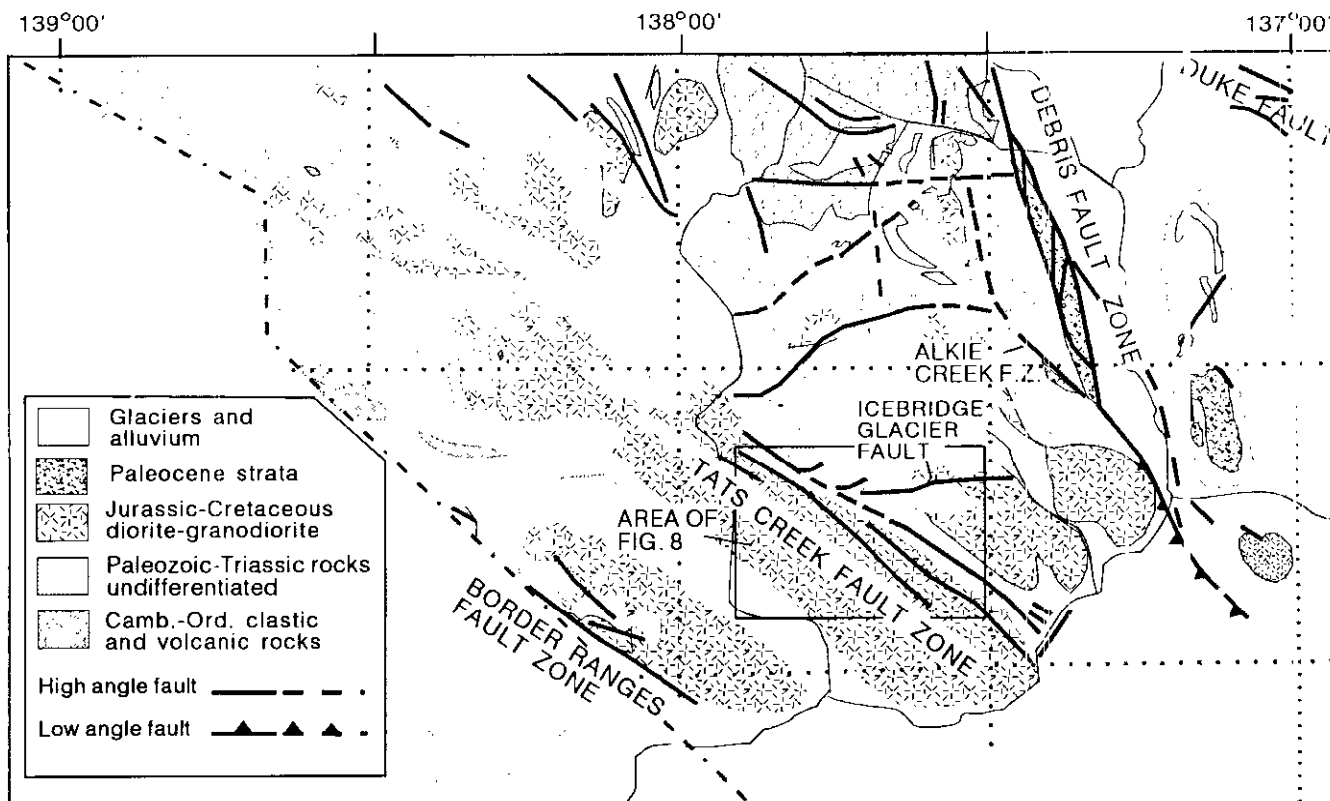


Figure 1-13-7. Simplified geological map showing the distribution of major faults in the map area.

However, excellent exposures in one locality in the Tkope River valley reveal a moderately south-southwest-dipping shear zone at least 30 metres wide, developed in a sequence of graphitic argillites juxtaposed against a relatively intact sequence of sandstones and calcsilicate rocks, which may be the continuation of the fault zone.

OTHER NORTH AND NORTHWEST-TRENDING FAULTS

The northwest-trending, anastomosing Alkie Creek fault zone is apparently a splay off the main Debris fault zone, which crosses, then parallels the northern margin of Alkie glacier (local name). It bounds another wedge of lower Tertiary sedimentary rocks. Several parallel high-angle faults also transect the South Range Creek area (114P/13N), the area of Easy Creek and Supercub Creek (114O/16) and the Silurian-Permian section north of the upper Tweedsmuir Glacier (informal: No Name glacier) on the same map sheet.

North-trending faults are mapped in the eastern part of 114O/16, north of the Alsek River, and in 114P/13, where they offset the Cambrian-Ordovician volcanic and lower Paleozoic carbonate contact. Similar faults also occupy the prominent north-trending glacial valleys on this map sheet. These faults lie within and are parallel to the tightened hinges of large north-trending folds. This phenomenon is well displayed in south-facing slopes north of the Alsek River and east of Easy Creek, where the hinge areas of several upright, kilometre-scale chevron folds in the megacycle sequence are faulted.

EAST-TRENDING (ANTITHETIC?) CROSS FAULTS

A series of east-trending cross faults dissects the map area, particularly on the 114P/12 and 114P/13 map sheets. They do not appear to offset the northwest-trending faults, and thus may be coeval and antithetic.

Southernmost and largest of the mapped east-west trending faults is the Icebridge Glacier fault (Figure 1-13-8). Near Icebridge Glacier, this fault is manifest as a discrete fault zone with approximately 1.5 kilometres of post Early Cretaceous sinistral strike-slip motion, probably antithetic to dextral motion on the Tats Creek fault zone. The timing and sense of motion are constrained by offset of a pluton contact and accompanying brittle deformation of its thermal aureole. This fault zone widens to the east where a zone of fault breccia and gouge within Jurassic-Cretaceous plutonic rocks is at least 1 kilometre wide (Plate 1-13-16). A series of four subparallel faults, spaced approximately a kilometre apart, are mapped to the northwest (Figure 1-13-8). Offset on each of these faults is unknown, but is expected to be less than on the Icebridge Glacier fault.

The recognition of the Icebridge Glacier fault and other east-trending faults in this area has important implications for mineral potential studies. The Tats showing (MacInyre, 1984) is terminated to the south along the Icebridge Glacier fault. The newly discovered Rainy Monday showing (see Part D) is terminated to the north along the fault. Further investigation may reveal that the two represent the same.

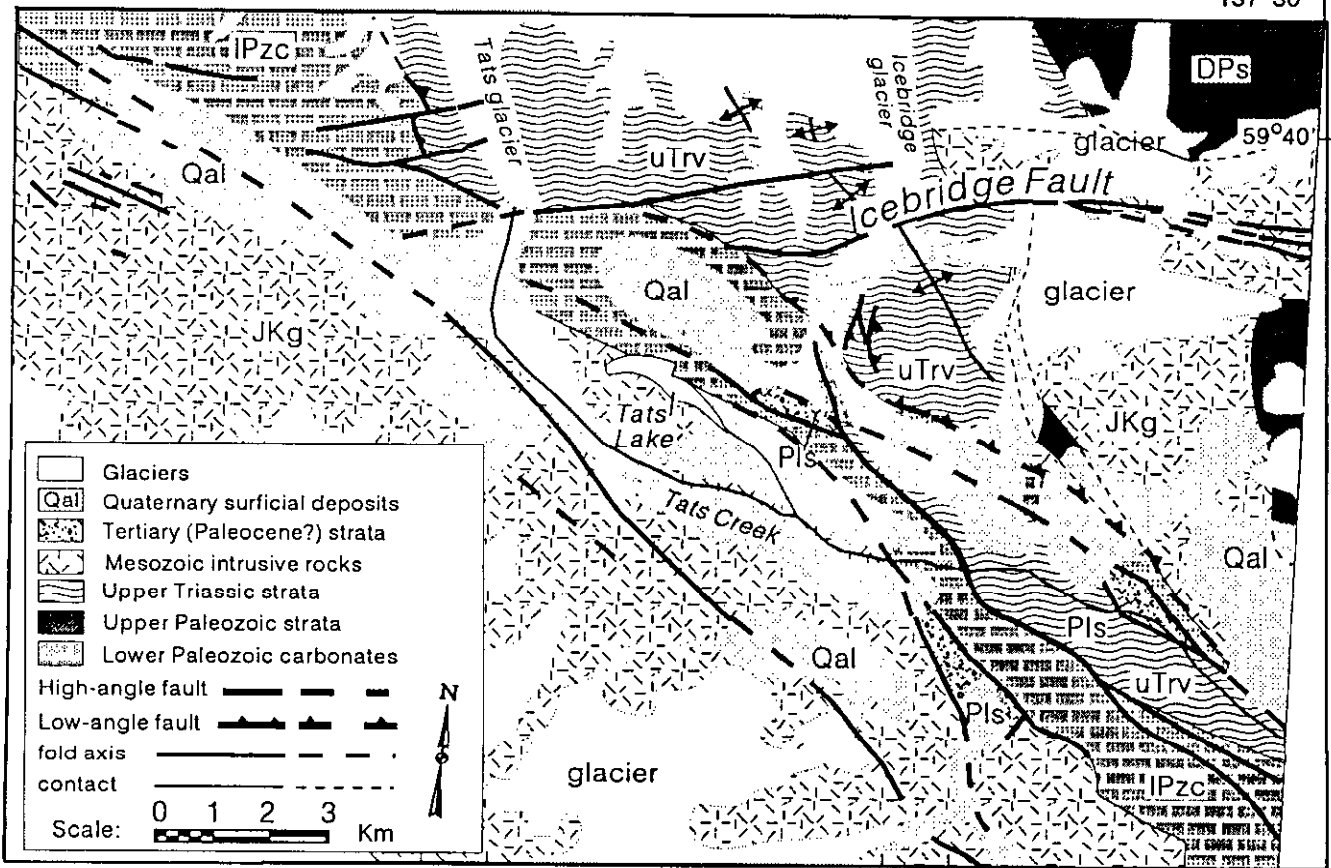


Figure 1-13-8. Detail of Tats Creek valley showing distribution of major northwest-trending strike-slip faults, and east-trending cross faults. See Figure 1-13-7 for location.



Plate 1-13-16. Icebridge Glacier fault zone near Henshi Creek. The lighter coloured rocks at left are brittily deformed granite. View is to the east, approximately parallel to the fault zone.

offset massive sulphide horizon. Other massive sulphide bodies, including the Windy Craggy orebody, may also be offset along these faults.

Approximately 20 kilometres to the north of the Icebridge Glacier fault, a large, arching, east-northeast-trending fault on the southern edge of 114P/13 may have relatively large displacement. It places Upper Triassic and Devonian-Permian rocks to the south against Paleozoic carbonate rocks to the north. Another fault with smaller displacement parallels it 10 kilometres to the north.

Lastly, a series of small, northeast to east-trending faults dissect the Cambrian-Ordovician volcanic units in 114P/13. These are most evident where they offset the contact between the volcanic unit and overlying Paleozoic carbonates. Overall, the sense of offset across many of these faults is north-side-up, with each block exposing deeper stratigraphic levels. Each individual block appears to be rotated slightly, with down-to-the-south sense of motion. Additional work will confirm this interpretation. Numerous smaller scale faults may show sense of motion similar to that described above.

THRUST FAULTS

Large numbers of thrust faults are not readily apparent in the map area, although cryptic thrust faults, particularly in the monotonous carbonate unit may be identified as we receive more biostratigraphic information. The north-western contact of the Tats group is an east-dipping thrust, and a series of stacked northeast-dipping thrust faults can be seen in the lower Paleozoic carbonate sequence at the mouth of Easy Creek. A thrust fault within the carbonate sequence at the mouth of Tough Creek is illustrated by Plate 1-13-14. As previously described, the Debris fault zone may merge to the south with a gently south to southwest-dipping zone with top-to-the-north (dextral reverse) displacement. Several southwest-dipping thrust faults have also been mapped in the Squaw Range.

PENETRATIVE SHEAR FABRICS

Evidence of penetrative ductile shear has been noted in several locations. In some cases, it is clearly related to a mapped fault, such as the zone of mylonitic rocks along Tats Creek. In other areas, diffuse zones of sheared rocks are not clearly related to any discrete fault. They consist of a series of closely spaced shears which disrupt the foliation or bedding, and form a penetrative fabric on outcrop and larger scales (Plates 1-13-17a and b). These zones are widely distributed throughout the map area, particularly on 114P/12 and 114P/13, are typically steeply dipping, oriented east-west to northwest-southeast, and show both dextral and sinistral shear sense.

DISTINCT STRUCTURAL DOMAIN IN 114O/9 and 114O/15

A distinct structural domain consisting of strongly deformed amphibolite-grade rocks underlies the nunatak and ridge system that divides the Vern Ritchie and Battle glaciers in 114O/9, and areas along the western margin of

114O/15. These rocks consist of medium-grained plagioclase-hornblende gneiss, calcilicatic gneiss and biotite-quartz-feldspar schist. In 114O/9, they form a series of northwest-striking, steeply southwesterly dipping compositional bands, with foliation parallel to compositional layering. Tight to isoclinal folds and mineral lineations also follow this northwesterly trend and dip gently to moderately to the southeast. Competent layers within this package are isoclinally folded and refolded, then boudinaged, testifying to a complicated strain history (Plate 1-13-18). Sinistral-shear-sense indicators predominate in the area of the nunatak, however, there is evidence for both dextral and sinistral shear in other locations.

It is uncertain how this domain relates to the rest of the study area. The contact between these and lower grade rocks to the northeast is intruded by a linear diorite body in one locality; elsewhere it is ice covered. The zone of high-grade rocks is parallel to a ductile shear zone in the Tats Creek valley with sinistral shear sense; thus the former may represent the deeper levels of a northwest-trending sinistral shear zone of late Mesozoic age. This hypothesis may be important from a mineral potential standpoint as it implies significant offset of the presumed western continuation of Tats group stratigraphy. Alternatively, these rocks may be analogous to the pre-Ordovician Wales Metamorphic Suite of Gehrels (1990), which forms the basement to the rest of the Alexander Terrane in southeast Alaska, and with which the rocks in the present study area share many lithologic and structural characteristics. However, we have not as yet identified any appropriate candidates for radiometric determination of protolith age in order to test this hypothesis.

METAMORPHISM

As with structural styles, the metamorphic history of rocks in the map area is difficult to summarize due to the large area, the presence of numerous plutons, which underlie over 30 per cent of the area, and the predominance of lithologic types such as limestone and argillite that do not facilitate recognition of isograds at subamphibolite metamorphic grades. The presence of authigenic albite, chlorite and epidote in mafic rocks interbedded with the above indicates that most rocks in the study area are subgreenschist to low greenschist facies. Adjacent to the margins of large plutons, foliated pelitic rocks contain fine-grained biotite and rare garnet, and mafic rocks contain fine-grained actinolite, suggestive of low to middle greenschist facies conditions. Contact metamorphic aureoles are also present around the margins of some plutons, suggesting that, in at least some cases, intrusion of the Jurassic-Cretaceous suite outlasted metamorphism.

Gneissic and coarse schistose rocks in the southwestern part of the study area record metamorphic conditions distinctly different from those elsewhere. Rocks with mafic protoliths are amphibolite-grade hornblende+plagioclase+biotite±garnet gneiss or schist and pelitic assemblages contain the assemblage biotite+muscovite+garnet+plagioclase+quartz. Rocks in some areas contain a weak greenschist facies (actinolite+chlor-

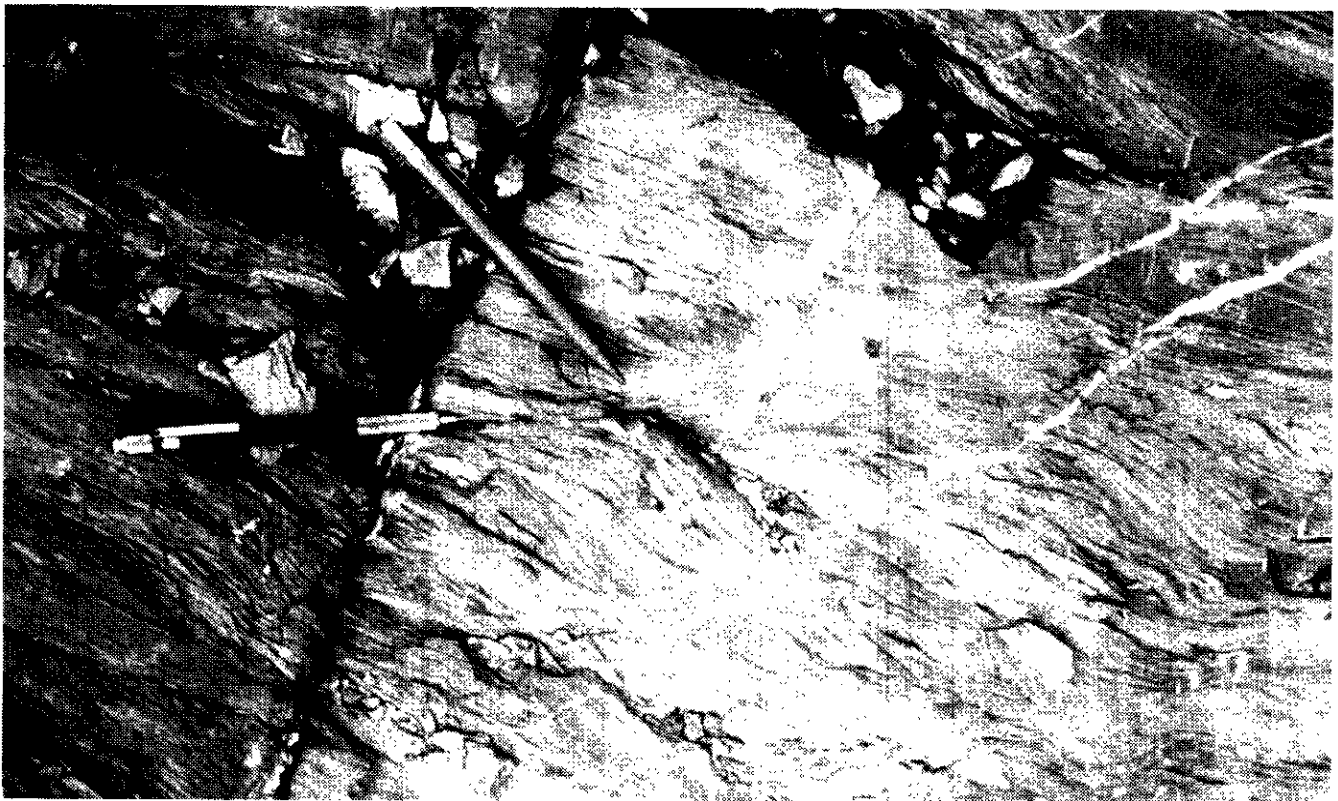
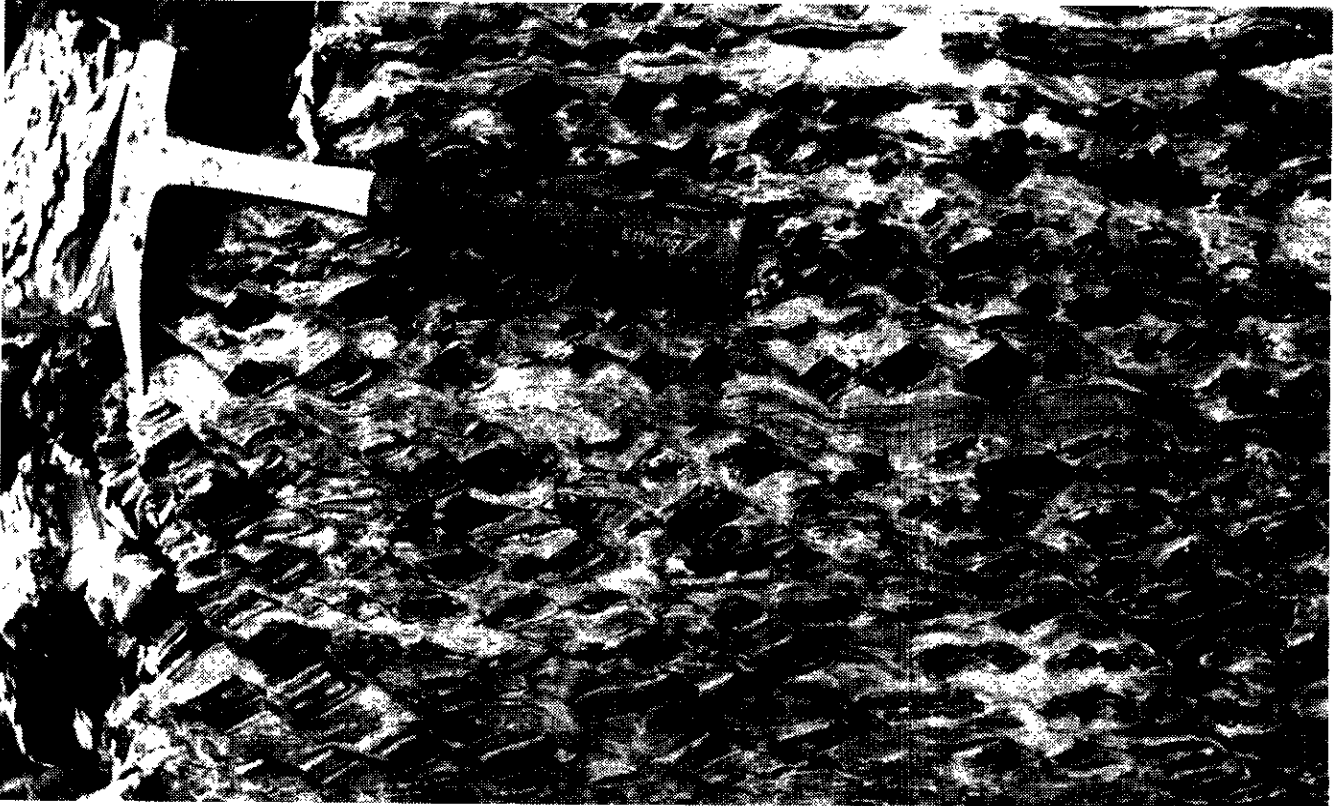


Plate 1-13-17. (A) Shear fabric developed in a sequence of thin-bedded argillite and limestone. The limestone has flowed, whereas the argillite has deformed brittly. The photo was taken between the Alsek River and south Range Creek. The shears are oriented roughly north-south, and the sense of shear is sinistral and east side up. (B) Shear fabric developed in argillaceous limestone of the megacycle sequence, east bank of the Alsek River west of Mount Blackadar. Shears are oriented roughly west-northwest, and the sense of shear is sinistral.



Plate 1-13-18. Fabric developed in calcsilicate gneiss in the amphibolite-grade package south of the Vern Ritchie Glacier. Note coarsely recrystallized texture, rootless folds, conflicting senses of shear, and rotation and extreme boudinage of the competent boudin in the upper half of the photograph.

ite+epidote) overprint, apparently related to or postdating emplacement of granitic dikes, which contain only this assemblage.

DEFORMATIONAL AND TECTONIC HISTORY

A structure versus time diagram (Figure 1-13-9) illustrates our preliminary interpretation of the structural and metamorphic history of the map area, based on the relationship of deformational phases to each other and to rocks of known ages. Other evidence used to construct this diagram (discussed in Part B) includes fossil age data and the extrapolation of relationships interpreted from adjacent areas. Locally developed conglomeratic horizons and a change in depositional environment from carbonate platform to siliciclastic-dominated reef and backreef during Late Silurian or Early Devonian time suggests the possibility of nearby tectonic activity. This time period corresponds to the Klakas Orogeny of Gehrels *et al.* (1987) in southeastern Alaska. The earliest documented phase of deformation, manifest by intrafolial isoclinal folds may be related to a Pennsylvanian-Permian plutonic event documented to the north and south of the study area (Dodds and Campbell, 1988; Hudson, 1983). A depositional hiatus or period of erosion of unknown duration lasted from late Paleozoic through Middle Triassic time. Basalt and fine-grained sedimentary rocks of the Upper Triassic Tats group were deposited in graben-type basins, suggesting an overall extensional regime and rifting. Peter (1992) equated the depositional

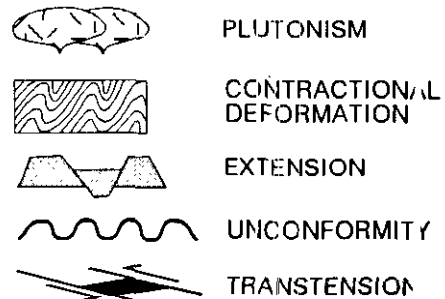
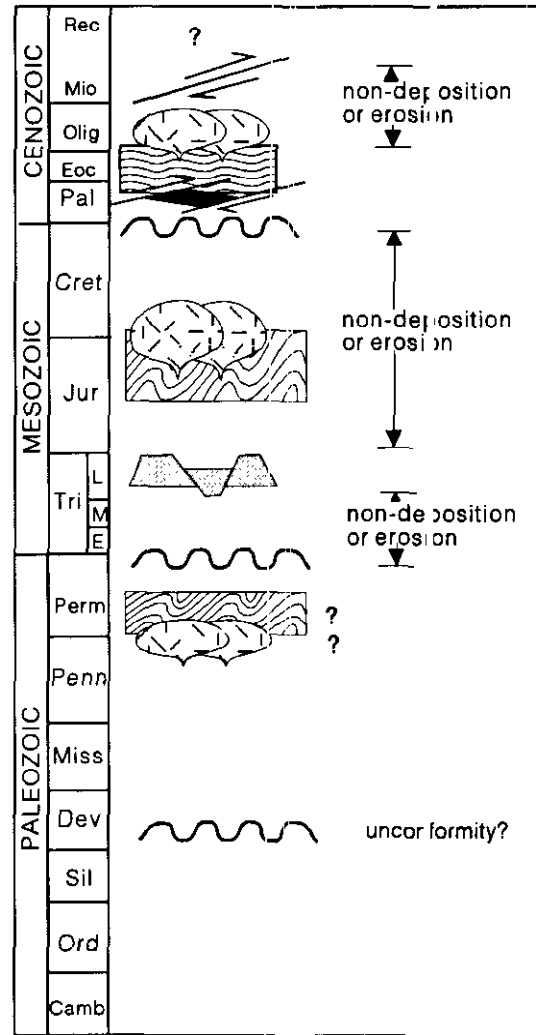


Figure 1-13-9. Structure versus time diagram showing postulated timing of plutonism, unconformities, contractional, strike-slip, and extensional episodes in the study area. See text for explanation.

setting of the Tats group to the modern day Guaymas Basin. A major episode of contractional deformation and metamorphism began post Late Triassic (Norian) deposition but prior to Late Jurassic plutonism. In places significant deformation accompanied an extensive episode of Late Jurassic to Early Cretaceous plutonism (Dodds and Campbell, 1988). These plutons are calcalkalic and are interpreted to be related to northeast-directed subduction along the

present-day Boundary Ranges fault zone (Plafker *et al.*, 1989; Hudson, 1983). During middle to Late Cretaceous time, northwest-trending zones of ductile shear, with mainly sinistral offset, cut both the plutons and older rocks. Brittle to ductile shears with dextral offsets are imposed on these early ductile shear fabrics. This episode of faulting continued from Late Cretaceous to Early Tertiary time, based on the presence of synorogenic clastic rocks in pull-apart(?) basins and the postulated relationship of these faults to other crustal-scale dextral strike-slip faults in the region (Lan-

phere, 1977; Pavlis *et al.*, 1989). The synorogenic clastic rocks are themselves folded and faulted, suggesting that orogenesis outlasted sedimentation. The Oligocene Tkope intrusions followed this episode of strike-slip faulting. The Tkope intrusions are also brittly deformed, testifying to continued tectonic instability in the region. Miocene to Recent motion on these faults cannot be documented with certainty, however, some geomorphic features suggest the possibility of relatively recent movement.

PART D: MINERAL INVENTORY UPDATE (114P AND 114O)

By D.G. MacIntyre, M.G. Mihalynuk and M.T. Smith

INTRODUCTION

A key objective of the Tatshenshini project is the creation of an up to date inventory of the mineral resources of the project area. Unlike some parts of British Columbia, the Tatshenshini area is not as well explored and the documented mineral occurrences in the MINFILE database do not represent an accurate inventory of the mineral endowment of the region. In order to obtain a more complete assessment of known mineral occurrences, James J. McDougall was engaged to assist ministry crews in locating and sampling occurrences that for the most part are undocumented. Mr. McDougall is credited with the discovery of the Windy Craggy copper-cobalt massive sulphide deposit in 1958 and has spent many years exploring the Tatshenshini area. His contribution to the Tatshenshini mineral assessment project was invaluable and helped ministry crews develop a more complete mineral inventory of the area. Much of the information that follows is derived from unpublished reports and verbal communications provided by Mr. McDougall, particularly for the Buck, Jo and Pup properties (McDougall *et al.*, 1989; McDougall, 1990a, b).

The following descriptions are of properties and showings visited and sampled during the 1992 field season. The descriptions include location, mineralization and alteration, hostrocks, previous work and potential for additional discoveries. The descriptions are arranged according to deposit type. An updated list of mineral occurrences is given in Table 1-13-1; mineral occurrence locations discussed in this report are shown in Figure 1-13-10. Note that several of the occurrences described below are new discoveries made during the 1992 mineral assessment project.

STRATIFORM DEPOSITS

VOLCANOGENIC MASSIVE SULPHIDE (Cu±Zn, Ag, Au, Co)

The most economically significant exploration targets in the Tatshenshini project area are volcanogenic massive sulphide deposits of the Windy Craggy type. These deposits are hosted by Late Triassic submarine volcanic and sedimentary rocks of the Tats group (informal, see Part B). The world-class Windy Craggy deposit, which is owned by Geddes Resources Ltd., is estimated to contain reserves of nearly 300 million tonnes grading 1.38 per cent copper (Geddes Resources, 1992). Approximately \$47 million has been spent on exploration of this deposit to date.

WINDY CRAGGY AREA

Five new copper occurrences were discovered while mapping the Alsek-Tatshenshini area during the 1992 field season. Four of these are located in a 20 square kilometre area centred approximately 15 kilometres southeast of Windy Craggy and 5 kilometres northeast of Tats Lake

(Figure 1-13-11). Here, as at Windy Craggy, the host stratigraphy includes interbedded pillowed flows, calcareous siltstones and sills of the middle Tats member of the Tats group. Assays of up to 20 per cent copper have been obtained from the most extensively mineralized of these

TABLE 1-13-1
MINERAL OCCURRENCES, TATSHENSHINI PROJECT
AREA, 114O AND 114P (NORTH)

MINFILE	Name	Map	Easting	Northing	Status	Cl #	Comments
1	BUCK'S FACIE	114P10E	349274	6629308	showing	Gypse n	Gypsum
2	WINDY CRAGGY	114P10E	349274	6629308	dev prospect	Van	Cu,Ag,Zn
3	TATS	114P10E	349300	6610157	prospect	VMS	Cu,Ag,Co,Zn,Au
4	SQUAW CREEK PLACER	114P10E	363638	6651175	past prod	Place	Au,Cu,Ag
5	O'CONNOR RIVER	114P10E	402302	6611501	dev prospect	Gypse n	Gypsum,Amphibole
6	KIM	114P10E	404133	6611507	showing	Van	Zn
7	MIND OF ERIN (L 722)	114P10E	410487	6610177	past prod	Skarn	Ag,Cu,Au,Zn,Pb
8	STATE OF MONTANA (L 283)	114P10E	412496	6601965	past prod	Skarn	Ag,Cu,Au,D
9	VICTORIA (L 903)	114P10E	412082	6601948	prospect	Skarn	Ag,Zn,Pb,Au,Cu
10	ADAMS (L 727)	114P10E	414051	6601110	prospect	Skarn	Pb,Zn,Ag
11	LAWRENCE (L 964)	114P09W	415038	6607151	prospect	Skarn	Ag,Pb,Zn,Au,Cu
12	SMOKE (L 705)	114P09W	421281	6607329	showing	Skarn	Au,Cu,Fe,Mo
13	MILDRED (L 213)	114P09W	420560	6601980	showing	Skarn	Ag,Cu,Fe
14	CANADIAN VERDE	114P09W	420528	6601035	showing	Skarn	Ag,Cu,Zn,Au,B,Fe
15	GOLD CORO	114P07E	414635	6593319	showing	Van	Au,Ag,Cu
16	GOLD RUN CREEK PLACER	114P07E	388294	6642389	past prod	Place	Au
17	WINDSOR (L 804)	114P10E	412257	6601816	showing	Skarn	Cu,Zn
18	HUMBERD - DISCOVERY	114P10W	398989	6623537	showing	Van	Ag,Pb,Zn,Cu
19	BORNITE	114P10E	409648	6602885	prospect	Skarn	Cu,Pb,Zn
20	WAR EAGLE (L 901)	114P10E	412332	6603690	showing	Skarn	Fe
21	SHEEP	114P10E	382310	6621221	showing	Dist r	Cu
22	KELSAL 24	114P10W	416773	6628730	showing	Van	Cu
23	KELSAL 32	114P10W	418008	6628312	showing	Van	Cu
24	HUMBERD - CREEK	114P10W	398924	6621775	showing	Van	Ag,Zn,Pb,Cu
25	HUMBERD - SOUTH	114P10W	398923	6619750	showing	Van	Ag,Cu,Zn,Pb
26	HERBERT - CAMP	114P10W	398911	6617461	showing	Van	Ag,Cu,Zn,Pb
27	LUNAR	114P10E	409638	6616133	showing	Van	Ag,Pb,Zn
28	NADAHINI MOUNTAIN	114P10E	403636	6617790	showing	Alter at	Asthenite
29	HIBERNIAN	114P10E	411378	6617063	showing	Skarn	Cu,Pb,Zn,Ag
30	MOUNT MARSH FELD	114P10E	407533	6615544	showing	Cu	Cu
31	C AND E NORTH	114P10W	409271	6617408	showing	Skarn	Cu,Pb
32	C AND E SOUTH	114P10W	401949	6617257	showing	Skarn	Zn,Pb,Sn
33	WC 17	114P10E	348854	6614221	showing	Skarn	Au,Ag
34	TATS CREEK	114P10E	356082	6605700	showing	VMS	Cu,Ag
35	BARKER MOUNT	114P10E	352783	6601967	showing	Van	Ag,Cu,Au
36	KLEIN RIVER SW	114P10E	403614	6612811	showing	Van	Zn,Ag,Cd
37	ALTA K IBERIATAY	114P10W	378573	6616510	showing	Cond. J	Cu,Au,Ag
38	FAULT CHALK	114P10W	387210	661759	showing	Van	Ag,Pb,Zn,Au
39	CAMP CHALK	114P10E	405095	6616108	showing	Van	Ag,Cu,Au
40	ALTA IBERIATAY	114P10E	405318	6617382	showing	Van	Ag,Pb,Zn,Cu
41	ALSEK	114P10E	345438	6614091	showing	VMS	Cu,Au,Ag
42	INSPIRATION CHALK	114P10E	412472	6614087	showing	Cond. I	Cu,Au,Ag
43	BASE M N1 - JUNE 24	114P09W	368709	6610037	showing	VMS	Ag,Au,Cu,Pb,Zn,Au,Cu
44	BASE M N1 - JUNE 21	114P09W	367678	6610742	showing	VMS	Au,Ag
45	BASE M N1 WEST	114P09W	367480	6609275	showing	VMS	Cu,Ag,Au,Co,Zn
46	HUMBERD - DOME	114P10W	389987	6610662	showing	Repl	Ag,Cu,Zn,Pb,Au
47	SAM - NORTH GLACIER	114P10W	394130	6610222	showing	Van	Cu,Zn,Pb
48	SAM - MAIN GLACIER	114P10W	394027	6610298	showing	Skarn	Cu,Pb,Zn,Ag,Au
49	ICE	114P09W	421987	6610267	showing	Van	Ag,Cu,Zn
50	VALLA	114P07W	406811	6591831	showing	Ind m	Cu,Pb,Zn,Ag,Fe
51	MOUNT BIGGER	114P07W	406385	6591896	showing	Van	Pb,Ag,Cu,Zn
52	PENDANT GLACIER	114P10E	356309	6610778	showing	Van	Zn,Cu,Ag,Au,Pb
53	PAMPERO RIDGE	114P10E	350159	6610375	showing	Van	Zn,Cu,Ag
54	CAMP'S CRAG	114P10E	352211	6610156	showing	Van	Cu,Zn,Ag
55	AEOLIAN STEEPLE	114P10E	356625	6613344	showing	VMS	Zn,Cu,Ag
56	VEGA (L 145)	114P10E	417589	6610582	showing	Skarn	Ag,Cu,Zn,Au
57	ALLI	114P09E	364583	6611124	showing	Skarn	Cu,Mo,Wo
58	ICE	114P09E	378427	6611564	showing	Heavy	Van
59	HARNS ROAD	114P10E	403449	6610000	showing	VMS	Bi
60	SQUAW VALLEY	114P10E	387157	6610596	showing	Alter at	Asthenite
61	RIME	114P10E	352959	6610083	prospect	VMS	Au,Ag,Cu,Pb,Zn,Co
62	HERBERT WEST	114P07E	412437	6617854	showing	VMS	Au,Ag,Cu,Co,Pb
63	HERBERT EAST	114P07E	412880	6617831	prospect	VMS	Ag,Cu,Zn,Au,Cd,Pb
64	LOW HERBERT	114P07E	414892	6617408	prospect	VMS	Cu,Ag,Au,Zn,Pb,Co,Bi
65	MOUNT HENRY CLAY	114P08W	418004	6512753	prospect	VMS	Au,Ag,Cu,Zn
66	JARVIS SOUTH	114P08W	416010	6513679	showing	Dist m	Cu
67	HIGH JARVIS	114P07E	413228	6610812	showing	VMS	Zn,Ag,Au
68	GRIZZLY HEIGHTS	114P07E	410872	6518319	prospect	Van	Au,Ag
69	KUD	114P14E	387089	6618074	showing	Van	Cu,Ag,Au
70	FARR	114P11E	378854	6620288	prospect	Skarn	Cu,Zn,Pb,Au,Ag
71	LOW JARVIS	114P07E	415935	6610430	showing	VMS	Cu,Zn,Bi
72	EMPIRE (L 268)	114P10E	413074	6615190	showing	Skarn	Ag,Cu
73	ARIZONA (L 285)	114P10E	411960	6605481	showing	Skarn	Ag,Cu,Pb
74	GRROY (L 730)	114P10E	414490	6605312	showing	Skarn	Ag,Cu,Zn
75	MOCKING BIRD (L 264)	114P10E	414005	6614704	showing	Skarn	Ag,Cu,Zn
76	NEW YORK (L 261)	114P10E	412637	6614844	showing	Skarn	Ag,Cu
77	EVENING (L 900)	114P10E	414489	6614384	showing	Skarn	Ag,Cu,Zn
78	FRISCO (L 154)	114P10E	414938	6614219	showing	Skarn	Ag,Cu,Zn,Pb,Au
79	FAIRFIELD (L 821)	114P10E	413210	6614258	showing	Skarn	Ag,Cu
80	SADDLE 344	114P10E	411202	6615904	showing	Van	Au,Ag
81	SADDLE 2	114P10E	411510	6615954	showing	Skarn	Ag,Cu,Au
82	KR 1	114P10E	407159	6600841	showing	Van	Au,Ag,Cu
83	KR 4	114P10E	407109	6610834	showing	Van	Au,Ag,Cu
84	KR 7	114P10E	413288	6617446	showing	Van	Au,Ag,Cu
85	VARENCE LIMESTONE	114P10E	415288	6618845	showing	Van - dome	Malachite, limonite
none	Buck	114P7	403200	6617500	showing	Hyd r	Cu,Au
none	Pup	114P8	399200	6616951	showing	Hyd r	Cu,Au (Zn,Pb)
none	Goldun	114P15	394750	6610850	showing	VMS	Cu
new	Jo	114P11	371500	6610400	showing	Skarn	Van
new	Carmie	114P11	378150	6614300	showing	Van	Pb,Cu,Zn,Ag,Au
new	Randy Monday	114P12	350520	6615300	showing	VMS	Cu,Au,Ag
new	Tequila Sunset	114P12	352850	6614825	showing	VMS	(Cu)
new	Ice Bridge	114P12	351400	6618000	showing	VMS	Cu,Zn
new	Skus	114P12	352275	6614900	showing	VMS	Cu,Zn
new	Norm	114P15	641950	6610261	showing	Van	Ag,Pb,Au
new	Van	114P16	645000	6610200	showing	VMS	(Cu)
new	Wounded Hedgehog	114O9	564900	6610801	showing	Skarn	(Cu)
new	Lomely	114P13	364750	6618000	showing	Skarn	(Cu)
new	Misty	114P13	341950	6610851	showing	Skarn	(Cu)

Abbreviations: VMS = volcanogenic massive sulphide, Disten = disseminated, Hyd r = hydrothermal.

Notes: - MINFILE data from 1986 release
- elements enclosed in parentheses are suspected based on observed mineralogy, however, analyses are not yet available
- occurrences with MINFILE = "none" are from J. McDougall, unpublished data
- occurrences with MINFILE = "new" were discovered by BCOS mapping in 1992.

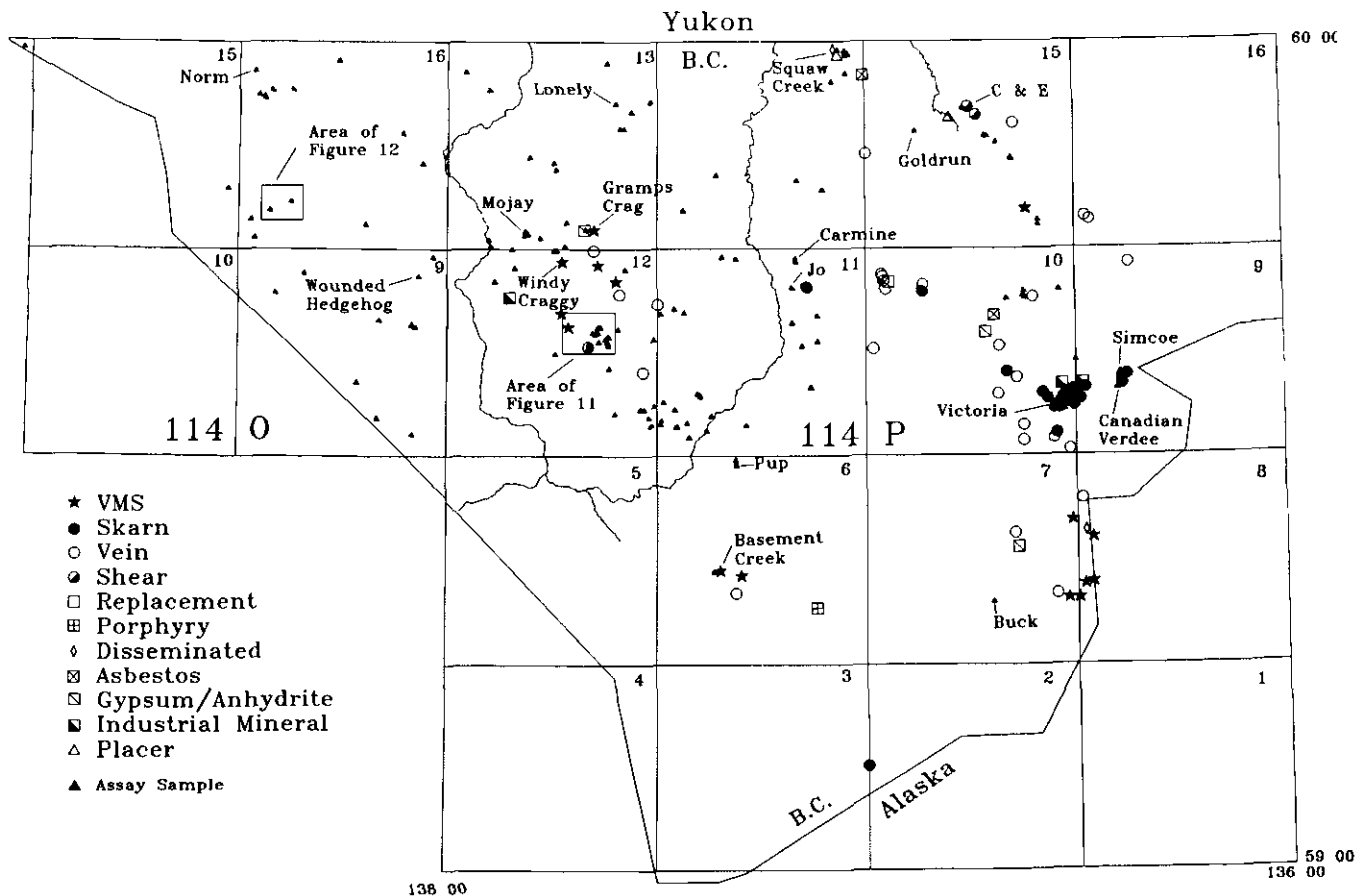


Figure 1-13-10. Location of assay samples and occurrences discussed in text. See Figures 1-13-11 and 1-13-12 for locations of the Rainy Monday, Ice Bridge, Skid, Tequila Sunset and Vern showings.

new occurrences, the Rainy Monday deposit. Such new discoveries demonstrate the very high mineral endowment of the Upper Triassic Tats group and the high potential for the discovery of new reserves.

The new discoveries can be subdivided into two different types of stratiform deposits. The first, which includes the Rainy Monday, Tequila Sunset and Skid occurrences is characterized by chalcopyrite and pyrite stringers and lenses, and stratiform, banded chalcopyrite and pyrrhotite-rich layers within foliated, chloritized basalt and lesser cherty argillite. The second type, which includes the Ice Bridge showing, is characterized by pyrite and pyrrhotite laminae with minor chalcopyrite in calcareous to cherty argillites and siltstone. The latter is probably at a stratigraphically higher level than the main massive sulphide bearing sequence and may represent a waning phase of sulphide deposition.

RAINY MONDAY

The Rainy Monday showing was discovered while the authors (MacIntyre and Mihalynuk) were mapping the area west of the Ice Bridge glacier (local name). The discovery showing is located on the west side of a north-trending ridge just above the valley floor (Figure 1-13-11). Here, a resi-

stant, rusty weathering outcrop of massive to semimassive sulphide protrudes from a scree and grass-covered slope. Pillowed flows crop out to the north and south of the sulphide zone and calcareous siltstone talus occurs upslope to the northeast. The hostrocks are typical of the middle Tats member of the Late Triassic Tats group. The host stratigraphy is contained within a northwest-trending belt that is offset by an east-striking fault north of Tats Lake. The most likely fault restoration solution places the Rainy Monday deposit on strike with the mineralogically similar Tats showing (Figure 1-13-11), thus increasing the overall length of the prospective horizon.

The Rainy Monday discovery showing dips steeply to the northeast and is about 8 metres wide. Within the zone are lenses of porous iron oxide and hydroxide 5 metres wide that locally contain remnants of coarse-grained pyrite and partly oxidized chalcopyrite stringers up to 20 centimetres thick. Mineralization persists over a slope distance of 30 metres but the strike continuation of the zone is lost beneath alpine vegetation and scree to the west and east. Although the surface showing is extensively weathered and oxidized, samples of coarse-grained pyrite and chalcopyrite were obtained for assay (Table 1-13-2, Nos. 12-15, 112). These contained copper concentrations up to 13.5 per cent and gold up to 0.72 gram per tonne.

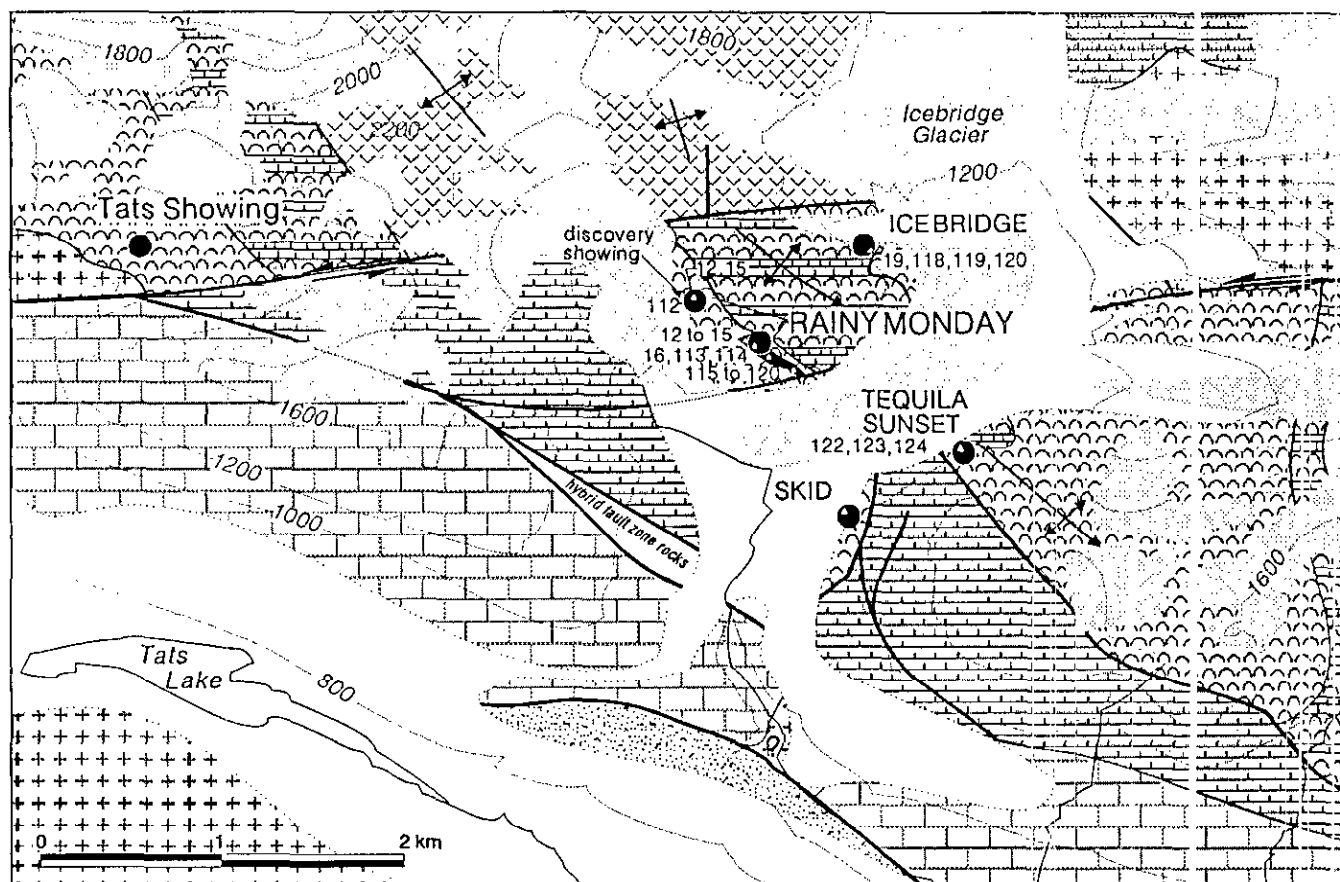
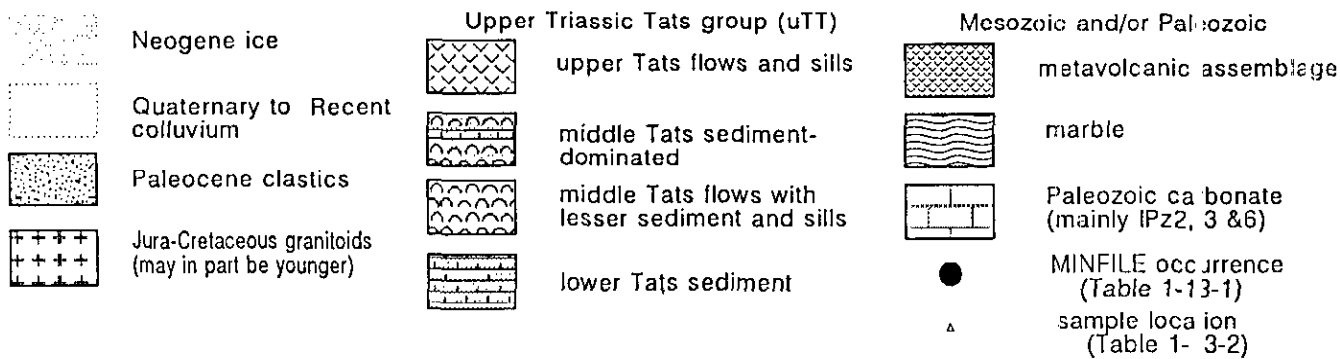


Figure 1-13-11. Generalized geologic setting of newly discovered copper occurrences in the vicinity of Tats Lake (cent al 114P/12). Thick lines indicate fault contacts.

The southeast strike of the discovery showing suggests that the host stratigraphy may crop out on the east side of the ridge where a steep but accessible scree slope extends from the ridge crest to just above lateral moraines covering the base of the slope. Several rusty weathering, resistant knobs protrude from the scree slope and each of these exposures were found to be oxidized massive to semimassive sulphide similar to the discovery showing. The lenses are interbedded with intensely chloritized flows and calcareous, carbonaceous siltstone and argillite. The host stratigraphy strikes north-northwest and dips steeply to the northeast.

Overall mineral content within the eastern zone is difficult to determine due to the high degree of oxidation and, in

places, scree cover. The oxidized sulphide lens occurs within a northwest-trending zone that is over 100 metres wide. The mineralized zone comprises stringers and lenses of massive chalcopyrite and pyrite up to 30 centimetres thick and, where adequately exposed, such lenses can be seen to comprise up to 15 per cent of gossanous zones. Some of the lenses are cut by postmineral mafic dikes or sills which may have recrystallized an original fine-grained protolith. Grab samples collected from several different localities on the slope (Table 1-13-2, Nos. 16-18, 113-117) contained up to 20.2 per cent copper, 2.4 grams per tonne gold and 39 grams per tonne silver.

Mineralization within the southeastern zone has a visible vertical extent of 150 metres and appears to continue

TABLE 1-13-2
PRELIMINARY ASSAY RESULTS, TATSHENSHINI PROJECT AREA, 1140 AND 114P (NORTH)

Text ref. #	Sample No.	NTS#	Easting	Northing	rock type	minerals	sulph %	Au (g/t)	Ag g/t	Cu ppm	Pb ppm	Zn ppm	Co ppm	As ppm	Ni ppm	comments		
5	DMA92	3 12	114P/6	365600	6582700	mass. sulph.	po,cpy	50		1.1	0.59%	9	300			McDougal showing, Basemnt Ck.		
9	DMA92	5 22 1	114P/11	378200	6623900	float/semi-mass	py,gn	20		196	272	13.13%	0.53%			float in saddle, west Carmine Mtn.		
10	DMA92	6 33	114P/7	403200	6577500	volc breccia	py	2		0.4	22	187	51			Buck property		
12	DMA92	12 64 1	114P/12	350500	6615300	mass. sulph.	py,cpy	25-30	0.02	<.5	0.01%	<.5	38	349	<.50	41 Rainy Monday		
13	DMA92	12 64 2	114P/12	350500	6615300	mass. sulph.	cpy,cpy	35-40	0.43	18	5.44%	8	74	650	117	38 Rainy Monday		
14	DMA92	12 64 3	114P/12	350500	6615300	mass. sulph.	py,cpy	25-30	0.27	11	5.32%	9	74	488	50	30 Rainy Monday		
15	DMA92	12 64 4	114P/12	350500	6615300	dissem. sulph.	py,cpy	10-15	1.71	11	0.10%	7	699	238	98	41 Rainy Monday		
16	DMA92	12 65	114P/12	350850	6615150	oxidized sulph.	cpy,mt	60	2.00	31	6.68%	<.5	919	80	<.50	34 Rainy Monday		
17	DMA92	13 66 1	114P/12	350500	6615300	mass. sulph.	py,py	60	1.70	11	2.37%	<.5	312	280	<.50	63 Rainy Monday		
18	DMA92	13 66 2	114P/12	350500	6615300	banded sulph.	cpy,py	20	0.14	5	0.79%	5	214	80	<.50	55 Rainy Monday		
19	DMA92	13 69	114P/12	351400	6616000	lam. sulph.	po,cpy	15	0.62	4	0.46%	63	935	138	196	65 Ice Bridge Glacier showing		
20	DMA92	14 72	114P/6	369200	6596950	breccia	py	5		<.2	132	14	75			Pup breccia		
21	DMA92	14 73	114P/6	369200	6596750	breccia	py	5		<.2	86	10	85			Pup breccia		
24	DMA92	15 78 2	114P/15	394750	6640850	barite-carb.	py,sp,mt	<.1		72	23	513	450			Goldrun property		
25	DMA92	15 78	114P/15	394750	6640850	barite-carb.	py,sp,mt	<.1		19	71	508	0.12%			Goldrun property		
27	JO SHO		114P/11	377500	6620400	limestone	bc	5		8	1.20%	12	190			Jo showing		
28	JT92	3 2	114P/10	415050	6604000	skarn	py,sp,gn	40		13	490	476	17.70%			Night showing, Copper Butte		
29	JT92	4 3	114P/9	420900	6605650	skarn	mg,sp,bo	50								Canadian Verdee		
30	JT92	4 5	114P/9	421325	6607700	skarn	mg,sp,bo	50		42	0.40%	10	0.11%			Simcoe		
35	JT92	6 7	114P/9	415400	6609450	alaskite	mt,az	?		7	0.27%	15	32			Stonehouse Ck.		
38	JT92	16 4	114P/14	367800	6635850	mylonitic carb.	bc,herm,mt	2	3.08	2	619	19	125	94	2900	<.50	fault zone	
52	MDE92	3 1 B	114P/10	413750	6602850	skarn	gn,sp,mt	80		175	11	1.12%	3.00%				near Adams prospect	
53	MDE92	3 5	114P/10	412150	6604075	greenstone	po	3		3	0.16%	23	200				State of Montana	
54	MDE92	3 6	114P/10	412800	6604350	skarn	bnt, mt	10		710	13.10%	50	136				State of Montana	
56	MDE92	3 8	114P/10	413450	6603600	skarn	sph	10		61	233	0.91%	0.24%				near Adams prospect	
57	MDE92	4 4	114P/9	415500	6606350	skarn	cpy,gn	45		14	301	0.35%	6.70%				Lawrence prospect	
58	MDE92	4 5	114P/9	415550	6606550	skarn	gn, sph	30									Lawrence prospect	
64	MDE92	15 6	114Q/16	641850	6650250	vein	gl,py	15	2.07	540	196	10.50%	83	34	63000	<.100	Norm showing	
79	MDE92	30 6 B	114Q/9	664900	6623600	amphibolite	po,cpy,bo	70									Wounded Hedgehog showing	
80	MDE92	32 1 2	114P/13	354750	6646000	skarn	po,cpy	50									Lonely showing	
97	MM92	1 4	114P/10	408750	6618100	argillite	po,sp	up to 80		1.5	81	71	65				Lunar showing	
99	MM92	3 4	114P/10	414400	6604250	basalt?	py,sp,gn	40		19	365	0.11%	3.00%				Evening showing	
101	MM92	3 10	114P/10	413800	6603900	skarn	py,trace cpy,po	95		2	920	12	0.40%				NewYork/Cariboo	
102	MM92	3 11	114P/10	413800	6603350	skarn	gn,sp,py	?		32	365	6.18%	8.80%				Adams	
112	MM92	20 4 2	114P/12	350500	6615300	basalt	py > cpy	15	0.72	15	13.50%	5	192	0.27%	0.18%		197 Rainy Monday	
113	MM92	20 5	114P/12	350850	6615200	basalt	cpy	? 0.12		18	8.60%	<.5	589	38	<.50		20 Rainy Monday	
114	MM92	20 6	114P/12	350800	6615100	basalt	cpy	? 0.96		25	13.60%	<.5	359	56	<.50		7 Rainy Monday	
115	MM92	21 2	114P/12E	351200	6616000	basalt	py	25	0.19	5	0.36%	<.5	99	264	76		43 Rainy Monday	
116	MM92	21 3 1	114P/12E	351250	6615250	basalt	cpy	85	2.37	36	10.20%	<.5	136	273	50		5 Rainy Monday	
117	MM92	21 3 2	114P/12E	351250	6615250	basalt	cpy	90	1.29	39	20.20%	<.5	321	175	50		5 Rainy Monday	
118	MM92	21 5 1	114P/12E	351550	6616050	argillite	po > cpy	10	0.33	3	0.43%	49	0.29%	127	50		74 Ice Bridge Gl. showing	
119	MM92	21 5 2	114P/12E	351550	6616050	argillite	po > cpy	10	0.70	3	0.36%	59	0.41%	122	65		73 Ice Bridge Gl. showing	
120	MM92	21 6	114P/12E	351550	6616000	argillite	cpy,po	10	0.24	1	0.13%	52	815	52	289		52 Ice Bridge Gl. showing	
122	MM92	22 7	114P/12	352650	6614625	hornfels lim.	cpy	10	0.037	0.8	870	7	80	450	41		320 Tequila Sunset	
123	MM92	22 9 1	114P/12	352125	6614400	basalt	cpy >> py	10	0.41	6	0.86%	20	0.22%	710	380		120 Tequila Sunset	
124	MM92	22 9 2	114P/12	352125	6614400	basalt	cpy >> py	15	0.56	12	1.56%	9	173	78	11		<.50	Tequila Sunset
144	MSM92	1 3 B	114P/10	408500	6618350	skarn	mt, py, po	80			78	9	400					
146	MSM92	3 6	114P/10	412800	6604100	skarn	gn,+?	5-10		55	1.06%	1.02%	1.43%					State of Montana
147	MSM92	3 8	114P/10	412150	6603450	skarn	gn,sp,py,mt	80		235	0.54%	17.90%	30.00%					Victoria
148	MSM92	4 3	114P/9	420950	660550*	skarn	bo,mt,az	20		375	17.95%	230	1.60%					Canadian Verdee
151	MSM92	10 1	114P/13	341050	6628850	skarn	po,py,bo,cpy	80	0.007	4	523	5	41	550	4.2	240		Mojay showing
167	MSM92	13 13	114P/11	378150	6624300	qtz vein	galena qvm	15	5.81	150	0.37%	4.37%	0.13%	34	63000	<.100		Carmine

beneath lateral moraine near the valley floor. Assuming that the discovery showing and lenses exposed on the east-facing scree slope are at the same stratigraphic level, the Rainy Monday mineralized zone has a strike length of at least 600 metres, is up to 100 metres thick and extends down dip at least 150 metres. These dimensions suggest the deposit has significant tonnage potential. This combined with the high copper, gold and silver values obtained from assay samples suggest that the Rainy Monday is a significant new volcanogenic massive sulphide deposit.

ICE BRIDGE

The Ice Bridge showing is located approximately 1000 metres north of the Rainy Monday deposit (Figure 1-13-11). Here, rusty, calcareous, cherty argillite and siltstone are interbedded with massive to pillowed flows. The clastic rocks contain fine-grained pyrrhotite laminae 0.5 to 2 centimetres thick that contain variable amounts of chalcopyrite. Over intervals of a few centimetres the sulphide content is as much as 10 per cent. Analyses of samples from this occurrence return values of up to 0.46 per cent copper and

0.41 per cent zinc. The laminated nature of the mineralization, the argillaceous hostrocks and the higher zinc values distinguish these showings from the Rainy Monday. The Ice Bridge showing is at a higher stratigraphic level, assuming no major fault or fold complications within the intervening succession.

TEQUILA SUNSET

The Tequila Sunset showing is located southeast of the Ice Bridge glacier (Figure 1-13-11). The showing includes discrete, yellow and orange gossanous zones, 0.5 to 3 metres wide of tectonically admixed fine-grained sediment and foliated basalt (now chlorite schist) that occur within the hinge zone of a faulted, south-plunging anticline. A sequence of an echelon mineralized zones is exposed across about 20 metres and may extend over 100 metres of a cliff face south of the Ice Bridge glacier terminus. Malachite-stained chalcopyrite and pyrite occur as stratabound stringers within the pods. Chalcopyrite may comprise up to 15 per cent of the rock over intervals of less than 0.2 metre.

Controls on the distribution of the sulphides appear to be predominantly structural. This showing is similar in style to the *Rainy Monday* and the anticline is on trend with the *Rainy Monday* showing. Extents of the mineralization both above and below the immediate discovery zone are untested; such testing will require technical climbing and drilling.

SKID

A thin veneer of foliated basalt forms the steep cliff faces at the base of the ridge southeast of the Ice Bridge glacier. Chalcopyrite occurs as stringers and blebs within the foliated basalt. Lateral moraine is plastered on the slopes both above and below the showing. Bedrock is exposed in a series of waterfalls that erode through the moraine. Assays from grab samples yield up to 1.56 per cent copper and 0.22 per cent zinc (Table 1-13-2). Further exploration may require trenching and technical climbing.

GRAMPS CRAG (MINFILE 114P 054)

The Gramps Crag showing is located in rugged terrain in the extreme southwestern corner of 114P/14. It lies northwest of a belt of rocks correlated with the Upper Triassic Tats group. A field check indicates that the showing is marginal to a dioritic intrusive unit, in a sequence of meta-sedimentary rocks intruded by abundant mafic sills or flows. In this sense, the sequence resembles the lower or middle Tats volcanic sequence, to which it has been correlated (Warwick *et al.*, 1984). However, the metasedimentary rocks, which make up less than 10 per cent of the sequence, include marble and chert-pebble conglomerate, lithologies more typical of the Silurian-Permian sequence, which crops out to the north and east. The showing is hosted in vesicular basalt, and consists of a massive sulphide layer or lens approximately 20 centimetres thick, consisting of massive pyrrhotite and pyrite, chalcopyrite, malachite and azurite. Assay results are pending.

OCCURRENCE WEST OF THE ALSEK RIVER

Another showing was discovered on a small, remote nunatak 35 kilometres west-northwest of the Windy Craggy deposit, near the head of the Vern Ritchie Glacier.

VERN

The Vern showing occurs in Palaeozoic to Mesozoic greenstones on the south side of a small nunatak. (Figure 1-13-12). Chalcopyrite occurs as malachite-stained blebs within wacke (?) near the gradational contact between dominantly *plagioclase-porphyritic basalt flows and buff to brown-weathering banded marble*. The copper grades are visually estimated to be up to 5 per cent in places. The extent of the mineralization is not known. Other rocks within the contact zone are lapilli and block tuff and volcanic breccia, all cemented by carbonate. Very fine-grained basalt dikes up to 40 centimetres thick crosscut the succession.

On the north side of the nunatak the succession is mainly chert or siliceous volcanic rocks (tuff?) and pyritic sericite schist. A bright orange gossanous zone is exposed over

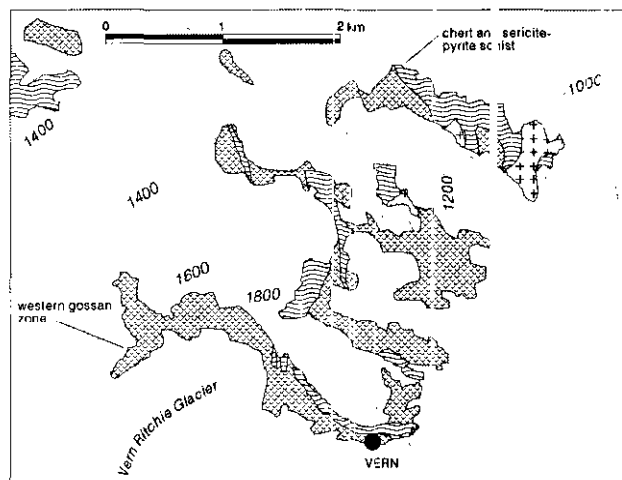


Figure 1-13-12. Geologic setting of the Vern occurrence: (see Figure 1-13-11 for legend).

several tens of metres below an ice fall on the western end of the nunatak.

MELBERN LAKE – BASEMENT CREEK AREA

Several copper showings are known in the watershed of Basement Creek, a northwest-flowing tributary of the Tashshini River. The upper part of the creek is incised into a broad U-shaped valley exposing a nearly continuous section of *northwest-trending, steeply dipping, interbedded marine sedimentary and volcanic rocks of possible Triassic age*. Numerous bright orange and red gossans occur along the trend of the creek, several of which are known sulphide occurrences. These rocks are part of a narrow belt of gossans and copper showings that extends from Melbern Lake, northwest across the Tikki Glacier, down Basement Creek and northward toward Tomahnow Creek. A section through the belt is exposed on the cliffs north of the Tikki Glacier. Here the beds dip steeply and malachite staining occurs locally on cliff faces. A white-weathering gypsum bed is exposed near the top of the cliff section. This belt of marine sedimentary and volcanic rocks is bounded by granitic plutons and may be a roof pendant.

BASEMENT CREEK (MINFILE 114P 043, 044, 045)

Three showings have been located on the Basement Creek property – the Basement West or McDougall (MINFILE 114P 045), June 21st (MINFILE 114P 044) and June 24th (MINFILE 114P 043). Only the McDougall showing, which is exposed on both banks of an east-flowing creek, approximately 100 metres from its confluence with Basement Creek, was examined during the 1992 program. This showing is a vertical, resistant, north-trending coarse-grained, massive to semimassive sulphide lens up to 5 metres thick. The massive sulphide is predominantly pyrrhotite with lesser chalcopyrite and pyrite. The lens is interbedded with steeply dipping chlorite schist, mafic sills and limestone. A grab sample from the southern exposure of the lens contained 0.59 per cent copper and slightly anomalous zinc and silver (Table 1-13-2, No. 5).

The June 21 showing is mainly pyrrhotite veins and stringers with some anomalous copper and gold values in a garnet-tremolite-bearing marble; the June 24 showing is a bedded barite-carbonate exhalite that contains weakly disseminated sphalerite, pyrite, chalcopyrite and galena (Perkins, 1985). The hostrocks are interbedded chlorite schist, mafic volcanics and limestone with numerous mafic sills and dikes.

The belt of possible Triassic rocks that hosts the Basement Creek baritic exhalite and massive sulphide showings extends over 50 kilometres along strike and has high potential for the discovery of additional stratiform massive sulphide deposits.

SQUAW CREEK AREA

Squaw Creek has historically been an important placer mining camp with a reputation for producing large nuggets of both gold and copper. It occupies a linear valley which follows the trace of a major terrane-bounding fault, the Duke fault (Figure 1-13-1). This fault separates part of Wrangellia from the Alexander Terrane (Campbell and Dodds, 1983a). Bedrock mineralization is believed to occur within rocks of Wrangellia Terrane affiliation.

SHEEP (MINFILE 114P 021)

A zone of copper-iron sulphide pods hosted in foliated and unfoliated aphanitic basalt flows and calcareous marine sediments is exposed on the north end of Barrier Ridge, east of upper Squaw Creek. Showings are mainly within a contorted basalt-dominated section near the steeply dipping contact with a less deformed package of calcareous to shaly argillite and wacke. Lithologies associated with predominantly dense, locally pillowed, nonmagnetic, aphanitic basalt flows are: interpillow, laminated micrite; massive white to black and green banded chert (exhalite? or tuff); rusty, well laminated cherty argillite; calcareous siltstone and brown to black, fetid limestone.

Pods of pyrrhotite are up to 1 by 5 metres in size, but commonly 10 to 30 centimetres. Chalcopyrite typically occurs as blebs or veinlets within pyrrhotite, and locally within basalt and chert where it may comprise up to 2 per cent of the rock over a width of 9 metres. Chalcopyrite veinlets also contain pyrite, calcite and subordinate quartz. The mineralized zone is exposed in a series of trenches within east-flowing creek gullies over a strike length of approximately 200 metres. Continuity across strike is about 50 metres, but due to Quaternary cover, its eastern limit is not known to within a kilometre. Smaller zones of massive sulphide mineralization crop out to the northwest within the stream-bed of the eastern fork of Squaw Creek.

Past exploration on the zone includes six diamond-drill holes totalling less than 200 metres (Bapty, 1968) together with airborne and electromagnetic surveys, but the results of the program are not available. In later years, additional geophysical and geochemical work was done on areas peripheral to or overlapping the Sheep property. These programs were aimed at locating the lode source of the Squaw Creek placers.

Mineralized rocks on the Sheep property are probably Late Triassic in age; similar in age and lithology to the Tats group (*see* Part B) which hosts the Windy Craggy deposit. However, these rocks are believed to be part of Wrangellia Terrane (Campbell and Dodds, 1983a) and as such probably belong to a slightly older stage (Carnian) than the Norian Tats group of the Alexander Terrane (*e.g.*, MacIntyre, 1983). Since such a correlation has mineral potential significance, samples for rare-earth element and microfossil analyses were collected as part of this study to test the correlation. The results of these analyses are pending as this paper goes to press.

POLYMETALLIC BARITE-SULPHIDE DEPOSITS (Cu-Zn-Pb-Ag-Au)

GOLDRUN

The Goldrun property (Dat and Bar claims) extends from Goldrun Creek southwestward to Datlasaka Creek. Access to the property is by a dirt road which connects to the Haines Highway approximately 3 kilometres to the east. The property was located in 1988 after prospector Ted Hayes discovered an isolated outcrop of bedded barite with weak sulphide mineralization protruding from the grassy, east-facing slope of a rounded, northwest-trending ridge. The property was briefly visited and sampled as part of the Tatshenshini mineral assessment project.

The Goldrun property covers part of a narrow, fault-bounded, northwest-trending, southwest-dipping belt of poorly exposed, possibly Late Triassic volcanic and sedimentary rocks that extends from Squaw Creek to southeast of Datlasaka Creek. A crinoidal limestone of possible Devonian age crops out along the southwest edge of the property and may be the basal member of a southwest-dipping thrust panel.

The Discovery showing is bedded, calcareous baritic exhalite with minor concentrations of fine-grained pyrite, galena, sphalerite, chalcopyrite, pyrrhotite and argentite. Christopher (1990) reports assays up to 6.7 grams per tonne gold, 227.0 grams per tonne silver and 51 per cent barium. Other showings on the property include the "Massive Sulphide Creek" and "Zinc Mountain" neither of which were visited during the 1992 program. Christopher reports analyses from the Zinc Mountain showing up to 94 447 ppm zinc, 60 289 ppm lead and 150.7 ppm silver. The Massive Sulphide Creek occurrence is a gossanous zone of greater than 15 per cent sulphide in mafic volcanics. No anomalous base or precious metal values are reported for this occurrence (Christopher, 1990). Assay results for two samples collected from the discovery outcrop are given in Table 1-13-2 (Nos. 24 & 25). These barite-rich samples contained 19 and 72 ppm silver with anomalous concentrations of zinc and lead. Sulphides are less than 5 per cent and are very fine grained. The hostrocks are sericite-quartz-talc-carbonate schists that may have formed by alteration of a felsic volcanic protolith. The occurrence of talc and an enrichment in nickel suggests some of the protolith rocks may have been mafic volcanics (Naciuk, 1991). Chloritic schists crop out to the northeast and presumably down section from the baritic exhalite horizon.

The Goldbank Ventures Ltd. - Sutton Resources Ltd. joint venture completed 12 diamond-drill holes totalling 1134 metres, an induced polarization survey, trenching, mapping and rock geochemistry on the Goldrun property in late 1990. The drilling intersected a 10-centimetre bed of massive pyrite with trace to minor argentite, sphalerite and chalcopyrite within the calcareous baritic exhalite zone. The stratiform mineralization assayed 0.27 gram per tonne gold, 1087 grams per tonne silver, 1.14 per cent copper, 0.22 per cent lead and 2.14 per cent zinc (Naciuk, 1991). Regional exploration led to the discovery of another baritic zone up to 130 metres thick, 14 kilometres to the southeast of the Discovery showing. Naciuk (1991) reports analyses from this zone up to 3000 ppb gold, 57.0 ppm silver, 24 350 ppm copper, 31 512 ppm lead and 41 610 ppm zinc. This zone was not visited during the 1992 program.

The mineralization and hostrocks at the Discovery showing on the Goldrun property are very similar to those at the Late Triassic Haines barite-lead-zinc deposit in the Mount Henry Clay area, just south of the International Boundary and the Greens Creek polymetallic massive sulphide deposit in southeast Alaska. The Goldrun showings are also on strike with other sulphide occurrences in the Squaw Creek area to the northwest. The hostrocks for these occurrences, which crop out in a narrow northwest-trending belt, have obvious high potential for undiscovered stratiform barite-sulphide and polymetallic massive sulphide deposits.

HYDROTHERMAL ALTERATION ZONES (Cu-Au-Ag)

Buck

The Buck property, located 69 kilometres southeast of Windy Craggy, consists of 54 claim units that were staked in 1989 to cover a large brown to orange-weathering gossanous zone at the confluence of the Tkope River and Tsirku Glacier (McDougall *et al.*, 1989). The property was visited briefly with Mr. McDougall during a reconnaissance of the area.

A mineralized and altered zone approximately 4 kilometres long and up to 3 kilometres wide is exposed along a northwest-trending ridge that is bounded to the east by the Buckwell Glacier, to the south by the Tsirku Glacier and to the west by the Tkope River. McDougall *et al.* (1989) suggest the zone continues up to 8 kilometres to the south under the Tsirku Glacier but do not clearly state the basis for this conclusion. Where exposed, the zone includes brecciated quartz-carbonate-altered volcanic and sedimentary rocks of possible Triassic age. Bedding, as defined by pyritiferous sediments, trends northwest and dips steeply east. Intensely deformed black argillaceous sediments and limestones that may be correlative with the lower part of the Tats group outcrop to the west of the Tkope River, presumably at a lower stratigraphic level. Rugged ridges and peaks north of the zone appear to be mainly volcanic and could be the upper part of the Tats group.

Sulphide mineral assemblages within the zone include varying proportions and concentrations of fine-grained disseminated to coarse-grained, interstitial pyrite, pyrrhotite and rare chalcopyrite. Manganese oxide coats fracture sur-

faces. Within the zone, intense silica flooding and development of mariposite are reported. Secondary silica is apparently present as grey chert to opaline masses rather than as veins and veinlets. The style of alteration has been described as listwanitic but there is no evidence for an ultramafic protolith and elsewhere within the zone the alteration assemblages suggest a high-level hydrothermal system of possible epithermal origin. Many of the rocks within the altered zone are light coloured and are mapped as felsic volcanics but this coloration probably reflects intense silica-sericite-clay alteration rather than original rock composition.

Samples from various locations within the zone are reported to contain anomalous gold, copper and silver values (McDougall *et al.*, 1989). A sample from a pyritic shear zone near the crest of the ridge apparently assayed 18.41 grams per tonne gold, 0.58 per cent copper and 25.5 grams per tonne silver. Other samples from the area contained up to 0.9 per cent copper, 0.22 per cent zinc 4.1 grams per tonne silver, 0.23 per cent manganese and 176 ppm arsenic with generally low but anomalous gold values. A single grab sample collected during a short visit to the property contained slightly anomalous lead (Table 1-13-2, No. 10)

Additional sampling in 1990 failed to delineate any continuous zones of gold, silver or copper concentration although isolated samples returned copper values between 0.15 and 0.85 per cent and zinc values to 2.44 per cent (McDougall, 1990a). Small zones of massive to semimassive pyrite occur along northwest and northeast-trending shear zones. Northwest-trending basaltic dikes and sills up to 35 metres wide also appear to be intruded along these zones. Brecciation is apparently associated with these basaltic intrusions and narrow copper-bearing shears parallel their northeastern contacts.

The Buck hydrothermal system represents a large and relatively unexplored exploration target in the Tatshenshini mineral assessment area. It appears to be a high-level, possibly epithermal hydrothermal system, with indications of potentially economic concentrations of gold, silver and copper. Because of the areal extent of the zone of mineralization and alteration, much more work will be required to fully assess the mineral potential of this property.

PUP

The Pup property, which includes 40 claim units, was staked in 1989 to cover a zone of intensely brecciated and pervasively mineralized volcanic rock that crops out at the confluence of Pup (local name) and Tomahous creeks (McDougall *et al.*, 1989; McDougall, 1990a). The breccia zone was sampled as part of the Tatshenshini mineral assessment.

Clasts within the breccia are 1 to 5 centimetres in diameter, subangular to subrounded and are crudely stratified. They are predominantly dark grey, fine-grained chlorite and sericite-clay-altered volcanic rocks with minor oxidized quartz and calcareous sediments. In places, oxidation and leaching has produced a porous, poorly consolidated mass of breccia fragments with coarse-grained, oxidized sulphide clusters occupying solution cavities. Minerals identified

include cuprite, copper carbonates, fine-grained pyrite and chalcopyrite. Late quartz veins cut the breccia. Iron oxide cemented boulders occur in the lower part of Pup Creek and clay-rich fault gouge was observed in the bed of Tomahnous Creek. Quartz-carbonate veining is reported north of the creek but was not examined.

Samples from the mineralized breccia are reported to contain up to 1.03 grams per tonne gold, 12.4 grams per tonne silver, 1.67 per cent copper and 0.07 per cent molybdenum (McDougall *et al.*, 1989). Assays results for two samples collected from the breccia zone during the 1992 program are summarized in Table 1-13-2 (Nos. 20 & 21). Neither of these samples returned significant metal values. However, the mineralized zone is large and much additional sampling and possibly drilling is required to fully evaluate the significance of the Pup breccia zone.

The Pup breccia is located along a major fault zone that trends parallel to Tomahnous Creek and may connect with a strand of the Tats Creek fault zone northwest of the Tatshenshini River. Intensely fractured granitic rocks crop out downstream from the breccia zone. The breccia is believed to have formed by explosion of a high-level cupola above a subvolcanic intrusion that may have been emplaced into the fault zone (McDougall, 1990b).

The poorly consolidated nature of the Pup Creek breccia and its location along a fault zone that offsets Early Tertiary sediments in Tats Creek suggests brecciation and mineralization are post-Paleocene to Recent in age. This type of fault-controlled hydrothermal activity may occur along other major Tertiary to Recent faults in the Tatshenshini area. For example, a similar, but untested fault breccia is exposed 6 kilometres north of Sediments Creek.

In addition to the breccia zone, a bedded gypsum-andrydrite deposit occurs in calcareous sediments exposed immediately north of the breccia and adjacent to a quartz diorite stock. There is probably no relationship between the evaporite deposit, which is most likely Triassic in age, and the mineralized breccia.

C AND E NORTH (MINFILE 114P 031) AND C AND E SOUTH (MINFILE 114P 032)

The C and E North and South showings are located east of the Haines Highway near Stanley Creek. Hostrocks are a sequence of strongly altered, mafic volcanic rocks of Wrangellian affinity and Paleozoic or Mesozoic age (Dodds and Campbell, 1983a). The showings are located immediately west of the main strand of the Denali fault, and are apparently genetically related to it. Rocks are light orange weathering and strongly carbonate altered, with numerous quartz-carbonate veinlets. Protolith types are difficult to distinguish over an area at least 1 kilometre wide and several kilometres long. Neither "showing" was located with certainty. They may correspond to the northern and southern baselines of an extensive grid of cut lines. Quartz-carbonate alteration is common along the Denali fault zone to the south of these showings. Three samples of orange-weathering, intensely quartz-carbonate altered rocks did not return anomalous values of silver, lead, copper or zinc (not listed in table).

MINERAL DEPOSITS RELATED TO PLUTONS

QUARTZ-CARBONATE VEINS (Pb, Ag±Zn)

NORM

The Norm showing is a new discovery located on the steep northwest-facing slope of a nunatak in the north-eastern part of the Tweedsmuir Glacier, 4 kilometres south of the Yukon border (NTS 1140/16, northwest corner). The nunatak is underlain by a pluton 2.5 kilometres wide consisting of layered and massive hornblende gabbro and diorite. Its age is not known, but it may be related to abundant Jurassic-Cretaceous plutonic rocks in the area. The contact of the pluton is covered by ice but it presumably intrudes fossiliferous limestone, argillite, sandstone and volcanic rocks of probable Devonian age.

The gabbroic host contains reddish weathering gossanous zones composed of quartz-carbonate veins and altered selvages. A west-trending vein, 1 metre wide, that was examined in the course of this study contains up to 30 per cent coarse galena as small veinlets and lenses, as well as disseminated pyrite. A single grab sample from this vein assayed 10.5 per cent lead, 2.07 grams per tonne gold and 540 grams per tonne silver, and is also anomalous with respect to arsenic, antimony and tin (Table 1-13-2, No. 64). Other gossanous zones within this body were not investigated.

CARMINE

Small (2 - 10 cm thick) quartz veins with coarse galena were found in a north-trending gully on the north side of a small divide on the northwest side of the Carmine Mountain plateau (114P/11N), approximately 5 kilometres north of the Jo showing (*see* below). Hostrocks are rhyolite and dacite flows and tuff intruded by biotite-quartz-feldspar porphyry with accessory hornblende. The flows unconformably overlie lower Paleozoic marble and may be Tertiary in age. A single sample returned 150 grams per tonne silver, 5.8 grams per tonne gold, 0.37 per cent copper, 4.37 per cent lead and 0.13 per cent zinc, and is also anomalous with respect to arsenic and antimony (Table 1-13-2, No. 167).

SKARN DEPOSITS

SHOWINGS NORTH AND WEST OF WINDY CRAGGY

The potential for skarn-hosted mineral deposits north and west of Windy Craggy has not been previously investigated in any detail, although up to 30 per cent of the area is underlain by plutonic rocks, mostly of Jurassic-Cretaceous age, that cut Paleozoic limestone. The plutonic rocks can be divided into two broadly defined map units: relatively homogeneous quartz monzonite or granodiorite, with rare potassium feldspar megacrystic granite, and a relatively heterogeneous complex of tonalitic to dioritic or gabbroic rocks (*see* Plate 1-13-7 for an example of the latter). The more felsic plutons generally do not have skarn mineralization associated with them. Their contacts are usually sharp, but from a distance the intrusions can be difficult to dif-

ferentiate from the country rock where they intrude massive limestone or marble. The heterogeneous, dioritic plutons, in contrast, have abundant alteration and skarn mineralization associated with them, and contacts, particularly where they intrude argillite units, can be mapped from a distance by the presence of wide, red-orange-weathering zones of alteration. Most of the alteration within both the argillite sequences and the plutons up to several tens of metres from the contacts consists of disseminated pyrrhotite (up to 30% but more commonly 2-5%), with associated garnet-epidote-pyroxene skarn in calcareous rocks. In some areas, however, massive sulphide layers or pods are present. Three of the most significant prospects investigated to date are briefly described below. In addition to the new discoveries several other skarn localities have yielded copper values in the 500 ppm range.

WOUNDED HEDGEHOG

The newly discovered Wounded Hedgehog mineral occurrence is located near the toe of the Vern Ritchie Glacier approximately 4 kilometres northwest of Vern Ritchie Lake, on 114O/9NW. The area is underlain by a sequence of massive, recrystallized carbonate rocks intruded by Jurassic-Cretaceous plutonic rocks. At the showing, coarse white marble is intruded by a north-northwest-trending body of hornblende amphibolite, which is moderately to strongly foliated. Red-weathering altered zones occur along this contact, the colour primarily the result of weathering of disseminated pyrrhotite. A brief examination of one of these zones revealed a 1 by 2 metre pod containing approximately 70 per cent very fine grained massive pyrrhotite, chalcopyrite, and lesser bornite. Assay results are pending.

MOJAY

The Mojay showing is located on the southern border of 114P/13, 4 kilometres east of the Asek River on the west side of a narrow glacial canyon. At this locality, coarse, white marble is intruded by Jurassic-Cretaceous(?), variably foliated hornblende diorite and gabbro. At least four intrusive phases were noted in this area. The contact with host marble is extremely irregular, and numerous dikes with skarn-mineralized (mainly garnet+epidote+hornblende±pyroxene) selvages are present. Northwest-trending rusty weathering, resistant lenses of sulphide-bearing skarn are exposed in the canyon, mainly developed within the dioritic pluton contact zone and numerous marble screens. The sulphides are primarily disseminated pyrrhotite and pyrite. One such zone measures approximately 10 metres by 200(?) metres. Lenses of massive sulphide within these zones consist primarily of pyrite, pyrrhotite, chalcopyrite and bornite(?). The extent and distribution of massive sulphide mineralization is largely unknown, as most outcrops are inaccessible in cliff faces or were mapped only by aerial reconnaissance. One sample returned an analysis of 4 ppm silver, 550 ppm cobalt and 523 ppm copper (Table 1-13-2, No. 151). Although the mineralization seems to be of a skarn type, the consistent northwest trend to these bodies suggests a degree of structural control as well.

There are similar showings in the next valley to the east, where at least three large west-northwest-trending rusty weathering skarn lenses are exposed. One such lens developed within the marble at the contact between the marble and the diorite body, consists of very fine grained disseminated and massive pyrite and pyrrhotite, with slightly coarser, disseminated pyrite and pyrrhotite within the diorite body. Only minor development of calcisilicate skarn was observed here, in contrast to the first locality. Two samples collected from this locality did not yield anomalous assays for silver, copper, lead or zinc.

LONELY

The Lonely showing is located approximately 4 kilometres south of the confluence of Range and South Range creeks, where the lower Paleozoic carbonate and Paleozoic argillite units are intruded by a Jurassic-Cretaceous heterogeneous dioritic pluton. Argillaceous rocks host up to 50 per cent pyrrhotite and chalcopyrite as pods and lenses. Calcisilicate skarn alteration is pervasive along this contact. The sulphide zone has a northwest trend and may be in part structurally controlled. Assay results are pending.

Several other localities along the margin of this pluton were also examined and sampled. Most of the sulphide mineralization consists of disseminated pyrrhotite.

CARMINE MOUNTAIN AREA

Jo

The Jo showing was briefly visited and sampled during the 1992 program. It is located on the crest of a small north-trending ridge approximately 2 kilometres west of Red Mountain and 1.5 kilometres south of Frederickson Creek.

Red Mountain is underlain by rusty red weathering, pyritic andesite to basalt flows and related sills of probable Late Cretaceous to Tertiary age. These rocks sit with angular discordance on intensely folded Paleozoic carbonates. Outcrops of carbonate form rounded crests of several north-trending hills on the west slope of the mountain. A northwest and north-trending swarm of dikes, sills and plugs of basalt, diorite and quartz monzonite porphyry cuts the carbonates.

The Jo showing is a disseminated bornite skarn developed near the contact of a dioritic plug. Several small pits probably record exploration work at the showings many years ago. Three samples collected by Geddes Resources Limited in 1990 contained 0.7 to 1.18 per cent copper and 5.9 to 7.0 grams per tonne silver and up to 0.18 per cent zinc. A grab sample collected during a brief stop at the showing assayed 1.20 per cent copper and 3 grams per tonne silver (Table 1-13-2, No. 27).

McDougall (1990) describes the location of a showing in Frederickson Creek, approximately 1.5 kilometres north of the Jo showing and 3.5 kilometres southwest of Carmine Mountain. It occurs in a deep gorge and is not easily accessible and was not visited during the current project. According to McDougall (1990), interest in Frederickson Creek was generated by the discovery of bornite-rich float near its confluence with the Tatshenshini River. Subsequent

work located a copper-stained outcrop in a steep gorge that apparently yielded assays of up to 6.8 grams per tonne gold. Follow-up work by Geddes Resources in 1990 failed to relocate the showing due to high water levels in Fredrickson Creek.

Outcrop in Fredrickson Creek is reported to be mainly limestone with lesser intercalations of shale and cherty argillite of probable Paleozoic age. Sedimentary strata strike northerly and dip steeply; they are cut by basalt dikes and sills and small diorite plugs. The showing is assumed to be a skarn related to emplacement of these intrusions.

RAINY HOLLOW AND THREE GUARDSMEN AREA (114P/10W AND 9E)

The Rainy Hollow and Three Guardsmen areas (114P/10W and 9E) contain abundant skarn prospects, generally believed to be associated with intrusion of the Oligocene Tkope intrusions, and have been the target of mineral exploration efforts since the late 1800s (Watson, 1948). Field checks were made of approximately half of the MINFILE localities in these areas. Several localities were visited by Webster *et al.* (1992) and are not included here, but many more have never had the benefit of a field check. Three of the latter are briefly described below. Most of these prospects are now located to within approximately 100 metres, in contrast to previous investigations which placed them only within 0.5 to 1 kilometre of their correct position.

VICTORIA (MINFILE 114P 009)

The Victoria prospect is located on a west-facing hill slope a few hundred metres south of the War Eagle showing. An adit has been driven into the hillside, and approximately 50 metres above it, a small pit has been excavated in skarn-mineralized marble. The skarn consists of coarse garnet and wollastonite, with lenses of massive sulphide consisting primarily of coarse galena and sphalerite. Watson (1948) reported 188 grams per tonne silver from a sample from this locality. A single grab sample consisting of approximately 80 per cent coarse galena, sphalerite, pyrite and malachite returned 235 grams per tonne silver, 17.90 per cent lead, and 30.0 per cent zinc (Table 1-13-2, No. 147). Lead isotope analysis of this sample will help to determine the timing of mineralization.

SIMCOE (MINFILE 114P 012)

The Simcoe showing is located approximately 150 metres above Clayton Creek on the east side. A trail leads to an adit driven into the steep mountainside an unknown distance, with a small waste dump at the portal. Copper staining is obvious around the portal, however massive and disseminated sulphides were observed mainly in the dump. Rusty weathering zones project up the hillside above the adit, and in part delineate an east-trending, high-angle contact between foliated quartz diorite and greenish metasedimentary rock. Greenish, unfoliated, porphyritic dikes crop out throughout the area. A grab sample of semimassive sulphide containing sphalerite and bornite returned 42 grams per tonne silver, 0.40 per cent copper, and 0.11 per cent lead (Table 1-13-2, No. 30).

We were unable to locate the Mildred showing (MIN-FILE 114P 013) in this area. Its approximate recorded location corresponds to the contact between the Three Guardsmen batholith and metasedimentary country rocks where it changes orientation from north-south to roughly east-west. The contact is rusty weathering and contains disseminated sulphides, apparently a continuation of the skarn mineralization at the Canadian Verdee showing (*see* below).

CANADIAN VERDEE (MINFILE 114P 014)

The Canadian Verdee showing is located along a ridge crest south of Three Guardsmen peak, in a sequence of metamorphosed argillite, quartzite and marble, intruded by quartz diorite. Metasediments and intrusive rocks are strongly foliated along a north to north-northeast trend, and dip steeply to the west. The intrusive body is locally mylonitized along the contact, with amount of strain decreasing to the west, away from the contact. Most of the skarn alteration is a garnet-epidote-diopside-actinolite assemblage developed within the marble unit. Pods and lenses of massive magnetite and malachite, azurite and bornite are developed within the foliation. Massive pyrite-pyrrhotite-chalcocopyrite skarn was observed in float. Iron and copper-stained rocks are visible in cliff faces to the south of the showing, and continue along strike for at least a kilometre north of the showing. Evidence of drilling was noted in several locations along the strike of the mineralized zone. A single grab sample containing bornite, malachite and azurite returned 375 grams per tonne silver, 17.95 per cent copper and 1.6 per cent zinc (Table 1-13-2, No. 148).

The foliated plutonic rocks are part of the Three Guardsmen batholith, for which the unfoliated parts are demonstrably Oligocene in age (Dodds and Campbell, 1988) and related to the Tkope intrusions, with which most of the skarn showings in the Rainy Hollow camp are associated. However, Dodds (1988) has suggested that some of the rocks in the Three Guardsmen batholith (presumably the more foliated ones) may be Cretaceous.

Several other skarn localities were noted in the course of our survey of the Rainy hollow area that are not presently part of the MINFILE inventory. One is located approximately 500 metres southwest of the Adams prospect (MIN-FILE 114P 010), and consists of a weathered roadcut and nearby exposures of galena-sphalerite-magnetite and massive magnetite skarn in a mixed sedimentary sequence intruded by granitic dikes. A grab sample returned 175 grams per tonne silver, 1 per cent lead and 3 per cent zinc. Several reddish weathering, resistant skarn lenses are located along the east side of Wilson Creek, of the Adams prospect.

PRELIMINARY MINERAL POTENTIAL ASSESSMENT

The following constitutes our preliminary assessment of the Alsek-Tatshenshini area. As only a small number of assays have been completed, this assessment is based almost entirely on geological observations recorded during a 2-month field season in the areas outlined in Figure

1-13-1. With the exception of visits to showings and prospects described, our observations (and hence interpretations) do not extend to the southern part of the Tatshenshini map area. Additional data will be provided by completion of regional geochemical surveys.

- Rocks with high mineral potential are Late Triassic in age and occur in a relatively restricted, northwest-trending belt approximately 7 kilometres wide (Figure 1-13-4). They may have formed in an ancient rift system not unlike the present-day Red Sea or Gulf of California (*e.g.*, Peter, 1992). Parts of this belt of Upper Triassic rocks contain significant copper deposits, such as Windy Craggy. To emphasize this, our mapping alone resulted in the discovery of four new copper occurrences within 15 kilometres of the Windy Craggy deposit. Most significant of these is the Rainy Monday showing. It is over 600 metres long, over 150 metres deep, and is up to 100 metres thick. Assay samples from this zone have yielded up to 20 per cent copper, up to 2 grams per tonne gold, up to 28 grams per tonne silver and up to 0.27 per cent cobalt.
- Metamorphic rocks exposed near the southwestern border of the map area may also have significant mineral potential. A mineral occurrence that we discovered in this area is visually estimated to contain up to 5 per cent copper in rocks that were originally much like those at Windy Craggy. However, the area is remote, rugged and icebound.
- Paleozoic limestone underlies a significant portion of the map area but contains only a few scattered mineral occurrences that appear to be of limited extent. Therefore, areas dominantly underlain by these rocks are tentatively assigned a low mineral potential. Assay and regional geochemical survey results to test these observations are pending.
- The third major rock type in the map area, Jura-Cretaceous granitic rock, is associated in some instances with iron-copper skarn or lead-silver vein mineralization at intrusive contacts. These occurrences tend to be small and irregular, and therefore offer relatively low mineral potential. However, high-grade veins such as the newly discovered Norm occurrence could have economic significance.

ACKNOWLEDGMENTS

We would like to thank the other members of the Team Tatshenshini field crew: Paul Schiarizza, Jay Timmerman and Dean Mason, who assisted in gathering the information contained in this report and Guy Deschne, who put most of our field data into digital format. Norm Graham (Discovery Helicopters), our eagle-eyed helicopter pilot, transported us quickly and safely through the clag and ice for which the area is notorious. Likewise, relief pilot Delmar Washington (Capital Helicopters, Whitehorse) capably and amicably moved us to wherever we needed to go.

We are indebted to R.B. Campbell and C.J. Dodds for having established a comprehensive geological framework within the Tatshenshini-Elsek and adjacent areas. Chris

Dodds shared with us some of his personal experience and made many useful logistical recommendations. Dave Brew kindly provided unpublished information from adjacent parts of Alaska and shared his personal reference library. For shelter and a secure base of operations we are grateful to the highways maintenance crew at Blanchard, to Keith Summerville for use of the Geddes Resources exploration camp at Tats Lake and the DIAND MDA office staff for free run of their Whitehorse office.

Very timely macrofossil identification has once again proven to be an invaluable contribution to the construction of our stratigraphic framework. We have thus benefited from the paleontologic expertise of Drs. E.W. Bamber, B.S. Norford and A.W. Norris.

Many other people helped to facilitate our field program through unsolicited kindness, volunteering valuable information and other means of support. An inexhaustive list includes: Haley Holzer (Discovery Helicopters), Lance Goodwin, and Carl Zeihe (Heli Dynamics, Whitehorse).

This paper has benefited from a thorough review by John Newell.

REFERENCES CITED

- Bapty, H. (1968): Sheep, Rouge Point Mines Ltd. in Minister of Mines Annual Report 1967, *B.C. Ministry of Energy, Mines and Petroleum Resources*, page 24.
- Berg, H.C., Jones, D.L. and Coney, P.J. (1978): Map Showing Precambrian to Cenozoic Tectonostratigraphic Terranes of Southeastern Alaska and Adjacent Areas; *U.S. Geological Survey, Open File Report 78-1085*, 2 sheets.
- Brew, D.A. and Morrell, R.P. (1979): The Wrangell Terrane ("Wrangellia") in Southeastern Alaska: The Tur Inlet Subarc Zone and its Northern and Southern Extensions; in *The United States Geological Survey in Alaska: Accomplishments During 1978*, Johnson, K.M., and Williams, J.F., Editors, *U.S. Geological Survey, Circular 804-B*, pages B111-B123.
- Brisco, J. (1987): Diamond Drill, Geological and Geophysical Report on the East Arm Project (Rime 1-29 Claims); *B.C. Ministry of Energy, Mines and Petroleum Resources, Assessment Report 17 014*.
- Campbell, R.B. and Dodds, C.J. (1979): Operation Saint Elias, British Columbia; in *Current Research. Part A, Geological Survey of Canada, Paper 79-1A*, pages 17-20.
- Campbell, R.B. and Dodds, C.J. (1983a): Geology, Tatshenshini River Map Area (114P); *Geological Survey of Canada, Open File 926, Scale 1:125 000*.
- Campbell, R.B. and Dodds, C.J. (1983b): Geology Yakutat Map Area (114O); *Geological Survey of Canada, Open File 927, Scale 1:125 000*.
- Campbell, R.B. and Dodds, C.J. (1983c): Geology, Saint Elias Map Area (115 B and C); *Geological Survey of Canada, Open File 830, Scale 1:125 000*.
- Campbell, R.B. and Eisbacher, G.F. (1974) Operation Saint Elias, Yukon Territory; in *Report of Activities. Part A, Geological Survey of Canada, Paper 74-1A*, pages 11-12.
- Christopher, P.A. (1990): Geochemical and Geological Report Goldrun Creek Property; *B.C. Ministry of Energy, Mines and Petroleum Resources, Assessment Report 19 56*, 11 pages.
- Coney, P.J., Jones, D.L. and Monger, J.W.H. (1980): Cordilleran Suspect Terranes; *Nature*, Volume 288, pages 329-333.

- Dodds, C.J. (1988): Geological Mapping in Tatshenshini River Map Area, British Columbia; in Current Research, *Geological Survey of Canada*, Paper 88-1E, pages 65-72.
- Dodds, C.J. and Campbell, R.B. (1988): Potassium-Argon Ages of Mainly Intrusive Rocks in the Saint Elias Mountains, Yukon and British Columbia; *Geological Survey of Canada*, Paper 87-16, 43 pages.
- Downing, B.W. and McDougall, J.J. (1991): History of Windy Craggy, Tatshenshini River Area, British Columbia; *Geddes Resources Limited*, unpublished report, 29 pages.
- Gammon, J.B. and Chandler, T.E. (1986): Exploration of the Windy Craggy Massive Sulphide Deposit, British Columbia, Canada; in *Geology in the Real World - The Kingsley Dunham Volume*, *The Institute of Mining and Metallurgy*, pages 131-141.
- Gardner, M.C., Bergman, S.C., Cushing, G.W., MacKevett, E.M., Jr., Plafker, G., Campbell, R.B., Dodds, C.J., McClelland, W.C. and Mueller, P.A. (1988): Pennsylvanian Pluton Stitching of Wrangellia and the Alexander Terrane, Wrangell Mountains, Alaska; *Geology*, Volume 16, pages 967-971.
- Geddes Resources (1992): Visitors' Briefing, Windy Craggy Project, *Geddes Resources Limited*, August 1992, 9 pages.
- Gehrels, G.E. (1990): Late Proterozoic - Cambrian Metamorphic Basement of the Alexander Terrane on Long and Dall Islands, Southeast Alaska; *Geological Society of America*, Bulletin, Volume 102, pages 760-767.
- Gehrels, G.E., Saleeby, J.B. and Berg, H.C. (1987): Geology of Annette, Gravina, and Duke Islands, Southeastern Alaska; *Canadian Journal of Earth Sciences*, Volume 24, pages 866-881.
- Horner, R.B. (1989): Low Level Seismic Monitoring at the Windy Craggy Deposit in Northwestern British Columbia; in Current Research, Part E, *Geological Survey of Canada*, Paper 89-1E, pages 275-278.
- Hudson, T. (1983): Calc-alkaline Plutonism along the Pacific Rim of Southern Alaska; *Geological Society of America*, Memoir 159, pages 159-169.
- Jackaman, W. (1993): 1992 Regional Geochemical Survey Program: Review of Activities; in Geological Fieldwork, 1992, Grant, B. and Newell, J.M., Editors, *B.C. Ministry of Energy, Mines and Petroleum Resources*, Paper 1993-1, this volume.
- Jacobsen, B., Parrish, R.R., and Armstrong, R.L. (1980): Geochronology and Petrology of the Tkope River Batholith in the Saint Elias Mountains, Northwestern British Columbia; in Current Research, Part B, *Geological Survey of Canada*, Paper 80-1B, pages 195-206.
- James, H.T. (1928): North-western Mineral Survey District (No. 1) in Minister of Mines Annual Report 1927, *B.C. Ministry of Energy, Mines and Petroleum Resources*, pages C57-C115.
- James, N.P. (1984): Shallowing Upward Sequences in Carbonates; in *Facies Models*, Second Edition, Walker, R.G., Editor, *Geoscience Canada*, Reprint Series 1, pages 209-212.
- Johnson, H.D. (1981): Shallow Siliciclastic Seas; in *Sedimentary Environments and Facies*, Reading, H.G., Editor, *Elsevier*, New York, pages 207-258.
- Lanphere, M.A. (1977): Displacement History of the Denali Fault System, Alaska and Canada; *Canadian Journal of Earth Sciences*, Volume 15, pages 817-822.
- MacIntyre, D.G. (1983): A Comparison of the Geologic Setting of Stratiform Massive Sulphide Deposits of the Gataga District with the Midway and Windy-Craggy Deposits, Northern British Columbia (94F, L; 104O/16; 114P/12); in Geological Fieldwork 1982, *B.C. Ministry of Energy, Mines and Petroleum Resources*, Paper 1983-1, pages 149-170.
- MacIntyre, D.G. (1984): Geology of the Alsek-Tatshenshini Rivers Area; in Geological Fieldwork 1983, *B.C. Ministry of Energy, Mines and Petroleum Resources*, Paper 1984-1, pages 173-184.
- MacIntyre, D.G. (1986): The Geochemistry of Basalts Hosting Massive Sulphide Deposits, Alexander Terrane, Northwest British Columbia (114P); in Geological Fieldwork 1985, *B.C. Ministry of Energy, Mines and Petroleum Resources*, Paper 1985-1, pages 197-210.
- MacIntyre, D.G. and Schroeter, T.G. (1985): Mineral Occurrences in the Mount Henry Clay Area (114P/7, 8); in Geological Fieldwork 1984, *B.C. Ministry of Energy, Mines and Petroleum Resources*, Paper 1985-1, pages 365-379.
- McDougall, J.J. (1990a): Tatshenshini Area Exploration; *Geddes Resources Limited*, unpublished report, 8 pages.
- McDougall, J.J. (1990b): Geological Report on Pup Mineral Claims; *B.C. Ministry of Energy, Mines and Petroleum Resources*, Assessment Report 20 409, 11 pages.
- McDougall, J.J., Potter, A. and Kowall, C. (1989): Results of Alsek-Tatshenshini Area Exploration, *Geddes Resources Limited*, unpublished report, 18 pages.
- Monger, J.W.H., Wheeler, J.O., Tipper, H.W., Gabrielse, H., Harms, T., Struik, L.C., Campbell, R.B., Dodds, C.J., Gehrels, G.E. and O'Brien, J. (1991): Part B. Cordilleran Terranes; in *Upper Devonian to Middle Jurassic Assemblages*, Chapter 8 of *Geology of the Cordilleran Orogen in Canada*, Gabrielse, H. and Yorath, C.J., Editors, *Geological Survey of Canada*, Geology of Canada, Number 4, pages 281-327.
- Naciuk, T.M. (1991): Report on Phase I Geology, Geophysics, Geochemistry, and Diamond Drilling, Goldrun Creek Project; *B.C. Ministry of Energy, Mines and Petroleum Resources*, Assessment Report 21.065, 26 pages.
- Norford, B.S. (1992): Report on Five Collections of Fossils from the Tatshenshini River and Yakutat Map-Areas, Northwestern British Columbia; *Geological Survey of Canada*, Unpublished report Number O-D 7 BSN 1992, 2 pages.
- Norris, A.W. (1992): Report on One Lot of Fossils from Lower Section of Henshi Glacier (North Side), British Columbia; *Geological Survey of Canada*, Unpublished report Number 2-AWN-92, 2 pages.
- Pavlis, T.L., Roeske, S.M., Sisson, V.B. and Smart, K. (1989): Evidence for Cretaceous Dextral Strike-slip on the Border Ranges Fault in Glacier Bay National Park, Alaska; *American Geophysical Union*, Transactions, Volume 70, page 1337.
- Perkins, D.A. (1985): Geological Report on the Basement Group; *B.C. Ministry of Energy, Mines and Petroleum Resources*, Assessment Report 13.523, 17 pages.
- Peter, J.M. (1989): The Windy-Craggy Copper-Cobalt-Gold Massive Sulphide Deposit, Northwestern British Columbia; in Geological Fieldwork 1988, *B.C. Ministry of Energy, Mines and Petroleum Resources*, Paper 1989-1, pages 455-467.
- Peter, J.M. (1992): Comparative Geochemical Studies of the Upper Triassic Windy-Craggy and Modern Guaymas Basin Deposits: A Contribution to the Understanding of Massive Sulphide Formation in Volcano-sedimentary Environments; unpublished Ph. D. dissertation, *University of Toronto*.
- Plafker, G., Jones, D.L., Hudson, T. and Berg, H.C. (1976): The Border Ranges Fault System in the St. Elias Mountains and Alexander Archipelago; in *The United States Geological Survey in Alaska: Accomplishments during 1975*, Cobb, E.H., Editor, *U.S. Geological Survey*, Circular 733, pages 14-16.

- Plafker, G., Nokleberg, W.J. and Lull, L.S. (1989): Bedrock Geology and Tectonic Evolution of the Wrangellia, Peninsular, and Chugach Terranes along the Trans-Alaska Crustal Transect in the Chugach Mountains and Southern Copper River Basin, Alaska; *Journal of Geophysical Research*, Volume 94, pages 4255-4295.
- Prince, D.R. (1983): Report on Reconnaissance Geological Mapping of the Windy Craggy Area, B.C., NTS 114P; unpublished company report, *Falconbridge, Limited*.
- Roeske, S.M., Pavlis, T.L., Snee, L.W. and Sisson, V.B. (1990): $^{40}\text{Ar}/^{39}\text{Ar}$ Isotopic Ages from the Combined Wrangellia-Alexander Terrane along the Border Ranges Fault System in the Eastern Chugach Mountains and Glacier Bay, Alaska; in *Geologic Studies in Alaska*, U.S. Geological Survey, Bulletin 1999, pages 180-195.
- Schielly, H., Banninger, C. and Della Valle, G. (1976): Report on Geological Mapping, including a Consideration of a Report on Geophysical Mag and EM Surveys, in the Area of the Mus Claims; *B.C. Ministry of Energy, Mines and Petroleum Resources*, Assessment Report 5841.
- Souther, J.G. and Stanciu, C. (1975): Operation St. Elias, Yukon Territory: Tertiary Volcanic Rocks; in *Current Research, Part A*, *Geological Survey of Canada*, Paper 75-1A, pages 63-70.
- Warwick, M.R., Kennedy, D.R., Pigott, J.A. and Isherwood, D. (1984): Geological, Geochemical, and Geophysical Report on the East Arm Property (Rime 1-20 Claims); *B.C. Ministry of Energy, Mines and Petroleum Resources*, Assessment Report 12,225.
- Watson, K.DeP. (1948): The Squaw Creek - Rainy Hollow Area, Northern British Columbia; *B.C. Ministry of Energy, Mines and Petroleum Resources*, Bulletin 25, 74 pages, 2 plates.
- Webster, I.C.I., Ray, G.E. and Pettipas, A.R. (1992) An Investigation of Selected Mineralized Skarns in British Columbia; in *Geological Fieldwork 1991*, *B.C. Ministry of Energy, Mines and Petroleum Resources*, Paper 1992-1, Grant, B. and Newell, J.M., Editors, pages 235-252.
- Wheeler, J.O., Brookfield, A.J., Gabrielse, H., Mønger, J.W.H., Tipper, H.W. and Woodsworth, G.J. (1991): Terrane Map of the Canadian Cordillera; *Geological Survey of Canada*, Map 1713A, Scale 1:2 000 000.

NOTES



KATIE – AN ALKALINE PORPHYRY COPPER-GOLD DEPOSIT IN THE ROSSLAND GROUP, SOUTHEASTERN BRITISH COLUMBIA (82F/3W)

By M.S. Cathro, B.C. Geological Survey Branch
K.P.E. Dunne, Mineral Deposit Research Unit, U.B.C.
and T.M. Naciuk, CME Consulting Ltd.

KEYWORDS: Economic geology, Katie, Jim, alkaline porphyry, copper, gold, silver, Rossland Group, Elise Formation, potassic alteration, propylitic alteration, sericitic alteration, mylonite, shear zone.

INTRODUCTION

The Katie deposit (49°08'00", 117°19'50", MINFILE 82FSW290) is located 7.0 kilometres southwest of the town of Salmo (Figure 2-1-1). Access to the property is via the 6-kilometre Hellroaring Creek logging road, which leaves Highway #3, 2 kilometres south of Salmo. Topography consists of gentle to moderately steep slopes ranging in elevation from about 1250 to 1700 metres. Outcrop on the property is sparse due to extensive glacial deposits which locally attain thicknesses of up to 50 metres.

Low-grade porphyry copper-gold mineralization is hosted by mafic to intermediate alkaline to subalkaline volcanic rocks of the Lower Jurassic Elise Formation of the Rossland Group. The rocks exhibit variable potassic and propylitic alteration associated with disseminated and stockwork pyrite, chalcopyrite and magnetite. This geological setting is similar to that of the alkaline suite of porphyry copper deposits as defined by Barr *et al.* (1976) and McMillan (1991), which includes Copper Mountain, Afton, Mount Milligan and Galore Creek. Katie is the most easterly significant example of this deposit class found to date in the Canadian Cordillera. Similar showings in the Rossland Group occur near Nelson and include the Star (Dawson *et al.*, 1989) and Shaft (Andrew and Höy, 1989).

Distinct but relatively minor gold and silver-bearing quartz-dolomite veins with minor pyrite, chalcopyrite, tetrahedrite, arsenopyrite and molybdenite crosscut the porphyry stockwork. Specular hematite has also been tentatively identified. These veins follow mylonitic shear zones which are altered to an assemblage of sericite, quartz and carbonate.

This paper presents a summary of the property geology and exploration results to date and details the results of core logging and petrography completed during 1992.

EXPLORATION HISTORY

Anomalous copper values in Hellroaring Creek stream sediments were first indicated by the 1977 National Geochemical Reconnaissance Survey (GSC Open File 514). The earliest recorded exploration work in the area was a geochemical survey completed on the Jim claims by Amoco Canada Petroleum Company Limited in 1980. This survey indicated "a zone of anomalous copper values in soils ...

with values over 100 ppm over an area of 1200 m by 300-400 m" (MacIsaac, 1980). No further work was done and the claims were allowed to lapse. From 1982 onwards, exploration on the adjacent Gus, Swift, Elise and Lisa claims was focused on shear-hosted gold-silver targets (Andrew and Höy, 1990).

The Katie claim group (Figure 2-1-1) was staked by prospector Ken Murray in 1985 to cover the Amoco copper anomaly. Soil geochemistry carried out by Murray further defined the anomaly and established the presence of partially coincident gold anomalies (Murray, 1987). Balliol Lassiter Petroleum Limited optioned the property in 1983 and completed geological and geophysical surveys and drilled four diamond-drill holes totalling 105 metres in 1989. The best intersection, in hole KT-89-4, assayed 0.24 per cent copper and 0.20 gram per tonne gold over 6.0 metres (McIntyre and Bradish, 1990).

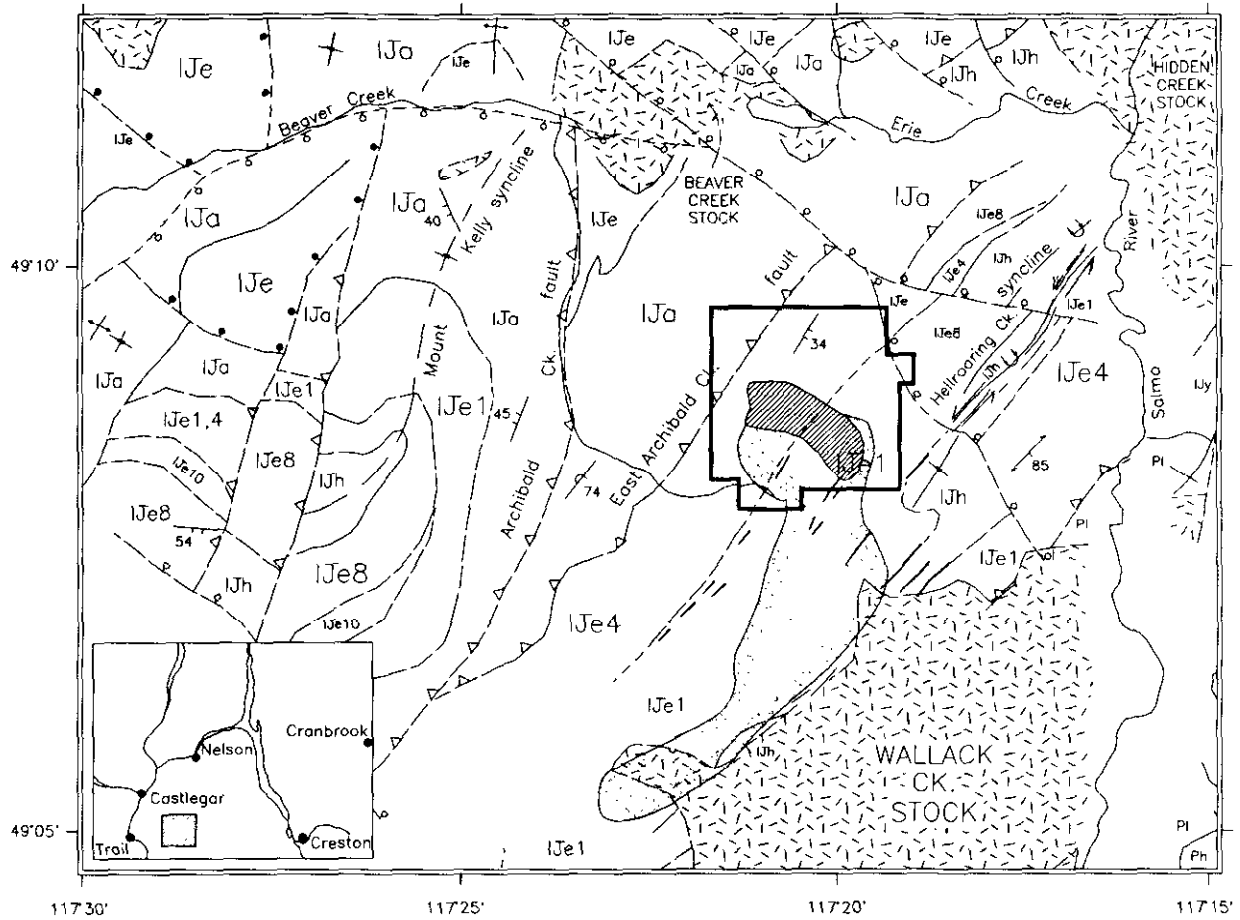
Yellowjack Resources Limited acquired Balliol's interest in 1990 and formed a joint venture with Hemlo Gold Mines Inc. and Brenda Mines Limited to explore the property. As operator, Noranda Exploration Company, Limited conducted further geological, geochemical and geophysical surveys and drilled 34 diamond-drill holes totalling 8260 metres (McIntyre and Bradish, 1990; McIntyre, 1991; Kemp, 1992). Yellowjack took over as operator in 1992 and drilled an additional 18 holes totalling 4477 metres.

The drilling has delineated three areas of low-grade porphyry copper-gold mineralization, named the "Main", "West" and "17" zones (Figure 2-1-2). To date, no mineral inventory figure has been released by the owners.

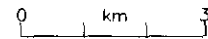
REGIONAL GEOLOGY

The Katie property is underlain mainly by mafic to intermediate volcanic rocks of the Lower Jurassic Rossland Group, the easternmost part of the Quesnel Terrane. Just a few kilometres south of the property the Rossland Group is juxtaposed against Paleozoic rocks of the Kootenay Terrane by the Waneta fault, a steep west-dipping thrust fault (Figure 2-1-1).

The Rossland Group in the Salmo area comprises a basal succession of fine and coarse-grained clastic rocks of the Archibald Formation, volcanic and epiclastic rocks of the Elise Formation and overlying fine-grained clastic rocks of the Hall Formation. These rocks have been well described by Little (1950; 1960; 1965; 1985), Frelbold and Little (1962), Frelbold and Tipper (1970), Höy and Andrew (1988; 1989a; 1989b; 1989c; 1990a; 1990b), Andrew *et al.* (1991) and Dunne and Höy (1992).



LEGEND



JURASSIC - CRETACEOUS

granite, granodiorite

LOWER JURASSIC

ROSSLAND GROUP

IJh HALL FORMATION; argillite, siltstone

IJe ELISE FORMATION

IJe10 siltstone, argillite

IJe8 intermediate to mafic tuff

IJe1,4 mafic flows, tuff; Katie intrusions

IJa ARCHIBALD FORMATION; siltstone, conglomerate, argillite, tuff

LOWER JURASSIC AND UPPER TRIASSIC (?)

IJy YMIR GROUP

PALEOZOIC

Pi LAIB FORMATION

Ph HAMILL GROUP

>58,000 gamma aeromagnetic contour

area of drilling

Figure 2-1-1. Location and regional geology map of the Katie property (after Höy and Andrew, 1990a). Katie claim group is shown by bold line. Magnetic data from GSC Map 8479G.

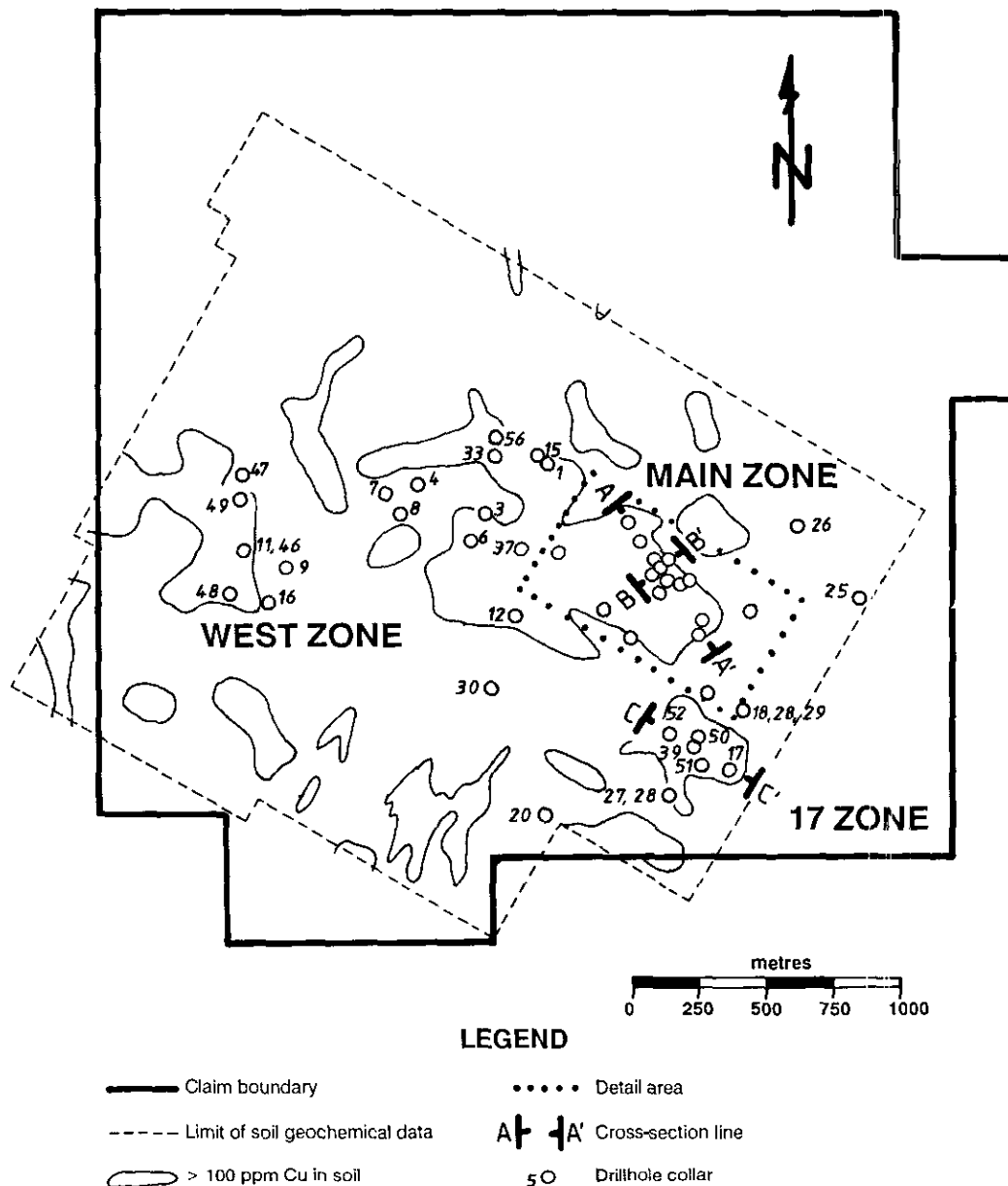


Figure 2-1-2. Drillhole plan for the Katie property. The location of Figure 2-1-3 is shown by the heavy dotted line. The locations of cross-section lines are also shown (see Figure 2-1-4).

Drill information from the Katie property indicates that the Elise Formation in this area is composed of mafic to intermediate volcanic rocks intruded by numerous sub-volcanic gabbro to monzonite dikes and sills. These intrusive rocks, informally known as the “Katie intrusions”, are assumed to be roughly syn-Elise in age. They are described in detail below.

The earliest structures in the Katie area (*ca.* 180 Ma) are tight folds, locally associated with a penetrative mineral foliation and intense shearing and thrusting (Höy and Andrew, 1990a). These structures are more pronounced and evident near the Waneta fault where the Hellroaring Creek syncline, an overturned, east-dipping syncline exposes Hall Formation in its core and sheared Elise Formation in its

limbs. This syncline may be the southern extension of the Hall Creek syncline in the Neison area (Höy and Andrew, 1990a).

To the south of the Katie claims, a number of northeast-trending shear zones formed during this early deformation event. Several of these can be seen in surface exposures and are characterized by intense carbonate-sericite-silica alteration (Andrew and Höy, 1990). Northwest-trending shear zones interpreted from Katie drill core may be the folded equivalents of these surface exposures.

North to northeast-trending, east-verging thrust faults post-date shearing along the Waneta fault. These include the steeply west dipping Archibald and East Archibald Creek faults on the west side of the Katie property (Figure 2-1-1).

The compressional structures are sealed by Middle Jurassic and Late Cretaceous intrusions such as the Beaver Creek, Wallack Creek and Salmo stocks (Figure 2-1-1). Late northwest-trending normal faults offset earlier thrust faults and cut both Jurassic and Cretaceous intrusions. These late faults are probably related to Eocene extensional tectonics (Parrish *et al.* 1988; Corbett and Simony, 1984).

Despite proximity to the tectonic boundary between Quesnellia and North America, Rossland Group rocks are relatively undeformed except within about 2 kilometres of the Waneta fault where they are penetratively deformed. Regional metamorphic grade of the Rossland Group is low in the Salmo area, but increases to the north in the Nelson area.

A strong (250 gamma), northeast-trending regional magnetic anomaly measuring 2 by 8 kilometres (Figure 2-1-1), overlies the property and probably reflects a magnetite-rich intrusion or volcanic unit (GSC Map 8479G).

ROCK TYPES

Outcrops on the property are rare and rock types are described mainly from drill core. Lithologies are described in order from oldest to youngest.

LOWER JURASSIC ROSSLAND GROUP

UNIT IJev: ANDESITIC TO BASALTIC FLOWS AND TUFFS

The property is mainly underlain by variably altered volcanic rocks of the Lower Jurassic Elise Formation. They are medium to dark greenish grey in colour, weakly to moderately magnetic and generally massive to vaguely laminated. Although alteration has partially obscured the original textures, large pyroxene and feldspar phenocrysts are common and easily discernible in hand specimen. Pyroxene phenocrysts are subhedral to euhedral, range in size from 1 to 10 millimetres and average 2 to 3 millimetres. Feldspar phenocrysts are subhedral to euhedral and lath-like, average 2 to 3 millimetres in length and usually appear altered. The dominance of pyroxene and feldspar-phyric rocks suggests that most of this unit is part of the lower member of the Elise Formation (Höy and Andrew, 1988).

This unit is further subdivided into flow and flow breccia (IJe4), monolithic pyroclastic breccia (IJe2) and lapilli (IJe8l), crystal (IJe8x) and fine (IJe7f) tuff (Table 2-1-1) corresponding to the nomenclature of Andrew *et al.* (1991). Petrographically, flow units are distinguished from tuffs by trachytic alignment of feldspars, local calcite or quartz-filled amygdules and absence of broken crystals. Despite the apparent presence of pyroxene in hand sample, primary pyroxene phenocrysts are completely altered and replaced by actinolite, chlorite, epidote and biotite (Plate 2-1-1). Plagioclase varies from andesine to labradorite; the anorthite content is often obscured by saussuritization or sericitization of feldspar cores (Plate 2-1-2), replacement of rims by potassium feldspar or plagioclase zoning. Apatite is an accessory mineral in virtually all the Elise volcanic rocks. In tuffs, apatite phenocrysts are often broken (Plate 2-1-3).

UNIT IJga: KATIE INTRUSIONS

Intrusive rocks at the Katie property are generally pale green and grey spotted, moderately magnetic and medium to coarse grained. They range in composition from gabbro to monzonite and are composed of nearly equal proportions of anhedral to subhedral pale grey to greenish grey feldspar and subhedral dark green mafic minerals, mainly hornblende and lesser pyroxene. Grain size ranges from about 1 to 3 millimetres. In drill core, these intrusive lithologies alternate with volcanic rocks suggesting that they probably occur as thick sills or dikes. The rock often has a heterogeneous appearance with partially assimilated fragments of gabbroic or volcanic material: a texture that is more typical of a hybrid border phase than an intrusive breccia (V.A. Preto, personal communication, 1992).

In thin sections, intrusive rocks are mainly equigranular and granophyric (Plate 2-1-4), although porphyritic phases are also represented. They range from mafic to intermediate in composition. The mafic phases contain 15 to 40 per cent plagioclase (An₅₀₋₆₅) and lesser potassium feldspar (5 to 15%; Table 2-1-1). Primary quartz is generally absent. Pyroxene and hornblende are altered to actinolite, epidote, chlorite and carbonate. Feldspars are commonly sericitized (Plate 2-1-4) or saussuritized. Apatite occurs as an accessory mineral.

More intermediate phases comprise 15 to 40 per cent plagioclase (An₁₀₋₄₅) and 15 to 30 per cent potassium feldspar, including perthite (Plate 2-1-5). The abundance of potassium feldspar and perthite is probably due to potassic alteration. Hornblende is rarely partially preserved as ragged grains. Commonly chlorite, epidote and calcite replace primary amphibole and pyroxene. Sphene is often present as an accessory mineral; apatite is notably absent.

Based on primary mineral assemblages in thin section, the Katie intrusions are mainly gabbro to monzogabbro in composition with some more monzonitic varieties (Table 2-1-1). The variation, however, may be due to the increase in the potassium feldspar (and quartz) content in some specimens and could in part be an effect of the strong potassic alteration. Due to this alteration, discrimination of the protolith by whole-rock analysis is inappropriate.

The lack of sharp intrusive contacts and chilled margins, and the similar overall petrographic composition, suggest that the Katie intrusions were emplaced into the Rossland Group as synvolcanic intrusions. They incorporate partially assimilated gabbroic or volcanic phases and occur near a major regional structure (in the core of the Hellroaring Creek syncline). These features are characteristic of other complex subvolcanic intrusions in the Rossland Group including the Eagle Creek Complex (Dunne and Höy, 1992) and the Shaft gabbro (Andrew and Höy, 1989).

UNIT IJh: BLACK ARGILLITE AND SILTSTONE

Fissile black carbonaceous argillite and siltstone of the Lower Jurassic Hall Formation outcrops on the east side of the property (Höy and Andrew, 1990a). Similar black argillite and greywacke are also present in hole 25 to the northeast of the Main zone and are interpreted to be Hall Formation.

TABLE 2-1-1
 PETROGRAPHIC CHARACTERISTICS OF THE LOWER JURASSIC ROSSLAND GROUP AT THE KATIE
 PROPERTY (082F/03W), SOUTHEASTERN BRITISH COLUMBIA

Unit	Primary		Alteration		
	Phenocrysts%	Groundmass%	Replacement% (of phenocrysts)	Pervasive%	Vein%
VOLCANIC ROCKS:					
andesite/basalt flow/flow breccia (IJe4)	plagioclase 10 apatite 1	opagues 2	sericite 10 chlorite 10 calcite 10	quartz 30 sericite 25	calcite 2 quartz 1 opagues 1
andesite/basalt lapilli tuff (IJe8l)	plagioclase 3 (An45-60) apatite 1-2	opagues 1-3	epidote 20-40 chlorite 5-10 actinolite 2-5 sphene trace	k-spar 10-20 quartz 10-15 chlorite 0-20 epidote 5-7	quartz 2 epidote 1-3 k-spar 1 biotite 1
andesite/basalt crystal tuff (IJe8x)	plagioclase 15-30 (An55-62) k-spar 2 apatite 1-2	hornblende 0-10 opagues 1-7	chlorite 1-15 albite 0-15 epidote 0-7 sericite 5 calcite 0-5 biotite 0-5 actinolite 0-5 k-spar 1-5	quartz 25-35 sericite 0-10	calcite 0-5 quartz 0-5 k-spar 0-1 opagues 1
latite fine tuff (Je7f)	plagioclase 20 (An45-60) k-spar 15-20 apatite 1	opagues 2-3	calcite 20 sericite 10 chlorite 10 biotite 0-5 albite 0-2	sericite 0-40 chlorite 0-15 quartz 2	

INTRUSIVE ROCKS:					
gabbro (Umga)	plagioclase 15-25 (An 50) apatite 1	perthite 15 opagues 5	actinolite 25 quartz 5-15 k-spar 3-25 calcite 1-10 sericite 1-5	chlorite 40	calcite 1 opagues 1
monzogabbro (Umga)	apatite 1	plagioclase 15-40 (An 55-60) k-spar 5-15 opagues 0-2	chlorite 15 sericite 10 leucoxene 1-7 calcite 2-3 actinolite 2 epidote 1-3 quartz 1	albite 1	epidote calcite 1 quartz 1 opagues 1
monzodiorite (Umga)		plagioclase 15-40 (An30-45) perthite 30 quartz 10 k-spar 3 opagues 0-5	chlorite 10 epidote 5 calcite 5 actinolite 0-20 leucoxene 3 sericite 1	chlorite 0-5	calcite 3 epidote 1-3 quartz 1
monzonite (Umga)		plagioclase 20-30 (An10-30) k-spar 15-20 quartz 10 opagues 2	k-spar 30 actinolite 10 epidote 5 sericite 5 quartz 3-10 calcite 3 sphene 3	calcite 5 chlorite 2 quartz 1	calcite 2 epidote quartz 1 calcite 1

1. Based on analyses of 20 thin sections from DDH 13, 39, 53 and 56 and private report for YellowJack Resources Ltd. by Getsinger (1992)
 2. Table format after Ross (1992)

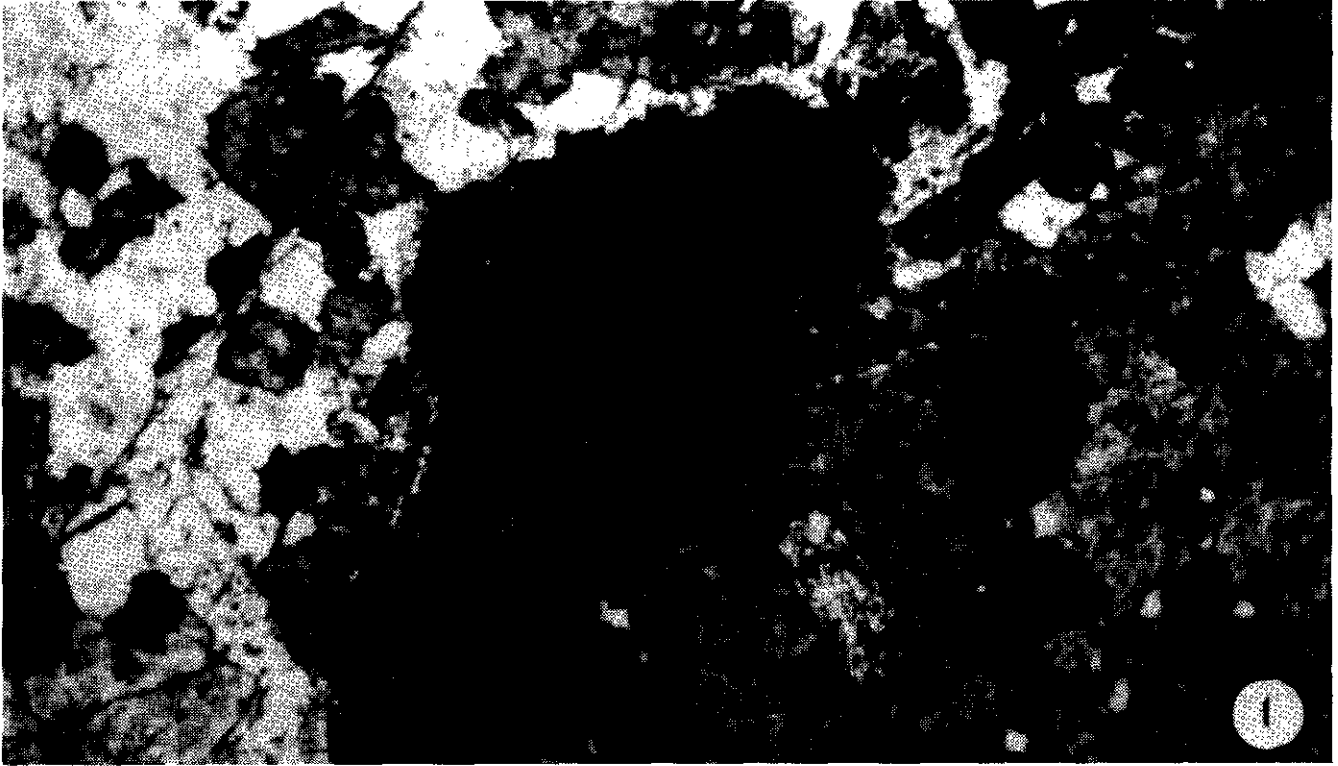


Plate 2-1-1. Pyroxene replaced by actinolite and carbonate in monzogabbro. Matrix dominated by potassium feldspar. Also note primary magnetite grains (dark grey) with needles of rutile. Katie DDH 41-176.7 metres (from McDonald, 1992: ppl + reflected light, field of view = 5.1 mm).

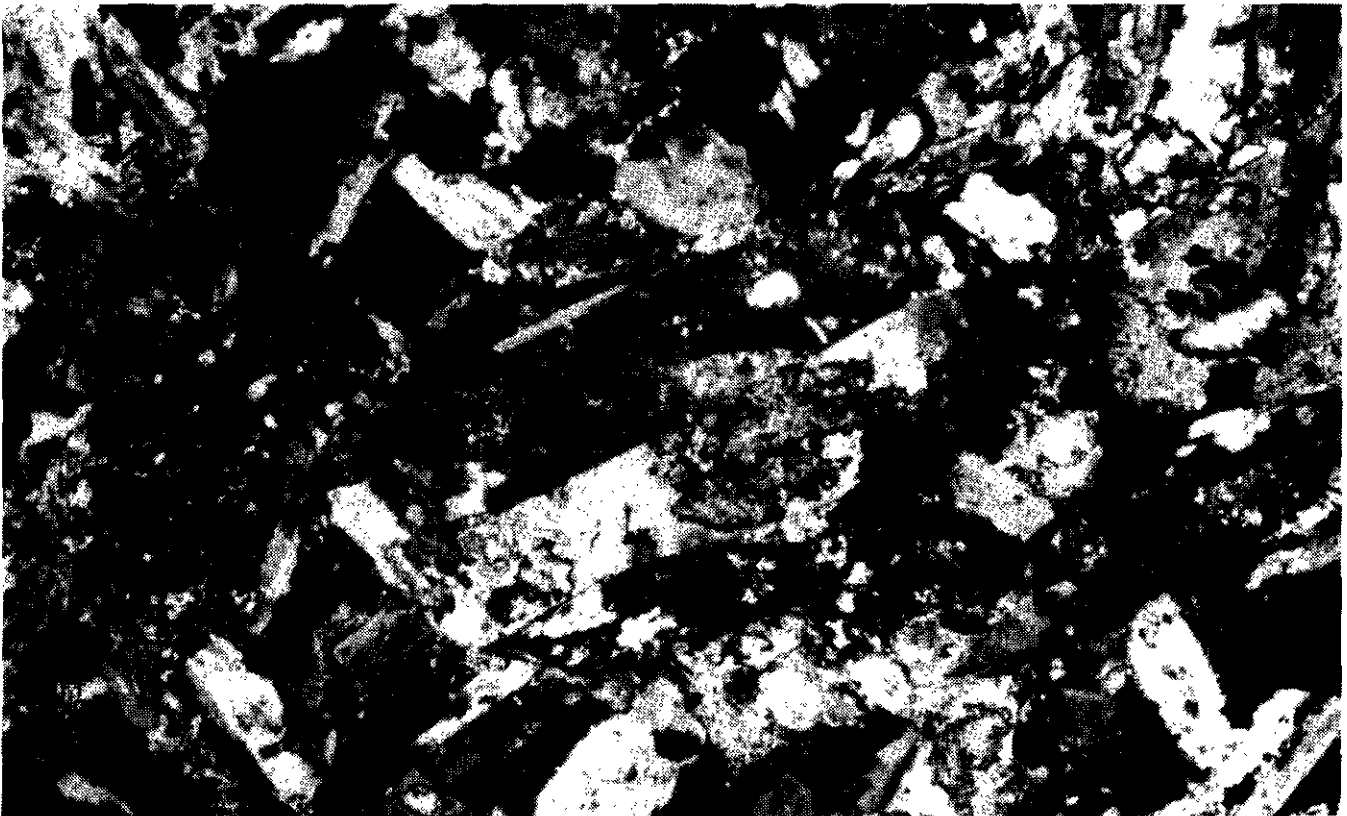


Plate 2-1-2. Saussuritized albite in plagioclase-augite crystal tuff; albite phenocryst in centre of photo is 0.7 millimetre long. Katie DDH 53-223.5 metres (xp, field of view = 1.3 mm).

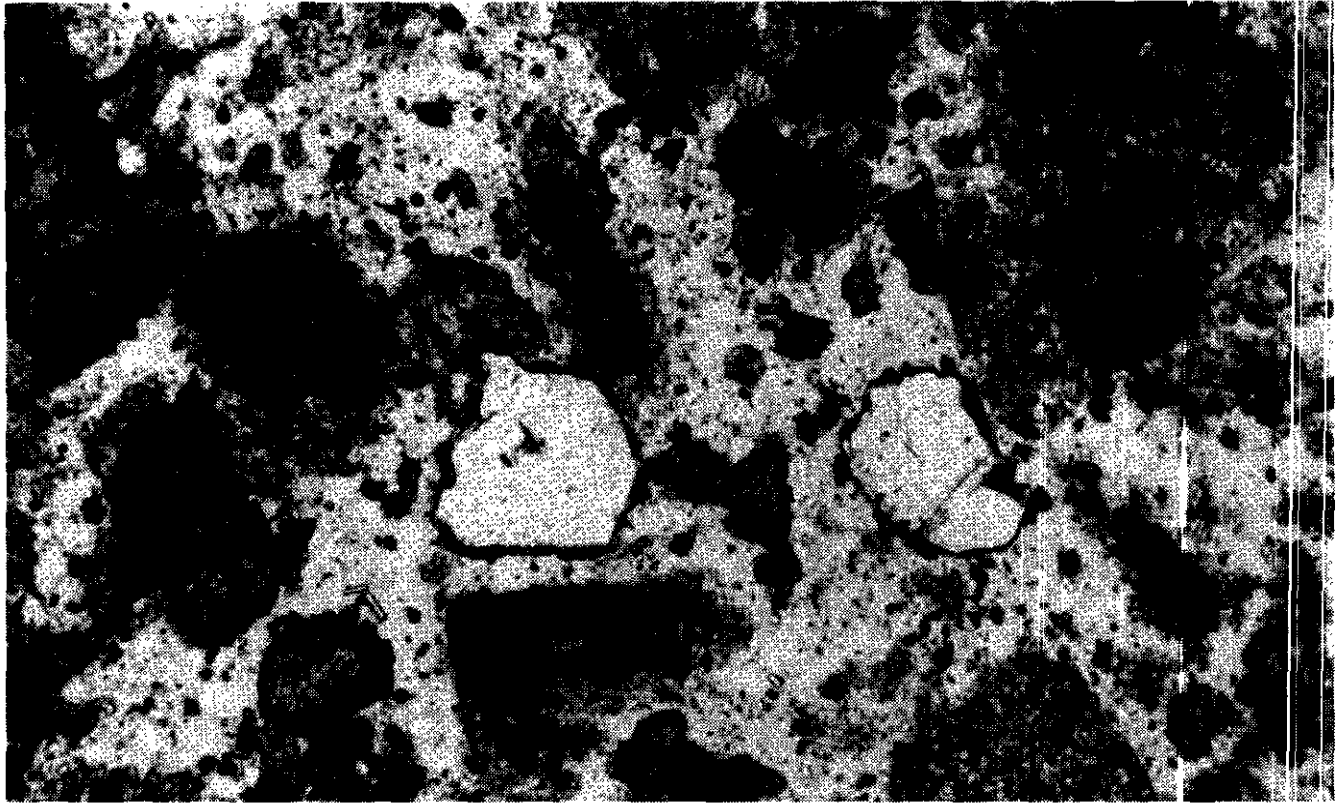


Plate 2-1-3. Broken apatite phenocrysts in crystal tuff; apatite crystals are 2 millimetres in diameter.
Katie DDH 53-109.2 metres (ppl, field of view = 1.3 mm).

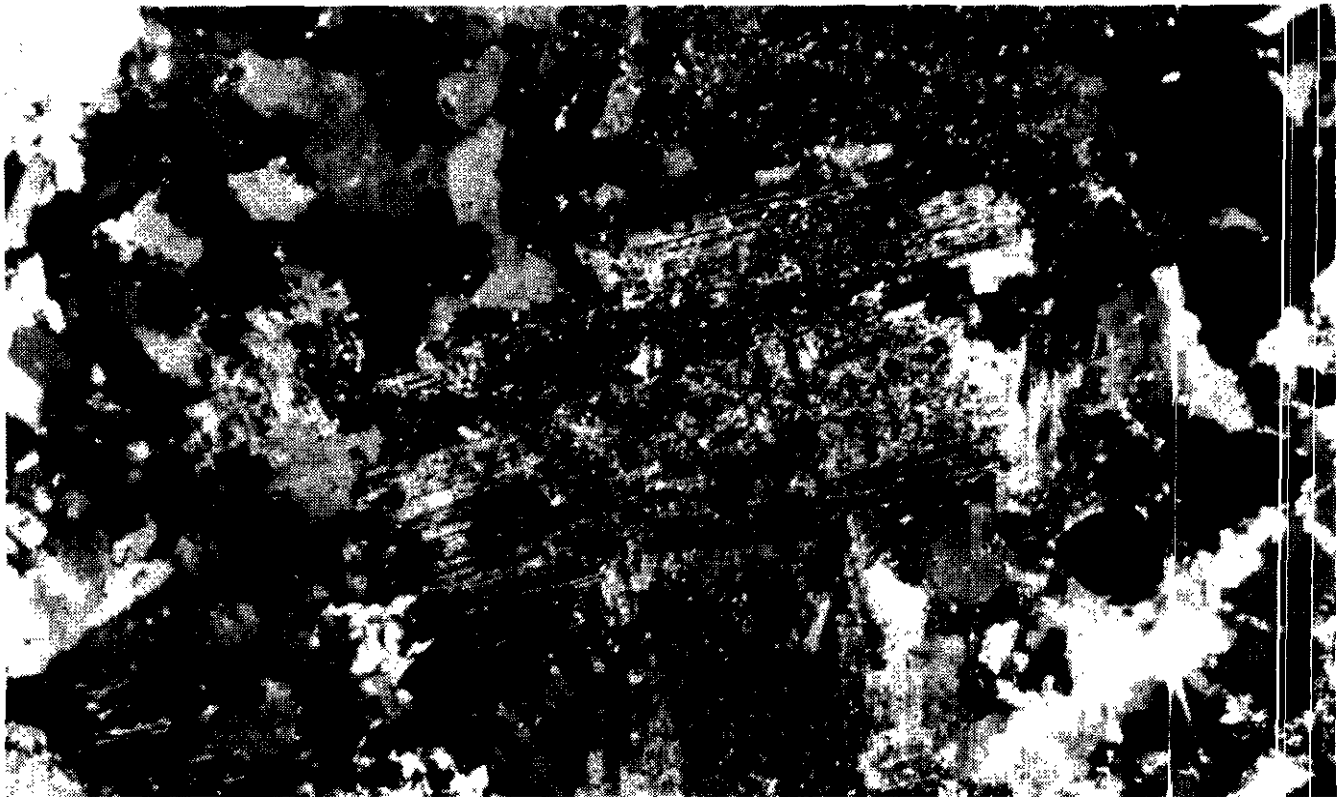


Plate 2-1-4. Sericitized plagioclase phenocryst in granophyric monzonitic matrix, Katie DDH 53-90.3 metres
(xp, field of view = 2.6 mm).

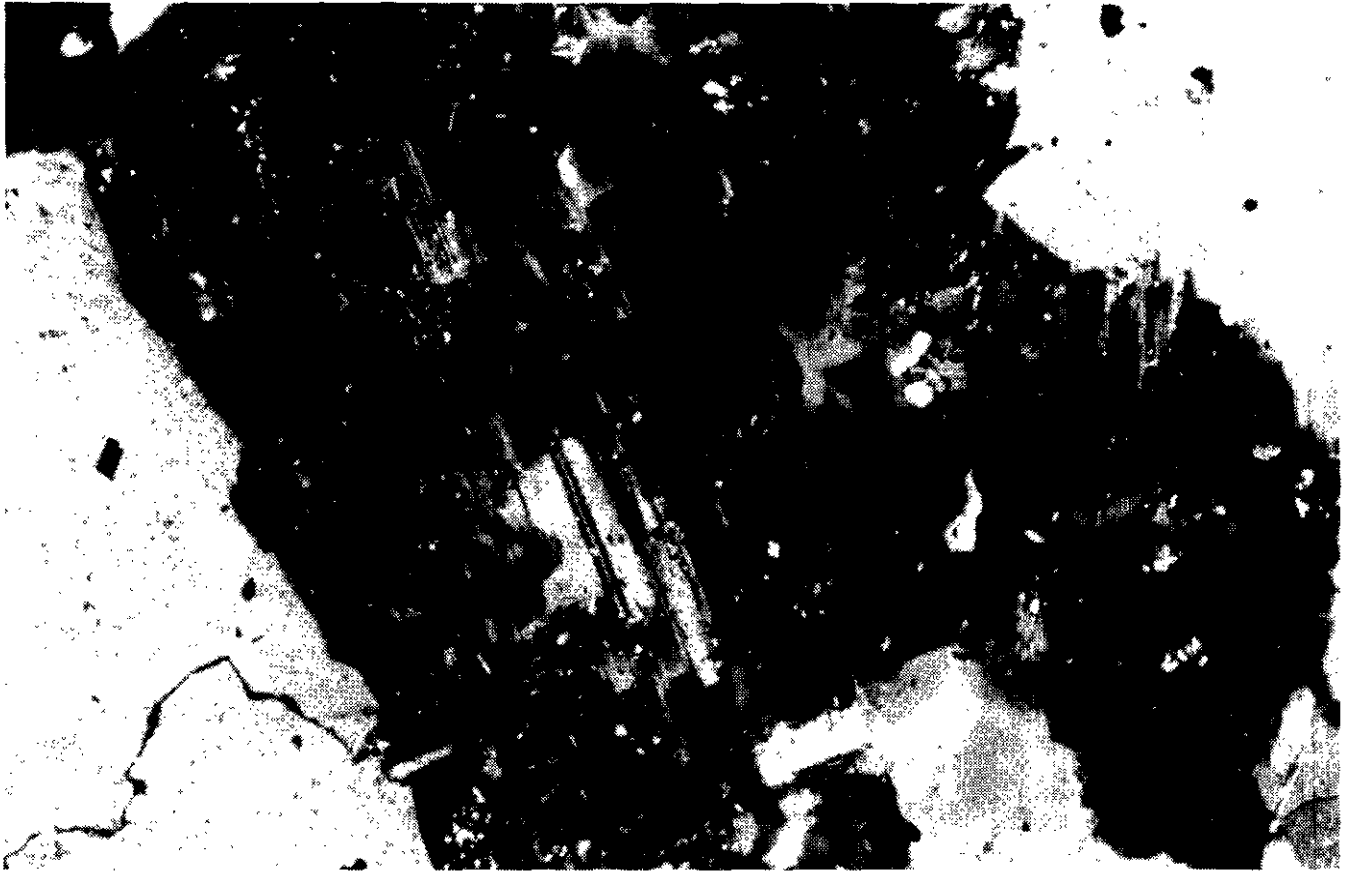


Plate 2-1-5. Perthitic texture of plagioclase in potassium feldspar. Alternatively, this may be potassium feldspar replacing a primary plagioclase phenocryst. Katie DDH 53-90.3 metres (xp, field of view = 0.65 mm).

UNIT IJsk? FELDSPAR PORPHYRY

Pale grey and greenish grey plagioclase porphyry is occasionally present in the drill core. In hand specimen it is generally foliated and mottled in appearance, with 5 to 7 per cent subhedral to euhedral feldspar phenocrysts 6 to 10 millimetres in size in a medium to dark greenish grey groundmass. Chloritized hornblende laths 1 to 2 millimetres long comprise 5 to 15 per cent of the rock. In thin section, sericitized labradorite phenocrysts are seen in a groundmass of plagioclase, potassium feldspar and quartz; hornblende needles are virtually all altered to chlorite. Several per cent magnetite grains show a poikilitic texture. The protolith for this rock was probably a dacite. It is similar in appearance to the post-Elise (*ca.* 186 Ma) Silver King porphyry near Nelson (Höy and Andrew, 1988) but may be a synvolcanic dike rock. It contains 1 to 2 per cent pyrite but has only background levels of copper and gold; this infers that it is a post-mineral intrusion.

LATE DIKES

Late dikes of lamprophyre, microdiorite and feldspar porphyry are minor but ubiquitous; they are generally unmineralized and unaltered or only weakly altered. None of these dikes has been dated at Katie or in the immediate area, but they are post-mineralization and may be related to

the Nelson (Middle Jurassic) or Coryell (Middle Eocene) plutonic suites.

UNIT mJnd?: PLAGIOCLASE MICRODIORITE, HORNBLLENDE MICRODIORITE

Narrow dikes of fine-grained porphyritic microdiorite are common in the drill core. These dike rocks are spotted light and dark grey, are nonmagnetic to moderately magnetic and contain 0.5 to 2-millimetre pale green or grey, anhedral to subhedral phenocrysts of feldspar and 0.5 to 1-millimetre needles of black hornblende.

UNIT mJfp?: FELDSPAR PORPHYRY

Fine to medium-grained, nonmagnetic to weakly magnetic, beige-grey to pale beige feldspar porphyry dikes are locally present. This unit is distinguished by 0.5 to 2-millimetre subhedral to anhedral phenocrysts of white to pale green feldspar in a greenish beige aphanitic groundmass.

UNIT mEl?: BIOTITE LAMPROPHYRE, BIOTITE-HORNBLLENDE LAMPROPHYRE

Lamprophyre dikes or sills up to 15 metres thick, but generally less than 3 metres thick, are locally present in drill core. They are dark grey, relatively fresh and nonmagnetic to weakly magnetic. These dikes have a fine-grained

groundmass with 3 to 5 millimetre biotite phenocrysts, less common hornblende phenocrysts and angular to sub-rounded, grey, fine-grained rock fragments up to 5 millimetres in diameter. Fine-grained chilled margins are usually evident. Staining shows that this unit contains 10 to 20 per cent potassium feldspar in the groundmass and that the rock fragments contain no potassium minerals.

STRUCTURAL GEOLOGY

The Katie property is within a generally northeast-trending, southeast-dipping panel of lower Elise rocks on the western limb of the Hellroaring Creek syncline. Lack of outcrop hinders more detailed structural interpretations. Bedding is difficult to recognize in the volcanic rocks, partially because of pervasive alteration. Correlation of bedding contacts in the Main zone suggests they strike northwest and dip northeast. A weakly developed foliation is recognizable in drill core as chloritic partings along microfractures.

Several zones of sheared and mylonitic rocks have been recognized in the Main zone. These shears are 5 to 20 metres wide and appear to crosscut porphyry-stage alteration and mineralization. Their relationship to post-mineral dikes is not known and their attitude and distribution are unclear. Some drillhole correlations suggest that they may have a predominantly northwest strike and northeast dip (Figures 2-1-3 and 2-1-4).

The mylonitic rocks have an intense penetrative fabric, are wavy banded, pale beige and greenish beige, strongly slickensided and may grade into chlorite-sericite schist. In thin section, the cataclastic fabric is marked by rounded feldspar boudins and rotated sulphide grains with quartz pressure shadows (Plate 2-1-6). Compositionally, the mylonite comprises over 70 per cent sericite as pervasive alteration and replacement of feldspar, 10 per cent quartz, 10 per cent sulphides, 2 to 3 per cent carbonate (possibly ankerite) and several per cent leucoxene. Folded and sheared quartz-dolomite-sulphide veins, which are described below, are also present.

Drillhole 25 intersected a fault in the northeast part of the property which juxtaposes andesites of the Elise Formation against black argillite of the Hall Formation. This is probably a steeply dipping northwest-trending fault mapped by Höy and Andrew (1990b).

MINERALIZATION AND ALTERATION

At least two stages of mineralization are present; an alkalic porphyry copper-gold stage and a later, shear-hosted gold-silver-copper-antimony-arsenic stage.

ALKALINE PORPHYRY STAGE

Porphyry-stage mineralization is simple, consisting mainly of pyrite and lesser chalcopyrite (Plate 2-1-7). Traces of bornite, pyrrhotite, sphalerite and tetrahedrite have been noted and chalcocite has been tentatively identified in drillhole 37. Total sulphide content ranges from 1 to 10 per cent and averages about 2 per cent. The sulphides

occur as subhedral disseminations in the volcanic and intrusive rocks or in narrow veinlets with quartz, calcite, potassium feldspar, chlorite and epidote. Chalcopyrite also occurs locally with pyroxene which is commonly altered to actinolite (McDonald, 1992). Good correlation of copper and gold analyses suggests that gold occurs mainly in chalcopyrite. Limonite, malachite and azurite are common on fractures high in drillholes; in some holes partial oxidation extends to depths of over 100 metres.

In terms of metal content, the altered volcanic and intrusive rocks contain a maximum of about 1 per cent copper and 0.5 gram per tonne gold. Copper contents are rarely less than 400 ppm, except in late dikes which generally contain less than 100 ppm. Other elements, such as silver, lead, zinc, arsenic and antimony, are relatively low.

Up to several per cent magnetite is present in most rock types. The main exception to this is strongly potassium feldspar altered zones which are often nonmagnetic. Magnetite occurs mainly as rounded and corroded primary (?) grains 0.1 to 2.0 millimetres in diameter (Plate 2-1-1), or as secondary grains to 50 microns, veins, irregular aggregates and breccia fillings (Plate 2-1-8; McDonald, 1992). Narrow zones of coarsely crystalline secondary magnetite are locally well developed, especially above mineralized intervals (Figures 2-1-3 and 2-1-4). Locally these contain up to 50 per cent magnetite (Plate 2-1-8). A slightly oxidized surface sample of this material returned analyses of 14 200 ppm copper and 2800 ppb gold. Other trace accessory minerals include rutile, sphene, ilmenite and leucoxene. These are generally associated with magnetite (Plate 2-1-1) and ferromagnesian minerals, although rutile is also found locally in veins carrying chalcopyrite (Getsinger, 1992; McDonald, 1992).

Alteration mineral assemblages in the Katie area are consistent with both propylitic alteration and greenschist facies metamorphic grade. However, as the regional metamorphic grade is low in the Salmo area and penetrative deformation of the volcanic rocks is generally lacking on the property, propylitic alteration is more likely. On the Katie property, this alteration is characterized by saussurization of feldspars to a greenish grey mixture of chlorite, epidote, sericite and calcite. Pyroxene grains have been altered to chlorite, sericite and actinolite. Albite is locally developed adjacent to sulphides (Getsinger, 1992). In addition, calcite, epidote and chlorite-pyrite stringers crosscut the rock, although many of these appear to be later than the main stage of mineralization.

Pervasive potassic alteration is locally well developed (Figures 2-1-3 and 2-1-4) and is characterized by a grey, green, pink and purplish brown mottled, vaguely granular rock composed of potassium feldspar, plagioclase and lesser quartz, biotite and chlorite. Petrography indicates that potassium feldspar has replaced the groundmass and forms rims on primary plagioclase grains (Getsinger, 1992). Coarse secondary biotite is also locally present. In some places, potassium feldspar may be confined to narrow (1 to 5 cm) veins, quartz vein selvages, or irregular flooded zones associated with quartz, pyrite and chalcopyrite (Plate 2-1-9).

A late, retrograde, hydrous alteration appears to overprint the prograde alteration types. Sericite replaces plagioclase

**KATIE MAIN ZONE
SURFACE PROJECTION OF
ALTERATION AND MINERALIZATION**

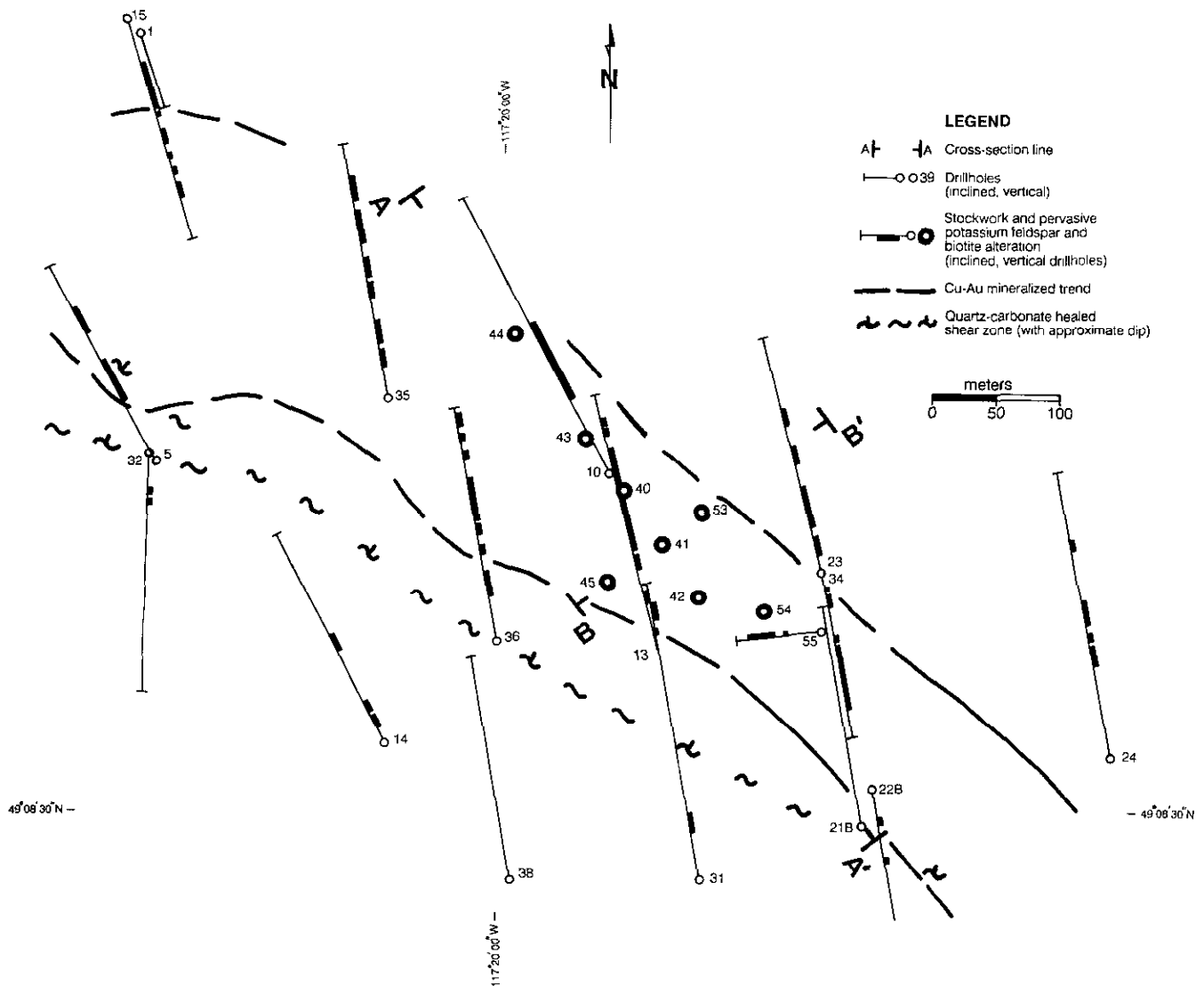


Figure 2-1-3. Drillhole plan for the Main zone, Katie property. Drillhole traces and the extent of alteration zones and mineralization are shown projected to surface.

and secondary potassium feldspar and chlorite replaces secondary biotite and amphibole (Getsinger, 1992). The abundant late calcite, epidote and chlorite-pyrite stringers mentioned above crosscut the potassic alteration and may also be part of this late retrograde stage.

SHEAR-RELATED AU-AG-CU-SB-AS STAGE

Although not common, mylonitic shear zones carry significant gold values (1 to 3 ppm), silver (10 to 60 ppm) and copper (up to 1 per cent) and anomalous levels of arsenic and antimony. These sheared rocks are pervasively altered to an assemblage of quartz, sericite and carbonate and contain weakly to strongly contorted quartz-dolomite-sulphide veins. The veins contain minor but locally abundant concentrations of pyrite, chalcopyrite, tetrahedrite and

arsenopyrite and traces of molybdenite. Specular hematite has been tentatively identified.

The mylonitic shears appears to be younger than the porphyry stage and may displace porphyry mineralization in some places. As outlined above, the attitude of these structures is not well known, although at least one set appears to strike northwest and dip northeast (Figures 2-1-3 and 2-1-4).

EXPLORATION RESULTS

Ground geophysical surveys and soil geochemistry have detected numerous anomalies on the Katie claims. Geophysical surveys include a 28 line-kilometre pole-dipole induced polarization survey (a = 50 m, n = 1 to 5, line-

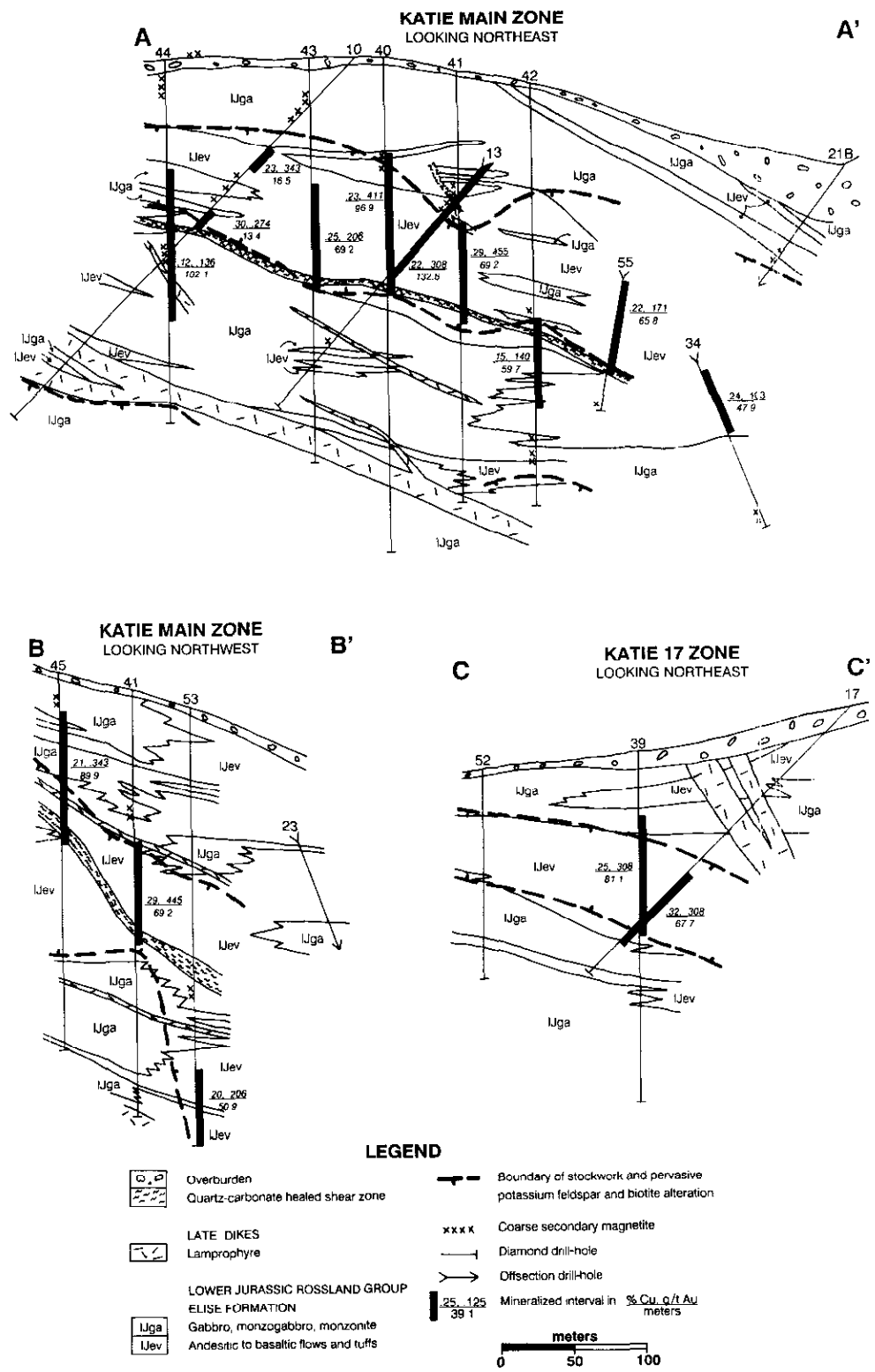


Figure 2-1-4. Cross-sections through the Main and 17 zones, Katie property. The locations of cross-section lines are shown on Figures 2-1-2 and 2-1-3.

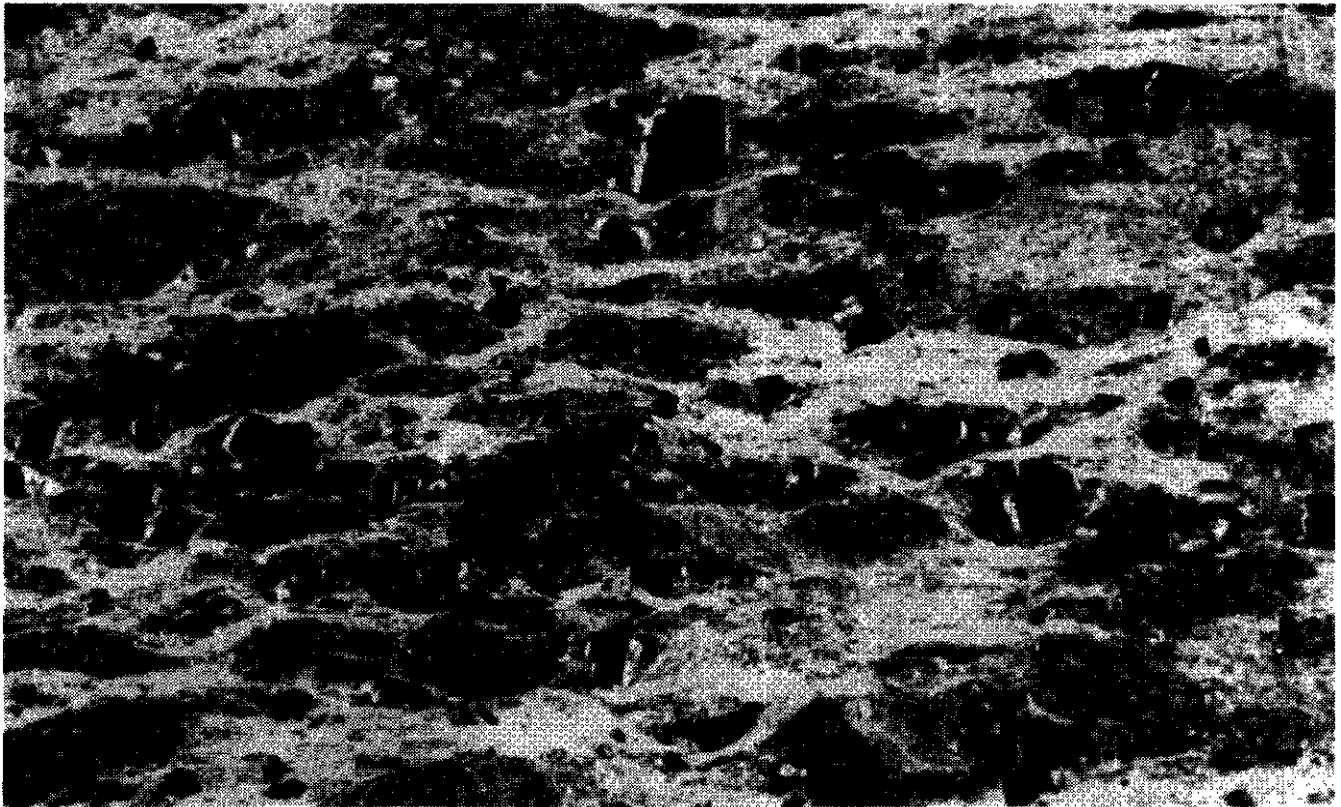


Plate 2-1-6. Protomylonite. Note rotated sulphide grains with quartz pressure shadows and replacement of feldspar by sericite and carbonate. Katie DDH 13-100.4 metres (ppl, field of view = 5.1 mm).



Plate 2-1-7. Matrix chalcopyrite and lesser pyrite (both white) in quartz-albite alteration replacing sericitized plagioclase. Katie DDH 41-124.2 metres (from McDonald, 1992; ppl + reflected light, field of view = 5.1 mm).

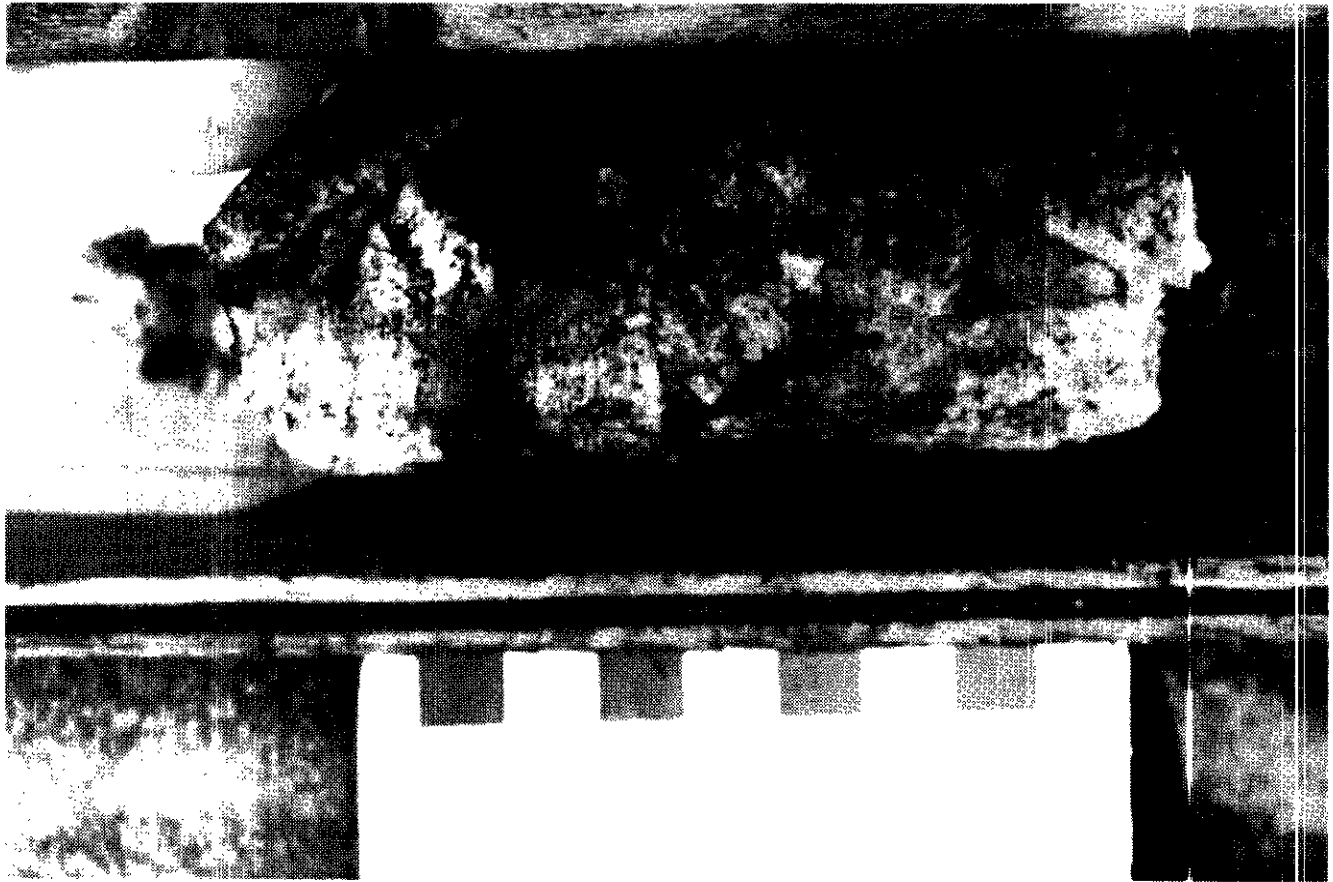


Plate 2-1-8. Coarse-grained magnetite-cemented breccia. Fragments are 2 to 3 centimetres in diameter. Katie DDH 40-77.0 metres.

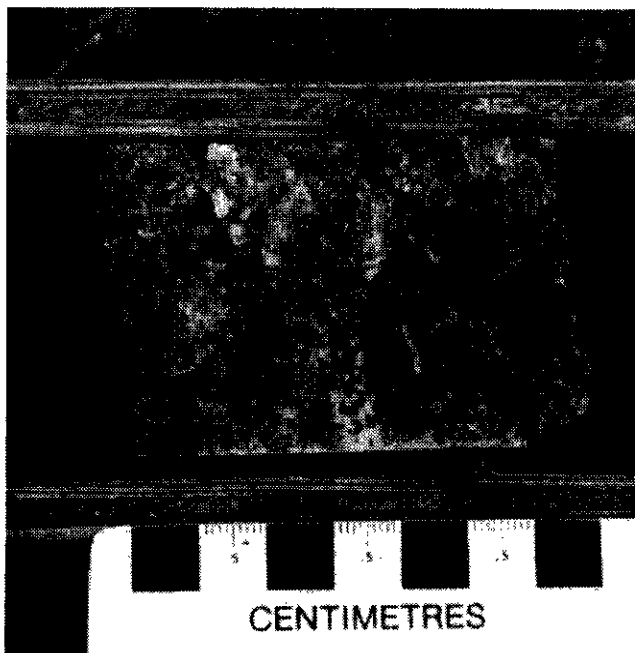


Plate 2-1-9. Pinkish brown mottled potassic alteration comprising fine-grained potassium feldspar and biotite with 1 to 2-centimetre quartz-chalcopyrite stringers and patches. Katie DDH 41-103.8 metres.

spacing = 200 m) and a 41 line-kilometre magnetometer survey (25 m stations, line spacing = 100 m). In addition, a total of 36 line-kilometres of soil sampling (100 x 100 m grid) has been carried out but was hindered somewhat by thick overburden. Several large areas of anomalous copper (100 ppm) have been outlined (Figure 2-1-2). There are no large contiguous gold anomalies, although spots of high (10 ppb) are coincident with the copper zones. Details of the geophysical and geochemical work can be found in McIntyre and Bradish (1990) and McIntyre (1991).

Three anomalous zones were identified by the ground geophysics and extend over an area of at least 1800 by 500 metres. An anomaly over the Main zone consists of coincident high chargeability, moderate resistivity and moderate to strong magnetic responses. The true dimensions of this geophysical anomaly were not ascertained because its stratigraphic and mineralized trends strike subparallel to the grid lines. A roughly coincident copper-gold soil anomaly (Figure 2-1-2) is also present. Drilling has shown that the Main zone strikes northwest, has an apparent true thickness of 70 to 135 metres and is at least 500 metres long (Figures 2-1-2, 2-1-3, 2-1-4). It has been intersected in drillholes to 350 metres below surface. Copper-gold enrichment is mainly confined to intensely potassically altered andesitic volcanic rocks (for grades *see* Figure 2-1-4). Local enrichments in gold and silver are associated with late mylonitic shear zones as previously described.

The 17 zone anomaly is located 670 metres south of the the Main zone, has a strong magnetic response but is outside the area of induced polarization coverage. It is geologically similar to the Main zone, with copper-gold mineralization associated with intense potassium feldspar and biotite alteration. Limited drilling has outlined an altered and locally mineralized area measuring at least 300 by 100 metres (Figure 2-1-4). The zone appears to strike northwest and dip at a low angle to the northeast (Figures 2-1-2 and 2-1-4). *It may be a faulted extension of the Main zone.*

The West zone anomaly is 1.6 kilometres west of the Main zone and comprises a north-trending zone of high resistivity, high chargeability and locally high magnetic responses. Potassic alteration is not as well developed in this area although one drillhole, NKT-89-9, cut a 170.3 metre intercept grading 0.16 per cent copper and 0.171 gram per tonne gold.

CONCLUSIONS

- The Katie property hosts low-grade, alkaline porphyry copper-gold mineralization within variably potassic and propylitically altered intermediate to mafic volcanic rocks and gabbro to monzonite synvolcanic intrusions of the Lower Jurassic Elise Formation. Drilling to date is insufficient to close off the area of mineralization and alteration but it measures at least 1800 by 500 metres.
- The early porphyry-stage mineralization is mineralogically simple, consisting mainly of pyrite and chalcopyrite with traces of bornite, pyrrhotite, molybdenite, tetrahedrite and sphalerite. Highest copper grades are associated with zones of potassium feldspar and biotite alteration and potassium feldspar-quartz-calcite-sulphide veining. Strong positive correlation between copper and gold suggests that gold probably occurs in chalcopyrite. The potassic alteration zones are surrounded by a much wider area of pervasive propylitic alteration. Zones of coarse secondary magnetite cemented breccia are locally present and occur most commonly above mineralized intervals. Late calcite, epidote and chlorite-pyrite veins transect the prograde alteration assemblages and may be part of a late, hydrous, retrograde alteration phase.
- A later, relatively minor stage of Au-Ag-Cu-Sb-As mineralization crosscuts the porphyry mineralization and is at least partially controlled by northwest-striking, northeast-dipping mylonitic shear zones. These shear-hosted zones result in local enrichments in gold and silver.
- The Katie porphyry deposit has numerous similarities to other alkaline porphyry deposits in volcanic arc terranes in the Cordillera (Copper Mountain, Afton, Mount Milligan, Galore Creek); specifically with respect to its Jurassic age, calcalkaline to alkaline hostrocks, potassic and propylitic alteration and relatively high gold and magnetite content.
- The mineralized area lies within a 2 by 8 kilometre, northeast-trending, 250 gamma aeromagnetic anomaly, which probably reflects magnetite-rich intrusive or

volcanic rocks. Exploration for similar deposits in the Rossland Group should focus on coincident magnetic, chargeability, resistivity, copper and gold anomalies, as well as the recognition of characteristic alteration assemblages and synvolcanic gabbro to monzonite intrusions.

ACKNOWLEDGMENTS

The authors would like to thank Paul Wilton and Trygve Höy of the British Columbia Geological Survey Branch for suggesting this study, providing guidance and supervision throughout and for reviewing the manuscript. Ken Murray and the management of Yellowjack Resources Limited contributed confidential information, historical details and allowed access to the drill core. The support of Greg Hawkins of CME Consulting Limited is also acknowledged. The editorial comments of Vic Preto, Brian Grant and John Newell are appreciated.

REFERENCES

- Andrew, K.P.E. and Höy, T. (1989): The Shaft Showing, Elise Formation, Rossland Group; *in* Exploration in British Columbia 1988, *B.C. Ministry of Energy, Mines and Petroleum Resources*, pages B21-28.
- Andrew, K.P.E. and Höy, T. (1990): Geology and Exploration of the Rossland Group in the Swift Creek Area; *in* Exploration in British Columbia 1989, *B.C. Ministry of Energy, Mines and Petroleum Resources*, pages 73-80.
- Andrew, K.P.E., Höy, T. and Simony, P. (1991): Geology of the Trail Map Area, Southeastern British Columbia; *B.C. Ministry of Energy, Mines and Petroleum Resources*, Open File 1991-16.
- Barr, D.A., Fox, P.E., Northcote, K.E. and Preto, V.A. (1976): The Alkaline Suite Porphyry Deposits - A Summary; *in* Porphyry Deposits of the Canadian Cordillera, Sutherland-Brown, A., Editor, *Canadian Institute of Mining and Metallurgy*, Special Volume 15, pages 359-367.
- Corbett, C.R. and Simony, P.S. (1984): The Champion Lake Fault in the Trail-Castlegar Area of Southeastern British Columbia; *in* Current Research, Part A, *Geological Survey of Canada*, Paper 84-1A, pages 103-104.
- Dawson, G.L., Augsten, B.E.K. and Heinrich, S.M. (1989): Great Western Star Gold-Copper Project; *B.C. Ministry of Energy, Mines and Petroleum Resources*, Assessment Report 19503.
- Dunne, K.P.E. and Höy, T. (1992): Petrology of Pre to Syntectonic Early and Middle Jurassic Intrusions in the Rossland Group, Southeastern British Columbia (82F/SW); *in* Geological Fieldwork 1991, Grant, B. and Newell, J.M., Editors, *B.C. Ministry of Energy, Mines and Petroleum Resources*, Paper 1992-1, pages 9-19.
- Frebald, H. and Little, H.W. (1962): Paleontology, Stratigraphy, and Structure of the Jurassic Rocks in Salmo Map-area, British Columbia; *Geological Survey of Canada*, Bulletin 81, 31 pages.
- Frebald, H. and Tipper, H.W. (1970): Status of the Jurassic in Canadian Cordillera of British Columbia, Alberta and Southern Yukon; *Canadian Journal of Earth Sciences*, Volume 7, pages 1-21.
- Getsinger, J.S. (1992): Petrography of Fourteen Samples from the Katie Project; unpublished report for CME Consulting Limited and Yellowjack Resources Limited.

- Höy, T. and Andrew, K.P.E. (1988): Preliminary Geology and Geochemistry of the Elise Formation, Rossland Group, between Nelson and Ymir, Southeastern British Columbia; in *Geological Fieldwork 1987, B.C. Ministry of Energy, Mines and Petroleum Resources*, Paper 1988-1, pages 19-30.
- Höy, T. and Andrew, K.P.E. (1989a): The Rossland Group, Nelson Map Area, Southeastern British Columbia; in *Geological Fieldwork 1988, B.C. Ministry of Energy, Mines and Petroleum Resources*, Paper 1989-1, pages 33-43.
- Höy, T. and Andrew, K.P.E. (1989b): Geology of the Rossland Group, Nelson Map Area, Southeastern, British Columbia; *B.C. Ministry of Energy, Mines and Petroleum Resources*; Open File 1989-1.
- Höy, T. and Andrew, K.P.E. (1989c): The Great Western Group, Elise Formation, Rossland Group; in *Exploration in British Columbia 1988, B.C. Ministry of Energy, Mines and Petroleum Resources*, pages B15-B20.
- Höy, T. and Andrew, K.P.E. (1990a): Structure and Tectonic Setting of the Rossland Group, Mount Kelly - Hellroaring Creek Area, Southeastern British Columbia (82F/3W); in *Geological Fieldwork 1989, B.C. Ministry of Energy, Mines and Petroleum Resources*, Paper 1990-1, pages 11-17.
- Höy, T. and Andrew, K.P.E. (1990b): Geology of the Mount Kelly - Hellroaring Creek Area, Southeastern British Columbia; *B.C. Ministry of Energy, Mines and Petroleum Resources*, Open File 1990-8.
- Kemp, R. (1992): Report of the Drilling Activities carried out on the Katie Group of Claims, Nelson Mining Division, NTS 82F/3; *B.C. Ministry of Energy, Mines and Petroleum Resources*, Assessment Report 22200.
- Little, H.W. (1950): Salmo Map-area, British Columbia; *Geological Survey of Canada*, Paper 50-19, 43 pages.
- Little, H.W. (1960): Nelson Map-area, West-half, British Columbia; *Geological Survey of Canada*, Memoir 308, 205 pages.
- Little, H.W. (1965): Geology, Salmo, British Columbia; *Geological Survey of Canada*, Map 1145A.
- Little, H.W. (1985): Geological Notes, Nelson West Half (82F, W1/2) Map Area; *Geological Survey of Canada*, Open File 1199.
- MacIsaac, B. (1980): Soil Geochemistry Report Jim Group, Nelson Mining Division, 82F 3W; *B.C. Ministry of Energy, Mines and Petroleum Resources*, Assessment Report 82:58.
- McDonald, J.A. (1992): Opaque Mineralogy of 24 samples from the Katie Project; unpublished report for CME Consulting Limited and Yellowjack Resources Limited.
- McIntyre, T.J. (1991): Report on the Drilling Activities carried out on the Katie Group of Claims, Nelson Mining Division, NTS 82F/3; *B.C. Ministry of Energy, Mines and Petroleum Resources*, Assessment Report 21704.
- McIntyre, T.J. and Bradish, L. (1990): Geological and Geochemical Survey on the Katie Group of Claims, Nelson Mining Division, NTS 82F/3; *B.C. Ministry of Energy, Mines and Petroleum Resources*, Assessment Report 203: 1.
- McMillan, W.J. (1991): Porphyry Deposits in the Canadian Cordillera; in *Ore Deposits, Tectonics, and Metallogeny in the Canadian Cordillera*; *B.C. Ministry of Energy, Mines and Petroleum Resources*, Paper 1991-4, pages 25. -276.
- Murray, K. (1987): Soil Geochemistry of the Katie Group Area, Salmo, B.C., NTS 82F/3W; *B.C. Ministry of Energy, Mines and Petroleum Resources*, Assessment Report 15781.
- Parrish, R.R., Carr, S.D. and Parkinson, D.L. (1988): Eocene Extensional Tectonics and Geochronology of the Southern Omineca Belt, British Columbia; *Tectonics*, Volume 7, pages 181-212.
- Ross, K. (1992): Major Lithologies and Alteration Zonation of the Ajax West Pit, an Alkalic Copper-Gold Porphyry Deposit, Kamloops, South-Central British Columbia in *Porphyry Copper-Gold Systems of British Columbia, Annual Technical Report - Year 1, Mineral Deposit Research Unit, The University of British Columbia*, 28 pages.

NOTES

PETROLOGY OF THE EVENING STAR CLAIM, ROSSLAND, B.C. (82F/4)

By P. Stinson and D.R.M. Pattison
University of Calgary

KEYWORDS: Economic geology, Rossland, Evening Star, petrology, skarn, gold, arsenopyrite, paragenesis.

INTRODUCTION

The Rossland mining camp of southeastern British Columbia has been one of the most important gold producers in the province's history. Most of the camp's production was during the period 1895 to 1928, 98 per cent of this from four large, connected mines (Le Roi, Centre Star, Josie, and War Eagle). During this period and for a few years after, minor production was recorded on about 30 other claims.

The Evening Star claim, about 1.5 kilometres northwest of the town of Rossland, has been one focus of renewed exploration in the Rossland camp. A drilling program carried out by Antelope Resources Inc. from 1988 to 1990 has revealed significant gold potential on this claim (approximately 20 000 tonnes averaging 17 grams per tonne gold; Wehrle, 1991). A petrographic study of samples from surface and drill core was undertaken to determine the mineralogy and paragenesis of the deposit, and to compare it to the rest of the Rossland camp.

GEOLOGY OF THE ROSSLAND AREA

The geology of the Rossland area has been well studied due to the importance of its mineral deposits (Figure 2-2-1). Drysdale (1915) described the geology of the camp and the

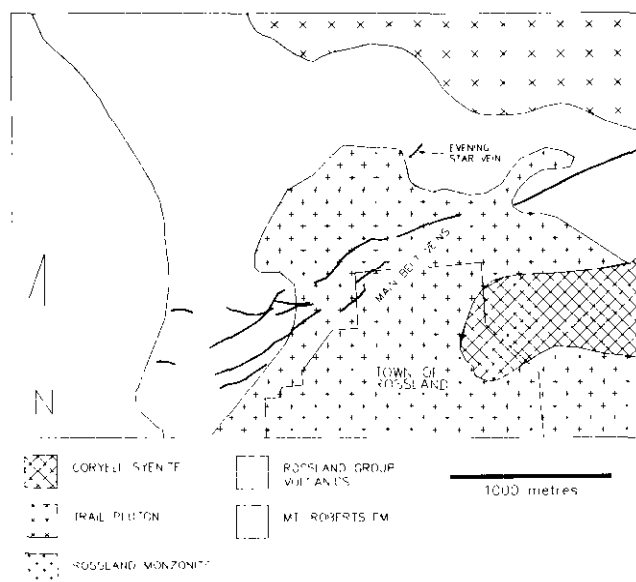


Figure 2-2-1. Schematic geological map of the north part of the Rossland mining camp, showing the location of the Evening Star vein and the main belt veins (after Höy *et al.*, 1992, and Little, 1982).

mineral deposits when the underground mines were active. More recently the geological setting of the camp has been described by Fyles (1984) and Höy *et al.* (1992) and the regional geology by Little (1982). The Rossland area is underlain by late Paleozoic sediments of the Mount Roberts Formation and the Jurassic Rossland Group, comprising volcanics and volcanic sediments. These rocks have been intruded by three distinct igneous suites – the Early Jurassic Rossland monzonite, the Middle Jurassic Trail pluton, and Eocene dikes and stocks, probably related to the large Coryell batholith to the west.

Gold mineralization at Rossland is roughly centred on the Rossland monzonite and is mainly hosted by Rossland Group metavolcanics and metasediments, which are possibly comagmatic with the monzonite (Höy *et al.*, 1992). The camp has traditionally been divided into three belts based on the structural trends of the mineralized fractures. The main belt contains all the large producers and runs east-northeast across the north side of the monzonite. The north belt, containing the Evening Star claim, appears to be a northeast splay of the main belt. The south belt parallels the southern margin of the monzonite. The Crown Point deposit within this belt was recently described by Wilson *et al.* (1990).

Thorpe (1967) proposed a mineralogical zonation of the Rossland camp based on ore petrology and copper, silver and gold ratios of the ores. He divided it into central, intermediate and outer zones centred on the Le Roi - Centre Star main vein. The central zone ores are mostly massive pyrrhotite and chalcopyrite. The intermediate zone is characterized by arsenopyrite and pyrite, and the outer zone by galena, tetrahedrite and sphalerite. Thorpe placed the Evening Star deposit in the intermediate zone based on two samples taken from the old workings.

EVENING STAR CLAIM

The Evening Star deposit (Figure 2-2-2), located on the north belt, saw minor production from 1896 to 1907 and from 1932 to 1939. Total output was 56.7 kilograms of gold, 21.5 kilograms of silver and 1276 kilograms of copper from 2859 tonnes of ore (Fyles, 1984). Production was mainly from shallow surface workings following a strong mineralized trend across the claim, representing the surface expression of a steeply dipping tabular ore body near the contact of the Rossland monzonite. The ore is crosscut by several north-striking porphyritic syenite dikes which are probably Eocene.

The ore is hosted by strongly altered Rossland Group volcanics. The main alteration types include silicification, local formation of andraditic garnet, diopside and epidote (skarn), and patchy amphibole-chlorite-calcite alteration. Early sulphide mineralization appears to have been spatially associated with the skarn alteration. The genetic association

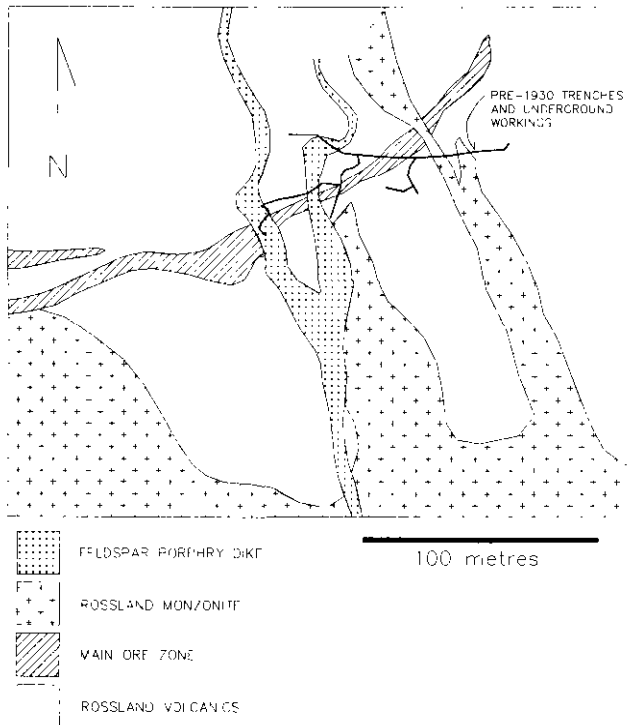


Figure 2-2 2. Map of the Evening Star deposit. Mineralization dips steeply to the north (from Wehrle, 1991).

between the ore and the contact metasomatism associated with the Rossland monzonite has only been recognized recently in this camp (Wilson *et al.*, 1990), and its overall significance is not yet well understood.

PETROLOGY

METAMORPHIC HOSTROCKS

The Evening Star deposit is hosted by contact metamorphosed and hydrothermally altered Jurassic volcanic sediments. There is a general gradation in mineral assemblages outward from the contact of the monzonite across the tabular orebody.

Pockets of garnetiferous skarn, the highest metamorphic grade observed, occur locally in the ore zone within 10 metres of the igneous contact. These exhibit a coarse-grained skarn assemblage of andraditic garnet, diopside and plagioclase, which in turn is overprinted by hornblende along growth zones in garnet (Plate 2-2-1), and by quartz, calcite and zeolites. Minor arsenopyrite and pyrite are disseminated in this rock, and chalcopyrite and pyrrhotite are mainly confined to late quartz-carbonate veins.

Farther out from the monzonite contact (20 to 40 m) pockets of lower grade skarn are found within the hydrothermally altered country rock. The skarn consists of diopside and plagioclase, overprinted by actinolite and later epidote and clinozoisite. Minor minerals present include sphene, apatite, sericite and tourmaline. These assemblages



Plate 2-2-1. Hornblende alteration (dark) of garnet (light) along growth zones. Both minerals are cut by pyrrhotite-bearing calcite veins. Transmitted light, width of photo 2 mm.

are cut by carbonate and quartz-carbonate veins. In the ore zone arsenopyrite, pyrrhotite, chalcopyrite and other opaque minerals are disseminated in highly variable amounts.

Still farther out from the monzonite (40+ m) the volcanics are dominantly fine grained and strongly silicified. These are cut by veins of diopside, wollastonite and/or actinolitic amphibole, 0.5 to 5 millimetre wide, which are partly replaced by calcite. Some actinolite veins contain arsenopyrite along their margins, suggesting it might have been formed at the same time as the actinolite alteration. Pyrrhotite is present in the veins as a replacement of arsenopyrite and actinolite (Plate 2-2-2).

These assemblages are crudely arranged outward from the Rosslund monzonite, in a similar fashion to skarn zones in the Hedley district as described by Ray *et al.* (1987). This marked spatial association with the monzonite provides evidence in favour of it being the source of heat and possibly mineralizing fluids for the Evening Star deposit.

ORE PETROLOGY

The ore assemblages consist of variable proportions of a few common minerals. There appear to be two main stages of sulphide mineralization. The first is characterized by pyrite, arsenopyrite and gold; the second by chalcopyrite

and pyrrhotite. Locally magnetite is a late replacement of the sulphide phases, and hematite and marcasite are present as minor alteration products.

Arsenopyrite and pyrite occur mainly as fine to coarse-grained subhedral crystals and crystal aggregates in the silicate host and in zones of massive pyrrhotite. Early formation of arsenopyrite and pyrite relative to pyrrhotite and chalcopyrite is indicated by several textures. Blebs of optically continuous arsenopyrite often occur within massive pyrrhotite. Grains of pyrite and arsenopyrite are commonly traversed by irregular veinlets of pyrrhotite and chalcopyrite with irregular or cusped walls (Plate 2-2-2). Textures between arsenopyrite and pyrite are equivocal, possibly indicating that they are contemporaneous.

Gold appears to be related to the earlier arsenopyrite-pyrite stage. There is a strong correlation of high gold values with high arsenic contents (Wehrle, 1991). It generally occurs as small (10-40 μm) subhedral grains in arsenopyrite, or disseminated with it in the silicate host. This strong association suggests that gold precipitated at the same time as arsenopyrite, either as free gold or in solid solution with it.

Locally, gold visible within arsenopyrite grains forms small subparallel elongate blebs which might be indicative

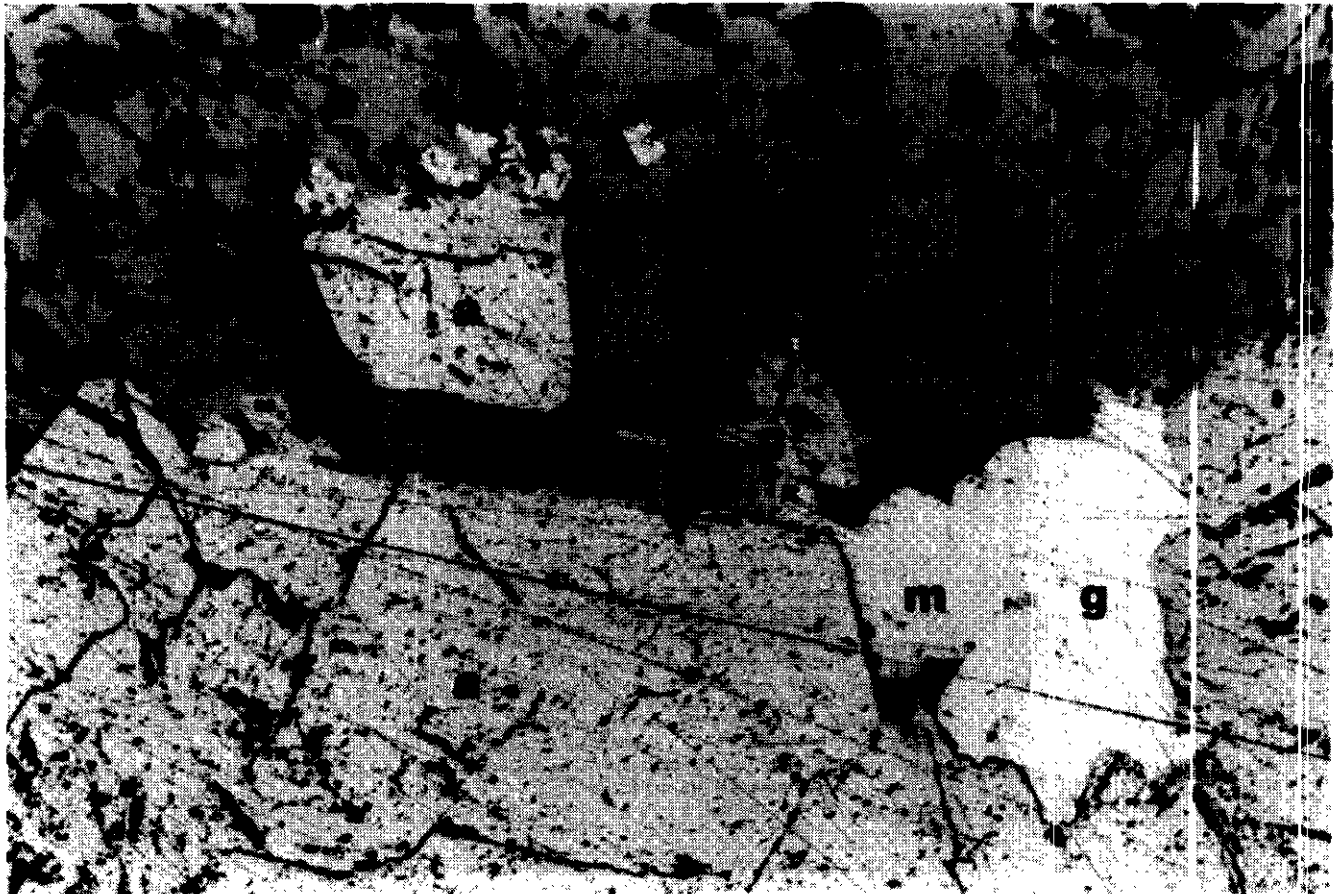


Plate 2-2-2. Pyrrhotite (top, dark grey) replacing gold-bearing arsenopyrite (bottom, light grey) along an irregular contact. The cavity in arsenopyrite near the interface contains gold (g) intergrown with maldonite (m). Arsenopyrite and gold (small arrow, right of centre) are contained in pyrrhotite. Reflected light, width of photo 400 microns.

of exsolution. In one instance native gold is intergrown with a mineral which preliminary microprobe work indicates is maldonite, Au_2Bi (Plate 2-2-2).

The second mineralizing episode is represented by deposition of pyrrhotite and chalcopyrite. These minerals occur in three associations: in quartz-carbonate veins; as coarse disseminations in the metamorphic host; and as large massive sulphide veins. Pyrrhotite and chalcopyrite generally appear to envelope or replace the earlier arsenopyrite-pyrite-gold assemblage. Textures between chalcopyrite and pyrrhotite are inconsistent, suggesting generally coeval formation.

Rarely, native gold occurs in chalcopyrite veins cutting arsenopyrite (Plate 2-2-3). Although this could represent a second influx of gold it may also be the result of local remobilization. Cook and Chryssoullis (1990) indicate that, in general, arsenopyrite can carry significantly more gold in solid solution than chalcopyrite (by several orders of magnitude). In this case, significant replacement of auriferous arsenopyrite could result in the solid solution gold being reprecipitated with the chalcopyrite as visible gold.

Several other late phases are locally present. In places magnetite forms a massive replacement of the sulphide minerals. Hematite is a minor replacement of all the other opaque minerals in surface grab samples, and marcasite is a local alteration product of pyrite.

LINK BETWEEN SKARN AND SULPHIDE MINERALIZATION

The relationships between the sulphide minerals and the host rock alteration are important in determining the origin of this deposit. The occurrence of arsenopyrite along the margins of actinolite-rich veins suggests it was deposited during the initial stages of vein opening, followed by further deposition of actinolite and calcite during continued vein widening. Pyrrhotite and calcite also occur in these veins as partial replacements of arsenopyrite and actinolite (Plate 2-2-4). Late quartz-carbonate veins which crosscut garnetiferous skarn contain chalcopyrite and pyrrhotite. Mineral relationships indicate that arsenopyrite and pyrite are probably contemporaneous with actinolite and epidote alteration and that pyrrhotite and chalcopyrite are later and might be synchronous with quartz-carbonate alteration and veining. The overall paragenetic interpretation of the alteration types and mineralization is presented in Figure 2-2-3.

CONCLUSIONS AND DISCUSSION

Gold-bearing sulphide mineralization occurred in two main stages in the Evening Star deposit. The first resulted in deposition of pyrite, arsenopyrite and gold. The second consisted of partial replacement of these phases by pyr-

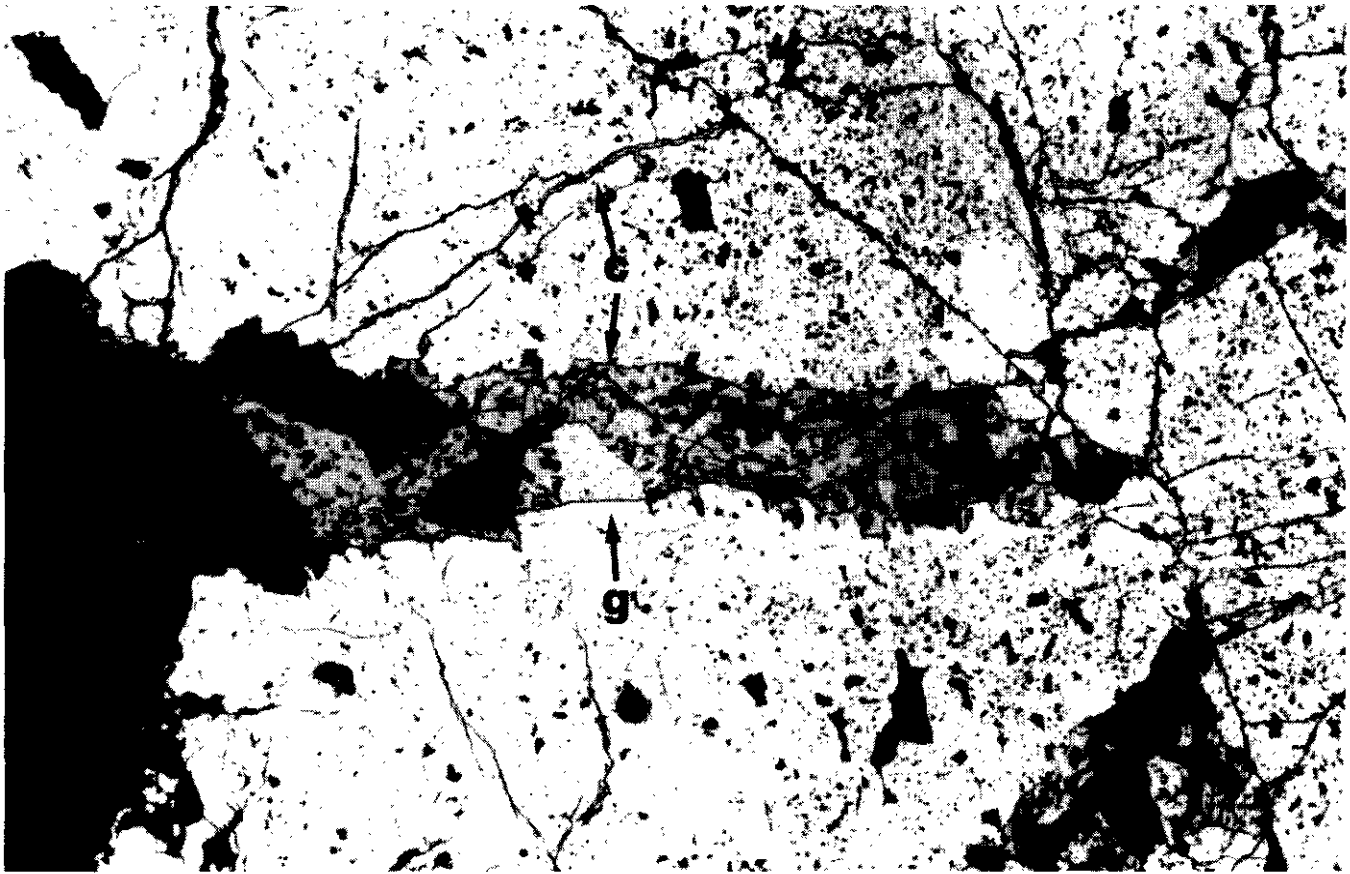


Plate 2-2-3. Chalcopyrite veins (c) cutting arsenopyrite. A large bleb of gold (g) is contained in the larger vein. Reflected light, width of photo approximately 2.5 mm.



Plate 2-2-4. Actinolite replaced by pyrrhotite (bright white) along cleavage. Reflected light, width of photo 2 mm.

Mineral	Prograde Skarn	Retrograde skarn/veins	Early Mineralization	Later Mineralization and Alteration
Garnet	—			
Diopside	—			
Plag.	—			
Amph.		—		
Epidote		—		
Quartz			—	—
Calcite			— ?	
Pyrite			—	
Arsenopyrite			—	
Gold			—	
Pyrrhotite				—
Chalcopyrite				—
Magnetite				—
Hematite				—

Figure 2-2-3. Paragenetic diagram for the Evening Star deposit.

pyrrhotite and chalcopyrite, possibly with some reprecipitation of gold.

One conspicuous aspect of the Evening Star deposit is the strong association of gold with arsenopyrite. Although this association is well known from many gold camps, previous work at Rosslund has mainly suggested a gold-chalcopyrite

association. Thorpe (1967) concluded from work mainly in the central zone that much of the Rosslund gold was in solid solution with chalcopyrite. However, recent microanalytical work from a variety of gold deposits (Cook and Chryssoulis, 1990) has shown that, in general, chalcopyrite and pyrrhotite are limited in their ability to carry gold in solid solution (maximum about 7 ppm) compared to arsenopyrite.

The gold-arsenopyrite mineralization is contemporaneous with the formation of retrograde skarn assemblages in the aureole of the Rosslund monzonite, and consequently may be temporally and genetically related to it. This is consistent with recent work on the Rosslund camp pointing to a genetic link between the gold ores and the monzonite, rather than with the later intrusions or large-scale regional structures (Höy *et al.*, 1992; Thorpe, 1967).

ACKNOWLEDGMENTS

The authors would like to thank D. Wehrle and F. Fowler for providing field trips, samples and information over the last several years. This study was a graduate student project at the University of Calgary. Research was funded by National Science and Engineering Research Council Operating Grant 0037233 to D.R.M. Pattison. Thanks are also due to J.M. Newell for a constructive review.

REFERENCES

- Cook, N.J. and Chryssoulis, S.L. (1990): Concentrations of "Invisible Gold" in the Common Sulphide Minerals; *Canadian Mineralogist*, Volume 28, pages 1-16.
- Drysdale, C.W. (1915): Geology and Ore Deposits of Rossland, British Columbia; *Geological Survey of Canada*, Memoir 77.
- Fyles, J.T. (1984): Geological Setting of the Rossland Mining Camp; *B.C. Ministry of Energy, Mines and Petroleum Resources*, Bulletin 74.
- Höy, T., Dunne, K.P.E. and Werhle, D. (1992): Tectonic and Stratigraphic Controls of Gold-Copper Mineralization in the Rossland Camp, Southeastern British Columbia; in *Geological Fieldwork 1991*, Grant, B. and Newell, J.M., Editors, *B.C. Ministry of Energy, Mines and Petroleum Resources*, Paper 1992-1, pages 261-272.
- Little, H.W. (1982): Geology of the Rossland-Trail Map-area, British Columbia; *Geological Survey of Canada*, Paper 79-26.
- Ray, G.E., Dawson, G.L. and Simpson, R. (1987): The Geology and Controls of Skarn Mineralization in the Hedley Camp, Southern British Columbia; in *Geological Fieldwork 1986*, *B.C. Ministry of Energy, Mines and Petroleum Resources*, Paper 1987-1, pages 65-79.
- Thorpe, R.I. (1967): Mineralogy and Zoning of the Rossland Area; unpublished Ph.D. thesis; *University of Wisconsin*.
- Wehrle, D.M. (1991): Recent Development on the North Belt Property, Rossland, B.C.; internal report for *Vangold Resources, Inc.*
- Wilson, G.C., Rucklidge, J.C. and Kilius, L.R. (1990): Sulphide Gold Content of Skarn Mineralization at Rossland, British Columbia; *Economic Geology*, Volume 85, pages 1252-1259.



MINERAL CHEMISTRY OF SOME METAMORPHOSED SHUSWAP-AREA MINERAL DEPOSITS (82L,M)

By Paul R. Bartholomew
Yale University

KEYWORDS: Economic geology, Shuswap deposits, Cottonbelt, CK, Goldstream, Big Ledge, mineralogy, geobarometry, mineral chemistry.

INTRODUCTION

This paper is an initial report on the mineral chemistry of four metamorphosed stratabound mineral deposits which are located within or adjacent to the Shuswap Complex. These are commonly referred to as Cottonbelt, CK, Goldstream and Big Ledge deposits. Rock specimens were selected from those collected by Trygve Höy of the British Columbia Geological Survey Branch. The particular specimens chosen were not selected specifically to be representative of each deposit as a whole but rather as examples of the assemblage sphalerite-pyrrhotite-pyrite, in order to test the proposed sphalerite geospeedometer (Bartholomew and Lasaga, 1992). However, since very few data on the chemistry of minerals within these deposits has previously been reported, this paper was written in order to begin to correct this deficiency. After reviewing the mineralogy of each of the selected specimens, one was chosen from each deposit for analysis. Only these four specimens are described here.

GEOLOGIC SETTING

The four deposits covered by this report are all located in southeastern British Columbia (Figure 2-3-1). All four are

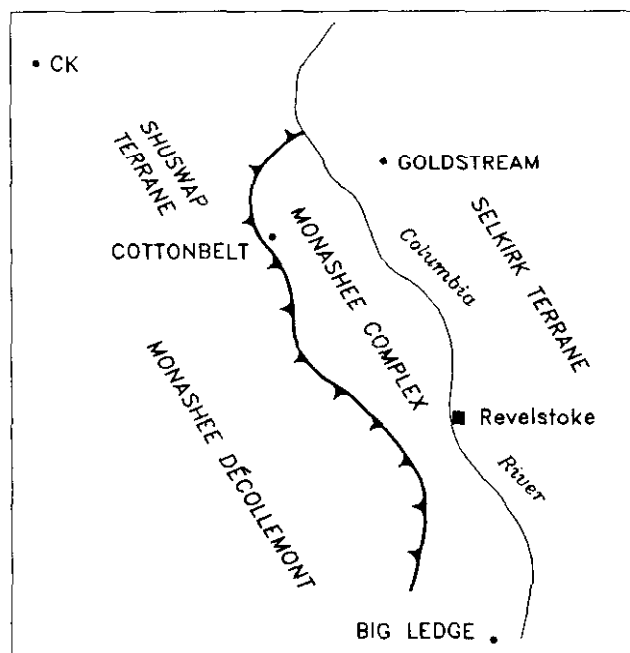


Figure 2-3-1. Sketch map showing the location of the four deposits.

interpreted to be of syngenetic exhalative origin (Höy *et al.*, 1984; Höy, 1987). They are all stratabound and exhibit structures and textures indicative that mineralization pre-dates regional deformation and metamorphism and, most likely, was syngenetic with the enclosing sediments. Three of the deposits, Cottonbelt, Big Ledge and CK, are lead-zinc deposits situated within the Shuswap Complex. Cottonbelt and Big Ledge are within the Monashee Complex which is bounded by the Columbia River fault on the east and the Monashee décollement on the west. The CK deposit is in the Shuswap Terrane to the west and north of the Monashee Complex. Goldstream is a copper-zinc deposit in the Selkirk Terrane on the east side of the Columbia River fault.

Big Ledge and Cottonbelt are both hosted by strongly deformed and metamorphosed sedimentary and volcanic rocks which conformably overlie Precambrian basement gneisses which core the Monashee Complex (Höy, 1977, 1987). Their age is not known with certainty, however Pb-Pb dating of the Cottonbelt deposit suggests a Cambrian age (Höy and Godwin, 1987). Both of these deposits have experienced upper amphibolite grade metamorphism. Each lies within a metasedimentary sequence which includes quartzites, pelitic schists, calcareous gneisses and marbles. Big Ledge is a massive sulphide deposit, dominated by sphalerite, in calcareous, graphitic schists. Cottonbelt is a sulphide-magnetite deposit in a calcareous gneiss succession.

The CK showings are also hosted by calcareous gneisses (Höy, 1979, 1987). However, this deposit is hosted by younger allochthonous rocks of the Shuswap Terrane which structurally overlie the Monashee Complex. Here the calcareous hostrock succession is underlain by metavolcanic hornblende gneisses and amphibolites. The grade of metamorphism which the CK deposit has been subjected to is broadly amphibolite facies.

The Goldstream deposit and other copper-zinc deposits in the Goldstream area are interpreted to be volcanic exhalative in origin due to a close association with basic metavolcanic rocks (Höy *et al.*, 1984). At Goldstream, a massive sulphide layer is hosted by chloritic phyllite in a metasedimentary sequence which includes chloritic and sericitic phyllites, carbonaceous phyllites and limestones. The metamorphic grade is greenschist facies.

METHODS

Polished thin sections were examined optically and with a JEOL JXA-8600 electron microprobe. Under the microprobe, backscattered electron (BSE) imaging was used in combination with energy-dispersive x-ray spectrometry in order to corroborate optical mineral identification and to identify mineral grains too small to be identified optically. Wavelength-dispersive x-ray spectrometry was used for quantitative analysis.

MINERALOGY AND MINERAL CHEMISTRY

GOLDSTREAM

The specimen from the Goldstream deposit is designated GS-Ha. Its mineralogy includes actinolite, calcite, quartz, pyrrhotite, chalcopyrite, sphalerite, galena, biotite, muscovite and traces of silver and bismuth tellurides. The tellurides are only found intergrown with galena. Chemical analyses show that the amphibole is 80 to 90 mole per cent tremolite and slightly aluminous. The calcite contains minor amounts of manganese, magnesium and iron, the sphalerite contains 16 mole per cent iron and 1 mole per cent manganese, the biotite is phlogopitic containing 16 mole per cent annite, 15 mole per cent of the hydroxyl in the biotite is replaced by fluorine, and the galena contains 5 weight per cent selenium. The amphibole is zoned with grain cores slightly higher in aluminum and iron.

CK

The specimen from the CK deposit which was examined is designated CK-H67. Its mineralogy includes sphalerite, pyrrhotite, galena, potassium feldspar, plagioclase, quartz, biotite and both sphene and rutile. Chemical analyses reveal that the sphalerite contains 18 to 21 mole per cent iron; the plagioclase is An₄₉; the potassium feldspar is a hyalophane containing 11 mole per cent albite and 9 mole per cent celsian. The biotite is titanian containing 35 mole per cent annite, 3 mole per cent replacement of potassium by barium and 25 per cent replacement of hydroxyl by fluorine.

BIG LEDGE

The specimen from the Big Ledge deposit is designated BL-H555. Its mineralogy includes pyrrhotite, sphalerite, pyrite, galena, diopside, tremolite, calcite, potassium feldspar, phlogopite, chlorite, sphene, apatite and graphite. Chemical analyses show that the sphalerite contains 16 mole per cent iron; the diopside, tremolite and phlogopite are highly magnesian, being 95 to 98 mole per cent of their magnesium end-members. Phlogopite has 3 per cent replacement of potassium by barium and 50 per cent replacement of hydroxyl by fluorine. Calcite is nearly pure, and the potassium feldspar is hyalophane containing 3 per cent albite and 5 to 17 mole per cent celsian.

The hyalophane grains are, in fact, distinctly zoned with respect to the barium content (Plate 2-3-1). This zoning has a recognizable sequence beginning with a discrete high-barium phase which is overgrown by a phase distinctly lower in barium. Further feldspar growth resulted in continuous gradational zoning increasing in barium content. This phase is locally overgrown by a phase distinctly lower in barium. A late, high-barium phase is also present locally with some fracture control on its distribution.

COTTONBELT

The specimen from the Cottonbelt deposit is designated CB-H12. Its mineralogy includes magnetite, sphalerite, pyr-

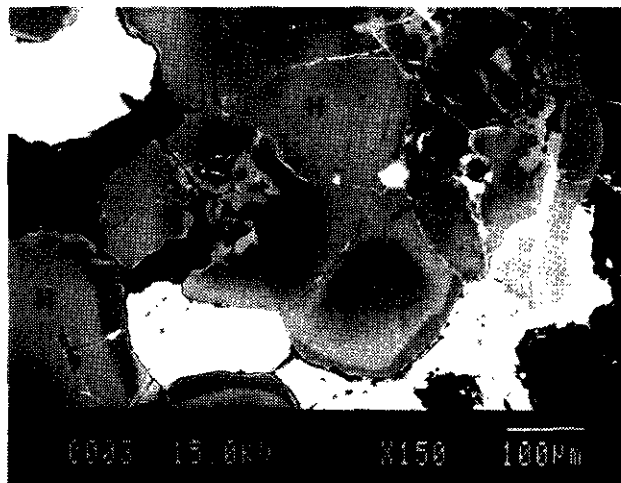


Plate 2-3-1. BSE photograph of hyalophane grains (H) from specimen BL-H555. The brighter regions of the hyalophane are relatively rich in barium.

rotite, galena, olivine, biotite, rhodochrosite, kutnohorite, apatite and graphite. Chemical analyses confirm the high abundance of manganese in gangue minerals reported by Höy (1987) and reveal a significant manganese content in the ore minerals as well. These analyses show that the sphalerite contains 24 to 27 mole per cent iron and 5 per cent manganese, the olivine is 50 per cent fayalite, 30 per cent tephroite and 25 per cent forsterite, and the biotite is 35 per cent annite with 8 per cent of the hydroxyl replaced by fluorine and 1.5 per cent of the hydroxyl replaced by chlorine.

The carbonates exhibit a distinct zoning sequence with textures indicative that the latest generations formed by infilling small open spaces (Plate 2-3-2). The most voluminous phase is a manganese-rich dolomitic carbonate (kutnohorite) which is approximately 50 mole per cent kutnohorite, 30 per cent dolomite and 20 per cent ankerite.

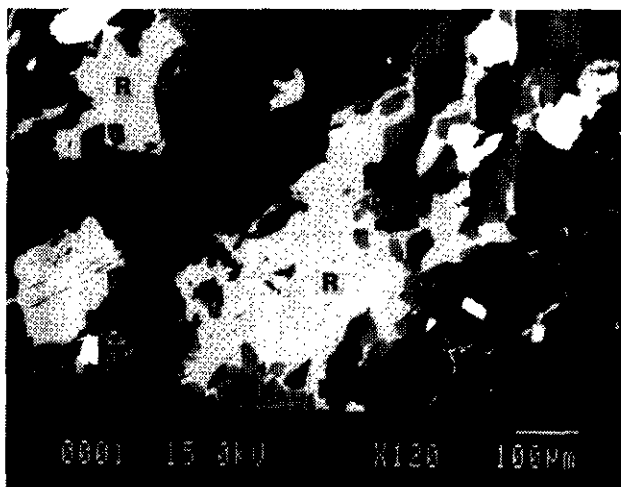


Plate 2-3-2. BSE photograph showing manganese carbonate zoning in specimen CB-H12. Indicated are early kutnohorite (EK), late kutnohorite (LK) and rhodochrosite (R).

Near the centre of areas filled with carbonate this intermediate kutnohorite generally has regular terminations and is overgrown with small amounts of a distinct high-manganese kutnohorite (90% kutnohorite) phase which also has crystal-face type terminations. The small remaining central volume is filled with a high-manganese rhodochrosite (80 to 90% rhodochrosite).

The magnetites have an exsolution texture, undoubtedly a response to solubility shifts during cooling from the maximum metamorphic temperature (650°-700°C, Höy, 1987). The exsolved phase is an aluminous spinel containing 48 mole per cent gahnite, 32 per cent hercynite, 12 per cent spinel ($MgAl_2O_4$) and 8 per cent galaxite ($MnAl_2O_4$). Very small grains of this spinel speckle the interior of magnetite grains (Plate 2-3-3). However, within about 20 micrometres of grain edges the magnetite is free of spinel inclusions. The identification of aluminous spinel grains along these grain boundaries (intergrown with the surrounding phases) indicates that within this edge region the spinel components have migrated to the grain boundary rather than nucleating within the magnetite. The magnetite itself contains almost 3 weight per cent MnO.

DISCUSSION

Although it is beyond the scope of this report to extensively discuss any implications of the mineral chemistry described above, there are several features worthy of note: the selenium content of the Goldstream galena, the manganese content of the Cottonbelt specimen, the fluorine content of the biotites, the occurrence of hyalophane, the preservation of compositional zoning in the Big Ledge and Cottonbelt specimens, and the implications of the buffered sphalerite composition in the Big Ledge specimen.

The high manganese content of the Cottonbelt specimen is reflected in the chemistry of nearly all minerals which are known to take up manganese; even the magnetite and the sphalerite contain significant amounts.

Feldspars containing essential barium, such as at the Big Ledge deposit, occur exclusively in mineral deposit settings, especially metamorphosed mineral deposits (Deer *et al.*, 1966).

Despite the high metamorphic temperatures experienced by the specimens from Cottonbelt and Big Ledge, compositional zoning in the carbonate, kutnohorite (CB-H12), and the potassium feldspar, hyalophane (BL-H555), have not been significantly modified by diffusion. Growth zoning features in both of these minerals are locally sharply defined implying that diffusion of the zoned components (Mn in kutnohorite and Ba in hyalophane) is relatively slow.

The specimen from Big Ledge contains the assemblage necessary for pressure-sensitive buffering the composition of sphalerite – the sphalerite geobarometer (sphalerite + pyrrhotite + pyrite). Assuming that the peak metamorphic temperature experienced at Big Ledge was similar to that at Cottonbelt (650°-700°C, Höy, 1987) the 16 mole per cent FeS in the sphalerite in BL-H555 implies a forma-

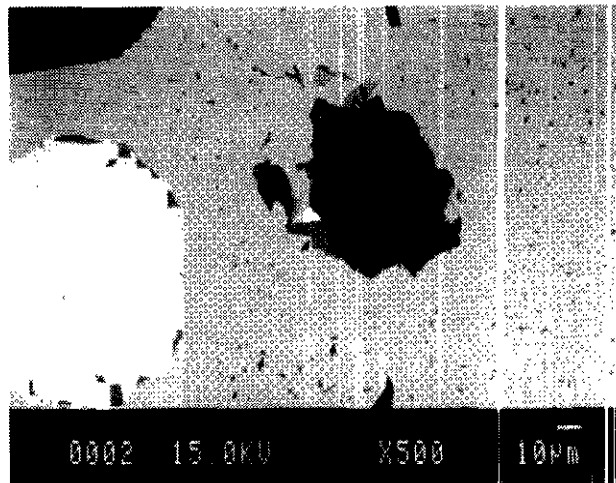


Plate 2-3-3. BSE photograph showing spinel exsolution textures in magnetite in specimen CB-H 2.

tional pressure less than 40 megapascals (4 kilobars) whether the thermodynamic calibration or the experimental calibration is used (Toulmin *et al.*, 1991). This is in distinct contrast with the 70 megapascals (7 kilobars) peak metamorphic pressure estimated for the Cottonbelt region and may imply significant resetting of the sphalerite composition during cooling.

REFERENCES

- Bartholomew, P.R. and Lasaga, A.C. (1992): Sphalerite Geospeedometry; *Geological Society of America, Abstracts with Programs*, Volume 24:7, page A218.
- Deer, W.A., Howie, R.A. and Zussman, J. (1966): *An Introduction to the Rock Forming Minerals*, Longman, London, 528 pages.
- Höy, T. (1977): Big Ledge (82L/8E); in *Geology in British Columbia 1975*, B.C. Ministry of Energy, Mines and Petroleum Resources, pages G12-G18.
- Höy, T. (1979): CK Prospect, Shuswap Metamorphic Complex; in *Geological Fieldwork 1978*, B.C. Ministry of Energy, Mines and Petroleum Resources, Paper 1979-1, pages 23-27.
- Höy, T. (1987): Geology of the Cottonbelt Lead-Zinc-Magnetite Layer, Carbonatites and Alkaline Rocks in the Mount Grace Area, Frenchman Cap Dome, Southeastern British Columbia; B.C. Ministry of Energy, Mines and Petroleum Resources Bulletin 80, 99 pages.
- Höy, T. and Godwin, C.I. (1987): Significance of a Cambrian Date from Galena Lead-Isotope Data for the Stratiform Cottonbelt Deposit in the Monashee Complex, Southeastern British Columbia; *Canadian Journal of Earth Sciences*, Volume 25, pages 1534-1541.
- Höy, T., Gibson, G. and Berg, N.W. (1984): Copper-Zinc Deposits, Associated with Basic Volcanism, Goldstream Area, Southeastern British Columbia; *Economic Geology*, Volume 70, pages 789-814.
- Toulmin, P. III, Barton, P.B. Jr. and Wiggins, L.B. (1991): Commentary on the Sphalerite Geobarometer; *American Mineralogist*, Volume 76, pages 1038-1051.

NOTES



GEOLOGY, GEOCHEMISTRY, HYDROTHERMAL ALTERATION AND MINERALIZATION IN THE VIRGINIA ZONE, COPPER MOUNTAIN COPPER-GOLD CAMP, PRINCETON, BRITISH COLUMBIA (92H/7)

By Clifford R. Stanley and James R. Lang,
Mineral Deposit Research Unit, U.B.C.

(MDRU Contribution 024)

KEYWORDS: Economic geology, Copper Mountain, Princeton, Quesnellia, porphyry, copper, gold, veins, magnetite, hematite, albite, potassic, propylitic.

INTRODUCTION

The Virginia zone is one of several copper-gold mineralized zones in the Copper Mountain camp, located 15 kilometres south of Princeton, British Columbia. Reserves consist of 4.5 million tonnes grading 0.39 per cent copper (Tim Carew, personal communication, 1992) and approximately 0.17 gram gold and 1.49 grams silver per tonne (calculated from median Cu/Au and Cu/Ag ratios in samples within the deposit). This zone has special interest because it contains higher gold grades than other previously or currently mined zones in the camp and because it is in the initial stage of production. As a result, there is currently an opportunity to document the geology of this zone more fully, and to use this information to understand the genetic controls on copper and gold deposition.

This report presents the results of surface geological mapping, drill-core logging of lithologies, vein types and alteration, and statistical analysis of a 30-element lithogeochemical database from the Virginia zone. These data and subsequent analytical research will be used to determine the ore controls within the Virginia zone. They should also provide broader insight into the genetic controls on other deposits in the Copper Mountain camp.

GENERAL GEOLOGY

Detailed descriptions of the regional setting and local geology of the Copper Mountain camp are presented by Takeda (1976), Preto (1972), and Fahrni *et al.* (1976). The discussion that follows summarizes these descriptions and new observations made during 1992. A generalized geological map of the Copper Mountain camp is presented in Figure 2-4-1.

Volcanic rocks of the Nicola Group are exposed in a northwesterly oriented belt 1100 metres wide by 4300 metres long that is bounded by several large intrusive bodies. Rock types within the Nicola Group include coarse agglomerates, tuff breccia, tuff, massive flows and minor sedimentary units. Compositions of the volcanic rocks in this belt range from basalt to rhyolite.

To the south the Nicola Group is intruded by the Copper Mountain stock, a large, concentrically zoned pluton that grades from a chilled margin of diorite into monzodiorite, monzonite and ultimately into syenite and pegmatitic per-

thosite in its core. The Smelter Lake and Voigt stocks, and the Lost Horse complex lie to the north of the belt of Nicola Group rocks. The Voigt and Smelter Lake stocks are not compositionally zoned, but have an overall composition that is similar to the marginal diorite phase of the Copper Mountain stock.

The Lost Horse complex is a composite body of dikes that range in composition from diorite to monzonite. Two principal phases of the complex have been recognized. The LH1 phase is a set of equigranular diorite dikes that comprise most of the volume of the complex. The LH2 phase represents a later intrusive episode characterized by diorite to monzonite dikes with subporphyritic to strongly porphyritic textures. Both phases of dikes dip steeply and strike roughly east.

All volcanic rocks and large intrusions within the Copper Mountain camp yield Late Triassic to Early Jurassic K-Ar radiometric dates (Preto, 1972). A group of post-mineral felsite dikes which cut the entire system along a general northerly orientation are, however, probably Cretaceous or Tertiary in age.

MINERALIZATION

Copper-gold mineralization occurs predominantly as chalcopyrite, with or without, bornite in veins, both within the Nicola volcanic rocks and at the contact of the Nicola Group with the bordering intrusions (Figure 2-4-1). The major ore zones, from west to east, are the Ingerbelle, Pit 1, Pit 2, Pit 3 and Virginia deposits. Sub-economic mineralization occurs farther to the east in the Voigt zone and the economic potential of several other areas (Orrole, Alabama and Mill zones) is currently being assessed. The intensity of copper mineralization within the Nicola volcanic belt diminishes to the east as the distance between the Copper Mountain stock and Lost Horse complex increases. The Copper Mountain stock is not mineralized beyond its outer few metres and apparently formed a barrier to the migration of hydrothermal fluids (Fahrni *et al.*, 1976).

The Virginia zone is located in the northeastern sector of the camp, near the contact of the Lost Horse complex and the Nicola Group (Figure 2-4-1). Ore in the Virginia zone is hosted primarily by the LH1 phase of the Lost Horse complex, with lesser volumes in the Nicola Group and the LH2 phase. The Virginia zone orebody is composed of a variety of different crosscutting and closely spaced chalcopyrite veins with orientations strongly influenced by east-trending structures. Copper, gold and silver grades in the Nicola

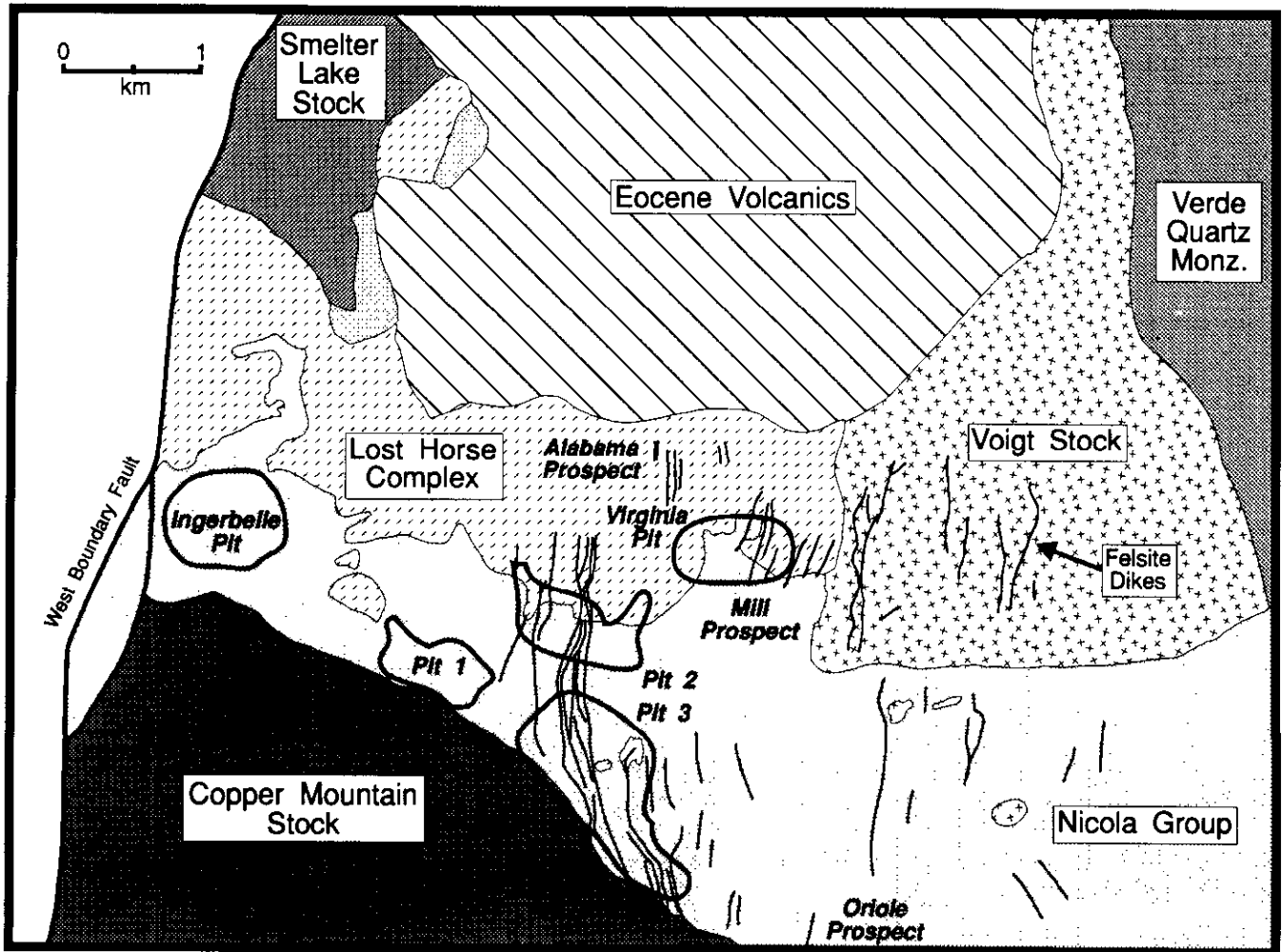


Figure 2-4-1. Simplified geology and the location of mineral deposits and prospects in the Copper Mountain Camp (modified after Preto, 1972).

Group and the LH1 phase are similar but are higher, on average, than grades in the LH2 phase (Stanley, 1992). The LH1 dikes are thought to be pre-mineral intrusions whereas the LH2 dikes have been interpreted by Huyck (1986, 1990, 1991) as syn-mineral intrusions which may be related to mineralization. However, field data also suggest that at least some of the LH2 dikes are post-mineral and intruded along the same structures that host vein mineralization (Stanley, 1992).

OPEN PIT GEOLOGY

During 1992, the three benches comprising the Virginia zone open pit were mapped at 1:200 scale (Figure 2-4-2). Data were collected from traverses of the pit walls and from drill-core logs at depths corresponding to the elevation of the pit floor. Three general rock types occur within the open pit. These consist of steeply dipping, easterly striking volcanic flows and tuffs of the Nicola Group which were intruded by a steeply dipping, easterly striking diorite dike swarm of the Lost Horse complex. These rocks were subsequently intruded by steeply dipping, northerly striking, post-mineral felsite dikes.

The Nicola volcanic rocks consist of light-coloured, very fine grained felsic (cherty) ash tuffs and massive, dark green to black mafic flows. These rocks now exist as screens up to 100 metres thick between thick sections of Lost Horse dikes that are composed of multiple cooling units which range from 2 to 15 metres thick. The dikes probably intruded parallel to and along contacts between and within the volcanic rocks and earlier dikes. The Lost Horse dikes can be subdivided into a number of petrologically distinct varieties that are distinguished by the presence and size distribution of plagioclase, augite and biotite phenocrysts. Whereas only four Lost Horse dike varieties are observed in the Virginia open pit, at least seven different varieties have been mapped in the Lost Horse complex. The diorite dikes are equigranular to subporphyritic with very fine to medium-grained textures, and contain numerous xenoliths of both Nicola mafic volcanic rocks and earlier Lost Horse dikes. Subporphyritic varieties exhibit both hiatal and seriate grain size distributions.

Within the Virginia open pit, a general chronology of dike emplacement can be determined using contact and crosscutting relationships, types of contained xenoliths, degree and

type of hydrothermal alteration, and degree and type of veining. Earliest to intrude were the LH1 diorite dikes of the equigranular phase. These comprise roughly 65 per cent of the volume of the Lost Horse complex within the pit. They were followed by the intrusion of biotite-phyric, plagioclase-phyric and plagioclase-biotite-phyric subporphyritic diorite dikes of the LH2 phase. These later dikes comprise approximately 20, 10 and 5 per cent of the intrusive volume, respectively. The emplacement of these later dikes probably overlapped significantly in time.

From south to north across the open pit, there appears to be a general increase in grain size and thickness of each Lost Horse dike phase, and a decrease in the width and textural contrast of chilled margins in the equigranular diorite dikes. Furthermore, the LH1 dikes usually have more distinct chilled margins than the LH2 dikes.

The textural variations within the open pit indicate that the Virginia zone is located at the southern margin of the Lost Horse complex (Figure 2-4-1). Furthermore, the emplacement of early Lost Horse dikes into relatively cool country rocks north of the zone probably introduced suffi-

cient heat to cause later Lost Horse dikes to exhibit limited chilled margin development due to emplacement into a relatively hotter environment. The textural variations also constrain the age difference between the earliest and latest Lost Horse dikes to be less than the time necessary for the decay of this thermal aureole. Finally, the occurrence of subporphyritic textures and biotite phenocrysts in later Lost Horse dikes may indicate that fractionation of the Lost Horse parental magma(s) resulted in an increase in volatile concentrations.

Contact orientations of Lost Horse dikes indicate that they were emplaced along a subvertical to steep northerly dipping, east-southeast-striking fracture system (Figure 2-4-3A). The large volume of dikes relative to the enclosed volcanic rocks also indicates that significant extension accompanied intrusion. One fault set within the open pit has this same general attitude and exhibits both apparent dextral and sinistral displacements. A second, subvertical, northerly striking fault set controls the emplacement of the post-mineral felsite dikes and appears to have predominantly dextral offset.

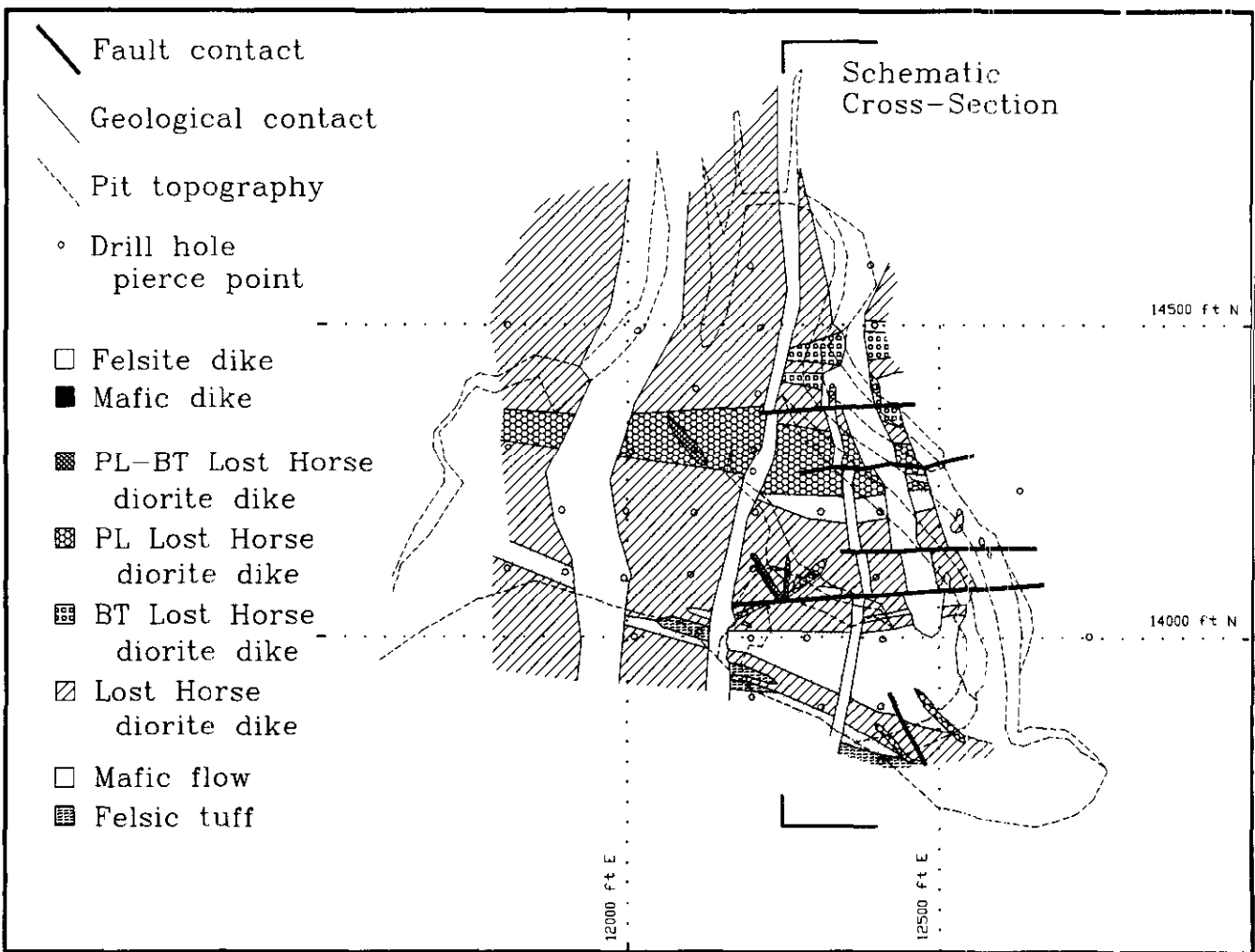


Figure 2-4-2. Virginia zone open pit geology mapped originally at 1:200-scale

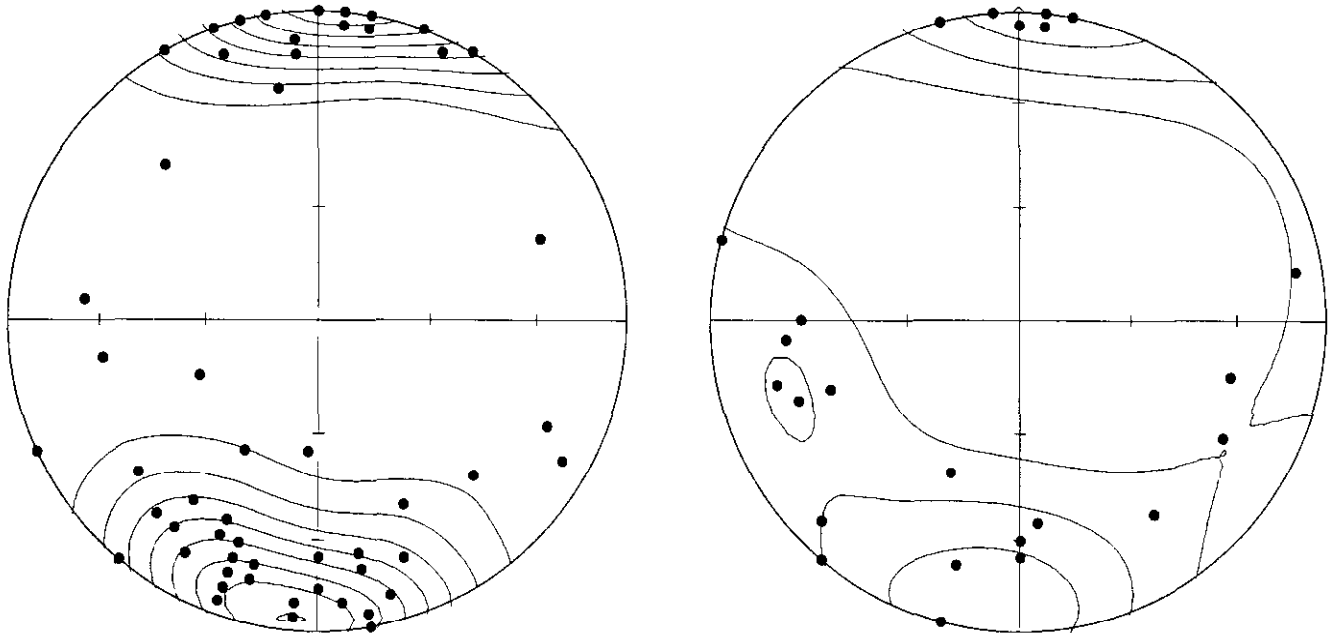


Figure 2-4-3. Poles to the orientations of intrusive contacts of (A) Lost Horse dikes and (B) mineralized veins measured in the Virginia zone open pit.

Within the open pit, the veins which carry the greater proportion of copper mineralization are magnetite+pyrite±chalcopyrite and chlorite+pyrite±chalcopyrite veins. These cut both Nicola Group rocks and most of the early Lost Horse dikes. Measured orientations of these veins in the pit walls indicate that they also strike west-northwest and dip steeply north (Figure 2-4-3B).

Post-mineral felsite dikes exhibit flow banding, columnar jointing, strongly chilled margins, variable amounts of quartz and feldspar phenocrysts and late, disseminated clots of chlorite alteration. Thick felsite dikes also appear to have produced a biotite hornfels envelope with disseminated pyrite cubes extending up to 10 metres from their margins. These dikes are clearly late (Fahrni *et al.*, 1976) and were intruded into cold country rocks.

VEINS AND HYDROTHERMAL ALTERATION

Hydrothermal alteration in the Virginia zone consists of demonstrably veinlet-controlled alteration and pervasive alteration that cannot yet be ascribed to a specific vein stage. Several types of veins were observed in drill core and the following descriptions distinguish these on the basis of their mineralogy and associated hydrothermal alteration of the adjacent wallrocks (Lang, 1992). The informal vein nomenclature derives from the most abundant and distinctive vein mineral(s). Sufficient crosscutting relationships have been observed among the veins to present a preliminary paragenetic sequence (Table 2-4-1). Several styles of pervasive alteration have also been observed (Table 2-4-2) but their spatial distribution and genetic controls are not yet well defined.

VEINLET-CONTROLLED ALTERATION

MAGNETITE STRINGERS

This stage of veining comprises narrow, irregular, discontinuous stringers that typically occur in clusters or zones. The veinlets are commonly less than 2 millimetres wide and consist solely of magnetite. They commonly have no recognizable alteration envelope, but in some cases a narrow zone of pink potassium feldspar is present.

MAGNETITE-SULPHIDE VEINS

These veins differ markedly from the magnetite stringers. Individual veins range from one centimetre to several metres wide with steep dips (Huyck, 1990). Huyck suggests that they occur in wide zones with significant vertical extent. Magnetite is the most abundant mineral in these veins and commonly has a coarse-grained, bladed habit adjacent to vein margins but less well defined and more equant habit in the centres of the veins. Hematite commonly occurs in the cores of magnetite blades but the relative timing of these minerals is not yet clear (personal communication, Huyck, 1992). Pyrite and chalcopyrite are commonly less abundant. Pyrite usually occurs as large, subhedral to euhedral grains. Chalcopyrite has irregular grain shapes and appears to post-date pyrite; its relationship to magnetite is less clear. Calcite is the most abundant gangue mineral, is commonly coarse grained and is generally interstitial to the metallic minerals. Other gangue minerals include variable but minor amounts of epidote, potassium feldspar, apatite, chlorite and sphene. In one sample a 30-micron grain of native gold was observed as an inclusion within a large pyrite grain. These veins typically have

TABLE 2-4-1
 PETROGRAPHIC CHARACTERISTICS OF HYDROTHERMAL VEIN TYPES IN THE VIRGINIA ZONE CU-AU DEPOSIT

Vein Stage	Mineral Assemblage ^{1,2}	Envelopes	Morphology
<i>Earlier Veins</i>			
Magnetite Stringers	mag-(hem)	K-fld	irregular
Magnetite-Sulphide	mag-py-cpy-calc-(ep-K-fld-apt-chl-sphn-Au-hem)	K-fld-chl-alb?-(ep)	planar
K-Feldspar	K-fld-chl-calc-(mag-py-cpy-qtz-apt-sphn-hem)	K-fld-alb?	variable
K-Feldspar-Epidote	K-fld-ep-chl-(mag-py-cpy-hem)	K-fld-alb?	irregular
Chlorite	chl-py-cpy-(calc-mag-hem)	chl-calc-py-cpy	variable
Calcite-Sulphide-Chlorite	calc-py-cpy-chl-(ep)	K-fld	planar
Epidote	ep-py-cpy-calc-(chl)	K-fld-alb	planar
Quartz	qtz-calc-(cpy-py-chl-bt)		planar
Calcite-Hematite	calc-hem-(chl)		planar
Calcite	calc-(py)		planar
Breccia Matrix	calc-K-fld-py-cpy-hem-(chl-qtz-bt)	?	
<i>Later Veins</i>			

¹sphn = sphene

²Parentheses indicate mineral species of minor to trace abundance.

TABLE 2-4-2
 PETROGRAPHIC CHARACTERISTICS OF PERVASIVE STYLES OF ALTERATION IN THE VIRGINIA ZONE CU-AU DEPOSIT

Alteration Type	Mineral Assemblage	Distribution
Potassic/Deuteric	Kfld	Locally strong; LH intrusions only
Potassic	Kfld± alb± bio± py± cpy	Wide distribution; in all rock types
Albitic	alb± ep± chl± diop± scap	Minor overall; locally strong
Propylitic	calc-chl-ep-py-hem	Evenly distributed; in all rock types
SCC	ser-clay± calc	Spotty; locally strong
Hornfels	bio± py	Adjacent to felsite dikes only

alteration envelopes of pink potassium feldspar and chlorite after primary igneous biotite. In addition, they, together with the magnetite stringers, are cut by all other vein types with the possible exception of potassium feldspar veins. Magnetite-sulphide veins introduced a large proportion of the sulphides in the Virginia zone.

POTASSIUM FELDSPAR VEINS

These common, widely distributed veins are usually planar and continuous and may reach several centimetres in width. More rarely they appear to form the matrix of 'breccias'; however, these may represent zones of intense, multiple phases of veining rather than true breccias with rotated fragments. The veins are dominated by deep salmon-pink potassium feldspar and contain lesser chlorite and calcite.

Minor phases include pyrite, chalcopyrite, magnetite, apatite and sphene. Quartz and biotite occur in trace amounts. Alteration envelopes are usually distinct zones dominated by potassium feldspar; associated light-coloured, very fine grained minerals that do not stain are interpreted to be albite. Calcite and epidote are locally stable.

POTASSIUM FELDSPAR + EPIDOTE VEINS

This style of alteration may be transitional between the potassium feldspar and epidote vein types. They are both common and widespread and usually occur as numerous, wispy stringers and veinlets with an overall vein-like expression. The major minerals are potassium feldspar and epidote, which occur either intimately intergrown or in textures suggesting that epidote post-dates potassium feld-

spar. Chlorite is common in the vein structure and adjacent wallrock. This vein type is nearly devoid of sulphides, and magnetite is either absent or occurs only in trace amounts. Contacts between this vein type and wallrock are often indistinct and no significant alteration envelopes are apparent. These veins formed before the epidote-dominated alteration but their relationship to other vein types is unknown.

CHLORITE VEINS

Chlorite veins are very common and widely distributed. They typically range from hairline fracture coatings to veins a few millimetres wide. They vary from discontinuous, sinuous stringers to planar veins and are characterized by abundant chlorite, with lesser but variable amounts of calcite, and minor epidote, magnetite and hematite. They commonly carry abundant pyrite and chalcocopyrite and are distinguished from other chlorite-bearing vein types by prominent, narrow chlorite alteration envelopes. In the envelopes, abundant pyrite and chalcocopyrite were introduced and magnetite was not destroyed. Chlorite veins exhibit mutually crosscutting relationships with calcite-sulphide-chlorite veins. Their abundance and high sulphide concentrations demonstrate that they were an important mineral-forming stage in the hydrothermal system.

CALCITE-SULPHIDE-CHLORITE VEINS

These veins are similar to the chlorite veins in distribution, mineralogy and position in the paragenetic sequence. They are distinguished from them by a greater proportion of calcite relative to chlorite, by the presence of an epidote selvage within the vein structure, by the absence of a chlorite-bearing alteration envelope and the presence of a pink potassium feldspar envelope. These veins were also important in the introduction of copper and gold into the system.

EPIDOTE VEINS

Epidote veins are typically regular, continuous fracture fillings and range from a millimetre to more than a centimetre wide. They can be entirely composed of epidote, or epidote with any combination of calcite, chlorite, potassium feldspar, pyrite and chalcocopyrite. Alteration envelopes range from absent through a faint pinkish zone, to strong development of pink potassium feldspar. Potassium feldspar may yield outward to albite in some vein envelopes.

QUARTZ VEINS

Quartz veins are uncommon. They are planar, regular, continuous, and 1 to 3 millimetres wide. Quartz and calcite dominate the veins in subequal amounts and pyrite and chalcocopyrite are trace to minor constituents. These veins do not have obvious alteration envelopes and although they formed late in the paragenetic sequence, their timing relative to late calcite veins is unknown.

CALCITE VEINS

These veins comprise three subtypes that together form the latest episode of veining. They are regular, continuous veins and vary from hairline fracture fillings to veins up to

tens of centimetres wide. Only rarely do they have visible alteration envelopes. The first subtype contains only coarse-grained calcite that commonly grew as euhedral crystals into open space. The second subtype is composed primarily of calcite but contains significant pyrite and chalcocopyrite, and minor chlorite. Although well mineralized, these veins are not volumetrically important and their timing relative to the barren calcite veins is unknown. The third subtype contains calcite, earthy hematite and, rarely, minor chlorite.

BRECCIAS

Breccias are a minor component of the Virginia zone and their distribution and timing are poorly understood. The matrix of breccias is coarse grained and consists of abundant calcite, potassium feldspar, pyrite, chalcocopyrite and earthy hematite, and trace amounts of chlorite, quartz and biotite. Fragments consist of LH1 dike rocks and Nicola volcanic rocks altered to potassium feldspar, calcite and trace chlorite and biotite. Pyrite and chalcocopyrite are evenly disseminated throughout fragments and matrix. Primary igneous magnetite has not been destroyed in altered fragments.

PERVASIVE ALTERATION

Potassic alteration is expressed by two distinct assemblages (Table 2-4-2). The earliest occurs as washes of light pink coloration that are erratically distributed within, but confined to, the Lost Horse intrusions. Original igneous magnetite is almost always obliterated. This assemblage is thought to represent an early deuteritic alteration and is not associated with sulphide mineralization. The second type of pervasive potassic alteration occurs in patches related to microveinlets. The primary alteration mineral is also potassium feldspar accompanied by various combinations of albite, biotite, pyrite and chalcocopyrite; magnetite is not typically destroyed. This second style of potassic alteration appears, at least in part, to overprint the deuteritic alteration. A significant portion of the potassic alteration may be due to coalescing alteration envelopes of potassium feldspar veins. In other cases, it appears to be distributed in zones independent of vein type. In places, significant sulphide mineralization accompanies this potassic alteration.

Pervasive albitic alteration has been observed locally, but in much smaller volumes than potassic alteration. The primary alteration assemblage is white albite, usually with epidote and chlorite, and locally with diopside and, possibly, scapolite. Zones of albitization affect both the Lost Horse intrusions and Nicola volcanic rocks. Some albitic alteration zones may represent overlapping envelopes of epidote veins. Albitization does not appear to be related to sulphide introduction.

Propylitic alteration is widely and evenly distributed throughout the deposit. It consists of calcite, chlorite, pyrite, epidote and hematite and affects both intrusive and volcanic rocks. The timing of propylitic alteration is poorly constrained. It shows evidence of being both early and late in the sequence of alteration, possibly as a result of early expansion and later contraction of the hydrothermal system.

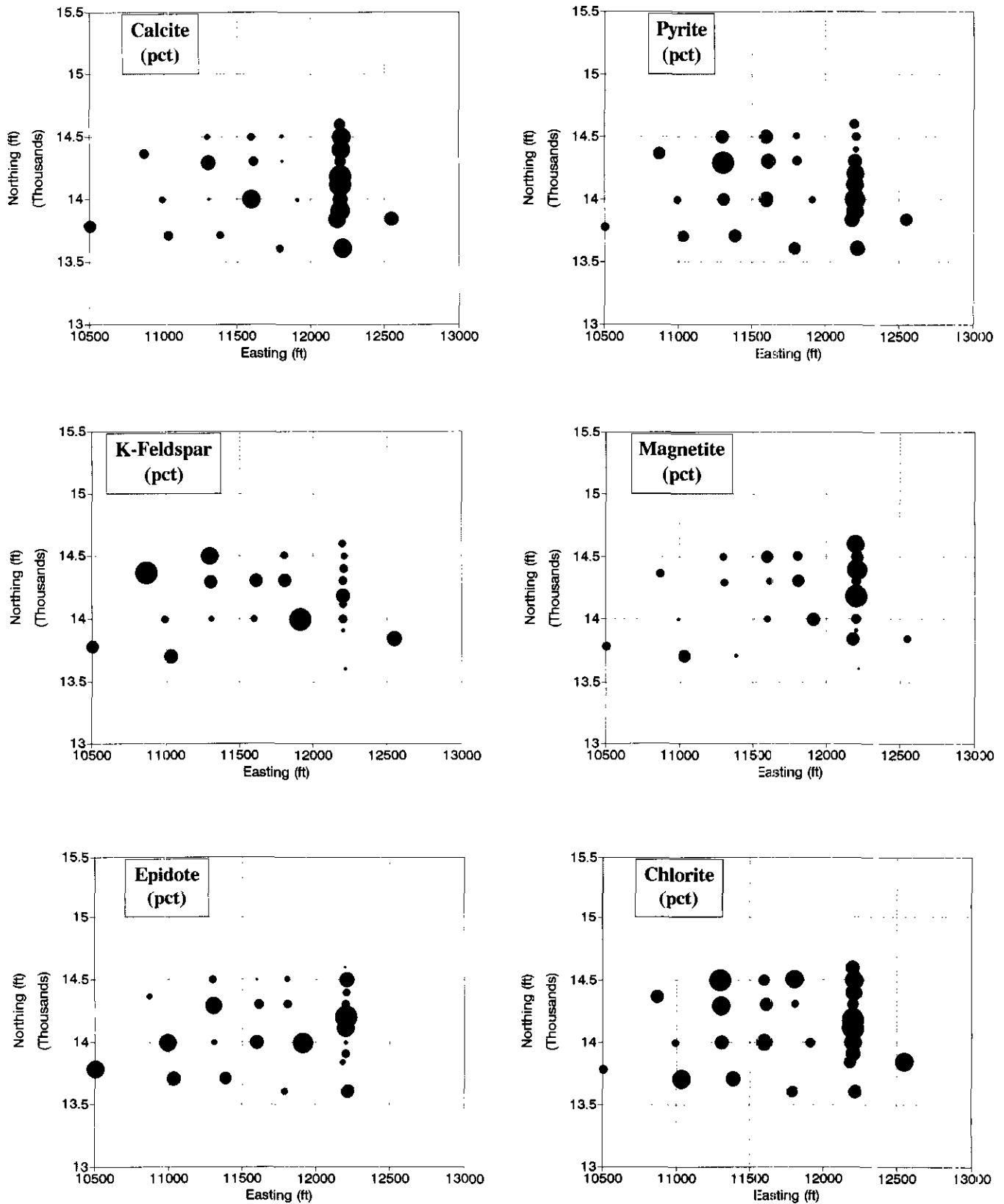


Figure 2-4-4. Bubble plots of hydrothermal alteration minerals in the Virginia zone of the Copper Mountain Cu-Au deposit. The size of the bubbles varies proportionally with the abundance of each mineral species. On these diagrams, the smallest and largest bubbles represent the minimum and maximum mineral concentration observed in the drill holes at the 3300-foot elevation. These are 0.68 and 21.25 % calcite, 0.36 and 4.50 % pyrite, 0.00 and 50.00 % potassium feldspar, 0.00 and 10.00 % magnetite, 0.00 and 8.90 % epidote, and 2.50 and 17.78 % chlorite.

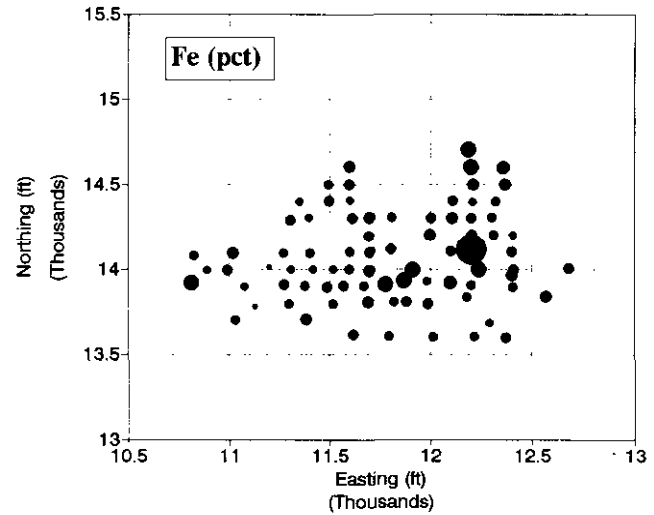
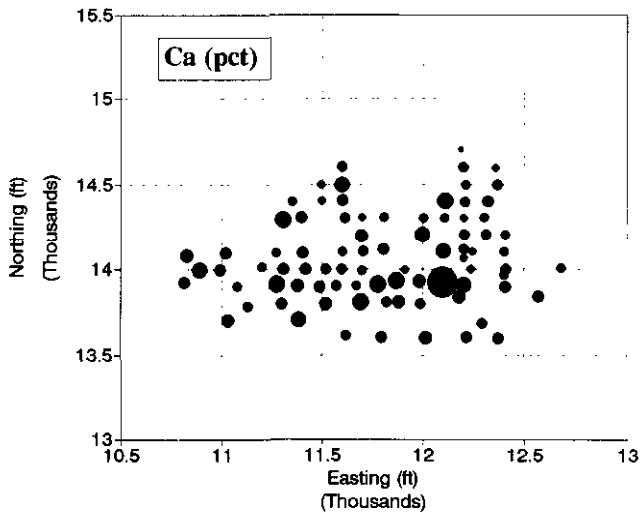
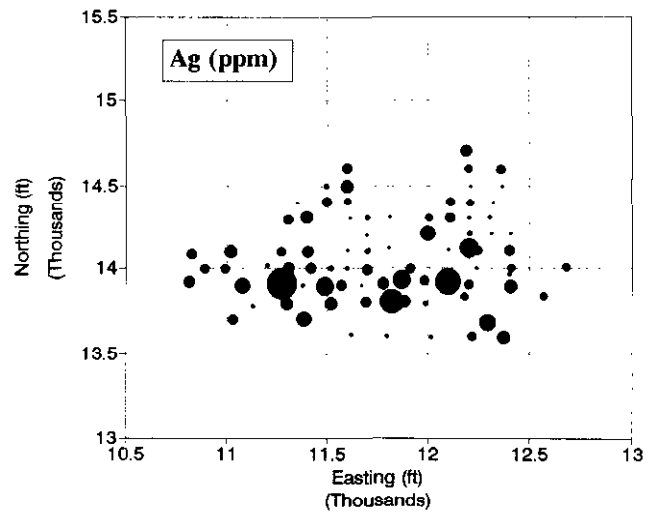
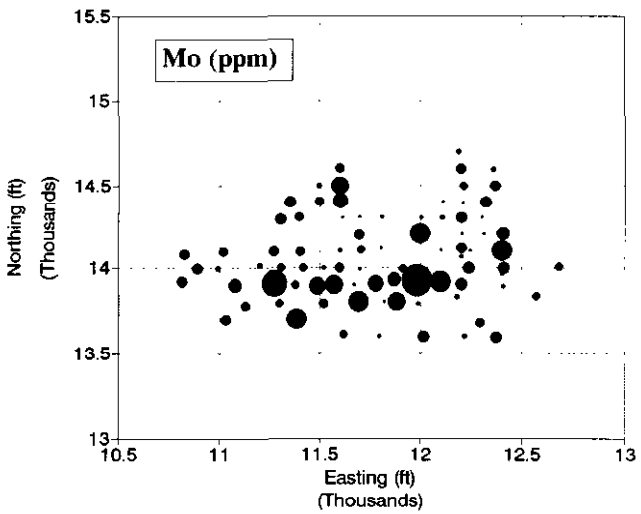
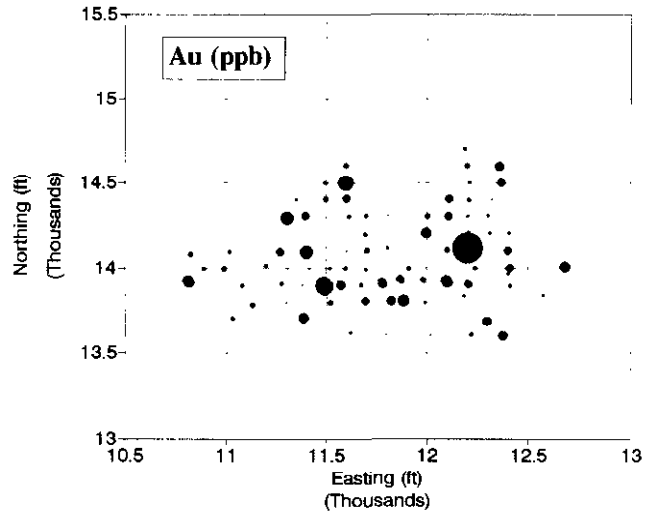
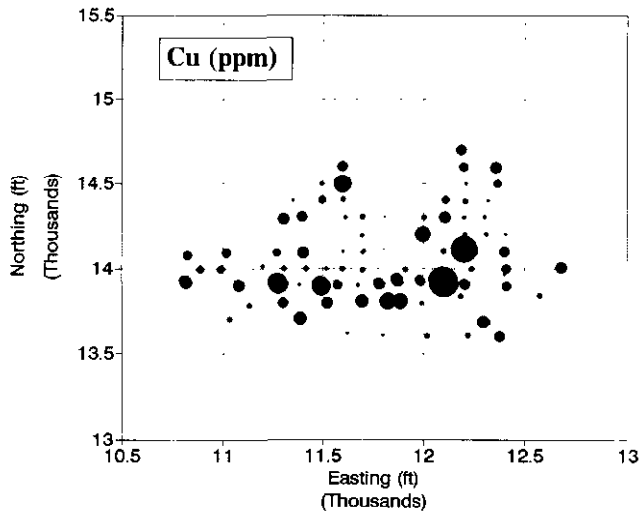


Figure 2-4-5. Bubble plots of Cu, Au, Mo, Ag, Ca and Fe geochemical concentrations in the Virginia zone of the Copper Mountain Cu-Au camp. The size of the bubbles varies proportionally with concentration of each element. On these diagrams, the smallest and largest bubbles represent the minimum and maximum concentration observed in the drill holes at the 3300-foot elevation. These are 150 and 18753 ppm Cu, 2 and 1165 ppb Au, 1 and 95 ppm Mo, 0.1 and 6.6 ppm Ag, 1.15 and 21.28 % Ca, and 2.06 and 41.13 % Fe.

Minor alteration types include a very late stage hydrothermal overprint consisting of sericite, calcite and a brown clay mineral. It is locally strong but very unevenly distributed. A biotite hornfels with disseminated pyrite is developed adjacent to thicker felsite dikes.

HYDROTHERMAL ALTERATION AND GEOCHEMICAL ZONING

Detailed drill-core logging and statistical analysis of a multi-element geochemical database provided data to produce hydrothermal alteration and geochemical zoning maps of the 3300-foot elevation.

Evaluation of mineral zoning patterns was based on visual estimations of the percentage of alteration minerals logged in intervals of core from 27 diamond-drill holes distributed across the deposit. Results are summarized in Figure 2-4-4. Fifty-foot intervals were logged in core along the 12250E cross-section, which is perpendicular to the main ore zone. Twenty-foot sections were examined in all other holes. All intervals were centred on piercing points through the 3300-foot elevation; some intervals were offset slightly from this level to avoid post-mineral felsite dikes. Emphasis was given to estimating the bulk percentage of alteration minerals in several assay intervals in each hole; the means of these intervals are plotted on bubble plots (Figure 2-4-4). Results indicate that no significant alteration zoning is evident in the Virginia zone. This may be due, in part, to the sparse sampling of drill holes through the deposit and to the dominance of fracture-controlled alteration and mineralization.

The geochemical database consists of 5436 samples from approximately 3-metre drill-core intervals from 110 drill holes. The samples were analyzed for a suite of 29 elements (Cu, Pb, Zn, Mo, Ag, Ni, Co, Mn, Fe, As, U, Th, Sr, Cd, Sb, Bi, V, Ca, P, La, Cr, Mg, Ba, Ti, B, Al, Na, K, and W) by aqua regia digestion with an inductively coupled plasma spectrophotometry finish; gold was determined by aqua regia digestion and atomic absorption finish. These data were composited across a 50-foot interval at the 3300-foot elevation. A number of statistical procedures (histograms,

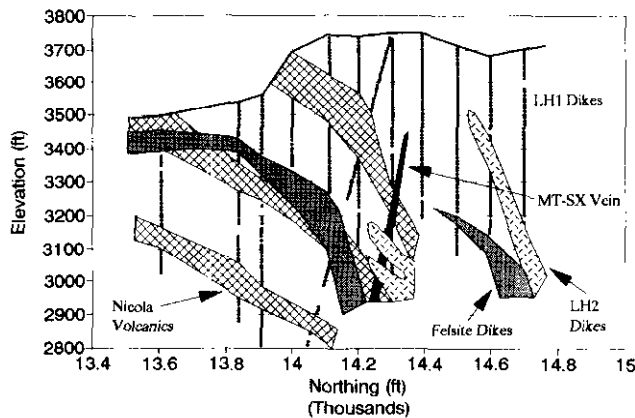


Figure 2-4-6. Generalized geological cross-section of the Virginia zone, at 12 250E, with drill-hole sample locations. Geologic correlations inferred from lithologic codes in the lithochemical data base.

probability plots, bubble plots, scatterplots) were applied to each lithology to determine if any zoning or geological control on mineralization was present.

Results indicate that only limited geochemical zoning is apparent. A single easterly oriented (ore) zone with generally anomalous copper concentrations at the 3300-foot elevation also exhibits generally anomalous gold, silver and molybdenum concentrations (Figure 2-4-5). Iron and calcium concentrations, thought to represent the abundance of magnetite and calcite as gangue minerals in productive veins, do not correlate with this zone (Figure 2-4-5). Similarly, no other elements define haloes about this high-grade zone.

The high-grade part of the ore zone occurs within Nicola volcanics (Figure 2-4-6). Additional evidence in support of similar lithological grade control can be seen in the copper and gold grade distributions of the volcanic flows, fragmentals and tuffs, and early equigranular and late subporphyritic Lost Horse diorite dikes (Figure 2-4-7). Higher copper and

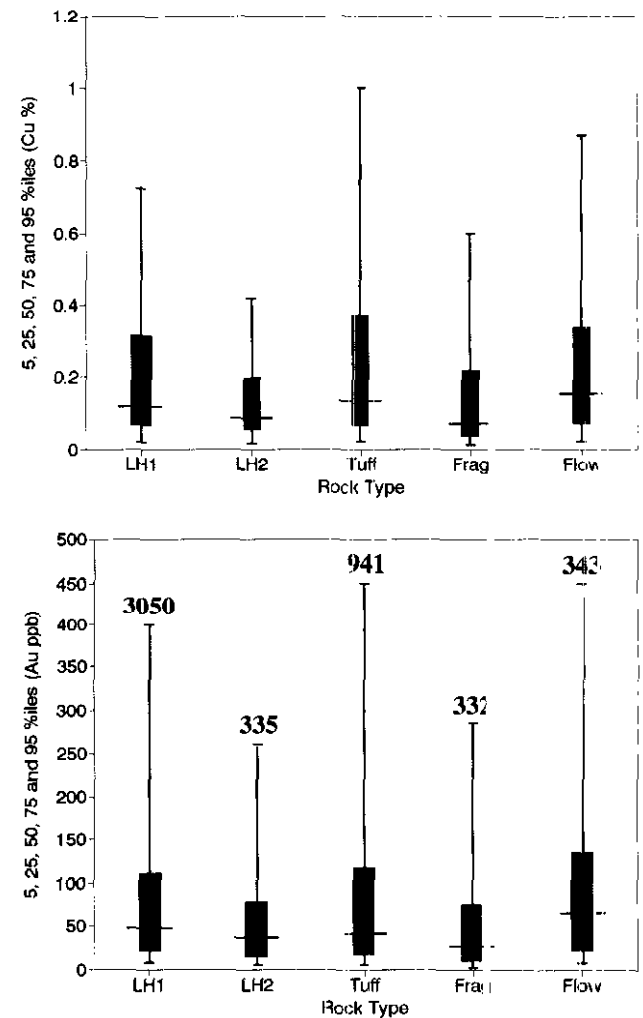


Figure 2-4-7. Plots of concentration percentiles for Cu (%) and Au (ppb) for equigranular (LH1) and subporphyritic (LH2) Lost Horse diorite dikes, Nicola volcanic felsic tuffs (TUFF), mafic flows (FLOW) and mafic lapilli tuffs, breccias and agglomerates (FRAG). The number of samples from each unit are indicated.

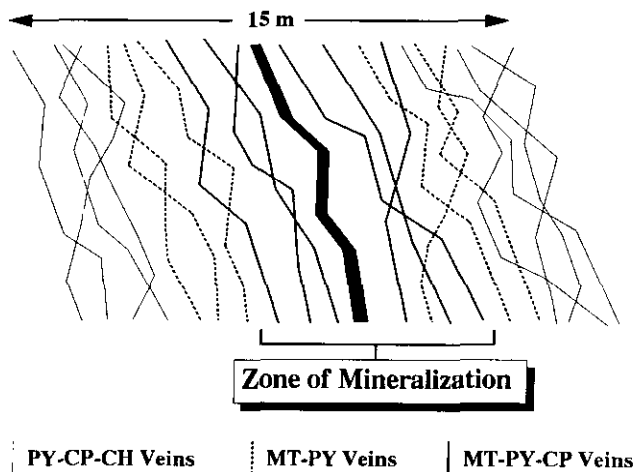


Figure 2-4-8. Schematic cross-section of a major mineralized structure within the Virginia zone.

gold concentrations in the massive flows and tuffs may be due to their tendency to fracture more readily than the less massive fragmental volcanics. Similarly, the pre-mineral, equigranular Lost Horse diorite dikes have higher copper and gold grades than the younger subporphyritic Lost Horse diorite dikes.

Despite the lack of deposit-scale zoning in the Virginia zone, geologic mapping in the open pit does indicate that there is a crude zoning of vein types across mineralized structures. Specifically, major magnetite-sulphide veins (>30 cm wide) which contain significant chalcopyrite are generally bounded by similar magnetite sulphide veins without chalcopyrite. These relatively barren veins are themselves bounded by calcite-sulphide-chlorite veins (as schematically illustrated in Figure 2-4-8). Furthermore, the thick magnetite-sulphide veins exhibit abundant conjugate magnetite-sulphide veins within zones up to two times the vein width from the major vein margins. These 'parasitic' veins are thinner, but contain a mineralogy which is identical to the major magnetite-sulphide veins.

CONCLUSIONS

Geological mapping, drill-core logging and geochemical analysis of samples indicates that the Virginia zone is a bulk tonnage copper-gold deposit hosted by Nicola volcanics which have been intruded by diorite dikes of the Lost Horse complex. Copper and gold mineralization is hosted by a

series of closely spaced, easterly striking, steeply dipping veins and occurs with significant amounts of magnetite gangue. Geochemical and mineralogical zoning within the deposit is limited, but zoning of vein types about mineralized structures has been observed. Mineralization does appear to be controlled to some extent by host lithology and early Lost Horse dikes and massive volcanics appear to be the most favourable host rocks.

ACKNOWLEDGMENTS

The authors thank Princeton Mining Corporation for access to the Virginia zone and associated drill core, and for its assistance in support of the fieldwork undertaken in the course of this research. The assistance of Dr. Holly Huyck in locating property information and for helpful discussions of camp geology is also gratefully acknowledged.

REFERENCES

- Fahmi, K.C., Macauley, T.N. and Preto, V.A.G. (1976): Copper Mountain and Ingerbelle; in *Porphyry Deposits of the Canadian Cordillera*, Sutherland Brown, A., Editor, *Canadian Institute of Mining and Metallurgy*, Special Volume 15, pages 368-375.
- Huyck, H.L.O. (1986): Geologic Observations at Copper Mountain; private report, *Similkameen Mining Division, Newmont Mines Ltd.*
- Huyck, H.L.O. (1990): Virginia Area Geologic Model; private report, *Princeton Mining Corporation*.
- Huyck, H.L.O. (1991): Exploration Proposal for the 1991 Field Season, Copper Mountain; private report, *Princeton Mining Corporation*.
- Lang, J.R. (1992): Petrographic Observations in the Virginia Zone, Copper Mountain; in *Annual Technical Report — Year 1, Copper-Gold Porphyry Systems of British Columbia*, Chapter 9, *Mineral Deposit Research Unit, The University of British Columbia*.
- Preto, V.A.G. (1972): Geology of Copper Mountain, B.C.; *B.C. Ministry of Energy, Mines and Petroleum Resources*, Bulletin 59, 87 pages.
- Stanley, C.R. (1992): Geochemistry of the Virginia Zone, Copper Mountain; in *Annual Technical Report — Year 1, Copper-Gold Porphyry Systems of British Columbia*, Chapter 8, *Mineral Deposit Research Unit, The University of British Columbia*.
- Takeda, T. (1976): On the Exploration and Structural Control of the Ingerbelle Deposit, British Columbia, Canada; *Mining Geology (Japan)*, Volume 26, pages 179-190.



A GEOLOGICAL OVERVIEW OF THE HEDLEY GOLD SKARN DISTRICT SOUTHERN BRITISH COLUMBIA (92H)

By G.E. Ray, I.C.L. Webster, B.C. Geological Survey Branch
G.L. Dawson, The University of British Columbia
A.D. Ettlinger, Santa Fe Pacific Mining Inc.

KEYWORDS: Economic geology, gold skarn, Hedley, Upper Triassic, Nicola, stratigraphy, back-arc basin, slump breccias, Mount Riordan, garnet skarn, industrial minerals.

INTRODUCTION

This paper presents an updated overview of the geology and mineral deposits in the Hedley mining district, south-central British Columbia. The district contains the Nickel Plate gold skarn deposit, which is currently being operated by Homestake Canada Ltd. (formerly Corona Corporation), as well as several past-producing gold skarns: the French, Canty and Good Hope mines (Figure 2-5-1). It also includes the Mount Riordan (Crystal Peak) skarn which is being evaluated as a potential industrial garnet deposit by Polestar Exploration Inc.

Early mapping of the district geology was completed by Bostock (1930) and Rice (1947, 1960), and more recently by Ray and Dawson (1987, 1988, 1993, in preparation), and Monger (1989). Studies on the various gold skarns include early work by Camsell (1910), Bostock (1930), Warren and Cummings (1936), Billingsley and Hume (1941), Dolmage and Brown (1945), and Lee (1951); recent investigations have been completed by Ray *et al.*, (1987, 1988), Webster (1988), Ettlinger and Ray (1989), Ettlinger (1990), Dawson *et al.*, (1990a, 1990b), Ettlinger *et al.*, (1992), and Ray and Dawson (1993 in preparation). In addition, details on the Mount Riordan industrial garnet deposit have been published by Mathieu *et al.*, (1991), Grond *et al.*, (1991) and Ray *et al.*, (1992).

REGIONAL GEOLOGY

The Hedley mining district lies within the allochthonous Quesnel Terrane of the Intermontane Belt. It is situated at the eastern edge of the Upper Triassic Nicola Group, close to its contact with Paleozoic and Triassic oceanic rocks of the Apex Mountain Complex (Figure 2-5-1), which is believed to be a deformed ophiolite (Milford, 1984). Elsewhere in south-central British Columbia, the Nicola Group unconformably overlies this package (Read and Okulitch, 1977), but at Hedley the contact is either faulted or occupied by the mid-Jurassic Cahill Creek pluton.

The Nicola Group consists largely of island-arc supracrustal rocks that were deposited in an elongate and rifted marginal marine basin associated with an easterly dipping subduction zone (Preto, 1979; Mortimer, 1986, 1987). West of the Hedley district, along the main axis of the arc, the group reaches 6000 metres in thickness and is dominated by mafic, subaerial to submarine volcanic flows and tuffaceous rocks in which limestones are uncommon (Preto, 1979). Farther east at Hedley, however, the group is

thinner (maximum 3000 m), lacks volcanic flows, and is dominated instead by sedimentary rocks that include bedded tuffs, calcareous and turbiditic siltstones and thick, extensive limestones.

Immediately following the termination of the Late Triassic Nicola arc volcanism, a variety of intrusions ranging from dikes and sills to major batholiths were emplaced into the Nicola Group. These intermediate to high-level intrusions, which vary from gabbro to granodiorite and alkaline to calcalkaline in composition, range from 194 to 210 Ma in age, (Preto *et al.*, 1979; Monger, 1989; Parrish and Monger, 1992). Some of the alkalic intrusions (*e.g.*, Copper Mountain stock) are related to porphyry copper-gold deposits, while some of the calcalkaline plutons (*e.g.*, Brenda stock) are associated with gold-poor porphyry copper-molybdenum orebodies (Carr, 1968; Preto, 1972; Soregaroli and Whitford, 1976). In the Hedley district, the Bromley batholith, the Hedley intrusions and the Mount Riordan stock (Figure 2-5-1) were all emplaced during this Late Triassic to Early Jurassic plutonic episode.

DISTRICT STRATIGRAPHY

The Nicola Group at Hedley is a westerly thickening, late Carnian to late Norian calcareous sedimentary and arc-related volcanoclastic sequence that was deposited on a tectonically active, west-dipping paleoslope (Figures 2-5-2 and 2-5-3). Sedimentary facies changes and paleocurrent indicators suggest that the sediments in the group were derived largely from an eastern source, although the alkaline and calcalkaline pyroclastic rocks higher in the succession may have originated from the Nicola arc to the west. The Nicola Group in the Hedley area is believed to have been laid down across the structural hinge zone that marked the rifted margin of the westerly deepening, shallow-marine Nicola basin.

At Hedley, the Nicola Group sedimentary succession contains a number of newly recognized formations for which formal nomenclature is now proposed (Ray and Dawson, 1993, in preparation). The succession (Figure 2-5-2) includes an upper, widely developed and thick (at least 1200 m) unit, the Whistle Formation; the formation consists largely of alkalic and subalkalic tuffs and tuffaceous sediments, and its base is occupied by an extensive limestone-boulder deposit, the Copperfield breccia, which reaches 200 metres in thickness. The angular to well-rounded limestone clasts are commonly 1 metre in diameter although, rarely, they reach up to 15 metres across; they contain shallow-water bivalves, as well as conodonts that are slightly older (late Carnian to early Norian) than the early to middle Norian faunas in the underlying Chuchwayana and Hedley

formations (M.J. Orchard, personal communication, 1989) (Figure 2-5-3). One of the rare chert clast from the breccia yielded radiolarians of Permian age (F. Cordey, personal communication, 1985).

Limestone makes up 95 per cent of the clasts but rare clasts of chert, argillite, siltstone, and volcanic and plutonic rock are present. Many of the elongate argillite and siltstone clasts are deformed which suggests they were un lithified when they were incorporated into the breccia. Some appear to have been scoured from the immediately underlying sedimentary units, and many of these units show chaotically

disturbed bedding, presumably caused when the breccia ploughed into the unconsolidated silty and argillaceous sediments.

The Copperfield breccia probably represents a chaotic gravity-slide deposit formed by the catastrophic slumping of an unstable accumulation of shallow-marine reef debris down the submarine paleoslope. This mass ploughed into, and was deposited on the unconsolidated deeper water sediments of the Hedley, Chuchuwayha and Stemwinder formations (Figure 2-5-4). The breccia is probably analogous to the modern megabreccias described along the Nicaraguan

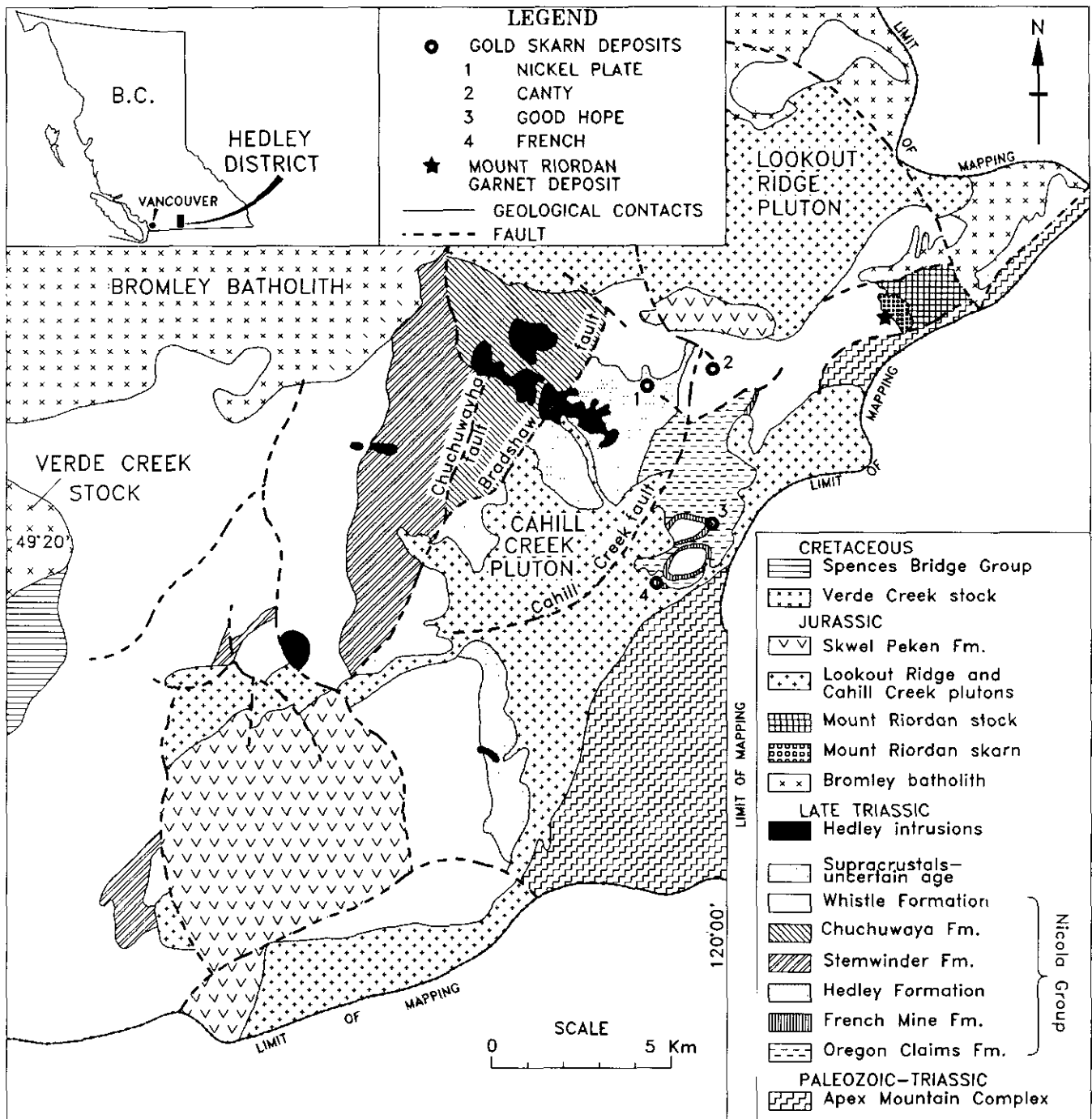


Figure 2-5-1. Geology of the Hedley district and location of the skarn deposits.

Rise in the Western Caribbean (Hine *et al.*, 1992). These megabreccias form thick (up to 120 m) and extensive (27 km by 16 km) units and are believed to represent seismically triggered bank-margin collapse features that took place along the edges of low-relief carbonate platforms (Hine *et al.*, 1992).

The Whistle Formation is underlain by a succession in which four sedimentary facies are distinguished from east to west: the thin (up to 200 m), shallow-marine, limestone-dominant French Mine Formation in the east, the thicker, siltstone-dominant Hedley and Chuchuwayha formations in the central part of the area, and the thick (up to 2200 m), deeper water and argillite-dominant Stemwinder Formation in the west. Conodonts from the French Mine, Hedley and Chuchuwayha formations indicate they are Late Triassic (Carnian-Norian) in age (M.J. Orchard, personal communication, 1989; Figure 2-5-3). The sedimentary facies were separated from one another, and partly controlled by northerly trending active growth faults (Figures 2-5-2 and 2-5-4); these fractures, which were probably related to the basin-margin rift structures, were precursors of the Chuchuwayha, Bradshaw and Cahill Creek faults.

The Chuchuwayha, Hedley and French Mine formations are underlain by a poorly understood sequence of mafic tuffs with minor flows, limestone and chert-pebble conglomerate, the Oregon Claims Formation (Figure 2-5-2; Ray and Dawson, 1993, in preparation). The age of this unit and its contact relationship with the overlying Nicola rocks are uncertain. It may represent the oldest exposed section of the Nicola Group, but it is more likely to be an older basement on which the Nicola Group was unconformably deposited, and could be a western extension of the Apex Mountain Complex.

A newly recognized mid-Jurassic unit, the Skwel Peken Formation, overlies the Nicola Group at Hedley (Figure 2-5-1). It has two members. The lower member, 1500 metres thick, is dominated by calcalkaline andesitic to dacitic lapilli and ash tuffs that commonly contain glassy, strongly embayed and fractured quartz crystals. Minor amounts of epiclastic sediments, welded tuffs and pyroclastic surge deposits are also present. The thinner (maximum 400 m) upper member is dominated by massive andesitic crystal tuffs.

We believe that the Skwel Peken Formation is the first mid-Jurassic supracrustal unit recognized in south-central British Columbia. The formation was laid down in a non-marine, subaerial to shallow-water environment and is believed (Ray and Dawson, 1993, in preparation) to represent extrusive volcanism related to the mid-Jurassic Cahill Creek and Lookout Ridge plutons (Figure 2-5-1). Zircons extracted from quartz-rich tuffs in the lower member give a maximum U-Pb age of 187 ± 9 Ma (J.E. Gabites, personal communication, 1992). Minor amounts of Cretaceous Spences Bridge Group and Eocene Springbrook and Marron formations are also exposed in the area (Figure 2-5-1).

Several episodes of plutonism are recognized. The oldest resulted in the quartz dioritic and gabbroic Hedley intrusions that are associated with widespread gold skarn mineralization, including the Nickel Plate, Canty, French and Good Hope deposits. Field evidence and equivocal radi-

ometric U-Pb dating suggest they were intruded during Late Triassic to Early Jurassic times, between 219 to 194 Ma (J.E. Gabites, personal communication, 1992). The intrusions occur as large and small stocks, as sill dike swarms and as isolated minor bodies; the swarms are preferentially developed in the thinly bedded Chuchuwayha and Hedley

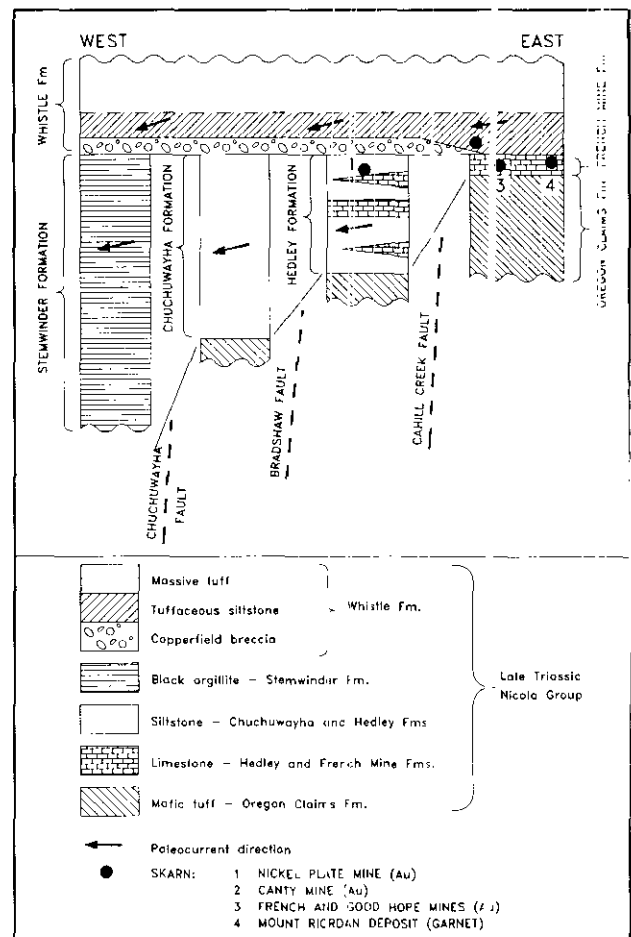


Figure 2-5-2. Schematic east-west section across the Hedley district showing sedimentary facies changes in the Nicola Group and stratigraphic location of the skarn deposits.

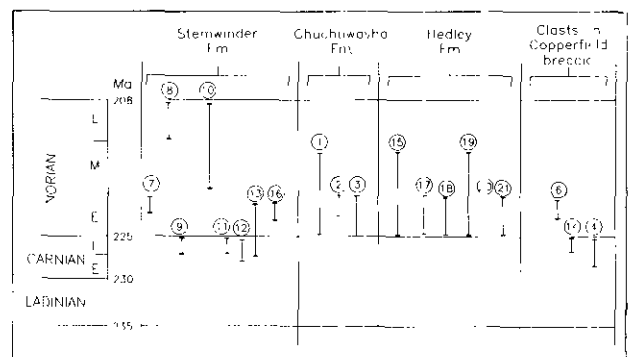


Figure 2-5-3. Age range of conodont microfossils collected from the Nicola Group, Hedley district. Numbers in circles refer to fossil sample numbers listed in Ray and Dawson (1993, in preparation). (Fossils identified by M.J. Orchard, Geological Survey of Canada).

formations. Some elongate bodies, such as the Toronto stock, were intruded along easterly trending lineaments that may have been late Triassic transform faults related to the rifted basin margin.

A slightly younger plutonic episode resulted in the large, granodioritic Bromley batholith and a related marginal body, the granodioritic to gabbroic Mount Riordan stock. The latter is genetically associated with the large, garnet-rich Mount Riordan (Crystal Peak) skarn that contains minor tungsten-copper occurrences. A radiometric U-Pb zircon age of 194.6 ± 5 Ma (Early Jurassic) is indicated for the Mount Riordan stock (J.E. Gabites, personal communication, 1992), and a similar age of 193 ± 1 is obtained from the Bromley batholith (Parrish and Monger, 1992).

A subsequent phase of granodioritic to quartz monzonitic magmatism is represented by the Lookout Ridge and Cahill Creek plutons. The latter, which commonly separates the Nicola Group to the west from the Apex Mountain Complex farther east, yields a U-Pb zircon mid-Jurassic date of 168.8 ± 9 Ma (J.E. Gabites, personal communication, 1992). These high-level plutons are spatially related to a suite of minor aplites and quartz porphyry intrusions that yield a Late Jurassic U-Pb zircon date of $154.5 \pm 8 - 43$ Ma. The plutons are believed to be the magmatic source of the

volcaniclastic package in the nearby Skwel Peken Formation (Ray and Dawson, 1993, in preparation).

The youngest major intrusion in the district is the granitoid Verde Creek stock (Dolmage, 1934) which is coeval with the Early Cretaceous Spences Bridge Group (Preto, 1972); it intrudes the Nicola Group in the western part of the district (Figure 2-5-1).

A rare, distinctive suite of leucocratic, calcalkaline minor intrusions (or possible volcanic flows) is spatially associated with the Skwel Peken Formation. These rocks contain magmatic garnet phenocrysts with almandine-rich cores and spessartine-rich margins that are chemically and optically distinct from the grossular-andradite garnets in the gold skarns.

STRUCTURAL GEOLOGY

Two deformational episodes are identified in both the Apex Mountain Complex and Nicola Group, although the temporal relationship of the episodes between one rock package and the other is unknown. The first and most intense episode identified in the Apex Mountain Complex resulted in tight to isoclinal minor folds with moderate to strong, northerly to northeast-striking and subvertically

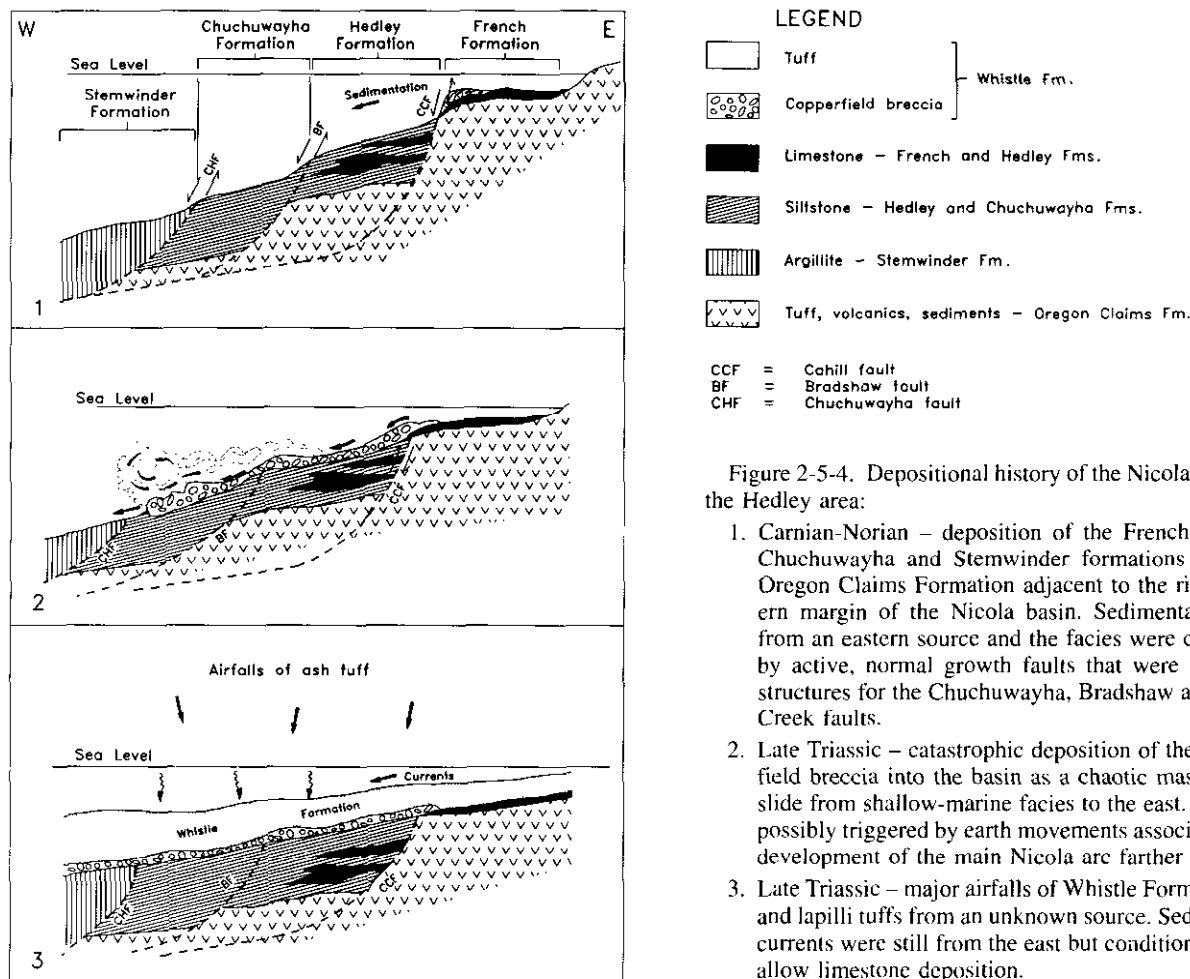


Figure 2-5-4. Depositional history of the Nicola Group in the Hedley area:

1. Carnian-Norian - deposition of the French, Hedley, Chuchuwayha and Stemwinder formations onto the Oregon Claims Formation adjacent to the rifted eastern margin of the Nicola basin. Sedimentation was from an eastern source and the facies were controlled by active, normal growth faults that were precursor structures for the Chuchuwayha, Bradshaw and Cahill Creek faults.
2. Late Triassic - catastrophic deposition of the Copperfield breccia into the basin as a chaotic mass-gravity slide from shallow-marine facies to the east. This was possibly triggered by earth movements associated with development of the main Nicola arc farther west.
3. Late Triassic - major airfalls of Whistle Formation ash and lapilli tuffs from an unknown source. Sedimentary currents were still from the east but conditions did not allow limestone deposition.

inclined penetrative axial planar fabrics; no major folds of this age are recognized. The second period of deformation is only locally developed in the Apex Mountain rocks. It resulted in northerly striking, subvertical open folds, but is not associated with any penetrative fabrics.

Both of the deformational episodes identified in the Nicola Group predate the Skwel Peken Formation and the Cahill Creek pluton which suggests they are pre-Middle Jurassic in age. The first episode, which was only locally developed in the Nicola Group, produced west to northwest-

striking minor flexures that were probably related to the forcible emplacement of the Hedley intrusion. At Nickel Plate, these structures partly controlled the gold skarn mineralization (Billingsley and Hurne, 1941).

The second deformation in the Nicola Group was the dominant structural event in the district. It resulted in easterly overturned minor and major asymmetric folds with northerly striking, steep westerly dipping axial planes. It produced a large anticlinal structure with its axis just east of the Nickel Plate deposit. Locally, argillites in the Ste-

TABLE 2-5-1
COMPARISON BETWEEN THE NICKEL PLATE AND MOUNT RIORDAN SKARNS

	Nickel Plate	Mt. Riordan
Host formation and age	Upper Triassic Hedley Fm.	?Upper Triassic French Mine Fm?
Hostrock lithology	Predominantly siltstone, minor limestone	?Massive limestone and carbonate breccia?
Associated Intrusive rocks	Hedley intrusions (gabbro, diorite)	Mount Riordan stock (granodiorite-gabbro)
Age of intrusions	Post 219 and pre 194 Ma (Late Triassic - Early Jurassic)	194.6 ± 5 Ma (Early Jurassic)
Initial ⁸⁷ Sr/ ⁸⁶ Sr of intrusions	0.7038*	0.7044*
Skarn mineralogy	Banded, clinopyroxene-dominant skarn with sulphides and scapolite. Garnets generally anhedral and brown coloured. No scheelite present.	Massive, garnet-dominant skarn. Coarse, euhedral garnets with highly variable colour. Generally low sulphide content. Minor pyroxene, actinolite, epidote. Scheelite present.
Opaque minerals	Pyrrhotite, arsenopyrite, minor chalcopyrite and rare pyrite	Magnetite, pyrrhotite, pyrite minor chalcopyrite.
Degree of skarn alteration	Original sedimentary bedding commonly preserved in skarn.	Virtually no primary structures preserved.
Approximate exposed area of skarn	4 km ²	0.3 km ²
Maximum thickness of skarn	300 m	At least 175 m
Geochemistry of mineralization	Anomalous Au,As,Cu,Co,Bi,Te,Ag,Sb	Anomalous Cu,W,Ag,Mo
Garnet composition	Low Mn (< 0.5% MnO) Grossularitic cores, andraditic margins Ad 15-80	Low Mn (< 1.0 % MnO) Andraditic cores, grossularitic margins Ad 45-98
Pyroxene composition	Low Mn (< 1.0% MnO) Hd 40-95	Low Mn (< 1.3 % MnO) Hd 41-51

* R.L Armstrong, personal communication 1989.

winder and Chuchuwayha formations contain a fracture cleavage related to this deformation, although elsewhere axial planar penetrative fabrics are absent.

In addition to the above two episodes, a younger period of folding has gently deformed the Skwel Peken Formation. This post-mid-Jurassic deformation resulted in open minor flexure folds with northeasterly striking axial planes.

ECONOMIC GEOLOGY

The Hedley district has important skarn deposits (Figures 2-5-1 and 2-5-2) as well as some minor gold-bearing quartz-carbonate veins. The skarns are separable into two types: older and more economically important gold skarns such as the Nickel Plate, Carty, French and Good Hope deposits

TABLE 2-5-2
PRODUCTION FROM GOLD SKARN
DEPOSITS - HEDLEY DISTRICT

Deposit	Ore milled (t)	Gold (kg)	Silver (kg)	Copper (t)	Grade (Au g/t)
Nickel Plate					
1904-1963 ^a (Underground)	2 983 900	41 705	4 160	981	13.97
Nickel Plate* (Open pit)					
1987 ^b	481 454	1512.4	832.4	0	3.14
1988 ^b	879 645	2714.9	2955.7	0	3.08
1989 ^b	1 065 026	2463.8	3246.0	0	2.31
1990 ^b	1 141 255	2382.1	844.6	0	2.08
1991 ^b	1 166 039	2842.7	677.7	0	2.43
Hedley Mascot (Underground) 1936-1949 ^{a,c}	619 022	7 248	1 707	871	11.70
Total	8 336 341	60 868.9	14 423.4	1 852	7.30
French					
1950-1965 ^a	29 450	786	NA	NA	26.68
1957-1961 ^d	48 158	817	66	NA	16.96
1982-1983 ^a	4 438	26	135	20	5.86
Total	82 046	1629	201	20	19.85
Good Hope					
1946-1948 ^d	4 241	89	NA	NA	20.98
1982 ^a	6 874	77	119	0.6	11.20
Total	11 115	166	119	0.6	14.93
Carty					
1939-1941 ^{a,c}	1 483	16	NA	NA	10.78
Grand total from skarn	8 430 985	82 679.9	14 743.4	1872.6	7.43

NA = Data not available

*Note: includes some open pit production from the Carty deposit.

Sources

(a) MINIFILE

(b) Mineral Statistics, EMPR Mineral Policy Branch

(c) Rice (1947, 1960)

(d) National Mineral Inventory - NMI 92H/8

TABLE 2-5-3
PRODUCTION FROM VEINS - HEDLEY DISTRICT

Vein	Ore milled (t)	Gold (kg)	Silver (kg)	Copper (kg)	Lead (kg)
Maple Leaf; Pine Knot 1937	5 897	29.4	13.3	846	891
1982 (Banbury Mines Ltd.)	1 179	4.1	NA	NA	NA
Total	7 076	33.5	13.3	846	891

that generally have low garnet/pyroxene ratios, and younger skarns that have high garnet/pyroxene ratios, and contain minor tungsten and copper but little or no gold. The Mount Riordan (Crystal Peak) skarn is the largest of this second type: it is a potential industrial garnet deposit with drill-indicated reserves of 40 million tonnes averaging 78 per cent by volume garnet (Mathieu *et al.*, 1991; Grond *et al.*, 1991). Differences between the gold skarns, represented by the Nickel Plate deposit, and the garnet-dominant Mount Riordan skarn are listed in Table 2-5-1.

Gold skarns have produced over 62 tonnes of gold from 8.4 million tonnes of ore (Table 2-5-2); over 97 per cent of the gold was derived from the Nickel Plate deposit. By contrast, the quartz-carbonate veins, such as the Pine Knot, Maple Leaf and Gold Zone veins, have produced only 33 kilograms of gold (Table 2-5-3). The gold grade of the Nickel Plate ore, worked during the early underground operations, ranged from 12 to 14 grams per tonne gold, whereas the ore currently mined by open-pit methods ranges between 2 and 3.1 grams per tonne gold (Table 2-5-2). The overall grade of all the gold skarn deposits mined in the district is 7.43 grams per tonne gold.

The gold skarns are genetically and spatially related to diorite-gabbro stocks and dike-sill swarms of the Hedley intrusions. Economic gold skarns are hosted only in the Nicola Group, and on both a district and mine scale are structurally, stratigraphically and lithologically controlled. They favour areas where the Hedley intrusions cut the calcareous, shallower marine sedimentary facies of the Hedley and French Mine formations (particularly rocks that are flat lying or gently dipping) but are absent in the deeper water sediments of the Stemwinder Formation farther west (Figure 2-5-2).

Economic gold mineralization is almost wholly confined to the exoskarn, although locally the endoskarn is cut by late, thin veinlets of auriferous sulphides. Exoskarn alteration varies from narrow zones less than 10 metres wide to large envelopes hundreds of metres thick. The largest exoskarn envelope is at Nickel Plate where it outcrops over 4 square kilometres (Figure 2-5-5), is up to 300 metres thick, and is estimated to contain between 0.75 and 1.5 cubic kilometres of altered rock. Alteration is characterized by pyroxene-garnet-carbonate-scapolite assemblages, and mineralogical zoning is present in both the mineralized and barren skarns. This zoning generally consists of coarser grained garnet-rich proximal assemblages and finer grained pyroxene-rich distal assemblages (Figure 2-5-5). Gold-pyrrhotite-arsenopyrite mineralization is preferentially developed in the distal, pyroxene-dominant skarn, and is associated with a geochemical enrichment in arsenic, copper, bismuth, tellurium, cobalt, zinc, antimony, molybdenum, and nickel.

Significant geochemical and mineralogical variations are seen throughout the gold skarns. At Nickel Plate, chalcopyrite and Cu/Au ratios increase westwards towards the Hedley intrusion Toronto stock, and Au/Ag ratios are greater than 1 in the northern part of the deposit and less than 1 in the south.

Bismuth tellurides (hedleyite, tetradymite), arsenopyrite and high pyrrhotite/pyrite ratios characterize the gold ore;

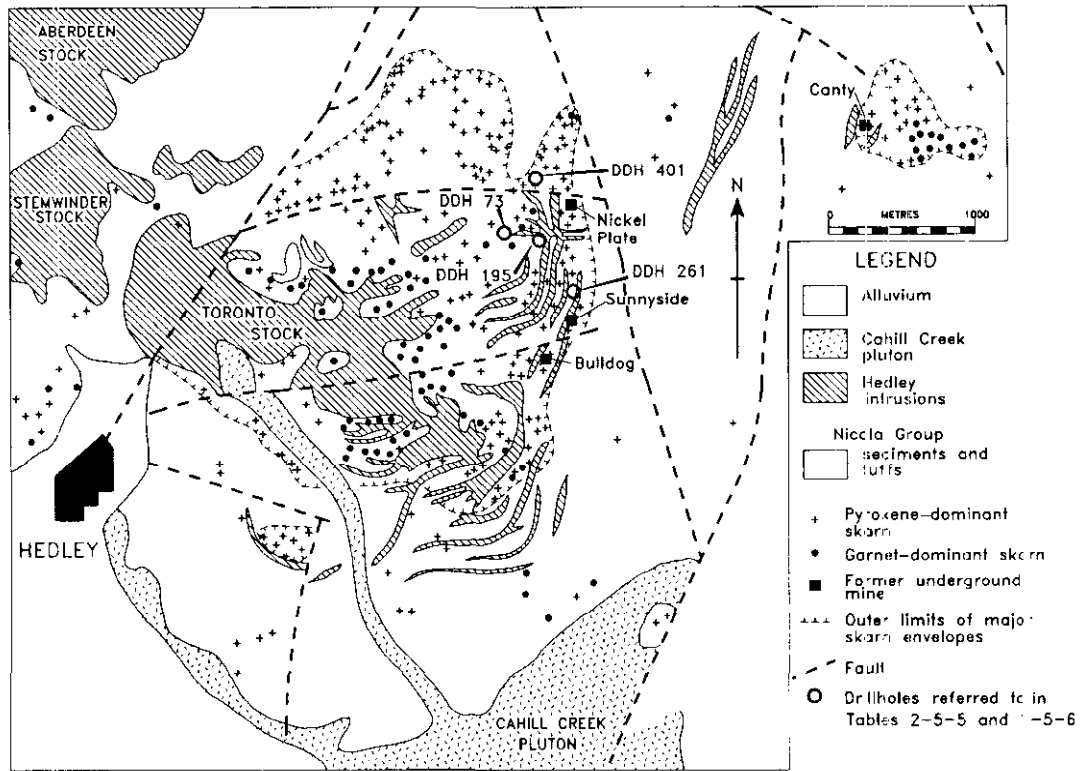


Figure 2-5-5. Outcrop distribution of the exoskarn envelopes surrounding the Nickel Plate and Canty deposits. Note: location of drillholes listed in Tables 2-5-5 and 2-5-6.

TABLE 2-5-4
CHEMICAL COMPOSITIONS OF THE HEDLEY INTRUSIONS COMPARED TO IGNEOUS ROCKS ASSOCIATED WITH BASE AND FERROUS METAL SKARNS

	SKARN DEPOSIT CLASSES													
	Au (Hedley)		Fe		Cu		Zn-Pb		W		Mo		In	
	mean	range	mean	range	mean	range	mean	range	mean	range	mean	range	mean	range
SiO ₂	54.56	(48.27-59.48)	61.5	(47.2-74.7)	63.5	(55.2-73.7)	66.2	(57.1-76.3)	68.9	(62.6-72.8)	74.8	(73.1-76.0)	76.6	(75.4-78.0)
TiO ₂	0.67	(0.51-1.04)	0.8	(0.2-3.1)	0.5	(0.0-1.0)	0.6	(0.2-1.6)	0.4	(0.1-0.7)	0.2	(0.1-0.3)	0.13	(0.01-0.04)
Al ₂ O ₃	18.49	(15.51-20.24)	17.3	(13.1-22.3)	16.6	(14.3-20.4)	15.4	(12.1-16.3)	15.5	(14.0-16.8)	14.3	(13.0-15.1)	12.6	(10.5-13.4)
Fe ₂ O ₃	1.39	(0.37-3.14)	2.0	(0.5-5.6)	1.9	(0.03-3.2)	2.1	(1.0-3.0)	1.3	(0.2-2.3)	-	-	0.4	(0.0-0.9)
FeO	5.86	(4.15-7.90)	3.8	(0.4-11.2)	2.8	(0.7-5.8)	2.4	(0.2-5.0)	2.0	(0.8-3.2)	0.5	(0.0-1.5)	1.1	(0.2-1.4)
Fe ₂ O ₃ T	7.85	(5.83-10.94)	6.2	-	5.0	-	4.7	-	3.5	-	-	-	1.5	-
MnO	0.14	(0.07-0.19)	0.1	(0.0-0.3)	0.2	(0.0-1.8)	0.1	(0.0-0.3)	0.1	(0.0-1.0)	0.03	(0.0-0.05)	0.1	(0.0-0.2)
MgO	4.00	(2.51-8.51)	2.3	(0.2-4.9)	2.2	(0.7-4.2)	1.8	(0.1-4.2)	1.1	(0.1-2.6)	0.5	(0.3-0.9)	0.1	(0.1-0.4)
CaO	8.56	(6.48-11.88)	5.7	(0.7-11.4)	4.3	(1.8-7.6)	4.0	(0.4-6.3)	3.2	(1.9-4.6)	1.2	(0.5-2.0)	0.1	0.4-0.7
Na ₂ O	3.17	(2.04-4.79)	4.4	(2.9-7.7)	3.3	(1.0-5.3)	3.5	(1.6-4.3)	3.4	(2.7-4.0)	3.1	(1.9-4.2)	2.1	(0.8-3.6)
K ₂ O	1.40	(0.53-2.54)	1.7	(0.3-3.4)	3.4	(1.3-5.4)	3.6	(2.0-5.2)	3.5	(2.4-5.4)	5.0	(2.8-7.9)	4.1	(4.2-5.0)
P ₂ O ₅	0.18	(0.14-0.26)	0.27	(0.0-0.4)	0.25	(0.0-0.4)	0.26	(0.0-0.6)	0.15	(0.1-0.3)	0.06	(0.0-0.1)	0.1	(0.0-0.03)
Fe ₂ O ₃ /FeO	0.24	(0.05-0.44)	0.53	(0.12-2.36)	0.68	(0.01-1.04)	0.87	(0.49-6.18)	0.65	(0.09-1.23)	-	-	0.0	(0.01-1.34)
K ₂ O/Na ₂ O	0.44	(0.20-0.66)	0.39	(0.05-0.85)	1.03	(0.38-1.71)	1.03	(0.53-3.06)	1.03	(0.61-1.87)	1.6	(0.67-4.16)	1.4	(1.17-6.24)
Number of samples	28		18		17		9		17		3		9	

*Data for base and ferrous metal skarns compiled by Meinert (1983)
Fe₂O₃T = Total iron as Fe₂O₃

also present throughout the ore are chalcopyrite and trace sphalerite together with traces of bismuth, nickel and cobalt minerals (native bismuth, maldonite, breithauptite, gersdorffite and cobaltite). Native gold, intimately associated with tellurides, occurs as minute blebs (maximum 25 microns across) in arsenopyrite and less commonly in pyrrhotite (Warren and Cummings, 1936). The gold-sulphide mineralization is generally coeval with widespread scapolitization (Billingsley and Hume, 1941; Dolmage and Brown, 1945; Ettliger *et al.*, 1992). The close temporal and spatial association between gold and scapolite suggests that chlorine-rich fluids may have been important in the transportation and precipitation of gold in the Hedley skarns.

The proposed model for the Nickel Plate deposit (Figure 2-5-6) involves metals being derived from the Hedley intrusions and transported by large volumes of reduced magmatic fluid into a strongly reduced calcareous sedimentary sequence. Formation of the large exoskarn envelope was accompanied by an early, high-temperature mineral sequence of (1) biotite and orthoclase, followed in turn by (2) manganese-poor, generally hedenbergitic clinopyroxene (Hd₃₅₋₉₅), and (3) grandite garnet (Ad₁₅₋₁₀₀). The overall compositional zoning in the larger Nickel Plate garnets is from grossularitic cores to andraditic margins, and both they and the pyroxene tend to have a low manganese content (<1 and 1.5 weight %, respectively). Garnets are mostly birefringent although some crystals have isotropic cores and birefringent margins. Subsequently, at lower temperatures, gold, sulphides, tellurides and scapolite, together with minerals such as prehnite, were deposited. Fluid inclusion studies (Ettliger, 1990) indicate the main pyroxene-garnet skarn at Nickel Plate formed at temperatures (pressure corrected) between 460° and 480°C, with average fluid salinities of 18.3 and 9.7 weight per cent NaCl equivalent for garnet and pyroxene, respectively. Homogenization temperatures for scapolite associated with gold and sulphide minerals were in the range of 320° to 400°C.

Compared to other magmatic rocks related to either copper, iron, tungsten, zinc-lead, molybdenum or tin skarns, the Hedley intrusions are enriched in iron and have the lowest amounts of total alkalis and silica, and highest amounts of calcium, magnesium and iron (Ray and Webster, 1991; Table 2-5-4). The coarse porphyritic textures of some of the Hedley intrusions suggest these rocks were emplaced at shallow to intermediate depths. Low Fe₂O₃/FeO ratios and the presence of ilmenite and pyrrhotite in the unaltered Hedley intrusions, and high pyrrhotite/pyrite ratios in the ore indicate that both the intrusions and the skarn-forming fluids were strongly reduced. This conclusion is also supported by the presence of iron-rich biotite (Ettliger, 1990), native bismuth and hedenbergitic pyroxene.

Skarn overprinting of the intrusions, to produce endoskarn, was accompanied by variable increases in the potassium and silica content and the K₂O/Na₂O ratios, decreases in magnesium and total iron, and sharp declines in the Fe₂O₃/FeO ratios (Table 2-5-5). Many of these chemical changes are related to the breakdown of the primary ferromagnesian minerals and their replacement by biotite, orthoclase, quartz and clinopyroxene. Initial skarn overprinting of the Nicola siltstones, with the appearance of

orthoclase, biotite and lesser albite, leads to gains in potassium and sodium (*see* DDH401, Table 2-5-6). However, as skarn alteration increases, these minerals are replaced by clinopyroxene and garnet, leading to relative losses in potassium and sodium and gains in iron, magnesium and manganese, together with increased K₂O/Na₂O ratios (*see* DDH's 195 and 261, Table 2-5-6). The dramatic decrease of iron in the Nickel Plate endoskarn with progressive skarn overprinting is matched by a corresponding increase of iron in the adjacent exoskarn. This suggests that the destruction of the magmatic ferromagnesian minerals in the intrusions led to the iron enrichment in the nearby exoskarns. Thus, these minerals are probably the main source of the iron in the ore zones and may also be the source of the gold.

TABLE 2-5-5
COMPARATIVE CHEMISTRY (USING MEAN VALUES) OF THE UNALTERED HEDLEY INTRUSIONS AND MODERATELY AND INTENSELY ALTERED ENDOSKARN IN THE NICKEL PLATE DEPOSIT

Element	Unaltered Hedley intrusions	Moderately altered endoskarn DDH401	Intensely altered endoskarn DDH195 and DDH261
SiO ₂	54.56	52.45	58.79
TiO ₂	0.67	0.71	0.52
Al ₂ O ₃	18.49	17.16	17.05
Fe ₂ O ₃	1.39	0.3	0.24
FeO	5.86	5.77	2.89
Fe ₂ O ₃ T	7.85	6.66	3.45
MnO	0.14	0.11	0.07
MgO	4.00	4.76	3.10
CaO	8.56	9.80	8.70
Na ₂ O	3.17	2.92	3.61
K ₂ O	1.40	2.54	3.33
P ₂ O ₅	0.18	0.19	0.14
LOI	1.30	1.53	1.01
Fe ₂ O ₃ /FeO	0.24	0.05	0.08
K ₂ O/Na ₂ O	0.44	0.87	1.19
No. of samples	28	9	12

Fe₂O₃T = Total iron as Fe₂O₃
For drillhole locations see Figure 2-XX-5.

TABLE 2-5-6
COMPARATIVE CHEMISTRY (USING MEAN VALUES) OF THE UNALTERED NICOLA GROUP SEDIMENTARY ROCKS AND MODERATELY AND INTENSELY ALTERED EXOSKARN IN THE NICKEL PLATE DEPOSIT

Element	Unaltered limestone	Unaltered siltstone	Moderately altered exoskarn		Intensely altered exoskarn
			DDH401		DDH195 and DDH261
SiO ₂	8.11	57.97	55.01		42.41
TiO ₂	0.03	0.35	0.55		0.27
Al ₂ O ₃	0.80	6.29	12.45		5.37
Fe ₂ O ₃	0.06	0.82	0.20		3.35
FeO	0.22	1.51	4.06		8.92
Fe ₂ O ₃ T	0.29	2.50	4.79		13.26
MnO	0.11	0.09	0.10		0.44
MgO	1.37	1.90	3.91		2.82
CaO	49.02	18.48	12.27		26.19
Na ₂ O	0.09	1.28	1.76		0.16
K ₂ O	0.15	1.17	3.76		1.30
P ₂ O ₅	0.09	0.21	0.21		0.31
LOI	39.53	9.64	3.63		6.35
Fe ₂ O ₃ /FeO	0.30	0.63	0.07		0.83
K ₂ O/Na ₂ O	1.65	1.06	5.02		36.84
No. of samples	5	6	23		29

Fe₂O₃T = Total iron as Fe₂O₃
For drillhole locations see Figure 2-XX-5.

It is postulated that a large thermal cell formed around the Nickel Plate skarn (Figure 2-5-6). This probably resulted in the influx of cooler, more oxygen-rich meteoric waters into the bottom of the system which mixed with the magmatic fluids and resulted in the deposition of sulphides and gold. Consequently, ore horizons are preferentially developed near the base and lateral margins of the alteration envelope, close to its contact with underlying limestones. By contrast, the upper and middle portions of the skarn tend to be barren (Figure 2-5-6). This zoning has relevance regarding future exploration of other, apparently barren, skarn outcrops that may mask mineralization at depth.

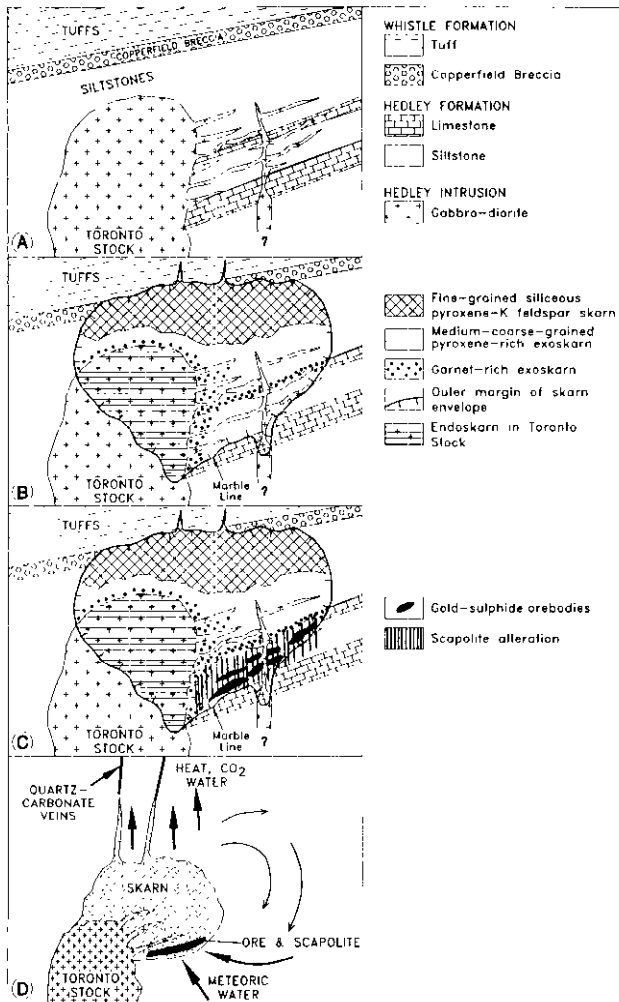


Figure 2-5-6. Schematic diagram showing postulated development of the Nickel Plate skarn envelope:

A: intrusion of the Toronto stock and associated sill-dike complex.

B: Infiltration of hydrothermal fluids to produce a 300-metre-thick, pyroxene-rich prograde skarn envelope with upper fine-grained siliceous zone. Coarser grained and garnet-dominant skarn developed adjacent to intrusions.

C and D: The formation of a large thermal cell around the skarn leads to an influx of meteoric water into the base of the system causing precipitation of the sulphide-gold-scapolite orebodies. Some quartz-carbonate veins develop along fractures above the envelope.

A district-wide, east-to-west change in the metallogeny, mineralogy and oxidation state of the skarns is suggested. Pyroxene-dominant and strongly reduced skarns containing gold, arsenopyrite and bismuth tellurides occur in the west and central parts of the district, while more oxidized tungsten-bearing and garnet-dominant skarn such as the Mount Riordan skarn occur in the east (Ray *et al.*, 1992). This zoning is partly due to the different sedimentary protoliths of the various skarns which reflect the original sedimentary facies changes in the Nicola Group across the district. It is also related to the different age and compositions of the associated intrusions responsible for the gold skarns and the Mount Riordan garnet skarn.

CONCLUSIONS

The Hedley district straddles the eastern tectonic edge of the Late Triassic Nicola back-arc basin, and its geology provides an insight into how rifting controlled the basin margin, the easterly derived sedimentation, and development of several economically important sedimentary facies. Dramatic evidence of syntectonic sedimentation is displayed in one distinct marker horizon, the Copperfield breccia, which represents a chaotic gravity-slide deposit of carbonate reefal debris. The breccia was probably derived from a shallow-marine, carbonate platform that originally lay immediately east of Hedley. Similar gravity-slide breccias could be expected to mark proximity to the eastern boundary of the Nicola basin elsewhere in British Columbia. The Copperfield breccia probably has a similar origin as the extensive modern megabreccia units that occur along the margins of low-relief carbonate platforms in the western Caribbean (Hine *et al.*, 1992).

In addition to several minor gold-bearing veins, the district contains some major gold skarn deposits as well as the Mount Riordan garnet skarn which has industrial mineral potential. The latter is associated with the 184 Ma (Early Jurassic) Mount Riordan stock whereas the gold skarns are genetically related to the slightly older Hedley intrusions. The Hedley intrusions, in comparison with other igneous rocks related to iron, copper, zinc-lead, tungsten, molybdenum and tin skarns, are the least differentiated and have the highest content of iron, magnesium, aluminum and calcium. This chemistry reflects their derivation from primitive oceanic crust in an island arc environment.

In contrast to the rarer oxidized gold skarns, such as the McCoy deposit in Nevada (Kuyper, 1987; Erockes *et al.*, 1990), and the McLymont property in northern British Columbia (Ray *et al.*, 1991), the Nickel Plate, French, Canty and Good Hope deposits represent classical reduced-type gold skarn systems. Their reduced state is demonstrated by high pyrrhotite/pyrite and low Fe_2O_3/FeO ratios in the ore, and the presence of native bismuth, iron-rich biotite and hedenbergitic pyroxene. Progressive skarn overprinting of the intrusions and calcareous siltstones at Nickel Plate is accompanied by a sharp decrease in the iron content of the endoskarn and a corresponding increase in iron in the adjacent exoskarn. It is believed that the magmatic ferromagnesian minerals in the Hedley intrusions, which were broken down during skarn alteration, were the main source of the iron enrichment in the exoskarn.

The Hedley district still has good exploration potential for gold-skarn discoveries, particularly as the Nickel Plate model suggests that some of the larger, untested and apparently barren skarn envelopes in the district may overlie mineralization at depth. While underground mining would not be economically feasible on the Nickel Plate ore currently being worked by open-pit methods, it should be remembered that the ore extracted between 1904 and 1963 by underground mining graded 12 to 14 grams per tonne gold.

The deposit model and ore controls postulated at Hedley are applicable to other areas of the Cordillera. Tectonic hinge zones marking rifted margins of island-arc or marginal basins are considered to be highly favourable for gold skarns. Such areas containing abrupt facies changes with reduced calcareous sediments and porphyritic ilmenite-bearing dioritic to gabbroic intrusions are ideal for gold skarn development. In particular, exploration should be directed to intrusions that are iron-rich (greater than 7% total iron), have low $\text{Fe}_2\text{O}_3/\text{FeO}$ ratios and are associated with pyroxene-dominant exoskarn systems containing early orthoclase-biotite alteration, high pyrrhotite/pyrite ratios, arsenopyrite, bismuth tellurides and scapolite.

ACKNOWLEDGMENTS

Part of the mapping and study costs were financed by the Canada - British Columbia Mineral Development Agreement 1985-1990. We wish to thank the management, staff and former staff of the following companies and organizations for their considerable assistance and co-operation: Homestake Canada Ltd. (formerly Corona Corporation and Mascot Gold Mines Ltd.), particularly J. Bellemy, A.H. Ransom, R. Simpson, W. Wilkinson, H.G. Ewanchuk and L.W. Saleken; Polestar Exploration Inc., particularly H.C. Grond and R. Wolfe; Banbury Gold Mines Ltd., particularly M.R. Sanford; Chevron Canada Resources Limited, particularly E. D. Dodson and L.A. Dick; and the Similkameen Indian Band, particularly Chief B. Allison and G. Douglas. M.J. Orchard and F. Cordey of the Geological Survey of Canada, identified the microfossils. The zircon U-Pb analyses were completed at the Department of Geology, The University of British Columbia, by J.E. Gabites, D. Murphy and P. Van der Hayden. Assistance in the field was given by M.E. MacLean, M. Mills and M. Fournier. Informative discussions with J.W.H. Monger, L.A. Dick, J. Hammack and the late R.L. Armstrong are appreciated. The figures were drafted by I.C.L. Webster, A.R. Pettipas and M.S. Taylor, and the paper was considerably improved by the editing of J.M. Newell.

REFERENCES

Billingsley, P. and Hume, C.G. (1941): The Ore Deposits of Nickel Plate Mountain, Hedley. B.C.; *Canadian Institute of Mining and Metallurgy*, Bulletin, Volume. 44, pages 524-590.

Bostock, H.S. (1930): Geology and Ore Deposits of Nickel Plate Mountain, Hedley, B.C.; in Summary Report 1929, Part A, *Geological Survey of Canada*, pages 198A-252A.

Bostock, H.S. (1940): Map of the Hedley Area. B.C.; *Geological Survey of Canada*, Map 568A.

Brookes, J.W., Meinert, L.D., Kuyper, B.A. and Lane, M.L. (1990): Petrology and Geochemistry of the McCoy Gold Skarn, Lander County, Nevada; in *Geology and Ore Deposits of the Great Basin*, Symposium Proceedings, *Geological Society of Nevada*, April 1990.

Camsell, C. (1910): Geology and Ore Deposits of the Hedley Mining District. B.C.; *Geological Survey of Canada*, Memoir 2.

Carr, J.M. (1968): The Geology of the Brenda Lake Area, B.C. *Minister of Mines and Petroleum Resources*, Annual Report 1967, pages 183-212.

Dawson, G.L., Godwin, C.I., Ray, G.E., Hammack, J. and Bordin, D., (1990a): Geology of the Good Hope - French Mine Area, South-central British Columbia, in *Geological Fieldwork 1989*, B.C. Ministry of Energy, Mines and Petroleum Resources, Paper 1990-1, pages 271-277.

Dawson, G.L., Godwin, C.I. and Ray, G.E. (1990b): Gold Skarn Mineralization Associated with a Sediment-sill Complex, French Mine, South-central B.C.; *Geological Association of Canada - Mineralogical Association of Canada*, Program with Abstracts, Volume 15, page A30, Annual Meeting, May 16-18 1990, Vancouver, B.C.

Dolmage, V. (1934): Geology and Ore Deposits of Copper Mountain, British Columbia; *Geological Survey of Canada*, Memoir 171.

Dolmage, V. and Brown, C.E. (1945): Contact Metamorphism at Nickel Plate Mountain, Hedley, B.C.; *Canadian Institute of Mining and Metallurgy*, Bulletin, Volume 48, pages 27-67.

Ettlinger, A.D. (1990): A Geological Analysis of Gold Skarns and Precious-metal-enriched Iron and Copper Skarns in British Columbia, Canada; unpublished Ph.D thesis, *Washington State University*, Pullman.

Ettlinger, A.D. and Ray, G.E. (1989): Precious Metal Enriched Skarns in British Columbia: An Overview and Geological Study; *B.C. Ministry of Energy, Mines and Petroleum Resources*, Paper 1989-3.

Ettlinger, A.D., Meinert, L.D. and Ray, G.E. (1992): Skarn Evolution and Hydrothermal Fluid Characteristics in the Nickel Plate Deposit, Hedley District, British Columbia; *Economic Geology*, Volume 87, pages 1541-1565.

Grond, H.C., Wolfe, R., Montgomery, J.H. and Giroux, G.H. (1991): A Massive Skarn-hosted Andradite Deposit near Penticton, British Columbia; in *Industrial Minerals of Alberta and British Columbia*, Canada, Proceedings 27th Forum on the Geology of Industrial Minerals, Banff, Alberta, Hora, Z.D., Hamilton, W.N., Grant, B. and Kelly, P.D., Editors, *B.C. Ministry of Energy, Mines and Petroleum Resources*, Open File 1991-23, pages 131-133.

Hine, A.C., Locker, S.D., Tedesco, L.P., Mullins, H.T., Hallock, P., Belknap, D.F., Gonzales, J.L., Neumann, A.C. and Snyder, S.W. (1992): Megabreccia Shedding from Modern, Low-relief Carbonate Platforms, Nicaraguan Rise; *Geological Society of America*, Volume 104, pages 928-943.

Kuyper, B.A. (1987): Geology of the McCoy Gold Deposit, Lander County, Nevada; *Symposium on Bulk Mineable Precious Metal Deposits of the Western United States*, April, 1987, Program with Abstracts, page 40.

Lee, J.W. (1951): The Geology of Nickel Plate Mountain, B.C.; unpublished Ph.D. thesis, *Stanford University*.

- Mathieu, G.I., Boisclair, M.R. and Wolfe, R., (1991): Geology, Mineralogy and Processing of Mount Riordan Garnet Ores; in *Industrial Minerals of Alberta and British Columbia, Canada, Proceedings 27th Forum on the Geology of Industrial Minerals*, Banff, Alberta. Hora, Z.D., Hamilton, W.N., Grant, B. and Kelly, P.D., Editors, *B.C. Ministry of Energy, Mines and Petroleum Resources*, Open File 1991-23, pages 135-145.
- Meinert, L.D. (1983): Variability of Skarn Deposits: Guides to Exploration; in *Revolution in the Earth Sciences – Advances in the Past Half-Century*, Boardman, S.J., Editor, *Kendall/Hunt Publishing Company*; pages 301-316.
- Milford, J.C. (1984): Geology of the Apex Mountain Group, North and East of the Similkameen River, South-central British Columbia; unpublished M.Sc. thesis, *The University of British Columbia*.
- Monger, J.W.H. (1989): Geology of Hope and Ashcroft Map Areas, British Columbia; *Geological Survey of Canada*, Map 42-1989.
- Mortimer, N. (1986): Late Triassic, Arc-related, Potassic Igneous Rocks in the North American Cordillera; *Geology*, Volume 14, pages 1035-1038.
- Mortimer, N. (1987): The Nicola Group: Late Triassic and Early Jurassic Subduction-related Volcanism in British Columbia; *Canadian Journal of Earth Sciences*, Volume 24, pages 2521-2536.
- Parrish, R.R. and Monger, J.W.H. (1992): New U-Pb Dates from Southwestern British Columbia; in *Radiogenic Age and Isotope Studies: Report 5*; *Geological Survey of Canada*, Paper 91-2, pages 87-108.
- Preto, V.A. (1972): Geology of Copper Mountain; *B.C. Ministry of Energy, Mines and Petroleum Resources*, Bulletin 59.
- Preto, V.A. (1979): Geology of the Nicola Group between Merritt and Princeton; *B.C. Ministry of Energy, Mines and Petroleum Resources*, Bulletin 69.
- Preto, V.A., Osatenko, M.J., McMillan, W.J. and Armstrong, R.L. (1979): Isotopic Dates and Strontium Isotopic Ratios for Plutonic and Volcanic Rocks in the Quesnel Trough and Nicola Belt, South-central British Columbia; *Canadian Journal of Earth Sciences*, Volume 16, Number 9, pages 1658-1672.
- Ray, G.E. and Dawson, G.L. (1987): Geology and Mineral Occurrences in the Hedley Gold Camp; *B.C. Ministry of Energy, Mines and Petroleum Resources*, Open File 1987-10, Scale 1:20 000.
- Ray, G.E. and Dawson, G.L. (1988): Geology and Mineral Occurrences in the Hedley Gold Camp; *B.C. Ministry of Energy, Mines and Petroleum Resources*, Open File 1988-6, Scale 1:25 000.
- Ray, G.E. and Dawson, G.L. (1993, in preparation): The Geology and Mineral Deposits of the Hedley Gold Skarn District, Southern British Columbia; *B.C. Ministry of Energy, Mines and Petroleum Resources*, Bulletin.
- Ray, G.E. and Webster, I.C.L. (1991): An Overview of Skarn Deposits, in *Ore Deposits, Tectonics and Metallurgy in the Canadian Cordillera*; *B.C. Ministry of Energy Mines and Petroleum Resources*, Paper 1991-4, pages 213-252.
- Ray, G.E., Dawson, G.L. and Simpson, R. (1987): The Geology and Controls of Skarn Mineralization in the Hedley Gold Camp, Southern B.C.; in *Geological Fieldwork 1986*, *B.C. Ministry of Energy, Mines and Petroleum Resources*, Paper 1987-1, pages 65-79.
- Ray, G.E., Dawson, G.L. and Simpson, R. (1988): Geology, Geochemistry and Metallogenic Zoning in the Hedley Gold Skarn Camp; in *Geological Fieldwork 1987*, *B.C. Ministry of Energy, Mines and Petroleum Resources*, Paper 1988-1, pages 59-80.
- Ray, G.E., Grond, H.C., Dawson, G.L. and Webster, I.C.L. (1992): The Mount Riordan (Crystal Peak) Garnet Skarn, Hedley District, Southern British Columbia; *Economic Geology*, Volume 87, pages 1862-1876.
- Ray, G.E., Jaramillo, V.A. and Ettlinger, A. D. (1991): The McLymont Northwest Zone, Northwest British Columbia: A Gold-rich Retrograde Skarn?; in *Geological Fieldwork 1990*, *B.C. Ministry of Energy, Mines and Petroleum Resources*, Paper 1991-1, pages 255-262.
- Read, P.B. and Okulitch, A.V. (1977): The Triassic Inconformity of South Central British Columbia; *Canadian Journal of Earth Sciences*, Volume 14, pages 1127-1145.
- Rice, H.M.A. (1947): Geology and Mineral Deposits of the Princeton Map-area, B.C.; *Geological Survey of Canada*, Memoir 243.
- Rice, H.M.A. (1960): Geology and Mineral Deposits of the Princeton Map-area, B.C.; *Geological Survey of Canada*, Memoir 243.
- Soregaroli, A.E. and Whitford, D.F. (1976): Brendt; in *Porphyry Deposits of the Canadian Cordillera*, Sutherland-Brown, A., Editor, *Canadian Institute of Mining and Metallurgy*, Special Volume No. 15, pages 186-194.
- Warren, H.V. and Cummings, J.M. (1936): Mineralogy at the Nickel Plate Mine, *The Miner*, Volume 9, pages 27-28.
- Webster, I.C.L. (1988): Skarn and Ore Mineralogy at the Hedley Amalgamated Mine, Hedley, B.C.; unpublished B.Sc. thesis *Brock University*.

NOTES

FIELD CONSTRAINTS ON DIVERSE IGNEOUS PROCESSES IN THE IRON MASK BATHOLITH (92I/9, 10)

By Lori D. Snyder and J.K. Russell
Mineral Deposit Research Unit, U.B.C.
(MDRU Contribution 022)

KEYWORDS: Petrology, Iron Mask batholith, field relationships, magmatic differentiation, hybridization.

INTRODUCTION

The Iron Mask batholith is an Early Jurassic composite alkaline intrusion located southwest of Kamloops in south-central British Columbia (Figure 2-6-1). It lies in the southern portion of the Quesnel trough in the Intermontane tectonic belt. It is a northwest-trending body approximately 22 kilometres long and 5 kilometres wide intruding volcanic and sedimentary rocks of the eastern belt of the Upper Triassic Nicola Group (Preto, 1979). Emplacement is interpreted to have been controlled by major northwesterly and northeasterly trending fault systems and previous workers have suggested that the batholith is subvolcanic and coeval with the Nicola Group (Northcote, 1977b).

Two plutons comprise the batholith; the Iron Mask pluton in the southeast, and the smaller Cherry Creek pluton in the northwest (Figure 2-6-1). The two plutons are separated by a belt 6 kilometres wide, probably a graben structure, containing Tertiary volcanics of the Kamloops Group (Kwong, 1987). Erosional remnants of these same Tertiary rocks are found overlying the batholith.

The Iron Mask batholith has historically and recently been a focus of mineral exploration for porphyry copper-gold deposits. Major deposits include the Afton and Ajax orebodies although there have also been numerous smaller producers within the batholith (Carr, 1957; Preto, 1968; Kwong, 1987). Surrounding Nicola rocks are also host to abundant copper showings.

The current nomenclature of the Iron Mask intrusive rocks derives from Preto (1968) and Northcote (1975, 1977a,b) who divided the batholith into four comagmatic intrusive rock types and a single unrelated intrusion. Their comagmatic intrusive units, listed from oldest to youngest, include Iron Mask hybrid, Pothook diorite, Sugarloaf diorite and Cherry Creek diorite-syenite. Previous workers also delineated small amounts of serpentinized picrite basalt, inferred to have intruded the Iron Mask batholith between emplacement of the Pothook and Sugarloaf phases (Northcote, 1977b). This paper maintains the names and basic subdivisions of these five map units. However, in two of the units, the Iron Mask hybrid and the Sugarloaf diorite, important mineralogical and textural variations necessitate further subdivision.

One of the main objectives of this fieldwork is to corroborate, re-evaluate and strengthen the relative age rela-

tionships between the intrusions comprising the Iron Mask batholith. Additionally, field observations and mapping have been directed at detailing the nature and origins of the enigmatic hybrid and picrite units. During the 1992 season, fieldwork by the senior author comprised reconnaissance mapping of the batholith and surrounding Nicola Group rocks and detailed mapping (1:300 and 1:2500) of five selected areas (Figure 2-6-1). These detailed geological maps (Figures 2-6-3 to 2-6-7) address several broad questions concerning the Nicola - Iron Mask relationship and the magmatic history of the batholith, which includes the formation of the hybrid and the petrologic relationships between the intrusive phases.

MAP UNITS

The five geological maps (Figures 2-6-3 to 2-6-7) portray seven major map units. A composite legend for these maps is provided in Figure 2-6-2. The following descriptions pertain to the rocks located in these map areas and also reflect reconnaissance observations.

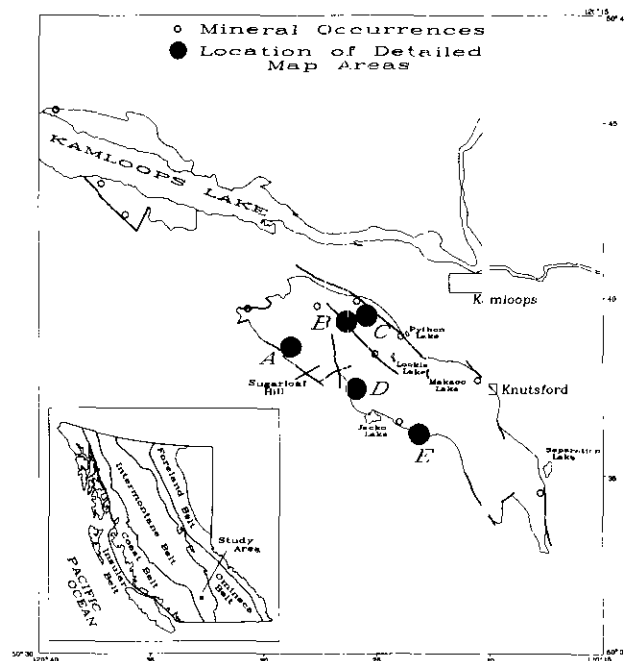


Figure 2-6-1. Location of the Iron Mask batholith showing the two separate plutons which make up the batholith and main geographical features (modified from Kwong, 1987). Inset shows tectonic setting within the Canadian Cordillera.

NICOLA GROUP

Nicola Group rocks in the vicinity of the Iron Mask batholith consist primarily of green and purple andesitic flows, flow breccias, massive tuffs, and medium and fine-grained bedded tuffs. All rock types are metamorphosed to greenschist facies. Typical assemblages include chlorite, epidote, actinolite and calcite; locally, well-developed cleavage is observed. Nicola rocks are hornfelsed adjacent to the batholith. In contrast to other workers (*e.g.*, Cockfield, 1948; Northcote, 1977b) no plutonic rock clasts with definite Iron Mask affinities were seen in Nicola Group lithologies.

PICRITE(?)

A volumetrically minor amount of serpentinized picrite basalt is found within the Iron Mask batholith. The rock consists of 15 to 30 per cent olivine phenocrysts and subor-

dinate, rarely preserved clinopyroxene microphenocrysts in a groundmass of iron oxides and serpentine and/or talc. These serpentinized picrites occur as small pods and lenses associated with fault zones. The serpentinization is pervasive and pseudomorphic and in some instances totally replaces the original mineral assemblage.

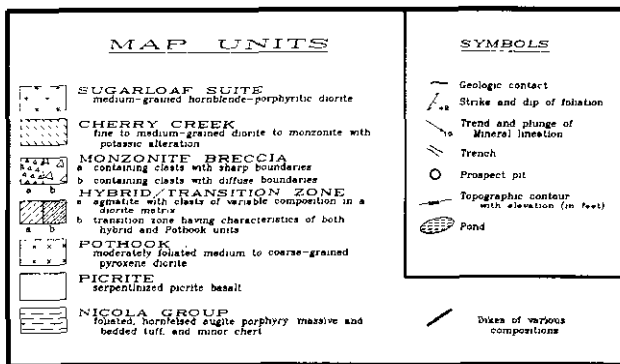


Figure 2-6-2. Map units and symbols for Figures 2-6-3 to 2-6-7.

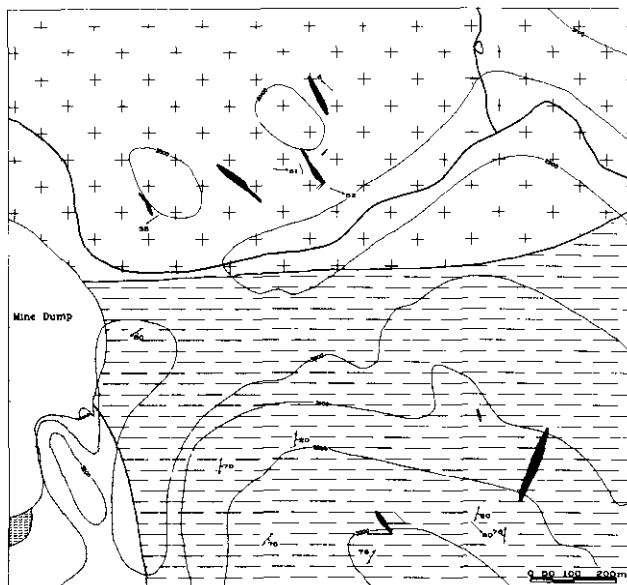


Figure 2-6-3. Map area E. This location establishes the relationship between picrite found outside the boundary of the Iron Mask batholith, Nicola Group rocks, and the Sugarloaf suite. Dikes shown on this map have been assigned to the Sugarloaf suite.

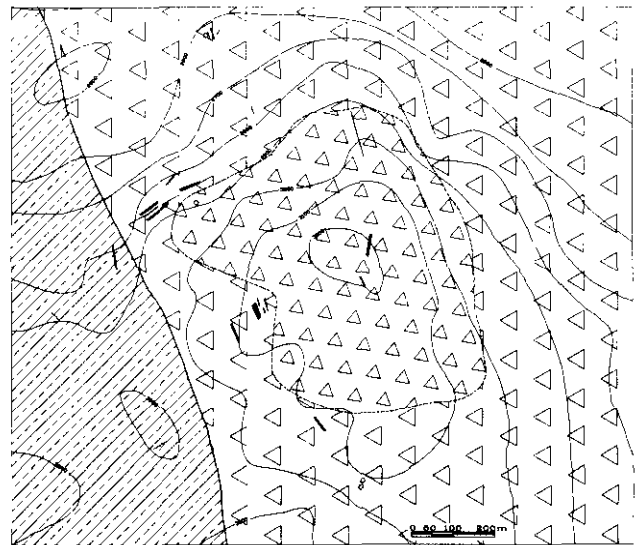


Figure 2-6-4. Map area C. This map area comprises the monzonite breccia unit. The dashed line shows the approximate boundary between clasts with sharp boundaries and clasts with diffuse boundaries.

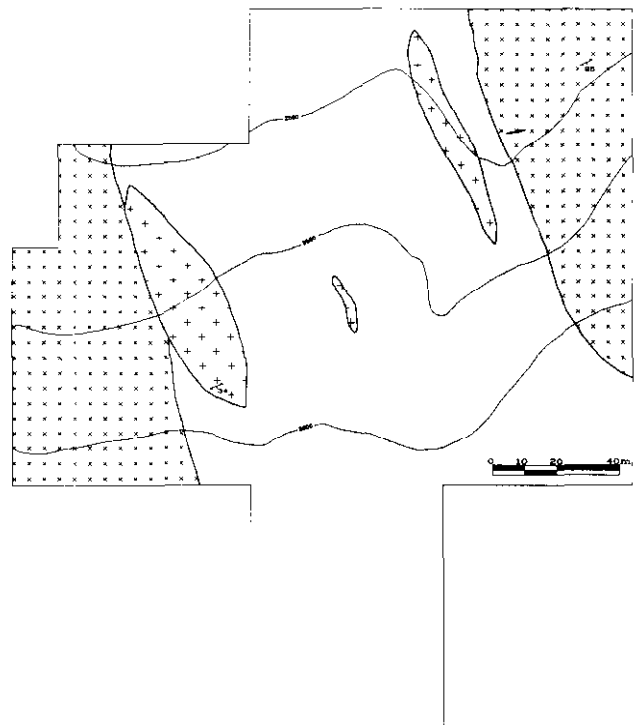


Figure 2-6-5. Map area B. Located in the north-central part of the Iron Mask pluton, this area comprises picrite basalt within the Pothook diorite. Small volumes of Sugarloaf rocks intrude the picrite.

Outside of the batholith, mineralogically and texturally similar picrite basalt is exposed at three localities. These rocks have the attribute that they are much less serpentinized and modal phenocrystic pyroxene is more commonly preserved. The first is located just outside the margin of the batholith on a small, isolated knoll southeast of Jacko Lake (Figure 2-6-3). This occurrence was mapped by Mathews (1941) as a peridotite which: "may conceivably be a part of the Nicola Formation, although similar rocks have not yet been found elsewhere in this volcanic series. On the other hand, it may represent a phase of the Ironmask batholith . . . The writer is, however, inclined to consider the peridotite as a minor intrusive unrelated to either the Nicola or Ironmask rocks." Two other occurrences are along Carabine Creek and Watching Creek on the north side of Kamloops Lake (Cockfield, 1948). Both localities are approximately 20 kilometres north-northwest of the northern contact of the Iron Mask pluton.

POTHOOK UNIT

The Pothook unit is a greenish coloured, moderately foliated, medium to coarse-grained pyroxene diorite. It generally contains poikilitic biotite on which basis it was defined. Potassic alteration in this unit is widespread and occurs mainly as well defined, potassium feldspar veinlets and, less commonly, as pervasive potassic alteration. Pothook rocks always contain abundant magnetite, mainly as disseminations and centimetre-sized veinlets. Locally, magnetite and apatite accumulations occur as dikes creating lode deposits such as the Magnet showing (Cann, 1979).

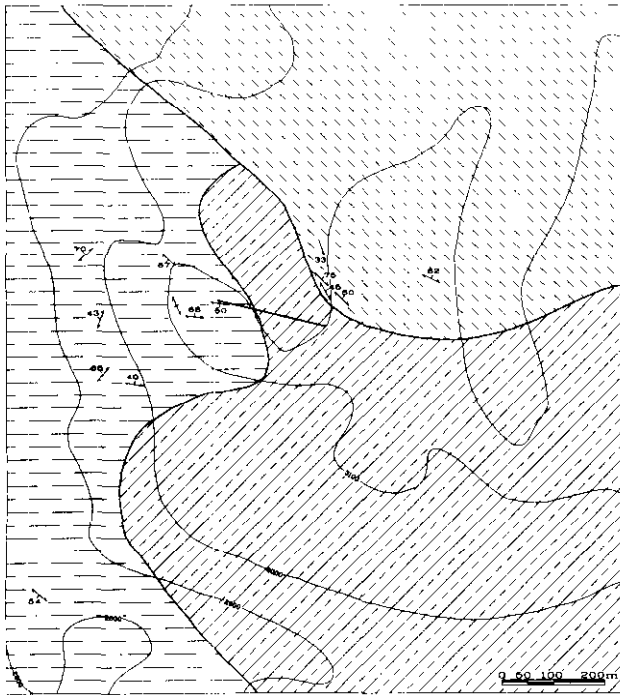


Figure 2-6-6. Map area D. Situated north of Jacko Lake, this location has exposures of the hybrid unit, Nicola Group rocks and Cherry Creek diorite which elucidate the nature of the batholith margin.

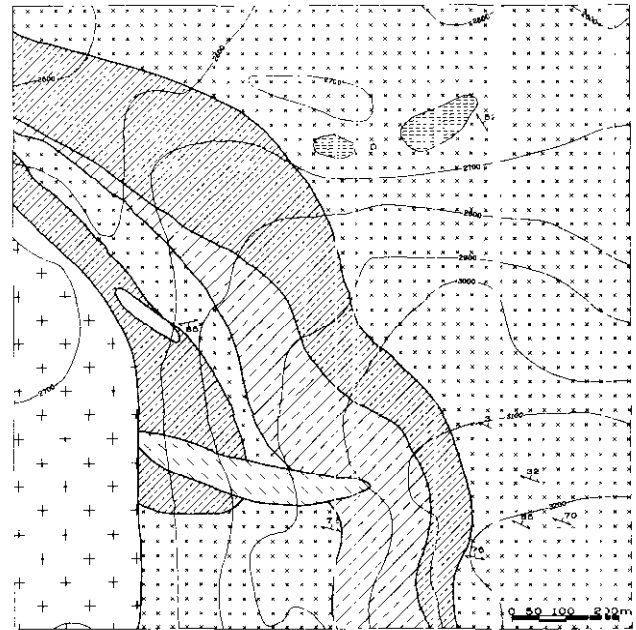


Figure 2-6-7. Map area A. This area delineates a gradational zone between the Pothook and hybrid units. Both of these units are intruded by Sugarloaf diorite.

This unit occurs as fairly small bodies in the northern part of the Iron Mask pluton roughly along the northern margins of the exposures of the Iron Mask hybrid unit. The contacts between the Pothook unit and the hybrid and Cherry Creek units are gradational.

IRON MASK HYBRID UNIT

The Iron Mask hybrid unit is of dioritic to gabbroic composition with pyroxene or hornblende ± biotite as the dominant mafic components. The textural variation in this unit is striking, ranging from fine grained to pegmatitic on an outcrop scale. In the western and central parts of the batholith, this unit is agmatitic, with clasts of coarse gabbro, medium and coarse-grained diorite, and fine-grained amphibolite in a diorite matrix. Locally, the interclast material is almost exclusively fine to coarse-grained plagioclase. In the eastern part of the batholith, the unit is more consistent in texture and composition; here it is a fine to medium-grained, unfoliated light grey diorite which contains very few clasts.

The hybrid unit is areally extensive, covering approximately one-half of the surface area of the batholith, according to Kwong's (1987) compilation. One of the results of this fieldwork is that the hybrid unit has been subdivided to allow recognition of a transitional member.

CHERRY CREEK UNIT

Rocks of the Cherry Creek unit are diorite to monzonite in composition. Generally, they are fine to medium grained and characterized by prominent, tabular, interlocking feldspar crystals. Mineralogically Cherry Creek rocks carry pyroxene, hornblende or biotite as the principal mafic phase

but never contains all three phases. Fine-grained disseminated magnetite and epidote are characteristic accessory minerals.

In addition to any primary igneous compositional variations within the Cherry Creek unit there is apparent chemical variation induced by extreme potassium metasomatism. The secondary alteration is manifest as partial replacement of the ferromagnesian minerals, complete replacement of plagioclase, and a pervasive pink coloration of weathered outcrop surfaces.

The Cherry Creek unit is distributed throughout the Iron Mask batholith but the two main bodies are the Cherry Creek pluton and along the northern margin of the Iron Mask pluton. The latter area hosts the Afton copper-gold deposit which is situated on the extreme northern contact of the Iron Mask pluton.

SUGARLOAF SUITE

The Sugarloaf unit is a suite of hornblende-porphyrific diorites occurring as lenticular bodies and dikes along the western margin of the Iron Mask pluton and in the nearby Nicola rocks. We have subdivided the suite on the basis of texture. On Sugarloaf Hill, the Sugarloaf rocks are light grey in colour, hornblende and plagioclase porphyritic with an aphanitic groundmass. Texturally the rocks are characterized by trachytic plagioclase and aligned stubby euhedral hornblende phenocrysts. A similar sized body of Sugarloaf rocks is exposed south of Sugarloaf Hill near Jacko Lake. These rocks are light tan in colour, and contain abundant, bladed hornblende phenocrysts commonly occurring as radial aggregates with rare anhedral plagioclase phenocrysts. These diorites are themselves intruded by numerous northwest-trending dikes which, on the basis of mineralogy, have also been assigned to the Sugarloaf suite (Figure 2-6-3). The dikes are dark grey, fine-grained diorite with abundant magnetite veinlets and disseminated chalcopyrite. Secondary alteration of this suite is generally minimal except within the Ajax deposit where albitization is extensive (Ross *et al.*, in press).

MONZONITE BRECCIA UNIT

The monzonite breccia unit is a volumetrically minor part of the Iron Mask batholith which has not been reported previously. The relative age relationship and chemical affinity to the rest of the batholith is uncertain. The unit consists of fragments of hybrid unit rocks ranging in size from 0.03 to 1 metre in a fine to medium-grained biotite monzonite matrix. The boundaries between fragments and matrix are sharp or diffuse with the sharpest contacts found in exposures at the highest elevations. This difference in the nature of the boundaries forms the basis of subdivision for the breccia unit as seen in Figure 2-6-4. The breccia is cut by northwest and northeast oriented, fine-grained, light grey, biotite monzonite dikes 0.5 to 15 metres wide, which generally contain clasts of hybrid rocks at their margins.

The monzonite breccia body is somewhat teardrop shaped, trending northwest and tapering off to the south near Lockie Lake (Figure 2-6-1).

DISCUSSION

Detailed geological maps for five selected areas of the Iron Mask batholith are shown in Figures 2-6-3 to 2-6-7. These areas were chosen because of relationships within the map areas that were critical to resolving a number of key research questions concerning the units and genesis of the Iron Mask batholith. Among these questions are: the nature and origin of the picrite; the nature and variation of the spatially dominant Iron Mask hybrid unit; the relationship of the batholithic units to the host Nicola Group rocks; and, the age and genetic relationships between the major batholithic units. Preliminary results are discussed below.

PICRITE – IRON MASK RELATIONSHIP

The picrite unit occurs as septa, pendants and xenoliths within Iron Mask batholithic rocks and has been intruded by Sugarloaf suite rocks (Figure 2-6-5). In addition, it has been observed that the inclusions of picrite occur in the Iron Mask hybrid unit (Northcote, 1977b) and that it predates mineralization at the Ajax East pit (Ross *et al.*, in press). Therefore, the picrite unit is interpreted to be older than the batholith.

The occurrences of picrite outside the batholith have not been subjected to greenschist facies metamorphism, lack a penetrative fabric and are always found structurally overlying Nicola Group rocks (*e.g.*, Figure 2-6-3). North of Kamloops Lake picrite basalts are overlain by Tertiary Kamloops Group rocks. These observations indicate that the picrite basalts cannot be correlated with the Nicola Group and that they are probably younger. The age of this unit is therefore postulated to be post-Nicola and pre-Sugarloaf.

These interpretations conflict with several previous ideas. Firstly, the tentative correlation between the Watching Creek - Carabine Creek ultramafic rocks and the Iron Mask batholith made on the 1:250 000 Ashcroft map sheet (Monger and McMillan, 1989) is not supported. Secondly, the picrite basalts do not represent a series of plutonic bodies intruding the Iron Mask (*e.g.*, Northcote, 1977b).

NATURE OF THE IRON MASK HYBRID

The Iron Mask hybrid unit comprises approximately 40 per cent of the outcrop of the batholith. The contact features of Nicola rocks and hybrid unit are illustrated by Figure 2-6-6. At this location, the Nicola rocks are hornfelsed fine-grained tuffs and augite porphyry. Closer to the contact, the Nicola rocks are coarsely recrystallized and contain abundant secondary(?) magnetite. Finally, at the contact, coarsely recrystallized Nicola rocks are intruded and brecciated by diorite.

Figure 2-6-7 illustrates the nature of the relationship between the Iron Mask hybrid unit and the Pothook unit. The spatial association and mineralogical similarity of these two units has already been described. Typically, they are separated by a zone of intermediate characteristics, which, if present, may be up to 250 metres wide. This transition zone comprises two end-members: partially digested mafic igneous fragments hosted in a diorite (Pothook) matrix; and foliated, fine to coarse-grained, biotite hornblende diorite

with fewer fragments. The latter end-member is distinguished from the Pothook unit by the presence of hornblende and from the hybrid unit by the presence of poikilitic biotite.

Textural and mineralogical variation within the hybrid unit is dramatic and increases with clast abundance. The clast boundaries are generally nebulous and irregular with plagioclase grains commonly growing across them. The matrix can be granitic to pegmatitic in texture. Matrix material is highly variable in plagioclase content and locally is anorthositic.

These field observations record a sequence of steps associated with the generation of hybrid rocks. These steps include: the interaction of Nicola Group rocks with intrusive rocks of the Iron Mask batholith, the incorporation and disaggregation of older (Nicola?) materials into the batholith, the partial assimilation and recrystallization of these materials and, finally, the contamination and crystallization of the original magmatic material.

YOUNGEST PHASE OF THE IRON MASK PLUTON

Previous workers have argued that the Cherry Creek unit is the youngest phase of the Iron Mask batholith (*e.g.*, Preto, 1968; Northcote, 1977b). This premise was founded on the presence of fine-grained dioritic dikes which were observed to cut all other intrusive rocks. These dikes, especially prominent in the vicinity of the Ajax property northeast of Jacko Lake, have historically been correlated with the Cherry Creek unit, thereby giving the Cherry Creek a young age by association. The correlation between these late felsic dikes and rocks of the Cherry Creek unit is subjective in that it is based on macroscopic features alone. The affinity of these late dikes can be tested further with petrography, mineral and rock chemistry, and isotopes (MDRU, in preparation). The implication is that the Cherry Creek unit probably is not as young as the late felsic dikes commonly referred to as Cherry Creek dikes (*e.g.*, Ross *et al.*, 1992).

Contacts between the Cherry Creek and Pothook units are not commonly exposed, however, there is sufficient exposure in areas near Makaoo Lake and north of Sugarloaf Hill to suggest that the contacts are gradational. This observation, together with the mineralogical and textural similarities of these units, implies a closer petrologic relationship than previously described. This would suggest that these two units are close together in age and previous workers have always considered the Pothook unit to be one of the older intrusive phases of the batholith. Furthermore, if the Cherry Creek and the Pothook are similar in age and character it is unlikely that the age of Sugarloaf suite, which is petrologically dissimilar, lies between them in time.

CONCLUSION

In view of the work conducted during the field season, a tentative reordering of the relative age relationships of the Iron Mask units is proposed. The proposed sequence of events for the major phases of the batholith is: 1) Nicola

volcanic phase, 2) magmatism generating rocks of picritic composition, 3) Pothook/hybridization event followed very shortly by or consanguineous with, 4) the Cherry Creek event, and 5) intrusion of the Sugarloaf phase.

Further data in the form of detailed petrography, major, minor, trace, and rare-earth element chemistry of each of the above described units is in progress. Relevant mineral compositions will also be determined. These laboratory data will aid in describing and constraining the processes involved in the genesis of the Iron Mask batholith. Tests for cogenetic affinity and the processes of differentiation, partial melting and assimilation will be investigated using these data.

ACKNOWLEDGMENTS

Funding for this study was supplied by Natural Sciences and Engineering Research Council, the Science Council of British Columbia, and industry through the Mineral Deposit Research Unit at The University of British Columbia on the research project "Copper-Gold Porphyry Deposits of British Columbia."

REFERENCES

- Cann, R.M. (1979): Geochemistry of Magnetite and the Genesis of Magnetite-Apatite Lodes in the Iron Mask Batholith, British Columbia: unpublished M.Sc. thesis, *The University of British Columbia*, 196 pages.
- Carr, J.M. (1957): (Copper) Deposits Associated with the Eastern Part of the Iron Mask Batholith near Kamloops, B.C. *Minister of Mines Annual Report 1956*, pages 47-69.
- Cockfield, W.E. (1948): Geology and Mineral Deposits of Nicola Map-area, British Columbia: *Geological Survey of Canada*, Memoir 249, 157 pages.
- Kwong, Y.T.J. (1987): Evolution of the Iron Mask Batholith and its Associated Copper Mineralization; *B.C. Ministry of Energy, Mines and Petroleum Resources*, Bulletin 77, 55 pages.
- Mathews, W.H. (1941): Geology of the Iron Mask Batholith; unpublished M.Sc. thesis, *The University of British Columbia*, 42 pages.
- Monger, J.W.H. and McMillan, W.J. (1989): Geology, Ashcroft, British Columbia: *Geological Survey of Canada*; Map 42-1989, Sheet 1, Scale 1:250 000.
- Northcote, K.E. (1975): Geology of the Northwest Half of the Iron Mask Batholith; in *Geological Fieldwork 1974 B.C. Ministry of Energy, Mines and Petroleum Resources*, Paper 1975-1, pages 22-26.
- Northcote, K.E. (1977a): Geology of the Southeast Half of the Iron Mask Batholith; in *Geological Fieldwork 1976 B.C. Ministry of Energy, Mines and Petroleum Resources*, Paper 1977-1, pages 41-46.
- Northcote, K.E. (1977b): Preliminary Map No. 16 (Iron Mask Batholith) and accompanying notes; *B.C. Ministry of Energy, Mines and Petroleum Resources*, 8 pages.
- Preto, V.A. (1968): Geology of the Eastern Part of the Iron Mask Batholith; *B.C. Minister of Mines and Petroleum Resources*, Annual Report 1967, pages 137-147.
- Preto, V.A. (1979): Geology of the Nicola Group between Merritt and Princeton; *B.C. Ministry of Energy, Mines, and Petroleum Resources*, Bulletin 69, 90 pages.

Ross, K.V., Dawson, K.M., Godwin, C.I. and Bond, L. (1992): Major Lithologies of the Ajax West Pit, an Alkalic Copper-Gold Porphyry Deposit, Kamloops, British Columbia; *in* Current Research, Part A, *Geological Survey of Canada*, Paper 92-1A, pages 179-183.

Ross, K.V., Dawson, K.M., Godwin, C.I. and Bond, L. (in press): Major Lithologies and Alteration of the Ajax East Orebody, a Sub-alkalic Copper-Gold Porphyry Deposit, Kamloops, South Central British Columbia; *in* Current Research, *Geological Survey of Canada*.

ADVANCED ARGILLIC ALTERATION IN BONANZA VOLCANIC ROCKS, NORTHERN VANCOUVER ISLAND — TRANSITIONS BETWEEN PORPHYRY COPPER AND EPITHERMAL ENVIRONMENTS (92L/12)

By Andre Panteleyev and Victor M. Koyanagi

KEYWORDS: Economic geology, Bonanza volcanics, porphyry copper, copper-gold, epithermal, advanced argillic, acid sulphate, alunite, hydrothermal alteration, mineralization.

INTRODUCTION

Hydrothermally altered Bonanza volcanic rocks in the Quatsino map area (NTS 92L/12) were examined in order to describe the style of copper-gold mineralization in the extensive zones of argillic and advanced argillic alteration that occur in the area. This work is part of a province-wide study of intrusion-related advanced argillic, acid sulphate mineralization started in 1991 (Panteleyev, 1992). It is intended to investigate the potential for precious metal and copper-gold deposits in these settings and to develop genetic models.

Magmatic hydrothermal systems associated with sub-volcanic porphyry intrusions can produce mineralization ranging from high-level porphyry copper to near-surface epithermal and hot-spring types. Between the deep and shallow hydrothermal levels is a 'transitional' environment in which strongly saline, relatively high temperature hydrothermal fluids of largely magmatic origin are active. These robust fluids are not representative, in a strict sense, of either porphyry copper or most epithermal systems. The associated mineral deposits and alteration are characterized and recognized by the presence of phyllic and/or (high-temperature) advanced argillic alteration and abundant sulphide minerals in a distinctive mineral suite. The copper and precious metal ores, in addition to abundant pyrite, may contain chalcocite, covellite, bornite and chalcopyrite as well as arsenic and antimony minerals, typically enargite/luzonite and tetrahedrite/tennantite and minor sphalerite, galena, arsenopyrite, gold and numerous other complex sulphosalt minerals. Characteristic gangue consists of abundant silica with kaolinite, dickite, sericite/illite, pyrophyllite, diaspore, alunite, barite and various other aluminous, sulphate and phosphate minerals including zunyite ($Al_{13}Si_5O_{20}(OH,F)_{18}Cl$). The mineralization has been variably referred to as *acid sulphate*, *high sulphidation*, *quartz-alunite*, *alunite-kaolinite* (pyrophyllite), *enargite-type*, *Nansatsu-type* and a number of other names. This type of mineralization can be considered to be a distinct deposit type or a subset of epithermal deposits (White, 1991).

The hydrothermally altered rocks typically contain quartz and vuggy to massive, residual 'slaggy' silica with kaolinite, dickite, alunite and, in some cases pyrophyllite, diaspore and zunyite. This alteration assemblage forms in zones of acid sulphate alteration, a product of sulphuric acid

leaching. The sulphuric acid is formed in three ways, as summarized by Rye *et al.* (1992): as a product of magmatic vapour-derived SO_2 interaction with water - a potentially mineralizing magmatic-hydrothermal setting; a steam-heated system where H_2S is oxidized to sulphuric acid above the water table - usually an unmineralized zone, common in geothermal settings; and a supergene leaching environment. The alteration zones produced by these three processes can be large and visually striking. However discovery of ore is a difficult task unless the origin of the alteration and the depth-zoning relationship of the hydrothermal systems are understood.

Mineral deposit types found to date in advanced argillic Bonanza rocks in northern Vancouver Island include the Island Copper mine, Hushama/Mount McIntosh (EXPO) and the Red Dog porphyry copper-gold-molybdenum deposits. In addition, a number of large siliceous zones with advanced argillic alteration have been explored in the Wanokana River - Pemberton Hills area and regions both to the east and west. These mineralized environments, among others in the province, are similar to a number of the high-level Andean (Sillitoe, 1991a) and southwest Pacific porphyry copper and related deposits with advanced argillic overprints (Sillitoe, 1989, 1991b). Potential for ore in this environment also occurs in deposits far removed from plutons, such as the structurally controlled high-grade veins at El Indio, Chile, the lithologically controlled replacement bodies at Lepanto, Philippines and the bulk mineable breccia zones at El Tambo, Chile. The extensive silica-clay replacement bodies at the tops of the high-level hydrothermal systems have been mined in Japan for ceramic materials. Some Japanese silica deposits such as in the Nansatsu district, are known to contain or be underlain at slight depth by both bulk-mineable and bonanza-type precious metal mineralization Izawa (1991).

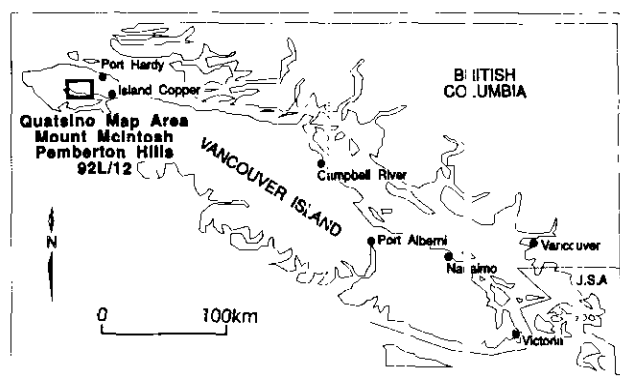


Figure 2-7-1. Location map.

THE BONANZA VOLCANIC BELT, QUATSINO MAP AREA

STRATIGRAPHY AND LITHOLOGIES

We mapped an area of about 125 square kilometres in the west-central part of Quatsino map area, between Nahwitti Lake on the north and Holberg Inlet on the south (Figure 2-7-1). Mapping was focused mainly in the northwest-trending belt of Lower Jurassic Bonanza Group volcanics and Jurassic Island Plutonic Suite. To the north, the Bonanza rocks are underlain by older rocks, part of the Upper Triassic Vancouver Group. This underlying unit comprises, in sequence, progressively older rocks of the Parson Bay, Quatsino and Karmutsen formations. In the south of the map area, along Holberg Inlet, are patches of sedimentary rocks of the Lower Cretaceous Longarm Formation, part of the Kyuquut Group. A simplified geological map of the area is shown on Figure 2-7-2.

Bonanza volcanics of northwestern Vancouver Island have been described in some detail by Muller *et al.* (1974) and Muller (1977). The rocks are generally considered to be

andesitic to rhyodacite lava, tuff (and) breccia (Muller and Roddick, 1983). These volcanic units are exemplified by the apparently bimodal basalt-rhyolite assemblage near Quatsino Sound in the Mahatta Creek map area (NTS 92L/5), described by Nixon *et al.* (1993, this volume). In contrast, our mapping to the north, in the Quatsino map area, shows the volcanic assemblage to consist almost entirely of pyroxene-phyric basalt and pyroxene-plagioclase-phyric basaltic andesite flows, breccia and minor tuffaceous sediments. Only one small area with rhyodacite and rhyolite was noted in the succession: it is probably part of a local flow-dome complex. The mainly basaltic rocks in the volcanic belt north of Holberg Inlet are similar to the lithologies farther to the east in the Rupert Arm area near the Island Copper mine. The geology there is described by Northcote (1971), Northcote and Robinson (1973) and Cargill *et al.* (1976).

In our map area the Middle to Upper Triassic Karmutsen Formation consists of a succession of thick flows, dikes or sills and some pillow basalt, pillow breccia and tuff. Local intercalation of limestone towards the top of the unit is reported elsewhere (Muller *et al.*, 1974). The top of the unit

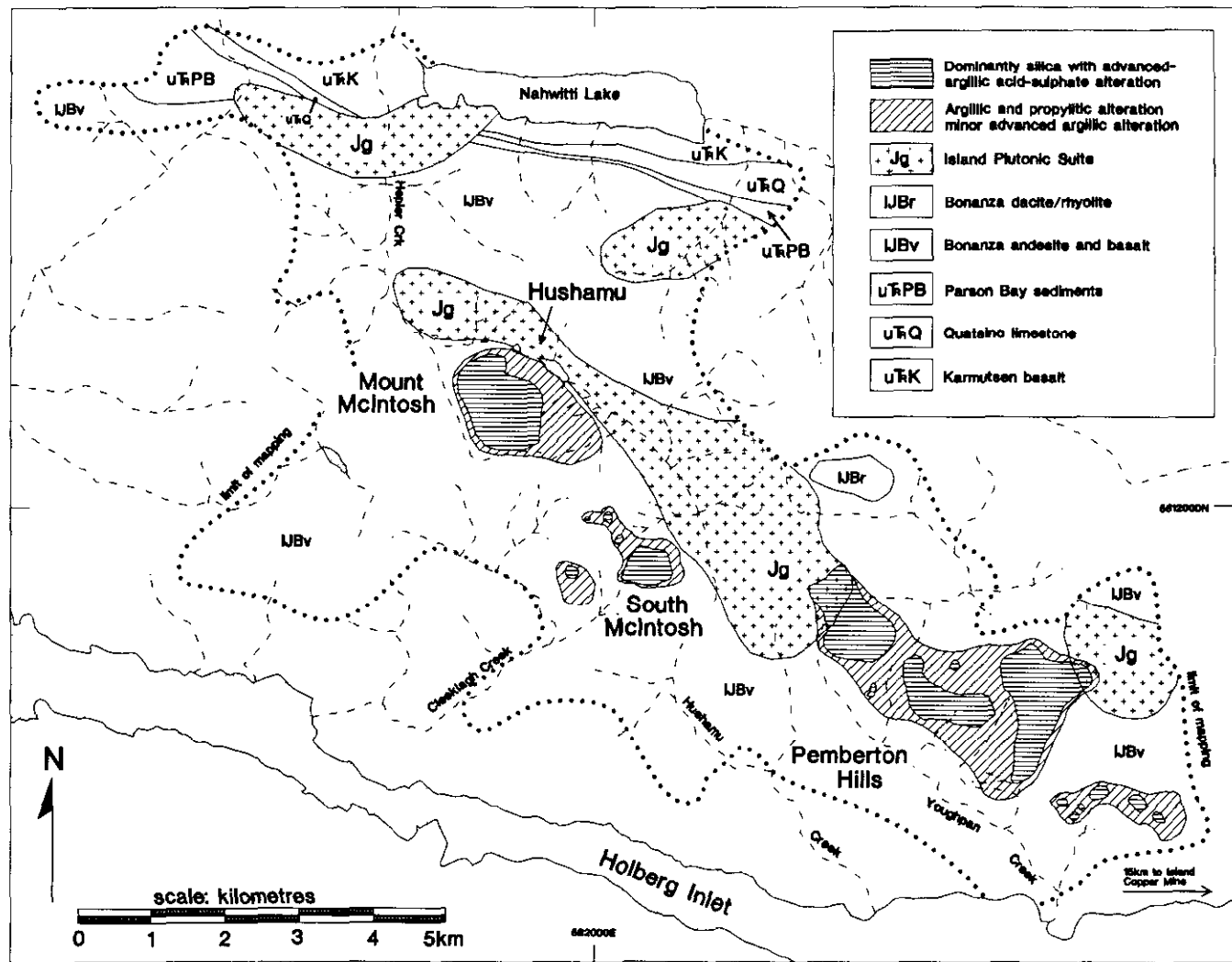


Figure 2-7-2. Generalized regional geology map with alteration patterns, part of NTS 92L/12.

is marked by a paraconformable contact with Quatsino limestone. The thick-bedded to massive, grey to black limestone grades upward into the Upper Triassic Parson Bay Formation that consists of thin-bedded to finely laminated dark grey argillite, shale and siltstone. These rocks are extensively intruded and altered to a calcisilicate assemblage throughout the Nahwitti Lake area. Muller *et al.* (1974) state that thicknesses of the Quatsino and Parson Bay units are up to 760 metres and 600 metres, respectively. In our map area both the units appear to be considerably thinner. The base of the overlying Lower Jurassic Bonanza Formation is difficult to establish precisely because the lower units of the Bonanza Formation consist of thin-bedded, tuffaceous sediments. These differ only slightly in appearance from the Parson Bay beds. The distinction between the units is, therefore, largely arbitrary when rock outcroppings are examined. The boundary between the two map units is further complicated by the presence of large intrusive bodies and the altered nature of the rocks, especially the calcisilicate members of the Parson Bay. We considered that the base of the Bonanza Formation is marked by the first presence of (chloritic) volcanic detritus; this seems to coincide with the presence of volcanic dust and ash-tuff beds and pyroxene basalt sills or flows in the Bonanza succession. The basal part of the Bonanza succession can be regarded as a transition from mixed sedimentary, volcanoclastic and tuffaceous deposition to dominantly volcanic conditions with pyroclastic, flow and lesser volcanoclastic accumulations. Fahey (1979) has estimated a thickness of about 1200 metres for the Bonanza volcanics near the Island Copper mine.

Rocks of the Island Plutonic Suite in the map area are medium-grained quartz diorite to porphyritic granodiorite

stocks, with minor but economically important quartz feldspar porphyry dikes. A comagmatic relationship with the Bonanza volcanics is suggested by their compositions, contact relationships and range of Jurassic radiometric K-Ar dates (Muller *et al.*, 1974). Rubidium-strontium isochron ages of 174 ± 10 Ma reported by Muller (1977) and 180 Ma obtained by R.L. Armstrong (J. Fleming, personal communication, 1992) provide the strongest support for an Early to Middle Jurassic age of magmatism.

CHEMICAL COMPOSITIONS

Descriptions by Muller *et al.* (1974) of 19 samples from the Cape Parkins section, Alert Bay - Cape Scott map area, on the map sheet to the south of our study area, suggest an overall andesitic composition for Bonanza volcanics with lesser dacite, rhyodacite and minor basalt. A calcalkaline petrogenetic character is interpreted, but some sodium enrichment due to albitization is recognized.

The chemical compositions of 17 of the least-altered rocks in our map area are listed in Table 2-7-1 and illustrated on Figure 2-7-3; an additional 11 hydrothermally altered rocks are also shown to portray the effects of hydrothermal alteration. The analyses are representative of the abundance and distribution of compositional types in the map area. The rocks are mainly basalt and basaltic andesite. The less common samples of rhyolite and dacite were collected from one area, a ridge in the northern part of the map area that probably represents a flow-dome centre. Chemical compositions shown on the total alkali-silica (TAS) diagram indicate subalkalic, possibly tholeiitic rocks.

Both the Karmutsen and the basal part of the Bonanza Formation contain abundant pyroxene basalts of similar

TABLE 2-7-1
WHOLE-ROCK MAJOR OXIDE PETROCHEMICAL DATA

SAMPLE	Map Unit*	Rock Type**	Eastng	Northing	SiO ₂	TiO ₂	Al ₂ O ₃	Fe ₂ O ₃ ***	MnO	MgO	CaO	Na ₂ O	K ₂ O	P ₂ O ₅	LOI	Total	CO ₂	S	F+D
Unaltered																			
92AP01/1-1	1	1	578214	5612680	51.90	0.83	17.67	8.17	0.18	2.96	7.89	3.24	1.36	0.24	4.77	99.21	2.20	0.004	5.38
92AP01/2-2	1	1	578159	5611115	50.79	1.01	17.09	9.54	0.19	2.91	9.47	2.75	0.22	0.20	5.25	99.42	2.10	0.001	4.81
92AP01/5-53	1	1	578534	5612376	51.47	0.80	17.50	9.12	0.19	4.50	7.74	3.05	1.04	0.20	3.69	99.30	0.40	0.004	5.15
92AP8/5-30	1	1	576128	5617652	46.37	0.81	15.34	10.13	0.17	10.09	10.94	1.52	0.85	0.12	2.93	99.27	0.20	0.01	7.79
92AP5/8-18	1	1	581873	5616109	51.65	0.75	18.19	8.84	0.16	5.25	9.21	3.28	0.67	0.15	1.28	99.43	0.07	0.10	6.42
92AP01/5-5	1	2	578644	5611570	54.14	0.86	16.60	8.13	0.16	2.60	5.01	3.42	1.25	0.17	7.16	99.50	0.20	0.001	2.16
92AP13/10-68	1	2	582167	5611310	55.28	0.86	18.74	6.80	0.27	2.44	7.52	3.15	1.13	0.19	3.07	99.45	1.00	0.11	4.02
92AP20/8-128	1	2	586784	5609612	54.36	0.81	15.97	8.05	0.19	4.94	3.65	3.04	1.95	0.15	6.22	99.33	1.17	0.04	3.98
92AP21/7-132	1	2	589941	5608133	53.48	0.78	15.95	8.36	0.25	5.88	6.63	2.66	1.80	0.15	3.55	99.49	0.70	0.003	4.98
92AP16/1-77	1	2	586791	5610934	53.64	0.83	17.54	8.52	0.16	3.01	7.31	3.05	1.72	0.23	1.76	99.77	0.40	0.014	3.88
92VK08-1	1	2	585921	5611889	54.46	0.77	17.49	8.60	0.20	3.57	7.61	2.84	1.32	0.23	2.64	99.73	0.10	0.10	4.88
92VK08-4	1	3	585900	5612159	74.22	0.27	13.05	2.09	0.11	0.86	1.72	3.27	1.87	0.08	1.84	99.38	0.07	0.24	0.84
92AP16/7-83	1	3	585130	5612360	69.80	0.30	14.60	2.52	0.12	1.34	2.40	3.32	2.86	0.07	2.05	99.38	0.00	1.09	1.00
92AP07/1-27	2	1	578376	5617526	48.68	2.33	13.19	14.34	0.29	6.21	10.63	2.63	0.27	0.19	0.65	99.41	0.00	0.007	5.06
92AP22/1-140	2	1	579223	5618229	49.22	1.51	16.79	11.01	0.18	5.71	11.14	2.84	0.23	0.12	0.82	99.57	0.07	0.013	7.97
Spilitized Matched Pair																			
92AP19/2-119	1	1	586779	5608443	49.23	0.90	19.21	9.01	0.19	3.05	10.03	2.63	0.44	0.20	4.45	99.34	1.70	0.003	5.06
92AP19/2-120	1	4	586779	5608443	48.34	0.86	17.76	9.22	0.26	3.26	6.09	5.24	0.31	0.19	7.94	99.47	2.30	0.006	5.46
Hydrothermally Altered																			
91AP41a	1	4	580931	5613075	73.80	0.83	18.67	0.08	0.00	0.00	0.08	0.00	0.01	0.12	5.05	99.64	0.00	0.05	0.00
91AP20/6-95	1	4	580931	5613075	96.34	1.67	0.95	0.17	0.00	0.00	0.01	0.00	0.00	0.01	0.59	99.74	0.00	0.02	0.00
92AP19/1-109	1	4	587379	5609236	60.54	1.11	15.49	10.63	0.00	0.00	0.17	0.00	0.01	0.23	11.22	99.40	0.10	8.16	0.00
92AP19/1-110	1	4	587379	5609236	70.16	1.45	18.65	1.34	0.00	0.02	0.16	0.00	0.01	0.20	7.42	99.41	0.20	0.19	0.00
92AP19/1-111	1	4	587379	5609236	86.24	2.04	2.03	7.94	0.00	0.00	0.03	0.00	0.00	0.04	2.53	100.85	0.20	0.10	0.22
92AP19/1-112	1	4	587379	5609236	93.90	2.81	2.13	0.74	0.00	0.00	0.03	0.00	0.00	0.03	1.12	100.76	0.07	0.036	0.17
92AP19/1-113	1	4	587379	5609236	63.66	0.84	17.06	7.09	0.00	0.25	0.16	0.00	1.36	0.20	9.06	99.68	0.10	5.78	0.07
92AP19/1-114	1	4	587379	5609236	66.68	0.67	12.92	8.55	0.00	0.21	0.14	0.00	1.51	0.21	8.38	99.27	0.00	6.87	0.07
92AP19/1-115	1	4	587379	5609236	63.38	1.05	6.95	7.47	0.13	2.46	6.11	0.30	0.36	0.11	13.81	99.13	3.40	6.99	0.37
92AP19/1-116	1	4	587379	5609236	54.59	0.94	15.51	7.46	0.11	5.78	3.36	1.01	1.13	0.21	9.11	99.21	0.80	1.72	0.23
92AP19/1-117	1	4	587379	5609236	56.74	0.83	16.02	8.44	0.17	4.48	3.56	2.62	2.60	0.17	3.60	99.23	0.20	0.57	0.15
92AP19/1-118	1	4	587379	5609236	55.84	0.83	15.84	8.38	0.08	4.30	4.54	2.29	1.07	0.17	5.92	99.26	0.80	1.82	0.00

* Map Unit: 1 = Bonanza volcanics; 2 = Karmutsen basalt;

** Rock Type Classification from TAS diagram: 1 = basalt; 2 = basalt/andesite; 3 = rhyolite/dacite; 4 = hydrothermally altered

*** Fe₂O₃ = total iron

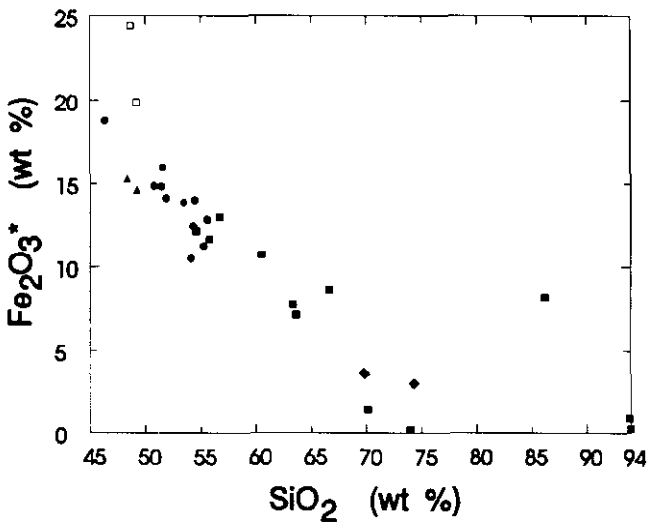
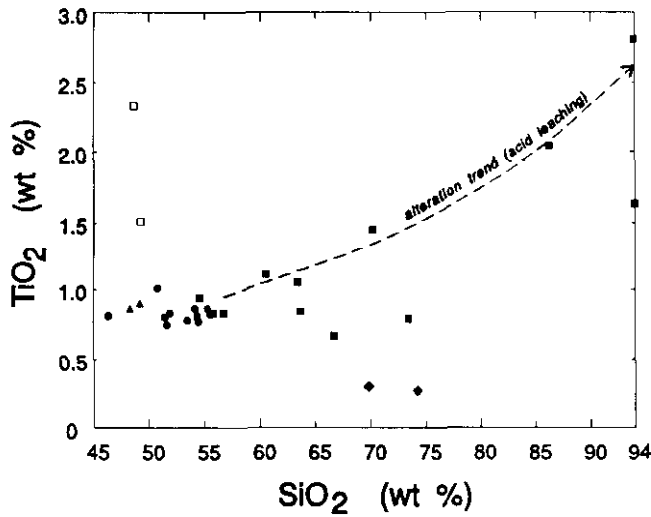
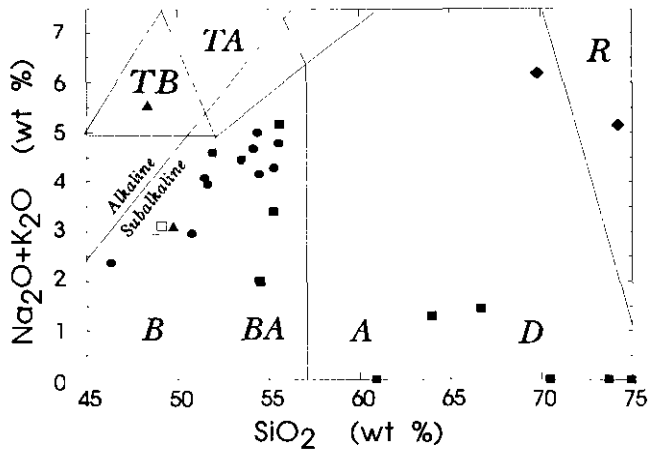


Figure 2-7-3. Whole-rock petrochemical plots. List of symbols: empty square = Karmutsen basalt; circle = Bonanza basalt/andesite; diamond = Bonanza rhyolite/dacite; triangle = spilitized Bonanza basalt; square = hydrothermally altered Bonanza volcanics.

appearance. The two units can be distinguished on the basis of TiO_2 content. It appears that Bonanza rocks contain less than 1 per cent TiO_2 and Karmutsen rocks have more than 1.5 per cent. The effects of large-scale spilitization are shown by a pair of samples (119 and 120, triangles on Figure 2-7-3). In the field, spilitized rocks that appear to predate the more intense argillic hydrothermal alteration can be recognized in the map area by their pronounced pervasive greenish cast and the abundance of chlorite and epidote. The effects of more intense hydrothermal alteration are profound base leaching with resulting silicification and (residual) alumina and titania increases. Chemical compositions of some hydrothermally altered rocks are shown as square symbols on Figure 2-7-3.

STRUCTURE

All the Bonanza rocks in the map area dip moderately to the south or southwest. The notable exception is in the Youghpan Creek area where an abundance of flat-lying sedimentary and tuffaceous beds is noted. These rocks possibly mark the site of a graben or caldera-like structure that disrupted the continuity of volcanic lava deposits along the trend to the volcanic arc. The bounding structures have

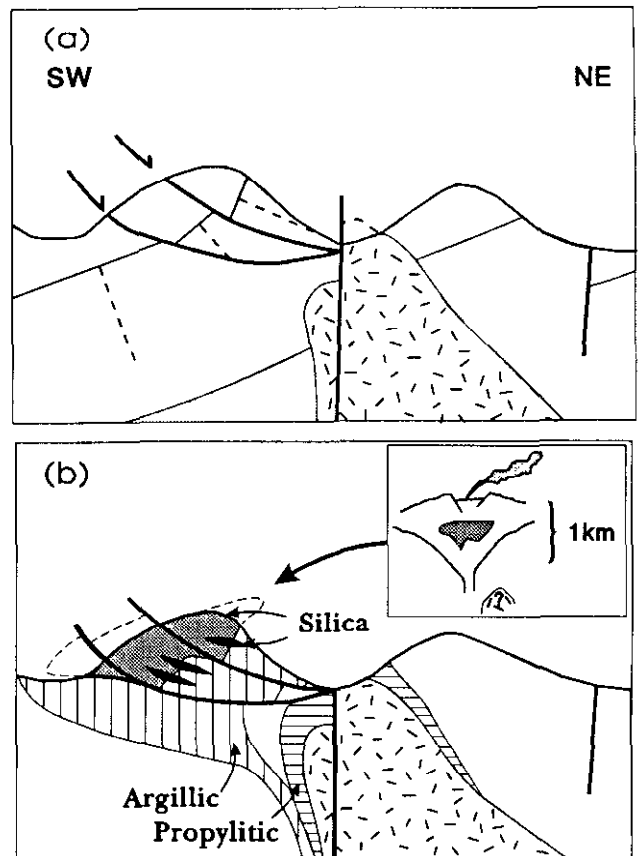


Figure 2-7-4. Structural style, diagrammatic cross-section; (a) large-scale fault block displacements of south and southwesterly dipping beds results in exposure of similar lithologies and stratigraphy in the map area; (b) tilting and low-angle normal faulting of hydrothermally altered rocks result in compression (telescoping) of alteration zones.

apparently acted as channelways for hydrothermal fluids as the bedded rocks are extensively and, in some cases, pervasively clay-altered.

The major regional structures are high-angle faults. The most prominent, and evidently the older, structural trends are west-northwest. The north to northeasterly trending structures are probably considerably younger. The northwesterly trending faults control the major valleys in the area and appear to bound fault blocks in which displacements are upward on the southwest side. Consequently everywhere in the map area it appears that the exposed rocks represent the basal, basaltic part of the Bonanza section. No other type of structural repetition of stratigraphic units is evident. A diagrammatic cross-section (Figure 2-7-4) illustrates the structural style and manner of juxtaposition of the structural and stratigraphic blocks in the map area. Some higher stratigraphic units are exposed on ridges in the southern part of the map area. There amphibole-bearing basaltic andesites occur in coarse breccia, lithic lapilli tuff and debris-flow slump-type deposits. The presence of carbonaceous wood fragments and the laharic appearance of some units suggests near-shore to subaerial depositional conditions.

HYDROTHERMAL ALTERATION

Porphyry copper-molybdenum-gold mineralization and hydrothermal alteration at Island Copper mine have been described by Cargill *et al.* (1976), Fleming (1983), Perello (1987) and Perello *et al.* (1989). Ore is associated with a high-level quartz feldspar porphyry dike, but is most extensively developed in the surrounding, brecciated Bonanza rocks. The mineralization and alteration took place during a series of hydrothermal events in which there was multiple overprinting of early-formed assemblages by later ones. The early alteration consists of stockworks carrying quartz, magnetite, amphibole and albite with later biotite, magnetite, chalcopyrite, pyrite, molybdenite and chlorite with peripheral epidote. An intermediate stage of structurally controlled quartz stockworks with sericite, chlorite, kaolinite and intermediate clay minerals is superimposed on the older alteration, together with some additional pyrite, chalcopyrite and molybdenite. A late-stage alteration is associated with emplacement of hydrothermal breccias containing an advanced argillic alteration assemblage with kaolinite, pyrophyllite, sericite and dumortierite. All these centrally located and relatively early alteration types are flanked by chlorite and epidote-bearing rocks and are overlapped by veinlets with carbonate minerals, zeolites and hydrocarbon compounds.

The alteration and style of mineralization at the Hushamu deposit is similar in many respects to the early magnetite-bearing alteration at the Island Copper mine but appears to be related to a large intrusive body of quartz diorite. Adjoining and to the south of the Hushamu deposit, hydrothermal alteration on Mount McIntosh consists of argillic and advanced argillic assemblages containing quartz stockworks with flanking propylitic Bonanza rocks around a core of pervasively silicified to vuggy siliceous rocks, 1 kilometre wide. The Mount McIntosh siliceous rocks contain kaolinite, zunyite, diaspore, pyrophyllite, alunite, abundant pyrite and locally enargite with traces of chalcopyrite,

covellite, chalcocite and bornite (J. Perello and J. Fleming, personal communication, 1992). This alteration represents mineralization related to the Hushamu porphyry deposit but at a higher structural level. Mineralization appears to have taken place in a telescoped, that is, a compressed hydrothermal system. Late low-angle normal faults in the Hushamu area have tilted and further contracted the underlying porphyry body and the higher level alteration zones on the west, as illustrated diagrammatically on Figure 2-7-4.

Argillic and siliceous altered Bonanza rocks similar to those at Mount McIntosh also form large, resistant ridges or 'ledges' up to a kilometre long in the South McIntosh, Pemberton Hills and Wanokara River areas to the east-southeast of Hushamu and Mount McIntosh. The zones of siliceous clay alteration outline a belt of advanced argillic, argillic and flanking propylitic alteration at least 8 kilometres in length. The rocks are of exploration interest for their potential for epithermal gold-silver deposits and buried porphyry copper-gold mineralization. The silicified zones consist of both residual, acid leached, vuggy porous rocks as well as hydrothermally silicified rocks. In addition to abundant silica, the rocks contain kaolinite, dickite, pyrophyllite, white micaceous minerals including sericite, illite and paragonite, abundant alunite (mainly natroalunite), zunyite and locally native sulphur. In one quartz stockwork native gold was observed to occur together with alunite, possibly an arsenian variety, schlossmacherite. The amount of sulphide minerals in these altered rocks varies from trace amounts to patches and lenses of massive, fine-grained pyrite. Large areas of argillic, silicified rock containing between 5 and 10 per cent, and locally up to 30 per cent, fine-grained disseminated pyrite with lesser marcasite are common. Weathering and leaching of the pyritic rocks is actively taking place. Surface waters and streams in the vicinity of the hydrothermally altered rocks are markedly acidic. For a discussion of natural acidic waters in the area see the accompanying discussion by Koyanagi and Panteleyev (1993, this volume).

DISCUSSION

The presence of advanced argillic, acid sulphate hydrothermal alteration containing quartz-kaolinite-alunite-pyrophyllite with diaspore and zunyite mineral assemblages is confirmed in large areas of hydrothermally altered Bonanza rocks in the Quatsino map area north of Holberg Inlet. Mineralization of the acid sulphate or high sulphidation type is present containing enargite, some chalcopyrite and minor chalcocite, covellite, bornite with **an abundance of pyrite**. The deposits resemble relatively high temperature, acid fluid related 'Temora' type high sulphidation epithermal gold deposits as described by Thonson *et al.* (1986) and White (1991). The siliceous, argillic and advanced argillic zones are also similar to the high-level silica-clay caps found in the Nansatsu district of Japan (Izawa, 1991). The intrusive-related mineralization and some of the fracture-controlled sericite-rich quartz-pyrite alteration assemblages bear a closer affinity to intrusion-related porphyry copper-gold and porphyry gold mineralization. Similar deposits with phyllic alteration elsewhere are the Thorn property in northwestern British Columbia (NTS

104K) and the La Joya deposit (Inti Raymi mine), Bolivia (Long *et al.*, 1992).

The siliceous, hydrothermally altered rocks in the Quatsino map area can be referred to as siliceous caps but they are not siliceous sinters (subaerial deposits). White (1991) considers from genetic models based on the equivalent Nansatsu deposits that the tops of the siliceous bodies form at depths of 200 to 300 metres below the surface. The vertical extent of the siliceous bodies might be up to 1000 metres. Sillitoe (1993, in press) describes siliceous sinter as a product of subaerial geothermal systems. He contrasts this to the deeper origin of siliceous caps that form at or near the paleo-watertable. Sillitoe considers that the lensoid or planar siliceous caps can be up to 50 metres in thickness. Clearly the north Vancouver Island siliceous caps are larger than this, probably because they have a strong vertical to subvertical structural component related to hydrothermal channelways from porphyry intrusions at depth. As well there is additional potential for stratabound and bedding plane replacement deposits in these environments that remains to be tested.

The types of exploration targets in the large clay-silica altered zones are elusive. Certainly no ore is evident at surface in the well-exposed, resistant and topographically high-weathering siliceous zones. Erratic small silicified patches with high-grade gold can be expected to occur in narrow hydrothermal conduits that form breccias and vuggy quartz veins, for example, in outcroppings on the west bank of Youghpan Creek and the more widespread quartz stockworks on McIntosh Mountain. Most likely, the large clay-silica alteration zones might be leakage from deeper porphyry copper-gold deposits. Deeper mineralized zones contained within the silica caps, as in the Nansatsu district, Japan with aggregate resource of 1.5 million tonnes with 4.4 grams per tonne gold and 8.5 grams per tonne silver (Izawa, 1991) might be economically marginal in British Columbia, especially if the deposits are not oxidized and therefore refractory. However ore in structurally controlled high-grade veins that are hydrothermal feeder zones or fluid conduits, as at El Indio, Chile, are superb discoveries (Jannas *et al.*, 1990). Also stratigraphic (lithologic) permeability possibly combined with structurally controlled massive sulphide replacements such as the auriferous enargite deposits of Lepanto, Philippines and the nearby intrusion and breccia-related Far Southeast porphyry copper-gold deposit (Garcia, 1991) would be highly attractive exploration targets in this environment.

ACKNOWLEDGMENTS

It is a pleasure to acknowledge the assistance in the field and access to information provided by John Fleming, Island Copper mine; Peter Dasler, Daiwan Engineering Limited on behalf of Jordex Resources; and Jose 'Pepe' Perello, Minera BHP de Chile. We particularly benefitted from the discussions and insights these individuals shared with us and we value highly the interest they show in this project.

REFERENCES

Cargill, D.G., Lamb, J., Young, M.J. and Rugg, E.S. (1976): Island Copper; in *Porphyry Copper Deposits of the Canadian Cor-*

- dillera, Sutherland Brown, A., Editor. *Canadian Institute of Mining and Metallurgy*, Special Volume 15, pages 206-218.
- Fahy, P.L. (1979): *The Geology of Island Copper Mine*, Vancouver Island, British Columbia; unpublished M.Sc. thesis, *University of Washington*, Seattle, 52 pages.
- Fleming, J. (1983): *Island Copper*; in *Mineral Deposits of Vancouver Island*, *Geological Association of Canada*. Field Trip Guidebook, pages 21-35.
- Garcia, J.S., Jr. (1991): *Geology and Mineralization of the Mankayan Mineral District, Benguet, Philippines*; in *High-temperature Acid Fluids and Associated Alteration and Mineralization*, *Geological Survey of Japan*, Report Number 277, pages 21-30.
- Izawa, E. (1991): *Hydrothermal Alteration associated with Nansatsu-type Gold Mineralization in the Kasuga Area, Kagoshima Prefecture, Japan*; in *High-temperature Acid Fluids and Associated Alteration and Mineralization*, *Geological Survey of Japan*, Report 277, pages 49-52.
- Jannas, R.R., Beane, R.E., Ahler, B.A. and Brosnahan, D.R. (1990): *Gold and Copper Mineralization at the El Indio Deposit, Chile*; in *Epithermal Gold Mineralization of the Circum-Pacific: Geology, Geochemistry, Origin and Exploration, II*; *Journal of Geochemical Exploration*, Volume 36, Number 1-3, pages 233-266.
- Koyanagi, V.M. and Panteleyev, A. (1993): *Natural Acid Drainage in the Mount McIntosh - Pemberton Hills Area, Northern Vancouver Island, NTS 92L/12*; in *Geological Fieldwork 1992*, Grant, B. and Newell, J.M., Editors, *B.C. Ministry of Energy, Mines and Petroleum Resources*, Paper 1993-1, this volume.
- Long, K.R., Ludington, S., du Bray, E.A., Orlando, A.R. and McKee, E. (1992): *LaJoya District*; in *Geology and Mineral Resources of the Altiplano and Cordillera Occidental, Bolivia*; *U.S. Geological Survey*, Bulletin 1975, pages 131-136.
- Muller, J.E. (1977): *Evolution of the Pacific Margin, Vancouver Island and Adjacent Regions*; *Canadian Journal of Earth Sciences*, Volume 14, pages 2062-2085.
- Muller, J.E., Northcote, K.E. and Carlisle, D. (1974): *Geology and Mineral Deposits of Alert Bay - Cape Scott Map-area, Vancouver Island, British Columbia*; *Geological Survey of Canada*, Paper 74-8, 77 pages.
- Muller, J.E. and Roddick, J.A. (1983): *Alert Bay - Cape Scott*; *Geological Survey of Canada*, Map 1552A.
- Nixon, G.T., Hammack, J.L., Hamilton, J. and Jennings, H. (1993): *Preliminary Geology of the Quatsino Sound Area, Northern Vancouver Island, 92L/5*; in *Geological Fieldwork 1992*, Grant, B. and Newell, J.M., Editors, *B.C. Ministry of Energy, Mines and Petroleum Resources*, Paper 1993-1, this volume.
- Northcote, K.E. (1971): *Rupert Inlet - Cape Scott*; in *Geology, Exploration and Mining in British Columbia 1970*, *B.C. Ministry of Energy, Mines and Petroleum Resources*, pages 254-258.
- Northcote, K.E. and Robinson, W.C. (1973): *Island Copper Mine*; in *Geology, Exploration and Mining in British Columbia 1970*, *B.C. Ministry of Energy, Mines and Petroleum Resources*, pages 293-303.
- Panteleyev, A. (1992): *Copper-Gold-Silver Deposits Transitional Between Subvolcanic Porphyry and Epithermal Environments*; in *Geological Fieldwork 1991*, Grant, B. and Newell, J.M., Editors, *B.C. Ministry of Energy, Mines and Petroleum Resources*, Paper 1992-1, pages 231-234.

- Perello, J. A. (1987): The Occurrence of Gold at Island Copper Mine, Vancouver Island, British Columbia; unpublished M.Sc. thesis, *Queen's University*, 85 pages.
- Perello, J.A., Arancibia, O.N., Burt, P., Clark, A.H., Clarke, C., Fleming, J., Himes, M.D., Leitch, C. and Reeve, A. (1989): Porphyry Cu-Mo-Au Mineralization at Island Copper, Vancouver Island, B.C.; *Geological Association of Canada Cordilleran Section, Porphyry Copper Workshop*, Vancouver, April 1989, Abstract.
- Rye, R.O., Bethke, P.M. and Wasserman, M.D. (1992): The Stable Isotope Geochemistry of Acid Sulfate Alteration; *Economic Geology*, Volume 87, pages 225-262.
- Sillitoe, R.H. (1989): Gold Deposits in the Western Pacific Island Arcs: The Magmatic Connection; *Economic Geology*, Monograph 6, pages 274-291.
- Sillitoe, R.H. (1991a): Regional Setting of Epithermal Gold Deposits, Chile; *Economic Geology*, Volume 86, pages 1174-1186.
- Sillitoe, R.H. (1991b): Intrusion-related Gold Deposits; in *Metallogeny and Exploration of Gold*; Foster, R.P., Editor, *Blackie and Sons*, Glasgow, pages 165-209.
- Sillitoe, R.H. (1993): Epithermal Models: Genetic Types, Geometric Controls and Shallow Features; in *IJGS/UNESCO Deposit Modeling Program Conference*, Ottawa 1990, Proceedings Volume, *Geological Association of Canada*, in press.
- Thompson, J.F.H., Lessman, J. and Thompson, A.J.B. (1986): The Temora Gold-Silver Deposit: A Newly Recognized Style of High Sulfur Mineralization in the Lower Paleozoic of Australia; *Economic Geology*, Volume 81, pages 732-738.
- White, N.C. (1991): High Sulfidation Epithermal Gold Deposits: Characteristics and a Model for their Origin; in *High-temperature Acid Fluids and Associated Alteration and Mineralization*, *Geological Survey of Japan, Report 277*, pages 9-20.

NOTES



GEOLOGY AND ALTERATION OF THE MOUNT POLLEY ALKALIC PORPHYRY COPPER-GOLD DEPOSIT, BRITISH COLUMBIA (93A/12)

By Theresa M. Fraser, Colin I. Godwin, John F.H. Thompson and Clifford R. Stanley
Mineral Deposit Research Unit, U.B.C.
(MDRU Contribution 021)

KEYWORDS: Economic geology, porphyry Cu-Au, Mount Polley, Quesnellia, breccia, alteration, alkaline, calc-potassic, propylitic.

INTRODUCTION

The Mount Polley deposit in south-central British Columbia (52°30'N, 121°35'W) is an alkaline porphyry copper-gold deposit (Hodgson *et al.*, 1976). The deposit, located 56 kilometres northeast of Williams Lake, is accessible from Highway 97 at 150 Mile House by 90 kilometres of secondary paved road.

Imperial Metals Corporation (Gorc *et al.*, 1992) has estimated geological reserves at 48.8 million tonnes grading

0.383 per cent copper and 0.556 gram per tonne gold in the proposed S19 open pit (Figure 2-8-1A).

Fieldwork was undertaken to study alteration zoning and its relationship to the various rock units. This was accomplished by detailed surface mapping, logging of eleven drill holes on a cross-section, and logging of 10-metre intervals from 105 drill holes at piercing points through the 1110-metre elevation, which is approximately 100 metres below the surface. Lithologies, hypogene alteration and associated mineralization are described. Preliminary statistical analyses and related plots are presented; these illustrate the spatial relationship of alteration mineral assemblages and rock types. Supergene characteristics are ignored in this paper.

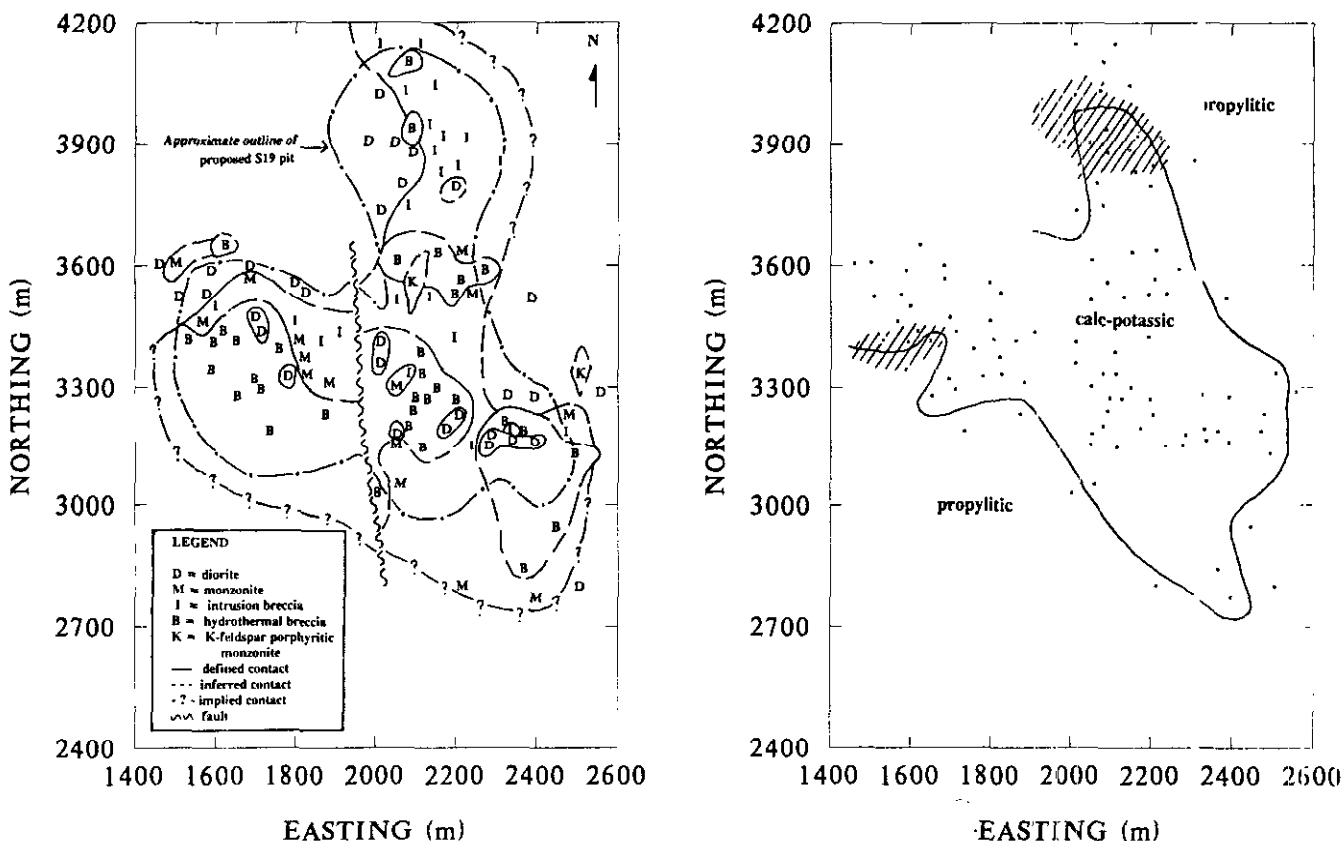


Figure 2-8-1. Geology and alteration at the 1110-metre plan level, Mount Polley, south-central British Columbia. This level is about 100 metres below the surface. (A) Rock units are plotted at drill-hole piercing points. Post-mineral dikes have been removed. Diorite outside the pit boundary may contain minor volcanic screens. (B) Distribution of the calc-potassic and propylitic alteration zones. The core of the system is characterized by a copper-gold (chalcopyrite±bornite), potassium feldspar, magnetite, diopside±albite assemblage. A peripheral propylitic zone defines a pyrite, epidote and albite assemblage. Hatched areas represent regions of overlap. The dashed-dot line is the surface outline of the proposed S19 pit.

EXPLORATION HISTORY

Copper showings were first documented at Mount Polley in 1964 during investigation of an aeromagnetic anomaly by Mastodon - Highland Bell Mines Limited and Leitch Gold Mines Limited. From 1966 to 1972 Cariboo - Bell Copper Mines Limited drilled 215 holes and conducted geophysical surveys, mapping, geochemistry and trenching. In 1979 Teck Corporation drilled six percussion holes. During 1981 and 1982, E & B Explorations Inc. confirmed and expanded the tonnage of low-grade copper-gold mineralization by drilling 42 additional holes, following ground geophysical and soil geochemistry surveys. E & B was joined by Imperial Metals Corporation in a joint venture that drilled a further 22 holes and conducted magnetometer, induced polarization, VLF-EM and soil geochemistry surveys (Imperial Metals Corporation, 1989). Imperial Metals Corporation acquired the Mount Polley property in 1988, and conducted an extensive diamond drilling program over 1988 and 1989 that totaled 238 holes. Six bulk samples were collected from surface trenches for metallurgical testing. A total of 528 drill holes (61884 metres) have been completed since 1964 (Gorc *et al.*, 1992).

REGIONAL GEOLOGY

The deposit is located within Quesnellia on the eastern margin of the Intermontane Belt. This part of Quesnellia consists of a sequence of volcanic units that dip east to northeast 5 kilometres west of the property, and dip predominantly to the west or southwest 4 kilometres east of the property (Bailey, 1987). The volcanic rocks include flows, breccias and tuffs. Volumetrically the most important are augite-porphyrific basalts to trachybasalts that locally form pillowed units. Less common are purple and maroon poly-mictic volcanic breccias, and green crystal and lapilli tuffs. An analcite-bearing flow and flow breccia are interpreted to be the youngest volcanic units in the area (Bailey, 1987).

An extensive intermediate to alkaline intrusive complex is exposed in the Bootjack - Polley Lakes area, more or less at the centre of the synclinorium that defines Quesnellia in this region. The complex is divisible into two major bodies both of which intrude a variety of volcanic rock types. A diorite intrusion, with lesser monzonite and pyroxenite, forms the hills between Polley and Bootjack lakes. This body hosts the Mount Polley deposit (Figure 2-8-1A). Three kilometres south of the deposit the diorite is intruded by a large alkaline stock. This body varies upwards, west to east, from pseudoleucite syenite porphyry through crowded orbicular syenite porphyry to granophyric syenite. The orbicules consist of pseudoleucite cores with concentric overgrowths of potassium feldspar and range up to 4 centimetres in diameter. Granophyric syenite partially overprints orbicular textures. This, combined with the concentration of granophyre in the upper part of the intrusion, apparently reflects fluid build-up during late crystallization. The granophyric syenite contains xenoliths of diorite. Thus, the granophyre is closely related in age to mineralization. It may be a source for hydrothermal fluids.

DEPOSIT GEOLOGY

The Mount Polley deposit lies within the diorite intrusive complex between Bootjack and Polley lakes. It is hosted largely by breccias of various types and related intrusive phases. Breccias and mineralization are cut by post-mineral intrusions, the most prominent being a swarm of augite porphyry dikes. Veinlet copper-gold mineralization is concentrated within the breccias and the associated alteration zone. Figure 2-8-1 represents the generalized geology and distribution of units at the 1110-metre elevation. Post-mineral dikes have been removed. A prominent north-striking fault (Hodgson *et al.*, 1976) separates the deposit into two zones, the west and central zones of the proposed S19 pit. Rock types are described from oldest to youngest.

Diorite is homogeneous, equigranular, medium to dark grey and fine grained. It consists of up to 70 per cent plagioclase and varying percentages of biotite, green pyroxene and finely disseminated magnetite. Xenoliths of volcanic country rock occur locally. Peripheral to the deposit, the diorite is relatively fresh with only minor (<5%) crosscutting albite veins with potassium feldspar envelopes. Within the deposit, diorite is characteristically pervasively flooded with potassium feldspar (up to 25%) and amphibole-diopside-magnetite veinlets with pink potassium feldspar envelopes.

Monzonite and intrusion breccia are complexly related and intrusive into the diorite. They occupy the centre of the proposed pit. The intrusion breccia has a monzonite matrix and is dominated by rounded to subangular fragments and blocks of diorite that range from 3 centimetres to 12 metres in diameter. Fragments of volcanic rock occur locally. The breccia is matrix supported and locally contains up to 35 per cent clasts. The monzonite is characterized by 40 per cent rounded plagioclase phenocrysts, about 1 millimetre in diameter, in a fine-grained matrix dominated by pink potassium feldspar with lesser pyroxene and magnetite, and traces of biotite. In the strongly brecciated areas, the matrix of the monzonite is interpreted to be largely secondary with intense pink potassium feldspar alteration. Larger areas of homogeneous monzonite are pinkish grey in colour and plagioclase has a seriate texture.

Hydrothermal breccia occurs in three main areas at the plan level. These are generally at the contact between diorite and monzonite or intrusion breccia. The breccia is polyolithic and is characterized by clasts of diorite, monzonite and intrusion breccia. It is therefore younger than the intrusion breccia. Hydrothermal breccia weathers recessively because of intense alteration and is poorly exposed at surface. In drill core, more compact phases of the breccia are mottled with potassium feldspar and pale albite. This obliterates primary textures and clast boundaries. Hydrothermal breccia is characteristically vuggy and porous. Coarse-grained secondary biotite, prismatic albite crystals (up to 1.5 cm long), and fine-grained magnetite and diopside commonly fill vugs.

The hydrothermal breccia is syn-mineral and is strongly stockworked with chalcopyrite + diopside + magnetite ± amphibole veinlets. The matrix also contains finely dissemi-

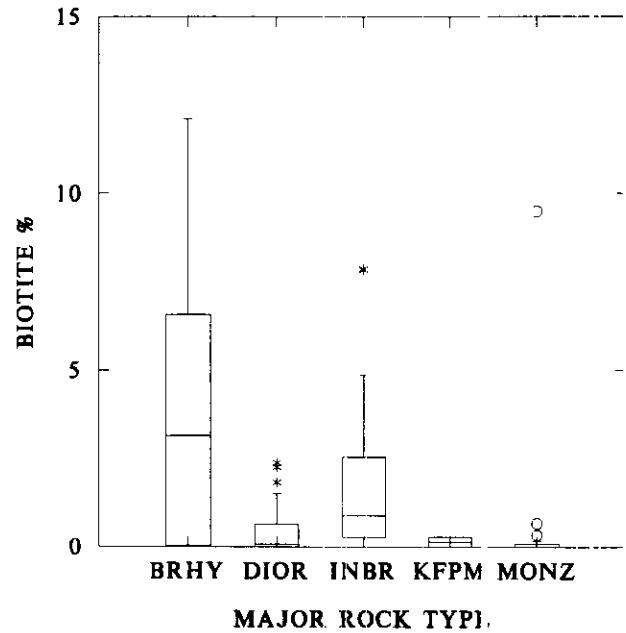
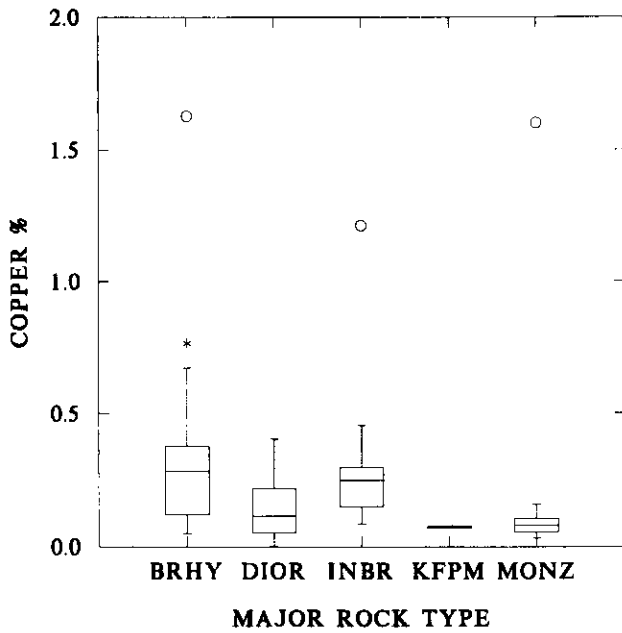


Figure 2-8-2. Box plots of total copper assay value and biotite versus major rock type. BRHY = B (in Figure 2-8-1) = hydrothermal breccia, DIOR = D = diorite, INBR = I = intrusion breccia, KFPM = K = potassium feldspar porphyritic monzonite, PLPP = P = monzonite. (A) Highest copper assays are in the hydrothermal and intrusive breccias. (B) Secondary biotite is rock specific. It is well developed in the hydrothermal breccia, and to a lesser degree, in the intrusive breccia.

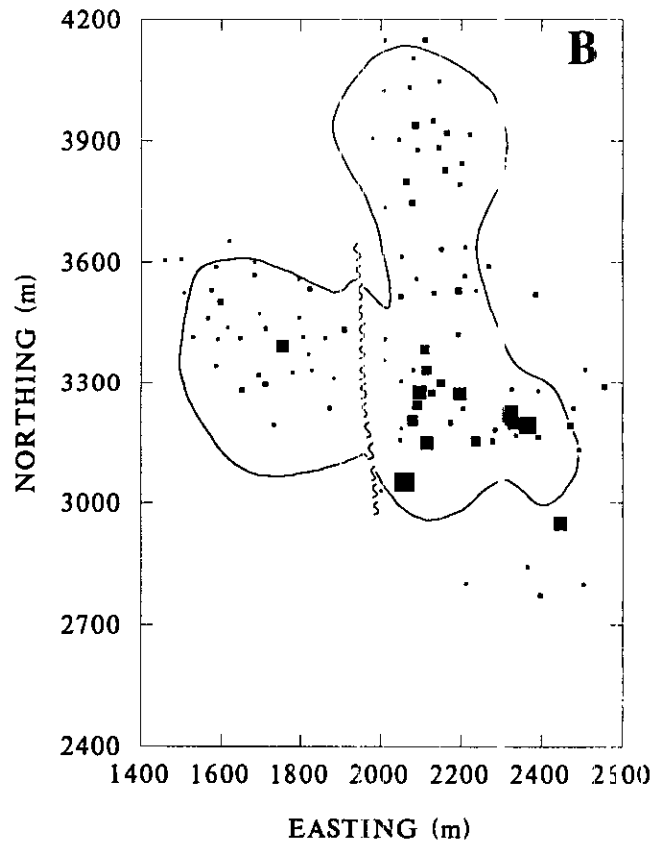
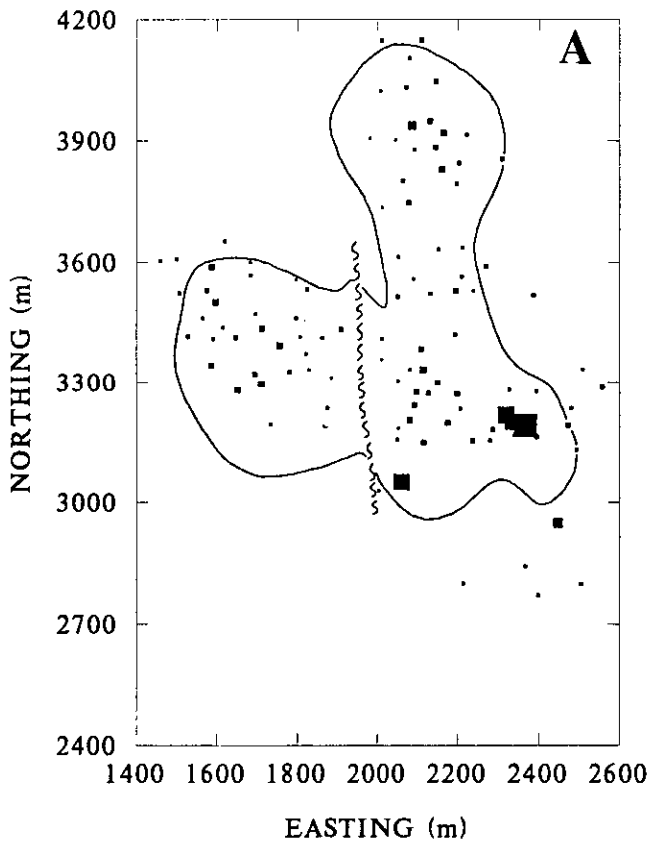


Figure 2-8-3. Bubble plots of total copper assay value and gold (ppb) at the 1110-metre plan level, Mount Polley. (A) The highest copper grade is in the south-central zone of the pit. Bubble size is proportional to percentage; largest bubble = 2.33%, and smallest bubble = 0%. (B) The highest gold grade is in the south-central zone of the pit and correlates with copper. Bubble size is proportional to grade; largest bubble = 2560 ppb, and smallest bubble = 0 ppb. The solid line is the surface outline of the proposed S19 pit.

nated chalcopyrite. Generally the highest copper and gold assays can be correlated with these breccias (Figures 2-8-2 and 2-8-3).

Potassium feldspar porphyritic monzonite occurs as dikes and pods in the centre of the proposed pit area. This unit is weakly altered and probably late-mineral. Hostrock xenoliths are found at the margins of these intrusive bodies. About 20 per cent of the porphyritic monzonite is trachytic with zoned, euhedral potassium feldspar phenocrysts that average 6 millimetres long by 1 millimetre wide. Locally, these phenocrysts have dimensions up to 2 centimetres by 2 millimetres. The potassium feldspar phenocrysts in less altered rock are translucent to beige; more altered specimens have opaque, pink to white phenocrysts. The groundmass consists of 50 per cent subhedral plagioclase laths, approximately 1 by 0.5 millimetre, with minor disseminated magnetite and augite.

Augite porphyry dikes are unaltered and clearly post-mineral. They occur as swarms throughout the deposit, striking north and dipping steeply to the east, with an average thickness of 4 metres. On surface, the dikes are continuous along strike for at least 100 metres.

Chilled margins of most dikes are up to 15 centimetres in width and are aphanitic, dark reddish brown, with approximately 3 per cent very fine grained plagioclase laths aligned parallel to the contact. Trace augite phenocrysts are occasionally present in the chilled margin. The visual appearance of the dikes varies with groundmass composition; two end members are prominent. The first has 40 per cent fine grained euhedral augite phenocrysts, 1 per cent disseminated magnetite and rare plagioclase laths in a dark grey, very fine grained groundmass. The second has 55 per cent augite phenocrysts, 3 per cent disseminated fine-grained magnetite, and a felsic groundmass consisting of fine-grained plagioclase with sparse subhedral plagioclase phenocrysts.

Intermediate dikes are numerous, friable, grey-green to yellow, fine grained and locally vesicular. They are concentrated in the western part of the pit. The dikes vary from biotite lamprophyre to andesite or dacite in composition and are probably of Tertiary age. Their orientation is similar to the augite porphyry dikes.

ALTERATION AND MINERALIZATION

Visual estimates of the percentages of alteration minerals were made during core logging of intervals on the 1110-metre level. Statistical analysis is restricted to data from this level. SYSTAT-SYGRAPH software (Wilkinson, 1990), was used to analyse and display this data. Two distinct alteration suites are defined: a copper-gold bearing calc-potassic alteration zone that is centred on intrusive and hydrothermal breccias, and a peripheral propylitic zone with low levels of copper and gold. An inferred contact between the calc-potassic and the propylitic zones is shown in Figure 2-8-1B; hatched areas represent areas of overlap. The propylitic zone is peripheral to the deposit but its lateral extent is poorly defined due to a lack of drill holes outside the proposed S19 pit. Post-mineral anhydrite and calcite veins are a widespread component of both alteration zones. The

alteration pattern is a refinement of that presented by Hodgson *et al.* (1976). Future analysis will investigate the detailed relationship of alteration to different lithologies, particularly breccias, and the spatial distribution of all alteration minerals.

CALC-POTASSIC ALTERATION

Calc-potassic alteration, coincident with copper-gold mineralization, is concentrated within the proposed pit area. It is dominated by chalcopyrite, pervasive potassium feldspar, biotite, diopside, albite and magnetite.

Copper and gold assay values are closely correlated and are highest in the hydrothermal and intrusion breccias (Figure 2-8-2A). Copper and gold distributions on the plan level are shown in Figure 2-8-3. The highest copper and gold grades occur in the southern part of the central zone in the eastern part of the proposed pit. Copper occurs dominantly as chalcopyrite with traces of bornite. The most common vein assemblage consists of chalcopyrite, magnetite and diopside with or without pyrite. Chalcopyrite also occurs as fine-grained disseminations in the matrix of hydrothermal breccia, and rarely as breccia cement. Bornite is rare, but is found in chalcopyrite-rich areas. Gold is not macroscopically visible, but may be contained within chalcopyrite because of the close copper-gold association (Figure 2-8-3).

Potassium feldspar is present throughout the deposit but is concentrated in the breccias. This alteration is pink, fine grained and usually pervasive. Visually estimated percentages vary from 15 to 70. Minor potassium feldspar occurs as vein envelopes. Potassium feldspar correlates poorly with other alteration minerals; this may reflect the difficulty of distinguishing primary from secondary potassium feldspar.

Biotite is abundant, averaging 5 per cent in vugs in the hydrothermal breccia. Flakes from 1 millimetre to 1 centimetre in width are common. The association of visible secondary biotite with the hydrothermal breccias is illustrated by Figure 2-8-2B. Secondary biotite has developed to a lesser extent within the intrusion breccia, possibly due to its more competent nature. Secondary biotite coincides with the spatial distribution of breccia; concentrations are generally higher in the central zone than the west zone.

Magnetite occurs as fine-grained disseminations, up to 5 per cent, and in veinlets throughout the deposit; it also forms the matrix to some breccias. The distribution of vein magnetite (Figure 2-8-4A) is erratic, and is less specific to rock type than biotite. Veinlet assemblages commonly consist of: magnetite + diopside ± amphibole ± chalcopyrite, diopside + magnetite + chalcopyrite ± pyrite and magnetite + chalcopyrite ± pyrite.

Diopside is a ubiquitous alteration mineral and occurs as fine-grained disseminations (5%) within the hydrothermal and intrusion breccias. It typically occurs as diopside + magnetite ± chalcopyrite ± amphibole + albite veinlets, usually with potassium feldspar envelopes.

Albite (field term) is an important alteration mineral, with concentrations up to 30 per cent. It is particularly abundant in the west zone where it causes pervasive bleach-

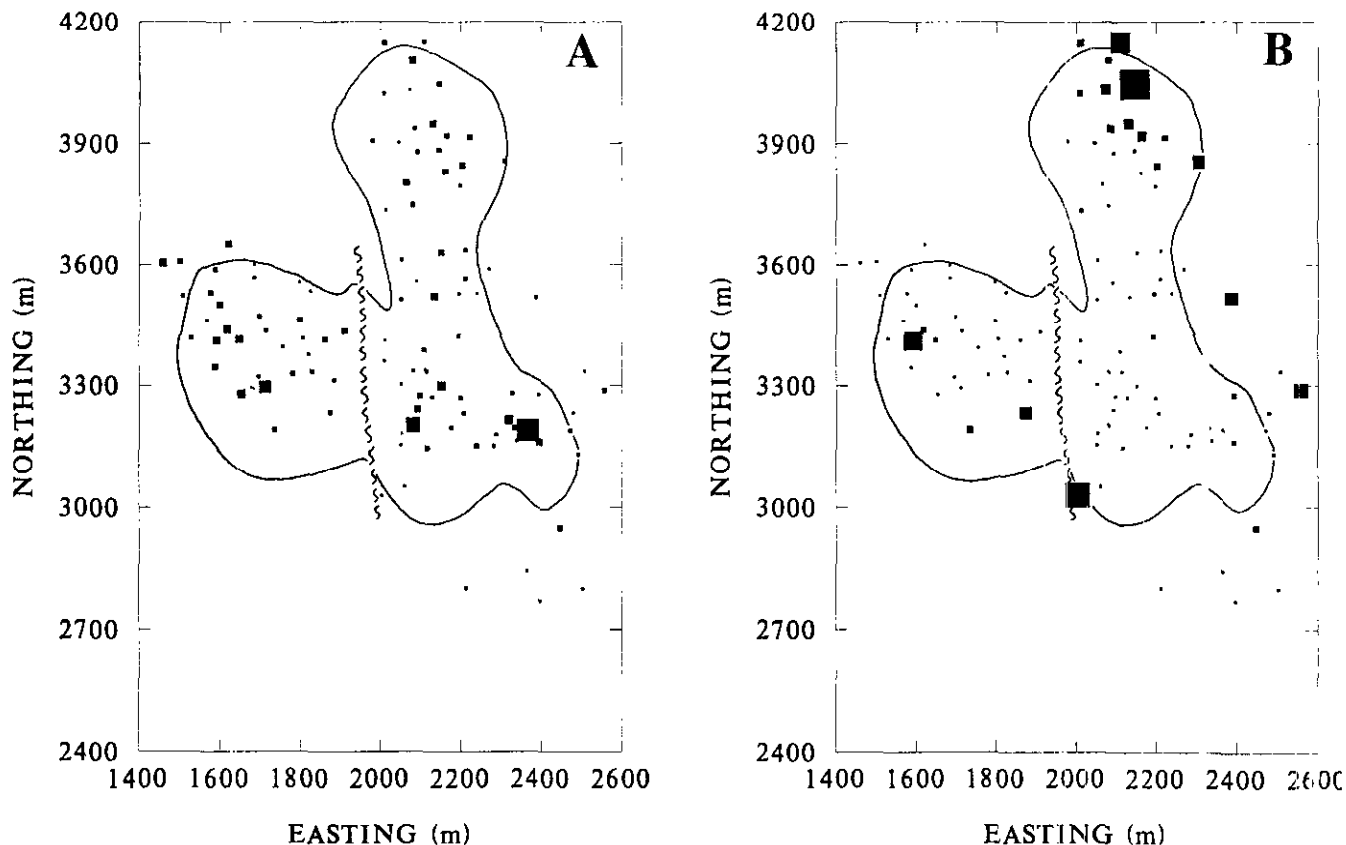


Figure 2-8-4. Bubble plots of visually estimated secondary magnetite and pyrite at the 1110-metre plan level, Mount Polley. (A) The distribution of magnetite is irregular, and is not rock specific. Magnetite veining is present in all rock units. Bubble size is proportional to percentage; largest bubble = 13.63%, and smallest bubble = 0%. (B) Pyrite is peripheral to the deposit and marks the propylitic assemblage. There is some overlap on the calc-potassic zone. Bubble size is proportional to percentage; largest bubble = 4.2%, and smallest bubble = 0%. The solid line is the surface outline of the proposed S19 pit.

ing. Vugs in hydrothermal breccias in both the central and west zones contain euhedral albite. Albite also occurs in the propylitic zone.

PROPYLITIC ALTERATION

Propylitic alteration, peripheral to the calc-potassic alteration zone, is developed outside the proposed pit area. Generally, the rocks are weakly altered compared with the calc-potassic zone. Pyrite, epidote and albite dominate most assemblages.

Pyrite forms veinlets up to 2 millimetres wide and averages approximately 1 per cent of the rock volume. Pyrite distribution is not rock specific and occurs as veinlets in both breccias and the diorite. The highest concentrations of pyrite are on the northeast and southwest margins of the calc-potassic alteration zone (Figure 2-8-4B), suggesting the development of a pyrite halo within peripheral propylitic alteration.

Epidote is present in minor quantities and occurs as fine-grained disseminations throughout all syn-mineral units. It characteristically occurs in veinlets with calcite. The spatial distribution of epidote correlates closely with that of pyrite on the periphery of the mineralized zones. This relationship was noted by Hodgson *et al.* (1976).

Albite, often associated with diopside, occurs locally as minor veins accounting for less than 2 volume per cent of the altered diorite.

CONCLUSIONS

The alkalic porphyry copper-gold system at Mount Polley is associated with a series of intrusions and breccia bodies. The intrusive suite that hosts the deposit ranges from pyroxenite to monzonite and is dominated by diorite. Breccias are divisible into intrusion breccias with an igneous monzonitic matrix, and hydrothermal breccias with a porous and vuggy matrix. The emplacement of the monzonite, formation of the intrusion breccia and alteration probably represent a continuum of orthomagmatic processes. Specifically, hydrothermal breccias containing a calc-potassic vug-filling alteration assemblage probably are of orthomagmatic origin. Hydrothermal breccias are also the major host for better grade mineralization, which consists of disseminated and stockwork chalcopyrite, bornite and magnetite.

The calc-potassic alteration zone dominates the core of the deposit. Pervasive potassium feldspar commonly obliterates primary textures. Disseminated magnetite, diopside-amphibole-chalcopyrite veinlets and coarse biotite in hydrothermal breccias are characteristic. Peripheral pro-

pylitic alteration overlaps the outer margin of the potassic zone and is prominent outside the proposed S19 pit. The assemblage consists of pyrite veinlets, epidote disseminations and albite-diopside veins.

ACKNOWLEDGMENTS

Imperial Metals Corporation is thanked for granting permission to work on its property, and for providing drill-log information and assays. This M.Sc. thesis study is part of the Mineral Deposit Research Unit (MDRU) project "Porphyry Copper-Gold Systems of British Columbia". All direct funding has been by MDRU. Members of the MDRU group are thanked for violent discussions about bubble plots.

REFERENCES

- Bailey, D.G. (1987): Geology of the Hydraulic Map Area (NTS 93A/12). *B.C. Ministry of Energy, Mines and Petroleum Resources*; Preliminary Map No. 67, Scale 1:50 000.
- Gorc D., Nikic. Z.T. and Pesalj, R. (1992): Mount Polley; unpublished report, *Imperial Metals Corporation*, 11 pages.
- Hodgson, C.J., Bailes, R.J. and Verzosa, R.S. (1976): Cariboo-Bell; in *Porphyry Deposits of the Canadian Cordillera*, Sutherland Brown, A., Editor, *Canadian Institute of Mining and Metallurgy*, Special Volume 15, pages 388-396.
- Imperial Metals Corporation (1989): Mount Polley Copper/Gold Property; *Imperial Metals Corporation and Corona Corporation*, Prospectus, 37 pages.
- Wilkinson, L. (1990): SYSTAT: The System for Statistics; *SYSTAT Inc.*, Evanstone, Illinois, 676 pages.

RARE-EARTH ELEMENT BEARING PEGMATITES IN THE WOLVERINE METAMORPHIC COMPLEX: A NEW EXPLORATION TARGET (93N/9E, 93O/12W, 5W)

By A.A.D. Halleran, Inzana Resources Inc. and
J.K. Russell, The University of British Columbia

KEYWORDS: Economic geology, Mount Bisson, rare-earth elements, pegmatites, Wolverine Complex, petrology, exploration targets.

INTRODUCTION

Both alkaline and subalkaline rare-earth element (REE) bearing pegmatites occur within the Wolverine Metamorphic Complex of the Omineca crystalline belt west of Williston Lake (Figure 2-9-1). Detailed geological mapping (1:5000) of the Mount Bisson area between the Manson River and Munroe Creek has delineated a number of small REE-bearing intrusions (Figure 2-9-2) that are the topic of this study. The major REE-bearing phases are allanite and

monazite. Indeed, in some of the REE-bearing pegmatites allanite occurs as a rock-forming phase. REE concentrations in such pegmatites range as high as 17 per cent rare-earth oxides.

The REE pegmatites, especially the alkaline pegmatites, represent a new exploration target within the Wolverine Complex. Rare-earth mineralization was discovered on Mount Bisson in 1986 and 1987 and Chevron Minerals Ltd. conducted a limited exploration program for rare-earth elements in 1988 (Halleran, 1988). Subsequently, the Mount Bisson REE-bearing units were investigated in more detail by Halleran and Russell (1990) and Halleran (1991). The objective of this paper is to present petrographic and geochemical data on these pegmatites and to elucidate their origins and economic potential. The regional framework for this research is derived entirely from recent regional mapping by Mansy and Gabrielse (1978), Ferri and Melville (1988, 1989, 1990), Deville and Struik (1993), and Struik and Northcote (1991).

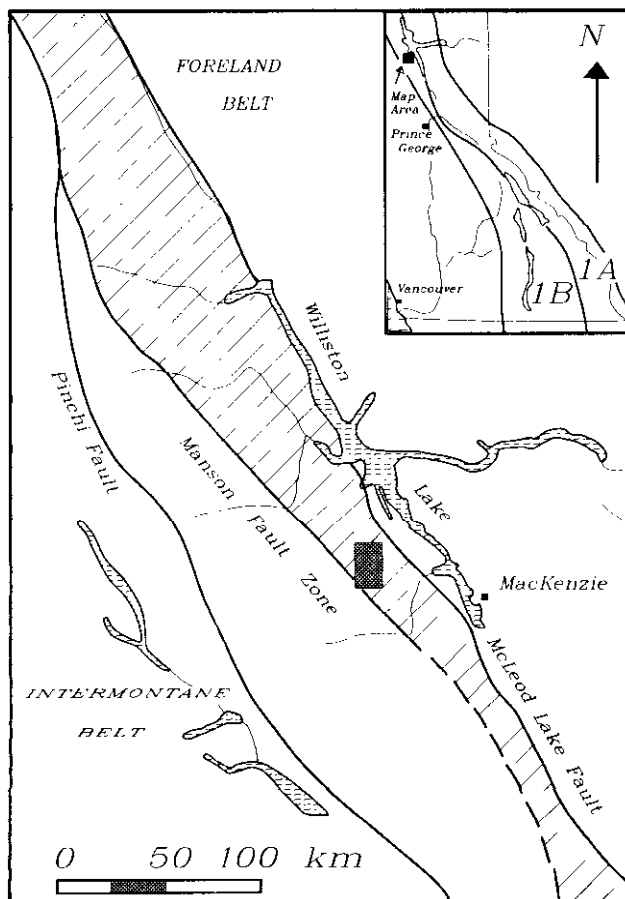


Figure 2-9-1. Location of Mount Bisson field area relative to tectonic framework of the Canadian Cordillera (modified from Ferri and Melville, 1988). Mount Bisson lies within the Omineca crystalline belt (lined pattern). Inset figure locates Mount Bisson area relative to belts of alkaline ultrabasic rocks types (1A and 1B) defined by Pell (1987).

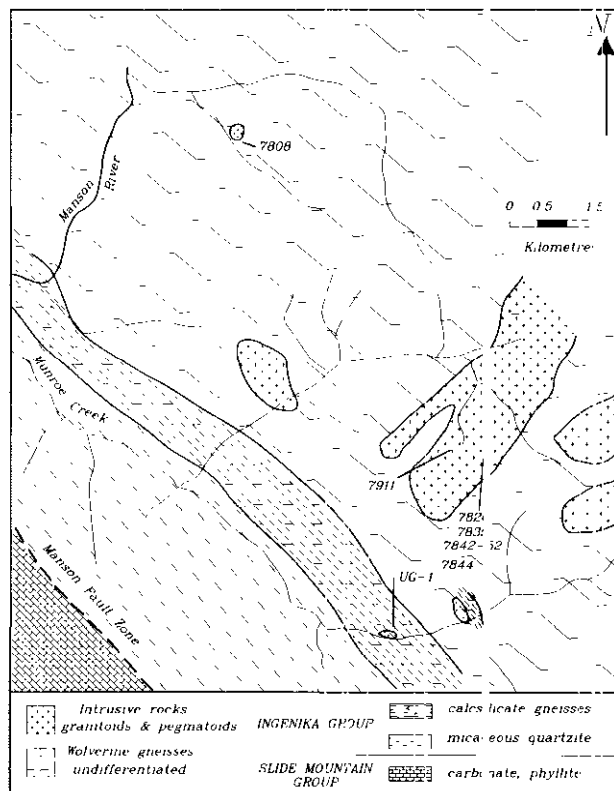


Figure 2-9-2. Geological map of the Mount Bisson area with pegmatite sample locations denoted by sample numbers (See Tables 2-9-1 and 2-9-2). Ingenika Group stratigraphy is from Ferri and Melville (1988).

GEOLOGICAL SETTING

The Mount Bisson study area lies mainly within the Omineca crystalline belt and is dominantly underlain by undifferentiated metamorphic rocks of the Wolverine Complex (Figure 2-9-2). Schists and gneisses of the Ingenika Group, including calcisilicate gneisses and micaceous quartzite, parallel Munro Creek to the southwest of Mount Bisson (Ferri and Melville, 1988). Farther to the southwest, the Ingenika Group rocks are in fault contact with phyllites and carbonates of the Slide Mountain Group (Figure 2-9-2). Both Wolverine gneisses and Ingenika rocks are intruded by apparently small granitic and pegmatitic intrusions. Pegmatite commonly occurs as small (<5 m thick) sills and dikes oriented subparallel to the metamorphic layering in the Wolverine gneisses and as larger (1 km diameter) irregular bodies.

Previous workers have argued for at least two separate periods of intrusive activity based on relative age relationships. Intrusive rocks affected by the amphibolite facies metamorphism and deformation which characterize the Wolverine Metamorphic Complex are considered to be at least Cretaceous in age (Tipper *et al.*, 1974; Parrish, 1976, 1979; Ferri and Melville, 1989; Deville and Struik, 1990). Deville and Struik (1990) ascribe the metamorphism and coincident intrusive activity to deep burial of the Wolverine rocks during Cretaceous crustal thickening. Intrusions within the Wolverine gneisses which clearly postdate the peak of metamorphism and deformation are most likely Tertiary (Parrish, 1976, 1979; Ferri and Melville, 1989; Deville and Struik, 1990; Struik and Northcote, 1991) and may be associated with crustal extension and regional uplift of the Wolverine Complex.

Based on mineralogy and chemical composition, both alkaline and subalkaline pegmatites are recognized in the Mount Bisson area and many are enriched in rare-earth elements. We distinguish three types of pegmatites as: alkaline versus subalkaline REE-bearing pegmatites and barren pegmatites. In addition to being chemically distinct, the alkaline and subalkaline REE-bearing pegmatites are not all the same age. Several of the subalkaline pegmatites are deformed or foliated, suggesting a minimum age of Cretaceous. In contrast, the alkaline REE pegmatites crosscut the Wolverine structural fabric and are themselves unfoliated, suggesting they are Tertiary.

Pell's (1987) regional synthesis of alkaline ultrabasic rocks in the Canadian Cordillera established three belts containing all significant carbonatite and related alkaline rock occurrences. The divisions reflect the age relationships, tectonic history and mineralogical and chemical characteristics of these igneous rocks. Mount Bisson lies within Belt 1B, which comprises the Devon-Mississippian syenites and carbonatites at Manson Creek, Blue River and Three Valley Gap. In contrast to these occurrences of alkaline ultrabasic rocks, the Mount Bisson REE pegmatites, based on field observations, are Cretaceous or younger in age, chemically basic to acidic and alkaline to subalkaline. Furthermore, they appear to be unrelated to carbonatite magmatism.

DESCRIPTION OF PEGMATITES

Mineralogically the REE pegmatites are diverse (Table 2-9-1). Chemical discrimination of the alkaline and subalkaline pegmatites (Macdonald and Katsura, 1964) is shown in Figure 2-9-3. The alkaline and subalkaline chemistry is expressed modally by the presence of nepheline or quartz, respectively. The alkaline pegmatites are also characterized by abundant sodic pyroxene (*e.g.* aegirine-augite) and accessory sphene. Mineralogical distinction can also be based on whether the dominant REE-bearing phase is allanite or monazite (Table 2-9-1).

REE ALKALINE PEGMATITES

The REE alkaline pegmatite group comprises numerous allanite-bearing dikes which outcrop at two localities in the Mount Bisson map area (Samples 7826 and 7911; Figure 2-9-2). These pegmatite bodies commonly occur as dikes 1 to 4 metres wide with minimum strike lengths of over 30 metres. In several places they crosscut the structural fabric of the Wolverine gneisses.

The REE alkaline pegmatites comprise perthitic potassium feldspar, plagioclase, green to brown pleochroic allanite (<35 volume %), titanite (<5 volume %), apatite, with minor aegirine-augite and trace zircon and opaques. One sample contains fresh nepheline. The allanite occurs as subhedral to euhedral grains 0.3 to 20 millimetres in size and is typically associated with titanite and apatite. The modal abundance of allanite varies substantially and the mineral commonly occurs in clusters and along the edges of the dikes.

TABLE 2-9-1
VISUALLY ESTIMATED MODAL MINERAL ABUNDANCES
(VOLUME PER CENT) FOR MOUNT BISSON PEGMATITES

Sample No.	Q	Pl	Ksp	Px	Hbl	Al	Ttn	Ap	Bi	Zr	Other
7826	-	33	33	11	-	15	5	2	tr	tr	Nepheline
7911	tr	40	30	16	-	10	tr	2	tr	tr	Opagues
7842-52	28	33	31	2	-	3	2	1	-	tr	Thorite
UG - 1	40	25	35	-	-	tr	tr	tr	tr	tr	Monazite
7835	2	75	2	-	20	tr	tr	tr	-	-	Epidote
7844	50	25	25	-	-	-	-	-	tr	tr	Monazite
7808	3	87	-	10	-	tr	tr	-	tr	-	Epidote

Q - quartz, Pl - plagioclase, Ksp - K-feldspar, Px - pyroxene, Hbl - homblende, Al - allanite, Ttn - titanite, Ap - apatite, Bi - biotite, Zr - zircon.

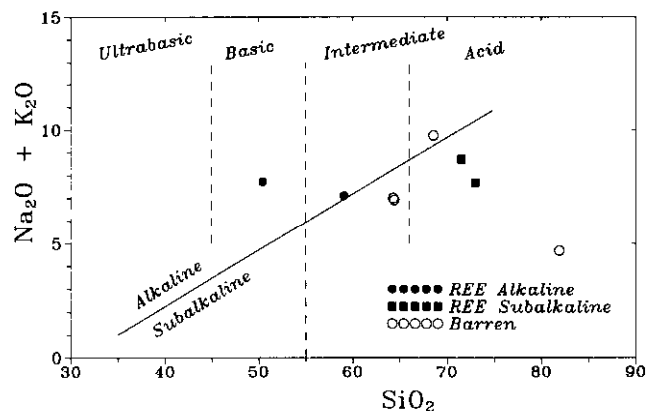


Figure 2-9-3. Chemical compositions of pegmatites plotted as $\text{Na}_2\text{O} + \text{K}_2\text{O}$ vs SiO_2 with superimposed silica-content classification.

The allanite pegmatites have little to no fabric, suggesting that they intruded the Wolverine metamorphic rocks after the peak metamorphic-deformational event and are presumed to represent Tertiary magmatism (Deville and Struik, 1990).

REE SUBALKALINE PEGMATITES

Monazite is the most abundant rare earth bearing mineral in the REE-enriched subalkaline pegmatites. A single exposure of quartz allanite pegmatite occurs at Mount Bisson (Sample 7842-52; Figure 2-9-2). It is 0.5 metre wide, tens of metres long, and has an internal fabric paralleling the metamorphic foliation of the Wolverine gneisses.

Although the quartz allanite pegmatite is chemically subalkaline (Figure 2-9-3), mineralogically it comprises heterogeneous clusters of mafic minerals including: allanite (5 volume %), titanite, euhedral apatite, pink pleochroic zircon and thorite. These intergrowths occur with uncommon aegirine-augite in a groundmass of potassium feldspar, quartz and minor plagioclase. The allanite occurrence is erratic and commonly limited to compositionally distinct bands. Anhedral polycrystalline quartz grains are elongate parallel to the mafic bands.

Sample UG-1 (Figure 2-9-2) is a representative monazite-bearing pegmatite taken from a body intruding calcisilicate gneisses of the Ingenika Group (Ferri and Melville, 1988). The pegmatite occurs as a strongly deformed to mylonitized dike, 1 to 2 metres wide. It comprises recrystallized potassium feldspar, quartz and oriented albite grains with more weakly oriented monazite. The monazite distribution is erratic with concentrations of up to 2 volume per cent occurring over tens of centimetres. The average monazite concentration of the rock type is less than 0.5 volume per cent. Biotite, chlorite, titanite, allanite and zircon occur as trace phases. The coexistence of monazite and allanite is of petrologic interest as these minerals rarely occur together (Parrish, 1990). Biotite occurs as irregularly shaped crystals intergrown with allanite and appears to be partly replaced by allanite. A similar textural relationship has been described between biotite and allanite in rocks of the Boulder Creek batholith and is ascribed to allanite replacement of biotite (Hickling *et al.*, 1970).

Field and petrographic observations show that at least the monazite pegmatites are affected by the last significant regional metamorphic-deformational event. This suggests that they are older than the alkaline intrusive rocks and may be Cretaceous or older in age.

BARREN PEGMATITES

Pegmatites devoid of significant REE concentrations also outcrop at Mount Bisson and make a useful petrologic contrast to the REE-bearing pegmatites. They include both alkaline and subalkaline rock types (Figure 2-9-3). Mineralogically this group ranges from quartz feldspar and hornblende pegmatites which are chemically subalkaline, to quartz syenite pegmatites which are alkaline (Table 2-9-1). The contact relationships between them are not known because mutually crosscutting relationships have not been

observed, although the rock types commonly outcrop together. Large xenoliths of Wolverine amphibolite are commonly incorporated within the pegmatite bodies.

Major constituents of the hornblende pegmatites are plagioclase, hornblende, potassium feldspar and quartz, with euhedral titanite, apatite, allanite and epidote occurring as trace phases. The quartz feldspar pegmatite contains 5 to 10-millimetre polycrystalline quartz grains, perthitic potassium feldspar, plagioclase and minor magnetite, biotite and chlorite. Trace phases include zircon, euhedral zoned monazite and opaques. The biotite is replaced by chlorite and exhibits slight kink banding. Coarse-grained quartz syenite pegmatite comprises plagioclase, hornblende, perthitic potassium feldspar, elongate quartz crystals and late fracture-filling epidote. Late stage recrystallization of quartz and plagioclase also occurs along fractures.

GEOCHEMISTRY

Table 2-9-2 lists the major, trace and rare earth element compositions of the Mount Bisson pegmatites. The pegmatite suite includes basic to acid rock types based on SiO₂ content (Figure 2-9-3). The majority of pegmatites are metaluminous (Table 2-9-3) and the normative mineralogy parallels the chemical classification used in Figure 2-9-3. The subalkaline REE pegmatites are silica oversaturated and characterized by normative quartz. The alkaline pegmatites are silica undersaturated to saturated depending on the presence or absence of normative nepheline (Table 2-9-3). The barren pegmatites are intermediate to acidic (Figure 2-9-3) and compositionally separate the alkaline (basic to intermediate) and subalkaline (acid) REE pegmatites. Normatively, they are oversaturated with respect to silica. Two pegmatites (UG-1 and 7844) are chemically peraluminous (normative corundum), although neither rock type contains any of the characteristic peraluminous phases.

The REE pegmatites have a wider range in barium content, compared to the barren pegmatites, from 350 to 5300 ppm, and a smaller range in strontium, from 450 to 1000 ppm (Table 2-9-2). The barren pegmatites have barium concentrations of 360 to 800 ppm and strontium concentrations of 100 to 750 ppm. There are also significant differences in trace element contents between the alkaline and subalkaline pegmatites. Alkaline REE pegmatites have 357 to 1841 ppm barium, whereas the subalkaline pegmatitic rocks have substantially higher barium concentrations of 3000 to 5290 ppm. Zirconium and rubidium are below the lower detection limits in the alkaline REE pegmatites but vary from 238 to 517 ppm zirconium and 62 to 83 ppm rubidium, respectively, in the subalkaline REE pegmatites.

Figure 2-9-4 illustrates the rare-earth element chondrite-normalized (REE_{cn}) abundance patterns (after Wakita *et al.*, 1971; Boynton, 1984) for representative samples of Mount Bisson pegmatites. As summarized in Table 2-9-3, the REE pegmatites have high total REE concentrations ranging from 2783 to greater than 35 000 ppm, whereas the barren pegmatites have lower values (128 to 607 ppm). The three groups of pegmatites differentiated on the basis of mineralogy, structural fabric and major element chemistry are so distinct in terms of REE_{cn} patterns (Figure 2-9-4): strongly

TABLE 2-9-2
MAJOR ELEMENT OXIDES, TRACE ELEMENT AND RARE-EARTH ELEMENT COMPOSITIONS OF
MOUNT BISSON PEGMATITES

Sample No.	REE Alkaline Pegmatites		REE Subalkaline Pegmatites		Barren Pegmatites		
	7826	7911	7842-52	UG-1	7835	7844	7808
SiO ₂	50.44	59.08	71.50	72.98	64.34	81.90	68.56
TiO ₂	2.96	1.25	1.17	0.12	0.19	0.15	0.03
Al ₂ O ₃	19.92	17.42	12.43	15.28	17.91	7.93	15.50
FeO	4.78	3.78	1.43	0.82	3.07	2.21	1.68
Fe ₂ O ₃	2.45	1.44	0.84	0.18	0.47	1.60	0.60
MnO	0.18	0.17	0.09	0.02	0.08	0.05	0.14
MgO	1.29	1.39	0.51	0.38	1.41	0.16	0.77
CaO	10.22	7.76	2.46	2.17	5.31	0.37	2.53
Na ₂ O	2.97	5.61	2.86	3.88	5.73	2.48	5.65
K ₂ O	4.75	1.51	5.86	3.80	1.28	2.20	4.09
P ₂ O ₅	0.67	0.42	0.14	0.17	0.13	0.03	0.03
Total	100.61	99.38	99.30	99.81	99.91	99.10	99.58
LOI	0.56	0.28	0.34	0.38	0.62	0.20	0.35
Trace Element Concentrations (ppm)							
Nb	358	241	554	bd	13	30	9
Zr	bd	bd	245	517	24	736	86
Y	342	157	138	16	21	14	16
Sr	444	474	1031	455	717	100	388
Rb	bd	bd	63	83	20	42	85
Ba	1841	357	5291	3010	416	493	797
Sc	26.1	28.7	7.6	1.3	24.9	0.3	19.9
Th	3050	1090	1910	305	33	58	5
U	91	25	93	6	1.6	10	3.5
Rare Earth Element Concentrations (ppm)							
La	>9000	>9000	1240	751	169	82	19
Ce	>20000	16400	2440	1370	290	150	38
Pr	1400	750	240	140	<50	<50	<50
Nd	4190	2630	430	450	77	35	13
Sm	>200	>200	77	61	11	5	2
Eu	77.8	30.0	18.0	2.7	1.6	0.8	0.6
Tb	24	12	6	2	<1	2	1.5
Dy	117	51	33	5	5	3	2.0
Ho	12	7.4	3.7	<1	<1	<1	<1
Yb	13	8.4	1.7	<0.5	1.4	1.8	1.5
Lu	2	1.3	0.15	<0.10	0.18	0.31	0.26
(La/Lu) _n	>450	>667	930	751	93	26.4	7.3
(La/Sm) _n	>26	>26	9.2	7.1	8.8	9.6	5.7
(Tb/Yb) _n	8.6	6.3	17.6	18.7	3.3	2.6	3.1
Eu/Sm	-	-	0.23	0.05	0.15	0.16	0.32

Major and trace elements were determined by XRF and rare-earth elements by neutron activation. FeO was measured by volumetric analysis. Ce, La and Sm have upper detection limits of >20000 ppm, >9000 ppm and >200 ppm respectively; bd denotes below lower detection limit

REE-enriched alkaline pegmatites, less REE-enriched sub-alkaline pegmatites and barren pegmatites which lack substantial REE concentrations.

The REE_{cn} patterns for the barren pegmatites are lower and flatter than the corresponding patterns for the REE-bearing pegmatites, indicating that the latter have undergone greater degrees of fractionation. The subalkaline REE pegmatites have lower overall REE concentrations than do the alkaline REE pegmatites (Figure 2-9-4).

Table 2-9-2 also lists several calculated parameters based on the measured REE concentrations which can chemically discriminate igneous rocks and elucidate their origins. These indexes (e.g., Haskin, 1984) monitor: overall rare-earth element fractionation (La/Lu)_{cn}; light rare-earth element (LREE) fractionation (La/Sm)_{cn}; heavy rare-earth element (HREE) fractionation (Tb/Yb)_{cn}; and the europium anomaly (Eu/Sm). For example, compared to the REE-bearing pegmatites, the barren pegmatites have much lower ratios of La/Lu and Tb/Yb, indicating that they have undergone significantly less LREE and HREE fractionation. The alkaline and subalkaline REE pegmatites have significantly different La/Lu, La/Sm and Tb/Yb indices. The REE data suggest that although the subalkaline pegmatites are less enriched and represent greater degrees of overall REE fractionation they have undergone less LREE fractionation and more HREE fractionation.

DISCUSSION

The alkaline REE pegmatites are virtually undeformed and are mineralogically and chemically distinct from the subalkaline REE pegmatites. They probably derive from Tertiary magmatism. REE concentrations are greater than

5 per cent and the dominant REE-bearing mineral is allanite. Based on their chemical and mineralogical composition, these pegmatites are inferred to derive from mantle melts (Heinrich, 1966; Currie, 1976; Bell, 1989). There are a variety of other alkaline intrusive rocks in the Mount Bisson study area which crosscut Wolverine structures and appear to have a similar age (Halleran, 1991). They are probably genetically related to the alkaline REE pegmatites and may represent part of a larger alkaline magmatic event. The pegmatites are quite numerous, have sizes consistent with other economic ore bodies and occur close together, presenting a reasonable exploration target.

The subalkaline REE pegmatites are deformed, suggesting a Cretaceous age. Rare-earth element concentrations are predominantly less than 2 per cent and the dominant rare-earth mineral is monazite. The subalkaline pegmatites may derive from melts produced through partial fusion of the upper crust. This is suggested by the normative character of the pegmatite (peraluminous and silica oversaturated) and by the abundance of monazite (e.g., White and Chappell, 1977). Monazite-bearing granitic pegmatites have been shown elsewhere to result from regional metamorphism in granulite facies migmatitic terrains (Shearer *et al.*, 1987). The large negative europium anomaly (Table 2-9-2) is attributable to plagioclase fractionation (e.g., McKay, 1989). The REE-bearing subalkaline pegmatites have lower total REE concentrations than the alkaline pegmatites, are only sporadically enriched in rare-earth elements and occur as small isolated bodies one or more kilometres apart. These characteristics result in the older (Cretaceous) REE pegmatites exposed at Mount Bisson being of little economic importance.

CONCLUSION

The spatial relationship of the pegmatites, their diverse mineralogy, and varying concentration of rare-earth minerals suggest the presence of more than one period of intrusion. The REE-bearing pegmatites which intrude Wolverine metamorphic rocks at Mount Bisson are divided into: Cretaceous or older monazite and allanite-bearing sub-alkaline pegmatites resulting from crustal anatexis during regional metamorphism and post-Cretaceous allanite-bearing alkaline pegmatites derived from mantle sources. The latter group, and other related alkaline rocks within the study area, may be associated with a larger unexposed alkaline body. The REE alkaline pegmatites represent economic REE targets for the following reasons: they are rich in rare earths, they have potentially economic width and lengths, and the dikes commonly occur together over hundreds of metres.

ACKNOWLEDGMENTS

Funding for this research was supplied in part by the Canada - British Columbia Mineral Development Agreement (1985-1990). A.A.D. Halleran acknowledges field support from Chevron Minerals and the Halleran Prospecting Partnership. We also acknowledge Stanya Horsky's technical assistance during chemical analysis of the rocks.

TABLE 2-9-3
CHEMICAL CHARACTERISTICS OF MOUNT BISSON
PEGMATITES

Sample No.	Pegmatite Type	Silica Normative Character	Alumina Normative Character	ΣREE(ppm)
7826	Allanite	Ne	Metaluminous	> 35036
7911	Allanite	Ne-Q	Metaluminous	> 29090
7842-52	Granite	Q	Metaluminous	4498
UG - 1	Quartz monzonite	Q	Peraluminous	2783
7835	Hornblende	Q	Metaluminous	607
7844	Quartz Feldspar	Q	Peraluminous	329
7808	Quartz Hedenbergite	Q	Metaluminous	128

Q - quartz, Ne - nepheline.

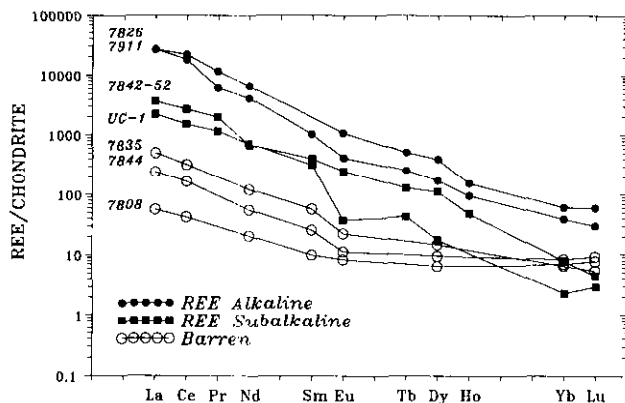


Figure 2-9-4. Chondrite-normalized REE abundance patterns for Mount Bisson pegmatites.

REFERENCES

- Bell, K. (1989): Carbonatites – Genesis and Evolution; *Unwin Hyman Publishing*, London, 618 pages.
- Boynton, W.V. (1984): Cosmochemistry of the Rare Earth Elements: Meteorite Studies; in *Rare Earth Geochemistry*, Henderson, P., Editor, *Elsevier Publishing Company*, pages 63-114.
- Currie, K. L. (1976): The Alkaline Rocks of Canada; *Geological Survey of Canada*, Bulletin 239, 278 pages.
- Deville, E. and Struik, L.C. (1990): Polyphase Tectonic, Metamorphic and Magmatic Events in the Wolverine Complex, Mount MacKinnon, Central British Columbia; in *Current Research, Part E, Geological Survey of Canada*, Paper 90-1E, pages 65-69.
- Ferri, F. and Melville, D.M. (1988): Manson Creek Mapping Project (93N/9); in *Geological Fieldwork 1987, B.C. Ministry of Energy, Mines and Petroleum Resources*, Paper 1988-1, pages 169-180.
- Ferri, F. and Melville, D.M. (1989): Geology of the Germansen Landing Area, British Columbia (93N/15, 94C/2); in *Geological Fieldwork 1988, B.C. Ministry of Energy, Mines and Petroleum Resources*, Paper 1989-1, pages 209-220.
- Ferri, F. and Melville, D.M. (1990): Geology between Nina Lake and Osilinka River, North-central British Columbia (93N/15, North Half and 94C/2, South Half); in *Geological Fieldwork 1989, B.C. Ministry of Energy, Mines and Petroleum Resources*, Paper 1990-1, pages 101-114.
- Halleran, A.A.D. (1988): Geology, Geochemistry and Geophysics of the Ursa Property; *B.C. Ministry of Energy, Mines and Petroleum Resources*, Assessment Report 17872.
- Halleran, A.A.D. (1991): Geology, Geochemistry and Origins of the Mount Bisson Alkaline Rocks, Munroe Creek, British Columbia, Canada; unpublished M.Sc. thesis, *The University of British Columbia*, 176 pages.
- Halleran, A.A.D. and Russell J.K. (1990): Geology and Descriptive Petrology of the Mount Bisson Alkaline Complex, Munroe Creek, British Columbia; in *Geological Fieldwork 1989, B.C. Ministry of Energy, Mines and Petroleum Resources*, Paper 1990-1, pages 297-304.
- Haskin, L.A. (1984): Petrogenetic Modelling – Use of Rare Earth Elements; in *Rare Earth Geochemistry*, Henderson, P., Editor, *Elsevier Publishing Co.*, pages 115-152.
- Heinrich, E.W. (1966): The Geology of Carbonatites; *Robert E. Krieger Publishing Company*, 585 pages.
- Hickling, N.L., Phair G., Moore, R. and Rose H.J. Jr (1970): Boulder Creek Batholith, Colorado Part I; Allanite and its bearing upon Age Patterns; *Geological Society of America Bulletin*, Volume 81, pages 1973-1994.
- Macdonald, G.A. and Katsura, T. (1964): Chemical Composition of Hawaiian Lavas; *Journal of Petrology*, Volume 5, pages 82-133.
- Mansy, J. L. and Gabrielse, H. (1978): Stratigraphy, Terminology and Correlation of Upper Proterozoic Rocks in Omineca and Cassiar Mountains, North-central British Columbia; *Geological Survey of Canada*, Paper 77-19, 17 pages.
- McKay, G.A. (1989): Partitioning of Rare Earth Elements Between Major Silicate Minerals and Basaltic Melts; in *Geochemistry and Mineralogy of Rare Earth Elements*, Lipin, B.R. and McKay, G.A., Editors, *Reviews in Mineralogy*, Volume 21, pages 45-77.
- Parrish, R.R. (1976): Structure, Metamorphism and Geochronology of the Northern Wolverine Complex near Chase Mount, Aiken Lake Map-area, British Columbia; unpublished M.Sc. thesis, *The University of British Columbia*, 89 pages.
- Parrish, R.R. (1979): Geochronology and Tectonics of the Northern Wolverine Complex, British Columbia; *Canadian Journal of Earth Sciences*, Volume 16, pages 1428-1438.
- Parrish, R.R. (1990): U-Pb Dating of Monazite and its Application to Geological Problems; *Canadian Journal of Earth Sciences*, Volume 27, pages 1431-1450.
- Pell, J. (1987): Alkaline Ultrabasic Rocks in British Columbia; Carbonatites, Nepheline Syenites, Kimberlite, Ultramafic Lamprophyres and Related Rocks; *B.C. Ministry of Energy, Mines and Petroleum Resources*, Open File 1987-17, 109 pages.
- Shearer, C.K., Papike, J.J., Redden, J.A., Simon B.S., Walker, R.J. and Laul, J.C. (1987): Origin of Pegmatitic Granite Segregations, Willow Creek, Black Hills, South Dakota; *Canadian Mineralogist*, Volume 25, pages 159-171.
- Struik, L.C. and Northcote, B.K. (1991): Pine Pass Map Area, Southwest of the Northern Rocky Mountain Trench, British Columbia; in *Current Research, Part A, Geological Survey of Canada*, Paper 91-1A, pages 285-291.
- Tipper, H.W., Campbell, R.B., Taylor, G.C. and Stott, D.F. (1974): Parsnip River, British Columbia; *Geological Survey of Canada*, Map 142A, Sheet 93.
- Wakita, H., Rey, P. and Schmitt, R.A. (1971): Abundances of the 14 Rare Earth Elements and 12 Other Trace Elements in Apollo XXII Samples: Five Igneous and One Breccia Rocks and Four Soils; *Proceedings of 2nd Lunar Science Conference*, pages 1319-1329.
- White, A.J.R. and Chappell, B.W. (1977): Ultrametamorphism and Granitoid Genesis; *Tectonophysics*, Volume 43, pages 2-22.

BASALTIC ROCKS OF THE MIDDLE JURASSIC SALMON RIVER FORMATION, NORTHWESTERN BRITISH COLUMBIA (104A, B, G)

By A. James Macdonald, Peter D. Lewis, Art D. Ettlinger, Roland D. Bartsch, Bruce D. Miller,
Mineral Deposit Research Unit, U.B.C., and Jim M. Logan, B.C. Geological Survey Branch

(MDRU Contribution 018)

KEYWORDS: Petrography, lithogeochemistry, Stikinia, Hazelton Group, Salmon River Formation, basalt; andesite, Eskay Creek.

INTRODUCTION

At Eskay Creek, in the Iskut River area of northwestern British Columbia (Figure 2-10-1), the bulk of the 21 zone is hosted within the Salmon River Formation; basaltic and andesitic rocks comprise a significant component of the Salmon River Formation in this locality. The mining reserve estimate at Eskay Creek is 1.04 million tonnes grading 63.8 grams per tonne gold, 986 grams per tonne silver (operator: International Corona Inc. prior to August 1992; Homestake Canada Ltd. thereafter). One of us (JML) has coordinated a regional mapping project in the Galore Creek, More Creek and Forrest Kerr Creek areas since 1988 (Logan and Koyanagi, 1989; Logan *et al.*, 1990, 1992); work by the remaining authors is part of The University of British Columbia (MDRU) project "Metallogeny of the Iskut River Area," which commenced in mid-1990 (Macdonald, 1991; Ettlinger, 1991; Bartsch, 1992; Miller, 1992; Lewis, 1992).

Volcanogenic massive sulphide deposits are frequently associated with either a bimodal, felsic-mafic volcanic assemblage, or a polymodal dacite-andesite-rhyolite-basalt assemblage (*e.g.*, Gibson and Watkinson, 1986; Large, 1992). Recently, Edmunds *et al.* (1992) proposed that both acid and mafic volcanism, together with sedimentation of fine-grained mudstones, are approximately contemporaneous with mineralization in the Eskay Creek 21 zones. In addition, Bartsch (1993, this volume, and manuscript in preparation) has described regional-scale alteration spatially associated with mineralization to the south of Eskay Creek, and on the Eskay Creek mining lease. These views and observations suggest collectively that it is critical to assess both the environment in which such volcano-sedimentary processes take place, and also the effects of alteration. Hydrothermal alteration is commonly more widespread than associated base and precious metal mineralization; if zonal patterns are present, alteration may provide useful vectors towards mineralized centres of hydrothermal systems.

In this paper we address: the stratigraphy of the volcanic components of the Salmon River Formation; the petrology and lithogeochemistry of intermediate to mafic volcanic rocks in Salmon River Formation, with the long term objective of determining their provenance and the environment in which they formed; and the effects of alteration in the vicinity of known mineralization, in order to assess the effectiveness of basalt lithogeochemistry as an exploration tool. Basaltic rocks are particularly well suited to a study of this nature, being more sensitive to alteration than the associated felsic rocks, because they are in greater disequilibrium with hydrothermal fluids (which are commonly in equilibrium with minerals such as quartz, carbonate, chlorite and potassium-bearing phases such as potassium feldspar and sericite; Franklin, 1990; Large, 1992).

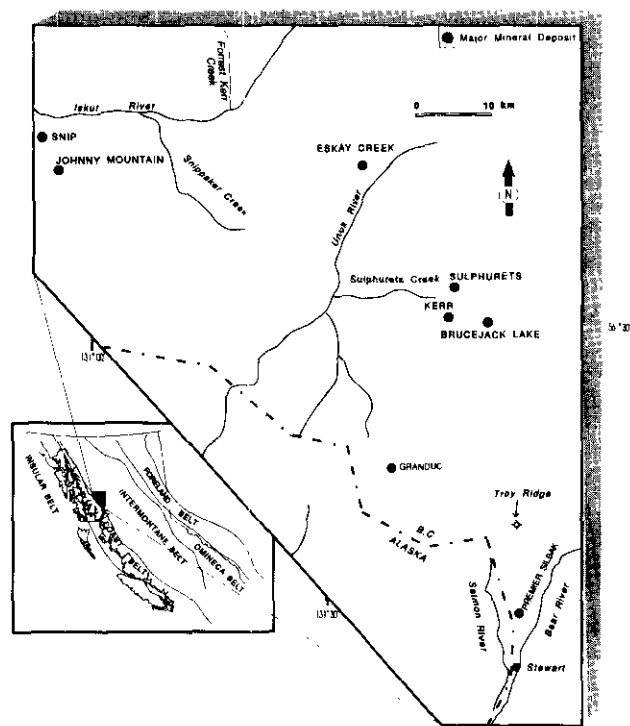


Figure 2-10-1. Location map.

BASALTIC ROCKS OF THE SALMON RIVER FORMATION

Basaltic rocks are a significant component of the Jurassic stratigraphic succession in the Iskut River area. Original mapping of the area included all of these mafic volcanic strata in the Unuk River and Betty Creek formations of the Hazelton Group, and reserved the Salmon River Formation for strictly sedimentary successions higher in section (Grove, 1986), consistent with Schofield and Hanson's (1922) original definition for that unit. Second generation regional mapping by provincial and federal government surveys revised the lithologic definitions of Hazelton Group units, and recognized that the Salmon River Formation contained an upper, basaltic member in the eastern Iskut

River area (Eskay Creek facies of Anderson and Thorkelson, 1990). Descriptions of the Mount Dilworth formation by Alldrick and Britton (1988) and Alldrick *et al.* (1989) provided a regional marker unit dividing the Salmon River Formation from older Hazelton Group rocks, and greatly assisted in its recognition. We now know that the basaltic portion of the Salmon River Formation is quite extensive in the eastern Iskut River, Unuk River and Forrest Kerr Creek areas, (*e.g.*, Anderson and Thorkelson, 1990; Logan *et al.*, 1990; Lewis, 1992) and that it locally forms accumulations up to 2000 metres thick (Read *et al.*, 1989). Anderson and Thorkelson (1990), and more recently Lewis *et al.* (1992) suggest that a belt of pillowed basaltic rocks along the eastern bank of the Unuk River, previously defined as the Unuk River formation, are probably part of the Salmon River Formation and may extend southward to the Granduc area. This correlation implies a significantly younger age for the Granduc deposit than previously assumed.

Salmon River Formation basalts vary significantly in lithologic character and thickness. Sections of pillowed flows hundreds of metres thick occur immediately adjacent to stratigraphic sections completely lacking correlative strata, suggesting either local volcanic centres or considerable basin relief during deposition. The most common

lithotype in the eastern Iskut River area is pillowed to massive volcanic flows. At Treaty Creek, possible correlatives to these flows pass upward into a thick sequence of hydroclastic volcanic breccias. On the western Prout Plateau, basaltic rocks undergo a southward transition from pillowed flows on Mount Shirley, to broken-pillow breccias and volcanic breccias just south of Mount Shirley, to massive volcanic flows farther south.

North of the Iskut River, rocks of the Salmon River Formation underlie the area east of the Forrest Kerr fault (Read *et al.*, 1989), and extend 30 kilometres northward into the More Creek area, where fossil collections indicate early Middle Jurassic (Aalenian) ages (Logan *et al.*, 1992). The volcanic succession comprises up to 2000 metres (Read *et al.*, 1989) of well-preserved, predominantly pillowed lava flows, sparsely pyroxene-phyric, mafic lava flows, scoriaceous lapilli-tuff breccia (Logan *et al.*, 1992) and subordinate, interbedded, cherty, black siltstones and white tuffs (pajama beds) characteristic of the Eskay Creek facies (Anderson and Thorkelson, 1990). Flow tops and facing directions are easily recognized. Interbedded fine-ash tuff and siltstone constitute less than 10 per cent of the section. The basalt is dense, amygdaloidal and made up of fine-grained vitreous plagioclase and rare pyroxene phenocrysts. Subvolcanic gabbroic sills and dikes intrude the volcanic



Plate 2-10-1. Pillow lavas, Eskay Creek mining lease.

pile. Their mineralogy and textures are similar to pillowed and brecciated extrusive rocks for which they probably represent feeders.

Contact relationships between the Salmon River Formation basaltic rocks and enclosing strata are varied through the area: one of the most extensively studied localities is Eskay Creek, where pillowed (*e.g.*, Plate 2-10-1) and brecciated basaltic flows (*see* Plate 2-12-4, in Roth, 1993, this volume) are separated from underlying felsic volcanic rocks of the Mount Dilworth formation by a thin mudstone layer. Well-bedded siltstone to fine-grained wacke overlies the mafic rocks in the Argillite Creek watershed; it is not clear whether these sediments are part of the Salmon River Formation or the overlying Bowser Lake Group (*see* Bartsch, this volume). On the southern Prout Plateau, Salmon River basalts overlie a mudstone and volcanic rock sequence similar in character to Eskay Creek, and the upper contact is

eroded. At John Peaks and Mount Mudge, east of the Unuk River, Salmon River basalts are tectonically interleaved with mudstones and felsic volcanic rocks along an imbricate thrust fault system, and original stratigraphic contacts are obliterated.

PETROGRAPHY

Thin sections of basalt from the Eskay Creek mining lease contain plagioclase as microphenocrysts and radiating microlites, very locally accompanied by minor pyroxene, which is more commonly obliterated by alteration (*e.g.*, Plate 2-10-2). There is no petrographic evidence for the timing of pyroxene-destructive alteration. Along the western edge of the Prout Plateau, where the unit forms a thick succession of pillowed flows on Mount Shirley, textures are characterized by ophitic pyroxene enclosing feldspar (Plate 2-10-3). Basalts in the hanging wall of the 21 zone retain



Plate 2-10-2. Sample AJM-ISK90-117. Plagioclase microphenocrysts and radiating microlites, pillowed basalt flow, Argillite Creek, southern margin of Eskay Creek property; field of view = 1.15 mm.



Plate 2-10-3. Sample S106. Ophitic pyroxene enclosing plagioclase from basalt flow, Mount Shirley area, north Prout Plateau, field of view = 2.5 mm.

primary volcanic textures and plagioclase laths, although plagioclase and glass groundmass are locally altered by sericite and chlorite, respectively. Very locally, carbonate alteration is considerable (visual estimates to 20%), resulting in a buff-grey, fine-grained rock (e.g., exposed in Tom MacKay Creek on the Eskay Creek mining lease) in which carbonate (+ quartz) veinlets cut earlier magnetite veinlets in the mafic rock.

North of the Iskut River, in quenched basaltic rock (close to pillow margins), acicular plagioclase laths form an open intersertal texture with dark iron oxide stained, devitrified glass and variolitic intergrowths of clinopyroxene and plagioclase. In other thin sections, an intergranular texture of randomly oriented, interlocking, subhedral grains of plagioclase and clinopyroxene is more common. Alteration is mainly lower greenschist facies: calcite, chlorite, chalcidonic quartz and rare epidote line vesicles. Prehnite + quartz + chlorite \pm albite assemblages occur in thinly bedded, intraflow volcanic siltstone and tuffs. Radiating and "bow-tie" structures of prehnite (Plate 2-10-4) are similar to the "crystallites" described at Eskay Creek (Ettliger, 1991). North of the Iskut River, however, these assemblages are not associated with known mineralization. Locally, plagioclase laths and microlite groundmass are altered to sericite, and chlorite forms pseudomorphs after clinopyroxene.

LITHOGEOCHEMISTRY

The locally pillowed and brecciated volcanic rocks associated with tuffaceous turbidites and argillaceous rocks of the Salmon River Formation in the Eskay Creek area were termed, informally, "andesites" by earlier workers (e.g., Idziszek *et al.*, 1990). Lavas at a similar stratigraphic level in the Forest Kerr Creek area, on the other hand, are basaltic, subalkaline tholeiitic composition, lying on an iron-enrichment trend on an AFM diagram (Logan and Drobe, in preparation). In addition, the Forrest Kerr Creek basaltic rocks plot as ocean-floor basalts on the discrimination diagrams of Pearce and Cann (1973).

Here we present data (Table 2-10-1) comparing relatively unaltered and altered lavas from the Prout Plateau and Forrest Kerr Creek areas, including samples of subvolcanic dikes interpreted to be feeders to overlying flows within the Salmon River Formation. These mafic dikes do not intrude overlying Bowser Lake Group sediments. The Prout Plateau samples have been further divided into a set collected from surface and samples from diamond-drill core in the vicinity of the Eskay Creek 21 zone. Total weight per cent oxides for a small number of samples (e.g., AJM-ISK90-040, total = 96.8 weight %) are low; in most of these cases, carbonate alteration (and, hence, loss on ignition) is considerable, commonly greater than 10 per cent. Other samples included a significant sulphide component (e.g., CA-90-423-55.5, S



Plate 2-10-4. Sample 89-JDR-4-5 : Prehnite in low-grade volcanic rocks from the Forrest Kerr area.

TABLE 2-10-1
OXIDE AND SELECTED TRACE ELEMENT ANALYSES OF VOLCANIC ROCKS, SALMON RIVER FORMAT ON,
NORTHWESTERN B.C.

	89-JLO-12-3	89-JLO-12-4	89-JLO-12-5	89-JLO-33-7	89-JLO-7-11	89-JLO-9-2.2	89-JLO-9-2.2	89-YKO-11-4	90-YKO-4-1	91-PL-425	AJM-1SK90-008	AJM-1SK90-016	AJM-1SK90-018a	AJM-1SK90-018b	AJM-1SK90-031	AJM-1SK90-044
(Wt %)																
SiO2	46.00	49.10	48.20	47.50	43.60	48.70	46.50	46.70	46.80	56.50	49.40	51.00	43.70	44.90	57.50	39.71
TiO2	2.00	1.15	2.30	1.44	0.73	1.51	1.48	1.58	1.58	1.28	1.77	1.85	1.75	1.81	1.08	1.31
Al2O3	13.50	16.00	13.80	17.80	13.20	15.30	14.30	15.50	15.50	16.00	15.00	15.40	13.30	16.80	13.20	12.81
Fe2O3	2.08	1.53	2.27	1.12	1.58	1.74	1.83	1.97	1.71	1.07	2.01	1.85	1.85	2.13	1.52	1.31
FeO	10.48	7.80	11.55	5.73	7.95	8.87	9.33	10.02	8.72	5.48	10.25	9.33	9.16	10.88	7.72	6.85
MnO	0.21	0.17	0.22	0.17	0.24	0.17	0.22	0.18	0.18	0.12	0.21	0.19	0.17	0.22	0.22	0.21
MgO	6.70	7.02	6.90	5.93	10.50	6.26	9.72	8.37	5.92	3.24	6.92	3.33	5.14	6.19	2.43	2.71
CaO	9.40	10.70	9.28	8.65	10.80	10.80	8.53	10.40	10.90	4.01	8.18	7.24	5.01	3.78	4.40	16.01
Na2O	2.50	2.66	2.30	3.71	1.08	2.58	2.16	2.84	2.37	6.18	1.66	3.39	3.01	3.31	3.01	0.71
K2O	0.11	0.62	0.02	1.03	0.97	0.43	0.58	0.23	0.23	0.59	0.32	0.37	0.70	0.53	1.50	2.11
P2O5	0.16	0.11	0.20	0.36	0.11	0.23	0.22	0.21	0.15	0.83	0.23	0.23	0.29	0.28	0.48	0.21
LOI	2.54	2.08	3.23	4.39	7.63	3.39	3.93	2.85	3.54	3.82	3.54	2.30	3.54	4.23	5.54	12.81
Sum	97.87	98.94	97.66	97.83	98.48	97.99	98.78	98.85	99.38	96.92	97.49	98.35	85.59	95.14	98.80	98.71
CO2(Wt %)	1.00	0.80	0.78	2.03	4.47	1.05	0.04	0.47	1.80	1.22	0.87	1.09	2.80	2.12	4.84	12.41
S(ppm)	0	0	155	0	363	0	150	0	54	0	1040	27200	162	154	0	4111
Al	36.40	36.38	35.31	38.02	49.55	33.32	49.02	33.60	31.67	27.32	48.01	25.82	42.14	48.66	34.86	22.61
Au (ppb)	8	0	10	0	0	5	0	0	0	<DL	2	1	0	1	0	0
Nb(ppm)	22	<DL	26	12	<DL	<DL	35	<DL	31	19	11	11	16	21	20	11
Zr(ppm)	108	63	123	122	32	81	75	60	86	184	85	78	81	64	112	73
Tl(ppm)	11980	8884	13789	8833	4368	9052	6733	8532	9352	7674	10611	8682	13481	11450	8475	8061
Y(ppm)	22	15	28	23	11	30	27	34	19	32	31	31	32	34	22	23
Nb/Y	1.00	-	0.93	0.52	-	-	1.30	-	1.83	0.59	0.35	0.35	0.50	0.82	0.91	0.81
Zr/Y	0.01	0.01	0.01	0.01	0.01	0.01	0.01	0.01	0.01	0.02	0.01	0.01	0.01	0.01	0.02	0.01

	AJM-1SK90-005	AJM-1SK90-065	AJM-1SK90-067	AJM-1SK90-068	AJM-1SK90-069	AJM-1SK90-070	AJM-1SK90-081	AJM-1SK90-082	AJM-1SK90-083	AJM-1SK90-086	BDM91-S109	BDM91-S115	BDM91-S46	BDM91-F15	BDM91-C11
(Wt %)															
SiO2	48.90	47.20	49.20	48.00	49.20	48.10	48.90	43.50	48.10	44.20	48.20	51.50	48.80	45.10	51.50
TiO2	1.88	1.85	1.78	1.72	1.85	1.91	1.75	1.95	1.93	1.55	1.02	1.21	1.97	0.42	0.19
Al2O3	14.70	16.90	15.20	15.40	15.90	18.20	15.00	18.30	19.50	16.70	16.90	14.20	5.50	6.15	17.30
Fe2O3	1.85	1.86	1.85	1.74	1.82	1.82	1.97	1.71	1.82	1.20	1.79	1.84	2.28	0.79	0.30
FeO	9.41	9.64	9.41	8.87	9.25	9.25	10.02	8.72	8.26	6.13	9.10	8.34	1.83	4.01	4.10
MnO	0.21	0.23	0.20	0.20	0.22	0.19	0.22	0.08	0.11	0.08	0.21	0.20	0.19	0.28	0.39
MgO	5.89	5.74	5.43	4.84	5.23	5.81	5.21	10.20	7.14	6.58	8.19	6.58	5.78	6.38	2.14
CaO	9.75	8.05	8.14	8.85	6.45	5.78	8.01	0.18	0.57	6.22	6.41	10.90	8.53	13.00	7.73
Na2O	2.81	3.40	2.97	3.50	4.90	4.69	4.05	1.87	2.75	5.41	2.94	2.08	2.83	2.25	6.50
K2O	0.34	1.87	0.91	1.29	0.34	0.15	0.28	3.84	2.22	0.55	1.25	0.22	1.04	0.91	0.35
P2O5	0.28	0.19	0.24	0.23	0.26	0.25	0.24	0.20	0.21	0.48	0.17	0.16	0.19	0.10	0.33
LOI	1.77	4.23	2.47	3.77	2.93	3.47	2.47	8.23	5.54	8.40	5.23	2.47	0.38	17.50	7.36
Sum	97.36	98.48	97.77	98.21	97.65	97.16	98.08	98.58	97.95	97.47	99.41	99.28	89.11	99.84	99.41
CO2(Wt %)	0.59	1.37	0.81	2.20	0.55	0.33	0.10	0.00	0.02	6.30	0.36	0.84	0.40	15.70	5.40
S(ppm)	0	130	3880	57	15100	150	0	14000	0	0	0	1	0	0	0
Al	33.51	43.95	36.33	32.44	33.72	36.62	31.20	87.10	73.82	37.64	80.24	34.36	17.44	32.28	17.84
Au (ppb)	0	0	0	5	7	0	0	19	0	-2	<DL	<DL	18	4	7
Nb(ppm)	11	<DL	<DL	24	15	23	23	19	<DL	2	<DL	4	4	4	3
Zr(ppm)	78	78	80	80	81	90	84	92	91	<DL	59	85	137	62	55
Tl(ppm)	10072	8692	10651	10311	11091	11450	10491	11690	11570	9262	6115	7254	1610	2524	4119
Y(ppm)	32	32	33	33	35	32	32	27	28	37	32	41	31	-999	46
Nb/Y	0.34	-	-	0.73	0.43	0.72	0.72	0.70	-	0.38	-	0.38	0.13	0.00	0.07
Zr/Y	0.01	0.01	0.01	0.01	0.01	0.01	0.01	0.01	0.01	0.01	0.01	0.01	0.01	0.02	0.02

	BDM91-S101	BDM91-S105	BDM91-S106	CA89-89-34.3	CA89-89-42.1	CA89-291-15.9	CA89-291-9.2	CA89-291-87.0	CA89-423-29.3	CA89-423-35.9	CA89-423-57.0	D91-186	E81-117	G81-181	G91-175	GM-82	X1	GM-82-002	GM-82-013	
(Wt %)																				
SiO2	56.00	43.70	47.70	47.20	39.90	47.00	27.70	45.10	48.70	35.80	35.90	50.50	50.80	51.80	48.10	4.50	47.30	43.30		
TiO2	2.10	0.48	0.50	1.52	0.83	1.47	0.87	1.61	1.90	0.87	1.77	1.67	1.67	1.24	1.50	1.8	1.84	1.54		
Al2O3	11.80	17.00	19.70	15.50	9.90	15.30	9.15	15.50	16.00	11.10	16.80	15.40	15.40	16.40	14.70	1.30	14.90	14.30		
Fe2O3	1.94	0.98	1.13	1.85	1.31	1.88	1.40	1.83	1.92	1.68	1.53	1.89	1.92	1.28	1.62	0.6	1.91	1.79		
FeO	9.97	5.07	5.77	9.41	6.99	8.57	7.11	9.33	9.79	8.57	7.90	9.94	8.79	9.40	6.28	1.46	9.71	9.10		
MnO	0.24	0.12	0.22	0.21	0.24	0.21	0.18	0.18	0.14	0.15	0.14	0.21	0.21	0.14	0.23	0.19	0.21	0.19		
MgO	4.22	4.92	6.73	5.95	3.75	5.31	3.23	11.30	6.70	7.86	18.80	4.22	4.23	4.33	5.08	1.10	4.88	8.33		
CaO	5.44	19.90	9.83	9.37	19.80	10.40	28.90	3.01	3.48	9.99	1.85	7.37	1.42	7.52	8.40	7.2	10.20	8.30		
Na2O	3.88	1.23	1.85	3.68	2.38	3.80	0.38	2.89	2.95	0.17	0.48	3.73	3.88	5.08	4.47	24	3.91	1.34		
K2O	0.20	0.10	2.45	0.43	0.02	0.50	0.18	0.08	0.58	3.96	2.03	0.27	0.28	0.36	0.14	44	0.25	1.22		
P2O5	0.36	0.08	0.08	0.17	0.14	0.19	0.13	0.17	0.18	0.23	0.19	0.23	0.23	0.89	0.18	14	0.24	0.24		
LOI	2.83	6.23	3.77	2.70	12.50	3.39	16.50	6.54	3.77	4.77	6.39	3.54	2.54	2.93	4.62	77	4.16	7.36		
Sum	98.75	90.53	99.52	97.88	97.32	97.82	95.51	97.32	95.81	84.75	95.48	98.87	98.15	98.35	98.30	9.11	99.11	97.83		
CO2(Wt %)	0.18	2.36	0.13	1.19	13.10	2.72	17.90	2.17	1.16	8.21	1.23	0.88	1.88	0.30	2.98	.15	2.01	3.12		
S(ppm)	0	0	0	827	5290	1370	12100	305	-50	47300	11300	17000	19300	960	2500	0	0	0		
Al	32.22	19.42	44.43	31.78	14.94	29.33	10.44	86.83	53.10	53.35	89.84	28.80	26.80	27.13	27.34	8.73	25.89	52.82		
Au (ppb)	33	<DL	<DL	11	3	<DL	<DL	3	6	780	100	6	3	6	2					

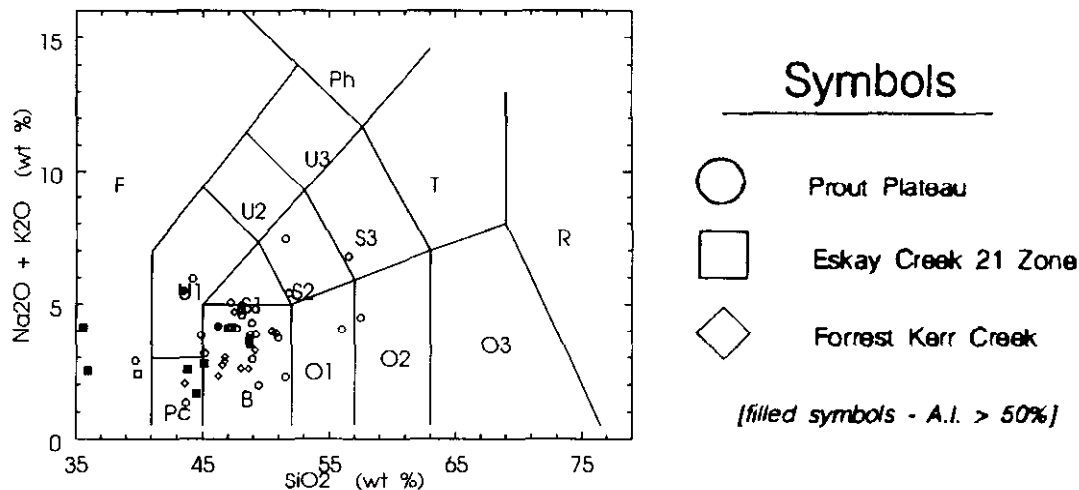


Figure 2-10-2. Total alkali – silica diagram (after LeMaitre, 1989); classification of volcanic rocks (Le Bas *et al.*, 1986). Circles are volcanic rock samples from the Prout Plateau, squares are from diamond-drill core at Eskay Creek, diamonds are from Forest Kerr Creek; filled symbols are those registering with AI>50% (refer to Table 2-10-1).

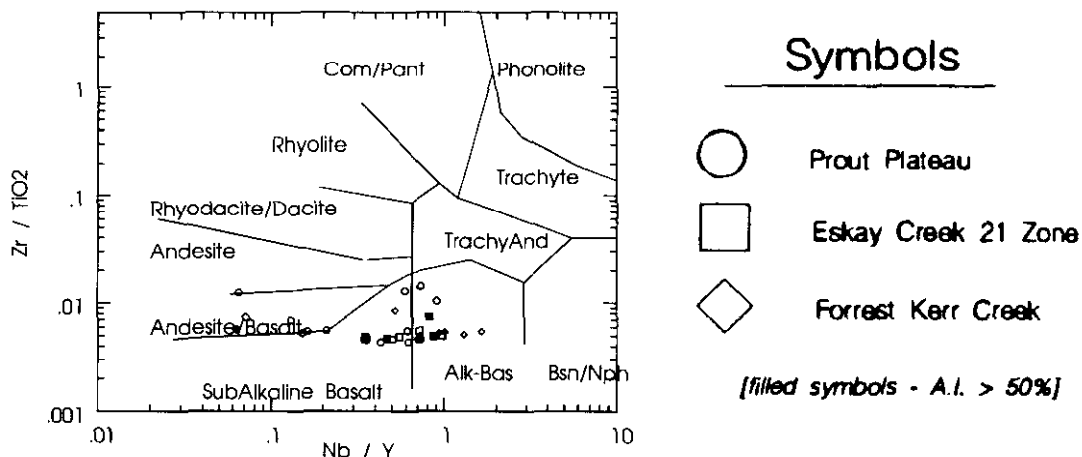


Figure 2-10-3. Zr/TiO₂ vs. Nb/Y diagram (after Winchester and Floyd, 1977), basaltic and intermediate rocks in the Iskut River and Forest Kerr Creek areas. Circles are samples from the Prout Plateau, squares are from diamond-drill core at Eskay Creek, diamonds are from Forest Kerr Creek; filled symbols are those registering with AI>50% (refer to Table 2-10-1).

= 47 300 ppm, or 4.7 %). Caution is required in interpretation of data from samples that contain elevated quantities of elements resulting from alteration.

An “index of alteration” (included in Table 2-10-1) is the percentage ratio $(K_2O + MgO) \times 100 / (K_2O + MgO + Na_2O + CaO)$, established originally for felsic rocks by Ishikawa *et al.* (1976). The index is an assessment of alteration phenomena including “addition” of potassium and magnesium, with “removal” of sodium and calcium. This method can only be considered as a first-pass technique as it does not consider conservation of species, nor the effects of closure. Gemmell and Large (1992) demonstrated that the alteration index (AI) is applicable to intermediate and mafic rocks in the Hellyer mine, Tasmania.

Figure 2-10-2 (silica - total alkalis diagram, with rock nomenclature after Le Bas *et al.*, 1986) indicates that most of the rocks are basaltic in composition. Outliers, with silica less than 41 per cent, are samples that have suffered considerable carbonate alteration (Table 2-10-1), most of which are from diamond-drill core in the vicinity of the Eskay Creek deposits. A small number of samples (4) are picobasaltic, including one from the Forrest Kerr Creek area; the remainder of the Forrest Kerr data cluster tightly within the basaltic field. Prout Plateau rocks, on the other hand, exhibit a range in composition from picobasalt, through basalt to trachyandesite and andesite. Two samples within the tephrite-basalt field have suffered alkali alteration and are discussed separately below.

Trace element contents suggest alkaline basalt to sub-alkaline basaltic compositions (Figure 2-10-3; Winchester and Floyd, 1977). Basalts from the Forrest Kerr Creek area again show a restricted composition, whereas Prout Plateau rocks show a range of compositions from basaltic to andesitic. More data are required to assess whether these differences reflect different, time-equivalent volcanic centres; unrelated volcanic events; a natural variation in basalt chemistry; or hydrothermal alteration.

The alteration index data (Table 2-10-1) suggest that the Forrest Kerr Creek sample set comprises a relatively unaltered suite. One sample (BDM91-109) from the Mount Shirley area of the Prout Plateau has an index of 50.24 per cent. Six samples from diamond-drill core in the vicinity of the Eskay Creek 21 zone and also two samples collected from surface in Tom McKay Creek, to the north of the Eskay Creek 21 zone, registered high alteration indices. The two outcrop samples (AJM-ISK90-082, -083; AI = 87.1% and 73.82%, respectively) were collected from the projection to surface of the hangingwall above the Eskay Creek 21 mineralized zone. Gold contents in these two rocks are less than 20 ppb. Another basaltic sample from a nearby exposure in Tom McKay Creek (AJM-ISK90-086, AI = 37.9%) did not register a significant AI using this approach, as the rock has apparently suffered carbonate alteration ($\text{CO}_2 = 6.3 \text{ wt. } \%$) and possible sodium addition ($\text{Na}_2\text{O} = 5.4 \text{ wt. } \%$; Table 2-10-1).

SUMMARY

Intermediate to mafic volcanic rocks are a key component of Salmon River Formation hostrocks to the Eskay Creek precious and base metal deposits in the Iskut River area of northwestern British Columbia. An initial appraisal of basalt petrology and geochemistry from the Prout Plateau and Forrest Kerr Creek areas suggests that hydrothermal alteration related spatially and, by inference, genetically to mineralization, may be recorded in the basaltic rocks. The alteration signatures are revealed by a crude measure of alteration involving the oxides of potassium, magnesium, sodium and calcium. These preliminary results encourage us to investigate further the effects of mass transfer that accompanied alteration in the Eskay Creek mineralizing system, through the employment of more rigorous and quantitative analysis, such as that proposed by Pearce (1968).

ACKNOWLEDGMENTS

We wish to acknowledge the several mining and exploration companies whose logistic assistance has made this project possible: Prime Resources Inc. (now Prime Equities Inc.), Granges Inc. and International Corona Inc. (now Homestake Canada Ltd.). The assistance of Gerry McArthur (Consultant to Prime) in providing samples from diamond-drill core, technical assistance and much valuable discussion is gratefully appreciated. J.F.H. Thompson and A.J. Sinclair are thanked for review of an earlier draft.

REFERENCES

- Alldrick, D.J. and Britton, J.M. (1988): Geology and Mineral Deposits of the Sulphurets Area (104A/5, 104A/12, 104B/8, 104B/9); *B.C. Ministry of Energy, Mines and Petroleum Resources*, Open File 1988-4.
- Alldrick, D.J., Britton, J.M., Webster, I.C.L. and Russell, C.W.P. (1989): Geology and Mineral Deposits of the Unuk River Area, (104B/7E, 8W, 9W, 0E); *B.C. Ministry of Energy, Mines and Petroleum Resources*, Open File 1989-10.
- Anderson, R.G. and Thorkelson, D.J. (1990): Mesozoic Stratigraphy and Setting for some Mineral Deposits in Iskut River Map Area, Northwestern British Columbia; in *Current Research, Part E., Geological Survey of Canada*, Paper 90-1E.
- Bartsch, R.D. (1992): Prout Plateau - Lithology Petrology and Geochemistry; in MDRU Project: *Metallogenesis of the Iskut River Area, Northwestern B.C., Mineral Deposit Research Unit, The University of British Columbia*, Annual Report for period June 1991 - May 1992.
- Ettlinger, A.D. (1991): Eskay Creek - 21 Zone; in MDRU Project *Metallogenesis of the Iskut River Area, Northwestern B.C.; Mineral Deposit Research Unit, The University of British Columbia*, Annual Report for period June 1990 - May 1991.
- Edmunds, F.C., Kuran, D.L. and Rye, K.A. (1992): The Geology of the Eskay Creek Property and the #21 Zone Deposits; abstract, *Canadian Institute of Mining, Metallurgy and Petroleum*, Second Annual Field Conference, Kamloops, B.C., September 28-29.
- Franklin, J.M. (1990): Volcanic-associated Massive Sulphide Deposits; in *Gold and Base Metal Mineralization in the Abitibi Subprovince, Canada. University of Western Australia*, Publication No. 24, pages 211-243.
- Gemmell, J.B. and Large, R.R. (1992): Stringer System and Alteration Zones Underlying the Hellyer Volcanic-hosted Massive Sulphide Deposits, Northwestern Tasmania; *Economic Geology*, Volume 87, No. 3, pages 623-649.
- Gibson, H.L. and Watkinson, D.H. (1986): Volcanogenic Massive Sulphide Deposits of the Noranda Cauldron and Shield Volcano, Quebec; in *The Northwestern Quebec Polymetallic Belt, Canadian Institute of Mining and Metallurgy*, Special Volume 43, pages 119-132.
- Grove, E.W. (1986): Geology and Mineral Deposits of the Unuk River - Salmon River - Anyox Area; *B.C. Ministry of Energy, Mines and Petroleum Resources*, Bulletin 63, 152 pages.
- Ishikawa, Y., Sawaguchi, T., Iwaya, S. and Horuchi, M. (1976): Delineation of Prospecting Targets for Kuroko Deposits Based on Modes of Volcanism of Underlying Dacite and Alteration Halos; *Mining Geology*, Volume 26, pages 105-117.
- Idziszek, C., Blackwell, J., Fenlor, R., McArthur, G. and Mallo, D. (1990): The Eskay Creek Discovery; *Mining Magazine*, March 1990, pages 172-173.
- Large, R.R. (1992): Australian Volcanic-hosted Massive Sulphide Deposits: Features, Styles, and Genetic Deposits; *Economic Geology*, Volume 87, pages 471-510.
- Le Bas, M.J., Le Maitre, R.W., Streckeisen, A. and Zanettin, B. (1986): A Chemical Classification of Volcanic Rocks Based on the Total Alkali - Silica Diagram; *Journal of Petrology*, Volume 27, Part 3, pages 745-750.
- Le Maitre, R.W. (1989): Some Problems of the Projection of Chemical Data into Mineralogical Classifications; *Contributions to Mineralogy and Petrology*, Volume 56, pages 181-189.

- Lewis, P.D. (1992): Geology of the Eastern Half of the Iskut River Map Area; poster, *British Columbia & Yukon Chamber of Mines*, Cordilleran Round-up, January 1992.
- Lewis, P.D., Macdonald, A.J. and Bartsch, R.D. (1992): Hazelton Group/Bowser Lake Group Stratigraphy in the Iskut River Area: Progress and Problems; in MDRU Metallogeneses of the Iskut River Area, Northwestern, B.C., *Mineral Deposit Research Unit, The University of British Columbia*, Annual Report for period June 1991 - May 1992.
- Logan, J.M. and Drobe, J.R. (in preparation): The Geology of Mess Lake, More Creek and Forrest Kerr Map Areas, Northwestern British Columbia; *B.C. Ministry of Energy, Mines and Petroleum Resources*, Bulletin.
- Logan, J.M. and Koyanagi, V.M. (1989): Geology and Mineral Deposits of the Galore Creek Area, Northwestern B.C. (104G/3, 4); in *Geological Fieldwork 1988*, B.C. Ministry of Energy, Mines and Petroleum Resources, Paper 1989-1, pages 269-284.
- Logan, J.M., Drobe, J.R. and Elsby, D.C. (1992): Geology of the More Creek Area, Northwestern British Columbia (104G/2); in *Geological Fieldwork 1991*, Grant, B. and Newell, J.M., Editors, *B.C. Ministry of Energy, Mines and Petroleum Resources*, Paper 1992-1, pages 161-178.
- Logan, J.M., Koyanagi, V.M. and Drobe, J.R. (1990): Geology of the Forrest Kerr Creek Area, Northwestern British Columbia (104B/15); *Geological Fieldwork 1989*, B.C. Ministry of Energy, Mines and Petroleum Resources, Paper 1990-1, pages 127-139.
- Macdonald, A. J. (1991): Lithostratigraphic Reconnaissance – Eskay Creek Area; in MDRU Metallogeneses of the Iskut River Area, Northwestern, B.C., *Mineral Deposit Research Unit, The University of British Columbia*, Annual Report for period June 1990 - May 1991.
- Miller, B.D. (1992): Structural History and Evolution of the Northern Prout Plateau; in MDRU Metallogeneses of the Iskut River Area, Northwestern, B.C., *Mineral Deposit Research Unit, The University of British Columbia*, Annual Report for period June 1991 - May 1992.
- Pearce, J.A., and Cann, J.R. (1973): Tectonic Settings of Basic Volcanic Rocks Determined Using Trace Element Analyses; *Earth and Planetary Sciences Letters*, Volume 19, pages 290-300.
- Pearce, T.H. (1968): A Contribution to the Theory of Variation Diagrams; *Contributions to Mineralogy and Petrology*, Volume 19, pages 142-157.
- Read, P.B., Brown, R.L., Psutka, J.F., Moore, J.M., Journeay, M., Lane, L.S. and Orchard, M.J. (1989): Geology of parts of the Snippaker Creek (104B/10), Forrest Kerr Creek (104B/15), Bob Quinn Lake (104B/16), Iskut River (104G/1), and More Creek (104G/2); *Geological Survey of Canada*, Open File 2094.
- Schofield, S.J. and Hanson, G. (1922): Geology and Ore Deposits of the Salmon River District, British Columbia; *Geological Survey of Canada*, Memoir 132.
- Smith, P.L. and Carter E. S. (1990): Jurassic Correlations in the Iskut River Map Area, British Columbia, and the Age of the Eskay Creek Deposit; Current Research, Part E; *Geological Survey of Canada*, Paper 90-1E, pages 149-151.
- Winchester, J.A., and Floyd, P.A. (1977): Geochemical Discrimination of Different Magma Series and their Differentiation Products using Immobile Elements; *Chemical Geology*, Volume 20, pages 325-343.

**LITHOSTRATIGRAPHY AND GEOCHRONOMETRY, BRUCEJACK LAKE,
 NORTHWESTERN BRITISH COLUMBIA (104B/8E)**

By A. James Macdonald, Mineral Deposit Research Unit,
 U.B.C.

(MDRU Contribution 017)

KEYWORDS: Economic geology, Hazelton Group, Stikine assemblage, geochronometry, metallogeny, silver, gold, Brucejack Lake, stratigraphy, flow-dome complex.

INTRODUCTION

This paper describes lithostratigraphy and two new U-Pb dates from the Brucejack Lake area, located in the southeast portion of the Bruceside property (Newhawk Gold Mines Ltd. 60%; Granduc Mines Ltd. 40%), part of the Sulphurets copper-gold-silver district (Figure 2-11-1). The study is part of the Mineral Deposit Research Unit's Project "Metallogeny of the Iskut River Area, Northwestern British Columbia". The Sulphurets area is important to the project due to the occurrence of mineral deposit types ranging from porphyry deposits (Cu, Cu-Au, and possibly Au-only), "mesothermal" veins to "epithermal" veins (*N.B.* usage of "mesothermal" and "epithermal" is based upon textural features) within a restricted area. It is not known whether

this spectrum of mineral deposits is co-temporal. Britton and Alldrick (1988) suggest that some mineralization in the Sulphurets area is coeval with intrusive activity, and intrusive activity is both syn and post-volcanic. Therefore, one part of this project is designed to understand the geological environment(s) prevailing during volcanic activity, intrusion of plutonic and hypabyssal rocks, base and precious metal mineralization, and finally, whether any or all of these events are related. Here, volcanic and subvolcanic igneous rocks and associated sediments in the Brucejack Lake area are described, with an emphasis on the volcanic environment.

The exploration history of the Sulphurets property to late 1991 is given by Roach and Macdonald (1992). Significant mineral deposits with published reserves in the immediate area include the Kerr porphyry copper-gold deposit (Placer Dome Inc., 125.7 million tonnes, 0.27 g/t Au, 0.62% Cu), and the West zone (Newhawk Gold Mines Ltd., 750 000 tonnes, 15.4 g/t Au, 644 g/t Ag).

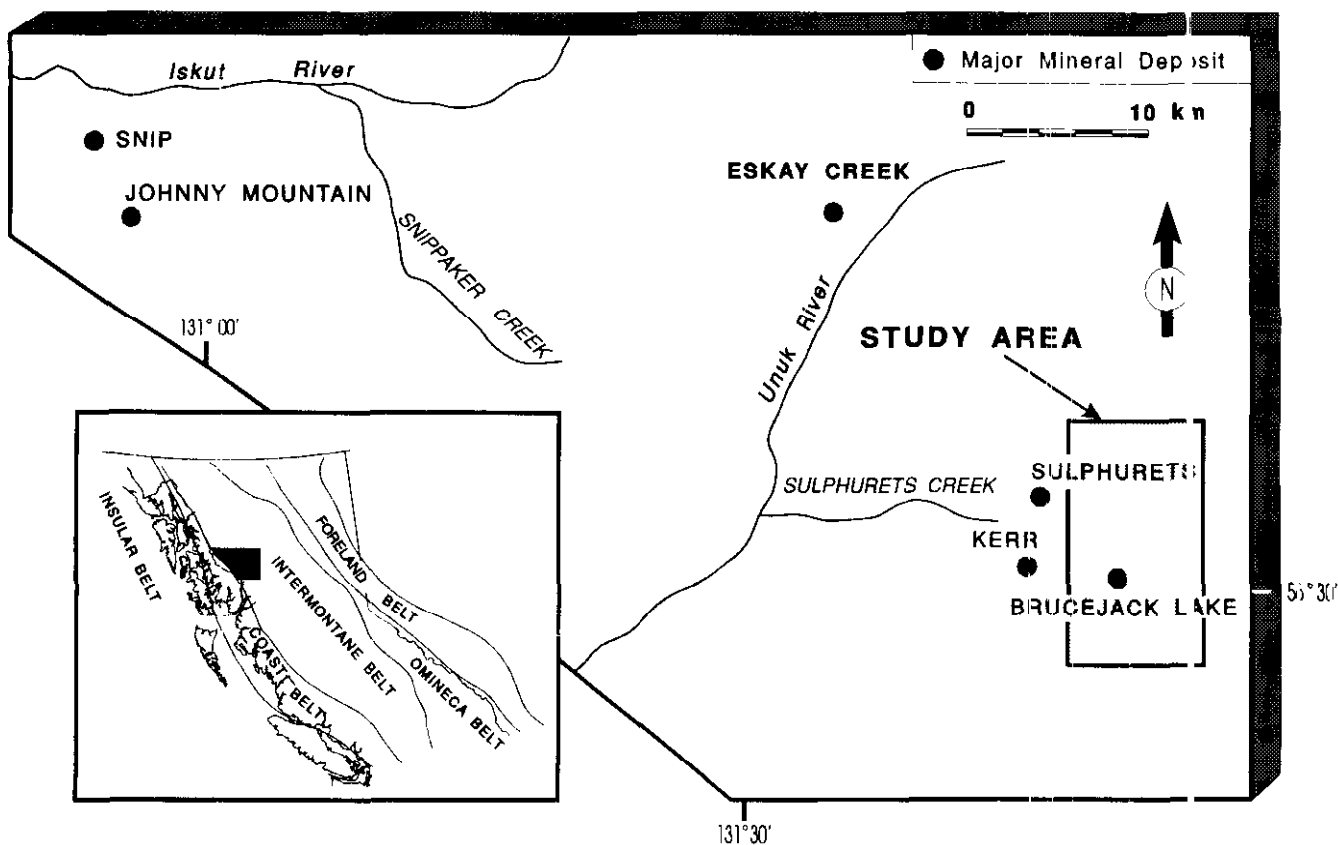


Figure 2-11-1. Location map, Brucejack Lake, Northwestern British Columbia

REGIONAL GEOLOGY

The results of recent studies (Aldrick and Britton, 1988; Henderson *et al.*, 1992; Kirkham, 1991, 1992; Lewis, 1992) collectively suggest that Upper Triassic Stuhini Group in the Sulphurets area is overlain unconformably by the Lower to Middle Jurassic Hazelton Group, at the base of which is a heterogeneous clastic sedimentary unit, comprising locally fossiliferous limy sandstone, siltstone and heterolithic conglomerate; the unit has been termed the Jack formation (named informally after the Jack Glacier) by Henderson *et al.* (*ibid.*). Overlying the Jack formation is the bulk of the Hazelton Group, comprising at lower levels a succession of dominantly intermediate volcanic and volcanoclastic rocks, with minor sediments, overlain by an intermediate to felsic extrusive unit (Mount Dilworth formation) and capped by a mixed sedimentary/mafic volcanic assemblage (Salmon River Formation). Overlying the Hazelton Group is an on-lap sedimentary unit, the Middle to Upper Jurassic Bowser Lake Group, comprising rhythmically bedded sandstone and argillite, and laterally discontinuous conglomerate; the assemblage is interpreted to be a turbidite succession by Henderson *et al.* (1992).

In this paper facies relationships are described from exposures within a small interval of the Sulphurets stratigraphy, comprising Hazelton volcanic, volcanoclastic and sedimentary rocks associated with a flow dome.

ECONOMIC GEOLOGY

In the vicinity of Brucejack Lake, precious metal mineralization occurs in two modes: semi-brittle, shear vein systems (*e.g.*, West zone), and brittle extension and breccia veins (*e.g.*, Quartz Hill, 367 zones). There are no data available to suggest that the two styles reflect two discrete, unrelated hydrothermal events. Galena lead-lead isotopes from both styles of mineralization are essentially identical; data fall within the Jurassic cluster defined by Godwin *et al.* (1990). The West zone crops out approximately 200 metres south of Brucejack Creek (draining the west end of Brucejack Lake) and plunges to the north under the creek. The geology and structure of the syntectonic, shear zone hosted West zone has been described by Lefebure (1987), Britton and Aldrick (1988), Roach and Macdonald (1992) and Macdonald and Roach (1992). Other shear-related vein structures are exposed to the north and northeast, for example, Gossan Hill and Shore zones.

Along strike to the northwest of the West zone and extending for in excess of 2 kilometres in its footwall (to the south-southwest), stockworks, extension veins and breccia veins are locally developed; for example, Galena Hill, 367, North Spine, Napoleon, Electrum, Mammoth, Quartz Hill, Bridge, Agatha, Jessica, and Fletcher veins and zones (Kirkham, 1992). The veins and their hostrocks are characterized by a lack of penetrative fabric, in contrast with intense schistosity developed in spatially restricted, quartz-sericite-pyrite hostrock near the West zone. Gangue mineralogy is dominated by quartz (locally microcrystalline) and locally by carbonate, and very locally, barite; in places, bladed carbonate is replaced by quartz, a feature that has been recognized in epithermal environments such as Mount

Skukum in the Yukon Territory (McDonald and Godwin, 1986) and Pajingo in Queensland, Australia (Dowling and Morrison, 1989). Lefebure (1987) first pointed out that quartz-carbonate veins are developed peripherally to the intense quartz-sericite-pyrite alteration around the ductily deformed West zone vein mineralization. This spatial relationship suggests that the two styles may be related.

LITHOSTRATIGRAPHY – BRUCEJACK LAKE

The Hazelton Group in the Brucejack Lake area consists of a thick (>2 km) sequence of interbedded sedimentary and volcanic rocks including both flows and pyroclastic deposits (Britton and Aldrick, 1988). The sedimentary rocks vary from fine-grained argillaceous rocks (*e.g.*, in the footwall of the West zone: Roach and Macdonald, 1992) to conglomerate with fine-grained muddy matrix, to epiclastic rocks (Britton and Aldrick, 1988). Conglomerate matrix is locally a hematitic, finely banded siltstone (*see* below).

Crystal tuffs, lapilli tuffs and blocky tuff breccias of intermediate composition are volumetrically the most significant volcanic rock type in the Brucejack Lake area; they are commonly well layered (Plate 2-11-1), exhibit graded bedding, locally reverse grading (coarsening upwards), with local development of tractional bed forms such as ripples (Plate 2-11-2), small troughs associated with low-angle cross-stratification and erosional contacts formed during the emplacement of overlying deposits (Plate 2-11-3). The volcanoclastic deposits are interlayered with marine sedimentary units; in addition, Britton and Aldrick (1988) note the presence of air-fall tuffs, although these have not been observed during this study. Accretionary lapilli are preserved locally, and are concentrated in the upper part of bedded, intermediate volcanoclastic deposits (location marked in Plate 2-11-1). The lapilli are "rim-type" under the classification of Schumacher and Schminke (1991), in which a fine to medium-grained core of each ash lapillus is surrounded by an extremely fine grained rim of ash (Plate 2-11-4). Multiple banding is not seen in the fine ash rims; rare lapilli have no obvious core, composed only of fine ash.

In the lithic and breccia tuffs, both clasts and matrix may contain plagioclase, potassium feldspar and/or hornblende phenocrysts. Flow rocks may also contain similar phenocryst assemblages and, as described below, show local interdigitations with volcanoclastic rocks, suggesting that the two are closely related. Mafic pillow lavas are present (Britton and Aldrick, 1988), but are volumetrically insignificant. Clast size in blocky tuff breccias reaches in excess of 3 metres to the south of Brucejack Lake.

Superficially similar to pyroclastic lithic tuffs and tuff breccias, although genetically quite different, complex poly-lithic units are interpreted to form from the juxtaposition and admixture of more than one pyroclastic deposit, either as an intrusion breccia, in which a younger flow brecciates an older flow or pyroclastic deposit (Plate 2-11-5), or by the disaggregation of an unconsolidated deposit during introduction of subsequent flow(s) (Plate 2-11-6). Complex breccias resulting from the process of interaction of volcanic or volcanoclastic rocks with unconsolidated precursor volcanic, volcanoclastic or sedimentary rocks, have been

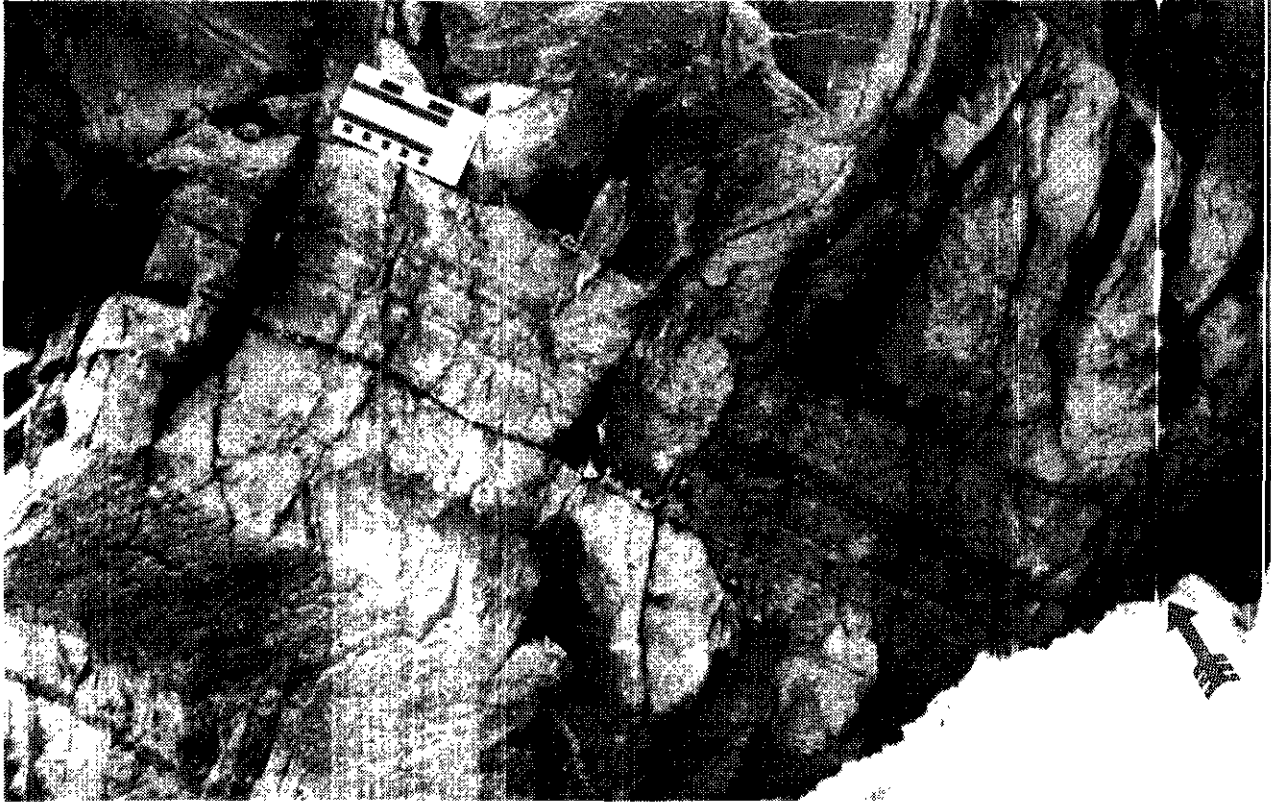


Plate 2-11-1. Layered intermediate pyroclastic rocks, south of Brucejack Lake.
Arrow notes stratigraphic level of accretionary lapilli (refer to Plate 2-11-6).

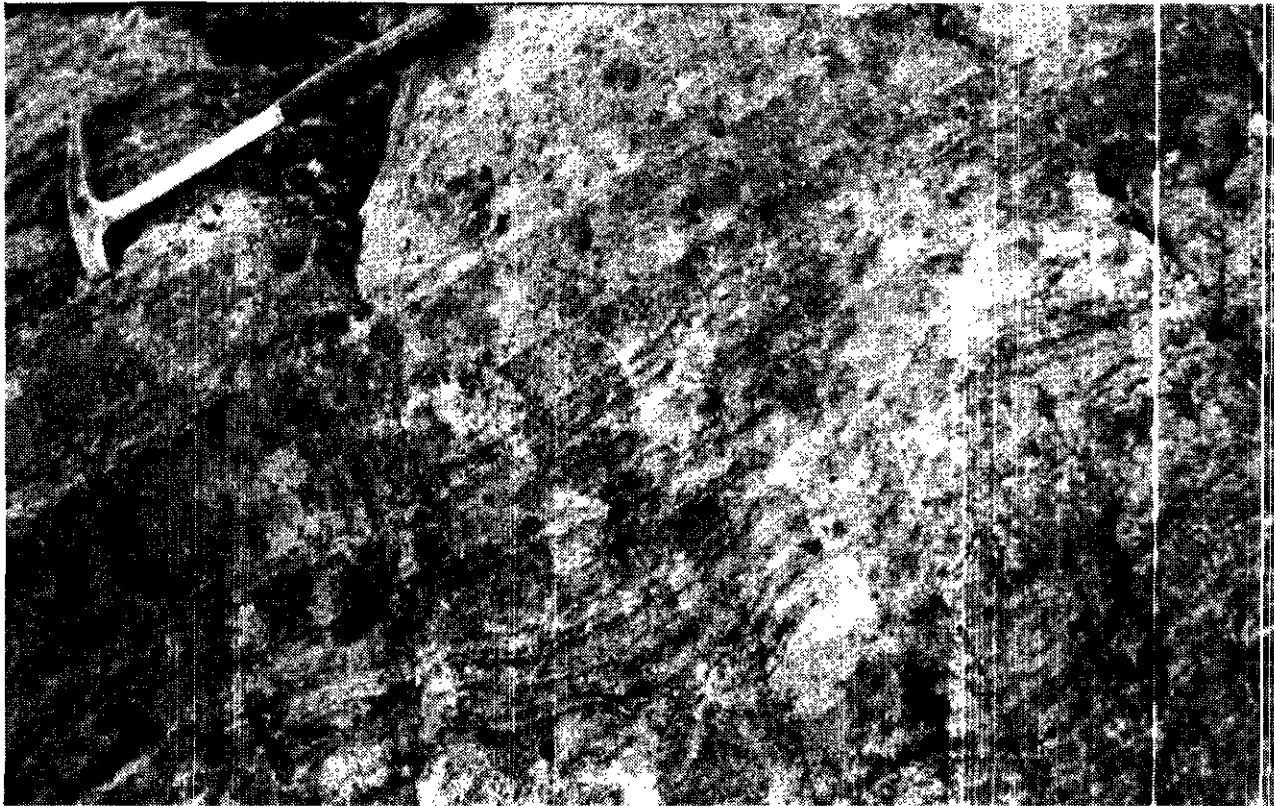


Plate 2-11-2. Ripple bed-forms in intermediate pyroclastic rocks,
southeast of Brucejack Lake.



Plate 2-11-3. Erosional relationships exhibited by pyroclastic deposits, south wall of Hanging Glacier valley.

described elsewhere in the Iskut River map area, such as the Eskay Creek mining lease (Macdonald, 1990), and the Treaty nunatak (Lewis *et al.*, 1993).

A felsic flow-dome complex within the Hazelton rocks outcrops near Brucejack Lake (Roach and Macdonald, 1992); both intrusive and extrusive components of the complex are well exposed. The intrusive component is flow banded and locally flow folded (Plate 2-11-7); the attitude of flow banding is highly variable in the body of the intrusive phase, but becomes aligned subparallel to intrusive contacts with enclosing, heterogenous, bedded to massive pyroclastic rocks; faulted contacts with enclosing volcanoclastic rocks are also common. The appearance of flow banding is enhanced in hand specimen by reddish, hematitic alteration spatially related to millimetre to centimetre-scale, sigmoidal fractures developed preferentially in the fine-grained flow bands and not in intervening feldspar-phyric material.

The flow-banded unit has gradational, diffuse, irregular and interfingering contacts with a voluminous breccia unit (Plate 2-11-8) comprising clasts and boulders of massive and flow-banded felsic material identical in hand specimen to the intrusive phase, in a hematitic, muddy and locally finely laminated matrix. Higher in the section to the south of Brucejack Lake, the flow-banded felsic unit rests in apparent stratigraphic contact upon maroon, blocky tuff and the above-mentioned breccia unit; flow banding in this extrusive component of the unit is generally subparallel to both the contact with underlying breccias and tuffs, and bedding in other pyroclastic and sedimentary units south of Brucejack Lake (Aldrick and Britton, 1991). The thickness of the breccia unit is variable, but is best developed, in excess of 30 metres, on the south and southwest flank of Mount John

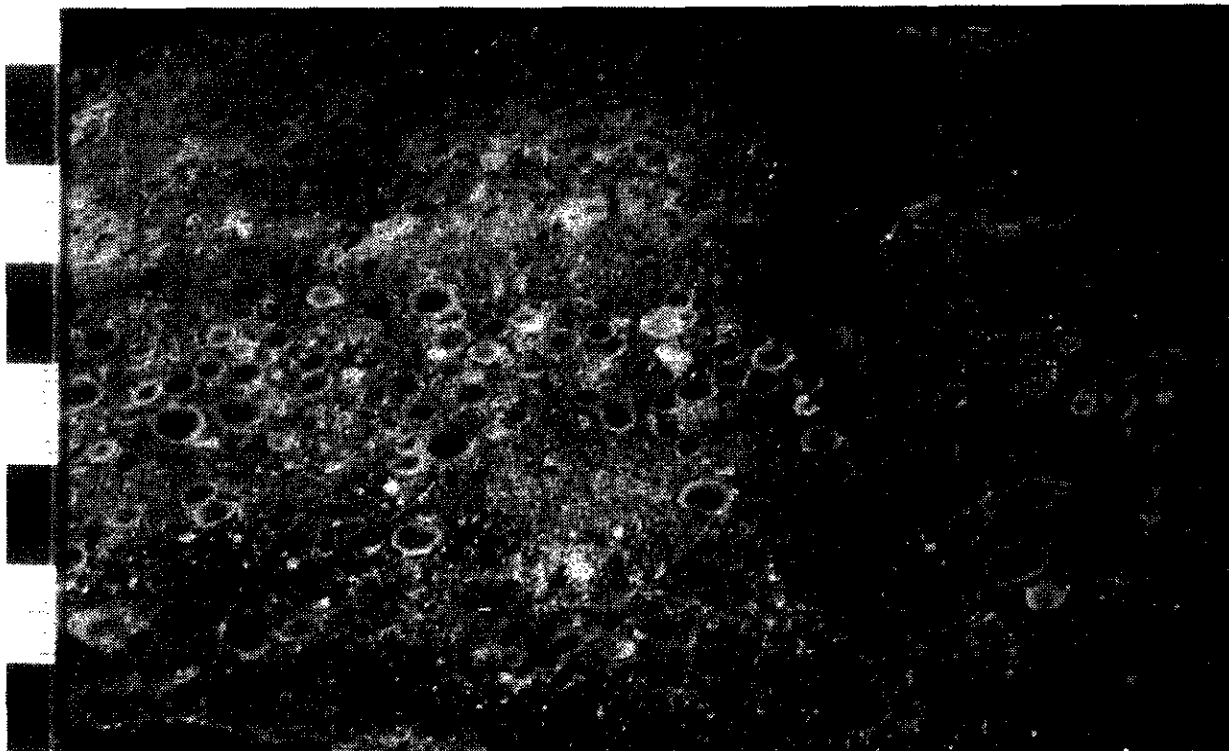


Plate 2-11-4. Accretionary lapilli from outcrop in Plate 2-11-1.



Plate 2-11-5. Breccia of light grey intermediate volcanic rock intruding dark intermediate pyroclastic rock, south of Brucejack Lake. Scale: measuring tape (decimetre scale on outcrop).

Walker, north of Brucejack Lake, from where the unit can be traced intermittently around the east end of Brucejack Lake to the intrusive and extrusive components of the flow dome described above, and northwest to the south wall of Hanging Glacier (referred to as Freegold Glacier in some pre-1990 publications) a strike length of approximately 4 kilometres.

In thin section, the flow banded rock is seen to contain (a) 35 to 40 per cent plagioclase phenocrysts to 4 millimetres exhibiting minor sericite alteration along fractures, and local epidote and hematite alteration; the hematite is manifest as a curious "peppering" of altered feldspar (?plagioclase), the significance of which is not yet clear; (b) conspicuous, trace apatite (<0.2%) needles to 400 microns; (c) approximately 60 per cent groundmass of quartz \pm feldspar \pm clay \pm sericite \pm carbonate; the rock is cut by sericite-carbonate veinlets, locally up to 5 millimetres wide.

The flow dome is intruded by felsic dikes, striking north-northwesterly, dipping steeply, and generally less than 50 centimetres wide (visible under the measuring tape in Plate 2-11-7). Locally the dikes disaggregate into bulbous, ovoid bodies, less than a metre in long dimension (Plate 2-11-9). Although these bodies exhibit some geometric similarities to boudins, the host rock (flow-banded felsic unit) shows no visible strain.

In thin section, the felsic dike rock exhibits pervasive alteration of plagioclase (approximately 30%, to 3 mm in long dimension) by epidote. This rock, like the flow-banded rock it intrudes, contains strongly altered grains of feldspar (?plagioclase), partially replaced by hematite; the groundmass comprises 65 to 70 per cent of the rock, similar to the flow-banded unit; the dike rock (including epidote after plagioclase) is cut by quartz veinlets.

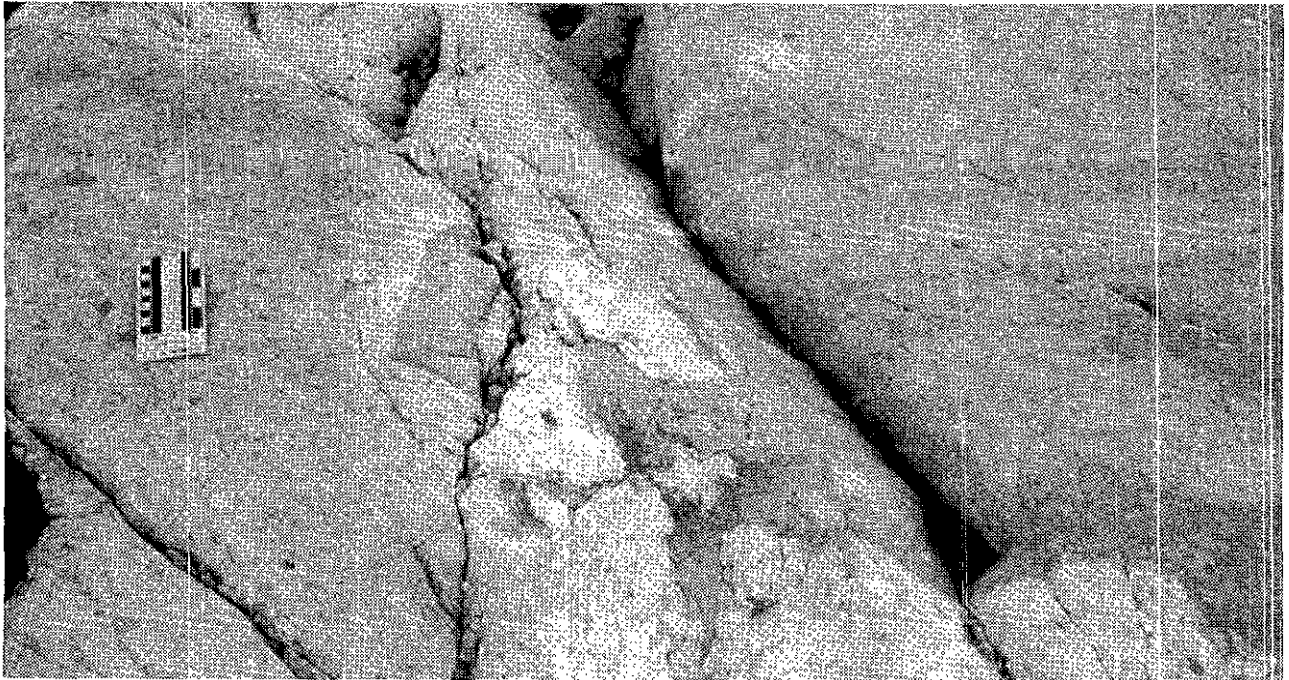


Plate 2-11-6. Disaggregation of unconsolidated pyroclastic deposit during influx of subsequent pyroclastic deposit, south wall of Hanging Glacier valley.



Plate 2-11-7. Flow-folded, intrusive component of flow-dome complex, south of Brucejack Lake. Microgranite dike visible beneath tape measure. Scale:measuring tape (decimetre scale on outcrop).

Lithochemical analyses of the flow dome and dike are described elsewhere (Macdonald, 1992); in brief, both the flow dome and dike have similar modal proportions, and may be classified as granodiorite and microgranite, respectively (after the method of LeMaitre, 1989).

GEOCHRONOMETRY

Two samples from the flow-dome complex were selected for U-Pb zircon geochronometry: AJM-ISK91-388 (intrusive component of flow dome) and AJM-ISK91-399 (disaggregated felsic dike from within intrusive component of flow dome). Analytical procedures are those described by Macdonald *et al.* (1991); the only modification pertains to the total procedural blanks, which are approximately 30 picograms for lead and 6 picograms for uranium. The analyses were performed by Dr. D. Ghosh in the Geochronometry Laboratory, Department of Geological Sciences at The University of British Columbia; results are reported in Table 2-11-1.



Plate 2-11-8. Boulder breccia marginal to flow-dome complex; boulders of flow-dome granodiorite in a hematitic, finely laminated, muddy matrix.

The flow-dome sample is interpreted to be 185.6 ± 1.0 Ma (2σ) based on the lower intercept of the well-defined discordia with a mean squared weighted deviation (MSWD) of 0.16 (Figure 2-11-2). The upper intercept of about $1013 + 261/-241$ Ma suggests incorporation of a lead component from an older source.

The dike sample is interpreted to be 185 ± 1.0 Ma ($2s$) based also on the lower intercept of the well-defined discordia with an MWSD of 0.03 (Figure 2-11-3). For this sample also, incorporation of an old lead component is suggested by the upper intercept of the discordia at about $1058 + 386/-342$ Ma.

Interpreted ages of these two samples from the Sulphurets area are similar within errors and suggest plutonic activity during the late Early Jurassic (Toarcian; Harland *et al.*, 1989) in the Stikine Terrane. Inheritance of an old (about 1000 Ma) lead component in the zircon fractions from both the samples suggests presence of a basement on which Toarcian magmatic arc developed (Ghosh, 1992). This basement might be part of the Nisling Terrane or its equivalent.



Plate 12-11-9. Disaggregated microgranite dike within intrusive component of flow-dome complex.

This terrane has been recently defined as a metamorphosed Proterozoic to lower Paleozoic(?) passive continental-margin assemblage in the western part of the Cordillera (Wheeler *et al.*, 1991).

These ages are similar to 186 ± 2 Ma obtained from the Eskay porphyry (Eskay Creek area) by Macdonald *et al.* (1991) suggesting that Toarcian magmatism was widespread. It is interesting to note that even though the samples from the Sulphurets area show lead inheritance, dated samples from the Eskay Creek, Inel and Iskut River (Macdonald *et al.*, *ibid*) rather show lead loss.

INTERPRETATION

Henderson *et al.* (1992) infer the presence of considerable topographic relief during Hazelton Group volcanism in the Sulphurets area, with ensuing rapid facies changes over small distances along strike; these relationships suggest that the Sulphurets area was a probable volcanic centre during deposition of Hazelton rocks, a suggestion made earlier by Alldrick (1989). The presence of rim-type accretionary lapilli in the upper parts of individual pyroclastic units indicates deposition by a pyroclastic flow or surge (as opposed to co-ignimbrite ashfall), and deposition within less than 4 kilometres from the volcanic source (based on Schumacher and Schminke, 1991), again consistent with the hypothesis of proximity to a volcanic centre.

Both crosscutting and conformable relationships exhibited by the flow-banded unit indicate a progression

from intrusive at depth, to complex interdigitations with related ejecta at intermediate levels, to extrusive at the highest observed level. Microgranite dikes intrude the flow-dome complex, but become disaggregated within the body of the feldspar-phyric, flow-banded rock. These field relationships suggest that the two (flow dome and dike) are coeval, an hypothesis confirmed by U-Pb geochronometry. The presence of both intrusive and extrusive components of a flow-dome complex is additional evidence for a local magmatic centre in the vicinity of Brucejack Lake during the Toarcian. Mud-cemented breccias are the lateral equivalent of the flow dome, with which they interfinger; the breccias are also overlain by the extrusive component of the flow-dome complex. The breccias are interpreted to be talus material formed by erosion of the emergent dome. In turn, the morphology and geometry of the breccias suggests conformity with enclosing flow rocks, including potassium feldspar, plagioclase and hornblende-phyric flows.

Available geological evidence, when considered collectively, is consistent with deposition of volcanic and volcanoclastic rocks in a submarine environment, and includes the rhythmic interbeds of sediment containing marine fossils, the finely laminated nature of muddy matrix to breccias peripheral to the flow-dome complex, tractional bed forms, such as ripples. Oxidation of units that imparted a prominent reddish colouration to the rocks, resulting from hematite alteration, occurred at some period subsequent to original deposition; it is not known when this event occurred, although it is speculated that the Jurassic volcanic edifice in the Sulphurets area may have been wholly or

TABLE 2-11-1
U-Pb ANALYTICAL DATA

Sample/ Fraction ²	Wt (mg)	U (ppm)	Pb ³	Isotopic abundance ⁴ ²⁰⁶ Pb=100			206/204 ⁵	Isotopic ratios ⁶ ±2 sigma errors		
				208	207	204		²⁰⁶ Pb*/ ²³⁸ U	²⁰⁷ Pb*/ ²³⁵ U	²⁰⁷ Pb*/ ²⁰⁶ Pb
								Dates (Ma) ⁷ ±2 sigma errors		
AJM-ISK91-388⁸										
a. M2/1	0.6	354	10.9	16.11	5.80	0.0559	1563	0.02920±14	0.20053±106	0.04981±10
ABR, +74m								185.5±0.8	185.6±0.8	186.3±5.0
b. NM2/1	0.7	309	9.4	16.24	5.30	0.0229	3250	0.02906±14	0.19886±104	0.04963±12
ABR, -74+44m								184.7±0.8	184.2±0.8	177.7±5.4
c. M2/1, NM1.5/3	0.3	445	14.1	18.21	5.25	0.0161	3534	0.02967±14	0.20546±108	0.05022±14
ABR, -74m								188.5±0.8	189.7±1.0	205.3±6.4
AJM-ISK91-389⁹										
a. NM2/1	0.4	389	11.7	14.85	5.16	0.0131	4196	0.02910±12	0.19967±104	0.04976±16
ABR, 149+74m								184.9±0.8	184.8±0.8	183.7±7.2
b. M2/1 NM1.5/3	0.4	413	13.0	17.91	5.61	0.0404	1980	0.02950±14	0.20403±102	0.05017±12
ABR, -74+44m								187.4±0.8	188.5±0.8	202.9±5.4
c. NM1.5/3 M1.0/5	0.3	586	18.1	17.36	5.19	0.0146	4147	0.02917±14	0.20036±106	0.04982±10
ABR, -74+44m								185.3±0.8	185.4±0.8	186.5±4.8

NOTES:

¹ Complete analytical data, including the measured ²⁰⁶Pb/²⁰⁴Pb errors, the mole % blank Pb and the Pb*/(Pb*+Pb_{common}) ratios in the analyses, the assumed Stacey-Kramers common Pb ages and their errors, and the correlation coefficients for the Pb/U ratios, are recorded on UBC Geochronometry Laboratory data sheets.

² NM= non magnetic, M=magnetic, -74+44m = size range in microns; ABR=abrased: all fractions were abrased for 2 hours to remove the outer rims

³ radiogenic + common Pb

⁴ radiogenic + common Pb, corrected for 0.43%/amu (atomic mass units) fractionation and for 30 pg Pb blank with composition 208:207:206:204=37.67:15.30:18.12:1

⁵ ²⁰⁶Pb/²⁰⁴Pb measured, corrected for 0.43%/amu fractionation.

⁶ corrected for fractionation (0.44%/amu for U and 0.43%/amu for Pb), blank Pb (see note above), and for common Pb using Stacey and Kramers (1975) growth curves; errors are 2 sigma, only last digits shown.

⁷ decay constants used in age calculation: $\lambda^{238}\text{U}=1.55125 \times 10^{-10}$, $\lambda^{235}\text{U}=9.8485 \times 10^{-10}$, $^{238}\text{U}/^{235}\text{U}=137.88$ (Steiger and Jager, 1977). Errors are 2 σ .

⁸ collected by AJM, Longitude: 130° 09' 21"; Latitude: 56° 27' 52".

⁹ collected by AJM, Longitude and Latitude: same as above.

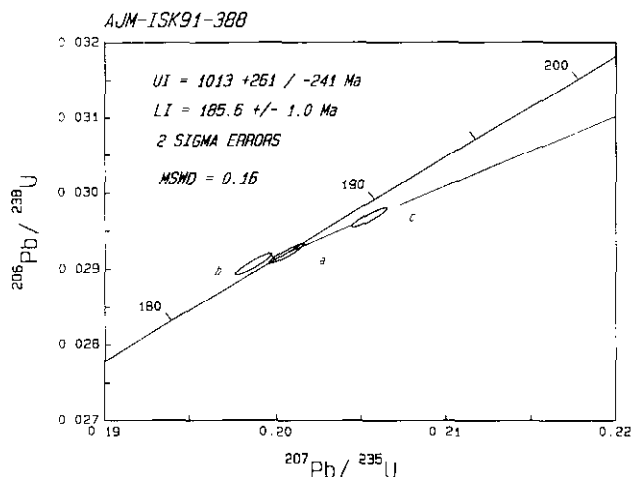


Figure 2-11-2. ²⁰⁶Pb/²³⁸U vs. ²⁰⁷Pb/²³⁵U concordia diagram for AJM-ISK91-388. LI = lower intercept, UI = upper intercept.

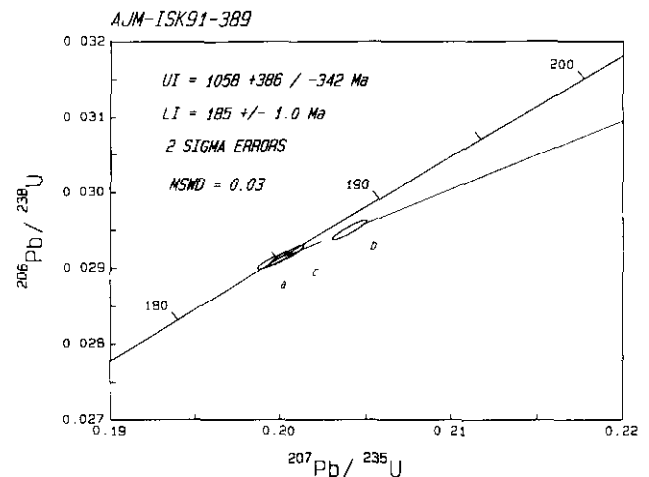


Figure 2-11-3. ²⁰⁶Pb/²³⁸U vs. ²⁰⁷Pb/²³⁵U concordia diagram for AJM-ISK91-389. LI = lower intercept, UI = upper intercept.

partially exposed to the atmosphere prior to burial by younger rocks.

ACKNOWLEDGMENTS

The management and exploration staff of Newhawk Gold Mines Ltd. are thanked for continuing logistical and technical support towards MDRU's Project "Metallogeny of the Iskut River Area, Northwestern British Columbia". Particular thanks are extended to F. Hewett and D. Visagie of Newhawk. Early drafts of the manuscript have benefitted from review by A.J. Sinclair and P.D. Lewis.

REFERENCES

- Alldrick, D.J. (1989): Volcanic Centres in the Stewart Complex (103P and 104A,B): in Geological Fieldwork 1988, B.C. Ministry of Energy, Mines and Petroleum Resources, Paper 1989-1, pages 233-240.
- Alldrick, D.J. and Britton, J.M. (1988): Geology and Mineral Deposits of the Sulphurets Area: B.C. Ministry of Energy, Mines and Petroleum Resources, Open File 1988-4
- Alldrick, D.J., and Britton, J.M. (1991): Sulphurets Area Geology: B.C. Ministry of Energy, Mines and Petroleum Resources, Open File 1991-21.
- Britton, J.M. and Alldrick, D. J. (1988): Sulphurets Map Area (104A/5W, 12W; 104B/8E, 9E); in Geological Fieldwork 1987, B.C. Ministry of Energy, Mines and Petroleum Resources, Paper 1988-1, pages 199-209.
- Dowling, K. and Morrison, G. (1989): Application of Quartz Textures to the Classification of Gold Deposits using North Queensland Examples; in *The Geology of Gold Deposits: The Perspective in 1988*, Keays, R.R., Ramsay, W.R.H. and Groves, D.I., Editors, *Economic Geology*, Monograph 16, pages 342-356.
- Ghosh, D. (1992): U-Pb Geochronometry of the Iskut River Project, Section 8.2; in MDRU Iskut Project Annual Report, May 1992; *Mineral Deposit Research Unit, The University of British Columbia*.
- Godwin, C.I., Pickering, A.D.R. and Gabites, J.E. (1990): Interpretation of Galena Lead Isotopes from the Stewart-Iskut Area (103O, P; 104A, B, G); in Geological Fieldwork 1990, B.C. Ministry of Energy, Mines and Petroleum Resources, Paper 1991-1, pages 235-243.
- Harland, W.B., Armstrong, R.L., Cox, A.V., Craig, I.E., Smith, A.G. and Smith, D.G. (1989): A Geologic Time Scale 1989; *Cambridge University Press*.
- Henderson, J.R., Kirkham, R.V., Henderson, M.N., Payne, J.G., Wright, T.O. and Wright, R.L. (1992): Stratigraphy and Structure of the Sulphurets Area, British Columbia, (104 B/8 and 9); in Current Research, Part A, *Geological Survey of Canada*, Paper 92-1A.
- Kirkham, R.V. (1991): Provisional Geology of the Mitchell-Sulphurets Region, Northwestern British Columbia (104 B/8, 9); *Geological Survey of Canada*, Open File 2416.
- Kirkham, R.V. (1992): Preliminary Geological Map of the Brucejack Creek Area, British Columbia (part of 104 B/8); *Geological Survey of Canada*, Open File 2550.
- Lefebure, D.V. (1987): Red River (Sulphurets); in Exploration in British Columbia 1986, B.C. Ministry of Energy Mines and Petroleum Resources, pages B57-B62.
- Le Maitre, R.W. (1989): Some Problems of the Projection of Chemical Data into Mineralogical Classifications; *Contributions to Mineralogy and Petrology*, Volume 56, pages 181-189.
- Lewis, P. D. (1992): Structural Geology of the Prout Plateau Region, Iskut River Map Area, British Columbia; in Geological Fieldwork 1991, Grant, B. and Newell, J.M., Editors, B.C. Ministry of Energy, Mines and Petroleum Resources, Paper 1992-1, pages 521-527.
- Lewis, P.D., Thompson, J.F.H., Nadaraju, G., Anderson, R.A. and Johansson, G. (1993): Lower and Middle Jurassic Stratigraphy in the Treaty Glacier Area and Geological Setting of the Treaty Glacier Alteration System, Northwestern British Columbia; in Current Research, Part A: *Geological Survey of Canada*, Paper 93-1A, in preparation.
- Macdonald, A.J. (1990): MDRU Iskut Project, Photo Atlas - 1990 Field Season; *Mineral Deposit Research Unit, The University of British Columbia*.
- Macdonald, A.J. (1992): Eskay Porphyry, Section 1.2; in MDRU Iskut Project Annual Report, May 1992, *Mineral Deposit Research Unit, The University of British Columbia*.
- Macdonald, A.J. and Roach, S. (1992): Mesothermal and Epithermal Styles of Mineralization at Brucejack Lake, Iskut River Area, Northwestern British Columbia; *Geological Association of Canada/Mineralogical Association of Canada*, Annual Meeting, May 1992, Wolfville, Nova Scotia, Abstracts page A70.
- Macdonald, A.J., van der Heyden, P., Lefebure, D.V. and Alldrick, D.J. (1991): Geochronometry of the Iskut River area: An Update (104A and B); in Geological Fieldwork 1991, Grant, B. and Newell, J.M., Editors, B.C. Ministry of Energy, Mines and Petroleum Resources, Paper 1992-1, page: 495-501
- McDonald, B. and Godwin, C.I. (1936): Geology of the Main Zone at Mt. Skukum, Wheaton River Area, Southern Yukon; in *Yukon Geology*, Volume 1, *Indian and Northern Affairs Canada*, pages 6-10.
- Roach, S. and Macdonald, A.J. (1992): Silver-Gold vein Mineralization, West Zone, Brucejack Lake, Northwestern British Columbia; in Geological Fieldwork 1991, Grant, B. and Newell, J.M., Editors, B.C. Ministry of Energy, Mines and Petroleum Resources, Paper 1992-1, pages 503-511.
- Schumacher, R. and Schmincke, H.-U. (1991): Internal Structure and Occurrence of Accretionary Lapilli - A Case Study at Laacher See Volcano; *Bulletin of Volcanology* Volume 53, pages 612-634.
- Stacey, J.S. and Kramers, J.D. (1975): Approximation of Terrestrial Lead Isotope Evolution by a Two-stage Model; *Earth and Planetary Science Letters*, Volume 26, pages 207-221.
- Steiger, R.H. and Jager, E. (1977): Subcommittee on Geochronology: Convention on the Use of Decay Constant; in *Geo- and Cosmochronology*; *Earth and Planetary Science Letters*, Volume 36, pages 359-362.
- Wheeler, J.O., Brookfield, A.J., Gabrielse, H., Moirer, J.W.H., Tipper, H. W. and Woodsworth, G.J. (1991): Terrain Map of the Canadian Cordillera, *Geological Survey of Canada*, Map 1713A.

NOTES

SURFACE GEOLOGY OF THE 21A ZONE, ESKAY CREEK, BRITISH COLUMBIA (104B/9W)

By Tina Roth, Mineral Deposit Research Unit, U.B.C.

(MDRU Contribution 016)

KEYWORDS: Economic geology, Eskay Creek, gold, silver, 21A zone, massive sulphides, stibnite, realgar, Hazelton Group.

INTRODUCTION

The Eskay Creek deposit (56°38'N, 130°27'W) is in the Iskut River area of northwestern British Columbia, approximately 80 kilometres north of Stewart (Figure 2-12-1). The deposit, known as the 21 zone, occurs in a bimodal volcanic sequence of the Lower to Middle Jurassic Hazelton Group. The 21 zone is comprised of several zones distinguished by differing ore mineralogies and gold grades.

Geological reserves for the 21 zone are 4.30 million tonnes grading 28.8 grams per tonne gold and 1027 grams per tonne silver (Edmunds *et al.*, 1992). The bulk of these reserves occur in the 21B zone as tabular, syndimentary sheets of graded and fragmental sulphides and underlying vein and disseminated zones. Mineralization in the 21A zone occurs as a massive to semimassive stratabound lens of stibnite-realgar-cinnabar-arsenopyrite underlain by footwall disseminations and veins of dominantly sphalerite-galenite-tetrahedrite-pyrite with minor amounts of chalcopyrite. The 21A zone is estimated to contain approximately 0.97 million tonnes grading 9.6 grams per tonne gold and 127 grams per tonne silver (A. Ransom, International Corona Corporation, personal communication, Dec. 1991). The property operator to August 1992 was International Corona Corporation. The current operator is Homestake Canada Ltd.

Preliminary geology of the 21A zone has been described by Roth and Godwin (1992). During the summer of 1992, an area including the 21A zone was mapped at a scale of 1:1000; results are presented here.

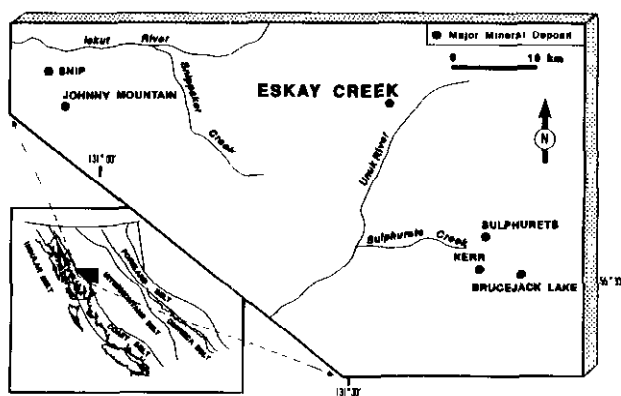


Figure 2-12-1. Location map of Eskay Creek, Iskut River area.

REGIONAL GEOLOGY

The area is underlain by Triassic Stuhin Group and Jurassic Hazelton Group sedimentary and volcanic rocks, which have been described by several workers including Alldrick *et al.* (1989), Anderson (1989), Anderson and Thorkelson (1990), Britton (1991), Lewis (1992) and Lewis *et al.* (1992). The detailed stratigraphy containing the Eskay Creek deposit has been described by Bartsch (1992a, 1992b, 1993, this volume).

SURFACE GEOLOGY OF THE 21A ZONE

Host stratigraphy of the 21A zone is a sequence of volcanic and sedimentary rocks that strike northeasterly and dip moderately to the northwest. The map of the 21A zone area is reproduced in Figure 2-12-2 at a reduced scale. A cross-section through the deposit is presented in Figure 2-12-3. Units 1 to 8 below are described from oldest to youngest. A zone of intense alteration obscures most lithologies in the northeastern part of the study area. However, the presence of distinctive amygdaloidal dacite allows extension of contacts through this part of the map.

Footwall sediments and volcanoclastic rocks (Unit 1) are the lowermost unit in the map area. Shale and sandy sediments were observed in the southeast part of the area, southeast of Eskay Creek. On the northwest side of the creek, volcanoclastic rocks are generally unsorted and consist of dominantly intermediate volcanic clasts and minor argillite clasts in a dark green chloritic matrix. Locally these clastic rocks are graded and bedded. Pyroclastic material, exposed near the south end of the map area shows well-developed, slightly flattened pumice fragments and intermediate volcanic clasts in a dark green matrix.

Dacite (Unit 2) overlies Unit 1 based on stratigraphy interpreted from drill core logged in 1991. Quartz, locally chlorite, amygdules are common and assist tracing this unit through zones of intense quartz-sericite-pyrite alteration. The dacite has a characteristically pinkish beige alteration, cut by a stockwork of pyrite and quartz-rich veins (up to 10 cm wide) with grey sericitic envelopes. The dacitic composition has been confirmed by geochemical analysis (Edmunds *et al.*, 1992). This unit may represent a flow or sill.

Argillite (Unit 3) occurs in most drill sections where it separates the dacite, sediments and volcanoclastic rocks from the overlying rhyolite. On surface, only two small shale outcrops were found in this stratigraphic position. The relationships between Units 1 to 3 depend upon an intrusive or extrusive interpretation for Unit 3. Coarser sedimentary

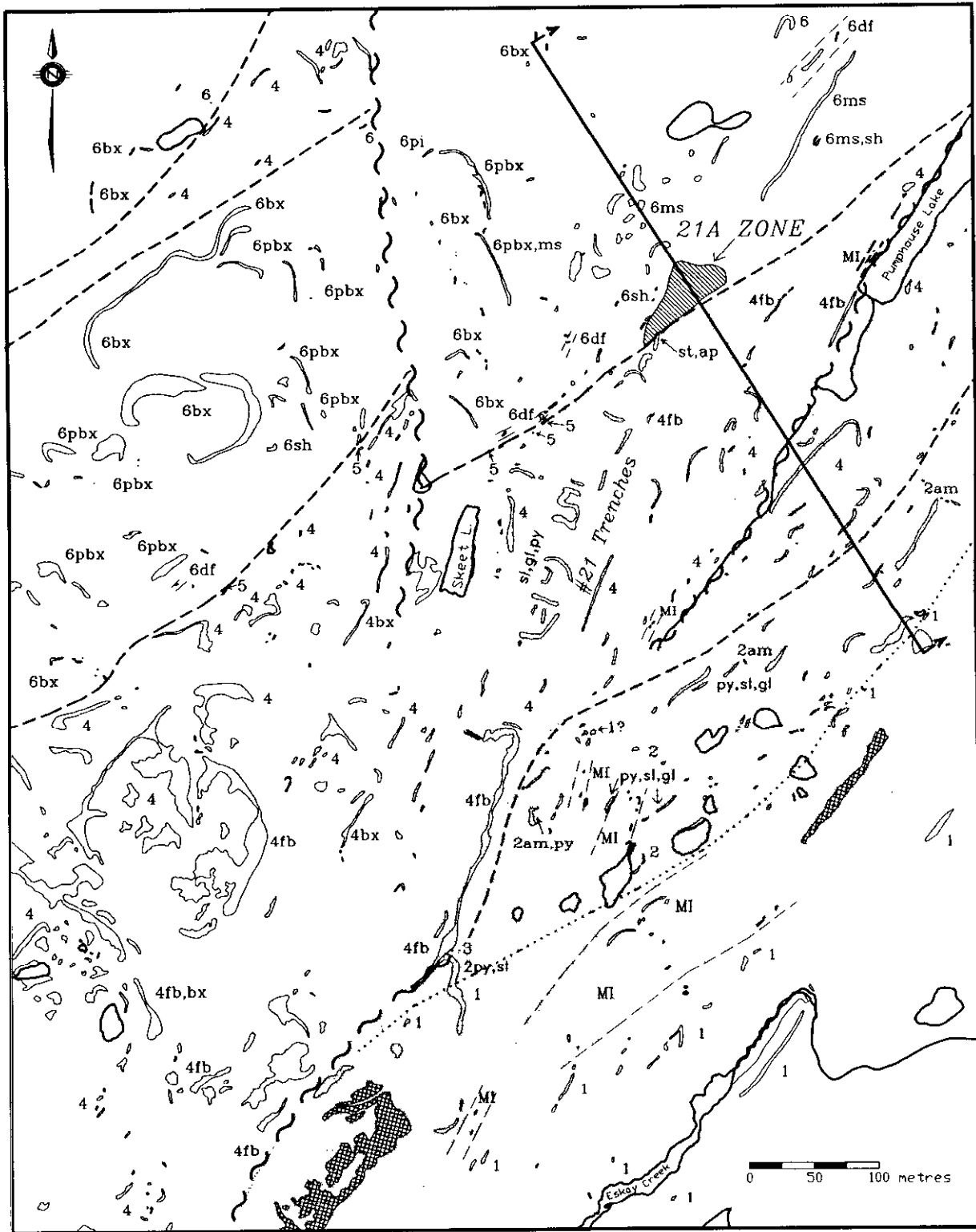


Figure 2-12-2. Map of the 21A zone area. Cross-section A-A' is shown in Figure 2-12-3.

LEGEND

- | | |
|----|--|
| 6 | Basalt and intercalated shale and argillite. |
| 5 | Contact shale and argillite. |
| 4 | Rhyolite. |
| 3 | Argillite. |
| 2 | Dacite. |
| 1 | Sediments and volcaniclastic rocks. |
| MI | Mafic intrusion. |
| | Altered felsic intrusion. |
| | Surface projection of massive to semi-massive st-re-ci mineralization. |
| | Quartz-sericite-pyrite alteration: moderate to intense. |

ABBREVIATIONS

am	amygdules
bx	breccia
df	debris flow
fb	flow banding
ms	massive
pbx	pillow breccia
pi	pillows
sh	shale
ap	arsenopyrite
ci	cinnabar
gl	galena
py	pyrite
re	realgar
sl	sphalerite
st	stibnite

- | | |
|--|--|
| | Outcrop |
| | Fault |
| | Geologic contacts:
interpreted, inferred,
approximate. |
| | Lake, pond, stream. |

rocks are observed locally in drill core at this stratigraphic horizon (Figure 2-12-3). In drill hole CA89-024, wacke overlies stockwork-altered dacite and grades up-hole to graphitic argillite.

Rhyolite (Unit 4) overlies the dacite and argillite. Contact relationships were not observed in surface mapping. In outcrop, most of the rhyolite appears to be massive and

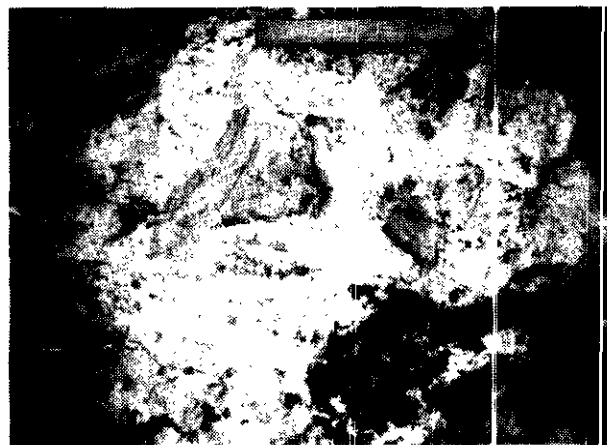


Plate 2-12-1. Rotated, flow-banded clasts of rhyolite in an altered rhyolite matrix (Unit 4).

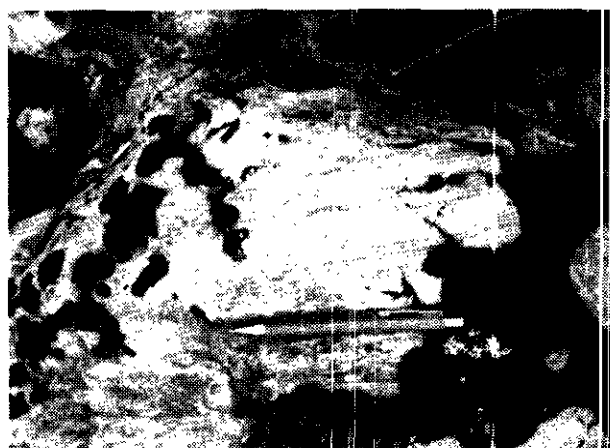


Plate 2-12-2. Flow-banded rhyolite (Unit 4). The texture becomes prominent on the weathered surface.

textureless. However, on surfaces that have been broken and exposed for a few years, flow banding and well-preserved breccias with rotated flow-banded clasts are common (Plates 2-12-1 and 2-12-2). Contorted flow bands occur at hand-specimen to outcrop scale. Attitudes of flow bands are inconsistent and locally chaotic.

The upper contact of the rhyolite with overlying siliceous, black argillite or chert (Unit 5) is exposed locally. At this contact, white siliceous rhyolite fragments are incorporated in a black siliceous matrix (Plate 2-12-3).

Rhyolite also occurs as a discrete lens within the basalt sequence in the northwest part of the map area. It is not obvious from surface mapping whether contacts between this rhyolite and the surrounding basalt are tectonic or stratigraphic, as they are not exposed. Evidence from diamond-drill core suggests that this rhyolite is intercalated with basalt at depth (Edmunds *et al.*, 1992). The relationship between the rhyolite and basalt is critical to understanding the Eskay Creek deposit.

Contact argillite and chert (Unit 5) occurs between the rhyolite and the overlying basalt and hosts massive to semi-massive stibnite-realgar mineralization of the 21A zone. In

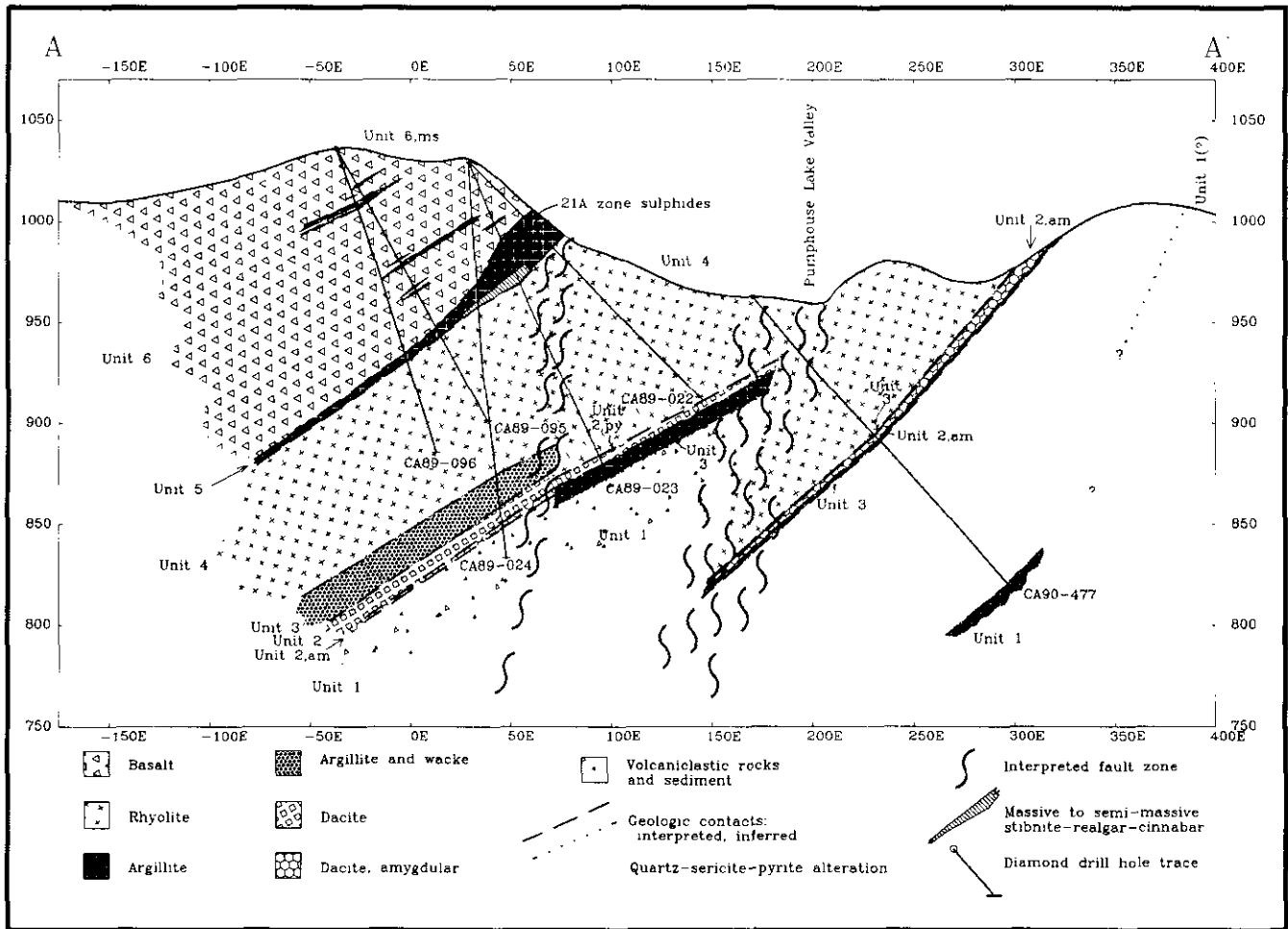


Figure 2-12-3. Schematic cross-section A-A' showing stratigraphy through the 21A zone.

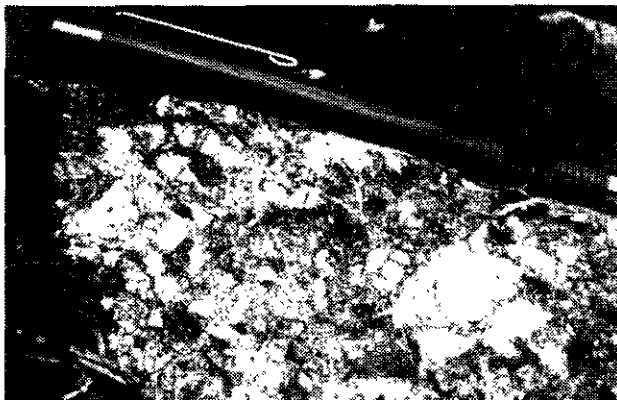


Plate 2-12-3. Siliceous, white rhyolite fragments in a siliceous, black matrix. This texture is characteristic of the top of the rhyolite (Unit 4) in contact with the overlying black, siliceous argillite (Unit 5).

drill core the argillite is usually laminated, variably calcareous, cherty or graphitic, and locally contains thin intervals of intercalated tuffaceous to brecciated rhyolite. At surface, only a few very hard and cherty black outcrops are exposed. Thin, white quartz veinlets generally cut perpendicular to bedding. In some exposures, thin cherty beds

weather white, giving the outcrop a banded appearance. The bedding in the unit is locally folded gently or disrupted.

Basalt (Unit 6) is massive to pillowed and brecciated. In the area immediately overlying the 21A zone the basalts are generally massive. Topographically and stratigraphically overlying the massive basalt are well-preserved pillow flows and pillow breccias showing chilled and amygdaloidal pillow margins (Plate 2-12-4). Well-formed pillows are commonly 80 centimetres to 1 metre in diameter; locally pillows are smaller and have irregular or elongate shapes. Massive to blocky and brecciated basalts also occur within the pillowed sequence, possibly as sills, flows or dikes.

Argillite intervals, rarely exposed at surface, are intercalated with the basalt sequence. A basalt debris flow, with clasts of basalt and argillite, crops out in the northeast corner of the map area near the base of the basalt sequence. In the central portion of the map, a debris flow immediately overlies the contact argillite (Unit 5). In the northeast, the debris flow is underlain by massive basalt.

INTRUSIVE ROCKS

Felsic intrusions cut across stratigraphy in the footwall rocks and are possible feeders for the rhyolite and/or the orebodies (Edmunds *et al.*, 1992; Bartsch, 1992b; 1993. this

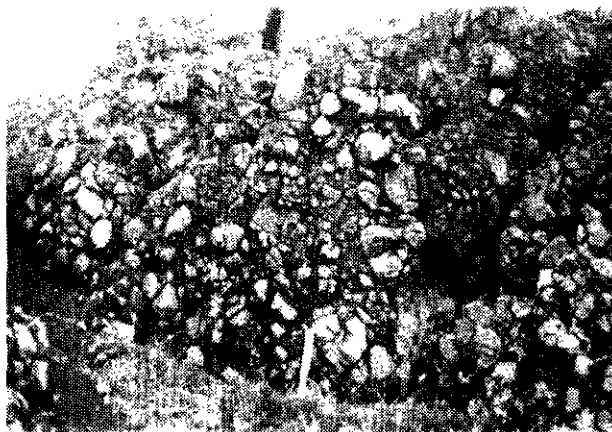


Plate 2-12-4. Brecciated pillow basalt fragments (Unit 6) in a calcareous matrix. The clasts show chilled and amygdaloidal margins.

volume). Within the map area, these intrusions are expressed on surface as two distinctive gossanous bluffs (marked by cross-hatching on Figure 2-12-2). They are pervasively altered to quartz-sericite-pyrite assemblages and primary textures are not evident. Hostrocks marginal to these intrusions are also intensely altered.

Mafic dikes and sills are exposed throughout the map area, in both the hangingwall and footwall of the 21A zone. The mafic intrusions appear to be generally weakly altered or fresh. Typically these rocks are dark green to grey and locally contain up to 5 per cent chlorite-filled amygdules. The mafic intrusions are comagmatic with the basaltic flows (Unit 6) (Edmunds *et al.*, 1992).

ALTERATION

Variably intense alteration (stippled pattern, Figure 2-12-2) extends along a generally northeast-trending zone in the Pumphouse Lake valley that includes the area between the gossanous bluffs. Intense silicification and variable secondary quartz-sericite-pyrite alteration has generally obliterated all primary textures and features in the rocks, making interpretation of a protolith difficult. Locally, relict features such as altered clasts and amygdules allow the interpretation of contacts within this zone.

In the 21 zone trenches sericite-pyrite alteration is dominant and is characterized by small white patches, generally 3 centimetres across, in a grey matrix. On the north end of the 21 zone trenches an area of intense sericite-chlorite-pyrite alteration, which immediately underlies the massive mineralization of the 21A zone in drill core, is exposed at surface.

STRUCTURES

Several faults transect the area. A north-trending dextral fault, with an apparent offset of about 120 metres, occurs in the centre of the map at the rhyolite-chert-basalt contact. Another fault is interpreted at the contact between the rhyolite and the felsic intrusion. A small, apparent dextral offset along this structure is indicated by shales of Unit 3,

which appear to be juxtaposed against altered dacite. This fault may be related to the major north-north west-trending fault zone which occurs along the Pumphouse Lake valley (Blackwell, 1990; Figure 2-12-3). Minor faults and shear zones, not shown in Figure 2-12-2, are also present in the map area.

The prevailing structural fabric in the map area is a moderate to intense foliation and cleavage most prominent in the Pumphouse Lake valley. This fabric trends about 030° and dips steeply. Footwall rocks to the 21A zone are more intensely foliated than the hangingwall basalts. Variable foliation intensity reflects the proportion of phyllosilicate development in the hydrothermal alteration zone related to base and precious metal mineralization.

MINERALIZATION

The Eskay Creek deposits have been described in detail by Britton *et al.* (1990) and Blackwell (1990); the 21A zone has been described by Roth and Godwin (1992) and Roth (1992). This discussion will be limited to a brief description of the general styles of mineral showings within the map area.

Veinlets and stringers of sphalerite, galena, tetrahedrite, and pyrite occur locally in the footwall rhyolite sequence. These veinlets are most evident in the #21 zone trenches, and also occur locally in outcrops in the Pumphouse Lake valley. Sulphides are sparse in the rhyolites in the southwest part of the map area.

The most prominent surface showings are pyrite veins on the dacitic volcanic rocks (Unit 2). Sphalerite and galena are commonly associated with these veins.

Disseminated stibnite and arsenopyrite, with associated gold and silver, is exposed at the north end of the #21 zone trenches in intensely sericite-chlorite-pyrite-altered rhyolite (Figure 2-12-2). They also occur in drill core from immediately beneath massive sulphides in the 21A zone contact argillite. Massive stibnite-realgar-cinnabar mineralization is not exposed at surface, although small weathered fragments can be found at the north end of the #21 zone trenches.

CONCLUSIONS

The map and cross-section presented here elaborate on earlier work by Roth and Godwin (1992) and Roth (1992). The stratigraphic sequence is comprised of sediments and volcanoclastic rocks, overlain by dacitic, rhyolitic and basaltic volcanic rocks. Intervals of argillite and shale occur between the volcanic units, and are intercalated with basalt. Rhyolite may also be intercalated with basalt. Felsic and mafic intrusions, which may be related to the rhyolite and basalt respectively, were outlined by surface mapping.

Within the map area, quartz-sericite-pyrite alteration is most intense in the 21A zone footwall and marginal to the felsic intrusions. Sericite-chlorite-pyrite alteration is prevalent in the area immediately underlying massive sulphide mineralization. Disseminated stibnite and arsenopyrite are locally associated with this footwall alteration. Veins and stringers of sphalerite, galena, tetrahedrite and pyrite cut the footwall rhyolite; veins in the underlying dacite are domi-

nated by pyrite, with sphalerite and galena. Studies are ongoing to characterize the alteration and mineralization associated with the 21A zone at Eskay Creek.

ACKNOWLEDGMENTS

I thank International Corona Corporation for re-establishing grid control and providing base map orthophotos. I also thank Colin Godwin for supervising my M.Sc. thesis, and for his help. Members of the Mineral Deposit Research Unit (MDRU) Iskut research team provided helpful discussions and regional insights. This study forms part of the MDRU project "Metallogenesis of the Iskut River Area, Northwestern B.C.," funded by mining and exploration companies, a Science Council of British Columbia Research and Technology Grant, and a Natural Science and Engineering Research Council (NSERC) CRD grant. Additional funding is provided to the author through an NSERC postgraduate scholarship.

REFERENCES

- Alldrick, D.J., Britton, J.M., Webster, I.C.L. and Russell, C.W.P. (1989): Geology and Mineral Deposits of the Unuk Area (104B/7E, 8W, 9W, 10E); *B.C. Ministry of Energy, Mines and Resources*, Open File 1989-10.
- Anderson, R.G. (1989): A Stratigraphic, Plutonic and Structural Framework for the Iskut River Map Area (NTS 104B), Northwestern British Columbia; in *Current Research, Part E, Geological Survey of Canada*, Paper 89-1E, pages 145-154.
- Anderson, R.G. and Thorkelson, D.J. (1990): Mesozoic Stratigraphy and Setting for some Mineral Deposits in the Iskut River Map Area, Northwestern British Columbia; in *Current Research, Part E, Geological Survey of Canada*, Paper 90-1E, pages 131-139.
- Bartsch, R.D. (1992a): Eskay Creek Area, Stratigraphy Update; in *Geological Fieldwork 1991*, Grant, B. and Newell, J.M., Editors, *B.C. Ministry of Energy, Mines and Petroleum Resources*, Paper 1992-1, pages 517-520.
- Bartsch, R.D. (1992b): Lithostratigraphy – Prout Plateau; in *MDRU Metallogenesis of the Iskut River Area, Northwestern B.C., Mineral Deposit Research Unit, The University of British Columbia*, Annual Technical Report for the period June 1991 - May 1992.
- Bartsch, R.D. (1993): A Rhyolite Flow Dome in the Upper Hazelton Group, Eskay Creek Area (104B/9, 10); in *Geological Fieldwork 1992*, Grant, B. and Newell, J.M., Editors, *B.C. Ministry of Energy, Mines and Petroleum Resources*, Paper 1993-1, this volume.
- Blackwell, J.D. (1990): Geology of the Eskay Creek #21 Deposits; *Mineral Deposits Division, Geological Association of Canada*, The Ganguer, Number 31, April 1990, pages 1-4.
- Britton, J.M. (1991): Stratigraphic Notes from the Iskut-Sulphurets Area; in *Geological Fieldwork 1990*, *B.C. Ministry of Energy, Mines and Petroleum Resources*, Paper 1991-1, pages 131-137.
- Britton, J.M., Blackwell, J.D. and Schroeter, T.G. (1990): #21 Zone Deposits, Eskay Creek, Northwestern British Columbia; in *Exploration in British Columbia 1989*, *B.C. Ministry of Energy, Mines and Petroleum Resources*, pages 197-223.
- Edmunds, F.C., Kuran, D.L. and Ryc, K.A. (1992): The Geology of the Eskay Creek Property and the #21 Zone Deposits; Abstracts of Technical Presentations; *Geological Society of the Canadian Institute of Mining and Metallurgy*, Second Annual Field Conference, Kamloops, B.C., September 28-29, 1992.
- Lewis, P.D. (1992): Structural Geology of the Prout Plateau Region, Iskut River Map Area, British Columbia; in *Geological Fieldwork 1991*, Grant, B. and Newell, J.M., Editors, *B.C. Ministry of Energy, Mines and Petroleum Resources*, Paper 1992-1, pages 521-527.
- Lewis, P.D., Macdonald, A.J. and Bartsch, R.D. (1992): Hazelton Group/Bowser Lake Group Stratigraphy in the Iskut River Area: Progress and Problems; in *MDRU Metallogenesis of the Iskut River Area, Northwestern B.C., Mineral Deposit Research Unit, The University of British Columbia*, Annual Technical Report for the period June 1991 - May 1992.
- Roth, T. and Godwin C.I. (1992): Preliminary Geology of the 21A Zone, Eskay Creek, British Columbia; in *Geological Fieldwork 1991*, Grant, B. and Newell, J.M., Editors, *B.C. Ministry of Energy, Mines and Petroleum Resources*, Paper 1992-1, pages 529-533.
- Roth, T. (1992): Geology of the 21A Zone – An Update; in *MDRU Metallogenesis of the Iskut River Area, Northwestern B.C., Mineral Deposit Research Unit, The University of British Columbia*, Annual Technical Report for the period June 1991 - May 1992.

A RHYOLITE FLOW DOME IN THE UPPER HAZELTON GROUP, ESKAY CREEK AREA (104B/9, 10)

By R.D. Bartsch
Mineral Deposit Research Unit, U.B.C.
(MDRU Contribution 015)

KEYWORDS: Economic geology, stratigraphy, upper Hazelton Group, rhyolite flow domes, Eskay Creek.

INTRODUCTION

Mapping at 1:5000-scale of an area surrounding the Eskay Creek precious and base metal deposit, initiated in 1991 and completed in 1992, emphasizes facies variations within the Lower to Middle Jurassic rocks of the Hazelton Group. This work is an integral part of the Mineral Deposit Research Unit's Iskut River Metallogeny project and is the basis of M.Sc. thesis research by the author at The University of British Columbia.

The study area is centred within the northern half of the Unuk River map area (Alldrick *et al.*, 1989) and extends south of the Eskay Creek deposit (Figure 2-13-1). Previous work in the Unuk and adjacent Snippaker and Sulphurets map areas was compiled by Britton (1990); work by the Mineral Deposit Research Unit (Bartsch, 1991, 1992; Lewis, 1991; Lewis *et al.*, 1992), provided stratigraphic updates.

Mapping indicates that the stratigraphic footwall to the Eskay Creek deposits comprises a rhyolite flow-dome complex which forms a linear belt several kilometres long. A major mineralized and intensely altered subvolcanic felsite dike can be mapped along the same strike length of stratigraphy. The felsic volcanic rocks and dike are interpreted to represent a fissure eruptive centre. This paper reports on stratigraphic relationships from a cross-section constructed from mapping and diamond-drill-hole data. The cross-section A-A' (Figures 2-13-2 and 2-13-3) is located 500 metres south of the McKay adit on property held by American Fibre Corporation and Silver Butte Resources Ltd.

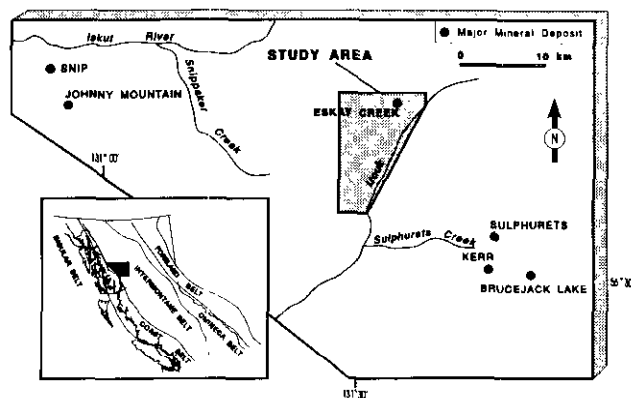


Figure 2-13-1. Location map showing the MDRU Iskut River Project area and area covered by the author's 1:5000-scale mapping.

STRATIGRAPHY

The Hazelton Group has been subdivided into lower and upper sections (Lewis *et al.*, 1992). The lower Hazelton rocks are dominated by volcanic flows, breccias and volcanoclastic rocks of intermediate composition, the upper Hazelton Group is characterized by a dominance of felsic volcanic rocks overlain by sedimentary and mafic volcanic rocks. Detailed stratigraphic subdivisions of the Hazelton Group have been proposed (Britton *et al.*, 1989; Bartsch, 1991, 1992; Lewis, 1992; Lewis *et al.*, 1992). Abrupt facies changes render regional stratigraphic correlations speculative.

Cross-section A-A' is located on the western limb of a regional anticline, 2 kilometres south and along strike from the Eskay Creek deposits. The regional and minor fold axes trend 035° and plunge gently to the northeast. The western limb of the anticline has a predictable, continuous stratigraphy (Bartsch, 1991, 1992; Lewis, 1991; Lewis *et al.*, 1992) and bedding dips vary from 50° to 70° northwest.

CROSS-SECTION A-A'

The Hazelton Group rocks are best mapped in terms of facies. Stratigraphic relationships described in cross-section A-A' represent a minimally disrupted section through proximal facies and a thick section of felsic volcanic rocks belonging to the upper Hazelton Group. Facies relationships of the rhyolites in plan view (Figure 2-13-2) through which section A-A' is drawn are interpreted to represent a flow dome tilted on its side. Broad characteristics from which the interpretation of a dome is based are:

- A multiphase felsite feeder dike and associated minor felsic and mafic dikes within footwall sedimentary rocks.
- Basal and peripheral fragmental felsic rocks, including heterolithic and monolithic breccias commonly containing pumaceous clasts.
- A central zone of rhyolite lava which forms a resistant topographic high and is dome-like in the cross-sectional exposure at surface.

The subvolcanic felsite dike cuts across bedding in the sedimentary rocks underlying the dome. The sedimentary rocks include interbedded shales, feldspathic wackes, conglomerates and minor bioclastic limestones of the upper Hazelton Group. Local abundance of shallow-marine fauna within the limestones and shales in conjunction with conglomerate beds with well-rounded, water worn pebbles, suggest that the sediments were deposited in a shallow-marine setting.

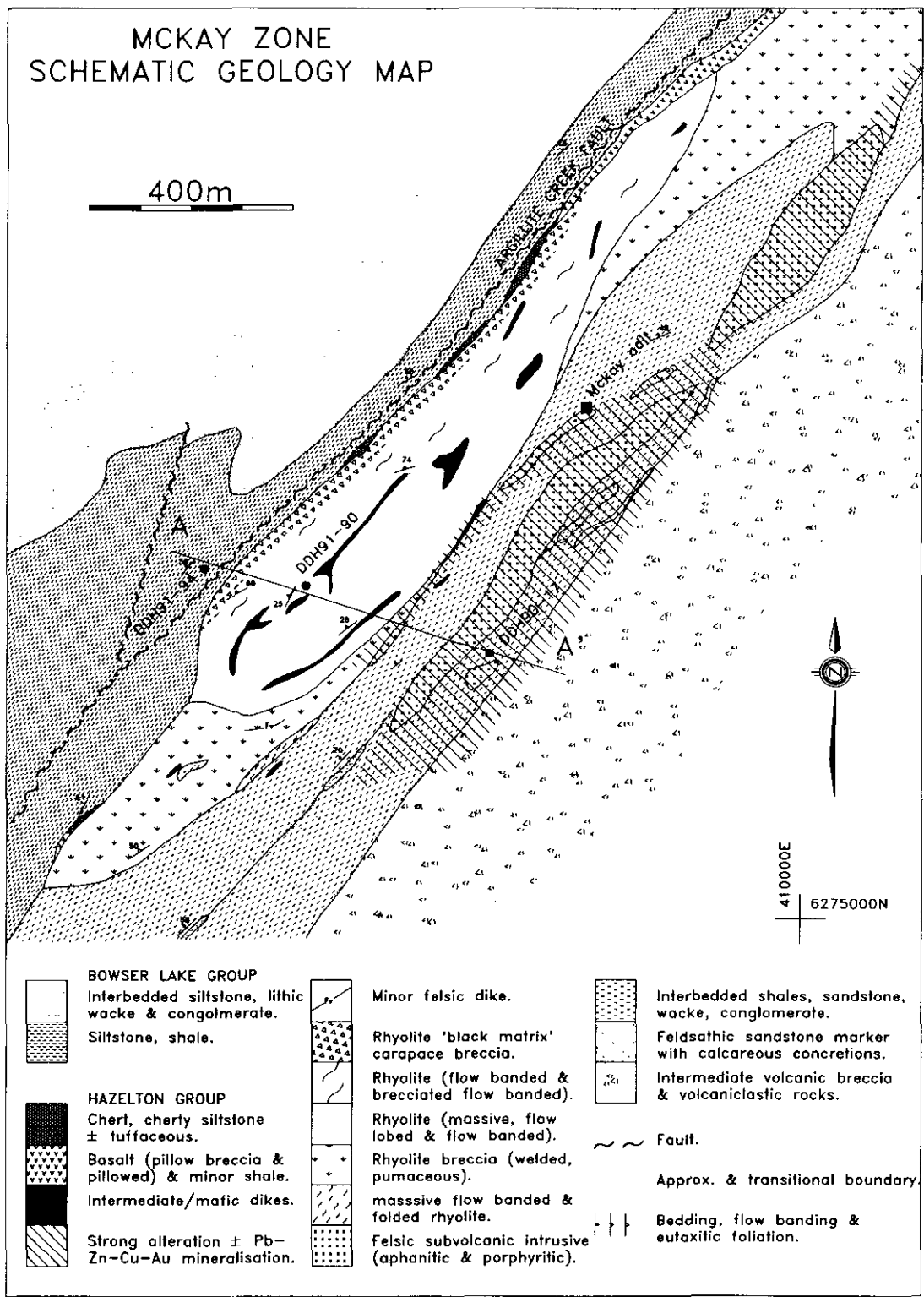


Figure 2-13-2. Geological interpretation map; broad facies distributions are interpreted to represent a rhyolite dome. The location of cross-section A-A' is indicated.

The intrusion is lensoid in shape and forms a prominent, radiant orange, gossanous knoll with 50 metres vertical relief. Similar discontinuous lensoidal intrusions extend in a linear belt south to the Coulter Creek thrust fault and north

to the immediate footwall of the Eskay Creek deposit (see Bartsch, 1991). The location of the 'dike lenses' spatially correlates with the thickest intervals of the felsic extrusions. The intrusion is pervasively altered and is composed pre-

dominantly of microcrystalline quartz, sericite and potassium feldspar. Ghosts of feldspar phenocrysts are commonly visible. The dike is multiphase, a minor late phase is potassium feldspar phyrlic, displays minimal alteration and has intrusive contacts with altered aphanitic felsite.

The base of the felsic succession comprises unsorted volcanic breccias. The breccias are thin (2-4 m) in the section (Figure 2-13-2), but thicken peripherally to the south and north. They are characterized by an abundance of pumice. Locally, at the base of the breccias, cherty devitrified clasts are strongly flattened. Intense alteration, in particular strong sericitization and structurally imposed fabrics, hinder confident interpretation of primary textures; however, the local development of breccias with flattened clasts at the base of the sequence suggests a probable zone of welding and development of eutaxitic textures. The contacts of the welded breccias are sharp, planar and locally discordant to bedding in the underlying sediments.

The greatest thickness of felsic rocks comprises a complex assemblage of flow-banded and brecciated, flow-banded rhyolites. The eastern exposures of the rhyolite, closer to the felsite intrusion and lower in the section, are massive with less well developed flow banding and breccias. Massive rhyolite comprises lobes less than 1 metre in diameter, which are fine grained and may display peripheral

autobreccia rinds, typically set in zones 10 centimetres thick containing fabrics which anastomose tangentially around the lobes.

Flow banding in the rhyolite is irregular with development of small and large-scale flow folds. The flow banding is generally flat throughout the section, but steepens markedly to the west where it is sub-parallel to the steep, westerly dipping rhyolite contact. The western contact of the rhyolite is marked by a rhyolite 'black matrix' carapace breccia. The breccia consists of matrix-supported angular rhyolite clasts in a matrix of black chert. The black matrix breccia is less than 5 metres thick and caps the section of rhyolite characterized by massive flow-banded lavas and breccias with flow-banded clasts.

Alteration and devitrification are pervasive throughout the felsic volcanic rocks; however, islands of minimally altered rhyolite occur within the core of large massive flow lobes. Alteration assemblages are dominated by quartz, sericite, potassium feldspar and pyrite, with or without chlorite. Alteration and mineralization are most intense within and along the margins of the felsite dike. Mineralization styles within the footwall are dominated by pyrite ± galena, chalcopyrite and sphalerite in quartz-vein stockworks within the dike, or at the contact of the dike,

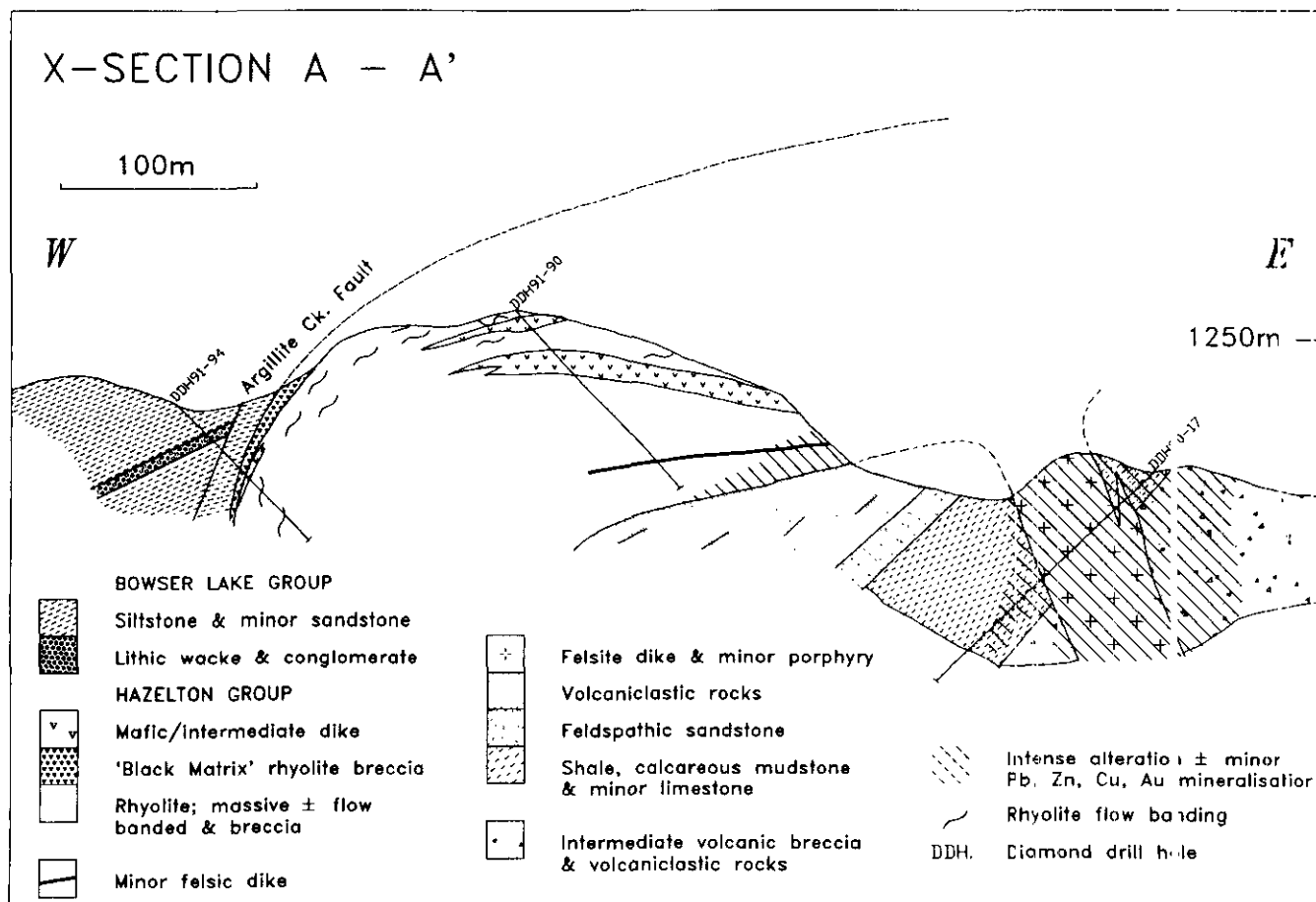


Figure 2-13-3. Cross-section A-A', schematically showing stratigraphic relationships between rhyolites and subvolcanic felsite dikes.

associated with intense silicification of calcareous mudstone.

The rhyolite dome is intruded by numerous small aphanitic rhyolitic and dacitic dikes and late chlorite-carbonate-altered, fine to medium-grained mafic dikes. The smallest dikes are discontinuous and intrude subparallel to the general orientation of the flow banding or within disrupted flow folded zones. The minor dikes fan out from the subvolcanic intrusions in the immediate footwall of the dome (Figures 2-13-2, 2-13-3).

Lenses of thinly laminated white and black cherty siltstone 1 to 2 metres thick occur locally along the rhyolite contact. The siltstones are correlative with the Salmon River Formation shales hosting the stratiform mineralization at Eskay Creek. Salmon River Formation basaltic flows which overlie the Eskay Creek 21 zone deposit pinch out 500 metres to the north of cross-section A-A'. Twenty metres west of the rhyolite contact is the Argillite Creek fault. Argillites to the east of the fault may be Salmon River correlative but are indistinguishable from argillites of the Bowser Lake Group west of the fault.

CONCLUSION

Rhyolitic rocks to the immediate south of the Eskay Creek deposits display facies relationships characteristic of rhyolite flow-dome complexes. Early explosive eruptions are represented by the basal and peripheral breccias and were followed by extrusion of rhyolite lava. Hydrothermal fluids derived from the magmas or resulting from convection initiated by the magmatic activity were concentrated along the fissure-eruptive feeder zone to the rhyolites.

ACKNOWLEDGMENTS

I am grateful to International Corona Corporation/Homestake Canada Ltd., Granges Inc., American Fibre Corporation, Silver Butte Resources Ltd., Prime Equities Inc., Copeland and Rebagliatti Consulting and their respective

staffs for ongoing logistical and technical support of this study. Thanks are also extended to Western Mining Corporation Limited and its generous study-leave program which enabled me to take two years leave to come from Australia to undertake an M.Sc. Assistance from Dr. A.J. Sinclair, my supervisor, Dr. A.J. Macdonald, the manager of the Iskut Project and co-workers in the Mineral Deposit Research Unit is deeply appreciated.

REFERENCES

- Alldrick, D.J., Britton, J.M., Webster, I.C.L. and Russell, C.W.P. (1989): Geology and Mineral Deposits of the Unuk Area (104B/7E, 8W, 9W, 10E); *B.C. Ministry of Energy, Mines and Petroleum Resources*, Open File 1989-10.
- Bartsch, R.D., (1991): Eskay Creek Area, Stratigraphy Update (104B/9, 10); in Geological Fieldwork 1991, Grant, B. and Newell, J.M. Editors, *B.C. Ministry of Energy, Mines and Petroleum Resources*, Paper 1991-1, pages 517-520.
- Bartsch, R.D. (1992): Lithostratigraphy – Prout Plateau; in MDRU Metallogenesis of the Iskut River Area, Northwestern B.C.; Annual Technical Report - Year 2, *The University of British Columbia*.
- Britton, J.M. (1990): Stratigraphic Notes from the Iskut-Sulphurets Area; in Geological Fieldwork 1990; *B.C. Ministry of Energy, Mines and Petroleum Resources*, Paper 1991-1, pages 131-137.
- Britton, J.M., Webster, I.C.L. and Alldrick, D.J. (1989): Unuk Map Area (104b/7E, 8W, 9W, 10E); in Geological Fieldwork 1988; *B.C. Ministry of Energy, Mines and Mineral Petroleum Resources*, Paper 1989-1, pages 241-250.
- Lewis, P.D., (1991): Structural Geology of the Prout Plateau Region, Iskut River Map Area, British Columbia; in Geological Fieldwork 1991, Grant, B. and Newell, J.M., Editors, *B.C. Ministry of Energy, Mines and Petroleum Resources*, Paper 1992-1, pages 521-527.
- Lewis, P.D., Macdonald, A.J. and Bartsch, R.D., (1992): Hazelton Group/Bowser Lake Group Stratigraphy in the Iskut River Area: Progress And Problems; in MDRU Metallogenesis of the Iskut River Area, Northwestern B.C., Annual Technical Report – Year 2, *The University of British Columbia*.



**REFINEMENT AND LOCAL CORRELATION OF THE UPPER SNIPPAKER
RIDGE SECTION, ISKUT RIVER AREA, B.C.
(104B/10W and 11E)**

By Paul Metcalfe and James G. Moors
Mineral Deposit Research Unit, U.B.C.
(MDRU Contribution 014)

KEYWORDS: Regional geology, stratigraphy, Iskut River, Snippaker Mountain, Johnny Mountain, Stuhini Group, Hazelton Group.

verses and flycamps utilized a helicopter, or ground transport along the Bronson - Johnny Mountain road.

INTRODUCTION

A 1:20 000-scale regional mapping project in the western part of the Iskut map area was carried out to augment the extensive regional work conducted by federal and provincial surveys in the area (Lefebvre and Gunning, 1989; Anderson, 1989; Anderson and Bevier, 1990; Anderson and Thorkelson, 1990; Alldrick *et al.*, 1990; Britton *et al.*, 1990; Fletcher and Hiebert, 1990) and to refine local and regional stratigraphic correlations. The study will provide an updated geological framework for mineral target identification and for specific economically related studies (*e.g.*, Rhys and Godwin, 1992; Rhys and Lewis, 1993, this volume). The "Bronson corridor", a structural trend along strike from the Snip gold mine operated by Cominco Metals Ltd., is of particular interest to this study because the Snip, Stonehouse and Inel gold deposits lie on or close to this trend.

The study area lies in the eastern Boundary Ranges of the Coast Mountains (Figure 2-14-1) and is bounded to the southwest by the Coast Mountains, to the east by the Snippaker Creek valley and to the north by the Iskut River. Elevations vary from 100 metres to 2300 metres above sea level, with steep-sided glaciated valleys. Treeline is at approximately 1000 metres. Vegetation below treeline includes Douglas fir and Sitka spruce, with abundant devil's club and slide alder.

Access to the area is by fixed-wing aircraft to the 1500-metre airstrip at Bronson Creek. Fieldwork was based at Cominco Metals' Snip camp by Bronson airstrip. Day tra-

STRATIGRAPHY

Alldrick (1989) noted that "Nomenclature for early to middle Mesozoic strata in northwest British Columbia is evolving". In the area of the Bronson corridor, rocks of Jurassic age comprise a discrete sequence of cliff-forming volcanic and volcanogenic rocks which are exposed on ridge crests along the corridor (Alldrick *et al.*, 1990; Britton *et al.*, 1990; Metcalfe *et al.*, in preparation). The age of the unit at the base of this succession has not yet been determined. The succession overlies a sequence of dominant clastic sedimentary rocks with minor intercalated volcanic rocks. Fossils obtained from this sequence on Snippaker Ridge indicate a Late Triassic age (Nadaraju and Smith, 1992a; 1992b). These rocks are therefore part of the Stuhini Group. Biostratigraphic data are not available for sedimentary strata on the southwest side of Bronson Creek and on the southwest side of Johnny Mountain, but their lithologic similarity to the rocks exposed on Snippaker Ridge suggests that they are coeval (J.R. Atkinson, Skyline Gold Corporation, personal communication, 1990; D. Rhys, personal communication, 1991).

This paper presents a section across the contact between the underlying sedimentary strata on Snippaker Ridge and the overlying intermediate volcanic and volcanogenic rocks. The location of the section is shown in Figure 2-14-2. This contact is also exposed on the southwest side of Bronson Creek and has, in that area, been interpreted either as a low-angle fault or an angular unconformity (Alldrick *et al.*, 1990). An unconformable stratigraphic contact between overlying intermediate to felsic volcanic rocks and underlying baked clastic sedimentary rocks was observed at the break of slope on Johnny Ridge during the course of 1992 fieldwork, indicating that this basal contact is an angular unconformity. A detailed description of the Johnny Ridge section is included in a study by Metcalfe *et al.* (in preparation).

SNIPPAKER RIDGE SECTION

A section from northwest to southeast along Snippaker Ridge, through Snippaker Mountain and the unnamed peak immediately to the south, is shown in Figure 2-14-3. The strata at the top of this section are relatively flat lying and are weakly deformed. The section is based upon information from four traverses carried out in the vicinity of Snip-

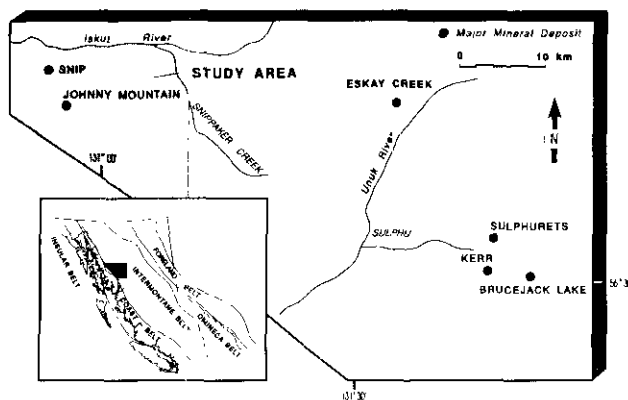


Figure 2-14-1. Location of study area.

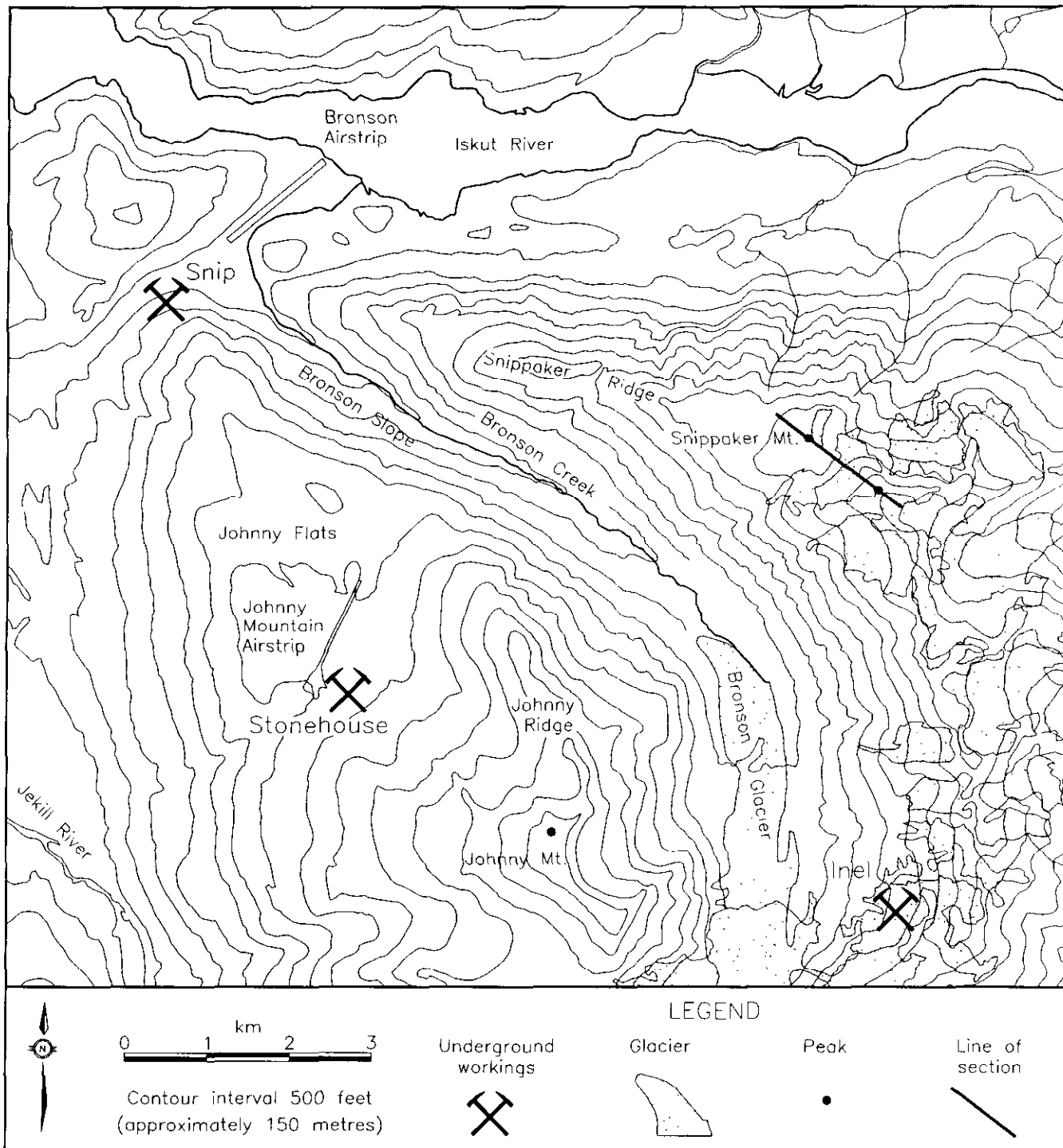


Figure 2-14-2. Location of Snippaker Ridge section (see Figure 2-14-3).

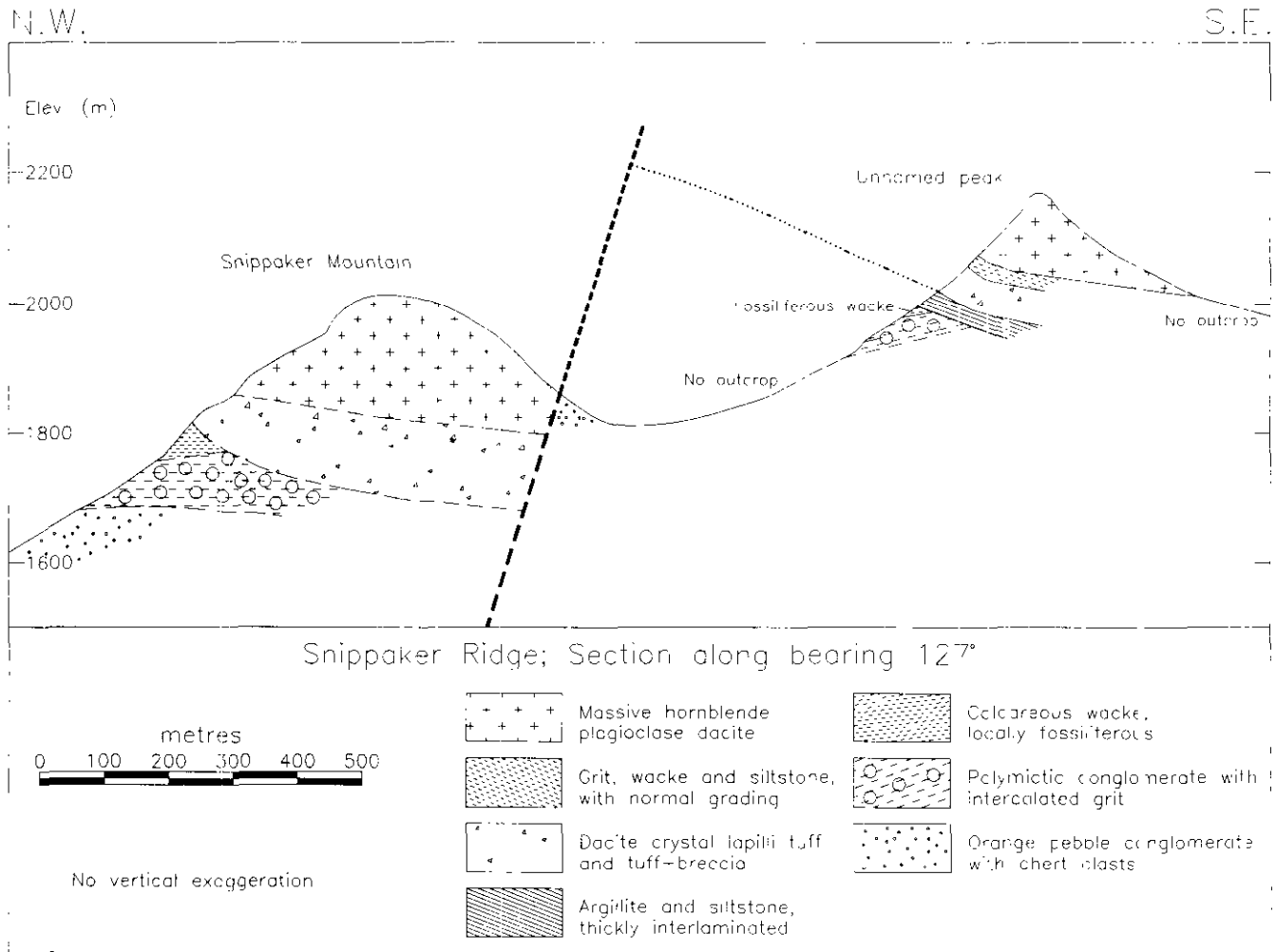


Figure 2-14-3. Snippaker Ridge section.

TABLE 2-14-1
STRATIGRAPHIC SUMMARY

THICKNESS	LITHOLOGY	CONTROL
—	Skyline rhyolite, not exposed on Snippaker Ridge	192 ± 3 Ma
>180 m	Massive plagioclase hornblende phryic dacite	
-----	unconformity, horizontal basal contact of dacite	
25 m	Grey siltstone grading downsection to grit	
=====	loss of exposure	
50 m	Pale green, orange-weathering dacite crystal lapilli tuff	
-----	unconformity, horizontal sedimentary rocks at basal contact of dacite	
30 m	Thickly laminated dark grey siltstones and wackes	
-----	unconformity	
15 m	Orange-weathering wacke with fossiliferous horizon	Nonan
No base	Polymictic boulder conglomerate with grit horizons and some calcite matrix, weakly fossiliferous	

paker Mountain. Lithologic descriptions and stratigraphic observations are summarized in Table 2-14-1.

SILTSTONE-WACKE SEQUENCE

The most commonly occurring lithology on Snippaker Ridge is a thick sequence of thinly bedded to thickly laminated siltstone and wacke with less common argillite, grit

and conglomerate horizons. Previous mapping (Graf, 1985, unpublished data) indicates that the sequence near Snippaker Peak is well bedded; bed thickness varies from 1 centimetre to as much as 200 metres. At the top of the siltstone-wacke sequence is a paraconformable series of coarse grits and polymictic conglomerates which contain chert pebbles and weather to a distinctive orange colour near Snippaker Mountain. The upper contact was not observed.

POLYMICTIC CONGLOMERATE

The siltstone-wacke sequence is overlain by a series of coarse grits and polymictic conglomerates. The basal contact of this unit was not observed. The unit is a mottled dark greenish grey, weathering to a medium grey or brownish grey. The largest clasts are 2 metres across, but clast size ranges down to small cobbles or, locally, gravel. The clasts are angular to rounded and are dark green, maroon or medium to light grey in colour. Clast lithologies include intermediate to mafic feldspar-phryic volcanic rocks and thickly to thinly laminated siltstone and wacke. The unit is

massively bedded, locally with thick interlaminae of siltstone, scour surfaces and graded bedding.

The conglomerate unit includes both clast and matrix-suspended facies. Locally, the matrix is calcareous and, less commonly, fossiliferous, containing unidentified bivalve shell fragments. The contact with the overlying unit is gradational.

FOSSILIFEROUS WACKE

The conglomerate grades upsection, over a thickness of approximately 10 metres, to a calcareous wacke. This unit is massively bedded and weathers to a distinctive orange or ochre. An estimate of the thickness of this unit is hindered by poor exposure, but the total thickness does not exceed 15 metres. The wacke contains a horizon rich in macrofossils. These include scleractinian corals, gastropods, bivalves, brachiopods and ammonites that have been identified as Norian in age (Nadaraju and Smith 1992a, 1992b). The fossiliferous wacke is therefore part of the Stuhini Group and the date is a minimum age for the underlying sedimentary strata. The upper contact of this unit with the overlying sedimentary rocks was observed in only one outcrop and appears unconformable.

BANDED SILTSTONE/ARGILLITE

Overlying the fossiliferous wacke with apparent unconformity is a sequence of thickly laminated to thinly bedded black argillites and siltstones. The sedimentary rocks are medium to dark grey on fresh and weathered surfaces, dip gently to moderately to the south and are exposed in the section on the north slope of the peak to the south of Snippaker Mountain (Figure 2-14-3). The unit was not seen in the Snippaker Mountain section. In the section to the south of Snippaker Mountain, it is recessively weathering, with incomplete exposure, but the thickness is estimated to be 30 metres.

DACITE CRYSTAL-LAPILLI TUFF

The sedimentary succession is overlain by a massive unit of crystal-lapilli tuff of intermediate, probably dacitic composition, with a measured thickness of approximately 50 metres. The unit is pale green in colour and weathers to a rusty orange or beige. Lapilli are commonly 0.5 to 1 centimetre in size, angular to subrounded and matrix supported. Phenocrysts are dominantly feldspar.

The basal contact of the dacite is subparallel with bedding in the underlying clastic sedimentary sequence and dips moderately to the south in most exposures. The contact locally cuts bedding surfaces. The underlying sedimentary rocks are well cleaved but are also baked adjacent to the contact, which is therefore an unconformity rather than a tectonic contact and marks the base of the volcanic succession on Snippaker and Johnny ridges.

VOLCANIC GRIT-WACKE-SILTSTONE

The top of the lower dacite unit on the peak to the south of Snippaker Mountain is not exposed. Overlying this unit is a thin sequence of epiclastic conglomerate and grit, grading

upsection to siltstone. The unit dips moderately to gently to the south. The total thickness of this unit does not exceed 25 metres. The clastic sedimentary rocks are interpreted as representative of local reworking of the underlying dacite and are absent from the Snippaker Peak section. Similar epiclastic horizons occur in the lower part of the dacite succession on Johnny Ridge (Metcalf *et al.*, in preparation).

MASSIVE HORNBLENDE PLAGIOCLASE DACITE

The epiclastic sedimentary unit is unconformably overlain by a massive unit interpreted as a lava flow or, possibly, a recrystallized crystal tuff. The top of the unit is eroded on Snippaker Mountain but a total thickness of 180 metres is exposed. In the section preserved on Johnny Ridge, the thickness of the dacite unit is in excess of 300 metres.

The rock is a plagioclase±hornblende-phyric dacite. Fresh surfaces are medium to dark grey, weathering through dark grey-green to grey or light grey. Phenocrysts comprise 20 per cent subhedral plagioclase, 1 to 4 millimetres in size, and 5 per cent subhedral hornblende, 1 to 3 millimetres in size, in a grey to grey-green aphanitic groundmass. Epidote alteration causes the greenish hue and is patchy to pervasive after both plagioclase phenocrysts and groundmass. Rare flow-banding is visible on lightly weathered surfaces.

The unit is apparently without sedimentary interbeds or structures at all locations examined on Snippaker Ridge. The dacite is a cliff-former and caps the sedimentary sequence at least as far south as the Inel workings (Figure 2-14-2).

CORRELATION OF THE SNIPPAKER RIDGE SECTION

The 1992 fieldwork carried out on the Snippaker Ridge section permits a correlation to be made across the valley of Bronson Creek, using previously acquired information. Both sections are of intermediate to felsic volcanic or volcanogenic rocks, each overlying a predominantly sedimentary succession. Contacts on either side of the valley are stratigraphic and unconformable rather than structural. One U-Pb zircon date of 192 ± 3 Ma has been obtained (M.L. Bevier, unpublished data) from a rhyolite unit stratigraphically above the massive dacite on Johnny Ridge, suggesting that the volcanism is Early Jurassic in age. The unconformity described here is therefore interpreted as marking the onset of Early Jurassic volcanism in the Snippaker Mountain - Johnny Mountain area.

One structural observation can be made regarding the flat-lying basal contact of the dacite. On Snippaker Ridge, this contact is exposed at an elevation of 1800 to 1900 metres; on the Johnny Mountain side, the contact is exposed at an elevation of 1100 metres. The disparity of elevations is not caused by an observable southwest dip to the contact on either ridge and supports the hypothesis of a significant structural discontinuity in the valley of Bronson Creek (Lefebvre and Gunning, 1989), with the Johnny Mountain block being downthrown.

Outcrops of dacitic volcanic rocks occur near the base of slope, on the southwest side of Bronson Creek, overlying a

steeply northeasterly dipping sedimentary sequence. It is not certain that these units are equivalent to the Snippaker and Johnny Ridge dacites. If a correlation is made, this will imply still greater displacement along the Bronson Creek structure.

MINERALIZATION

Three significant gold deposits and a number of interesting prospects lie within or close to the Bronson corridor. Each of the three deposits contains galena with lead isotope compositions that suggest the lead separated from its radioactive parents during the Early Jurassic (Godwin *et al.*, 1991). The onset of intermediate to felsic volcanism during this period is therefore of considerable significance. The heat source (or sources) associated with the volcanic rocks and their intrusive equivalents probably generated and maintained the hydrothermal systems which supplied the base and precious metal mineralization present in this area.

ACKNOWLEDGMENTS

The authors are indebted to Cominco Metals Ltd., to Skyline Gold Corporation and to Gulf International Minerals Ltd. for logistical support. Our sincere thanks go to Terry Hodson and Nick Callan of Cominco Ltd., Dave Yeager of Skyline Gold Corporation, Mike Jones of Cathedral Gold Corporation, Bob Gifford and Victor Jaramillo of Gulf International Minerals Ltd., Chris Graf of Ecstall Mining Corporation and Bob Hewton of Vector Industries International Inc. for generous donations both of their time and of geological information.

REFERENCES

- Alldrick, D.J. (1989): Volcanic Centres in the Stewart Complex (103P AND 104A, B); in Geological Fieldwork 1988, *B.C. Ministry of Energy, Mines and Petroleum Resources*, Paper 1989-1, pages 233-240.
- Alldrick, D.J., Britton, J.M., Maclean, M.E., Hancock, K.D., Fletcher, B.A. and Hiebert, S.M. (1990): Geology and Mineral Deposits - Snippaker Area (NTS 104B/6E, 7W, 10W, 11E); *B.C. Ministry of Energy, Mines and Petroleum Resources*, Open File 1990-16.
- Anderson, R.G. (1989): A Stratigraphic, Plutonic and Structural Framework for the Iskut River Map Area, Northwestern British Columbia; in Current Research, Part E, *Geological Survey of Canada*, Paper 89-1E, pages 145-154.

- Anderson, R.G. and Bevier, M.L. (1990): A Note on Mesozoic and Tertiary K-Ar Geochronometry of Plutonic Suites, Iskut River Map Area, Northwestern British Columbia; in Current Research, Part E, *Geological Survey of Canada*, Paper 90-1E, pages 141-147.
- Anderson, R.G. and Thorkelson, D.J. (1990): Mesozoic Stratigraphy and Setting for some Mineral Deposits in the Iskut River Map Area, Northwestern British Columbia; in Current Research, Part E, *Geological Survey of Canada*, Paper 90-1E, pages 131-139.
- Britton, J.M., Fletcher, B.A. and Alldrick, D.J. (1990): Snippaker Map Area; in Geological Fieldwork 1989, *B.C. Ministry of Energy, Mines and Petroleum Resources*, Paper 1990-1, pages 115-125.
- Fletcher, B.A. and Hiebert, S.N. (1990): Geology of the Johnny Mountain Area; *B.C. Ministry of Energy, Mines and Petroleum Resources*, Open File 1990-19.
- Godwin, C.I., Pickering, A.D.R., Gabites, J.E. and Alldrick, D.J. (1991): Interpretation of Galena Lead Isotopes from the Stewart-Iskut Area (103O & P and 104/A B & G); in Geological Fieldwork 1990, *B.C. Ministry of Energy, Mines and Petroleum Resources*, Paper 1991-1, pages 235-243.
- Lefebvre, D.V. and Gunning, M.H. (1989): Geology of the Bronson Creek Area, British Columbia; *B.C. Ministry of Energy, Mines and Petroleum Resources*, Open File 1990-16.
- Metcalfe, P., Anderson, R.G., Yeager, D.A., Bevier, M.L. and Atkinson, J.R. (in preparation): Stratigraphy, Structure and Mineral Deposits at Johnny Mountain, Northwestern British Columbia.
- Nadaraju, G.T. and Smith, P.L. (1992a): Jurassic Biochronology in the Iskut River Map Area, British Columbia: A Progress Report; in Current Research, Part A, *Geological Survey of Canada*, Paper 92-1A, pages 333-335.
- Nadaraju, G.T. and Smith, P.L. (1992b): Triassic-Jurassic Biochronology of the Iskut River Map Area, Northwestern British Columbia; Abstracts, *Canadian Paleontology Conference II*, Ottawa, Ontario, September 26th-28th, 1992.
- Rhys, D. and Godwin, C. (1992): Preliminary Structural Interpretation of the Snip Mine (104B/11); in Geological Fieldwork 1991, Grant, B. and Newell, J.M., Editors, and *B.C. Ministry of Energy, Mines and Petroleum Resources*, Paper 1992-1, pages 549-554.
- Rhys, D. and Lewis, P.D. (1993): Geology of the Inel Deposit, Iskut River Area, Northwestern British Columbia (104B/11); in Geological Fieldwork 1992, Grant, B. and Newell, J.M., Editors, *B.C. Ministry of Energy, Mines and Petroleum Resources*, Paper 1993-1, this volume.

NOTES



GEOLOGY OF THE INEL DEPOSIT, ISKUT RIVER AREA, NORTHWESTERN BRITISH COLUMBIA (104B/11)

By David A. Rhys and Peter D. Lewis, Mineral Deposit Research Unit, U.B.C.
(MDRU Contribution 013)

KEYWORDS: Economic geology, Inel, Snip, Stonehouse, shear vein, potassic alteration, mesothermal gold.

INTRODUCTION

The Bronson Creek area (Figure 2-15-1) contains several significant mineral deposits and showings, including Snip, the largest currently operating gold producer in British Columbia, owned by Cominco Metals (60%) and Prime Resources Group Inc. (40%). These occurrences underscore the importance of understanding controls on mineralization as a guide to further exploration. For example, the Snip, Johnny Mountain and Inel deposits are all examples of structurally controlled deposits spatially associated with syntectonic porphyry intrusions. Work by D. Rhys on the Snip deposit (Rhys and Godwin, 1992) and recent mapping by P. Metcalfe and James Moors (1993; this volume) is presently defining the stratigraphic and structural evolution of the entire western Iskut River area, and a comprehensive isotopic and geochemical examination of Mesozoic plutons in the area is in progress (Macdonald *et al.*, 1992).

The Inel property was originally staked by R.G. Gifford in 1969, and subsequently acquired by Skyline Explorations Limited. Surface exploration was carried out under option by Texasgulf Inc. in the mid-1970s, and later by Skyline. In 1987 the property was optioned, and later acquired by Inel Resources Ltd. Between 1987 and 1990, two adits were driven (AK and Discovery levels; Figure 2-15-1), and a total of 1200 metres of drifting and 11 500 metres of diamond drilling were completed (Gifford, 1991). During 1990, Inel Resources amalgamated with Gulf International Minerals Limited, which is now the sole property owner.

To better constrain the geological evolution of the Inel deposit and explore possible similarities with the nearby producing Snip and past-producing Johnny Mountain deposits, we examined the underground workings during the 1992 field season. The underground program included sampling and structural mapping at 1:500-scale through most of the two exploration drifts. Low oxygen levels at the end of the Discovery drift limited access.

GEOLOGICAL SETTING

The Inel property lies near the centre of the Snippaker map area within Intermontane Belt rocks just northeast of their boundary with Tertiary plutons of the Coast Plutonic Complex. Regional geologic maps (Lefebure and Gunning, 1989; Alldrick *et al.*, 1990) show the property to be underlain by a mixed volcanic and sedimentary succession, characterized by fine-grained marine sedimentary strata and mafic porphyritic flows and other volcanic rocks. Numerous intermediate to felsic dikes and stocks, associated with both

Jurassic and Tertiary magmatism, intrude the e rocks. Previous workers disagree on the age of the strata: Lefebure and Gunning (1989) suggest a Late Triassic age, and assignment to the Stuhini Group, whereas Alldrick *et al.*, (1990) prefer the Jurassic Hazelton Group. Recent mapping by P. Metcalfe (personal communication, 1992) indicates that rocks at Inel are lateral equivalents to strata exposed at Snippaker Peak, which contain Upper Triassic ammonites (Nadaraju and Smith, 1992).

The Inel property is on the southwestern flank of the south end of Snippaker Ridge, overlooking the Bronson Glacier. Jurassic strata on the upper part of Snippaker Ridge, and to the west on the upper part of Johnny Ridge, are flat lying to moderately tilted. Gold-bearing veins of the Stonehouse deposit at the Johnny Mountain gold mine occur in the lower part of this sequence. On Johnny Ridge, unconformably underlying Triassic sedimentary and volcanic strata are complexly folded and bedding attitudes range from flat lying to overturned. In contrast, the two packages are more nearly concordant on Snippaker Ridge, where Triassic strata are mostly flat lying to gently dipping. This folded Triassic sequence contains the Snip deposit at the base of Johnny Ridge.

Major structures in the Inel area include steep orthogonal fault sets striking northeasterly and northwesterly (Lefebure and Gunning, 1989; Alldrick *et al.*, 1990). These faults do not appreciably offset stratigraphic contacts, and displacements are probably a few hundred metres or less. Mappable folds are limited to tight, locally overturned, northwesterly-trending folds in the Triassic strata at Johnny Mountain, and to broad, upright open warps in the overlying Jurassic rocks.

GEOLOGY OF THE AK DRIFT

Rocks exposed in the AK drift (1650-metre mine level, Figure 2-15-2) are dominantly laminated to thinly bedded, graded siltstones and mudstones, with subordinate interbeds of matrix-supported cobble conglomerate and breccia up to 5 metres thick. Clasts within these coarser layers range from 0.5 to 60 centimetres in diameter and consist of rounded, massive medium-grained tonalite and angular mudstone. The clasts comprise between 5 and 30 per cent of the unit and are surrounded by a massive siltstone to mudstone matrix. Rare fining-upward beds within the laminated siltstone and mudstone sequence grade from a clast-rich basal conglomerate into massive mudstone. Isolated rounded tonalite to diorite clasts, 1 to 3 centimetres in diameter, are common throughout the siltstone and mudstone unit. Medium-grained, medium to thickly bedded greywacke occurs at the southeast end of the drift. Intrusive lithologies in the AK zone are limited to a medium to fine-grained

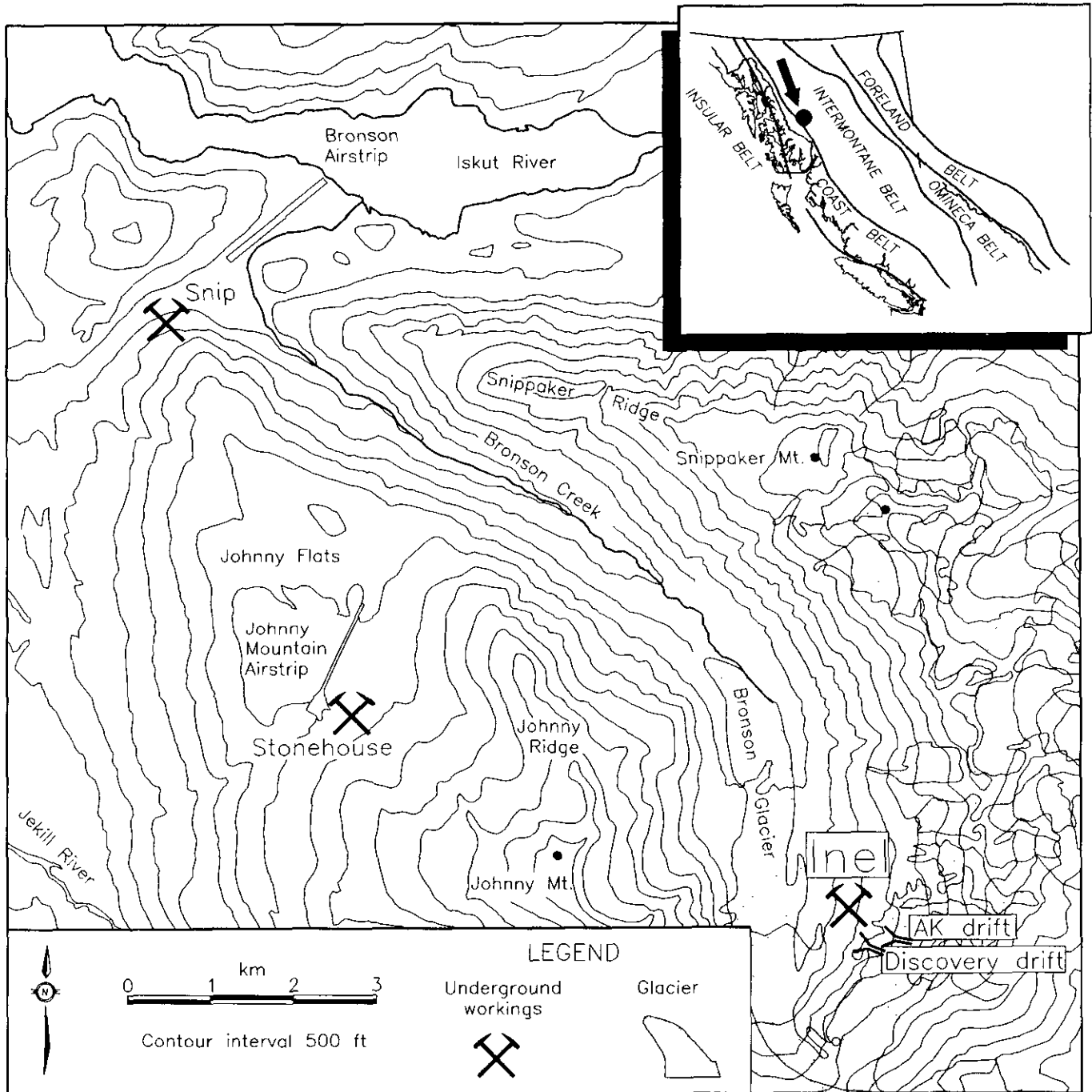


Figure 2-15-1. Location map of the Bronson Creek area, showing the locations of the Inel property, and the Snip and Stonehouse mines.

plagioclase-porphyritic stock which intrudes the siltstone and mudstone unit near the portal.

Rocks previously described as heterolithic intrusive breccias are exposed in the west end of the AK drift (Figure 2-15-2). These rocks have concordant contact relationships to mudstones underground, and a matrix composition similar to that in conglomeratic rocks observed elsewhere in the drift. Rounded massive to medium-grained tonalite to diorite clasts and angular mudstone to siltstone clasts occur in a medium to coarse-grained lithic greywacke matrix

(Plate 2-15-1). The sedimentary clasts display variable degrees of pyrite alteration, and often have 1 to 4-millimetre bleached haloes. Surface exposures of this unit show it forming a tabular body discordant to bedding in enclosing strata, forming the basis for its suggested intrusive breccia origin (V. Jaramillo, K. Illerbrun; personal communication, 1992).

Throughout the AK workings, beds dip gently easterly to northeasterly, except in locally disrupted areas. Structural features superimposed on these strata include stockwork

veinlet systems, thick sulphide veins, localized folds and brittle faults. Zones of potassium feldspar - sericite alteration bleach the laminated siltstones and are spatially associated with a pyrrhotite-sphalerite stockwork. Feldspar staining indicates that potassium feldspar occurs irregularly in this altered zone, and is absent from some strongly bleached samples. The veinlets have both moderate southeast and shallow north-northeast bedding-parallel dips. Several steep southwest-striking pyrite + calcite + sphalerite ± biotite ± chlorite veins, up to 40 centimetres wide, are associated with potassium feldspar alteration. Some of these steep veins are folded about flat-lying axial surfaces. Gouge-filled faults, locally with rusty bleached envelopes and thin calcite vein fill, cut all other structures. These have variable orientations, but most commonly dip moderately to steeply to the northwest. Slip direction and amount for these late structures could not be determined from available exposures:

Galena from a thin sulphide veinlet at the southeast end of the AK drift returned an Early Jurassic Pb-Pb relative age (Godwin *et al.*, 1991).

Near the east end of the exploration drift, bedding is deformed by disharmonic, overturned minor folds with variably oriented axial surfaces. A phyllitic bedding-parallel foliation is developed locally within this zone.

Exploration drilling from the AK drift intersected a southwest-dipping orthoclase-porphyritic dike 7 to 15 metres wide, 50 metres northeast of the drift (Figure 2-15-2 inset; compiled from Gifford, 1991). This dike is not exposed in the workings. An altered, mineralized heterolithic breccia or conglomerate, 5 to 12 metres thick, in its immediate footwall, known as the AK zone, strongly resembles the "intrusive breccia" at the west end of the AK drift. It consists of tonalite, diorite and siltstone/mudstone clasts in a sandy matrix and has contacts discordant to bedding in surface exposures. Drill-core samples often have a porous to pyritized matrix. Areas of highest pyrite content carry sub-economic copper, lead and zinc values associated with significant gold content. On the basis of current drilling information, a resource of 57 600 tonnes with an average grade of 11.7 grams per tonne gold has been calculated for this zone (Gifford, 1991).

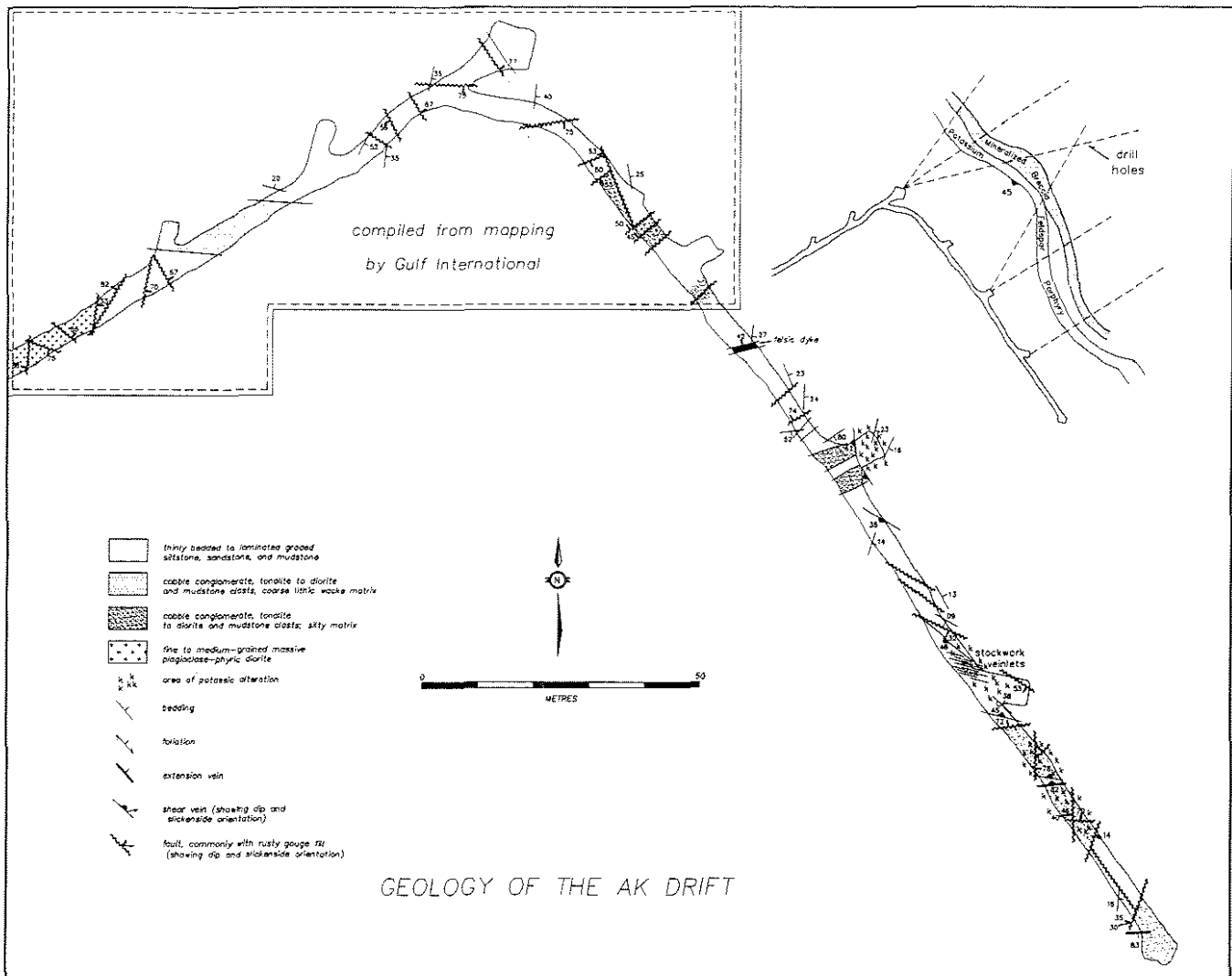


Figure 2-15-2. Geology of the AK drift, based on 1992 underground mapping.

GEOLOGY OF THE DISCOVERY DRIFT

The Discovery drift (1510-metre mine level; Figure 2-15-3) contains many of the same lithotypes present in the AK drift. Bedded to laminated siltstones and greywackes, generally coarser grained than equivalent units in the AK drift, are the dominant rock types. Greywackes in the Discovery drift are massive to medium bedded and generally poorly sorted, and contain scattered siltstone interbeds. Local coarser grained layers contain granule-sized angular mudstone fragments and well-rounded quartz grains.

Epidotized volcanic breccia at the eastern end of the mapped Discovery workings contains angular porphyritic fragments with black, biotite-altered mafic phenocrysts and epidote spots. The fragments are typically 0.5 to 3 centimetres in diameter, with highly angular, pitted margins that commonly interlock with adjacent fragments. The breccia matrix is a fine-grained mixture of epidote, calcite, and locally, potassium feldspar. A drill-hole intersection of this unit clearly shows that the epidote-calcite matrix material has replaced a fine to medium-grained mafic rock along fractures, indicating that the texture observed has probably resulted from intense alteration of a fractured basaltic protolith.

Two intrusive bodies are exposed at the southern end of the workings, outside the mapped area (Figure 2-15-3, inset map). A steeply southwest-dipping orthoclase-porphyritic dike, 6 metres wide, is exposed at the far southern end. This dike contains 5 to 10 per cent, 0.3 to 3-centimetre potassium feldspar crystals in a chloritic, medium-grained plagioclase-rich matrix (Plate 2-15-2). It is texturally and compositionally similar to the dike associated with the AK zone mineralization, of which it may be an offset extension. Five metres north of this dike, a parallel medium-grained massive, plagioclase-porphyritic dike, 10 metres wide, intrudes the greywackes. The fine-grained matrix of the dike is moderately to strongly potassium feldspar altered. In addition, medium-grained plagioclase-porphyritic diorite dikes intrude the north-central portion and the southeastern portion of the mapped workings.



Plate 2-15-1. Cobble conglomerate with tonalite to diorite and siltstone clasts, from the west end of the AK drift. Note the bleached alteration haloes around some siltstone clasts.

Bedding in the mapped portion of the Discovery drift is upright and has shallow to moderate northeasterly and southeasterly dips that define two broad, west-trending upright folds. Mesoscopic structural features in this area include sheeted shear veins, faults, foliation and extension veins. Shear veins are most common and generally have moderate southwest, northeast and southeast dips. There are two main varieties of vein infillings: calcite-chlorite veins, with subordinate quartz, biotite, pyrite and sphalerite; and massive pyrite-calcite-quartz veins with lesser chlorite and biotite. Calcite-chlorite veins are the most abundant, and range up to 40 centimetres in thickness. These commonly have a laminated fill of alternating chlorite and calcite-rich layers (Plate 2-15-3) and rarely have narrow biotite alteration envelopes. Massive pyrite veins are mostly thicker (up to 2.0 m) and commonly have biotite alteration envelopes 0.2 to 1.5 centimetres wide. Pyrite veins strike 090° to 110° , and are locally cut by calcite-chlorite veins, which usually strike 120° to 140° . Calcite-chlorite veins often contain a subhorizontal internal foliation oblique to vein walls. This foliation also occurs in adjacent footwall rocks, but rotates to steeper dips along the vein-footwall contact. In one vein, pyrite grains have well-developed pressure shadows aligned on the flat foliation surface. In several veins, the layered vein-filling material is disrupted by asymmetric, down-dip verging folds with shallow fold axes. Slickenside lineations on chlorite foliation surfaces in the veins mostly record dip-slip movement. Offset markers are rare; one southwest-dipping pyrite-rich calcite-biotite-chlorite vein, 15 centimetres wide at the southeast corner of the mapped area offsets one of the potassium feldspar altered dioritic dikes by 1.5 metres in an apparent normal sense. A sample of galena collected from a 1-metre quartz-sulphide vein at 46.95 metres in Discovery drillhole U-87 (Figure 2-15-3) returned an Early Jurassic Pb-Pb relative age (A. Pickering, personal communication, 1992).

A strong spaced cleavage in siltstones in the north-central section of the workings is defined by closely spaced (0.3, 3 cm) bedding-parallel chlorite-calcite > pyrite + quartz + biotite veinlets and stringers.

Blocky quartz-calcite extension veins occur rarely in all rock units. The veins have various orientations; a well-developed moderately southeast-dipping set occurs at the central east end of the mapped area. Some extension veins crosscut shear-vein fabrics, but are also offset along them.

Rusty gouge-filled faults cut all other structures and form northwest and northeast-striking sets. Faults of both sets dip moderately to steeply to both sides and rarely have down-dip slickensides. Sense and amount of displacement, and relative chronology of fault sets could not be determined from the mapped exposures.

Several zones of potassium feldspar alteration that affect the siltstones are spatially associated with stockwork veinlets of pyrite, chlorite, biotite and calcite. In the southeastern part of the mapped area (Figure 2-15-3), four bedding-parallel altered zones range from 0.2 to 2.5 metres thick, and have common southwest-dipping veinlet orientations. A similar alteration style surrounds the two dikes at the south end of the Discovery drift, and is coincident with several thick pyrite veins. This alteration cuts bedding and

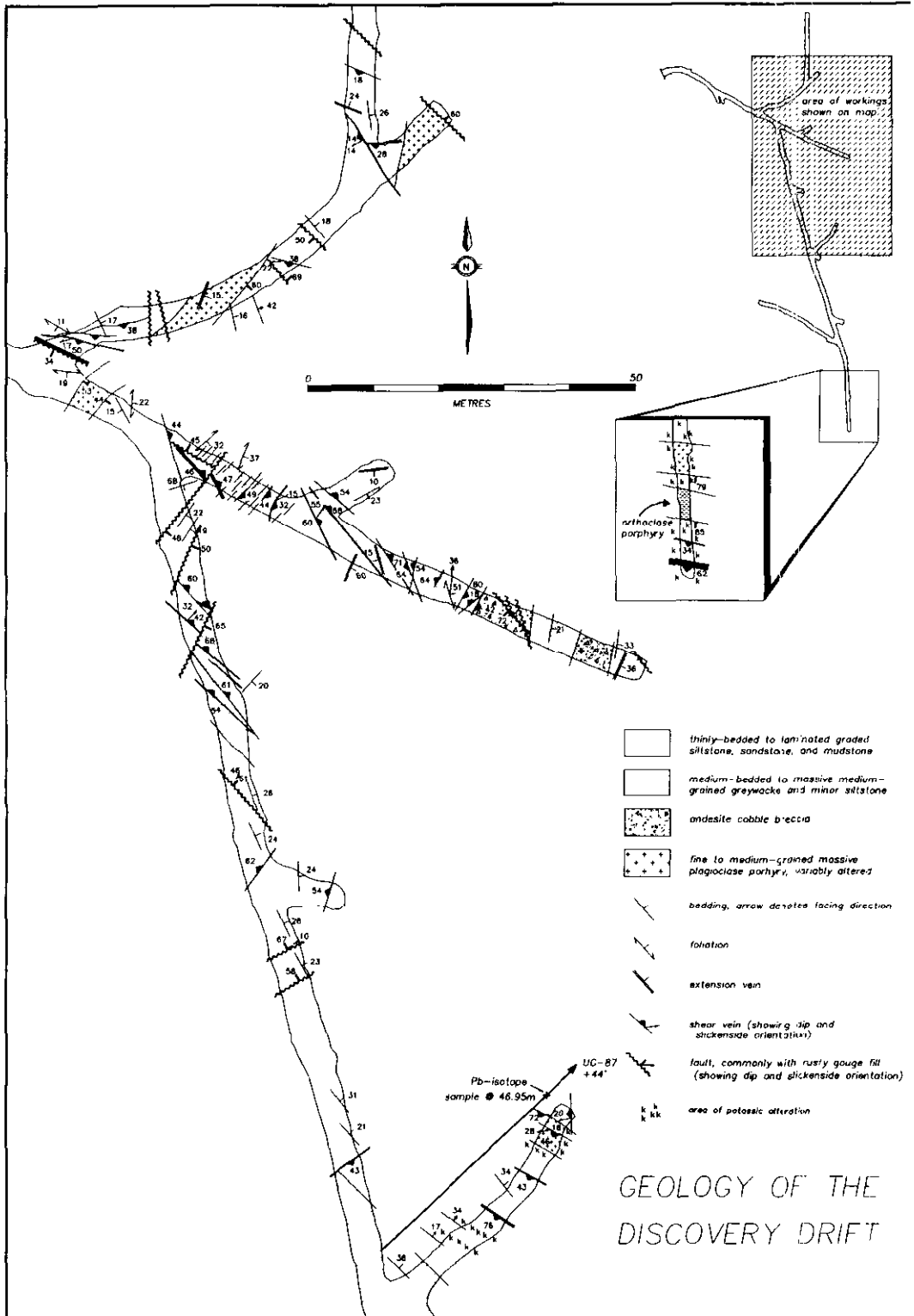


Figure 2-15-3. Geology of the Discovery drift, based on 1992 underground mapping.

is parallel to dike contacts. In contrast, no alteration is associated with the diorite dike in the northern part of the Discovery workings.

DISCUSSION

New underground mapping at Inel highlights some important similarities to other deposits in the Bronson Creek area. The mine sequence is dominantly sedimentary, with the possible exception of an altered volcanic breccia in the Discovery drift. The AK zone breccia or conglomerate is enigmatic, and requires further investigation to determine its origin. The clast type, abundance, and texture are identical to that of siltstone-mudstone matrix sedimentary conglomerates in the AK drift. If this unit is truly discordant to bedding, it may have an origin similar to the pebble dikes described in some copper porphyry systems (e.g., El Salvador; Gustafson and Hunt, 1975). Mineralization overprints this unit, and the spatially associated orthoclase-porphyratic dike probably intruded synchronous with both mineralization and alteration on the AK and Discovery levels.

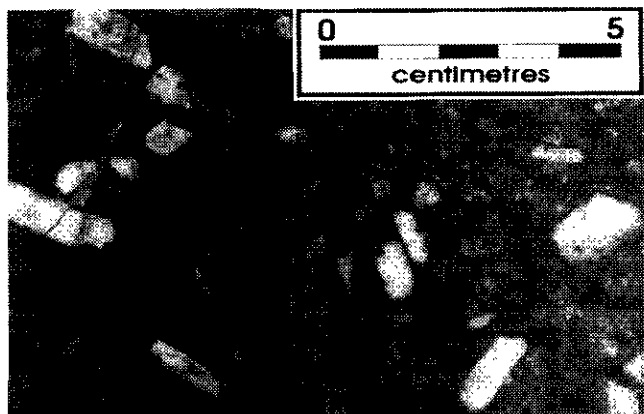


Plate 2-15-2. Porphyritic dike, from the south end of the Discovery drift. Coarse orthoclase phenocrysts are enclosed in a chloritic medium-grained plagioclase-phyric groundmass.

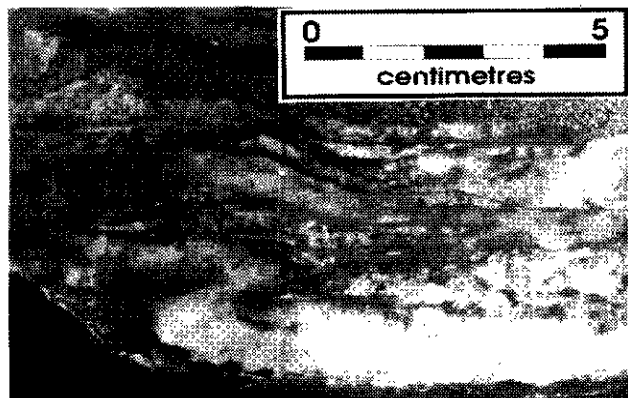


Plate 2-15-3. Laminated calcite-chlorite-pyrite-quartz vein from the northeastern Discovery drift, with an asymmetric fold outlined by a quartz vein. A massive pyrite band runs through the top of the picture, beside the scale bar.

The northeast and southwest-dipping orientations of shear veins on the Discovery level may represent a conjugate array. The normal sense of motion for both sets is consistent with this interpretation. Minor, southeast-dipping shear-veins are parallel to bedding, suggesting rheologically controlled failure and movement along bedding surfaces during formation of the conjugate vein sets. Crosscutting relationships show the massive pyrite veins predate the calcite-chlorite veins.

The irregularity of fold axes and axial planes, and the presence of internally folded siltstone and mudstone clasts in conglomerates of the AK drift suggest that soft-sediment deformation may have been occurring during or slightly after deposition. Later folding of sphalerite-pyrite veins about subhorizontal axial surfaces is kinematically consistent with and may be linked to formation of the shear veins.

Two styles of alteration are developed in both mine levels: bedding parallel to discordant zones of predominantly potassic alteration associated with sulphide-chlorite-calcite stockwork veins; and biotite - potassium feldspar - chlorite-silica envelopes developed around shear veins. Both styles occur together, but the broad, stockworked alteration zones may slightly predate the shear veins in some places, as demonstrated by their local offset by shear veins. The broad alteration zones may represent a channeling of fluids along permeable rock units that were superseded by flow along the shear veins once they developed. The spatial association of the orthoclase porphyry dike with alteration and mineralization implies that it may be a potential source of fluid and/or heat for at least part of the hydrothermal system. Dioritic dikes in the Discovery workings are offset by shear veins and are potassium feldspar altered, indicating that they predate the mineralizing event.

COMPARISON WITH THE SNIP AND STONEHOUSE DEPOSITS

The geology of the Inel deposit contains notable similarities to published descriptions of the Snip and Stonehouse deposits. Structures at both Snip and Inel are dominated by shear veins with layered calcite, chlorite and biotite fill hosted by probable Triassic sedimentary rocks (Rhys and Godwin, 1992). Kinematic indicators in both locations indicate a large component of down-dip simple shear associated with vein formation. In contrast, the Stonehouse deposit consists of a set of parallel, tabular, extensional quartz-sulphide veins cutting Jurassic volcanic and volcanoclastic strata (Britton *et al.*, 1990).

At all three deposits, porphyritic intrusions are co-spatial with alteration and mineralization. At Snip, the Red Bluff porphyry, a potassium feldspar megacrystic quartz monzonite to monzodiorite body, intrudes footwall sandstones approximately 1 kilometre from the ore deposits of the Twin zone. At Stonehouse, two-feldspar porphyry dikes (Britton *et al.*, 1990) cut the volcanoclastic sequence, and are in turn cut by mineralized veins. Our descriptions above note the occurrence of altered potassium feldspar megacrystic and dioritic dikes within the mine sequence at Inel. Isotopic data are consistent with intrusion broadly coeval with mineralization. Uranium-lead analyses for the Red

Bluff porphyry (195 ± 1 Ma, Macdonald *et al.*, 1992), the Inel stock (190 ± 3 Ma, Macdonald *et al.*, 1992), and the Stonehouse two-feldspar porphyry dikes (194 ± 3 Ma, M-L. Bevier, personal communication, 1992) are consistent with Early Jurassic galena Pb-Pb ages from all three deposits (Godwin *et al.*, 1991).

Finally, potassic alteration is widespread at Stonehouse, Snip and Inel. Biotite envelopes are common around veins at Snip and Inel, as are wide zones of potassium feldspar alteration associated with sulphide-calcite-chlorite stockwork veining. Mineralized veins at Stonehouse are enveloped by potassium feldspar alteration zones 5 to 10 metres thick, and this alteration hosts well-developed pyrite-quartz-chlorite-calcite veins and veinlets.

ACKNOWLEDGMENTS

This contribution has benefited greatly from discussions with V. Jaramillo and R.G. Gifford of Gulf International Minerals Ltd., Cominco geologists N. Callan and T. Hodson, D. Yeager of Skyline Gold Corporation, and with P. Metcalfe, J. Moors and J. Macdonald at The University of British Columbia. P. Carter and R.G. Gifford of Gulf International are thanked for permission to visit the property, and for logistical help. Cominco Metals provided accommodation at the Snip mine. A. Pickering analysed the Discovery drift galena Pb-Pb sample at the U.B.C. Geochronology Laboratory. Funding for this study is provided by the Science Council of British Columbia and Natural Sciences and Engineering Research Council of Canada under the Mineral Deposit Research Unit project "Metallogenesis of the Iskut River Area".

REFERENCES

Alldrick, D.J., Britton, J.M., MacLean, M.E., Hancock, K.D., Fletcher, B.A. and Hiebert, S.N. (1990): *Geology and Mineral Deposits of the Snippaker Map Area (104B/6E, 7W, 10W,*

11E); B.C. Ministry of Energy, Mines and Petroleum Resources, Open File 1990-16.

Britton, J.M., Fletcher, B.A. and Alldrick, D.J. (1990): Snippaker Map Area (104B/6E, 7W, 10W, 11E); *in Geological Fieldwork 1989, B.C. Ministry of Energy, Mines and Petroleum Resources, Paper 1990-1, pages 115-125.*

Gifford, R.G. (1991): Report on the Inel Property, British Columbia, Canada; *Gulf International Minerals Limited, unpublished company report*

Godwin, C.I., Pickering, A.D.R. and Gabites, J.E. (1991): Interpretation of Galena Lead Isotopes from the Stewart-Iskut Area (103O, P; 104A, B, G); *in Geological Fieldwork 1990, B.C. Ministry of Energy, Mines and Petroleum Resources, Paper 1991-1, pages 235-243.*

Gustafson, L.B. and Hunt, J.P. (1975): The Porphyry Copper Deposit at El Salvador, Chile; *Economic Geology, Volume 70, pages 857-913.*

Lefebvre, D. and Gunning, M. (1989): Geology of the Bronson Creek Area; *B.C. Ministry of Energy, Mines and Petroleum Resources, Open File 1989-28*

Macdonald, A.J., van der Heyden, P., Alldrick, D. and Lefebvre, D. (1992): Geochronometry of the Iskut River Area - An Update; *in Geological Fieldwork 1991, Grant B. and Newell, J.M., Editors, B.C. Ministry of Energy, Mines and Petroleum Resources, Paper 1992-1, pages 495-501.*

Metcalfe, P. and Moors, J.G. (1993): Refinement and Local Correlation of the Upper Snippaker Ridge Section, Iskut River Area, B.C. (104B/10W and 11E); *in Geological Fieldwork 1992, Grant, B. and Newell, J.M., Editors, B.C. Ministry of Energy, Mines and Petroleum Resources, Paper 1993-1, this volume.*

Nadaraju, G. and Smith, P. (1992): Jurassic Biocronology of the Iskut River Map Area: A Progress Report; *in Current Research, Geological Survey of Canada, Paper 1992-1A, pages 333-335.*

Rhys, D.A. and Godwin, C.I. (1992): Preliminary Structural Interpretation of the Snip Mine; *in Geological Fieldwork 1991, Grant, B. and Newell, J.M., Editors, B.C. Ministry of Energy, Mines and Petroleum Resources, Paper 1992-1, pages 549-554.*

NOTES

PRELIMINARY GEOLOGY OF THE HANK PROPERTY, NORTHWESTERN BRITISH COLUMBIA (104G/1, 2)

By Andrew W. Kaip, Mineral Deposit Research Unit, U.B.C.
and
Margaret D. McPherson, Homestake Canada Ltd.
(MDRU Contribution 019)

KEYWORDS: Economic geology, stratigraphy, Stuhini Group, megacrystic porphyry, alteration, natroalunite.

INTRODUCTION

The Hank property is situated in northwestern British Columbia approximately 20 kilometres northwest of Bob Quinn Lake (Figure 2-16-1). The property lies along a broad, northeast-trending ridge southeast of Ball Creek and varies in elevation from 900 metres in the northeast corner of the property to 2050 metres in the southwest. Access to the property is by helicopter from Bob Quinn Lake; the

claims are served by a network of cat trails developed by Lac Minerals Ltd. between 1985 and 1989.

The objective of this study is to define the stratigraphy, structure and alteration on the Hank property, leading to an understanding of the style and timing of precious metal mineralization.

Fieldwork conducted as a part of a Homestake Canada Ltd. exploration program between July and September, 1992, consisted of geologic mapping of the property and relogging of selected diamond-drill core. Mapping was conducted at two scales, 1:5000 property-scale mapping and 1:2000 detailed mapping of the informally named Fe site Hill, Bald Bluff and Rojo Grande areas. Subsequent research at the University of British Columbia will comprise part of an M.Sc. thesis supervised by Dr. A. Sinclair and Dr. J.F.H. Thompson

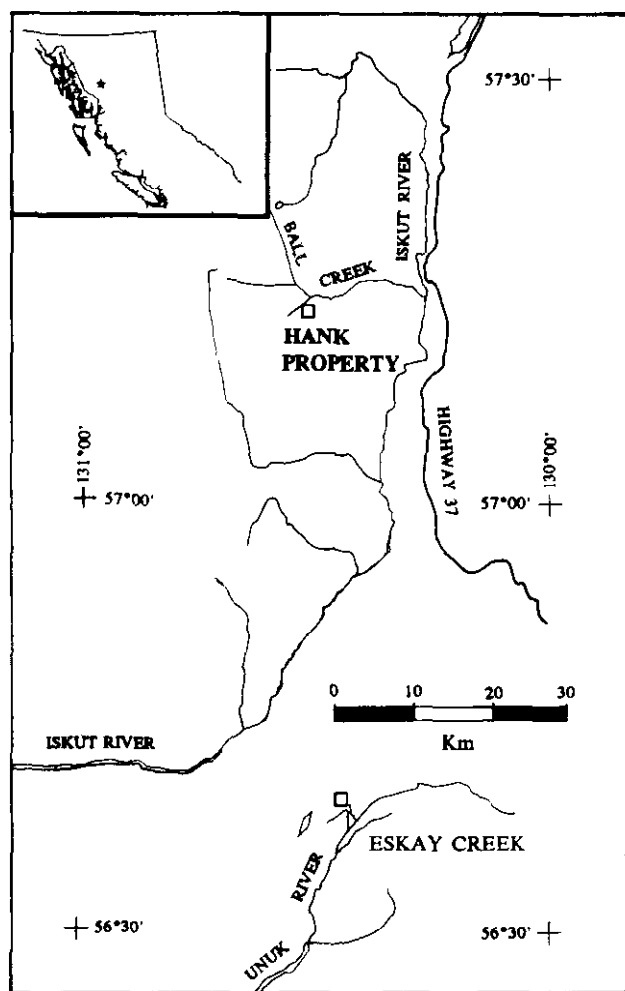


Figure 2-16-1. Property location map adapted from Anderson and Thorkelson, 1990.

EXPLORATION HISTORY

The Hank property comprises two groups of claims totaling 91 units. The Hank claims, owned by Lac Minerals Ltd., cover a large hydrothermal system that extends to the south and east onto the Panky claims, owned by Cominco Ltd. Homestake Canada Ltd. optioned both groups of claims in 1992.

The Hank prospect was initially identified and staked by Lac Minerals Ltd. in 1983, based on regional stream-sediment geochemical anomalies and the presence of prominent gossans along the ridge. Preliminary geological mapping and sampling that year outlined several broad zones of anomalous gold and arsenic values.

Lac Minerals Ltd. completed more extensive geologic mapping, sampling, trenching and geophysical surveys resulting in the discovery of two subparallel, northeast-trending alteration zones, the upper and lower alteration zones (Figure 2-16-2). Trenching identified a zone of gold mineralization which averaged 3.3 grams per tonne gold over 13 metres, coincident with a broad gold anomaly (> 300 ppb) in soils within the upper zone. Four diamond-drill holes totalling 288.1 metres tested this zone and hole 84-2 cut an intercept assaying 1.98 grams per tonne gold over 18 metres (Turna, 1985).

Lac Minerals completed additional mapping, trenching, sampling and geophysical surveying during 1984 to 1985 and 1987 to 1989. Additional diamond drilling totaled 11604.1 metres in 88 holes, in both the upper and lower alteration zones and several other targets. Drilling outlined a geologic reserve of 245 000 tonnes with an average grade of 4.0 grams per tonne gold and 218 000 tonnes with an

LEGEND FOR FIGURES 2, 3 AND 4

EAST SIDE OF FAULT

WEST SIDE OF FAULT

STRATIFIED ROCKS

LOWER JURASSIC (?)

4 Undivided siltstones, well-bedded sandstones and heterolithic conglomerates.

LATE TRIASSIC STUHINI GROUP

2A Undivided magnetic pyroxene-feldspar-phyric flows and breccias.

3 Undivided aphyric flows, rusty pyritic flow-banded rhyolites and minor well-bedded siltstones and fine-grained sandstones.

2b Bioclastic and silty limestone.

1a,d Undivided hornblende \pm feldspar-pyroxene flows, feldspar-hornblende \pm pyroxene phyric ash tuffs, lapilli tuff and tuff breccias and volcanic-derived siltstones and fine-grained sandstones.

1b Siltstones interbedded with well-bedded sandstones.

1c Feldspar \pm biotite-phyric ash tuffs and biotite-phyric massive flows and breccias.

INTRUSIVE ROCKS

A Orthoclase-megacrystic, hornblende-phyric monzonite.

B Medium-grained hornblende diorite.

ALTERATION

 Quartz+clay+pyrite

 Quartz+clay+pyrite

 Clay \pm quartz

 Quartz \pm pyrite

SYMBOLS

 Fault (defined, approximate, assumed)

 Geologic contact (defined, approximate, assumed)

 Alteration contact (defined)

average grade of 2.0 grams per tonne gold in the 200 and 440 pit areas (Figure 2-16-2).

Carmac Resources Ltd. (now Camnor Resources Ltd.) optioned the Hank claims in 1990 and drilled five holes totalling 1090.5 metres in the upper and lower zones, then terminated the option.

The Panky claims were staked by Cominco Ltd. in 1988, and geological mapping and sampling were completed in 1988 and 1990.

Homestake Canada Ltd. optioned the Hank and Panky claims in 1992, and completed a program of soil and rock sampling, an induced polarization survey and both property-scale and detailed geological mapping. Work concentrated on exploring the extensive alteration zones lying topographically and stratigraphically above the previously explored upper and lower alteration zones, with most of the detailed work in the Felsite Hill and Rojo Grande areas (Figure 2-16-2).

REGIONAL GEOLOGY

The Hank Property lies within the Stikine Terrane along the western margin of the Intermontane Belt and the eastern margin of the Skeena fold belt. Regional mapping in the area (Logan *et al.*, 1992.; Evenchick, 1991.; Souther, 1972) has defined the stratigraphy as predominately Upper Triassic: augite andesite flows, pyroclastic rocks and volcanic-derived sediments overlain by Lower Jurassic grits, con-

glomerates and greywackes (Units 5, 7, 8 and 13, Souther, 1972). Sedimentary rocks of the Middle Jurassic Ashman Formation of the Bowser Lake Group are exposed along the Iskut River valley to the east (Evenchick, 1991). Augite-phyric flows, andesite tuffs and volcanic-derived wackes and sandstones of the Upper Triassic Stuhni Group are exposed along the western margin of the property (Units uTSv, uTSs, and uTSsn, Logan *et al.*, 1992).

To the west of the property a large-scale northwest-striking fault is mapped at the head of Hank Creek (Souther, 1972). A subparallel fault, informally named the West Hank fault, adjacent and to the east of the large-scale fault, is exposed on the ridge to the northwest of the claims and continues along the western boundary of the property (Figure 2-16-2). A syncline trending southeast along the top of Hank Ridge is exposed in the saddle northeast of Goat Peak (Souther, 1972).

PROPERTY GEOLOGY

The Hank property is underlain by a succession of flows, pyroclastic and minor sedimentary rocks divided into four units (Figure 2-16-2). On the northeast side of the West Hank fault the stratigraphy consists of Upper Triassic Stuhni Group pyroxene-phyric flows and breccias overlying hornblende±pyroxene flows, pyroclastic rocks, siltstones, sandstones and biotite-phyric flows and breccias. Lower Jurassic carbonaceous siltstones, sandstones, wackes and pebble conglomerates which locally contain fossilized wood fragments unconformably overlie the volcanic succession (Souther, 1972).

On the west side of the fault Upper Triassic Stuhni Group interlayered aphyric flows and flow-banded rhyolites are overlain by siltstone and fine-grained sandstone.

Two intrusive plugs are exposed on the property, an orthoclase-megacrystic, hornblende-phyric monzonite which outlines the prominent knoll, Bald Bluff, and a medium-grained hornblende diorite which crops out on Goat Peak.

STUHNI GROUP

UNIT 1a

On the northeastern side of the West Hank fault, the most volumetrically abundant unit on the property is green to maroon, lapilli and tuff breccia. Rocks in this unit are poorly sorted and display weak normal grading from lapilli to breccia-sized fragments. Individual layers are difficult to identify, imparting an overall massive appearance to the rock. The fragments are feldspar-hornblende±pyroxene-phyric, typically angular and vary in size from 2 to 50 centimetres. Feldspar laths vary from 1 to 4 millimetres and make up 20 to 35 per cent (this and all subsequent mineral percentages are based on field estimates) of the fragments. Hornblende varies from 2 to 5 millimetres and pyroxene from 1 to 2 millimetres; together they comprise 15 per cent of the fragments. The matrix of lapilli and tuff breccia is composed of a fine-grained mass of broken feldspar crystals and aphanitic ash.

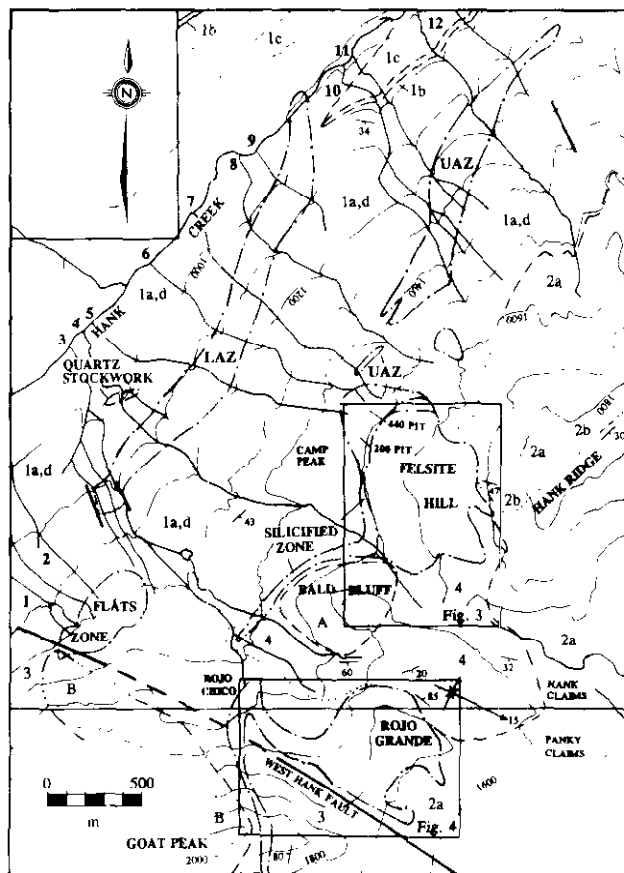


Figure 2-16-2. Generalized geology of the Hank property.

Within this sequence isolated lenses of well-bedded ash tuff, composed of broken feldspar laths and ash are exposed in Creeks 4 and 7 and on Camp Peak and vary from 0.5 to 1 metre wide. Poorly indurated, well-bedded, maroon and green calcareous siltstones and volcanic sandstones crop out at the top of Creek 13.

UNIT 1b

At the base of Creeks 8, 9 and 10 a lens of feldspar±biotite-phyric ash and lapilli tuff interfingers with Unit 1a. On the ridge to the north these tuffs are interbedded with black biotite and feldspar-phyric flows and breccias. Fragments are subrounded to rounded and vary in size from 2 to 20 centimetres. The groundmass is composed of fine-grained ash and isolated shards of volcanic glass. Flows, 20 to 30 metres thick, are massive to amygdaloidal and medium grained with euhedral 2 to 5-millimetre biotite phenocrysts.

UNIT 1c

Overlying Unit 1b are black, finely laminated siltstones interbedded with grey and brown fine to medium-grained sandstones. Individual sandstone beds vary in thickness from 2 to 20 centimetres and occasional load structures indicate that beds are upright. The thickness of this unit varies along strike from 20 to greater than 50 metres.

UNIT 1d

Interfingering with Unit 1a are maroon to grey, magnetic, hornblende-feldspar±pyroxene-phyric flows. On the west side of the property these flows are volumetrically minor forming thin lenses which are discontinuous over 100 metres strike length. On the east side of the property, a series of flows up to 70 metres thick dominates the stratigraphy. The flows are massive with amygdaloidal bases, best exposed in Creeks 6 and 7. Hornblende phenocrysts vary from 2 to 20 millimetres in size and comprise up to 15 percent of the rock. Feldspars are commonly pale green and form single crystals or radiating masses with magnetite inclusions. Pyroxene occurs as equant crystals 2 to 4 millimetres in size. The groundmass is maroon, aphanitic and contains disseminated magnetite.

UNIT 2a

Overlying Unit 1, interlayered pyroxene and feldspar-phyric, dark green to grey, magnetic flows and maroon to green breccias are best exposed along Hank Ridge (Figure 2-16-2). The flows are massive and amygdaloidal and range in thickness from 5 to greater than 100 metres. Isolated limestone clasts are observed in the flows near the top of the section on Hank Ridge. The breccias are poorly sorted and consist of angular to well-rounded fragments up to 1.5 metres in size derived from the flows. Recessively weathering pyroxene crystals are equant, vary in size from 2 to 10 millimetres and comprise 10 to 30 per cent of these rocks. Feldspars occur as crowded white laths up to 3 millimetres in size and forming 20 to 40 per cent of the rock. The groundmass is aphanitic and contains fine-grained disseminated magnetite.

UNIT 2b

A lens of partially recrystallized, bioclastic and silty limestone crops out near the top of the exposed section of Unit 2a on Hank Ridge (Figure 2-16-2.). The limestone contains bivalve and gastropod fossil fragments in strongly bioturbated layers interbedded with well-laminated, fine-grained silty limestone. This unit overlies tuff breccia and underlies pyroxene-feldspar-phyric flows.

UNIT 3

Dark green to black amygdaloidal aphyric flows and flow breccias interlayered with rusty, pyritic, flow-banded rhyolites are exposed on the east flank of Goat Peak along the southwest side of the West Hank fault. These volcanic rocks underlie brown to black, well-bedded, calcareous siltstones and fine-grained sandstones with carbonaceous plant fragments along bedding planes. The sediments are exposed west of Creek 1 and at the base of Goat Peak on the southwest side of the West Hank fault.

LOWER JURASSIC

UNIT 4

Unconformably overlying Unit 2 are poorly indurated, maroon and green siltstones, brown and green well-bedded sandstones, and heterolithic pebble to cobble conglomerates. Fossilized wood fragments up to 2 metres are common and rare *Weyla* are reported (Turna, 1985). Siltstones are well laminated and individual beds vary from 0.5 to 5 metres thick. The sandstones are calcareous and display low-angle, cross trough bedding with pebble lags along foresets. Clasts in the conglomerates are well rounded and vary in size from 0.5 to 10 centimetres. Clasts are dominantly intraformational and derived from the underlying volcanic rocks.

INTRUSIVE ROCKS

UNIT A

An orthoclase-megacrystic, hornblende-porphyrific intrusive is exposed on Bald Bluff. The intrusive is well foliated and locally flow banded with the strike of the foliation subparallel to the margins of the plug and dipping near vertically. On the top of Bald Bluff the foliation flattens and well-banded orthoclase-megacrystic intrusive rock underlies silicified breccia derived from it. A contact breccia with angular fragments of the foliated intrusive cemented by calcite, iron-bearing carbonate and grey to red silica is exposed on the margins of the intrusive. The Bald Bluff porphyry has intrusive contacts with the surrounding sediments and breccia dikes related to it intrude sedimentary rocks adjacent to the contact. Minor hornfelsing of Unit 4 is observed in outcrop adjacent to the intrusion and represented by the occurrence of black, euhedral biotite and fine-grained, disseminated pyrite.

UNIT B

A plug of relatively homogeneous, medium-grained equigranular diorite which locally contains more pegmatitic phases, crops out on Goat Peak west of the West Hank fault.

STRUCTURE

The West Hank fault was identified during mapping along the southwestern boundary of the Hank property. This fault is recognized as an extension of a fault previously mapped on the ridge to the northwest (Logan *et al.*, 1992). In outcrop the fault is marked by abundant white calcite veining, brecciation and contorted bedding in sedimentary rocks adjacent to it.

Bedding in the volcanic succession on the northeast side of the West Hank fault strikes northeast and dips 20° to 40° to the southeast along Hank Ridge. On the ridge to the north, bedding strikes southwest and dips 20° to the northwest. Within Unit 2b, above Felsite Hill, bedding strikes southeast and dips 50° to the southwest. Local variations in bedding are also recorded within Unit 1b at the base of Creeks 10 and 12.

Within Unit 4 bedding is more variable due to doming, caused by the intrusion of the Bald Bluff porphyry and folding along the east side of Rojo Grande. Along the margins of the intrusion, east to northeast-striking bedding steepens from 30° to 60°. On the east side of Rojo Grande an asymmetric syncline trending southeast probably corresponds to one mapped by Souther (1972).

Bedding on the southwest side of the West Hank fault strikes south and dips steeply to the west. Bedding in the sedimentary rocks adjacent to the fault and along Hank Creek strikes east and dips steeply south.

Within the volcanic succession along the northwest side of Hank Ridge local faults have been identified in outcrop and drill core. These faults strike north-northwest and have offsets of less than 100 metres.

ALTERATION AND MINERALIZATION

Seven alteration zones were identified during mapping and examination of drill core. The use of sericite and clays are field terms only. Preliminary x-ray diffraction work has indicated that most of the sericite is illite and clays are kaolinite ± dickite.

LOWER ALTERATION ZONE

The lower alteration zone is a broad northeast-striking zone of sericite + pyrite ± carbonate alteration which dips steeply to the southeast and cuts stratigraphy (Figure 2-16-2). The intensity of alteration increases toward the lower boundary of the alteration zone from weak chlorite + pyrite + carbonate alteration to strong sericite + pyrite + carbonate alteration. The lower boundary of the alteration zone is based on a decrease in the estimated percentage of carbonate and the prominent change in the colour of the gossans in the creeks along the northeast side of Hank ridge. The upper contact of the lower alteration zone is gradational and marked by a gradual decrease in the intensity of alteration to weak chlorite + pyrite + carbonate ± sericite with discontinuous pods of stronger alteration.

The northern boundary of the lower alteration zone terminates between creeks 9 and 10 along Hank Creek (Figure 2-16-2). Reconnaissance mapping on the ridge to the north of the property indicates that it does not extend across Hank

Creek. The southwest limit of the lower zone is a fault contact with unaltered hornblende and feldspar-phyric lapilli tuff.

Altered rocks are typically pale grey in colour and very uniform. Pyrite is euhedral, 1 to 10 millimetres in size, comprises 10 to 15 per cent of the rock and is commonly disseminated or concentrated within relict lapilli. Sericite is predominantly white and less commonly pale green to brown and comprises up to 80 per cent of the alteration assemblage. The predominant carbonate mineral is fine-grained calcite which comprises less than 10 per cent of the assemblage.

Within the lower alteration zone gold has been found in quartz-carbonate veins which also carry sphalerite-galena + pyrite ± chalcopyrite and vary from 2 to 50 centimetres in width. In drill core these veins appear to be localized along dilational zones which pinch and swell, while on surface they appear to be discontinuous over tens of metres. Where zoned the veins consist of fine-grained, grey quartz on their margins and coarse-grained, white to pale pink calcite and sulphides in their cores. Wall-rock alteration typically increases to soft pyritic clay adjacent to the margins of the veins.

Pyrite stringers, less than 1 centimetre wide cut calcite stringers and in turn are cut by late pink to white carbonate veins up to 30 centimetres wide. Gypsum and anhydrite fill the latest set of fractures with crystal growth typically perpendicular to the fracture walls.

QUARTZ STOCKWORK

Below the lower alteration zone in Creek 4, a 10 by 150 metre zone of quartz stockwork is exposed within chlorite + iron-carbonate + pyrite altered lapilli tuff of Unit 1a. The zone appears to terminate to the east of Creek 4 and is covered by talus to the west. Both milky white quartz veins up to 2 centimetres wide and silica flooding of the rock are observed in outcrop. Sheeted quartz veins in the core of the stockwork strike 170° and dip vertically.

UPPER ALTERATION ZONE

The upper alteration zone is less continuous than the lower zone and forms a series of northeasterly trending zones from the head of Creek 4 to the west side of Creek 12 (Figure 2-16-2). Alteration varies from strong sericite + pyrite ± carbonate to strong sericite + chlorite + pyrite + carbonate. In Creeks 10, 11 and 12 the footwall of the zone is very sharp; in drill core within the 200 and 440 pit areas this lower boundary coincides with the top of maroon hornblende ± pyroxene-phyric flows. In Creek 12 the upper contact of the alteration zone coincides with the base of a thick pile of hornblende-phyric flows. This suggests that the upper alteration zone may be stratigraphically controlled.

The alteration assemblage in the upper zone comprises pale green, sericite + chlorite + pyrite + carbonate with localized pods of intense pale grey, sericite + pyrite ± carbonate similar to the lower zone. Gold in the upper zone appears to be related to pyrite concentration. Disseminated pyrite varies from 10 to 15 per cent, is very fine-

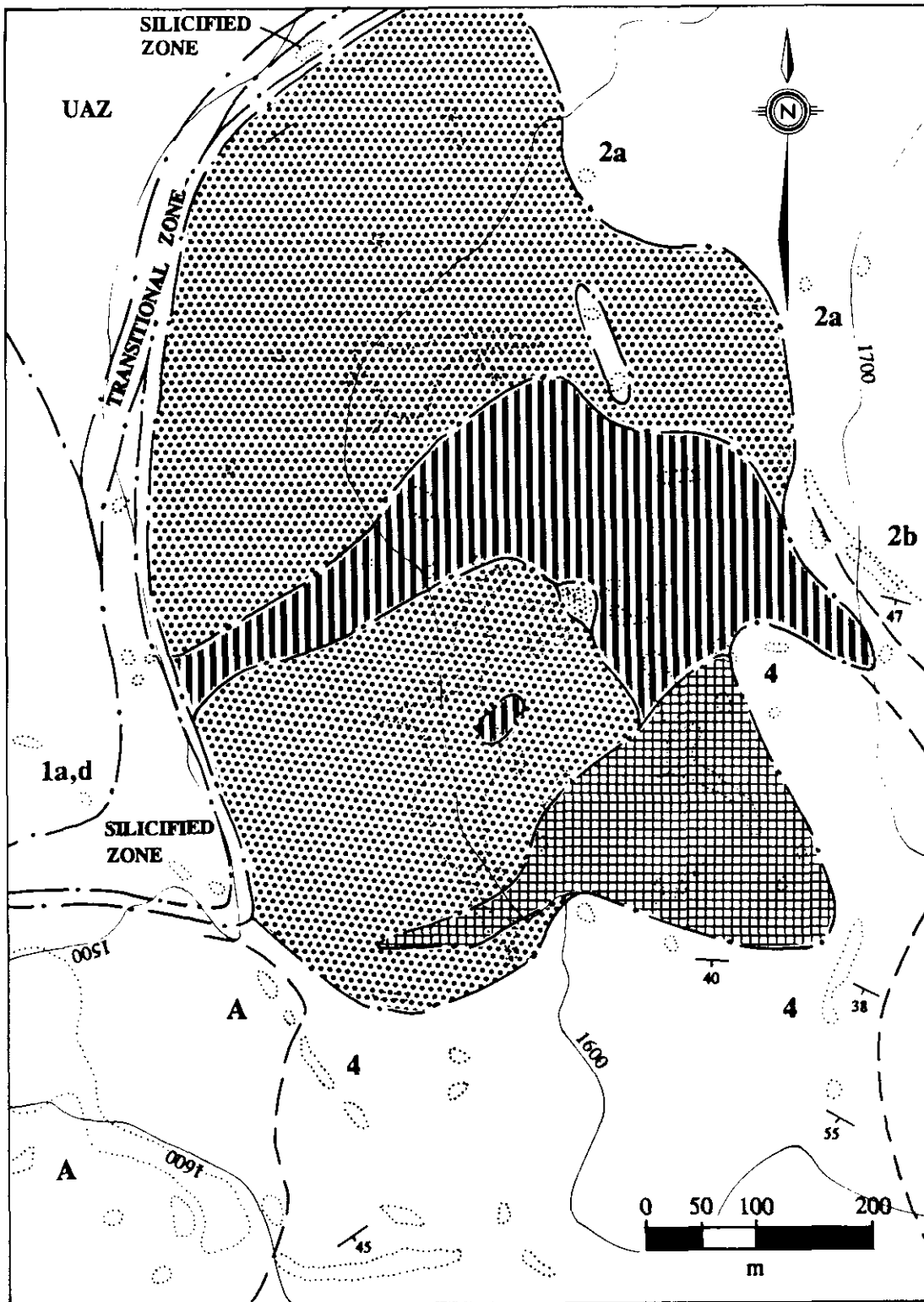


Figure 2-16-3. Distribution of alteration assemblages on Felsite Hill.

grained (<1mm) and appears to be concentrate in relict lapilli. Pyrite stringers up to 1 centimetre wide cut calcite stringer veins. Disseminated carbonate varies from 5 to 15 per cent of the alteration assemblage with an increase in

calcite occurring along the margins of quartz-carbonate veins.

Quartz-carbonate veins carrying sphalerite±galena±pyrite±chalcopyrite, similar to those in the lower

alteration zone are present but less abundant. Late, coarse-grained, milky white to pale pink, crustiform calcite \pm pyrite veins up to 50 centimetres in width cut these veins. Gypsum and anhydrite fill the latest set of fractures. Discontinuous zones of grey silicification are seen in core and correspond to an increase in the percentage and grain size of pyrite. These zones are usually related to an increase in the amount of veining and are up to 10 metres in width.

Between the upper alteration zone and quartz-clay-pyrite alteration on Felsite Hill there is a poorly exposed zone, up to 100 metres wide, of transitional alteration best seen in drill core within and above the 200 pit area (Figure 2-16-3). In drill core there is a general decrease in the degree of silicification downward from quartz+clay+pyrite alteration to friable clay+pyrite \pm quartz. Crumbly clay+pyrite \pm quartz grades downward into sericite+clay+pyrite \pm carbonate and into typical upper zone alteration. An interval of diffuse silica flooding within this transitional zone may correspond with the position of the silicified zone described below.

SILICIFIED ZONE

The "silicified zone" consists of intense silicification, sometimes accompanied by disseminated pyrite, exposed at the base of Bald Bluff and extending along the western margin of Felsite Hill (Figure 2-16-2). Below Bald Bluff the silicified zone appears stratigraphically controlled within sedimentary rocks of Unit 4; it strikes 100° and dips 30° to the south. It may pinch and swell along strike, as indicated by the absence of this type of alteration in drill core below Felsite Hill (Figure 2-16-3). The zone is bounded by a poorly exposed zone of strong sericite+clay+pyrite \pm quartz alteration of unknown width. Below Bald Bluff this zone contains cavities lined with drusy quartz and quartz veins similar to those observed in the "flats zone" described below.

Alteration in the silicified zone is composed of pale grey to dark blue-grey, very fine grained quartz. Pyrite is present as very fine grained disseminations within grey quartz and coarse-grained pyrite within blue-grey quartz. At least three phases of brecciation are recognized in the zone. The earliest phase is characterized by white to grey angular fragments in a grey silica matrix. The second phase is characterized by rebrecciation and partial cementation by silica. Drusy cavities occurring at the interstices between angular fragments and chalcedonic veinlets up to 2 millimetres wide are associated with this phase. The latest phase is characterized by the brittle fracturing of silicified outcrops and the presence of barite in open cavities.

FELSITE HILL

Alteration on Felsite Hill forms a broad oval zone with a north-trending long axis cutting across stratigraphic contacts (Figure 2-16-3). Along the margins of the zone are altered sedimentary rocks of Unit 4 and pyroxene and feldspar-phyric flows of Unit 2a. The dominant alteration is intense quartz+clay+pyrite followed by quartz+clay \pm pyrite and clay \pm quartz. A small zone of quartz+pyrite alteration, similar in appearance to the silicified zone, is exposed on the top of Felsite Hill.

Quartz+clay+pyrite alteration is texturally destructive with relict feldspar and fragment outlines present only on weathered surfaces. Near the margins of quartz+clay+pyrite alteration zones, the intensity of silicification decreases and clay-altered feldspars and fragments are visible. Texturally this alteration type is composed of fine grained blue to grey silica, grey to white clay and up to 15 per cent very fine grained disseminated pyrite. A small pod of clay \pm quartz-altered, fine-grained sediments with carbonaceous partings is exposed within quartz+clay+pyrite alteration on the west side of Felsite Hill. This alteration varies from clay \pm quartz to brown clay which appears more granular than the typical soft amorphous clay described below.

Quartz+clay \pm pyrite alteration varies from texturally destructive vuggy, quartz+clay alteration to less intense alteration with relict primary textures and isolated pods of fine-grained pyrite. In the former, intensely altered rock, fine-grained white to buff quartz comprises to 10 per cent of the rock which has small cavities throughout. These cavities contained clay which has since been leached out. Where textures are more visible there is an increase in clay \pm pyrite alteration. Pyrite occurs as fine-grained euhedral grains in localized disseminations of up to 15 per cent pyrite. Small pods of chalcedonic grey silica and white amorphous clay veinlets have been identified in outcrop.

Clay \pm quartz alteration varies dramatically in intensity along the southern margin of the alteration zone on Felsite Hill (Figure 2-16-3). In this area clay \pm quartz alteration preserves primary sedimentary textures in the maroon siltstones and conglomerates. Clay varies from green to maroon in colour and occurs initially as soft amorphous clay alteration of the matrix. With an increase in alteration intensity, clasts in the conglomerates are altered to fine-grained clay similar to the matrix.

Patchy zones of moderate quartz+clay+pyrite \pm sericite \pm chlorite alteration with textural similarities to alteration on Felsite Hill and in the upper alteration zone are exposed on the top of Bald Bluff.

ROJO GRANDE

Alteration on Rojo Grande forms a more irregular zone than on Felsite Hill, extending from Rojo Chico eastward to Rojo Grande and southward onto Goat Peak (Figure 2-16-4). The style of alteration is similar to alteration on Felsite Hill with quartz+clay+pyrite the dominant assemblage, followed by quartz+clay \pm pyrite and minor clay \pm quartz. On Rojo Grande zones of intense quartz \pm pyrite alteration are more abundant and occur as north-striking linear zones.

Rojo Chico is situated to the west of Rojo Grande and is altered to quartz+clay+pyrite (Figure 2-16-4). Altered rocks are typically massive and granular in appearance with fine-grained, blue-grey quartz, disseminated pyrite and white clay.

Along the east-northeast side of Goat Peak a prominent zone of quartz+clay+pyrite alteration appears to strike towards Rojo Chico. This linear zone cuts across the West Hank fault along the base of Goat Peak with no observable offset. Along the ridge line, a quartz-clay-pyrite assemblage

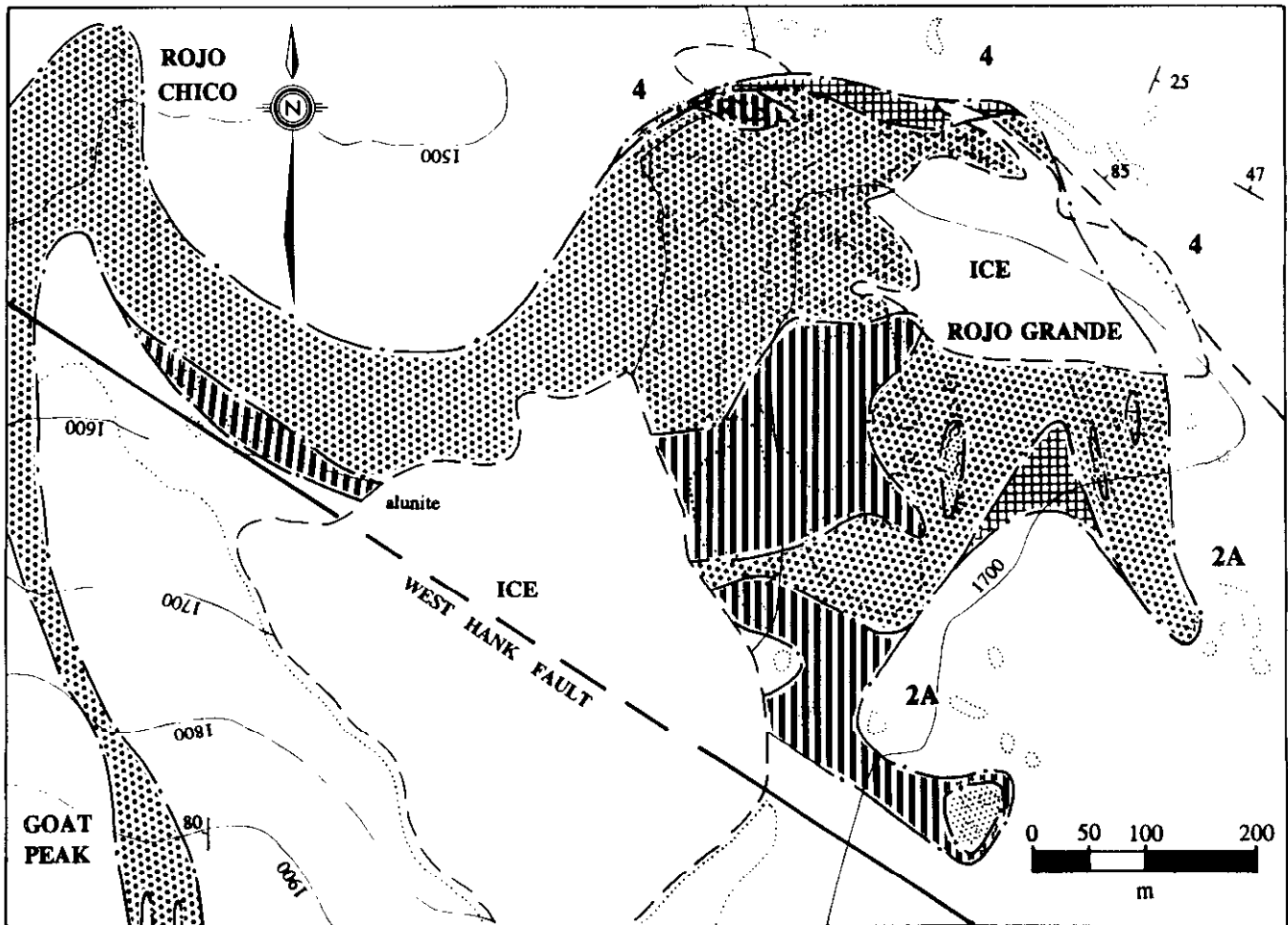


Figure 2-16-4. Distribution of alteration assemblages on Rojo Grande, Rojo Chico and Goat Peak.

alters aphyric amygdaloidal flows of Unit 3. This zone includes linear bands of unaltered flows striking 170° and dipping vertically (Figure 2-16-4).

Quartz+clay \pm pyrite altered rocks occur along the base of Goat Peak adjacent to the fault. Within this zone, white amorphous clay pods and veins up to 2 centimetres wide are observed adjacent to a zone of brecciation measuring 1.0 by 4.0 metres. The clasts in this breccia are altered to quartz and clay and cemented by fine-grained grey quartz. A vein of light brown sugary crystals 1.0 centimetre wide also occurs adjacent to the breccia. X-ray diffraction of this material has identified it as a combination of natroalunite and dickite.

FLATS ZONE

A poorly exposed zone of quartz+sericite+pyrite alteration hosting pods of clay+pyrite \pm quartz alteration is exposed at the head of Creeks 1 to 3 (Figure 2-16-2). Alteration in the flats zone is composed of pale grey, fine-grained sericite, quartz and pyrite with milky white, druzy quartz cavities and crustiform veining up to 3 centimetres wide. Fine-grained disseminated pyrite comprises 5 to 20 per cent of the rock. Clay+pyrite \pm quartz alteration is seen

in small outcrops of friable white to grey rock with very fine grained disseminated pyrite. Within this zone are discontinuous pods of grey silica which are recognized by an increase in the competence of the rock. These pods are surrounded by a broad zone of yellow and white, clayey soil.

In drill hole 87-7, collared in this zone, quartz+potassium-feldspar+pyrite alteration has been confirmed at a depth of 46.5 metres by x-ray diffraction. This alteration assemblage occurs as more competent intervals within friable quartz-sericite-pyrite alteration.

DISCUSSION

The Hank property is underlain by Upper Triassic Stuhini Group andesitic to basaltic flows, pyroclastic rocks, volcanic-derived sediments and minor limestone, overlain unconformably by poorly indurated, well-bedded Jurassic sediments. These rocks have been intruded by the Bald Bluff orthoclase-megacrystic porphyry and diorite. Three main alteration assemblages have been identified, possibly representative of a low-sulphidation epithermal system. They include: the sericite+pyrite+carbonate assemblage of the upper and lower alteration zones, where gold is concen-

trated in narrow quartz-carbonate veins in the lower parts of the system, and is related to disseminated pyrite in the upper parts of the system; pervasive multiphase silicification within a transitional zone of decreasing carbonate+sericite and increasing quartz+clay alteration and; variable quartz±clay±pyrite alteration of the broad Felsite, Rojo Chico and Rojo Grande zone, where gold mineralization is restricted to quartz-clay zones. This alteration may represent the upper levels of an epithermal system. Weak quartz+clay+pyrite±sericite alteration within the Bald Bluff porphyry suggests that it intruded during the final phases of the mineralizing event. Future geochronometry, petrology, x-ray diffraction and whole-rock geochemistry work will help to constrain these temporal relations.

ACKNOWLEDGMENTS

The authors would like to thank Homestake Canada Ltd. for the technical and logistical support of this study. We are grateful to R. Britten and H. Marsden of Homestake for insight and ideas on the Hank property and to Lac Minerals Ltd. and Cominco Ltd. for access to data. Thanks to J.F.H. Thompson, A.J. Sinclair and A.J. Macdonald for constructive editing. Continued financing for this study is

provided under the Mineral Deposit Research Unit project "Metallogenesis of the Iskut River Area".

REFERENCES

- Anderson, R.G. and Thorkelson, D.J. (1990): Mesozoic Stratigraphy and Setting for some Mineral Deposits in Iskut River Map Area, Northwestern British Columbia; in *Current Research, Part E, Geological Survey of Canada*, Paper 90-1F, pages 131-139.
- Evenchick, C.A. (1991): Jurassic Stratigraphy of East Telegraph Creek and West Spatsizi Map Areas, British Columbia; in *Current Research, Part A, Geological Survey of Canada*, Paper 91-1A, pages 155-162.
- Logan, J.M., Drobe, J.R. and Elsby, D.C. (1992): Geology of the Moore Creek Area, Northwestern British Columbia (104G/2), in *Geological Fieldwork 1991*, Grant, B. and Newell, J.M. Editors, *B.C. Ministry of Energy, Mines and Petroleum Resources*, Paper 1992-1, pages 161-178.
- Souther, J.G. (1972): Telegraph Creek Map Area, British Columbia; *Geological Survey of Canada*, Map 1623A.
- Turna, R. (1985): Geological, Geochemical and Diamond Drilling Report on the Hank Claim Group; *B.C. Ministry of Energy, Mines and Petroleum Resources*, Assessment Report 135-94, 374 pages.

NOTES

GEOLOGY OF SEVERAL TALC OCCURRENCES IN MIDDLE CAMBRIAN DOLOMITES, SOUTHERN ROCKY MOUNTAINS, BRITISH COLUMBIA (82N/1E, 82O/4W)

By Gary Benvenuto

KEYWORDS: Industrial minerals, talc, Cambrian dolomite, stratabound, Red Mountain, Gold Dollar, Silver Moon, Cathedral escarpment.

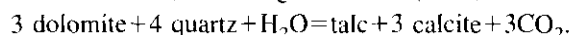
INTRODUCTION

The basal Middle Cambrian dolomites of the Southern Canadian Rocky Mountains host significant occurrences of stratabound microcrystalline talc varying from black and chloritic to white and nearly pure. The two groups of occurrences examined are at Talc Lake and nearby Mount Whymper in Kootenay National Park in British Columbia. The occurrences include the Red Mountain, Gold Dollar and Silver Moon. This preliminary study presents descriptions of the occurrences and guides to exploration, in the hope that they will encourage exploration for similar deposits outside the park.

All talc used in British Columbia is imported. As much as 2.3 tonnes of talc per day are consumed by 25 pulp and paper mills for pitch control and as a filler for paper coating (MacLean, 1988). Most is imported from southwestern Montana, where it is mined from conformable, commonly chloritic replacement lenses in Precambrian dolomitic marble.

The talc at Talc Lake and Mount Whymper, like that of the Montana deposits, is massive and microcrystalline to cryptocrystalline (steatite grade), but strongly fractured. It is either white or, more commonly, a darker coloured "soft platy talc" variety with minor chlorite. This study indicates that the white talc replaced dolomite and approaches pure talc in composition (ideally $Mg_6[Si_8O_{20}(OH)_4]$), but contains minor pyrite. The black and grey chloritic talc replaced variably argillaceous, carbonaceous dolomite.

Numerous authors suggest talc formed by the replacement of dolomite, following Winkler's (1974) reaction:



This requires the addition of 32 volume per cent quartz to pure dolomite, which is rarely documented.

The Mount Whymper (NTS 82N/1E) and Talc Lake (NTS 82O/4W) talc occurrences are 20 kilometres apart and 35 and 25 kilometres west and southwest, respectively, of Banff, Alberta (Figures 3-1-1 and 3-1-2). They are 1 to 2.5 kilometres southwest of the border between British Columbia and Alberta, which follows the Continental Divide.

In the decade after the initial staking in 1915 to 1917, four adits were driven 10 to 15 metres into the talc bodies. In 1930, 150 metres of diamond drilling was done at Red Mountain, the main occurrence at Talc Lake. The last geologic report on the occurrences was based on a 1937 visit by Spence (1940; see also Wilson, 1926).

The locations of the talc occurrences at Stanley Creek and near Shadow Lake (Figure 3-1-2) are described in a letter

(Scruggs, 1970) to the Research Council of Alberta. Talc talus in Stanley Creek valley could not be located; the Shadow Lake occurrence was not examined.

The descriptions that follow are based on field mapping, examination of 18 thin sections, x-ray fluorescence (XRF), x-ray diffraction (XRD) and inductively coupled argon plasma (ICP) analyses of 12 rock samples collected during mapping. In addition, two silt and two soil samples were collected at Talc Lake and Mount Whymper, respectively.

GEOLOGIC SETTING

The talc occurrences are in the Foreland tectonostratigraphic belt of the southern Canadian Rocky Mountains, at and just east of the boundary between the eastern and western Main Ranges (Figure 3-1-1). All are along or near northwest-trending normal faults and major Cambro-Ordovician facies boundaries.

STRATIGRAPHY

The boundary between the eastern and western Main Ranges is marked by the abrupt, generally discordant facies change from the Middle and Upper Cambrian carbonate-

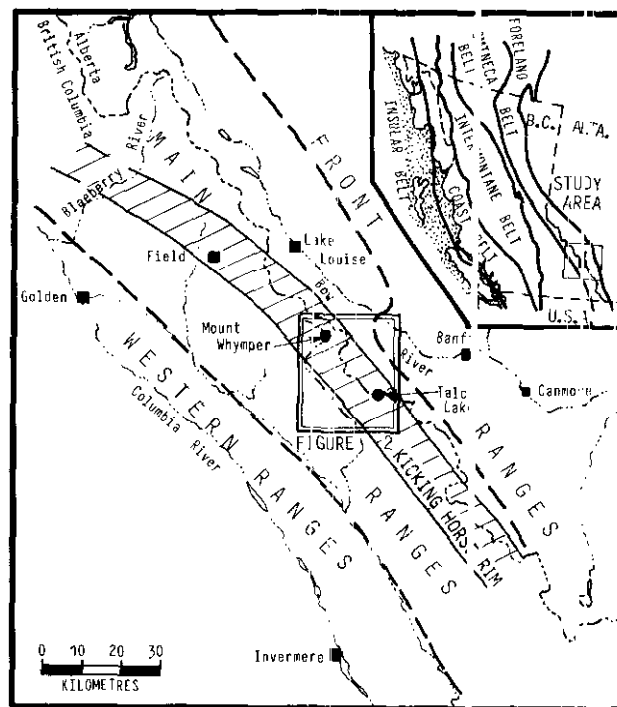


Figure 3-1-1. Location of the Talc Lake and Mount Whymper talc occurrences in the Southern Canadian Rocky Mountains on maps of the tectonostratigraphic belts of the Canadian Cordillera in British Columbia and of the Kicking Horse rim of the western Main Ranges (after Aitken, 1971).

dominated platformal margin sequence in nine formations to the east, to thicker, slope then predominantly basal shales of the Chancellor Formation to the west. Cambrian and Precambrian strata of the eastern Main Ranges form massifs with spectacular castellated peaks. The facies change occurs along the Kicking Horse rim, a northwest-trending, narrow (11 km) positive paleotopographic feature first active in Early Cambrian time (Figures 3-1-1 and 3-1-4). Lower Cambrian strata were bevelled by erosion and weathered along the crest of the rim. The rim may have continued to act as a hinge between more rapid subsidence on the west and less rapid on the east throughout the Middle and Late Cambrian and into the Ordovician (Aitken, 1971).

A regolith is formed at the top of the Lower Cambrian quartz arenites and interbedded varicoloured pelites of the Gog Group, with local significant relief. The Gog Group is overlain unconformably, locally with angularity, by Middle Cambrian strata (Aitken, 1971). It is unconformably underlain by Upper Proterozoic slates and pebble conglomerates of the Miette Group of the Windermere Supergroup.

At the crest of the rim, shales and interbedded limestones of the basal Middle Cambrian Mount Whyte Formation pinch out to the west (Figure 3-1-3). Farther to the west, coeval mudstones and shale with gravity-slump structures and a local basal limestone form the westward-thickening wedge of the Naiset Formation (Aitken, 1971, 1981; Stewart, 1989). At Mount Whympier, both formations appear to be absent. At Talc Lake, the black argillites sharply overlying the Gog Group could be the Naiset Formation (W.D. Stewart, personal communication, 1992).

In the Middle Cambrian, platformal growth of the Cathedral Formation of variably dolomitized peritidal carbonates

was initiated on the crest of the Kicking Horse rim and prograded basinward. The lower two-thirds (240 m) of the Cathedral Formation grades westward into the Takakkaw tongue of the lower Chancellor succession. It comprises sooty limestones with debris flows and slide surfaces – the deposits of a deep water ramp-like slope (Aitken, 1989). The upper third of the Cathedral Formation terminates westward (seaward) in the almost vertical Cathedral escarpment (Figure 3-1-3). Near Field, British Columbia, 33 kilometres north of Mount Whympier (Figure 3-1-1), the escarpment is the edge of a constructional organic reef up to 200 metres high that controlled the platform margin. The reef is altered to coarsely crystalline dolomite (Aitken and McIlreath, 1984). A pyritic halo up to 2 kilometres wide and 1.2 kilometres high surrounds the escarpment, but has not been mapped in detail (J.D. Aitken, personal communication, 1992).

Just west of Talc Lake, a cliff shows the escarpment was destructive in this area rather than constructive. Large-scale collapse of the outer platform during late Cathedral time created an embayment about 2.5 kilometres to the east (Figure 3-1-2). Dolomitized blocks up to 90 metres across fell from an escarpment 250 metres high and were deposited on the lower Cathedral carbonates then covered by strata of the upper Takakkaw tongue (Figure 3-1-5; Stewart, 1991).

STRUCTURE

The Cambro-Ordovician facies change and nearby tectonic occurrences are entirely within the gently west-dipping Simpson Pass thrust sheet of the mid-Jurassic to Eocene Cordilleran orogeny (Figures 3-1-2 and 3-1-4). The compo-

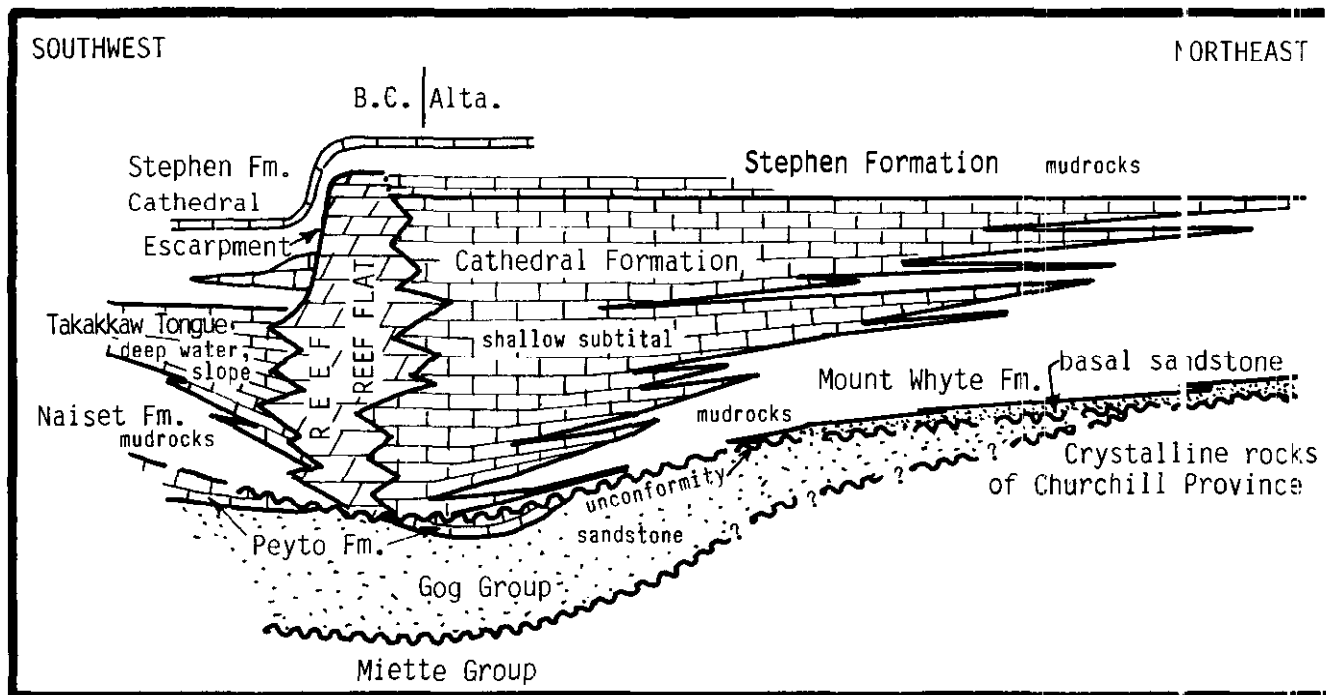


Figure 3-1-3. Schematic stratigraphic cross-section of the facies change at the Cathedral escarpment between the platformal Middle Cambrian Cathedral and Mount Whyte formations to the basal Takakkaw tongue (slope facies of the Cathedral Formation) and Naiset Formation to the west (after Figure 4a of Aitken, 1989). Horizontal length of section is about 475 kilometres.

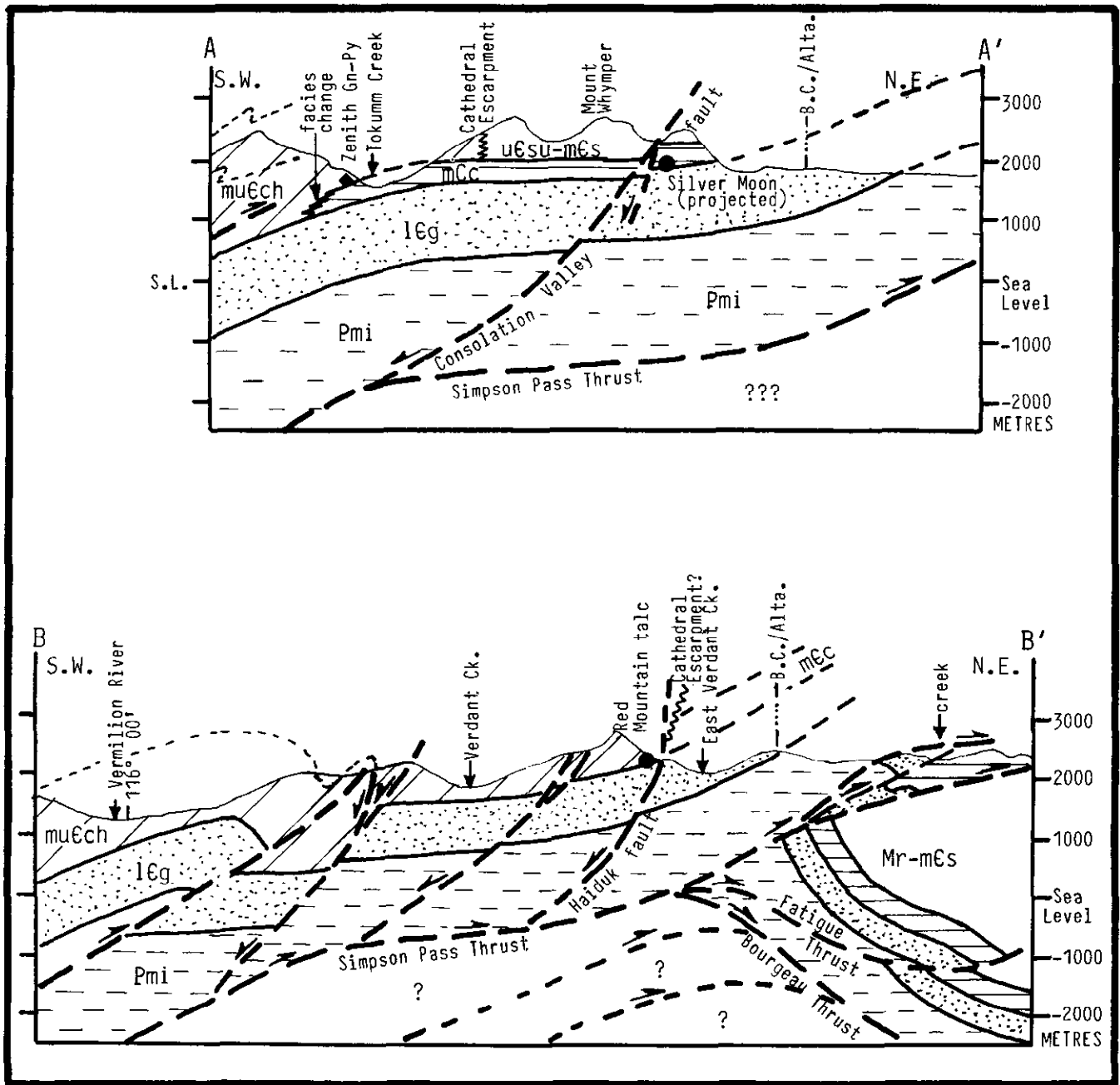


Figure 3-1-4. Geologic cross-sections through the area of the Silver Moon and Red Mountain talc occurrences (after Price and Mountjoy, 1972; Price *et al.*, 1978). See Figure 3-1-2 for location of the section lines.

tent sequence east of the facies boundary is broadly and concentrically folded and cut by normal faults.

The normal faults trend northwest to north, obliquely across the more west-northwest regional structural grain (Figure 3-1-2). They form a system of subparallel, branching and en echelon faults. Their map pattern suggests they formed in a regime of transtension, with components of northeast extension and northwest right-lateral strike-slip displacement. The normal offset was followed by minor subhorizontal displacement. The faults truncate and offset secondary thrusts, but apparently not the basal Simpson

Pass thrust (Cook, 1975). Concordant wedges of dolomitization locally extend away from the normal faults into adjoining carbonates (Westervelt, 1979).

ECONOMIC GEOLOGY

The Cathedral escarpment played an important role in localizing lead-zinc-silver mineralization at the Monarch and Kicking Horse mines and magnesite at the Mount Brussilof mine. The mines are 33 kilometres north and 37 kilometres south of the talc occurrences, respectively. Mineralization replaced and filled dolomitized and brecci-

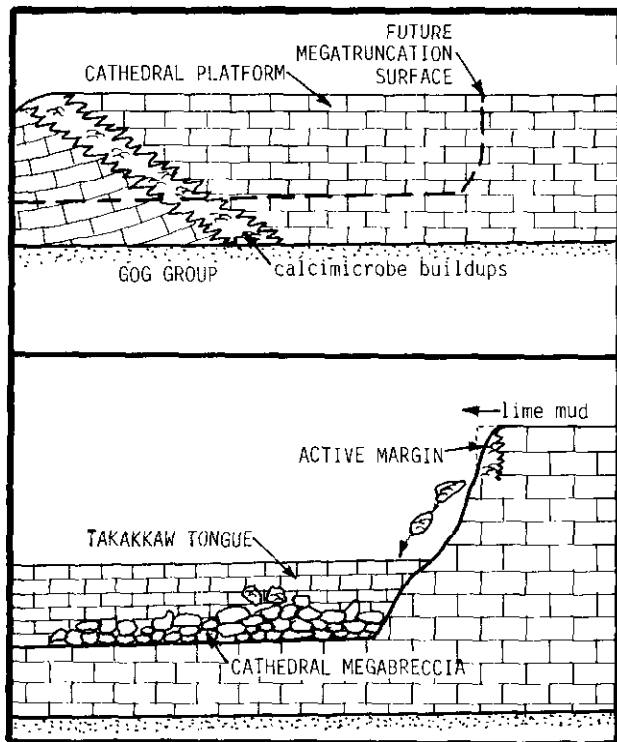


Figure 3-1-5. Model for the development of the Cathedral escarpment at Talc Lake (from Stewart, 1991, Figure 54: a, c).

ated Cathedral carbonates adjacent to the escarpment and near normal faults. The geologic setting of these deposits is analogous to that of the talc occurrences.

GEOLOGY OF THE TALC LAKE OCCURRENCES

A series of talc bodies is exposed at elevations of 2315 to 2375 metres on three spurs 1 kilometre to the southeast and northwest of Talc Lake (Figure 3-1-6). They may represent erosional remnants of once more continuous and extensive zones. The bodies are in the hangingwall, and 20 to 325 metres southwest of the northwest-trending informally named Haiduk normal fault. The fault cuts through saddles along the spurs, two of which mark the contact between the Gog Group and Takakkaw tongue. The talc bodies are also just southeast and north of the northeast corner of an embayment in the Cathedral escarpment (Figure 3-1-2). The Red Mountain and Gold Dollar occurrences are at the base of the Takakkaw tongue (or Naiset Formation), whereas the saddle occurrences are at the base of the Cathedral Formation.

RED MOUNTAIN OCCURRENCE

LOCATION AND GEOLOGIC SETTING

The Red Mountain talc occurrence is on the north side of an easterly spur of Red Mountain and 250 to 300 metres south of Talc Lake (Figures 3-1-2, 3-1-4 and 3-1-6). The talc is exposed along steep, mostly inaccessible bluffs above

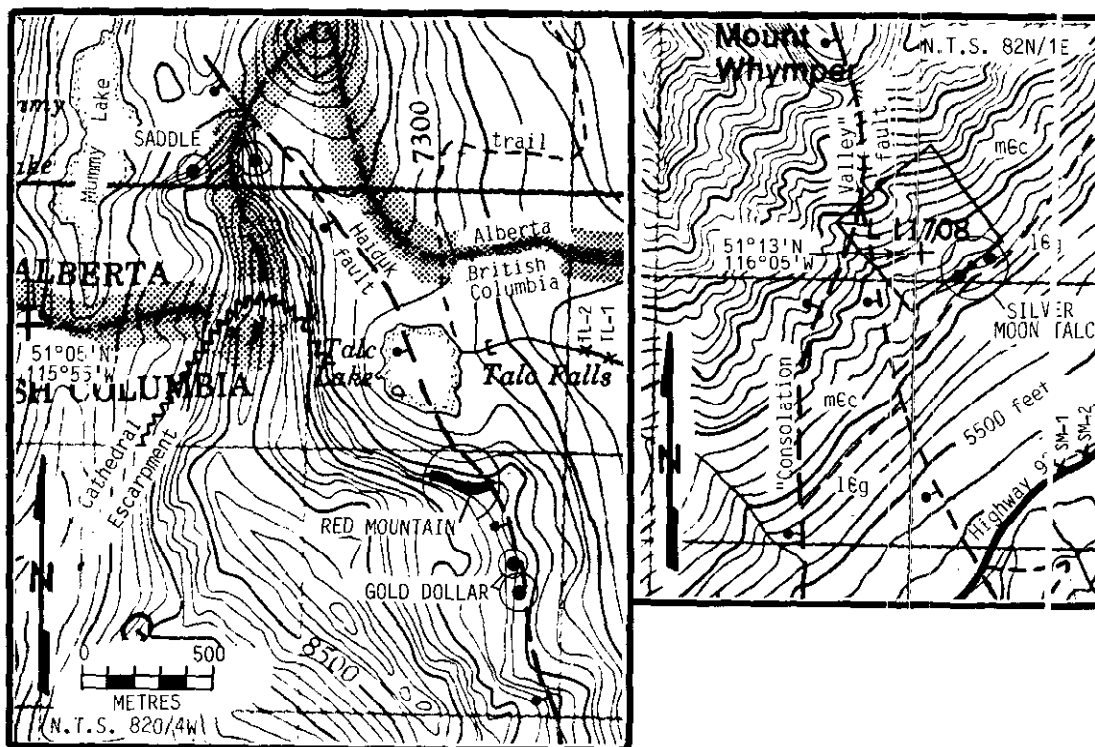


Figure 3-1-6. Locations of the Talc Lake (left) and Mount Whymper (right) talc occurrences on enlargements of 1:50 000 topographic maps with contour intervals of 100 feet (~30 m).

an extensive talus slope and below a cliff of the Takakkaw tongue and younger rocks (Figure 3-1-7). The cliff exposing the Cathedral escarpment is 550 metres to the north.

In 1927, ten years after the occurrence was first staked, two short (10 and 15 m) adits, 50 metres apart, were driven southerly into it by the National Talc Company (Figure 3-1-7). In 1930, Western Talc Holdings drilled five holes totalling 152 metres into the talc (Spence, 1940). The location of the core is unknown. In 1944, Wartime Metals Corporation developed a stope and raise at the end of the western adit.

The Red Mountain occurrence is the most extensive of those examined, with a length of 260 metres and height of up to 30 metres. The gently southwest-dipping body appears stratabound and formed as replacement of dolomite in interbedded and intergradational thin-bedded dolomite, argillaceous dolomite and dolomitic carbonaceous argillites. In general, it is just above the lowermost occurrence of dolomite and 0 to 20 metres above the unconformity at the top of the Gog Group quartz arenites. However, scattered exposures of the footwall beds suggest the lower contact of the talc is complex in detail. This may in part result from rapid vertical and horizontal facies changes in the footwall.

The extreme eastern end of the talc body appears to be offset with a minimum dip-slip displacement of 10 metres

along the Haiduk fault. The talc is also strongly deformed by steep to gently dipping shears and intersecting sets of fracture cleavage. The term "fracture cleavage" is used here to describe a series of non-pervasive subparallel fractures commonly spaced 0.5 to 15 centimetres apart.

TALC GEOLOGY

The talc body weathers a dark rusty brownish orange resulting from oxidized pyritic shears and fractures. Weathered rocks in the immediate footwall are surprisingly difficult to distinguish from talc. The talc, however, tends to form more rounded, hummocky but very rough weathered surfaces because of the well-developed fracture cleavages and shears.

Most of the talc is dark grey to near-black on fresh surfaces, with 2 to 10 per cent dirty white and up to 50 per cent very light grey patches, lenses, spots and specks (Plate 3-1-1). Thin sections and x-ray diffraction analyses indicate the near-black colour results from a carbon compound and a few per cent chlorite (Table 3-1-1). A distinct 18-metre interval of light grey talc with dirty white patches and lenses forms the hangingwall of the Haiduk fault. Locally the talc comprises a striking breccia with black angular fragments up to 10 centimetres in diameter floating in an off-white talc matrix. Thin sections indicate that spotted talc results from

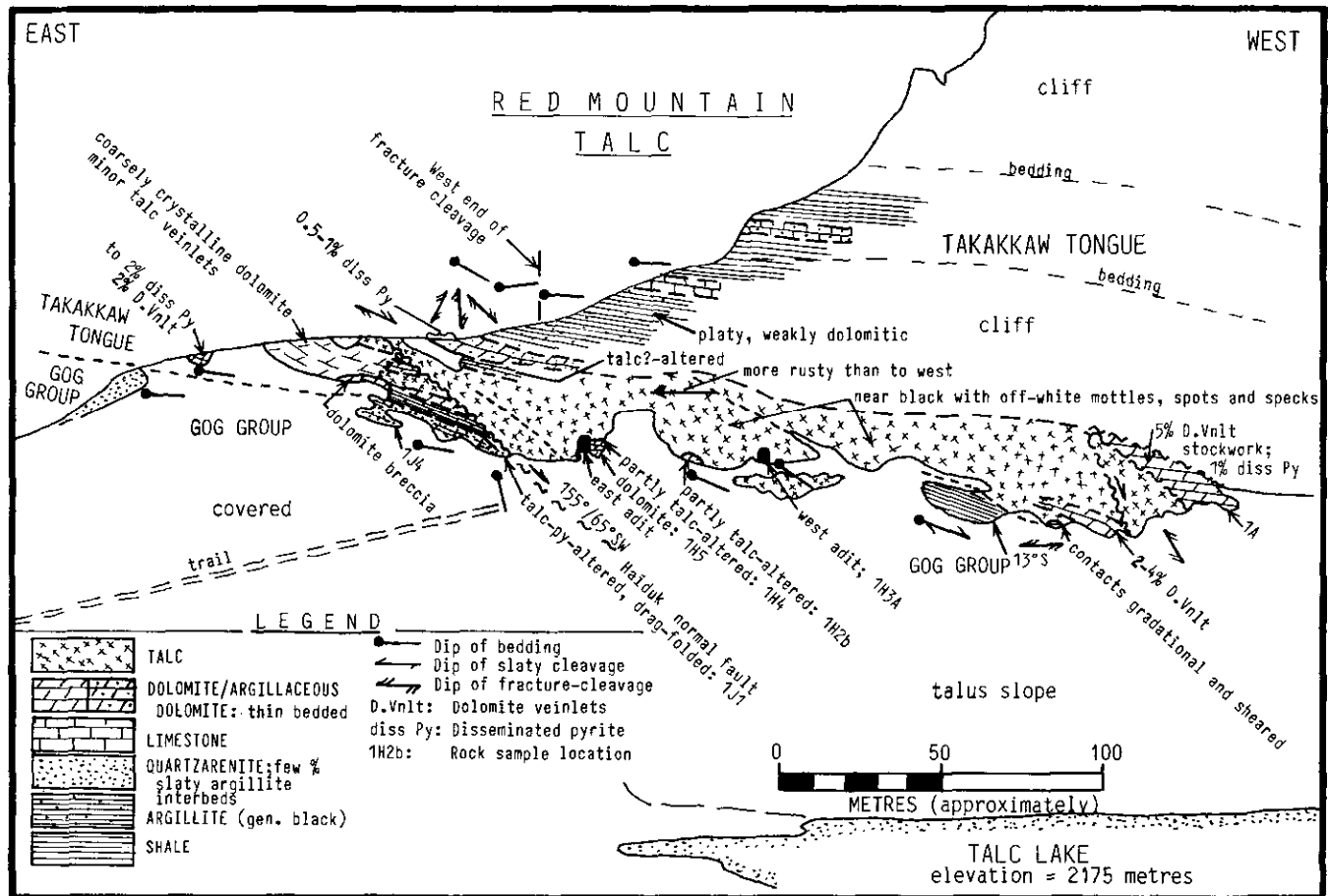


Figure 3-1-7. Geology of the Red Mountain talc occurrence at Talc Lake. The pseudosection is traced from a photograph looking south. The legend also applies to Figures 3-1-8 through 3-1-11 and 3-1-14.



Plate 3-1-1. Photomicrograph (crossed nichols) of pyritic white and light grey talc from east end of the Red Mountain talc body (sample 112). Coarser grained partial sprays of white talc are surrounded by a very fine grained mass of randomly oriented plates and fibres of talc.

alteration of a brecciated, variably carbonaceous argillaceous dolomite, and later shearing. However, unbrecciated talc with very delicate graded laminations resembling bedding is conspicuous on one polished shear surface.

Pyrite is very irregularly disseminated in the lighter coloured talc, commonly forming 0.5 to 1 per cent, to locally 3 per cent, fine to medium-grained disseminations. Very locally, sheared pyrite grains form up to 60 per cent of irregular zones of "rotten" talc to 5 centimetres or more thick. Thin sections indicate that the black talc does not contain pyrite.

An irregular, criss-crossing network of white talc veinlets, commonly 1 millimetre thick but locally to 1 to 2 centimetres, forms up to 4 per cent of the talc in several intervals. Rare(?) veins contain coarsely crystalline (to 3 by 10 cm) dolomite cut by minor veinlets of clear quartz, 1 millimetre thick. Vugs up to 3 by 12 centimetres occur very locally in the talc. They are lined with drusy to botryoidal dolomite(?) crystals and pyrite grains. The talc also contains a few sheared lenses of bedded dolomite to 20 by 50 centimetres, cut by dolomite veinlets.

The talc is generally moderately to strongly fractured and sheared. Intersecting fractures and fracture cleavages commonly result in a brecciated texture. An anastomotic

sheared fracture cleavage with a spacing of 3 to 15 millimetres, is developed near and subparallel to moderately southwest-dipping normal faults. It intersects a shallow-dipping slaty cleavage subparallel to bedding in nearby beds, to yield an irregular pencil cleavage.

FOOTWALL ROCKS

The lithology of the rocks in the footwall of the talc varies along the spur from east to west, as follows.

EAST OF THE HAIDUK FAULT

Coarsely crystalline dolomite: In the footwall of the Haiduk fault, talc overlies a very distinct coarsely crystalline, weakly pyritic dolomite unit about 8 metres thick. Similar dolomite forms large (0.4 m diameter to 2 by 5 m) inclusions in the talc overlying and west of the main unit. The dolomite is described in detail because it may be related to talc alteration, although it is not exposed at the other Talc Lake occurrences. However, similar dolomite forms a 90 by 250 metre outcrop between the Red Mountain and saddle occurrences, about 380 metres northwest of Talc Lake. It contains rare talc veinlets to 2 millimetres thick, and a few per cent iron oxide nodules to 10 by 30 centimetres. The dolomite adjoins Cathedral dolomite and does not appear to have a simple relationship to the Cathedral escarpment. However, it is in the hangingwall (southwest) of the Haiduk fault, suggesting it may be related to the fault and the talc alteration event.

The recrystallized dolomite is opaque white to medium rusty orange on fresh surfaces. It contains 5 per cent or less, very irregular patches with 5 per cent fine grained(?) grains surrounded by light grey to dirty white fine-grained (primary?) dolomite. Pyrite forms about 0.5 to 2 per cent, very fine to fine to locally medium-grained, irregularly distributed disseminations. The dolomite is strongly brecciated. It contains minor talc veinlets that are bright rusty orange, irregular, discontinuous and commonly up to 1 millimetre thick. Their origin and relationship to the overlying talc body are uncertain.

An east-dipping covered fault(?) separates the coarse dolomite from a succession to the west that is the most complete, although poorly accessible exposure of the footwall rocks. It is also in the immediate footwall of the Haiduk fault. The succession comprises, from the base of exposure: quartz arenite (10 m) of the Gog Group in beds 2 to 20 centimetres thick with 4 per cent partings and interbeds of argillite; black meta-argillite (8 m); thin-bedded dolomite (several metres); and grey talc. The quartz arenites in the 5 metres below the Haiduk fault appear partly talc-pyrite altered. Irregular polygonal outlines of replaced grains in a thin section of talc suggest a dolomite protolith. However, the talc (sample 111) contains 0.1 per cent sphene, minor zircon and perhaps fluorapatite (Table 3-1-1), suggesting a protolith of dolomitic(?) quartz sandstone.

Gog Group: The rocks of the uppermost 50 metres of the Gog section are quartz arenite with interbedded, somewhat slaty argillite and locally dolomitic quartz sandstone. The quartz arenite is generally a dirty white to less commonly subtranslucent light to medium grey on fresh surfaces. It

TABLE 3-1-1
RESULTS OF X-RAY FLUORESCENCE AND X-RAY DIFFRACTION ANALYSES OF TALC AND DOLOMITE HOSTROCKS
AT TALC LAKE AND MOUNT WHYMPER

X-RAY FLUORESCENCE ANALYSES											X-RAY DIFFRACTION MINERALS			
LITHOLOGY	Sample	SiO ₂	Al ₂ O ₃	MgO	CaO	Fe ₂ O ₃	TiO ₂	MnO	P ₂ O ₅	L.O.I.	Total	Major	Minor	Trace
Deposit	Number													
TALC														
Red Mountain	1H3A	58.22	2.52	31.87	0.32	0.25	0.09	0.01	0.14	6.52	100.01	tc	chl	f-ap
	1J1	56.35	2.42	30.81	0.52	2.01	0.56	0.01	0.35	6.91	100.00	tc	chl,py,sid	zr,spn?,f-ap?
Gold Dollar	3A	50.99	7.26	32.25	0.16	0.97	0.32	0.01	0.03	8.12	100.16	chl-tc		spn
	3B	60.74	1.03	31.66	0.37	0.23	0.02	0.01	0.31	5.47	99.92	tc	chl	f-ap
	4-45	61.50	0.08	30.84	0.06	1.32	0.01	0.01	0.01	5.95	99.87	tc		py
Saddle	5C	62.25	0.18	31.74	0.11	0.24	0.01	0.01	0.01	5.25	99.87	tc,qtz	chl,py	
Silver Moon	10A	62.58	0.01	31.38	0.09	0.66	0.01	0.01	0.01	5.16	100.00	tc		
Theoretical		63.36		31.89						4.75 ²				
DOLOMITE														
Red Mountain	1A	0.21	0.02	21.19	30.14	0.63	0.03	0.07	0.04	47.25	99.65	dol	chl, py	
	1H2B	32.55	1.81	28.17	12.27	0.39	0.07	0.01	0.04	24.25	99.68	tc,dol	chl,qtz	cal
	1H4	2.80	1.11	21.79	28.36	0.55	0.03	0.07	0.03	44.70	99.52	dol	tc,chl	qtz,cal
Silver Moon	10B	0.11	0.01	20.01	30.12	2.24	0.02	0.30	0.02	46.59	99.48	dol	chl,tc	cal, py,qtz ³
	12A	3.02	0.05	21.22	28.95	1.29	0.02	0.07	0.03	44.99	99.75	dol	tc,qtz	py,chl
(Haley, Ont.)				21.1	31.3					47.20				
CLINOCHLORE ¹		18.2	18.2	31.1		6.8				12.7 ²				

NOTES:

1. From Willow Creek talc mine in southwestern Montana (Berg, 1979).

2. % H₂O.

3. Also minor goethite and lepidocrocite identified.

All percentages are wet weight.

Na₂O analyses are all 0.01 or 0.02%.

K₂O are from 0.01 to 0.06%.

XRF analyses by Cominco Ltd. Exploration Research Laboratories in Vancouver, B.C., September, 1992.

XRD analyses by B.C. Ministry of Energy, Mines and Petroleum Resources laboratory, October, 1992.

ABBREVIATIONS OF MINERALS:

cal: calcite

f-ap: fluorapatite

sid: siderite

zr: zircon

chl: chlorite

py: pyrite

spn: sphene

dol: dolomite

qtz: quartz

tc: talc

ROCK SAMPLE NOTES

1H3A: near black; mottled, spotted with dirty white talc.

1J1: light grey; 1 to 2% pyrite; occurs in Gog Group, just east of Haiduk fault; 0.1% zircon, locally zoned.

3A: north occurrence; resembles partly talc-altered black argillite; 2% sphene(?).

3B: north occurrence; black, light grey and white spotted; relic dolomite(?) grain outlines.

4-45: south occurrence; 2% pyrite; medium grey with white spots. Talc coarser grained; relic dolomite(?) outlines.

5C: east occurrence; sub-opaque, pale orangish white; 2%, oxidized pyrite.

10A: southwest adit; frosty white with pale greenish grey tinge.

1A: hanging wall of talc, west end; 5% dolomite veinlets; 0.25% pyrite.

1H2B: footwall; partly talc altered, laminated, intergraded dolomite, argillaceous dolomite and carbonaceous argillite.

1H4: footwall, at east adit; weakly talc-altered, laminated dark grey dolomite; penninite(?) in dolomite veinlet.

10B: footwall, 3.5 m below talc at southwest adit; fenestral dolomite; 0.25%, oxidized pyrite; 2% dolomite veinlets.

12A: northeast occurrence, dolomite inclusion in quartz; subtranslucent medium grey; 0.25% pyrite; quartz-dolomite-replaced, prismatic mineral; trace interstitial quartz.

NOTE:

The theoretical composition of pure talc is included for comparison. That of the high magnesium end-member of the chlorite group, clinocllore, is also included because it may contain most of the aluminum in the first three samples of talc.

weathers dirty white to medium grey. The uppermost 10 metres show a conspicuous increase (to 90%) of rusty orange limonitic patches on shears and fractures. This characterizes the regolith at the top of the Gog Group (J.D. Aitken, personal communication, 1992).

The quartz arenite is very thin through medium bedded (1 to 50 cm). It is weakly laminated and banded with light grey, and generally very fine to fine grained. It commonly contains minor to 0.25 to locally 2 per cent, very fine to fine, disseminated, iron oxide coated pyrite or iron oxide specks with limonitic halos. Dolomite locally forms the matrix of the arenite and is dark buff on fresh surfaces.

Slaty argillite forms 1 to 5-millimetre partings and interbeds to 35 centimetres thick. They comprise about 2 to 4 per cent of the uppermost 20 metres of the Gog Group. In intervals below that they form 5 to 30 to locally 85 per cent of the succession. The argillite is light greenish grey to medium brownish grey (with black laminations) on fresh surfaces. The slaty cleavage is parallel or slightly oblique to bedding which dips gently (5°) to the west.

Quartz veinlets in Gog Group: Quartz veinlets are common in the quartz arenites of the Talc Lake area. It is unclear whether they represent channels for the introduction of silica to the dolomite during talc alteration. Locally, at least, they appear related to shearing. However, more study is required to establish their age and significance.

Intervals of the quartz arenite commonly contain 1 to 5 per cent veinlets, even 200 metres or more below the talc. The milky white veinlets are commonly 1 to 10 millimetres wide, but locally 3 to 15 centimetres thick. Although quartz veinlets are common regionally in the Gog Group, they are usually only 1 to 2 millimetres thick (J.D. Aitken, personal communication, 1992). The veinlets are irregular, discontinuous and commonly sheared and fractured. Locally, they resemble shear and tension gash veins related to simple shear couples. Near the talc, the veinlets commonly strike 155° , 070° and 035° (with decreasing frequency) and dip vertically.

The veinlets must be Middle Cambrian or younger. They cut the lowest part of a 3-metre interval of black platy argillite of the Naiset(?) Formation immediately overlying the Gog Group on the spur 850 metres southeast of the Red Mountain deposit.

WEST OF THE HAIDUK FAULT

Sheared footwall rocks are exposed in four main areas along 210 metres of the ridge spur. Just west of the eastern adit, black talc is underlain by about 2 metres of laminated to very thin bedded, graded carbonaceous dolomite and dolomite that are partly altered to talc. X-ray diffraction analysis (sample 1H2B) indicates that the black laminations contain talc and minor chlorite. The carbonaceous mineral was not identified as graphite. The talc-altered dolomite is underlain by several metres of thin and very thin-bedded dolomite.

West of the eastern adit 105 to 160 metres, the footwall rocks resemble those east of the Haiduk fault except for the very top of the Gog Group. Here, it comprises medium grey,

somewhat slaty, thin bedded argillite. It contains two intervals with three to five interbeds of quartz arenite with 0.5 per cent disseminated pyrite. The interbeds are 3 to 50 centimetres thick. Ten metres to the east, a lens of dark grey argillite 1 metre thick appears to grade upwards and laterally into talc, however, shearing along fracture cleavage disrupts its contacts.

HANGINGWALL ROCKS

Accessible exposure just below the crest of the spur indicates black talc is overlain by gently (25° to 30°) southwest-dipping, platy, black meta-argillite (3 m thick) and very thin bedded (0.5 to 5 cm) dolomite (7 m thick). The basal 4 metres of the dolomite unit is distinctly pyritic: 3 per cent very fine to coarse-grained (to 7 mm) disseminations of subhedral crystals are commonly coated with iron oxide.

Fracture cleavages are locally well developed at a high angle to bedding up to 33 metres west of the talc body and 40 metres west of the possibly related Haiduk fault (Figure 3-1-7). They dip northeast to southwest and are locally filled with dolomite or slickensided graphite(?), and spaced 2 to 15 millimetres apart.

At its western end, the talc body is structurally overlain by rusty orange weathering, thin-bedded, flat-lying dolomite 15 metres wide. The dolomite contains 5 per cent, white dolomite veinlets forming a stockwork. The veinlets are paper thin to 1 centimetre thick. Dolomite grains in several veinlets are elongated perpendicular to the walls. The dolomite also contains 0.25 per cent pyrite disseminated along stringer-like fractures. The pyrite is subhedral and up to 4 millimetres in diameter. The faulted contact between the dolomite and talc is irregular, stepped but sheared and truncates bedding in the dolomite.

GOLD DOLLAR – NORTH OCCURRENCE

Black talc is poorly exposed in several sloughed hand-cuts on the north side of the (next) spur 300 metres southeast of the Red Mountain occurrence (Figure 3-1-6). The showings are at the top of an extensive talus apron below a cliff (Figure 3-1-8).

Fifty metres east of the talc, the Haiduk fault is inferred to cut through the broad saddle between quartz arenites of the Gog Group to the east, and cliff-forming dolomites of the Takakkaw tongue to the west (Stewart, 1991, Section DS-23).

TALC GEOLOGY

This near-black, very rubbly weathering talc is at least 3 metres thick. The talc is weakly to strongly sheared and cut by a well-developed slaty cleavage. It is very fine grained and moderately to very soft.

A breccia of black talc fragments in 15 to 40 per cent matrix of white talc occurs in float. There are also pieces of light grey talc with 10 per cent black and 3 per cent white spots. A thin section (sample 3B) reveals relic polygonal grains outlined by carbonaceous material, suggesting a protolith of brecciated carbonaceous dolomite. The XRF analysis indicates that the black colour probably results from

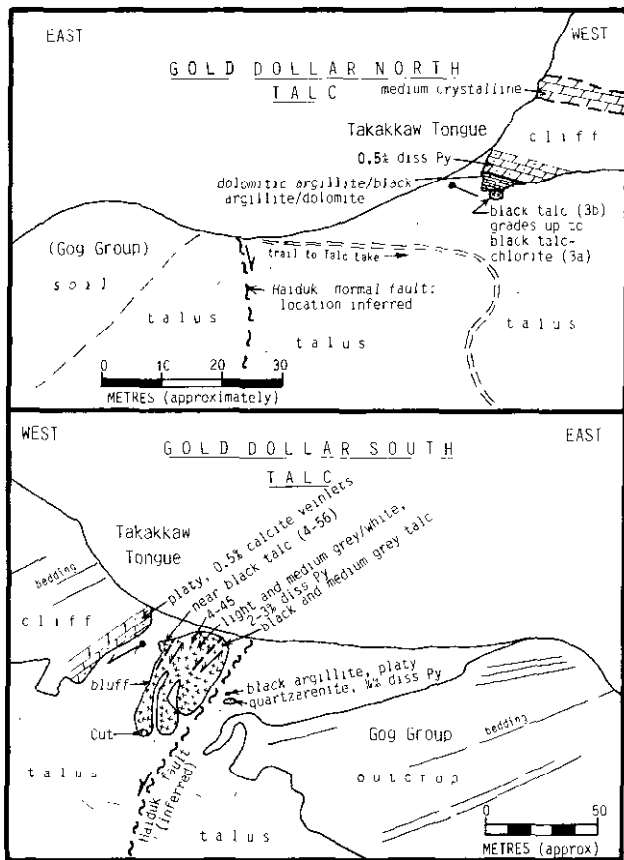


Figure 3-1-8. Geology of the Gold Dollar north (upper frame) and Gold Dollar south talc occurrences on opposite sides of a spur southeast of Talc Lake. The pseudosections are traced from photographs.

extremely fine grained chlorite as well as the carbonaceous mineral (Table 3-1-1). The white spots are coarser grained, partially formed sprays of talc.

Another sample (3A) from the same interval resembles weakly talc-altered black argillite in hand sample. Thin section and XRF analyses indicate it consists of very finely intergrown chlorite and talc. A carbon compound forms 0.5 per cent irregular coplanar wisps to 0.5 millimetre long. Sphene forms 2 per cent, extremely fine, uniformly disseminated, locally clustered grains. The relatively high alumina content (7.3%) may result in part from the large proportion of chlorite.

The slaty cleavage comprises irregular discontinuous hairline fractures that follow relic carbonate grain boundaries. The white-appearing fractures are 2 to 4 millimetres apart and filled with an opaque mineral and talc-altered grain fragments.

HANGINGWALL GEOLOGY

The talc grades upward into several metres of black argillite cut by a few per cent white talc veinlets. The argillite grades upward to a few metres of dolomitic argillite with intervals of black argillite and dolomite, into slaty argillaceous dolomite with 0.5 per cent, fine to medium-grained disseminated pyrite. All are thin to very thin bedded and laminated.

GOLD DOLLAR - SOUTH OCCURRENCE

The second largest body of talc in the Talc Lake area is exposed in a bluff that is 30 metres wide and 100 metres south and on the opposite side of the spur from the Gold Dollar - North occurrence (Figures 3-1-6 and 3-1-8). A cut was made several metres into the talc at the base of the bluff.

The contacts of the talc body are covered. The sheared body appears to occupy the hangingwall of the Haiduk fault and occurs between the top of the Gog Group to the east, and the Takakkaw tongue to the west.

TALC GEOLOGY

The talc weathers dark rusty orangish brown and has a very irregular, rough weathered surface. The eastern 7 metres of the talc body is medium to light grey with streaks and lenses of black on fresh surfaces. Partly talc-altered, very thin bedded and laminated dolomite interbedded with carbonaceous(?) argillaceous dolomite is locally apparent.

The central 19 metres of talc is light grey and white with variable proportions of medium to dark grey and a few per cent near-black carbonaceous lenses and patches. The interval is variably pyritic, 0.5 to 4 per cent, to very locally 10 per cent, but averaging 2 to 3 per cent. The pyrite is very fine to medium grained (dust size to 6 mm) and tends to cluster in irregular patches. The talc is harder than normal. However, in thin section (sample 4-45) there is only a minor dusting of impurities. Distinct outlines of relic anhedral carbonate grains indicate they are replaced by randomly oriented single grains of talc 0.1 to 0.5 millimetre in diameter.

The western 5 metres of talc is carbonaceous and near black with a few per cent white spots and a few, thin (to 3 mm), sheared lenses of white talc. In thin section, relic dolomite(?) grains are outlined by a carbon compound forming 5 per cent angular patches (Plate 3-1-2). They suggest the dolomite protolith had a high porosity prior to talc alteration and filling of interstices by the carbon compound. Original polysynthetic twins in the grains are replaced by single, slightly bent talc grains. The remainder is replaced by extremely fine, randomly oriented talc. A white veinlet of extremely fine talc has diffuse boundaries suggesting talc replaced a dolomite veinlet with no impurities to show grain boundaries.

The talc body is strongly sheared along a well-developed, moderately west-dipping (45° to 60°) fracture cleavage. Locally, stepped slickensides on cleavage surfaces indicate dip-slip displacement with the west side down. This may be subparallel to displacement on the Haiduk normal fault.

FOOTWALL GEOLOGY

Ten metres east of the talc bluffs, and presumably in the immediate footwall of the Haiduk fault, 3 metres or more of black argillite overlie gently west-dipping (10° to 20°), somewhat rusty weathering quartz arenite and argillite of the Gog Group. The black argillite is platy (1 to 3 mm) and cut, together with the quartz arenite, by abundant limonitic



Plate 3-1-2. Photomicrograph (crossed nichols) of near-black talc from west end of the southern Gold Dollar talc body (sample 4-56). The boundaries of the protolith dolomite(?) grains are preserved after alteration to very fine grained talc and chlorite(?). The original polysynthetic twins (light bands) are replaced by single grains of talc. A black carbonaceous material fills the angular protolith grain interstices. Very fine grained talc replaces(?) a dolomite veinlet on right side of photograph.

shears and fractures. The quartz arenite is weakly translucent white. It contains 0.25 per cent disseminated pyrite and a few per cent irregular veinlets of white quartz.

HANGINGWALL GEOLOGY

A covered interval 14 metres wide separates the talc bluffs from a cliff of argillaceous dolomite of the Takakkaw tongue to the west. The dolomite locally grades into weakly dolomitic black argillite. The beds in the basal 10 metres are gently west-dipping (30°), very thin (1 to 4 cm) and laminated and platy weathering. They are cut by thin (15 to 40 cm) intervals of slaty cleavage parallel to bedding, and 0.5 per cent white calcite veinlets (to 6 mm thick). Rare veinlets of dolomite, with or without quartz, step across and follow bedding.

SADDLE OCCURRENCES

Two small exposures of white talc are located 1.4 kilometres northwest of the Red Mountain occurrence (Figure 3-1-6). They are 230 metres apart and on the east and west

sides of a steep ridge. The exposures are just above talus aprons, at a narrow break in slope between a lower cliff of rusty weathering quartz arenites of the Gog Group to the north and a cliff of bedded dolomites of the Cathedral Formation to the south (Figures 3-1-9 and 3-1-10). They are 750 metres north of the Cathedral escarpment and 130 and 300 metres southwest, respectively, of the Ha duk fault that cuts through the prominent saddle between the Talc Lake and Mummy Lake basins.

There is a prominent angular discordance between the subhorizontal Gog Group bedding and the overlying gently southwest-dipping (15°) Cathedral dolomite (Figures 3-1-9 and 3-1-10). This may reflect an angular unconformity between the two units. There is shearing at the top of the talc that locally truncates bedding in the overlying dolomite at low angles. However, the substantial offset that would be required on a low-angle fault to account for the discordance between units is not evident.

The talc differs markedly from that at the Red Mountain and Gold Dollar occurrences. It is a much more uniform near-white and strongly resembles the Silver Moon talc 19 kilometres to the northwest.

EAST OCCURRENCE

An interval of white talc 2.5 metres thick, is stratobound in thin-bedded dolomite of the basal Cathedral Formation 2.5 metres above pyritic, possibly weakly talc-altered quartz arenite. These relationships are poorly exposed along 15 metres and disrupted by offsets of up to 2.5 metres of dip slip on steeply dipping, northwest-trending (345°) faults.

TALC GEOLOGY

The talc is subopaque, pale orangish white to limonitic and rusty orange on fresh surfaces. Shear and fracture surfaces cutting the talc weather medium to dark, rusty orange-brown. Very strong fracturing yields a rough and rubbly weathering surface.

A thin section of the talc (sample 5C) indicates it comprises very fine plates and fibres. The quartz identified by XRD analysis probably causes the somewhat increased hardness of this talc. It appears to form a very small fraction because the XRF analysis resembles that of nearly pure talc. The section contains 2 per cent, commonly completely oxidized pyrite as generally uniformly disseminated, but locally clustered, subhedral grains to 0.15 millimetre in diameter. The grains have halos of limonitic stain 0.05 millimetre wide.

The talc is weakly sheared. Strongly developed fracture cleavages cut the talc into fragments 0.5 to 3 centimetres in diameter. The most prominent and regular fracture cleavage is spaced 1 to 2 centimetres apart and dips gently southwest (15°), parallel to the upper contact of the talc. The other prominent cleavage is anastomotic and dips steeply southwest.

FOOTWALL GEOLOGY

The talc is underlain by 2.6 metres of dolomite resting on quartz arenites of the Gog Group (Figure 3-1-9). In one exposure the footwall contact is sharp and appears to follow

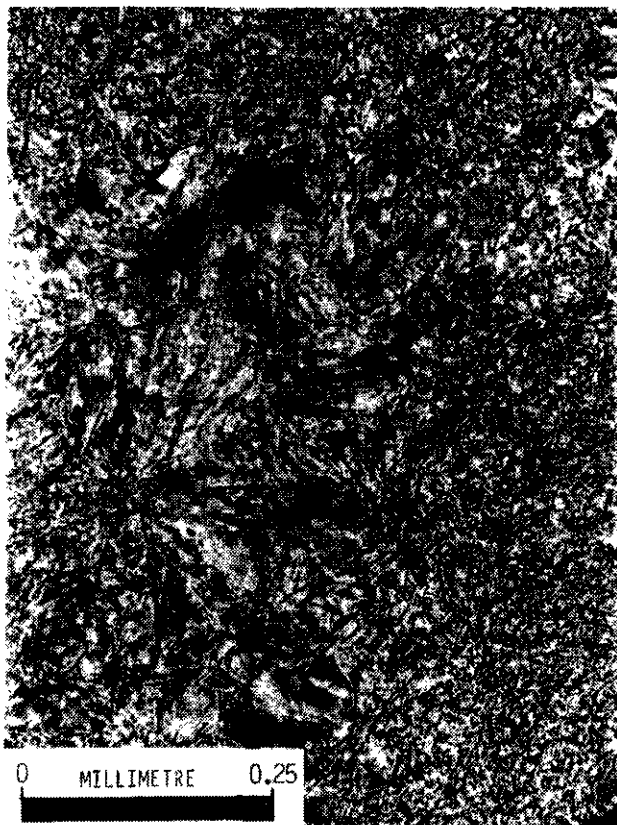


Plate 3-1-3. Photomicrograph (crossed nichols) of partly talc-altered pyritic quartz arenite of the Gog Group from just below the easterly saddle talc occurrence (sample 5A). Very fine grained talc appears to replace the rims of quartz grains with various deformation features. Pyrite (black) overgrows quartz and talc.

is very fine grained and disseminated irregularly in the talc. Pyrite is concentrated to 25 to 40 per cent in patches 0.5 to 4 millimetres in diameter. It has irregular subangular to subrounded outlines and appears to have overgrown and replaced quartz grains.

HANGINGWALL GEOLOGY

The upper contact of the talc is parallel overall to the gently southwest-dipping (15°) bedding in the overlying dolomite and to the fracture cleavage in the talc. Locally it is irregular and crosscuts bedding in the dolomite or is offset by steep-dipping faults. The contact is marked by a zone, of sheared talc 1 to 2 centimetres wide, or locally, an unsheared argillaceous rock.

The dolomite beds are 1 to 13 centimetres thick and have irregular surfaces. The dolomite is light orangish buff on fresh surfaces, very fine grained and contains 2 per cent rounded, clear, grey, fine quartz grains.

WEST OCCURRENCE

The poorly accessible west occurrence of white talc appears stratabound in a faulted interval, 7 metres wide and more than 20 metres long, between dolomite and argillite at the base of the Cathedral Formation (Figure 3-1-10). The talc resembles that of the eastern occurrence.

A dolomite unit, 0.75 metre thick, is exposed near the base of the talc interval. However, 2 metres away the dolomite is absent and the talc is underlain by 3 metres of medium greenish grey, platy argillite that weathers similar to the talc. The argillite is underlain by 0.3 metre of white talc and, in turn, an exposure of pyritic quartz arenite 0.5 metre high.

The lower contact of the talc interval appears to parallel the underlying, very gently west-dipping beds of quartz arenite. The upper contact of the talc is inferred to be a fault that truncates the overlying dolomite beds at 0° .

GEOLOGY OF THE SILVER MOON OCCURRENCE, MOUNT WHYMPER

LOCATION AND GEOLOGIC SETTING

Three talc occurrences were examined on the southeast slope of Mount Whympier, 20.2 kilometres northwest of the Red Mountain occurrence. They are 2.5 kilometres southwest of the Alberta border, and 840 metres northwest of, and 270 metres above Highway 93 (Figures 3-1-2, 3-1-4 and 3-1-6). The occurrences were originally staked by the Banff Talc Company in about 1915 (Spence, 1940) and later Crown granted (Lot 11708). Several cuts and two short access roads were driven into the talc bodies.

The irregular bodies of white talc are 10 to 20 metres high and contain a complex series of large, sheared inclusions of quartz-dolomite and bedded dolomite. They are at nearly the same elevation (1890 m) along 150 metres of the slope, near the base of horizontally bedded dolomites of the Cathedral Formation. The upper and lower contacts of the Silver Moon talc bodies appear parallel to bedding.

The lateral contacts of the bodies are covered but appear irregular, stepped and interfingering, and in part bounded by fracture cleavage. The bodies coincide with, and perhaps are localized along zones of well-developed northwest-striking fracture cleavage. The two northeast bodies have exposures elongated to the northwest.

The geologic setting most resembles that of the saddle occurrences. The base of the talc is about 15 metres above the rarely exposed Gog Group. They are 5.5 kilometres northeast of the inferred location of the facies change between the Cathedral and lower Chancellor Formations on the lower ramp(?) of the Cathedral escarpment (Price *et al.*, 1978; see Figure 3-1-3), and 2.5 kilometres northeast of the escarpment (Figures 3-1-2 and 3-1-4).

The informally named Consolation Valley fault is 475 to 550 metres west of the occurrences (Figures 3-1-2, 3-1-3 and 3-1-6). The northwest-trending, southwest-dipping normal fault has about 300 metres of dip separation at Mount Whympier (Price *et al.*, 1978; Figure 3-1-3). It is parallel to and 4 to 6 kilometres southwest of the Haiduk fault. The talc bodies are also near what appears to be a significant change in dip of the Consolation Valley fault from very steep, north of the talc, to about 40° south of it. A steeper dipping normal fault is inferred to splay southwards from the main fault from an apparent offset of the top of the Gog Group (Figure 3-1-6). A few talc veinlets were found in the immediate footwall of the splay.

The southwest talc body is 10 metres high (vertical) and 30 to 37 metres wide. An adit 7 metres from the southwest end of the body was driven northwesterly 9 metres. The middle body is 8 metres high and 23 to 29 metres northeast of the southwest body. The northeast body is 40 metres northeast of the middle body and up to 16 metres wide and 23 metres high. An adit was driven northwesterly 6 metres into the talc.

TALC GEOLOGY

Only 15 to 40 per cent of the complex Silver Moon bodies is exposed. The outcrops have low relief on moderately steep slopes between bluffs of the more competent bedded dolomite (Figure 3-1-11). The footwall contacts are locally exposed; other contacts are not. The talc bodies contain irregularly distributed, sheared lenses, pods and veins of highly variable proportions of quartz and dolomite. In addition, bedded dolomite forms lenses and intervals in the bodies.

The southwest body is 15 per cent exposed, but appears to contain the highest proportion of talc, with about 10 per cent bedded dolomite lenses and locally to 10 per cent quartz pods and lenses.

The talc is generally weakly translucent, frosty white with a pale greenish grey tinge on fresh surfaces. Locally, it is limonite stained and light to medium rusty orange in zones 1 metre or more wide. Very locally, the talc contains dark grey bands to 2 centimetres thick. Fracture and shear surfaces bounding talc weather medium to dark brown and are smooth. Otherwise, fracturing produces a very jagged, off-white weathered surface with patches of limonitic stain. The very strongly fractured talc is cut by a complex mosaic of criss-crossing fractures producing pieces measuring 0.5 by 1 by 1 centimetre. Slickensided shears commonly cut the talc. The more prominent strike northwest; one displays slickensides plunging 40° southeast. The talc between quartz-dolomite pods and lenses generally is cut by strongly developed fracture cleavage and shears that wrap around the pods.

Pyritic lenses are surrounded by talc at both the southwest and northeast occurrences, 1 to 3 metres above the basal contact. The lenses are up to 13 centimetres thick and 1 metre long, and dip subhorizontally to 25° southwest. The southwest lens of talc contains 10 per cent, very fine to fine anhedral pyrite irregularly scattered along stringers and within patches. The northeast lens consists of gossanous talc with patches of clear grey dolomite with 8 per cent disseminated pyrite.

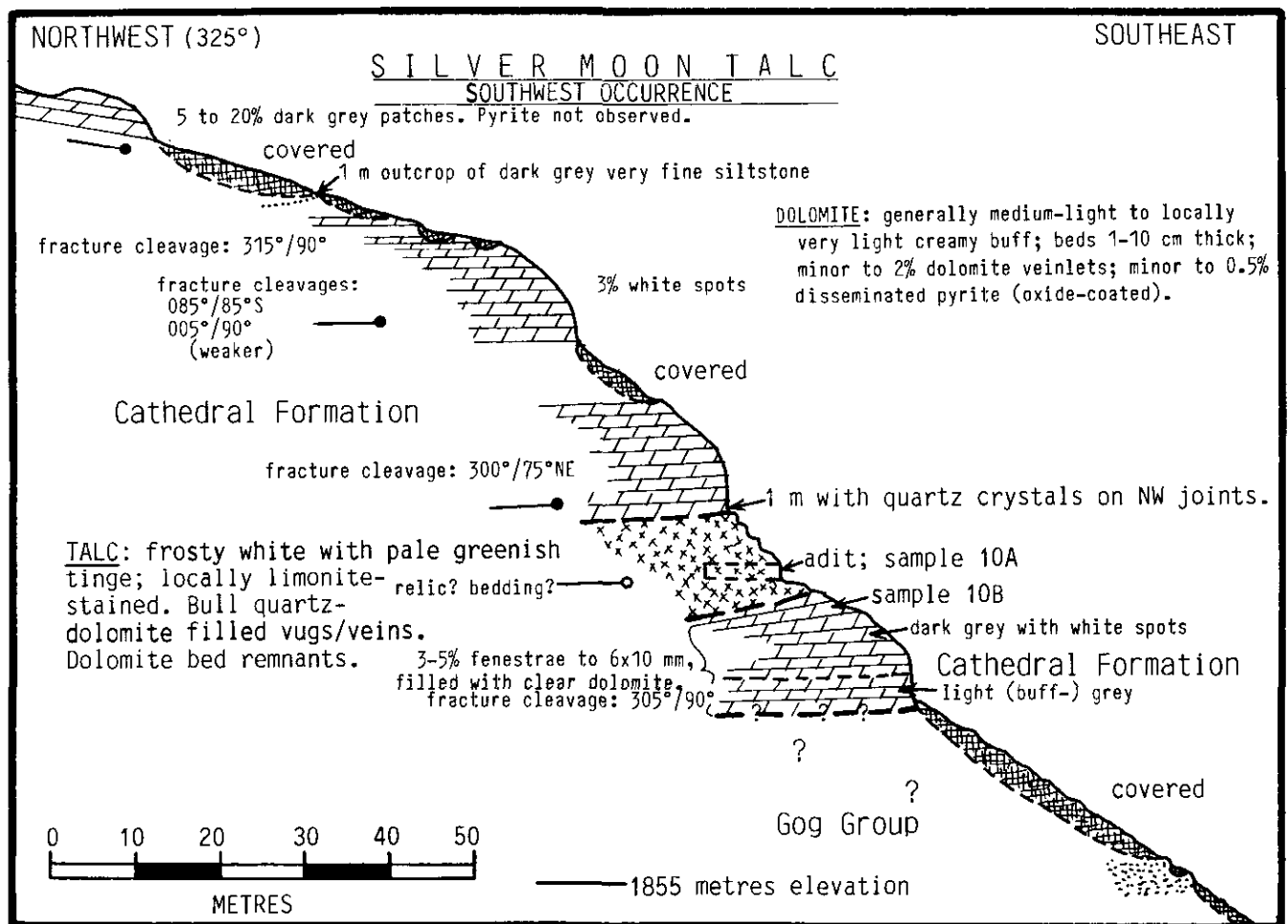


Figure 3-1-11. Cross-section of the southwesterly exposure of the Silver Moon talc occurrences on Mount Whymper. The section is based on a hip chain and compass traverse.

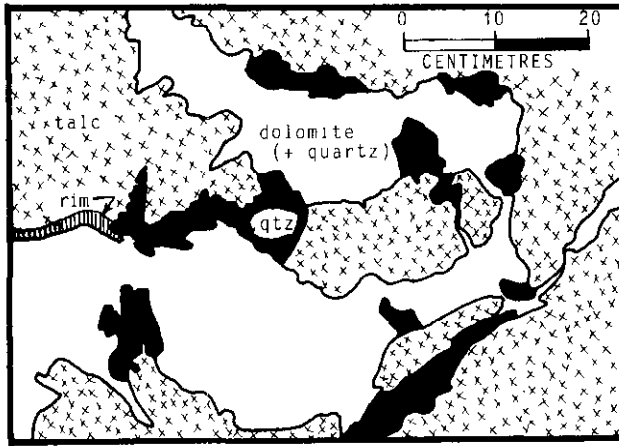


Figure 3-1-12. Coarse-grained dolomite and quartz fills irregular vugs in microcrystalline white talc. The tracing is from a photograph of a cut 20 metres northeast of the adit at the southwest Silver Moon talc body. Note the fine-grained recrystallized talc rim on the margin of a dolomite-filled vug.

Vugs and filled vugs in talc are a local feature (Figure 3-1-12). They are flattened, shallow dipping and range up to 0.7 metre long. Several are lined with dirty white botryoidal talc. They are filled with coarsely crystalline dolomite and white quartz.

In thin section the talc (sample 10A) comprises very fine elongate, irregular and weakly fibrous grains in a complex interlocking mosaic (Plate 3-1-4). A talc-replaced dolomite(?) veinlet is apparent in thin section but not in hand sample because it has the same grain size as the host talc. The thin section also contains hairline talc veinlets along a criss-crossing mosaic of fractures. They comprise very fine fibrous and non-fibrous talc grains elongated perpendicular to the veinlet walls.

Quartz-dolomite veins, pods and lenses have uncertain relationships to the talc because their contacts are generally sheared (Figure 3-1-13). However, at the southwest adit less deformed talc shows clearly that quartz and dolomite not only fill vugs, but form the matrix to coarsely fractured talc. They also form an anastomotic network of sheared and irregular fracture-offset veins to 15 centimetres thick. The quartz is moderately to very strongly shattered, coarse grained and milky white with limonitic fractures. The dolomite is generally coarsely crystalline and either surrounds or is intergrown with large quartz grains.

The quartz-dolomite bodies commonly contain 10 to 15 per cent angular to lens-shaped fragments of bedded dolomite measuring up to 0.4 by 1 metre. A thin section (sample 12A) indicates one fragment consists of a mosaic of variably sized, anhedral dolomite grains and 0.25 per cent, fine-grained, disseminated iron oxide coated pyrite. The XRD analysis indicates the dolomite is weakly altered to talc (Table 3-1-1).

Talc also encloses tabular, gently dipping, shear-bounded bodies of dolomite from 0.2 to 3 metres thick and 8 metres or more long. The weakly to moderately fractured dolomite



Plate 3-1-4. Photomicrograph (crossed nicols) of white, relatively pure talc from the southwestern Silver Moon body (sample 10A). The talc comprises a complex interlocking mosaic of elongated to irregular very fine grains and short fibres.

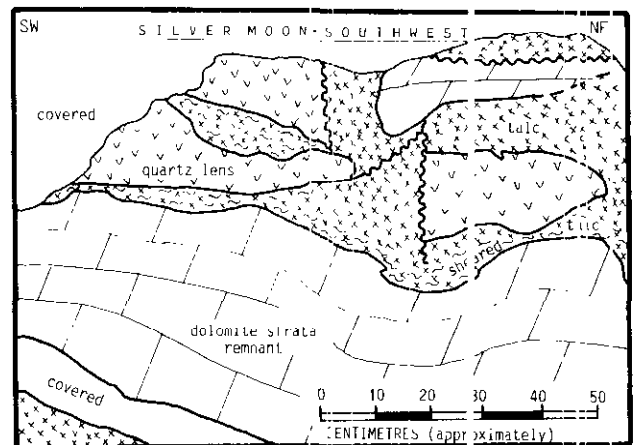


Figure 3-1-13. The complex, sheared, faulted and inter-layered relationships between talc, coarse-grained quartz and lenses of bedded dolomite in the southwest Silver Moon talc body. The pseudosection is traced from a photograph of the steep slope 8 metres northwest of the adit.

is subtranslucent, dark grey to irregularly banded light buff and medium buff-grey. One dolomite lens is cut by a few per cent (early?) dolomite veinlets and several talc veinlets 1 millimetre thick, within a few centimetres of its contacts. Another dolomite layer contains 7 per cent quartz and quartz-dolomite veinlets and pods. The veinlets are 1 to 20 millimetres thick and irregular, but commonly parallel bedding or fill a northwest-striking fracture cleavage. The pods measure up to 0.6 by 1 metre or more.

Quartz crystals commonly occur on fracture cleavages and joints cutting the dolomite. The quartz forms up to 10 per cent randomly oriented prismatic crystals to 1 by 20 millimetres in subhorizontal zones 4 centimetres wide on the joints.

The contact between talc and the underlying dolomite is sharp, locally weakly sheared and overall parallel to bedding. However, in detail it is irregular and locally stepped 0.4 metre or more and crosscuts bedding. Limonite fills small (1 by 1.5 cm) pockets in the dolomite surface.

FOOTWALL GEOLOGY

The talc is underlain by a bluff to 13 metres high of moderately fractured fenestral dolomite of the Cathedral Formation (Figure 3-1-11). It is thin to medium thin bedded and very fine grained but subtly laminated.

The dolomite contains minor to 0.5 per cent pyrite as very fine to locally fine, subhedral to anhedral grains. The pyrite is commonly rimmed or completely altered to goethite and lepidocrocite (both iron hydroxides identified by x-ray diffraction). Lens to eye-shaped fenestrae form 3 to 5 to locally 10 per cent of the rock. They commonly measure 0.5 by 1 to 6 by 10 millimetres and are filled with clear, fine-grained dolomite. X-ray diffraction analyses of dolomite from 3.5 metres below the talc body (sample 10B) identified minor amounts of chlorite and talc and traces of quartz; they are not apparent in thin section.

Dolomite veinlets form up to 2 per cent of the dolomite. They are fine grained, discontinuous, coplanar and en echelon, and criss-crossing.

At the southwest occurrence, a talus interval 20 metres high separates the base of the dolomite bluff from the small uppermost outcrop of quartz arenite of the Gog Group. The top of the Gog may be immediately below the base of the cliff because 530 metres to the southwest it is exposed at the base of a similar dolomite section.

HANGINGWALL GEOLOGY

Prismatic quartz crystals occur on northwest-striking fracture cleavage surfaces in the 1-metre interval of dolomite immediately above the southwest talc body (Figure 3-1-11). These have the same habit as those in the dolomite inclusions previously described.

The dolomite in the three bluffs in the 50 metres above the southwest talc body, resembles that below the talc with some variations. The gently dipping (10° to 5°) to horizontal beds are 1 to 10 centimetres thick. Bedding surfaces are irregular and wavy. Oxide-coated pyrite forms up to 0.5 per cent disseminations. Up to 2 per cent dolomite

veinlets commonly occur along fracture cleavages and bedding surfaces. They are hairline to 1 to locally 15 millimetres thick.

The covered intervals between the dolomite bluffs are probably underlain by platy siltstone, at least in part.

FRACTURE CLEAVAGES

Coplanar and complexly intersecting fracture cleavage sets are generally well developed in the rocks under and over, as well as in the talc bodies. The most prominent generally strike northwesterly (305° to 345°). Two additional sets of vertical fracture cleavage are locally prominent: an east-striking (085° to 105°) set and a northerly (005°) set. The spacing between the fractures commonly varies between 1 and 15 centimetres.

The fracture cleavages are probably of several generations and appear to have strongly influenced the geometry and perhaps localization of the talc bodies. An early fracture cleavage hosts dolomite(?) veinlets that were later altered to talc, together with the host.

Two of the talc bodies have exposures elongated sub-parallel to the northwest-striking fracture cleavage. The irregular sides of the bodies are probably in part controlled by this cleavage. Their upper and lower contacts jog up to 1 metre or more along fractures. Later fracture cleavages cut and offset the talc and enclosed lenses of dolomite. Talc fills those cutting talc, quartz and dolomite.

CHEMISTRY AND MINERALOGY OF TALC AND DOLOMITIC STRATA

Table 3-1-1 summarizes the results of XRF and XRD analyses on seven samples of talc and five samples of dolomite and argillaceous dolomite wallrocks from the occurrences described above.

A comparison between the theoretical compositions of talc (Table 3-1-1) and the Silver Moon white talc (sample 10A) indicates only minor impurities of calcium and iron. Interestingly, the lighter grey to white talc generally contains pyrite (up to 2%) whereas the black talc rarely does. Perhaps the iron is captured by chlorite.

CHLORITE

Three samples of black talc contain higher alumina (2.5%, 7.3% and 1.0% Al_2O_3 in 1H3A, 3A and 3B, respectively) and minor or major amounts of chlorite. It appears that the black colour may result as much as from the chlorite as the locally conspicuous carbon compound. The XRD analyses did not detect graphite, indicating that the carbon compound identified in hand samples and thin section is amorphous.

Chlorite was not positively identified in thin sections. It is, therefore, probably intergrown with the extremely fine grained talc. The maximum amount of chlorite might be 14, 40 and 6 per cent in the three talc samples if all the aluminum is in clinocllore (Table 3-1-1). This is a high magnesian member of the chlorite group common in the talc deposits in Precambrian dolomites of Montana (Berg, 1979). The precursor of the chlorite may clay.

FLUORAPATITE

X-ray diffraction analyses identified minor amounts of fluorapatite ($\text{Ca}_5(\text{PO}_4)_3\text{F}$) in one grey and two black talc samples from the Talc Lake area. All three (1H3A, 1J1 and 3B) have significantly higher percentages of P_2O_5 (0.14%, 0.35% and 0.31%) and contain chlorite. Grains resembling apatite were not recognized in thin section. Roe and Olson (1983) noted that 22 talc samples from deposits in sedimentary rocks worldwide contained 0.11 to 0.48 per cent fluorine.

TRACE ELEMENTS

Inductively coupled plasma analyses for 35 trace elements in three black and four white talc samples from Talc Lake and Mount Whympier indicate they contain low background levels of the more common metals and lack an obvious geochemical signature. The talc samples contain 1 to 15 ppm copper, 4 to 9 ppm lead, 1 to 64 ppm zinc, 4 ppm arsenic, 2 to 12 ppm tungsten, 0.2 to 0.5 ppm silver.

The black talc samples contain more zinc (22 to 64 ppm) than the white talc (1 to 12 ppm). This probably reflects the argillaceous and carbonaceous nature of the dolomite protolith.

SILT AND SOIL SAMPLES

Four samples suggest there are no obvious trace element indicators in the silt or soil downslope from the talc deposits. The two silt samples (TL-1 and -2) are from the creek that drains Talc Lake, 650 metres northeast of the Red Mountain talc occurrence (Figure 3-1-6, left). The two soil samples (SM-1 and -2) are from two low-relief draws 800 metres southeast of the Mount Whympier talc bodies (Figure 3-1-6, right). The samples contain low background levels of copper (18 to 24 ppm), lead (18 to 33 ppm), zinc (113 to 180 ppm), arsenic (4 to 11 ppm) and tungsten (3 ppm) which is similar to the talc.

TALC EXPLORATION GUIDELINES

The following preliminary exploration guidelines are based on the major similarities between the modes of occurrence of talc in the Talc Lake area and at Mount Whympier summarized in Figure 3-1-14. Although they may have similar origins, the significant differences between them cannot be explained without additional study. The considerable amount of vein-quartz and dolomite mixed with the talc at Mount Whympier distinguishes it from the other occurrences.

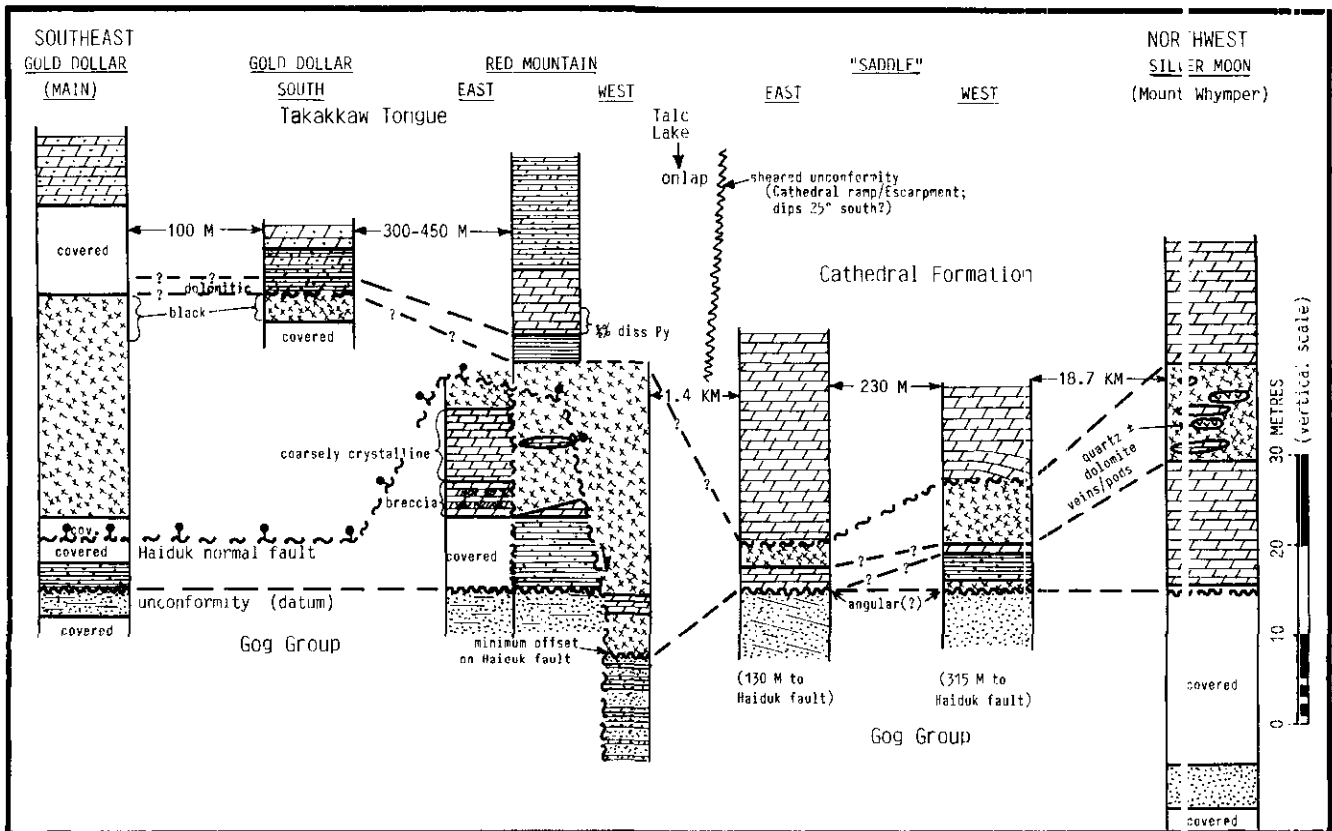


Figure 3-1-14. Correlations between schematic lithostratigraphic columns for the main talc occurrences at Talc Lake and Mount Whympier. Note the proximity of the talc bodies to the unconformity at the top of the Gog Group and their relationship to the Haiduk fault.

Permeable reef facies along the Cathedral escarpment are thought to have channeled fluids that formed the Kicking Horse, Monarch and Mount Brussilof deposits. The talc deposits, however, are below the stratigraphic level of the steep (reefoid) part of the escarpment. Evidence is lacking for structures channeling the fluids in rocks beneath the escarpment at the lead-zinc and magnesite deposits. However, the proximity of the talc deposits to the escarpment is probably more than fortuitous and it appears reasonable to conclude:

- The escarpment reflects prominent structures in the underlying Lower Cambrian and older rocks, which mark the hinge between platformal and basinal sedimentation.
- These structures localized the talc alteration.

The proximity of the talc deposits to one of two north-northwest trending normal faults probably is also not fortuitous. They are probably old structures with more than one episode and sense of displacement (Cook, 1975). The faults may have, in fact, channeled alteration fluids, as suggested by Westervelt (1979). If the faults predate the Cretaceous to Eocene shortening, then the Simpson Pass thrust must offset the upper part of the normal faults from their lower extensions.

The talc deposits appear to be localized by the following structural and lithologic controls (Figure 3-1-14):

- The Talc Lake bodies occur within 1 kilometre of the northeast end of an embayment in the Cathedral escarpment which appears to have an anomalous southerly dip. An embayment in the escarpment is not apparent near the Silver Moon occurrence but the location of the escarpment is not well constrained in this locality. The Talc Lake embayment may reflect an underlying pre-Middle Cambrian transverse (east-west) structure that controlled the location of the escarpment and caused permeable regions of dilatancy. Overburden in the Vermilion River valley conceals any large-scale northeasterly cross structure that might control the location of the talc occurrences.
- The Talc Lake bodies are in the hangingwall of the northwest-trending Haiduk normal fault. South of the escarpment the fault marks the contact between the Gog Group and the Takakkaw tongue. The main exposures of the Mount Whymper talc are east of a similar fault where it appears to change its southwest dip by 40°, and splay. These faults may have channeled the alteration fluids.
- Sets of closely spaced fracture cleavages of several ages are well developed in the talc bodies and enclosing rocks. The northwest-trending sets at Mount Whymper appear to have strongly influenced the geometry, elongation and perhaps localization of the talc deposits. At Talc Lake, quartz veinlets in quartz arenite parallel several northeast-trending fracture sets that may have channelled silica-bearing fluids into the overlying dolomite during talc alteration.
- Brecciation of the protolith dolomite at the Red Mountain deposit may have provided porosity at a small scale. Intergranular porosity is locally indicated at the microscopic scale.

- Talc is commonly strongly sheared and cleaved although upper and lower contacts appear to show relatively small offsets. The relatively incompetent talc may occur along fault-controlled linear topographic depressions, as at Talc Lake.
- Talc alteration appears stratabound at larger and smaller scales although it cuts bedding locally. Its upper and lower contacts vary from knife sharp and weakly sheared to gradational over a few metres or less. It is difficult to infer the amount of control the lithologies exercised on its extent because the most favourable hosts are presumably completely altered.
- Talc occurs near the base of the Middle Cambrian Cathedral Formation and its slope-facies equivalent, the Takakkaw tongue.
- The base of the talc is about 2.5 to 8 metres (at Talc Lake), to 15 metres (at Mount Whymper) above, or locally at the unconformity at the top of the Lower Cambrian Gog Group.
- The uppermost Gog quartz arenite at Talc Lake is locally partly to completely altered to talc, and contains disseminated pyrite. Quartz veinlets and veins form up to several per cent of the rock, which may be unusual for the Gog.
- Talc overlies the lowermost occurrence of dolomite. South and west of the Cathedral escarpment at Talc Lake it is in an interval of very thin bedded and laminated, graded black argillite, dolomite and argillaceous dolomite. The black argillite in thin intervals above and below the talc bodies is partly to completely altered to chlorite, talc and a carbon compound.
- A distinct, coarsely recrystallized dolomite immediately underlies the Red Mountain deposit at the Haiduk fault. The unit contains up to 2 per cent pyrite and minor talc veinlets. It is older than the talc but may be related to the same alteration event.
- Prismatic quartz crystals occur on fractures in the 1-metre interval of dolomite immediately above the Silver Moon occurrence.
- Pyrite generally forms 1 per cent disseminations in the lighter coloured talc. This and the pyrite in the footwall rocks might be detected by an induced polarization survey.
- Coarser pyrite is disseminated in the lower 4 metres of the dolomite unit overlying the Red Mountain deposit.

ACKNOWLEDGMENTS

I am pleased to acknowledge Z. Dan Hora of the British Columbia Ministry of Energy, Mines and Petroleum Resources for the background information and his ongoing assistance; he also conceived the study. I am also grateful to Peter Fischl for his assistance in field mapping. Finally, I would like to thank Perry Jacobson, Chief Park Warden of Kootenay National Park and Environment Canada (Parks) for permitting the fieldwork. The project was funded under contract number 93-663 by the British Columbia Ministry of Energy, Mines and Petroleum Resources.

REFERENCES

- Aitken, J.D. (1971): Control of Lower Paleozoic Sedimentary Facies by the Kicking Horse Rim, Southern Rocky Mountains; *Bulletin of Canadian Petroleum Geology*, Volume 19, pages 557-569.
- Aitken, J.D. (1981): Cambrian Stratigraphy and Depositional Fabrics, Southern Canadian Rocky Mountains, Alberta and British Columbia; in Guidebook for Field Trip 2, Taylor, M.E., Editor, *Second International Symposium on the Cambrian System*, pages 1-27.
- Aitken, J.D. (1989): Birth, Growth and Death of the Middle Cambrian Cathedral Lithosome, Southern Rocky Mountains; *Bulletin of Canadian Petroleum Geology*, Volume 37, pages 316-333.
- Aitken, J.D. and McIlreath, I.A. (1984): The Cathedral Reef Escarpment, A Cambrian Great Wall with Humble Origins; *Geos*, Volume 13, pages 17-19.
- Berg, R.B. (1979): Talc and Chlorite Deposits in Montana; *Montana Bureau of Mines and Geology*, Memoir 45, 65 pages.
- Cook, D.G. (1975): Structural Style Influenced by Lithofacies, Rocky Mountain Main Ranges, Alberta - British Columbia; *Geological Survey of Canada*, Bulletin 233, 73 pages.
- MacLean, M. (1988): Talc and Pyrophyllite in British Columbia; *B.C. Ministry of Energy, Mines and Petroleum Resources*, Open File 1988-19, 108 pages.
- Price, R.A. and Mountjoy, E.W. (1972): Geology, Banff, Alberta - British Columbia (West Half); *Geological Survey of Canada*, Map 1295A.
- Price, R.A., Mountjoy, E.W. and Cook, D.G. (1978): Geology, Mount Goodsir (East Half), British Columbia - Alberta; *Geological Survey of Canada*, Map 1476A.
- Roe, L.A. and Olson, R.H. (1983): Talc; in *Industrial Minerals and Rocks*, Fifth Edition, Volume 2, Lefond J.S., Editor-in-Chief, *American Institute of Mining, Metallurgical, and Petroleum Engineers*, pages 1275-1301.
- Scruggs, G.G. (1970): Letter to R. Green of Research Council of Alberta, from Scruggs, Chief Geologist of United Canso Oil & Gas Limited, dated August 25, 1970.
- Spence, H.S. (1940): Talc, Steatite, and Soapstone; Pyrophyllite; in Mines and Geology Branch Report Number 803, *Canada Department of Mines and Resources*, pages 57-61.
- Stewart, W.D. (1989): A Preliminary Report on Stratigraphy and Sedimentology of the Lower and Middle Chancellor Formation (Middle to Upper Cambrian) in the Zone of Facies Transition, Rocky Mountain Main Ranges, Southeastern British Columbia; in *Current Research, Part D, Geological Survey of Canada*, Paper 89-1D, pages 61-68.
- Stewart, W.D. (1991): Stratigraphy and Sedimentology of the Chancellor Succession (Middle and Upper Cambrian), Southeastern Canadian Rocky Mountains; unpublished Ph.D. thesis, *University of Ottawa*.
- Westervelt, T.N. (1979): Structural Superposition in the Lake O'Hara Region, Yoho and Kootenay National Parks, British Columbia, Canada; unpublished Ph.D. thesis, *University of Wyoming*, 266 pages and Appendix.
- Wilson, M.E. (1926): Talc Deposits of Canada; *Geological Survey of Canada*, Economic Geology Series Number 2, pages 51-52.
- Winkler, H.G.F. (1974): *Petrogenesis of Metamorphic Rocks*; Springer-Verlag, 320 pages.

NOTES

GEOLOGY OF THE ANZAC MAGNESITE DEPOSIT (93J/16W, 93O/1W)

By K.D. Hancock and G.J. Simandl

KEYWORDS: Industrial minerals, magnesite, Anzac, Gog Group, Misinchinka Group, Cambrian, refractories.

INTRODUCTION

Examination of the Anzac magnesite deposit is part of an ongoing study of sediment-hosted magnesite deposits in British Columbia. Other work is documented by Hancock and Simandl (1992), Simandl and Hancock (1991, 1992) and Simandl *et al.* (1992a). Magnesite is used in the production of refractory materials, magnesium chemicals and magnesium metal, and has significant potential in environmental applications (Simandl *et al.*, 1992b). Ministry work included mapping of lithologic sections across known magnesite-bearing units together with geochemical sampling, x-ray and petrographic analysis. This paper is a summary of field observations and preliminary laboratory results from work on the Anzac magnesite showings.

LOCATION

The Anzac magnesite deposit is on the western slopes of Mount Emmet, 122 kilometres north-northeast of Prince George and 43 kilometres due east of McLeod Lake (Figure 3-2-1), in the Misinchinka Ranges of the Rocky Mountains.

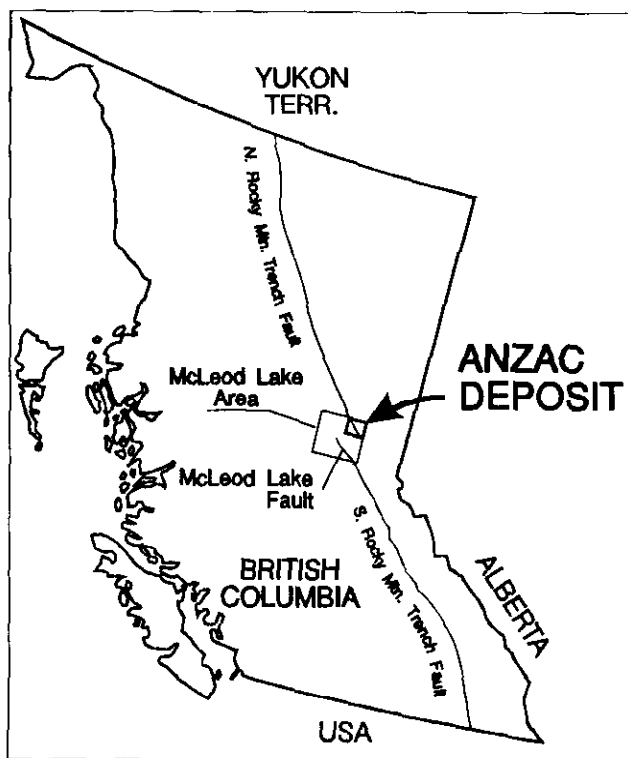


Figure 3-2-1. Location of the Anzac deposit and major regional structures.

There is no road access to the site; the property can be reached by secondary roads from Highway 97 which passes through the Anzac siding of the B. C. Electric Railway and flying the last 22 kilometres, or by air directly from Prince George.

HISTORY

The magnesite occurrences were first reported by Muller and Tipper (1969) of the Geological Survey of Canada. They were staked and reconnaissance mapped by MineQuest Exploration Associates Ltd. for Norsk Hydro in 1986. Additional mapping, sampling and drilling of three holes for a total of 287 metres were completed in 1989. Core was stored on site but the boxes have since been used by animals. The work identified six large showings: from north to south, Hela, Odin, Emmet, Knob, Knoll and Fria. Further mapping and sampling by MineQuest Exploration Associates Ltd. and section mapping with sampling by the Geological Survey Branch were done in 1991.

REGIONAL GEOLOGY

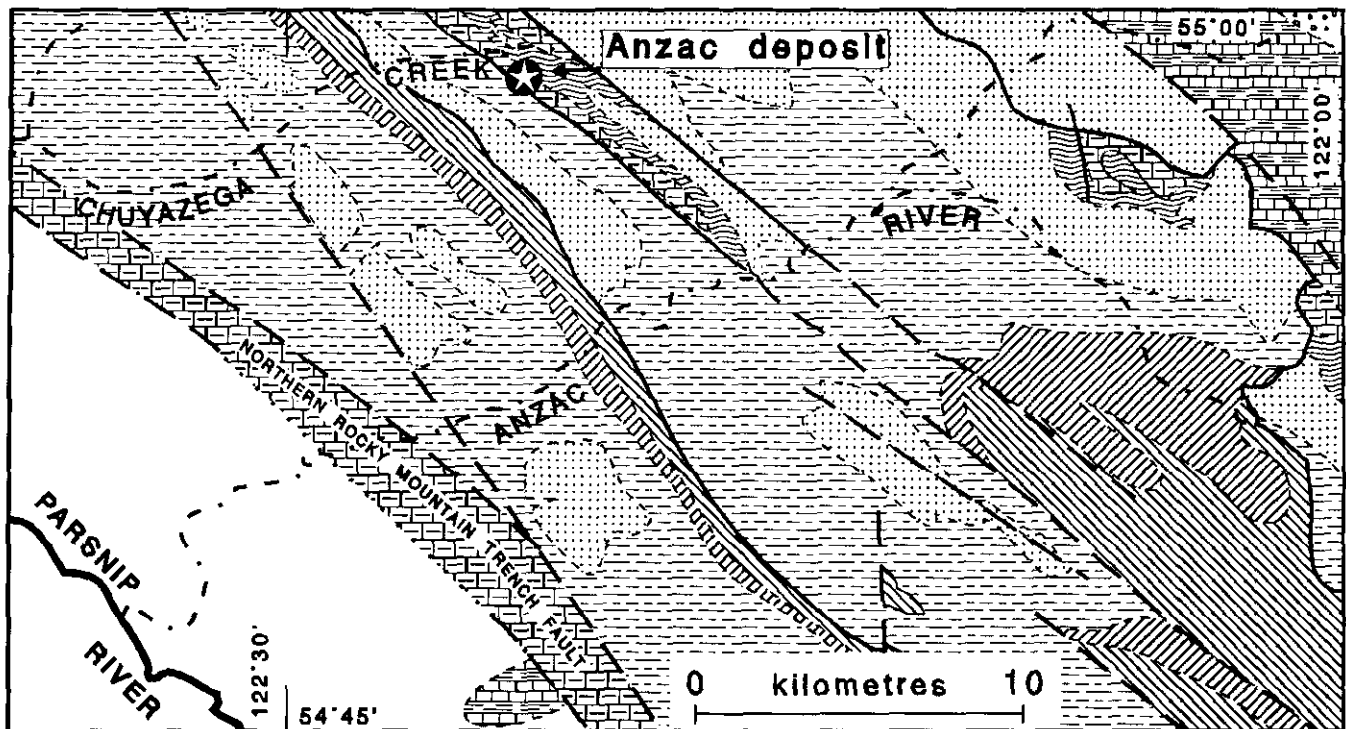
The region is transected by a major structural break defined by the Northern Rocky Mountain Trench and the McLeod Lake fault (Figure 3-2-1). This divides the area into Precambrian and Paleozoic sediments to the east with lower Paleozoic sediments and suspect terranes to the west. The McLeod Lake fault may have transferred dextral strike-slip movement along the northern part of the Southern Rocky Mountain Trench to the Northern Rocky Mountain Trench (Price and Carmichael, 1986). East of these major structures, thrusts and folds are typically east vergent although some folds verge west (McMechan, 1987). Northeast-trending extensional faults crosscut the northwest-trending faults. These structures are associated with Late Cretaceous to Early Tertiary east-vergent shortening (McMechan, 1987).

The Anzac magnesite deposit is located in the northeast corner of the McLeod Lake map sheet mapped by Muller and Tipper (1969), Struik (*in press*, 1989, 1990) and Struik and Fuller (1988). Equivalent stratigraphy occurs to the northwest (Struik, 1992; Struik and Northcote, 1991; McMechan, 1987). Three major stratigraphic units are present in the Anzac area: the Misinchinka, Gog and Kechika groups (Figure 3-2-2).

The Precambrian Misinchinka Group consists of fine to coarse-grained, marine clastic rocks separated into four subdivisions by Struik (*in press*). The lower two subdivisions consist of grey slate, fine quartzite, grit, diagenite, phyllite and minor carbonate rocks of Hadrynian age. The upper two subdivisions consist of white quartzite, grey slate and black slate of Hadrynian to Early Cambrian age. There is a glacial change from the Misinchinka Group into the Gog Group. The Lower Cambrian Gog Group is separated into

two divisions (Struik, in press). The lower division consists of quartzite, dolomite, sandy dolomite and slate. The upper member consists of limestone, dolomite, shale and siltstone. Poorly preserved *Archeocyathid* fossils are present sporadically in carbonate rocks of the Gog Group (McMechan, 1987; Muller and Tipper, 1969; Struik, 1989). Magnesite occurs within the Gog Group. Struik (1989) measured several sections across the transition from the Misinchinka Group through the Gog Group, east of the Anzac deposit. These sections provide detailed descriptions of the groups in the Anzac area. The Ketchika Group consists of Upper Cambrian to Lower Ordovician slate, phyllite and platy limestone together with some undifferentiated Cambrian to Devonian carbonates with minor clastics (Struik, in press; Muller and Tipper, 1969).

Magnesite-bearing rocks occur within a down-faulted block of both the Gog and Misinchinka groups (Figure 3-2-2). The block is bounded by west-dipping normal faults with the centre slightly down dropped. Rocks within the graben are folded into an open east-verging antiform. The Gog Group outcrops over most of the fault block and the upper Misinchinka Group forms the core of the antiform. The upper member of the Gog Group forms the northeastern and southwestern limbs of the antiform. The lower member of the Gog Group is mostly quartzite and the upper member is mostly carbonate. The Misinchinka Group consists of black and dark green slate and phyllite. To the east and west of the block are rocks of the Misinchinka Group. Axial planar cleavage is well developed in fine-grained clastic rocks and absent in quartzites and carbonates.



LEGEND

Cambrian to Devonian

 Undifferentiated carbonate and minor clastics

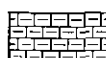
U. Cambrian & L. Ordovician

Ketchika Group

 Green-grey slate, phyllite and platy limestone

Lower Cambrian

Gog Group

 Archeocyathid limestone, shale and siltstone

 Quartzite, dolomite, sandy dolomite, slate

Misinchinka Group

 White quartzite, olive-grey slate and fine-grained quartzite

 Slate, white quartzite and black slate

Precambrian

Hadrynian

 Grey and dark grey slate, fine-grained quartzite

 Grit, slate, phyllite

Figure 3-2-2. Regional geology of the Anzac deposit (modified from Struik, in press).

THE ANZAC DEPOSIT

The Anzac deposit consists of six showings (Figure 3-2-3). The Fria, Knoll and Knob showings are isolated outcrops of massive, sparry magnesite. Sections were prepared across the Hela, Emmet and Odin showings (Figures 3-2-4, 5 and 6). Due to possible structural thickening or fold repetition these are lithologic sections only. From the sections, eleven lithofacies were identified which are grouped into three units. These are, in descending order, units of carbonate, argillite and quartzite. The argillite and quartzite are probably part of the lower member of the Gog Group. The carbonates are most probably correlative with an *Archaeocyathid* carbonate unit of the upper Gog Group (Struik, in press) and host the magnesite deposits. Grab samples were taken from the sections and isolated outcrops for whole-rock geochemical analysis. Chemical analyses are listed in Table 3-2-1. Lithologic correlation between sections is poor, possibly as a result of interfingering of lithofacies or structural complications.

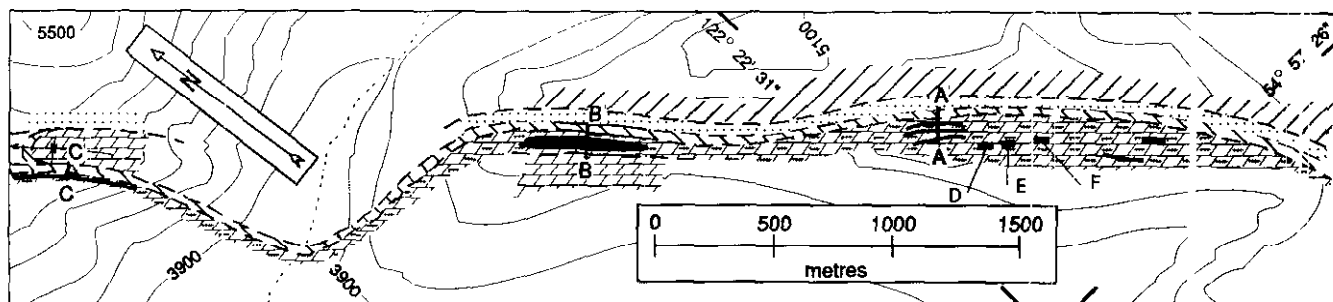
Magnesite at the Anzac deposit is massive, sparry and has few preserved sedimentary features. Rocks containing more than 80 per cent bladed crystals, with more than 36.5 per cent MgO, are referred to as magnesite (Table 3-2-1) and approach stoichiometric magnesite composition. The value of 36.5 per cent MgO is equivalent to 70 per cent MgO in calcined product. This is considered as the minimum grade for economic development in the current magnesia products market. A scatter plot of CaO versus MgO shows a tight cluster over 36.5 per cent MgO (Figure 3-2-7).

Zones of magnesite range from 3 to 11 metres wide. Contacts with host rock are gradational across up to 50 centi-

metres. Individual crystals are bladed, range in size from 5 to 20 millimetres and are usually randomly oriented, but they also form fans or rosettes. Magnesite is either white to buff or medium to light grey in colour on fresh surfaces. The buff to white, sparry magnesite is similar to that seen in southeast British Columbia, however, the medium grey magnesite has not previously been recorded in the province. Thin section analysis of grey, "high-grade" magnesite rock shows that small amounts of dolomite are present in the matrix as well as abundant, micron-scale inclusions within the magnesite crystals. X-ray analysis also shows the presence of talc and chlorite. Chlorite is absent in white magnesite. The grey colour is due to matrix dolomite and accessory minerals. Common impurities are dolomite, pyrite, limonite and hematite. Dolomite occurs as either scattered remnant matrix or masses of white, rhombic crystals. Pyrite occurs in or near small fractures, either as disseminated crystals or thin coatings, and is usually partially oxidized. Occasionally, limonite and hematite occur as fist-sized, amorphous masses.

Drill holes below the Emmet showing, 80 metres south of section A-A', cut several magnesite sections separated by dolomite, over lengths of 1 to 21 metres, with MgO concentrations between 31 and 43 per cent (Gcurly, 1989). Correlations between drill intersections and surface exposures are speculative. Broad zones can be distinguished but segment by segment correlations are impossible. This suggests that the magnesite may occur as discrete lenses or braided zones.

Dolomite is the most common rock type in the sections. It is typically massive, dark to medium grey, weathers light



LEGEND

	Grey dolomite, massive to thin bedded, some oolitic / pisolitic beds		Massive, white quartz arenite
	Grey to buff dolomite, massive to thin bedded, contains lenses, pods and disseminations of sparry carbonate		Grey to black argillite and phyllite
	Sparry carbonate		Geologic contact (approximate)
	Olive-green shale, argillite or phyllite, poor to well developed cleavage		Stream
			Contour, 200 foot interval
			A — A'

Figure 3-2-3. Geology of the Anzac deposit (modified from Gourlay, 1989, 1991). AA' = Emmet showing; BB' = Odin showing; CC' = Hela showing; D = Knob showing; E = Knoll showing; F = Fria showing.

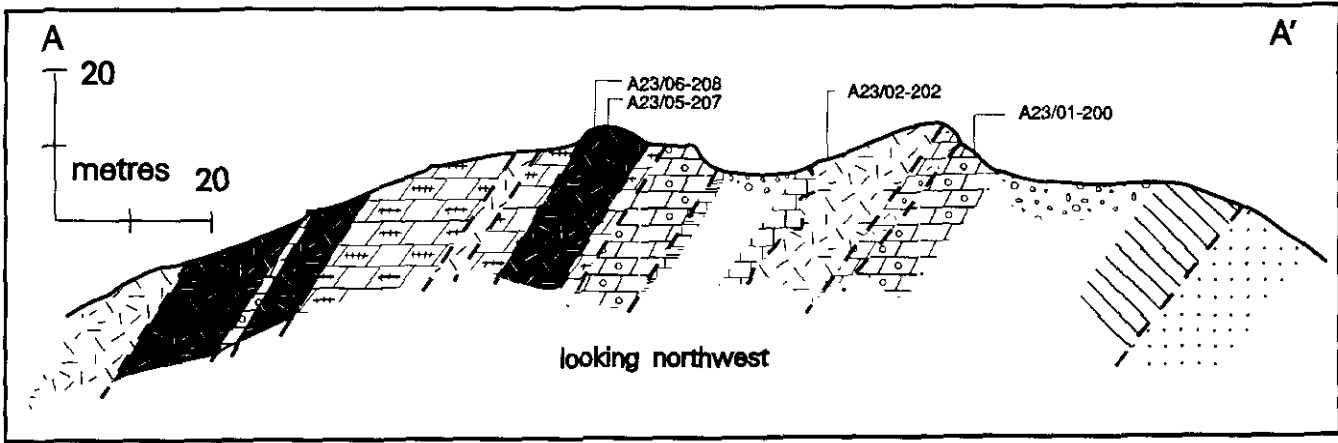


Figure 3-2-4. Lithologic section of the Emmet showing with sample locations.

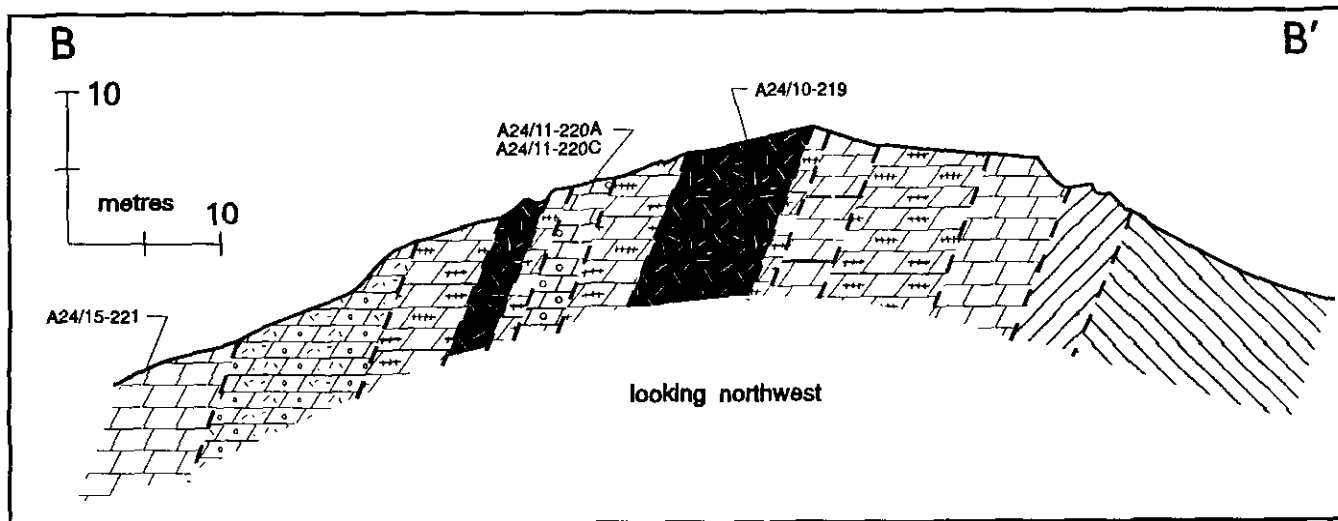


Figure 3-2-5. Lithologic section of the Odin showing with sample locations.

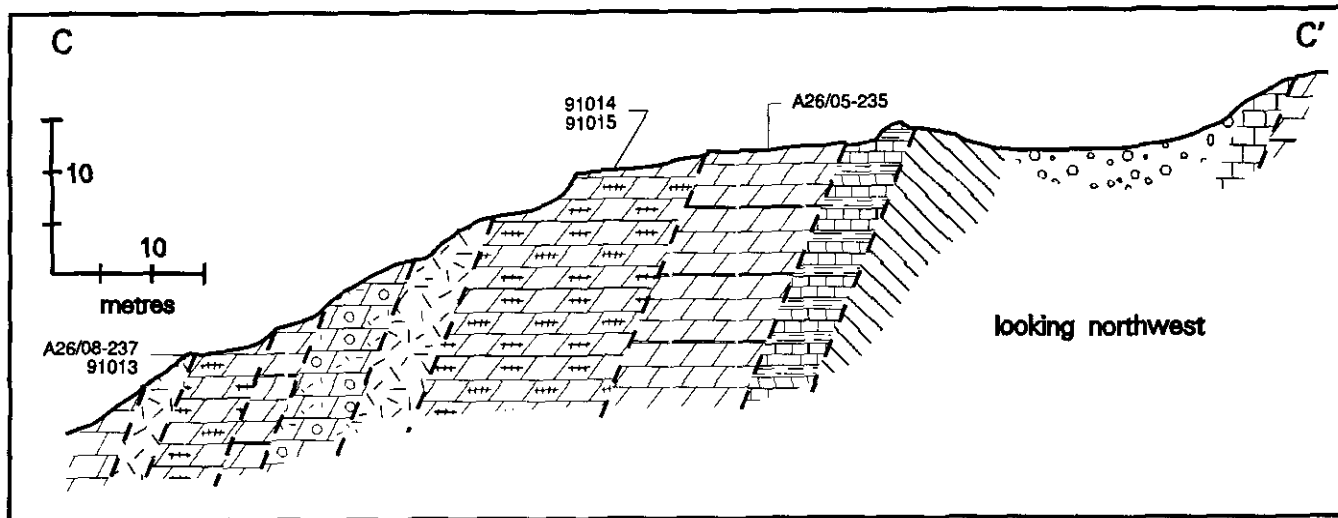


Figure 3-2-6. Lithologic section of the Hela showing with sample locations.

TABLE 3-2-1
WHOLE-ROCK GEOCHEMISTRY FROM THE ANZAC DEPOSIT

SAMPLE	SHOWING	ROCKTYPE	MgO	CaO	Al ₂ O ₃	Fe ₂ O ₃	SiO ₂	TiO ₂	MnO	Na ₂ O	K ₂ O	P ₂ O ₅	LOI	TCIAL	CaO/MgO
A23/5-207	Emmet	magnesite	43.99	0.72	0.11	0.98	2.23	0.01	0.02	0.01	0.01	0.86	50.01	91.95	0.016
91001	near Emmet	magnesite	39.70	6.74	0.22	1.30	1.62	0.01	0.03	0.05	0.06	0.10	50.00	91.24	0.169
A23/8-210	Knob	magnesite	43.05	1.89	0.09	0.61	0.74	0.01	0.01	0.02	0.01	0.87	53.25	101.55	0.044
91003	near Knob	magnesite	41.02	5.52	0.11	1.10	0.36	0.01	0.03	0.05	0.07	0.08	50.80	91.14	0.135
91004	Knoll	magnesite	42.76	3.15	0.21	1.01	0.64	0.01	0.03	0.05	0.06	0.08	51.10	91.11	0.074
91005	near Fria	magnesite	40.68	5.48	0.22	0.90	1.22	0.01	0.03	0.05	0.06	0.10	50.40	91.13	0.135
91006	near Fria	magnesite	42.92	3.20	0.20	0.97	0.56	0.02	0.02	0.05	0.07	0.09	51.10	91.19	0.074
91007	near Fria	magnesite	43.56	1.86	0.26	0.96	1.28	0.01	0.02	0.05	0.09	0.08	51.00	91.15	0.043
91008	near Fria	magnesite	38.55	4.17	0.49	1.76	5.53	0.02	0.04	0.06	0.05	0.14	48.50	91.30	0.108
91011	near Fria	magnesite	43.81	1.04	0.24	0.98	1.93	0.01	0.02	0.06	0.08	0.09	50.80	91.06	0.024
91012	near Fria	magnesite	44.81	1.23	0.14	0.87	0.46	0.01	0.02	0.05	0.05	0.10	51.40	91.06	0.027
A24/10-219	Odin	magnesite	43.79	3.14	0.21	1.16	0.44	0.01	0.02	0.01	0.01	1.04	50.36	101.19	0.072
91009	near Odin	magnesite	39.35	6.36	0.36	1.48	1.36	0.02	0.04	0.05	0.10	0.13	50.00	91.23	0.162
91010	near Odin	magnesite	41.47	3.52	0.37	1.55	1.17	0.01	0.04	0.05	0.05	0.14	50.50	91.11	0.085
A23/1-200	Emmet	dolomite	22.03	31.12	0.11	0.89	0.36	0.01	0.11	0.04	0.03	0.53	46.75	10.98	1.413
A23/2-202	Emmet	dolomite	25.32	27.12	0.56	0.71	0.94	0.02	0.06	0.03	0.01	0.55	46.00	10.32	1.071
A23/6-208	Emmet	dolomite	14.32	31.54	0.16	13.29	0.15	0.01	0.03	0.01	0.01	0.57	41.27	10.36	2.203
A24/11-220A	Odin	dolomite	21.84	31.18	0.01	0.84	0.39	0.01	0.06	0.02	0.01	0.49	46.78	10.63	1.428
A24/1-220C	Odin	dolomite	26.16	25.76	0.02	0.81	0.01	0.01	0.05	0.01	0.01	0.62	47.92	10.38	0.985
A24/15-221	Odin	dolomite	22.25	31.01	0.14	0.75	0.24	0.01	0.06	0.03	0.02	0.52	46.83	10.86	1.394
91002	near Knob	dolomite	30.10	18.80	0.19	0.88	0.59	0.01	0.03	0.05	0.11	0.13	48.50	91.40	0.625
A26/5-235	Hela	dolomite	21.15	30.73	1.00	0.88	1.58	0.04	0.08	0.04	0.29	0.49	45.82	10.10	1.453
A26/8-237	Hela	dolomite	34.23	16.70	0.08	0.76	0.39	0.01	0.02	0.01	0.01	0.82	48.95	10.98	0.438
91013	Hela / *237	dolomite	32.26	16.11	0.13	1.25	0.67	0.01	0.04	0.05	0.05	0.08	48.80	91.38	0.439
91901	dup 91013	dolomite	33.81	13.81	0.27	1.20	1.21	0.01	0.02	0.01	0.04	0.04	48.40	91.82	0.438
91014	Hela / #235	dolomite	20.33	29.85	0.13	0.96	3.22	0.01	0.03	0.05	0.05	0.08	45.10	91.74	1.458
91015	Hela / #235	dolomite	19.47	29.33	0.27	0.74	5.57	0.02	0.04	0.05	0.05	0.08	44.10	91.67	1.506
91016	Hela / #237	dolomite	19.65	32.47	0.06	0.68	0.96	0.04	0.04	0.05	0.05	0.06	45.70	91.72	1.652
91017	near Hela	dolomite	19.10	32.44	0.13	0.74	0.86	0.01	0.03	0.05	0.05	0.06	46.00	91.40	1.638
A23/7-209	near Emmet	limestone	1.05	48.30	0.30	0.01	13.00	0.01	0.03	0.01	0.12	0.01	37.89	101.73	46.000

Samples prefixed "A" are the authors and samples prefixed "91" are from Gourlay (1991.) Minequest.

grey to buff and is recrystallized. Grain size ranges from 0.1 to 0.5 millimetre and is usually around 0.25 millimetre. Sedimentary features are only visible on fresh surfaces; stylolites are common though poorly developed. The lithologic descriptions below are all variants of this massive dolomite.

Pisolithic dolomite contains variable amounts of pisolites and oolites, ranging from 5 to 20 millimetres in diameter. Where well preserved, the concentric nature of the grains is

readily apparent and core grains are visible. The texture ranges from scattered oolites or pisolites to rock approaching grainstone. Two further variants include massive dolomite and pisolithic dolomite with bladed crystals. The crystal abundance is less than 20 per cent. Chemically the rock composition is that of the massive dolomite. Bladed crystals vary from 5 to 25 millimetres in length, are light grey to white and are found as scattered grains or bipolar growths along stylolites or fractures. Massive dolomite and pisolithic dolomite with bladed crystals are commonly found adjacent to massive, sparry magnesite or massive dolomite with abundant bladed crystals. The latter consists of a framework of 20 to 80 per cent bladed crystals in massive dolomite. This rock is similar in colour and texture to massive, sparry magnesite when the bladed crystal content reaches the upper limit. Chemically, the MgO content is less than 36.5 per cent, often less than 30 per cent. Dolomite with bladed crystals approaching 80 per cent of the rock mass plots as magnesium-rich rock on Figure 3-2-7. X-ray and thin-section analysis shows that the high magnesium content is due to the abundance of magnesite crystals rather than high-magnesium dolomite. The magnesite is interstitial to and replaces dolomite. Other dolomite samples, either with few or no bladed crystals, plot near the stoichiometric dolomite composition. Contacts between massive, sparry magnesite, magnesite crystal rich dolomite and the crystal-poor (<20%) dolomites are distinct though gradational over

LEGEND

cross-sections

	Magnesite: > 80 % bladed crystals		Limestone
	Dolomite: 20-80 % bladed crystals		Interbedded limestone and argillite
	Dolomite: < 20 % bladed crystals		Calcareous argillite
	Pisolithic dolomite < 20 % bladed crystals		Argillite
	Dolomite		Quartzite
	Pisolithic dolomite		Overburden

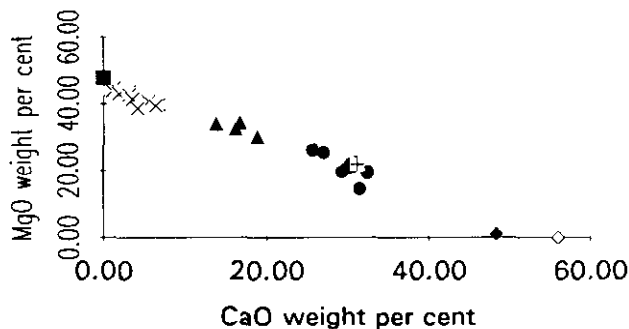


Figure 3-2-7. CaO/MgO plot for the Anzac deposit. Data are in Table 3-2-1. Square = stoichiometric magnesite; x = magnesite; Triangle = high-magnesium carbonate; Filled circle = dolomite; Cross = stoichiometric dolomite; Filled diamond = limestone; Diamond = stoichiometric calcite.

0.5 metre. The contacts are generally bedding parallel and subplanar although in some locations are highly irregular.

Limestone is rarely exposed at the Anzac deposit (Figure 3-2-6). Where found, it is medium to light grey and fine grained with a platy parting along bedding spaced at 10 to 20 millimetres. At the Hela showing there is a colour variation to beige at the downslope side of the outcrop. At or near the base of the carbonate unit are either interbedded limestone and argillite or calcareous argillite. The interbedded limestone and argillite consists of rust-coloured, fine-grained, recessive weathering limestone and green, thinly cleaved argillite. The calcareous argillite consists of interbedded brown and green, thinly cleaved argillite. The brown argillite is dolomitic and the green argillite is calcareous. Bedding is less than 5 millimetres thick.

Slaty argillite and quartzite underly the carbonate member. Argillite is olive green, thinly bedded and well cleaved. It is recessive weathering and only the parts adjacent to the more competent carbonate or quartzite units are exposed. Quartzite is resistant and forms low bluffs. It is white weathering and light grey on fresh surfaces. Grains are well rounded and fairly uniform in size, ranging from 0.1 to 0.25 millimetre in diameter. Where visible, planar bedding is 10 to 15 millimetres thick but the rock appears generally massive.

CONCLUSIONS

Magnesite at the Anzac showings is hosted by carbonate of the upper division of the Lower Cambrian Gog Group. The geological setting of the deposit is similar to that of the Lower Cambrian strata at Mount Brussilof and the Marysville area and the Helikian strata in the Brisco area. The MgO content of the high-grade material is also similar to the southeastern British Columbia deposits. The silica content is similar to the Brisco deposits and less than that of the Marysville deposit. Mapping shows that a magnesite-bearing unit extends over a length of several kilometres but continuity between individual showings is not established. Further exploration along strike to the north and south is justified. Equivalent carbonate units of the Gog Group

elsewhere in the area may host similar magnesite mineralization. Our work also suggests that favourable conditions within the Cambrian carbonates may extend northward from the Anzac River area to the Selwyn Basin.

ACKNOWLEDGMENTS

The authors would like to thank A. Gourlay and G. Vernon for their logistical support and cooperation in the field. Norsk Hydro kindly permitted our investigation of the site. Dr. L.C. Struik kindly provided a draft copy of his map of the regional geology in the McLeod Lake map area.

REFERENCES

- Gourlay, A.W. (1989): Anzak Magnesite Property, Diamond Drilling; *B.C. Ministry of Energy, Mines and Petroleum Resources*, Assessment Report 19213, 22 pages plus maps and appendices.
- Gourlay, A.W. (1991): Anzak Magnesite Property, Geology and Geochemistry; *B.C. Ministry of Energy, Mines and Petroleum Resources*, Assessment Report 21712, 18 pages plus maps and appendices.
- Hancock, K.D. and Simandl, G.J. (1992): Geology of the Marysville Magnesite Deposit, Southeastern British Columbia; in *Exploration in British Columbia 1991*, *B.C. Ministry of Energy, Mines and Petroleum Resources*, pages 71-80.
- McMechan, M.E. (1987): Stratigraphy and Structure of the Mount Selwyn Area, Rocky Mountains, Northeastern British Columbia; *Geological Survey of Canada*, Paper 85-28, 34 pages.
- Muller J.E. and Tipper H.W. (1969): Geology, McLeod Lake, 93J, British Columbia; *Geological Survey of Canada*, Map 1204A, scale 1:253 440.
- Price, R.A. and Carmichael, D.M. (1986): Geometric Test for Late Cretaceous-Paleogene Intracontinental Transform Faulting in the Canadian Cordillera; *Geology*, Volume 14, pages 468-471.
- Simandl, G.J. and Hancock, K.D. (1991): Geology of the Mount Brussilof Magnesite Deposit, Southeastern British Columbia (82J/12, 13); in *Geological Fieldwork 1990*, Paper 1991-1, *B.C. Ministry of Energy, Mines and Petroleum Resources*, pages 269-278.
- Simandl, G.J. and Hancock, K.D. (1992): Geology of Dolomite-hosted Magnesite Deposits of the Brisco and Driftwood Creek Areas, British Columbia; in *Geological Fieldwork 1991*, Grant, B. and Newell, J.M., Editors, *B.C. Ministry of Energy, Mines and Petroleum Resources*, Paper 1992-1, pages 461-478.
- Simandl, G.J., Hancock, K.D., Fournier, M., Koyanagi, V.M., Vilkos, V., Lett, R., and Colbourne, C. (1992a): Geology and Geochemistry of the Mount Brussilof Magnesite Deposit, Southeastern British Columbia, (82J/12E, 13W); *B.C. Ministry of Energy, Mines and Petroleum Resources*, Open File 1992-14, 14 pages.
- Simandl, G.J., Jakobsen, D. and Fischl, P.S. (1992b): Refractory Mineral Resources in British Columbia, Canada: A Fresh Look; *Industrial Minerals*, No. 296, pages 67-77.
- Struik, L.C. (1989): Devonian, Silurian, Cambrian and Precambrian Stratigraphy, McLeod Lake Map Area, British Columbia; in *Current Research, Part E*, *Geological Survey of Canada*, Paper 89-1E, pages 119-124.
- Struik, L.C. (1990): Stratigraphic Setting of Late Paleozoic and Mesozoic Fossils, McGregor Plateau, McLeod Lake Map Area, British Columbia; in *Current Research, Part E*, *Geological Survey of Canada*, Paper 90-1E, pages 55-58.

Struik, L.C. (1992): Further Reconnaissance Observations in the Pine Pass Southwest Map Area, British Columbia; *in* Current Research, Part A, *Geological Survey of Canada*, Paper 92-1A, pages 25-31.

Struik, L.C. (in press): Geology of the McLeod Lake Map Area, 093J, B. C., Bedrock Geology; *Geological Survey of Canada*, Open File Map 439, Sheet 2 of 4.

Struik, L.C. and Fuller, E.A. (1988): Preliminary Report on the Geology of McLeod Lake Area, British Columbia; *in* Current Research, Part E, *Geological Survey of Canada*, Paper 88-1E, pages 39-42.

Struik L.C and Northcote B.K. (1991): Pine Pass Map Area, Southwest of the Northern Rocky Mountain Trench, British Columbia; *in* Current Research, Part A, *Geological Survey of Canada*, Paper 91-1A, pages 285-291.

NOTES



THE AA GRAPHITE DEPOSIT, BELLA COOLA AREA, BRITISH COLUMBIA: EXPLORATION IMPLICATIONS FOR THE COAST PLUTONIC COMPLEX
(92M/15)

By Nathalie Marchildon, George J. Simandl and Kirk D. Hancock

KEYWORDS: Industrial minerals, graphite, crystalline flake, granulite facies, Coast Plutonic Complex, thermobarometry, retrograde metamorphism, exploration.

INTRODUCTION

Natural graphite is a well known high unit-value industrial mineral with a wide range of applications (Taylor, 1992; Simandl, 1992; Simandl *et al.*, 1992). The major uses are shown in Figure 3-3-1. Commercial graphite concentrates are classified into four major categories: crystalline lumps, crystalline flakes, powder and "amorphous" powder. Crystalline flake graphite is hosted by amphibolite to granulite grade metasedimentary rocks. The term "lump and chip" graphite refers to high-grade vein-type ore fragments typically 0.5 to 0.8 centimetre in size. Crystalline powder is produced as the result of excessive milling of flake graphite. Microcrystalline graphite, commonly called "amorphous" graphite, is produced from metamorphosed coal seams.

The most important technical parameters governing the price of graphite flake concentrate are graphitic carbon content, flake size, degree of crystallinity and the types of impurities. Prices of typical graphite concentrates are illustrated in Table 3-3-1. The long and medium-term outlooks for graphite consumption are positive. In the short term,

TABLE 3-3-1
TYPES OF GRAPHITE CONCENTRATES AND COSTS PER TON (US DOLLARS)

	Grade	Price
Crystalline lumps	92/95 %C	750-1500
Crystalline large flakes	85/90 %C	650-1200
Crystalline medium flakes	85/90 %C	450-1000
Crystalline small flakes	80/95 %C	400-600
Powder (200 mesh)	80/85 %C	325-360
	90/92 %C	520-600
	95/97 %C	770-1000
	97/99 %C	1000-1300
Amorphous powder	80/85 %C	220-440

CIF UK port

(Source: *Industrial Minerals*, 1992, Number 301, page 68.)

there is an oversupply, as with most other industrial minerals, due to reduced manufacturing activity worldwide (Harries-Rees, 1992). Prices of natural graphite are expected to recover faster than most other industrial minerals as many industries have kept inventories low during the recession (Hand, 1992) and if, as forecast, China reduces graphite exports to satisfy increasing internal needs (Holroyd and McCracken, 1992). In industrialized countries the areas of fastest growth for natural graphite use are likely to be the automotive and nuclear industries (Kanan, 1992).

This study focuses on a crystalline flake graphite deposit located in southwestern British Columbia. This case study, combined with published regional data, indicates that there is excellent geological potential for world-class crystalline flake graphite deposits within the Coast Plutonic Complex. This paper discusses geological and exploration considerations and the technical aspects of metamorphism and geothermobarometry will be addressed elsewhere. Specific economic considerations, such as to mine, grade continuity and average grade for this deposit are beyond the scope of this paper.

LOCATION AND ACCESS

The AA graphite deposit is located in the Bella Coola area, approximately 500 kilometres north-northwest of Vancouver. The property is approximately 2 kilometres north of the head of South Bentinck Arm, on its western shore (Figure 3-3-2).

The fastest access to the deposit is by floatplane from the town of Port Hardy, at the northern tip of Vancouver Island, approximately 200 kilometres to the south. Alternatively, the deposit can be reached by driving to Bella Coola, 45 kilometres north of the deposit, and by floatplane from there.

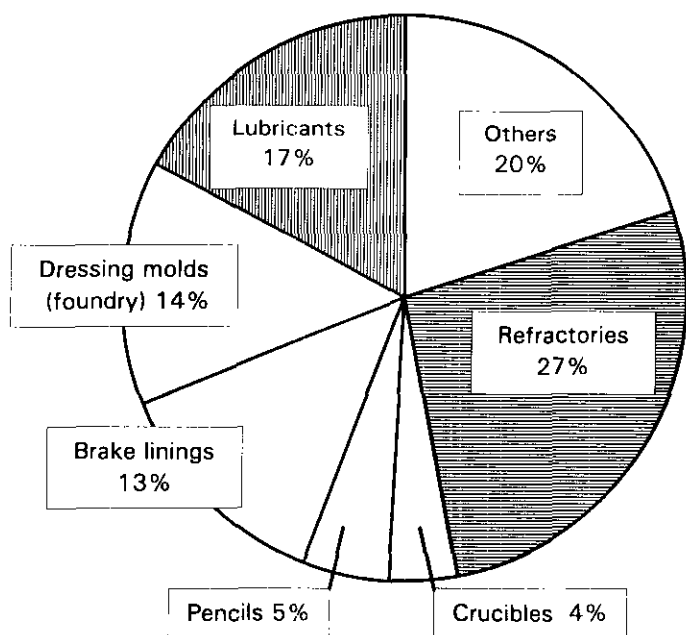


Figure 3-3-1. Natural graphite applications in the United States (from Taylor, 1992).

METHODS

Fieldwork was completed over 12 days in early July, 1992. A series of ten, 400 to 750-metre traverses, spaced 200 metres apart, were made perpendicular to the regional structural grain (northwest) on a grid centred on the graphite deposit, and more than 130 outcrops were described.

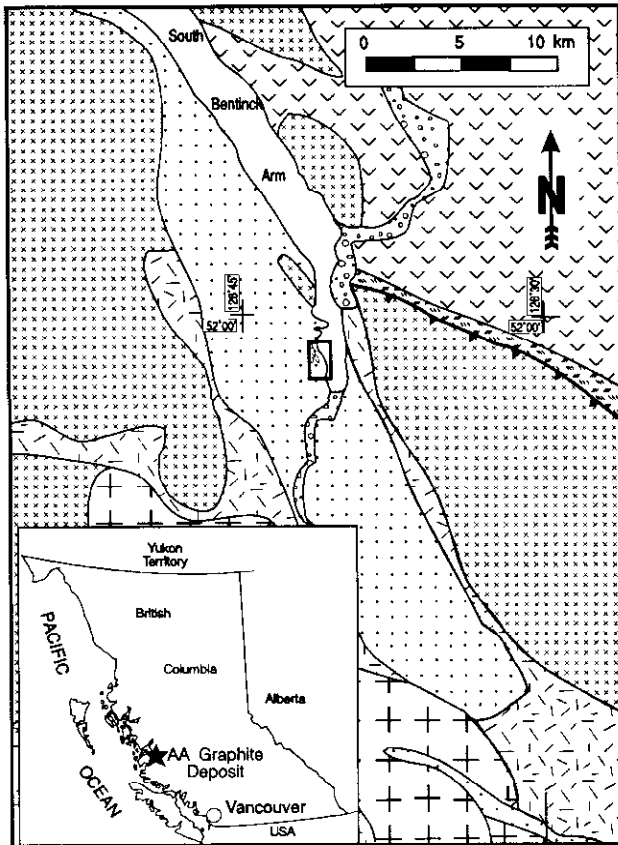
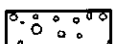
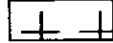
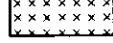
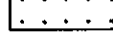
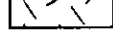


Figure 3-3-2. Regional geology of the South Bentinck Arm area, B.C. Heavy box shows area covered by Figure 3-3-3; inset shows geographical position of map area. Modified from Baer (1973) and Roddick (in preparation).

Legend

-  Quaternary alluvial and glacial deposits
-  Lower Cretaceous volcanic rocks
-  Dioritic complex
-  Undifferentiated plutonic rocks
-  Metasediments
-  Granitoid gneiss
-  Thrust fault zone

Trenches in high-grade graphitic rock were sampled and mapped in detail (1:100).

More than 50 thin sections of graphitic rocks and graphite-free country rocks and 20 thin sections of rocks from the deposit were described. Of these, six garnet-bearing rocks were analyzed using a JEOL Superprobe 733 electron microprobe to determine mineral compositions used in thermobarometric calculations. Back-scattered electron micrographs of graphite-bearing rocks were also obtained. Chemical analyses for major, minor and selected trace elements and for graphitic carbon were obtained for 13 samples from the deposit (Table 3-3-2).

REGIONAL GEOLOGY

The geological setting of the AA graphite deposit, based on 1:250 000 compilations of Baer (1973) and Roddick (in preparation), is described below and summarized in Figure 3-3-2. The volumetrically dominant rocks in the area are intrusions of the Coast Plutonic Complex (Early Cretaceous to Eocene; Baer, 1973). These rocks vary in composition from tonalite to diorite, and their precise ages are unknown. The plutons are surrounded by granitoid gneisses. The AA graphite deposit is located in a north-northeast-trending belt of metasediments running through the middle of the area covered by Figure 3-3-2. The northeast part of the area is underlain by Lower Cretaceous volcanic rocks. They are separated from intrusive rocks to the south by a regional thrust fault.

The granitoid gneisses are probably related to the intrusion of the plutons which they surround. They may represent strongly deformed intrusive material at the margins of plutons or they may have resulted from partial melting and deformation of the country rock. The metasedimentary sequences represent country rock to the intrusive complexes.

DEPOSIT GEOLOGY

The geology of the area surrounding the AA deposit is shown in Figure 3-3-3. The northern part of the map is dominated by moderately to strongly deformed granodioritic rocks. The southern part of the area is underlain by biotite-amphibole schists of metasedimentary origin. Locally, decametre to metre-scale mafic to ultramafic lenses, characterized by centimetre-scale concentrations of leucosomatic rims and crosscutting veins, may represent boudinaged mafic dikes intruding the schists and granodioritic rocks. Graphite-rich rocks outcrop in the central part of the map area, specifically in the crests of folds.

The dominant structural grain in the area is a subvertical north-northwest-trending foliation with decametre-scale folds (Figure 3-3-3). The dominant foliation trend is summarized in Figure 3-3-4. Late-kinematic folding synchronous with the development of retrograde chlorite has resulted in crenulation of this north-northwest foliation. Fold axes and resulting intersecting lineations are typically subvertical. Shear zones in the area are generally aligned with the regional foliation. Except for one extending over at least 700 metres (Figure 3-3-3), they can not be traced over any significant distance.

TABLE 3-3-2
CHEMICAL ANALYSES OF GRAPHITE-RICH ROCKS; AA GRAPHITE DEPOSIT, BRITISH COLUMBIA.

	G2/1-15	G10/2-86	G2/1-15DUP	G10/4-89	G10/1-84	G1/5-10	G2/1-16	G2/2-17	G6/2-48	G6/3-49	G10/2-85	G11, 1-94	G2/2-17/DUP
SiO ₂	66.34	64.41	66.66	66.00	62.59	65.14	59.49	62.95	47.61	58.67	64.42	70.34	64.63
Al ₂ O ₃	4.91	13.93	4.86	9.83	4.88	10.66	5.61	9.79	20.24	17.19	16.41	10.67	9.20
CaO	1.06	3.93	1.06	7.21	0.99	2.33	1.60	4.64	5.91	2.67	5.06	2.83	4.77
Cr ₂ O ₃	<0.01	<0.01	<0.01	<0.01	<0.01	<0.01	<0.01	<0.01	<0.01	<0.01	<0.01	<0.01	<0.01
Fe ₂ O ₃	4.06	3.87	4.02	3.76	2.23	3.46	2.78	2.06	9.24	6.99	3.14	1.33	2.14
K ₂ O	1.25	2.67	1.27	1.50	1.25	2.58	1.10	2.05	2.20	1.84	2.69	0.95	1.38
MgO	1.06	2.20	1.05	2.38	1.18	1.89	1.17	2.34	4.37	4.56	2.23	0.71	2.41
MnO	0.02	0.08	0.02	0.02	0.02	0.04	0.02	0.06	0.15	0.10	0.09	0.01	0.06
Na ₂ O	0.95	1.62	0.95	0.67	0.86	1.60	0.83	0.70	4.76	5.43	2.00	2.78	0.76
P ₂ O ₅	0.09	0.16	0.08	0.12	0.19	0.47	0.26	0.24	0.56	0.14	0.19	0.11	0.25
TiO ₂	0.37	0.42	0.37	0.41	0.30	0.57	0.21	0.41	1.07	0.43	0.41	0.12	0.41
LOI	19.60	6.02	19.49	9.65	24.51	9.35	26.83	13.46	2.32	1.24	3.13	10.59	13.61
C(gr)*	16.20	3.16	16.50	6.41	23.10	6.34	23.90	8.77	0.06	0.05	1.17	9.33	8.35
Ag **	0.2	<0.2	<0.2	<0.2	<0.2	<0.2	<0.2	<0.2	<0.2	<0.2	<0.2	<0.2	<0.2
Bi **	<5	<5	<5	<5	<5	<5	<5	<5	<5	<5	<5	5	<5
Cd **	2	7	1	<1	<1	6	<1	22	<1	<1	<1	1	21
Co **	189	57	191	61	35	36	45	79	67	53	32	54	78
Cr **	244	30	249	50	207	166	190	108	5	124	17	37	107
Cu **	342	114	338	84	11	136	349	124	118	188	55	37	129
Mo **	<1	12	<1	24	67	35	<1	37	<1	<1	8	24	37
Ni **	253	38	263	82	25	73	120	104	1	27	16	11	104
Pb **	44	54	40	56	38	74	54	78	134	194	240	206	42
Sr **	172	317	175	238	94	163	175	154	636	176	381	211	157
V **	287	469	296	925	1500	1827	300	1300	212	129	144	39	1320
Zn **	453	786	421	503	210	654	238	1681	133	121	239	106	1647

* graphitic carbon

** minor elements in ppm

GRANODIORITIC ROCKS

Granodioritic rocks in the area are generally coarser grained than the schists (2-5 mm grain size). The regional foliation, defined by a coarse layering of thin (<2 mm) biotite and/or amphibole-rich bands and thicker (>3 mm) quartzofeldspathic bands, is not as well expressed in these rocks as it is in the finer grained schists. The intensity of the foliation tends to decrease westwards within the granodiorite; to the northwest, the granodioritic body is essentially undeformed. In outcrop, weathered surfaces are typically yellowish white; fresh surfaces are pale to medium grey. The granodioritic rocks are more leucocratic than the schists although their mineralogy is similar except that clinopyroxene is found only in mafic and ultramafic lenses included in the granodiorite.

BIOTITE SCHISTS

Schists are usually fine to medium grained (0.5-2 mm) and display a penetrative schistosity, consistent with the regional trend and defined by the alignment of biotite and amphibole grains. These rocks weather pale grey to yellowish or brownish white. Fresh surfaces are medium to dark grey. They may display porphyroblastic textures; garnet and amphiboles are common porphyroblastic minerals. They are divided into two groups, garnet-bearing and garnet-free biotite-amphibole schists (Figure 3-3-3). Systematic trends in the distribution of these garnet-free and garnet-bearing schists suggest that the presence or absence of garnet is constrained by the bulk chemistry of the rock (aluminum content) rather than by variation in metamorphic conditions. The graphite deposit is hosted by the schists. Biotite,

hornblende, plagioclase, quartz, tremolite, actinolite, cummingtonite and clinopyroxene are the common constituent minerals of both garnet-bearing and garnet-free schists, although they may not all be present in the same rock. Sillimanite has been found in several outcrops in the southeastern part of the map area. Epidote (generally zoisite, rarely pistacite), chlorite, titanite and white mica are locally observed as minor constituents. Graphite, ilmenite, pyrite, chalcopyrite and sphalerite are the common opaque minerals and pyrrhotite has been observed as an included phase. Common accessory minerals are zircon, allanite and apatite.

Quartz and plagioclase are present in variable concentrations in all of the thin sections of schists examined. Plagioclase is locally replaced by fine-grained epidote and white mica. Biotite constitutes up to 20 volume per cent of the biotite schists. The orientation of biotite flakes generally defines the main foliation. In several instances, a late generation of biotite is developed along a later foliation. Bright red-brown biotite commonly forms less than 10 per cent of the volume in graphite-rich rocks where it is intergrown with graphite flakes (Plate 3-3-1). Green or greenish brown biotite occurs predominantly in the southern part of the mapped area. Garnet is present only locally. It generally comprises less than 5 volume per cent of the rock. It occurs in biotite-amphibole schists as strongly xenoblastic porphyroblasts (1-5 mm; in rare examples, up to 1 cm in diameter) commonly overgrown by biotite aligned with the regional schistosity. Late tectonic to post-tectonic chlorite and, less commonly, zoisite are also found as overgrowths on garnet porphyroblasts. In the southern part of the map area, it constitutes large, pre-tectonic porphyroblasts in aluminous, sillimanite-bearing schists. In all instances

garnet is pre-tectonic to early tectonic with respect to the main, regional foliation expressed in the rock. Several garnet-bearing rocks have been used to constrain metamorphic temperatures; the results are discussed below. Clinopyroxene is occasionally found as poikiloblastic relict crystals in amphibole-bearing schists. It is replaced by tremolite or hornblende. Also, it is associated with high-grade graphite concentrations where it is replaced by tremolite (Plate 3-3-2). Cummingtonite occurs as medium-sized (<2 mm) relict crystals representing less than 5 volume per cent of the schists. It is typically overgrown and replaced by tremolite (\pm actinolite) and, less commonly, by hornblende.

At least some of the cummingtonite and hornblende is present as prograde metamorphic phases. Cummingtonite has also been identified in several thin sections from

graphite-rich zones. Typically, euhedral hornblende (2–5 mm) comprises up to 15 volume per cent of the schists and colours vary from pale green to pale brown to dark brown-green. Together with biotite flakes, they define the principal foliation in the rock. The most common brownish green variety is optically zoned and often has a narrow actinolite rim (especially in strongly strained rocks). Less commonly, it is overgrown by biotite or tremolite. Locally it replaces clinopyroxene and is interpreted to be retrograde. Tremolite is fine to medium grained, generally acicular and overgrows cummingtonite, hornblende and clinopyroxene. It is interpreted as a retrograde phase.

Sillimanite represents trace to 5 volume per cent of the rock and occurs as fine prisms (2–3 mm in length and less than 500 μ m in width) aligned with the main foliation in biotite schists from the southern part of the area (Figure 3-3-3). Epidote is occasionally found in minor amounts overgrowing biotite, garnet or plagioclase. In several instances it forms fine-grained strings after biotite and is aligned with a late(?) foliation indicating syntectonic development. It was also observed in intergrowths with graphite in thin sections from graphite-rich rocks. Chlorite is pervasive as a minor retrograde phase after biotite or, less typically, after garnet. In one outcrop at the eastern margin of the map area, chlorite flakes are developed along a late cleavage which cuts and crenulates the regional foliation and is associated with outcrop-scale folds. This indicates

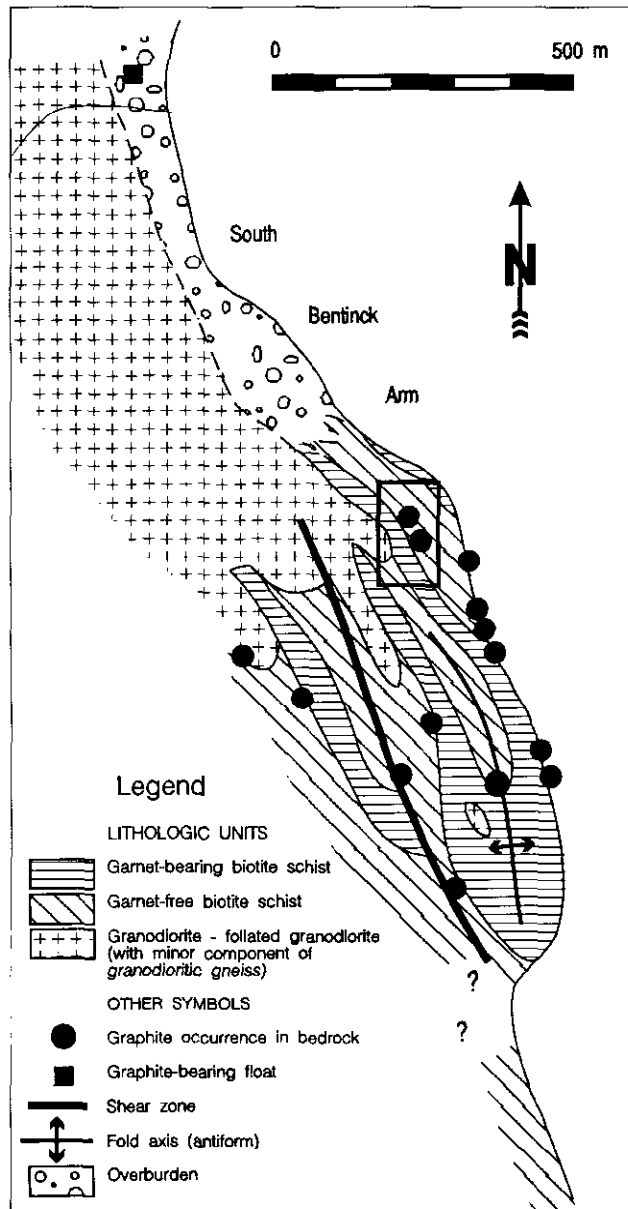


Figure 3-3-3. Local geology of the AA graphite deposit. Box is position of detailed map in Figure 3-3-5.

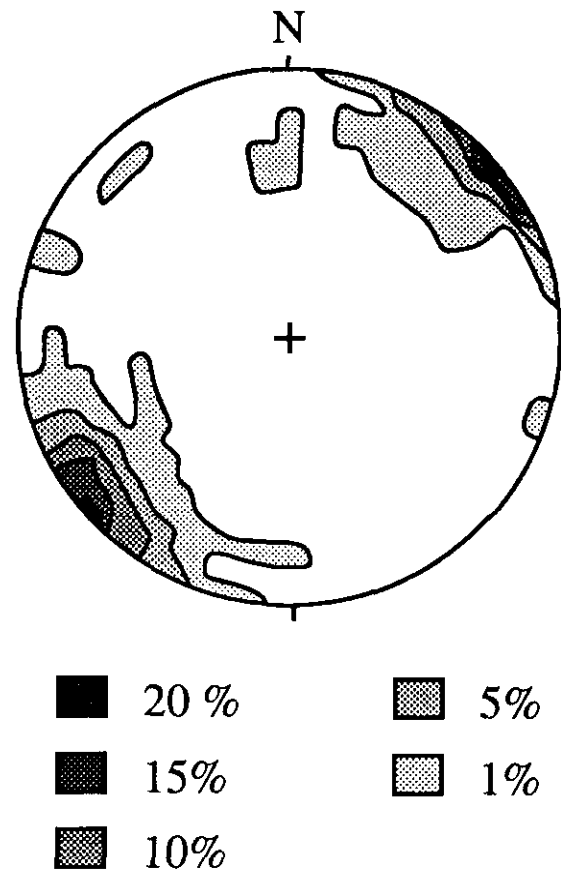


Figure 3-3-4. Stereonet projection of poles to main foliation in the area of the AA graphite deposit. n = 68.

that deformation was continuing during retrograde metamorphic recrystallization in rocks of the area. Chlorite is extensively developed in thin, post-tectonic veinlets.

Titanite is a relatively abundant (2–3 volume %) late phase in graphite-poor and graphite-free rocks where it is concordant with the regional foliation and developed at edges of hornblende and biotite grains. Traces of zircon are pervasive in the schists. It occurs in two varieties which often coexist in the same thin section. The first variety consists of large (200–500 μm), sometimes zoned, rounded to euhedral grains that are erratically distributed in the matrix. These are interpreted to be premetamorphic zircons. The second variety of zircon forms clots of very small (<100 μm) euhedral grains commonly found at the interface between biotite grains and other matrix minerals. The latter variety may overgrow euhedral zircon grains and is interpreted to be synmetamorphic.

Pyrite is found in two texturally distinct generations, commonly in rocks containing graphite. An early pyrite is present in trace concentrations, as fine-grained, subhedral to anhedral grains in the schists. It shows no particular textural association with graphite. Locally, it is overgrown and replaced by sphalerite. A late generation of pyrite is well

developed in graphite-bearing rocks where it may represent several volume per cent of the rock.

Graphite occurs in minor or trace amounts in biotite-amphibole schists throughout the area mapped. It is mainly present as fine to medium-sized, folded or kinked flakes aligned with the latest foliation and is often intergrown with concordant biotite (Plate 3-3-1) and, less commonly, with pyrite. Graphite occurs preferentially in garnet-free schists or at the contact between garnet-free schists and garnet-bearing schists or granodiorite (Figure 3-3-3). The association of chlorite with high concentrations of graphite in the crests of folds indicates that graphite formed during retrograde metamorphism. Also, some graphite precipitated during early retrograde metamorphism as indicated by the textural intergrowth of graphite and tremolite in clinopyroxene replacement textures (Plate 3-3-2).

A small amount of fine-grained, matte graphite is present along late shear zones cutting the regional foliation, and in narrow veins. This graphite formed during the last stages of retrograde metamorphism and stabilized at lower temperatures than the coarse flake graphite. The presence of pre-peak metamorphic graphite, early retrograde graphite and late retrograde graphite suggests that graphite precipitation took place during almost all stages of metamorphism.



Plate 3-3-1. Back-scattered electron micrograph of graphite-rich sample displaying close textural relationship between biotite (bt) and graphite (GP). Also shown is late, optically zoned pyrite (PY2) developed at the contact between graphite-rich and graphite-free layers. Width of field is 2.5 millimetres.



Plate 3-3-2. Natural light photomicrograph of sample G6/12-62 showing textural relationship between clinopyroxene, tremolite and graphite. See text for discussion. Width of field is 0.8 millimetres.

GRAPHITE-RICH ROCKS

Graphite-rich rocks are dark grey or rusty brown on weathered surfaces and locally characterized by a thin jarosite coating. Fresh surfaces are steel grey. The rocks are layered and have a lepidoblastic texture. Graphite occurs as flakes within the schists. Grades, expressed in terms of graphitic carbon content, are given in Table 3-3-2 (see also Figures 3-3-5 and 3-3-6). Individual layers may be graphite-rich or nearly barren. The graphite-rich rocks are soft and split along a foliation defined by the alignment of graphite flakes. Individual graphite flakes measure from 0.3 to 1.5 millimetres in diameter. The concentration of graphitic carbon reaches up to 24 weight per cent (Table 3-3-2 and Figures 3-3-5 and 3-3-6). The flakes have a metallic lustre, but locally are dull, indicating a lower degree of crystallinity.

Other major constituents, present in variable proportions, are quartz, feldspar, biotite and hornblende. Pyrite, either anhedral and optically zoned or cubic and unzoned, sphalerite and chalcopyrite comprise up to 5 per cent of the rock volume. The late-stage pyrite is the most abundant sulphide and occurs as optically zoned, medium to fine-grained patches in close textural association with graphite (Plate 3-3-3). Microprobe investigation of the optically zoned crystals reveals no variation in trace elements. The zoning is interpreted a result of to be variations in oxidation (de-sulphidation) of pyrite from core to rim. This zoned pyrite is intimately associated with sphalerite (Plates 3-3-4 and 3-3-3). Late pyrite also overgrows strongly resorbed pyrrhotite (Plate 3-3-3). It is also concentrated at the boundary between graphite-rich and graphite-free layers (Plate 3-3-1). These observations indicate that this pyrite and, by association, sphalerite, grew late with respect to graphite crystallization. Pyrrhotite has been identified in one sample as resorbed cores in late, optically zoned pyrite grains (Plate 3-3-3). Texturally, it appears to be associated with graphite flakes. Chalcopyrite is found in trace amounts, in rocks which also contain late pyrite and sphalerite. Sphalerite is present almost exclusively in graphite-bearing rocks as anhedral, undeformed grains. It is commonly associated with late pyrite. The base metal content of the graphite-rich samples is anomalous (Table 3-3-2), but not of economic interest. Sphalerite, chalcopyrite and zoned pyrite post-date graphite. Subhedral, bright pink to pale brown pleochroic titanite is a common mineral in graphitic rocks. Other minerals present in trace amounts are zircon and allanite. Biotite and sulphides are locally intergrown with graphite flakes. High-grade, coarse, crystalline graphite is found in the noses of outcrop-scale folds. Matte, finely crystalline graphite concentrations are also found in shear zones and late, post-ductile deformation veins (Plate 3-3-4).

PETROLOGIC INTERPRETATION

The presence of metamorphic clinopyroxene in hornblende-bearing rocks indicates minimum peak metamorphic temperatures were in excess of 750°C, consistent with granulite-grade metamorphism (Spear, 1981). In addition, garnet-biotite thermometry was used to constrain metamorphic conditions. Garnets from sillimanite-bearing

rocks exhibit a very gently decreasing Fe/Fe+Mg trend from core to rim that is consistent with increasing ambient temperature. It is interpreted to represent prograde zoning (Spear, 1991). The calculated peak metamorphic garnet-biotite temperature is $825 \pm 25^\circ\text{C}$ at a pressure of 750 ± 100 MPa (7.5 ± 1 Kbar) using the garnet-sillimanite-quartz-plagioclase barometer (Figure 3-3-7a), indicating conditions of granulite facies metamorphism.

Garnets from sillimanite-free, hornblende-bearing rocks display unzoned cores and increasing Fe/Fe+Mg trends at their rims. This is interpreted to be the result of diffusional re-equilibrium near the peak of metamorphism or during subsequent cooling (Spear, 1991). Calculated garnet-biotite temperatures for three sillimanite-free hornblende-bearing

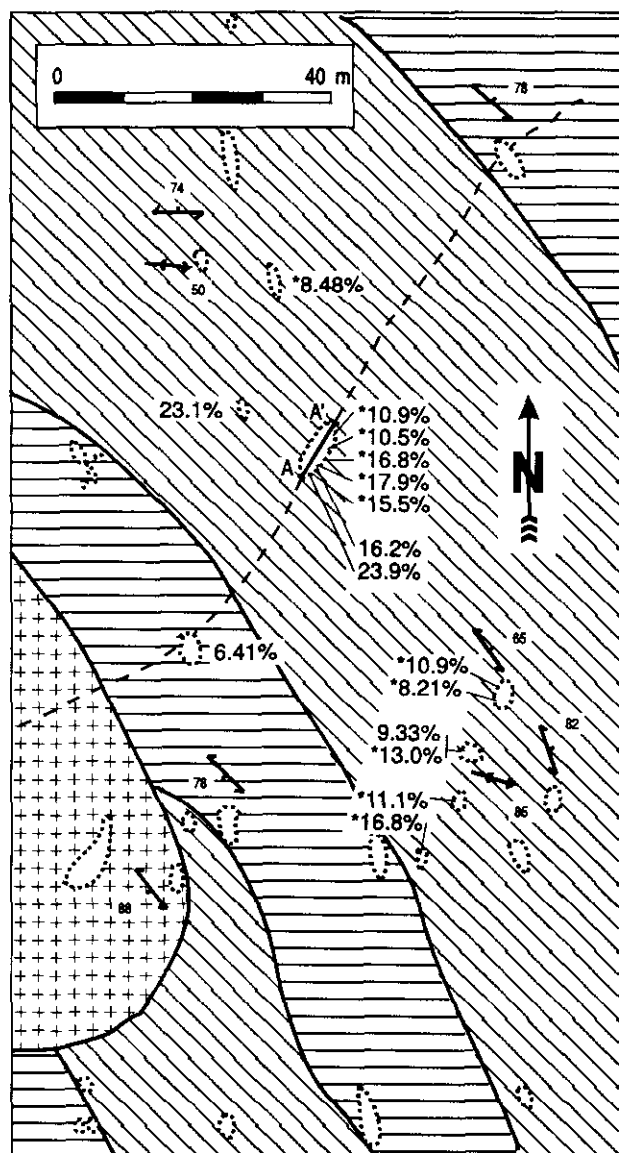


Figure 3-3-5. Detail of Figure 3-3-3 showing geology around the AA graphite deposit and graphitic-carbon contents from a number of trenches. A-A' is position of cross-section in Figure 3-3-6. * = data from Demczuk and Zbitnoff (1991).

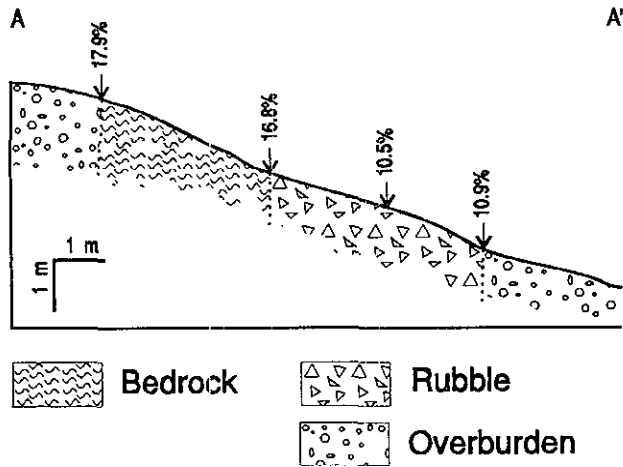


Figure 3-3-6. Cross-section through Trench 1 of the graphite deposit showing weight percentage of graphitic carbon. See Figure 3-3-5 for location.

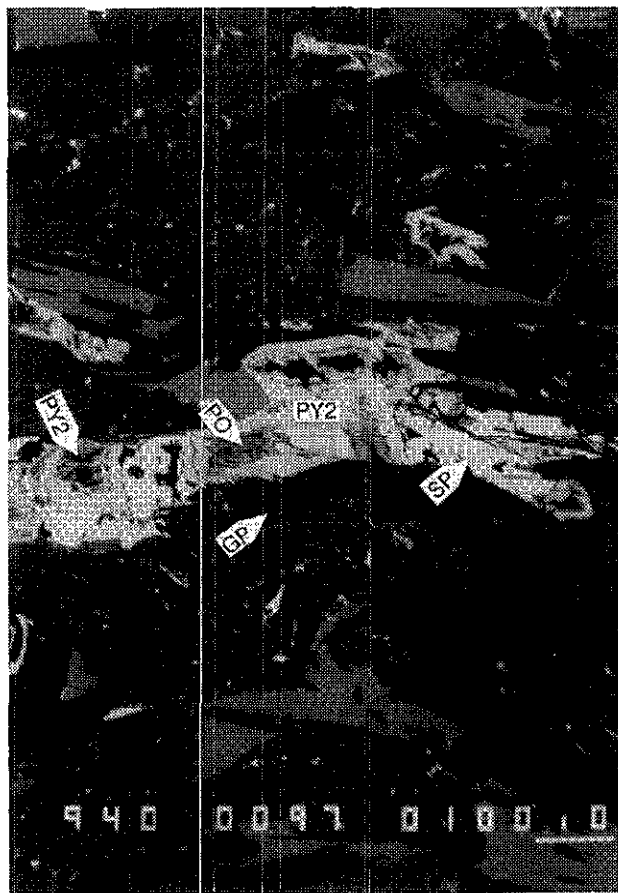


Plate 3-3-3. Back-scattered electron micrograph of late pyrite (PY2) cored by pyrrhotite (PO) and intergrown with sphalerite (SL). Note the close association of sulphides with graphite flakes (black). Scale bar is 100 microns.

rocks from different parts of the map area fall between 725° and 875°C, consistent with the presence of clinopyroxene and the sillimanite-schist calculated temperature (Figure 3-3-7b). Rare inclusions of graphite within these garnets suggest that some graphite persisted through metamorphic conditions well into the granulite field. Calculated retrograde (rim) temperatures for garnet-hornblende assemblages, Figure 3-3-7c, are consistently lower than garnet core - biotite temperatures. The stability field of titanite, as determined by Spear (1991), suggests that the graphite in equilibrium with titanite crystallized below 700°C, assuming a pressure of 500 MPa.

Replacement of clinopyroxene or cummingtonite by hornblende indicates that hornblende recrystallized extensively during the retrograde stages of metamorphism. Retrograde graphite is locally closely intergrown with tremolite (Plate 3-3-2), but such an association has not been found between graphite and hornblende. Clinopyroxene break-

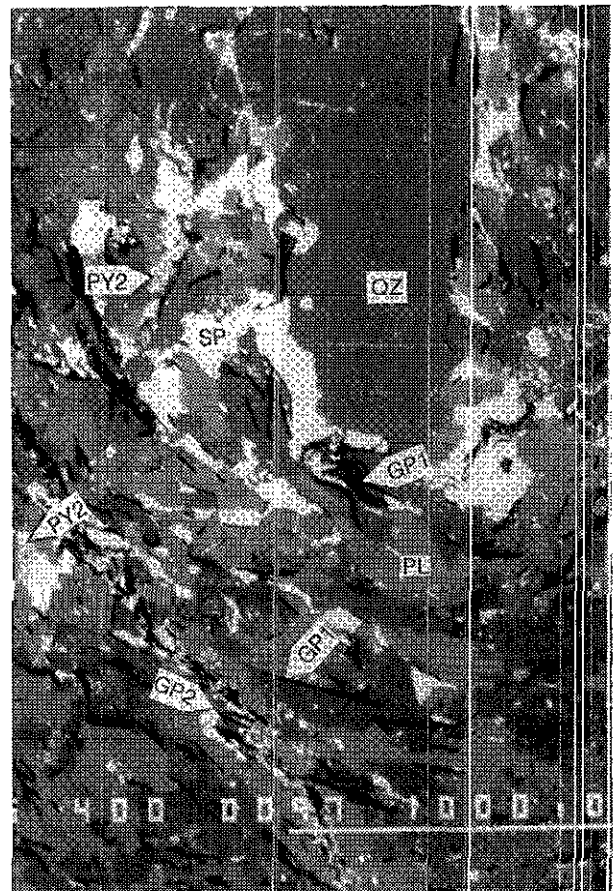


Plate 3-3-4. Back-scattered electron micrograph of graphite-bearing sample. (Brightness is proportional to density: GP1: pre to syntectonic graphite; GP2: post-tectonic vein graphite; SP: sphalerite; PY2: late pyrite; QZ: quartz; PL: plagioclase.) Quartz is concentrated in the core of a fold. Pre or syntectonic graphite coexists with post-tectonic graphite in a late vein. Coexistence of early and late pyrite is also shown (see text). Notice sphalerite concentration near graphite-free core part of fold. Scale bar is 1000 microns (1 mm).

down to tremolite occurs between 500° and 600°C, assuming $X_{CO_2} = 0.25$ and 0.75 (Tracy and Frost, 1991). This provides an upper temperature limit for the formation of retrograde graphite consistent with that calculated from garnet-hornblende retrograde temperatures.

ORIGIN OF GRAPHITE MINERALIZATION

There are a number of possible sources of carbon from which the graphite may have originated:

- *in situ* reduction of organic matter during metamorphism;
- devolatilization of organic matter to produce CO_2 or CH_4 (or both) in the fluid phase;
- destabilization of early graphite to produce carbon-bearing volatiles (CO_2 and CH_4);
- decarbonation of carbonate minerals;
- injection of carbon-bearing fluids from the deep crust or mantle;
- a combination of the above.

In and around the deposit, low concentrations of prograde metamorphic graphite were probably derived by *in situ* graphitization of organic matter concentrated in discrete layers. Retrograde graphite involved migration of carbon dioxide and/or methane-bearing fluids prior to graphite precipitation. The fluids were derived from oxidation of pre-existing graphite or from the devolatilization of carbonate minerals. Calculations by Ohmoto and Kerrick (1977) indicate that the reaction:

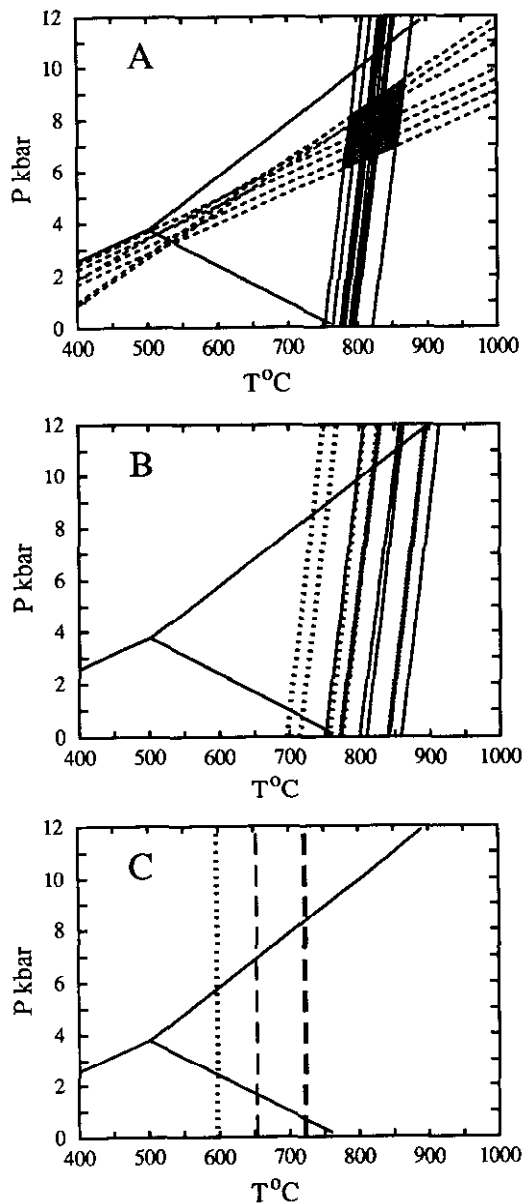


will proceed to the right with increasing temperature, favouring fluid enrichment in methane in a reducing environment and carbon dioxide in an oxidizing environment, at the expense of graphite. Hence, in a prograde metamorphic environment in which dehydration reactions take place, carbon will be concentrated in the fluid phase. Concentration of carbon in the fluid phase during prograde metamorphism followed by precipitation of graphite on cooling could account for remobilization and high graphite concentrations in permeable channels such as the crests of folds. Graphite could also have precipitated by the mixing of two fluids, one with a high X_{CO_2} and the other with either a high X_{H_2O} and/or X_{CH_4} . The hypothesis is based on a curved stability field of graphite in the C-O-H phase relation, as described by Rumble *et al.* (1982).

SUMMARY AND CONCLUSIONS

GENESIS OF GRAPHITE

The AA graphite deposit is hosted by metasedimentary biotite and biotite-hornblende schists intruded by granodioritic rocks. Medium to coarse-grained, premetamorphic graphite found as concentrations in discrete beds in the schists and as inclusions in prograde metamorphic minerals was subjected to temperatures in excess of 800°C at 750 MPa. This is well within the range of granulite facies metamorphism. Medium to coarse-grained, retrograde, syn-



Biotite - garnet (Ferry and Spear, 1978;
Hodges and Spear, 1982)

Hornblende - garnet (Graham and Powell, 1984)

Garnet - sillimanite - plagioclase - quartz
(Newton and Hazelton, 1981; Hodges and Spear,
1982; Ganguly and Saxena, 1984; Hodges and
Crowley, 1985)

Figure 3-3-7. (a) Calculated K_{eq} isopleths for iron-magnesium exchange between biotite and garnet and for the reaction: $2 \text{ anorthite} = 2 \text{ grossular} + \text{ sillimanite} + 4 \text{ quartz}$, for sillimanite-bearing, hornblende-free biotite schist. (b) Calculated K_{eq} isopleths for iron-magnesium partitioning between biotite and garnet for three hornblende-bearing biotite-schists from the AA graphite deposit area. (c) Calculated K_{eq} isopleths for iron-magnesium partitioning between garnet and hornblende for three hornblende-bearing biotite-schists from the AA graphite deposit area.

tectonic graphite precipitated in the 500° to 700°C temperature range, as constrained by the textural associations between graphite and the minerals hornblende, tremolite and titanite. Concentration of syntectonic, early retrograde graphite at the crests of outcrop-scale folds indicates a structural control on graphite mineralization. Fine-grained graphite, post-dating ductile deformation, concentrated in shear zones and thin veins is the latest graphite generation observed in the area. It formed at low temperatures, consistent with the development of coexisting chlorite. This suggests that graphite mineralization took place through a wide range of temperatures during retrograde metamorphism.

EXPLORATION IMPLICATIONS

This study indicates that medium to high-grade crystalline flake graphite concentrations can be found within metasedimentary roof pendants of the Coast Plutonic Complex. Peak metamorphic conditions near the AA deposit reached granulite facies. The degree of crystallinity of natural graphite is directly related to the grade of metamorphism. High-grade graphite mineralization at the AA deposit is partly prograde metamorphic and partly retrograde metamorphic in origin. Because of the retrograde nature of some of the graphite and common intergrowths with micas, it is recommended that metallurgical studies be performed in the early stages of deposit evaluations. At the AA deposit, graphite-rich rocks occur along the crests of folds, a feature that is commonly observed in most of the eastern Canadian crystalline flake graphite deposits. Fold axes are vertical here, indicating that graphite-rich zones will be steeply plunging. Attention should be given to similar settings where fold axes plunge more gently to maximize efficient recovery by open-pit mining. Detailed investigation of graphite grade, continuity of graphite-bearing rocks, deposit size, shape and tonnage are beyond the scope of this work.

Granulite facies metamorphism is considered rare in the Coast Plutonic Complex. Only three other locations have been identified in a recent compilation by Read *et al.* (1991). This study may indicate that rocks of granulite facies could be more abundant than previously recognised. Prograde metamorphic graphite, if present in such metamorphic conditions, would have an excellent degree of crystallinity. In summary, there is excellent geological potential for economic crystalline flake graphite deposits within schists of the Coast Plutonic Complex.

ACKNOWLEDGMENTS

J.A. Roddick of the Geological Survey of Canada kindly provided preliminary information on the regional geology. J.M. Newell, B.C. Geological Survey Branch, and J.A. Roddick, Geological Survey of Canada, improved earlier versions of this manuscript.

REFERENCES

Baer, A.J. (1973): Bella Coola - Laredo Sound Map-areas, British Columbia; *Geological Survey of Canada*, Memoir 372, 122 pages.
 Demczuk, L. and Zbitnoff, G.W. (1991): Geological and Geochemical Assessment Report on the AA 1-22 Claim Group;

B.C. Ministry of Energy, Mines and Petroleum Resources, Assessment Report 21,649.
 Ferry, J.M. and Spear, F.S. (1978): Experimental Calibration of the Partitioning of Fe and Mg between Biotite and Garnet; *Contributions to Mineralogy and Petrology*, Volume 66, pages 113-117.
 Ganguly, J. and Saxena, S.K. (1984): Mixing Properties of Aluminosilicate Garnets: Constraints from Natural and Experimental Data, and Applications to Geothermobarometry; *American Mineralogist*, Volume 69, pages 88-97.
 Graham, C.M. and Powell, R. (1984): A Garnet-Hornblende Geothermometer: Calibration, Testing and Application to the Pelona Schist, Southern California; *Journal of Metamorphic Geology*, Volume 2, pages 13-21.
 Hand, G.P. (1992): Graphite; *Mining Engineering*, pages 560-561.
 Harries-Rees, K. (1992): Refractory Majors; *Industrial Minerals* Number 300, pages 23-43.
 Hodges, K.V. and Crowley, P.D. (1985): Error Estimation and Empirical Geothermobarometry for Pelitic Systems; *American Mineralogist*, Volume 70, pages 702-709.
 Hodges, K.V. and Spear, F.S. (1982): Geothermometry Geobarometry and the Al₂SiO₅ Triple Point at Mt. Moosilauke, New Hampshire; *American Mineralogist*, Volume 67, pages 1118-1134.
 Holroyd, W.G. and McCracken, W.H. (1992): Refractory Materials from China; *Industrial Minerals*, Number 293, pages 59-67.
 Kenan, W.M. (1992): Carbon and Changing Technologies; in Proceedings, Industrial Minerals '92, Toronto, *Blondon Information Services*, pages
 Newton, R.C. and Haselton, H.T. (1981): Thermodynamics of the Garnet-Plagioclase-Al₂SiO₅-Quartz Geobarometer; in Newton, R. C. *et al.*, Editors, Thermodynamics of Minerals and Melts, *Elsevier*, New York, pages 131-147.
 Ohmoto, H. and Kerrick, R. (1977): Devolatilization Equilibria in Graphitic Systems; *American Journal of Science*, Volume 277, pages 1013-1044.
 Read, P.B., Woodsworth, G.T., Greenwood, H., Grant, E.D. and Evenchick, C.A. (1991): Metamorphic Map of the Canadian Cordillera; *Geological Survey of Canada*, Map 1714A.
 Roddick, J. (in preparation): Rivers Inlet; *Geological Survey of Canada*, Open File Map.
 Rumble D., Ferry, J.M., Hoering, T.C. and Bouclet, A.J. (1982): Fluid Flow During Metamorphism at the Beaver Brook Fossil Locality, New Hampshire; *American Journal of Science*, Volume 282, pages 886-919.
 Simandl, G.J. (1992): Gîtes de Graphite de la Région de Gatineau; unpublished Ph.D. thesis, *École Polytechnique de Montréal*, 359 pages.
 Simandl, G.J., Jakobsen, D. and Fischl, P. (1992): Refractory Mineral Resources in British Columbia, Canada; *Industrial Minerals*, Number 296, pages 67-77.
 Spear, F.S. (1981): An Experimental Study of Hornblende Stability and Compositional Variability in Amphibolite; *American Journal of Science*, Volume 281, pages 697-714.
 Spear, F.S. (1991): On the Interpretation of Peak Metamorphic Temperatures in Light of Garnet Diffusion During Cooling; *Journal of Metamorphic Geology*, Volume 9, pages 379-388.
 Taylor, H.A., Jr. (1992): Graphite (Natural); in Mineral Commodity Summaries 1992, *U.S. Department of Interior, Bureau of Mines*, pages 76-77.
 Tracy, R.J. and Frost, B.R. (1991): Phase Equilibria and Thermobarometry of Calcareous, Ultramafic and Mafic rocks and Iron formations; in Contact Metamorphism, Kerrick, D.M., Editor, *Reviews in Mineralogy*, Volume 26, pages 207-290.

NOTES



**1992 REGIONAL GEOCHEMICAL SURVEY PROGRAM:
REVIEW OF ACTIVITIES**

By W. Jackaman

KEYWORDS: Regional Geochemical Survey, reconnaissance, multi-element, stream sediment, stream water, Mount Waddington, Taseko Lakes, Bonaparte Lake, Skagway, Yakutat, Tatshenshini, Hope, Ashcroft, Pemberton.

INTRODUCTION

During the past twelve months, the British Columbia Regional Geochemical Survey Program (RGS) has continued to develop, maintain and disseminate a comprehensive geochemical database. Additions to the RGS database have included results from reconnaissance-scale stream-sediment and water programs conducted in areas not previously surveyed and, as part of the RGS Archive Program, new analytical data for sediment pulps saved from RGS programs conducted prior to 1986. Currently, the database contains multi-element determinations for stream-sediment and water samples, field observations and sample location information for 39 000 sample site locations covering over 65 per cent of the province (Figure 4-1-1 and Table 4-1-1). The data are used in the exploration and development of the province's mineral resources, resource management and land-use planning, and environmental assessments.

Activities conducted during 1992 include:

- Publication of results from the 1991 RGS program conducted in the Mount Waddington (NTS 92N) map area.
- Publication of new analytical results from joint federal-provincial surveys originally conducted on map sheets Taseko Lakes (NTS 92O) and Bonaparte Lake (NTS 92P) during 1979.
- Completion of RGS programs conducted on map sheets Skagway (NTS 104M), Yakutat (NTS 114O) and Tatshenshini (NTS 114P).

- Preparation of RGS data packages presenting new analytical results from joint federal-provincial surveys previously conducted on map sheets Hope (NTS 92H), Ashcroft (NTS 92I) and Pemberton (NTS 92J).

**1992 RGS RELEASE – CENTRAL B.C.
(92N, 92O, 92P)**

Despite a recent decline in mineral exploration activity in British Columbia, the July 7 release of RGS Open File 34 – Mount Waddington (NTS 92N), RGS Open File 35 – Taseko Lakes (NTS 92O) and RGS Open File 36 – Bonaparte Lake (NTS 92P) received a positive response. Over 75 data packages have been distributed and several companies have actively pursued identified RGS anomalies.

The data packages present multi-element determinations for stream sediments and waters, field observations, sample location information, bedrock associations, statistics and data analyses for 2568 sample sites covering 15 000 square kilometres in central British Columbia. Results identified 38 sample sites with gold values exceeding 100 ppb and 57 sample sites listing copper values greater than 100 ppm (Jackaman *et al.*, 1992a, b, c).

A review of staking activity during the period of July to August found that 65 per cent of the 831 claim units recorded are directly associated with RGS anomalies. Table 4-1-2 lists the claim status of the top ten single-element gold anomalies, top ten single-element copper anomalies and the top ten multi-element base and precious metal anomalies located in the survey areas. Although RGS anomalies were staked immediately following the release, numerous areas with anomalous concentrations for both precious and base metal values remain open as of September 1. Field site visits have resulted in the discovery of mineralization in bedrock in several drainage basins with RGS anomalies (Sibbick and Delaney, 1993, this volume).

**1992 RGS – NORTHWEST B.C.
(104M, 114O, 114P)**

As part of the Ministry of Energy, Mines and Petroleum Resources contribution to the Corporate Resource Inventory Initiative (CRII), a reconnaissance-scale stream-sediment and water survey was conducted in northwestern British Columbia. The objective of the 1992 RGS program is to provide a geochemical database which will assist in the evaluation of the mineral potential of this relatively unexplored region.

SAMPLE COLLECTION

McElhanney Engineering Services Limited (Surrey) was selected by competitive bid to collect stream-sediment samples, stream-water samples and field observations in the

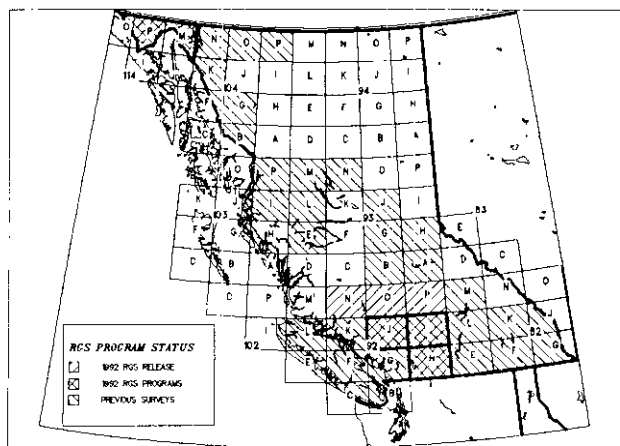


Figure 4-1-1. Current status of RGS program.

TABLE 4-1-1
SUMMARY OF RGS DATABASE

MAP	RGS OF	COLLECTION			ROUTINE		ADDITIONAL ANALYSES	RELEASE		
		GSC OF	YEAR	SITES	SUITE	YEAR		INAA	YEAR	
82E	RGS 29	OF 409	1976	1545	•			1977	•	1991
82F	RGS 30	OF 514	1977	1318	•	Sn,Hg		1978	•	1991
82G	RGS 27		1990	924	•	Sn,W,Hg,As,Sb,Cd,V,LOI,F,Bi,Cr		1991	•	1991
82J	RGS 28		1990	588	•	Sn,W,Hg,As,Sb,Cd,V,LOI,F,Bi,Cr		1991	•	1991
82K	RGS 31	OF 515	1977	1225	•	Sn,W,Hg		1978	•	1991
82L	RGS 32	OF 410	1976	1309	•			1977	•	1991
82M	RGS 33	OF 516	1977	1151	•	Hg		1978	•	1991
92B/C	RGS 24	OF 2182	1989	599	•	Sn,W,Hg,As,Sb,Cd,V,LOI,F,Bi,Cr,Au		1990		
92E	RGS 21	OF 2038	1988	386	•	Sn,W,Hg,As,Sb,Ba,Cd,V,LOI,F,Bi,Cr,Au		1989		
92F	RGS 25	OF 2183	1989	909	•	Sn,W,Hg,As,Sb,Cd,V,LOI,F,Bi,Cr,Au		1990		
92G	RGS 26	OF 2184	1989	855	•	Sn,W,Hg,As,Sb,Cd,V,LOI,F,Bi,Cr,Au		1990		
92H	RGS 07	OF 865	1981	941	•	Hg,W,As,Sb		1982	•	1993
92I	RGS 08	OF 866	1981	572	•	Hg,W,As,Sb		1982	•	1993
92J	RGS 09	OF 867	1981	805	•	Hg,W,As,Sb		1982	•	1993
92K	RGS 22	OF 2039	1988	1216	•	Sn,W,Hg,As,Sb,Ba,Cd,V,LOI,F,Bi,Cr,Au		1989		
92L/102I	RGS 23	OF 2040	1988	1144	•	Sn,Hg,W,As,Sb,Ba,Cd,V,LOI,F,Bi,Cr,Au		1989		
92N	RGS 34		1991	868	•	Sn,W,Hg,As,Sb,Cd,V,LOI,F,Bi,Cr,SO4		1992	•	1992
92O	RGS 35		1979	935	•	Hg,W,As		1980	•	1992
92P	RGS 36		1979	913	•	Hg,W,As		1980	•	1992
93A	RGS 05	OF 776	1980	1226	•	Hg,W,As,Sb		1980	•	FUTURE
93B	RGS 06	OF 777	1980	715	•	Hg,W,As,Sb		1980	•	FUTURE
93E	RGS 16	OF 1360	1986	1112	•	Hg,W,As,Sb,Ba,Cd,LOI,Au		1987		
93G	RGS 13	OF 1214	1984/85	1095	•	Sn,W,Hg,As,Sb,Ba,Cd,V,LOI		1986	•	FUTURE
93H	RGS 14	OF 1215	1984/85	1119	•	Sn,W,Hg,As,Sb,Ba,Cd,V,LOI		1986	•	FUTURE
93J	RGS 15	OF 1216	1985	1088	•	Sn,W,Hg,As,Sb,Ba,Cd,V,LOI		1986	•	FUTURE
93L	RGS 17	OF 1361	1986	1093	•	Sn,W,Hg,As,Sb,Ba,Cd,V,LOI,F,Au		1987		
93M	RGS 10	OF 1000	1983	1035	•	Hg,W,As,Sb		1984	•	FUTURE
93N	RGS 11	OF 1001	1983	1061	•	Hg,W,As,Sb		1984	•	FUTURE
103M/J	RGS 01	OF 772	1978	2216	•	Hg,W,AS		1979	•	FUTURE
103O/P	RGS 02	OF 773	1978	1784	•	Hg,W,AS		1979	•	FUTURE
104B	RGS 18	OF 1645	1987	661	•	Sn,W,Hg,As,Sb,Ba,Cd,V,LOI,F,Bi,Cr,Au		1988		
104F/G	RGS 19	OF 1646	1987	1218	•	Sn,W,Hg,As,Sb,Ba,Cd,V,LOI,F,Bi,Cr,Au		1988		
104K	RGS 20	OF 1647	1987	847	•	Sn,W,Hg,As,Sb,Ba,Cd,V,LOI,F,Bi,Cr,Au		1988		
104M			1992	748	•	Hg,As,Sb,Cd,V,LOI,F,Bi,SO4		1993	•	1993
104N	NGR 28	OF 517	1977	885	•	Sn,W,Hg		1978	•	FUTURE
104O	NGR 41	OF 561	1978	892	•			1979	•	FUTURE
104P	NGR 42	OF 562	1978	802	•			1979	•	FUTURE
104M	NGR 42	OF 562	1978	802	•			1979	•	FUTURE
114O/P			1992	1069	•	Hg,As,Sb,Cd,V,LOI,F,Bi,SO4		1993	•	1993

ROUTINE SEDIMENT ANALYTICAL SUITE : Zn, Cu, Pb, Ni, Co, Ag, Mn, Fe, Mo, U
ROUTINE WATER ANALYTICAL SUITE : U, F, pH
INAA SEDIMENT ANALYTICAL SUITE : Au, Sb, As, Ba, Br, Ce, Cs, Cr, Co, Hf, Fe, La, Lu, Mo, Ni, Rb, Sm, Sc, Na, Ta, Tb, Th, W, U, Yb, Zr

areas surveyed. Base camps and sample processing facilities were set up in Atlin. British Columbia and at the Government of Yukon highways maintenance camp located on the Haines Highway. Crews, stationed at each camp included a pilot, two samplers and a camp manager responsible for cataloguing and field processing of the samples. Helicopter support was provided by Trans North Air Limited and Vancouver Island Helicopters Limited. The program commenced on July 27 with the mobilization of crews to the base camps and was completed on August 22 with the delivery of the samples to a laboratory in Burnaby. Ministry

representation by the author was maintained throughout the program to ensure all aspects of the sample collection, data recording, sample drying, packing and shipping were in accordance with standards set by the National Geochemical Reconnaissance Program.

A total of 1924 stream-sediment and stream-water samples were systematically collected from 1817 sample sites. Field-site duplicate samples were routinely collected at 107 sites. The survey covered an area of approximately 16 500 square kilometres at an average density of one sample site every 9.5 square kilometres. The program also included the

TABLE 4-1-2
TOP RGS ANOMALIES FOR MAP SHEETS 92N, 92O AND 92P

Au STATUS				Cu STATUS				Au-Sb-As-Hg-Ag STATUS				Cu-Pb-Zn-Ag STATUS			
MAP	ID	(ppb)	STATUS	MAP	ID	(ppm)	STATUS	MAP	ID	(anomaly rating*)	STATUS	MAP	ID	(anomaly rating)	STATUS
			June Sept				June Sept				June Sept				June Sept
92N14	917034	3130	staked staked	92N11	915315	471	open open	92N05	915125	9	open staked	92N12	911229	9	open staked
92N13	915220	557	open staked	92N14	913100	330	open staked	92N10	915307	9	open open	92N05	915125	9	open staked
92N10	913024	407	open open	92N06	911157	325	staked staked	92N01	913028	8	open open	92N12	915253	9	open staked
92N08	913190	375	open open	92N10	817133	289	open open	92N14	913085	7	staked staked	92N10	913008	8	open open
92N08	913137	353	open open	92N05	915133	285	open open	92N08	913137	7	open open	92N14	913100	8	open staked
92N10	913057	296	staked staked	92N10	913008	236	open open	92N15	911279	7	open open	92N10	917133	8	staked staked
92N16	917018	164	open open	92N14	913085	225	staked staked	92N01	913026	7	open open	92N11	915315	8	open open
92N05	911078	164	open open	92N11	911244	176	open open	92N08	913130	6	staked staked	92N11	915280	7	open staked
92N10	911014	130	staked staked	92N14	917038	170	open open	92N05	917025	6	open open	92N05	915124	6	open staked
92N05	915122	120	open open	92N14	917036	146	staked staked	92N14	917034	6	staked staked	92N08	913131	6	open open
92O02	795362	588	staked staked	92O03	793134	1100	staked staked	92O03	793135	15	staked staked	92O03	793136	9	staked staked
92O02	795400	484	open open	92O03	795297	675	staked staked	92O03	793137	14	staked staked	92O03	795194	9	staked staked
92O16	795414	369	open open	92O02	793054	400	staked staked	92O01	795695	12	staked staked	92O03	793135	8	staked staked
92O13	795024	357	staked staked	92O02	793055	390	staked staked	92O06	795305	12	staked staked	92O03	793137	8	staked staked
92O07	795311	337	open staked	92O03	795287	310	staked staked	92O03	793136	11	staked staked	92O03	795288	8	staked staked
92O15	795430	319	open open	92O03	795464	240	staked staked	92O01	791008	10	open open	92O03	795502	8	staked staked
92O05	795071	293	open open	92O03	795285	240	staked staked	92O11	795045	10	staked staked	92O06	795306	8	staked staked
92O15	795431	277	open open	92O03	795465	230	staked staked	92O02	793055	10	staked staked	92O03	795499	8	staked staked
92O05	795135	276	open open	92O01	795695	210	staked staked	92O07	795395	9	open open	92O03	795388	7	staked staked
92O05	793147	269	staked staked	92O01	795696	210	staked staked	92O01	795646	9	staked staked	92O03	795389	7	staked staked
92P01	795319	251	staked staked	92P08	793300	200	open open	92P08	795278	10	staked staked	92P01	795310	11	reserve reserve
92P08	791189	247	staked staked	92P09	791132	182	staked staked	92P09	795111	10	staked staked	92P08	795291	10	open open
92P01	791212	222	staked staked	92P08	795278	178	staked staked	92P07	791119	9	open open	92P01	791234	9	staked staked
92P01	795318	200	staked staked	92P09	791131	174	staked staked	92P09	791132	9	staked staked	92P08	795238	9	staked staked
92P01	791214	190	staked staked	92P09	795111	166	staked staked	92P08	795333	9	staked staked	92P16	793192	9	staked staked
92P08	791148	140	open open	92P09	795118	166	staked staked	92P08	791148	9	open open	92P08	795296	9	open open
92P09	795111	130	staked staked	92P09	795269	156	open open	92P08	795283	9	staked staked	92P16	793216	9	open open
92P08	791166	130	open open	92P01	791213	154	staked staked	92P08	791120	8	open open	92P09	795118	9	staked staked
92P14	795013	120	open open	92P01	795318	146	staked staked	92P01	791234	8	staked staked	92P09	791132	8	staked staked
92P08	791126	120	open staked	92P06	795084	144	staked staked	92P09	791154	8	staked staked	92P16	793128	8	park park

(* after Jackaman *et al.*, 1992a,b,c)

collection of 40 stream-sediment and water samples in Atlin Provincial Park and Recreation Area. Ninety-eight per cent of the sample sites were accessed by helicopter and the remaining 2 per cent by truck.

The majority of primary and secondary drainage basins having catchment areas of less than 10 square kilometres were sampled. At each site samples weighing 1 to 2 kilograms were collected within the active (subject to flooding) stream channel and placed in kraft-paper bags. Unfiltered water samples free of suspended material were collected in 250-millilitre bottles. Field observations regarding sample media, sample site and local terrain were recorded and, to assist follow-up, aluminum tags inscribed with a unique RGS sample identification number were fixed to permanent objects, when available, at each site.

Stream-sediment samples were primarily composed of fine-grained material mixed with varying amounts of coarse sand and gravel, glacial sediments and organic material. Changes in sample composition often reflected physiographic variations in the survey area. Primary physiographic zones in northwest British Columbia include the St. Elias Mountains, the Coast Mountains and the Tagish Highlands (Holland, 1976). Most of the survey area is characterized by extremely rugged mountains largely covered with glaciers and snowfields. Creeks in these areas tend to be fast flowing and are often charged with sediments

from melting glaciers. To minimize the glacial flour component of samples collected from glacial streams the coarser grained material below the surface layer was sampled. In contrast, the Tagish Highland is a relatively smooth, gently sloping upland. Creeks in this region flow much slower and samples contain a slightly higher amount of organic material.

FIELD SAMPLE PREPARATION

Field sample preparation involved the drying and processing of sediment samples at facilities established at each of the field camps. Sediment samples were dried at a temperature range of 30°C to 50°C. All sediment material finer than 1 millimetre was recovered by sieving each of the dried samples through a -18 mesh ASTM screen. As a result of sediment samples for quality and content of fine-grained sediment resulted in a total of 10 sediment samples being rejected due to insufficient quantity of fine-grained material or unacceptable sample composition.

LABORATORY SAMPLE PREPARATION

Field-processed sediment and water samples were shipped to Rossbacher Laboratory Limited (Burnaby) for final preparation for analysis. Sediment samples were further sieved to -80 mesh ASTM fraction and analytical

TABLE 4-1-3
SUMMARY OF ANALYTICAL DETERMINATION METHODS

ELEMENT	DETECTION LIMITS	SAMPLE WEIGHT	DIGESTION TECHNIQUE	DETERMINATION METHOD
Gold (Au)	1 ppb	10 g	fire assay fusion	atomic absorption spectrophotometry after degestion of doré bead by aqua regia
Cadmium (Cd)	0.2 ppm	1 g	3 mL HNO ₃ let sit overnight, add 1 mL HCl in 90°C water bath, for 2 hrs. cool, add 2 mL H ₂ O, wait 2 hrs.	atomic absorption spectrophotometry using air-acetylene burner and standard solutions for calibration, background corrections made for Pb, Ni, Co, Ag, Cd
Cobalt (Co)	2 ppm			
Copper (Cu)	2 ppm			
Iron (Fe)	0.02 %			
Lead (Pb)	2 ppm			
Manganese (Mn)	5 ppm			
Nickel (Ni)	2 ppm			
Silver (Ag)	0.2 ppm			
Zinc (Zn)	2 ppm			
Molybdenum (Mo)	1 ppm	0.5 g	Al added to above solution	
Barium (Ba)	10 ppm	1 g	HNO ₃ - HCl - HF taken to dryness, hot HCl added to leach residue	
Vanadium (V)	5 ppm			
Chromium (Cr)	5 ppm			
Bismuth (Bi)	0.2 ppm	2 g	HCl - KClO ₂ digestion, KI added to reduce Fe, MIBK and TOPO for extraction	organic layer analyzed by atomic absorption spectrophotometry with background correction
Antimony (Sb)	0.2 ppm			
Tin (Sn)	1 ppm	1 g	sintered with NH ₄ I, HCl and ascorbic acid leach	atomic absorption spectrophotometry
Arsenic (As)	1 ppm	0.5 g	add 2 mL KI and dilute HCl to 0.8M HNO ₃ and 0.2M HCl	2 mL borohydride solution added to produce AsH ₃ gas which is passed through heated quartz tube in the light path of atomic absorption spectrophotometer
Mercury (Hg)	10 ppb	0.5 g	20 mL HNO ₃ and 1 mL HCl	10% stannous sulphate added to evolve mercury vapour, determined by atomic absorption spectrometry
Tungsten (W)	1 ppm	0.5 g	K ₂ SO ₄ fusion, HCl leach	colorimetric: reduced tungsten complexed with toluene 3, 4 dithiol
Fluorine (F)	40 ppm	0.25 g	Na ₂ CO ₃ - KNO ₃ fusion, H ₂ O leach	citric acid added and diluted with water, fluorine determined with specific ion electrode
Uranium (U)	0.5 ppm	1 g	nil	neutron activation with delayed neutron counting
LOI	0.1 %	0.5 g	ash sample at 500°C	weight difference measured
pH - water	0.1	25 mL	nil	glass - calomel electrode system
Uranium - water	0.05 ppb	5 mL	add 0.5 mL Fluran solution	place in Scintrex UA-3
Fluoride - water	20 ppb	25 mL	nil	fluorine measured by an ion specific electrode
Sulphate - water	1 ppm	50 mL	add 0.3 mL of Sulfaver reagent	turbidity measured by spectrometer absorption cell

duplicate samples and control reference materials were inserted into each analytical block of 20 sediment samples. In addition, a quantity of -80 mesh material and a representative sample of the +80 to -18 mesh fraction was archived for future studies. Control reference water standards were inserted into each analytical block of 20 water samples.

ANALYTICAL PROCEDURES

Sediment samples will be analyzed for cadmium, cobalt, copper, iron, lead, manganese, nickel, silver, zinc, molybdenum, vanadium, bismuth, antimony, arsenic, mercury, fluorine and loss on ignition. Water samples will be ana-

lyzed for pH, uranium, fluoride and sulphate. Table 4-1-3 details the determination methods and detection limits for the 1992 analytical suite of elements as well as element determinations utilized during previous RGS analytical programs. A 10-gram subsample will also be analyzed by instrumental neutron activation analysis (INAA). Elements determined by INAA are listed in Table 4-1-4.

Analytical results for field-site duplicates, analytical duplicates and control reference materials within each analytical block of 20 samples are closely monitored and evaluated. Blocks of 20 samples containing quality control samples which fail to satisfy established guidelines for precision and accuracy are re-analyzed.

TABLE 4-1-4
ELEMENTS ANALYZED BY INAA

ELEMENT	DETECTION LIMIT	ELEMENT	DETECTION LIMIT
Gold (Au)	2 ppb	Molybdenum (Mo)	1 ppm
Antimony (Sb)	0.1 ppm	Nickel (Ni)	10 ppm
Arsenic (As)	0.5 ppm	Rubidium (Rb)	5 ppm
Barium (Ba)	100 ppm	Samarium (Sm)	0.5 ppm
Bromine (Br)	0.5 ppm	Scandium (Sc)	0.5 ppm
Cerium (Ce)	10 ppm	Sodium (Na)	0.1 %
Cesium (Cs)	0.5 ppm	Tantalum (Ta)	0.5 ppm
Chromium (Cr)	5 ppm	Terbium (Tb)	0.5 ppm
Cobalt (Co)	5 ppm	Thorium (Th)	0.5 ppm
Hafnium (Hf)	1 ppm	Tungsten (W)	2 ppm
Iron (Fe)	0.2 %	Uranium (U)	0.2 ppm
Lanthanum (La)	5 ppm	Ytterbium (Yb)	2 ppm
Lutetium (Lu)	0.2 ppm	Zirconium (Zr)	200 ppm

RGS ARCHIVE PROGRAM – SOUTHERN B.C. (92H, 92I, 92J)

The RGS Archive Program involved the analysis by INAA of stream-sediment samples collected during joint federal-provincial surveys conducted prior to 1986. Samples weighing an average of 20 grams were analyzed for gold and other previously undetermined elements (Table 4-1-4). To date, 24 000 samples from nineteen 1:250 000-scale map sheet areas have been analyzed. The publication of this important data was initiated in 1991 with the release of five RGS data packages covering southeastern British Columbia. During 1992, results for map sheets 92O and 92P were published. Map sheets 92H, 92I and 92J are now scheduled for release in the spring of 1993. Future release areas are listed in Table 4-1-1. Data packages published as part of the RGS Archive Program include the new analytical data as determined by INAA, together with the original sample-site information and analytical results. The publication of these packages supersedes all previous reports.

RGS OPEN FILE FORMAT

RGS Open File data packages include a data booklet and a 1:500 000-scale map booklet. The data booklet presents survey details, data listings, summary statistics and data interpretations. The map booklet contains sample location maps, bedrock and surficial geology maps, symbol and value maps for each element, and multi-element anomaly maps. Also included in each package are 1: 00 000-scale sample location maps and 1:500 000-scale clear overlays showing sample locations and bedrock geology. Raw data are provided as ASCII files on 5.25-inch high-density diskettes.

ACKNOWLEDGMENTS

Acknowledgements are extended to all government agencies and private companies who contributed to the successful completion of the 1992 RGS and RGS Archive programs.

REFERENCES

- Holland, S.S. (1976): Landforms of British Columbia. A Physiographic Outline; *B.C. Ministry of Energy, Mines and Petroleum Resources*, Bulletin 48.
- Jackaman, W., Matysek, P.F. and Cook, S.J. (1992a): British Columbia Regional Geochemical Survey – Mount Waddington (NTS 92N); *B.C. Ministry of Energy, Mines and Petroleum Resources*, BC RGS 34.
- Jackaman, W., Matysek, P.F. and Cook, S.J. (1992b): British Columbia Regional Geochemical Survey – Taseko Lakes (NTS 92O); *B.C. Ministry of Energy, Mines and Petroleum Resources*, BC RGS 35.
- Jackaman, W., Matysek, P.F. and Cook, S.J. (1992c): British Columbia Regional Geochemical Survey – Bonaparte Lake (NTS 92P); *B.C. Ministry of Energy, Mines and Petroleum Resources*, BC RGS 36.
- Sibbick, S.J. and Delaney, T.A. (1993): Investigation of RGS Anomalies in South-central British Columbia (92N, O, P); in *Geological Fieldwork 1992*, Grant, B. and Nevell, J.M., Editors, *B.C. Ministry of Energy, Mines and Petroleum Resources*, Paper 1993-1, this volume.

NOTES



QUATERNARY GEOLOGY OF SOUTHEASTERN VANCOUVER ISLAND AND GULF ISLANDS (92B/5, 6, 11, 12, 13 AND 14)

By H.E. Blyth and N.W. Rutter

KEYWORDS: Economic geology, surficial geology, aggregate, Gulf Islands, hazards, Saanich Peninsula, stratigraphy, Quaternary, Vancouver Island.

INTRODUCTION

This report presents preliminary results of the first of a two-year Quaternary geological study involving surficial mapping and a regional geologic synthesis on southeastern Vancouver Island and the Gulf Islands. The location was selected for study in response to the need for more information on land resources and geologic hazards in an area of intensive urbanization.

The study area covers the region south of latitude 49°00' to the Juan de Fuca Strait, and from longitude 124°00' west to the east coast of Saturna Island (*see* Figure 4-2-1).

Growing urban pressures in the southeastern Vancouver Island and Gulf Island areas are forcing marginal land areas, such as poorly drained lowlands, to be considered as future urban development sites. At the same time urban and rural parkland is being identified for green space preservation and exploration programs are being conducted for aggregate and liquid and solid waste management sites. Furthermore, southwestern British Columbia's precarious position over an active subduction zone (Rogers, 1988) requires a clear identification of potential geologic hazards such as land susceptibility to earthquake induced liquefaction or ground failure. A land use and resource evaluation conducted around the expanding urban area is the first step towards maximizing the land's potential and preventing land-use conflicts.

To evaluate the resource and land-use potential of southeastern Vancouver Island and the Gulf Islands, the regional geological history of the area must be understood. This involves study of the Quaternary sediments and landforms in the region and their stratigraphic and chronologic relationships.

This project has four main objectives:

- To construct a comprehensive surficial geology map of southeastern Vancouver Island based on air photo interpretation and field investigation with special emphasis being placed on the Saanich Peninsula, a region that has not been mapped since 1913 and which is undergoing intensive urbanization.
- To characterize surficial deposits using textural, physical and lithological data in order to elucidate the material properties for engineering projects, hazard potential and chronological correlation.
- To establish a Quaternary history by integrating stratigraphic and morphological information with absolute dating results.

- To map and input data into a geographical information system (G.I.S.) to facilitate information accessibility.

Of these four objectives the air photo and field checking were completed in 1992. The detailed Quaternary history, maps and digital information base are presently in progress.

BEDROCK GEOLOGY AND PHYSIOGRAPHY

Low-relief areas (averaging 200-300 m above sea level) are found on the eastern Vancouver Island coast and northern Saltspring Island and Gulf Islands and are underlain by a conformable sequence of marine and nonmarine sedimentary rocks of Late Cretaceous age known as the Nanaimo Group (Muller, 1980). They consist of sandstone, shale, siltstone, conglomerate and often coal (van Vliet *et al.*, 1991). Bedrock controlled north to south-trending ridges separated by narrow valleys are typical of this area. Differential erosion of weak shale and mudstone is responsible for the formation of the valleys, whereas the ridges are formed by the resistant sandstones and conglomerates.

South of Fulford Valley on Saltspring Island and south-westward toward Victoria and Sooke, the bedrock consists of Paleozoic metasediments and metavolcanics (Ryder, 1978; Muller, 1980). These more resistant metamorphic rocks form topographic highs with elevations from 600 to 900 metres above sea level (van Vliet *et al.*, 1987).

Although the basic topography is controlled by bedrock formations, glacial processes have greatly altered the landscape. Thick sequences of Quaternary sediment found along the eastern coast from Ladysmith to Victoria and on James and Sidney Islands, have subdued the overall landscape. The bedrock terrain has also been reshaped by erosional glacial processes. Roche moutonnée, striated and fluted bedrock are dominant features in the landscape of southeastern Vancouver Island and on most of the Gulf Islands.

PREVIOUS WORK

Quaternary studies in British Columbia began with G.M. Dawson's general overview in 1881 and his later discovery, in 1887, of two tills separated by stratified sands and silts (Dawson, 1881, 1887). Willis' work in the Puget Lowland subdivided the Quaternary sediments into an older Admiralty glaciation, a "Puyallup" nonglacial interval and a more recent, Vashon glaciation (Willis, 1898). Many studies followed but only those most relevant to southeastern Vancouver Island and the Gulf Islands are cited here.

Clapp (1912, 1913 and 1917) not only expanded the known stratigraphy of southeastern Vancouver Island, by subdividing the Puyallup interglacial into the Maywood (marine) clays and the Cordova sands and gravels, he also

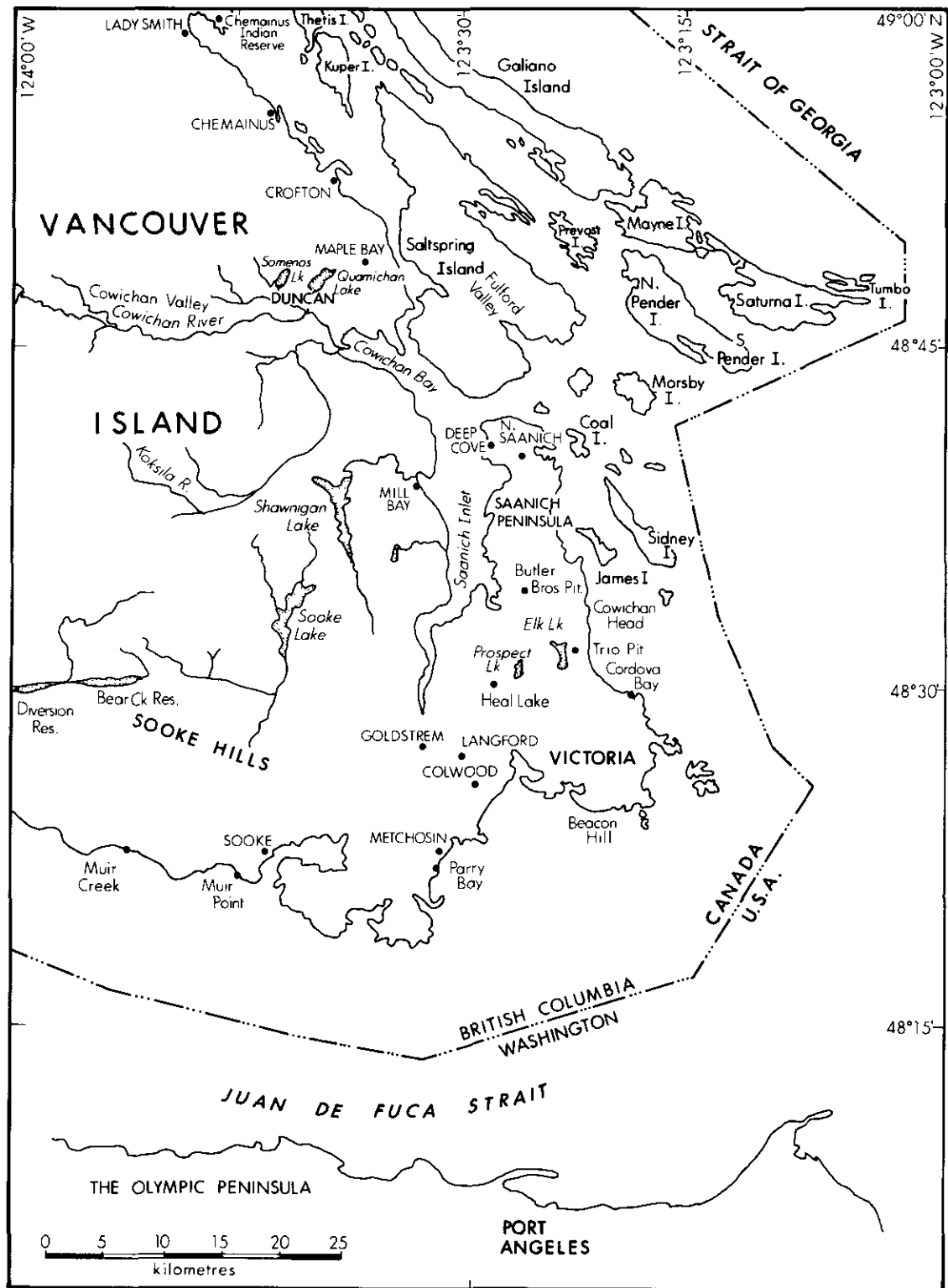


Figure 4-2-1. Map of study area and section locations.

produced surficial geologic maps for the Victoria, Saanich, Sooke and Duncan map areas. Fyles (1963) presented evidence from central Vancouver Island for two major glaciations and three nonglacial intervals. In the Fraser Lowlands

an evolution of stratigraphic sequences was developed by Armstrong (1956, 1957, 1960, 1961, 1965, 1975a, 1975b) and Armstrong *et al.* (1965). Revisional works by Armstrong and Hicoek (1975, 1976), Hicoek (1976) and Arm-

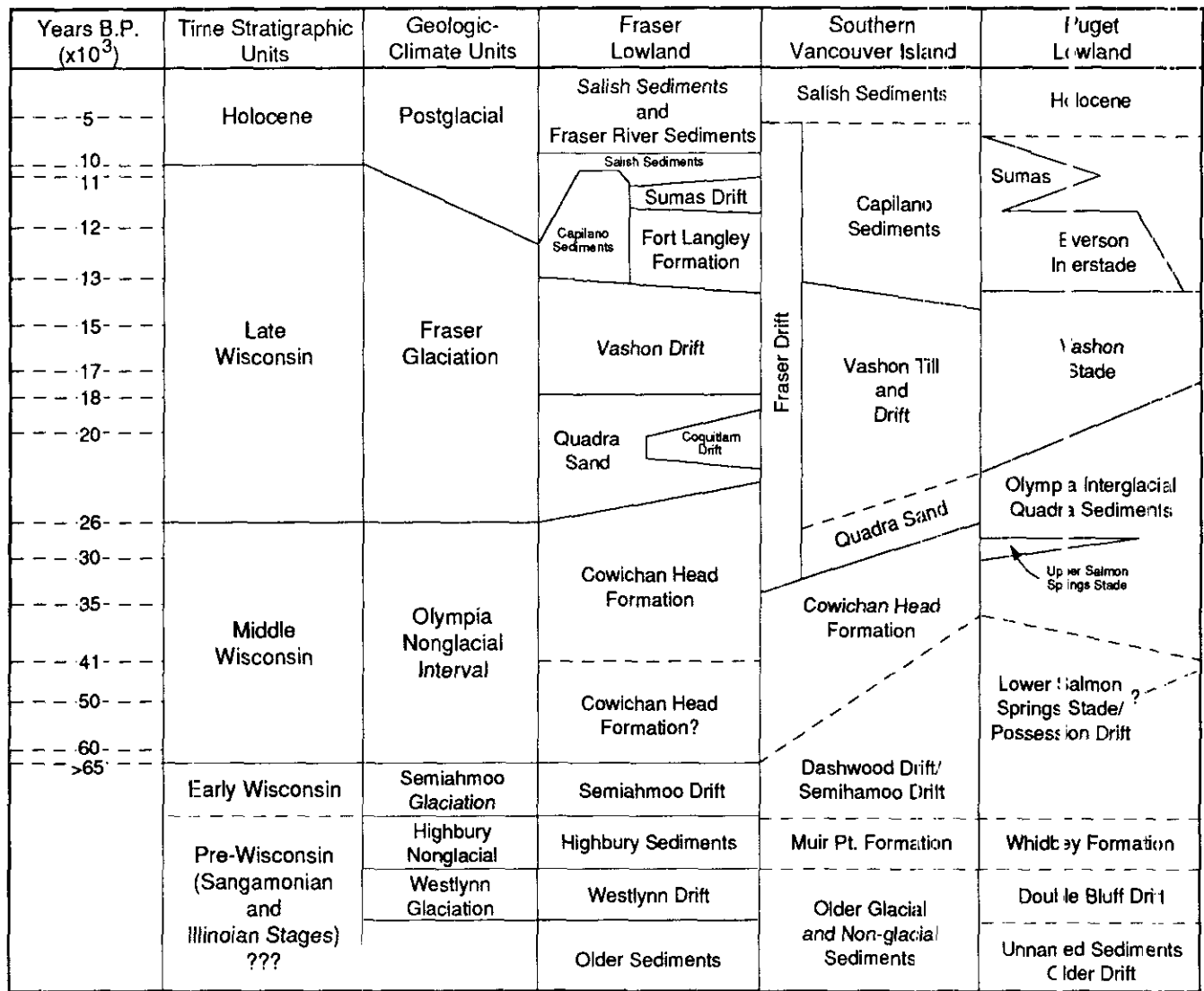


Figure 4-2-2. The Quaternary stratigraphic sequences in southwestern British Columbia and northwestern Washington (After: Fyles, 1963; Armstrong and Clague, 1977; Alley, 1979; Armstrong, 1981; Hicock and Armstrong, 1983; and Alley and Hicock, 1986).

strong (1981) established three major glacial events: the Westlynn, Semiahmoo and Fraser glaciations; and four major interglaciations. Meanwhile, Armstrong and Clague (1977), Clague (1976, 1977) and Alley (1979) worked to define the interglacial Cowichan Head Formation using stratigraphic and palynological investigation. Using Fyles' (1963) research as a framework, Hicock *et al.* (1979) compiled a summary of the Quaternary stratigraphy on southeastern Vancouver Island that included the detailed works of Clague (1977), Alley (1979) and his own research. Some of the most detailed work on pre-Fraser Pleistocene stratigraphy, geochronology and paleoecology to encompass Vancouver Island and the Fraser and Puget lowlands was completed by Hicock (1980). Alley and Hicock (1986) presented a review of the Quaternary history and stratigraphy of Vancouver Island, the Fraser lowlands and the Puget lowlands as did Hicock and Armstrong (1981, 1983, 1985) and Hicock (1990). A compilation of established Quaternary

stratigraphic sequences for southern Vancouver Island, the Fraser and Puget lowlands is presented in Figure 4-2-2.

Surficial mapping and geomorphic studies in the study area have been presented by Bretz (1920), Halstead (1968), Senyk (1972), Foster (1972) and Energy, Mines and Resources Canada (1981). Soils and surficial materials of the Gulf Islands were reviewed by van Vleet *et al.* (1987, 1991). General Quaternary overviews of the Cordilleran ice sheet were compiled by Ryder *et al.* (1991), Ryder and Clague (1989), Booth (1987, 1991) and Clague (1985).

Other research on specific Quaternary subjects includes: the sea level history has been developed by Clague and Bobrowsky (1990) and Clague *et al.* (1991); improvements in chronological control have been made by Clague (1981), Easterbrook and Rutter (1982), Hicock and Rutter (1986) and most recently, in Washington State, by Easterbrook (1986, 1992). Paleoclimatic studies have been undertaken by Clague (1978), Alley and Hicock (1986) and Alley and Chatwin (1979).

METHODS

A preliminary air photo interpretation of the surficial geology was conducted at a scale of 1:50 000 on NTS map sheets 92B/ 5, 6, 11, 12, 13 and 14 prior to fieldwork. More than 400 field sites were visited in order to check the accuracy of mapping and to describe stratigraphic and sedimentological features of Quaternary exposures. Section descriptions include field characteristics such as: colour, texture, unit thickness, large clast (\geq pebble) lithology, clast and matrix mineralogy, primary and secondary structures such as bedding and fabric, and unit contact descriptions. Unit provenance will be determined later by interpreting section descriptions and matching information to possible source localities or correlative units.

Samples for age determination were taken and will be analyzed in the manner most suitable for the material found. For example, amino acid analysis of shells will be used to provide relative dating control; radiocarbon analysis of organic matter will be used for absolute dating control; and tephrochronological methods will be used to identify and date samples of volcanic ash.

A geographical information system (TerraSoft) will be used to combine areal and point-form data with stratigraphic information to produce a three dimensional map of the study area.

SURFICIAL GEOLOGY

The majority of surficial materials in the study area were deposited during the last glaciation (the Vashon Stage of the Fraser Glaciation) between 25 000 and 15 000 years ago (Easterbrook, 1992; van Vliet *et al.*, 1987). Low-lying coastal areas in the southeastern Vancouver Island region are covered by glaciomarine drift, beach materials, till and/or glaciofluvial/fluvial sand and gravel. Higher elevations (*i.e.*, from 600 to 900 m above sea level) are covered by till or colluviated till, glaciofluvial sand and gravel and more recent colluvium.

DIAMICTON DEPOSITS

Much of the low-lying coastal areas, including Ladysmith, Chemainus, Victoria, the Saanich Peninsula and James and Sidney islands are draped by 1 to 2 metres of silty diamicton. In places it directly overlies bedrock; in low-lying areas it is found directly over a silty clay unit; and in upland areas it is found over what appears to be glaciofluvial sand and gravel.

In low-lying areas (less than 175 m above sea level) this diamicton is characterized by: high percentages of clay and silt (10-40 and 40-50 % respectively); approximately 10 to 15 per cent fine to medium sand and less than 5 per cent coarse sand. Clast content ranges from 5 per cent at the base to 30 per cent at the top and maximum clast size ranges from 0.1 to 1.0 metre in diameter. The diamicton is generally well indurated and a grey to dark greyish brown colour (Munsell code 2.5Y 4/2, moist). The dominant lithologies of the clasts are, in order of abundance: plagioclase porphyry, granite, quartzite, sandstone, siltstone and basalt (*i.e.*, mostly local and Coast Mountain lithologies).

The diamicton is interpreted to be a basal till deposited by ice that overrode and incorporated subaqueous silts and clays. From lithological and striae data it appears to have Cowichan Valley and/or Coast Mountain sources.

In the Ladysmith area, up to 12 metres of massive, very indurated, clay-rich diamicton occurs at surface. It contains 25 to 30 per cent clasts, 5 to 10 per cent clay, approximately 40 per cent silt, approximately 40 per cent fine sand and approximately 5 per cent medium to coarse sand. It differs slightly from diamictons in the Victoria area in both colour (*i.e.*, grey, Munsell code 5Y 5/1, moist) and lithology: plagioclase porphyry, diorite, fine-grained mafic volcanics and siltstone compose the majority of the clasts. Locally this diamicton shows signs of colluviation in the form of decreased clay content and rare bedding planes. This deposit is very similar to the surficial diamictons found in Deep Cove and Chemainus.

A diamicton with similar texture and colour characteristics as that in the Ladysmith area occurs near Shawnigan Lake. However, the abundance of basalt and fine-grained volcanic, sandstone and siltstone clasts in the diamicton denotes a more local source.

Throughout lowland regions, from Ladysmith to Victoria and in parts of Metchosin, outcrops of an unconsolidated, sandy, poorly bedded diamicton occur sporadically. Good examples can be found in sea cliffs in Beacon Hill Park and at the tops of sections at Parry Bay, Cordova Bay, the Trio gravel pit and the Butler Brother's gravel pit (Figure 4-2-1). Due to the low elevation of each of these sections (none above 90 m above sea level and all below the late glacial marine high stance of 175 metres (Ryder, 1978), poor sorting, the presence of bedding and the sandy texture of the diamicton, they are tentatively interpreted as subaqueous debris-flow deposits, most likely derived from a proglacial environment.

SAND AND GRAVEL DEPOSITS

Surface concentrations of sand and gravel exist in the Metchosin, Langford and Goldstream areas 15 kilometres west of Victoria, in an area just northwest of Muir Creek about 20 kilometres west of Sooke, along the Chemainus river approximately 21 kilometres west of Chemainus and throughout the lower and upper Cowichan Valley (Figure 4-2-1). They are thick, aggradational sequences of steeply dipping (25-28°) sands and gravels overlain by channelled, cut-and-fill sands and gravels resembling those of glaciofluvial deltaic and braided stream environments, respectively. They were most likely deposited in the recessional phase of the last glaciation.

Not all sand and gravel deposits in the field area are attributable to glaciofluvial processes, some appear to have originated in ice-contact environments. Convoluted, interbedded sand, gravel and diamicton combined with pitted, kame and kettle topography just south of Duncan, provides evidence for ice stagnation and downwasting in the area. Halstead (1966) attributes this to ice stagnation of a partially grounded Cowichan Valley glacier.

The economic viability of these aggregate deposits has been established in Metchosin, Langford, Goldstream, Dun-

can and in parts of the Cowichan Valley. Further study may also prove the Muir Creek and Chemainus sites to be of economic significance.

UPLAND COLLUVIAL AND RELATED DEPOSITS

The mountainous inland areas of southeastern Vancouver Island appear to have been completely covered by ice during the last glaciation. The surficial materials in this part of southeastern Vancouver Island consist of colluviated diamicton over bedrock. Exposures of well indurated, clay-rich diamicton or sandy diamicton can sometimes be found around valley basins such as in the Sooke Lake region. However, these diamictons are most often overlain by recent fluvial sands, gravels and lacustrine silts and clays.

STRATIGRAPHIC HISTORY OF SOUTHERN VANCOUVER ISLAND AND THE GULF ISLANDS

The following is a chronological interpretation of the most complete Quaternary sections on southeastern Vancouver Island. No reference will be made to either time or geologic-climatic units as these have yet to be accurately established. Without the results of chronologic analysis, there is little evidence to alter the Quaternary history established by Alley and Hicock (1986).

The Quaternary history of southeastern Vancouver Island and the Gulf Islands begins with what may have been an extensive glaciation. It is evidenced by diamicton deposits interpreted as till that occur at or near sea level in the bases of the Parry Bay, Cordova Bay and Muir Point sections. A period of interglaciation followed in the coastal areas with a sequence of erosion and possible subaqueous deposition of clay and beach lag deposits. A coarsening upward sequence of fine sands and gravels, inferred to be subaerial fluvial and alluvial deposits, indicates isostatic rebound and/or eustatic sea level rise associated with deglaciation. Overlying deposits of strongly oxidized, thinly crossbedded and laminated sands with syndepositional, interbedded silts and organic sediments indicate climatic warming comparable to the area's present climate (R. Hebda, personal communication, 1992; Hicock, 1980). Decreasing organics in the overlying silt and sand units appears to indicate a cooling climatic trend. This is followed by deposition of proglacial sands and gravels that are evident throughout the southeastern Vancouver Island area. They are directly overlain by a thick unit of diamicton, interpreted to be till and glacial debris-flow deposits associated with the last major glaciation. The uppermost units in the sequence vary with topography and elevation and consist mainly of sands and gravels deposited during ice recession. Holocene organic deposits found in the Heal Lake section on the Saanich Peninsula show a distinct climatic warming, prior to and after the deposition of the 6800 B.P. (Clague, 1990) Mazama ash marker.

CONCLUSIONS

Preliminary evidence from the 1992 field season confirms the existence of two glacial and three interglacial periods during the Quaternary on southeastern Vancouver

Island and the Gulf Islands. The longest Quaternary records in the area (the Parry Bay, Muir Point, Cowichan Head and Cordova Bay sections) begin with a sequence of pre-Sangamon diamicton overlain by pre-Wisconsinan or pre-Sangamon interglacial sediments (Alley and Hicock, 1986) belonging to the Muir Point Formation. These are overlain in turn by late glacial and proglacial sands and gravels which are most likely part of the Cowichan Head Formation. The upper units are composed mostly of till and outwash associated with the Late Wisconsinan Fraser glaciation. Late Wisconsinan and Holocene interglacial deposits dominate the modern landscape. Thick deposits of silt, sand, gravel and diamicton are found in valley bottoms and coastal areas; upland areas are veneered with colluvium and modern fluvial sand and gravel.

Fyles (1963) found evidence from central Vancouver Island for a mid-Wisconsinan glaciation known as the Dashwood. We have, at this stage of the project, found no evidence for this advance. More detailed chronological and paleoclimatic control should elucidate the issue of mid-Wisconsinan geologic history.

With the completion of this project we hope to resolve:

- The distribution of surficial and stratigraphic materials.
- The extent of surficial resources and geologic hazards.
- How the Dashwood drift is represented in this area.
- Where the effects of valley glaciation end and Cordilleran glaciation begin.

ACKNOWLEDGMENTS

This study was a joint research project between the Surficial Geology Unit of the British Columbia Geological Survey Branch and the University of Alberta. The authors would like to thank: Thurber Engineering Ltd.; Peter Bobrowsky; Tim Giles for his managing skill and his great ability to get things done; Vic Levson for reviewing this manuscript and for his assistance and guidance throughout this project; Beverly Brown for her patience and organizational skills; and friends and family for their support and assistance throughout the summer. Special thanks to Lisa Sankeralli for her enthusiastic and beneficial assistance in the field.

REFERENCES

- Alley, N.F. (1979): Middle Wisconsin Stratigraphy and Climatic Reconstruction, Southern Vancouver Island, British Columbia; *Quaternary Research*, Volume 11, pages 213-237.
- Alley, N.F. and Chatwin, S.C. (1979): Late Pleistocene History and Geomorphology, Southwestern Vancouver Island, British Columbia; *Canadian Journal of Earth Sciences*, Volume 16, pages 1645-1657.
- Alley, N.F. and Hicock, S.R. (1986): The Stratigraphy, Palynology, and Climatic Significance of Pre-middle Wisconsinan Pleistocene Sediments, Southern Vancouver Island, British Columbia; *Canadian Journal of Earth Sciences*, Volume 23, pages 369-382.
- Armstrong, J.E. (1956): Surficial Geology of the Vancouver Area, British Columbia; *Geological Survey of Canada*, Paper 53-40.

- Armstrong, J.E. (1957): Surficial Geology of the New Westminster Map Area, British Columbia; *Geological Survey of Canada*, Paper 57-5.
- Armstrong, J.E. (1960): Surficial Geology of the Sumas Map Area, British Columbia; *Geological Survey of Canada*, Paper 59-9.
- Armstrong, J.E. (1961): Soils of the Coastal Area of Southwest British Columbia; in *Soils in Canada*, Leggett, R.F., Editor, *Royal Society of Canada*, Special Publication No. 3, pages 22-32.
- Armstrong, J.E. (1965): Days 10, 12 and 13 in Guidebook of Field Conference J., Pacific Northwest; INQUA VIIIth Congress, USA; *Nebraska Academy of Science*, pages 80-86 and 102-108.
- Armstrong, J.E. (1975a): Quaternary Geology, Stratigraphic Studies, and Revaluation of Terrain Inventory Maps, Fraser Lowland, British Columbia; *Geological Survey of Canada*, Paper 75-1A.
- Armstrong, J.E. (1975b): Days 7 and 8 in The Last Glaciation; Guidebook for Field Conference, International Geological Correlation Program; Easterbrook, D.J., Editor, *Western Washington State College*, pages 74-97.
- Armstrong, J.E. (1981): Post-Vashon Wisconsin Glaciation, Fraser Lowland, British Columbia; *Geological Survey of Canada*, Bulletin 322.
- Armstrong, J.E. and Clague, J.J. (1977): Two Major Wisconsin Lithostratigraphic Units in Southwest British Columbia; *Canadian Journal of Earth Sciences*, Volume 14, pages 1471-1480.
- Armstrong, J.E. and Hicock, S.R. (1975): Quaternary Landscapes: Present and Past – at Mary Hill, Coquitlam, British Columbia; *Geological Survey of Canada*, Paper 75-1B.
- Armstrong, J.E. and Hicock, S.R. (1976): Quaternary Multiple Valley Development of the Lower Coquitlam Valley, Coquitlam, British Columbia; *Geological Survey of Canada*, Paper 76-1B.
- Armstrong, J.E., Crandell, D.R., Easterbrook, D.J. and Noble, J.B. (1965): Late Pleistocene Stratigraphy and Chronology in Southwestern British Columbia and Northwestern Washington; *Geological Society of America*, Bulletin, Volume 76, pages 321-330.
- Booth, D.B. (1987): Timing and Processes of Deglaciation Along the Southern Margin of the Cordilleran Ice Sheet; in *The Geology of North America*, Volume K-3, North America and Adjacent Oceans During the Last Deglaciation, *The Geological Society of America*, pages 71-90.
- Booth, D.B. (1991): Glacier Physics of the Puget Lobe, Southwest Cordilleran Ice Sheet; *Geographie Physique et Quaternaire*, Volume 45, No. 3, pages 301-315.
- Bretz, J.H. (1920): The Juan de Fuca Lobe of the Cordilleran Ice Sheet; *Journal of Geology*, Volume 28, pages 333-339.
- Clague, J.J. (1976): Quadra Sand and the Timing of the Late Wisconsin Glacial Advance in Southwest British Columbia; in *Quaternary Glaciations in the Northern Hemisphere*, Easterbrook, D.J. and Sibrava, V., Editors, *IUGS-Unesco International Geological Correlation Program*, Project 73-1-24, Report 3, pages 315-326.
- Clague, J.J. (1977): Quadra Sand: A Study of the Late Pleistocene Geology and Geomorphic History of Coastal Southwest British Columbia; *Geological Survey of Canada*, Paper 80-13.
- Clague, J.J. (1978): Mid-Wisconsinan Climates of the Pacific Northwest; in *Current Research*, Part B; *Geological Survey of Canada*, Paper 78-1B, pages 95-100.
- Clague, J.J. (1981): Late Quaternary Geology and Geochronology of British Columbia. Part 2: Summary and Discussion of Radiocarbon-dated Quaternary History; *Geological Survey of Canada*, Paper 80-35.
- Clague, J.J. (1986): The Quaternary Stratigraphic Record of British Columbia – Evidence for Episodic Sedimentation and Erosion Controlled by Glaciation; *Canadian Journal of Earth Sciences*, Volume 23, pages 885-894.
- Clague, J.J. (1990): Pleistocene Tephra in Central British Columbia; in *Current Research*, Part E, *Geological Survey of Canada*, Paper 90-1E, pages 257-261.
- Clague, J.J. and Bobrowsky, P.T. (1990): Holocene Sea Level Change and Crustal Deformation, Southwestern British Columbia; in *Current Research*, Part E, *Geological Survey of Canada*, Paper 90-1E.
- Clague, J.J., Lichti-Federovich, S., Guilbault, J.-P. and Mathewes, R.W. (1991): Holocene Sea Level Change, South-coastal British Columbia; in *Current Research*, Part A, *Geological Survey of Canada*, Paper 91-1A.
- Clapp, C.H. (1912): Southern Vancouver Island; *Geological Survey of Canada*, Memoir 13.
- Clapp, C.H. (1913): Geology of the Victoria and Saanich Map-areas, Vancouver Island, B.C.; *Geological Survey of Canada*, Memoir 36.
- Clapp, C.H. (1917): Sooke and Duncan Map-areas, Vancouver Island, British Columbia; *Geological Survey of Canada*, Memoir 96.
- Dawson, G.M. (1881): Additional Observations on the Superficial Geology of British Columbia and Adjacent Regions; *Quaternary Journal of Geology Society*, Volume 37, pages 272-285.
- Dawson, G.M. (1887): Report on a Geological Examination of the Northern Part of Vancouver Island and Adjacent Coasts; *Geological Survey of Canada*, Annual Report, 1886, Volume 2, Part B.
- Easterbrook, D.J. (1986): Stratigraphy and Chronology of Quaternary Deposits of the Puget Lowland and Olympic Mountains of Washington and the Cascade Mountains of Washington and Oregon; in *The Quaternary Glaciations of the Northern Hemisphere*, Sibrava, V., Bowen, D.Q. and Richmond, G.M., Editors, *Quaternary Science Reviews*.
- Easterbrook, D.J. (1992): Advance and Retreat of Cordilleran Ice Sheets in Washington, U.S.A.; *Geographie Physique et Quaternaire*, Volume 46, No.1, pages 51-68.
- Easterbrook, D.J. and N.W. Rutter (1982): Amino Acid Analysis of Wood and Shells in Development of Chronology and Correlation of Pleistocene Sediments in the Puget Lowland, Washington; *Geological Society of America*, Abstracts with Programs, Volume 14.
- Energy, Mines and Resources Canada (1981): Sooke, British Columbia; *Surveys and Mapping Branch*, Map No. 92B/5, 1:50 000 scale.
- Foster, H.D. (1972): *Geomorphology and Water Resource Management: Portage Inlet, a Case Study on Vancouver Island*; *Canadian Geographer*, Volume 16, pages 128-143.
- Fyles, J.G. (1963): Surficial Geology, Parksville, British Columbia; *Geological Survey of Canada*, Map 1112A.
- Halstead, E.C. (1966): Surficial Geology of Duncan and Shawnigan Map-areas, British Columbia; *Geological Survey of Canada*, Paper 65-24. Includes Maps 14-1965 and 15-1965.
- Halstead, E.C. (1968): The Cowichan Ice Tongue, Vancouver Island; *Canadian Journal of Earth Sciences*, Volume 5, pages 1409-1415.

- Hicock, S.R. (1976): Quaternary Geology, Coquitlam - Port Moody Area, British Columbia; unpublished M.Sc. thesis, *The University of British Columbia*.
- Hicock, S.R. (1980): Pre-Fraser Pleistocene Stratigraphy, Geochronology, and Paleocology of the Georgia Depression, British Columbia; unpublished Ph.D. thesis, *The University of Western Ontario*, London.
- Hicock, S.R. (1990): Last Interglacial Muir Point Formation, Vancouver Island, British Columbia; *Geographie Physique et Quaternaire*, Volume 44, pages 337-340.
- Hicock, S.R. and Armstrong, J.E. (1981): Coquitlam Drift: A Pre-Vashon Glacial Formation in the Fraser Lowland, British Columbia; *Canadian Journal of Earth Sciences*, Volume 18, pages 1443-1451.
- Hicock, S.R. and Armstrong, J.E. (1983): Four Pleistocene Formations in Southwest British Columbia: Their Implications for Patterns of Sedimentation of Possible Sangamonian to Early Wisconsinan Age; *Canadian Journal of Earth Sciences*, Volume 20, pages 1232-1247.
- Hicock, S.R. and Armstrong, J.E. (1985): Vashon Drift: Definition of the Formation in the Georgia Depression, Southwest British Columbia; *Canadian Journal of Earth Sciences*, Volume 22, pages 748-757.
- Hicock, S.R. and Rutter, N.W. (1986): Pleistocene Aminostratigraphy of the Georgia Depression, Southwest British Columbia; *Canadian Journal of Earth Sciences*, Volume 23, pages 383-392.
- Hicock, S.R., Dreimanis, A., Armstrong, J.E., Palmer, H.C. and Rutter, N.W. (1979): Pre-Fraser Stratigraphy, Georgia Depression, British Columbia; *Geological Society of America*, Abstracts with Programs, Volume 11.
- Muller, J.E. (1980): Geology: Victoria Map Area, Vancouver Island and Gulf Islands, British Columbia; *Geological Survey of Canada*, Map No. 92B/NW and part of B/SW, Open File 701.
- Rogers, G.C. (1988): An Assessment of the Megathrust Potential of the Cascadia Subduction Zone; *Canadian Journal of Earth Sciences*, Volume 25, pages 844-852.
- Ryder, J.M. (1978): Geology, Landforms - Surficial Materials: in *The Soil Landscapes of British Columbia*; Valentine, K.W.G., Sprout, P.N., Baker, T.E. and Lavkulich, L.M., Editors. *B.C. Ministry of Environment*.
- Ryder, J.M. and Clague, J.J. (1989): British Columbia -- Quaternary Stratigraphy and History, Cordilleran Ice Sheet; in Chapter 1 of *Quaternary Geology of Canada and Greenland*, Fulton, R.J., Editor. *Geological Survey of Canada*, Geology of Canada, No. 1, pages 48-58 (also *Geological Society of America*, *The Geology of North America*, Volume K-1).
- Ryder, J.M., Fulton, R.J. and Clague, J.J. (1991): The Cordilleran Ice Sheet and the Glacial Geomorphology of Southern and Central British Columbia; *Geographie Physique et Quaternaire*, Volume 45, No. 3, pages 365-377.
- Senyk, J. (1972): Sooke Terrain Map; *Environment Canada*, Map No. 92B/5 Terrain.
- van Vliet, L.J.P., Green, A.J. and Kenney, E.A. (1937): Soils of the Gulf Islands of British Columbia - Soils of Sooke Island; *Agriculture Canada*, Report No. 43, Volume 1, British Columbia Soil Survey, Research Branch.
- van Vliet, L.J.P., Kenney, E.A. and Green, A.J. (1931): Soils of the Gulf Islands of British Columbia; *Agriculture Canada*, Report No. 43, Volume 5, British Columbia Soil Survey.
- Willis, B. (1898): Drift Phenomena of Puget Sound; *Geological Society of America*, Bulletin, Volume 9, pages 111-162.

NOTES

APPLIED SURFICIAL GEOLOGY PROGRAM: AGGREGATE POTENTIAL MAPPING, SQUAMISH AREA (92G)

By V. M. Levson

KEYWORDS: Economic geology, surficial geology, land use, aggregate, stratigraphy, sand and gravel, exploration, Squamish.

INTRODUCTION

This paper outlines a new program of the British Columbia Geological Survey Branch in the field of applied surficial geology. Its objectives are to develop methodologies whereby information from about 2000 existing surficial geology maps, in conjunction with subsurface data, can be used to produce derivative products in applied fields such as aggregate resources, geological hazards, waste disposal and groundwater resources. Some of the most common applications of surficial geology maps are outlined in this paper; this project will define minimum information requirements and standards for producing derivative products in these

applied fields. The program is designed principally to address the needs of land-use planners. Case study areas will represent regions experiencing high rates of urban growth where detailed surficial geologic data are required for resource management and planning.

The Squamish - Sunshine Coast area (Figure 4-3-1) was selected as a case study area for the first phase of this program. The surficial geology of the area was mapped in the late 1970s by an experienced team of terrain mappers during the Quadra project which covered a large part of the southern Coast Mountains (30 NTS 1:50 000 sheets). The region is characterized by diverse and multiple land uses such as forestry, recreation and mineral exploration and was the focus of recent environmental science workshops and public meetings (Ferguson and McPhee, 1992). The area is also experiencing increasing land use pressures from new housing developments, recreational facilities and new highway alignments and major upgrades. Finally, the region is subject to a wide variety of geologic hazards such as debris torrents, floods, rockslides, earthquakes and glacial hazards.

This study will exemplify the multifaceted uses of existing 1:50 000 scale surficial geology data beginning with the field of aggregate resource management. Rapid urban expansion in many parts of British Columbia has resulted in increased pressures on existing sand and gravel reserves. This and related issues, such as a poor understanding of the three-dimensional configuration of exposed and buried aggregate deposits, can be addressed through the production of derivative products which take into account subsurface records. This type of information is needed for regional planning purposes in order to properly identify areas suitable for development, prevent sterilization of valuable resources and avoid unnecessary importing of sand and gravel supplies. Rapidly developing areas deserve immediate attention as post-development appraisal will not contribute to sound resource management and land-use planning.

APPLICATIONS OF SURFICIAL GEOLOGY MAPS

Surficial geology maps provide data on the areal distribution of different types of sediment, their geologic origin, texture (per cent clay, silt, sand and gravel), geomorphology, drainage and active geologic processes (e.g., avalanching, gullying, flooding, ground subsidence, volcanism, etc.). This information can be used for a number of different applications including exploration for mineral resources, the study of geologic hazards, engineering and environmental applications. Examples of each of these are outlined in Table 4-3-1.

The applications and users of surficial geology data in British Columbia have recently been discussed by Boydell (1992) and Walmsley (1992). The principal users of surficial

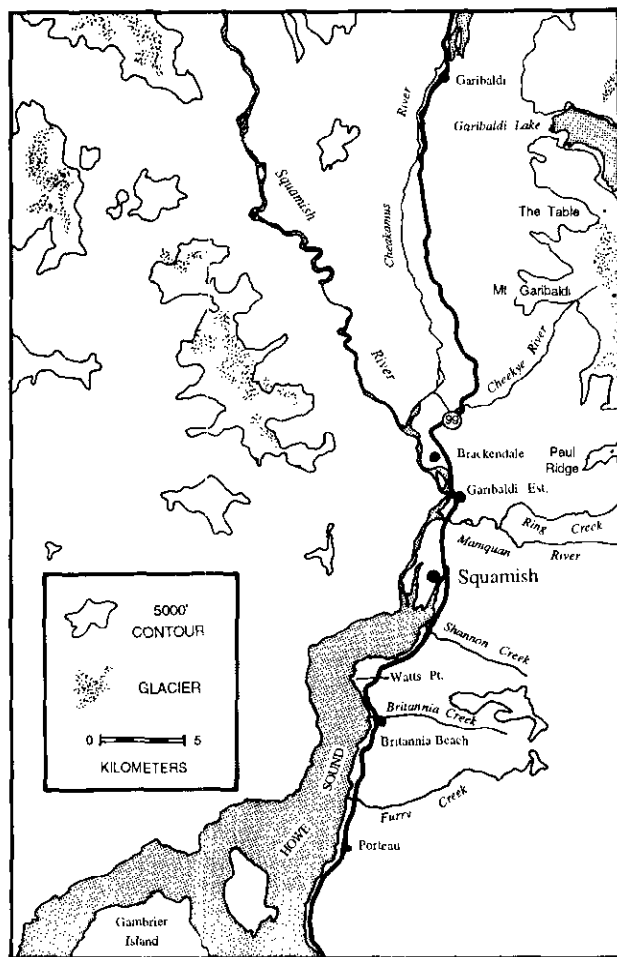


Figure 4-3-1. Location map of Squamish study area.

TABLE 4-3-1
APPLICATIONS OF SURFICIAL GEOLOGY MAPS

Mineral Resource Applications:

- determining aggregate (sand and gravel) potential
- evaluating earth-borrow potential (for roads, hydro developments, building foundations *etc.*)
- locating sources of mineral deposits (origin of geochemical anomalies and mineral-rich float in surface deposits)
- determining placer potential

Environmental Applications:

- identification of environmentally safe liquid and solid waste disposal sites
- determining groundwater aquifer potential
- evaluating contaminant migration hazard (as determined primarily by the permeability and porosity of the surficial materials)

Geologic Hazards Applications:

- susceptibility to flooding, shoreline erosion, gullyng, piping and solution collapse
- susceptibility to mass movements (landslides, slumps, debris flows, debris torrents *etc.*)
- areas sensitive to earthquake-induced liquefaction, slope failure, settling and amplification of ground motions
- sites susceptible to surface soil erosion
- areas of recent volcanism and other geologic hazards

Engineering Applications:

- general construction capability (*e.g.*, for buildings)
- engineering characteristics (*e.g.*, soil compressibility, shear strength and plasticity)
- susceptibility to frost heave, ground ice degradation and solifluction
- ease of excavation (depth to bedrock, boulder content, water content *etc.*)
- evaluation of overburden drilling conditions

Other Applications:

- land-use planning (*e.g.*, municipal development planning and zoning)
- routing of transportation, pipeline, utility and communication corridors (for highways, forestry, mines, hydroelectric developments *etc.*)
- evaluating land capability for agriculture (*e.g.*, stoniness, clay content, relief, drainage *etc.*)
- locating areas with surficial materials such as peat and clay that are of potential economic significance
- fisheries applications (*e.g.*, preventing stream sedimentation and turbidity affecting fish and habitat)
- forestry uses (*e.g.*, identifying sites susceptible to logging-induced disturbance)
- wildlife uses (*e.g.*, biophysical inventory)

cial geology information in the province at present are the forest and mineral industries and there is a projected trend of increasing use by government agencies. Government organizations presently using surficial geology data include: Transportation and Highways; Forests; Energy, Mines and Petroleum Resources; Environment, Lands and Parks; British Columbia Hydro; Geological Survey of Canada; and regional and municipal planning departments. Surficial geology data are required by these users mainly for the design of transportation and utility corridors, layout of forest cutblocks, erosion control in community watersheds, protection of fish and wildlife habitat, waste management, aggregate resource identification and production of slope stability maps (Boydell, 1992; Walmsley, 1992). The surficial geology of approximately 60 per cent of the province has been mapped at a scale of 1:50 000 or larger. This database has been compiled by the British Columbia Geological Survey Branch and a listing of these maps was recently presented by Bobrowsky *et al.* (1992).

BEDROCK GEOLOGY

The bedrock geology of the study area was mapped by Roddick and Woodsworth (1979) and the geology of the Coast Mountains has recently been summarized by Monger (1990). The area is underlain mainly by Middle to Late Jurassic and Early to mid-Cretaceous granodiorite and quartz diorite of the Coast Plutonic Complex. These plutons intrude Early Cretaceous rocks of the Gambier Group (mainly andesite, greenstone and argillite with minor conglomerate, limestone and schist) and pre-Late Jurassic greenstone (with minor chert and greywacke) of the Bowen Island Group. The structural geology of the region is characterized by north-northwest trending shear zones such as the Ashlu Creek shear zone north of Squamish and the Britannia shear zone southeast of Britannia. Pliocene to Recent volcanic rocks of the Garibaldi Group dominate the Garibaldi Park area northeast of Squamish. The late Cenozoic history of volcanism in this area was discussed by Green (1990). The presence of these young volcanic rocks has important implications for the study of both geologic hazards and aggregate resources in this region.

QUATERNARY GEOLOGY

The surficial geology of the Squamish area was mapped by Thomson (1980a, b), McCammon (1977), Ryder (1980) and Thomson (1980c) mapped the surficial geology of the Sechelt region. Sand and gravel deposits on the Sunshine Coast area were investigated by McCammon (1977). Exposed bedrock and colluvial deposits dominate the region as a result of the typically high relief and steep slopes. Morainal deposits are restricted mainly to small valleys and lower slopes in large valleys. The bottoms of main valleys such as the Squamish and Cheakamus River valleys are dominated by fluvial and alluvial fan deposits.

Glaciers covered the study area during the Late Wisconsinan up to an elevation of about 2000 metres. Glacial erosional features resulting from this period of ice cover typify the landscape. During glaciation a number of volcanic eruptions occurred producing several unusual ice-

contact volcanic features including collapsed supraglacial tuff-breccia cones, anomalously thick lava flows formed by ponding of lava against ice, a table-shaped complex developed by flooding of lava into a thawed pit in the glacier and esker-like basaltic flows possibly formed by extrusion of lava into tunnels thawed in the ice by heated meltwaters (Mathews, 1951, 1952a, b, 1958; Green, 1990). Glacial depositional features such as well developed mor-

aines are relatively rare, presumably reflecting the rapid retreat of glaciers from the region.

Immediately following deglaciation, sea level was up to about 200 metres higher than present due to glacial isostatic depression (Clague, 1989). Raised glaciofluvial deltas, formed during this period of relatively high sea level, are a major source of sand and gravel deposits in the region today. Postglacial volcanic activity resulted in a number of

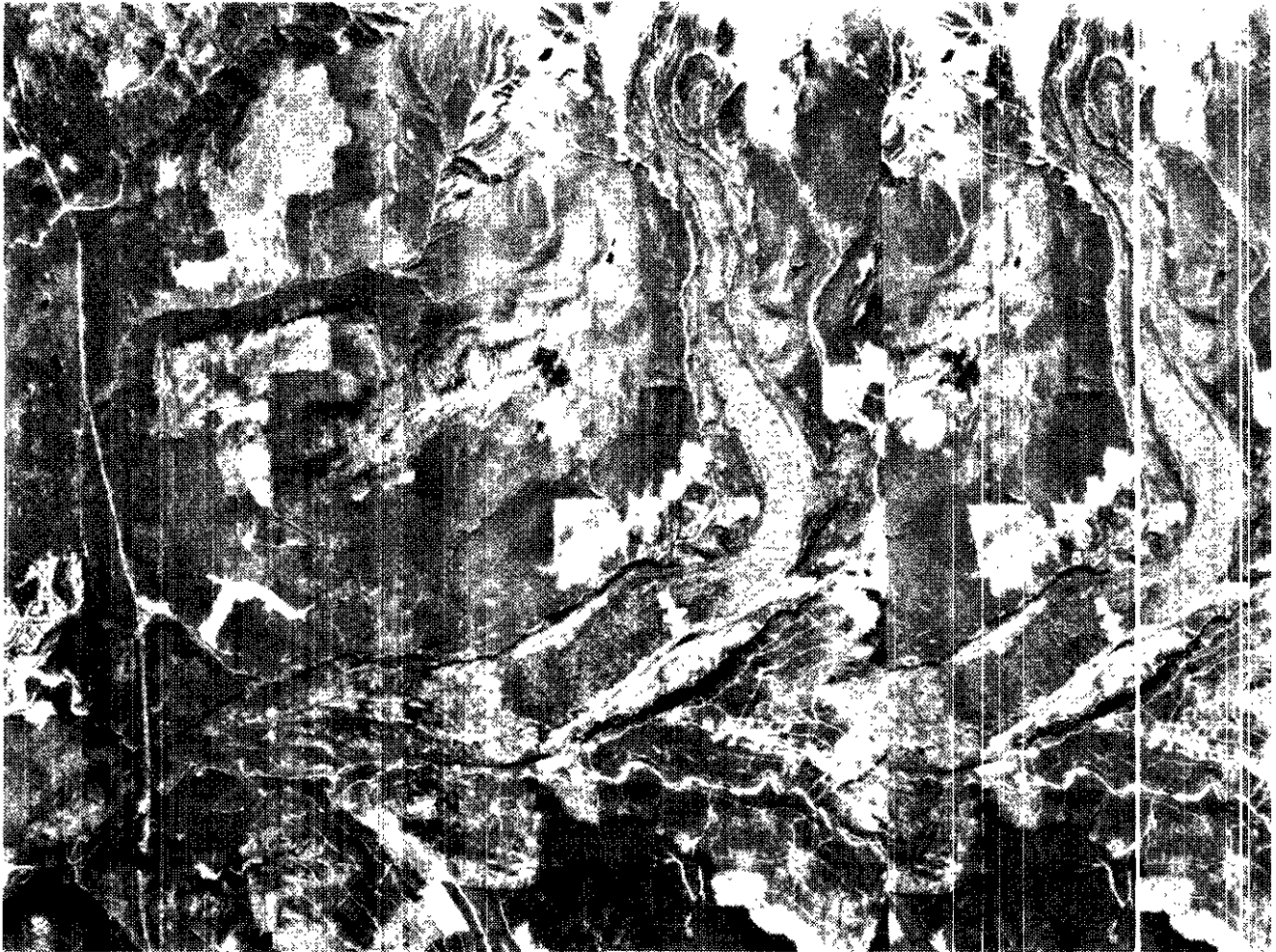


Plate 4-3-1. Postglacial lava flow deposits south of Mount Garibaldi in the Ring Creek area. Note the excellent preservation of morphologic features such as transverse flow ridges and lateral levees. The communities of Squamish, Garibaldi Estates and Brackendale occur directly west of toe of the lava flow. The largest sand and gravel operation in the area can be seen in the southwest corner of the photo.



Plate 4-3-2. Bouldery debris-flood deposits from the August, 1991 event on Furry Creek. Note the large size of the boulders (up to a few metres in diameter) in this abandoned channel that is now entirely above present discharge levels. The upper level of the boulder levees indicates that flow levels almost reached the top of the buttresses of the railroad bridge in the distance and the highway bridge from which the photo was taken.



Plate 4-3-3. One of several engineering structures built along the Sea to Sky Highway (#99) to control debris torrents in high-gradient streams flowing off the Coast Mountains into Howe Sound.

well preserved lava flow deposits in the Mount Garibaldi and Garibaldi Lake areas such as the Ring Creek lava (Plate 4-3-1) which issued from a volcanic cone on the southeast slope of Mount Garibaldi and flowed more than 15 kilometres around the east and south sides of Paul Ridge (Mathews, 1958; Green, 1990).

The southern Coast Mountains were subjected to at least three phases of glaciation during the Holocene including: an early Neoglacial advance known as the Garibaldi phase that occurred between about 6000 and 5000 ¹⁴C years BP; a middle Neoglacial phase (Tiedemann advance) that began about 3300 ¹⁴C years BP and ended some time after 1900 ¹⁴C years BP; and a late Neoglacial phase (Little Ice Age advance) that began before 900 ¹⁴C years BP and reached a maximum between 1800 and 1900 A.D. (Ryder and Thomson, 1986). Moraines, trim lines and other glacial features from this latter advance are well preserved in areas near modern glaciers throughout the region.

GEOLOGIC HAZARDS

The study area has been the focus of numerous investigations of geologic hazards including published studies on debris torrents along Howe Sound (Hungry *et al.*, 1984, 1987), landslides in the Rubble Creek area (Moore and Mathews, 1978) and volcanism in the Mount Garibaldi area (Mathews, 1952a, b; Green, 1990). Numerous other unpublished studies have also been conducted including recent investigations of debris torrents, floods and other geologic hazards along proposed and existing highway corridors (Thurber Engineering Ltd., 1983; Buchanan, 1990, 1991) and an ongoing study of the Cheekye River alluvial fan (Thurber Engineering Ltd. and Golder Associates Ltd., 1992). A summary discussion of geologic hazards in the Howe Sound, Squamish and Whistler areas was recently presented by Hungry and Skermer (1992).

The climate of the region is characterized by high and episodic precipitation as well as sudden large-magnitude snowmelt events; glaciers cover a large part of high-elevation areas (Figure 4-3-1). The combined effects of these climatic factors, as well as the abundance of relatively unstable surficial materials, makes the study area particularly susceptible to slope hazards such as debris flows, debris torrents, rock avalanches and rockfalls. Poorly consolidated volcanic rocks of the Garibaldi Group are especially prone to mass movements.

Evidence of the current susceptibility of the Squamish area to flooding and slope hazards was observed at a number of sites during the course of this study as a result of an unusually high summer rainfall event in 1991 (Hungry and Skermer, 1992). Debris flows and floods during that time occurred on a number of streams in the area including Britannia Creek, Mamquam River, Cheekye River and Furry Creek (Plate 4-3-2). Extensive channel clearing and stabilizing activities were observed at these and other sites in the region as a result of debris deposition in and along stream and alluvial-fan channels at some sites and lateral channel shifting and erosion at other sites during the 1991 event.

Debris torrents are particularly common in the Howe Sound area. They typically have volumes of about 20 000

cubic metres and can attain discharges more than an order of magnitude greater than those of the largest floods (Hungry and Skermer, 1992). Approximately \$35 million was spent on engineering structures along Howe Sound (Plate 4-3-3) in response to three debris torrent disasters in the early 1980s.

A well known example of a rock avalanche occurred on Rubble Creek in the Mount Garibaldi area. The slide involved about 25 million cubic metres of rock derived from the steep, unstable margin of a lava flow that formed by ponding against glacial ice at the end of the Late Wisconsinan (Moore and Mathews, 1978).

The Porteau Cove bluffs provide an excellent example of an area susceptible to rockfall hazards. The likelihood of rockfalls in this region is increased by steeply dipping sheet joints in the plutonic rocks (Plate 4-3-4). Several people have been killed by rockfalls at this site, the most recent fatality occurring in the spring of 1991. Approximately 3000 metres of steel anchors were installed in the steep rock slopes at this site in 1991 by the Ministry of Transportation and Highways (Hungry and Skermer, 1992).

1992 PROGRAM – AGGREGATE RESOURCES

The initial component of this study involves the development of techniques for deriving aggregate resource maps from existing terrain maps. Sand and gravel resources generate between \$130 and \$150 million per year within the province (B.C. Ministry of Energy, Mines and Petroleum Resources, 1990). Although the Ministry of Transportation and Highways currently supports a sand and gravel inventory suitable for provincial government needs, local and regional needs are not currently examined. Rapidly expanding urban development and future transportation corridors require an accessible sand and gravel database.

METHODS

Terrain units with varying levels of sand and gravel resource potential were identified on existing surficial geology maps (Thomson, 1980a, b) of the Squamish area (NTS sheets 92 G/11 and G/14) by an evaluation of the following geologic characteristics: genesis of the surficial material, grain-size distribution (if available), geomorphologic expression, stratigraphic position, unit thickness and deposit size. This information was supplemented with water-well data for several 1:50 000 NTS sheets (92G 5, 11 and 14), obtained from the Ministry of Environment, Lands and Parks. The well logs were summarized and entered into a computer database. Well locations on 92G/11 were identified in the field where possible.

Reconnaissance geomorphologic, sedimentologic and stratigraphic field investigations were conducted to test the validity of the aggregate potential designations (*see below*) and the utility of the compiled borehole data. Sand and gravel deposits were investigated at about 20 different sites including several active pits and a number of abandoned operations. Sediment samples were collected in order to determine the lithological and textural characteristics of the deposits and assess aggregate potential. Associated wood



Plate 4-3-4. Sheet joints in quartz diorite bluffs at Porteau Cove along Highway 99, the site of a number of rockfall disasters. An ambitious slope-stabilization program was conducted at this site in 1991 by the Ministry of Transportation and Highways.

and shell materials were obtained from critical horizons for radiocarbon dating to aid in interpretations of deposit genesis. Physical properties of the deposits, important for determining aggregate quality (such as particle shape, maximum clast-size, grain-size distribution and the presence of deleterious substances including structurally weak particles, clay, organics, chert and chemically reactive particles), were also described. Qualitative determinations of aggregate quality used in this study are based on these physical properties. Although the relative importance of each property varies with different construction applications (Barksdale, 1991), good quality aggregates generally are well graded and contain few large clasts, little silt or clay and few deleterious substances. Detailed laboratory tests, including specific gravity, adsorption, degradation, abrasion, sulphate soundness, sand equivalent and freeze-thaw tests, used to examine aggregate suitability for specific applications (Barksdale, 1991) are beyond the scope of this study.

RESULTS

DESCRIPTION OF AGGREGATE DEPOSITS

The results of field investigations in the area indicate that the most common sources of aggregate presently or previously exploited in the region are glaciofluvial sediments

deposited in braided stream, delta and fan-delta environments. Terrain units consisting of glaciofluvial deposits are relatively easily identified and accurate mapping of these units appears to be more consistent than other terrain units. These sand and gravel deposits provide good quality aggregates as they generally are well graded and contain few fines or deleterious substances. Deltaic deposits are characterized by thick sequences of moderately to well sorted gravels with well developed foreset bedding (Plate 4-3-5). Beds of sandy matrix-filled gravels typically alternate with open-work gravels; silts and clays are rare. Fan-delta deposits are similar but tend to have a greater range in clast sizes with a larger number of cobbles and boulders (Plate 4-3-6). Fan-delta deposits in the area are typically smaller than glaciofluvial deltaic deposits and they are mainly restricted to areas along the lower slopes of mountains bordering Howe Sound. Braided stream deposits are generally dominated by pebble to cobble gravels with horizontal bedding and cut-and-fill channel structures on all scales (Plate 4-3-7). Braided stream deposits occur as progradational sequences overlying glaciofluvial delta deposits at several sites (Plate 4-3-8).

Alluvial fan deposits are the second most abundant aggregate source in the region, comprising nearly 25 per cent of

the gravel pits visited. These deposits are generally lower quality aggregates than glaciofluvial deposits because they tend to have an overall wider range in clast size and more variability in grain-size distribution from bed to bed. For example, they often contain diamicton units with relatively high proportions of silt and/or clay interbedded with the sand and gravel. The proportion of large boulders in these deposits is also generally higher than in most of the productive glaciofluvial sequences in the area.

Talus deposits have been worked at a number of sites in the area and are an unexpectedly common source of sand and gravel. These deposits are characterized by crudely bedded, angular, pebble to cobble-sized gravels (Plate 4-3-9). They are typically monolithologic, consisting of fragments of basalt or other volcanic rocks. They are derived mainly from steep exposures of Garibaldi Group volcanics. Closely spaced columnar jointing (in some cases on the order of a few centimetres) in these young volcanic rocks has allowed for the development of relatively thick talus accumulations of pebble to small cobble-sized material. At some sites the deposits are relatively uniform in size and they are a potential source of aggregate as they contain virtually no fine-grained matrix materials.

SUBSURFACE (WATER-WELL) DATA

The British Columbia water-well database, housed with the Ministry of Environment, Lands and Parks, is an excellent source of subsurface surficial geology data but a preliminary evaluation of the utility of the data for the purpose of producing aggregate potential maps indicates a number of problems. First, the database is incomplete as there is no provincial legislation requiring submission of well logs. Data are supplied gratuitously to the province, mainly by companies and drilling contractors. In addition, the data provided are not independently confirmed by the province and consequently all data released to users by the Ministry is qualified with a cautioning disclaimer. The database includes a computerized listing of well logs and a manually plotted series of maps showing well locations. The well owner, date and method of construction and well depth are recorded for all sites in the computerized listing. However, detailed location data, well yield information, water table depth and water quality data are only available for some wells. Well locations have been plotted using the British Columbia Geographic System (BCGS) of mapping at scales ranging from about 1:12 000 to 1:16 000 in the study area. Unfortunately plotted locations have not been verified and field checking of these maps in the Squamish area revealed a number of misplotted wells. In addition, cross-referencing of well locations in the computer database with locations on the maps is problematic as, in some cases, one or more sites with the same well number have been plotted in the same BCGS map unit and in a few cases not all well locations have been plotted.

In spite of these difficulties, the provincial water-well database can be used at sites where there are no discrepancies between recorded and plotted locations or where detailed location data are available and can be verified. Similarly, although the quality of the well logs in the

database generally has not been independently verified, many of the logs have been provided by professional groundwater geologists, as in the example provided in Figure 4-3-2. Although there are obvious problems with using unverified data, the database is nevertheless considered to be a valuable source of subsurface data because of the good quality of many of the logs and the possibility of verification of the data by field studies and by stratigraphic comparisons of independent logs with published data.

AGGREGATE POTENTIAL

Terrain units in the study area having high, medium and low potential for aggregate deposits were identified on the basis of the geologic criteria outlined above from existing data. The relative terms high, medium and low are used because this type of classification can easily be used by land-use planners. Regional variations in factors controlling aggregate potential, such as natural abundance, quality, accessibility and degree of man-induced alienation, can also be accommodated. In addition, although the classification is qualitative, it can be derived by quantitative methods, with a degree of sophistication that varies with the level of data available.

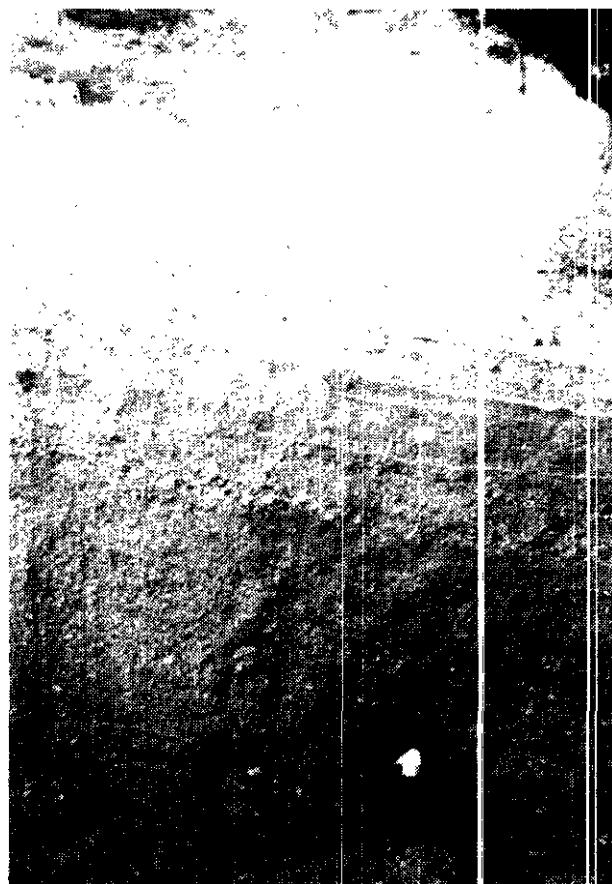


Plate 4-3-5. Well sorted deltaic gravels at the Coast Aggregate Ltd. pit east of Squamish. Foresee bedding is defined by alternating strata of sandy matrix-filled gravels and open-work gravels.



Plate 4-3-6. Glaciofluvial fan-delta deposit at a small gravel pit approximately 500 metres north of Shannon Falls. The boulder at the base of the exposure is 1.1 metres in diameter. Note the high degree of clast rounding.

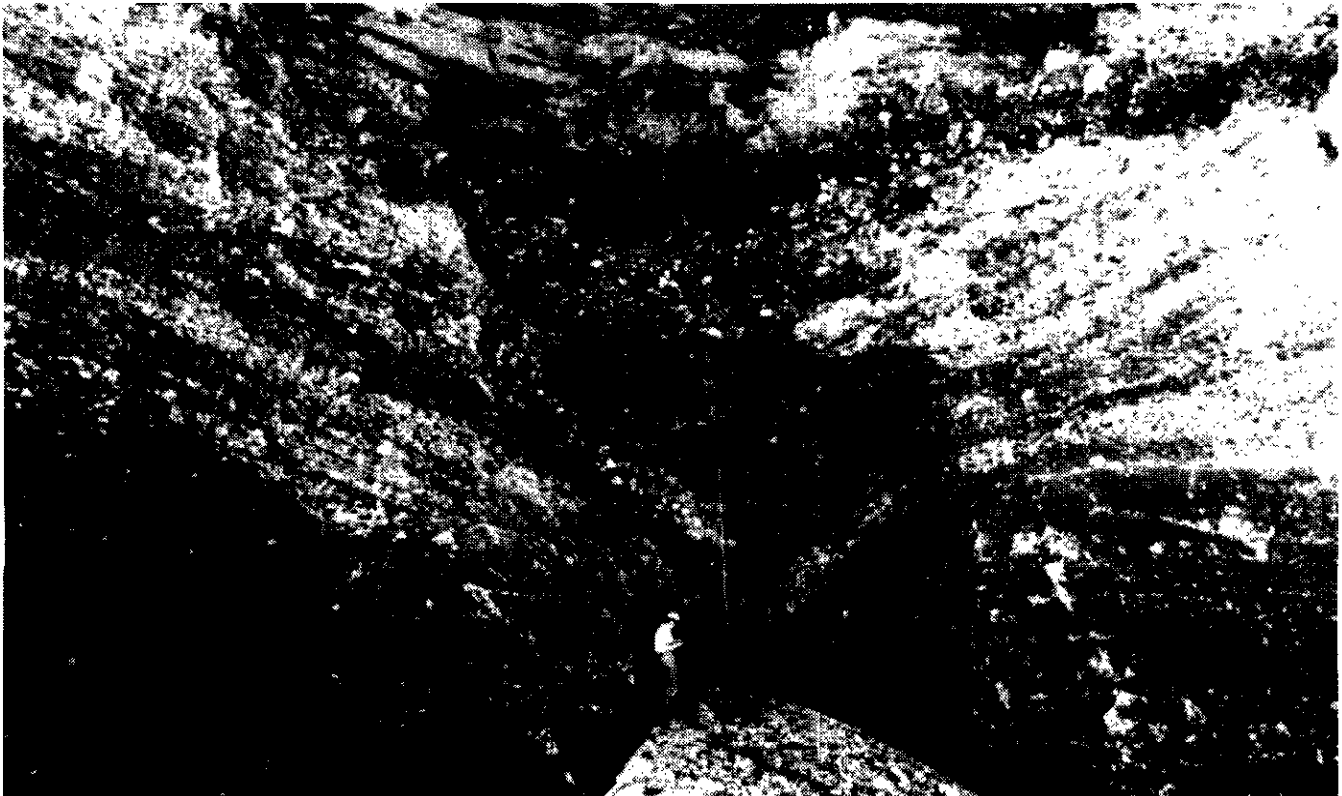


Plate 4-3-7. Well developed channel structures in braided stream deposits. Dark layers are open-work gravels stained with manganese oxides. The photo is taken at the same site as Plate 4-3-5 but at a higher stratigraphic level.

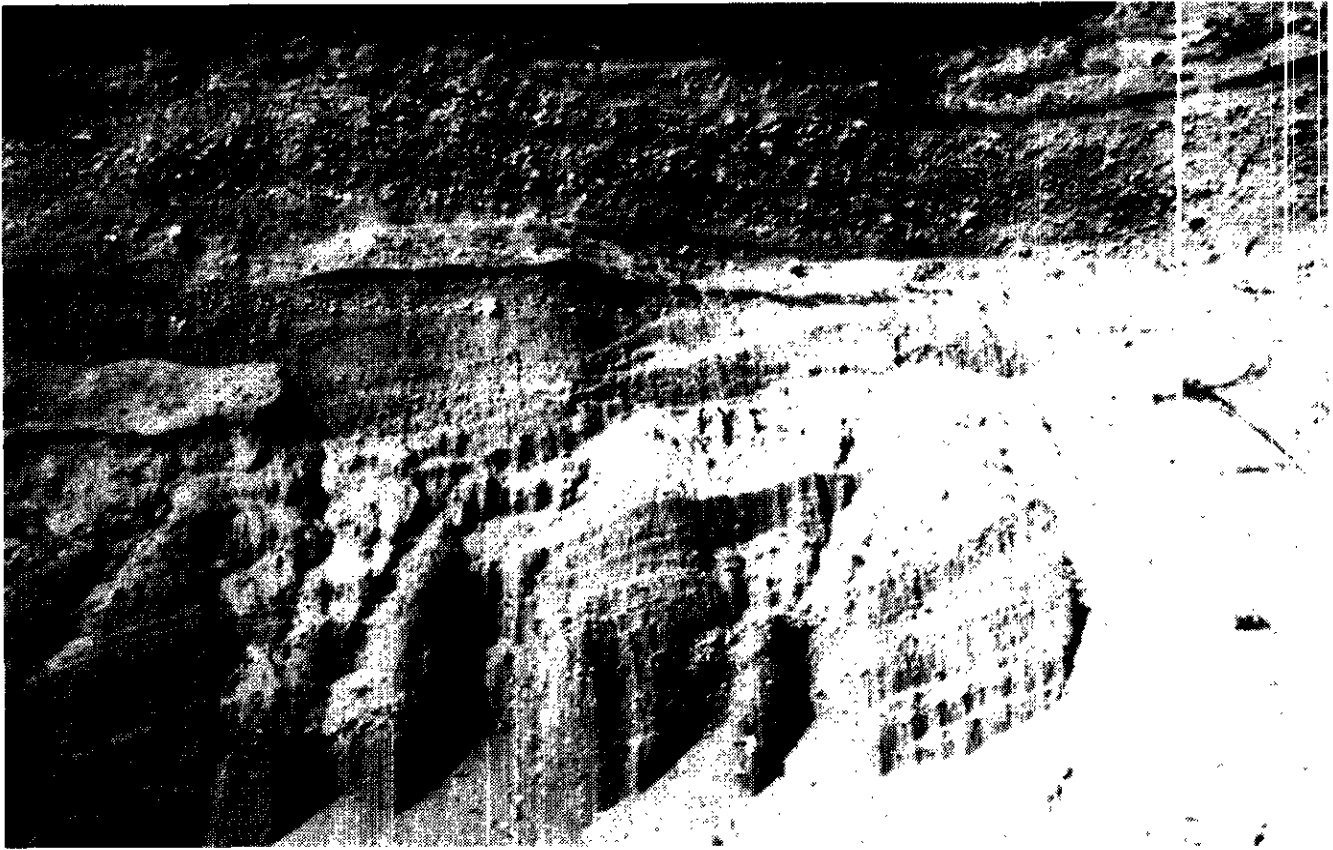


Plate 4-3-8. Glaciofluvial deltaic gravels with steep foreset bedding overlain by braided stream deposits with horizontal bedding and large-scale, low-angle, trough crossbedding along the north side of the Mamquam River about 4 kilometres up stream of its confluence with the Squamish River.

Terrain units identified as having high potential for aggregate deposits include glaciofluvial terrace and deltaic deposits (F^G). Fluvial low-terrace deposits (F^t) and alluvial fan deposits (F^f) identified with sand, pebble and/or general gravel textural modifiers or those known to be composed mainly of sand and/or gravel on the basis of drill logs were classified as moderate potential aggregate deposits. Floodplain deposits (F^A) were identified as low potential sand and gravel deposits because of the shallow water table. The latter can be inferred from terrain maps by the presence of a qualifying descriptor (identified with the ^A superscript) indicating active modifying processes such as flooding, or from subsurface data such as water-well records (e.g., Figure 4-3-2). Other map units with low aggregate potential include alluvial fans dominated by muddy debris-flow deposits, colluvial deposits including gravelly landslide and talus deposits (C^f), and gravelly or sandy morainal deposits. Terrain units with moderate or high potential occurring as secondary or tertiary units within a map polygon, those occurring as veneers over bedrock or morainal deposits and those with thick overburden were classified as low potential units. There are several other types of surficial materials that have potential mainly as sandy aggregates but that were not mapped in the study area. These include: thick sandy eolian deposits (e.g., sand dunes), sandy lacustrine beach

deposits, proximal glaciolacustrine sediments, marine spits, bars and beaches, and glaciomarine raised-beach and near-shore deposits.

CONCLUSIONS

Uses of surficial geology data briefly outlined in this paper include applications in the fields of mineral exploration and development, forestry, environmental studies (including fisheries, wildlife, recreation, parks and groundwater applications), engineering, geologic hazard studies and land-use planning. Surficial geology data in the form of maps and drill logs currently exist for much of British Columbia but the information is complicated and commonly must be scientifically evaluated, synthesized and in some cases supplemented with new data before it can be readily utilized in these applied fields.

From descriptions of existing and potential aggregate deposits in the study area, it is concluded that glaciofluvial braided stream and deltaic deposits are the highest potential aggregates because they are extensive, well sorted and contain little silt or clay. Low-terrace fluvial deposits and gravelly alluvial fan sediments are considered to be moderate potential aggregates as they tend to be more poorly sorted than glaciofluvial deposits. Gravelly colluvium and morainal



Plate 4-3-9. Angular, monolithologic talus deposits exposed along the shoreline of Howe Sound near Watts Point. These deposits are derived from steep cliffs of strongly jointed basalt and have been quarried at several sites in the area. Note the wood fragment directly below the rock hammer.

deposits are low potential units as are moderate or high potential sand and gravel deposits that occur as thin veneers or with thick overburden.

Preliminary results of field evaluations of aggregate potential maps prepared in the office indicate that, in general, potential sand and gravel areas identified from existing data were much larger than those identifiable in the field. The main reason for this is that sand and gravel deposits typically comprise small areas within larger, more generalized terrain units. In addition, many large map units with good potential for sand and gravel are not exploitable because of shallow groundwater tables. These map units include intermittently active fluvial channels and bars, and low terraces and floodplains. Classification of sand and gravel potential from mapped surficial geology data will have to take these factors into account. For example, map units containing relatively small areas with high potential for aggregate that occur within a larger region of lower potential will have to be distinguished from map units dominated by areas with high potential for sand and gravel deposits. Similarly, map units with near-surface water

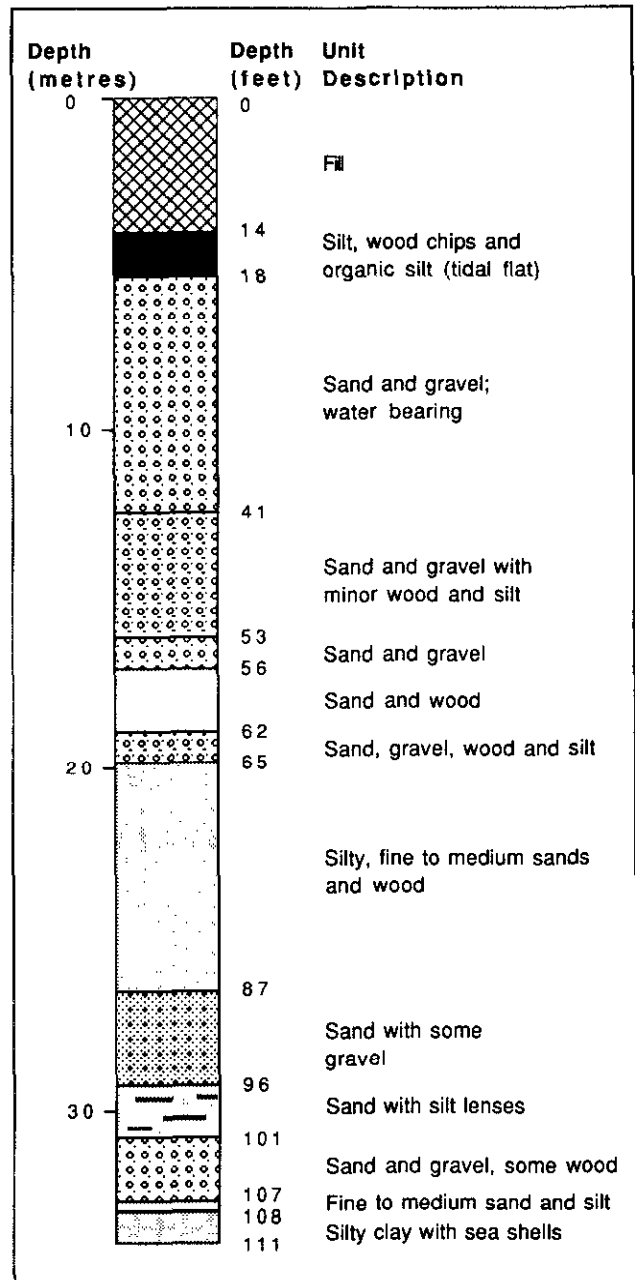


Figure 4-3-2. Sample well log from the British Columbia water-well database maintained by the Ministry of Environment, Lands and Parks. The shallow water table, indicated by the presence of water-bearing sand and gravel near the surface, limits the potential of these deposits for aggregate purposes.

should be distinguished from those with deep groundwater tables. Information on high groundwater table levels may have to be derived from sources other than surficial geology maps, such as water-well records. Additional data on slope, topography and depth to bedrock should also be incorporated into the classification. Other regional factors, such as the abundance of gravelly talus deposits derived from recent volcanics in this region, will also have to be considered.

FUTURE WORK

Methodologies for the production of derivative products such as 1:50 000 aggregate distribution maps which include volume and shape estimates are currently being developed. Further research in the aggregate component of this program will include:

- Testing the accuracy of these methodologies for producing aggregate potential maps and their applicability to different areas of the province.
- An evaluation of the utility of using existing subsurface data for three-dimensional reconstructions.
- An investigation of techniques for capturing surficial geology data in digital format and producing derivative algorithms.

In addition to providing information on aggregate deposits, data collected during this study will be used to elucidate the Quaternary history of the area and to investigate the frequency and nature of geologic hazards in the region. Studies to develop methodologies for combining surface and subsurface data to produce other applied products such as geologic hazard potential maps will be conducted in a subsequent phase of this project.

ACKNOWLEDGMENTS

Colleen Bauer provided outstanding assistance in the field. Diagrams were capably drafted by Scott Henthorn. The manuscript was reviewed by John Newell, Peter Bobrowsky, Brian Grant and Paul Matysek. This study was initiated on the basis of a recommendation of an independent advisory panel to the Surficial Geology Unit. Panel members are Rob Buchanan, John Clague, Kay Fletcher, Bob Gerath, Nat Rutter, June Ryder, Ian Thompson and Doug VanDine. Their contributions to this and related projects is gratefully acknowledged as is the assistance of Peter Bobrowsky, Tim Giles, Dan Kerr and Paul Matysek in the development of the program.

REFERENCES

- Barksdale, R.D. (Editor) (1991): The Aggregate Handbook; *National Stone Association*, Washington, D.C.
- Bobrowsky, P.T., Giles, T. and Jackaman, W. (1992): Surficial Geology Map Index of British Columbia; *B.C. Ministry of Energy, Mines and Petroleum Resources*, Open File 1992-13.
- B.C. Ministry of Energy, Mines and Petroleum Resources (1990): British Columbia Mineral Statistics, Annual Summary Tables, Historical Mineral Production to 1990; prepared by the Mineral Statistics Section, 86 pages.
- Boydell, A.N. (1992): Surficial Geology and Land Use; unpublished report prepared for the Surficial Geology Task Group, Resource Inventory Committee, Victoria, 15 pages.
- Buchanan, R.G. (1990): Preliminary Geotechnical Investigation, Indian Arm Corridor (East Alternative), Sea to Sky Highway Project; unpublished report, *B.C. Ministry of Transportation and Highways*, 22 pages.
- Buchanan, R.G. (1991): Geotechnical Investigation, Squamish to Whistler Village, Preliminary Planning and Design; unpublished report, *B.C. Ministry of Transportation and Highways*, 33 pages.
- Clague, J.J. (1989): Quaternary Sea Levels (Canada in Cordillera); in *Quaternary Geology of Canada and Greenland*, Fulton, R.J., Editor, *Geological Survey of Canada*, Geology of Canada, Number 1, pages 43-47.
- Ferguson, A. and McPhee, M. (1992): Howe Sound Watershed Environmental Science Workshops and Public Meetings, Summary of Proceedings; unpublished report, *Environment Canada*, 107 pages.
- Green, N.L. (1990): Late Cenozoic Volcanism in the Mount Garibaldi and Garibaldi Lake Volcanic Fields, Garibaldi Volcanic Belt, Southwestern British Columbia; *Geoscience Canada*, Volume 17, pages 171-175.
- Hungr, O. and Skermer, N.A. (1992): Debris Torrents and Rockslides, Howe Sound to Whistler Corridor; in *Geotechnique and Natural Hazards, Technical Tours Guidebook*, *BiTech Publishers Ltd.*, pages 4-46.
- Hungr, O., Morgan, G.C. and Kellerhals, R. (1984): Quantitative Analysis of Debris Torrent Hazards for Design of Remedial Measures; *Canadian Geotechnical Journal*, Volume 21, pages 663-667.
- Hungr, O., Morgan, G.C., VanDine, D.F. and Lister, D.R. (1987): Debris Flow Defenses in British Columbia; *Reviews in Engineering Geology*, Volume 7, pages 201-223.
- Mathews, W.H. (1951): The Table, a Flat-topped Volcano in Southwestern British Columbia; *American Journal of Science* Volume 249, pages 830-841.
- Mathews, W.H. (1952a): Mount Garibaldi, a Supra-glacial Volcano in South-western British Columbia; *American Journal of Science*, Volume 250, pages 81-103.
- Mathews, W.H. (1952b): Ice-dammed Lavas from Clinker Mountain, South-western British Columbia; *American Journal of Science*, Volume 250, pages 553-565.
- Mathews, W.H. (1958): Geology of the Mount Garibaldi Map Area, South-western British Columbia - II, Geomorphology and Quaternary Volcanic Rocks; *Geological Society of America, Bulletin*, Volume 69, pages 179-198.
- McCammon, J.W. (1977): Surficial Geology and Sand and Gravel Deposits of Sunshine Coast, Powell River and Campbell River Areas; *B.C. Ministry of Energy, Mines and Petroleum Resources*, Bulletin 65, 36 pages.
- Monger, J.W.H. (1990): Georgia Basin: Regional Setting and Adjacent Coast Mountains Geology, British Columbia; in *Current Research, Geological Survey of Canada*, Paper 90-1F, pages 95-107.
- Moore, D.P. and Mathews, W.H. (1978): The Ruble Creek Landslide, British Columbia; *Canadian Journal of Earth Sciences*, Volume 15, pages 1039-1052.
- Roddick, J.A. and Woodsworth, G.J. (1979): Geology of Vancouver, West Half, and Mainland Part of Alberta; *Geological Survey of Canada*, Open File 611.
- Ryder, J.M. (1980): Terrain Map of Sechelt, 92G/5; unpublished map, *B.C. Ministry of Environment, Lands and Parks*, 1:50 000-scale.
- Ryder, J.M. and Thomson, B. (1986): Neoglaciation in the Southern Coast Mountains of British Columbia: Chronology Prior to the Late Neoglacial Maximum; *Canadian Journal of Earth Sciences*, Volume 23, pages 273-287.
- Thomson, B. (1980a): Terrain Map of Squamish, 92C/11; unpublished map, *B.C. Ministry of Environment, Lands and Parks*, 1:50 000-scale.
- Thomson, B. (1980b): Terrain Map of Cheakamu River, 92G/14; unpublished map, *B.C. Ministry of Environment, Lands and Parks*, 1:50 000-scale.

- Thomson, B. (1980c): Terrain Map of Sechelt Inlet. 92G/12; unpublished map. *B.C. Ministry of Environment, Lands and Parks*, 1:50 000-scale.
- Thurber Engineering Ltd. (1983): Debris Torrent and Flooding Hazards Along Highway 99; unpublished report for *B.C. Ministry of Transportation and Highways*.
- Thurber Engineering Ltd. and Golder Associates Ltd. (1992): Cheekye River Terrain Study; unpublished report for *B.C. Ministry of Lands, Parks and Housing*.
- Walmsley, M.E. (1992): Report of the Soils, Geology and Archaeology Task Force; unpublished report prepared for the Resource Inventory Committee by *Westland Resource Group*, Victoria, 24 pages.

DRIFT EXPLORATION STUDIES, VALLEY COPPER PIT, HIGHLAND VALLEY COPPER MINE, BRITISH COLUMBIA: STRATIGRAPHY AND SEDIMENTOLOGY (92I/6, 7, 10 and 11)

By P.T. Bobrowsky, D.E. Kerr, S.J. Sibbick,
B.C. Geological Survey Branch
and K. Newman, Highland Valley Copper Ltd.

KEYWORDS: Applied geochemistry, lake sediments, Highland Valley Copper, Interior Plateau, drift exploration, surficial geology, Quaternary, stratigraphy, sedimentology, till, lacustrine, ¹⁴C dating.

INTRODUCTION

During the 1992 field season, drift exploration studies were undertaken by staff of the British Columbia Geological Survey Branch at the Highland Valley Copper mine (Figure 4-4-1). The project is part of a drift-prospecting program integrating surficial geology and applied geochemistry in the search for mineral deposits in areas of glaciated and drift-covered terrain in the province. Related studies this year include a case study documenting geochemical dispersion in till, conducted at the Galaxy deposit south of Kamloops, and the Anahim Lake map sheet, where reconnaissance till geochemical data were collected and terrain maps were produced (Proudfoot, 1993; Giles and Kerr, 1993; both this volume). The objectives of the program are summarized as follows:

- Develop, evaluate and recommend methods and techniques applicable to mineral exploration.

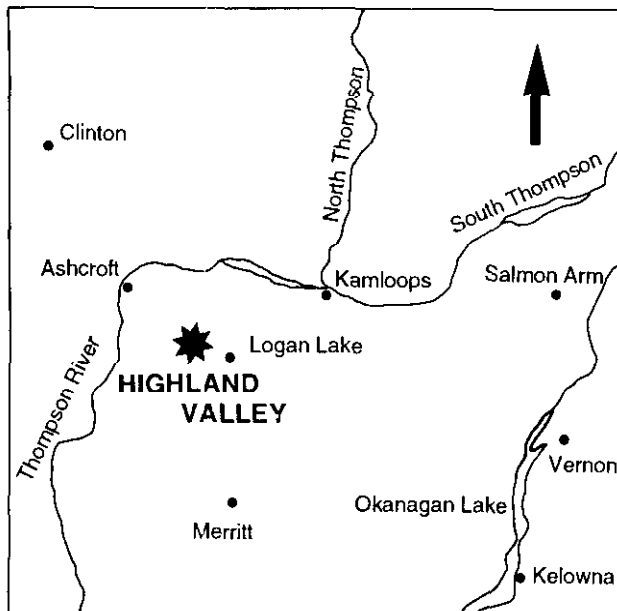


Figure 4-4-1. Location of the Highland Valley study area, southern British Columbia.

- Stimulate mineral exploration activities in glaciated and drift-covered regions of the province through specialized surficial geology techniques.
- Develop interpretive drift-exploration models founded on principles of Quaternary geology.
- Produce surficial geology and applied derivative maps at a scale of 1:50 000 which will be of practical use to the exploration community.

Previous studies relevant to the general drift-exploration program and its objectives have been detailed or summarized elsewhere (e.g., Kerr and Bobrowsky, 1991; Sibbick *et al.*, 1992). The present report provides a summary of field activities and details of the stratigraphy and sedimentology in the Valley pit area of Highland Valley Copper mine located some 370 kilometres northeast of Vancouver. Detailed interpretive results of the ancillary geochemical and surficial data will appear elsewhere, following completion of several analytical procedures now in progress.

Highland Valley Copper mine was selected for investigation during this field season given:

- Easy access to a lengthy and complex overburden sequence which overlies strongly mineralized bedrock (as recently exposed by mining in the Valley pit).
- The fortuitous occurrence of organic materials scattered throughout the deposits, which are suitable for radiocarbon dating and thus chronological control.
- The opportunity to evaluate modern methods of lake-sediment geochemistry sampling by analogy to an ancient lake sediment sequence (in direct contact with the mineralized bedrock).
- The possibility of obtaining proxy Quaternary data through paleomagnetic and pollen analyses.
- The occurrence of economic mineral deposits in the region.

A detailed study of the geology and geochemistry of a preserved lake sediment sequence overlying the Valley Copper orebody was undertaken, as a complement to the Applied Geochemistry Unit's lake sediment program (Cook, 1993, this volume). The goal of this research is to define controls on metal transport and deposition in a drained lake directly overlying ore. The results of these investigations will provide us with information (*i.e.*, geochemical dispersion characteristics) for evaluating the viability of modern lake sediment geochemistry. The underlying premise of modern lake sediment sampling assumes that these samples provide regional geochemical data representative of the underlying lithologies and reliable indica-

tions of local mineral occurrences. The occurrence of ancient lake sediments in direct contact with a known orebody provides a standard against which methods of modern lake sediment sampling can be compared. The success of this investigation depends to a large extent on the detail and accuracy of interpretation provided by complementary stratigraphic and sedimentological research. The present paper describes this research work.

PREVIOUS WORK

Excluding the work of early geologic explorers working in the Interior Plateau of southern British Columbia, it is the notable mineral deposits in the area (including Bethlehem, Lornex, Valley Copper, Highmont and JA; Figure 4-4-2) which have significantly influenced ongoing geological and mineral exploration studies. These studies have added immensely to the geological database.

Previous studies on the bedrock geology of the Highland Valley deposits and surrounding area have been detailed in several publications (*cf.* Sutherland Brown, 1976 for review articles as well as discussion below). Previous surficial studies are, however, less well known. During the 1960s and

1970s, R.J. Fulton (Geological Survey of Canada) mapped the surficial sediments directly east of the study site and developed a good understanding of the regional patterns of glaciation and deglaciation for the southern Interior Plateau. Based on his work (Fulton, 1969, 1975; Fulton and Smith, 1978), the Quaternary stratigraphy for this region can be summarized as typically consisting of Okanagan Centre Drift deposits (type locality near Okanagan Lake) of Early Wisconsinan age (>65 000 years old), overlain by Bessette Sediments (type locality near Lumby) of mid-Wisconsinan age (>20 000 - 65 000 years old) and Kamloops Lake Drift deposits (type locality near Kamloops Lake) correlative with the Late Wisconsinan (10 000 to 20 000 years old). Much older sediments, including deposits with reversed polarity (Matuyama age; >790 000 years), have recently been identified south of Merritt (Fulton *et al.*, 1992). Stratigraphy in the Merritt area (Table 4-4-1) is better understood and, therefore, much more detailed than elsewhere, but the essential components remain similar to the generalized stratigraphy of the Interior Plateau.

Perhaps the greatest attention has been paid to the history of deglaciation of the southern Interior Plateau and surficial deposits associated with the event (Fulton, 1967, 1969,

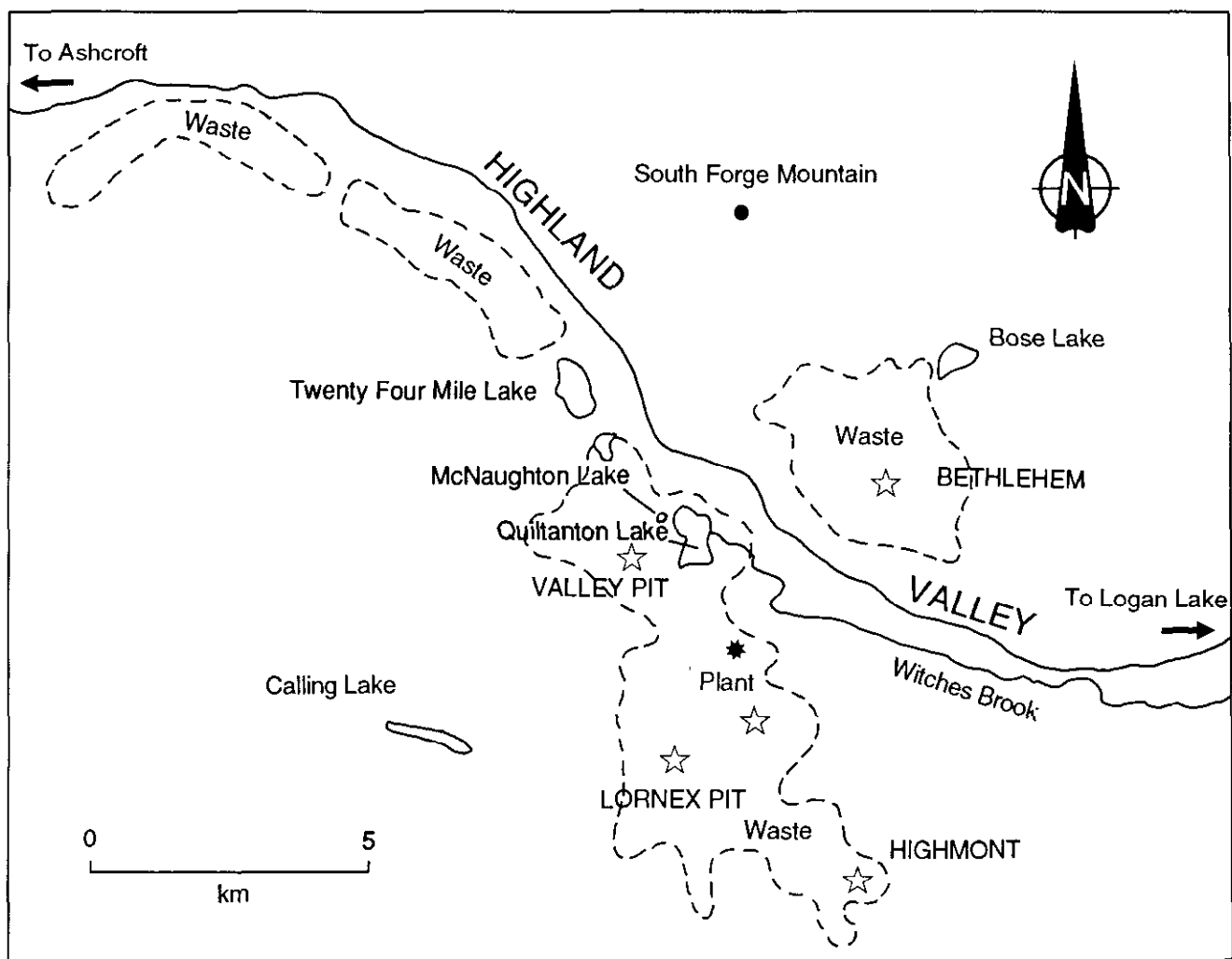


Figure 4-4-2. Location of the Valley pit and other deposits and features referred to in the text.

TABLE 4-4-1
QUATERNARY STRATIGRAPHIC UNITS IN THE
VICINITY OF MERRITT, BRITISH COLUMBIA

UNIT NAME	LOCALITY	INTERPRETATION	AGE
Merritt silts (Kamloops Lake Drift)	Merritt Lily Lake Road Coldwater	Glacial lake sediments	111 ka
Till (Kamloops Lake Drift)	Lily Lake Road Coldwater	Glacial deposit	11-20 ka
Proglacial Sediments (Kamloops Lake Drift)	Lily Lake Road	Proglacial deposits	120-25 ka
Brown Drift	Coldwater River	Glacial deposits	> 25 to < 790 ka
Valley basalts	Chutter Ranch Quilchena Creek valley	Volcanic eruption	100 to < 790 ka
Coutlee sediments	Lily Lake Road	Interglacial basin fill deposits	≥790 ka
Sub-Coutlee sediments	Lily Lake Road	Glacial lake deposits	> 790 ka
Coldwater silts	Coldwater	Glacial lake deposits	> 790 ka

According to Fulton et al. (1992)
Age is given in thousands of years before present (ka)

1991; Church and Ryder, 1972). The present day physiography, characterized by rolling uplands, steep-walled, flat-floored valleys, as well as open grassland and pine forested slopes, is strongly influenced by the style of deglaciation. Most of the major valleys and tributaries in the Interior Plateau supported large ice-dammed lakes as ice retreated northward at the end of the Pleistocene (Ryder *et al.*, 1991). These glaciolacustrine deposits typically consist of sand and silt, are of varying thickness and pose considerable hazard to transportation corridors and structures given their propensity to slope failure (Evans and Buchanan, 1976). From an exploration perspective the pervasive glaciolacustrine sediments conceal mineral deposits. As noted elsewhere in this paper, glaciolacustrine deposits are an integral component of stratigraphy of the valley-fill sequences of the study area and must be adequately understood.

At Highland Valley Copper, an early Quaternary geological investigation by J. Mollard (Ripley, Klohn and Leonoff, 1972) included air photo study and surficial map generation (scale of 1:31 680) as well as an interpretation of borehole drilling results from Witches Brook, east of the present mine area (Figure 4-4-2). More recently, Golder Associates Ltd. (1992) drilled a 245-metre hole in the valley floor north of the Highland Valley Copper mine. One other recent surficial study completed near the mine area is that of Clague (1988) who examined tephra and organic remains exposed in sediments of McNaughton Lake which was drained and trenched in early 1985 to allow for mine expansion (Figure 4-4-2).

BEDROCK GEOLOGY

The Valley orebody is located in the central core of the Late Triassic Guichon Creek batholith. The multiphase intrusions within the batholith are progressively younger from the border to the core. The core, or Bethsaida phase, is a coarse porphyritic granodiorite (Figure 4-4-3). The main alteration types are argillic, potassic and sericitic. The copper sulphides are bornite and chalcopyrite. In the central part of the orebody bornite:chalcopyrite ratios are 3:1 and decrease away from the core to the fringes. Bornite and

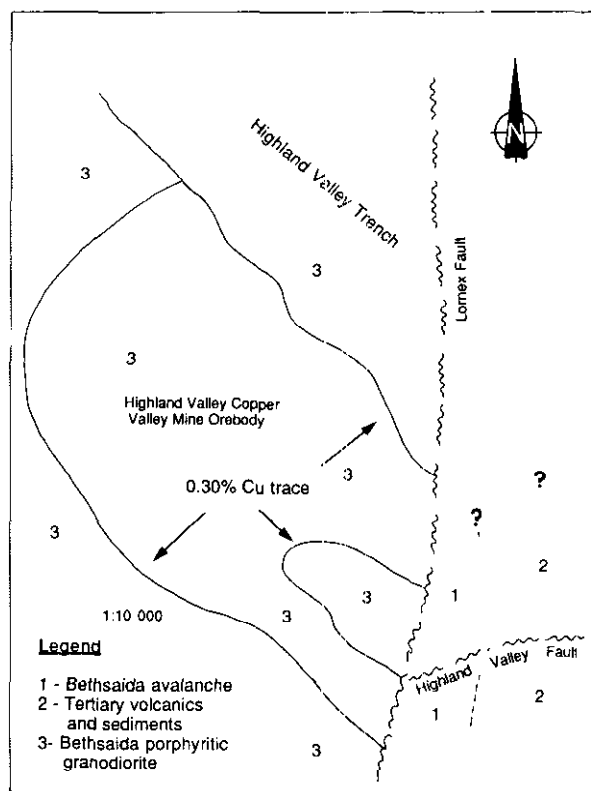


Figure 4-4-3. Bedrock geology of the Valley pit area. See text for details.

chalcopyrite are associated with a stockwork of quartz-sericite and crystalline sericite veins. The fracture sets are related to the north-striking Lornex fault and the east-striking Highland Valley fault. The southeast extension of the orebody is terminated by the Lornex fault. Drilling data indicate that the Lornex fault formed a 70° to 80° escarpment facing east with a height of at least 280 metres. Erosion and subsequent "bedrock avalanching" along the escarpment deposited ore-bearing boulders and debris on exposed Tertiary volcanics which are down-faulted against the Bethsaida phase. Glaciation and general erosion have modified the escarpment (*cf.* McMillan, 1976; Walcne: *et al.*, 1976; Osatenko and Jores, 1976).

METHODS

Surficial data and geochemical samples were collected at the western margin of the Valley open pit (Figure 4-4-2). Ongoing mining in this area provides access to both mineralized bedrock outcrop and deep valley-fill sediments. Mining procedures provided ready access to exposures of unconsolidated sediments including the deepest deposits which are directly in contact with underlying mineralized outcrop. Each mining bench is exactly 12.5 metres above the underlying bench, thereby providing accurate positioning and elevation data for the study. The benches also provide steep faces accessible for detailed stratigraphic and sedimentologic analysis (Table 4-4-2). During this summer, the east wall of the pit provided the best exposure of unconsolidated sediments, including evidence of the rela-

TABLE 4-4-2
FREQUENCY DISTRIBUTION OF DRIFT
EXPLORATION DATA

FACE	ELEVATION	LITHO.	PEBBLE	TEXTURE	GEOCHEM	POLLEN	¹⁴ C	FABRIC
13	1250.0-1262.5	VII	1	1	-	-	-	1
12	1237.5-1250.0	VII	-	-	-	-	-	-
11	1225.0-1237.5	VI, VII	1	1	-	-	-	1
10	1212.5-1225.0	VI	1	1	-	-	-	1
09	1200.0-1212.5	VI(VIII,IX)	4	1	(20)	-	-	1
08	1187.5-1200.0	IV,V(VIII)	-	1	-	1	1	-
07	1175.0-1187.5	IV	1	-	-	-	-	1
06	1162.5-1175.0	IV	1	-	-	-	-	-
05	1150.0-1162.5	IV	1	-	-	-	-	1
04	1137.5-1150.0	III, IV	2	1	-	2	4	-
03	1125.0-1137.5	II, III	-	-	41	3	1	-
02	1112.5-1125.0	II	-	-	34	-	4	-
01	1100.0-1112.5	I, II	3	2	21	3	1	1

In relation to exposure face, elevation (metres above sea level), lithostratigraphic unit and type of sample information for the Highland Valley Copper mine study. Note: Holocene lake sediments (lithostratigraphic unit IX) and underlying oolite deposits (lithostratigraphic unit VIII) which have cross-cut older deposits at a lower elevation are listed in brackets.

tionship of the lowest sediments to the mineralized bedrock. Excavation depth had reached 1100 metres above sea level, which provided access to a total of 13 faces for a cumulative vertical exposure of 162.5 metres.

Surficial studies included detailed descriptions of the nature and extent of the major lithostratigraphic units and beds exposed in the pit faces. Characteristics described include types of contacts, lateral and vertical extent of units and beds, internal structures and bedding style, sediment texture, as well as clast lithologies, shape, size and fabric. Bulk samples were taken from major units and unique beds for textural analysis. Similarly, palynological samples were taken from nonglacial deposits for relative dating and paleoecological analysis. Samples of wood were collected for conventional ¹⁴C analysis. Pebble samples (100 clasts/sample) were taken from representative units and beds for lithologic analysis. Sample provenance relative to pit face, elevation and lithostratigraphic unit is summarized in Table 4-4-2. Palynological, textural, paleomagnetic and radiocarbon samples have been submitted for analysis.

Geochemical sampling was primarily directed toward exposures of the oldest lacustrine sediments. Ninety-six bulk samples (2 to 3 kg) were taken from six profiles exposed on the eastern face of the 1100, 1112.5 and 1125-metre benches (cf. Table 4-4-2; Figure 4-4-4). Samples were taken at 1-metre intervals depending on access and exposure. Fifteen additional samples were taken at 10-metre intervals along a well-defined horizon within the lowest sequence in order to study lateral variation in lake sediments. These samples have been sieved to -250+125 micron, -125+63 micron and -63 micron size fractions for analysis by inductively coupled plasma (ICP) and instrumental neutron activation (INA) analysis. The -63-micron fraction will also undergo a sequential partial extraction procedure to identify the residence sites of copper and other metals within the silty clay fraction. Representative sampling of the modern lake sediments (Quiltanton Lake) was also undertaken. A total of 20 bulk samples were obtained from various horizons in the calcareous peat and marl-dominated modern rhythmites (Table 4-4-2). These samples are now in process.

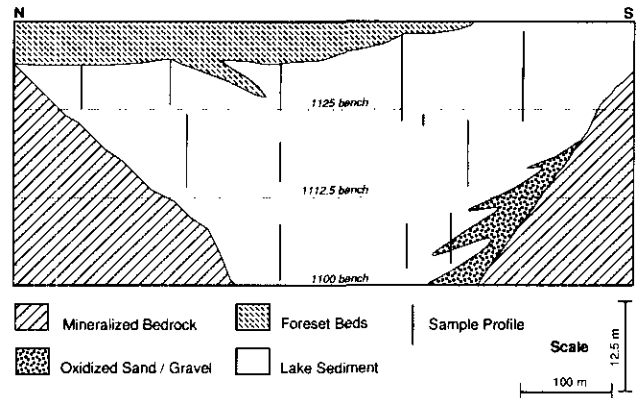


Figure 4-4-4. Schematic view of Valley pit illustrating location and relationship of geochemical profiles in lithostratigraphic Unit II.

RESULTS

STRATIGRAPHY AND SEDIMENTOLOGY

Mapping of the unconsolidated sediments in the Valley pit and surrounding area resulted in the identification of nine lithostratigraphic units (Figure 4-4-5). Bearing in mind the borehole data discussed earlier, the valley-fill sediments probably extend to a greater depth than that described in this report (most likely an additional 100 metres or more) which is limited to pit excavation depth.

UNIT I

The oldest exposed lithostratigraphic unit in the pit area directly overlies the mineralized granodiorite and averages 6 to 10 metres in thickness (Plate 4-4-1). This unit is characterized by poorly sorted, alternating beds of strongly oxidized, silty sand and sandy gravel. Oxidation lines crosscut the natural bedding planes. All beds dip steeply toward the valley floor. Most clasts are strongly weathered, subrounded to subangular and of local provenance, the basal part includes a *grus*. Occasional rip-up clasts of laminated silty clay beds are interspersed in the lower part of the unit. An unoxidized, discontinuous, gravel-supported diamicton with a silty sand matrix, 30 to 150 centimetres thick, and containing both local and exotic unstriated clasts, occurs at the base of the unit in one part of the pit. Sand and gravel beds in the upper part of the unit interfinger with rhythmites and therefore grade into the overlying unit over a short distance (~1 m). The sediments in this unit are interpreted to represent *in situ* bedrock weathering, colluviated bedrock, sand with organics and fluvial fan deposits which typically form on steeply inclined slopes of deep valleys.

UNIT II

Unit II (35 m) consists of an intercalated rhythmite assemblage of silty clay and clayey silt laminae and beds, ranging in thickness from less than 0.1 to 15 centimetres (Plate 4-4-2). Individual rhythmites are primarily horizontally stratified, show graded bedding and sharp, planar contacts. The lowest rhythmites drape over bedrock and

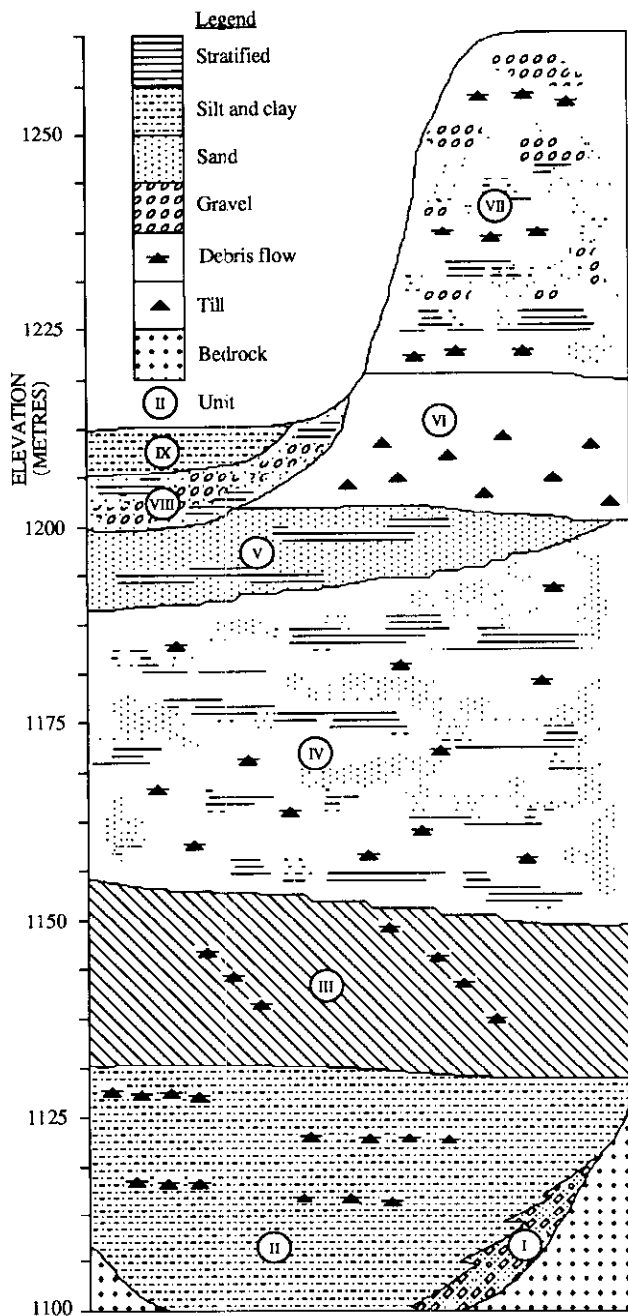


Figure 4-4-5. Composite stratigraphic column of Quaternary sediments from the Valley pit, Highland Valley Copper mine, B.C. See text for details regarding lithostratigraphic units.

deposits of Unit I. Rhythmites become progressively coarser and thicker up section. Localized examples of Type B climbing ripples were observed in one location supporting sandy silt bed sets 5 centimetres thick dipping towards 120°. Rare dropstones with drape laminations and minor penetrative structures are also present. Laterally discontinuous interbeds of massive, matrix-supported and clast-supported diamicton are evident and increase in thickness and frequency towards the top in the unit. Diamictons range from 1 to 35 centimetres in thickness, although one bed 1.1

metres thick was observed. A pebble fabric sample from one of the diamicton lenses has a trend of 169.3° and plunge of 07.3° (S1=0.546). Charcoal fragments and fine organics are conspicuous throughout the unit. Along the southern margin of the pit, rhythmites grade into a soil which preserved a paleosol (A-horizon) at three locations. The basal contact is gradational over a distance of approximately 1 metre as estimated from intertongues of rhythmic and sand and gravel beds. This unit is interpreted to represent glaciolacustrine sediments of a proglacial lake environment (cf. Ashley, 1988).

UNIT III

Unit III consists of steeply inclined, alternating planar crossbeds of sand and sandy gravel (Plate 4-4-3) and is up to 25 metres thick. Beds dip at angles averaging 25° to 38° toward 145° to 180° on the northeast side of the pit and toward 25° to 60° on the southeast side of the pit. Matrix-supported beds of gravelly sand are mainly medium to coarse sand with minor percentages of pebbles scattered along internal bedding planes. Clast-supported beds of sandy gravel consist mainly of granule to small pebble-sized clasts with a medium to coarse sand matrix. Rarer clast-supported beds with cobbles and boulders supporting an open-work structure are also evident. All types of beds average 60 centimetres in thickness and all show internal fining-upwards sequences (Plate 4-4-4). Very rare occurrences of silty clay and clayey silt laminae, rich in organic detritus including wood, are intercalated with the coarse beds. Rare boulder-sized dropstones and discontinuous beds of diamicton are present and increase in frequency in the upper part of the unit. Fine grained near the base, individual beds become progressively coarser, upward through the unit. Minor normal faulting and occasional rip-up clasts of laminated clay and silt blocks (up to 20 cm in diameter) are present near the base. At one location, evidence for local glaciotectionic deformation was observed. The steeply inclined beds change to a curvilinear form at their base, resulting in low-angle tangential contacts with the underlying sediments. The basal contact is, therefore, gradational over a few tens of centimetres with the rhythmically laminated sediments of Unit II. This unit is interpreted to represent a foreset bed complex formed by a series of prograding coalescing delta fronts (cf. McPherson *et al.*, 1987).

UNIT IV

Unit IV consists of up to 55 metres of poorly sorted sand and gravel beds interbedded with poorly stratified matrix and clast-supported diamicton (Plate 4-4-5). Silty sand beds alternate with sandy gravel lenses, both extremes showing variable contacts, gradation and sorting. Gravel-dominated beds up to 2 metres thick are rare, most beds and lenses are less than 1 metre thick. Occasional dropstones, up to 17 centimetres in diameter, are present in the sandy layers. Contacts between sand and gravel beds and diamicton beds are irregular, wavy and sharp. One matrix-supported diamicton bed is up to 15 metres thick, predominantly comprising a silty sand matrix (Face 5). This particular bed had a pebble fabric sample trending 183.1° and plunging 11.2° (S1=0.560). A thinner diamicton bed higher (Face 7)



Plate 4-4-1. View of fractured bedrock (A) and lithostratigraphic units (I) and (II) at base of Valley pit excavation, Highland Valley Copper mine, British Columbia. Exposure is 12.5 metres high. Pebbly diamicton at top of photo is modern road fill (B). Unit I is interpreted as slope wash and grus.

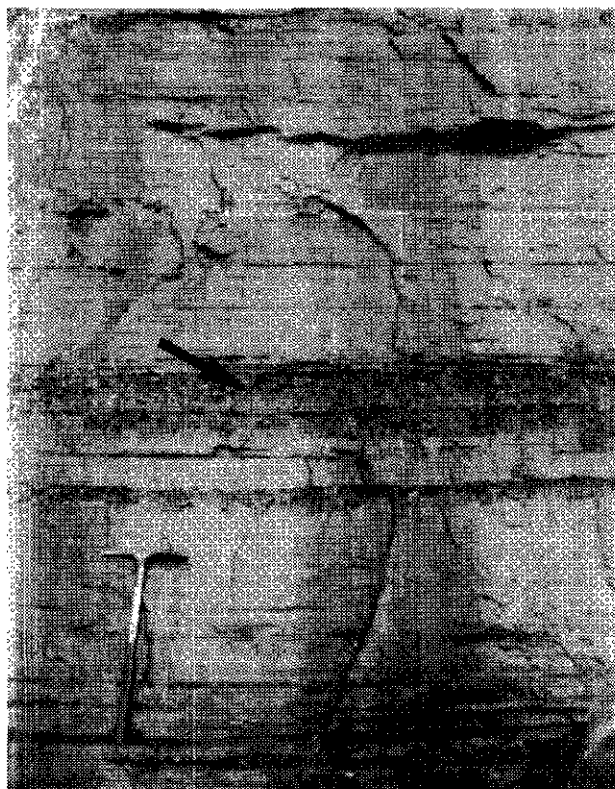


Plate 4-4-2. View of rhythmic sequence in lithostratigraphic Unit II consisting of alternating beds of silty clay and clayey silt. Pick for scale is 65 centimetres long. Arrow points to group of discontinuous matrix-supported beds. Unit is interpreted to represent glaciolacustrine sediments.

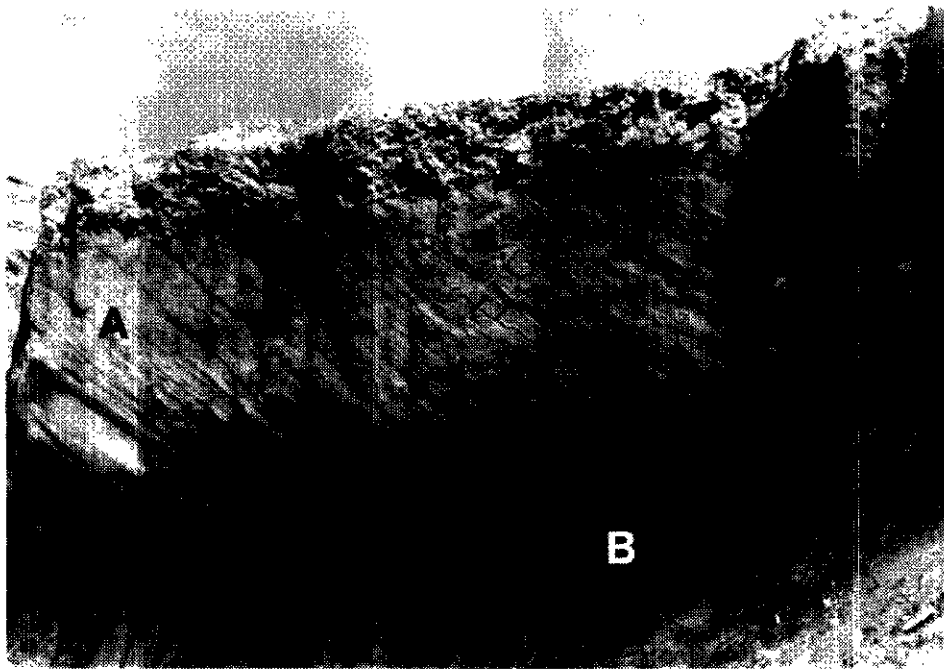


Plate 4-4-3. View of steeply inclined, alternating planar crossbeds of sand and sandy gravel of lithostratigraphic Unit III interpreted as fan-delta accumulation (A). Note transition into underlying rhythmic sequence (B).

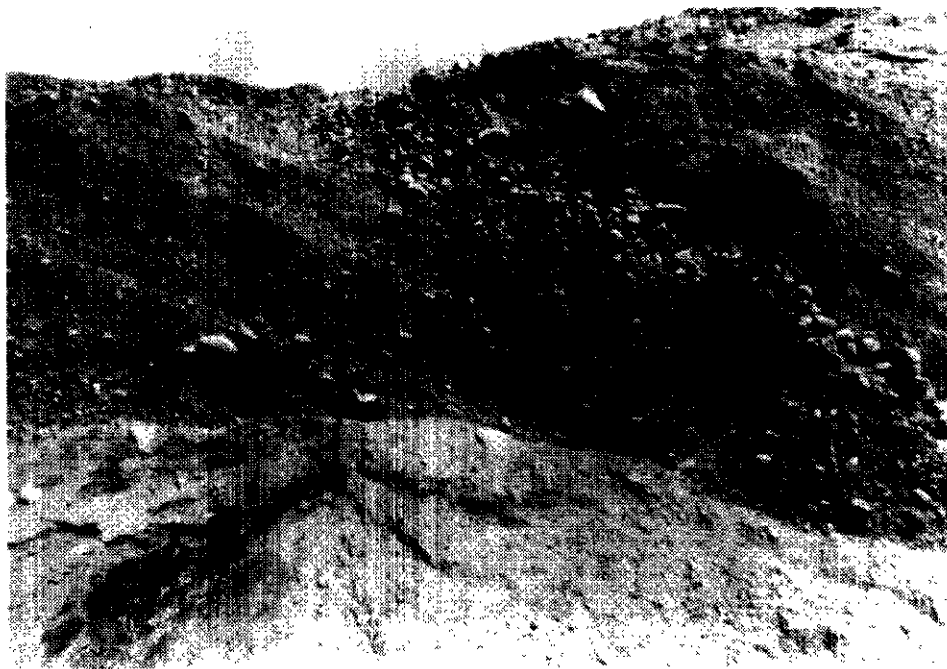


Plate 4-4-4. View of coarser beds in foreset complex of Unit III. Shovel for scale. Note fining-upwards sequences in the beds and diffuse over-sized clasts.

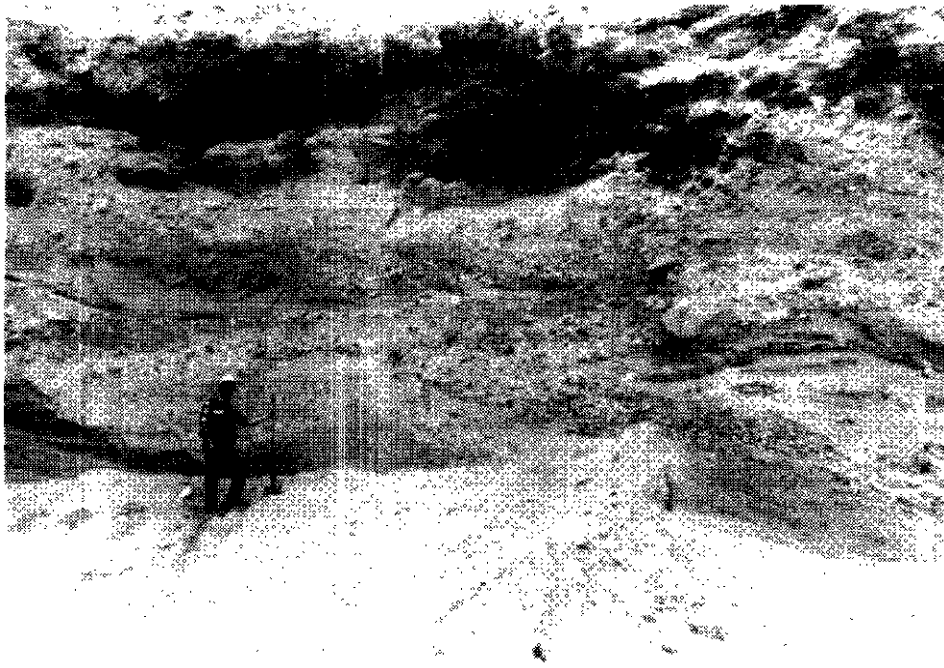


Plate 4-4-5. View of poorly sorted sand and gravel beds interbedded with poorly stratified matrix and clast-supported diamictics. Unit is interpreted as subaqueous outwash and debris flow deposits.

in the unit had a pebble fabric trending 163.9° and plunging 11.5° ($S1=0.711$). Clasts in all of the diamictons range in size from granules to boulders (<1 m in diameter), are angular to subrounded and are of mixed lithologies. This unit is interpreted as representing outwash deposits in a proglacial and subglacial environment (*cf.* Miall, 1977) and resedimented debris-flow accumulations in a subaqueous environment (*cf.* Eyles *et al.*, 1987).

UNIT V

This discontinuous unit consists of up to 10 metres of intercalated beds of sand and gravel. The dominant beds are moderately well sorted, stratified sandy silt and silty sand, ranging in thickness from 2 to 40 centimetres. The upper sand beds contain rare, over-sized clasts and thin (<15 cm thick) discontinuous lenses of matrix-supported diamicton. Clast-supported deposits are poorly sorted, pebbly cobble gravel beds, with openwork structure near their base. Many beds show internal grading. Inter-bed contacts are all sharp. Crossbeds dip regularly in variable directions, for example, up to 16° towards 90° and 15° towards 185° . The upper contact of this unit is indeterminate to truncated. The lower contact is sharp, erosive and curvilinear into the underlying sediments. The deposits in this unit are interpreted to represent subglacial outwash facies of an actively advancing ice mass (*cf.* Miall, 1977).

UNIT VI

Unit VI consists of up to 25 metres of diamicton beds, intercalated with isolated lenses of sand and gravel. Lenses are primarily stratified coarse sand and pebbly granules. Crossbedding in the lenses dips on average 22° towards

235° . Fine-textured horizons are discontinuous and less than 10 centimetres thick. Most of the unit is a massive to poorly stratified, matrix-supported diamicton. This poorly sorted deposit has a silty sand matrix, very low stone content (maximum clast diameter 0.7 m), and is relatively dense and compact. Clasts are subangular to subrounded. Rare pockets of sorted sand are present. A pebble fabric sample from the diamicton provided a trend of 305.7° and plunge of 05.9° ($S1=0.523$). Sandy interbeds support rafted diamicton rip-up clasts. Near the base of the unit, pebbles in a diamicton bed were measured and observed to have a strong ($S1=0.835$) fabric trending 139.6° and plunging 12.1° (Table 4-4-4). Where visible, part of this unit rests directly on bedrock, and the remaining part sharply overlies and truncates the lower sand and gravel unit. This unit is interpreted to represent a basal till accumulation (*cf.* Dreimanis, 1988).

UNIT VII

Unit VIII consists of approximately 33 metres of stratified sand, gravel and diamicton. The lower part of the unit contains beds of massive diamicton, ranging from 0.2 to 4 metres in thickness, separated by silt and fine sand beds averaging 50 centimetres in thickness (ranging from 15 to 100 cm) and 5 metres in length. Pebble fabric data from the lower diamictons provide a trend of 19.6° and plunge of 13.3° ($S1=0.742$). Rare over-sized clasts are present in the sandy beds. The diamicton beds are massive to stratified, poorly sorted, with a silty sand matrix, and rare clasts which are predominantly subangular to subrounded pebble to boulder size. The predominance of stratified sandy horizons (beds up to 2 m thick) increases in the middle part of the unit (Face 12) where beds are laterally extensive and contin-

uous for distances of hundreds of metres. In the upper part of the unit, the diamicton beds show greater stratification and lack obvious sand interbeds. One of the uppermost diamictons has a pebble fabric trending 24.8° and plunging 11.3° (S1=0.853). Rare sand and gravel cut-and-fill structures, up to 2 metres thick with crossbedding dipping 14° towards 045°, are present in the uppermost exposures (Face 13). The lower contact of this unit is gradational with the underlying deposits over several metres. These sediments are interpreted to represent various depositional facies of a supraglacial environment (cf. Eyles, 1979).

UNIT VIII

This unit is a thin (~6 m thick), disrupted and complex assemblage of stratified sand, gravel and diamicton beds. Sandy to pebbly cobble layers are interbedded with diamicton beds (30 to 300 cm thick) near the base as a lateral facies change. These lower diamicton provided a pebble fabric sample trending 142.6° and plunging 16.1° (S1=0.657). Higher up the section, the gravel beds alternate with discontinuous lenses and beds of pebbly sand which contain rare over-sized clasts. The finer textured beds show both planar and trough crossbedding dipping 20° towards 120° and 11° towards ~90°. Clasts are predominantly rounded to sub-rounded throughout the unit. The basal contact is inclined, sharp and crosive to transitional with intertonguing of beds. The unit locally shows a gradual fining-upwards sequence. This unit is interpreted as representing deposits associated with *in situ* ice decay in a braided stream environment (cf. Ashley *et al.*, 1985).

UNIT IX

Unit XI is confined to the recently drained lakes. Deposits consist of subhorizontally stratified sand and marl and interbeds of peat and bryophytes. Freshwater shells were observed throughout the unit, but those at the base provided a date of 9600±70 years BP (TO-215). The unit represents a Holocene lacustrine accumulation which formed shortly after deglaciation and stayed in existence until the lake was drained in 1985.

GEOCHRONOLOGY

Several specimens of wood and mollusc shell were collected from Units II and III and submitted for ¹⁴C dating. Previous chronologic control at the mine site has been obtained from wood samples collected by S. Daly (Highland Valley Copper Ltd.) from the base of Unit II. Resultant dates on the *Picea* specimens submitted by him are greater than 44 450 years BP (Beta-47216) and greater than 45 070 years BP (Beta-48735). The dates imply that the glaciolacustrine sediments are mid-Wisconsinan or older in age. Absolute dates are necessary to confirm the chronostratigraphy.

PALEOECOLOGY

Wood, shells and organic sediments collected by S. Daly have been analyzed previously. Wood submitted for ¹⁴C dating (*see above*) has been identified as *Picea* sp. (spruce; H. Jett, personal communication to S. Daly, 28 October,

TABLE 4-4-3
HIGHLAND VALLEY COPPER MINE POLLEN SPECTRA

TAXA	FREQUENCY
<i>Picea</i> sp. (Spruce)	86
<i>Pinus</i> (White pine)	38
<i>Pinus contorta</i> (Lodgepole pine)	2
<i>Pinus</i> sp. (species indetermin.)	53
<i>Abies</i> sp. (Fir)	5
<i>Betula</i> sp. (Birch)	3
<i>Alnus</i> sp. (Alder)	2
<i>Salix</i> sp. (Willow)	1
Graminae (Grasses)	13
Tubuliflorae	1
<i>Artemisia</i> (Sage)	91
Chenopodiineae (Chenopods)	3
Unidentified	1

(from H. Jetté, personal communication)

TABLE 4-4-4
PEBBLE FABRIC ORIENTATIONS FROM DIAMICTONS,
HIGHLAND VALLEY COPPER MINE

NUMBER	TREND	PLUNGE	S1	S2	S3	N
A	139.6	12.1	0.815	0.142	0.023	25
B	169.3	07.3	0.546	0.435	0.019	25
C	183.1	11.2	0.560	0.396	0.044	37
D	163.9	11.5	0.711	0.265	0.024	25
E	024.8	11.3	0.853	0.123	0.024	25
F	019.6	13.3	0.742	0.234	0.020	45
G	305.7	05.9	0.523	0.345	0.032	25
H	142.6	16.1	0.657	0.323	0.020	25

Notes: S1, S2 and S3 are eigenvalues, N is sample size
See text for location of samples

1991). Mollusc shell fragments were identified as freshwater gastropod and bivalve fragments (J. Tojpin, personal communication to H. Jett, 22 October, 1991). Pollen analysis of a single organic bulk sample contained high percentages of *Artemisia* (sage), *Picea* (spruce) and *Pinus* (pine) (Table 4-4-3). The environment at the time of deposition was interpreted to have been dry and cooler than present, with grasses and sagebrush in the valley bottoms and spruce, pine and fir on the slopes. The assemblage is marginally similar to pollen spectra from Meadow Creek (about 280 kilometres due east) where Bessette sediments were dated at 41 800±600 years BP (GSC-716; Alley *et al.*, 1986).

DISCUSSION AND CONCLUSIONS

The purpose of this paper was to review the 1992 drift-exploration program field activities at the Valley pit of Highland Valley Copper mine and detail the stratigraphic and sedimentologic data now available. Ancillary results on paleoecology, geochronology and geochemistry await laboratory analysis. Given the results of this study and those of previous publications, an interpretation can be offered regarding the Quaternary history and environments of deposition in and near the Highland Valley.

Ice-flow patterns in south-central British Columbia suggest that an ice-divide may have existed some 150 kilometres to the north-northwest of Highland Valley during the last glaciation (Ryder *et al.*, 1991). During the final glaciation, ice-flow directions, as interpreted from large-scale ground features (drumlins, drumlinoid ridges, *etc.*), indicate a regional flow toward the south-southeast (Fulton, 1975). This orientation is confirmed by pebble fabrics from the diamictons in the Valley pit. Fabrics are variable in the light of differing genesis, however, sediments interpreted as till deposits agree with a depositional direction toward the southeast. We further infer that, ice thickness over the study area may have been 1000 metres or more during the last glaciation and probably much thicker during earlier glaciations, given ice-limit indications of 2000 metres elevation south of Merritt and 2500 metres west of the Thompson River and Fraser River confluence.

Pre-Late Wisconsinan glaciation(s) may have significantly eroded and overdeepened Highland Valley without leaving depositional evidence of the event (*see* Mullins *et al.*, 1990, for a discussion of glacially overdeepened valleys and lakes in the southern Interior). During the mid-Wisconsinan, Highland Valley may have supported small streams or a river at a depth considerably below the modern surface (>250 m below modern surface). At the start of the Late Wisconsinan, ice present to the northwest would have resulted in increased water flow through the valley. Ice most likely filled the Guichon Creek valley to the east first, locally damming Highland Valley and resulting in the formation of a large and deep glaciolacustrine sequence. As ice advanced from the northwest, a prograding fan-delta complex developed leaving foreset and topset bed deposits. Ice eventually overrode the area leaving behind a discontinuous till sheet. As ice retreated from the area at the end of the Late Wisconsinan, a variety of glacial sediments accumulated in the valley and along its slopes, including subaqueous sediment gravity-flow deposits, outwash and ablation till. Further retreat of the ice resulted in the incision of pre-existing valley-fill sediments and deposition of distal outwash deposits. These deposits were eventually covered by local lake sediments which developed in depressions previously occupied by stagnating ice blocks.

DRIFT PROSPECTING IMPLICATIONS

Three issues pertinent to drift prospecting arise from the observations reviewed in this report. First, it is axiomatic that most glacially eroded valleys parallel preglacial features which in turn owe their existence to tectonic events such as large-scale faulting.

Second, the exceptional thickness of valley-fill sediments documented in Highland Valley indicates a configuration exists which mimics the overdeepened lakes of the southern Interior Plateau. We know that large lakes such as Kamloops, Okanagan and Shuswap, as well as several others in the region, occupy structurally controlled valleys which were glacially eroded to depths exceeding 400 metres below the present surface (Mullins *et al.*, 1990). Highland Valley provides another example of this pattern, differing only in that it does not support an active lake environment but is instead filled with a complex sequence of glacial and non-

glacial sediments. It is reasonable to suggest that most of the glaciated valleys in the region are similar insofar as they are probably overdeepened and now filled with complex Quaternary deposits. In the immediate vicinity of Highland Valley, this could include Pimainus Lakes valley, Guichon Creek valley and Nicola valley. The near-surface sediments in these valleys likely bear little resemblance (genetically or geochemically) to the underlying surficial deposits and bedrock. Finally, one can expect drilling costs to be high considering the potentially thick accumulation of sediment.

Third, most of the valley-fill sediments in the Highland Valley consist of glaciolacustrine deposits, a characteristic shared by the large lakes listed above and a feature probably typifying other valleys. We anticipate the results of our geochemical study will illustrate that these ancient lake sediments do indeed provide a reliable sampling medium for exploration. As such, we suggest that exploration strategies in the valleys sample lake sediments which are present at depth beneath the uppermost glacial sediment cover.

ACKNOWLEDGMENTS

The authors appreciate the able assistance of Colleen Bauer and Tracy Delaney in collecting field data. Sean Daly and Nelson Holowachuk provided assistance at the mine. Ron Arksey provided assistance with assessment reports. The manuscript benefited considerably from the editorial improvements proposed by Paul Matysek and John Newell.

REFERENCES

- Alley, N.F., Valentine, K.W.G. and Fulton, R.J. (1986): Paleoclimatic Implications of Middle Wisconsinan Pollen and a Paleosol from the Purcell Trench, South Central British Columbia; *Canadian Journal of Earth Sciences*, Volume 23, pages 1156-1168.
- Ashley, G.M. (1988): Classification of Glaciolacustrine Sediments; in *Genetic Classification of Glacial Deposits*, Goldthwait, R.P. and Matsch, C.L., Editors, A.A. Balkema, Rotterdam, pages 243-260.
- Ashley, G.M., Shaw, J. and Smith, N.D. (1985): Glacial Sedimentary Environments; *Society of Paleontologists and Mineralogists*, Tulsa, Oklahoma, Short Course No. 16, 246 pages.
- Church, M. and Ryder, J.M. (1972): Paraglacial Sedimentation: A Consideration of Fluvial Processes Conditioned by Glaciation; *Geological Society of America*, Bulletin, Volume 83, pages 3059-3072.
- Clague, J.J. (1988): Holocene Sediments at McNaughton Lake, British Columbia; in *Current Research, Part E, Geological Survey of Canada*, Paper 88-1E, pages 79-83.
- Cook, S.J. (1993): Preliminary Report on Lake-sediment Studies in the Northern Interior Plateau, Central British Columbia (93C, E, F, K, L); in *Geological Fieldwork 1992*, Grant, B. and Newell, J.M., Editors, B.C. Ministry of Energy, Mines and Petroleum Resources, Paper 1993-1, this volume.
- Dreimanis, A. (1988): Tills: Their Genetic Terminology and Classification; in *Genetic Classification of Glacial Deposits*, Goldthwait, R.P. and Matsch, C.L., Editors, A.A. Balkema, Rotterdam, pages 17-83.
- Evans, S.G. and Buchanan, R.G. (1976): Some Aspects of Natural Slope Stability in Silt Deposits near Kamloops, British Columbia; in *Proceedings, 29th Canadian Geotechnical Conference*, Session 4, pages 1-32.

- Eyles, N. (1979): Facies of Supraglacial Sedimentation on Icelandic and Alpine Temperate Glaciers; *Canadian Journal of Earth Sciences*, Volume 16, pages 1341-1361.
- Eyles, N., Clark, B.M. and Clague, J.J. (1987): Coarse-grained Sediment Gravity Flow Facies in a Large Supraglacial Lake; *Sedimentology*, Volume 34, pages 193-216.
- Fulton, R.J. (1967): Deglaciation Studies in the Kamloops Region, an Area of Moderate Relief, British Columbia; *Geological Survey of Canada*, Bulletin 154, 36 pages.
- Fulton, R.J. (1969): Glacial Lake History, Southern Interior Plateau, British Columbia; *Geological Survey of Canada*, Paper 69-37, 14 pages.
- Fulton, R.J. (1975): Quaternary Geology and Geomorphology, Nicola-Vernon Area, British Columbia (82L W1/2 and 921 E1/2); *Geological Survey of Canada*, Memoir 380, 50 pages.
- Fulton, R.J. (1991): A Conceptual Model for Growth and Decay of the Cordilleran Ice Sheet; *Géographie et Physique et Quaternaire*, Volume 45, Number 3, pages 281-286.
- Fulton, R.J. and Smith, G.W. (1978): Late Pleistocene Stratigraphy of South-central British Columbia; *Canadian Journal of Earth Sciences*, Volume 15, pages 971-980.
- Fulton, R.J., Irving, E. and Wheadon, P.M. (1992): Stratigraphy and Palcomagnetism of Bruhnes and Matuyama (>790 ka) Quaternary Deposits at Merritt, British Columbia; *Canadian Journal of Earth Sciences*, Volume 29, pages 76-92.
- Giles, T.R. and Kerr, D.E. (1993): Surficial geology in the Chilanko Forks and Chezacut Areas (93C/1, 8); in *Geological Fieldwork 1992*, Grant, B. and Newell, J.M., Editors, *B.C. Ministry of Energy, Mines and Petroleum Resources*, Paper 1993-1, this volume.
- Golder Associates Ltd. (1992): A Review of the Valley Pit, East Wall Overburden Slope Design Criteria; *Golder Associates Ltd.*, Vancouver, Report No. 922-1409.
- Kerr, D.E. and Bobrowsky, P.T. (1991): Quaternary Geology and Drift Exploration at Mount Milligan (93N/1E, 93O/4W) and Johnny Mountain (104B/6E, 7W, 10W, 11E), British Columbia; in *Exploration in British Columbia 1990, Part B*, *B.C. Ministry of Energy, Mines and Petroleum Resources*, pages 135-152.
- McMillan, W.J. (1976): Geology and Genesis of the Highland Valley Ore Deposits and the Guichon Creek Batholith; in *Porphyry Deposits of the Canadian Cordillera*, Sutherland Brown, A., Editor, *Canadian Institute of Mining and Metallurgy*, Special Volume 15, pages 85-104.
- McPherson, J.G., Shanmugam, G. and Moiola, R.J. (1987): Fandeltas and Braid Deltas: Varieties of Coarse-grained Deltas; *Geological Society of America*, Bulletin, Volume 99, pages 331-340.
- Miall, A.D. (1977): A Review of the Braided-river Depositional Environment; *Earth Science Reviews*, Volume 3, pages 1-62.
- Mullins, H.T., Eyles, N. and Hinchley, E.J. (1990): Seismic Reflection Investigation of Kalamalka Lake: a "Fiori Lake" on the Interior Plateau of Southern British Columbia; *Canadian Journal of Earth Sciences*, Volume 27, pages 1225-1235.
- Osatenko, M.J. and Jones, M.B. (1976): Valley Copper: in *Porphyry Deposits of the Canadian Cordillera*, Sutherland Brown, A., Editor, *Canadian Institute of Mining and Metallurgy*, Special Volume 15, pages 130-143.
- Proudfoot, D.N. (1993): Drift Exploration and Surficial Geology of the Clusko River and Toit Mountain Map Sheets (93C/16); in *Geological Fieldwork 1992*, Grant, B. and Newell, J.M., Editors, *B.C. Ministry of Energy, Mines and Petroleum Resources*, Paper 1993-1, this volume.
- Ripley, Kohn and Leonoff (1972): J.A. Mine Feasibility Study Groundwater Control, Waste Dump Design, Highway and Witches Brook Relocation; report submitted to *Bethlehem Copper Corp.*, Report VA 1655.
- Ryder, J.M., Fulton, R.J. and Clague, J.J. (1991): The Cordilleran Ice Sheet and the Glacial Geomorphology of Southern and Central British Columbia; *Géographie Physique et Quaternaire*, Volume 45, Number 3, pages 365-377.
- Sibbick, S.J., Rebagliati, C.M., Copeland, D.J. and Lett, R.E. (1992): Soil Geochemistry of the Keress South Porphyry Gold-Copper Deposit (94E/2E); in *Geological Fieldwork 1991*, Grant, B. and Newell, J.M., Editors, *B.C. Ministry of Energy, Mines and Petroleum Resources*, Paper 1992-1, pages, 349-361.
- Sutherland Brown, A., Editor. (1976): Porphyry Deposits of the Canadian Cordillera; *Canadian Institute of Mining and Metallurgy*, Special Volume 15, 510 pages.
- Waldner, M.W., Smith, G.D. and Willis, R.O. (1976): Lorne; in *Porphyry Deposits of the Canadian Cordillera*, Sutherland Brown, A., Editor, *Canadian Institute of Mining and Metallurgy*, Special Volume 15, pages 120-129.

NOTES



PRELIMINARY RESULTS OF GLACIAL DISPERSION STUDIES ON THE GALAXY PROPERTY, KAMLOOPS, B.C.

(92/9)

By D.E. Kerr, S.J. Sibbick, B.C. Geological Survey Branch
and G.D. Belik, Getchell Resources Inc.

KEYWORDS: Applied geochemistry, Iron Mask batholith, Galaxy, porphyry Cu-Au, drift exploration, surficial geology, till, soil geochemistry, glacial dispersion, biogeochemistry.

INTRODUCTION

This report describes the 1992 field season preliminary results of a glacial dispersion study on the Galaxy porphyry copper-gold deposit in the Iron Mask batholith, 5 kilometres southwest of Kamloops (Figure 4-5-1). The project involves three drift-exploration techniques: till geochemistry, till-pebble lithology and biogeochemistry. This investigation is designed to demonstrate the applicability of a combined surficial geology - exploration geochemistry program in the search for mineral deposits in areas of glaciated terrain with thick till cover.

Successful drift-exploration strategies require an accurate interpretation and understanding of the genesis and distribution of surficial materials, and ice-flow history (DiLabio, 1989). Drift sampling in the Galaxy area documents glacial patterns of geochemical and lithological dispersion in till. The Galaxy deposit was selected due to its physiographic environment, geological setting, well understood Quaternary glacial history and overburden stratigraphy, all of which make it suitable for a glacial dispersion

case study. This work complements similar surficial geology and geochemical dispersion investigations carried out on porphyry copper-gold deposits at Mount Milligan (Kerr and Bobrowsky, 1991; Gravel and Sibbick, 1991) and at the Island Copper mine (Kerr *et al.*, 1992).

The objective of the Galaxy till-sampling program is to determine the style of dispersion and the rate at which anomalous elements are diluted to background concentrations within a till sheet. Studies of soil profiles will illustrate the effects of soil formation on the geochemistry of till sediments. Relationships of glacial dispersion to size-fraction element concentrations, surficial geology and glacial history will also be assessed.

REGIONAL GEOLOGY

The Galaxy deposit is one of seven porphyry copper-gold deposits located within the Afton camp. These deposits, as well as the Afton and Ajax orebodies, are hosted within the Iron Mask batholith (Preto, 1968), an elongate, northwest-trending, alkaline subvolcanic intrusive complex about 20 kilometres long by 4 kilometres wide, that intrudes comagmatic and coeval andesitic to basaltic flows, pyroclastics and sedimentary rocks of the Triassic Nicola Group. The batholith comprises four intrusive phases ranging in composition from pyroxenite and gabbro to diorite to monzonite and syenite. Emplacement of the intrusive units and the subsequent mineralizing events were controlled by a complex system of recurring northwesterly, northeasterly and northerly trending faults and related fracture zones.

Primary mineralization within the deposits consists of fracture-controlled chalcopyrite and bornite accompanied by pyrite, pyrrhotite and magnetite. The Afton deposit, prior to mining, contained a large supergene zone of native copper, chalcocite and cuprite.

PROPERTY GEOLOGY

Copper mineralization on the Galaxy property consists of chalcopyrite and minor bornite with only minor, near-surface oxidation. The main deposit occurs within a keel-shaped zone, about 150 metres wide, 400 metres long and up to 70 metres thick, which is part of a northwest-trending, graben-like structure composed of sheared and strongly fractured Nicola Group volcanics and dioritic phases of the Iron Mask batholith (Figure 4-5-2). Irregular shaped bodies of sheared, serpentinized olivine-pyroxene-rich basic intrusive, referred to as picrite, are exposed along the southwest margin of the graben. The graben is bounded on the southwest and northeast by fine-grained syenite and micro-syenite.

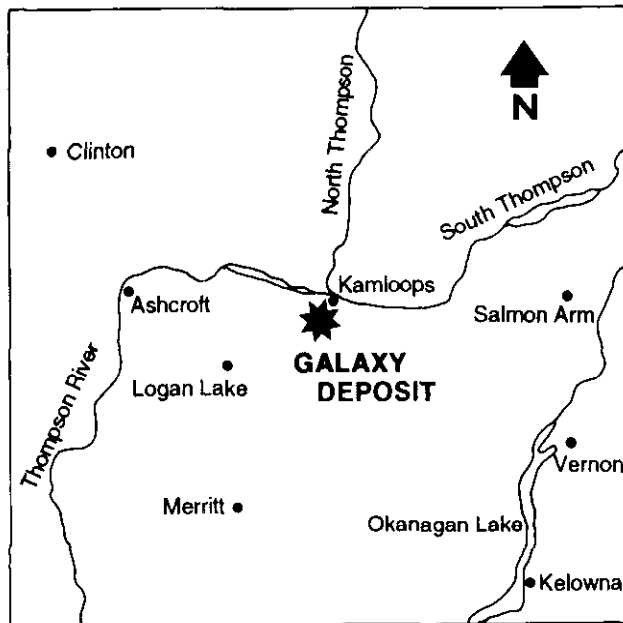


Figure 4-5-1. Location of the Galaxy property.

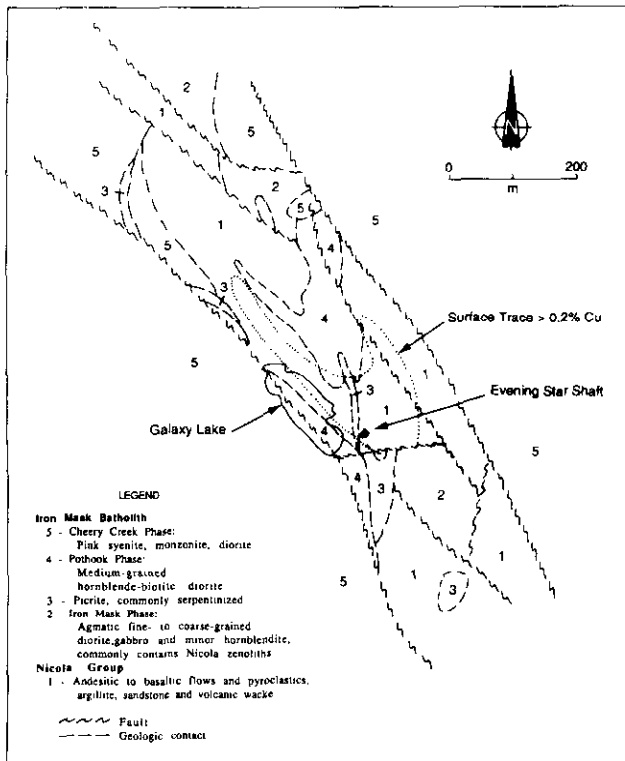


Figure 4-5-2. Simplified sketch of bedrock geology, Galaxy zone. Modified from Blanchflower (1978).

FIELD METHODS

Preliminary airphoto interpretation of the surficial geology of the Galaxy area at a scale of 1:70 000 was undertaken prior to fieldwork. Surficial sediment types and large-scale geomorphological ice-flow directional features (*i.e.*, drumlinoid ridges) were identified and plotted on a 1:5 000-scale base map. Additional ice-flow patterns were obtained from striated bedrock and till-pebble fabrics at two sites over the deposit in order to further define the direction of ice movement across the study area. Detailed stratigraphic investigations of trenches and hand-dug pits at 100 sites were undertaken to identify changes in the overburden sub-surface record.

A sampling grid was established over the areas of known mineralization, extending to a distance of 1500 metres in the down-ice direction of the deposit (Figure 4-5-3). The orientation of the grid was established on the basis of inferred ice-flow direction, so that sample sites would theoretically cover the expected dispersal trains. The oxidized C-horizon, commonly occurring 0.5 to 0.75 metre below the surface, was sampled at approximately 170 sites. Along the long axis of the grid, A and B-horizon samples were also collected to contrast differences with the underlying oxidized C-horizon. Three detailed soil profiles were also sampled to identify geochemical variations with depth. The 80 mesh (-177 micron) fraction of each drift sample will be analyzed by instrumental neutron activation analysis (INAA) and inductively coupled plasma analysis (ICP) for forty elements.

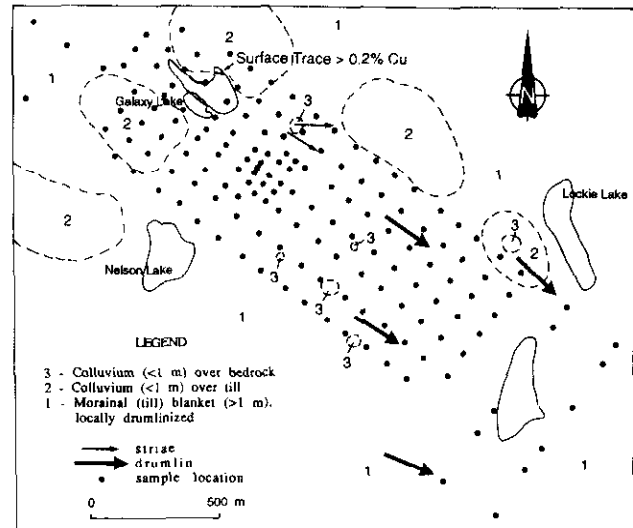


Figure 4-5-3. Surficial geology map of the Galaxy area, showing sampling grid location.

At 11 sites along the long axis of the grid, 25 pebbles were collected for lithological analyses and provenance studies. In addition, the stems, leaves and flowers of rabbit-bush (*Chrysothamnus nauseosus*) plants were sampled for comparison with soil data. Rabbitbush is a compact (50 cm high), olive-green shrub topped by a mass of small yellow flowers which is common in the dry interior of British Columbia (Lyons, 1991). Field observations show that the taproot of this shrub may extend 1 metre or more below the surface. Rabbitbush samples were analysed by ICP for 30 elements and results are expressed on an ashed basis.

RESULTS

SURFICIAL GEOLOGY

The last glacial episode in the Kamloops region occurred during the Late Wisconsinan (Fraser Glaciation) between $20\ 230 \pm 270$ years B.P. (GSC-194) and $10\ 500 \pm 170$ years B.P. (GSC-1524). Ice movement during this final event was primarily to the southeast, as interpreted from ice-flow indicators such as well-developed drumlin fields developed in till. This observation of regional flow is in accordance with earlier studies by Fulton (1963) in the Kamloops Lake area. Fulton (1975) also mapped the extent of glacial and nonglacial sediments and noted the presence of ice-flow indicators to the east, southeast and south of the study area. Previous glacial episodes also affected the area, but the conditions surrounding these older events can only be interpreted from more deeply buried deposits preserved in bedrock depressions and larger valleys. During deglaciation phases, ice appears to have retreated towards the north and northwest.

Drumlinized till sediments are widespread throughout the Kamloops area occurring primarily as a blanket (1 m) in the northern and southern plateaus along the South Thompson Valley, as well as in range country which continues discontinuously south to Princeton. The shape and size of the flutings are variable, but the dominant trend of these land-



Plate 4-5-1. Gently rolling topography developed on till south of the Galaxy property; view southeast.

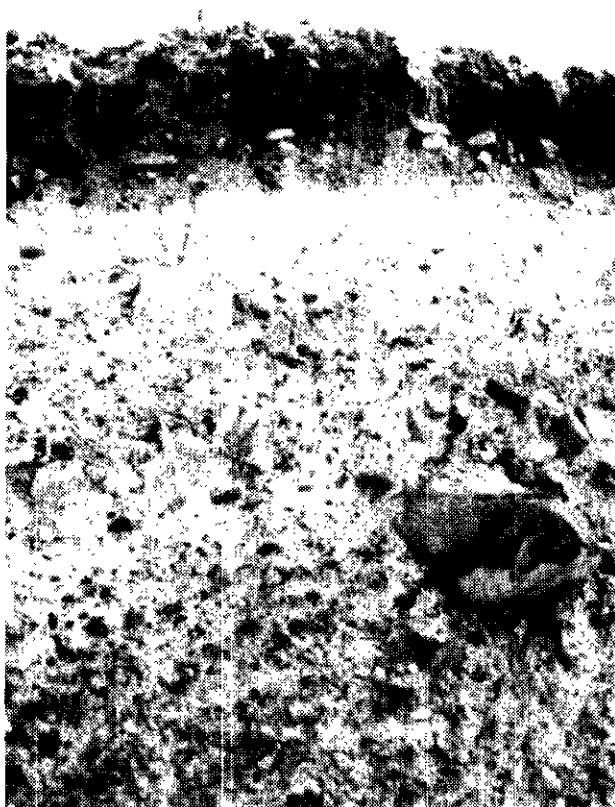


Plate 4-5-2. Massive till and soil development exposed in a trench; large boulder measures 40 centimetres.

forms is to the southeast. Surficial sediments identified in the Galaxy area include fluted diamicton (till) of variable thickness, thin veneers (m) of colluviated till over till on steeper slopes, and less than 5 per cent bedrock (Plate 4-5-1). Drift cover ranges from less than 1 metre to tens of metres in thickness. Near the deposit, surficial sediment cover averages 3 to 5 metres, obscuring much of the bed-

rock near the deposit. Drill-hole data from assessment reports show that significant thicknesses of unconsolidated sediments, in excess of 20 to 30 metres, are common southeast and south of the deposit (Blanchflower, 1978; Belik, 1990a, b). For most areas, the till is compact, very poorly sorted and consists of angular to well-rounded pebbles to boulders in a sand-silt-clay matrix (Plate 4-5-2).

GEOCHEMISTRY

Soils developed in the area of the Galaxy deposit consist of orthic dark brown chernozems in the grasslands and eutric brunisols under areas of forest cover. Results for copper in soil samples collected along the sample baseline indicate that soil copper contents are generally highest in the C-horizon (till) and lowest in the A-horizon (Figure 4-5-4). This feature may be due to the addition of loess to the upper soil horizons (H. Luttmerding, personal communication, 1992) which would dilute the original metal (*i.e.*, copper) content of the upper soil horizons. As depositor of loess in the postglacial period was controlled by factors such as wind patterns and topography, dilution of the upper soil horizons (and their metal concentrations) would be highly variable and bear no relation to the original A and B-horizon metal contents.

Rabbitbush samples reported higher copper contents than corresponding soils at eight of eleven sites, but show no consistent trend with distance from the deposit (Figure 4-5-4). Rabbitbush was also found to contain higher mean concentrations of boron, calcium, lead, magnesium, molybdenum, strontium and zinc. Additional biogeochemical studies are suggested in order to more accurately define the reliability and accuracy of this technique.

Preliminary results (Figure 4-5-5) indicate the existence of a strongly anomalous (200 ppm), ribbon-shaped dispersion train of copper extending for up to 1 kilometre down-ice from the deposit. Copper concentrations along the farthest down-ice sample line (approximately 1500 m from the deposit) average 136 ppm copper, suggesting that a significant (100 ppm) anomaly may extend for a greater distance.

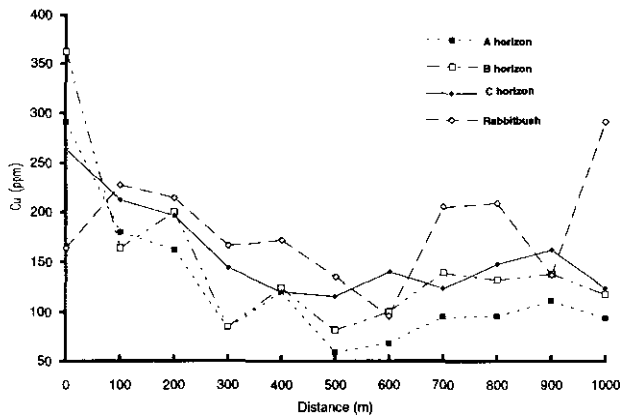


Figure 4-5-4. Down-ice dispersion of copper in A, B and C-horizon soils and rabbitbush.

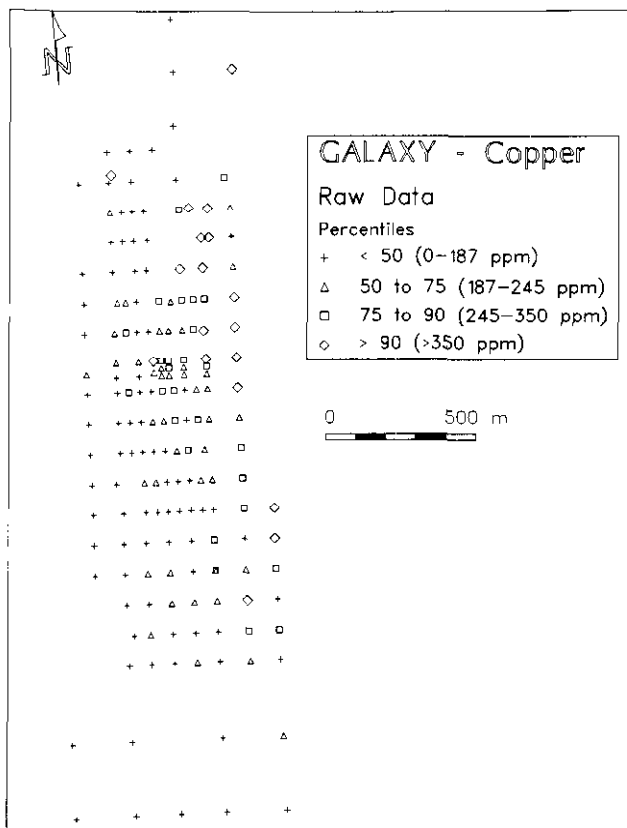


Figure 4-5-5. Copper concentrations overlying and down-ice from the Galaxy deposit.

These early results suggest similarities with the work described by Young and Rugg (1971) at the Island Copper mine; a linear geochemical anomaly, developed in till less than 9 metres thick over the orebody, extends for more than 600 metres in the down-ice direction parallel to ice flow. Fox *et al.*, (1987) describe a well-defined dispersion train developed in till over the Quesnel River gold deposit; this linear down-ice soil anomaly has been defined for approximately 1 kilometre.

CONCLUSIONS AND IMPLICATIONS

Studies at the Galaxy property focus on the controls of glacial dispersion and soil formation on geochemical anomaly formation. Data collected from this project will be used to develop a conceptual model of glacial dispersion and soil processes applicable to the search for porphyry copper-gold deposits. These studies will aid in the design and interpretation of drift-prospecting and geochemical soil surveys conducted in the province. Geochemical, lithological and biogeochemical orientation surveys will highlight the effects of mechanical and chemical dispersion and will define the grain-size fractions which provide the highest anomaly contrast. These surveys characterize the sediments over and down-ice from the deposit and may serve as a guide to similar mineral deposits with comparable surficial geology cover elsewhere in the southern Interior, notably in the Kamloops - Aspen Grove - Princeton region. Ongoing studies investigate the hypothesis that significantly higher metal values are associated with the oxidized C-horizon in till as opposed to oxidized B-horizon soils developed from the same parent material. Mapping of ice-flow patterns and an understanding of the nature and origin of surficial sediments are essential in the interpretation stages of soil geochemical surveys.

ACKNOWLEDGMENTS

The authors wish to thank Tracy Delaney and Colleen Bauer for their assistance in the field, as well as Paul Matysek, Peter Bobrowsky and Herb Luttmending for their helpful comments in the initial stages of fieldwork. Laboratory preparations of till samples were gracefully completed by Kathy Colbourne.

REFERENCES

- Belik, G. (1990a): Percussion Drilling Report on the Evening Star and Golden Star Crown Grants; *B.C. Ministry of Energy, Mines and Petroleum Resources*, Assessment Report 20242, 83 pages.
- Belik, G. (1990b): Percussion Drilling Report on the Venus 2, 4 and 11 Fraction; *B.C. Ministry of Energy, Mines and Petroleum Resources*, Assessment Report 20663, 26 pages.
- Blanchflower, J.D. (1978): *Geophysical and Diamond Drill Report on the Evening Star, Golden Star, Shear and Venus Claims*; *B.C. Ministry of Energy, Mines and Petroleum Resources*, Assessment Report 6864.
- DiLabio, R.N.W. (1989): Terrain Geochemistry in Canada. Chapter 10; in *Quaternary Geology of Canada and Greenland*, Fulton, R.J., Editor; *Geological Survey of Canada*, Geology of Canada, No. 1, pages 647-663.
- Fox, P.E., Cameron, R.S. and Hoffman, S.J. (1987): *Geology and Soil Geochemistry of the Quesnel River Gold Deposit*, British Columbia; in *Geoexpo '86*, Elliot, I.L. and Smee, B.W., Editors, *The Association of Exploration Geochemists*, pages 61-71.
- Fulton, R.J. (1963): *Surficial Geology, Kamloops Lake*, British Columbia; *Geological Survey of Canada*, Map 9-1963.
- Fulton, R.J. (1975): *Quaternary Geology and Geomorphology, Nicola-Vernon Area*, British Columbia (82L W1/2 and 92I E1/2); *Geological Survey of Canada*, Memoir 380, includes Maps 1391A, 1392A, 1393A and 1394A.

- Gravel, J. and Sibbick, S. (1991): Mount Milligan: Geochemical Exploration in Complex Glacial Drift; in *Exploration in British Columbia 1990*, B.C. Ministry of Energy, Mines and Petroleum Resources, Part B, pages 117-134.
- Kerr, D. and Bobrowsky, P.T. (1991): Quaternary Geology and Drift Exploration at Mount Milligan and Johnny Mountain, British Columbia; in *Exploration in British Columbia 1990*, B.C. Ministry of Energy, Mines and Petroleum Resources, Part B, pages 135-152.
- Kerr, D. E., Sibbick, S.J. and Jackaman, W. (1992): Till Geochemistry of the Quatsino Area, 92L/12; B.C. Ministry of Energy, Mines and Petroleum Resources, Open File 1992-21, 104 pages.
- Lyons, C.P. (1991): Trees, Shrubs and Flowers to Know in British Columbia; *Fitzhenry and Whiteside Ltd.*, 194 pages.
- Preto, V.A.G. (1968): Geology of the Eastern Part of Iron Mask Batholith; B.C. Minister of Mines and Petroleum Resources Annual Report 1967, pages 137-141.
- Young, M.J. and Rugg, E.S. (1971): Geology and Mineralization of the Island Copper Deposit; *Western Miner.*, Volume 44, pages 31-40.

NOTES

NATURAL ACID-DRAINAGE IN THE MOUNT McINTOSH / PEMBERTON HILLS AREA, NORTHERN VANCOUVER ISLAND (92L/12)

By Victor M. Koyanagi and Andre Panteleyev

KEYWORDS: Applied geochemistry, acid water, Holberg Inlet, Vancouver Group, acid generation, sulphide weathering, water chemistry, Hushamu, Vancouver Island, sulphate.

INTRODUCTION

Natural acid-drainage can be generated from acidic atmospheric precipitation (acid rain) and by both organic and inorganic acid-generating processes. The greater extent of natural acid generation occurs as the product of oxidation of sulphide minerals when rock is exposed to water and air.

The purpose of this study is to identify and measure the source and extent of natural acid waters draining from the altered and mineralized rocks in the Mount McIntosh - Pemberton Hills area of northern Vancouver Island. An advanced-argillic, acid-sulphate, copper-gold system of alteration and mineralization related to a porphyry intrusion forms a belt trending northwesterly across the area of study. During the 1991 and 1992 field seasons, a total of 77 water samples were tested for pH, and 34 selected waters analyzed for sulphate and metal content. Waters draining altered and mineralized areas are contrasted with those from relatively unmineralized areas revealing a focused mineralization-related acid-generating system.

LOCATION AND ACCESS

The Mount McIntosh - Pemberton Hills area is located on northern Vancouver Island about 25 kilometres west of Port Hardy on the north side of Holberg Inlet (Figure 4-6-1). The area encompasses watersheds bordered by Hushamu and Clesklagh creeks to the south, Hepler Creek on the west, Nahwitti Lake to the north and the Pemberton Hills to the east (Figure 4-6-2). Well-maintained logging roads provide access to the area from either Coal Harbour (southern access) or Port Hardy (northern access).

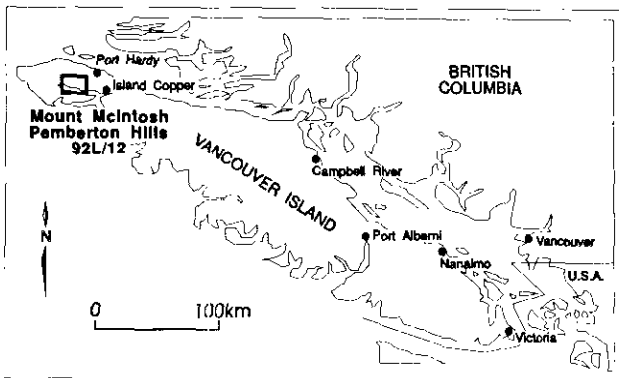


Figure 4-6-1. Location map.

GEOLOGIC SETTING

The study area is underlain by Upper Triassic to Lower Jurassic rocks of the Vancouver Group and Lower Cretaceous Kyuquot Group sediments (Figure 4-6-2). Muller *et al.*, (1974) describes the Vancouver Group as a sequence of Karmutsen basalt, Quatsino limestone, Parson Bay sediments and Bonanza volcanics. Upper Triassic (Carnian) Karmutsen basalts crop out along the south side of Nahwitti Lake and extend northward from the study area. This formation consists of basalt flows, pillow basalts, breccia, aquagene tuff, greenstone and minor limestone. East-trending outcrops of Upper Triassic (Carnian) Quatsino Formation limestones overlie the Karmutsen basalts and grade upward to calcareous siltstones, argillite and locally chert. These limestones are typically massive, locally fossiliferous and altered to skarn. The Quatsino limestone is an easily identifiable marker between Karmutsen volcanics and Parson Bay sediments. The Upper Triassic (Norian) Parson Bay Formation consists of well-bedded calcareous siltstone, shale, limestone, greywacke, conglomerate and breccia. Locally these sediments are skarn altered and mineralized. Lower Jurassic Bonanza Formation volcanics stratigraphically overlie the Parson Bay sediments. In the study area the lower part of the Bonanza Formation consists of well-layered, tuffaceous, commonly pyroxene-bearing, epiclastic and pyroclastic volcanics. Higher in the section Bonanza rocks are dominated by massive pyroxene-bearing andesite to basalt flows, tuffs and volcanoclastics with minor and localized dacite to rhyolite flows and pyroclastics (Panteleyev and Koyanagi, 1993, this volume). Lower Cretaceous Kyuquot Group conglomerate, siltstone and greywacke (Muller *et al.*, 1974) crop out in the southeast part of the study area along the shore of Holberg Inlet. Intrusive rocks are mainly the Jurassic Island Plutonic Suite (Muller, 1974 *et al.*). These intrusions are commonly quartz diorite to granodiorite in composition and intrude all rocks of the Vancouver Group.

ALTERATION AND MINERALIZATION

The study area includes mineral prospects and deposits of various types, mainly porphyry copper-gold, base metal skarns and advanced-argillic acid-sulphate epithermal mineralization.

Lower Jurassic Bonanza Formation volcanics host advanced-argillic, acid-sulphate alteration and mineralization that is transitional between porphyry and epithermal environments. This alteration and mineralization is related to the emplacement of the Jurassic Island Plutonic Suite. Hydrothermally altered and leached silica caps form physiographically prominent bluffs outcropping from Mount McIntosh to the Pemberton Hills, revealing a linear system

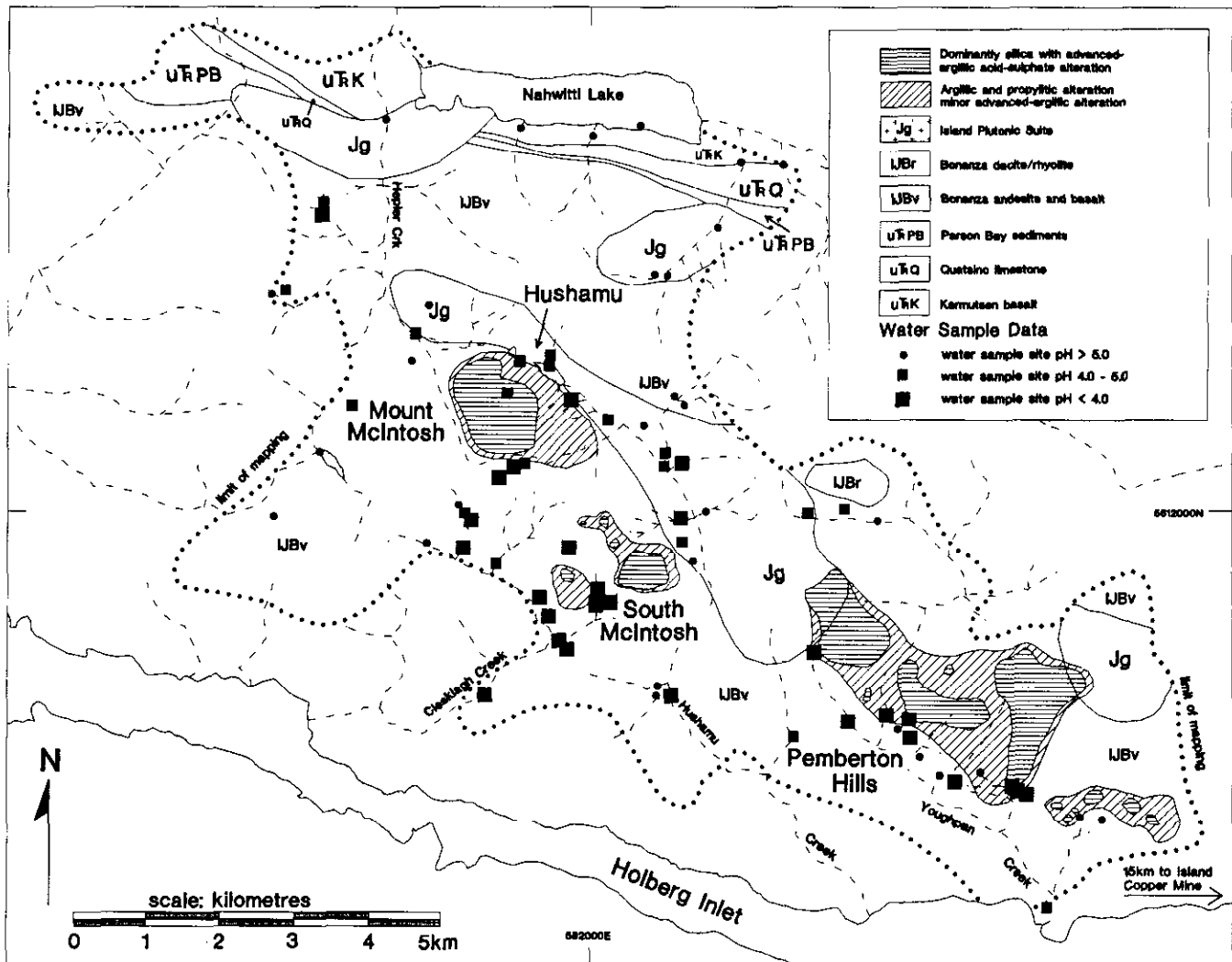


Figure 4-6-2. Geology and alteration map of the Mount McIntosh - Pemberton Hills area (92L/12) with water sample sites.

of alteration zones (Figure 4-6-2). Advanced-argillic, acid-sulphate alteration with quartz-alunite-kaolinite-pyrophyllite-zunyite mineral assemblages underlie and extend beyond higher level, barren siliceous rocks. The acid-sulphate environment is confirmed by the presence of sulphate minerals including alunite, jarosite, gypsum, anhydrite, barite and melanterite. The acidic and strongly oxidized character of the hydrothermal system creates an environment for high-sulphidation base and precious metal deposition. Sulphide mineralization consists of abundant disseminated and massive stratabound iron sulphides (dominantly pyrite and probably marcasite) with minor amounts of enargite and copper sulphides. Propylitic zones with characteristic epidote-chlorite-zeolite-pyrite mineral assemblages have formed peripheral to the advanced-argillic alteration zones. Sulphide mineralization of propylite is significant but occurs in lesser amounts than within the argillic zone. Rare phyllic alteration with quartz and sericite occur locally.

Porphyry copper mineralization close to the contact with a granodiorite stock of the Island Plutonic Suite occurs west of Hepler Creek. There propylitic Bonanza volcanics host

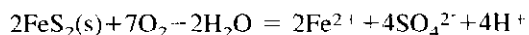
small, massive lenses and disseminations of pyrite representing an outer alteration envelope of a porphyry system. Outcrops of quartz diorite near Hushamu Lake also host porphyry copper-gold mineralization.

Calcareous sediments of the Upper Triassic Parson Bay and Quatsino formations contain extensive calcisilicate alteration and host skarn mineralization related to the Island Plutonic Suite (Dasler, 1990). Parson Bay sediments are also host to bedding-replacement massive pyrite mineralization.

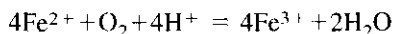
ACID GENERATION FROM SULPHIDE OXIDATION

The largest source of natural acid generation is the oxidation of sulphide minerals. This oxidation process begins with the exposure of sulphide-rich rock to air and water. Stumm and Morgan (1970) describe the reaction process as follows:

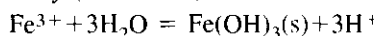
Iron sulphides, mainly pyrite, react with oxygen and water to produce ferrous iron, sulphate and free hydrogen (reaction A).



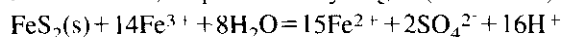
With continued oxidation the ferrous iron will oxidize to ferric iron (reaction B).



As the level of acidity increases (to around pH of 3.2) ferrous iron oxidation may be catalyzed by certain acidophilic bacteria, primarily *Thiobacillus ferrooxidans* (Steffen, Robertson and Kirsten (B.C.) Inc., 1989, pp. 2-5) and *Ferrobacillus ferrooxidans* (Stumm and Morgan, 1970, p. 542). When combined with water, ferric iron will precipitate ferric hydroxide that coats stream beds and creates additional acidity (reaction C).



Ferric iron then combines with additional pyrite to produce ferrous iron, sulphate and hydrogen (reaction D).

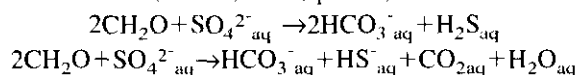


Provided that there are no other major external sources of sulphate, sulphate concentrations may be used as an overall indicator of the amount of acid generated from sulphide dissolution (Stumm and Morgan, 1970 p. 540). If acidity is neutralized, sulphate content is not affected (unless mineral saturation with respect to gypsum is attained) and the correlation is preserved (Steffen, Robertson and Kirsten (B.C.) Inc., 1989, pp. 2-7). Alternatively, if conditions of high acidity and low sulphate coincide, the source of acid is most likely not sulphide oxidation. Overall, if an extensive amount of pyrite is dissolved and the buffering capacity of the surrounding environment is exceeded, the result will be *sustained acid generation*.

The decomposition of pyrite is among the most acidic of all weathering reactions. Marcasite, a dimorph with pyrite and common in the study area, usually disintegrates more easily than pyrite, generating acid at a higher rate (Hurlbut and Klein, 1977).

The rate of dissolution of sulphides within stream drainages is variable. Extensive surface area exposure of sulphide-rich rock to air and water combined with low pH levels and elevated temperatures accelerates the process of acid generation. Under acidic conditions the presence of abundant acidophylic bacteria can also accelerate the process.

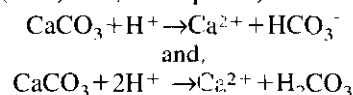
Organic generation of acid is also a contributor to natural acid-drainage. In our study area this process is likely to be much less significant than the weathering of sulphide minerals. Fermentation reactions and sulphate reduction results in acid generation. Sulphate introduced into an area of decomposing organic material will undergo bacterial reduction (by genus *Desulfovibrio*, Berner, 1971, p. 123). This bacteria utilizes organic carbon as a reducing agent. The reduction of sulphate forms acid by the following generalized reactions (Berner, 1971, p. 123):



ACID NEUTRALIZING PROCESS

The level of acidity produced from sulphide oxidation is dependent upon the ability of the surrounding environment to neutralize acid. Carbonate bedrock such as limestone is

an excellent acid neutralizer. Soils rich with carbonate minerals also have neutralizing capacities. The neutralization of acid by calcium carbonate is as follows (Steffen, Robertson and Kirsten (B.C.) Inc., 1989 p. 2-7):



FIELD STUDY AND ANALYTICAL PROCEDURE

Acidity levels in stream drainages were measured using a Corning CheckMate™ M90 portable microprocessor-based pH, conductivity and dissolved oxygen meter. Readings were taken and recorded in the field submersing the meter directly into streams.

Samples were collected during the summer months of 1991 and 1992. Low rainfall and warmer temperatures during July and August of 1992, in comparison to the same months in 1991, resulted in a reduced volume of water in many streams. This, in some instances, may result in higher acid levels as well as elevated conductivity and total dissolved solids (TDS) in 1992. Standing water in a swamp on Mount McIntosh was measured in 1991 and 1992 (samples EC91AP-37 and EC92AP-18, Table 4-6-1). Acid levels were slightly higher in 1992 with conductivity and TDS significantly higher.

The pH sensor was calibrated on a daily basis using prepared standard solutions. Plastic 250-millilitre bottles were used to collect water samples from selected sites. Samples were preserved with nitric acid but were not filtered.

RESULTS

Natural acid levels in drainages throughout the Mount McIntosh - Pemberton Hills area range between pH 6.5 and 2.0 (Table 4-6-1). Background acidity is considered to be the acid level in waters draining relatively unmineralized areas and lake waters in some of the larger lakes, for example Nahwitti Lake. This level is about pH 5.6 (sample EC92AP-01, Table 4-6-1). Atmospheric precipitation, organic fermentation and the oxidation of ubiquitous pyrite in the underlying rocks are contributors to acid generation resulting in the lower pH background level in the study area.

A strong correlation between high acidity (low pH) in waters and sulphide-bearing rocks is recognized. Several locations within the study area contain vast amounts of sulphides reflecting this correlation (Figure 4-6-2). Youghpan Creek for example, drains fine-grained, advanced-argillite altered Bonanza rocks hosting disseminated and massive stratabound pyrite and marcasite (Panteleyev and Koyanagi, 1993, this volume). This creek system transports a relatively high volume of water and drains a large watershed. Within a stream system of this size it may be expected that acidity is diluted by the large volume of water. Contrary to this prediction, measurements within the main course of Youghpan Creek returned acid levels of pH 3.1 (sample EC92AP-27, Table 4-6-1). A tributary to

TABLE 4-6-1
 WATER CHEMISTRY DATA FOR THE MOUNT MCINTOSH - PEMBERTON HILLS AREA, QUATSINO MAP AREA, NORTHERN VANCOUVER ISLAND (92L/12)

Sample No.	pH	Cond μ s	TDS g/ml	Temp $^{\circ}$ C	Location	SO4	Fe	Sl	Ba	Ca	Cu	Pb	Zn	Al	Mg
EC91AP-16	3.9	163.2	81.8	13.1	Hushamu Creek	31	0.01	6.78	0.03	5.18	0.12	0.02	0.01	1.89	1.70
EC91AP-17	5.4			12.2	Hushamu Creek Trib.										
EC91AP-18	4.0			11.2	Hushamu Creek Trib.										
EC91AP-19	3.8	176.5	92.0	14.6	Hushamu Creek Trib.	39	0.01	8.66	0.04	4.01	0.00	0.01	0.01	1.90	2.18
EC91AP-20	4.3	120.0	61.1	13.7	Hushamu Creek	18	0.01	5.90	0.01	4.66	0.01	0.00	0.01	0.96	1.88
EC91AP-21	5.8	48.1	24.2	14.1	Hushamu Creek Trib.										
EC91AP-22	3.5	244.0	126.0	9.4	Hushamu Creek Trib.	50	0.21	8.92	0.02	0.19	0.01	0.02	0.01	6.26	1.38
EC91AP-23	4.3	141.2	70.8	15.8	Hushamu Lake	32	0.01	5.84	0.01	6.43	0.02	0.02	0.01	1.48	2.28
EC91AP-24	3.7	53.9	27.3	9.1	Hushamu Creek Trib.	228	0.55	21.49	0.01	23.31	0.32	0.05	0.04	16.49	10.90
EC91AP-25	6.2	50.5	25.3	13.0	Hushamu Creek Trib.	1	0.10	1.86	0.05	2.06	0.00	0.01	0.03	0.08	0.64
EC91AP-26	6.0	61.3	36.9	10.6	Hushamu Creek Trib.										
EC91AP-29	5.5	48.4	28.1	10.0	Hepler Creek Trib.										
EC91AP-30	4.1	100.0	50.0	11.2	Hepler Creek Trib.	18	0.01	3.67	0.01	2.98	0.07	0.01	0.01	0.82	0.93
EC91AP-31	3.9	119.4	61.7	11.7	Hepler Creek Trib.	20	0.07	3.73	0.03	3.24	0.00	0.01	0.01	1.16	1.21
EC91AP-32	5.8	133.7	67.2	8.4	Hepler Creek Trib.										
EC91AP-33	4.8	47.3	24.0	10.4	Goodspeed River Trib.										
EC91AP-34	5.6	40.1	19.9	17.0	Goodspeed River Trib.	3	0.01	1.41	0.01	1.54	0.00	0.00	0.03	0.18	0.49
EC91AP-35	4.8	15.3	7.6	10.8	Mount McIntosh	7	0.29	0.31	0.01	0.01	0.00	0.01	0.01	0.28	0.12
EC91AP-36	4.7	28.0	14.0	11.3	Mount McIntosh										
EC91AP-37	3.6	88.0	44.7	12.2	Mount McIntosh	14	0.56	0.72	0.02	0.01	0.00	0.00	0.01	1.02	0.78
EC91AP-38	3.6	111.1	55.8	9.5	Mount McIntosh										
EC91AP-39	3.3	342.0	176.0	13.1	South McIntosh										
EC91AP-40	3.2	459.0	244.0	17.7	South McIntosh										
EC91AP-41	3.5	255.0	128.0	13.9	South McIntosh										
EC91AP-42	3.9	159.2	79.2	15.0	South McIntosh	29	0.01	5.36	0.03	6.89	0.00	0.01	0.01	1.87	1.65
EC91AP-43	4.1	215.0	107.0	12.9	South McIntosh										
EC91AP-44	3.1	442.0	219.0	14.3	South McIntosh										
EC91AP-45	3.6	282.0	149.0	12.6	South McIntosh										
EC91AP-46	5.1	44.4	22.3	9.6	Hushamu Creek Trib.										
EC91AP-47	5.9	43.7	15.9	10.4	Hushamu Creek Trib.										
EC91AP-48	5.8	60.0	30.3	12.2	Hushamu Creek Trib.										
EC91AP-49	3.8	198.0	98.5	14.3	Hushamu Creek Trib.										
EC92AP-1	5.6	75.7	37.9	11.5	Goodspeed River Trib.	13	0.13	3.92	0.06	9.04	0.01	0.01	0.03	0.19	1.18
EC92AP-2	5.2	21.9	10.9	11.0	Mead Creek										
EC92AP-3	5.6	23.4	11.7	9.9	Mead Creek	10	0.41	2.19	0.05	1.83	0.00	0.01	0.04	0.52	0.23
EC92AP-4	5.7	56.4	28.1	19.6	Mead Creek										
EC92AP-5	6.0	57.3	28.2	12.2	Nahwitti River Trib.										
EC92AP-6	6.5	35.1	17.6	11.7	Mead Creek	10	0.19	2.93	0.03	4.30	0.01	0.01	0.11	0.20	0.47
EC92AP-7	5.7	38.3	19.0	19.4	Nahwitti Lake										
EC92AP-8	6.1	64.8	30.0	16.8	S. Nahwitti Lake										
EC92AP-9	6.0	63.9	32.8	12.5	S. Nahwitti Lake										
EC92AP-10	5.0	73.5	36.4	13.8	Hepler Creek	26	0.45	5.29	0.05	5.73	0.01	0.01	0.01	0.52	1.20
EC92AP-11	4.7	58.6	29.5	15.2	Hepler Creek Trib.										
EC92AP-12	5.1	55.1	27.5	14.3	Hepler Creek Trib.										
EC92AP-13	3.9	152.1	75.4	15.3	Hepler Creek Trib.	51	0.35	7.83	0.05	7.48	0.03	0.01	0.08	3.47	1.07
EC92AP-14	4.2	77.0	38.7	13.6	Hepler Creek Trib.										
EC92AP-15	4.7	51.2	25.6	19.1	Hushamu Creek Trib.	17	0.29	4.47	0.04	3.80	0.00	0.01	0.02	0.29	0.61
EC92AP-16	4.4	151.3	75.2	12.8	Mount McIntosh	54	9.20	8.49	0.10	7.59	0.02	0.01	0.02	1.59	2.83
EC92AP-17	4.5	92.4	44.9	19.6	Hushamu Lake										
EC92AP-18	3.2	259.0	128.0	23.4	Mount McIntosh	58	0.14	3.29	0.30	5.51	0.01	0.01	0.06	0.10	0.70
EC92AP-19	5.4	55.0	27.4	15.6	Clesklagh Creek	10	2.30	1.08	0.14	1.43	0.01	0.01	0.01	2.90	1.83
EC92AP-20	3.9	184.2	92.9	14.9	Clesklagh Creek	72	0.68	8.21	0.08	14.30	0.01	0.01	0.03	3.22	2.33
EC92AP-21	2.0	2400.0	1190.0	28.9	South McIntosh	1300	88.80	36.60	0.06	165.00	0.15	0.11	0.65	45.70	9.62
EC92AP-22	4.3	157.0	78.5	14.0	South McIntosh										
EC92AP-23	5.3	71.1	35.5	12.0	South McIntosh										
EC92AP-24	3.5	219.0	105.0	12.7	South McIntosh	67	0.29	5.37	0.10	14.00	0.01	0.01	0.02	1.74	1.96
EC92AP-25	3.4	197.0	97.8	12.9	South McIntosh										
EC92AP-26	4.8	53.1	25.4	13.7	Hushamu Creek Trib.	12	2.98	3.50	0.05	4.45	0.00	0.01	0.01	0.61	0.94
EC92AP-27	3.1	252.0	124.0	12.4	Youghpan Creek	72	2.23	6.94	0.09	11.70	0.01	0.01	0.02	3.54	1.28
EC92AP-28	2.9	311.0	157.0	15.4	Youghpan Creek Trib.	113	5.60	11.30	0.12	14.70	0.01	0.01	0.03	3.95	2.72
EC92AP-29	3.4	347.0	175.0	11.5	Youghpan Creek Trib.										
EC92AP-30	5.3	89.9	28.3	12.6	N. Youghpan Creek	17	0.17	2.93	0.06	2.96	0.00	0.01	0.01	0.27	0.73
EC92AP-31	4.4	117.5	57.5	15.4	N. Youghpan Creek										
EC92AP-32	5.0	50.0	25.1	11.2	N. Youghpan Creek										
EC92AP-33	4.2	165.7	82.8	14.9	Mouth Youghpan Creek	69	0.89	8.38	0.09	17.90	0.01	0.01	0.02	1.71	1.91
EC92AP-34	5.1	40.4	20.3	13.3	Youghpan Creek Trib.										
EC92AP-35	3.9	77.2	38.5	17.7	Youghpan Creek Trib.										
EC92AP-36	4.0	90.7	43.1	14.8	Youghpan Creek Trib.	18	1.21	5.16	0.10	2.81	0.01	0.06	0.01	0.68	0.94
EC92AP-37	5.7	77.7	38.7	19.1	Youghpan Creek Trib.										
EC92AP-38	6.1	348.0	174.0	19.4	Youghpan Creek Trib.										
EC92AP-39	3.4	240.0	119.0	16.7	Youghpan Creek Trib.	60	2.25	6.98	0.09	5.45	0.01	0.01	0.03	2.35	1.69
EC92AP-40	5.4	82.9	42.0	16.1	Youghpan Creek Trib.										
EC92AP-41	3.7	330.0	171.0	18.8	Youghpan Creek Trib.										
EC92AP-42	3.5	264.0	131.0	16.1	Youghpan Creek Trib.	84	2.73	7.83	0.11	13.90	0.01	0.02	0.03	3.87	1.80
EC92AP-43	3.5	260.0	130.0	16.5	Youghpan Creek Trib.										
EC92AP-44	5.4	145.7	70.2	17.7	Youghpan Creek Trib.	49	1.12	6.68	0.05	16.40	0.01	0.01	0.01	0.40	1.48
EC92AP-45	5.5	774.0	385.0	25.3	Youghpan Creek Trib.										
VICT.RAIN	4.1	188.8	92.8	24.5	Victoria Rain										

TABLE 4-6-2

PEARSON CORRELATION MATRIX FOR ELEMENT PAIRS, pH, CONDUCTIVITY (COND) AND TOTAL DISSOLVED SOLIDS (TDS)

	Al	Ba	Ca	COND	Cu	Fe	Mg	Pb	pH	Si	SO4	TDS	Zn
Al	1.000												
Ba	-0.100	1.000											
Ca	0.562	0.176	1.000										
COND	0.181	0.494	0.402	1.000									
Cu	0.822	-0.192	0.477	-0.108	1.000								
Fe	0.084	0.315	0.212	0.290	-0.061	1.000							
Mg	0.905	0.089	0.662	0.077	0.872	0.154	1.000						
Pb	0.536	0.024	0.265	-0.029	0.569	0.001	0.528	1.000					
pH	-0.403	-0.293	-0.322	-0.777	-0.187	-0.181	-0.301	-0.203	1.000				
Si	0.854	-0.031	0.750	0.397	0.716	0.235	0.869	0.511	-0.492	1.000			
SO4	0.880	0.168	0.817	0.431	0.725	0.236	0.876	0.457	-0.540	0.916	1.000		
TDS	0.195	0.476	0.395	0.997	-0.101	0.289	0.086	-0.030	-0.785	0.409	0.433	1.000	
Zn	0.093	0.221	0.130	-0.018	0.101	-0.053	0.019	-0.027	0.203	0.076	0.156	-0.013	1.000

Level of significance (95th percentile)=0.306 calculated for N=30

Youghpan Creek transports a lower volume of water and returns a pH value of 2.9 (sample EC92AP-28, Table 4-6-1). These low pH levels indicate the presence of an extensive amount of sulphide minerals that are being leached into the drainage system. Sample EC92AP-33 (Table 4-6-1) is located near the mouth of Youghpan Creek, 3 to 4 kilometres downstream from the sample sites mentioned above. A pH level of 4.2 indicates dilution, but continues to reflect a large source of acid upstream.

Clesklagh Creek drainages include streams flowing from the South McIntosh area where abundant silicified and advanced-argillic altered Bonanza flows and tuffaceous volcanics strongly mineralized with disseminated pyrite are present. A sample of standing water in a ditch at the base of a sulphide-bearing, argillic-altered and strongly weathered outcrop (sample EC92AP-21, Table 4-6-1) returned a pH value of 2.0. Creeks draining the South McIntosh area average pH levels of 3.3. Upstream from South McIntosh, a southeasterly trending tributary of Clesklagh Creek drains unmineralized and unaltered Bonanza volcanics. Measurements in this tributary returned pH values of 5.4 (sample EC92AP-19, Table 4-6-1) indicating acid contributions limited to background levels. Downstream, below South McIntosh, Clesklagh Creek holds acid concentrations of pH 3.9 (Sample EC92AP-20, Table 4-6-1). The slight dilution of acidity at this location is a result of mixing waters from mineralized and unmineralized sources. These results indicate that the source of acid in the Clesklagh drainage is the altered and mineralized rocks of the South McIntosh area.

A tributary on the west side of Hepler Creek returned acid levels of pH 3.9 (sample EC92AP-13, Table 4-6-1). The sample site is flanked by propylitically altered Bonanza volcanics containing disseminated and massive pyrite in a porphyry copper setting. Acid here is being visibly generated by oxidizing iron sulphides adjacent to the stream.

Acidity of waters draining Parson Bay and Quatsino calcareous sediments (samples EC92AP-05 to EC92AP-09, Table 4-6-1) average well above pH 6.0. The Parson Bay Formation is locally mineralized with bedding-replacement iron sulphides, and Quatsino limestones are skarn altered

and mineralized. Acid is most likely generated from these sulphide-bearing rocks but the presence of the carbonate bedrock neutralizes this added acidity. The presence of carbonate strata produces pH levels generally well above the defined regional background levels.

WATER CHEMISTRY

Under natural weathering conditions, in which acid neutralization does not take place, there is a correlation between acidity and sulphide dissolution. Sulphate content can be correlated to levels of sulphide dissolution under neutralizing or non-neutralizing conditions. Sulphate minerals within acid-sulphate alteration zones (such as alunite, melanterite and gypsum) contribute some sulphate to the drainages. However, their insolubility and relative sparseness compared to pyrite suggests that their significance is negligible in comparison to contributions from pyrite oxidation. Water sample analyses in the study area show sulphate levels varying between 1 and 1300 ppm (Table 4-6-1). The sulphate levels show a strong positive correlation with acidity (Table 4-6-2). This correlation indicates that acid-producing sulphide oxidation takes place in a non-neutralizing environment. A low-acidity (high pH) high-sulphate relationship would indicate sulphide-generated acid in a neutralizing or diluted environment. Conversely, a high-acid (low pH) low-sulphate relationship reflects acid generation originating from a non-sulphide source of possibly organic origins. A Pearson correlation matrix (Table 4-6-2) illustrates correlations between pH and sulphate as well as other correlation data.

CONCLUSIONS

Natural acid is generated in surface waters in the Mount McIntosh - Pemberton Hills area. Clear-cut logging and road building indirectly increase acid generation by increasing the amount of fresh rock exposed to weathering. The primary source of acidity is the oxidation of the abundant iron sulphides contained within advanced-argillic acid-sulphate altered rocks as well as nearby porphyry copper

and skarn-mineralized rocks. Measurements of acidity in conjunction with sulphate levels can be used to locate sulphide-rich rocks that may contain ore deposits.

ACKNOWLEDGMENTS

The authors would like to thank Ray Lett, Steve Cook and Steve Sibbick of the Geological Survey Branch Environmental Geology Section for their assistance providing background information and reference materials and general insights during the preparation of this paper. Keith Mountjoy is acknowledged for developing field methods for the acid generation study in 1991. Editorial comments about technical content from Jan Hammack and Kirk Hancock were appreciated. This paper has benefitted from final editorial input from Dave Lefebure, Brian Grant and John Newell.

REFERENCES

- Berner, R.A. (1971): Principles of Chemical Sedimentology; *McGraw-Hill International Series in the Earth and Planetary Sciences*, New York, pages 123.
- Dasler, P.G. (1990): Report on the Expo Claim Group Northern Vancouver Island British Columbia, Canada; private report for *Moraga Resources Limited* (now Jordex Resources Inc.).
- Hurlbut, C.S. and Klein, C. (1977): Manual of Mineralogy, 19th Edition; *John Wiley and Sons, Inc*; New York, page 252.
- Muller, J.E., Northcote, K.E. and Carlisle, D. (1974): Geology and Mineral Deposits of the Alert - Cape Scott Map Area, Vancouver Island, British Columbia; *Geological Survey of Canada*, Paper 74-8, 77 pages, including Map 1552A.
- Panteleyev, A. and Koyanagi, V.M. (1993): Advanced Argillic Alteration in Bonanza Volcanic Rocks, Northern Vancouver Island - Transitions Between Porphyry Copper and Epithermal Environments (NTS 92L/12); in *Geological Fieldwork 1993*, Grant, B. and Newell, J.M., Editors, *B.C. Ministry of Energy, Mines and Petroleum Resources*, Paper 1993-1, this volume.
- Steffen, Robertson and Kirsten (B.C.) Inc. (1989): Draft Acid Rock Drainage Technical Guide, Volume 1; *B.C. Acid Mine Drainage Task Force Report*, pages 2-5, 2-7.
- Stumm, W. and Morgan, J. (1970): Aquatic Chemistry: An Introduction Emphasizing Chemical Equilibria in Natural Waters; *Wiley-Interscience*, New York, pages 540-542.



INVESTIGATION OF ANOMALOUS RGS STREAM SEDIMENT SITES IN CENTRAL BRITISH COLUMBIA (92N, O and P)

By S.J. Sibbick and T.A. Delaney

KEYWORDS: Regional Geochemical Survey, reconnaissance stream sampling, stream sediment, Mount Waddington, Taseko Lakes, Bonaparte Lake.

INTRODUCTION

Multi-element data for three Regional Geochemical Surveys covering approximately 45 000 square kilometres of central British Columbia were released on July 7, 1992. These data comprise the re-release of data from two previous surveys in NTS map sheets Taseko Lakes (92O) and Bonaparte Lake (92P), new data based on the analysis (by neutron activation) of archived stream sediment from these surveys, and the results of a new survey conducted in NTS map sheet Mount Waddington (92N) during the 1991 field season (Jackaman *et al.*, 1992a, b, c). Over 121 000 analytical determinations on samples from 2568 sites are presented in these three map areas.

Sampling densities for the Regional Geochemical Survey program are designed to provide information on regional geochemical trends. Identification of individual drainages hosting mineralization, although proven through years of use, is not the primary goal of the program. Rather, geochemical data from these surveys are a tool to direct detailed geological and geochemical investigations into geochemically favourable regions. The rapid and efficient evaluation of large multi-element geochemical databases, such as the RGS, poses a significant problem to explorationists. Further, the validity of geochemical anomalies generated by a survey of this type can be cast into doubt by the failure to detect mineralization expeditiously. As part of the Regional Geochemical Survey program, significant stream sediment anomalies which are not associated with known mineralization or in areas of exploration activity are evaluated in order to:

- Determine the effectiveness of the RGS program to detect regions of high mineral potential;
- Document the tendency of the RGS program to generate false anomalies, and;
- Define the geological and geochemical controls on anomaly generation.

Cook *et al.* (1992) conducted an analysis of data from the 1991 Regional Geochemical Survey release (NTS map sheets 82E, F, G, J, K and M). Their results indicated that a large number of gold and multi-element base and precious metal anomalies found within the release area remained unstaked and probably unexplored. Although nine of the ten highest gold concentrations (470-3530 ppb) were staked, seven of the next ten highest gold values (335-446 ppb) remained unstaked or partially staked. As the majority of these watersheds contain no known mineralization, the source of these anomalies is either due to the presence of

undiscovered mineralization or they are false anomalies resulting from a variety of mechanical, chemical and physiographic variables within the watershed.

This study details the investigation of seven watersheds hosting anomalous RGS sample sites within the 1992 Regional Geochemical Survey release area which host no known mineralization and were unstaked (save one) as of July 7, 1992 (release day). The objective of the study was to determine the origin of the anomalies and, if not attributable to a bedrock source, assess their impact on the Regional Geochemical Survey program.

INVESTIGATION OF ANOMALOUS SITES

SITE SELECTION

Selection of watersheds for investigation was based primarily upon four criteria: magnitude of the base or precious metal RGS anomaly; number of coincident anomalies in the surrounding drainages; lack of recent staking activity; absence of known mineralization; and the location and geologic setting of the watershed.

In its present form, the base and precious metal anomaly rating system developed for the Regional Geochemical Survey program has been included in all RGS releases since 1989 as both map and hardcopy output. A thorough description of this interpretive method is included in each Regional Geochemical Survey release. In summary, the method involves calculating the 90th, 95th and 98th percentile for each metal in each geological formation containing ten or more sample sites in the survey area. Samples exceeding the 98th percentile for a particular metal are assigned an anomaly rating of 3. Samples with concentrations between the 95th and 98th percentiles are given a value of 2, and samples between the 90th and 95th percentiles are assigned a rating of 1. Samples falling below the 90th percentile are given a rating of 0. Precious metal (Sb-As-Au-Ag) and base metal (Cu-Pb-Zn-Ag) scores are then summed for each sample. Anomaly ratings are not calculated for lithologies with less than 10 sites.

All watersheds selected for investigation are in regions characterized by multiple RGS sites with elevated or anomalous levels of metals. Of the seven sites, six were chosen based upon the magnitude of their base or precious metal rating (Table 4-7-1). The seventh site, Mamot Towers (92O/04 RGS site 795211), was chosen because of its unusual combination of anomalous, well-reproducing gold values (234 and 201 ppb), concentrations of uranium, zirconium, hafnium and several rare-earth elements (Ce, La, Sm) above the 95th percentile, and thorium and tungsten above the 90th percentile (Table 4-7-1).

Only one site, Klooqut Lake (92O/11 RGS Site 5045) had been staked before the release.

SAMPLING, PREPARATION AND ANALYTICAL METHODOLOGY

Where possible, the original RGS site was resampled at each drainage. Sampling programs within each drainage basin varied depending upon orientation of the stream, local topography, presumed style(s) of mineralization, and access. Investigation of each drainage was directed toward locating the mineral showings presumed to exist within the watershed. Stream sediment samples were taken above the confluence of streams, at 500-metre intervals, or at locations deemed appropriate. Samples were taken of rocks suspected to be mineralized or altered. Till samples were taken in areas of where drift cover thoroughly masked the underlying bedrock. In total, 25 stream sediments, 22 till and 69 rock samples were collected during the course of the project.

Sample preparation was carried out at the Analytical Sciences Laboratory of the British Columbia Geological Survey Branch. Stream sediment and till samples were dried at room temperature and dry sieved to -177 microns (-80 mesh). Rock samples were pulverized and ground in a tungsten carbide mill. Analytical duplicates and standards were inserted at the laboratory before analysis. Stream sediment and till samples were analyzed by aqua regia extraction and inductively coupled plasma emission spectrography analysis (ICP-ES) for 30 elements and gold by fire assay and ICP-ES at Eco-Tech Laboratories, Kamloops. Rock samples were analyzed by aqua regia extraction and ICP-ES for 30 elements and gold by fire assay and ICP-ES at Acme Analytical Laboratories, Vancouver.

RESULTS AND INTERPRETATION

BARNEY CREEK (92P/04; RGS SITES 791250, 791251)

Barney Creek is located approximately 25 kilometres west of Clinton and 16 kilometres downstream from Big Bar Creek on the Fraser River (Figure 4-7-1). It is accessible from Clinton via the Big Bar Creek road. The creek descends 450 metres over its length of 5 kilometres as it drains westwards into the Fraser River. Most of the elevation loss takes place in the final 2 kilometres as the creek descends the steep valley walls of the Fraser River. RGS sites 791250 and 791251 were sampled above the Big Bar Creek road at an approximate elevation of 460 metres. Sample site 791250 is on Barney Creek whereas site 791251 is in a dry creek 500 metres to the south. No trace of the original 1979 RGS sample sites was found during the investigation. Sample locations for this investigation are shown in Figure 4-7-2.

Barney Creek is underlain along its length by massive black to dark green argillites and cherty argillites of the Permian-Triassic lower Pavillion Group (Trettin, 1961). These rocks contain quartz-filled tension fractures and gash veins; joint and bedding planes in outcrop are often iron stained and gossanous. Gash veins and tension fractures are occasionally iron stained. Sulphides are not evident with

TABLE 4-7-1
ELEMENT CONCENTRATIONS AND
BASE AND PRECIOUS METAL ANOMALY RATINGS
USED IN SITE SELECTION

Location	NTS Map	RGS Site	Precious Metals						Base Metals				
			Sb	As	Au	Ag	Hg	Rating	Cu	Pb	Zn	Ag	Rating
Barney Creek	92P/04	1250	4.0	12.0	28	0.2	110	5	106	9	260	0.2	6
	92P/04	1251	3.1	7.5	15	0.2	90	76	7	220	0.2	3	
Klooqut Lake	92O/11	5045	3.3	7.0	68	0.1	150	10	18	2	78	0.1	
Bidwell Creek	92N/16	9017	0.3	3.0	12	0.5	80	5	86	2	58	0.5	5
Valleau Creek	92N/10	7025	37.0	43.0	5	0.2	730	6	54	3	91	0.2	
Trophy Lake	92N/12	1229	0.2	6.0	2	1.5	20	6	131	3	210	1.5	6
		5253	0.2	1.5	2	1.0	10	3	101	3	406	1.0	9
Dorothy Creek	92N/05	5125	0.2	9.0	31	0.7	10	9	51	33	208	0.7	9
Marmot Towers	92O/04	5211	Au	W	La	Ce	Th	Zr	U	Hf			
			234	15	34	49	7.2	1200	7.1	32			
			231 [repeat]										

Note: All elements listed in ppm except Au and Hg (ppb).
Values in bold are above the 90th percentile. Ratings <3 not listed

the exception of sample BN-RX-09 where fine-grained authigenic(?) pyrite was observed. Malachite was visible along the edge of a quartz vein 2 to 4 millimetres thick (sample BN-RX-10) in argillite, and a minor amount of malachite was noted on a talus fragment of argillite on a scree slope draining into Barney Creek below sample site BN-RX-15. This sample reported a copper concentration of 1454 ppm (Table 4-7-2). A series of recessively weathering parallel shear zones is exposed on the northern slope of the creek within 500 metres of the Big Bar Creek road over a north-south width of approximately 100 metres (samples BN-RX-15, BN-RX-16 and BN-RX-17). They are subvertical, strike at 238°, and consist of crushed argillite and clay gouge with abundant limonite, lesser jarosite and irregular white quartz veins which are generally subparallel to the strike of the shear. Molybdenum, copper and arsenic concentrations were anomalous in sample BN-RX-15. Another shear was noted along the roadcut farther up Barney Creek (sample BN-RX-08). Similar to the shears near the base of Barney Creek, this subvertical shear zone is approximately 10 metres wide and strikes at approximately 285°. Material in this shear varies from strongly jointed black argillite to hematitic argillite with fault gouge and minor quartz veining. Anomalous levels of molybdenum, zinc and cadmium together with elevated levels of copper were detected in this sample (Table 4-7-2). Another shear is exposed south of Barney Creek on the Big Bar Creek road switchback (samples BN-RX-11 and BN-RX-12). It is 9 metres wide, subvertical, strikes at 220° and consists of argillite fragments in a limonitic-jarositic clay gouge matrix. Anomalous concentrations of molybdenum and arsenic were found in these samples (Table 4-7-2).

In general, elevated to anomalous levels of molybdenum, copper, zinc, silver, cadmium and arsenic are associated with the shear or fault gouge zones discovered within the watershed. Trettin (1961) has noted the presence of shear zones throughout the lower Pavillion Group and attributes their existence to regional folding events, possibly related to emplacement of the Coast intrusions.

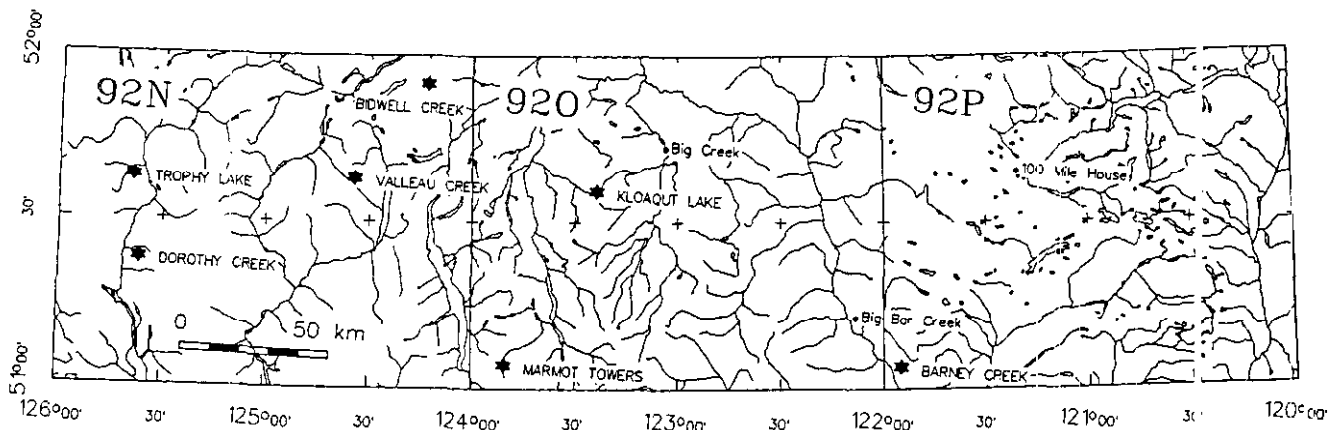


Figure 4-7-1. Anomalous RGS sites investigated within the 1992 release area.

Stream sediments sampled along the length of Barney Creek (Figure 4-7-2) indicate that anomalous values of molybdenum, copper, zinc, silver, arsenic and gold are present downstream from sample site BN-SS-04 (Table 4-7-3). These concentrations are comparable to the anomalous metal contents reported from the original RGS site (Table 4-7-1). The source of the anomalies at RGS sites 791250 and 791251 is undoubtedly the shear zones which outcrop in the creek and contribute altered, mineralized rock fragments and fault gouge directly to the stream.

KLOAOUT LAKE (92O/11; RGS SITE 795045)

Kloaout Lake is located on the Chilcotin Plateau approximately 40 kilometres southwest of Hanceville and is accessible by logging road (Figure 4-7-1). RGS site 795045 is on a creek draining a low, forested ridge south of the lake (Figure 4-7-3). Glacial drift (till) covers most of the slope between Kloaout Lake and the ridge crest. This cover thins towards the ridge, permitting the limited exposure of Kamloops Group basalt and mid-Jurassic granodiorite. Outcrop of granodiorite is restricted to the ridge crest and upper slopes separating the anomalous creek (795045) from the adjoining creeks. An outcrop of silicified quartz feldspar dacite porphyry was found along this ridge. Mineralized float is evident in the till covering the slope; most abundant is an angular light grey-green aphanitic silicified greenstone with up to 5 per cent disseminated pyrite, abundant limonite and lesser jarosite staining along surfaces and fractures (sample VL-RX-09). Analysis of this sample reported an exceptionally high concentration of zinc (12 795 ppm or 1.28%) and an anomalous level of cadmium (36 ppm; Table 4-7-2). Other mineralized float samples consist of a subangular silicified diorite (sample VL-RX-01) containing approximately 1 per cent pyrite, an intensely silicified, sheared felsite (sample VL-RX-02) and an angular pyritic mudstone (sample VL-RX-04). One fragment of gossanous silicified dacite (sample VL-RX-06), uncovered from the till, contains 821 ppm zinc and 56 ppm arsenic. Generally, however, metal concentrations in bedrock and float samples are within background limits.

Stream sediment and till samples taken upstream from the original RGS sample site contained background or near

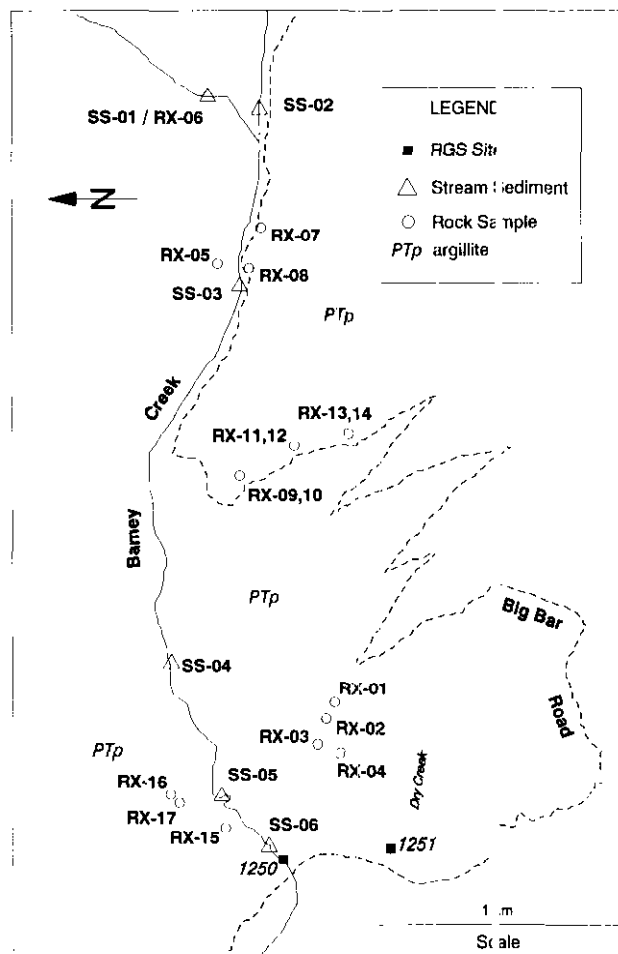


Figure 4-7-2. Sample locations, Barney Creek site.

background concentrations of all elements (Table 4-7-3). Abnormally high concentration of manganese (2700 ppm) from the original RGS site suggests that iron-manganese oxides may have precipitated and concentrated antimony, arsenic, mercury, zinc and, possibly, gold to anomalous levels. However, the presence of mineralized clasts in till within the drainage basin implies that the source of the RGS anomaly may have been glacially transported from outside

TABLE 4-7-2
 SELECTED GEOCHEMICAL RESULTS FOR ROCKS FROM BARNEY CREEK (BN), KLOAQT
 LAKE (VD), BIDWELL CREEK (BW), VALLEAU CREEK (VL), TROPHY LAKE (DB) AND
 DOROTHY CREEK (DY)

Sample	Type	Description	Sulphide Minerals	Mo ppm	Cu ppm	Pb ppm	Zn ppm	Ag ppm	Mn ppm	Fe % ppm	As ppm	Cd ppm	Sb ppm	Bi ppm	Ba ppm	Au ppb
BN-RX-01	Outcrop	Fe-stained argillite		1	115	8	70	0.6	339	2.55	5	0.4	2	2	103	13
BN-RX-02	Outcrop	Argillite		1	43	6	41	0.3	365	2.02	4	0.2	2	2	62	4
BN-RX-03	Outcrop	Quartz vein		1	1	3	7	0.1	144	0.39	2	0.2	2	2	49	1
BN-RX-04	Float	Argillite w. quartz vein stockwork		1	25	9	74	0.2	595	1.84	3	0.9	2	2	26	5
BN-RX-05	Outcrop	Fe-stained argillite		1	62	5	45	0.2	282	1.86	3	0.2	2	2	89	7
BN-RX-06	Float	Dacite		1	29	2	78	0.3	690	5.13	3	0.4	3	2	240	1
BN-RX-07	Outcrop	Argillite w. Fe-stained qtz veins		1	35	8	234	0.4	538	2.61	9	1	2	2	115	14
BN-RX-08	Outcrop	Sheared argillite		19	112	11	354	0.6	2451	3.86	8	9.2	2	2	243	4
BN-RX-09	Outcrop	Fe-stained argillite w. quartz veins		4	45	11	145	0.4	623	3.47	5	1.6	2	2	53	3
BN-RX-10	Outcrop	Malachite stained argillite		1	1454	9	85	1	553	2.84	12	0.2	2	2	53	20
BN-RX-11	Outcrop	Sheared argillite		66	45	9	104	0.6	222	1.6	18	0.7	6	2	149	8
BN-RX-12	Outcrop	Limonic-jarositic fault gouge		36	31	9	41	0.7	19	1.77	24	0.2	8	2	131	12
BN-RX-12D	Outcrop	Limonic-jarositic fault gouge		31	28	9	39	0.8	26	1.68	23	0.2	6	2	124	10
BN-RX-13	Outcrop	Gossanous argillite		6	34	6	20	0.2	158	1	3	0.2	2	2	108	5
BN-RX-14	Outcrop	Silicified argillite		1	16	6	45	0.1	462	0.96	2	0.2	2	2	179	13
BN-RX-15	Outcrop	Sheared Fe-stained argillite		11	123	5	154	0.1	41	6.56	37	0.2	2	2	62	6
BN-RX-16	Outcrop	Sheared Fe-stained argillite		1	52	4	97	0.1	347	2.89	2	0.7	2	2	163	2
BN-RX-17	Outcrop	Sheared Fe-stained argillite		20	30	7	47	0.9	24	1.51	13	0.2	4	2	157	8
VD-RX-01	Float	Silicified diorite	py	1	6	4	106	0.1	1225	2.83	2	0.2	2	2	108	2
VD-RX-02	Float	Silicified, sheared felsite	py	11	1	2	18	0.1	246	3.18	2	0.2	2	2	75	1
VD-RX-03	Float	Silicified porphyritic dacite		1	2	3	21	0.1	211	1.5	2	0.2	2	2	9	1
VD-RX-04	Float	Silicified Fe-stained mudstone	py	1	9	4	112	0.2	1031	2.67	2	0.3	2	2	73	2
VD-RX-05	Float	Limonic silicified breccia tuff		1	1	2	53	0.1	1275	2.59	4	0.2	2	2	80	1
VD-RX-06	Float	Gossanous silicified dacite		2	39	4	821	0.1	1186	16.8	56	1.5	8	2	273	1
VD-RX-07	Outcrop	Quartz-feldspar dacite porphyry		1	6	6	72	0.1	771	2.45	2	0.2	2	2	164	1
VD-RX-08	Outcrop	Quartz-feldspar dacite porphyry		2	11	3	61	0.2	671	2.45	7	0.2	2	2	159	1
VD-RX-09	Float	Silicified greenstone	py	1	66	5	12795	0.2	1432	3.93	8	36.1	2	2	26	1
VD-RX-10	Float	Fe-stained granodiorite		1	1	2	23	0.1	297	1.28	12	0.2	4	2	55	1
BW-RX-01	Outcrop	Intensely silicified felsite	py	21	11	4	15	0.1	24	1.43	2	0.2	2	2	41	3
BW-RX-02	Outcrop	Silicified schist	py	1	12	7	65	0.1	154	3.04	2	0.2	2	3	44	2
BW-RX-03	Outcrop	Fe-stained quartz vein		1	1	3	12	0.1	7	0.48	2	0.2	2	2	10	1
BW-RX-04	Float?	Intensely silicified felsite	py	6	1	2	1	0.1	2	1.01	2	0.2	2	2	72	1
BW-RX-05	Outcrop	Clay altered schist		1	20	4	67	0.1	284	3.83	2	0.3	2	2	108	1
BW-RX-06	Outcrop	Intensely silicified felsite	py	24	16	3	20	0.1	36	1.05	5	0.2	2	2	31	2
BW-RX-06D	Outcrop	Intensely silicified felsite	py	26	10	2	21	0.1	36	1.09	2	0.2	2	2	36	2
BW-RX-07	Float	Fe-stained felsic volcanic		5	8	6	34	0.1	79	2.18	4	0.2	2	2	94	1
VL-RX-01	Float	Malachite-stained basalt	py	1	2262	2	205	2.1	886	4.36	9	0.8	2	20	50	5
VL-RX-02	Float	Silicified(?) basalt		1	26	2	44	0.1	220	1.22	2	0.2	2	2	25	1
VL-RX-03	Outcrop	Granodiorite w. limonite vein		2	24	2	18	0.1	203	1.20	2	0.2	2	2	344	1
VL-RX-04	Subcrop	Fe-stained quartz diorite		1	5	3	5	0.1	81	0.48	2	0.2	2	2	66	1
VL-RX-05	Subcrop	Fe-stained quartz diorite		1	1	4	20	0.1	292	1.07	2	0.2	2	2	96	8
VL-RX-06	Float	Limonic calcite breccia		1	1	12	41	0.1	1279	1.65	2	0.2	2	2	452	1
VL-RX-07	Outcrop	Limonic hornfelsed basalt		1	14	7	162	0.1	1302	5.23	4	0.2	2	7	37	1
VL-RX-08	Subcrop	Skarned granodiorite	py, po	1	459	4	125	0.2	849	6.48	5	0.4	2	2	60	6
VL-RX-09	Outcrop	Limonic quartz vein gouge		5	24	9	186	0.1	1086	5.30	43	0.9	21	2	160	1
VL-RX-10	Outcrop	Intensely limonitic argillite		1	41	29	128	0.4	794	4.35	12	0.5	10	2	159	3
VL-RX-11	Outcrop	Gossanous pyritic argillite	py	2	70	2	33	0.1	559	3.73	27	0.2	2	2	7	3
DB-RX-01	Outcrop	Garniferous pelitic gneiss		1	28	2	88	0.3	562	3.82	3	0.2	2	2	501	1
DB-RX-02	Outcrop	Quartz-feldspar pegmatite		5	12	5	55	0.1	736	0.66	2	0.2	2	2	115	1
DB-RX-03	Outcrop	Fe-stained schist		38	88	2	7	0.5	192	2.87	2	0.2	2	2	33	1
DB-RX-04	Outcrop	Fe-stained schist		3	22	3	1	0.7	37	1.73	2	0.2	2	2	41	1
DB-RX-05	Outcrop	Fe-stained schist		6	13	4	4	0.4	179	1.15	2	0.2	2	2	34	1
DB-RX-06	Outcrop	Silicified metasediment		1	2	2	26	0.1	334	0.46	2	0.2	2	2	12	1
DB-RX-07	Outcrop	Silicified metasediment		4	36	6	20	0.2	82	1.47	2	0.2	2	2	78	1
DB-RX-08	Float	Fe-stained gneiss		4	35	2	13	0.1	120	0.83	2	0.2	2	2	109	1
DY-RX-01	Float	Brecciated epithermal(?) vein	gn	1	113	17511	235	146	93	1.26	264	0.5	11	4	53	565
DY-RX-02	Outcrop	Pegmatitic q.v. in granodiorite	py	2	133	21	15	2	24	1.5	2	0.2	2	6	101	9
DY-RX-03	Talus	Silicified pyritic schist	py	2	248	6	72	1.2	326	3.07	3	0.5	2	8	17	11
DY-RX-04	Float	Silicified pyritic schist	py	1	184	7	256	0.5	431	3.16	8	0.8	2	2	73	2
DY-RX-05	Float	Silicified, sheared pyritic schist	py	2	189	6	42	0.8	163	3.8	3	0.2	2	2	26	4
DY-RX-06	Float	Silicified granodiorite	py	1	259	15	210	0.9	448	6.02	7	1.3	2	7	39	2
DY-RX-07	Float	Silicified granodiorite(?) breccia	py, cpy	1	51	550	3472	49.8	48772	6.84	109	21.4	14	10	28	65
DY-RX-07D	Float	Silicified granodiorite(?) breccia	py, cpy	1	49	523	3409	48.3	46843	6.59	102	21.1	12	15	31	60
DY-RX-08	Float	Silicified granodiorite(?) breccia	gn, cpy	1	152	24341	6927	147	44232	9.61	292	35.4	15	9	20	487
DY-RX-09	Outcrop	V. altered silicified breccia (vein)		1	129	5568	1586	209	17598	4.22	21	9.1	2	5	32	69
DY-RX-10	Float	Intensely silicified breccia	gn, cpy	4	3235	25875	99999	96.9	9472	4.71	57	894	4	40	15	15528

TABLE 4-7-3
SELECTED GEOCHEMICAL RESULTS FOR STREAM SEDIMENTS
AND TILLS FROM BARNEY CREEK (BN), KLOAQT LAKE (VD),
BIDWELL CREEK (BW), VALLEAU CREEK (VL), TROPHY LAKE
(DB) AND DOROTHY CREEK (DY)

Sample	Type	Mo	Cu	Pb	Zn	Ag	Mn	Fe	As	Cd	Sb	Bi	Ba	W	Au
		ppm	ppm	ppm	ppm	ppm	ppm	%	ppm						
BN-SS-01	Stream sed.	1	47	4	113	0.8	596	3.10	<5	<1	<5	<5	160	<10	10
BN-SS-02	Stream sed.	1	37	4	110	<2	599	3.22	5	<1	<5	<5	120	<10	15
BN-SS-03	Stream sed.	2	42	4	111	0.4	643	3.02	5	<1	5	<5	140	20	5
BN-SS-04	Stream sed.	7	115	8	238	0.4	798	4.02	15	1	5	<5	125	<10	25
BN-SS-05	Stream sed.	10	116	8	272	0.4	802	4.41	20	2	5	<5	125	<10	40
BN-SS-06	Stream sed.	8	105	8	225	0.4	744	4.20	15	1	5	<5	105	<10	45
VD-SS-01	Stream sed.	1	20	2	64	<2	1940	3.68	10	<1	<5	<5	135	<10	5
VD-SS-02	Stream sed.	<1	18	4	59	<2	692	3.48	10	<1	<5	<5	80	<10	<5
VD-SS-03	Stream sed.	<1	43	4	56	<2	449	3.43	<5	<1	<5	<5	125	<10	5
VD-SS-04	Stream sed.	<1	21	<2	38	<2	733	3.66	5	<1	<5	<5	305	<10	<5
VD-SS-05	Stream sed.	1	33	4	47	<2	575	4.62	5	<1	<5	<5	95	<10	5
VD-SS-06	Stream sed.	<1	17	<2	57	<2	728	3.41	<5	<1	<5	<5	95	<10	<5
VD-TL-01	Till	<1	14	<2	36	<2	429	3.22	5	<1	<5	<5	90	<10	<5
VD-TL-02	Till	<1	17	2	45	<2	448	3.44	10	<1	<5	<5	75	<10	5
VD-TL-03	Till	1	36	4	122	<2	1529	5.69	20	<1	5	5	145	<10	5
VD-TL-04	Till	<1	17	4	44	<2	411	3.31	5	<1	<5	<5	90	<10	5
VD-TL-04D	Till	<1	17	6	43	<2	399	3.27	5	<1	<5	<5	90	<10	5
VD-TL-05	Till	<1	27	8	60	<2	501	3.94	<5	<1	5	<5	75	<10	5
VD-TL-06	Till	<1	32	6	81	<2	818	4.21	5	<1	5	<5	100	<10	10
VD-TL-07	Till	<1	26	2	54	<2	525	3.69	5	<1	<5	<5	90	<10	5
BW-SS-01	Stream sed.	1	142	<2	42	0.6	1069	4.18	5	<1	<5	<5	180	<10	5
BW-BK-01	Bank sed.	<1	19	4	49	<2	206	2.23	<5	<1	<5	<5	50	<10	<5
BW-TL-01	Till	1	46	2	31	<2	154	1.84	<5	<1	<5	<5	90	<10	<5
BW-TL-02	Till	6	60	<2	45	0.2	137	2.56	<5	<1	<5	<5	110	<10	<5
BW-TL-03	Till	3	50	2	36	<2	170	2.15	<5	<1	<5	<5	100	<10	<5
BW-TL-04	Till	<1	20	2	27	<2	151	1.62	<5	<1	<5	<5	65	<10	<5
BW-TL-05	Till	4	56	2	62	<2	162	2.30	<5	<1	5	<5	115	<10	15
BW-TL-06	Till	1	33	8	49	<2	167	1.86	<5	<1	<5	<5	65	<10	5
BW-TL-07	Till	1	32	<2	27	<2	131	1.59	5	<1	<5	<5	55	<10	10
BW-TL-08	Till	<1	27	2	52	<2	236	2.06	5	<1	5	<5	140	<10	5
BW-TL-09	Till	<1	20	2	39	0.2	195	2.00	5	<1	<5	<5	95	<10	5
BW-TL-10	Till	<1	21	<2	37	<2	179	1.92	5	<1	<5	<5	95	<10	5
BW-TL-11	Till	<1	16	<2	22	<2	127	1.65	5	<1	<5	<5	60	<10	5
BW-TL-12	Till	<1	11	<2	35	<2	169	1.57	<5	<1	<5	<5	65	<10	5
VL-SS-01	Stream sed.	1	48	2	69	<2	694	3.37	10	<1	5	<5	125	<10	5
VL-SS-02	Stream sed.	<1	43	<2	61	<2	580	3.00	10	<1	5	<5	50	<10	<5
VL-SS-03	Stream sed.	1	35	2	60	<2	549	2.03	<5	<1	<5	<5	45	<10	5
VL-SS-04	Stream sed.	1	61	2	80	<2	880	5.29	80	<1	25	<5	85	<10	10
VL-SS-04D	Stream sed.	1	53	2	75	<2	885	5.38	80	<1	20	<5	85	<10	10
VL-SS-05	Stream sed.	1	47	2	64	<2	720	3.61	<5	<1	5	<5	110	<10	5
VL-SS-06	Stream sed.	1	56	2	72	<2	945	5.14	80	<1	30	<5	85	<10	15
DB-TL-01	Till	3	82	2	68	<2	368	3.44	5	<1	5	<5	185	<10	5
DB-TL-01D	Till	3	82	2	67	<2	366	3.43	5	<1	5	<5	190	<10	5
DB-TL-02	Till	2	52	<2	33	<2	205	1.80	5	<1	<5	<5	105	<10	5
DY-SS-01	Stream sed.	<1	29	4	61	<2	304	1.56	5	<1	<5	<5	35	<10	15
DY-SS-02	Stream sed.	1	52	88	282	1.4	1258	2.08	20	2	<5	<5	60	<10	40
DY-SS-03	Stream sed.	<1	57	52	195	1.4	907	1.89	10	1	<5	<5	55	<10	140
DY-SS-04	Stream sed.	<1	71	10	225	0.8	492	1.64	5	1	<5	<5	55	<10	30

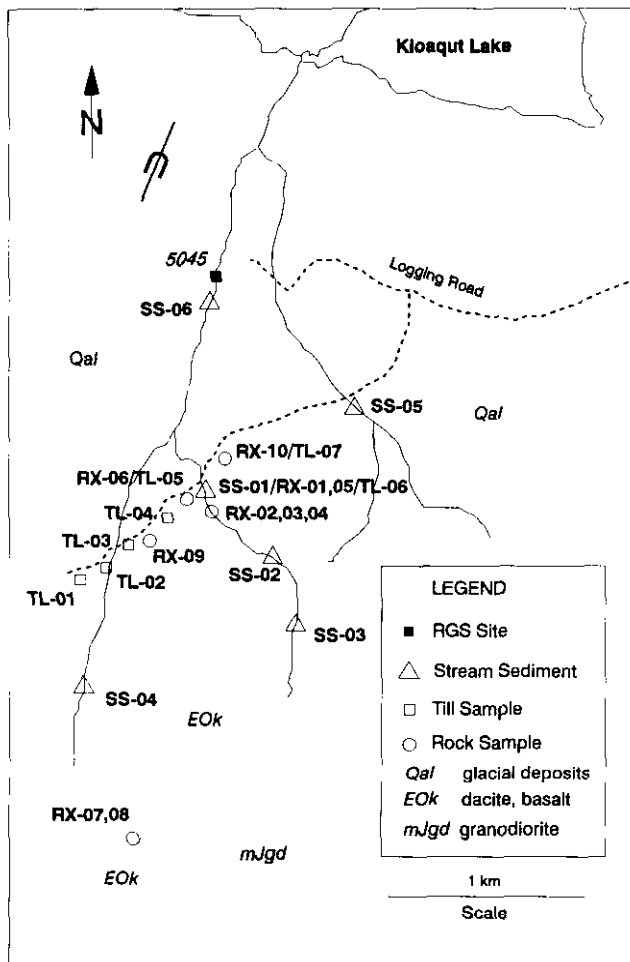


Figure 4-7-3. Sample locations, Kloaqt Lake site.

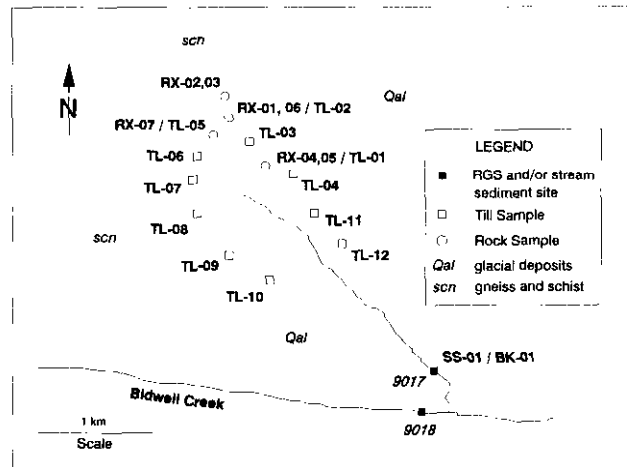


Figure 4-7-4. Sample locations, Bidwell Creek site.

the watershed. Glacial striae mapped in the area (Tipper, 1971) indicate that ice flow during the last glaciation was from the south-southwest in the vicinity of Kloaqt Lake.

BIDWELL CREEK (92N/16; RGS SITE 919017)

RGS site 919017 is on a tributary of Bidwell Creek 5 kilometres southeast of Eagle Lake and 12 kilometres east of Tatla Lake (Figure 4-7-1). Access to the site is by logging road. Gneissic to schistose rocks are exposed along a north-trending ridge at the headwaters of a tributary of Bidwell Creek. Granodiorite outcrop is exposed on the lower, southern ridge slope. Contact between the metamorphic and intrusive rocks, in most cases, is relatively sharp, with gradational changes in the texture of both rock types over several metres. Dikes of granodiorite are commonly observed cutting both the gneissic and schistose units. Fine-grained granodiorite to aplitic dikes crosscut both the granodiorite and metamorphic rocks. Metamorphic rocks range from a coarse-grained, mafic granitoid gneiss near the granodiorite contact to a fine-grained, felsic pelitic schist distal to the intrusive. Outcrop of an aphanitic, silicified rock containing 3 to 5 per cent pyrite (samples BD-RX-01 and BD-RX-06) was discovered along an old logging trail at

approximately 1585 metres elevation on the east-facing slope of the drainage (Figure 4-7-4). Clasts and boulders of this material are found along the logging trail for a distance of approximately 100 metres south of the outcrop. Significant amounts of this pyritic rock were found as float (sample BD-RX-04) near the outcrop of a barren quartz vein approximately 250 metres from the pyritic outcrop. A limited amount of trenching in the area by the authors failed to establish whether the pyritic float is derived from the pyritic outcrop 250 metres away or if it is related to the barren quartz vein in the immediate vicinity. One hundred and fifty metres north of the pyritic outcrop, a rusty coloured, limonitic subcrop of felsic pelitic schist (sample BD-RX-02) has been exposed by stripping. A rusty stained, glassy textured quartz vein 10 centimetres wide (sample BD-RX-03) is exposed in the outcrop over a length of approximately 2 metres. No visible sulphides were observed. Element concentrations in these outcrop and float samples are generally very low; however, elevated concentrations of up to 26 ppm molybdenum are found in the silicified, pyritic outcrop (samples BD-RX-01 and BD-RX-06) (Table 4-7-2).

Sediment at the original RGS site (sample BD-SS-01) consists of a fine-grained organic-rich muck which appears to be derived from the organic-rich, vegetated banks of the stream. Water flow was negligible. Poor quality (due to increasing organic content) of stream sediment upstream from this site prevented further sampling. Analysis of sample BD-SS-01 reported an anomalous copper concentration of 142 ppm whereas a bank sample from an exposure 15 metres away (sample BD-BK-01) contained only 19 ppm copper (Table 4-7-3). Contour till samples taken within the watershed (Figure 4-7-4) also reported background concentrations of copper and other elements. Anomalous concentrations of iron (4.50%), manganese (4810 ppm) loss on ignition (25.8%) and sulphate (17 ppm) from the original RGS site data (Jackaman *et al.*, 1992a) suggest that the anomalous levels of copper and mercury are the result of the precipitation and concentration of these elements from groundwater onto iron-manganese oxides and/or organic complexes.

VALLEAU CREEK (92N/10; RGS SITE 917025)

RGS site 917025 is on a tributary of Valteau Creek, 8 kilometres southeast of Bluff Lake (Figure 4-7-1). The lower reach of the stream is accessible by logging road and foot trail, while the upper section is best reached by helicopter. Approximately 4 kilometres long, the stream descends from 2450 metres elevation to its confluence with Valteau Creek at 1400 metres. Talus and felsenmeer predominate above treeline at 2000 metres elevation. In the upper reaches of the creek, Lower Cretaceous andesitic to basaltic rocks are intruded by quartz diorite. Dark green to black Lower Cretaceous argillite is exposed in the lower kilometre of the stream. These sediments are bounded on the east by the quartz diorite intrusion along the Tchaikazan fault (Rod-dick and Tipper, 1985). Near the headwaters of the stream, a hornfelsed contact between the volcanics and quartz diorite is exposed in the creek bed. This contact is occupied by an irregularly shaped limonitic pod (sample VL-RX-07) bounded by hornfelsed quartz diorite and basalt (Figure 4-7-5). Fifty metres to the north, quartz diorite with minor irregular pods of hornfels and/or skarn minerals crops out along the banks of a stream. Boulders and cobbles of pyrite and pyrrhotite-bearing skarn altered quartz diorite occur as talus or felsenmeer. Sample VL-RX-08, a talus clast of skarn-altered granodiorite, contains 459 ppm copper (Table 4-7-2). A large (1x1x0.5 m) boulder of pyritic, malachite-stained altered basalt (sample VL-RX-01), is located on a saddle between two peaks at 2400 metres elevation and has a reported copper content of 2262 ppm (Table 4-7-2). Although similar to nearby outcrop, no evidence of mineralization or alteration was found. This boulder is believed to be a glacial erratic; although it bears similarities to mineralization at the Math copper-silver occurrence (MINFILE 092N 021) located approximately 3 kilometres to the northeast, the source of this boulder is unknown.

The Tchaikazan fault is exposed in the bed and slope of the stream at an elevation of approximately 1700 metres. It consists of a rusty orange weathering alteration zone 30 metres wide, marking the contact between argillites and the quartz diorite intrusion. Alteration is most intense within the argillite along the contact, consisting of a strongly limonitic fault gouge with original textures and composition that are nearly destroyed (samples VL-RX-09 and VL-RX-10). Rock samples from this location contain anomalous values of arsenic and antimony (Table 4-7-2). This alteration decreases gradually over 30 metres within the argillite. Argillites along the edge of this zone contain spotty limonitic stains and minor pyrite (sample VL-RX-11). Alteration within the quartz diorite is less intense and restricted to an interval of approximately 5 metres from the fault contact.

Stream sediment data for this creek (Table 4-7-3) indicate a dramatic increase in arsenic and antimony values immediately downstream from the Tchaikazan fault (samples VL-SS-04 and VL-SS-06). Sample sites above the fault report background concentrations in all elements. Skarn mineralization exposed near the headwaters of the creek (samples VL-RX-07 and VL-RX-08) is not reflected in the stream sediment data. Clearly, the RGS anomaly is related to the

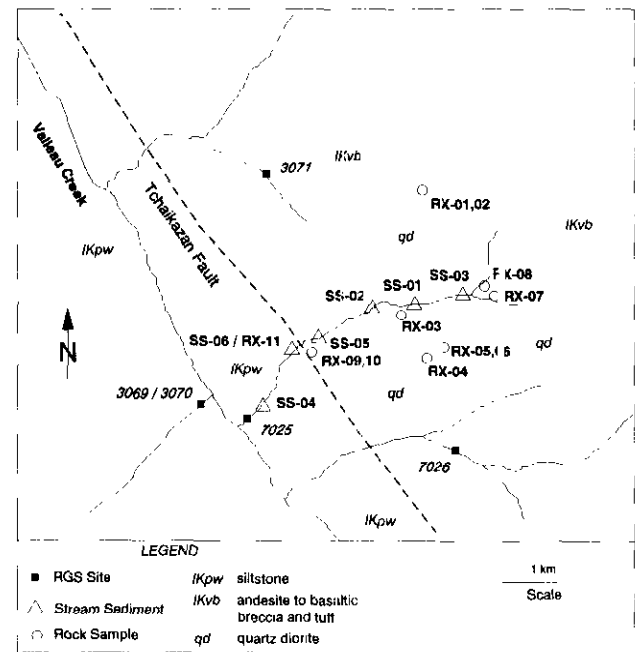


Figure 4-7-5. Sample locations, Valteau Creek site.

altered argillites and quartz diorites along the Tchaikazan fault. Fault and intrusive-related copper mineralization in volcanic and sedimentary rocks has been documented 10 to 15 kilometres to the southeast at the Nuit Mountain (MINFILE 092N 020) and Rusty (MINFILE 092N 044) showings and the Fly (MINFILE 092N 056) prospect. However, these mineral occurrences are associated with significant (133 and 289 ppm) RGS copper anomalies. The lack of stream sediments or rocks anomalous in copper suggests that this alteration zone does not host similar mineralization.

TROPHY LAKE (92N/12; RGS SITES 911229, 915253)

Granitoid gneisses and schistose pelitic metasediments form a ridge extending northwards from the cirque of an unnamed mountain approximately 5 kilometres west of Trophy Lake and the Kliniklini River (Figure 4-7-1). Granitic apophyses cut these rocks near the southern end of the ridge. Numerous crosscutting pegmatitic quartz-feldspar veins up to 5 metres wide dissect the metasediments. Iron-stained to gossanous outcrop is prevalent in the valley with the two anomalous RGS sites (911229, 915253). Both sites are located on streams which drain the precipitous, west-facing slope of the ridge. Elevation change between the sites and the ridge crest averages 800 metres over an interval of 1.5 kilometres, causing the streams to form near-vertical chutes for most of their length. Due to time and access limitations, investigation of the site was restricted to the ridge crest and adjacent slope of the cirque. The original RGS sites were not revisited. Sample sites are shown in Figure 4-7-6.

No clear indication of mineralization was observed. One sample of pelitic schist with abundant iron oxide staining (sample DB-RX-03) assayed 38 ppm molybdenum and 88 ppm copper (Table 4-7-2). Strongly gossanous gneisses

found in talus (sample DB-RX-08) within the cirque contained near-background concentrations of elements, most notably iron and manganese, suggesting that the gossan is only a thin patina on the exterior and on fractures within the sample. Samples of colluviated till downslope from these gossanous gneisses report background element concentrations (Table 4-7-3). RGS data for the two sample locations (Table 4-7-1) indicate that site 911229 is anomalous in arsenic, copper, silver and zinc whereas site 915253 is anomalous in copper, silver and zinc. The spatial proximity of these two similar anomalies is suggestive of mineralization and not an artifact of the stream environment. Anomalous sulphate (SO_4^{2-}) concentrations of 26 ppm at RGS site 911229 (95th percentile for all rock types is 21 ppm) further suggests the presence of oxidizing sulphides within this watershed. Elevation difference between the lowermost sample location and the RGS sample sites was on the order of 500 metres. It is possible that there are mineralized showings at a lower elevation than the area investigated.

DOROTHY CREEK (92N/05; RGS SITE 915125)

RGS site 915125 is approximately 37 kilometres north of Knight Inlet and 5 kilometres east of the Klinaklini River on a north-flowing tributary of Dorothy Creek (Figure 4-7-1). Access to the watershed is by helicopter. The upper half of the watershed is a cirque drained by three tertiary tributaries. Much of the cirque is underlain by a siliceous granitoid gneiss. A unit of iron-stained black pyritic schist is exposed on the western ridge of the watershed. These schists overlie the siliceous granitoid gneiss and are dissected by numerous barren quartz-feldspar veins which grade into the surrounding intrusive. Active glaciers ring the upper part of the drainage basin and a thick layer of boulder-rich talus and drift covers the cirque floor.

The Darlene lead-zinc-copper-silver-gold showing (MIN-FILE 92N 063) was discovered on August 25, 1992 by the authors. It consists of a vein 50 metres long and 0.3 to 0.5 metre wide on a narrow ridge of siliceous granitoid gneiss near the contact with altered pyritic schist at an elevation of 1850 metres (Figure 4-7-7). Vein material (sample DY-RX-09) consists of strongly altered and silicified wallrock with original textures destroyed (Plate 4-7-1). A grab sample of this vein contained 0.5 per cent lead and 0.15 per cent zinc (Table 4-7-2). No sulphides are visible. Weathered open spaces are lined with limonitic material. Limonite and iron-manganese staining is also prevalent along fractures and weathered surfaces. Numerous angular clasts and cobbles of galena-sphalerite-chalcopryrite-bearing vein material were found less than 50 metres away and immediately downslope from the vein, at the foot of a small glacier (samples DY-RX-07, DY-RX-08 and DY-RX-10). These samples are characterised by veins or stringers of galena and/or sphalerite containing occasional grains of chalcopryrite. Sample DY-RX-10 returned an assay of 0.36 per cent copper, 4.58 per cent lead and 15.3 per cent zinc. Similar fragments were found over a distance of several hundred metres down ice (north) from the glacier. A boulder of galena-bearing, brecciated vuggy quartz (sample DY-RX-01) was found on the crest of a lateral moraine approximately 2 kilometres down ice from

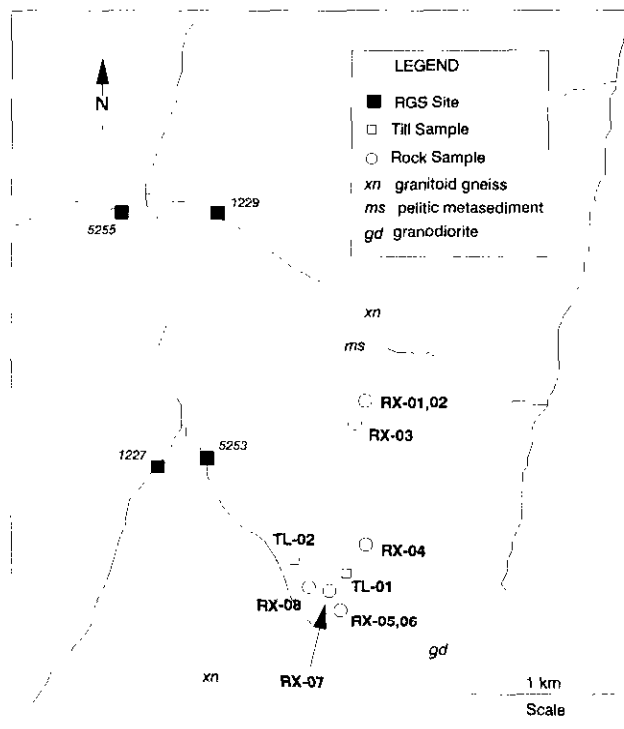


Figure 4-7-6. Sample locations, Trophy Lake site.

the vein. Samples of pyritic schist taken along the western ridge of the cirque contained from 1 (samples DY-RX-03 and DY-RX-05) to 10 per cent (sample DY-RX-04) pyrite and elevated concentrations of copper (Table 4-7-2).

Stream sediment samples collected from four locations (Figure 4-7-7) all reported anomalous values of lead, zinc and gold (Table 4-7-3). Data from these samples compares very closely with the results from the RGS site approximately 2 kilometres downstream. In this case, the RGS program has effectively detected a new area of mineralization. The proximity of mineralization at the Hoodoo North occurrence (MINFILE 92N 029) suggests that this occurrence may be related. Hoodoo North is a Tertiary porphyry copper-molybdenum prospect with associated chalcopryrite-sphalerite-galena-bearing quartz veins hosted by Mesozoic gneisses. Lead isotope values were calculated from galena acquired from samples DY-RX-01 and DY-RX-08 (Table 4-7-4). Unfortunately, these values cannot be used to define a unique date (C.I. Godwin, personal communication, 1992); a Mesozoic age is indicated based on similarity to lead from the Iskut area (Godwin *et al.*, 1991) whereas a Tertiary age is interpreted when compared to lead from the Silver Queen and Equity Silver lead isotope data (Godwin, 1988) or to Tertiary gold veins on Vancouver Island (Andrew and Godwin, 1989).

MARMOT TOWERS (92O/04; RGS SITE 795211)

A small tributary creek of the Tchaikazan River drains a cirque on the west-facing slope of a group of peaks known as the Marmot Towers. This site is approximately 20 kilometres southwest of the southern end of Upper Taseko Lake (Figure 4-7-1). Access to the area is by helicopter. The



Plate 4-7-1. Outcropping vein mineralization, Dorothy Creek site.

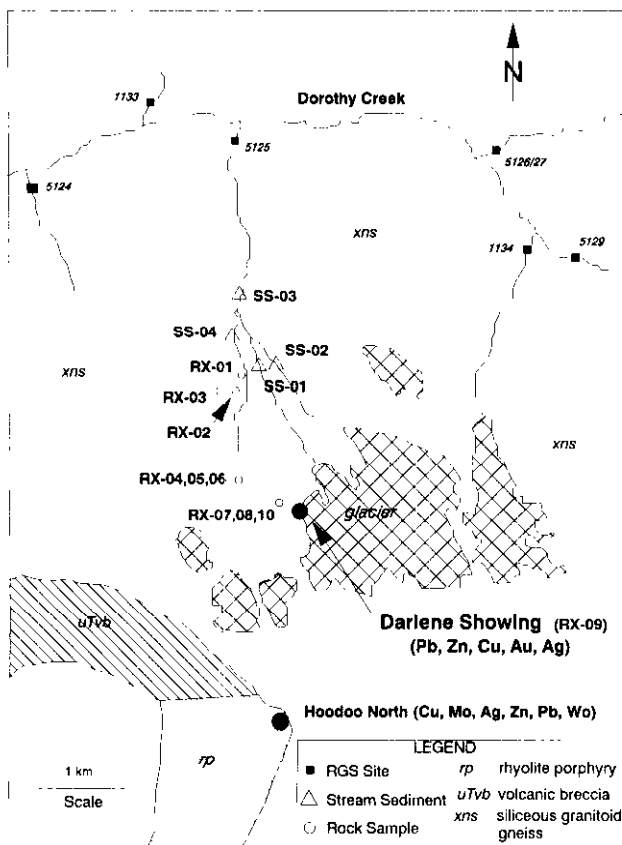


Figure 4-7-7. Sample locations, Dorothy Creek site.

watershed is underlain by granodiorites of the Coast Plutonic Complex (McLaren, 1989). Talus, felsenmeer and glacial drift cover the lower slopes and floor of the cirque. At its confluence with the Tchaikazan River, the creek is underlain by a thick sequence of alluvial sands and gravels. Investigation of this watershed was limited to the examination of a zone of strongly altered granodiorite at 2300 metres elevation and the sampling of the creek near the original RGS site (Figure 4-7-8).

Talus near the base of the alteration zone consists of silicified granodiorite containing hematitic breccia veins (samples TK-RX-02, TK-RX-03 and TK-RX-04), a buff-coloured, pervasively altered, fine-grained rock (granodiorite?) with flecks of limonite (samples TK-RX-05 and TK-RX-06) and a granodiorite cut by pyritic quartz-feldspar and calcite veins (sample TK-RX-01) (Figure 4-7-8). In general, the chemistry of the rock samples does not correspond to the anomalous values detected at the RGS site. Vein material (sample TK-RX-01) carries anomalous values of copper (170 ppm) and arsenic (168 ppm) but does not report elevated levels of gold, lanthanum, uranium or thorium (Table 4-7-5).

No trace of the original RGS site sampled in 1979 was found for resampling. Stream sediment sample TK-SS-01 was taken approximately 300 metres upstream from the confluence with the Tchaikazan River and probably 200 to 250 metres upstream from the original RGS site (Figure 4-7-8). A second stream sediment site (sample TK-SS-02) was sampled at the mouth of the cirque at 2250 metres elevation (Figure 4-7-8). Results from these two sites fall

TABLE 4-7-4
GALENA LEAD ISOTOPE RESULTS FROM THE
DARLENE SHOWING

Pb/Pb Ratio	DY-RX-01		DY-RX-08		
206/204	18.808	18.811	18.819	18.811	18.810
207/204	15.578	15.578	15.603	15.589	15.595
208/204	38.326	38.316	38.402	38.346	38.372
207/206	0.8283	0.8282	0.8291	0.8287	0.8291
208/206	2.03780	2.03698	2.04060	2.03860	2.04000

within background concentrations (Table 4-7-6). Analytical results for the RGS site (Table 4-7-1) suggest that the anomaly is the result of the accumulation of the heavy minerals electrum, gold (gold), scheelite (tungsten), monazite (lanthanum, cerium, thorium and uranium) and zircon (zirconium and hafnium) and may not be reflective of mineralization in the watershed. The poor correspondence of stream sediment and lithochemical results from this investigation support this hypothesis. Anomalous values at RGS site 795211 may have resulted from the reworking of alluvial material in the bed of the stream to form local concentrations of heavy minerals. However, the presence of pyritic quartz-feldspar veins in granodiorite (sample TK-RX-01) and the proximity of granodiorite-hosted veins at Discord Creek (MINFILE 0920 122) and Twin Creek (MINFILE 0920 121) (McLaren, 1989) suggests that there is potential for similar mineralization near this site.

CONCLUSIONS

Results of this investigation have shown that anomalous metal concentrations at three of the seven RGS sites (Barney Creek, Valleau Creek and Dorothy Creek) are directly attributable to a bedrock source. Of the remaining four sites, three (Kloaqt Lake, Bidwell Creek and Marmot Towers) do not appear to be directly associated with mineralization. The large precious metal anomaly near Kloaqt Lake appears to be derived from glacially transported material with a source area outside the watershed. Anomalous metal levels in Bidwell Creek may be the result of hydro-morphic transport and precipitation whereas high concentrations of elements at Marmot Towers appear to be the consequence of the mechanical concentration of background concentrations of heavy minerals within the streambed. Both Bidwell Creek and Marmot Towers may be classed as false anomalies resulting from unusual chemical or physical conditions which have amplified certain element concentrations to anomalous levels. Interpretation of these anomalous concentrations in light of other analytical or field variables available in the RGS dataset can provide an effective means to filter out false anomalies. The final site, Trophy Lake, is ambiguous; there is not enough information to confirm or deny the presence of mineralization.

Results of this study have shown that the Regional Geochemical Survey program is effective in defining watersheds hosting mineralization. However, the RGS program is designed to provide information on regional geochemical trends; identification of individual drainages hosting miner-

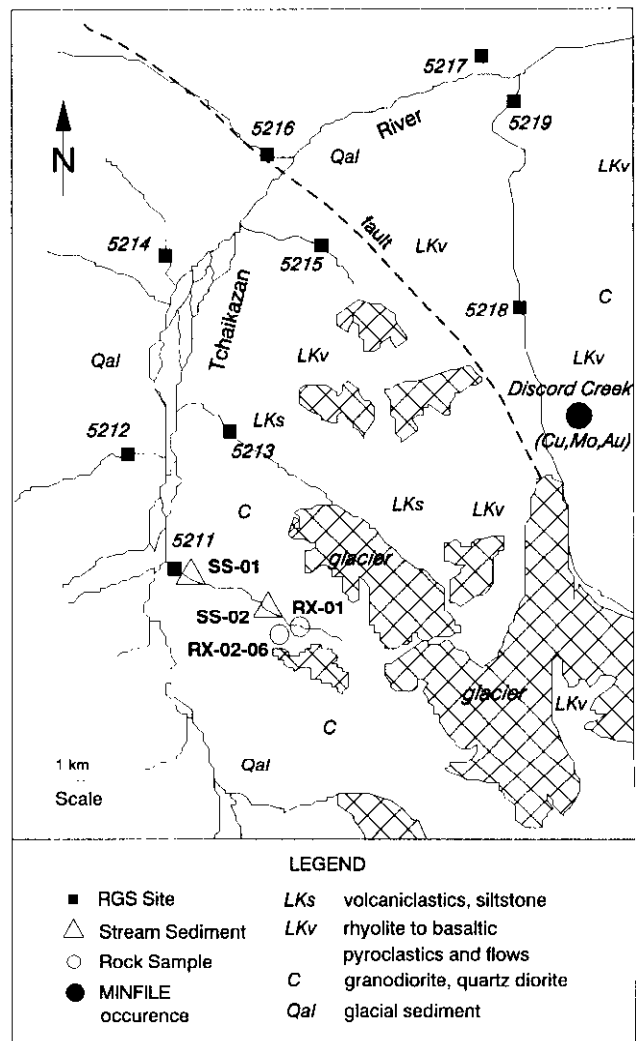


Figure 4-7-8. Sample locations, Marmot Towers site.

alization is not the primary goal of the program. Although new mineralization is often pinpointed by following up single RGS sites, geochemical data from these surveys should be utilized to direct detailed geological and geochemical investigations into geochemically favourable regions hosting multi-site anomalies. This approach will minimize the possibility of single-site false anomalies misleading an exploration program. Further, failure to detect mineralization within an individual watershed should not be viewed as a deterrent to a more comprehensive exploration program which includes surrounding watersheds. Successful application of the RGS database to mineral exploration requires an interdisciplinary approach focusing on favourable geological environments and multi-site RGS anomalies.

ACKNOWLEDGMENTS

The authors wish to thank Kathy Colbourne, Ray Lett and Bish Bhagwananai of the Analytical Sciences Laboratory for sample preparation and analysis, Anne Pickering and Colin Godwin at The University of British Columbia for

TABLE 4-7-5
SELECTED GEOCHEMICAL RESULTS FOR ROCKS FROM MARMOT TOWERS (TK)

Sample	Type	Description	Sulphide Minerals	Mo ppm	Cu ppm	Pb ppm	Zn ppm	Ag ppm	Mn ppm	Fe %	As ppm	Cd ppm	Sb ppm	Bi ppm	Ba ppm	Al ppm	La ppm	U ppm	Th ppm
TK-RX-01	Float	Quartz vein in granodiorite	py	1	170	2	82	0.2	507	5.4	168	0.2	2	2	20	1	4	5	2
TK-RX-02	Float	Hematitic silicified granodiorite (g.d.)		1	38	3	54	0.1	583	3	13	0.2	4	2	61		7	5	1
TK-RX-03	Float	Hematitic silicified g.d. breccia		1	84	2	62	0.2	716	2.8	6	0.2	2	2	347		4	5	1
TK-RX-04	Float	Hematitic silicified g.d. breccia		1	19	2	64	0.1	1275	3.4	4	0.3	10	2	1132		7	5	1
TK-RX-05	Float	Intensely altered(bleached) g.d.(?)		1	46	2	15	0.1	170	0.2	7	0.2	29	2	57		3	5	1
TK-RX-05D	Float	Intensely altered(bleached) g.d.(?)		1	42	6	14	0.1	157	0.2	7	0.2	31	2	51		3	5	1
TK-RX-06	Float	Silicified variant of TK-RX-05		1	1	6	6	0.1	159	0.1	2	0.2	2	2	212		2	7	1

TABLE 4-7-6
SELECTED GEOCHEMICAL RESULTS FOR STREAM SEDIMENTS FROM MARMOT TOWERS (TK)

Sample	Type	Mo ppm	Cu ppm	Pb ppm	Zn ppm	Ag ppm	Mn ppm	Fe %	As ppm	Cd ppm	Sb ppm	Bi ppm	Ba ppm	La ppm	W ppm	Au ppb
TK-SS-01	Stream sed.	1	63	2	61	<2	648	3.85	<5	<1	5	<5	100	<10	<10	10
TK-SS-02	Stream sed.	<1	55	<2	56	<2	544	3.54	<5	<1	5	<5	100	<10	<10	<5

analysis and interpretation of galena lead isotope data and Mike King of Whitesaddle Air. Wayne Jackaman provided advice and assistance with the interpretation of RGS data. Paul Matysek and John Newell provided insightful editorial comments.

REFERENCES

- Andrew, A. and Godwin, C.I. (1989): Galena Lead Isotope Model for Vancouver Island; in Geological Fieldwork 1988, B.C. Ministry of Energy, Mines and Petroleum Resources, Paper 1989-1, pages 75-79.
- Cook, S.J., Jackaman, W. and Matysek, P. (1992): Follow-up Investigation of Anomalous RGS Stream Sediment Sites in Southeastern British Columbia: Guide to Potential Discoveries; in Exploration in British Columbia 1991, B.C. Ministry of Energy, Mines and Petroleum Resources, pages 51-59.
- Godwin, C.I. (1988): LEADTABLE: A Galena Lead Isotope Data Base for the Canadian Cordillera, with a Guide to its Use by Explorationists; B.C. Ministry of Energy, Mines and Petroleum Resources, Paper 1988-4, 188 pages.
- Godwin, C.I., Pickering, A.D.R., Gabities, J.E. and Alldrick, D.J. (1991): Interpretation of Galena Lead Isotopes from the Stewart-Iskut Area; in Geological Fieldwork 1990, B.C. Ministry of Energy, Mines and Petroleum Resources, Paper 1991-1, pages 235-243.
- Jackaman, W., Cook, S.J. and Matysek, P. (1992a): British Columbia Regional Geochemical Survey - Mount Waddington (NTS 92N); B.C. Ministry of Energy, Mines and Petroleum Resources, RGS 34.
- Jackaman, W., Cook, S.J. and Matysek, P. (1992b): British Columbia Regional Geochemical Survey - Taseko Lakes (NTS 92O); B.C. Ministry of Energy, Mines and Petroleum Resources, RGS 35.
- Jackaman, W., Cook, S.J. and Matysek, P. (1992c): British Columbia Regional Geochemical Survey - Bonaparte Lake (NTS 92P); B.C. Ministry of Energy, Mines and Petroleum Resources, RGS 36.
- McLaren, G. P. (1989): A Mineral Potential Assessment of the Chilko Lake Planning Area; B.C. Ministry of Energy, Mines and Petroleum Resources, Bulletin 81, 117 pages.
- Roddick, J.A. and Tipper, H.W. (1985): Geology, Mount Waddington (92N) Map Area; Geological Survey of Canada, Open File 1163.
- Tipper, H.W. (1971): Surficial Geology, Taseko Lakes (92O) Map Area; Geological Survey of Canada, Map 1292A.
- Trettin, H.P. (1961): Geology of the Fraser River Valley between Lillooet and Big Bar Creek; B.C. Ministry of Energy, Mines and Petroleum Resources, Bulletin 44, 109 pages.

NOTES

EVALUATING BURIED PLACER DEPOSITS IN THE CARIBOO REGION OF CENTRAL BRITISH COLUMBIA (93A, B, G, H)

By V. M. Levson, B.C. Geological Survey Branch
R. Clarkson, New Era Engineering Corporation
and M. Douma, Geological Survey of Canada

KEYWORDS: Economic geology, Cariboo, placer gold, stratigraphy, reverse-circulation drilling, gamma logs, seismic, ground-penetrating radar, conductivity.

INTRODUCTION

This paper is a report on the field activities and preliminary results of the 1992 placer geology program conducted by the Surficial Geology Unit of the British Columbia Geological Survey Branch. The program is designed to test models of placer deposition and preservation (Levson and Giles, 1991, in preparation; Levson and Morison, in press) developed from geologic data collected at mines in the Cariboo region and other glaciated areas of the Canadian Cordillera (Clague, 1989a, b; Eyles and Kocsis, 1989a, b; Levson *et al.*, 1990; Levson and Morison, 1991; Levson, 1992a, b; Levson and Kerr, 1992). The program includes an investigation of the utility and limitations of various subsurface exploration techniques for evaluating buried placer deposits. The Cariboo region (Figure 4-8-1) was selected as the study area because of the relative wealth of geologic data available. Current exploration activities are focusing on deeply buried (~20-100 metres) deposits with high placer potential. Detailed geologic data are required to identify and evaluate promising settings for these deposits, but the potential for locating new occurrences is limited by the lack of an adequate stratigraphic database. This program addresses this need for data by investigating the geology of economic placer deposits in areas where they are deeply buried by surficial sediments. The results of these studies are provided to industry through conference presentations,

field trips and publications in both technical (*e.g.*, Levson 1991a) and non-technical formats.

The 1992 placer geology program consisted of the following components:

- A drilling program testing theoretical geologic models of buried placer deposits in glaciated areas.
- An evaluation of geophysical tools for logging boreholes (for natural gamma radiation, apparent conductivity and magnetic susceptibility) at sites with good subsurface lithologic records.
- A study of ground-penetrating radar methods for identifying subsurface placer gravels.
- Tests of the applicability of seismic reflection and refraction surveys for locating paleochannel gravels below till deposits, in areas with good stratigraphic control.
- An investigation of gold recovery from placer gravels by reverse-circulation drilling.
- A field conference on the geology of placer deposits in the Cariboo region for the mining and exploration industry.
- Property visits to compile stratigraphic, sedimentologic and geomorphic data on producing and prospective placer deposits.

PREVIOUS WORK

The bedrock geology of the study area was mapped by Sutherland Brown (1957, 1963), Tipper (1959, 1961), Campbell (1978), Struik (1982, 1986, 1983) and Bailey (1989). Regional compilation maps were produced by Tipper *et al.* (1979) and Bailey (1990). The Quaternary geology of the region was mapped by Tipper (1971) and recent investigations of the Quaternary and placer geology have been made by Clague (1987a, b; 1988; 1989a, b; 1991) and Clague *et al.* (1990). Depositional environments of Cariboo placer deposits have recently been discussed by Eyles and Kocsis (1988; 1989a, b), Levson (1990) and Levson *et al.* (1990). Some implications of these studies for lode gold exploration were presented by Levson (1991b). Descriptions of geologic settings representative of each of the main placer-producing environments in the Cariboo was presented by Levson and Giles (1991). Levson (1991b) discussed geologic controls on exploration, evaluation and mining of placer deposits in each of the main settings. Trace element geochemistry studies of lode and placer gold deposits were conducted in the region by Knight and McTaggart (1990).

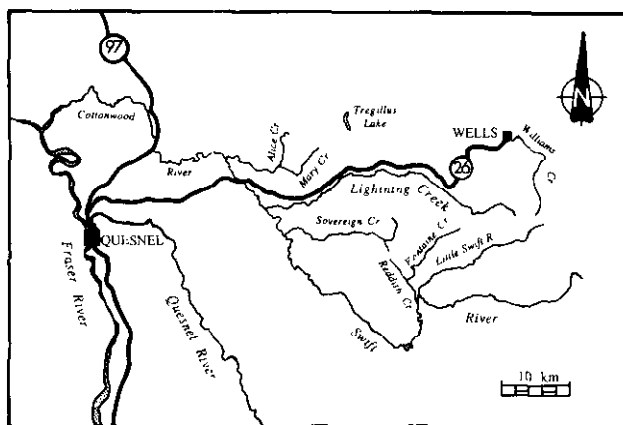


Figure 4-8-1. Location of study sites.

TABLE 4-8-1.

LOG OF DRILL-HOLE NUMBER VL92-1 AT THE GALLERY RESOURCES LTD. MINE ON LIGHTNING CREEK.

Drill Log - Hole Number VL92-1

Location: Gallery Resources Ltd. mine, Hannador property, Lightning Creek
 NTS: 93 G/1 Cottonwood
 Latitude and longitude: 53°01'25"N, 122°01'50"W
 UTM: 5875200m N, 565200m E

Notes: The drill site is on the south side of Lightning Creek, approximately 1 kilometre downstream from its confluence with Moustique Creek; the hole is at the eastern end of the minesite at the top of a high terrace paralleling Lightning Creek. This hole is the same as Gallery Resources hole number 6. Exposures of massive, matrix-supported diamicton are present on the hill side about 10 metres above the drill collar. The presence of striated clasts and the varied clast lithology (including quartzite, phyllite, granite, basalt, dacite, andesite, gneiss, biotite schist, sandstone, chert and pebble conglomerate) indicates a glacial derivation. The section measured in 1990 by Levson and Giles (in prep.) is located about 200 metres northeast (220°) of the drill site.

Unit	Depth (metres)	Description:
1	0 - 3.0	Fine sand and silt: light olive-brown colour (Munsell code: 2.5Y 5/4); well sorted; no clasts; poor sample recovery; Sample 6-0-10.
2	3.0 - 6.7	Silt and clay: olive-brown colour (Munsell code: 2.5Y 4/4); no gravel clasts; very well sorted; Samples 6-10-15, 6-15-20.
3	6.7 - 9.1	Pebble gravel; sandy matrix; clast lithologies varied; approximate proportions: 40% quartzite, 20% phyllite, 20% vein quartz, 10% sandstone, 10% schist, etc. Samples 6-20-25, 6-25-30.
4	9.1 - 12.2	Pebble to cobble gravel; sandy matrix; clast lithologies varied; similar to unit 3 except for coarser beds at top and bottom of unit; Samples 6-30-35, 6-35-40.
5	12.2 - 17.7	Pebble gravel; minor, thin, sand lenses; gravels have a sandy matrix; clast lithologies varied; similar to unit 3; Samples 6-40-45, 6-45-50, 6-50-55.
6	17.7 - 18.3	Boulder gravel; little matrix; clast lithologies varied; similar to unit 3 except coarser; Sample 6-55-60.
7	18.3 - 29.0	Pebble gravel; similar to unit 5; minor, thin, sand lenses; cobble bed in lowest 0.5 metre at base of unit; gravels have a sandy matrix; clast lithologies varied; pebble-chip count results (n=95): 54% quartzite (27% red micaceous quartzite, 27% other quartzite), 32% vein quartz, 7% black argillite/phyllite, 3% metasiltstone, minor (<1%) schist, minor sandstone, minor hornblende dacite; Samples 6-60-65, 6-65-70, 6-70-75, 6-75-80, 6-80-85, 6-85-90, 6-90-95, VL-92001 (at 23 metres depth), VL-92002 (at 29 metres depth).
8	29.0 - 35.1	Pebble to cobble gravel; similar to unit 7 but with cobble beds at 30.5 - 32 metres and 33 - 34 metres; matrix is clay rich from about 29 - 32 metres, otherwise is sandy; iron oxide (red) staining present in some gravels; sand beds rare; clast lithologies varied; Pebble-chip count results (n=100): 57% quartzite (34% red micaceous quartzite, 23% other quartzite), 26% vein quartz, 10% black argillite/phyllite, 2% metasiltstone, 2% schist, 1% metavolcanics, 1% chert, 1% hornblende dacite; Samples 6-95-100, 6-100-105, 6-105-110, 6-110-115, VL-92003 (at 31 metres depth), VL-92004 (at 35 metres depth).
9	35.1 - 39.6	Cobble to boulder gravel; unit appears to coarsen with depth; minor pebble beds at 35.7 - 36.3 metres and 37.5 - 37.8 metres; sandy matrix; clast lithologies varied; large clasts are mainly quartzites; pebble-chip count results (n=50): 57% quartzite (28% red micaceous quartzite, 22% other quartzite), 24% vein quartz, 24% black argillite/phyllite, 2% hornblende dacite; Samples 6-115-120, 6-120-125, 6-125-130, VL-92005 (at 38 metres depth), VL-92006 (at 39.5 metres depth).
10	39.6 +	Bedrock: very dark gray (Munsell code: 5Y 3/1) to black (Munsell code: 5Y 2.5/1); lithology mainly argillite; Samples 6-130-135, 6-135-140, 6-140-145.

METHODS

Sites with stratigraphic control and geologic evidence for buried placer potential were selected for field investigation by airphoto study and office review of existing data. Geologic data collected during previous studies in the Cariboo were used to help identify areas with high buried-placer potential. Fieldwork included a reverse-circulation drilling program to collect subsurface data needed to test stratigraphic correlations and depositional models. The efficiency of the drilling method for recovering gold was tested by New Era Engineering Corporation using radiotracers. Geophysical methods for evaluating buried placers (including borehole geophysics, seismic reflection and refraction techniques and ground-penetrating radar) were also investigated in conjunction with the Geological Survey of Canada. Shallow refraction hammer-seismic data were collected by Howard Myers. The effectiveness of these exploration techniques for evaluating buried deposits will be discussed elsewhere. Detailed descriptions of the procedures for each subsurface technique and preliminary results are described here.

DRILLING PROGRAM

A number of drill sites were selected in different geologic settings in order to test depositional models for placer deposits in British Columbia. Emphasis was placed on buried placer deposits in both trunk and tributary paleovalleys and two holes (VL92-5 and VL92-6) were drilled in a terrace-placer setting. The type of data collected during the drilling program is exemplified by the log of drill hole VL92-1 from Lightning Creek (Table 4-8-1).

The Mobile B80 drill used in this study (Plate 4-8-1) was fitted with a 115-millimetre (4.5-inch) diameter, skirted

rotary tri-cone bit and 89-millimetre (3.5-inch) diameter drill rods. The rods consisted of an inner tube to carry sample from the bottom of the hole to the surface and an outer annulus to carry the compressed air used to flush the drill cuttings from the hole. Approximately 1.60 litres per second (540 cubic feet per minute) of air compressed to 2.4 megapascals (350 pounds per square inch) was forced down the outer annulus of the rods. Water was added to the compressed air stream to lubricate the drill rods. Drill cuttings were forced up the inner tubing through the rotary head and hoses into a sampling cyclone and were collected in buckets. Holes remaining open after drilling was completed were cased with 5-centimetre (2-inch) diameter plastic (PVC) pipe to as great a depth as possible to accommodate the geophysical logging tools.

LIGHTNING CREEK AREA

Drill holes VL92-1 and VL92-2 were located in the Lightning Creek valley at the Hannador property of Gallery Resources Limited. An active exploration program at this site has targeted a buried deposit of probable interglacial age that is believed to lie parallel to and south of the modern Lightning Creek channel (Levson, 1991a). Preliminary results of the drilling program (Table 4-8-1) indicate that auriferous paleochannel gravels extend underneath a thick (30 m) sequence of glaciofluvial and fluvial deposits exposed on the south side of the valley.

ALICE CREEK AREA

Drill holes VL92-3 and VL92-4 were drilled to investigate buried river channel deposits in the Alice Creek area believed to be Tertiary in age (Rouse *et al.*, 1990). Deposits mined at Alice Creek are believed to be correlative with

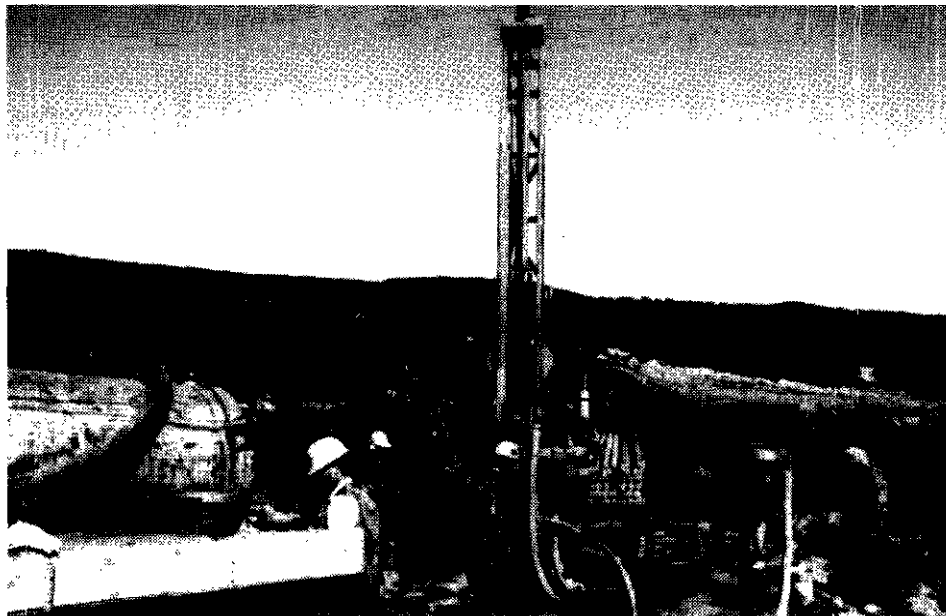


Plate 4-8-1. The reverse-circulation drill used in this study drilling hole number VL92-3, due west of the Alice Creek mine. The cyclone on the right hand side of the drill is used to catch the drill samples.

those at the nearby Mary Creek mine (Levson and Giles, 1991) but the extent and orientation of the paleochannel system is not known. Holes VL92-3 and VL92-4 were 'wildcat' holes drilled in an attempt to constrain the paleogeography of the buried channel. The location of hole VL92-3 (Plate 4-8-1), due west of the Alice Creek mine, was chosen on the basis of industry drill records (Ed Kruckowski and Jack Wyder, personal communication, 1992). These data defined a deep channel in the Alice Creek valley with a cross-sectional geometry suggestive of a west-trending paleochannel. Bedrock was intersected in hole VL92-3 under till at a depth of about 10 metres, well above base level in the Alice Creek paleochannel. These data, together with the known distribution of bedrock outcrops in the area, provide a new constraint on the orientation of the paleochannel system. These results lead to the hypothesis that placer gravels mined on the east side of Alice Creek must have been deposited in a paleochannel system that either extends to the north or swings sharply to the south. To test this, hole VL92-4 was drilled about 1 kilometre north of the Alice Creek mine. Several metres of gold-bearing gravels were encountered in this deep hole with bedrock occurring at 36 metres depth. These gravels are believed to be the deposits of a northerly extension, possibly a tributary channel, of the main paleochannel system.

COTTONWOOD RIVER AREA

Holes VL92-5 and VL92-6 were drilled along the Cottonwood River to investigate Holocene terrace gravels and possible older paleochannel deposits in that area. The holes were collared on opposite sides of a broad, low terrace on the south side of the Cottonwood River. The terrace is a few metres higher than the present channel and directly upstream from a bedrock-floored canyon into which the Cottonwood River valley narrows. High ridges on both sides of the canyon are comprised mainly of bedrock to the north of the river and unconsolidated Quaternary sediments to the south. Small bedrock knolls are also exposed at low water levels along the present course of the river upstream from the canyon. Gravels occur throughout the entire drilled sequence above bedrock which was intersected at a depth of about 20 metres in both holes. The gravels are gold bearing with the highest gold recovery occurring in coarse gravel beds at the bottom of the holes; the latter are interpreted to be erosional lag gravels.

Bedrock exposures in the modern channel of the Cottonwood River, particularly those along the canyon directly below the drill sites, constrain the depth of Holocene incision of the river to that of the present-day channel. Consequently, as bedrock is nearly 20 metres below the present channel base at the drill sites, the gravels in the lower part of the sequence must predate the Holocene. They are believed to be interglacial or preglacial gravels deposited in a paleochannel that presumably lies south of the present river and may extend under the thick Quaternary deposits south of the canyon. Deep-channel gravels on the southwest side of the terrace have been previously mined at one site near the valley side. Mining was stopped when the gravels could no longer be removed because they were covered by, and apparently extended underneath, a thick clay (glaciolacustrine?) sequence.

The placer operation at this site is currently evaluating the potential for mining these paleochannel gravels in areas where they may be preserved below Holocene terrace gravels.

SOVEREIGN CREEK AREA

Holes VL92-7 and VL92-8 were drilled in the Sovereign Creek region in an area with excellent potential for a large-volume buried paleochannel placer deposit of interglacial or preglacial age. This deposit occurs in a recently discovered buried valley that apparently trends northwesterly parallel to Sovereign Creek. The paleochannel gravels were intersected in drill hole VL92-7 at depths from 8 to 27 metres. They overlie bedrock and are overlain by diamicton units with interbedded silty clays interpreted, respectively, as till and glaciolacustrine sediments.

The paleovalley containing the auriferous deposits is separated from the modern Sovereign Creek valley by a bedrock high which has been exposed by recent mining and forms the northeast wall of the buried valley. Hole VL92-8 was drilled to help define the southern extent of the paleovalley and its general orientation. Drilling results indicate that the channel gravels thin substantially to the south. Bedrock was encountered at shallow depths (16.5 m), suggesting that the drill site is located near the southwest margin of the paleochannel.

REDDISH CREEK AREA

Holes VL92-9 and VL92-10 were drilled between Fontaine Creek and the Little Swift River to test the potential of a large buried "trunk" valley trending northwesterly parallel to the Reddish Creek valley. Previous stratigraphic studies in the Little Swift River area (Levson and Giles, 1991; Levson, 1991a; Levson and Giles, in preparation) suggested that a large paleovalley placer deposit may occur in the region. Past mining strategies have targeted southwesterly flowing streams such as the Little Swift River and Fontaine Creek, but little attention has been paid to the possibility of a northwesterly trending paleochannel, possibly following the strike of the Eureka thrust. This fault separates the Barkerville and Quesnel terranes (Struik, 1988) and may have provided a major structural control on preglacial drainage patterns in the area. Drill hole VL92-9 was drilled southeast of the Fontaine Creek valley and intersected gold-bearing gravels of similar thickness and type to those currently being mined along it. Hole VL92-10 was a 'wildcat' hole drilled part way between the Little Swift River and Fontaine Creek. The occurrence of auriferous gravels at the bottom of this hole provides new evidence that strongly supports the hypothesis that a large northwesterly trending paleovalley exists in this area.

GOLD RECOVERY TESTS

The reverse-circulation drill used in this study was tested at four sites using gold radiotracers as part of a broader research program on drilling methods conducted by R. Clarkson of New Era Engineering Corporation. Information on radiotracers (very low level radioactive gold particles) and their use in gold recovery research has been

provided by Clarkson (1991). The results and preliminary conclusions presented here apply only to the four sites tested during this study.

For each test, four sizes of radiotracers were used: 0.18 millimetre (-65+100 mesh), 0.36 millimetre (-35+48 mesh), 0.72 millimetre (-20+28 mesh) and 1.44 millimetres (-10+14 mesh). The radiotracers were placed in the middle of barren compacted gravels and frozen into a solid cylindrical shape. The test gravel cylinders were 300 millimetres (12 inches) long and 90 to 100 millimetres (3.5 to 4 inches) in diameter. The test procedure involved drilling to the desired depth (10 to 35 m) and pulling the drill rods out of the hole. The open hole depth was then measured and caved portions were redrilled until the desired depth was reached (where practical). The radioactive test cylinder was then dropped down the hole and the depth of penetration was determined and increased if necessary by pushing with the drill stem. Gravel stemming was then dumped into the hole and compacted before redrilling. The collar of the hole, drill cuttings, drill equipment, sample collection equipment and personnel were checked for radioactive gold during and after completion of the drilling (Plate 4-8-2). Radioactive particles were detected using a scintillometer. Their locations were recorded and all detected particles were collected. Drill samples containing tracers were processed in a small sluice and by hand panning until each radioactive particle present in the concentrate was recovered.

Most of the recovered radiotracers were out of the holes by the time the bit had reached 3 metres beyond the depth where the test cylinders were originally placed. The addition of water to the compressed air stream increased segregation and entrapment of gold tracers. Water addition also increased spillage losses and made it difficult to collect and

contain the samples. Although surges of high-pressure air were used to flush the system, many tracers were caught and remained in the hose fittings and sampling cyclone. To remove them, the cyclone and hose fittings were disconnected and cleaned out after the hole was completed. As the collars of the holes were not sealed a high proportion of the cuttings and tracers was forced up outside the drill rods onto the ground near the collars (blow-by).

Between 2 and 98 per cent of the tracers were recovered from the four holes tested. In the hole with the deepest sample depth (35 m) only 2 per cent of the tracers were recovered, one was on the ground next to the collar and the other was trapped in the cyclone. Even in shallower holes (10 m) with relatively high recoveries, many of the tracers were lost due to spillage and to blow-by around the collar of the hole. Some of the tracers were trapped in the sample cyclone and its plumbing.

Natural gamma logs (*see below*) were obtained from three of the four holes tested. In all three logs, anomalous peaks in the gamma radiation, indicating the presence of tracers, were observed at the approximate penetration depths that the test cylinders initially reached after being dropped down the holes. No anomalous peaks occurred more than 1 to 2 metres above these depths. This suggests that attempts to push the radioactive test cylinders to the bottom of the holes with the drill rods caused part of the samples to be lodged in the side of the hole at or near the depth of initial penetration. In this regard, it is interesting to note that the test with the highest initial penetration of the sample cylinder relative to the hole depth (10 m in a 10.5 m hole) yielded the best tracer recovery (98%). Similarly, the hole with the lowest initial penetration (4 m in a 36.5 m hole) yielded the lowest recovery (2%). In this latter case,



Plate 4-8-2. Searching drill-sample collection area for gold radiotracers using a scintillometer.

numerous anomalous gamma peaks were detected between the initial penetration depth and the base of the log (15 m) suggesting that the test cylinder was pushed at least part way down the hole. These results indicate that caving of open holes in wet, unfrozen materials presents a major difficulty in testing gold recovery in this method of reverse-circulation drilling.

Material derived from caving along the walls of the drill hole may also result in the introduction of significant amounts of sediment (and gold) into the sample over any one sample interval. Caving may occur when boulders are encountered or when saturated gravels are drilled. Gold values may be overestimated as a result of caving if all of the recovered gold is assumed to have come from a volume of sediment calculated on the basis of hole diameter. This problem can be avoided if the actual volume or weight of the recovered sample is used to determine gold concentrations. Up-hole contamination can also introduce errors in determining gold values for any one sampled interval. Up-hole contamination occurs, for example, when the blow-by is lost.

Although results of the four radiotracer tests suggest that unsealed, uncased reverse-circulation drilling is not a reliable method of determining gold values in unfrozen placer gravels, this method does provide samples which are suitable for determining the lithology and stratigraphy of the surficial deposits. Depth to bedrock is also readily determined as bedrock cuttings are generally easy to recognize. Losses due to blow-by can be reduced by drilling a short length (3 to 6 m) of casing (Odex) into the hole and sealing off the drill rods with a packing case. Losses in the drill hole may also be reduced if casing is used for the total length of the hole (especially if the casing is driven ahead of the bit). Losses and carry-over from the sampling hose, fittings and cyclone can be reduced with designs that eliminate gold traps and with frequent thorough cleaning. Other methods of reverse-circulation drilling should be tested at several locations to determine which drilling equipment and procedures maximize gold recovery on a consistent and predictable basis.

GEOPHYSICAL PROGRAM

BOREHOLE LOGGING

Seven cased drill holes (VL92-1, VL92-4, VL92-7, VL92-10, DH-14, DH-17, and TH-9) were logged by the Geological Survey of Canada using the Geonics EM-39 logging system (Plate 4-8-3). Apparent conductivity, naturally occurring gamma radiation and magnetic susceptibility were recorded in six of the seven holes. Only natural gamma radiation was measured in one of the holes at Sovereign Creek (DH-14) due to the presence of steel casing in the hole.

The radius of penetration for the conductivity probe is estimated to be 1 to 1.5 metres and, as the tool is claimed by the manufacturer to be unaffected by fluids in the plastic casing, the conductivity measured is taken to be that of the surrounding formation and associated groundwater. The results of a conductivity log of drill hole VL92-1 at the

Gallery Resources mine at Lightning Creek are given in Figure 4-8-2. High conductivity in the upper several metres of the hole corresponds well with lithologic data (Table 4-8-1) showing high silt and clay contents in Units 1 and 2. Low conductivity in the gravelly deposits underlying Unit 2 contrasts sharply with the high conductivity in the overlying fine-grained sediments.

The gamma tool detects the decay of uranium, thorium and potassium, although for practical purposes the tool measures, quantitatively, the abundance of clay in the strata surrounding the borehole. Low gamma readings are an indication of coarse-grained sediments, and high gamma readings are attributable to fine-grained materials. A natural gamma log for drill hole VL92-1 is provided in Figure 4-8-3. The natural gamma peak at 5 metres depth corresponds well with a similar peak in the conductivity log at the same depth. The natural gamma log shows more variability and fluctuations than the conductivity log, possibly reflecting a greater sensitivity to textural changes such as sand and silt content in the gravelly units at this site.

The magnetic susceptibility probe measures how strongly the material adjacent to the borehole is affected by a magnetic field, in this case the earth's field. It is accepted that the overall susceptibility of a lithology is dependent only on the amount of ferrimagnetic minerals present such as magnetite, pyrrhotite and ilmenite. Data collected with the magnetic susceptibility tool are currently being processed.

SEISMIC SURVEYS

Expanding-spread seismic refraction and/or common offset seismic reflection surveys were conducted by the Geological Survey of Canada at the following sites: Ballarat mine near Barkerville, Alice Creek property, Sovereign Creek area, Fontaine Creek mine, Reddish Creek area, Golden Bench mine on the Cottonwood River and Corless Tertiary mine on the Quesnel River. The surveys can be efficiently conducted with a two-person line crew and one person operating the seismograph (Plate 4-8-4). A portable, gas-powered auger drill was used to drill shot holes to a depth of about a metre and shotgun explosives were used as the signal source (Plate 4-8-4). For comparison purposes, shallow hammer-seismic refraction surveys were also conducted at two sites (Gallery Resources and Golden Bench mines) using hammer blows on a steel plate as the signal source. All refraction and reflection surveys were located near holes drilled during this program (VL92-4, VL92-6, VL92-7, VL92-9 and VL92-10) or near industry drill holes at the Gallery Resources Ltd., Ballarat, Corless Tertiary and Sovereign Creek mines. The drill-hole results will provide stratigraphic control and reference data for evaluation of the seismic results.

The purpose of the seismic surveys was to map the subsurface stratigraphy, in particular the thickness and lateral extent of gravel horizons that are known or believed to contain placer gold, and to evaluate the applicability of the various methods in different geologic conditions. Many buried auriferous gravel units pose a problem for interpretation because their acoustic velocity is lower than that of till units which they commonly underlie. These deposits constitute what is known as a 'hidden' layer. The preliminary



Plate 4-8-3. Geonics EM-39 logging system for apparent conductivity, naturally occurring gamma radiation and magnetic susceptibility. The apparent conductivity probe has been partially inserted into plastic (PVC) casing in the drill hole.

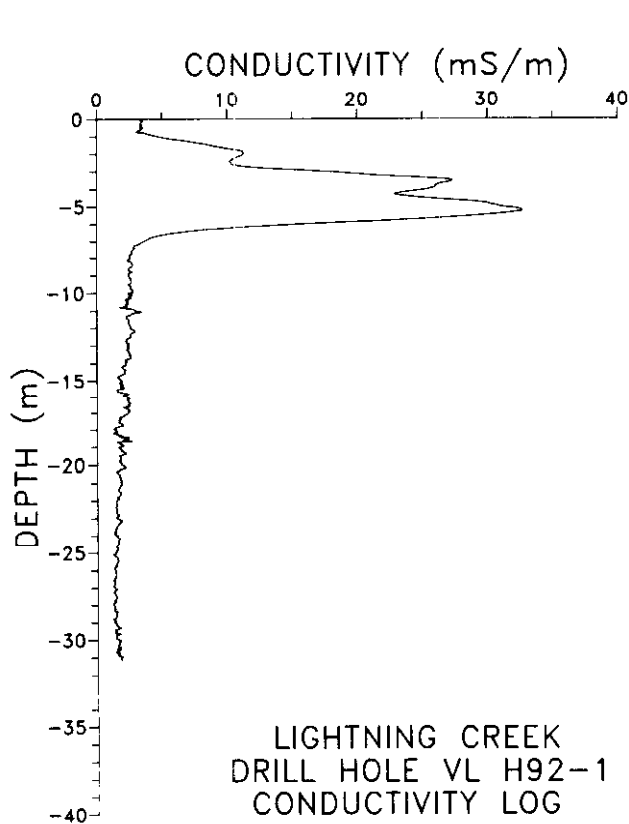


Figure 4-8-2. Conductivity log of drill hole VL92-1 at the Gallery Resources mine on Lightning Creek. High conductivity in the upper several metres of the hole reflects high silt and clay contents whereas low conductivity is indicative of gravelly deposits. (mS/m = millisiemens/metre).

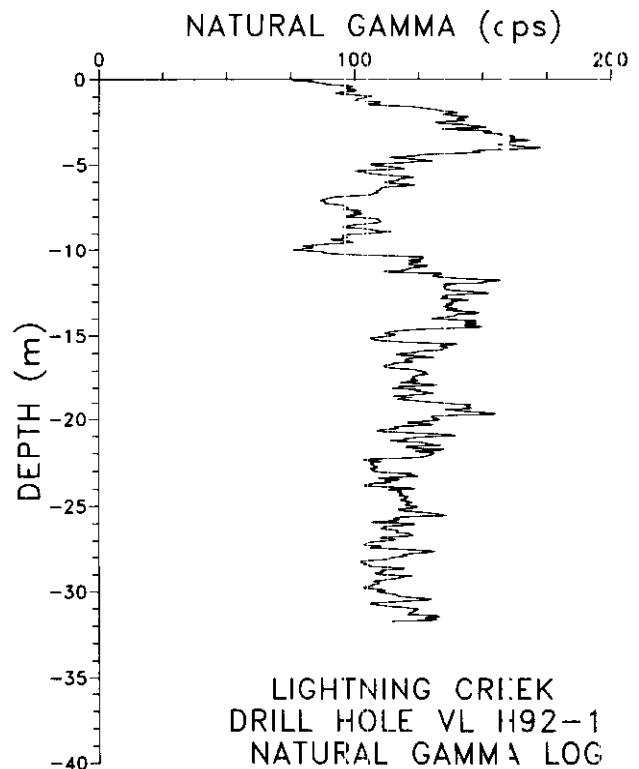


Figure 4-8-3. Natural gamma log of drill hole VL92-1. The natural gamma peak at 5 metres depth corresponds well with a similar peak in the conductivity log at the same depth (see Figure 4-8-2). Fluctuating values in the natural gamma log may reflect textural changes such as variations in sand and silt content in the gravels. (cps = counts per second).



Plate 4-8-4. Field crew conducting an expanding-spread seismic refraction and reflection survey on a high terrace of the Quesnel River above the Corless Tertiary mine site. The person on the left is operating the seismograph and the person on the right is releasing the firing pin into a shot hole. Geophones are spaced at equal intervals along the cables on the right. Note the portable, gas-powered auger drill in the middle of the road, used to drill shot holes.



Plate 4-8-5. Equipment used for ground-penetrating radar surveys. Transmitting and receiving antennas, in the foreground, are connected by fibre-optic cables to the data collection and processing equipment in the background.

seismic surveys conducted during this study will attempt to determine the potential of these techniques for locating these hidden layers. The seismic data are currently being processed and analyzed. The results of these analyses will indicate the potential for future studies.

GROUND-PENETRATING RADAR STUDY

Ground-penetrating radar surveys were conducted by Jean Pilon of the Geological Survey of Canada at six different mine sites (Gallery Resources Limited, Ballarat, Golden Bench, Pawnee, Tregillus Lake and Corless Tertiary mines). The survey equipment consists of two hand-carried antennas, one for transmitting and one for receiving the radar signals, connected to the data collection and processing equipment by fibre-optic cables (Plate 4-8-5). Data were collected from a total of 25 lines up to several 100 metres in length. The results of drilling data from these sites, collected during the 1992 program and by industry, were compiled in order to test the accuracy of the ground-penetrating radar data. Preliminary results indicate that the method is an excellent tool for determining depth to bedrock, water table level and major stratigraphic breaks and for investigating channel geometry in gravelly placer deposits. The main limitation of the method appears to be caused by the presence of clay-rich sediments that may overlie or be interbedded with auriferous gravel units.

FIELD CONFERENCE

A field conference on the geology of placer deposits in the Cariboo region was held for the mining and exploration industry as part of this program. The following topics were discussed: the bedrock geology of the Cariboo and relationships of lode gold and placer deposits (Chris Ash, B.C.

Geological Survey), the geology of the Alice and Mary Creek placer deposits (Jack Wyder), the composition of lode and placer gold in the Cariboo (John Knight and Ken McTaggart, The University of British Columbia), the formation of placers, depositional processes, paystreaks and sedimentary traps (Ted Faulkner, B.C. Geological Survey), the geology of buried placer deposits, field criteria for recognizing different types of placers and ways of identifying potential geologic settings conducive to placer deposition (Vic Levson, B.C. Geological Survey), placer gold recovery technologies, ways of reducing gold losses and sampling methods (Randy Clarkson, New Era Engineering), geophysical and other methods of locating and investigating buried placer deposits (Marten Douma, Susan Pullan and Jim Hunter, Geological Survey of Canada). The conference included a field trip to study the geology of local placer operations (Plate 4-8-6). Buried Quaternary and Tertiary placers were examined at three sites: the Ballarat, Gallery Resources and Alice Creek mines. High attendance at the conference (100 people) indicates that this is an excellent format for the exchange of geoscientific information between researchers and industry.

SUMMARY

Subsurface placer deposits were investigated using a number of techniques including reverse-circulation drilling, ground-penetrating radar, borehole geophysics and seismic studies. The utility and limitations of these techniques in different geologic settings were also evaluated. The investigations were conducted in conjunction with industry and the Geological Survey of Canada at the Gallery Resources Limited property, the Ballarat mine, the Golden Bench mine, in the Alice Creek area, south of Sovereign Creek, near Fontaine Creek, in the Reddish Creek region, in the



Plate 4-8-6. Some of the field conference participants examining the geology of a buried placer deposit at the Ballarat mine.

Quesnel Canyon area and near the Tregillus Lake mine. The main results of this program include:

- The intersection of auriferous paleochannel gravels in eight of the ten reverse-circulation holes drilled.
- The discovery of previously unknown gold-bearing paleochannel gravels at two sites (near Alice and Reddish creeks).
- Completion of the first phase of a program to investigate the applicability of ground-penetrating radar, borehole logging and geophysical studies to determining the subsurface stratigraphy and geometry of buried placers in a number of different settings.
- Completion of a preliminary evaluation of gold recovery in reverse-circulation drilling.

At most of the drill locations, the presence of subsurface paleochannels was not indicated by surface geomorphologic features. In addition, the auriferous deposits were buried by a thick glacial overburden sequence at all sites (except at the two drill holes along the Cottonwood River). The identification of buried channel deposits must therefore rely on the interpretation of existing geologic data from the area of interest and extrapolation of information from adjacent areas. The most critical data for successful results include information on the paleogeomorphic setting, depositional environment, source proximity and paleoflow direction. Useful subsurface data, such as paleoflow records and information on stratigraphy and depth to bedrock, can be obtained from natural and manmade exposures and from drilling programs. In addition, bedrock geology controls such as the locations of potential source rocks and favourable geologic structures need to be considered. The results of the drilling program conducted during this study indicate that these sources of information can be successfully used to identify new paleochannel deposits. Targets for drilling should be based on correlations of stratigraphic data and paleogeographic reconstructions of the buried channel systems.

Reverse-circulation drilling can provide valuable geologic data, such as lithologic composition of gravel units, stratigraphy and depth to bedrock, but the method is not recommended for accurate determinations of gold content. Potential errors may be reduced by determining gold content on the basis of the actual amount of sediment recovered (rather than on theoretical calculations of sediment volume based on the drill bit diameter and sample interval). Modifications to the drilling techniques and equipment used may also help eliminate potential sources of error. Results are apparently more reliable in compact gravels not subject to caving. However, determinations of gold values from drilling data, regardless of the method used, must be interpreted with caution due to the typically small sample size and other factors. Qualitative records of gold content, such as notes on presence or absence of gold and relative abundance, are considered to be more reliable than quantitative determinations based on small samples.

The preliminary results of the borehole logging component of this study indicate that subsurface gravel units can readily be distinguished from units with high silt and clay contents. Geophysical logging of abandoned holes from previous drilling programs, common on many placer prop-

erties, may be an economic way of obtaining useful stratigraphic information. Other methods of determining subsurface stratigraphy such as refraction and reflection seismic surveys and ground-penetrating radar surveys may also be useful for locating buried placer deposits. Preliminary results indicate that ground-penetrating radar is a particularly good method for investigating buried channel gravels provided that they are not overlain by clay-rich sediments.

ACKNOWLEDGMENTS

The authors would like to thank all the miners whose properties are discussed in this paper for providing information and access to their properties. Special thanks are extended to Stan Bergunder and Norm Olausen (Golden Bench mine), Bert Ball (Wilderness Resources), Debbie Corless and Lee Frank (Corless Tertiary mine), Bruce Costerd (Gallery Resources Ltd.), Don Kirkham and Stuart Spiers (Dragon Mountain Placers Ltd.), Ed Kruchkowski and Jack Wyder (Alice Creek mine), Dale Pauls (Beaver Pass Exploration and Development), Dan Romanow (Fontaine Creek mine) and Gunner Slack and Chris Armstrong (Tercon Contractors Ltd.). James and Greg Devins of Dateline Contracting Ltd. are especially thanked for providing efficient and excellent quality drilling services. Howard Myers provided information on shallow refraction seismic surveys. The support of the Geological Survey of Canada is acknowledged, particularly the efforts of Jim Hunter and Susan Pullan for assisting with the geophysical component of the program, Jean Pilon for conducting the ground-penetrating radar study and Jean-Serge Vincent for coordinating this collaborative research project. We acknowledge the support of the of Cariboo Mining Association. Other information and assistance were provided by Fred Andrusko (Yanks Peak Resources), Brian McClay (Mosquito Consolidated Gold Mines Ltd.), Marlene Van Halderen and numerous other members of the Cariboo placer mining community. Excellent field assistance was provided by Colleen Bauer. The manuscript was reviewed by John Newell and Peter Bobrowsky. Figure 4-8-1 was drafted by Scott Henthorn.

REFERENCES

- Bailey, D.G. (1989): Geology of the Swift River Map area, NTS 93A/12, NTS 93A/13, 93B/16, 93G/1; *B.C. Ministry of Energy, Mines and Petroleum Resources*, Open File 1989-20, 1:50 000.
- Bailey, D.G. (1990): Geology of the Central Quesnel Belt, British Columbia; *B.C. Ministry of Energy, Mines and Petroleum Resources*, Open File 1990-31, 1:100 000.
- Campbell, R.B. (1978): Quesnel Lake 93A Map Area; *Geological Survey of Canada*, Open File 574.
- Clague, J.J. (1987a): Quaternary History and Stratigraphy, Williams Lake, British Columbia; *Canadian Journal of Earth Sciences*, Volume 24, pages 147-158.
- Clague, J.J. (1987b): A Placer Exploration Target in the Cariboo District, British Columbia; *Geological Survey of Canada*, Paper 87-1A, pages 177-180.
- Clague, J.J. (1988): Quaternary Stratigraphy and History, Quesnel, British Columbia; *Géographie Physique et Quaternaire*, Volume 42, Number 3, pages 279-288.

- Clague, J.J. (1989a): Gold in the Cariboo District, British Columbia; *Mining Review*, September/October, pages 26-32.
- Clague, J.J. (1989b): Placer Gold in the Cariboo District, British Columbia; in *Current Research, Part E, Geological Survey of Canada*, Paper 89-1E, pages 243-250.
- Clague, J.J. (1991): Quaternary Stratigraphy and History of Quesnel and Cariboo River Valleys, British Columbia: Implications for Placer Gold Production; in *Current Research, Part A, Geological Survey of Canada*, Paper 91-1A, pages 1-5.
- Clague, J.J., Hebda, R.J. and Mathewes, R.W. (1990): Stratigraphy and Paleocology of Pleistocene Interstadial Sediments, Central British Columbia; *Quaternary Research*, Volume 34, pages 208-228.
- Clarkson, R. (1991): Placer Gold Recovery Research, Final Summary; report prepared for the Klondike Placer Miners Association, *New Era Engineering Corporation*, Whitehorse, Yukon, 49 pages.
- Eyles, N. and Kocsis, S.P. (1988): Gold Placers in Pleistocene Glacial Deposits; Barkerville, British Columbia; *Canadian Institute of Mining, Metallurgy, and Petroleum*, Bulletin, Volume 81, pages 71-79.
- Eyles, N. and Kocsis, S.P. (1989a): Sedimentological Controls on Gold Distribution in Pleistocene Placer Deposits of the Cariboo Mining District, British Columbia; in *Geological Fieldwork 1988, B.C. Ministry of Energy, Mines and Petroleum Resources*, Paper 1989-1, pages 377-385.
- Eyles, N. and Kocsis, S.P. (1989b): Sedimentological Controls on Gold in a Late Pleistocene Glacial Placer Deposits, Cariboo Mining District, British Columbia, Canada; *Sedimentary Geology*, Volume 65, pages 45-68.
- Knight J. and McTaggart K.C. (1990): Lode and Placer Gold of the Coquihalla and Wells Areas, British Columbia (92H, 93H); in *Geological Fieldwork 1989, B.C. Ministry of Energy, Mines and Petroleum Resources*, Paper 1990-1, pages 105-118.
- Levson, V.M. (1990): Geologic Settings of Buried Placer Gold Deposits in Glaciated Regions of the Canadian Cordillera; *Geological Association of Canada - Mineralogical Association of Canada*, Program with Abstracts, Volume 15, page A-76.
- Levson, V.M. (1991a). The Bullion Mine; a Large Buried-valley Gold Placer; *The Cariboo Miner*, Volume 2, Number 5, pages 8-9.
- Levson, V.M. (1991b): Geologic Controls on Alluvial Gold Mining in the Cariboo District, British Columbia, Canada; in *Alluvial Mining, Elsevier Science Publishers for Institute of Mining and Metallurgy*, London, England, pages 245-267.
- Levson, V.M. (1992a). Quaternary Geology of the Atlin Area (104N/11W, 104N/12E); in *Geological Fieldwork 1991*, Grant, B. and Newell, J.M., Editors, *B.C. Ministry of Energy, Mines and Petroleum Resources*, Paper 1992-1, pages 375-390.
- Levson, V.M. (1992b): The Sedimentology of Pleistocene Deposits Associated with Placer Gold Bearing Gravels in the Livingstone Creek Area, Yukon Territory; in *Yukon Geology - Volume 3*, Bremner, T., Editor, *Canada Department of Indian Affairs and Northern Development*, Whitehorse, 28 pages.
- Levson, V.M. and Giles, T.R. (1991): Stratigraphy and Geologic Settings of Gold Placers in the Cariboo Mining District (93A, B, G, H); in *Geological Fieldwork 1990, B.C. Ministry of Energy, Mines and Petroleum Resources*, Paper 1991-1, pages 331-344.
- Levson, V.M. and Giles, T.R. (in preparation): Geology of Cariboo Tertiary and Quaternary Gold-bearing Placers (93A, B, G, H); *B.C. Ministry of Energy, Mines and Petroleum Resources*, Paper.
- Levson, V.M. and Kerr, D.K. (1992): Surficial Geology and Placer Gold Settings of the Atlin - Surprise Lake Area, NTS 104N/11, 12; *B.C. Ministry of Energy, Mines and Petroleum Resources*, Open File 1992-7, 1:50 000.
- Levson, V.M. and S. Morison. (1991). Quaternary Gold Placers in the Canadian Cordillera; *International Union for Quaternary Research, XIII International Congress, Abstracts*, page 191.
- Levson, V.M. and Morison, S.R. (in press): Geology of Placer Deposits in Glaciated Environments; in *Glacial Environments - Processes, Sediments and Landforms*, Menzies, J., Editor, *Pergamon Press*, Oxford, U.K., 44 pages.
- Levson, V.M., Giles, T.R., Bobrowsky, P.T. and Matysck, P.F. (1990): Geology of Placer Deposits in the Cariboo Mining District, British Columbia; Implications for Exploration; in *Geological Fieldwork 1989, B.C. Ministry of Energy, Mines and Petroleum Resources*, Paper 1990-1, pages 519-530.
- Rouse, G.E., Lesack, K.A. and Hughes, B.L. (1990): Palynological Dating of Sediments Associated with Placer Gold Deposits in the Barkerville - Quesnel - Prince George Region, South-central British Columbia; in *Geological Fieldwork 1989, B.C. Ministry of Energy, Mines and Petroleum Resources*, Paper 1990-1, pages 531-532.
- Struik, L.C. (1982): Bedrock Geology of the Cariboo Lake (93A/14), Spectacle Lake (93H/3), Swift River (93A/13) and Wells (93H/4) Map Areas, Central British Columbia; *Geological Survey of Canada*, Open File 858.
- Struik, L.C. (1986): Imbricated Terranes of the Cariboo Gold Belt with Correlations and Implications for Tectonics in Southeastern British Columbia; *Canadian Journal of Earth Sciences*, Volume 23, pages 1047-1061.
- Struik, L.C. (1988): Structural Geology of the Cariboo Gold Mining District, East-central British Columbia; *Geological Survey of Canada*, Memoir 421, 100 pages and four 1:50 000 maps.
- Sutherland Brown, A. (1957): Geology of the Antler Creek Area, Cariboo District, British Columbia; *B.C. Ministry of Energy, Mines and Petroleum Resources*, Bulletin 38, 105 pages.
- Sutherland Brown, A. (1963): Geology of the Cariboo River Area, British Columbia; *B.C. Ministry of Energy, Mines and Petroleum Resources*, Bulletin 47, 60 pages.
- Tipper, H.W. (1959): Geology, Quesnel, Cariboo District, British Columbia; *Geological Survey of Canada*, Map 12-1959, 1:250 000.
- Tipper, H.W. (1961): Geology, Prince George, British Columbia; *Geological Survey of Canada*, Map 49-1960, 1:250 000.
- Tipper, H.W. (1971): Glacial Geomorphology and Pleistocene History of Central British Columbia; *Geological Survey of Canada*, Bulletin 196, 89 pages.
- Tipper, H.W., Campbell, R.B., Taylor, G.C. and Scott, D.F. (1975): Parsnip River, British Columbia; *Geological Survey of Canada*, Map 1424A, 1:1 000 000.

NOTES



**PRELIMINARY REPORT ON LAKE SEDIMENT STUDIES IN THE
NORTHERN INTERIOR PLATEAU, CENTRAL BRITISH COLUMBIA
(93 C, E, F, K, L)**

By Stephen J. Cook

*(Contribution to the Interior Plateau Program
Canada - British Columbia Mineral Development Agreement 1991-1995)*

KEYWORDS: Applied geochemistry, lake sediments, Nechako Plateau, mineral deposits, limnology.

INTRODUCTION

Stream sediments are the preferred sampling medium for reconnaissance-scale Regional Geochemical Surveys (RGS) over most of British Columbia, but the subdued topography, abundance of lakes and relatively poor drainage of the Nechako Plateau in the northern Interior suggest that lake sediments may be a more appropriate medium in this area. Mineral exploration in the region has been limited by extensive drift cover and poor exposure, and lake sediment geochemistry may provide an effective tool to delineate both regional geochemical patterns as well as anomalous metal concentrations related to potentially economic deposits.

Lake sediment orientation studies are an important prelude to successful application of the technique to exploration in the Cordillera. Most Canadian studies of lake sediment geochemistry have focused on Shield and Appalachian environments where there are considerable differences in climate, physiography and surficial geology relative to British Columbia. Publicly funded regional lake sediment surveys, covering an area of 1.2 million square kilometres (Friske, 1991), have been conducted primarily in central and Atlantic Canada. These, run to the standards of the Geological Survey of Canada's National Geochemical Reconnaissance (NGR) program, have provided a wealth of high-quality geochemical data for mineral exploration and contributed to the discovery of deposits such as the Strange Lake yttrium-zirconium-beryllium deposit in Labrador. Regional lake sediment surveys in British Columbia, jointly undertaken by the Geological Survey Branch and the Geological Survey of Canada have, in contrast, been restricted to relatively small areas of NTS map sheets 93E (Whitesail Lake) and 93L (Smithers) in the west-central Interior (Johnson *et al.*, 1987a, b), and 104N (Atlin) in the Teslin Plateau. There is consequently tremendous potential for the effective use of lake sediment geochemistry in central British Columbia, both for reconnaissance and detailed mineral exploration. Several regional surveys have been carried out in the northern Interior, including those of mineral exploration companies, Spilsbury and Fletcher (1974), Hoffman (1976) and Gintautas (1984). The scope and results of the latter three have been summarized by Earle (1992) in a study of the applicability of regional lake sediment surveys in the area. Prospects such as the Wolf gold-silver occurrence have been discovered through the use of lake sediment geochemistry. Nevertheless there is a paucity

of detailed orientation studies and case histories on which to formulate exploration models.

The purpose of the Interior Plateau lake sediment studies program, part of the federal-provincial mineral development agreement (MDA), is to evaluate the effectiveness of lake sediment geochemistry as a sample medium for a proposed reconnaissance survey (Figure 4-9-1) of 1:250 000 NTS map sheets 93C (Anahim Lake), 93F (Nechako River) and 93K (Fort Fraser). Results of the study will increase our understanding of controls on Cordilleran trace element geochemistry and optimize sampling and interpretive techniques for the proposed RGS survey, thus increasing the possibility of new mineral deposit discoveries in the northern Interior. It fulfills an important part of the Interior Plateau project objective of upgrading the existing geological database to assess the mineral potential of the region. This paper outlines the objectives of the study, describes fieldwork performed in 1992, and outlines the scope of planned work.

LAKE SEDIMENTS AND THEIR USE IN MINERAL EXPLORATION

Lake sediments consist of organic gels, organic sediments and inorganic sediments (Jonasson, 1976). Organic gels, or gyttja, are mixtures of particulate organic matter, inorganic precipitates and mineral matter (Wetzel, 1983). They are mature green-grey to black homogenous sediments charac-

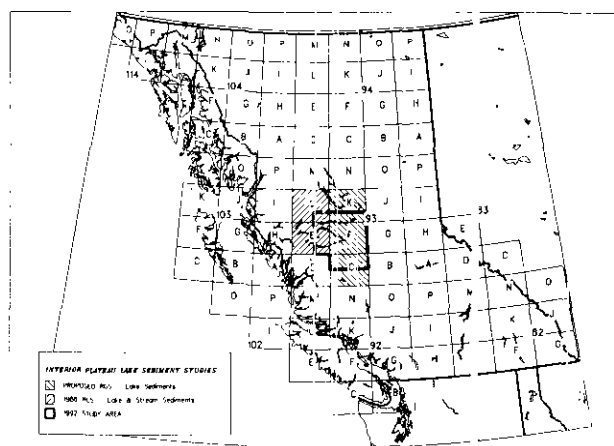


Figure 4-9-1. Location of proposed Regional Geochemical Survey, utilizing lake sediments, of NTS map sheets 93C, F and K, and of the 1986 lake and stream sediment RGS survey of NTS map sheets 93E and L. Outlined area indicates the extent of the current lake sediment study shown in Figure 4-9-2.

teristic of deep-water basins. Organic sediments are immature mixtures of organic gels, organic debris and mineral matter occurring in shallow water and near drainage inflows (Jonasson, 1976). Inorganic sediments, by contrast, are mixtures of mineral particles with little organic matter. Of the three, organic gels have been found the most suitable as a geochemical exploration medium; deep-water basins where they accumulate have been favoured as ideal sites for regional geochemical sampling (Friske, 1991).

Lake sediment composition is influenced by bedrock geology, surficial geology, climate, soils, vegetation, mineral occurrences and limnological factors. Sediment geochemistry in the Nechako Plateau, as in other areas of Canada, generally reflects bedrock variations (Hoffman, 1976; Gintautas, 1984). Sediment geochemistry also reflects the presence of weathering sulphide minerals from prospects near Capoose (Hoffman, 1976; Hoffman and Fletcher, 1981) and Chutanli (Mehrtens, 1975; Mehrrens *et al.*, 1972) lakes, and has been successful in locating potentially economic gold-silver mineralization at the Wolf occurrence (Andrew, 1988). The effect of limnological variations on trace element abundance and mineral exploration has, however, received relatively little attention in the Cordillera. The temperature and oxygen content of lake waters in northern temperate regions may stratify during the warm summer months, overturning with seasonal changes in the spring and fall. Of such thermally stratified, or dimictic, lakes, eutrophic lakes are those small nutrient-rich lakes with high organic production and almost complete oxygen depletion with increasing depth. Conversely, oligotrophic lakes are deep, large, nutrient-poor lakes with low organic production and a much more constant oxygen content with depth. Polymictic or unstratified lakes are relatively shallow and are not thermally stratified. Earle (1992) and Hoffman and Fletcher (1981) have shown that there are distinct geochemical differences between the sediments of eutrophic and oligotrophic lakes, particularly with respect to the abundance of organic matter and of iron and manganese oxides. Both may scavenge trace elements, and their abundance in lake sediments is largely influenced by water productivity, oxygen stratification in the water column and the rate of clastic sedimentation (Gintautas, 1984). High organic matter content is characteristic of eutrophic lakes, while manganese and iron oxide precipitates are products of the oxygen-rich conditions of oligotrophic lakes. The effect of within-lake limnological variations on these constituents, and on the transport and accumulation of trace elements, studied in southern Shield regions, has been summarized by Timperley and Allan (1974).

Limnological classification, or trophic status, may consequently have a major influence on interpretation of lake sediment geochemistry. Earle (1992) has recognized nine such classes in the Nechako Plateau. In the present study, trophic status was found to vary considerably even within separate sub-basins and channels of the same lake. As lakes in NTS map areas 93C, F and K for which limnological data are available are almost equally divided among the four most common classifications (oligotrophic, mesotrophic, eutrophic and polymictic types; Earle, 1992), the geochemical responses of each must be evaluated prior to carrying out a regional survey.

OBJECTIVES OF THE INTERIOR PLATEAU LAKE SEDIMENT STUDY

The main objective of this study is to assess the effect of limnological variations on sediment geochemistry in the Nechako Plateau region in order to optimize sampling and interpretive techniques for regional geochemical surveys:

Problems to be addressed include:

- The effect of limnological variations on sediment geochemistry of lakes within and between different geological units.
- The extent to which sediment geochemistry reflects the presence of nearby mineral occurrences.
- Operational problems concerning sample media and sampling strategies for a proposed RGS survey of the Nechako Plateau.

The first two problems are being addressed by evaluation of a systematic collection of case studies which, together with interpretation of regional lake sediment data from adjoining NTS map sheets 93E and L, will facilitate the development of interpretive models for lakes of varying trophic status in each geological unit. Operational problems to be resolved for future RGS surveys of the Nechako area include choice of the most suitable sample media, determination of minimum and maximum lake size, optimum sampling location, optimum number of samples per lake, and optimum size of field samples and analytical subsamples necessary to detect and reproduce anomalies related to potentially economic mineral deposits. Whereas a standard sampling methodology has been used to evaluate geochemical responses and limnological variations at each lake, some of the operational problems are the subject of specific substudies.

SCOPE OF 1992 FIELD STUDIES

Orientation studies of 16 lakes at 11 localities (Figure 4-9-2) were carried out in the period late July to mid-September, 1992. The program design was based partly on recommendations of Earle (1992). A total of 625 sediment samples were collected at 437 sites (Table 4-9-1). The lakes are characteristic of eutrophic, mesotrophic, oligotrophic and unstratified limnological environments above two different geological rock types. These units, areally extensive within the proposed survey area and of considerable economic interest, are:

- Jurassic, Cretaceous and Eocene plutonic rocks of the Francois Lake, Bulkley and Nanika plutonic suites, respectively, hosting porphyry copper-molybdenum deposits and occurrences.
- Eocene Ootsa Lake Group volcanic rocks, hosting epithermal gold-silver occurrences.

The lakes are adjacent to the Hanson Lake, Ken, Nithi Mountain and Dual copper-molybdenum and molybdenum occurrences, and to the Clisbako, Wolf and Holy Cross gold-silver prospects (Table 4-9-1). Lakes within each geological grouping were chosen on the basis of documented trophic status (Balkwill, 1991), proximity to known

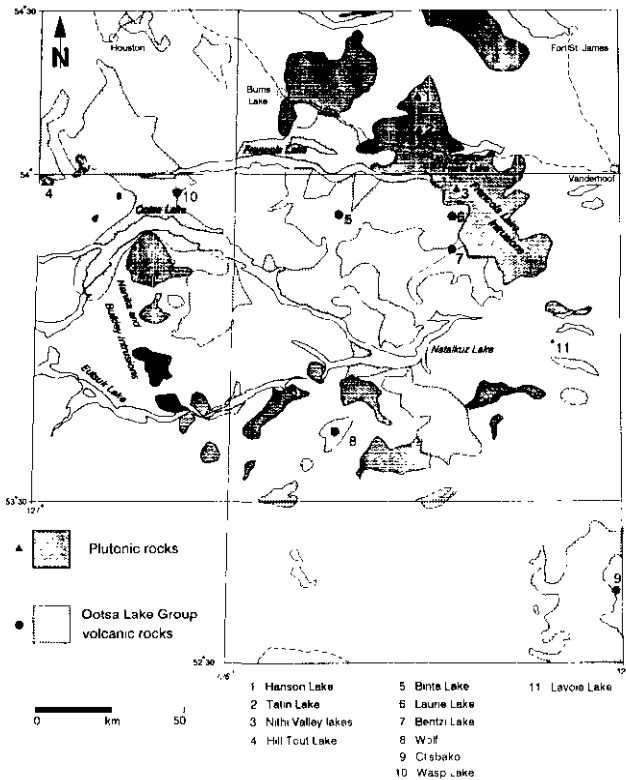


Figure 4-9-2. Locations of lake sediment survey areas in the Nechako Plateau, showing their relation to Eocene-Jurassic plutonic rocks and Eocene Ootsa Lake Group volcanic rocks (geology modified from Tipper *et al.*, 1979).

mineral occurrences, exploration industry lake sediment data and road access. Most were chosen from NTS map sheets 93C, F and K, but two lakes from map sheets 93E (Johnson *et al.*, 1987a) were also included on the basis of available RGS sediment geochemistry. These, Hill-Tout Lake and Wasp Lake, contain anomalous concentrations of copper and gold, respectively. One lake underlain by Miocene-Pliocene basalts was also surveyed as being representative of lakes above a widely occurring rock unit generally devoid of known mineral occurrences.

DESCRIPTION OF THE STUDY AREA

LOCATION, PHYSIOGRAPHY AND SURFICIAL GEOLOGY

The study area (Figures 4-9-1 and 4-9-2) is bounded east and west by Vanderhoof and Houston, respectively, and extends northward from the Clisbako River to the Babine and Stuart lakes area. Most of the area lies on the Nechako Plateau, the northernmost subdivision of the Interior Plateau (Holland, 1976), although its southern limit extends onto the Fraser Plateau. The low and rolling terrain generally lies between 1000 to 1500 metres elevation. The area is thickly forested and bedrock is obscured by extensive drift cover. Tipper (1963) noted that over 90 per cent of the Nechako River map area is drift covered. Till and glaciofluvial outwash are the predominant materials. Giles and Kerr (1993) and Proudfoot (1993) provide more detailed information on the surficial geology of the southernmost part of the proposed survey area.

TABLE 4-9-1
SUMMARY LISTING OF LAKES SURVEYED OVER CONTRASTING ROCK UNITS

Bedrock Lithology	Lake Name	NTS	Trophic Status	Lake Size (km ²)	Maximum Depth (m)	Sediment Sites	Sediment Samples	Temperature and Oxygen Profiles	Adjacent Mineral Occurrences
Eocene - Jurassic									
Plutonic Rocks (Cu, Mo)									
	Hanson	93K03	Unstratified	1 to 5	7	44	62	5	Hanson Lake (Mo, Cu)
	Tatin	93K03	Oligotrophic	1 to 5	22	38	52	6	Kerr (Mo, Cu)
	Hill-Tout	93E14, 15	Mesotrophic	1/4 to 1	14	52	74	5	Dal (Cu, Mo)
	Nithi Lakes (4)	93F15	Eutrophic	1/4 to 1	12	63	99	9	Nithi (Mo)
Eocene									
Ootsa Lake Group									
Volcanic Rocks (Au, Ag)									
	Binta	93F13, 14	Oligotrophic	> 5	> 40	37	50	3	None
	Bentzi (2)	93F15	Mesotrophic	1 to 5	35	66	92	7	Holy Cross (Au, Ag, Cu, Zn)
	Laurie	93F15	Eutrophic	1 to 5	22	25	35	5	None
	Wolf	93F03	Eutrophic	Pond	8	7	12	1	Wolf (Au, Ag)
	Clisbako	93C09		1/4 to 1	10.5	40	57	3	Clisbako (Au, Ag)
	Wasp (2)	93E 16		1/4 to 1	6	13	19	1	None
Miocene-Pliocene									
Volcanic Rocks									
	Lavoie	93F08	Unstratified	1 to 5	9	52	73	4	None
Total:						437	625	49	

REGIONAL GEOLOGY

The area covered by NTS map sheets 93C, F and K is almost entirely within the Intermontane Belt with the exception of the southwest corner which is in the Coast Belt. The area includes parts of the Stikinia, Cache Creek and Quesnellia terranes. Within the study area (Figure 4-9-2), volcanic and sedimentary rocks of the Lower to Middle Jurassic Hazelton Group are intruded by Late Jurassic, Late Cretaceous and Tertiary felsic plutonic rocks. These are overlain by Eocene volcanics of the Ootsa Lake Group, Oligocene and Miocene volcanics of the Endako Group, and Miocene-Pliocene basalt flows. The Anahim volcanic belt, a 600-kilometre belt of Miocene-Quaternary continental volcanic rocks (Souther, 1977), runs east-west through the southern part of the area.

GEOLOGY AND METALLOGENY

FRANCOIS LAKE, BULKLEY AND NANIKA PLUTONIC SUITES

Three of the lakes associated with plutonic rocks were sampled above Late Jurassic Francois Lake intrusions (133-155 Ma), the fourth is adjacent to quartz monzonite of either the Late Cretaceous Bulkley intrusions (70-84 Ma) or the Eocene Nanika intrusions (47-54 Ma). The Francois Lake Plutonic Suite, predominantly of quartz monzonite composition, hosts many porphyry molybdenum deposits and occurrences. The most significant is the Endako orebody west of Fraser Lake, where molybdenite is hosted by east-trending subparallel quartz veins (Kimura *et al.*, 1976). The Bulkley and Nanika intrusions comprise north-westerly belts of granodiorite, quartz monzonite and granite stocks in the western part of the study area (Figure 4-9-2). They are two of the four subparallel belts of plutonic rocks known to host porphyry copper-molybdenum deposits in west-central British Columbia (Carter, 1981).

OOTSA LAKE GROUP

Eocene continental volcanic rocks of the Ootsa Lake Group are exposed in two general regions of the study area. The first extends from the Nechako River to the west side of Francois Lake (Figure 4-9-2); the second, smaller area is west of Quesnel between the Chilcotin and West Road rivers (Duffell, 1959; Tipper, 1963). Diakow and Mihalynuk (1987) recognized six lithologic divisions in the Ootsa Lake Group, which comprises a differentiated succession of andesitic to rhyolitic flows and pyroclastic rocks. Sedimentary rocks, although not common, are interspersed throughout the sequence. Potassium-argon ages of approximately 50 Ma have been obtained from Ootsa Lake rocks (Diakow and Koyanagi, 1988).

Interest in the precious metal potential of the Ootsa Lake Group has increased in recent years. The Wolf and Clisbako prospects are epithermal gold-silver occurrences currently under exploration. The Wolf prospect is hosted by felsic flows, tuffs and subvolcanic porphyries, and is a low-sulphur silicified stockwork deposit (Andrew, 1988). The Clisbako prospect is hosted by Eocene basaltic to rhyolitic tuffs, flows and volcanic breccias exhibiting intense sil-

icification and argillic alteration. Gold mineralization in both areas is associated with low-sulphide quartz stockwork zones. The Clisbako prospect has been interpreted to be a high-level volcanic-hosted epithermal system similar to those in the western United States (Dawson, 1991; Schroeter and Lane, 1992).

FIELD AND LABORATORY METHODOLOGY

SAMPLE COLLECTION

Systematic collection of lake sediments and waters, and measurement of temperature and dissolved oxygen content of the water column was performed at each lake (Table 4-9-1). Sediment sampling was the main focus of activity; waters were collected primarily as a reconnaissance for possible future study of metal distribution in lake waters. Oxygen and temperature measurements were made to verify pre-existing Fisheries Branch (Ministry of Environment, Lands and Parks) data, to determine the trophic status of smaller lakes for which no data are otherwise available, and to investigate the variability of these measurements within separate sub-basins of individual lakes.

SEDIMENTS

Lake sediments were sampled from a zodiac or canoe with a Hornbrook-type torpedo sampler. Standard sampling procedures, as discussed by Friske (1991), were used. Samples were collected in kraft paper bags and sample depth, colour, composition and odour recorded at each site. Sites were located along profiles traversing deep and shallow-water parts of main basins and sub-basins, and at all stream inflows. The number of sites on each lake (Table 4-9-1) ranged from a minimum of seven in small ponds to a maximum of fifty-eight in larger lakes in order to evaluate the relationship between trace element patterns and mineral occurrence location, bathymetry, organic matter content, drainage inflow and outflow, and sediment texture.

Two substudies were incorporated into the sampling design to address specific sampling problems. First, an unbalanced nested sampling design similar to that described by Garrett (1979) was used to assess sampling and analytical variation. A modified version of the Regional Geochemical Survey sampling scheme was used for this. Each block of twenty samples (Figure 4-9-3) comprises twelve routine samples and:

- Five field duplicate samples, to assess sampling variability;
- Two analytical duplicate samples, inserted after sample preparation to determine analytical precision;
- One control reference standard, to monitor analytical accuracy.

Two of the five field duplicate samples in each block were randomly selected for further use as analytical duplicate splits.

Secondly, one lake was chosen for a comparative study of field sample size. At this locality, adjacent to the Clisbako gold-silver prospect (Figure 4-9-2), two samples were taken at each of 36 sites: one standard sample obtained from one

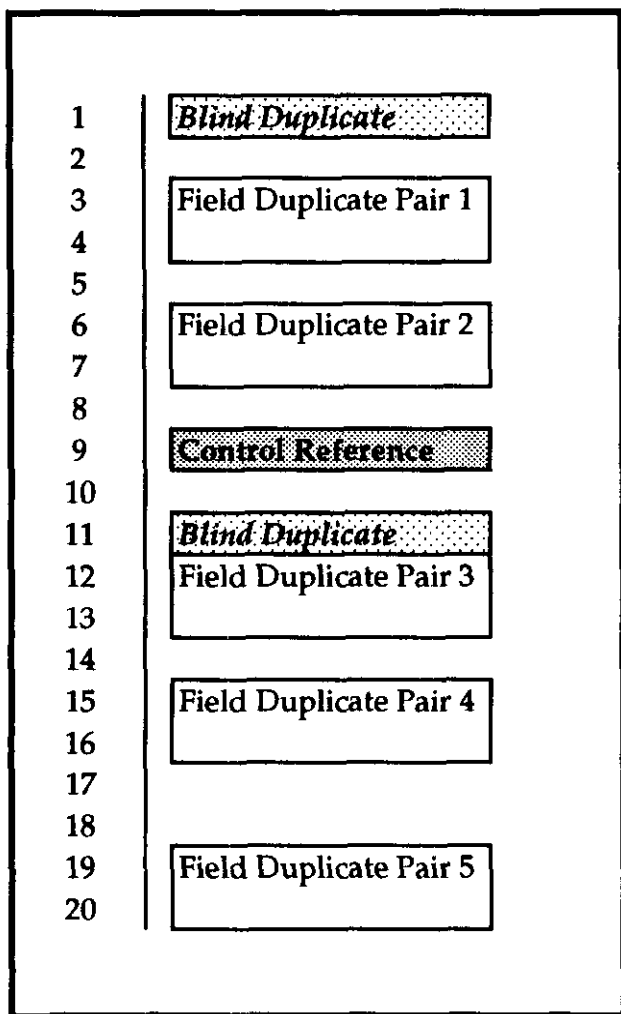


Figure 4-9-3. Typical sample collection scheme. The modified 20-sample collection block incorporates twelve routine samples and five field duplicates. Two blind duplicates and a control reference standard are inserted in the laboratory prior to analysis.

drop of the sampler, and a larger sample obtained from two drops. Standard lake sediment samples typically weigh 50 to 100 grams when dry (Friske, 1991). Due to the particle sparsity effect, larger field samples might be more representative of gold concentrations in sediments above auriferous Ootsa Lake Group rocks. The objective is to ascertain whether or not there are significant differences in gold concentrations with increasing sample size.

WATERS

Two water samples were collected in 250-millilitre polyethylene bottles from the centre of each lake: a surface sample and a deep sample. The first was taken approximately 15 centimetres beneath the surface, to minimize collection of surface scum, whereas the second was collected with a Van Dorn sampler 1 to 2 metres above the lake bottom. Bottles were rinsed in the water to be sampled prior

to collection, and observations of water colour and suspended matter recorded. The boat was anchored in place during both water sampling and temperature/oxygen profiling to prevent movement. Waters were stored in a cooler and refrigerator prior to analysis.

DISSOLVED OXYGEN AND TEMPERATURE MEASUREMENTS

Water column profiles of dissolved oxygen content and temperature were measured at one to five sites on each lake, using a YSI Model 57 oxygen meter with cable probe. Measurements were generally made, at 1-metre intervals, in the centre of all major sub-basins and at two near-shore sites to a maximum depth of 29 metres. A total of 49 profiles were surveyed (Table 4-9-1), comprising 619 sets of measurements. The instrument was calibrated for lake elevation and air temperature prior to measurement at each lake, and data collected only during the afternoon period so as to standardize measurement conditions. Prevailing weather conditions were also recorded at the beginning of each profile. Measurements generally corroborated earlier Fisheries Branch data at most lakes, although considerable within-lake variations were encountered. Measurements at the last two lakes surveyed (Clisbako and Wasp) were inconclusive due to the onset of cold weather in mid-September.

SAMPLE PREPARATION AND ANALYSIS

SEDIMENTS

Lake sediment samples were initially field dried and, when sufficiently dry to transport, shipped to Rossbacher Laboratory, Burnaby, for final drying at 60°C. Sample preparation was done at Bondar-Clegg and Company, North Vancouver. Dry sediment samples were disaggregated inside a plastic bag with a rubber mallet. The entire sample, to a maximum of 250 grams, was pulverized to approximately -150 mesh in a ceramic ring mill, and two analytical splits taken from the pulverized material. The first was submitted to Activation Laboratories, Mississauga, for determination of gold and 34 additional elements by instrumental neutron activation analysis (INAA) on a 30-gram subsample. The second was analyzed for 30 trace elements (including Zn, Cu, Pb, Co, Ag, Mn, Mo, Fe and Cd) by inductively coupled plasma - atomic emission spectrometry (ICP - AES) and for loss on ignition. Blind duplicates and appropriate ranges of copper and gold-bearing standards were inserted into each of the two analytical suites as part of a rigorous quality control program (Figure 4-9-3) to monitor analytical precision and accuracy.

WATERS

Water samples were filtered with 0.45 micron filters and submitted to Eco-Tech Laboratories, Kamloops. They were acidified and analyzed for 30 elements by inductively coupled plasma - atomic emission spectrometry (ICP-AES). Sulphate and pH were also determined. Standards and distilled water blanks were inserted into the sample suite to monitor analytical accuracy.

FUTURE WORK

No analytical results for lake sediments and waters from the 1992 field season are available at the time of writing. Analysis of regional lake and stream sediment data (Johnson *et al.*, 1987a, b) from adjoining NTS map sheets 93E and 93L comprises the second component of the study and is currently in progress. It will show the extent to which sediment geochemistry reflects bedrock geology, whereas the individual orientation studies have been designed to show how mineralization is reflected by trace element patterns in sediments, and how these patterns are modified by limnological factors. Recommendations regarding the suitability of the Nechako Plateau for lake sediment geochemistry, and the area, size and density of the proposed 1993 RGS survey, will be an important product of the study.

ACKNOWLEDGMENTS

The author wishes to acknowledge G. Mowatt, W. Jackman and T. Giles for assistance in the field, and S.J. Sibbick and P.F. Matysek for their perceptive comments and suggestions during development of the project. Staff of the Fisheries Branch, Ministry of Environment, Lands and Parks, especially J. Balkwill, R. Dabrowski and D. Coombes, are thanked for providing equipment, bathymetric maps and useful advice. P.W.B. Friske of the Geological Survey of Canada, Ottawa, loaned sediment sampling apparatus. Rio Algom Exploration Inc. and Minnova Inc. are thanked for providing access to information and properties, respectively.

REFERENCES

- Andrew, K.P.E. (1988): Geology and Genesis of the Wolf Precious Metal Epithermal Prospect and the Capoose Base and Precious Metal Porphyry-style Prospect, Capoose Lake Area, Central British Columbia; unpublished M.Sc. thesis, *The University of British Columbia*, 334 pages.
- Balkwill, J.A. (1991): Limnological and Fisheries Surveys of Lakes and Ponds in British Columbia: 1915-1990; *B.C. Ministry of Environment, Lands and Parks*, Fisheries Technical Circular No. 90, 157 pages.
- Carter, N.C. (1981): Porphyry Copper and Molybdenum Deposits – West-central British Columbia; *B.C. Ministry of Energy, Mines and Petroleum Resources*, Bulletin 64, 150 pages.
- Dawson, J.M. (1991): Geological and Geochemical Report on the Clisbako Property, Cariboo Mining Division, British Columbia; *B.C. Ministry of Energy, Mines and Petroleum Resources*, Assessment Report 20864.
- Diakow, L. and Koyanagi, V. (1988): Stratigraphy and Mineral Occurrences of Chikamin Mountain and Whitesail Reach Map Areas (93E/06, 10); in *Geological Fieldwork 1987*, *B.C. Ministry of Energy, Mines and Petroleum Resources*, Paper 1988-1, pages 155-168.
- Diakow, L. and Mihalynuk, M. (1987): Geology of Whitesail Reach and Troitsa Lake Map Areas (93E/10W, 11E); in *Geological Fieldwork 1986*, *B.C. Ministry of Energy, Mines and Petroleum Resources*, Paper 1987-1, pages 171-179.
- Duffell, S. (1959): Whitesail Lake Map-area, British Columbia; *Geological Survey of Canada*, Memoir 299, 119 pages.
- Earle, S. (1992): Assessment of the Applicability of Lake Sediment Geochemical Surveys for Mineral Exploration in the Nechako Plateau Area of British Columbia; *B.C. Ministry of Energy, Mines and Petroleum Resources*, unpublished internal report.
- Frisk, P.W.B. (1991): The Application of Lake Sediment Geochemistry in Mineral Exploration; in *Exploration Geochemistry Workshop*, *Geological Survey of Canada*, Open File 2390, pages 4.1-4.20.
- Garrett, R.G. (1979): Sampling Considerations For Regional Geochemical Surveys; in *Current Research, Part A*, *Geological Survey of Canada*, Paper 79-1A, pages 197-205.
- Giles, T.R. and Kerr, D.E. (1993): Surficial Geology in the Chilanko Forks (93C/1) and Chezacut (93C/8) Areas; in *Geological Fieldwork 1992*, Grant, B. and Newell, J.M., Editors, *B.C. Ministry of Energy, Mines and Petroleum Resources*, Paper 1993-1, this volume.
- Gintautas, P.A. (1984): Lake Sediment Geochemistry, Northern Interior Plateau, British Columbia; unpublished M.Sc. thesis, *University of Calgary*.
- Hoffman, S.J. (1976): Mineral Exploration of the Nechako Plateau, Central British Columbia, Using Lake Sediment Geochemistry; unpublished Ph.D. thesis, *The University of British Columbia*, 346 pages.
- Hoffman, S.J. and Fletcher, W.K. (1981): Detailed Lake Sediment Geochemistry of Anomalous Lakes on the Nechako Plateau, Central British Columbia – Comparison of Trace Metal Distributions in Capoose and Fish Lakes; *Journal of Geochemical Exploration*, Volume 14, pages 221-244.
- Holland, S.S. (1976): Landforms of British Columbia – A Physiographic Outline; *B.C. Ministry of Energy, Mines and Petroleum Resources*, Bulletin 48, 138 pages.
- Johnson, W.M., Hornbrook, E.H.W. and Friske, P.W.B. (1987a): National Geochemical Reconnaissance 1:250 000 Map Series – Whitesail Lake, British Columbia (NTS 93E); *Geological Survey of Canada*, Open File 1360.
- Johnson, W.M., Hornbrook, E.H.W. and Friske, P.W.B. (1987b): National Geochemical Reconnaissance 1:250 000 Map Series – Smithers, British Columbia (NTS 93L); *Geological Survey of Canada*, Open File 1361.
- Jonasson, I.R. (1976): Detailed Hydrogeochemistry of Two Small Lakes in the Grenville Geological Province; *Geological Survey of Canada*, Paper 76-13, 37 pages.
- Kimura, E.T., Bysouth, G.D. and Drummond, A.D. (1976): Endako; in *Porphyry Deposits of the Canadian Cordillera*, Sutherland Brown, A., Editor, *Canadian Institute of Mining and Metallurgy*, Special Volume 15, pages 444-454.
- Mehrtens, M.B. (1975): Chutanli Mo Prospect, British Columbia; in *Conceptual Models in Exploration Geochemistry*, Bradshaw, P.M.D., Editor, *Association of Exploration Geochemists*, Special Publication No. 3, pages 63-65.
- Mehrtens, M.B., Tooms, J.S. and Troup, A.G. (1972): Some Aspects of Geochemical Dispersion from Base-Metal Mineralization within Glaciated Terrain in Norway, North Wales and British Columbia, Canada; in *Geochemical Exploration 1972*, Jones, M.J., Editor, *The Institution of Mining and Metallurgy*, pages 105-115.
- Proudfoot, D.N. (1993): Drift Exploration and Surficial Geology of the Clusko River (93C/9) and Toil Mountain (93C/16) Map Sheets; in *Geological Fieldwork 1992*, Grant, B. and Newell, J.M., Editors, *B.C. Ministry of Energy, Mines and Petroleum Resources*, Paper 1993-1, this volume.
- Schroeter, T. and Lane, B. (1992): Clisbako; in *Exploration in British Columbia 1991*, *B.C. Ministry of Energy, Mines and Petroleum Resources*, pages 103-111.
- Souther, J.G. (1977): Volcanism and Tectonic Environments in the Canadian Cordillera – A Second Look; in *Volcanic Regimes*

- in Canada, Baragar, W.R.A., Coleman, L.C. and Hall, J.M., Editors, *Geological Association of Canada*, Special Paper 16, pages 3-24.
- Spilsbury, W. and Fletcher, W.K. (1974): Application of Regression Analysis to Interpretation of Geochemical Data from Lake Sediments in Central British Columbia; *Canadian Journal of Earth Sciences*, Volume 11, pages 345-348.
- Timperley, M.H. and Allan, R.J. (1974): The Formation and Detection of Metal Dispersion Halos in Organic Lake Sediments; *Journal of Geochemical Exploration*, Volume 3, pages 167-190.
- Tipper, H.W. (1963): Nechako River Map-area, British Columbia; *Geological Survey of Canada*, Memoir 324, 59 pages.
- Tipper, H.W., Campbell, R.B., Taylor, G.C. and Stott, D.F. (1979): Parsnip River, British Columbia (Sheet 93); *Geological Survey of Canada*, Map 1424A.
- Wetzel, R.G. (1983): *Limnology*. Second Edition; *Saunders College Publishing*, Philadelphia. 767 pages.

NOTES

SURFICIAL GEOLOGY IN THE CHILANKO FORKS AND CHEZACUT AREAS (93C/1, 8)

By T.R. Giles and D.E. Kerr

(Contribution to the Interior Plateau Program, Canada - British Columbia Mineral Development Agreement
1991-1995)

KEYWORDS: Surficial geology, drift exploration, till, glaciofluvial outwash, glaciolacustrine, applied geochemistry, mineral dispersion.

INTRODUCTION

This report describes the preliminary results of surficial geological mapping during the 1992 field season in the Chilanko Forks (93C/1) and Chezacut (93C/8) map areas (Figure 4-10-1). As part of the Canada - British Columbia Mineral Development Agreement, the British Columbia Geological Survey Branch proposed to map the surficial geology of these areas to derive drift exploration potential maps. The two map sheets to the north, Clusko River (93C/9) and Toil Mountain (93C/16) were also mapped as part of this program (Proudfoot, 1993, this volume). The project's main goals are:

- To produce 1:50 000 surficial geology maps of NTS sheets 93C/1 and 93C/8.
- To define the regional Quaternary stratigraphy and glacial history.
- To derive surficial drift exploration potential maps.

This project illustrates the use of baseline surficial geology data, combined with a drift sampling program, for mineral exploration on a low-relief plateau with thick till cover. The Chilanko Forks and Chezacut map areas were selected because mineral exploration in the region is hampered by the thick and variable cover of surficial sediment,

which masks the geological, geochemical and geophysical signatures of mineral occurrences. Furthermore, the surficial geology has not yet been mapped and little is known of the Quaternary geological history. Derivative drift exploration potential maps, which will aid in detailed planning of regional geochemical and drift exploration surveys, will be one of the products resulting from this investigation. A lack of mineral exploration has led to a low demand for geological data in the region and few mapping projects have been completed. Now, with increasing pressure on the mining and exploration industry in British Columbia as the inventory of easily explorable lands decreases, new methods are being tested in areas previously avoided.

The study region lies within the Fraser Plateau, in the west-central part of the Interior Plateau (Hollard, 1976). In the study area, the plateau is approximately 1 000 to 1 400 metres above sea level and is deeply dissected by the Talla Lake, Chilanko River and Chilcotin River valleys. The plateau has flat to gently rolling topography broken by occasional mountains or ridges (Plate 4-10-1). Elevations range from a high of 1 615 metres on Arc Mountain in the northwest of the Chezacut map sheet to a low of 900 metres in the Chilanko River valley in the southeast of the Chilanko Forks sheet. The topography becomes generally more diverse towards the north of the study area.

METHODS

Preliminary interpretation of the surficial geology of the study area was completed prior to fieldwork using 1:60 000-scale air photographs. Access in the region was by public and logging roads. All-terrain vehicles were used for traverses along logging roads and trails. A helicopter was used to reach isolated areas and complete sample coverage. Sample and map-unit verification sites consisted of borrow pits, roadcuts, streamcuts, uprooted trees, hand-dug pits and bed-rock exposures. Site locations were plotted on 1:50 000 base maps with the aid of air photographs. Ice-flow directions were obtained from striation measurements on exposed bed-rock and fluting or drumlin orientations on air photographs. At each exposure the nature of the deposit was determined and a brief description of the sediment was made. Descriptions include primary and secondary structures, matrix texture, pebble content, size and shape, and exposure of the site. Detailed stratigraphic and sedimentological information was collected at a few larger, well exposed sections.

Samples of till were collected for geochemical and grain-size analysis where a good exposure was available, and as needed to verify airphoto mapping. Till samples were

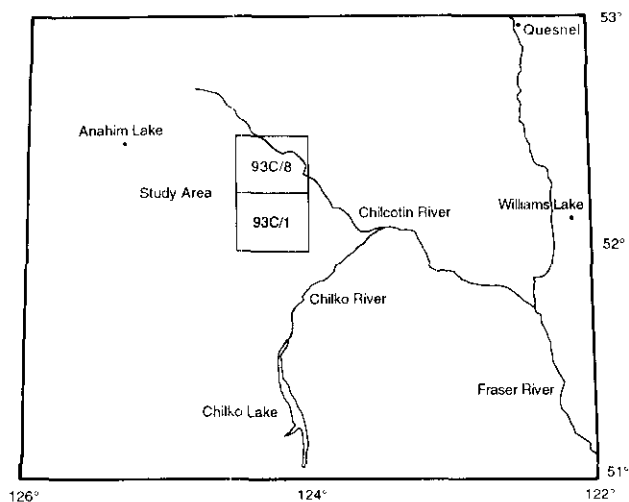


Figure 4-10-1. Location map of the Chilanko Forks (93C/1) and Chezacut (93C/8) map sheets.



Plate 4-10-1. Aerial view of topography in the northwest of 93C/8, looking northeast. In the foreground is Palmer Creek and the highest feature in the background is Arc Mountain.

recovered from sufficient depths to avoid subaerial or root contamination. Till samples will be analyzed by instrumental neutron activation analysis (INAA) and inductively coupled plasma analysis (ICP) for 32 elements. A total of 151 till or colluviated till samples were collected in the study area at a density of one sample per 12.6 square kilometres. Approximately 100 pebbles were collected for lithologic analysis and provenance studies from most till sample sites as well as from a number of glaciofluvial outwash exposures. Bedrock samples were taken to document exposures for future bedrock geology mapping surveys and to help establish a representative lithologic reference collection. In total, 146 pebble and 26 bedrock and exotic boulder samples were obtained. Sample and map-unit verification sites are shown in Figure 4-10-2. Table 4-10-1 shows information pertaining to each terrain unit: sites, samples, verifications, minimum and maximum thicknesses, and typical stratigraphic setting.

TABLE 4-10-1
SUMMARY OF SELECTED SURFICIAL GEOLOGY
DATA PERTAINING TO MAJOR TERRAIN UNITS

Terrain Units	Total Slope	Sampled	Verified	Thickness		Stratigraphic Position
				Minimum	Maximum	
Moraine blanket or veneer Mbv	188	126	62	50 cm	15 m	Surface, over R Basal, under FG and C
Hummocky moraine Mh	37	20	17	50 cm	5 m	Surface, over R Basal, under FG and C
Glaciofluvial outwash FG	91	11	80	50 cm	30 m	Surface, over Mbv and Mh Basal, under Mbv, Mh and C
Esker FG (ridge)	7	1	6	2 m	25 m	Surface, over Mbv, Mh and FG
Eolian E	4	0	4	1 m	5 m	Surface, over FG and LG
Glaciolacustrine LG	26	0	26	20 cm	5 m	Surface, over Mbv and FG
Colluvium C	35	5	30	20 cm	3 m	Surface, over R, Mbv, Mh and FG
Bedrock R	33	21	12	n/a	n/a	Basal, under Mbv, Mh and C
Ectites / exotics	14	6	8	n/a	n/a	Surface, in Mbv, Mh, FG and C

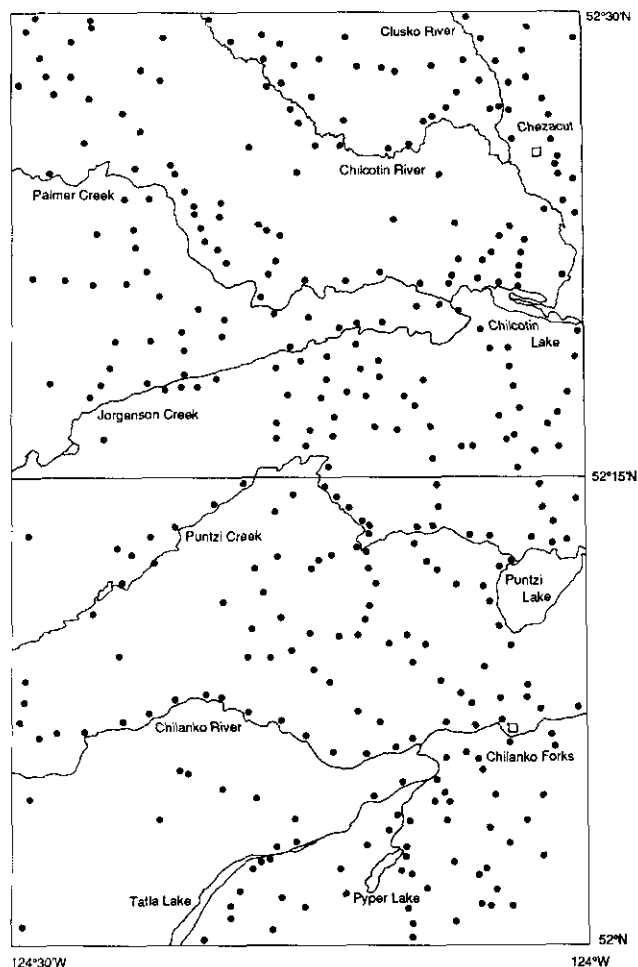


Figure 4-10-2. Location map of sample and verification sites in the study area.

BEDROCK GEOLOGY

A series of bedrock geology maps of the Interior Plateau, including the Anahim Lake sheet, have been published by the Geological Survey of Canada. Extrusive igneous rocks, rhyolitic to basaltic in composition, dominate the Fraser Plateau and are exposed as knobs and ridges throughout the study area (Tipper, 1969). The oldest rocks in the area are part of the mid-Jurassic Hazelton Group: exposed mostly in the south and central parts of the Chilanko Forks sheet, they consist of andesitic to basaltic tuffs or breccias and derived metamorphic and sedimentary rocks. These have been intruded by Jurassic or younger granodiorites and granites of the Coast Plutonic Suite and their metamorphic equivalents (quartz biotite and granite gneisses). Cretaceous to Tertiary Ootsa Lake Group extrusives are found in the west-central parts of the Chilanko Forks sheet and in the eastern half of the Chezacut map sheet. These are dominantly feldspar-porphyritic andesitic basalts, amygdaloidal basalts or rhyolitic and andesitic tuffs. The study area has only 5 per cent bedrock outcrops, most of which are on mountain tops. There is only one mineral occurrence in the study area listed in MINFILE and only five assessment reports have been filed. Exploration to both the north and south of the study area has been successful in locating mineral occurrences in similar geological settings.

GLACIAL HISTORY

There is a lack of knowledge of the surficial sedimentary cover in the east half of the Anahim Lake (93C) sheet with the exception of a 1:250 000 generalized surficial geology map (Tipper, 1971a). This map provides a regional understanding of glacial geomorphology, but does not provide information on the surficial sediments. The Chilanko Forks and Chezacut map areas were covered by Late Wisconsinan Cordilleran ice of the Fraser glaciation (Tipper, 1971b). Ice originated in the Coast Mountains before flowing north, northeast and east onto the Interior Plateau. Coast Mountain ice extended as far east as the Fraser River before coalescing with Cariboo Mountain ice flowing to the west and northwest. The two ice masses then turned northwards and extended as far as the Parsnip River area (Tipper, 1971b). During deglaciation in the Anahim Lake region, ice flow was increasingly controlled by topography as ice masses became isolated and stagnated.

A late glacial readvance covered much of the Anahim Lake area and is postulated to have reached the north-western edge of the Chezacut map area (Tipper, 1971a). This ice mass, named the Anahim Lake advance, originated to the west in the Coast Mountains and flowed onto the plateau through the Tusulko River valley before spreading out to the north, east and southeast. It is the eastward limit of this ice, identified on the basis of differential ice-flow directions and pitted or kettled terrain (Tipper 1971b), that is believed to have reached the study area. A second late glacial readvance may also have entered the Chilanko Forks map area from the south through the Tatla Lake valley (Tipper, 1971a). This Kleena-Kleene advance originated from the south in the Mount Waddington area (92N). The margins of the ice were topographically controlled as it

flowed north and northeast along the Tatla Lake, Tatlayoko Lake, Kleena-Kleene and Chilko valleys. Tipper (1971a) places the limit of this advance at an elevation of 1065 to 1220 metres on the slopes to the northwest and southeast of Tatla Lake Creek.

Fluted bedrock and drumlins developed in till are preserved in the Chilanko Forks map area on the west-central and southeast uplands. These large-scale directional features indicate a flow toward the northeast between 050° and 065°. Glacial striations measured in the southeast of the area trend between 059° and 082°. They may reflect lower elevation, topographically influenced, ice flow during waning stages of glaciation. Large boulders of exotic lithologies were found throughout the study region, the largest of which was a quartz-biotite gneiss of the Coast intrusive suite measuring approximately 10 by 6 by 3 metres. Rounded erratics, found up to elevations of 1400 metres in the south-central parts of the Chilanko Forks sheet, indicate ice completely covered the region during the Fraser glaciation. Hummocky terrain was identified in the northwestern part of the Chezacut sheet, but whether this is Fraser glaciation or late glacial sediment is uncertain. Geochemical signatures or pebble lithologic analysis may provide evidence of a late glacial readvance but at present only the Late Wisconsinan Fraser glaciation has been defined.

SURFICIAL SEDIMENTS

TILL DEPOSITS

Surficial geological mapping shows that till is the dominant deposit on the uplands of the Fraser Plateau. It forms a blanket of variable thickness across much of the area and is expressed as hummocky or kettled, fluted or relatively flat terrain. Surface exposures of till are up to 10 metres thick but are more commonly 1 to 2 metres or less. Tills on steep slopes have commonly been reworked into colluvial deposits. Till is rarely found in valley bottoms because most of the valleys are either late-glacial meltwater channels which have cut down into the surficial cover, or have been partially infilled by glaciofluvial outwash sediments.

Till deposits in the area generally have a silty to fine sandy matrix with minor clay and little medium or coarse sand. Clasts range in size from small pebbles to large boulders, although medium to large pebbles dominate. Sub-angular to subrounded clasts are most common but some exposures, notably those close to bedrock, are dominated by angular blocks; rounded clasts are quite rare. Some tills are comprised of up to 50 per cent clasts, but most exposures have between 10 and 30 per cent. Striated clasts are frequently found in the tills and may represent up to 10 per cent of the population.

Poorly to moderately compacted, massive, silty sand till with lenses and beds of silt, sand and pebbles is the most common till deposit. This till is interpreted to have had an englacial or supraglacial origin forming hummocky or flat moraine during retreat and stagnation of the glacier. Compact, platy structured clay, silt and sand till forms thick, prominent cliff-like exposures (Plate 4-10-2). These tills are massive with thin lenses and stringers of silt or sand and a



Plate 4-10-2. A cliff-like deposit of compact, platy till overlain by a glaciolacustrine sequence and colluvium. This section is located in the north of 93C/8 along the Chilcotin River. The exposure is approximately 8 metres thick.

clear, erosive basal contact. They are interpreted to be a blanket or veneer of basal meltout or lodgement till deposited at the base of the advancing ice.

SAND AND GRAVEL DEPOSITS

Sand and gravel was observed beneath the till in the study area. These sediments are over 5 metres thick on the upland between Tatla Lake Creek and Pyper Lake and are overlain by 1 to 2 metres of till. They are dominated by well-stratified, subangular to rounded, sandy, small-pebble to cobble gravels with thin lenses and beds of stratified sand and silt. They are interpreted as glaciofluvial sediments deposited during the advance phase of the Fraser glaciation.

Glaciofluvial outwash is found along most valleys; it varies from well-sorted fine sand to coarse-cobble gravel. There are two types of glaciofluvial outwash deposits: melt-water channel, and esker or esker complex sediments. Melt-water channels, associated with ice-margin areas, carried water away from the advancing or retreating glacier. Steep-sided valleys with terraces on the sides and coarse cobble or boulder lags in the base are typical. Terrace deposits attain thicknesses of 20 metres in the Chilcotin River valley (Plate 4-10-3) but more often are 1 to 5 metres thick. Well-sorted sand deposits are fairly common in the base of the larger meltwater channels of the Chilcotin and Chilanko valleys.

Sand and gravel ridges that branch and rejoin in braided patterns are interpreted as esker complexes. Deep depressions between the ridges are interpreted as kettles. The esker complex in the Chilanko River valley is 8 kilometres long and 1 kilometre wide and has ridges up to 30 metres high (Plate 4-10-4). More typically, they are 50 to 400 metres wide, 500 to 1500 metres long and ridges are 5 to 15 metres high. Esker complexes in the Chilanko River, Tatla Lake Creek and Puntzi Creek valleys are evidence of topographi-

cally controlled subglacial or englacial meltwater flow. Several single esker ridges with orientations oblique to regional ice flow were noted during mapping. They are located in the lee of mountains and ridges, on flat, open terrain or in valleys oblique to ice flow. These eskers are 10 to 15 metres high, 25 to 50 metres wide and up to 500 metres long. Eskers and esker-complex ridges are usually moderately sorted pebbly sand to cobbly gravel deposits with sub-rounded to rounded clasts.

LAKE DEPOSITS

Parallel-laminated sand, silt and clay deposits in the Clusko River, Chilcotin Lake and Tatla Lake valleys are interpreted as glaciolacustrine deposits. In the Clusko River area they occur as a ubiquitous veneer, 20 centimetres to 1 metre thick, overlying till. These deposits have up to 5 per cent isolated clasts and rare thin diamicton lenses which are interpreted to be dropstones and subaqueous sediment gravity-flows, respectively. In the Chilcotin Lake area, these deposits are finely laminated to thinly bedded fine sand and silt exhibiting climbing ripples or horizontal stratification (Plate 4-10-5).

COLLUVIAL, ORGANIC AND EOLIAN DEPOSITS

A loose cover of weathered and broken bedrock near the mountain tops grades downhill into a thin veneer of colluvial diamicton derived from weathered bedrock and till (Plate 4-10-6). A colluvial veneer is commonly found overlying till on steeper slopes in lower lying areas. Colluvial sediment is differentiated from till by its loose unconsolidated character, the presence of coarse angular blocks of bedrock, and crude stratification. Lenses of well-sorted and stratified sand and gravel are interbedded with the diamicton.



Plate 4-10-3. A thick deposit of glaciofluvial meltwater-channel terrace gravel. This section located in the northern Chilcotin River valley is over 20 metres high.



Plate 4-10-4. A part of the Chilanko Forks esker complex, the ridges here are approximately 10 to 15 metres high and branch and rejoin in a braided pattern. View is looking north across the Chilanko River near the townsite of Chilanko Forks.

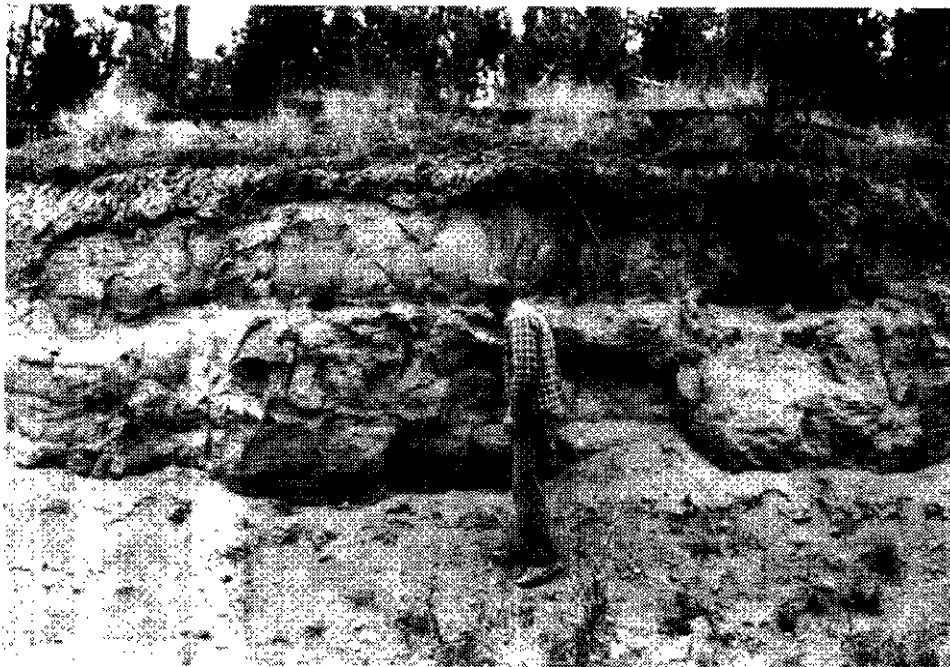


Plate 4-10-5. A thick sequence of glaciolacustrine sand and silt on the north side of Chilcotin Lake. Planar to wavy stratification can be seen in the lower 1.5 metres of the section. The upper metre consists of climbing ripple cross laminations and planar laminations.



Plate 4-10-6. Broken bedrock exposure in a roadcut with a thin layer of till and a capping veneer of colluvial diamicton.

The open, flat terrain in the northwest part of the Chilanko Forks map area and in the western half of Chezacut map area is characterized by marshes and shallow lakes filled with organic sediment. Organic deposits are also common throughout the deep, broad valleys of the Chilcotin and Chilanko rivers, and Puntzi, Pyper and Tatla lakes. The organic deposits consist of decayed marsh vegetation with minor sand, silt and clay. In the bases of some meltwater channels organic deposits occur as a thin veneer of decaying vegetation over cobble and boulder gravel. There was no subsurface organic material recoverable for dating of the sediments and providing a simple chronostratigraphic framework.

Well-sorted, massive to crudely laminated silt and fine sand in the valley bottoms are interpreted as eolian sediments. They are derived from glaciolacustrine deposits in the Puntzi and Pyper Creek valleys and usually occur as low-relief, dune-shaped forms which are not readily visible on air photographs.

CONCLUSIONS AND EXPLORATION IMPLICATIONS

Late Wisconsinan Fraser glaciation ice advanced across the study region from the southwest towards the northeast. Although multiple glacial advances are known to have occurred elsewhere in British Columbia (Clague, 1989), no evidence of any prior glaciation was found in the study area. A sequence of coarse-grained proglacial sand and gravel was deposited in front of the advancing ice. The contact between the outwash and the overlying till is sharp and unconformable, illustrating the erosive nature of the advancing glacier. During glaciation relatively dense till was deposited from the base of the glacier. Bedrock flutings, striations and drumlins attest to the erosive and sculpting capabilities of the ice and indicate a regional northeasterly direction of flow. Later, as the glacier began to stagnate, less compact, silty sandy till was deposited to form hummocky or kettled moraine.

Synchronous with stagnation, large quantities of glacial meltwater formed channels in the Chilanko, Tatla Lake, Pyper, Puntzi and Chilcotin valleys. Confined subglacial and englacial meltwaters created eskers and esker complexes on the valley floors. Unconfined flow in other areas deposited thick sequences of glaciofluvial sand and gravel in the channels. In the Clusko and Chilcotin River valleys, meltwaters appear to have been dammed by stagnant ice masses creating short-lived glacial lakes. Late-glacial readvances of ice from the Anahim Lake region and Mount Waddington may have reached the edge of the study area (Tipper 1971a). Hummocky morainal sediments may have been deposited along the margin of the late glacial advances but no distinct deposits of either are identified in the study area. Meltwaters from these advances followed existing valleys and deposited more sand and gravel. These deposits have since been incised by modern rivers. The growth and decay of vegetation in valleys and on the open uplands to the west has produced organic deposits. Colluvium has

been ongoing slowly since the retreat of ice, forming thin diamicton veneers on the steeper slopes.

Successful mineral exploration in this area will probably require the use of drift prospecting techniques due to limited bedrock exposures. Different genesis and transport histories of the various surficial sediments make some types of sediment more favorable than others for drift exploration (Fortescue and Gleeson, 1984). The thickness of the deposits will affect the ease of sampling and in some cases provides more information on genesis. The best sediments for drift sampling are basal meltout and lodgement tills. These deposits occur relatively close to their source so that boulder tracing and geochemical anomalies in these sediments can be good indicators of nearby mineral occurrences. Using ice-flow directional indicators (striations, flutings, drumlin and till fabrics) these tills can be used to trace dispersal ribbons and isolate mineral sources as demonstrated by DiLabio (1989) and Shilts (1976). Erglacially or supraglacially transported debris deposited in hummocky or flat terrain is usually more distally derived and the provenance of the anomaly is less easy to track. Primary colluvial sediments from local bedrock are good indicators of mineral provenance. Colluvium derived from a pre-existing sediment is less desirable as an indicator.

Glaciofluvial outwash sand and gravel deposits tend to have more complex transport histories and they may be less reliable indicators of mineral occurrence. Commonly these sediments are reworked from a variety of sources and determining their provenance may be difficult. These deposits also experience a much more rapid dilution downstream from mineralization due to high rates of sediment transport and deposition. In some cases however, they may contain concentrations of heavy minerals that can be used to detect and trace mineral occurrences. Eolian samples are the least useful sediments for drift exploration sampling.

ACKNOWLEDGMENTS

The authors would like to thank Milt Law at Mega Fuels for fixing everything we owned and Peter Bobrowsky for supervision. This manuscript benefitted from insightful reviews by Vic Levson, Paul Matysek and John Newell.

REFERENCES

- Clague, J.J. (Compiler) (1989): Cordilleran Ice Sheet, in Quaternary Geology of Canada and Greenland; Fulton, R.J., Editor, *Geological Survey of Canada*, Geology of Canada, No. 1, Chapter 1.
- DiLabio, R.N.W. (1989): Terrain Geochemistry in Canada; in Quaternary Geology of Canada and Greenland; Fulton R.J., Editor, *Geological Survey of Canada*, Geology of Canada, No. 1, Chapter 10.
- Fortescue, J.A.C. and Gleeson C.F. (1984): An Introduction to the Kirkland Lake (KLIP) Basal Till Geochemical and Mineralogical Study (1979-1982), Timiskaming District, *Ontario Geological Survey*, Geochemical Series, Map 80 714.
- Holland, S.S. (1976): Landforms of British Columbia, a Physiographic Outline; *B.C. Ministry of Energy, Mines and Petroleum Resources*, Bulletin 48, 138 pages.

- Proudfoot, D.N. (1993): Drift Exploration and Surficial Geology of the Clusko River and Toil Mountain Map Sheets (93C/9,16); in Geological Fieldwork 1992, Grant, B. and Newell, J.M., Editors, *B.C. Ministry of Energy, Mines and Petroleum Resources*, Paper 1993-1, this volume.
- Shifts, W.W. (1976): Glacial Till and Mineral Exploration; in Glacial Till. Legget, R.F., Editor, *Royal Society of Canada*, Special Publication No. 12, pages. 205-224.
- Tipper, H.W. (1969): Geology Anahim Lake (93C); *Geological Survey of Canada*, Map 1202A.
- Tipper, H.W. (1971a): Surficial Geology Anahim Lake (93C); *Geological Survey of Canada*, Map 1289A.
- Tipper, H.W. (1971b): Glacial Geomorphology and Pleistocene History of Central British Columbia; *Geological Survey of Canada*, Bulletin 196, 89 pages.

DRIFT EXPLORATION AND SURFICIAL GEOLOGY OF THE CLUSKO RIVER AND TOIL MOUNTAIN MAP SHEETS (93C/9, 16)

By D.N. Proudfoot, Geological Consultant

(Contribution to the Interior Plateau Program
Canada – British Columbia Mineral Development Agreement 1991-1995)

KEYWORDS: Drift exploration, surficial geology, Quaternary, sedimentology, geomorphology, surficial maps, Chilcotin.

INTRODUCTION

This report describes the details of field investigations carried out during 1:50 000-scale mapping of surficial geology on NTS map sheets 93C/9 and 16 (Figure 4-11-1). The area has good mineral potential but exploration is hindered in many areas by a thick cover of surficial sediment (Tipper, 1971). Surficial geology maps at a scale of 1:50 000 are available for the areas directly north and east of these map sheets but none exist for the current study area. The aim of this project is to provide 1:50 000-scale maps and surficial geology interpretation that will assist mineral exploration. Map products will be of two types: a terrain map, and a surficial exploration potential map. These maps and an accompanying report will be published separately. The project is funded by the Canada - British Columbia Mineral Development Agreement 1991-1995.

The only prior surficial geology map published for the area was based on fieldwork during the 1950s and 1960s conducted mainly for the purpose of mapping bedrock (Tipper, 1971). The map was published at a scale of 1:250 000 and described mainly surficial geology features, but not materials. Tipper's study was conducted prior to logging in the area and so could not take advantage of the many road exposures of surficial material now available.

Tipper interpreted an early, generally northward, glacial flow through the study area, which he equated with the Fraser glaciation of the Cordilleran ice sheet. Later eastward and northeastward ice flow in the western part of the area was interpreted as readvances by Fraser ice. As ice thinned during deglaciation, topography had an increasing effect on ice-flow direction, causing deflections around topographically high areas. Tipper described abundant sand and gravel deposits present in eskers and meltwater channels, that he suggested developed from a stagnant ice mass during deglaciation. He also mapped the approximate limit of readvancing ice based on the position of "pitted terrain", and the different directions of ice-flow indicators on either side of this terrain. This feature transects the western part of the map area.

PHYSIOGRAPHY AND ACCESS

The study area is located on the Interior Plateau (Mathews, 1986) of British Columbia. It consists of several broad valleys that dissect the plateau, and the intervening high areas. Elevations range from about 1065 metres in the

Clusko River valley at the southern boundary of 92C/9 to as high as 1770 metres above sea level at a hilltop southwest of North Hill (Figure 4-11-1). Most of the area lies between about 1220 and 1525 metres elevation.

Access to most of NTS 93C/9 is by Highway 39 west of Williams Lake to 100 Road which runs north from the highway on the east side of the bridge over the Chilcotin River at Redstone. The 100 Road follows the Clusko River Valley north of Chezacut, intersecting the southern boundary of the map sheet at about Kilometre 52 and traversing the map sheet from the southeast to the northwest. The northern and eastern parts of the map area contain a number of secondary logging roads and tracks that are easily traversed by four-wheeled all-terrain vehicle (ATV). Several

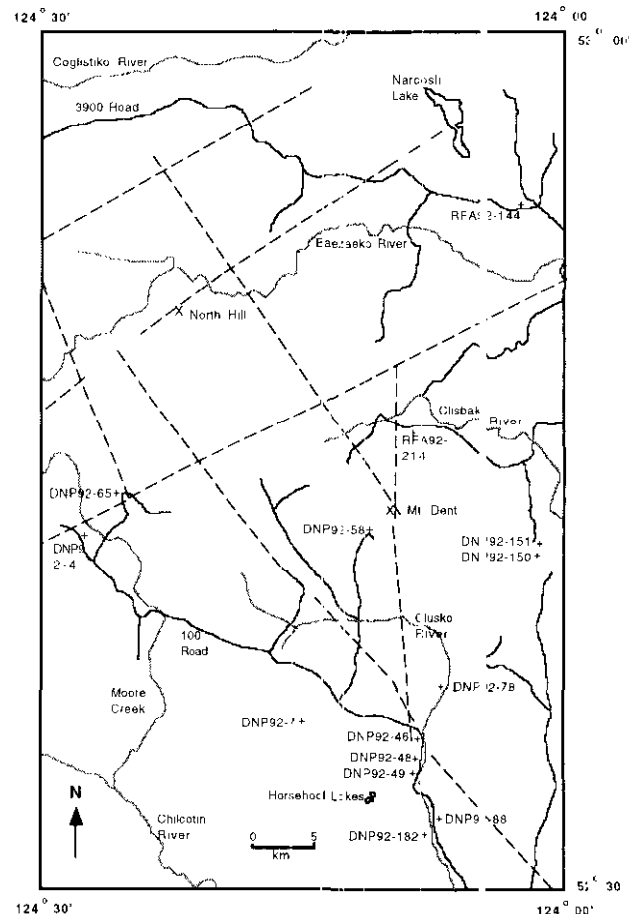


Figure 4-11-1. Location map of observation sites (+) and geographic names mentioned in the text. Dashed lines are seismic lines, solid lines are roads and grey lines are rivers.

seismic lines in the northern part of the map area were also traversed using ATVs. The southwestern quadrant of the map sheet and other areas with no road access were surveyed by helicopter for one half day.

MAPPING AND SAMPLING

A preliminary surficial geology map was prepared using 1:63 000-scale black and white aerial photographs. This was then verified in the field using natural and man-made exposures and hand-dug pits. A total of 187 bulk till samples, 1 to 2 kilograms in weight, and 145 pebble samples, each containing 100 pebbles (2 to 4 cm in diameter) were taken. Most bedrock outcrops were also sampled. Where till occurs along roads, tracks and seismic lines, till samples were taken every 1 to 2 kilometres. The interval between samples varied to take advantage of the best exposures or to verify changes in sediment type.

Sample depth varied according to the type and quality of exposure. For small road cuts (<2 m high) samples were taken near the base, generally at least 60 centimetres below the surface. For larger natural and man-made exposures samples were taken at least 1 metre below the surface and in most cases as close to the base as was possible. Where exposures were not available tree-throw pits were sought to gain easy access for sampling 50 to 75 centimetres below surface. Elsewhere pits were dug by hand to sample to at least 40 centimetres depth. About 75 per cent of all samples were taken from existing exposures. Detailed evaluations of the exposed stratigraphy and sedimentology were recorded at each sampling site. This involved the description of deposit type, internal units and beds, bed contacts, structures, texture, and clast content and shape.

RESULTS AND INTERPRETATIONS

ICE-FLOW HISTORY

Ice-flow directions were determined primarily from geomorphic terrain indicators such as flutings and drumlinoid ridges evident on aerial photographs, and also on two striated outcrops. Unfortunately bedrock in the area is so friable and easily weathered that striations are rarely preserved. The earliest ice-flow direction recorded in the area is determined from two striation sites and numerous stream-lined ridges. At site DNP92-7 in the south-central part of 93C/9, southeast of Thunder Mountain, striations on a polished metavolcanic rock trend 024° (Plate 4-11-1). The direction of flow is confidently interpreted from miniature crag-and-tail features in the rock. This direction of flow agrees with the orientation of numerous flutings in bedrock observed on aerial photographs about 7 kilometres to the east and in a zone 8 to 15 kilometres to the northeast (Plate 4-11-2). At site DNP92-150, in the northeastern part of 93C/9, striations occur on a small area of bedrock beneath a compact till exposed in a roadcut. They also trend 020° . The interpretation of ice-flow direction is based on stoss-and-lee features on the outcrop. This trend is parallel to numerous flutings in the east half of 93C/9 and near the southeastern border of 93C/16. It is the same direction as determined from a few crag-and-tail ridges observed on aerial photographs southeast of Mount Sheringham in the southeast part of 93C/9.

A limited number of easterly trending flutings (about 080°) observed on aerial photographs in the southwest corner of 93C/9 are interpreted to be the result of a subsequent advance. They are parallel to numerous flutings several kilometres to the west on NTS 93C/10. It is unlikely that



Plate 4-11-1. Striations on a bedrock surface at site DNP92-7.

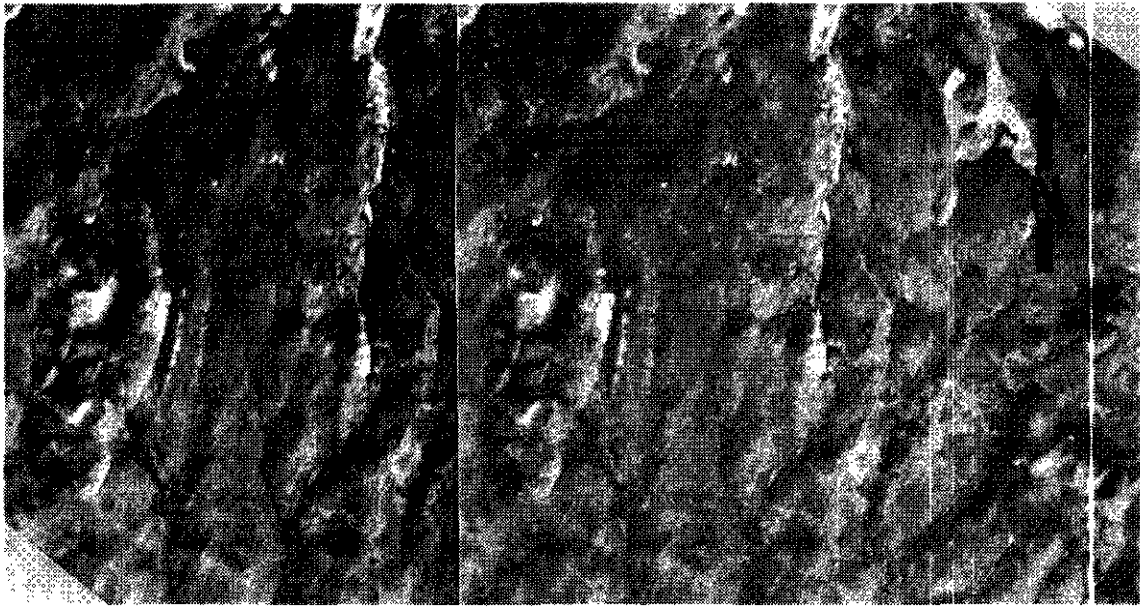


Plate 4-11-2. Photostereogram of north-northeast-trending glacial flutings on bedrock and till terrain southwest of Canyon Mountain (aerial photographs BC88041-206 and 207).

they were created at the same time as the north-northeastward flow that left flutings 17 kilometres to the east because the topography between them is not high enough to have caused deflection toward the northeast. Unfortunately the intervening area was subsequently eroded by subglacial and proglacial meltwater that would have removed this type of evidence. This second ice-flow direction is the same as Tipper's Fraser readvance.

There are also numerous northeast-oriented flutings in an area that extends northward from the north side of the Baezaeko River northwest of North Hill across the western third of 93C/16 to within 3 kilometres of the Coglistiko River. In the southern part of this area the flutings trend about 040° to 045° and gradually veer to 065° in the north. This gradual change in trend is probably due to topographic control of a relatively thin ice sheet as it deflected around the high area that includes a number of hills rising to above 1675 metres elevation.

A 500-metre band of short southeast trending low ridges that are tens of metres wide and about 100 to 200 metres long extends northwest from the northwest side of Narcosli Lake to beyond the northern boundary of the map sheet. They are only evident on aerial photographs. These ridges are most likely transverse moraines that formed perpendicular to northeastward flow. This feature transects a major northeast-trending esker system. The eskers must have been active during the ice flow that created the morainal feature.

There is no evidence in the map area from which to determine the relationship between the two areas of north-eastward ice flow.

SURFICIAL SEDIMENTS

This is a general description of surficial sediments observed in the map area. Greater detail will be provided with the maps.

TILL DEPOSITS

The term 'till' refers to diamicton of glacial origin and should not be confused with till-like diamicton that occurs as colluvium on many steep slopes or as debris-flow deposits in glaciolacustrine sediments. Till occurs on the surface in more than half of the map area and in most topographic settings, but is rare in valley floors. The geomorphology of areas of till cover varies from featureless to fluted or hummocky. Till generally has a silty sandy texture. Clasts are typically subangular to subrounded, range in size from small pebbles to boulders and form from 5 to 25 per cent of the volume of the till. Where till forms a veneer over friable or fractured bedrock, clasts are commonly more angular and comprise a much higher volume (up to 90%) of the sediment. Till deposit thickness ranges from less than a metre to several tens of metres. No multiple till sequences were found.

Where good till exposures occur in areas that are not hummocky, the sediment is generally massive, containing no lenses or beds of washed sediment. It is compact to very compact and in some places has a platy structure. This sediment is interpreted to have been deposited from the base of a moving glacier (Kruger, 1976).

Silty sandy till exposed in hummocks typically contains lenses or beds of sand and/or gravel or silt and is moderately to highly compact. This till is interpreted to have melted out from an englacial or supraglacial position within a glacier (Drewry, 1986). In some places, where sand and gravel deposits occur in close association with hummocky till, the till is low to moderately compact pebbly sand containing only minor silt. This sediment was probably also deposited from an englacial or supraglacial position. The coarser texture of the till may result if a larger proportion of sediment in transport was of glaciofluvial origin. At several sites (e.g., DNP92-151) a veneer of clast-rich (>7% by volume)

diamicton is dominated by angular cobbles (Plate 4-11-3). This sediment is interpreted to have been deposited from a supraglacial position.

A large area of hummocky moraine occurs in the north-western part of the map area (Plate 4-11-4) and could have formed as part of the terminal moraine of eastward and northeastward ice flow during glacial readvance. Elsewhere, hummocky moraine is confined to small areas.

In a few valley settings, (*e.g.*, DNP92-58; Plate 4-11-5), thin beds of diamicton (5 to 20 cm thick) containing relatively few clasts (5% by volume) are interbedded with moderately to poorly sorted sandy gravel and laminated fine

sand to silt beds. Contacts between these beds are sharp and drape underlying sediment. Laminations in silt-sand beds are commonly normally graded. This sequence was probably deposited in a glaciolacustrine environment relatively close to a source of meltwater. Sandy gravel and sand beds are probably high-density turbidity current deposits and sand and silt laminations are probably interflow deposits all of which emanated from a meltwater drainage system at the margin of the lake. The diamicton beds are interpreted as debris-flow deposits that slumped from valley walls and possibly a nearby glacier.

Sampling of tills was limited by the distribution of roads which tend to follow valleys that are almost all covered by



Plate 4-11-3. A veneer (80 cm thick) of cobbly sandy silty till containing about 80 per cent clasts overlying sandy silty till that contains about 15 per cent clasts most of which are pebble sized (DNP92-151). The pick is 90 centimetres long.

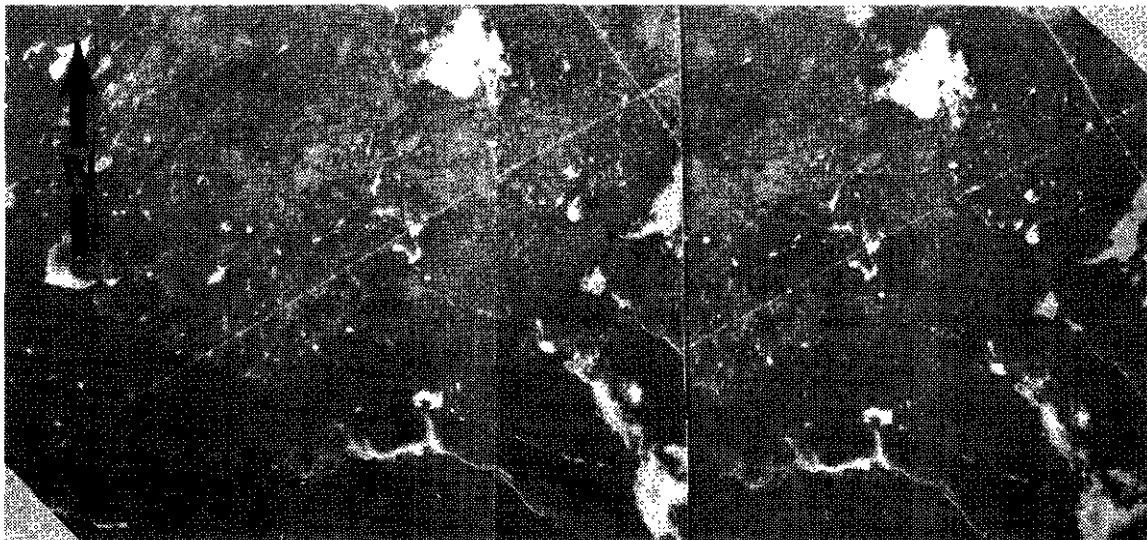


Plate 4-11-4. Photostereogram of hummocky moraine in the northwest corner of 93C/16 (aerial photographs BC88075-112 and 113).



Plate 4-11-5. Interbedded diamicton, sandy gravel and laminated fine sand and silt at site DNP92-58. The trowel is about 20 centimetres long.



Plate 4-11-6. A meltwater channel cut into sand and gravel and till at site DNP92-151. The channel is about 15 metres wide at the top.

sand and gravel. Geochemical analysis of bulk till samples and lithological analysis of pebble collections from most sample sites should help to clarify regional sediment dispersion by glacial transport.

SAND AND GRAVEL DEPOSITS

Sand and gravel deposits form a significant part of the surficial sediment cover in the area. They occur in two main settings: in most valleys, particularly tributaries to major river valleys; and in esker complexes that occur between

and within valleys. Most eskers or esker complexes lead out of or into meltwater channels. In many places, particularly where underlying bedrock is basalt, these channels cut into bedrock. Where till is cut by channels, the channel floor is commonly covered with a cobbly lag deposit.

There are numerous steep sided valleys in the map area (Plate 4-11-6). Some are occupied by small modern streams, others have no flowing water in them. They are all meltwater channels eroded by subglacial and proglacial meltwater. Most of these meltwater channels contain terraces and

blankets of sand and gravel that were deposited by flowing water with much higher energy than any of the modern rivers and streams in the map area. This sediment was probably deposited by glacial meltwater that was no longer confined by overlying ice.

Modern stream and river valleys also contain a significant volume of postglacial sand and fine gravel. Most of these deposits occur in channels and on the flood plain. The maximum grain size of these deposits is normally in the small pebble range, because of the considerably lower energy of the water flow.

Most eskers in the area are cobbly to pebbly sand and gravel that ranges from poorly to well sorted. Some are draped by a discontinuous veneer of till (Plate 4-11-7). Pebbles and cobbles are commonly subrounded to rounded. Thicknesses range up to about 15 metres but average 3 to 5 metres.

SAND AND SILT DEPOSITS

Sand and silt deposits cover less than 10 per cent of the surface in the map area. They occur in three settings: on the flood plains of modern drainage systems; as eroded remnants of glaciolacustrine valley fill in the Clusko and Clisbako River valleys; and as a veneer overlying till and glaciofluvial sand and gravel deposits. They are most significant in the Clusko River valley east and southeast of Horsehoof Lakes and in the headwaters of the Clusko River in the north-central part of NTS 93C/9.

The sediment on modern flood plains consists of interbedded fine to very fine sand and silt with minor clay, and occurs up to about 1.5 metres above present water level. Examples are well exposed along the Clusko River at site DNP92-78. Beds are discontinuous and vary in thickness up

to 20 centimetres. Cut-and-fill structures and buried organic detritus are common. Here sediment was probably deposited by modern drainage during peak discharge periods and was derived from the winnowing of pre-existing glaciofluvial and glacial deposits.

Good exposures up to 8 metres thick of laminated fine to very fine sand, silt and clayey silt beds occur in several places (*e.g.*, DNP92-88, DNP92-65 and RFA92-144). At RFA92-144 (Plate 4-11-8) massive fine to very fine silty sand beds 5 to 10 centimetres thick are interbedded with laminated sequences of very fine sand, silt and silty clay. Laminations are normally graded and 0.1 to 5 centimetres thick. A few pebbles occur in this exposure. All of this sediment was probably deposited by medium to high-density turbidity currents in a glaciolacustrine lake.

In many valleys a discontinuous veneer of interbedded to laminated silt and sand and clayey silt overlies diamicton or sand and gravel deposits. At DNP92-46, a large esker is draped by less than 1 metre of laminated sand and silt similar to the sediment described in the previous paragraph. At DNP92-49, a 3-metre exposure of compact massive diamicton, interpreted as till, is covered by 2 metres of laminated clayey silt and very fine sand. This surface material is interpreted to be glacial lake sediment deposited after the glacier had retreated.

In Moore Creek valley in the northwest corner of 93C/9, glaciofluvial sand and gravel and rhythmically bedded glaciolacustrine sand, silt and clayey silt deposits are covered by a discontinuous veneer of massive to weakly laminated very fine sand and silt with no clay. In this area, at DNP92-4, a steep sided ridge, 8 metres high and composed of weakly laminated fine to very fine sand and silt, rests on a flat plain of diamicton that is interpreted to be till. This

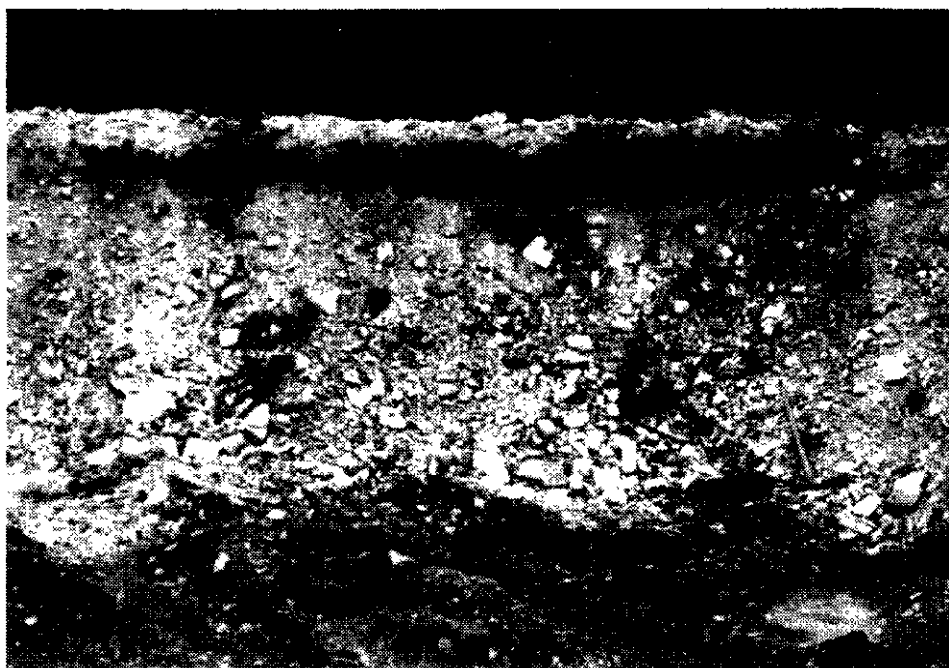


Plate 4-11-7. Glaciofluvial sand and gravel deposit overlying diamicton that is probably till. This is an example of a site in a broad area of sand and gravel where a reliable till sample could be taken (RFA92-214). The pick is 90 centimetres long.

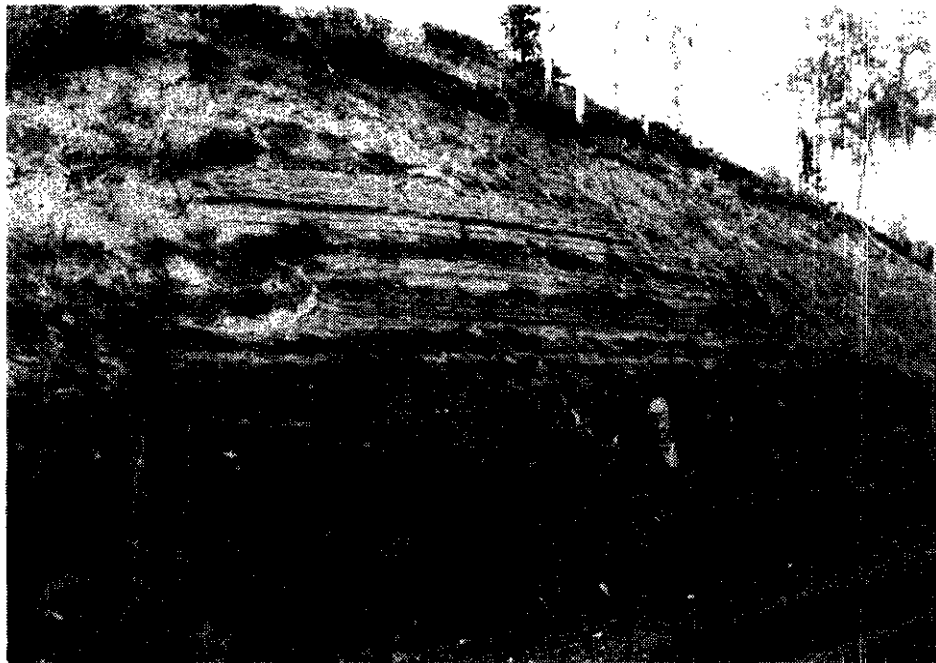


Plate 4-11-8. Interbedded fine to very fine sand and silt at site RFA92-144. Silty beds are dark grey because of higher moisture content than surrounding sand.

ridge is probably a dune and similar sediment found as a veneer in the area is also interpreted to be eolian in origin. Unfortunately this area is heavily treed and appears featureless on aerial photographs. Small dunes less than 1.5 metres high were, however, observed on a grass-covered silty sandy fluvial plain, directly west of North Hill. All of this eolian sediment was probably derived from the surrounding glaciolacustrine, outwash and fluvial plains. Areas where diamicton is at the surface probably had the veneer of glaciolacustrine sediment removed by wind after the lake basin dried and before the establishment of vegetation. The veneer of glaciolacustrine and eolian sediment is under-represented during mapping because of the difficulty in recognizing it on aerial photographs.

COLLUVIUM DEPOSITS

Numerous sites on or at the base of relatively steep hillsides contain a veneer of massive or thinly bedded diamicton (e.g., DNP92-48). Bedding planes and the broad side of flat pebbles are parallel to the local slope. Cut-and-fill lenses and stringers of sand and gravel are also common. This sediment was deposited by slope processes that occurred mainly when there was no vegetation, either in early postglacial time or after forest fires.

ORGANIC SEDIMENT

Organic sediment consists of a mixture of silt, sand and decayed plant remains (mainly bog plants and grasses). It occurs in poorly drained depressions, especially in abandoned meltwater channels, along the edge of ponds and on modern flood plains. Away from modern drainage it consists mainly of black organic mud, however, along active drainage the mud contains abundant silt and sand.

QUATERNARY HISTORY

The history of deposition and erosion of surficial sediment in the area has been constructed from deposit and landform field relationships and sediment genesis. There have been at least four glacial events recorded in this part of British Columbia (Fulton, 1984). In the absence of good multiple till exposures and dateable organic material, the simplest stratigraphic interpretation is used. These Quaternary geologic events are summarized below:

- (1) Deposition of proglacial sand and gravel during glacial advance. Fluvial sediment deposited during erosion of the area in late preglacial time would have been reworked during and after glaciation and has not been recognized.
- (2) Deposition of a till blanket or veneer by actively flowing ice during glaciation.
- (3) Deposition of hummocky moraine during glacial retreat or stagnation. Contemporaneous development of meltwater channels beneath and beyond glacier ice. Major pre-existing valleys would have been drainage conduits.
- (4) Ponding of meltwater behind ice dams and ice-cored moraines that blocked drainage. This resulted in the formation of relatively short-lived lakes along which deltas formed (DNP92-182) and finer sediment was deposited.
- (5) Drainage of glaciolacustrine lakes and re-establishment of regional drainage. Erosion of glaciolacustrine sediment by postglacial drainage.
- (6) Glacial readvance into the western margin of map area. Deposition of hummocky moraine along the ice margin?

- (7) Disintegration of readvance ice. Enhancement of drainage to east and northeast from this ice. Further deposition of sand and gravel in meltwater channels.
- (8) Drying out of lake basins and outwash plains. Reworking of fine sediment by wind.
- (9) Establishment of modern drainage, bogs and colluviation of hillsides.

IMPLICATIONS FOR MINERAL EXPLORATION

There are three major problems for drift exploration in the study area; first the problem of basal-till sampling. There are large areas that contain little or no basal till at the surface. In glaciated terrain, basal till is the most desirable sediment to sample because it is normally the shortest travelled of glacial sediment types and can be most easily traced to its source.

The sediment in hummocky terrain was probably deposited from debris well above the base of the glacier. This material is presumed to have travelled farther than basally derived till. The deposition of hummocky terrain occurs during melting and therefore has abundant meltwater associated with it. In the study area this meltwater has cut numerous channels (Plate 4-11-6) many of which expose till of probable basal origin. Detailed drift-sampling programs should therefore be devised to sample carefully along these channels. The resulting sample distribution would likely be less systematic but far more useful. In the absence of meltwater channels, samples should be taken between hummocks to a depth of at least metre. This will be much more time consuming than typical sampling programs and will provide less samples for the same cost, but the results should be more effective.

Secondly, what to do in a sampling program where till is scarce? Anomalies in glaciofluvial and fluvial deposits potentially have had a more complex history of transport from bedrock source to final deposition. They may have been derived from till or sand and gravel deposits and are thus at least a second derivative from their source (Shilts, 1975). In most of the study area till underlies or is adjacent to sand and gravel and glaciolacustrine deposits. However because roads follow valleys and outwash, due to the presence of sand and gravel, the only exposures are of sand and

gravel. Sampling programs should be offset to adjacent till covered terrain where possible. The map area is anomalous because of the abundance of meltwater channels. In some areas of sand and gravel cover, till is exposed in the side of the channels.

Finally, bedrock striation sites are rare and large-scale glacial-flow features only occur in a few places. These data have allowed for an interpretation of regional ice flow, however local variations due to topographic influences cannot be determined. Numerous detailed till-fabric measurements must be carried out to determine local flow directions.

ACKNOWLEDGMENTS

Rochelle Allison provided excellent field preparation and field assistance. Peter Bobrowsky, Tim Giles and Dan Kerr, all with the British Columbia Geological Survey Branch, assisted in several ways with the project. Clusko Logging Company Ltd. and Jacobson Brothers Limited provided us with fresh water and a place to park our trailer. Brian Dougherty, Northern Mountain Helicopters, Quesnel, helped us to finish our sampling program on schedule. This project was funded under contract No. 93-661 with the British Columbia Ministry of Energy, Mines and Petroleum Resources.

REFERENCES

- Drewry, D. (1986): *Glacial Geologic Processes*, Edward Arnold Ltd., London, U.K., 276 pages.
- Fulton, R.J. (1984): Quaternary Glaciation, Canadian Cordillera, in Quaternary Stratigraphy of Canada – A Canadian Contribution to IGCP Project 24, Fulton, R.J., Editor, *Geological Survey of Canada*, Paper 84-10.
- Kruger, J. (1976): Structures and Textures in Till Indicating Subglacial Deposition; *Boreas*, Volume 8, pages 323-340.
- Mathews, W.H. (1986): Physiographic Map of the Canadian Cordillera; *Geological Survey of Canada*, Map 1701A.
- Shilts, W. (1975): Principles of Geochemical Exploration for Sulphide Deposits Using Shallow Samples of Glacial Drift; *Canadian Institute of Mining and Metallurgy*, Bulletin, Volume 68, pages 73-80.
- Tipper, H.W. (1971): Surficial Geology Anahim Lake (93C); *Geological Survey of Canada*, Map 1289A, Bulletin 196.



PRELIMINARY EVALUATION OF MULTIELEMENT REGIONAL STREAM-SEDIMENT DATA, ISKUT RIVER AREA (104B)

By A. J. Sinclair and T. A. Delaney, Mineral Deposit Research Unit, U.B.C.

(MDRU Contribution 020)

KEYWORDS: Applied geochemistry, Iskut River, stream sediments, probability plots, anomaly discrimination.

INTRODUCTION

Multi-element geochemical data from regional stream-sediment surveys provide a useful base with which to determine geochemical characteristics of an area and thus, to assist in the design of more detailed, exploration oriented studies. The Eskay Creek area is of particular interest because of the enigmatic deposits found recently with abnormally high grades of gold and silver. The general area was sampled in 1988 as part of the Regional Geochemical Survey program of the Geological Survey Branch of the British Columbia Ministry of Energy, Mines and Petroleum Resources. Analytical data emerging from that survey were provided to us for evaluation.

The analytical data were obtained from the -80-mesh fraction of stream sediment samples analyzed by atomic absorption techniques for 21 constituents (Zn, Cu, Pb, Ni, Co, Ag, Mn, Fe, Mo, U, W, Sn, Hg, As, Sb, Ba, Cd, V, LOI, F and Au), and water samples (from stream-sediment sample sites) analyzed for uranium, fluorine and pH. In addition, a number of categorical variables were recorded for each sample site such as grain size, sediment colour, stream velocity and lithology underlying the basin contributing to a stream sediment sample site.

METHODOLOGY

Our initial work has been oriented toward the recognition and characterization of background populations for the various metals analyzed, and the identification of thresholds for those elements that are clearly anomalous in known mineralized areas. The approach we have taken includes:

- Updating the information pertaining to lithology underlying the drainage basin for each sample in the light of the most recent geological mapping.
- Grouping of samples with related lithologies to produce groups with sufficient data for the evaluation procedure to be used.
- Interpretation of particular groups of data using probability graphs.
- Examination of the spatial plots of those elements for which multiple populations were identified.

In particular, we examined the analytical data reported for 660 stream-sediment samples from map area NTS 104B, that is, the Iskut River area which embraces the Snip deposit, Eskay Creek area and the Sulphurets camp, and chose two extreme groups of data with which to begin our study: samples reflecting drainage basins underlain by sedi-

mentary rocks of the Bowser Lake Group, and samples which reflect volcanic lithologies of the Hazelton Group. These groups are coded SLSN and BRCC respectively in the publicly available government data file. The latter group includes units that locally have been referred to as Jack, Unuk River, Betty Creek, Mount Dilworth and Salmon River formations although the correlations are commonly uncertain. We edited these data groups substantially with the assistance of up-to-date geological information from Dr. P. Lewis. The resulting modified files were then examined sequentially using probability plots (Sinclair, 1976; Stanley, 1988).

RESULTS

Results of our study are discussed in terms of the shapes of the histograms (numbers of interpreted data subpopulations) and selection of thresholds for the variables studied.

In nearly all cases we were able to interpret the shapes of probability graphs (cumulative histograms) as indicative of either a single lognormal population or combinations of lognormal populations. In general, we can classify variables from each geologically defined group into four subgroups of increasing complexity of cumulative histograms.

The interpretation of probability plots is subjective, but experience has shown that different subpopulations of a particular geochemical variable are commonly the product of different processes. For example, high subpopulations of metals such as copper and lead in many cases are related to mineralization, whereas, the lower subpopulations for these metals represent samples derived from unmineralized terrains. Where sufficient independent data are available the various processes represented by data subpopulations can be identified with reasonable certainty. As a general rule, we have ignored two very specific types of population as follows: outlier values which we define for our purposes as representing less than 1 percent of a data set at either the high or low ends of a distribution, and pseudo-subpopulations that may appear where a significant proportion of values occurs near the detection limit of the analytical procedure. This latter situation is of little concern for the metal variables considered here because, in general, we are more interested in higher values than in lower values; this need not be true with such variables as loss on ignition (LOI) or pH.

Results of this preliminary study are listed in Table 4-12-1 for samples from sedimentary terrains and in Table 4-12-2 for samples from volcanic terrains. For each of these geological groups of data, variables are subdivided according to increasing complexity of cumulative histograms (*i.e.*, increasing numbers of modes). Thresholds are given for all variables (*cf.* Sinclair, 1991)

TABLE 4-12-1

SUMMARY OF SUBPOPULATIONS AND SOME IMPORTANT CHARACTERISTICS, REGIONAL GEOCHEMICAL SURVEY DATA FOR DRAINAGE BASINS UNDERLAIN BY HAZELTON GROUP ROCKS (SLSN) (NTS 104B)

ONE POPULATION (n = 194)

Variable	Geom Mean	95% range (units) (2nd figure is threshold)
Ag	0.14 ppm	0.03 - 0.65
Co	17 ppm	6 - 35
Cu	42 ppm	19 - 91
Fe	3.48%	2.32 - 5.21
Mn	638 ppm	285 - 1,430
Sn	0.9 ppm	0.2 - 3.7
W	2.1 ppm	1.0 - 4.4
pH	6.98	6.15 - 7.80
U	1.9 ppm	1.1 - 3.6

TWO POPULATIONS (n = 194)

Variable	Pop'n	Geom Mean %	Lower Threshold (units)
As	A	71 3%	27 ppm
	B	12 97%	
Mo	A	12 2%	4.7 ppm
	B	1.6 98%	
Au	A	32 5%	20 ppb
	B	2.5 95%	
Pb	A	52 2%	18 ppm
	B	7.7 98%	
V	A	126 7%	72 ppm
	B	45 93%	
Fw	A	93 10%	60 ppb
	B	34 90%	
Zn	A	525 4.5%	285 ppm
	B	124 95.5%	
LOI	A	9.4 23%	5.29%
	B	3.0 87%	
F	A	470 16%	368 ppb
	B	266 84%	
Sb	A	6.3 5%	2.0pp
	B	0.5 95%	
Ba	A	1260 22%	993 ppm
	B	842 78%	
Cd	A	1.5 16%	0.48pp
	B	0.1 84%	

THREE POPULATIONS (n = 194)

Variable	Pop'n	Geom Mean %	Lower Threshold (units)
Hg	A	630 3%	213 ppm
	B	84 93.5%	32 ppm
	C	5.6 3.5%	
Ni	A	166 2%	140 ppm
	B	97 84%	53 ppm
	C	18 14%	

* arithmetic mean

TABLE 4-12-2

SUMMARY OF SUBPOPULATIONS AND SOME IMPORTANT CHARACTERISTICS, REGIONAL GEOCHEMICAL SURVEY DATA FOR STREAM SEDIMENT SAMPLES FROM DRAINAGE BASINS UNDERLAIN BY VOLCANIC ROCKS (BRCC), NTS MAP AREA 104B

ONE POPULATION (n = 78)

Variable	Geom Mean	95% Range (units) (2nd figure is threshold)
Cd	0.5	.05 - 5 ppm
Sn	1.0	.2 - 3.6 ppm
Ag	0.4	.06 - 2.3 pp
Ni	33	5 - 227 ppm

TWO POPULATIONS (n = 78)

Variable	Pop'n	Geom Mean %	Threshold
pH	A	7.18 95%	6.35
	B	3.20 5%	
Zn	A	660 5%	295 ppm
	B	142 95%	
Fe	A	4.04 95%	2.48%
	B	1.55 5%	
Uw	A	0.32 14%	.08 ppb
	B	0.02 86%	
Mo	A	20 15%	7 pp
	B	2.7 85%	
U	A	6.7 10%	3.8 pp
	B	2.3 90%	
W	A	26 4%	5 ppm
	B	2.6 96%	

THREE POPULATIONS (n = 78)

Metal	Pop'n	Geom Mean %	Lower Threshold
Fw	A	121 (17%)	40 pp
	B	32.5 (71%)	19.5
	C	10 (12%)	
Ba	A	2510 (10%)	1720 ppm
	B	1270 (87%)	902
	C	630 (3%)	
As	A	282 (15%)	103 ppm
	B	26 (77%)	6.2
	C	1.7 (8%)	
V	A	117 (15%)	92 ppm
	B	65 (65%)	44
	C	33 (20%)	
F	A	794 (3%)	669 ppm
	B	501 (75%)	391
	C	324 (22%)	
Mn	A	1740 (5%)	1320 ppm
	B	747 (91%)	316
	C	126 (4%)	
Au	A	158 (27%)	34 ppb
	B	8.7 (64%)	2.3
	C	1.1 (9%)	

FOUR POPULATIONS (n = 78)

Metal	Pop'n	Geom Mean %	Threshold (units)
Cu	A	480 (6%)	229 ppm
	B	109 (26%)	63
	C	50 (65%)	27
	D	17 (3%)	
Pb	A	107 (7%)	58 ppm
	B	31 (23%)	20
	C	13 (65%)	6.3
	D	3.1 (5%)	
Hg	A	2510 (5%)	630 ppm
	B	169 (65%)	60
	C	32 (20%)	13
	D	4.7 (10%)	
Co	A	40 (5%)	29 ppm
	B	21 (50%)	15
	C	13 (36%)	8
	D	4.2 (4%)	

DISCUSSION

The two data groups dealt with represent surficial geochemical responses to two contrasting geological environments, that is, sedimentary and volcanic terrains. Even a cursory comparison of results in Tables 4-12-1 and 4-12-2 indicates that histograms of variables from the sedimentary group (Table 4-12-1) are less complex (*i.e.*, fewer modes) and metal abundances are generally much lower than for the volcanic group (Table 4-12-2). For about half the variables (*i.e.*, Ba, Cu, U, As, Mo, Au, Pb, V, F, Zn and Hg) the high abundance subpopulation for the volcanic-related group is substantially above the value at the 97.5 percentile of the corresponding population related to sedimentary terrains. The generally higher level of metal abundances in the volcanic-related data reflects both differing background populations for the two distinctive rock sequences and the presence of a substantial number of mineral showings and hydrothermal alteration zones localized within or at the margins of the volcanic sequence. It seems likely that for most metals with multiple subpopulations the upper subpopulation correlates with a mineralized source. An exception seems to be barium (*see* Table 4-12-2). In some cases, tin for example, the histograms from the two groups are comparable.

Examples of varying complexity of the form of cumulative histograms are given in Figures 4-12-1 to 4-12-4. Metals showing single lognormal populations are of limited practical use in identifying anomalous samples; we have adopted the mean plus two standard deviations of the lognormal population as an arbitrary threshold in such cases (Sinclair, 1991).

The foregoing observations are consistent with the known concentration of mineral deposits and occurrences in or marginal to the volcanic sequences in the area, and the general absence of showings in predominantly sedimentary terrains. However, there are several surprising results from our study:

- Silver and antimony values are remarkably low and their distributions are simple. This is particularly surprising because many showings in the area contain abundant sulphosalts and have high silver contents.
- Relatively few samples are anomalous in more than one or two elements. For example, among the volcanic-related samples, 27 are anomalous in one or more of copper, lead, zinc, mercury and arsenic (Table 4-12-3). This particular group of elements is important because all the metals are strongly concentrated in the Eskay Creek area and the Sulphurets camp. From a practical point of view results of our evaluation imply that multi-element analyses are essential for stream sediment samples to provide an acceptable level of anomaly recognition.

Despite the limitations discussed above regarding the inefficiency of using single elements for anomaly recognition, several metals are useful on a more regional scale. High zinc values, for example, clearly identify a large area including and extending south from the Eskay Creek deposits. High arsenic values are concentrated in the Sulphurets camp and are associated with high zinc values to the

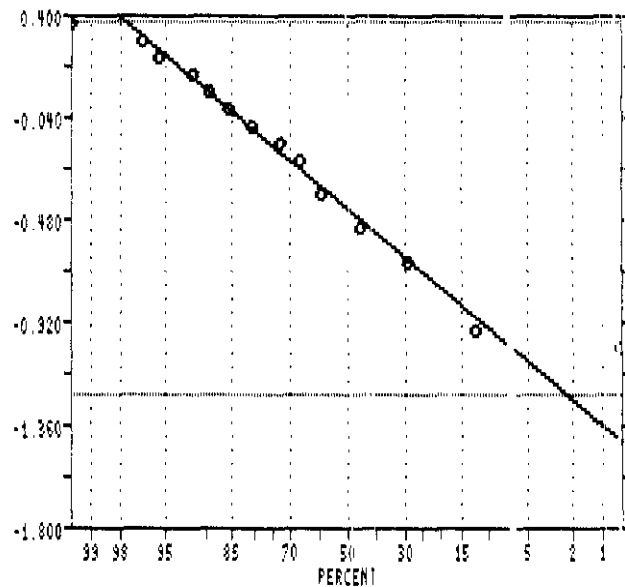


Figure 4-12-1. Log probability graph for silver in volcanic-derived stream sediment samples, Eskay Creek area. Ordinate is $\text{Log}_{10}(\text{metal abundance})$. Open circles are cumulative data; straight line through cumulative data is a visual, best fit, lognormal distribution; horizontal dotted lines are the 2.5 and 97.5 percentiles of the best fit distribution.

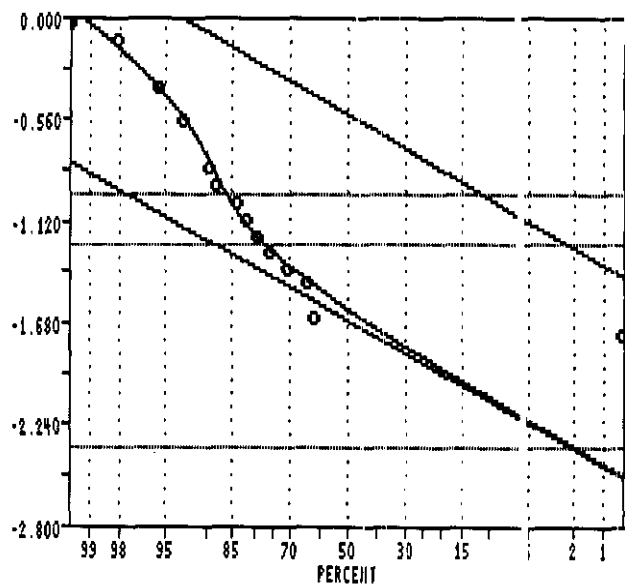


Figure 4-12-2. Log probability graph for uranium in water (U_w) at volcanic-derived stream sediment sites, Eskay Creek area. Ordinate is $\text{Log}_{10}(\text{metal abundance})$. Open circles are cumulative data; curve fitted to open circles is a visual best fit bimodal distribution; sloping straight lines are partitioned lognormal subpopulations; horizontal dotted lines are at the 2.5 and 97.5 percentiles of each of the partitioned subpopulations.

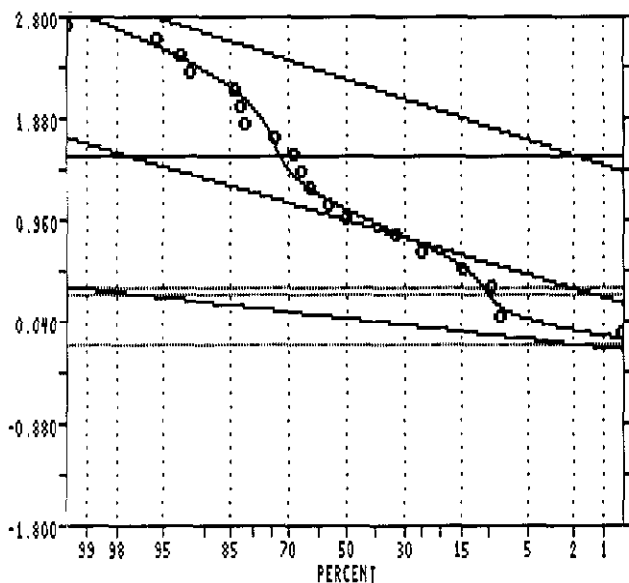


Figure 4-12-3. Log probability graph for gold in volcanic-derived stream sediment samples, Eskay Creek area. Ordinate is $\text{Log}_{10}(\text{metal abundance})$. See Figure 2 for explanation of symbols.

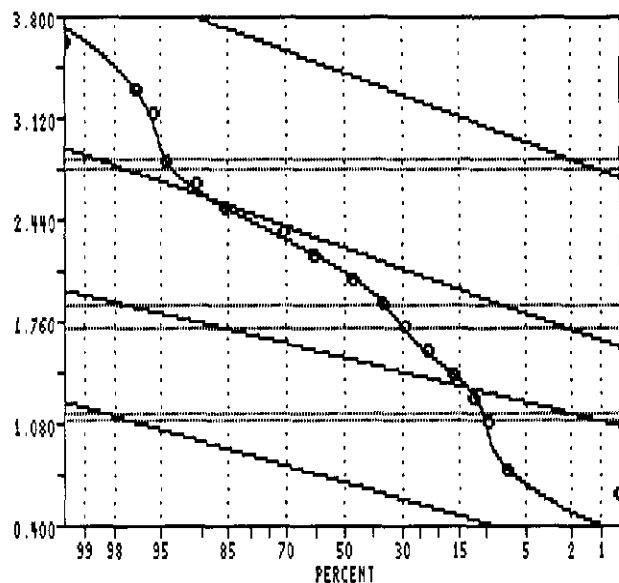


Figure 4-12-4. Log probability graph for gold in volcanic-derived stream sediment samples, Eskay Creek area. Ordinate is $\text{Log}_{10}(\text{metal abundance})$. See Figure 4-12-2 for explanation of symbols.

south of Eskay Creek. The fact that many samples are "one metal anomalous" may be partly related to mineral zoning and secondary dispersion patterns. If this is so, closer spaced samples are essential to identify such patterns.

The following comments relate to the volcanic-related data set: uranium in water, molybdenum and to a lesser degree uranium, have very similar cumulative distributions; of these uranium in water is particularly well defined as a mixture of two lognormal populations. Association of these elements is to be expected because of their geochemical similarity in surficial environments. A small percentage of values that represent a high subpopulation relates spatially to small intrusive bodies. Zinc background is normal for volcanic terrains.

Complex distributions are difficult to interpret with confidence. Several three-population variables (Sb, Au, Ba, F_w and Mn) seem to have one of their constituent populations generated artificially near the detection limit; hence, they are interpreted here as bimodal variables. Gold has two clearly defined and abundant populations. The relatively high abundance of an upper population (27%) probably reflects the widespread occurrence of mineralized and altered zones within the volcanic sequence and the biased location of samples relative to known mineralization.

Copper and lead (and possibly mercury) have very similar, complex histograms. The upper subpopulations of each of these three elements appears to be related spatially to known mineralization but, as indicated previously, stream-sediment samples are generally high in only one of the three metals.

Values for pH are largely concentrated near 7; however, a very small subpopulation (4 samples) of extremely low values ($\text{pH} < 5.4$) represents strongly acid conditions associated with extensive gossan development over pyritic zones.

These low (anomalous) pH values appear erratically located because of the scale of sampling combined with the short distances over which local acidities are diluted (neutralized).

CONCLUSIONS

Stream-sediment samples in the Iskut River area, taken as part of a Regional Geochemical Survey, provide useful information to guide further surveys and exploration. In particular, thresholds have been determined for all variables for the two geologically defined data groups in the publicly available data that we examined.

TABLE 4-12-3
NUMBERS OF SAMPLES (VOLCANIC TERRAINS) THAT ARE ANOMALOUS IN REGIONALLY IMPORTANT METALS AND COMBINATIONS OF THOSE METALS

Anomalous Metal Association	No. of Samples
Hg	3
Cu	3
Cu + Hg	1
Cu + Hg + As	1
Hg + As	1
As	6
As + Pb	1
Pb	4
Zn	7
Total Anomalous Samples	27

A need for more closely spaced stream-sediment samples has been demonstrated for follow-up work, to provide a basis for recognizing primary and secondary dispersion patterns.

Anomalous samples are rarely anomalous in more than one element. Clearly, multi-element analyses are essential; otherwise, many anomalous samples will not be recognized.

ACKNOWLEDGMENTS

Mr. Steve Sibbick of the British Columbia Ministry of Energy, Mines and Petroleum Resources kindly provided up-to-date computer files of the Regional Stream Survey data for the purposes of our study. Dr. P. Lewis assisted in the reclassification of lithologies underlying upstream

drainage basins of many of the sample sites. Comments by Dr. J.F.H. Thompson improved the manuscript.

REFERENCES

- Sinclair, A.J. (1976): Applications of Probability Graphs in Mineral Exploration; *Association of Exploration Geochemists*, Special Volume No. 4, 95 pages.
- Sinclair, A.J. (1991): A Fundamental Approach to Threshold Estimation in Exploration Geochemistry: Probability Plots Revisited; *Journal of Exploration Geochemistry*, Volume 41, pages 1-22.
- Stanley, C.R. (1988): PROBPLOT: An Interactive Computer Program to Fit Mixtures of Normal (or Lognormal) Distributions with Maximum Likelihood Procedures; *Association of Exploration Geochemists*, Special Volume No. 14, 40 pages (includes diskette).

NOTES



THE PREDICTED COKE STRENGTH AFTER REACTION VALUES OF BRITISH COLUMBIA COALS, WITH COMPARISONS TO INTERNATIONAL COALS

By Barry D. Ryan, B.C. Geological Survey Branch and
John T. Price, Canada Centre for Mineral and Energy Technology

KEYWORDS: Coal quality, coke strength after reaction (CSR), coke reactivity index (CRI), ash chemistry; base-acid ratio (BAR), pulverized coal injection (PCI), blending.

INTRODUCTION

This paper provides background to the coke strength after reaction (CSR) test and gives perspective regarding changes in the coking coal market. It provides a summary of some of the predicted relationships between the ash chemistry of coal, and coke properties of British Columbia coals.

A brief overview of the ash chemistry of British Columbia coking coals is presented. The data are used to comment upon the potential coke strength after reaction (CSR) of these coals based on their ash chemistry. Finally comparisons are made with coals from other parts of Canada, U.S.A and Australia.

BACKGROUND

Coke making is a major production step in the steel making process. The blast furnace operator must be able to assess the performance of the coke in the furnace in order to run the furnace efficiently. Blast furnaces are operated on a continuous basis with every effort made to reduce variations in the operating conditions. They are only shut-down for expensive relining or because of unforeseen circumstances. It is therefore almost impossible to measure the actual performance of coke in a furnace and the operator must depend on predictions of its performance.

A variety of tests have been developed to predict the performance of coke in blast furnaces. Historically attempts were made to predict the cold strength of coke (stability factor, SF) by measuring various petrographic and rheological properties of the parent coal. Fluidity, dilatation and FSI (free swelling index) are all useful pointers to the strength of coke that can be made from a parent coal. Unfortunately they do not cover all aspects of the quality control required in modern blast furnaces.

More recently, pilot coke ovens have been used to produce samples of coke that can be used for quality tests. The tests, such as stability factor, measure the resistance of the coke to breakage and abrasion, both problems in the top of the blast furnace where the sintered iron ore and coke are loaded into the furnace. As it sinks lower into the furnace it heats up, dissolving and reducing the iron ore by the solution loss reaction (Boudouard reaction) which in part provides carbon monoxide to reduce the iron. This reaction consumes coke which at the same time is still required to support the iron ore and maintain a permeable pathway for

the gases. Finally the coke descends to the raceway area of the blast furnace where it is totally consumed leaving an unvolatilized ash residue.

As blast furnace operation techniques evolved to make the process more efficient, so also have the techniques used to predict coke performance in blast furnaces. A recognition of the importance of evaluating the performance of coke in the mid-region of the furnace led to the development of a number of hot-coke evaluation tests (Ishakawa, 1983). The most accepted of these measure the coke strength after reaction (CSR) and coke reactivity index (CRI). The CSR test involves measuring the resistance of coke to breakage after it has been reacted in a carbon dioxide atmosphere at a temperature of 1100°C. The CRI test measures the loss of weight after this reaction. The acceptance of the CSR test recognizes the fact that coke performance must be evaluated in all parts of the blast furnace, not just the top, colder regions.

Coke is an expensive component in the steel-making process. It is made in coke ovens that most companies would like to see last as long as possible while they decide which new technology to invest in as a replacement. For both reasons there is incentive to reduce the amount of coke used to produce a ton of hot metal.

In the short term, pulverized coal injection (PCI) is the easiest way of replacing some of the coke used in the blast furnace. This technology provides heat and carbon monoxide but does not help maintain gas permeability in the furnace. This means that the remaining coke must be even stronger if it is going to support the same weight of iron ore. With increased use of PCI, coals with improved hot coke strengths will be required for continued efficient and consistent performance in the furnace. The CSR test will become an even more important measure of coke performance.

Figure 5-1-1 (from Chardon and Barry, 1991) illustrates the projected requirements of coke and PCI in European blast furnaces.

Steel producers are increasingly relying on the CSR values of coal to assess their value, which means that it is now important to know what properties in the parent coal influence the CSR value of coke. Fresh-coal physical properties that influence CSR are rheology, rank, ash content and major oxide chemistry of the ash. Oxidation "damages" the rheological properties of the coal and will result in lower CSR values. It should not be forgotten that the dynamics of the coke making process also influence CSR.

For CSR to be a useful screening test for coals, values of CSR obtained on coke from small test pilot coke ovens must be similar to results obtained on the same coal when it is

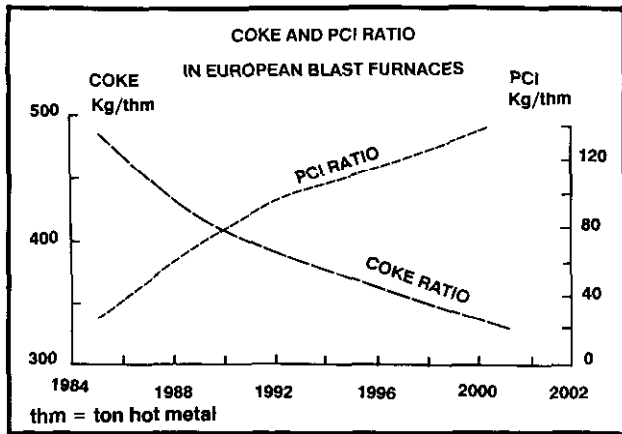


Figure 5-1-1. Plot of projected coke and PCI used in European blast furnaces.

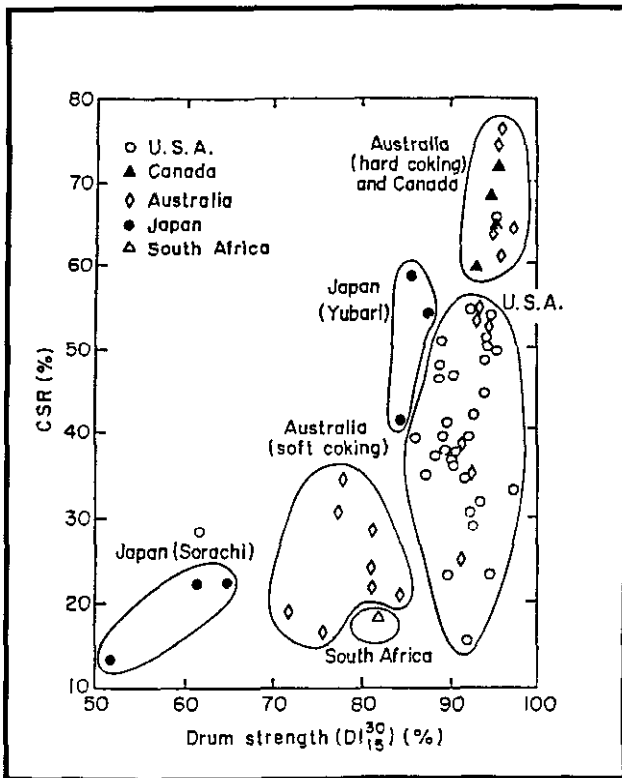


Figure 5-1-2. Plot of CSR versus JIS drum strength, adapted from Figure 5-1-1, Pearson (1989) data from Ishikawa (1983).

coked in an industrial coke oven battery. The experience of steel companies confirms that the CSR values obtained on coke from a pilot oven are in fact similar to values obtained on the same mixture of coal coked under similar conditions in an industrial coke battery.

The original comparison of CSR to other coke properties (Ishikawa, 1983) compared CSR to Japanese Industrial Standard (JIS) drum strength (D 30/15; Figure 5-1-2). This latter property is a measure of the resistance of cold coke to breakage and is similar to the ASTM stability factor test. Pearson (1980, Figure 14) illustrates that the ASTM and JIS

tests behave similarly with reference to petrography and rank. It is obvious from Figure 5-1-2 that CSR does not correlate with cold coke tests. One way of interpreting the diagram is to draw a line from the origin through the point providing the maximum slope so that all points are either on or below the line. If one assumes that under ideal conditions all points should plot on the line then there is some factor which is variably degrading CSR values but which has either no effect or constant effect on the cold coke strength. Canadian and Australian hard coking coals have the least degraded CSR values.

This is to some extent an intuitive and not a scientific argument, but it leads to two important conclusions. Firstly, CSR and cold strength values do not necessarily correlate. The blast furnace operator who wants good stability factors and good CSR values will have to perform both tests or have separate procedures available for predicting both values. Secondly, one must look for a coal parameter, one generally not used to predict cold coke properties, to help in predicting CSR values.

TABLE 5-1-1
EQUATIONS RELATING CSR TO COAL PROPERTIES

A: PRICE ET AL

$$CSR = 56.9 + 0.08268x(c+d) - 6.86 \cdot (MBI)^2 + 11.47 \cdot \bar{R}_{max}$$
 based on 33 Western Canadian Coals (Price et al., 1988)
 (Equation A)

$$CSR = 52.7 + .0882x(c+d) - 6.73x(MBI)^2 + 14.6x\bar{R}_{max}$$
 based on 33 Western Canadian and 22 Appalachian coals
 (Price et al., 1988)

RELATIONSHIP OF FLUIDITY TO DILITATION

$$\text{Log(fluidity)} = .994 + 0.0635x(c+d) - 0.00012x(c+d)^2$$
 (Price and Grandsen, 1987)

This Equation can be approximated by

$$\text{Log(fluidity)} = 0.3891x(c+d) - 0.5894$$
 or

$$(c+d) = 4.97x(\text{Log(fluidity)})^{1.695}$$

B: BHP AUSTRALIA

$$CSR = 133.8 - 15.56x\text{BAR} - 3.1x\text{VM} + 8.5x\text{log(fluidity)} - 0.22x\text{Inerts}$$
 (Equation B)
 (Pearson, 1989)

C: KOBE STEEL

$$CSR = 70.9 \times \bar{R}_{max}\% + 7.8 \times \text{Log(fluidity)} - 89 \times \text{BAR} - 32$$
 (Equation C)
 (Goscinski et al., 1985)

ABBREVIATIONS

c + d = total dilatation
 MBI = modified basicity index

$$MBI = \frac{100x\text{ash}x(\text{Na}_2\text{O} + \text{K}_2\text{O} + \text{CaO} + \text{MgO} + \text{Fe}_2\text{O}_3)}{(100 - \text{VM})x(\text{SiO}_2 + \text{Al}_2\text{O}_3)}$$

\bar{R}_{max} = Mean maximum reflectance
 VM = per cent volatile matter
 ash = per cent ash
 fluidity = maximum fluidity in drum dial divisions per minute (ddpm)
 Log = logarithm to base 10
 Inerts = total inert material in sample

CSR PREDICTION

A number of authors have investigated the possibility of using coal properties to predict CSR values of coke. Gosciniski *et al.* (1985) provide a good summary of some equations that have been developed. Pearson (1989) provides an equation used by BHP Australia. Price *et al.* (1988), have developed an equation for predicting CSR of British Columbia and Appalachian coals using rheology, base-acid ratio and rank. Equations developed by Price *et al.*, BHP and Kobe Steel are outlined in Table 5-1-1.

All three equations introduce ash chemistry as an important variable for predicting CSR. In all probability, ash chemistry is the extra variable that confuses the correlation between cold coke properties and CSR.

The Price Equation (Equation A, Table 5-1-1) uses a modified form of base-acid ratio (modified basicity index; MBI). The rheology term is a measure of total dilatation ($c+d$, Table 5-1-1), measured using a Ruhr dilatometer. It can be converted to an equivalent value of maximum fluidity measured with a Geisler plastometer using a relationship provided by Price and Gransden (1987). Rank is represented in the equation by the mean maximum reflectance of the coal (\bar{R}_{max}).

BHP Australia uses an equation described by Pearson (1989; Equation B, Table 5-1-1), that has some important differences from Equation A. It has terms for base-acid ratio, volatile matter, fluidity and total inerts.

Gosciniski *et al.* (1985) provide an equation (Equation C, Table 5-1-1) used by Kobe Steel which is similar to that of BHP but has no term for the amount of inert material in the sample and therefore cannot respond to changes in ash content.

A computer program has been written to calculate CSR values using Equations A, B and C. Equation A was modified to allow for input of either fluidity or dilatation. The program allows for the consideration of the uncertainties attached to each of the input variables (ash per cent, base-acid ratio, volatile matter, \bar{R}_{max} and maximum fluidity). A specific value of each variable is picked from a gaussian distribution of possibilities defined by a mean and standard deviation for the variable. A number of predictions of CSR using one of the equations scatter about a mean CSR with a standard deviation that is a result of the combined effect of the uncertainties of the input variables. This process illustrates the sensitivity of CSR to fluctuations in the values of variables such as base-acid ratio, fluidity, \bar{R}_{max} and ash per cent.

British Columbia product coking coals are characterized by moderate ash levels, low fluidity and low base-acid ratios. A hypothetical British Columbian coking coal is represented by the following properties: ash, 9.5 per cent; \bar{R}_{max} , 1.35 per cent; fluidity, 50 drum dial divisions per minute and base-acid ratio, 0.10. Table 5-1-2 indicates the sensitivity of CSR to these variables, as predicted by the three equations. At the starting values the three equations agree well with Equation A predicting the lowest values. This equation is also more sensitive to ash chemistry and less sensitive to rank and fluidity than the other two equations. Figure 5-1-3 illustrates the sensitivity of CSR to

changes in base-acid ratio as predicted by the three equations. A CSR value of 57.5 is usually considered to be an acceptable minimum (Price and Gransden, 1987) and this value is indicated in Figure 5-1-3.

The process of varying a single property while keeping the others fixed is not totally justified because the variables are not independent, but it does give an intuitive feeling of how the variables effect CSR over a limited range.

All three equations only apply to medium and low-volatile bituminous coals. The CSR is generally at a maximum in the range high-volatile bituminous to low-volatile bituminous and decreases either side of this rank window.

These coal quality parameters have uncertainties attached to them that derive from measurement errors and also variations from shipment to shipment. If the uncertainties are: ash, 9.5 ± 0.5 per cent; fluidity, 50 ± 10 ddp; \bar{R}_{max} , 1.35 ± 0.05 per cent; and base-acid, ratio 0.10 ± 0.03 , then the coal is predicted to make coke with CSR values of 64 ± 6.0 (Equation A) 64 ± 6.5 (Equation B), or 68 ± 4.3 (Equation C) at one standard deviation. These ranges in CSR values are acceptable when the mean value is high but could cause problems at lower CSR values.

Price *et al.* (1988), plot actual CSR values against CSR values predicted using Equation A. Data scatter about the best fit line. This scatter is caused by measurement errors in

TABLE 5-1-2
CSR PREDICTIONS USING EQUATIONS FROM TABLE 5-1-1

		STARTING COAL						
		Ash %	9.5					
		VM %	23.9					
		Organic Inerts %	30					
		Max Fluidity ddp	50					
		\bar{R}_{max}	1.35					
		BAR	0.10					
		BAR						
Equation	0.06	0.08	0.10	0.12	0.14	0.16	0.18	0.20
A	70.5	67.6	63.8	59.3	53.8	47.1	40.5	32.6
B	64.8	64.5	64.1	63.8	63.5	63.1	62.9	62.6
C	71.6	69.9	68.1	66.3	64.5	62.7	61.0	59.2
		\bar{R}_{max}						
Equation	1.15	1.25	1.35	1.45	1.55	1.65		
A	60.6	62.3	63.8	65.4	66.9	68.1		
B	53.9	59.0	64.1	69.3	74.4	79.1		
C	53.9	61.0	68.1	75.2	82.2	89.1		
		MAX FLUIDITY						
Equation	5	10	50	100	500	1000		
A	60.7	62.3	63.8	65.4	66.9	68.1		
B	55.6	58.2	64.1	66.7	72.6	75.2		
C	60.3	62.6	68.1	70.4	75.9	78.2		

Equations A, B and C from Table 5-1-1

BAR = base-acid ratio

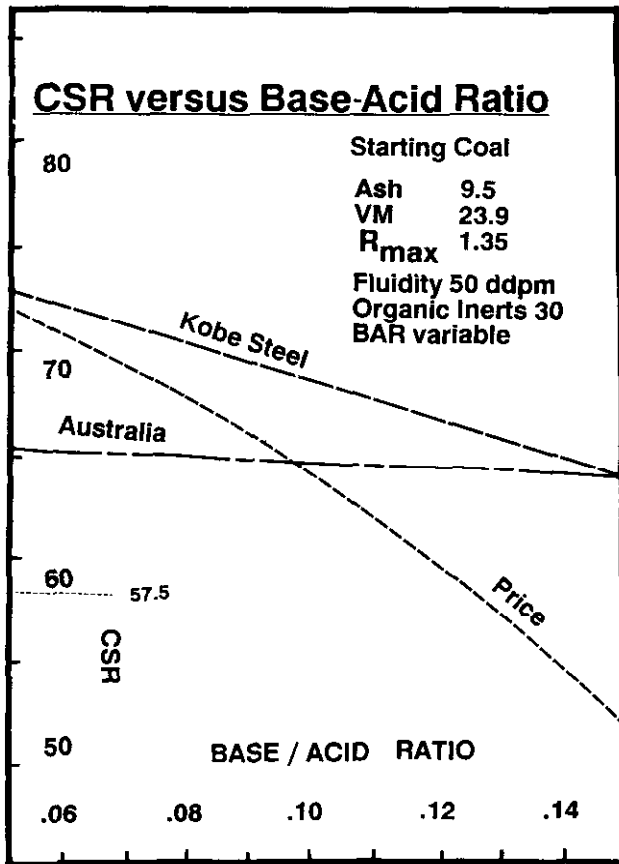


Figure 5-1-3. Plot of CSR versus base-acid ratio illustrating equations in Table 5-1-1.

actual CSR and by the inability of equation A to precisely predict CSR. The one standard deviation error about the line for the data is approximately ± 4.0 CSR units, which is similar to the calculated uncertainty of the predicted CSR values. Within the range of base-acid ratios represented by the samples, the equations can predict CSR well without the introduction of other important variables such as moisture and variations in the coke making process.

ASH CHEMISTRY OF BRITISH COLUMBIA COALS

The major formations in British Columbia that contain reserves of coking coal are the Upper Jurassic to Lower Cretaceous Mist Mountain Formation and the Cretaceous Gates and Gething formations. Possible resources of coking coal exist in the Jurassic Minnes Group and Cretaceous Currier, Comox and Red Rose formations. There is very little coking coal in Tertiary rocks.

Data in this paper illustrate that ash chemistry is probably the most important parameter affecting the CSR of British Columbia coking coals, but coal rank is also important. The rank of coal in the Mist Mountain Formation generally varies from low or medium-volatile bituminous at the base of the formation to high-volatile bituminous at the top. The range in rank in the Gates and Gething formations is similar.

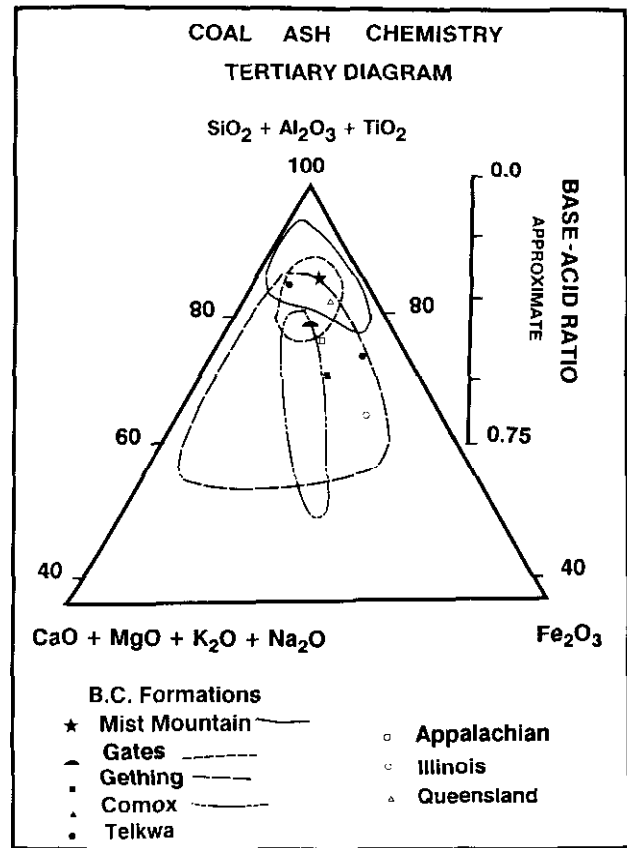


Figure 5-1-4. Tertiary diagram illustrating coal ash chemistry for British Columbia coals.

Coal in the Currier Formation varies from low volatile to anthracite. Coal in the Comox Formation is high-volatile bituminous whereas coal in the Red Rose Formation varies from high-volatile bituminous to semi-anthracite. Coal in these formations is generally not coking.

The ranges of base-acid ratio for most of these formations are illustrated in Figure 5-1-4, which is adapted from Figure 3.7 of Matheson (1986). Most coals from formations in British Columbia have base-acid ratios less than 0.3, although some values for the Gething and Comox formations are higher. Data from Pearson (1981) provide average base-acid ratios for the three major coking coal formations of 0.13 for the Mist Mountain Formation, 0.18 for the Gates Formation, and 0.33 for the Gething Formation (Figure 5-1-4 and Table 5-1-3).

In the Mist Mountain Formation it appears that the base-acid ratio increases up section. Data in Table 5-1-3 which are from the lower half of the formation indicate a weak trend towards higher base-acid ratios up section; average values range from 0.057 at the bottom of the section to 0.21 at the top.

Base-acid ratios from the upper coal-bearing section at Telkwa (Red Rose Formation) vary from 0.13 at the base of the coal section to 0.33 at the top (Table 5-1-3). A single analysis for the lower coal-bearing section provided a value of 0.05, indicating that the lower section might have coking

TABLE 5-1-3
BASE-ACID RATIOS OF COALS FROM SOME BRITISH
COLUMBIA FORMATIONS

Jura-Cretaceous Coking Coal Formations								
Formation	Base-acid ratio	% S.D	Count					
Mist Mountain	0.128	56	8					
Gates	0.179	28	11					
Gething	0.326	56	7					
	SiO ₂	Al ₂ O ₃	TiO ₂	Fe ₂ O ₃	CaO	MgO	Na ₂ O	K ₂ O
Mist Mt	53.3	30.9	1.5	6.2	2.8	0.8	0.15	1.05
Gates	54.5	22.6	1.7	7.0	4.3	1.26	0.75	0.77
Gething	47.2	22.4	1.2	13.4	4.9	1.4	1.1	0.96

Data from Pearson (1981)

Formation	Base-acid ratio	% S.D	Count					
Red Rose Formation Upper Coal-bearing section at Telkwa								
Top	0.327	49	4					
	0.16	69	24					
Base	0.13	25	10					
Mist Mountain Formation Lower Section								
top	0.213	89	8					
	0.07	14	4					
	0.094	35	8					
	0.09		3					
	0.077	60	5					
	0.075	45	20					
Base	0.057	28	4					

Data from assesment reports
S.D. = standard deviation

coal potential in areas where the rank is medium-volatile bituminous or higher.

Most of the coal in the Currier Formation is non-agglomerating because of the high rank. Some coal in the Comox Formation is reported to have good fluidity (Bickford and Kenyon, 1988), but the rank of high-volatile bituminous and moderately high base-acid ratios probably means that the coal will make a weak coke with low CSR values.

Coal in most of the Tertiary coal basins is not coking. One exception is the Seaton coal basin near Smithers which has base-acid ratios averaging 0.16.

PREDICTED CSR VALUES OF BRITISH COLUMBIA COKING COALS

The low base-acid ratios of coal from the Mist Mountain, Gates and Gething formations ensure that, despite low fluidity, cokes from British Columbia coking coals will generally have good CSR values.

Equation A is used to predict ranges of CSR values for possible British Columbian coking coals with 9.5 per cent ash. Figures 5-1-5 and 5-1-6 illustrate the relationship of base-acid ratio to CSR for different values of R_{max} when the

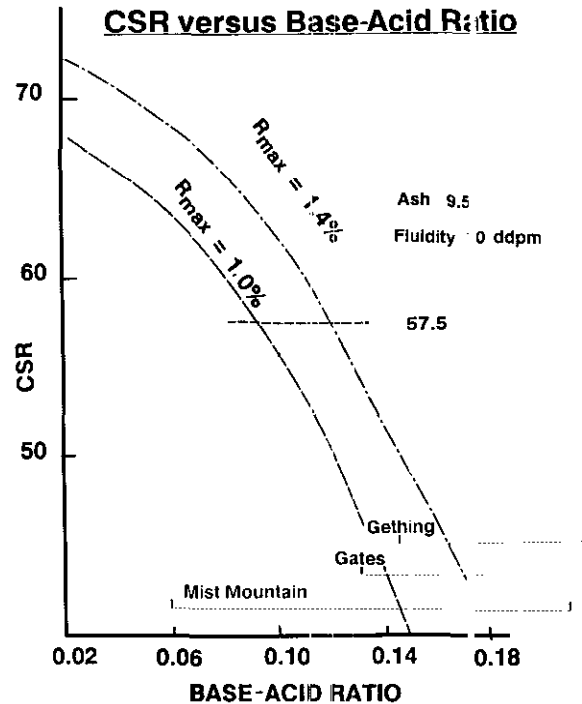


Figure 5-1-5. Plot of CSR versus base-acid ratio as predicted by Equation A for a coal with 9.5 per cent ash and a fluidity of 10 ddpm.

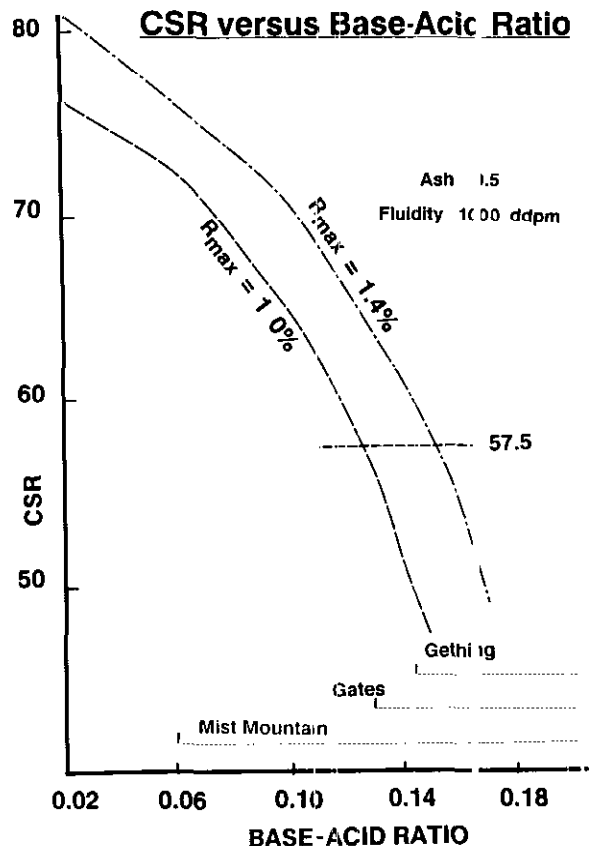


Figure 5-1-6. Plot of CSR versus base-acid ratio as predicted by Equation A for a coal with 9.5 per cent ash and a fluidity of 1000 ddpm.

fluidity is kept constant at 10 ddpm (Figure 5-1-5) and 1 000 ddpm (Figure 5-1-6). The ranges of base-acid ratio for the Mist Mountain, Gates and Gething formations are indicated on the figures. The CSR value of 57.5, which is an acceptable minimum value for coke (Price and Gransden, 1987), is also plotted on the figures. It is apparent that if the base-acid ratio is greater than 0.20 then the coals must be cleaned to an ash much lower than 9.5 per cent to obtain an acceptable CSR value.

The sample to sample variability of base-acid ratios is considerable (Table 5-1-3) and standard deviations are usually greater than 30 per cent. Figure 5-1-7 illustrates how a standard deviation of 30 per cent in base-acid ratio affects the scatter of possible CSR values. What appear to be insignificant changes in low to very low base-acid ratios from one coal batch to the next can cause major changes in CSR.

It is important to recognize which mineral phase in the coal is responsible for causing most of the variation in CSR values. Blast furnace operators require consistent coke quality. Anything that the mine operator can do to ensure this will make the coal more saleable.

The effect that variations in the concentration of an individual mineral phase have on the base-acid ratio of an ash depends on three things;

- the amount of the mineral already in the coal;
- the percentage of the mineral that remains in the ash as oxides after ashing;
- the base-acid ratio of the mineral.

For example, all the quartz in the coal will remain in the ash as SiO_2 and it has a base-acid ratio of 0.0 but because there is usually a lot of SiO_2 in the ash, removal or addition of small amounts of quartz will not have much effect on the base-acid ratio of the ash.

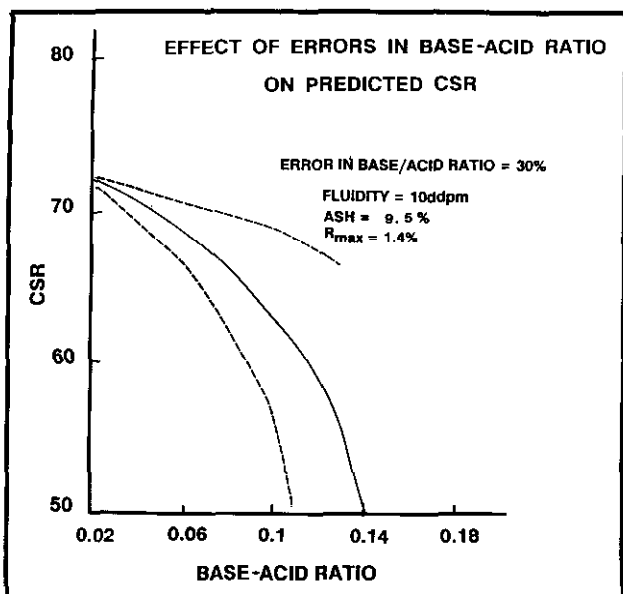


Figure 5-1-7. Plot of the effect of 30 per cent plus or minus errors in base-acid ratio on predicted CSR.

On the other hand pyrite in the coal will contribute all its iron (46.5 weight %) to the ash as Fe_2O_3 and this will have a base-acid ratio of infinity. If the iron content in the ash is not high then small changes in the pyrite concentration of the coal will cause large changes in the base-acid ratio of the ash. The situation is similar for carbonates; for example the calcium in calcite (40 weight %) will remain in the ash as CaO and it has a base-acid ratio of infinity.

Table 5-1-4 illustrates the effect of addition of small amounts of pyrite or carbonate on CSR. For a typical cleaned southeast British Columbia coal with 0.5 per cent sulphur (1.0% or less visible pyrite) a 0.2 per cent increase in pyrite will result in a 12 per cent increase in base-acid ratio and a decrease in CSR of 3 points. Similarly a 0.1 per cent increase in calcite in the coal will result in a 6.0 per cent change in base-acid ratio. Obviously apparently insignificant changes in the pyrite or calcite content of the raw coal can result in surprisingly large changes in CSR.

Minerals such as illite fall midway between quartz and pyrite in terms of their effect on the base-acid ratio of the ash. About 90 weight per cent of the illite remains in the ash

TABLE 5-1-4
EFFECT OF SOME MINERAL ADDITIONS TO COAL ON THE BASE-ACID RATIO OF THE ASH AND ON THE CALCULATED CSR VALUE

STARTING COAL		
Ash	=	10 %
BAR(Base-acid ratio)	=	0.10 %
Sulphur	=	0.5 %
R_{max}	=	1.4 %
Fluidity	=	10 ddpm

EFFECT OF ADDITION OF PYRITE
Pyrite = 46.5 % Fe and 53.5 % Sulphur

Add 0.19 % pyrite to sample
Sulphur of sample increases by 0.1 %
Iron concentration of the sample increases by 0.087 %
This reports to the ash as a 1.24 % increase in Fe_2O_3
BAR to change from 0.10 to 0.112
This causes CSR to decrease from 61.2 to 58.3

If pyrite increases by 0.93 % then sulphur increases 0.5 %
BAR changes from 0.10 to 0.167
This causes CSR to decrease from 61.2 to 41.4

EFFECT OF ADDITION OF CALCITE
Calcite is 56.0 % CaO 44.0 % CO_2

Add 0.1 % calcite to sample
This provides 0.056 % CaO to the coal or 0.56 % to the ash
BAR increases from 0.10 to 0.105
This causes CSR to decrease from 61.2 to 59.8

Addition of 0.5 % calcite to sample
BAR increases to 0.125
This causes CSR to decrease from 61.2 to 55.0

as oxides, but it has a base-acid ratio of about 0.2 which is not markedly different from the composite base-acid ratio of many ashes. Therefore generally small fluctuations in the concentration of illite will not cause major changes in the ratio of the ash.

Correlation analysis of ash oxide data from the lowermost seam in the Mist Mountain Formation indicates that much of the variability of base-acid ratios is related to changes in iron oxide concentrations. The best base-acid ratio versus oxide correlation is for Fe₂O₃ (Table 5-1-5). The iron oxide is negatively correlated with sulphur. Obviously not all of the iron is in the coal as pyrite.

The sulphur content of samples from this seam averages 0.43 and most of it is organic. It appears that as the organic sulphur content increases the iron content decreases. The iron oxide is correlated with calcium and magnesium oxides, indicating either a carbonate or mixed-layer clay

origin. Normative calculations indicate that variations in base-acid ratio are probably related to changes in the low concentration of iron carbonate and possibly pyrite.

Base-acid ratios for the Gates Formation (Table 5-1-5) correlate with iron, calcium and magnesium oxides. Variations in the base-acid ratios are probably caused by variations in the amount of calcite and to a lesser extent clays. Base-acid ratios for the Gething Formation correlate best with magnesium oxide, possibly indicating a chlorite/clay influence on variability in ratios. Iron oxide has a negative correlation to calcium oxide in the Gething Formation. Pearson (1981) did not report sulphur data for these formations although sulphur contents of washed Gates coals are typically less than 0.5 per cent.

Correlation analysis of base-acid ratio and oxide data for coal from the upper coal-bearing section in the Telkwa basin (Table 5-1-5) indicates that variations in base-acid ratios correlate with changes in iron and sulphur concentrations. Changes in the pyrite content must be influencing the variability in base-acid ratios. Normative calculations indicate that most of the iron is present as pyrite with minor amounts present in clays and carbonates.

Iron oxide seems to be one of the most important base oxides responsible for variations in base-acid ratio. Three possible mineral hosts for the iron are pyrite, mixed-layer clays and carbonates. It is obviously important to know the mineral form of the iron. Low-temperature washing of the coal and x-ray diffraction analysis of the residue mineral matter may be a way of identifying changes in the iron carbonate or pyrite content. Using this information it might be possible to influence the base-acid ratio and CSR values by changing the way the coal is mined or washed.

Some coal-washing plants now have on-line radioactive ash monitors that can also detect variations in iron content. Data from these instruments could be used to provide real-time estimates of the CSR values of the coal as it is washed.

A plot of iron versus sulphur in the total coal can help indicate if the iron is mostly in pyrite and can also indicate if there is excess sulphur or excess iron after accounting for pyrite in the coal. If all the iron and sulphur are in the coal as pyrite then the plot should produce a straight line with a slope of 0.871. If iron is in excess then carbonate or clay hosts are probable, and if sulphur is in excess then a pyrite host is probable. Iron in pyrite is probably most responsible for fluctuations in base-acid ratios. Iron versus sulphur data for the Mist Mountain and Red Rose formations are plotted in Figure 5-1-8. Coals from both formations have excess sulphur although the Red Rose (Telkwa) coals have the most.

Actual CSR values of clean coals are generally not published for obvious reasons, but there are sufficient data in the literature to make some estimates. Ash chemistry and rank data for many production coals are available in Price and Gransden (1987). Base-acid ratios for coals from the mines in southeast British Columbia range from 0.06 to 0.11 with Byron Creek higher at 0.285. Values for mines in the northeast range from 0.10 to 0.22. Values for metallurgical coals from Alberta range from 0.127 to 0.22.

TABLE 5-1-5
CORRELATION MATRIX FOR BASE-ACID RATIOS AND
OXIDE DATA

MIST MOUNTAIN FORMATION BASE SEAM (19)						
	Fe ₂ O ₃	CaO	MgO	Na ₂ O	K ₂ O	S
BAR	.954	.942	.819	.032	-.45	-.524
Fe ₂ O ₃		.850	.700	-.041	-.56	-.35
CaO			.830	-.120	-.53	-.56
MgO				-.170	-.38	-.47
Na ₂ O					.31	-.07
K ₂ O						-.19
GATES FORMATION (11)						
BAR	.842	.865	.845	.489	-.180	ND
Fe ₂ O ₃		.497	.697	.179	-.089	ND
CaO			.661	.657	-.332	ND
MgO				.227	.046	ND
Na ₂ O					-.735	ND
GETHING FORMATION (7)						
BAR	.635	.445	.720	.108	-.362	ND
Fe ₂ O ₃		-.408	-.05	-.595	.064	ND
CaO			.906	.819	-.500	ND
MgO				.575	-.324	ND
Na ₂ O					-.639	ND
RED ROSE FORMATION AT TELKWA (66)						
BAR	.802	.366	.4030	-.003	-.058	.681
Fe ₂ O ₃		-.24	-.038	-.004	-.2390	.930
CaO			.6290	-.072	-.555	-.33
MgO				.0050	-.213	-.19
Na ₂ O					.2260	-.02
K ₂ O						.282

BAR = Base-acid ratio
 $BAR = (Fe_2O_3 + CaO + MgO + K_2O + Na_2O) / (SiO_2 + Al_2O_3 + TiO_2)$
 Numbers in parentheses after formation names = data count

IRON VERSUS SULPHUR

IN TOTAL COAL

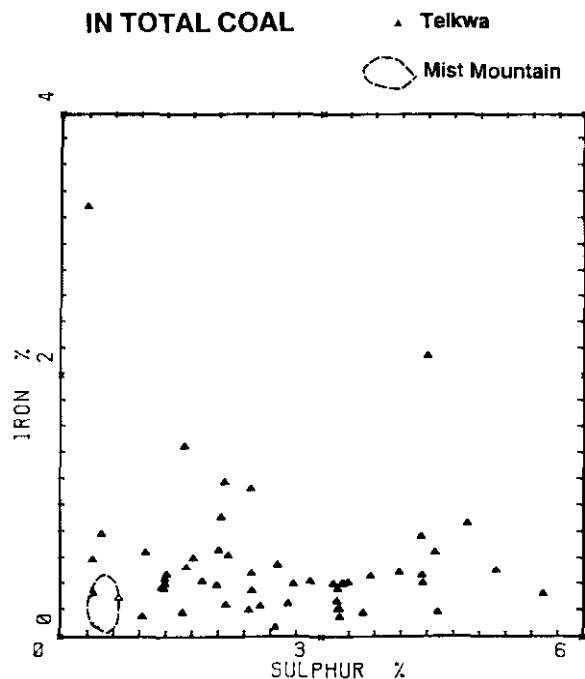


Figure 5-1-8. Plot of iron versus sulphur in Telkwa and Mist Mountain coal.

COMPARISON OF BRITISH COLUMBIA COALS TO OTHER CANADIAN AND INTERNATIONAL COALS

Most Upper Jurassic to Cretaceous coals of British Columbia formed in an environment with very little marine influence. Mineral matter in coal is therefore rich in kaolinite and quartz and has low base-acid ratios. In contrast, most of the bituminous coals in eastern North America formed in paralic environments. The marine influence caused moderate to high pyrite and illite contents, ensuring higher concentrations of iron, potassium and sodium in the ash compared to western Canadian coals.

Base-acid ratios for the Carboniferous coking coals from eastern Canada and eastern U.S.A. are reported in Table 5-1-6. Base-acid ratios of Nova Scotia coals are high, averaging 1.05 (average of 24 analyses reported by Cape Breton Development Corporation in Faurichou *et al.*, 1982) because of high iron oxide contents. The base-acid ratios of eleven Carboniferous coals from Illinois average 0.49 ± 0.11 and seven coking coals from the Appalachian region average 0.23 ± 0.05 (Abernethy *et al.*, 1969).

Eleven coking coals from Queensland, Australia have base-acid ratios averaging 0.21 ± 0.014 (Queensland Coal Board, 1975). This is somewhat higher than base-acid ratios for the Mist Mountain and Gates formations in British Columbia. It appears that some Australian Permian coals are similar to British Columbian coals but that they may contain slightly higher concentrations of iron.

In general eastern Canadian and eastern U.S.A. bituminous coals have high to very high fluidities and wash to a

TABLE 5-1-6
ASH CHEMISTRY DATA FOR EASTERN CANADIAN AND INTERNATIONAL COALS

Location	Base-acid ratio	% S.D.	Count
Nova Scotia	1.05	90	24
Appalachian	0.23	22	7
Illinois	0.49	22	11
Queensland	0.21	69	11

APPALACHIAN COKING COALS (7)

	Fe ₂ O ₃	CaO	MgO	Na ₂ O	K ₂ O	S
BAR	.773	.687	.805	.102	-.214	.45
Fe ₂ O ₃		.226	.354	-.144	-.081	.735
CaO			.68	-.103	-.731	.081
MgO				.405	-.141	.051
Na ₂ O					.503	-.306
K ₂ O						-.178

AVERAGE OXIDE ANALYSIS (7)

SiO ₂	Al ₂ O ₃	Fe ₂ O ₃	CaO	MgO	Na ₂ O	K ₂ O	S
47.2	28.8	10.0	3.23	1.44	0.73	1.97	0.79

QUEENSLAND COKING COALS (11)

	Fe ₂ O ₃	CaO	MgO	Na ₂ O	K ₂ O	S
BAR	.167	.931	.753	.113	-.06	.143
Fe ₂ O ₃		-.19	.099	.525	.185	.064
CaO			.673	-.134	-.173	.139
MgO				.400	-.236	-.175
Na ₂ O					.21	-.353
K ₂ O						-.180

AVERAGE OXIDE ANALYSIS (11)

SiO ₂	Al ₂ O ₃	Fe ₂ O ₃	CaO	MgO	Na ₂ O	K ₂ O	S
50.0	30.2	7.71	5.78	.76	0.5	0.68	0.58

% S.D. = per cent standard deviation

BAR = Base-acid ratio

Note: S is sulphur content in coal sample; oxides are per cent values in ash.

lower ash than western Canadian coals. The improved fluidities are not sufficient to overcome the detrimental effects of high base-acid ratios which will usually ensure that these coals produce cokes with lower CSR values than British Columbia coals.

Equation A was developed using British Columbia and Appalachian coals, which generally do not have base-acid ratios greater than 0.30. The equation cannot be used to predict meaningful CSR values for Nova Scotia coals.

Correlation analysis of the ash oxide data from Appalachian coals (Table 5-1-6) indicates that base-acid

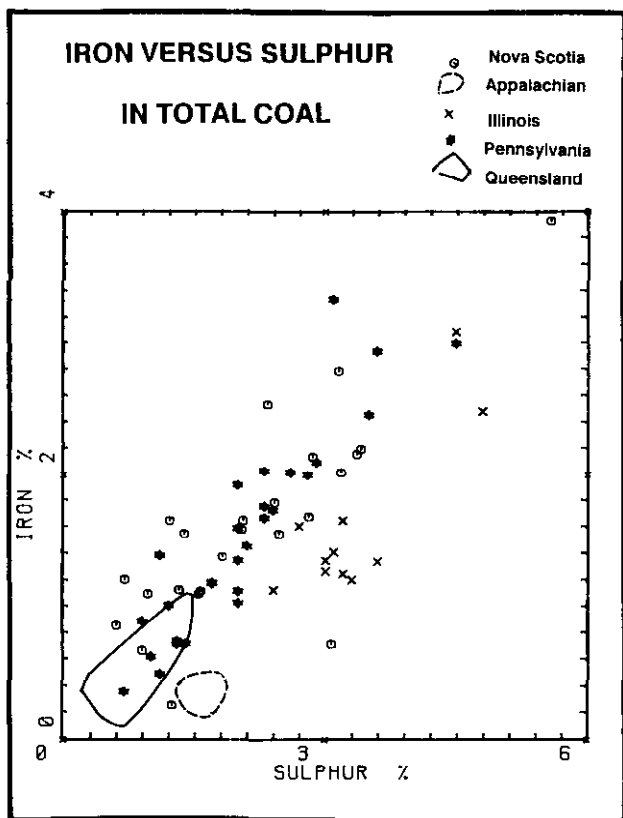


Figure 5-1-9. Plot of iron versus sulphur in some Canadian and international coals.

ratio correlates with iron, calcium and magnesium oxides and that iron oxide correlates with sulphur. Apparently most of the iron is in pyrite and the calcium and magnesium is in clays. In contrast to British Columbia coals calcium oxide correlates with base-acid ratios for the Queensland coals, possibly indicating a carbonate influence on base-acid ratio.

A plot of iron oxide versus sulphur concentrations (Figure 5-1-9) for Pennsylvania and Nova Scotia coals produces linear trends with data plotting near the pyrite line. Data from Illinois and Appalachian coals plot to the right of the pyrite line and indicate excess sulphur.

Base-acid ratios of eastern Canadian and eastern U.S.A. coals are high mainly because of varying amounts of pyrite and possibly iron carbonates. The coals do wash to a low ash and this provides flexibility for blending with British Columbia coals to reduce base-acid ratios.

BLENDING FOR IMPROVED CSR

Recent work investigated the effect on CSR values of coke of adding specific minerals to the parent coal samples (Price *et al.*, 1992). The addition of minerals such as calcite, pyrite and quartz changed the base-acid ratios of the doped coal sample and produced a change in the CSR values of the resultant coke. The CSR values were changed generally in amounts predicted by changes in the base-acid ratios and Equation A. This suggests that CSR values of coal blends can be estimated using the calculated blended base-acid

ratio as long as there is not a wide disparity of rank or rheology.

Equation A predicts that CSR decreases nonlinearly as base-acid ratio increases (Figure 5-1-3). This means that there will be a better than additive improvement in CSR if a high base-acid ratio coal is blended with a low base-acid ratio coal. Table 5-1-2 can be used to provide an example. If two coals A (57% of blend) and B (43% of blend) with BAR/CSR values of 0.06/70.5(A) and 0.20/32.5(B) (line 1, Table 5-1-2) are mixed, then the resulting BAR/CSR values are 0.12/59.3. This is an 82 per cent improvement in the CSR value of coal B and the blend has an acceptable CSR value. There is adequate flexibility to produce blends with good CSR values for the range of base-acid ratios of British Columbia coals.

The study by Price *et al.* (1992) also indicated that the mineral used to produce a change in CSR also had an effect on the CSR value independent of its effect on base-acid ratio. Thus if the base-acid ratio was changed a constant per cent by addition of the appropriate amount of apatite, gypsum, calcite or lime, the decrease in CSR value depended on the mineral (least for apatite most for lime). Similar results were observed for iron. Siderite addition had less effect than pyrite addition which had less effect than adding iron oxide.

This has interesting implications when considering the effect of weathering on CSR. For a property so dependent on ash chemistry one might expect it to be resistant to weathering, which mainly affects coal, not mineral matter. This is not the case, and an answer might be that weathering changes the form of some of the base oxides. For example, pyrite weathers to iron sulphate and in this way increases the detrimental effect of the ash on CSR without actually changing the base-acid ratio.

DISCUSSION

Coke strength after reaction is an important measure of coke quality, especially at a time when the ratio coke(kilogram)/ton hot metal is being decreased by the use of pulverized coal injection (PCI).

A sensitivity analysis using an empirical equation that predicts CSR values provides for a better understanding of the relative importance of ash content, base-acid ratio, rank and fluidity in influencing the resultant CSR. The base-acid ratio of the coal is one of the most important coal properties effecting the CSR of the resultant coke.

Correlation analysis of ash oxide data can indicate which oxides are responsible for variations in base-acid ratio. It then becomes important to identify the mineral host for these oxides. This can be achieved using correlation analysis, iron-sulphur plots, normative calculations or low-temperature ashing combined with x-ray diffraction. Often variations in base-acid ratio are correlated with variations in iron oxide concentration, probably present as pyrite or an iron carbonate. This information may lead to ways of selecting or washing run-of-mine coal for improved CSR.

On-line ash analyzers in coal wash-plants may be able to measure changes in iron content. From these data it might be possible to predict fluctuations in the CSR values of the clean coal before it reaches the customer.

Estimated values of CSR for coal from the major coal-bearing formations in British Columbia are good to excellent. Producers of British Columbian coking coals are fortunate; they generally have base-acid ratios which are lower than the competitor coals in the rest of Canada and in U.S.A. This is an important advantage that should help improve the marketability of British Columbia coals.

Data suggest that for coals with low to moderate base-acid ratios there is a better than additive advantage to blending for improved CSR.

There is a mineralogical influence on CSR which may help explain why CSR is sensitive to weathering while also being strongly dependent on ash chemistry.

CONCLUSIONS

- It is possible to predict CSR values using Equation A and these values compare favourably with measured values.
- For a limited range of bituminous coking coals base-acid ratio is one of the most important factors controlling CSR.
- British Columbia coals generally have good to excellent CSR values.
- It may be possible to predict the CSR of a coal blend using the calculated composite base-acid ratio.
- Because CSR decreases non-linearly with increasing base-acid ratio there is a better than additive advantage to blending for improved CSR.

REFERENCES

Abernathy, R.F., Peterson M.J. and Gibson F.H. (1969): Major Ash Constituents in U.S. Coals; *U.S. Department of the Interior; Bureau of Mines*, Report of Investigations, Number 7240.

Bickford, G.C. and Kenyon, C. (1988): Coalfield Geology of Eastern Vancouver Island (92F); in *Geological Fieldwork 1987*, *B.C. Ministry of Energy, Mines and Petroleum Resources*, Paper 88-1, pages 441-450.

Chardon and Barry (1991): Coal Injection. A Bright Future; *Coal Association of Canada*, 39th Canadian Conference on Coal, Banff, September 15-17th.

Faurschou, D.K., Bonnell, G.W. and Janke, L.C. (1982): Analysis Directory of Canadian Commercial Coals; Supplement Number 4; *Energy Mines and Resources Canada*, CANMET Report 82-13E.

Goscinski, J.S., Gay, R.J. and Robinson, J.W. (1985): A Review of American Coal, Quality and its Effect on Coke Reactivity and After Reaction Strength of Cokes; Part 1 and 2, *Journal of Coal Quality*, Volumes 2 and 4, pages 21-29 and 35-43.

Ishikawa, Y. (1983): Relationship between Coke Behavior in the Lower Part of the Blast Furnace and Blast Furnace Performance; 18th Iron and Steel Smelting Research Symposium at Tohoku University.

Matheson, A. (1986): Coal in British Columbia; *B.C. Ministry of Energy, Mines and Petroleum Resources*, Paper 1986-3.

Pearson, D.E. (1980): The Quality of Western Canadian Coking Coal; *Canadian Institute of Mining and Metallurgy*, Bulletin Volume 73, pages 70-84.

Pearson, D.E. (1981): Geology of Western Canadian Coals and Quality; Coal Preparation Course, *The University of British Columbia*, November 1981.

Pearson, D.E. (1989): Influence of Geology on CSR (Coke Strength After Reaction with CO₂); in *Advances in Western Canadian Coal Geoscience. Forum Proceedings*; Langenberg, W., Editor, pages 174-183.

Price, J.T. and Gransden, J.F. (1987): Metallurgical Coals in Canada: Resources, Research and Utilization; *Energy Mines and Resources Canada*, Canmet Report 87-2E.

Price, J.T., Gransden, J.F. and Khan, M. A. (1988): Effect of the Properties of Western Canadian Coals on their Coking Behaviour; *American Institute of Mining Engineers*, Proceedings.

Price, J.T., Gransden, J.F., Khan, M. A. and Ryan, B.D. (1992): Effect of Selected Minerals on High Temperature Properties of Coke; Abstract.

Queensland Coal Board. (1975): Physical and Chemical Properties and Classification; *Queensland Coal Board*, Brisbane, Australia.



WASHABILITY OF LITHOTYPES FROM A SELECTED SEAM IN THE EAST KOOTENAY COALFIELD, SOUTHEAST BRITISH COLUMBIA. (85J/2)

By Maria E. Holuszko

KEYWORDS: Coal geology, coal quality, Greenhills, washability, degree of washing, washability number, coal petrography, mineral matter, lithotypes.

INTRODUCTION

This study is part of the Coal Quality project, and involves washability characteristics of British Columbia coals. The first two parts of the project involved collection and analysis of washability data from assessment reports (Holuszko and Grieve, 1990; Holuszko, 1991). The washability characteristics of coals from different regions, geological formations and seams were studied using classical washability parameters, together with the washability number and degree-of-washing. The latter were found to be more appropriate for comparing inherent washability characteristics. This part of the study focuses on the analysis of the washability of different lithotype samples, collected from faces at producing coal mines.

During the 1991 field season a number of lithotype samples were collected from two mine sites: Line Creek and Greenhills in southeast British Columbia. All of the seams belong to the Mist Mountain Formation. The sampling was carried out in cooperation with Dr. A. Cameron of the Institute of Sedimentary and Petroleum Geology, Calgary. Samples collected from Greenhills 16-seam were chosen for the washability study using degree-of-washing and washability number parameters.

BACKGROUND

LITHOTYPES AS INDICATORS OF DEPOSITIONAL HISTORY OF THE COAL SEAM

Lithotypes are defined as macroscopically recognizable bands of coal, based on variations in brightness. They are assumed to reflect original contributions of organic material, and the physical and chemical conditions during and after peat accumulation (Kalkreuth and Leckie, 1989). For example, the height of the water table is believed to play an important role (Diessel, 1982; Cohen, 1984). The bright and banded bright coal lithotypes indicate formation in a wet forest mire, while banded and banded dull were formed in a moderately wet forest mire or in an open mire environment with a higher water table (Kalkreuth *et al.*, 1991).

Frequently, both lithotype description and maceral composition are used to provide information on depositional environment (Kalkreuth and Leckie, 1989). Based on maceral composition, a number of indices are derived, and these

are used to outline depositional environment with much greater precision (Diessel, 1986).

Detailed studies defining coal facies, using lithotype and maceral data, have been completed on coals from the Lower Cretaceous Gates Formation in Western Canada (Lamberson *et al.*, 1989, 1991). For these coals it was found that vitrinite content decreases from bright to dull while inertinite and liptinite increase in parallel with mineral matter. The most variation in petrographic composition is associated with dull lithotypes. Macroscopically similar dull coal bands show significant differences in their microscopic composition.

Generally, the petrographic composition of the individual lithotypes has been proved to be consistent for various coal seams (Hower *et al.*, 1990; Lamberson *et al.*, 1991; Kalkreuth *et al.*, 1991).

LITHOTYPES AS INDICATORS OF QUALITY VARIATIONS

The fundamental differences in maceral and lithotype composition account for differences in physical properties of coal (Jeremic, 1980; Stach *et al.*, 1982; Tsai, 1982; Hower *et al.*, 1987; Hower, 1988). This can have an influence on the mining, preparation and utilization of coal.

The density of lithotypes varies significantly, with the bright lithotypes having the lowest density and the dull lithotypes rich in mineral matter the highest. Porosity and mechanical properties such as strength, hardness and friability are also strongly dependent on lithotype composition (Hower *et al.*, 1987, 1990; Falcon and Falcon, 1987; Hower, 1988; Hower and Lineberry, 1988). The relationship between lithotypes and their variation in grindability index (GFI) has also been established (Hower *et al.*, 1987; Hower, 1988; Hower and Lineberry, 1988). Differences up to 40 units in grindability index have been observed between lithotypes. Dull lithotypes with a dominance of trimaceral microlithotypes, especially those rich in liptinite, are more resistant to breakage and grinding than those rich in vitrinite and inertinite.

The floatability of lithotypes has been studied, confirming that lithotypes have different responses to flotation, due to varying degrees of hydrophobicity (Horsley and Smith, 1951; Sun, 1954; Klassen, 1966; Holuszko, 1991).

It is also expected that the washability of a whole seam, as derived from density separation, will be influenced by the lithotype composition. Varying ease of washing for different lithotypes is expected due to their varying mineral and maceral composition (Falcon and Falcon, 1987).

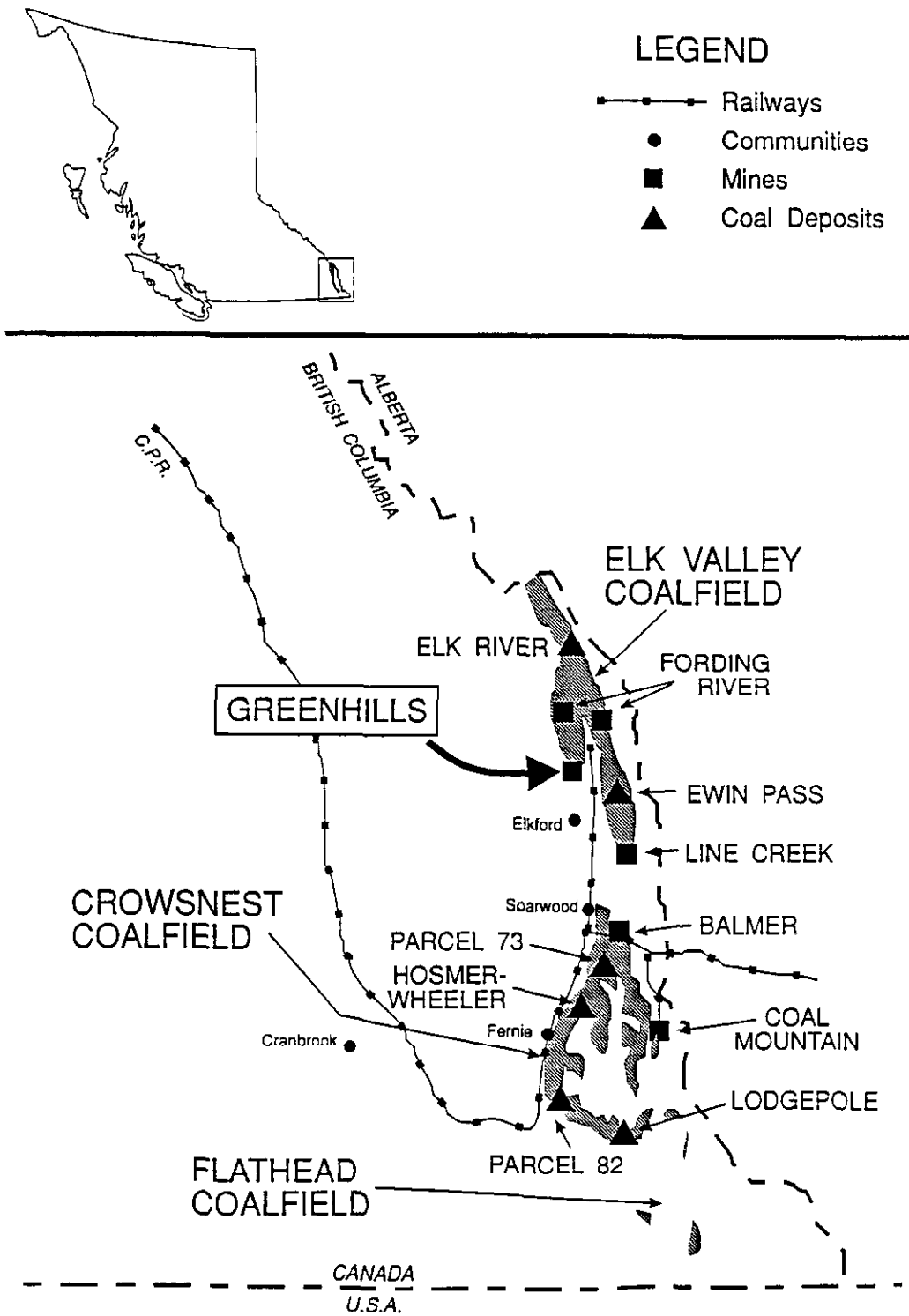


Figure 5-2-1. Location of Greenhills mine.

FACTORS INFLUENCING WASHABILITY AND MEANING OF WASHABILITY NUMBER

The washability of a coal seam is directly related to the amount, type and, most importantly, the association of minerals with the coal. The way in which mineral matter is incorporated in a coal seam is a direct result of the sedimentation conditions that prevailed during its formation. Mineral matter in coal originates from a variety of sources. Some is incorporated in original plant material (chemically bound), some is washed or blown into the mire during peat formation (epiclastic), some is precipitated during the very earliest peat accumulation stage (syngenetic), and some is subsequently introduced by migrating mineral-forming solutions (epigenetic).

Depending on the relative abundance of each type, liberation of these minerals will range from impossible (chemically bound minerals) to easy (epiclastic and epigenetic minerals). The ease of washing will depend on liberation of mineral matter at any given size range of coal. Breaking and crushing during coal preparation leads to separation first of minerals formed along the bedding planes, and successively the syngenetic minerals as the size approaches that of the mineral grains. Liberation of mineral matter from coal is also a function of the physical characteristics of the parent coal, and these are controlled by the lithotype composition (Hower and Lineberry, 1988).

The ease or difficulty of washing is usually related to the yield of clean coal at a particular ash level, and the amount of near-gravity material at the density of separation for a specified coal product. These parameters, however, are coal dependent, and they are not reliable when comparing coals of different origin. Two parameters, degree of washing and washability number, have been established to describe the inherent washability characteristics of a coal (Sarkar and Das, 1974; Sarkar *et al.*, 1977; Sanders and Brooks, 1986; Holuszko and Grieve, 1990; Holuszko, 1991).

The degree of washing, when calculated at each density of separation and plotted against density of separation or yield of clean coal, forms a curve. The maximum on this curve reflects the optimum cut-point for separation. In other words, the maximum advantage in separating coal is expected at this optimum point, giving the highest yield of the cleanest product possible. The ratio of optimum degree of washing to the clean coal ash at this point is the value described as the washability number.

The degree of washing at any specific gravity cut-point is expressed as follows:

$$N = w(a-b)/a$$

where: a = the ash content of the raw coal (feed)

b = the ash content of the clean coal at a given density of separation

w = the yield of clean coal at a given density of separation

The washability number is calculated from the following equation:

$$W_n = 10(N_{opt}/b_{opt})$$

where: b_{opt} = ash content at N_{opt} .

It has been shown that the washability number can be a very useful tool in the study of coal seams as rock units (Sarkar and Das, 1974; Sarkar *et al.*, 1977). The way it is

expressed defines the boundary between free (removable) mineral matter and mineral matter associated with coal (fixed) and at the same time it gives an idea of the optimal conditions for separation. According to Sarkar, washability number represents the effect of the depositional conditions on the association of coal with mineral matter. It has been shown by the same authors that washability numbers are higher for coal seams formed under quiescent conditions (autochthonous) as opposed to those formed under turbulent conditions (hypoautochthonous). Lateral changes in washability number were used to outline patterns of depositional environment for some Indian and North American coals.

Comparative studies of washability numbers for coal seams in different formations in British Columbia show significant diversity (Holuszko, 1991). Variations in the washability number are also evident among different seams from the same geological formations. For some formations, there is an apparent trend in increasing washability numbers for coal seams higher in the formation, while for others no trend is evident.

The variations in quality within each seam are lithotype dependent, and each lithotype represents a change in the depositional environment. Therefore, it is expected that ease of washing, as measured by washability number, will vary for different lithotypes.

SAMPLES AND PROCEDURES

Lithotype samples from the Mist Mountain Formation of southeast British Columbia were collected from a number of producing seams. These coals range from high-volatile A to low-volatile bituminous in rank. In general, they are characterized by low sulphur content. Metallurgical products have good to excellent coking properties, while thermal products are also attractive due to their high rank and low sulphur content.

In terms of depositional history, coals of the Mist Mountain Formation were deposited along a broad coastal plain with numerous high-energy wave-dominated deltas (Kalkreuth and Leckie, 1989). The coal seams in the lower part of the formation are believed to have formed in open swamps with free movement of water (Cameron, 1972). Seams from the upper part of the formation were deposited in a fluvial to upper delta plain. These are thinner and vitrinite dominated, which indicates formation under forest bog conditions in stagnant water (Kalkreuth and Leckie, 1989).

Samples of lithotypes from Greenhills 16-seam were chosen for the detailed washability studies. This seam is located in the upper part of the Mist Mountain Formation, and its thickness exceeds 10 metres. This seam has contributed more than 80 per cent of the recent coal production from this property. It is classified as medium-volatile bituminous and is used as metallurgical coal. The location of the Greenhills mine is shown in Figure 5-2-1.

A total of 33 lithotype samples from Greenhills 16-seam were collected. Due to the small size of some of the samples, only 18 samples were used for sink-and-float studies. These represented six lithotypes: bright; landed bright; banded coal; banded dull; dull and sheared coal (Table 5-2-1).

TABLE 5-2-1
LITHOTYPE CLASSIFICATION SCHEME
(modified from Diessel, 1965; Marchioni, 1980)

BRIGHT	subvitreous to vitreous lustre, conchoidal fracture, less than 10% dull coal laminae.
BANDED BRIGHT	predominantly bright coal with 10-40% dull laminae.
BANDED COAL	interbedded dull and bright coal in approximately equal proportions
BANDED DULL	dull coal with approximately 10-40% bright laminae.
DULL	matte lustre, uneven fracture, less than 10% bright coal laminae, hard.
FIBROUS	satiny lustre, very friable, sooty to touch.
SHEARED COAL	variable lustre, disturbed bedding, numerous slip/slickenside surfaces, very brittle.

SAMPLING TECHNIQUES

Lithotypes were collected according to the modified Australian classification (Diesel, 1965; Marchioni, 1980). As a general rule, a coal band is considered to be a mixture of bright and dull components, and lithotypes are defined according to the proportions of the basic ingredients. A minimum thickness of 5 centimetres was used to delineate lithotypes, following the procedure of Lamberson *et al.*, (1989). The lithotype profile of 16-seam is reconstructed in Figure 5-2-2.

ANALYSIS

All lithotype samples were processed for proximate, specific gravity and HGI analyses. The chemical and sink-and-float analyses were performed by Loring Laboratory in Calgary. The data in Table 5-2-2 represent analyses of Greenhills 16-seam. The average values were calculated for each lithotype group.

SINK-AND-FLOAT TESTS

Sink-and-float analyses were performed on the coarse size fraction (0.50 to 9.5 mm) prepared from each lithotype sample, in seven gravity fractions: 1.30; 1.35; 1.40; 1.45; 1.50; 1.60 and 1.70 grams per cubic centimetre. The ash content was determined on the float fractions and the cumulative yield and ash values were computed. These were further used to derive degree-of-washing values at each density of separation and washability number (W_n) at the density corresponding to the optimum degree of washing (N_{opt}).

MACERAL ANALYSIS

Maceral analyses were accomplished by counting 500 points on each sample. Petrographic composition on a mineral-matter-free basis was calculated as an average value for each lithotype. The average maceral composition of all lithotypes in Greenhills 16-seam is depicted in Figure 5-2-3.

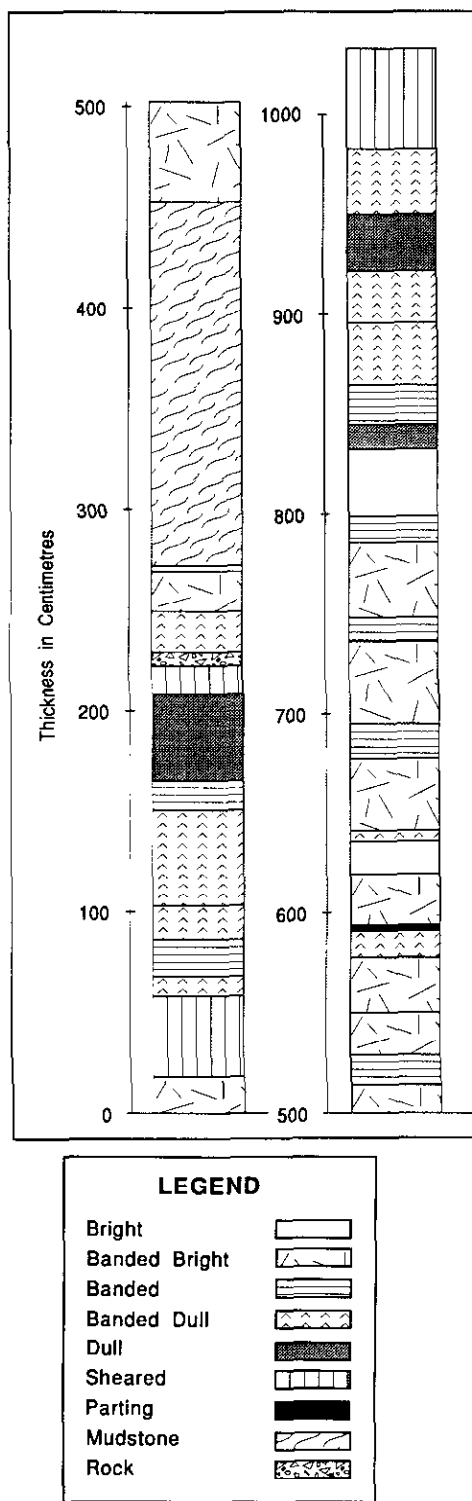
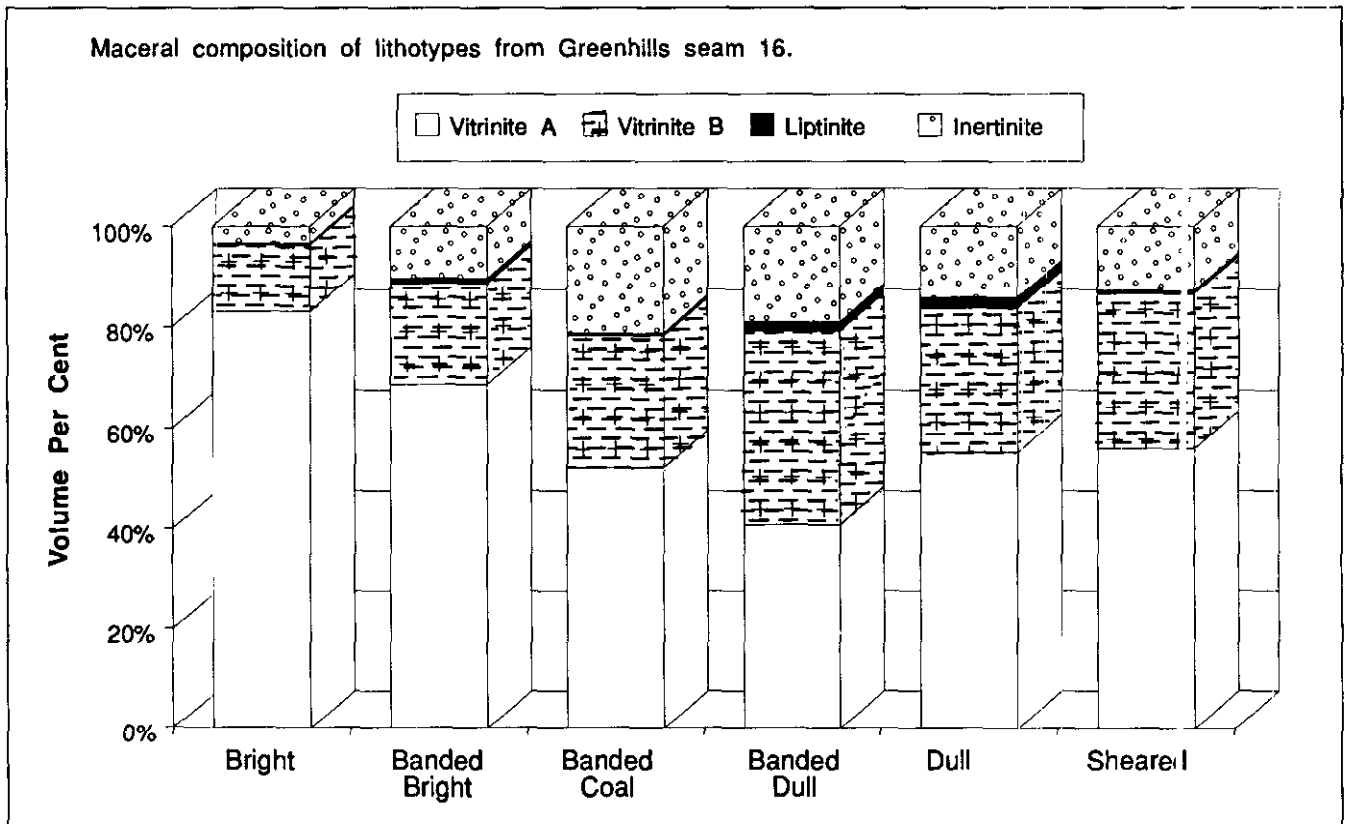


Figure 5-2-2. Profile of Greenhills 16-seam.

TABLE 5-2-2
 PROXIMATE ANALYSES, SPECIFIC GRAVITY
 AND HGI VALUES FOR GREENHILLS
 16-SEAM LITHOTYPES

Lithotype	Volatile Matter	Fixed Carbon	Ash	Specific Gravity	HGI
Bright (3)	28.02	68.44	3.53	1.26	99
Banded Bright (9)	28.31	65.21	6.48	1.29	91
Banded Coal (7)	26.61	68.40	4.99	1.29	101
Banded Dull (9)	25.37	61.35	13.28	1.36	90
Dull (3)	28.28	61.46	10.25	1.36	109
Sheared (3)	23.93	52.60	23.47	1.44	125



	Vitrinite A	Vitrinite B	Liptinite	Inertinite
Bright (3)	83.1	13.2	0.4	3.3
Banded Bright (9)	68.3	20.0	1.1	10.2
Banded Coal (7)	52.1	26.1	0.6	21.2
Banded Dull (9)	40.8	38.3	2.0	18.9
Dull (3)	55.2	28.4	2.3	14.1
Sheared (3)	55.9	30.7	0.7	12.7

Vitrinite A = Telinite, Collinite, Telocollinite

Vitrinite B = Vitrinite A + MM or Vitrodetrinite

Figure 5-2-3. Average maceral analyses of lithotypes in Greenhills 16-seam.

RESULTS

PETROGRAPHIC ANALYSES

The lithotype profile of Greenhills 16-seam (Figure 5-2-2) shows that it is composed predominantly of banded lithotypes, with banded bright as the most abundant. The base of the seam is rich in banded dull lithotypes, the middle part contains a thick mudstone parting, indicating frequent flooding, and above it the seam becomes predominantly banded bright. In the top of the seam the composition changes gradually to banded dull and dull. Sheared coal is present in the uppermost and lowermost parts of the seam.

On average, bright lithotypes are rich in total vitrinite (vitrinite A plus vitrinite B) reaching 96 per cent by volume (Figure 5-2-3). Vitrinite content decreases from bright to banded dull lithotypes; the average value in banded bright coal is 88.7 per cent, and in banded dull lithotypes its value decreases to 79 per cent. The ratio of vitrinite A to vitrinite B decreases in parallel with the decrease in total vitrinite, with the exception of the dull lithotype. Sheared coal is rich in vitrinite and its ratio of vitrinite A to vitrinite B is similar to that of dull coal. Plate 5-2-1 illustrates examples of macerals found in the lithotypes from Greenhills 16-seam.

The opposite trend is observed for intertinite in various lithotypes, the highest content being associated with the duller bands of coal. The exception again is for the dull lithotype. The liptinite content of these samples is negligible. The highest values, however, occur in banded and dull lithotypes (2.0 and 2.3% respectively).

CHEMICAL ANALYSIS

Proximate analytical values vary between different lithotypes (Table 5-2-2). Volatile matter decreases with decrease in brightness from bright to banded dull, and the lowest value is in sheared coal. Ash content increases from bright to banded dull lithotypes, with a discrepancy for the dull lithotype, and highest ash is associated with the sheared coal. The specific gravities follow a similar pattern of increase in value with decrease in brightness.

The grindability index (HGI) values are somewhat less predictable. The highest grindability is associated with the sheared coal and dull lithotypes, followed by the banded coal and bright lithotypes. Banded dull coal has the lowest grindability.

WASHABILITY CHARACTERIZATION

The washability numbers and optimum degree of washing, together with the parameters associated with the optimum cut point, such as density of separation and clean-coal ash at optimum, are presented in Table 5-2-3. For comparison, the average values are also calculated.

The highest washability numbers and the lowest clean-coal ash values (at the optimum) are associated with the bright lithotypes, and equal 289.4 and 1.62 per cent, respectively. The average washability number for the banded bright lithotype is 167.1, with clean-coal ash value of 2.75

TABLE 5-2-3
WASHABILITY NUMBER, DEGREE-OF-WASHING
AND OTHER WASHABILITY PARAMETERS
FOR SELECTED LITHOTYPES

Lithotype	Raw Ash	W_N	N_{opt}	d_{opt}	CC_{opt}
Bright	5.16	338.06	55.78	1.35	1.65
	2.88	240.54	39.93	1.35	1.66
	3.01	289.80	45.18	1.35	1.56
	Average	3.68	289.40	46.96	1.35
Banded Bright	11.69	89.90	43.69	1.35	4.86
	7.71	178.02	52.16	1.35	2.93
	5.70	173.18	47.45	1.35	2.74
	3.40	123.83	29.10	1.35	2.35
	1.76	295.61	33.70	1.35	1.14
	4.02	141.97	35.21	1.35	2.48
Average	5.71	167.09	40.22	1.35	2.75
Banded Coal	7.30	63.00	28.79	1.35	4.57
	10.19	61.67	30.96	1.35	5.02
	9.18	47.90	27.60	1.35	5.76
	4.07	200.64	42.15	1.35	2.08
	2.45	178.89	30.02	1.35	1.68
	Average	6.64	110.38	31.90	1.35
Banded Dull	6.79	82.19	30.82	1.35	3.75
	49.04	4.16	5.86	1.70	33.67
	13.55	51.08	35.91	1.40	7.03
	Average	23.13	45.81	24.20	1.48
Dull	5.92	90.20	31.66	1.35	3.51
Sheared	23.06	79.25	49.85	1.50	6.26

W_N = Washability number
 N_{opt} = Degree of washing @ optimum
 d_{opt} = Density of separation @ optimum
 CC_{opt} = Clean coal ash @ optimum

per cent. The banded coal washability number is about 110, with the clean-coal ash 3.82 per cent. A significant decrease in washability number is observed in the banded dull lithotype (45.81), with a sharp increase in ash content to 14.82 per cent for the clean coal at the optimum. The washability number for the dull lithotype is much higher than for banded dull, and does not follow the general trend. The sheared coal washability number (79.25 and ash of clean coal at 6.26%) was found to be higher than that for the banded dull lithotype, and lower than for banded coal.

From the analysis of maceral composition and washability numbers (Table 5-2-4), it is evident that washability numbers decrease with decrease in brightness from bright to banded dull lithotypes, and this is accompanied by a decrease in total vitrinite. The ratio of vitrinite A to vitrinite B follows the same trend.

SUMMARY AND CONCLUSIONS

Examination of washability characteristics of lithotypes collected from Greenhills 16-seam suggests the following conclusions.

The change in brightness of lithotypes is a result of changing maceral composition from vitrinite rich to intertinite rich, and generally the increase in mineral matter content (ash) from bright to dull lithotypes. Bright lithotypes are rich in vitrinite A and the ratio of vitrinite A to vitrinite B decreases with decrease in brightness.

The amount of total vitrinite in the dull lithotype is similar to that of the banded bright lithotype, while the ratio of vitrinite A to vitrinite B is similar to the banded coal category. According to Kalkreuth *et al.* (1991) there are two

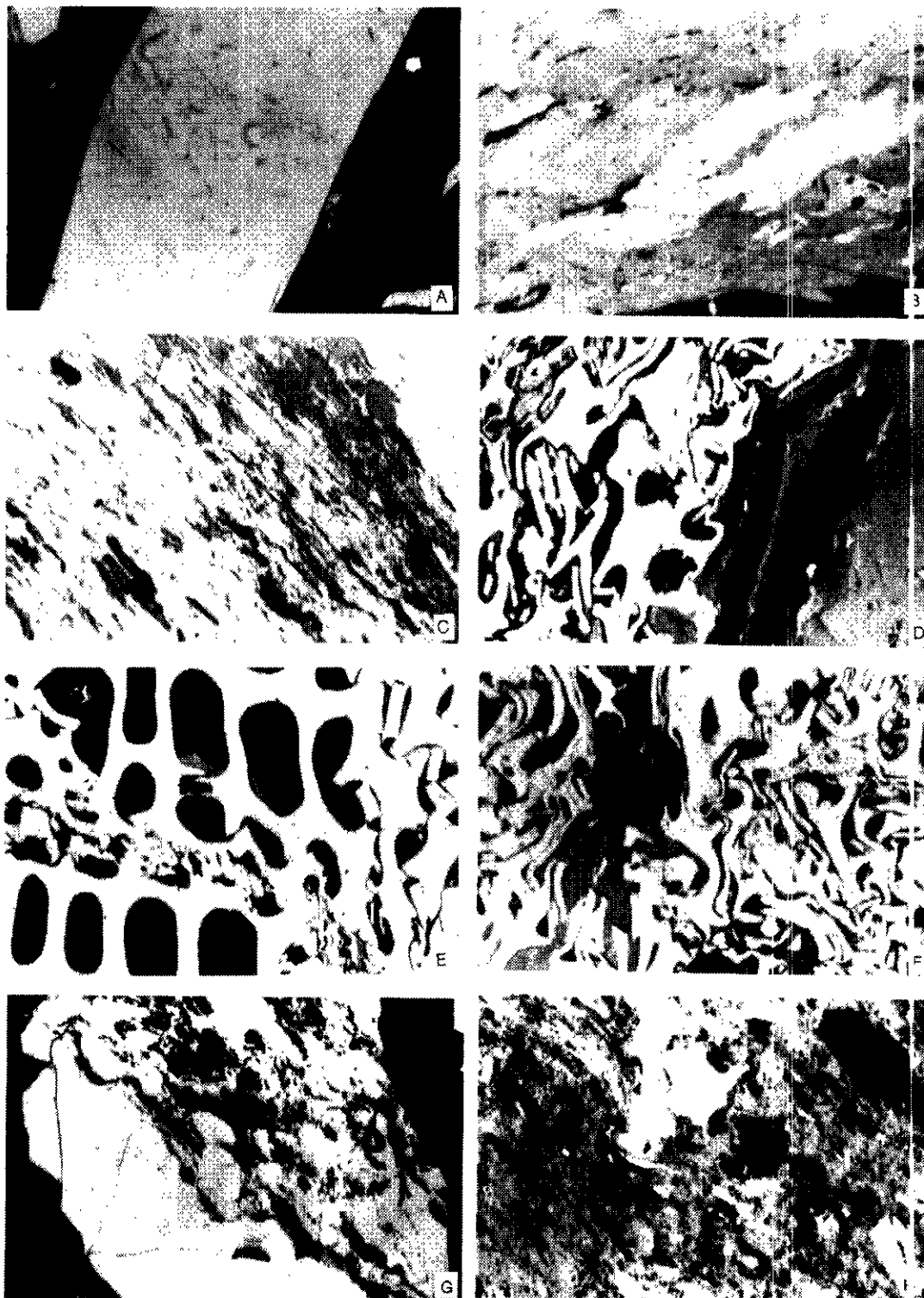


Plate 5-2-1. Macerals in Greenhills seam-16. A) Vitrinite A type. B) Vitrinite B type with semifusinite and liptinite macerals. C) Vitrinite and massive occurrence of liptinite. D) Fusinite (left) and mega-cuticle occurrence and vitrinite (right). E) Fusinite with cell structure preserved. F) Fusinite and resin (dark grey) filling the cavity in fusinite. G) Vitrinite A type with clays. H) Vitrodetrinite (matrix) with inertodetrinite macerals.

TABLE 5-2-4
WASHABILITY NUMBER AND MACERAL
COMPOSITION OF SELECTED LITHOTYPES
FROM GREENHILLS 16-SEAM

Lithotype	Raw Ash	W _N *	Maceral Composition			
			Vitrinite A	Vitrinite B	Inertinite	Liptinite
Bright	5.16	338.06	86.4	12.4	1.0	0.2
	2.88	240.54	80.8	14.6	4.2	0.4
	3.01	289.60	82.2	12.6	4.6	0.6
	Average	3.68	289.40	81.9	13.0	3.3
Banded Bright	11.69	89.90	53.6	37.2	7.8	1.6
	7.71	178.02	71.6	25.0	1.8	1.6
	5.70	173.18	73.6	16.2	9.8	0.4
	3.40	123.83	82.4	12.4	4.6	0.6
	1.76	295.61	83.6	3.6	12.2	0.2
	4.02	141.97	78.6	12.2	7.2	2.0
	Average	5.71	167.09	73.9	17.8	7.2
Banded Coal	7.30	63.00	37.4	34.6	27.2	0.8
	10.19	61.67	46.2	19.2	33.2	1.0
	9.18	47.90	23.0	48.4	27.6	1.0
	4.07	200.64	41.2	35.4	23.0	0.4
	2.45	178.69	91.0	5.4	2.0	-
	Average	6.64	110.38	47.8	28.6	22.8
Banded Dull	6.79	82.19	38.8	21.2	36.2	0.8
	49.04	4.16	18.4	79.4	1.6	0.6
	13.55	51.08	18.0	56.4	24.4	1.2
	Average	23.13	45.81	25.1	52.3	20.7
Dull	5.92	90.20	40.2	36.0	22.6	1.2
Sheared	23.06	79.25	80.8	12.4	5.6	0.8

* W_N = Washability number

types of dull lithotypes, one representing a moderately wet forest mire, and referred to as "dry", and the other "wet", indicating high water tables with a strong influence of open mire or marsh environments. In terms of maceral make-up the "wet" dull coal is similar to banded bright and banded coal lithotype composition. It is reasonable to assume that the dull lithotype studied here is the "wet" dull type.

For the dull lithotypes examined for washability, a combination of three factors may have controlled their appearance, as shown in Table 5-2-4. These are: increased inertinite, vitrinite B and, to some extent, liptinite content.

The variation in washability numbers among lithotypes observed here is very wide (Table 5-2-3). The washability numbers associated with the bright lithotypes are the highest, and are accompanied by the lowest ash content in clean coal at the optimum. In general, the variation in washability numbers is narrowest for the bright lithotypes, and this is also true for the ash of clean coal at the optimum. Bright lithotypes are vitrinite rich, with very low ash content. These were presumably formed under quiescent conditions with very little introduction of mineral matter, and this resulted in high washability numbers and low clean-coal ash at the optimum.

For banded bright lithotypes, the range of washability numbers is quite broad, with great variation in raw and clean coal ash content at the optimum. The variation in degree of washing and washability number becomes narrower for the banded coal. However, raw and clean-coal ash values still vary considerably.

The variation in washability numbers is always much greater for banded than for bright lithotypes. For the samples where an increase in raw ash is the probable cause of the dull appearance, the range of variation in washability number becomes narrower. This is because the amount and type of mineral matter (ash) has a major influence on the

magnitude of the washability number. It is also important to note that the density of separation at the optimum point, (d_{opt}), is constant and equal to 1.35 grams per cubic centimetre for all lithotypes, except those with high raw ash content, and sheared coal. This may indicate that for these lithotypes, the optimum point occurs at the same density, regardless of their composition. The clean-coal ash, however, increases from bright to banded dull, indicating different associations of mineral matter in different lithotypes.

The mineral matter and its association are the major factors in defining washability characteristics. It is not always the amount of mineral matter (raw ash) but type (association with coal) which contributes to the washability characteristics. For example, two different lithotypes, bright and banded bright, with similar raw ash contents, and similar maceral compositions, have quite different washability numbers (Table 5-2-4). This may indicate that the specific association of mineral matter with coal in one sample makes this coal look duller (due to its disseminated occurrence) and also contributes to the lower washability number, ($W_n=123.83$ for banded bright, compared to 289.60 for bright lithotype).

Assuming that washability numbers indicate variation in depositional environment, the actual decrease in the magnitude of this number, in conjunction with the decrease in the clean-coal ash at the optimum, suggest that moving towards the duller lithotypes the depositional conditions changed from wet forest mire to open mire. This is also in agreement with the change in maceral compositions, particularly the decreasing ratio of vitrinite A to vitrinite B towards duller lithotypes. Vitrinite A, representing structured vitrinite macerals, indicates a more preserving depositional environment, and reflects deposition conditions with less frequent changes in water level. This results in less mineral matter deposition. Vitrinite B, representing vitrodetrinite and vitrinite associated with mineral matter, indicates macerals of detrital origin, usually characterized by more degraded organic matter and a higher mineral matter content.

Knowledge of the variation in washability with change in lithotype composition may be a useful tool for predicting the washability characteristics of a seam. An attempt was made here to calculate a seam washability number from the washability numbers of component lithotypes. The weighted average washability number of the whole seam is 122.19. This compares with a washability number of 147 from a bulk washability test. The standard deviation of the weighted average value is 50.1.

FUTURE WORK

This paper presents a preliminary attempt to relate the washability characteristics of a coal seam to its lithotype composition. More comprehensive studies are needed to confirm the validity of these findings. This should involve more systematic washability analysis of other seams and linking them with identification of their depositional environments. This may lead to meaningful conclusions regarding the sedimentation patterns and the predictability of washability from lithology. In terms of the statistical

significance of the additivity of washability numbers from the respective lithotypes, more samples must be tested.

The next step in this study will be a more precise analysis of the association of mineral matter with macerals. This will be accomplished through microlithotype analysis of lithotype samples. This information will be used to better describe lithotype composition with respect to the original wetland environment and other quality characteristics.

ACKNOWLEDGMENTS

I wish to express my gratitude to geologists at Greenhills, Line Creek, Quintette and Quinsam mines for their assistance in collecting samples. I also would like to thank Dave Grieve for many valuable discussions and reading an earlier version of this paper and contributing to its improvement. I also extend my thanks to Mike Fournier for his assistance in preparation of technical drawings.

REFERENCES

- Cameron, A.R. (1972): Petrography of Kootenay Coals in the Upper Elk River and Crowsnest Areas, British Columbia and Alberta; *Research Council of Alberta, Information Series No. 60*, pages 31-45.
- Cohen, A.D., (1984): The Okefenokee Swamp: a Low Sulphur End Member of a Shoreline-related Depositional Model for Coastal Plain Coals; *International Association of Sedimentologists, Special Publication, Volume 7*, pages 321-340.
- Diessel, C.F.K. (1965): Correlation of Macro and Micropetrography of some New South Wales Coals; in *Proceedings, Volume 6, 8th Commonwealth Mineralogical and Metallurgical Congress*, Melbourne, Woodcock, J.T., Madigan, R.T. and Thomas, R.G., Editors, pages 669-677.
- Diessel, C.F.K. (1982): An Appraisal of Coal Facies Based on Maceral Characteristics; *Australian Coal Geology, Volume 4(2)*, pages 474-484.
- Diessel, C.F.K. (1986): The Correlation between Coal Facies and Depositional Environments. Advances in the Study of the Sydney Basin; in *Proceedings, 20th Symposium, The University of Newcastle*, pages 19-22.
- Falcon, L.M. and Falcon, R.M.S. (1987): The Petrographic Composition of Southern African Coals in Relation to Friability, Hardness and Abrasive Indices; *Journal of the South African Institute of Mining and Metallurgy, Volume 87*, pages 323-336.
- Holuszko, M.E. (1991): Wettability and Floatability of Coal Macerals as Derived from Flotations in Methanol Solutions; unpublished M.A.Sc. thesis, *The University of British Columbia*.
- Holuszko, M.E. and Grieve, D.A. (1990): Washability Characteristics of British Columbia Coals; in *Geological Fieldwork 1990, B.C. Ministry of Energy, Mines and Petroleum Resources, Paper 1991-1*, pages 371-379.
- Horsley, R.M. and Smith, H.G. (1951): Principles of Coal Flotation; *Fuel, Volume 30*, pages 54-63.
- Hower, J.C. (1988): Additivity of Hardgrove Grindability: A Case Study; *Journal of Coal Quality, Volume 7*, pages 68-70.
- Hower, J.C. and Lineberry, G.T. (1988): The Interaction of Coal Lithology and Coal Cutting on the Breakage Characteristics of Selected Kentucky Coals; *Journal of Coal Quality, Volume 7*, pages 88-95.
- Hower, J.C., Esterle, J.S., Wild, C.D. and Pollock, J.D. (1990): Perspectives on Coal Lithotypes Analysis; *Journal of Coal Quality, Volume 9, No. 2*, pages 48-52.
- Hower, J.C., Grease, A.M. and Klapheke, J.G. (1987): Influence of Microlithotype Composition on Hardgrove Grindability for Selected Eastern Kentucky Coals; *International Journal of Coal Geology, Volume 7*, pages 68-70.
- Jeremic, M.L. (1980): Coal Strengths in the Rocky Mountains; *World Coal, Volume 6, No. 9*, pages 40-43.
- Kalkreuth, W. and Leckie, D.A. (1989): Sedimentological and Petrographical Characteristics of Cretaceous Strandplain Coals: a Model for Coal Accumulation from North American Western Interior Seaway; *International Journal of Coal Geology, Volume 12*, pages 381-424.
- Kalkreuth, W.D., Marchioni, D.L., Calder, J.H., Lamberson, M.N., Naylor, R.D. and Paul, J. (1991): The Relationship between Coal Petrography and Depositional Environments from Selected Coal Basins in Canada; *International Journal of Coal Geology, Volume 19*, pages 21-76.
- Klassen W.I. (1966): Flotation of Petrographic Components; in *Flotacja Wegla, Slask, Katowice, Poland*.
- Lamberson, M.N., Bustin, R.M. and Kalkreuth, W. (1991): Lithotype (Maceral) Composition and Variation as Correlated with Paleo-wetland Environments, Gates Formation, Northeastern British Columbia, Canada; *International Journal of Coal Geology, Volume 18*, pages 87-124.
- Lamberson, M.N., Bustin, R.M., Kalkreuth, W. and Pratt K.C. (1989): Lithotype Characteristics and Variation in Selected Coal Seams of the Gates Formation, Northeastern British Columbia; in *Geological Fieldwork 1989, B.C. Ministry of Energy, Mines and Petroleum Resources, Paper 1990-1*, pages 461-468.
- Marchioni, D.L., (1980): Petrography and Depositional Environment of the Liddell Seam, Upper Hunter Valley, New South Wales; *International Journal of Coal Geology, Volume 1, No. 1*, pages 35-61.
- Sanders, G.J. and Brooks, G.F. (1986): Preparation of the "Gondwana" Coals. 1. Washability Characteristics; *Coal Preparation, Volume 3*, pages 105-132.
- Sarkar, G.G. and Das, H.P. (1974): A World Pattern of the Optimum Ash Levels of Cleans from the Washability Data of Typical Coal Seams; *Fuel, Volume 53*, pages 74-84.
- Sarkar, G.G., Das, H.P. and Ghose, S. (1977): Sedimentation Patterns: Do They Offer Clues to Coal Quality?; *World Coal*, pages 10-13.
- Stach, E., Mackowsky, M-Th., Teichmuller, M., Taylor, G.H., Chandra, D. and Teichmuller, R. (1982): Stach's Textbook of Coal Petrology, 3rd Edition; *Gebrüder Borntraeger, Berlin, Stuttgart*.
- Sun, S.C. (1954): Hypothesis for Different Floatability of Coals, Carbons, and Hydrocarbon minerals; *American Institute of Mining Engineers, Transactions, Volume 199*, pages 57-75.
- Tsai, S.C. (1982): Fundamentals of Coal Beneficiation and Utilization; in *Coal Science and Technology 2, Elsevier*, pages 17-30.

NOTES



PYRITE OCCURRENCES IN TELKWA AND QUINSAM COAL SEAMS

By Maria E. Holuszko, Alex Matheson and D.A. Grieve

KEYWORDS: Coal geology, sulphur, pyrite, Telkwa, Quinsam, coal cleaning.

INTRODUCTION

Sulphur in coal is a major environmental concern. The use of coal for combustion requires the control of sulphur dioxide emissions. To reduce these emissions, the total sulphur content in coal product must be decreased. This can be accomplished by using low-sulphur coal, cleaning coal prior to combustion, retaining sulphur during combustion, or by treatment of flue gases after combustion. The use of low-sulphur coal is limited to the areas where such coals are available, and retaining the sulphur during combustion is a process in the experimental stage. The remaining alternatives are to clean coal before combustion or reduce sulphur dioxide emissions by flue gas desulphurization. Physical cleaning before combustion, however, is still the most economical option.

Sulphur is found in coal in both inorganic and organic forms. The inorganic sulphur occurs: as iron disulphide, either pyrite (cubic) or marcasite (orthorhombic); as a sulphate, chiefly gypsum and iron sulphate; and as elemental sulphur. Elemental sulphur and sulphate are usually found in very small concentrations, generally less than 0.2 per cent and 0.1 per cent, respectively (Greer, 1979). The organic sulphur is bound to the coal structure. Pyritic and organic sulphur, however, account for most of the sulphur in coal.

Conventional cleaning is not adequate for the removal of organic sulphur, and chemical cleaning would be more appropriate. Pyritic sulphur is the only sulphur form which can be removed by physical methods. Therefore attention is usually focused on the forms of pyrite. For physical sulphur removal to be successful it is necessary to understand the nature and occurrences of pyrite in the coal.

The sulphur contents of most British Columbia coals are considered to be low (<1%). The two major coalfields, the Northeast and Southeast, produce coals with sulphur contents in the range 0.30 to 0.60 per cent. Coals from the Telkwa, Bowron River and Comox coalfields, have, on average, sulphur values greater than 1 per cent, and are exceptions.

British Columbia low-sulphur coal seams contain predominantly organic sulphur. Table 5-3-1(a) shows the distribution of sulphur forms in low-sulphur seams. Total sulphur ranges from 0.23 to 0.69 per cent and the organic sulphur comprises from 55.4 to 96.5 per cent of the total. A decrease in the proportion of organic sulphur is usually accompanied by an increase in pyritic sulphur. Organic sulphur is assumed to be part of the organic coal structure, and it is convenient to express it on a dry ash-free basis, to emphasize this association.

Coals from the Comox, Telkwa and Bowron River coalfields generally average between 0.5 and 1.6 per cent

sulphur. Compared with sub-bituminous coals, the coals from these areas are relatively high rank (higher kcal/kg), and therefore the elevated sulphur content in these seams will have much less effect on the possible sulphur dioxide emissions.

In coals with higher sulphur content an increase of total sulphur content is mainly due to an increase in pyritic sulphur (see part b of Table 5-3-1). The proportion of organic sulphur decreases drastically and may be as low as 4.5 per cent of the total sulphur in some cases. The organic sulphur content, as calculated on a dry ash-free basis, however, appears to be much higher than the organic sulphur in the low-sulphur coals. For Telkwa seams, organic sulphur is as much as 1.81 per cent of organic matter. For Quinsam No. 2 seam and No. 1-Rider seam it ranges from 0.80 to 0.87 per cent, whereas, for low-sulphur coals, organic sulphur on a dry ash-free basis averages 0.56 per cent.

The objective of this study is to investigate pyrite occurrences in Telkwa and Quinsam coals, as these coalfields produce higher sulphur coal. Pyrite occurrences will be discussed in terms of size and association with macerals (microlithotypes) with a view to assessing their possible influence on the cleaning processes.

BACKGROUND

ORIGIN OF SULPHUR IN COAL

Sulphur in coal may be either syngenetic or epigenetic. Most is syngenetic; the early syngenetic sulphur is introduced during the peat formation process, and late syngenetic sulphur is accumulated during the gelification-humification stage of coalification. Epigenetic sulphur, mostly pyritic, is present in cleats and fracture fillings (Renton and Bird, 1991).

Because organic and pyritic sulphur comprise most of the sulphur in coal, special attention is given to the origin of these two forms. The organic sulphur in low sulphur coals is derived primarily from sulphur contained in plants forming the peat deposit. Only a small part is derived from hydrogen sulphide generated by the microbial reduction of the sulphate of interstitial water. Coals rich in organic sulphur imply a syngenetic contribution from fluids with a high sulphate content (Querol *et al.*, 1991; Price and Casagrande, 1991). According to Casagrande and Nug (1979) organic sulphur originates from complexing of sulphur from sulphate ions and hydrogen sulphide by humic acids during coalification.

Organic sulphur in coal can be classified into four types (Markuszewski *et al.*, 1980):

- Aliphatic or aromatic thiols (mercaptans thiophenols);
- Aliphatic, aromatic or mixed sulphide (thioethers);

TABLE 5-3-1
 (A) DISTRIBUTION OF SULPHUR FORMS IN LOW-SULPHUR COAL SEAMS FROM BRITISH COLUMBIA
 (B) DISTRIBUTION OF SULPHUR FORMS IN HIGH-SULPHUR COAL SEAMS FROM BRITISH COLUMBIA

(A)			Moisture %	Ash %	Total	Sulphur %			% S _{org} / S _{tot}	% S _{org} d.a.f.*
Coalfield	Property	Seam				Organic	Sulphate	Pyritic		
Southeast	Byron Ck	Mammoth	0.96	21.70	0.23	0.21		0.02	91.30	0.27
		10A	0.72	12.40	0.52	0.50	0.01	0.01	96.20	0.58
		8	0.67	49.00	0.31	0.28	0.01	0.02	90.30	0.56
	Greenhills	16	0.93	16.80	0.56	0.46	0.02	0.08	82.14	0.56
		22	3.33	6.12	0.58	0.56	0.01	0.01	96.55	0.62
		20	0.80	32.70	0.60	0.46	0.02	0.12	76.67	0.69
		3	0.51	19.30	0.65	0.41	0.04	0.20	63.08	0.51
	Balmer	7RX	0.41	32.10	0.63	0.52	0.02	0.09	82.54	0.77
		7S	0.55	26.00	0.69	0.45	0.12	0.12	65.22	0.61
		4	0.57	24.80	0.62	0.48	0.01	0.13	77.44	0.64
Northeast	Bullmoose	A1	0.76	21.30	0.65	0.36	0.01	0.28	55.40	0.46
		D	1.00	22.10	0.58	0.42	0.03	0.13	72.41	0.55
		E	1.10	21.70	0.55	0.45	0.02	0.08	81.82	0.58
	Quintette	J3	0.86	13.80	0.60	0.38	0.08	0.14	63.33	0.45

* calculated on dry-ash-free basis

(B)			Moisture %	Ash %	Total	Sulphur %			% S _{org} / S _{tot}	% S _{org} d.a.f.*
Coalfield	Property	Seam				Organic	Sulphate	Pyritic		
Comox	Quinsam	Quinsam River (bulk)		14.40	1.57	0.07		1.50	4.50	0.08
		Hamilton Lake (bulk)		27.00	2.21	0.82		1.39	37.10	1.12
		2	2.30	30.90	2.63	0.53	0.08	2.02	20.20	0.79
		Rider	2.30	20.50	3.73	0.67	0.16	2.90	18.00	0.87
		1	2.50	9.80	0.58	0.33	0.01	0.24	56.90	0.38
Telkwa		Lower coal zone	0.49	23.12	3.52	1.38	0.15	1.99	39.20	1.81

* calculated on dry-ash-free basis

- Aliphatic, aromatic or mixed disulphides (bisthioethers);
- Heterocyclic compounds of the thiophene type (dibenzothiophene).

The proportion of different organic sulphur-bearing compounds is a function of rank and type of coal. The aliphatic (organic sulphur bound to the aliphatic hydrocarbon compound) to aromatic sulphur ratio varies significantly with maceral type and coal rank. Vitrinite macerals typically contain more of the aromatic-heterocyclic sulphur than either the inertinite or exinite macerals. An increase in rank increases the ratio of aromatic to aliphatic sulphur (Huggins, 1992). The distribution of organic sulphur in various macerals has been the subject of many studies (Raymond, 1982; Hippo *et al.*, 1987; Stock *et al.*, 1989).

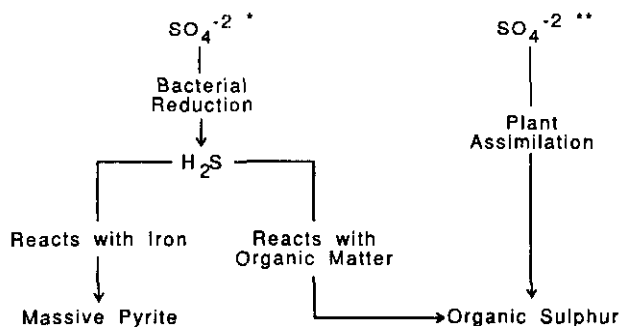
Generally, it was found that macerals from low-sulphur coals contain comparable amounts of organic sulphur. In contrast, the macerals of high-sulphur coals contain significantly different amounts of these substances. Sporinite has the highest content of organic sulphur, while vitrinite has significantly less. Furthermore, organic sulphur in sporinite was found to be more reactive than organic sulphur in vitrinite.

"Pyritic" sulphur includes sulphur contained in either of the two common iron sulphide minerals, pyrite and marcasite. The generation of sulphide in coal depends on the

availability of sulphur and iron, and on the intensity of the sulphate bacterial reduction (Figure 5-3-1). It is generally accepted that coals with the original peat or roof sediments formed in marine-influenced environments have a tendency to have a higher sulphide content than those accumulated in limnic areas (Williams and Keith, 1963). Considering that the sulphate content of seawater is 120 times greater than that of fresh water or ground water this is not surprising (McMillan, 1972).

According to Neavel (*in* Frankie and Hower, 1985) iron sulphide can only form in peats as a result of bacterial activity, because there is not enough energy for chemical reduction of sulphates to disulphides. The source of sulphur is plant and animal protein, largely bacterial protein, or sulphate ions in streams or sea water. Iron is derived from the weathering of silicate minerals or is carried in with groundwater as Fe-ions. The environmental conditions, especially pH, appear to have dramatic effect on pyrite formation (Casagrande, 1987).

The hydrogen sulphide which is transformed into iron disulphide is produced by sulphate-reducing bacteria, which thrive in high pH environments. The same swamp conditions that produce iron disulphide minerals determine the relative abundances of the various macerals in a particular coal seam. In other words, pH conditions in the swamp control the microbial degradation of plant debris to form the organic part of coal and, at the same time, control the



* Low Sulphur = Brackish to Fresh Water Source
High Sulphur = Marine Water Source

** Low and High Sulfur from Fresh Water Source

Figure 5-3-1. Sulphide formation in coal (Price and Shieh, 1979).

reactions that generate pyrite. For example, higher pH leads to increased microbial degradation of the plant and peat components and, as a result decreased content of pre-vitrinitic materials. Increased microbial reduction of sulphate ions subsequently results in the precipitation of iron disulphide minerals, mainly pyrite, in coal. The end result is that coal produced under high pH conditions is more exinite rich and higher in mineral matter, especially in pyritic sulphur. Typically the abundance of exinite and pyritic sulphur exhibit a strong statistical association with each other (Renton and Bird, 1991).

Low pH, by contrast, promotes accumulation of pre-vitrinitic woody tissues and suppresses exinite formation. In addition, metal ions, especially iron, are readily dissolved and removed from the peat, and bacterial reduction of sulphate to iron disulphide is simultaneously suppressed. Coals produced under these conditions are vitrinite rich and pyritic sulphur content is low; most of the sulphur is organic.

Strong relationships between petrographic composition and pyritic sulphur in coal exist due to the same chemical conditions controlling the pyrite formation and abundances of various macerals (Renton and Bird, 1991; Kalkreuth *et al.*, 1991).

PYRITE OCCURRENCES IN COAL

Pyrite may occur in a variety of forms, the most common being as narrow veins up to 150 millimetres thick and several hundred millimetres long, nodules resembling framboids, and discrete crystals. The framboids, which range from a few to several hundred microns in size, are aggregates of octahedral crystals; discrete crystals are usually much smaller (1-2 μm).

There are a number of different classifications of pyrite occurrence in coal. Neavel and Reyes-Navarro (*in* Frankie and Hower, 1985) classified pyrite as: framboidal, dendritic, euhedral, cleat and massive. Caruccio *et al.* (1977) consider two main categories, primary and secondary pyrite. Primary pyrite includes sulphur balls, finely disseminated pyrite, and primary emplacement pyrite. They also recognize five types of pyrite according to morphology: primary massive, plant

replacement, primary euhedral, secondary cleat coats and framboidal.

Lowson (1982) suggested that for many purposes it is adequate to consider pyrite as either framboidal or euhedral. In another classification, two types of pyrite morphology are defined: type 1 consists of submicron-size grains existing as loose particles or agglomerated in the form of framboids, typically 10 to 20 microns in diameter; type 2 includes larger individual crystals (often $>50 \mu\text{m}$) with no apparent sub-grain structures (Caley *et al.*, 1983). The latter are described as monolithic. These two types of pyrite morphologies coincide with framboidal and euhedral forms of pyrite discussed by Lowson (1982). It is also believed that these two types may be considered as the end members in a maturity range. The framboidal or submicron size pyrites are believed to be the least mature, whereas monolithic pyrites are the most mature.

In terms of pyrite reactivity it has also been established that framboidal pyrite is more reactive than other forms and, as result, responsible for forming acid solutions and causing acid mine-drainage problems (Carruccio *et al.*, 1977; McMillan, 1972). Similarly, the framboidal pyrite displays a higher level of reactivity upon pyrolysis than euhedral pyrite from the same coal (Caley *et al.*, 1989).

SAMPLES AND ANALYTICAL PROCEDURES

Samples were obtained from diamond-drilling projects in the Quinsam and Telkwa coalfields (Matheson, 1989; Matheson and Van Den Bussche, 1989). Locations of Quinsam mine and Telkwa coalfield are shown in Figures 5-3-2 and 5-3-3.

Samples representing Quinsam No. 1, 1-Rider and No. 2 seams were analyzed. These seams have a high pyrite content and are typical of seams which have been influenced by marine transgressions (Kenyon *et al.*, 1991). They are overlain directly by marine strata. A summary of analytical results is presented in Tables 5-3-2 and 5-3-3. Table 5-3-2 presents proximate analysis (Matheson, 1989). Table 5-3-3 shows the distribution of sulphur forms in these seams. Quinsam No. 1 seam, as presented in Table 5-3-3, has been subdivided into three intervals: upper, middle and lower (the first two are 80-centimetre intervals, the third 60 centimetres).

The Telkwa coal measures are part of an interbedded marine and nonmarine sedimentary sequence which is

TABLE 5-3-2
PROXIMATE ANALYSIS IN NO. 1, 1-RIDER AND 2 SEAMS
FROM QUINSAM

Seam	Moisture %	Ash %	Volatile Matter %	Fixed Carbon %
#2	2.30	30.90	30.00	36.80
#1	2.30	20.50	35.00	42.20
Rider #1	2.65	9.65	37.00	50.70

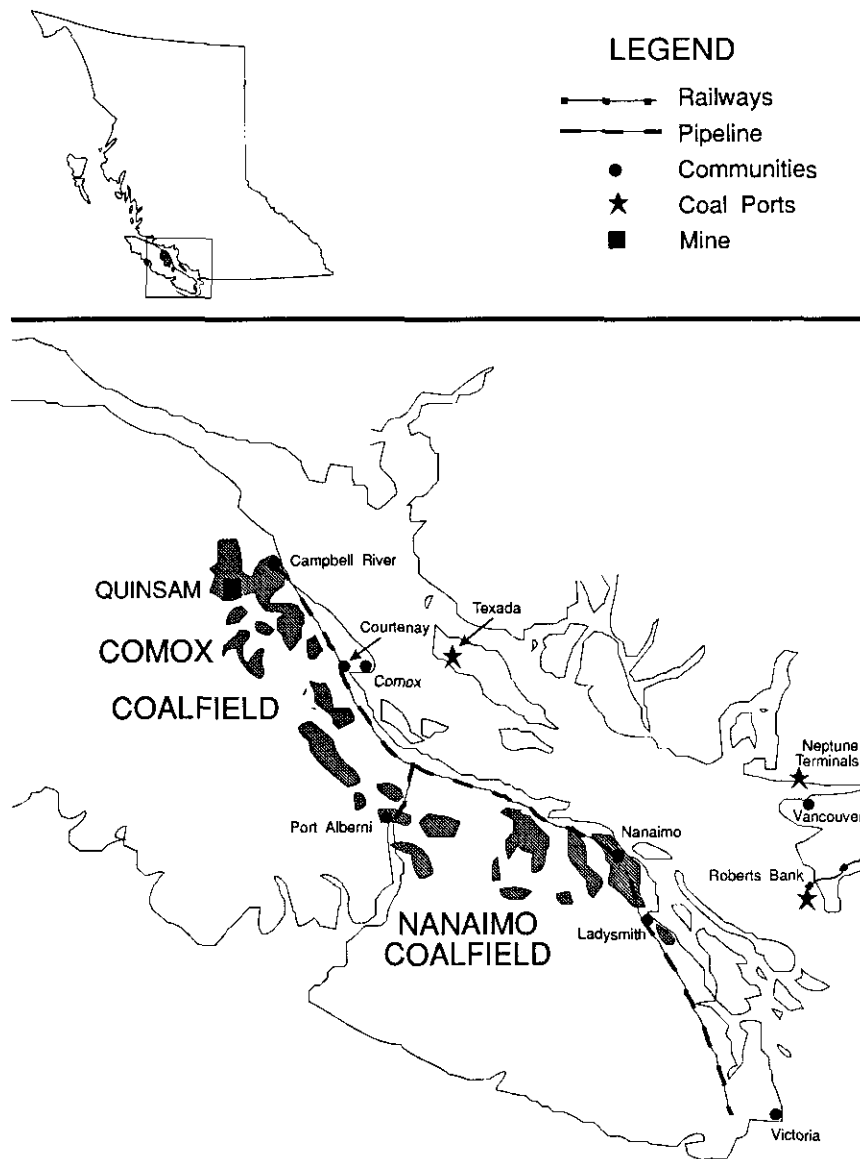


Figure 5-3-2. Location of Quinsam mine and Comox coalfield.

divided into three units (Koo, 1984; Matheson and Van Den Bussche, 1989). Only the lower and the upper unit contains coal measures. The coal seam No. 1 and some thin coal seams occur near the top of the lower unit (Matheson and Van Den Bussche, 1989). The upper unit contains ten seams. Palsgrove and Bustin (1991) described coal geology and quality of these seams in greater detail. In general, the uppermost six seams in the upper unit have the highest sulphur content, ranging from 2.00 to 3.80 per cent.

The incremental samples from the Telkwa No. 1 seam in the lower unit were analyzed for pyrite forms. Samples from the upper part of the seam have the highest sulphur contents, especially samples from the top of the seam, where sulphur reaches almost 10 per cent. In general, the sulphur content decreases downward within the seam. The average total sulphur content for this seam is 3.52 per cent; proximate and sulphur forms analyses are presented in Table 5-3-4. Sul-

phur, ash and moisture contents of samples taken in 20-centimetre intervals across the seam are reported in Table 5-3-5.

PETROGRAPHIC ANALYSIS

For detailed petrographic examination, epoxy pellets were prepared from coal samples taken in 10 to 15-centimetre increments from Quinsam No. 1, 1-Rider and No. 2 seams. The Telkwa seam was sampled in 20-centimetre increments. Maceral analyses were performed by counting 500 points on each pellet. Results are summarized in Tables 5-3-6 and 5-3-7. In addition, observations were made with respect to the size, form and association of pyrite with microlithotypes in vertical sequence of these seams. Table 5-3-8 summarizes the maceral composition of the various microlithotypes.

TABLE 5-3-3
DISTRIBUTION OF FORMS OF SULPHUR IN NO. 1, 1-RIDER AND NO. 2 SEAMS FROM QUINSAM

Coal Seam	Moisture %	Ash %	Total	Sulphur %			% S _{org} /S _{tot}	% S _{org} d.a.f.*
				Organic	Sulphate	Pyritic		
#2	2.30	30.90	2.66	0.54	0.08	2.04	20.30	0.80
Rider	2.30	20.50	6.08	0.67	0.27	5.14	11.00	0.87
#1 (first part; 80 cm from the top)	2.60	8.23	1.09	0.46	0.02	0.61	42.20	0.52
#1 (second part; next 80 cm from the top)	2.60	12.92	0.37	0.33	< 0.01	0.03	39.19	0.39
#1 (bottom part; last 60 cm)	2.81	8.84	0.29	0.27	< 0.01	0.01	93.10	0.31

* calculated on dry-ash-free basis

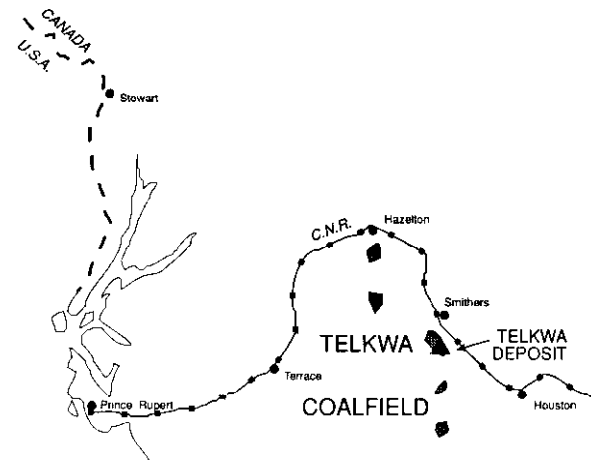
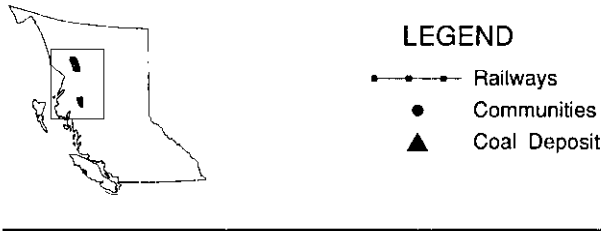


Figure 5-3-3. Location of Telkwa coalfield.

TABLE 5-3-4
PROXIMATE ANALYSIS AND SULPHUR FORMS IN TELKWA SEAM

Moisture %	Ash %	Volatile Matter %	Fixed Carbon %
0.49	23.01	28.21	48.29

Forms of Sulphur				% S _{org} /S _{tot}	% S _{org} d.a.f.*
Total	Organic	Sulphate	Pyritic		
3.52	1.38	0.15	1.99	36.9	1.79

TABLE 5-3-5
SULPHUR AND ASH DISTRIBUTION IN TELKWA SEAM

Sample No.	Moisture	Ash %	Sulphur %
1**	0.96	42.04	9.71
2	0.85	40.99	4.34
3	0.83	12.5	2.38
4	0.98	23.43	2.14
5	0.86	11.61	1.21
6	0.99	10.65	3.12
7	0.88	31.03	3.39
8	1.12	18.93	0.39
9	0.91	17.2	1.19

* analysis are on as received basis

** samples represent 20 cm intervals

DISTRIBUTION OF SULPHUR AND ASH

QUINSAM

The average total sulphur content for Quinsam No. 2 seam is 2.66 per cent. The highest sulphur content, 6.08 per cent, occurs in 1-Rider seam. The sulphur content of the upper part of No. 1 seam is much higher than the remainder of the seam and correlates with an increase in pyrite content (Table 5-3-3). The increasing trend of pyritic sulphur towards the top of the seam is evident and in agreement with other studies (Casagrande, 1987; Querol, 1991 *et al.*).

In the 1-Rider seam, pyritic sulphur comprises 89 per cent of the total sulphur, while in the sample with lowest sulphur content pyrite contributes only a little over 3 per cent of the total sulphur.

No. 2 seam has the highest ash content, followed by 1-Rider seam. The lowest ash content is associated with the uppermost 80-centimetre interval of the No. 1 seam, which is enriched in pyritic sulphur. An increase in ash content in

the samples from the middle part of No. 1 seam does not have a corresponding increase in the content of pyritic sulphur. There is no apparent correlation between total sulphur content or pyritic sulphur and the ash content.

TELKWA

The average total sulphur content for the Telkwa No. 1 seam is 3.52 per cent (Table 5-3-5). Pyritic sulphur comprises 56.5 per cent of the total sulphur content and organic sulphur contributes a further 39.2 per cent. Total sulphur decreases with depth down to the middle section of the seam (Table 5-3-5). This corresponds with a general decrease in

TABLE 5-3-6
MACERAL ANALYSIS OF SAMPLES FROM EXAMINED
QUINSAM SEAMS

Seam	Vitrinite Vol. % *	Exinite Vol. %	Inertinite Vol. %
2 (3)**	87.90	1.40	10.70
Rider (4)	72.90	2.40	24.70
1 (first 80 cm) (8)	80.00	2.50	17.50
1 (next 80 cm) (8)	78.80	2.20	19.00
1 (60 cm) (7)	80.20	2.30	17.50

* volume percent on mineral-matter-free basis

** average based on ()-number of samples

TABLE 5-3-7
MACERAL ANALYSIS OF SAMPLES FROM EXAMINED
TELKWA SEAM

Sample No.	Vitrinite Vol. % *	Exinite Vol. %	Inertinite Vol. %
1 **	94.60	1.20	4.20
2	81.50	0.60	18.10
3	40.80	1.80	57.40
4	69.60	1.40	29.00
5	60.60	2.20	37.20
6	61.20	1.00	37.80
7	69.60	2.20	28.20
8	59.80	0.60	39.40
9	68.40	0.40	31.20
Average	67.30	1.30	31.40

* Volume percent on mineral-matter-free basis

** Samples represent 20 cm intervals

TABLE 5-3-8
COMPOSITION OF VARIOUS MICROLITHOTYPES (after stach
et al., 1982)

Classification	Microlithotype	Mineral Group Composition
Monomaceral (mineral free)	Vitrite	V > 95%, E+I < 5%
	Liptite	E > 95%, V+I < 5%
	Inertite	I > 95%, V+E < 5%
Bimaceral (mineral free)	Clarite	V+E > 95%, I < 5%
	Vitrinertite	V+I > 95%, E < 5%
	Durite	I+E > 95%, V < 5%
	Trimacerite	V+I+E (each > 5%), > 95%
Maceral Association	Carbominerite	Any above microlithotype with 5-60% by volume mineral matter (5-20% if sulfides)

V - Vitrinite E - Exinite I - Intertinite

ash content, with some exceptions. The highest sulphur content (9.71%) is reported in the top sample, the corresponding ash content is 42.04 per cent.

DISTRIBUTION OF PYRITE FORMS

QUINSAM

Examination of samples from Quinsam No. 2 seam, representing the top of the coal sequence, revealed that the coal particles are very much contaminated with pyrite, predominantly framboidal, with an average size of approximately 13 microns. There are also massive framboids, 25 to 30 microns in size. Euhedral pyrite is found as very small, liberated particles, usually in cavities and cleats, indicating secondary origin. Some pyrite is intermixed with clays. Almost all particles are contaminated with pyrite, but only a few are heavily contaminated. Other minerals are clays and calcite. The latter is deposited in the cleats of coal particles. Examples of various pyrite forms in Quinsam coal seams are illustrated in Plate 5-3-1.

In 1-Rider seam, the framboidal pyrite appears mainly as large particles, up to 30 microns, while smaller framboids are up to 5 microns. There is also an increased abundance of euhedral pyrite, typically as tiny particles (1 to 2 μ m). In general, there is a high content of pyritic sulphur in various forms. Large framboids dominate the coal samples from 1-Rider seam. In the top of the section very tiny euhedral pyrites are found near larger framboids. This suggests that the euhedral pyrite may be the result of disintegration of framboidal pyrite (Figure 5-3-1). Liberation of pyrite in these samples is insignificant, considering the crushing process for pellet preparation (reducing the size down to -20 mesh). Most liberated pyrite particles are euhedral, but some framboidal pyrite is present in the cleats.

The top part of No. 1 seam (uppermost 80 cm) also contains substantial amounts of framboidal and euhedral pyrite. Framboidal pyrite quite often occurs in clusters and some clusters reach 25 microns in size. There are examples of larger euhedral pyrite. The trend in decreasing total sulphur content from the top to the lower part of No. 1 seam is accompanied by a decrease in size of the framboidal pyrite, and a parallel decrease in the ratio of framboidal to euhedral pyrite. In the middle 80-centimetre interval of the seam, there is almost no visible framboidal pyrite; the only pyrite present is very small euhedral grains.

TELKWA

Microscopic analysis of pyrite occurrences in the Telkwa high-sulphur seam shows a variety of its types. A total of nine samples were examined, covering the whole seam. Samples from the upper part of the seam are enriched in massive and very large framboids, some up to 250 microns in diameter. The first two samples appear to have an especially high mineral matter content. The first sample has abundant pyrite, whereas in the second the mineral matter is mostly clays. Plate 5-3-2 shows the pyrite forms found in the Telkwa coal seam.

There is an obvious trend from large framboidal to more irregular pyrite forms with depth. Somewhere in the middle

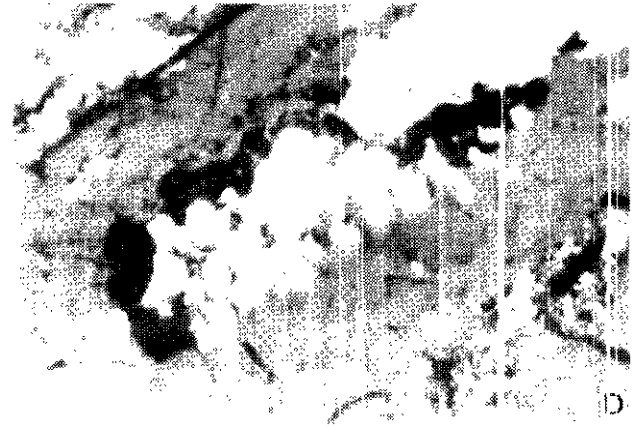
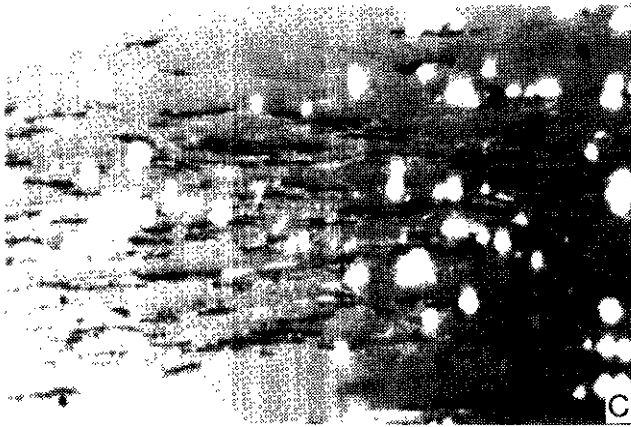
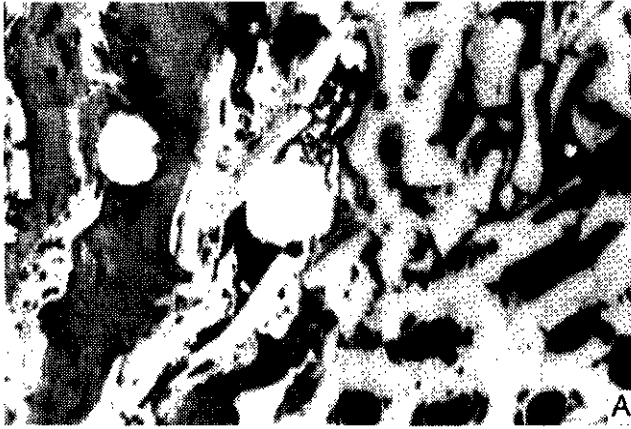


Plate 5-3-1. Pyrite occurrences in Quinsam coal seams, (250 m on horizontal). A. Regular framboids; B. Massive framboids; C. Disseminated small framboids; D. Euhedral pyrite.

of the seam, transformation of regular framboidal pyrite into massive "cauliflower-type" occurs. The size of irregular pyrite occurrences is somewhat smaller than the massive framboidal type, reaching on average 50 to 100 microns in diameter. The abundance of euhedral pyrite also increases with depth. This type is usually 4 to 5 microns in size, filling cavities in fusinite or semifusinite. It comprises almost 95 per cent of the total pyrite in the samples from the bottom of the seam.

In general, the liberation of pyrite increases with increase in euhedral grains. Liberated euhedral pyrite usually occurs in small cavities and cleats, but in some cases pyrite appears encapsulated in coal particles. In the part of the seam where the mineral matter is high and framboidal pyrite abundant, liberation of pyrite reaches up to 30 per cent, especially when pyrite particles are contained within the clay bands. Liberation is much less in the parts of the seam where irregular cauliflower pyrite occurs. The irregular form seems to have replaced semifusinite and is usually confined to this maceral.

ASSOCIATION OF PYRITE WITH MACERALS AND MICROLITHOTYPES

QUINSAM

Petrographic analysis (Table 5-3-6) of Quinsam No. 2 seam indicates that this coal is high in vitrinite. The average

exinite content is moderate, with a somewhat higher content of exinite in the top part of the seam. This also coincides very well with the larger occurrences of framboidal pyrite in this part of the seam. The lower part of the seam is enriched in smaller framboidal pyrite (5 to 7 μm) and secondary euhedral pyrite is found in cavities in fusinite and semifusinite. Framboidal pyrite is mostly associated with vitrinite-rich microlithotypes: vitrite, clarite and trimaccrite.

The 1-Rider seam has a lower vitrinite content than No. 2 seam. Its exinite content is higher and this is accompanied by an increase in abundance of inertinite, especially semifusinite. The average vitrinite content is 72.5 per cent by volume (Table 5-3-6), with an increasing trend from the top to the bottom of the seam. The highest exinite content is at the top of the seam and corresponds to the highest concentrations of pyrite, as in the No. 2 seam. Massive pyrite and large framboids appear to be always enclosed within the vitrinite particles. It is also evident that framboidal pyrites are usually aligned parallel to the bedding planes. In terms of microlithotype association, framboidal pyrite is usually a part of the vitrite and clarite microlithotype, whereas euhedral pyrite occurs in cavities in fusinite or semifusinite in the inertite lithotype.

Maceral composition throughout No. 1 seam is almost uniform. Vitrinite content is about 80 per cent by volume. exinite and inertinite contents are in the range of 2.2 to 2.5

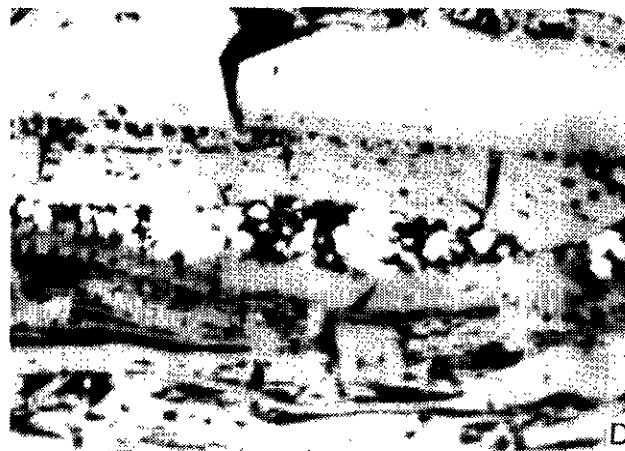
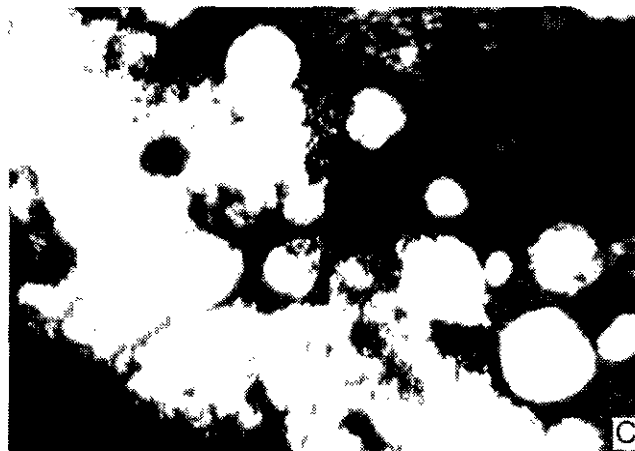
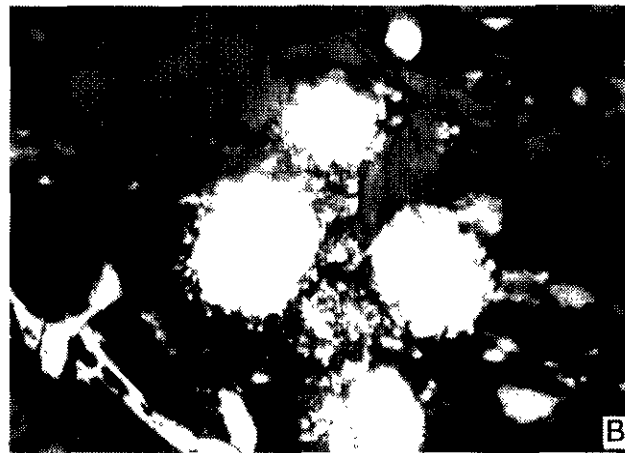
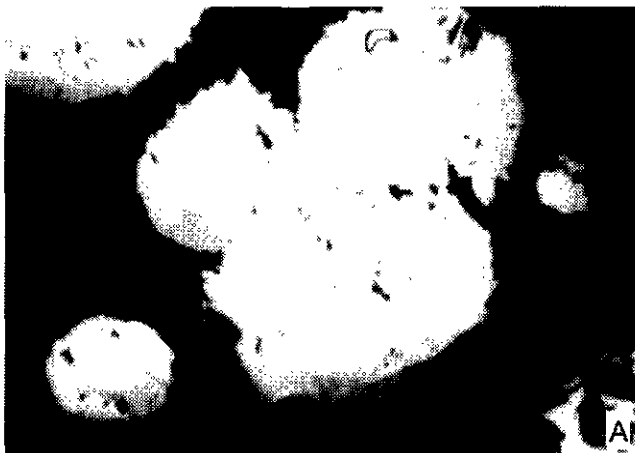


Plate 5-3-2. Pyrite occurrences in a Telkwa coal seam, (250 μm on horizontal). A. Large framboids; B. Regular framboids; C. Cauliflower-type; D. Small euhedral pyrite.

and 17.50 to 19.00 per cent, respectively. There is very little variation in association of pyrite with the macerals within the seam. Larger framboidal pyrite is almost always associated with vitrinite, while euhedral pyrite is found in cavities in vitrinite or fusinite. Framboidal pyrite is dominantly associated with vitrinite and trimacerites (V+E+I). The higher pyrite content in the top of the seam is not matched by an increased abundance of exinite, as observed in other seams.

TELKWA

In general, maceral composition of the Telkwa seam changes from vitrinite-rich in the top of the seam to inertinite-rich towards the bottom, with some irregularities in between (Table 5-3-7). The highest vitrinite content (94.6% by volume) is at the top of the seam. The variation in exinite content is even less regular. It ranges from 0.60 to 2.2 per cent by volume with no obvious correlation with the stratigraphy of the seam.

Occurrences of mega-framboids (up to 250 μm) of pyrite in the first 20-centimetre interval of the seam are almost exclusively confined to the vitrinite, as this maceral is dominant in this part of the seam. An obvious trend is observed moving downward in the seam; framboids become

more regular in shape and smaller in size (150 μm or less). Regular framboidal pyrite is typically confined to the vitrinite and clarite microlithotypes (V+E). In some instances, framboidal pyrite occurs in trimacerites (V+E+I). The cauliflower pyrite is commonly associated with semifusinite in inertite microlithotype.

SUMMARY AND CONCLUSIONS

The high sulphur content in the Quinsam and Telkwa seams reflects marine influence during the deposition. In terms of sulphur distribution within the individual seams, there are no systematic trends. The highest sulphur content, however, is always in the upper portions of these seams. The ash patterns are also variable, with the highest ash content usually accompanying high sulphur content.

High sulphur content is a direct result of increased pyritic sulphur. In the 1-Rider seam at Quinsam, pyritic sulphur comprises almost 90 per cent of total sulphur, while in the upper part of No. 1 seam pyritic sulphur comprises only 57.8 per cent of the total sulphur (Table 5-3-3). In the lower sections of No. 1 seam total sulphur decreases significantly. Here, organic sulphur is dominant and comprises more than 90 per cent of the total sulphur. This is in agreement with trends in other coals (Casagrande *et al.*, 1979; Given and

Miller, 1985); in coals with low total sulphur, the organic sulphur concentration exceeds that of pyritic sulphur, and in coals with higher total sulphur content pyritic sulphur is dominant.

The organic sulphur content of the Telkwa seam, calculated on a dry ash-free basis, is much higher than organic sulphur of Quinsam high-sulphur seams. Organic sulphur, as discussed by many (Renton and Bird, 1991; Price and Casagrande, 1991; Querol *et al.*, 1991), is derived from sulphur in plants or through the direct reaction between hydrogen sulphide derived from microbial reduction, and organic matter. Hydrogen sulphide may react with either organic matter or iron to form pyrite; however, it reacts preferentially with iron (Howarth, 1984; *in* Palsgrove and Bustin, 1991). Due to the deficiency of iron ions in the low pH peat, sulphur may be tied up in organic matter instead of in sulphides. Bacteria reactions are slower and, as a result, hydrogen sulphide is incorporated into the organic matter.

Lower pH promotes preservation of organic matter and, coupled with the high water table in the peat, leads to vitrinite-rich coal, as evident in the top of the Telkwa seam. Another observation is that a fair amount of pyritic sulphur in this part of the seam, up to 30 per cent, is liberated. This indicates introduction of secondary pyrite into the coal. There is also a possibility that pyrite was introduced during the humification and gelification stage, after formation of vitrinite.

According to the accepted model explaining pyrite formation in relation to the petrographic composition of coal, the chemical conditions favourable for pyrite formation result in exinite-rich and vitrinite-depleted coal. None of the examined seams appear to follow this pattern entirely. In parts of No. 2 and 1-Rider seams at Quinsam, some correlation between exinite and pyritic sulphur content can be observed. It is also noteworthy that these coals are impoverished in exinite, due to the type of vegetation contributing to the peat.

Distribution of various pyrite forms is quite similar for seams from Quinsam and Telkwa. The large framboidal pyrite is almost always dominant in the top of the seams. The size of framboids decreases with depth. The ratio of framboidal to euhedral pyrite also decreases with depth. The size of euhedral pyrite varies from 1 micron (Telkwa) in size to 5 microns (Quinsam). An irregular cauliflower form of pyrite was observed in the middle part of the Telkwa seam. The association of cauliflower pyrite with semifusinite may indicate the secondary replacement of semifusinite by pyrite.

It is evident from microscopic examination of Quinsam and Telkwa high-sulphur coal seams, that pyrite in the Telkwa seam is much coarser grained than the pyrite in the Quinsam seams. The size of pyrite in the Telkwa seam reaches up to 250 microns, whereas in Quinsam seams, the size of the framboidal pyrite averages between 13 and 15 microns, with a maximum size of 25 to 30 microns.

The examination of pyrite size and occurrences in high-sulphur seams from Quinsam and Telkwa suggests that pyrite in the Telkwa seams would be more amenable to removal in commercial cleaning. Large framboids would be much easier to liberate than those found in Quinsam seams.

Distribution of pyrite in the Telkwa seam is also more favourable. The largest framboids are concentrated at the top of the seam, allowing isolation of this section for selective mining, if necessary.

Petrographic analyses of samples from Quinsam and Telkwa seams indicate that in both cases pyrite occurs mostly in vitrite, clarite and trinacerites (V+I+E). Several studies (McCartney *et al.*, 1969; Frankie and Hower, 1935) correlating pyrite size and removal through the various physical cleaning circuits showed that fine pyrite (<20 μm) was always found in the clean coal fractions. It was also shown that clean coal was enriched in euhedral and framboidal pyrite associated with vitrite and clarite. Massive, large framboidal pyrite and pyrite associated with the mineral matter bands were usually concentrated in the refuse. Pyrite particles smaller than 10 microns in size remained in the clean coal.

It is expected that pyrite particles smaller than 20 microns in size and associated with vitrinite-dominated microlithotypes would tend to concentrate in clean coal product when gravity-based cleaning methods are used. Large particles of pyrite from the Telkwa seam would probably be much easier to remove when treated by conventional coal cleaning techniques. Microscopic analysis reveals that the large pyrite occurrences in the Telkwa seam are concentrated in the part of the seam enriched in vitrinite. This would indicate a better chance to release pyrite during the size reduction, as vitrinite is the softest maceral.

Greater reduction in top size would be required to liberate pyrite from Quinsam seams. Due to the fact that pyrite in Quinsam seams is more disseminated than in massive, more middlings will be produced during the preparation, and as a result the use of separators with sharper separation profiles would be necessary.

The coals examined here have weak floatability characteristics, therefore, froth flotation would not be adequate. This would also exclude the option of significant reduction in the top size of coal (*e.g.*, to liberate 25-micron pyrite grains in Quinsam coal), as there are few commercially available processes to treat fines for these coals.

The only viable alternative for treating the pyrite from Quinsam coal, if required, may be the use of the agglomeration process. This would allow further size reduction in order to liberate the pyrite (Pawlak *et al.*, 1987, 1988). Given the fact that larger framboidal pyrite is found mainly associated with the vitrite microlithotype, the probability of liberation and concentration in the fines would be much greater. To obtain maximum effect during agglomeration, the size of coal must be reduced. Size reduction may be impaired, however, by the fact that Quinsam coal has a low grindability index. Furthermore, the cost of adding agglomeration to the cleaning process will have to be balanced against the value of the improved coal quality. The end result may be that coarse coal will have lower sulphur contents, but the fines recovered in form of agglomerates will have to be incorporated into the final coal product.

For further reduction in pyritic sulphur in Quinsam coal, the Agglofloat technique would be far superior to agglomeration (Pawlak *et al.*, 1987, 1988). This technique combines both agglomeration and flotation into one pro-

cedure, and is more selective in pyrite removal. It claims to reject up to 70 per cent of pyrite during cleaning, with as high as 96 per cent recovery of combustibles. The main benefit of this technique is that it can treat very fine coal (well below 0.50 μm). The reduction to such fine sizes leads to greater liberation of pyrite particles and therefore greater chances of removal. The Agglofloat product, however, is finer and even more difficult to combine with the rest of the clean coal product.

ACKNOWLEDGMENTS

We would like to thank Steve Gardner of Brinco Mining Corporation for valuable comments on the sulphur occurrences in Quinsam coal. Mike Fournier and Anna Peakman are greatly acknowledged for their technical assistance in the preparation of this paper.

REFERENCES

- Caruccio, F.T., Ferm, J.C., Horne, J., Geidel, G. and Baganz, B. (1977): Paleoenvironment of Coal and its Relation to Drainage Quality; *U.S. Environmental Protection Agency*, Report No. R-802597-02, by Industrial Environmental Research Laboratory.
- Caley, W.F., Whiteway, S.G. and Steward, I. (1989): Variation of the Reactivity of FeS_2 in Eastern Canadian Coal as a Function of Morphology; *Coal Preparation*, Volume 7, pages 37-46.
- Casagrande, D.J. (1987): Sulphur in Peat and Coal; in *Coal and Coal Bearing Strata*, Scott, A.C., Editor, *U.K. Geological Society*, Special Publication 32, pages 87-105.
- Casagrande, D.J. and Nug, L. (1979): Incorporation of Elemental Sulphur in Coal as Organic Sulphur; *Nature*, Volume 282, pages 598-599.
- Casagrande D.J., Idosu, G., Friedman, J., Rickert, P., Siefert, K. and Schlenz, D. (1979): H_2S Incorporation in Coal Precursors: Origins of Organic Sulphur in Coal; *Nature*, Volume 282, pages 599-600.
- Frankie, K.A. and Hower, J., (1985): Pyrite/Marcasite Size, Form, and Microlithotype Association in Western Kentucky Prepared Coals; *Fuel Processing Technology*, Volume 10, pages 269-283.
- Given, P.H. and Miller, R.N. (1985): Distribution of Forms of Sulfur in Peats from Saline Environments in the Florida Everglades; *International Journal of Coal Geology*, Volume 5, pages 397-409.
- Greer, R.T. (1979): Organic and Inorganic Sulfur in Coal; *Scanning Electron Microscopy*, Volume 1, pages 477-486.
- Hippo, E.J., Crelling, J.C., Sarvela, D.P. and Mukerjee, J. (1987): Organic Sulfur Distribution and Desulfurization of Coal Maceral Fractions; in *Processing and Utilization of High Sulphur Coals*; Volume 2, Chugh, V.P. and Candle, D.C., Editors, Proceedings of the Second International Conference on Process and Utilization of High Sulphur Coals, 28 September to 1 Oct., 1987, *Elsevier*.
- Huggins, F. (1992): Differentiation of Organic Sulfur Forms in Fossil Fuels; *Highlights of the Energeia*, Volume 11, November 2, 1992.
- Kalkreuth, W.D., Marchioni, D.L., Calder, J.H., Lamberson, M.N., Naylor, R.D. and Paul, J. (1991): The Relationship Between Coal Petrography and Depositional Environments from Selected Coal Basins in Canada; *International Journal of Coal Geology*, Volume 19, pages 21-76.
- Kenyon, C., Cathyl-Bickford, C.G. and Hoffman, G.L. (1991): Quinsam and Chute Creek Coal Deposits; *B.C. Ministry of Energy, Mines and Petroleum Resources*, Paper 1991-3.
- Koo, J. (1984): Telkwa Coalfield, West-central British Columbia (93L); in *Geological Fieldwork 1983*, *B.C. Ministry of Energy, Mines and Petroleum Resources*, Paper 1984-1, pages 113-121.
- Lowson, R.T. (1982): Aqueous Oxidation of Pyrite by Molecular Oxygen; *Chemical Review*, Volume 82, pages 461-497.
- Markuszewski, R., Fan, C.W., Greer, R.T. and Wheelock, T.D. (1980): Evaluation of the Removal of Organic Sulfur from Coal; Symposium on New Approaches in Coal Chemistry, *American Chemical Society*, Pittsburg, PA, 12-14 November, 1980.
- Matheson, A. (1989): Subsurface Coal Sampling Survey, Quinsam Area, Vancouver Island, British Columbia; in *Geological Fieldwork 1989*, *B.C. Ministry of Energy, Mines and Petroleum Resources*, Paper 1990-1, pages 439-443.
- Matheson, A. and Van Den Bussche, B. (1989): Subsurface Coal Sampling Survey, Telkwa Area, Central British Columbia; in *Geological Fieldwork 1989*, *B.C. Ministry of Energy, Mines and Petroleum Resources*, Paper 1990-1, pages 445-448.
- McCartney, J.T., O'Connell, H.J. and Ergun, S. (1969): Pyrite Size Distribution and Coal Pyrite Association in Steam Coals; *U.S. Bureau of Mines*, Report 7231:18.
- McMillan, B.G. (1972): Sulfur Occurrence in Coal and its Relationship to Acid Water Formation; *Coal Research Bureau, West Virginia University*, Report No. 110.
- Palsgrove, R.J. and Bustin, R.M. (1991): Stratigraphy, Sedimentology and Coal Quality of the Lower Skeena Group, Telkwa Coalfield, Central British Columbia; *B.C. Ministry of Energy, Mines and Petroleum Resources*, Paper 1991-2.
- Pawlak, W., Turak, A., Briker, Y. and Ignasiak, B. (1987): Coal Upgrading by Selective Agglomeration; Proceedings of Twelfth Annual Electric Power Research Institute Contractor's Conference on Fuel Science and Conversion, May 1987, Palo Alto.
- Pawlak, W., Ignasiak, T., Briker, Y., Carson, D. and Ignasiak, B. (1988): Novel Application of Oil Agglomeration Technology; Proceedings of Thirteenth Annual Electric Power Research Institute Contractor's Conference on Fuel Science and Conversion, May 1988, Santa Clara.
- Price, F.T. and Casagrande, D.J. (1991): Sulfur Distribution and Isotopic Composition in Peats from the Okefenokee Swamp, Georgia and the Everglades, Florida; *International Journal of Coal Geology*, 17, pages 1-20.
- Price, F.T. and Shieh, Y.N. (1979): The Distribution and Isotopic Composition of Sulfur in Coals from the Illinois Basin; *Economic Geology*, Volume 74, pages 1445-1461
- Quercol, X., Fernandez-Turiel, J.L., Lopez-Soler, A., Hagemann, H.W., Dehmer, J., Juan, R. and Ruiz, C. (1991): Distribution of Sulfur in Coals of the Teruel Mining District, Spain; *International Journal of Coal Geology*, Volume 18, pages 327-346.
- Raymond, R., Jr. (1982): Electron Probe Microanalysis: A Means of Direct Determination of Organic Sulfur in Coal; in *Coal and Coal Products*, Fuller, E.L., Editor, *American Chemical Society*, Symposium Series 205, pages 191-203.
- Renton, J.J. and Bird, D.S. (1991): Association of Coal Macerals, Sulfur, Sulfur Species and the Iron Disulphide Minerals in Three Columns of the Pittsburg Coal; *International Journal of Coal Geology*, Volume 17, pages 21-50.
- Stach, E., Mackowsky, M-Th., Teichmuller, M., Taylor, G.H., Chandra, D. and Teichmuller, R. (1982): *Stach's Textbook of Coal Petrology*, 3rd Edition; *Gebrüder Borntraeger*, Berlin, Stuttgart.
- Stock, L.M., Wolny, R. and Bal, B., (1989): Sulfur Distribution in American Bituminous Coals; *Energy and Fuels*, Volume 3, Number 6, November/December 1989, pages 651-661.
- Williams, E.G. and Keith, M.L. (1963). Relationship Between Sulfur in Coals and the Occurrence of Marine Roof Beds; *Economic Geology*, Volume 58, pages 720-729.



**PEACE RIVER COALFIELD DIGITAL MAPPING PROJECT,
1992 FIELDWORK
(93I/9, 10)**

By J.M. Cunningham and B.W. Sprecher

KEYWORDS: Coal geology, Peace River, digital compilation, Belcourt Creek, Wapiti Lake, stratigraphy, coal exploration, Monkman Park, Kakwa Recreational Area, Belcourt Creek Park.

INTRODUCTION

The mapping completed during the 1992 field season covered the Belcourt Creek (93I/9) map sheet and half of the adjacent Wapiti Lake (93I/10) map sheet (Figure 5-4-1). These map areas straddle the foothills of the Rocky Mountains in northeast British Columbia, at the southeast end of the Peace River coalfield (Figure 5-4-2). This area is of particular interest because of proposed park additions and new parks in the Monkman Pass region which may include segments of the coalfield.

The work done this summer essentially completes the fieldwork for the Peace River coalfield digital mapping project. Since mapping began in 1986, nine maps have been released as Open Files. The Wapiti Lake and Belcourt Creek geology maps will be released as Open Files in early 1993. Maps completed in the Pine Pass - Chetwynd area by Peter Jahans, as part of a Master's thesis at the University of Alberta (Jahans, 1992), will also be released. Part or all of fourteen 1:50 000-scale map sheets will have been completed by the end of the project.

An important adjunct to the field mapping has been the digital compilation of data from previous work in the area. An extensive digital database (including virtually all the outcrop data from coal assessment reports, coal and petroleum drill-hole locations, as well as digital versions of some of the coal report maps) has been compiled for the Peace River coalfield.

LOCATION AND ACCESS

The total area mapped in the Belcourt Creek - Wapiti Lake area is approximately 1300 square kilometres, extending from the Outer Foothills in the east to the boundary of the Inner Foothills with the Rocky Mountain Main Ranges in the west. Elevations range from about 1000 to 2000 metres, with treeline at around 1800 metres. Vegetation varies from mature stands of pine and spruce to alpine tundra at higher elevations. Ridges trend predominantly northwest, reflecting the underlying geological control. The principal drainages in the area, the Wapiti River, Red Deer Creek and Belcourt Creek, follow wide valleys, and cut across the ridges in a northeasterly direction.

Outcrop is predominantly along the ridge tops, as well as in roadcuts and in the creek and river valleys. In 1987, a large forest fire burned almost 8000 hectares on the north side of Red Deer Creek, making outcrop in the area easier to find.

Road access from the city of Dawson Creek to the map area is by the Old Heritage Highway (52). Within the central part of the map area, logging and well-access roads provide access for four-wheel-drive truck. Mountain bikes were used where roads were impassable by truck. More remote areas in the west and south were reached by helicopter.

DIGITAL COMPILATION AND MAPPING

Most of the data collected during the compilation and field mapping have been incorporated into a digital database. The methodology used has been described to varying degrees in previous articles (Kilby and Wrightson, 1987a, b, c; Kilby and Johnston, 1988a, b, c; Kilby and Hunter, 1990; Hunter and Cunningham, 1991a, b; Cunningham and Sprecher, 1992a, b) and so will only be briefly summarized here.

The database has been compiled from several sources, including coal assessment reports (exploration maps, coal boreholes, exploration reports), oil and gas drill-hole data, earlier mapping by the British Columbia Geological Survey Branch (Gilchrist and Flynn, 1978) and the Geological Survey of Canada (McMechan and Thompson, 1985; Taylor and Stott, 1979). Outcrop data from all these sources have been digitized using an in-house program. Outcrop information collected in the field this year was also incorporated into the database.

Formation boundaries and structural traces were also digitized from coal assessment report maps using QUIK-Map, a Geographic Information System (GIS) program. QUIKMap was also used extensively during all phases of map compilation, editing and production for the Le Moray Creek and Carbon Creek map sheets (Cunningham and Sprecher, 1992a, b). Geological traces can be displayed in conjunction with outcrop data. Much of the coal exploration mapping in the area was done at 1:2500 scale. These large-scale, detailed geological maps can be digitized, then edited and incorporated into the final 1:50 000-scale map, preserving detail and accuracy. This ability to display and query all the outcrop data, drill-hole locations and previous mapping simultaneously on the computer screen, allows GIS programs to be used in the interpretive stage of map production, and not simply as a drafting tool.

GEOLOGY OF THE STUDY AREA

PREVIOUS WORK

Previous mapping in the Monkman Pass area includes 1:50 000-scale mapping completed by the Geological Survey of Canada which covers the southeast corner of 93I (McMechan and Thompson, 1985). Taylor and Stott (1979) published the 1:250 000-scale regional map covering all of

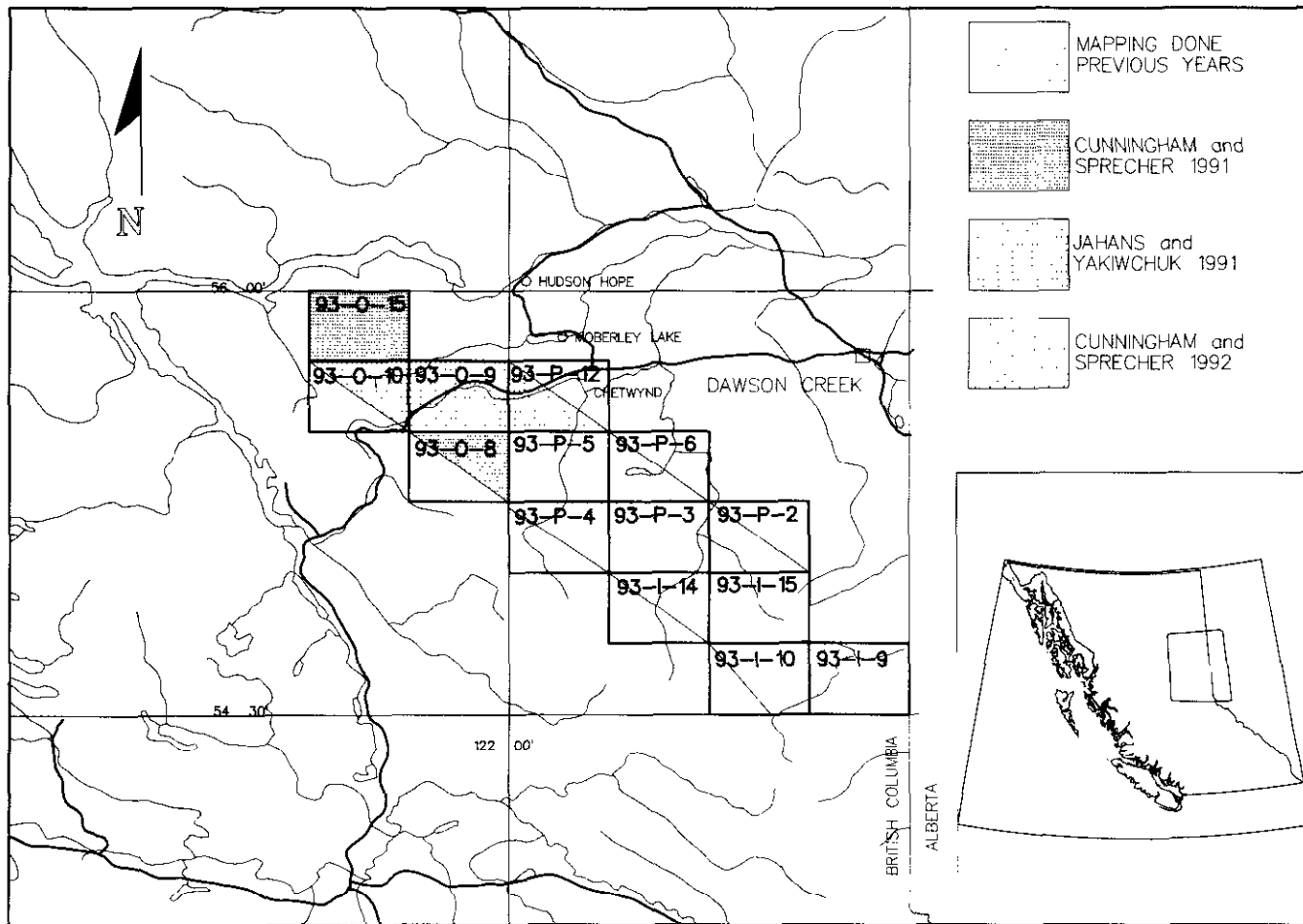


Figure 5-4-1. Location map indicating the area mapped in 1992. Areas mapped in previous years are also shown.

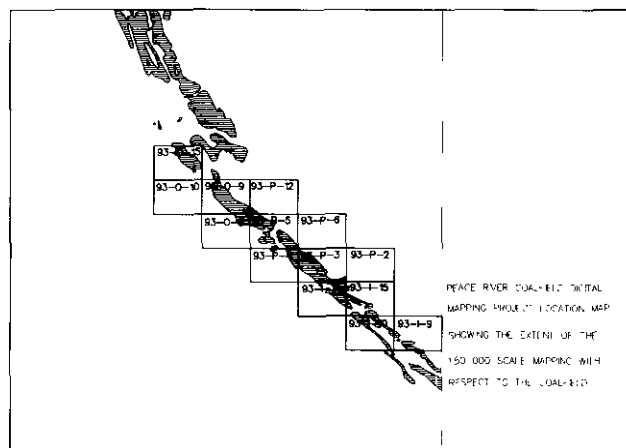


Figure 5-4-2. Map showing location of the Wapiti Lake (93I/10) and Belcourt Creek (93I/9) map areas relative to the Peace River coalfield.

931. Gilchrist and Flynn's (1978) compilation maps of the Peace River coalfield included the coal-bearing strata in the Monkman Pass area. Detailed mapping of the coal-measures in the Monkman Pass area has been done in previous years by coal exploration companies.

Detailed descriptions of the stratigraphy and structural geology, as well as interpretations of the paleogeography, have been published by Stott (1967, 1968, 1973, 1982) and Hughes (1964, 1967). The Gorman Creek Formation of the Minnes Group in the Monkman Pass area has been described by Stott (1981).

STRATIGRAPHY

Triassic to Upper Cretaceous strata are exposed in the study area. The younger Upper Cretaceous Smoky Group and Wapiti Formation are exposed in the eastern Belcourt Creek map area (Figure 5-4-3). Limited exposures of older Triassic limestones and Jurassic Fernie Formation, as well as Lower Cretaceous rocks of the Minnes Group, are found in the core of the broad, regional-scale Belcourt anticlinorium in the Wapiti Lake map area (Figure 5-4-4). Lower Cretaceous rocks of the Bullhead and Fort St. John groups are exposed in both limbs of the northwest-trending anticlinorium. The western limit of the area mapped is a

major fault which thrust Paleozoic carbonate rocks over the southwest-dipping Fort St. John Group. This fault marks the boundary between the Inner Foothills and the Rocky Mountain Main Ranges.

The formations found in the region are summarized in Table 5-4-1. The stratigraphic nomenclature used for the study area is that of the Geological Survey of Canada and is derived from the work of D.F. Stott (1967, 1968, 1973, 1981, 1982). This nomenclature is used to maintain continuity with previous mapping on this project (Kilby and Wrightson, 1987a, b, c; Kilby and Johnston, 1988a,b,c; Kilby and Hunter, 1990; Hunter and Cunningham, 1991a,b; Cunningham and Sprecher, 1992a,b). Previous descriptions of the stratigraphy are quite extensive, and only brief descriptions that highlight variations observed while mapping in various parts of the Peace River coalfield are provided here.

FERNIE FORMATION

The Fernie Formation consists predominantly of recessive, dark grey to black marine shale. Only limited exposures are found in the map area. Most outcrops of the Fernie Formation are found on the small tributary creeks that cut deeply into the overlying Minnes Group strata, in

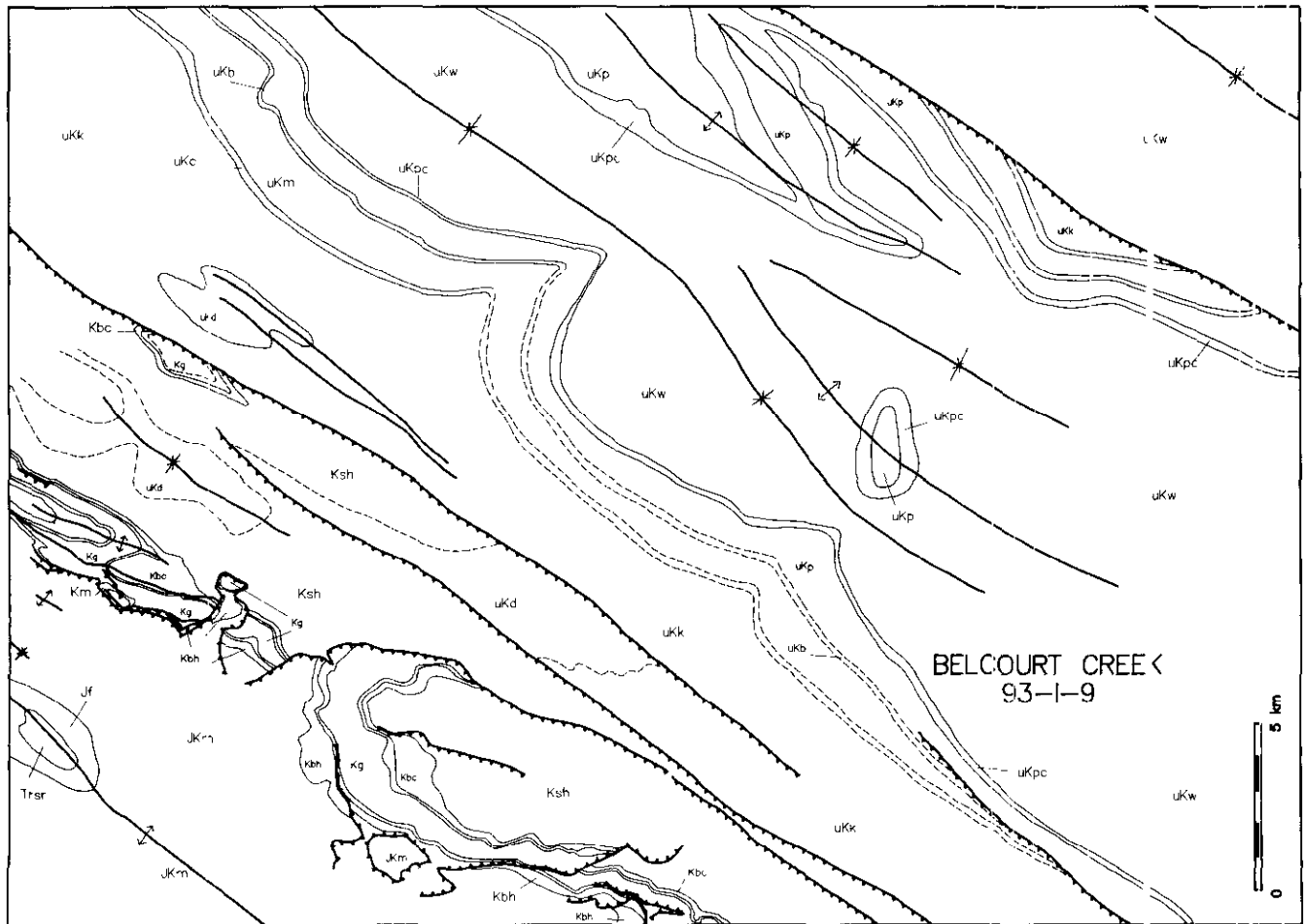


Figure 5-4-3. Preliminary compilation map of the Belcourt Creek map area. See Table 5-4-1 for key to map-unit symbols.

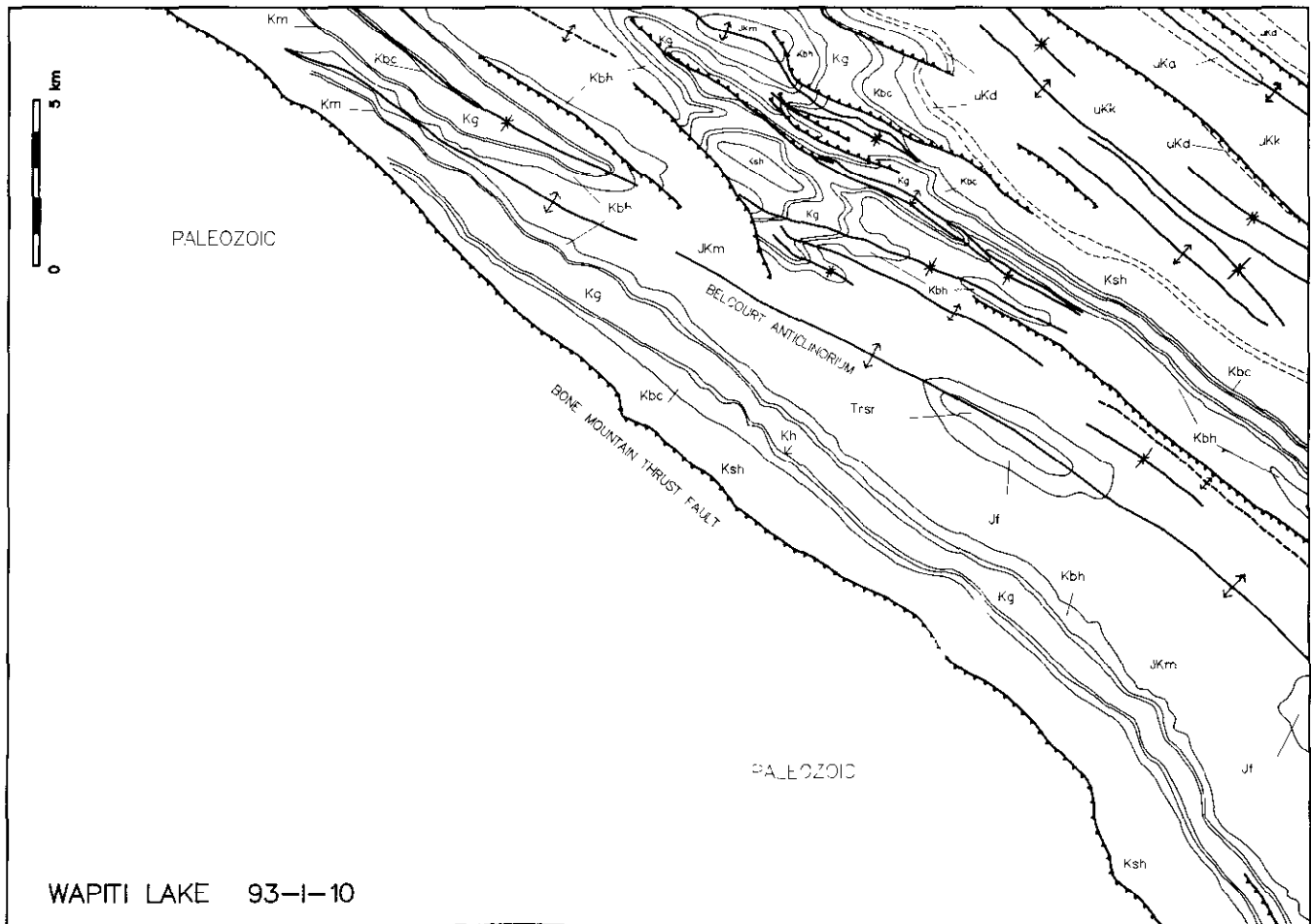


Figure 5-4-4. Preliminary compilation map of the Wapiti Lake map area. See Table 5-4-1 for key to map-unit symbols.

the valleys of Red Deer Creek and the Wapiti River, along the axis of the Belcourt anticlinorium.

MINNES GROUP

To the north, from the Pine River to the Peace Canyon, the Minnes Group can generally be divided into four units: the Jurassic to Lower Cretaceous Monteith Formation, and the Lower Cretaceous Beattie Peaks, Monach and Bickford formations (Stott, 1981, 1982). This is the nomenclature used for units in the Minnes Group in the Le Moray Creek map area (93O/8; Cunningham and Sprecher, 1991a,b) and in the Carbon Creek map area (93O/15; Legun, 1988; Cunningham and Sprecher, 1992a, b).

These divisions were not readily recognized in the Burnt River area, west of the Sukunka River (93P/5; Hunter and Cunningham, 1990a, b). The Minnes exposures there consist of interbedded sandstones, siltstones, mudstones, carbonaceous mudstones and thin coal seams and often display complex, mesoscopic-scale folding and faulting. In the Monkman Pass area, the upper part of the Minnes Group appears very similar to the deformed Minnes strata mapped in the Burnt River area.

South of the Pine River, Stott (1981) divides the Minnes Group into two units: the lower Monteith Formation and the

upper Gorman Creek Formation. This convention was continued by later workers mapping in the Monkman Pass area (McMechan and Thompson, 1985).

In the Wapiti Lake - Belcourt Creek map areas, the Gorman Creek Formation consists of sandstones, siltstones, mudstones, carbonaceous shales and mudstones, some conglomerates and a few thin coal seams. The Gorman Creek is somewhat similar in appearance to the Bickford Formation, but is considerably thicker. Stott (1981) equates the upper Gorman Creek Formation to the Bickford.

The Monteith Formation consists mostly of brown-grey weathering, resistant sandstones.

Minnes Group strata are generally tree covered and poorly exposed in the northern half of the map area, but are exposed along ridge tops in the south.

BULLHEAD GROUP

The Bullhead Group comprises two formations, the Cadomin and the Gething. In the map area, the Cadomin Formation consists predominantly of grey-weathering, pebble to cobble conglomerate, forming a resistant marker unit some 40 to 50 metres thick. This is similar to the Cadomin mapped in the Burnt River area. In the Le Moray Creek map area, the Cadomin thickens northward to about 250 metres

TABLE 5-4-1
TABLE OF STRATIGRAPHIC UNITS
THICKNESSES GIVEN ARE AVERAGE FOR THE MAP AREA

SERIES	GROUP	MAP KEY	FORMATION	THICK (m)	LITHOLOGY			
UPPER CRETACEOUS		uKw	WAPITI	1500	Nonmarine interbedded conglomerate; sandstone; siltstone and coal.			
	SMOKY	uKpc	CHUNGO MEMBER	20	Fine-grained, thick-bedded to massive, brown sandstone and gray siltstone.			
		uKp	PUSHWASKAU	250	Dark grey to black, rusty weathering marine shale; concretionary. Some calcareous shale in lower part.			
		uKb	BAD HEART	25	Fine-grained, brown sandstone; lower part includes siltstone and mudstone.			
		uKm	MUSKIKI	65	Grey marine shale; rusty weathering; concretionary.			
		uKc	CARDIUM	60	Marine and nonmarine sandstone; may be conglomerate in upper part.			
		uKk	KASKAPAU	750	Dark grey marine shales; interbedded sandstone and shale in lower half.			
		uKd	DUNVEGAN	150	Marine and nonmarine sandstone; shale and coal; some conglomerate.			
	LOWER CRETACEOUS	FORT ST. JOHN	Ksh	SHAFTSBURY	uKcr	CRUISER	120	Dark grey marine shale with sideritic concretions; some sandstone.
				Kgo	GOODRICH	190	Fine-grained, crossbedded sandstone; shale and mudstone.	
Kha				HASLER	250	Silty dark grey marine shale with sideritic concretions; siltstone in lower part.		
		Kbc	BOULDER CREEK	90	Fine-grained, well-sorted sandstone; massive conglomerate; nonmarine sandstone and mudstone and coal.			
		Kh	HULCROSS	20	Dark grey marine shale with sideritic concretions.			
		Kg	GATES	280	Fine-grained, marine and nonmarine sandstones; conglomerate; coal; shale and sandstone.			
		Km	MOOSEBAR	40	Dark grey marine shale with sideritic concretions; glauconitic sandstone and pebbles at base.			
		BULLHEAD	Kge	GETHING	80	Fine to coarse-grained, brown, calcareous carbonaceous sandstone; coal; carbonaceous shale, and conglomerate.		
		Kbh	Kcd	CADOMIN	40	Massive conglomerate containing chert and quartzite pebbles and sandstone.		
JURASSIC		MINNES	Kgc	GORMAN CREEK	900	Fine-grained sandstone; siltstone and mudstone; some conglomerate; carbonaceous shale and thin coal seams.		
	JKm	JKmt	MONTEITH	300	Fine-grained, brown-grey weathering sandstone; minor siltstone and mudstone.			
		Jf	FERNIE	200	Calcareous and phosphatic shales; rusty weathering shales; glauconitic siltstone; sideritic shales; and in upper part thinly interbedded sandstone, shale, and siltstone.			
TRIASSIC	SPRAY RIVER	Trer	(UNDIVIDED)	400	Resistant limestone and dolomite; some sandstone and siltstone.			

(After Stott 1967, 1981, 1982)

and includes increasing amounts of sandstone and mudstone. Farther north, in the Carbon Creek and Peace River Canyon areas, the Cadomin Formation consists principally of resistant sandstones and is about 250 to 280 metres thick (Stott, 1968; Legun, 1988).

In the Carbon Creek area, the Gething can be over 1000 metres thick (Legun, 1988; Gibson, 1985). To the south in the Monkman Pass region, it is much thinner, averaging about 80 metres thick. It comprises brownish grey weathering pebble to cobble conglomerate, brown-weathering sandstone, siltstone and mudstone and coal. Locally, conglomerate comprises approximately a third of the thickness and isolated outcrops of Gething conglomerate can be difficult to differentiate from Cadomin conglomerate. Only a few coal seams of interest have been noted in the Gething Formation within the map area. Gething coal seams are thicker and more abundant in the Burnt River map area, where the formation was a primary exploration target on coal properties in the area. Significant coal seams are found in the Gething in the Le Moray Creek as well as in the Carbon Creek area.

MOOSEBAR FORMATION

The Moosebar Formation is about 40 metres thick and is generally identified in the field and on airphotos as a recessive, (shaly) unit between the more resistant Gates and Gething formations.

GATES FORMATION

The Gates Formation consists mainly of interbedded sandstone, siltstone and mudstone, conglomerate and coal. Coal seams are up to 15 metres thick in some areas. Carbonaceous mudstones are also present, and siltstones and sandstones may contain carbonaceous material and woody imprints. The Torrens sandstone is a resistant unit, 15 to 25 metres thick, marking the base of the Gates Formation, which averages about 280 metres thick in the map area.

To the north, at the southern edge of the Burnt River map area, the Gates Formation contains only a few thin coal seams. Further north, across the Burnt River, there is little conglomerate or coal found in the Gates. In the Carbon Creek area, it consists of sandstones, siltstones and mudstones with little carbonaceous material or coal.

HULCROSS FORMATION

The Hulcross Formation is about 20 metres thick in the map area. It is generally recognized as a recessive band of shale between the resistant Boulder Creek and Gates formations. Farther to the south the Hulcross thins to only a few metres thick.

BOULDER CREEK FORMATION

The Boulder Creek Formation consists of light grey weathering pebble conglomerate and sandstone, as well as mudstone, and is approximately 90 metres thick. In the Burnt River area, it is slightly thicker, is dominated by two massive conglomerate units, and contains minor coal seams. In the Carbon Creek map area the formation consists mainly of finer sandstone, siltstone and mudstone.

YOUNGER FORT ST. JOHN GROUP STRATA

Along the foothills northwest of the map area, the Fort St. John Group above the Boulder Creek Formation is readily divided into the Hasler Formation (marine shale), the Goodrich Formation (sandstone, siltstone), and the topmost Cruiser Formation (marine shale). On the eastern limb of the Belcourt anticlinorium, the Goodrich sandstone units grade laterally into shales and the entire shale unit above the Boulder Creek is called the Shaftsbury Formation.

To the south of the Wapiti Lake area, the Goodrich Formation is exposed west of Mount Belcourt and Belcourt Lake, stretching along the western margin of the Inner Foothills (Taylor and Stott, 1979; McMechan and Thompson, 1985). No similar sandstone units are exposed in the map area, so for the present the Hasler, Goodrich, and Cruiser formations have not been differentiated. The recessive unit above the Boulder Creek Formation is mapped as the Shaftsbury Formation. Some sandstone outcrops on the north side of Red Deer Creek that have been exposed since the Red Deer Creek fire in 1987, and exposures along new logging roads on the south side of Red Deer Creek, may prove to be part of the Goodrich Formation.

STRUCTURE

The map area straddles the Inner and Outer Foothills of the Rocky Mountain thrust and fold belt in northeastern British Columbia. Structural elements in the area reflect the regional northwest structural trend.

The plunge of fold axes is generally very shallow. On a regional scale fold axes may undulate gently, with wavelengths of several kilometres as the plunge varies from northwest to southeast and back again along the length of the axial trace.

The Wapiti Lake map area is dominated by the Belcourt anticlinorium. The west limb of the anticlinorium is bounded by the thrust fault marking the boundary between the Inner Foothills and Rocky Mountain Main Ranges, informally called the Bone Mountain thrust fault. Paleozoic carbonate rocks are thrust over the southwest-dipping Fort St. John Group in the west limb of the anticlinorium. The east limb is structurally more complex, with megascopic-scale faulting and folding.

The style of folding varies from east to west. It reflects the transition from the broad, gentle folding and box folds found to the east in the Outer Foothills, to the tighter and more complex folding typical of the Inner Foothills to the west.

The incompetent strata of the Gorman Creek Formation show complex deformation. Tight mesoscopic chevron folds and faults are commonly seen in outcrop. The formation reflects a zone of disharmony. More competent Bullhead Group strata above, and Monteith Formation below, are not as deformed. Propagation of stress through the formations produced varying strain reflecting the competency of the layers.

Most of the faults mapped in the area dip steeply to the southwest. Some faults in the Dokken Creek and Red Deer Creek areas have been incorporated in later folding. For the most part, the Outer Foothills are less affected by faulting,

with most of the stress taken up in large-scale folds. The Inner Foothills contain faulting on all scales, with some of the faults involved in later folding. Most of the faults in the map area are high-angle reverse faults; the most prominent and continuous fault is the Bone Mountain thrust.

ECONOMIC CONSIDERATIONS

PREVIOUS EXPLORATION

Most of the coal exploration in the area mapped this summer took place between 1970 and 1985. The important coal horizons are found in the Gates Formation. Exploration was concentrated on two large coal properties, Monkman and Belcourt. In addition, some work was also done on the small Onion Lake property (Figure 5-4-5).

The Belcourt property extended southeastward from the Wapiti River to the Narraway River and the British Columbia - Alberta border, along the east-dipping limb of the Belcourt anticlinorium. The coal licences were originally acquired by Denison Mines Limited in late 1970, and in 1978 Denison and Gulf Oil Canada Limited formed the Belcourt Joint Venture. Earliest exploration on the property was in 1971, but most of the work took place in the middle to late 1970s. The extensive exploration program included detailed mapping, trenching and drilling. Test adits were driven for bulk sampling.

Significant potential reserves were identified, and in 1979 four areas amenable to surface mining were proposed. Two of the proposed pits are in the Belcourt Creek map area: the Red Deer pit, north of Red Deer Creek, and the Holtslander North pit, between Red Deer Creek and Holtslander Creek. The regional reserves calculated for the Red Deer block indicated almost 400 million tonnes of coal in place, with 72 million tonnes accessible by surface mining. (Johnson, 1981). Similarly, over 300 million tonnes of in-place raw coal reserves were calculated to exist in the Holtslander North block, with over 70 million tonnes targeted for removal in an open pit mine (Johnson, 1981). Farther to the south, two smaller pits were proposed on either side of

Flume Creek with combined reserves of about 43 million tonnes (Johnson, 1981). Coal outside these areas was targeted for possible underground mining. By 1980, the focus of the project had shifted to the two proposed pits near Red Deer Creek, with a preliminary feasibility study done to examine the existing and proposed infrastructure necessary for a mine. However, this was the last year any work was done on the Belcourt Property. None of the proposed open-pit mines were considered feasible due to economic considerations at the time.

The Petro-Canada Limited Monkman property extended southeastward in a narrow string of licence blocks from the area of Bone Mountain to Nekik Mountain, following ridges underlain by southwest-dipping Fort St. John and Bullhead Group strata on the west limb of the Belcourt anticlinorium. Two other major licence blocks were held covering coal-bearing strata in the Five Cabin Creek - Onion Creek area, and from Honeymoon Creek south to the Wapiti River. Exploration was carried out on the property by Petro-Canada on behalf of its other partners, Canadian Superior Exploration Ltd. and McIntyre Mines Ltd. McIntyre and Canadian Superior had done much of the initial work in the early 1970s. Most of Petro-Canada's work in the late 1970s and early 1980s concentrated on the Duke Mountain Block near Honeymoon Creek, north of the Wapiti River map area. In 1980, two open-pit mines, the Honeymoon and the Duke pits, were proposed and detailed mapping, trenching, drilling and structural interpretations helped to outline the extent of the coal deposit. Measured coal reserves calculated for the Honeymoon and Duke areas were 237 million tonnes and 146 million tonnes, respectively (Petro-Canada Coal Division, 1981). A third possible open-pit mine site was identified to the southwest of the Duke pit. Although by the mid-1980s it was apparent that significant reserves were indicated, mine development was uneconomic under prevailing market conditions.

The Onion Lake property was a small block of 5 licences acquired by Shell Canada Resources Ltd. in 1979 and operated by Crows Nest Resources Ltd. The property was located at the headwaters of Onion Creek, sandwiched between the south end of the Monkman property Onion Creek licence block on the east and the Rocky Mountain Main Ranges fault on the west. The property was relatively inaccessible with little outcrop. The exploration program was limited to mapping the licences and some of the surrounding area, and the drilling of two holes. Based on the results of this work, the licences were surrendered in the mid-1980s.

Gulf Canada Resources' Iris block in the Wapiti property extended as far south as the Wapiti River, but most of the interest was in coal in the Wapiti Formation on the Kaskatinaw block, farther to the north. Only a few holes were drilled and limited mapping was done in the Iris block.

COAL OCCURRENCES

The only producing coal mines in the Peace River coalfield are at Bullmoose and Quintette. Both are open-pit mines that are exploiting coal seams in the Gates Formation. The Gates seams are mostly medium-volatile bituminous

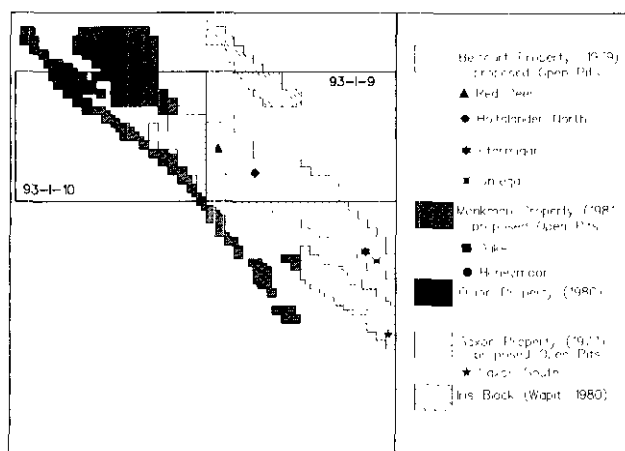


Figure 5-4-5. Map showing the various coal properties in relation to the Peace River coalfield and the areas mapped in 1992.

metallurgical coal. Oxidized coal is sold as thermal coal (Grieve, 1992).

Minor coal seams occur in several of the formations in the Monkman Pass area, but the principal coal-bearing strata are the Gorman Creek, Gething, and Gates formations; Wapiti Formation coal seams are mined in Alberta. In this area, only the Gething and Gates formations contain coal seams of potential economic interest, and it is the Gates which is the most promising.

Most of the Wapiti Formation coal seams in the map area are thin and of little interest. One thicker and relatively continuous seam is at the base of the formation, just above the resistant Chungo sandstone of the Puskwasau Formation. This 2-metre seam attracted some interest by Gulf Canada Resources on the Wapiti property farther to the north.

The coal seams in the Gorman Creek Formation are typically less than a metre thick. They are discontinuous, and the formation is often strongly deformed, making it very difficult to trace and correlate seams. The coal in the Gorman Creek has not yet proved to be of economic interest. Minnes coal ranks generally range from high to low-volatile bituminous in the Peace River coalfield. Minnes coals sampled on the Monkman property are low-volatile bituminous (Wright, 1981).

Coal in the Gething Formation is of more interest. Seam thicknesses vary, many are thin and discontinuous, but seams of possible economic significance have been noted. In the north part of the Wapiti Lake map sheet area, Gething coal may be up to a metre or two thick. In the south of the Belcourt Creek map area, seams range from a few metres to several metres thick. However, the number of thicker seams appears to decrease from north to south within the map area. Gething coals vary from medium to low-volatile in the area (Petro-Canada Coal Division, 1981).

The most important coal deposits in the region are in the Gates Formation. It contains several major seams and up to thirteen coal zones. Not all of these zones are continuous or potentially mineable. Thicknesses of the coal vary from a metre to several metres, and in some cases two or more closely associated seams form a coal zone. As many as five of these seams have been evaluated for by exploration companies. Gates Formation coals vary from high to low-volatile rank, but in the Monkman Pass area are mostly medium to low volatile (Gormley, 1977; Denison Mines Limited, 1979; Johnson, 1981).

Most of the coal horizons in the Gates Formation, and to a lesser extent the Minnes Group and Gething Formation, have been extensively sampled in drill-core, trenches and adits. For this reason, and because of a short field season, our sampling program was limited. Only a few samples of Minnes and Gates coal, as well as samples from thin seams in the Dunvegan and Bad Heart formations were collected, most in very shallow hand trenches. Samples were prepared and analyzed using methods outlined by Kilby (1986, 1989). Detailed analysis of the results has not been completed, but preliminary results indicate coal ranks fall within expected ranges.

PROPOSED PROVINCIAL PARKS AND ADDITIONS

"Parks and Wilderness for the 90s" is a cooperative program of BC Parks (Ministry of Environment, Lands and Parks) and the Forest Service (Ministry of Forests). As part of this initiative, the provincial government is proposing additions to various parks and recreational areas, as well as creating some new parks.

Additions have been proposed to Monkman Park and the Kakwa Recreational Area. A decision on these changes is planned for 1995. As well, a new park is proposed for the Belcourt Creek region; a decision will be made by the year 2000. Although the proposed boundaries are subject to revision during the planning process, the areas that have been designated for the Kakwa Addition and the new Belcourt Park include parts of the Peace River coalfield where potential coal reserves have been identified (Figure 5-4-6).

The proposed additions to the Kakwa Recreational Area would include the southern tip of the coalfield. The Saxon property, acquired by Saxon Coal Limited in late 1970, extended south from the Belcourt River to the Torrens River. The area was explored and drilled in the 1970s by Denison Mines Limited. In the middle to late 1970s, potential coal reserves were identified in two areas on the property. In the Saxon East block, calculations indicated reserves of 162 million tonnes of in-place raw coal (Jordan, 1977). Development of an open-pit mine was proposed on the Saxon South block between the Torrens River and Saxon Creek. Indicated reserves available to surface mining were calculated at 71 million tons of in-place raw coal (Jordan, 1977). A feasibility study was completed to assess the needed infrastructure to support a mine. As was the case for most of the mine development plans in the northeast at this time, economic considerations precluded mine development and continue to do so.

The proposed new Belcourt Park straddles the border of the Belcourt Creek and Belcourt Lake (93I/8) map areas, and also includes part of the southern Peace River Coalfield.

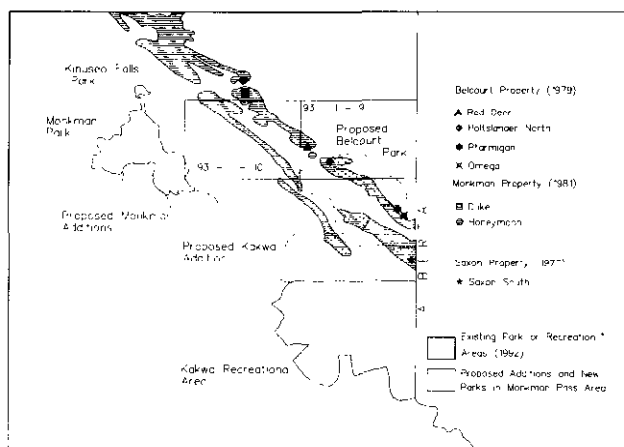


Figure 5-4-6. Map showing the boundaries of the proposed additions to Monkman Park, Kakwa Recreation Area and Belcourt Park.

This area was part of the Belcourt property explored in the 1970s and includes areas where open-pit mines were planned.

FUTURE CONSIDERATIONS

COAL EXPLORATION

Most of the coal-bearing strata in the northeast have been mapped piecemeal by various exploration companies at detailed scales, and several potentially economic deposits have been identified in the Monkman Pass area. However, present economic conditions do not encourage the development of these deposits. As a result, there has not been significant coal exploration in the area for several years.

COALBED METHANE

The high to low-volatile bituminous rank of the coals and the number of coal seams in the Peace River coalfield would make this area attractive for coalbed methane exploration. Thick coal zones in the Gates Formation might provide one source. Strain in response to the deformational stresses associated with the formation of the Rocky Mountains might provide increased permeability within coal seams. Coalbed methane production could provide a way to exploit coal which is too deep to mine.

The cold winters in the northeast could complicate water disposal from coalbed methane wells. This is an obstacle that would have to be overcome even if the geological factors are favourable. At present, there is little demand for coalbed methane in Canada, but as economic conditions change and the recovery technology improves, the coalfield may provide potential sites for coalbed methane production.

PARKS AND OTHER PROTECTED AREAS

Some of the most significant coal deposits in the southern Peace River coalfield are within the proposed boundaries for Belcourt Park and the Kakwa Addition. Although the mines that were proposed during the 1970s and 1980s could not be developed under current economic and market conditions, it is possible that in the future it will become feasible to develop these deposits. As well, the potential for coalbed methane production in this area should also be considered.

ACKNOWLEDGMENTS

The authors thank Ward Kilby and Dave Lefebure for their input into the project. Mike Malin of Canadian Helicopters in Dawson Creek provided expert helicopter support backed by years of flying experience in the Monkman Pass area. Dave Lefebure and Dave Grieve reviewed early versions of the manuscript.

REFERENCES

- Denison Mines Limited. (1979): Belcourt Project Geological Report; *B.C. Ministry of Energy, Mines and Petroleum Resources*, Coalfile 00463, 72 pages.
- Cunningham, J.M. and Sprecher, B. (1992a): Peace River Coalfield Digital Mapping Program (93O/8, 15); in *Geological Fieldwork 1991*, Grant, B. and Newell, J.M., Editors, *B.C. Ministry of Energy, Mines, and Petroleum Resources*, Paper 1992-1, pages 441-449.
- Cunningham, J.M. and Sprecher, B. (1992b): Geology of the Lemoray Creek and Carbon Creek Areas, Northeast British Columbia, NTS 93O/8,15; *B.C. Ministry of Energy, Mines and Petroleum Resources*, Open File 1992-1.
- Gibson, D.W. (1985): Stratigraphy and Sedimentology of the Lower Cretaceous Gething Formation, Carbon Creek Coal Basin, Northeastern British Columbia; *Geological Survey of Canada*, Paper 80-12.
- Gilchrist, R.D. and Flynn, B.P. (1978): Coal Resources, Peace River Coalfield, Northeastern British Columbia; *B.C. Ministry of Energy, Mines and Petroleum Resources*, Preliminary Map 33.
- Gormley, G.P. (1977): 1977 Exploration Assessment Report for Saxon Coal Limited; *B.C. Ministry of Energy, Mines and Petroleum Resources*, Coalfile 00628, 21 pages.
- Grieve, D.A. (1992): British Columbia Coal Quality Catalog, 2nd Edition; *B.C. Ministry of Energy, Mines and Petroleum Resources*, Information Circular 1992-20, 53 pages.
- Hughes, J.E. (1964): Jurassic and Cretaceous Strata of the Full-head Succession in the Peace River Foothills; *B.C. Ministry of Energy, Mines and Petroleum Resources*, Bulletin 51.
- Hughes, J.E. (1967): Geology of the Pine Valley, Mount Wabito Solitude Mountain, Northeastern British Columbia; *B.C. Ministry of Energy, Mines and Petroleum Resources*, Bulletin 52.
- Hunter, D.J. and Cunningham, J.M. (1991a): Burnt River Mapping and Compilation Project (93F/5,6); in *Geological Fieldwork 1990*, *B.C. Ministry of Energy, Mines and Petroleum Resources*, Paper 1991-1, pages 407-414.
- Hunter D.J. and Cunningham, J.M. (1991b): Geology of the Burnt River and Gwillim Lake (Southwest Half) Areas, Northeast British Columbia, NTS 93P/5, 6; *B.C. Ministry of Energy, Mines and Petroleum Resources*, Open File 1991-4.
- Jahans, P.C. (1992): Pine Valley Mapping and Compilation Project (93O/9,10; 93P12); in *Geological Fieldwork 1991*, Grant, B. and Newell, J.M., Editors, *B.C. Ministry of Energy, Mines and Petroleum Resources*, Paper 1992-1, pages 433-440.
- Johnson, D.G.S. (1981): Belcourt Joint Venture; *B.C. Ministry of Energy, Mines and Petroleum Resources*, Coalfile 00466, 31 pages.
- Jordan, G. (1977): Saxon Coal Company 1976 Exploration Report; *B.C. Ministry of Energy, Mines and Petroleum Resources*, Coalfile 00627, 34 pages.
- Kilby, W.E. (1986): Biaxial Reflecting Coals in the Peace River Coalfield (93O,P. 1); in *Geological Fieldwork 1985*, *B.C. Ministry of Energy, Mines and Petroleum Resources*, Paper 1986-1, Pages 127-137.
- Kilby, W.E. (1989): Tectonically Altered Coal Bank, Boulder Creek Formation, Northeastern British Columbia, (93P/3); in *Geological Fieldwork 1988*, *B.C. Ministry of Energy, Mines and Petroleum Resources*, Paper 1989-1, Page: 565-570.
- Kilby, W.E. and Hunter, D.J. (1990): Tumbler Ridge Northeastern British Columbia (93P/2, 3, 4; 93I/14, 15); in *Geological Fieldwork 1989*, *B.C. Ministry of Energy, Mines and Petroleum Resources*, Paper 1990-1, pages 451-459.
- Kilby, W.E. and Johnston, S.T. (1988a): Kinuseo Mapping and Compilation Project (93I/14,15;93P/3); in *Geological Fieldwork 1987*, *B.C. Ministry of Energy, Mines and Petroleum Resources*, Paper 1988-1, pages 463-470.
- Kilby, W.E. and Johnston, S.T. (1988b): Bedrock Geology of the Kinuseo Creek Area, Northeast British Columbia, NTS 93I/15; *B.C. Ministry of Energy, Mines and Petroleum Resources*, Open File 1988-21

- Kilby, W.E. and Johnston, S.T. (1988c): Bedrock Geology of the Kinuseo Falls Area, Northeast British Columbia, NTS93I/14; *B.C. Ministry of Energy, Mines and Petroleum Resources*, Open File 1988-22.
- Kilby W.E. and Wrightson, C.B. (1987a): Bullmoose Mapping and Compilation Project (93P/3.4); in Geological Fieldwork 1986, *B.C. Ministry of Energy, Mines and Petroleum Resources*, Paper 1987-1, pages 373-378.
- Kilby W.E. and Wrightson, C.B. (1987b): Bedrock Geology of the Bullmoose Creek Area, Northeast British Columbia, NTS 93P/3; *B.C. Ministry of Energy, Mines and Petroleum Resources*, Open File 1987-6.
- Kilby W.E. and Wrightson, C.B. (1987c): Bedrock Geology of the Sukunka River Area, Northeast British Columbia, NTS 93P/4; *B.C. Ministry of Energy, Mines and Petroleum Resources*, Open File 1987-7.
- Legun, A. (1988): Geology and Coal Resources of the Carbon Creek Map Area; *B.C. Ministry of Energy, Mines and Petroleum Resources*, Paper 1988-3.
- McMechan, M.E. and Thompson, R.I. (1985): Geology of Southeast Monkman Pass Area (93I/SE), British Columbia; *Geological Survey of Canada*, Open File 1150.
- Petro-Canada Coal Division (1981): Monkman Coal Project 1981 Exploration Report; *B.C. Ministry of Energy, Mines and Petroleum Resources*, Coalfile 00547, 77 pages.
- Stott, D.F. (1967): The Cretaceous Smoky Group, Rocky Mountain Foothills, Alberta and British Columbia; *Geological Survey of Canada*, Bulletin 132.
- Stott, D.F. (1968): Lower Cretaceous Bullhead and Fort St. John Groups between Smoky River and Peace River, Rocky Mountain Foothills, Northeastern British Columbia; *Geological Survey of Canada*, Bulletin 152.
- Stott, D.F. (1973): Lower Cretaceous Bullhead Group between Bullmoose Mountain and Tetsa River, Rocky Mountain Foothills, Northeastern British Columbia; *Geological Survey of Canada*, Bulletin 219.
- Stott, D.F. (1981): Bickford and Gorman Creek, Two New Formations of the Jurassic-Cretaceous Minnes Group, Alberta and British Columbia; in *Current Research, Part B. Geological Survey of Canada*, Paper 81-1B, pages 1-9.
- Stott, D.F. (1982): Lower Cretaceous Fort St. John Group and Upper Cretaceous Dunvegan Formation of the Foothills and Plains of Alberta, British Columbia, District of Mackenzie and Yukon Territory; *Geological Survey of Canada*, Bulletin 328.
- Taylor, G.C. and Stott, D.F. (1979): Geology of Monkman Pass Map-area (93I), Northeastern British Columbia; *Geological Survey of Canada*, Open File 630.
- Wright, J.Y. (1981): Monkman Coal Project 1980; *B.C. Ministry of Energy, Mines and Petroleum Resources*, Coalfile 00546, 53 pages.

UNIVERSITY RESEARCH IN BRITISH COLUMBIA

THE UNIVERSITY OF BRITISH COLUMBIA, 1992

- Chapman, A.E.: The Characterization of Porous Rocks with Nuclear Magnetic Resonance and the Confocal Laser Scanning Microscope. (M.Sc.)
- Clarkson, C.R.: Stratigraphy, Sedimentology, and Coal Quality of the Bowron River Coal Deposit (B.A.Sc.)
- Jakobs, G.K.: Toarcian (Lower Jurassic) Ammonite Biostratigraphy and Ammonite Fauna of North America. (Ph.D.)
- James, B.R.: The Worth of Data in Predicting Aquitard Continuity in Hydrogeological Design. (Ph.D.)
- McIntyre, C.A.: Construction on Paraglacial Fans: A Case Study of the Kipp Road Interchange. (B.A.Sc.)
- Miller, B.D.: Structural History and Evolution of the Northern Prout Plateau. (B.A.Sc.)
- Reilly, S.T.: Effects of Acquisition Parameters on Ground Penetrating Radar. (B.A.Sc.)
- Tercier, P.E.: Electrical Resistivity of Partially Saturated Sandstones. (M.Sc.)
- Woods, B.E.: Petrological and Geotechnical Stability Assessment of the B.C. Rail Mile 307 Rock Bluffs at Williams Lake, B.C. (M.Sc.)

UNIVERSITY OF ALBERTA, 1991

- Plint, H.E.: Metamorphism, Deformation, Uplift and their Tectonic Implications in the Horseshoe Range, North Central, British Columbia. (Ph.D.)

UNIVERSITY OF ALBERTA, 1992

- Carey, J.S.: Origin and Geologic Significance of Holocene Temperature Carbonates, British Columbia Continental Shelf. (M.Sc.)
- Hardy, R.V.: A Light Stable Isotope and Fluid Inclusion Study of the Sheep Creek Gold Camp, Salmo, British Columbia. (M.Sc.)

- Zaluski, G.S.: Hydrothermal Alteration and Fluid Sources Associated with the Babine Lake Porphyry Copper Deposits, West-central British Columbia. (M.Sc.)

UNIVERSITY OF OTTAWA, 1992

- Beaudoin, G.: Ag-Pb-Zn-Au Veins of Kokanee Range, British Columbia. (Ph.D.)

CARLETON UNIVERSITY, 1992

- Burbidge, S.: Late Quaternary Benthic Foraminifer of the Patton-Murray Seamount Group, Gulf of Alaska. (M.Sc.)
- Green, G.: Detailed Sedimentology of the Bowser Lake Group, Northern Bowser Basin, North-central British Columbia (M.Sc.)
- Thorkelson, D.: Volcanic and Tectonic Evolution of the Hazelton Group in Spatsizi River Map Area, North-central British Columbia (104H). (Ph.D.)

WESTERN WASHINGTON UNIVERSITY, 1992

- Alvarez, K.: Structure and Metamorphism in the Kwoiek Creek Area, British Columbia. (M.Sc.)

MCGILL UNIVERSITY, 1991

- Grasby, S.: Stratigraphy of the Miette Group and Tectonic History of the Southern Selwyn Range, Western Main Ranges, British Columbia. (M.Sc.)
- Klein, G.: Geology of the Northern Park Ranges and Porcupine Creek Anticlinorium, B.C. (M.Sc.)

UNIVERSITY OF SASKATCHEWAN, 1991

- Hudema, T.C.: Stratigraphy and Sedimentology of the Uppermost Frasnian Jean Marie Formation of Northeastern British Columbia and adjoining Northwest Territories. (M.Sc.)
- Zhu, C.: A Seismic Study of the Northern Williston Basin. (Ph.D.)

NOTES

**SELECTED RECENT EXTERNAL PUBLICATIONS ON
THE GEOLOGY OF BRITISH COLUMBIA
BY B.C. GEOLOGICAL SURVEY BRANCH STAFF**

Note: The following publications are by British Columbia Geological Survey Branch staff, or by staff in co-operation with other industry, government or university researchers.

- Birkett, T., Simandl, G.J. and Chaudhry, M. (1992): Ferromite, Goyazite and Apatite from the Mount Brussiloff Magnesite Deposit, B.C.; *Geological Association of Canada, Annual General Meeting, Wolfville, Nova Scotia, Abstracts*, page A9.
- Bobrowsky, P.T. and Rutter, N.W. (1992): The Quaternary Geologic History of the Canadian Rocky Mountains; *Géographie Physique et Quaternaire*: Volume 46, pages 5-50.
- Bobrowsky, P.T., Clague, J.J. and Hamilton, T.S. (1992): ¹³⁷cs Dating of a Tsunami Deposit at Port Alberni, British Columbia: The First Step Towards Establishing a Chronology of Holocene Great Earthquakes in the North Pacific; *American Quaternary Association, Program and Abstracts, 12th Biannual Meeting*, page 34.
- Brown, D.A., Greig, C.J., Bevier, M.L. and McClelland, W.C. (1992): U-Pb Zircon Ages for the Hazelton Group and Cone Mountain and Limpoke Plutons, Telegraph Creek Map Area (104G/11W, 12E and 13), Northwestern British Columbia: Age Constraints on Volcanism and Deformation; in *Radiogenic Age and Isotopic Studies: Report 6, Geological Survey of Canada, Paper 92-2*, in press.
- Dastal, J. and Church, B.N. (1992): Geology, Litho-geochemistry and Tectonic Setting of the Pioneer Basalts, Bridge River Area, British Columbia; *Geological Association of Canada, Annual General Meeting, Wolfville, Nova Scotia, Abstracts, Volume 17*, page A28.
- Dawson, K.M., Panteleyev, A., Sutherland Brown, A. and Woodsworth, G. (1991): Regional Metallogeny; in *A Decade of North American Geology; The Cordilleran Orogen, Geological Survey of Canada, Number 4, Chapter 19*.
- Diakow, L.J., Panteleyev, A. and Schroeter, T.G. (1991): Jurassic Epithermal Deposits in the Toodoggonne River Area, Northern British Columbia – Examples of Well Preserved, Volcanic-hosted, Precious Metal Mineralization; *Economic Geology*, Volume 86, Number 3.
- Drobe, J.R. (1992): Early Carboniferous Plutonism in Stikinia, Stikine and Iskut Rivers Area, Northwestern British Columbia; *Tectonics Workshop, University of Alberta, Number 24*, pages 85-86.
- Ettlinger, A.D., Meinert, L.D. and Ray, G.E. (1992): Skarn Evolution and Hydrothermal Fluid Characteristics in the Nickel Plate Deposit, Hedley District, British Columbia; *Economic Geology*, Volume 6, pages 1541-1565.
- Grieve, D.A. (1991): Biaxial Vitrinite Reflectance in Coals of the Elk Valley Coalfield, Southeastern British Columbia, Canada; in *Recent Advances in Organic Petrology and Geochemistry: A Symposium Honoring Dr. P. Hacquebard; Kalkreuth, W., Bustin, R.M. and Cameron, A.R., Editors, International Journal of Coal Geology*, Volume 19, pages 185-200.
- Hora, Z.D. and Hamilton, W.N. (1992): Native Sulfur Resource Potential of Western Canada; in *Native Sulfur - Developments in Geology and Exploration*, Wessel, G.R. and Wimberly, B.H., Editors, *Society for Mining, Metallurgy, and Exploration, Chapter 3*, pages 51-57.
- Hora, Z.D. (1992): Industrial Minerals of Western Canada – Export and Development Opportunities; *Industrial Minerals*, Volume 296, pages 55-64.
- Jessop, A.M. and Church, B.N. (1991): Geothermal Drilling in the Summerland Basin, British Columbia; *Geological Survey of Canada, Open File 2348*.
- Jones, L.D., Kortman, C.J., Pecnik, M. and Taylor, R.B. (1991): Guidelines for the Organization and Management of Earth Science Data on a Personal Computer; *International Atomic Energy Agency, Vienna, (IAEA-TECDOC- in preparation)*.
- Jones, L.D. and McPeck, C.B. (1991): MINFILE – A Mineral Deposit Information System for British Columbia, Canada; *Northwest Mining Association, 97th Annual Convention, Convention Paper 37, Computer Applications*.
- Jones, L.D., McArthur, J.G. and McPeck, C.B. (1991): MINFILE – A Mineral Deposit Information System; in *Proceedings of the Second Canadian Conference on Computer Applications in the Mineral Industry (CAMI)*, Poulin, R., Pakalnis, R.C.T. and Mular, A.L., Editors.
- Jones, L.D., McArthur, J.G., Smyth, W.R., Lowe, G.H., McPeck, C.B. and Wilcox, A.F. (1991): MINFILE – The British Columbia Solution to a Mineral Inventory Database; *Proceedings of the Fourth International Conference on Geoscience Information (GeoInfo IV); Geological Survey of Canada, Open File 2315*, in press.
- Kalnins, T.E., Wilcox, A.F., deGroot, L., McArthur, J.G., McPeck, C., Morrison, S., Guilbault, A. and Edgecombe, D. (1992): ARIS – A Mineral Assessment Report DataBase for the Public; *Proceedings for the Fourth International Conference on Geoscience Information (GeoInfo IV); Geological Survey of Canada, Open File 2315*, in press.
- Kerr, D.K., Leveson, V.M. and Smith, C.P. (1991): Applications of Quaternary Surficial Mapping to Archaeological Investigations in British Columbia; in *Current Research in the Pleistocene, Geological Survey of Canada, Volume 8*, pages 114-117.

- Kilby, W.E. (1991): Vitrinite Reflectance Measurement – Some Technique Enhancements and Relationships; *International Journal of Coal Geology*, Volume 19, pages 201-218.
- Leitch, C.H.B., Turner, R.J.W. and Höy, T. (1991): The District-scale Sullivan - North Star Alteration Zone, Sullivan Mine Area, B.C.: A Preliminary Petrographic Study; in *Current Research, Geological Survey of Canada*, Paper 91-1E, pages 45-57.
- Levson, V.M. and Morison, S. (1992): Geology of Placer Deposits in Glaciated Terrains; in *Glacial Environments – Processes, Sediments and Landforms, Pergamon Press*, 65 pages.
- Levson, V.M. (1992): The Sedimentology of Pleistocene Deposits associated with Placer Gold Bearing Gravels in the Livingstone Creek Area, Yukon Territory; *Yukon Geology*, pages 99-132.
- Levson, V.M. (1991): Geologic Controls on Alluvial Gold Mining in the Cariboo District, British Columbia, Canada; *Canadian Institute of Mining, Metallurgy and Petroleum*, Alluvial Mining, pages 245-267.
- Levson, V.M. (1991): The Bullion Mine; A Large Buried-valley Gold Placer; *The Cariboo Miner*, Volume 2, Number 5, pages 8-9.
- Levson, V.M. and Morison, S. (1991): Quaternary Gold Placers in the Canadian Cordillera; *International Union for Quaternary Research, XIII International Congress*, Abstracts, page 191.
- Levson, V.M. and Kerr, D.E. (1991): Quaternary Studies and Gold Exploration in the British Columbia Intermontane Belt; in *Late Glacial and Post-glacial Events in Coastal and Adjacent Areas, Canadian Quaternary Association*, Program and Abstracts, page 25.
- MacIntyre, D.G. (1992): Geological Setting and Genesis of Sedimentary Exhalative Barite and Barite-Sulfide Deposits, Gataga District, Northeastern British Columbia; in *Exploration and Mining Geology, Canadian Institute of Mining, Metallurgy and Petroleum*, Volume 1, Number 1, pages 1-20.
- McMillan, W.J. and Panteleyev, A. (1992): Tectonic Setting of Mesozoic Gold Deposits in the Canadian Cordillera; in *Basement Tectonics 8: Characterization and Comparison of Ancient and Mesozoic Continental Margins – Proceedings of the 8th International Conference on Basement Tectonics*, Bartholomew, M.J., Hyndman, D.W., Mogk, D.W. and Mason R., Editors, *International Basement Tectonics Association*, Publication 8, pages 633-651.
- Mihalynuk, M.G., Smith, M.T., Gabites, J., Runkle, D. and Lefebure, D. (1992): Age of Emplacement and Basement Characteristics of the Cache Creek Terrane as Constrained by New Isotopic Data; *Canadian Journal of Earth Sciences*, Volume 29, in press.
- Nelson, J. and Mihalynuk, M. (1992): Cache Creek Ocean: Closure or Enclosure?; *Geology*, November 1992.
- Pettipas, A.R., Church, B.N. and Dostal, J. (1992): Petrology and Age of the Bralorne Intrusions, Bridge River Area, British Columbia; *Geological Association of Canada*, Annual General Meeting, Wolfville, Nova Scotia, Abstracts, Volume 17, page A90.
- Ray, G.E. (1991): Vein Gold Mineralization Related to Mid-Tertiary Plutonism, Harrison Lake, British Columbia; *Economic Geology*, Volume 86, pages 883-891.
- Ray, G.E., Grond, H.C., Dawson, G.L. and Webster, I.C.L. (1992): The Mount Riordan (Crystal Peak) Garnet Skarn, Hedley District, Southern British Columbia; *Economic Geology*, Volume 7, in press.
- Simandl, G.J., Jakobsen, D. and Fischl, P.S. (1992): Refractory Mineral Resources in British Columbia, Canada – A Fresh Look; *Industrial Minerals*, May 1992.
- Simandl, G.J., Hancock, K.D., Paradis, S., Hora, Z.D. and McLean, M. (1991): Exploration for High-grade Magnesite Deposits in Mount Brussilof Area, Southeastern British Columbia; *Canadian Institute of Mining, Metallurgy and Petroleum*, Bulletin, Volume 84, Number 947, page 82.
- Simandl, G.J., Paradis, S., Valiquette, G. and Jacob, H.L. (1992): Crystalline Graphite Deposits, Classification and Economic Potential, Lachute - Hull - Mount Laurier Area, Quebec; *28th Forum on the Geology of Industrial Minerals*, West Virginia, Proceedings, in press.
- Simandl, G.J., Boucher, A.M., Macgregor, D.H., Fournier, M. and Hancock, K.D. (1992): Investment Opportunities in British Columbia Refractory Minerals and Related Value-added Products; *Fourth Annual Canadian Conference on Markets for Industrial Minerals*, Toronto, October 1992, Proceedings.
- Simandl, G.J., Jakobsen, D. and Fischl, P.S. (1992): Refractory Mineral Resources in British Columbia, Canada, A Fresh Look; *Industrial Minerals*, Number 296, May 1992, pages 67-77.
- Simandl, G.J., Hancock, K.D., Hora, Z.D., MacLean, M. and Paradis, S. (1991): Regional Geology of the Mount Brussilof Carbonate-hosted Magnesite Deposit, Southeastern British Columbia, Canada; *27th Forum on the Geology of Industrial Minerals*, Banff, Alberta, Proceedings, pages 57-65.
- Simandl, G.J., Hancock, K.D., Paradis, S., Hora, Z.D. and MacLean, M. (1992): Geology of the Mt. Brussilof Magnesite Deposit and some Exploration Considerations, Southern British Columbia, Canada; *Canadian Institute of Mining, Metallurgy and Petroleum*, Paper 6920, in press.
- Simandl, G.J., Hancock, K.D., Paradis, S. and Simandl, J. (1992): Field Identification of Magnesite-bearing Rocks Using Sodium Polytungstate; *Canadian Institute of Mining, Metallurgy and Petroleum*, Paper 6921, in press.
- Smith, M.T. (1991): Geologic Map of the Old Copper Hill - Butcher Mountain Area, Stevens County, Washington; *Washington Division of Geology and Earth Resources*, Open File Report 91-6.

- Smith, M.T. and Gehrels, G.E. (1992): Structural Geology of the Lardeau Group near Trout Lake, British Columbia: Implications for the Structural Evolution of the Kootenay Arc; *Canadian Journal of Earth Sciences*, Volume 29, Number 6, in press.
- Smith, M.T. and Gehrels, G.E. (1992): Stratigraphic Comparison of the Lardeau and Covada Groups: Implications for Revision of Stratigraphic Relations in the Kootenay Arc; *Canadian Journal of Earth Sciences* Volume 29, Number 6, in press.
- Smith, M.T., Gehrels, G.E. and Klepacki, D.W. (1992): Research Note: 173 Ma U-Pb Age of Felsite Sills near Kaslo, Southeastern British Columbia; *Canadian Journal of Earth Sciences*, Volume 29, pages 531-534.
- Smith, M.T. and Gehrels, G.E. (1992): Stratigraphy and Tectonic Significance of Lower Paleozoic Continental Margin Strata in Northeastern Washington; *Tectonics*, Volume 11, pages 607-620.
- Smith, M.T. and Gehrels, G.E. (1992): Detrital Zircon Constraints on the Provenance of the Harmony and Valmy Formations, Roberts Mountains Allochthon, Nevada; *Geological Society of America, Abstracts with Programs*, Volume 24.
- Turner, R.J.W., Leitch, C.H.B., Ames, D.E., Hoy, T., Franklin, J.M. and Goodfellow, W.D. (1991): Character of Hydrothermal Mounds and Adjacent Altered Sediments, Active Hydrothermal Areas, Middle Valley of Sedimented Rift, Northern Juan de Fuca Ridge, Northeastern Pacific: Evidence from ALVIN Push Cores, in Current Research, Part E, *Geological Survey of Canada*, Paper 91-1E, pages 99-108.

Queen's Printer for British Columbia®
Victoria, 1993